General Disclaimer

One or more of the Following Statements may affect this Document

- This document has been reproduced from the best copy furnished by the organizational source. It is being released in the interest of making available as much information as possible.

- This document may contain data, which exceeds the sheet parameters. It was furnished in this condition by the organizational source and is the best copy available.

- This document may contain tone-on-tone or color graphs, charts and/or pictures, which have been reproduced in black and white.

- This document is paginated as submitted by the original source.

- Portions of this document are not fully legible due to the historical nature of some of the material. However, it is the best reproduction available from the original submission.

Produced by the NASA Scientific and Technical Information Program

TABLE 4.8-12. SUMMARY OF HEATER SINGLE-FAILURE RESULTS (PARA. 4.8.16)

Series	LM Structure Temperature °F	Heater Voltage	Solar	Failure Mode	Temperature °F						Notes
					Injector		Ox Valve		Quad		
					Initial	Steady State	Initial	Steady State	Initial	Steady State	
VII S	100	32	NONE	ON	138	177	122	143	136	144	
F	100	32	NONE	ON	140	178	122	141	136	144	
U	100	32	NONE	ON	140	187	137	162	136	141	
D	100	32	NONE	ON	139	180	137	159	136	153	
VIII S	30	32	YES	ON	139	192	108	137	135	152	
F	30	32	YES	ON	141	192	107	135	135	152	
U	30	32	YES	ON	138	201	137	172	135	145	
D	30	32	YES	ON	138	195	137	170	135	161	
XV S	100	32	YES	ON	139	217	126	169	138	179	
F	100	32	YES	ON	138	217	126	168	138	179	
U	100	32	YES	ON	140	227	138	195	138	172	*
D	100	32	YES	ON	138	221	138	195	138	188	*

Note: (1) Only one heater on the engine shown has failed on. The other heater on the engine is off. The heaters on the other engines in the cluster are operating normally.

(2) Series shown in this table have parametric inputs similar to those in Table 4.8-10, except these are for single heater failure.

* On failure where Ox valve steady state temperature exceeds 175°F

Table 4.8.13. Forces and Moments due to RCS Plume Impingement (Para. 4.8.6.2)

Engine Quad Number	Impingement Force (lbs)			Pitch and Roll Impingement Moments* (ft-lbs)			
	Fx	Fy	Fz	Beginning of Powered Descent	Lunar Landing	CSM/LM Docked (CSM Full)	Reference Thruster Plane (x = 254, y=0 z=0)
Id	-10.4	41.7	-41.7	75.8	-28.4	-599.8	-167.4
IId	-10.4	41.7	41.7	75.8	-28.4	-599.8	-167.4
IIId	-31.4	-50.9	50.9	-52.0	-159.0	-868.6	-344.2
IVd	-10.4	-41.7	-41.7	75.8	-28.4	-599.8	-167.4

* Positive moments act in same direction as control torques

Table 4.8.14. Effect of RCS Thruster Plume Impingement on Attitude Control (Para. 4.8.6.2)

Attitude and Transition Control Mode	Mission Phase		
	Beginning Powered Descent c.g. (x=185 in, Y=0 in, z=0 in.)	Lunar Landing c.g.(x=210.2 in, y=0 in. z=0 in.)	CSM/LM Docked (CSM Full) c.g. (x=378in, Y=0 in, z=0 in.)
2-jet +X Translation force (lbs) (jets 2,10)	179.2	179.2	179.2
(jets 6,14)	137.0	137.0	137.0
4-jet +X Translation force (lbs)	318.0	318.0	318.0
2-jet Control Torque (ft-lbs) (pitch or roll)	1170.0	1083.0	500.1
using quad III	1048.0	946.0	231.3
4-jet Control Torque (ft-lbs) (pitch or roll)	2218.0	2029.0	731.4

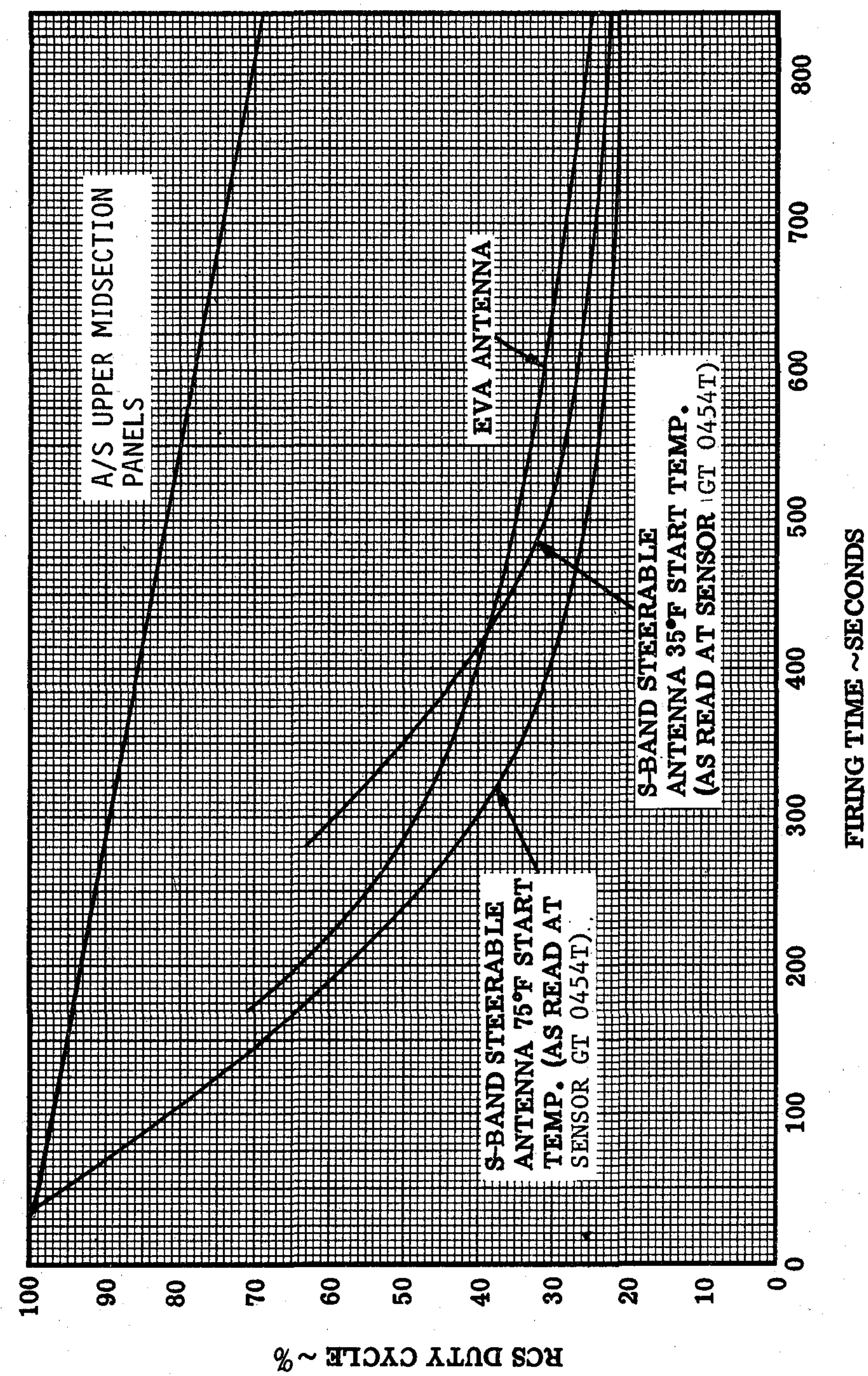

Figure 4.8-119. LM-8 and Subsequent RCS Plume Impingement Capability for Antennas (See Para. 4.8.6.1)

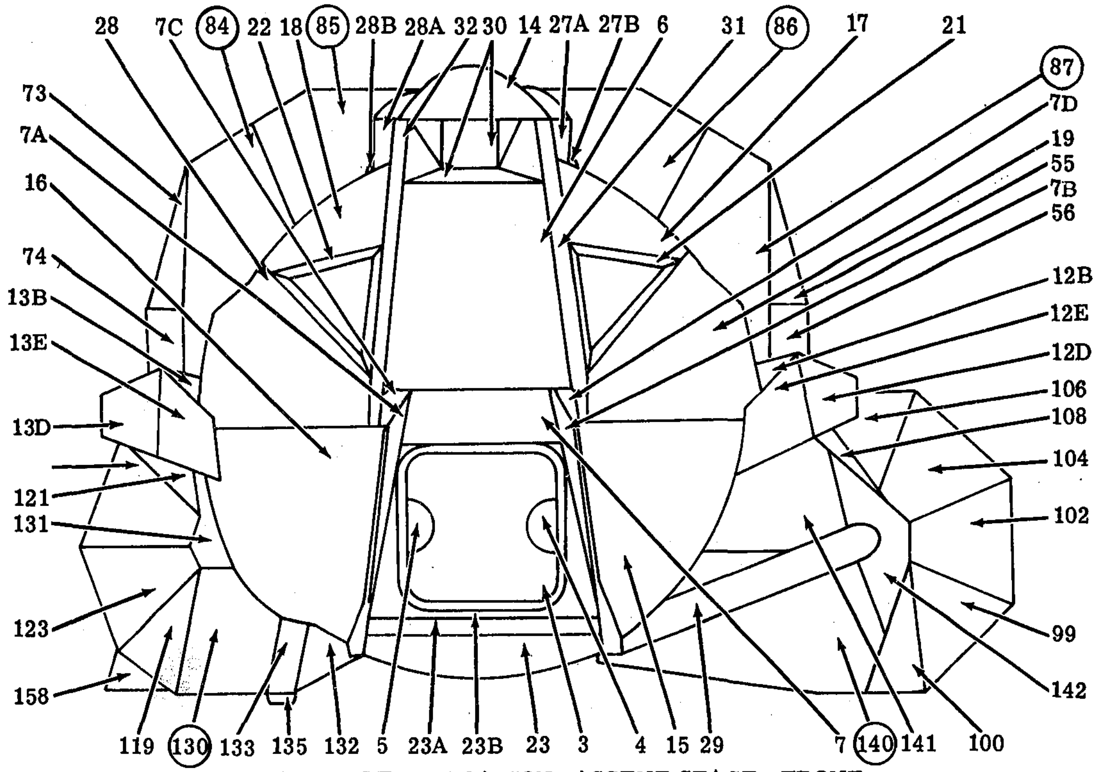

LM PANEL IDENTIFICATION, ASCENT STAGE, FRONT

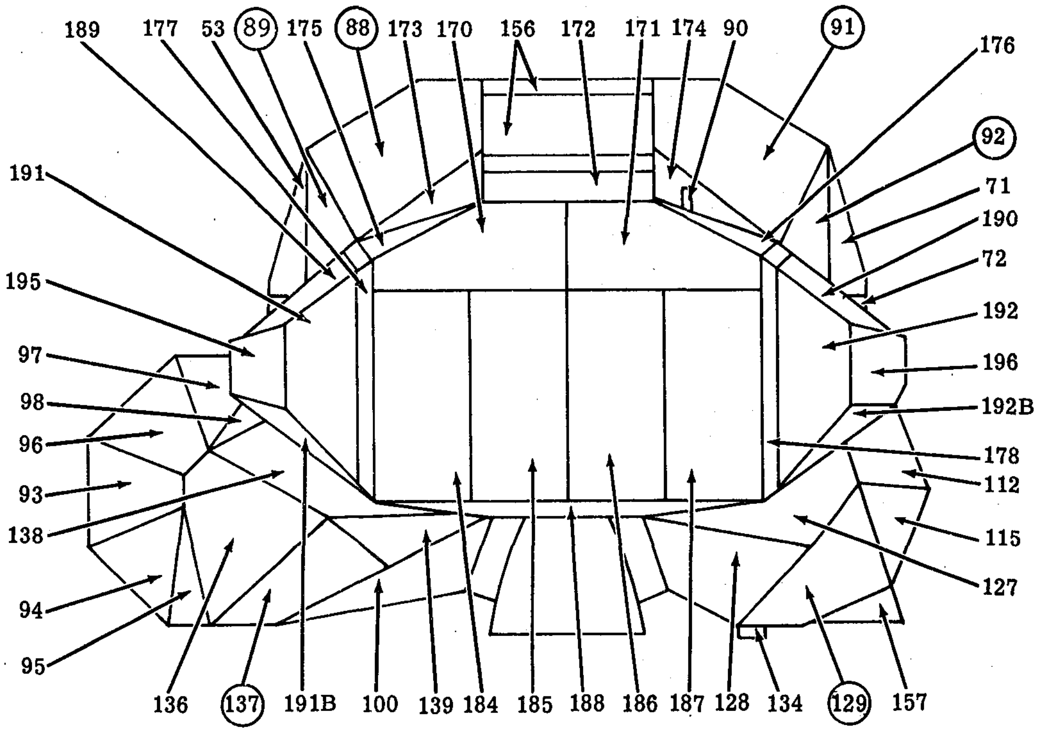

LM PANEL IDENTIFICATION, ASCENT STAGE, REAR

Figure 4.8-120. LM Panel Identification for Thermal Reference
(See paragraph 4.8.6.1.2)

Volume II LM Data Book
APPENDIX LM-7

TABLE OF CONTENTS

Changes to baseline data specific to LM-7 are included in this appendix.

1.0	No change
2.0	No change
3.1	Communications Constraints (TBS)
3.2	Crew/Equipment Constraints (TBS)
3.3	Environmental Control Subsystem Constraints (TBS)
3.6	APS Subsystem Constraints
3.7	DPS Subsystem Constraints
3.8	Reaction Control Subsystem Constraints
3.10	Thermal Constraints
4.1.2	S-Band Communications (TBS)
4.1.2.8	RCS Plume Impingement on Steerable Antenna (TBS)
4.2.4	Thermal Variations for the MESA
4.3.3	Lithium Hydroxide Consumption
4.3.4	Water Consumption (TBS)
4.3.8.1	Heat Transport Section Water Sublimators
4.3.11	Duty Cycle of LM Heaters
4.5.1.1	Uncertainty of LM IMU Alignment from CSM IMU
4.5.1.4	Guidance Computer Erasable Constants
4.5.1.5.2	Assembly Alignment Data of Spacecraft Docking Mating Surfaces to the Navigation Base
4.5.1.5.3	AOT Alignment Data
4.5.1.5.4	COAS Alignment Data (TBS)
4.5.2.1	Abort Sensor Assembly
4.5.2.1.2	AGS Angular Mounting Error
4.5.2.2	Abort Electronic Assembly
4.5.3.2.2.3	DPS Thrust Response at TTCA Minimum and Maximum Positions
4.5.3.4.3	GDA Drive Rates
4.5.4.2	RR Mechanical Alignment
4.5.4.3	RR Timeline Operations
4.5.4.4.11	RR and T AGC Voltage Versus Range
4.5.4.4.11.1	RR and T AGC Voltage Versus Range and LOS Angle
4.5.4.4.12	RR Self-Test
4.5.4.4.13	RR Power Monitor Calibration
4.5.4.4.16	Allowable Vehicle Acceleration During RR Power Off Periods
4.5.5.1.16	LR Power Monitor
4.5.5.1.17	Loss of LR Lock as a Function of Vehicle Pitch and Roll for Nominal Trajectory
4.5.5.1.18	Expected Altitude of LR Velocity and Range Initial "Data Good" Indication
4.5.5.1,21	LR Predicted Accuracy
4.5.5.2	LR Temperature Profile
4.5.5.3	LR Mechanical Alignment
4.5.5.4	Landing Radar Self-Test
4.6.1	APS Preflight Analysis
4.6.8	Thrust Vector Changes with Burn Time

Volume II LM Data Book
APPENDIX LM-7

TABLE OF CONTENTS

Changes to baseline data specific to LM-7 are included in this appendix.

4.6.9	Preflight Thermal Analysis of APS (TBS)
4.6.12	Ascent Engine Regulator Performance
4.7.1	DPS Preliminary Preflight Prediction
4.7.2	Supercritical Helium Tank Pressure (TBS)
4.7.5	DPS Propellant Tank Low Level Sensor Operation
4.7.6.1	DPS Engine Thrust Vector Orientation
4.7.8	Preflight Thermal Analysis of DPS (TBS)
4.7.12.1	DPS Propellant Tank Venting for Lunar Landing Mission
4.7.15	Descent Engine Regulator Performance
4.8.6.1	Multiple Steady State Firings Heating Effects
4.8.14	RCS Performance Limitations as a Result of Gimbal Drive Actuator (+ Pitch or + Roll) Failure During Powered Descent
4.8.14.1	Plume Impingement Constraints due to GDA Failure
4.8.14.2	Additional RCS Propellant Consumption as a Result of Gimbal Drive Actuator Failure During DPS Operation
5.0	No change
6.0	No change
7.0	No change
8.0	No change

LM7/3.6 PROPULSION - APS

OPERATIONAL LIMITATION OR PROCEDURE	RATIONALE
LM7/APS-1 Propellant Tank Pressure-Temperature Limit Relationship	
The propellant tank pressures should not exceed the values given in Figures LM7/3.6.1-1, LM7/3.6.1-2 and LM7/3.6.1-3.	Reliability is reduced below allowable value.
LM7/APS-9 Ambient Helium Storage Tank Pressure	
Helium tank pressure limitations are given in Figure LM7/3.6.1-4.	If maximum is exceeded, reliability is reduced below allowable value. If minimum is exceeded, there will be insufficient helium to complete a lunar mission duty cycle.

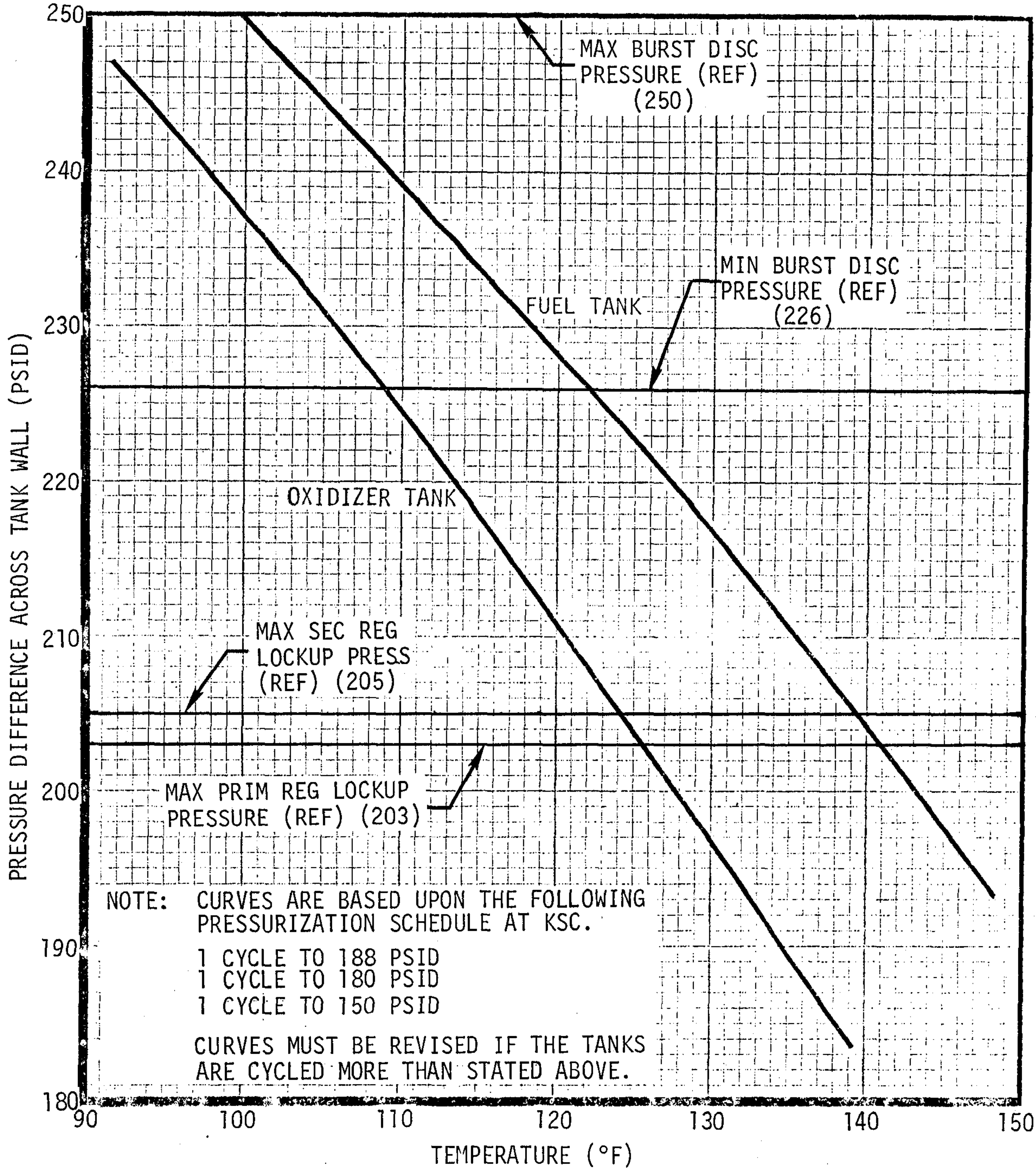

Figure LM7/3.6.1-1. Maximum Allowable Pressure-Temperature Limit Relationship for LM-7 Ascent Stage Propellant Tanks

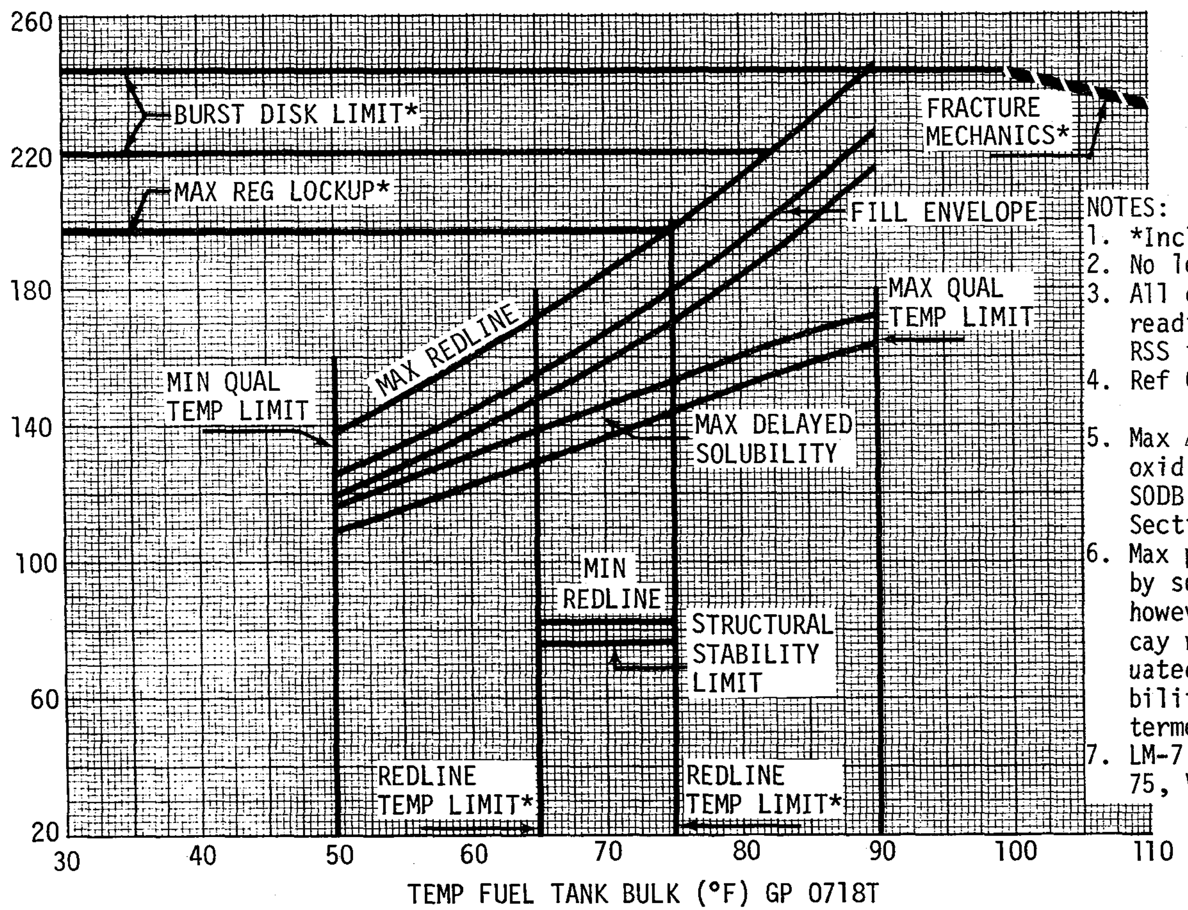

NOTES:
1. *Includes instr error
2. No leakage allowed
3. All data reflects CRT readings based on max RSS instr error
4. Ref GP 0718T/GP 1218T
5. Max ΔT between fuel & oxid is 10°F. Reference SODB Vol II, Part 1, Section 3.6
6. Max press decay defined by solubility curve, however, excessive decay rates must be evaluated considering solubility effects for intermediate points
7. LM-7 prop quan per amend 75, Vol III, SODB

Figure LM7/3.6.1-2. APS Fuel Tank Pressure-Temperature Limitations

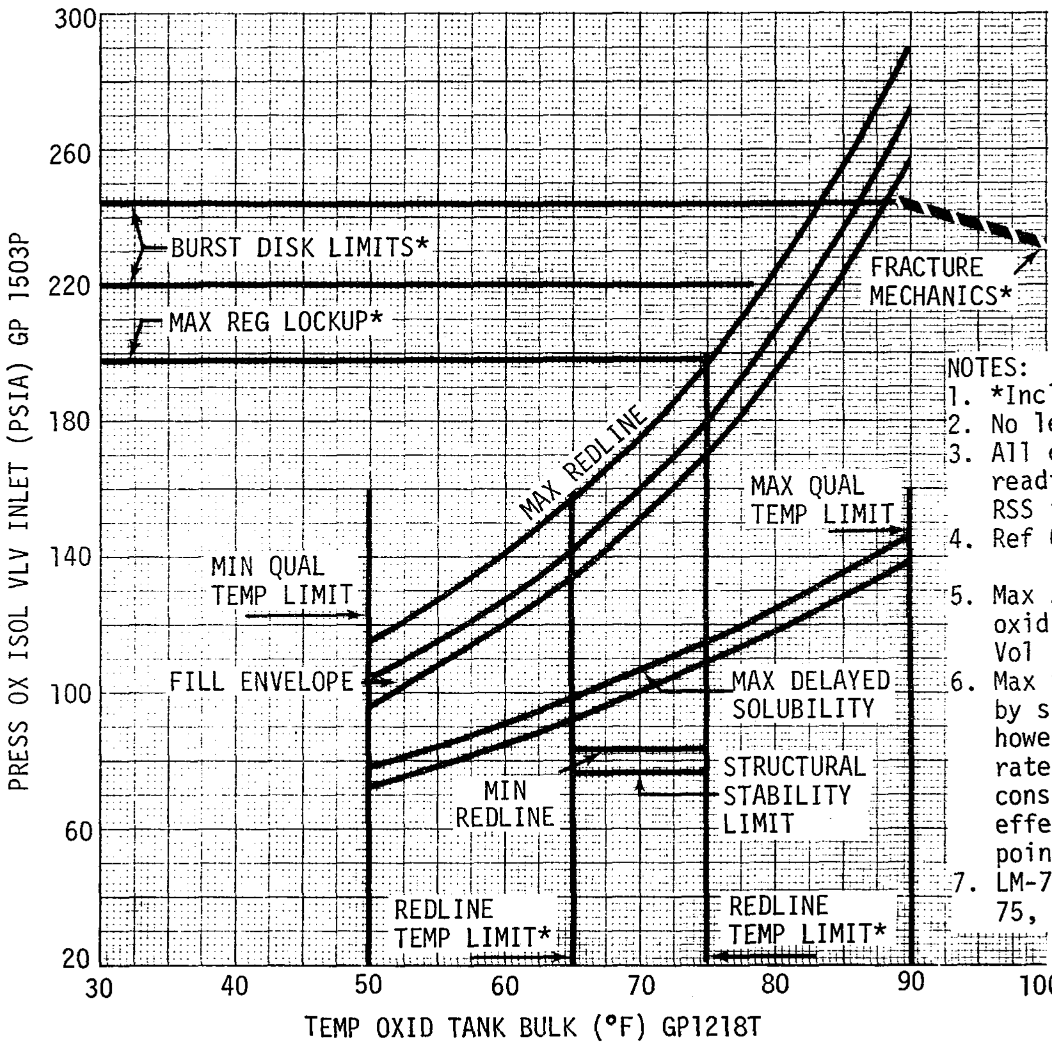

NOTES:
1. *Includes instr error
2. No leakage allowed
3. All data reflects CRT readings based on max RSS instr error
4. Ref GP 0718T/GP 1218T
5. Max ΔT between fuel & oxid is 10°F. Ref SODB Vol II, Part 1, Sec 3.6
6. Max press decay defined by solubility curve, however, excessive decay rates must be evaluated considering solubility effects for intermediate points
7. LM-7 prop quan per amend 75, Vol III, SODB

Figure LM7/3.6.1-3. APS Oxidizer Tank Pressure-Temperature Limitations

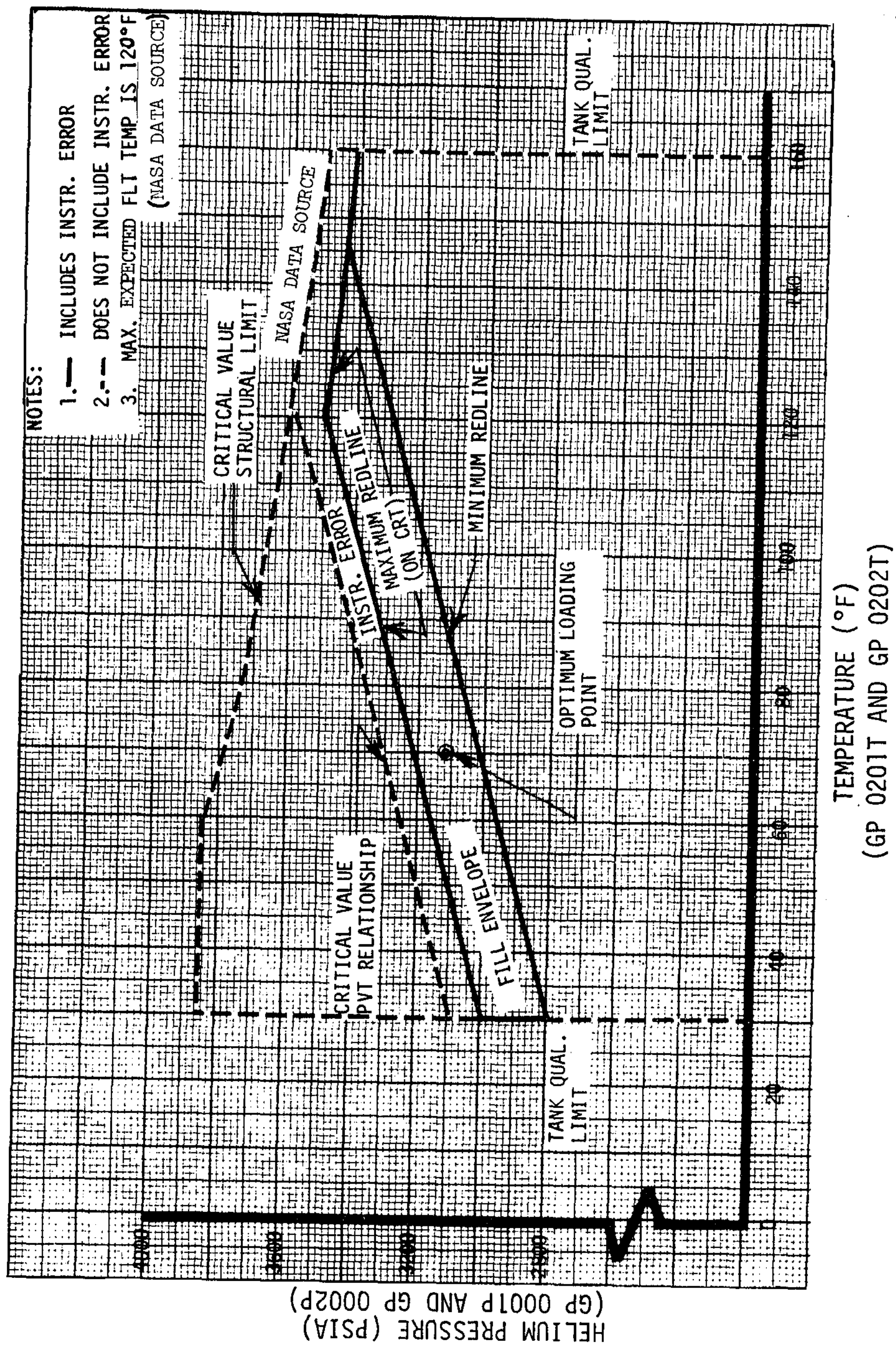

Figure LM7/3.6.1-4. APS Helium Tank Pressure-Temperature Limitations

LM7/3.7 PROPULSION - DPS

OPERATIONAL LIMITATION OR PROCEDURE	RATIONALE

LM7/DPS-6 Propellant Tank Pressure-Temperature Limit Relationship

The propellant tank pressure should not exceed the values given in Figures LM7/3.7.1-1, LM7/3.7.1-2 and LM7/3.7.1-3.

Rationale: Reliability is reduced below the allowable value.

LM7/DPS-8 Non-Throttling Range Engine Operation

See Table LM7/3.7.1-1

Rationale: Off-nominal mixture ratios may result, or the thrust chamber may burn through.

LM7/DPS-17 Engine Interface Pressure (Fuel and Oxidizer)

Event	Minimum	Maximum	Rationale
Preburn	30 psia	275 psia	If maximum is exceeded, burst disk pressure will be exceeded and helium supply will be reduced. If below minimum, freezing of fuel in heat exchanger may result.
During Burn	150 psia @ FTP	275 psia	If maximum exceeded, burst disk pressure will be exceeded and helium supply will be reduced.
	120 psia @ 10% to 65% thrust (see note)		If below minimum, extreme combustion roughness may result, which could cause engine damage.

Note: Severe chamber pressure spikes can occur as these limits are approached; therefore, operation near these limits should be minimized.

LM7/DPS-20 Ambient Helium Storage Tank Pressure-Temperature Limitations

Ambient helium tank pressure limitations are given in Figure LM7/3.7.1-4.

Rationale: If the maximum is exceeded, reliability is reduced below allowable value.

OPERATIONAL LIMITATION OR PROCEDURE	RATIONALE
LM7/DPS-24 Chamber Pressure at Throttle-Down	
The DPS Chamber pressure must be greater than 87 psia at FTP just prior to throttle down to complete the nominal mission duty cycle.	The reference chamber pressure corresponds to an erosion value equal to the maximum allowable 30% minus the predicted erosion between throttle down and landing.

Table LM 7/3.7.1-1 Non-Throttling Range Engine Operation

VEHICLE	ENGINE S/N	NOMINAL CONDITIONS		WORST CASE CONDITIONS*	
		Predicted Erosion **	Permissible Time In Non-Throttling Region ***	Predicted Erosion **	Permissible Time In Non-Throttling Region ***
LM-7	1041	17.6%	87.0 sec.	28.3%	33.5 sec.

* Worst Case erosions are applicable for MDC performed with cold propellants and high mixture ratios. (FTP 0/F = 1.63, 25% Thrust 0/F = 1.65, Propellant Bulk Temperature = 50° F)

** Predicted erosion is to propellant depletion with zero time in non-throttling range.

*** Operating time in the non-throttling range, as given, is permitted at any time during the lunar landing duty cycle.

Note: The permissible time in the non-throttling region is based on limiting the total mission duty cycle erosion to 35%, including normal and non-throttling range operations.

MDC - Mission Duty Cycle

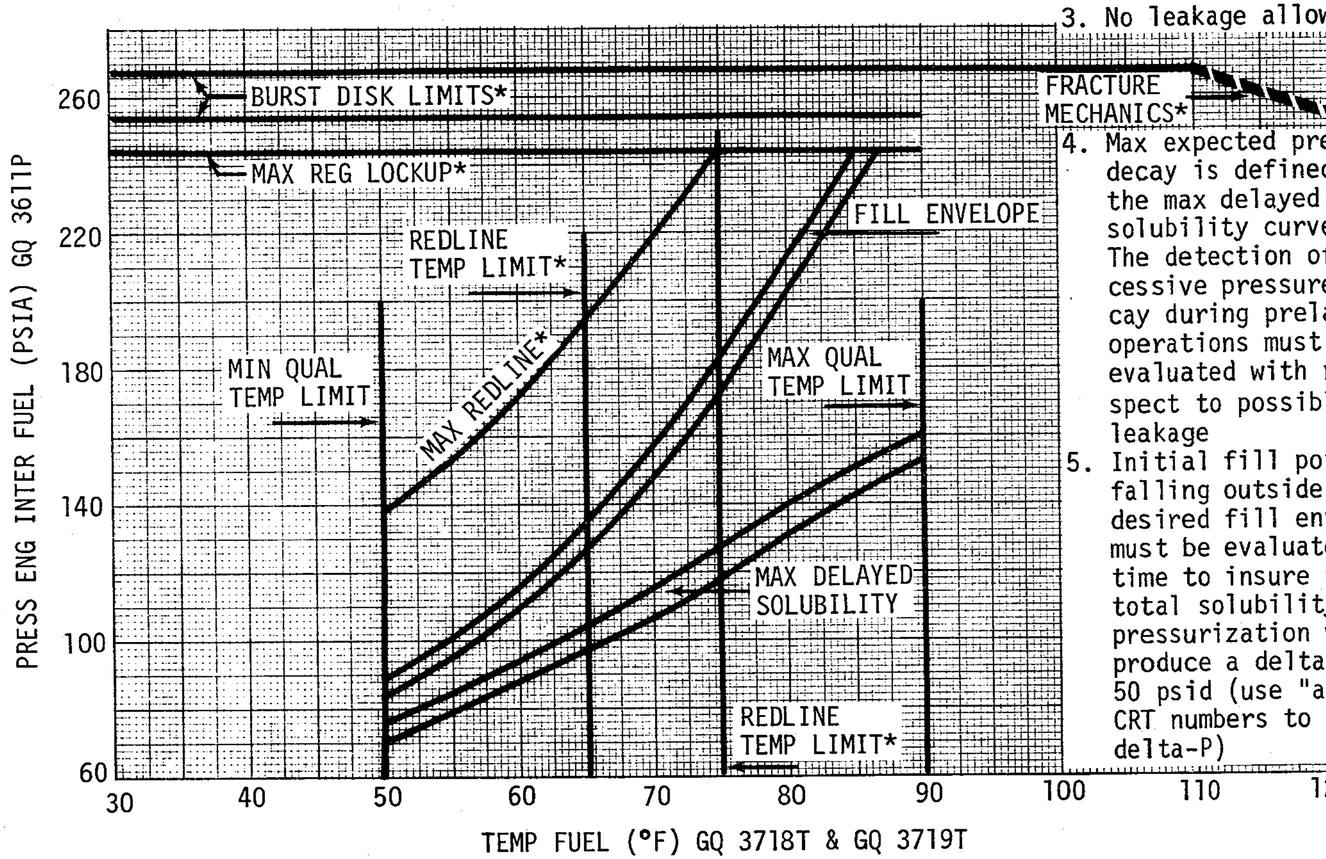

NOTES:

1. LM7 prop quan per amend 75, Vol III SODB
2. *Includes instr error
3. No leakage allowed
4. Max expected press decay is defined by the max delayed solubility curves. The detection of excessive pressure decay during prelaunch operations must be evaluated with respect to possible leakage
5. Initial fill points falling outside the desired fill envelope must be evaluated real time to insure that the total solubility at DPS pressurization will not produce a delta-P of 50 psid (use "as read" CRT numbers to determine delta-P)

Figure LM7/3.7.1-2. DPS Fuel Tank Pressure-Temperature Limitations

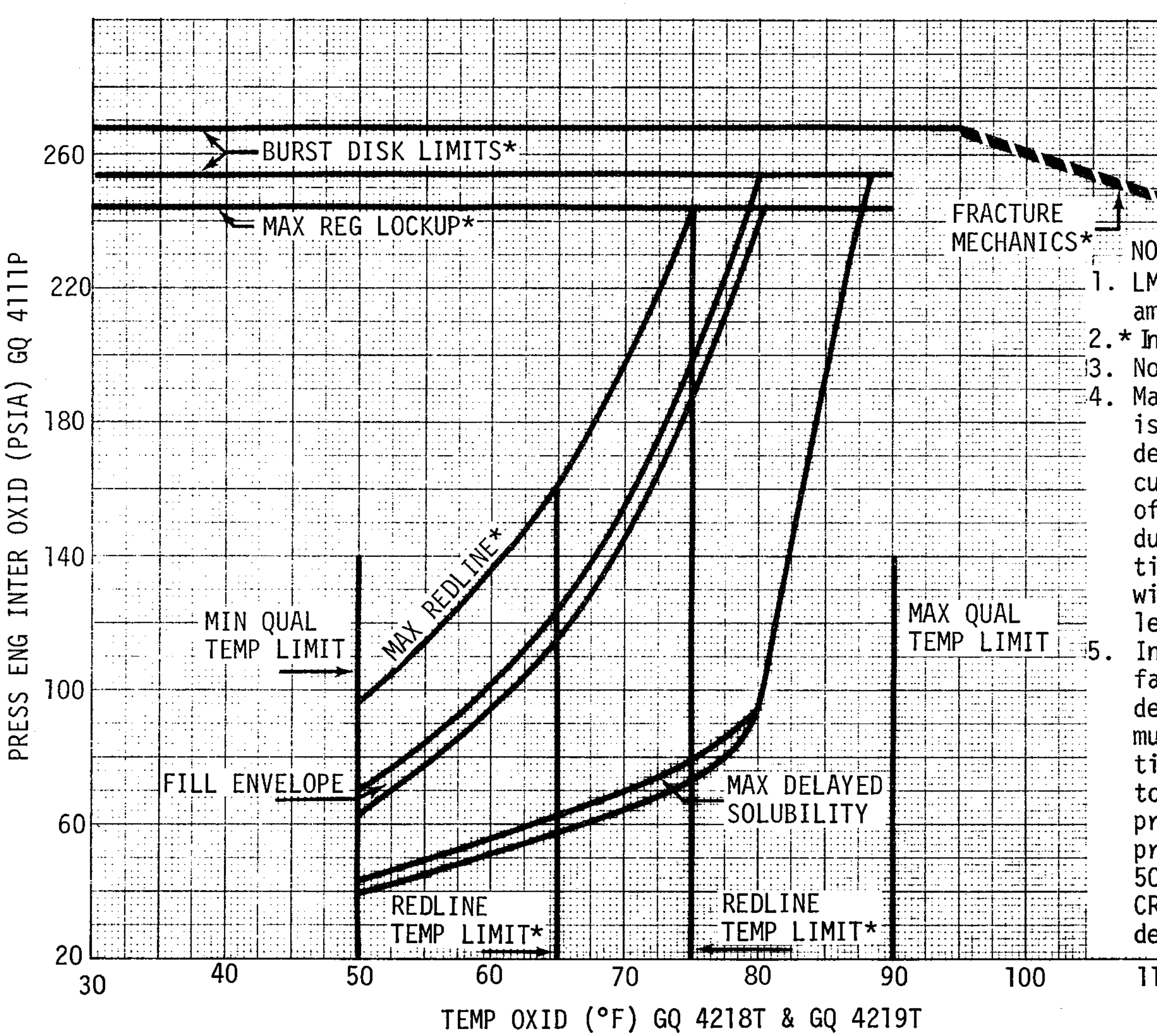

NOTES:

1. LM-7 prop quan per amend 75 Vol III SODB
2. * Includes instr error
3. No leakage allowed
4. Max expected pres decay is defined by the max delayed solubility curves. The detection of excessive pres decay during prelaunch operations must be evaluated with respect to possible leakage
5. Initial fill points falling outside the desired fill envelope must be evaluated real time to insure that the total solubility at DPS pressurization will not produce a delta-P of 50 psid (use "as read" CRT numbers to determine delta-P)

Figure LM7/3.7.1-3. DPS Oxidizer Tank Pressure-Temperature Limitations

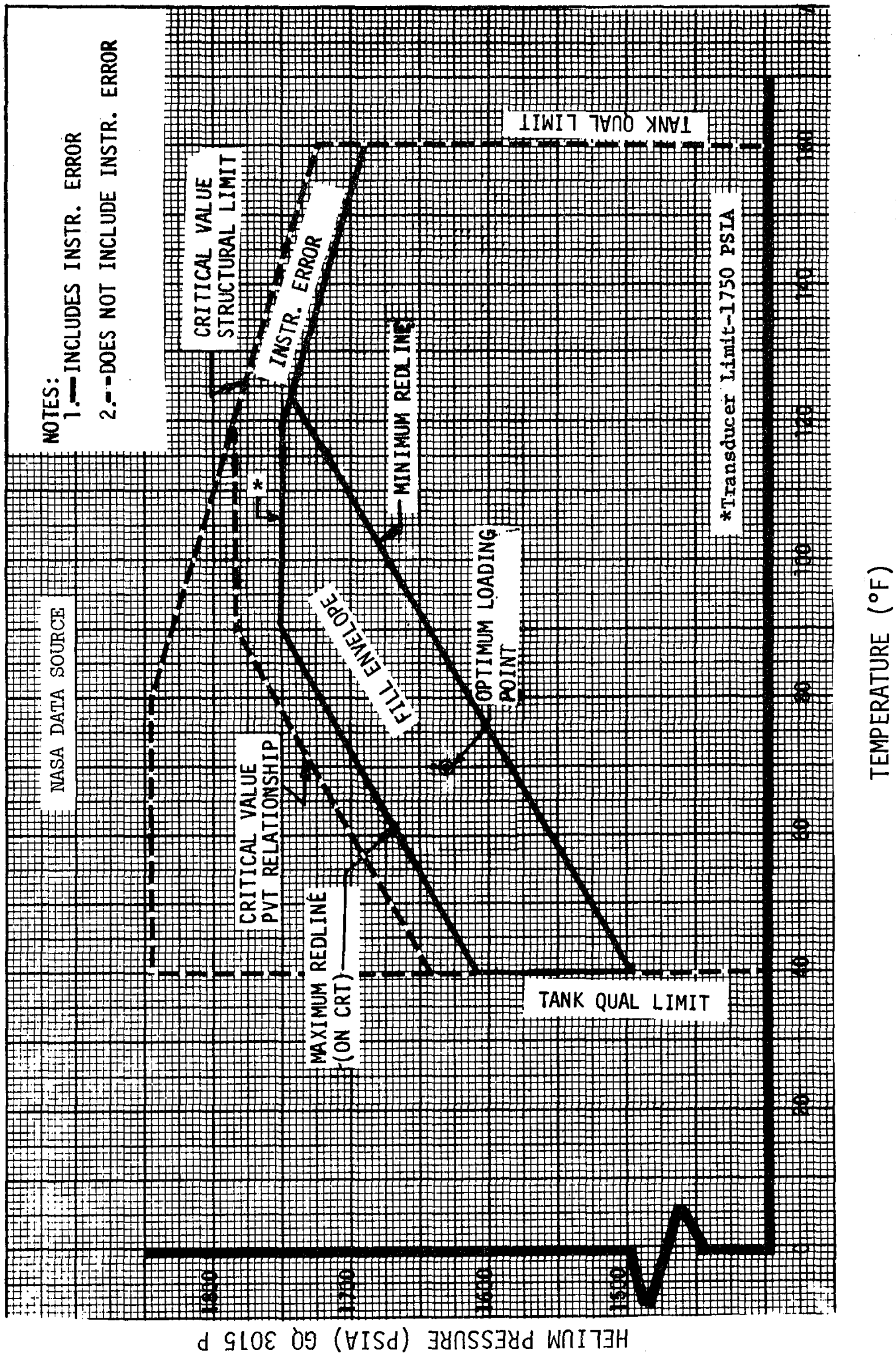

Figure LM7/3.7.1-4. DPS Ambient Helium Tank Pressure-Temperature Limitations

LM7/3.8 REACTION CONTROL SUBSYSTEM

LM7/RCS-13 Propellant Tank Pressure-Temperature Limit Relationship

The propellant tank pressure should not exceed the values given in Figure LM7/3.8.1-1.

Reliability is reduced below the allowable value.

LM7/RCS-17 RCS Helium Bottle Pressure-Temperature Limitations

RCS helium bottle pressure-temperature limitations are given in Figure LM7/3.8.1-2.

If the maximum is exceeded, reliability is reduced below allowable values.

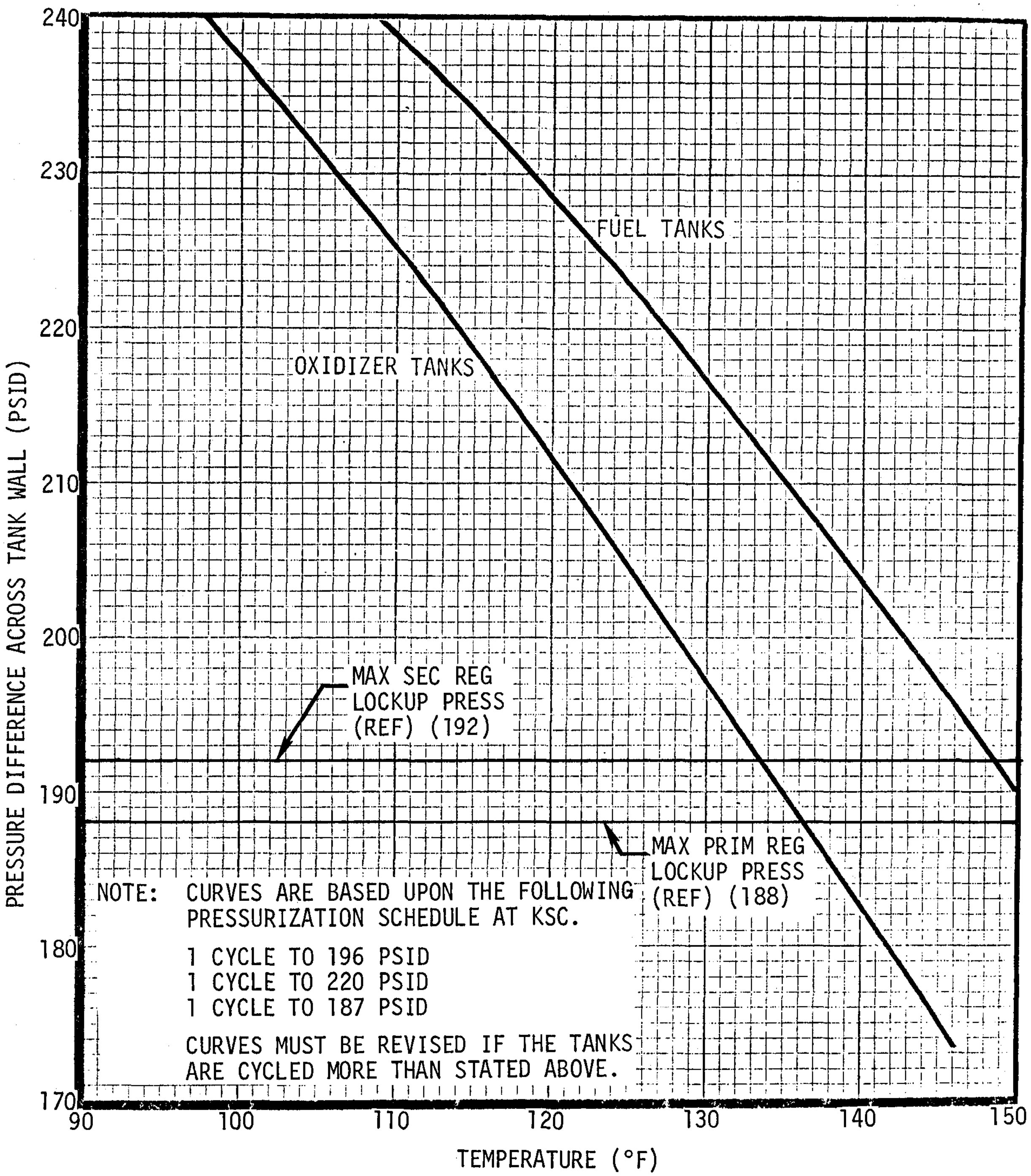

Figure LM7/3.8.1-1. Maximum Allowable Pressure-Temperature Limit Relationship for LM-7 RCS Propellant Tanks

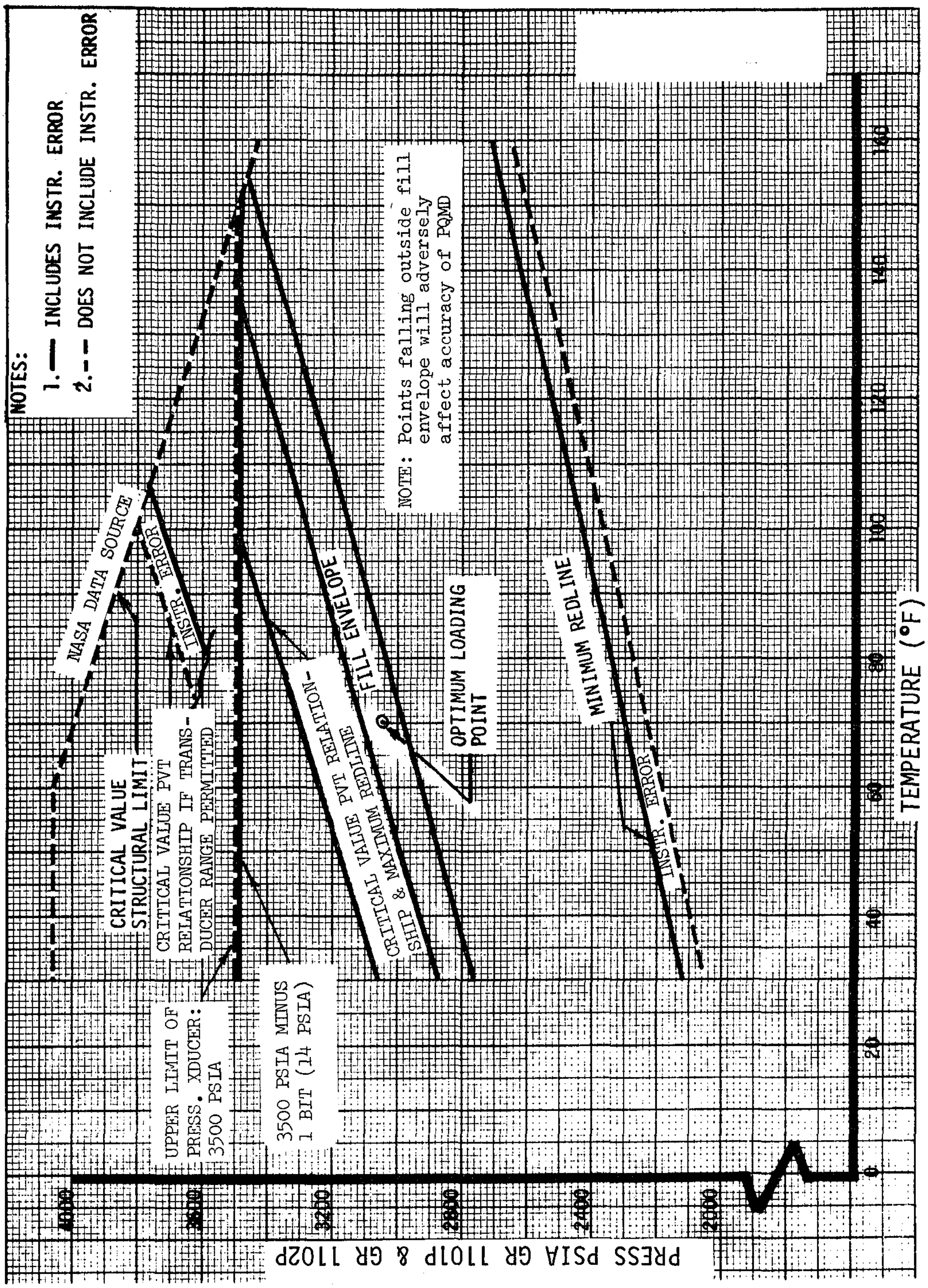

Figure LM7/3.8.1-2. RCS Helium Bottle Pressure-Temperature Limitations

Table LM7/3.10.1-1. Ascent Propulsion Subsystem (APS) Limitations

COMPONENT	TEMPERATURE LIMITS (°F)		LOW LIMIT REASON	HIGH LIMIT REASON	MEASUREMENT	
	LOW	HIGH			NUMBER	LOCATION
Fuel Tank		139		Fracture mechanics. Based upon secondary regulator lockup at 205 psid.	GP0718T	Fuel Tank Bulk
Oxidizer Tank		124			GP1218T	Ox Tank Bulk

NOTES:
1. Measurement number readings are valid only when tanks are at least 75% full.
2. See Figure LM7/3.6.1-1 for APS fracture mechanics pressure-temperature relationship curves.
3. See Table 3.10-6 for other APS temperature limitations.

Table LM7/3.10.1-2. Descent Propulsion Subsystem (DPS) Limitations

COMPONENT	TEMPERATURE LIMITS (°F)		LOW LIMIT REASON	HIGH LIMIT REASON	MEASUREMENT	
	LOW	HIGH			NUMBER	LOCATION
Fuel Tank		109		Fracture mechanics. Based upon burst disc pressure of 275 psid.	GQ3718T GQ3719T	Tank #1 Bulk Tank #2 Bulk
Oxidizer Tank		94			GQ4218T GQ4219T	Tank #1 Bulk Tank #2 Bulk

NOTES:
1. Measurement number readings are valid only when tanks are at least 75% full.
2. See Figure LM7/3.7.1-1 for DPS fracture mechanics pressure-temperature relationship curves.
3. See Table 3.10-7 for other DPS temperature limitations.

Table LM7/3.10.1-3. Reaction Control Subsystem (RCS) Limitations

COMPONENT	TEMPERATURE LIMITS (°F)		LOW LIMIT REASON	HIGH LIMIT REASON	MEASUREMENT	
	LOW	HIGH			NUMBER	LOCATION
Fuel Tank						
System A		100/148		Tank spec. limit and no engine firing experience above 100°F/Fracture mechanics. Based upon secondary regulator lock-up at 192 psid post-LOI.	GR2121T	Fuel Tank Outlet
System B		100/148			GR2122T	Fuel Tank Outlet
Oxidizer Tank						
System A		100/133		Tank spec. limit and no engine firing experience above 100°F/Fracture mechanics. Based upon secondary regulator lock-up at 192 psid post-LOI	GR2121T	Fuel Tank Outlet
System B		100/133			GR2122T	Fuel Tank Outlet

NOTES: 1. See Figure LM7/3.8.1-1 for RCS fracture mechanics pressure-temperature relationship curves.

2. See Table 3.10-8 for other RCS temperature limitations.

LM7/4.2.4 Thermal Variations of the MESA

Figures LM7/4.2.4-1 through LM7/4.2.4-3 indicate the thermal response of the MESA and temperature sensitive stowed equipment utilizing the following MESA and equipment optical properties.

	MESA Structure	ALSRC	LiOH	Batteries	ALSSC
α	0.63	0.30	--	0.54	--
ε	0.75	0.05	0.85	0.18	0.905

Data are provided for nominal, hot, and cold conditions. The nominal case is for a 7.25° sun angle and 60°F temperature at deployment. The hot case is for a 16° sun angle and 80°F temperature at deployment with sun incident on the MESA. The cold case is for a 7.25° sun angle and 45°F temperature at MESA deployment.

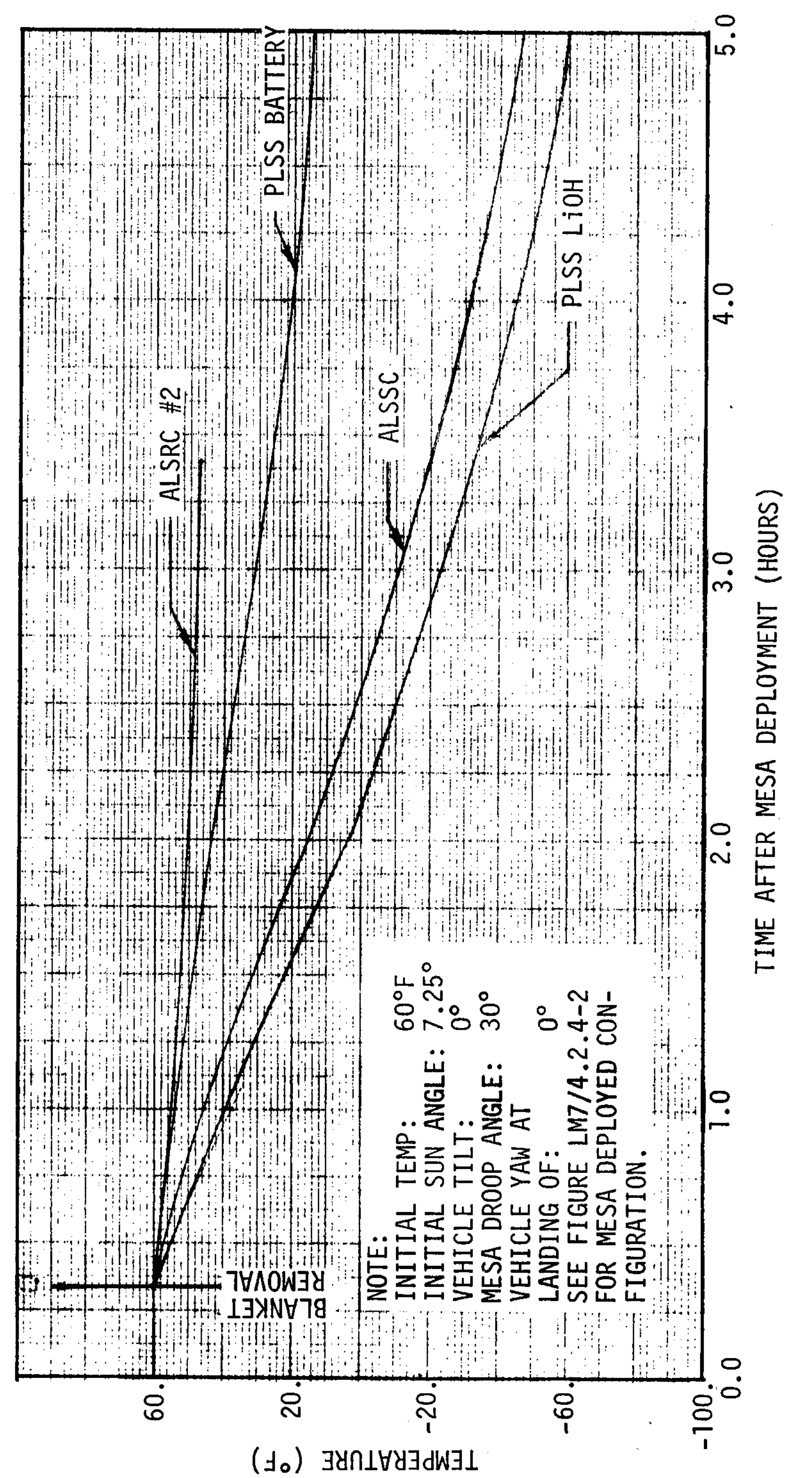

Figure LM7/4.2.4-1. Thermal Response of the MESA and Temperature Sensitive Stowed Equipment (Nominal Case)

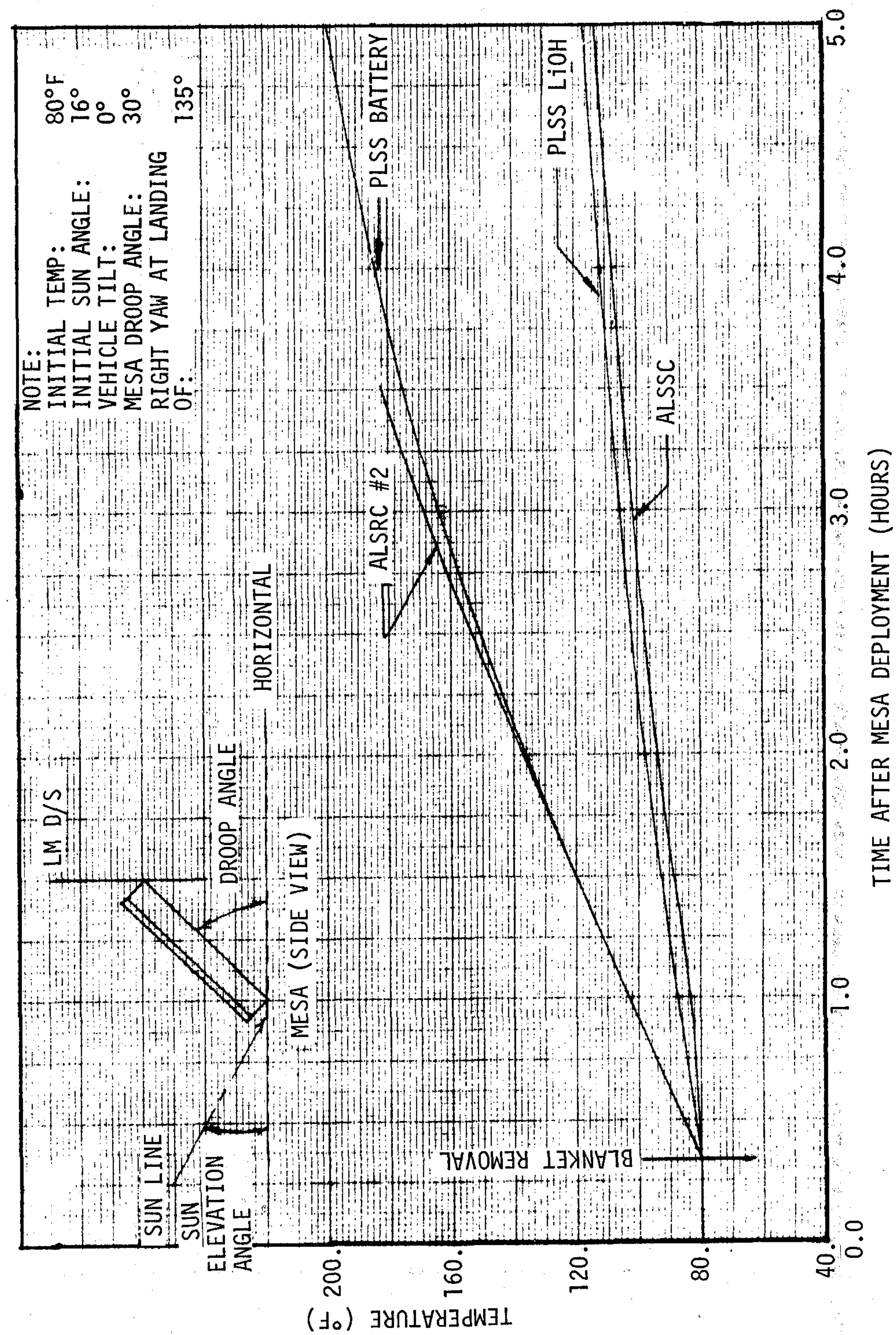

Figure LM7/4.2.4-2. Thermal Response of the MESA and Temperature Sensitive Stowed Equipment (Hot Case)

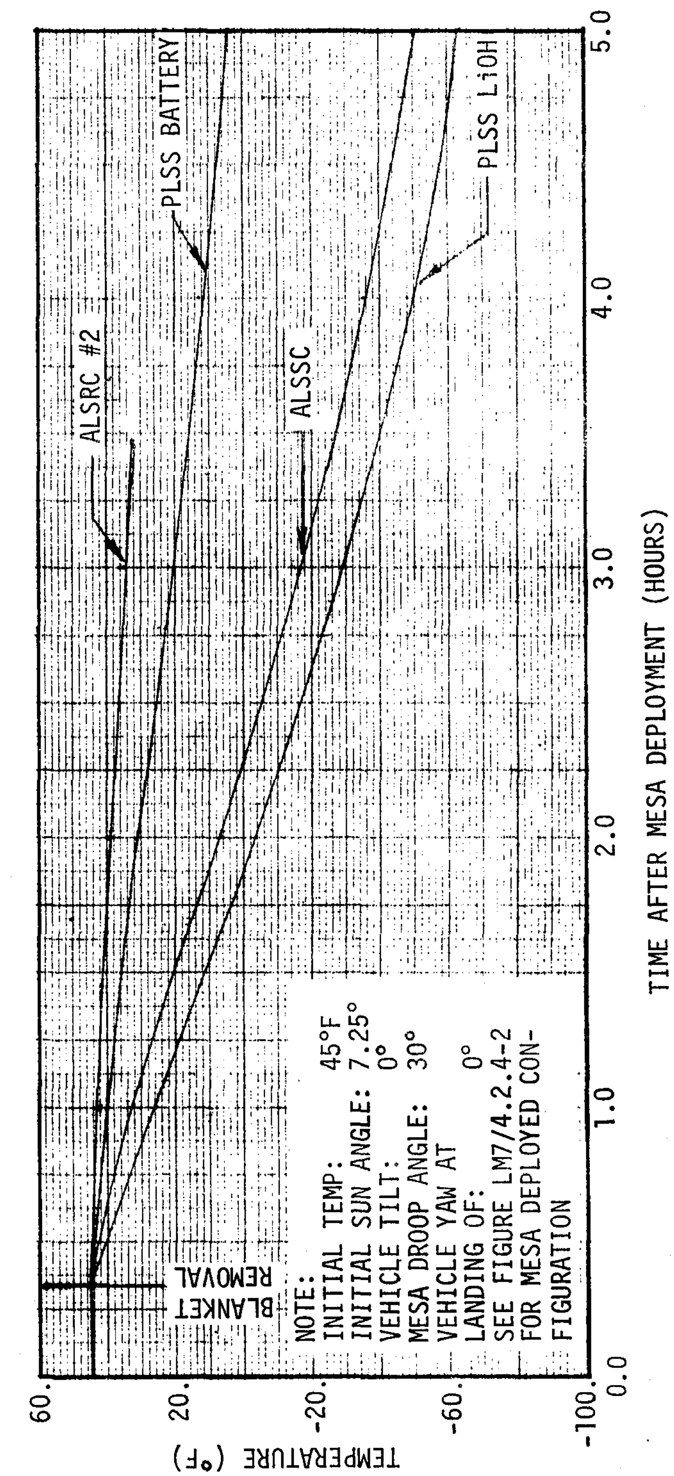

Figure LM7/4.2.4-3. Thermal Response of MESA and Temperature Sensitive Stowed Equipment (Cold Case)

LM7/4.2.5 Thermal Variation of the Sample Return Containers after Removal from the MESA (NASA DATA SOURCE)

The temperature response of the Sample Return Containers (SRC's) for the nominal timeline under nominal conditions is shown on Figure LM7/4.2.5-1. The responses for both hot and cold conditions are shown on Figure LM7/4.2.5-2.

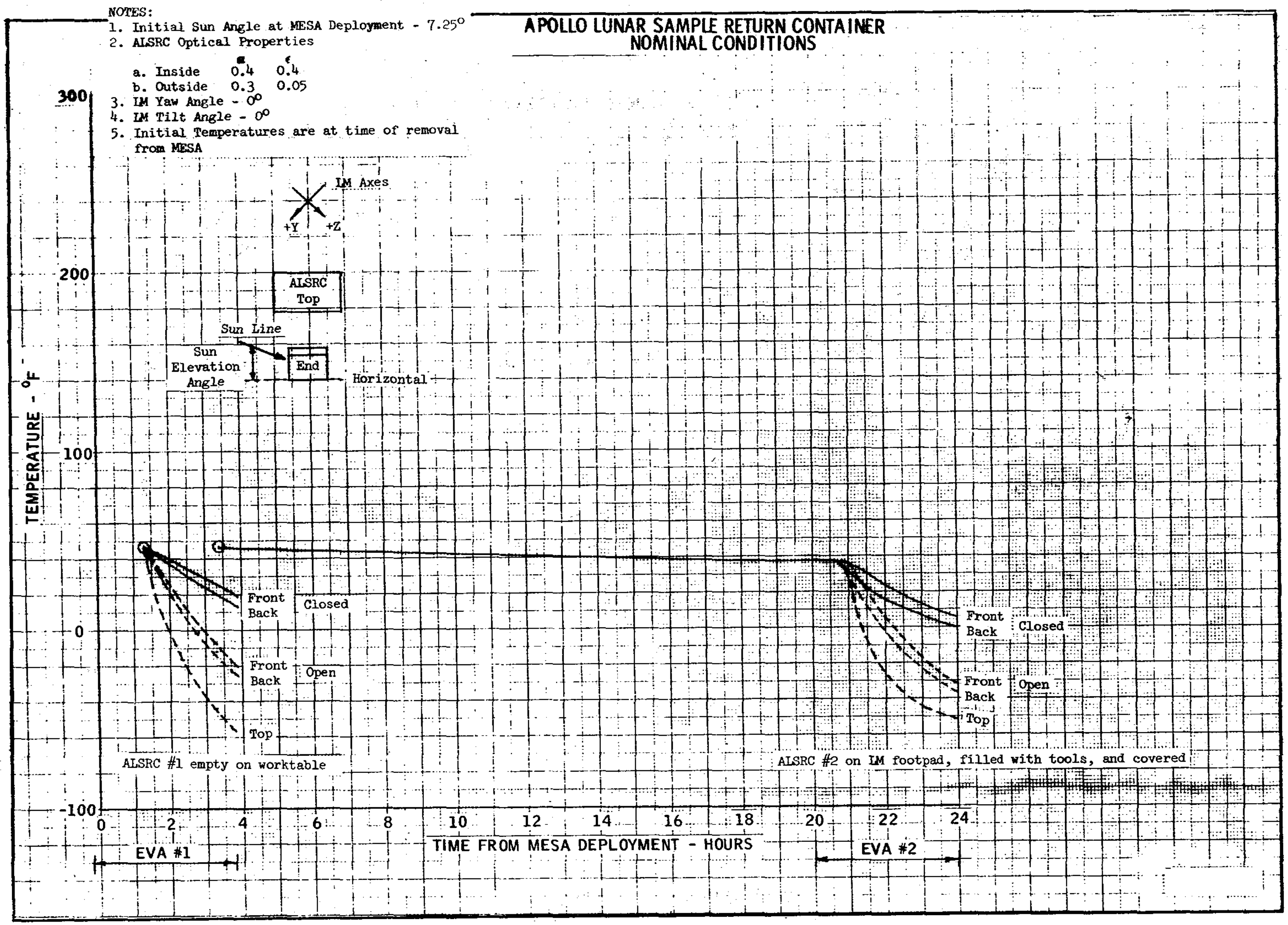

Figure LM7/4.2.5-1. Thermal Variation of the Sample Return Containers after Removal from the MESA (Nominal Timeline, Nominal Conditions)

(NASA DATA SOURCE)

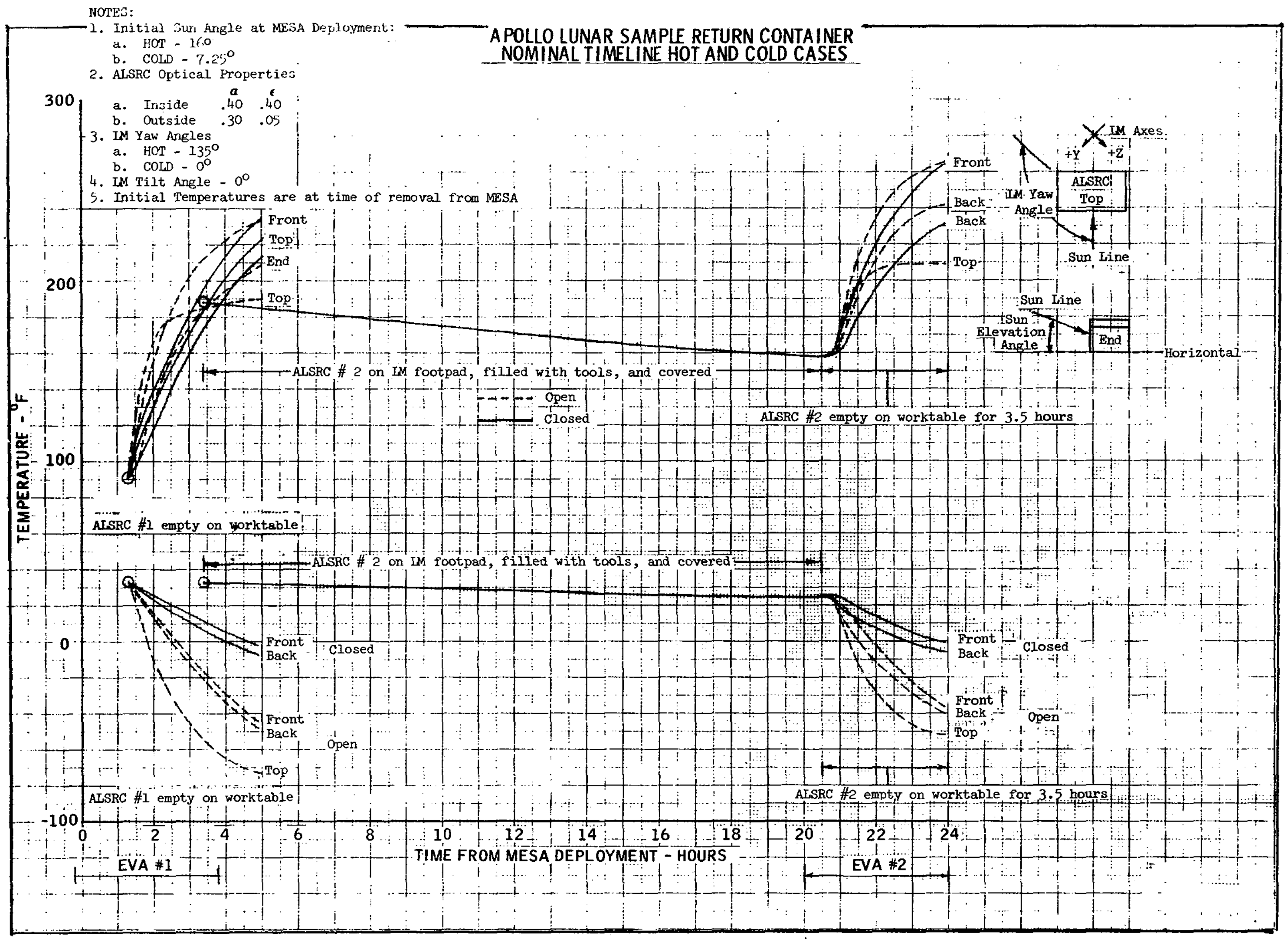

Figure LM7/4.2.5-2. Thermal Response of the Sample Return Containers after Removal from the MESA (Nominal Timeline, Hot and Cold Conditions)

LM7/4.2.6 Thermal Response of the Lunar Surface Color TV Camera (NASA DATA SOURCE)

Figure LM7/4.2.6-1 indicates the color TV camera thermal response while operating in the insulated MESA. The initial temperature at camera activation is 50°F.

Figure LM7/4.2.6-2 indicates the color TV camera thermal response while operating on the lunar surface with an initial camera temperature of 70°F at camera deployment, 10° sun angle, and local lunar surface slope of 15° into the sun.

(NASA DATA SOURCE)

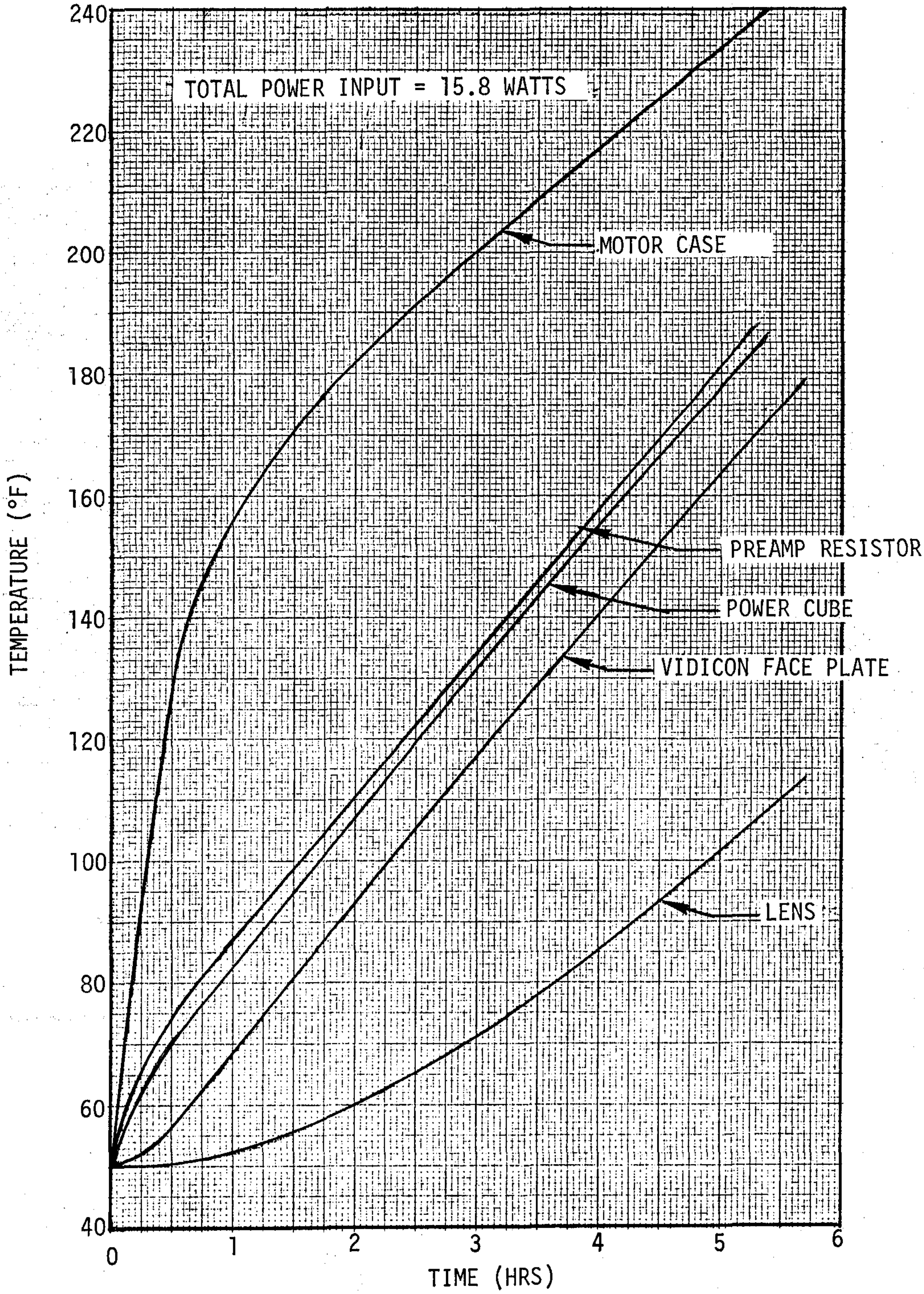

Figure LM7/4.2.6-1. Thermal Response of the Lunar Surface Color TV Camera while Operating in the Insulated MESA (See Para. LM7/4.2.6)

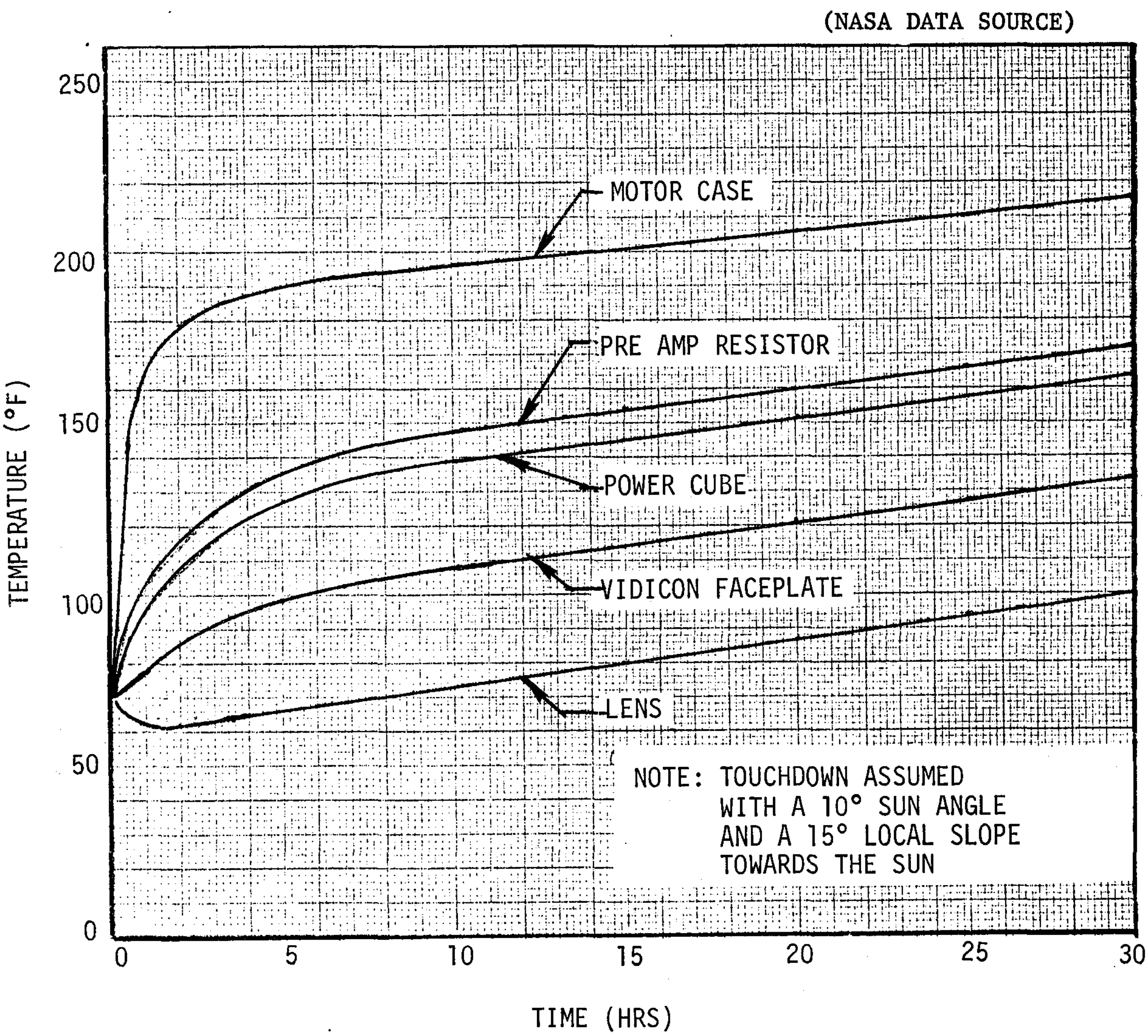

Figure LM7/4.2.6-2. Thermal Response of the Lunar Surface Color TV Camera While Operating on the Lunar Surface (See Para. LM7/4.2.6)

LM7/4.3.3 Lithium Hydroxide Consumption

Figures LM7/4.3.3-1 and LM7/4.3.3-2 show CO_2 partial pressure vs. mission time for nominal and worst flight-qualified cartridge, respectively. Figure LM7/4.3.3-3 presents LiOH hrs. remaining vs. mission time.

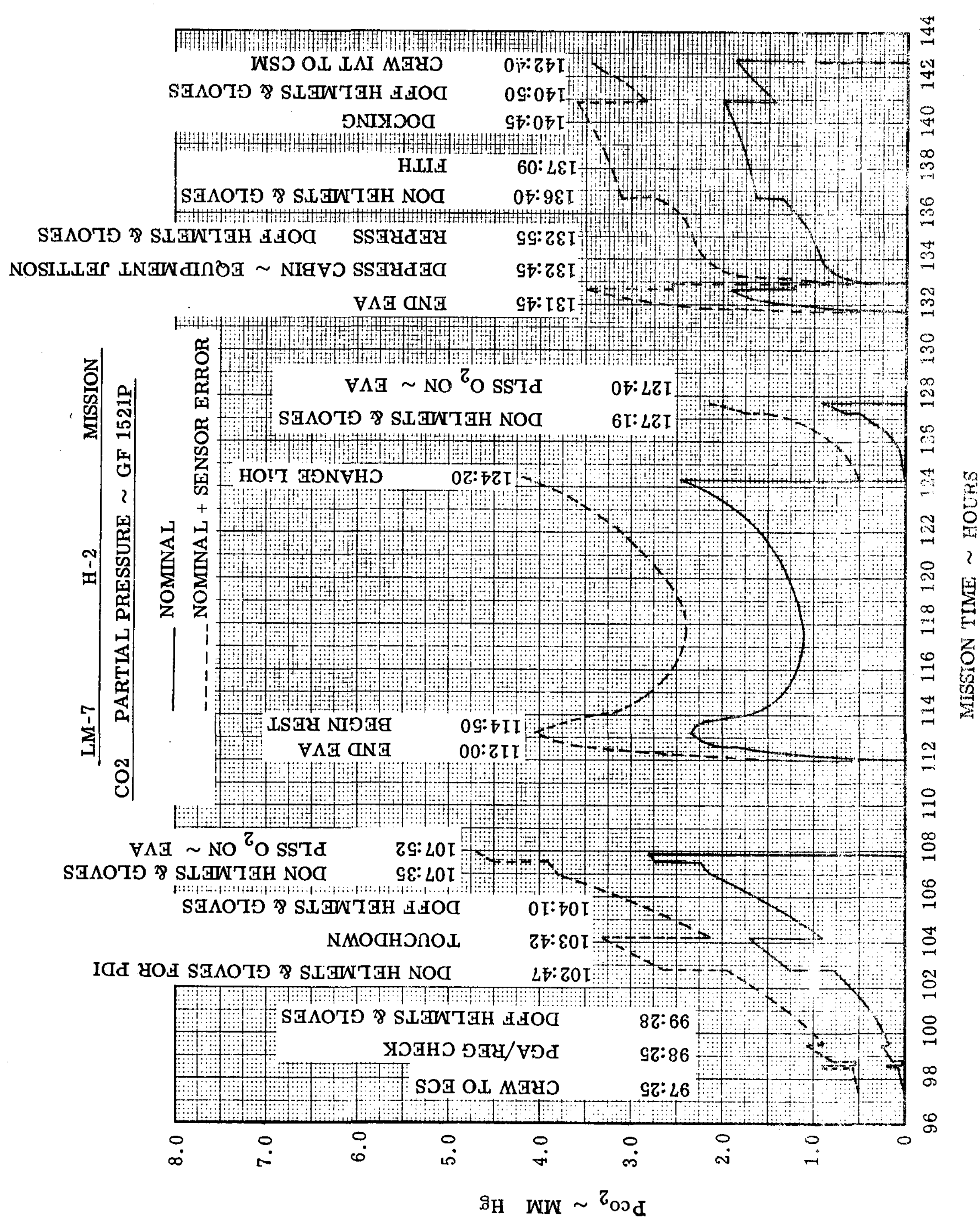

Figure LM7/4.3.3-1. CO_2 Partial Pressure Vs. Mission Time (Nominal Flight-Qualified LiOH Cartridge)

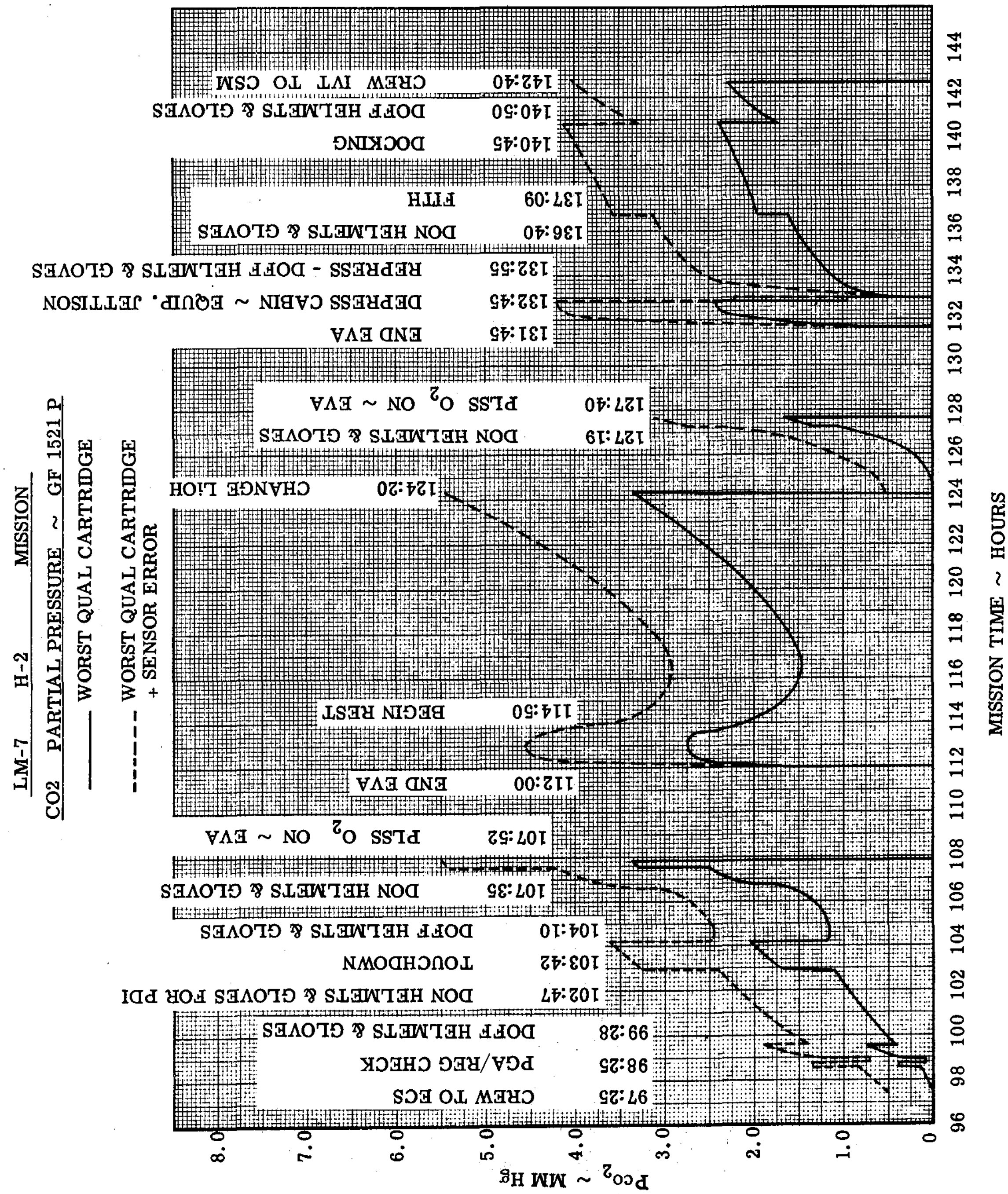

Figure LM7/4.3.3-2. CO_2 Partial Pressure Vs. Mission Time (Worst Flight-Qualified LiOH Cartridge)

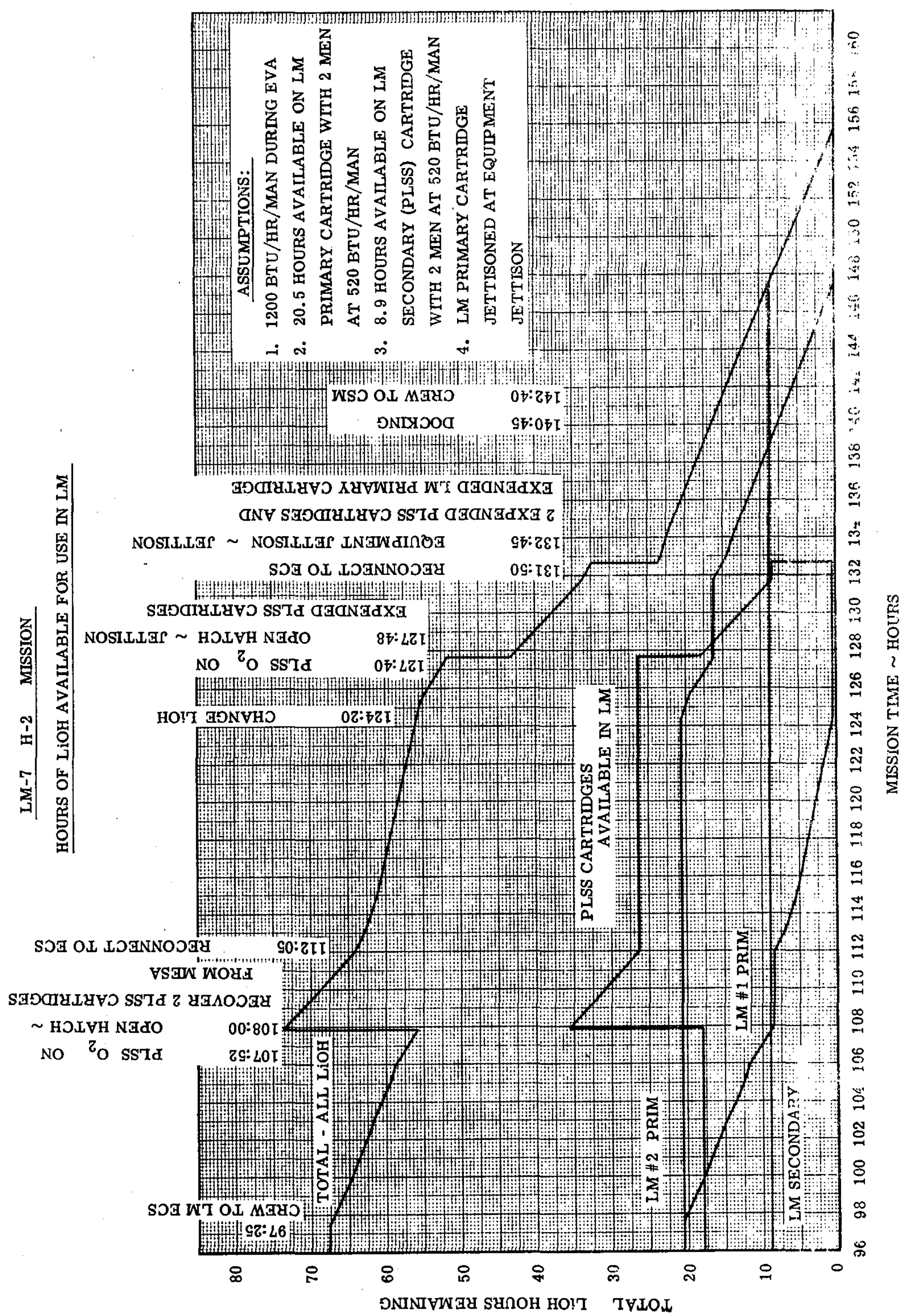

Figure LM7/4.3.3-3. LiOH Consumption

LM7/4.3.8 Environmental Control Equipment

LM7/4.3.8.1 Heat Transport Section Water Sublimators

Figures LM7/4.3.8-1 and LM7/4.3.8-2 present glycol outlet temperature as a function of glycol inlet temperature for primary HTS sublimator (209) and secondary HTS sublimator (224), respectively. Figures LM7/4.3.8-3 and LM7/4.3.8-4 represent heat rejection capabilities for primary HTS sublimator (209) and secondary HTS sublimator (224), respectively.

Figure LM7/4.3.8-5 presents pump load line and HTS ΔP characteristics as a function of glycol flow rate.

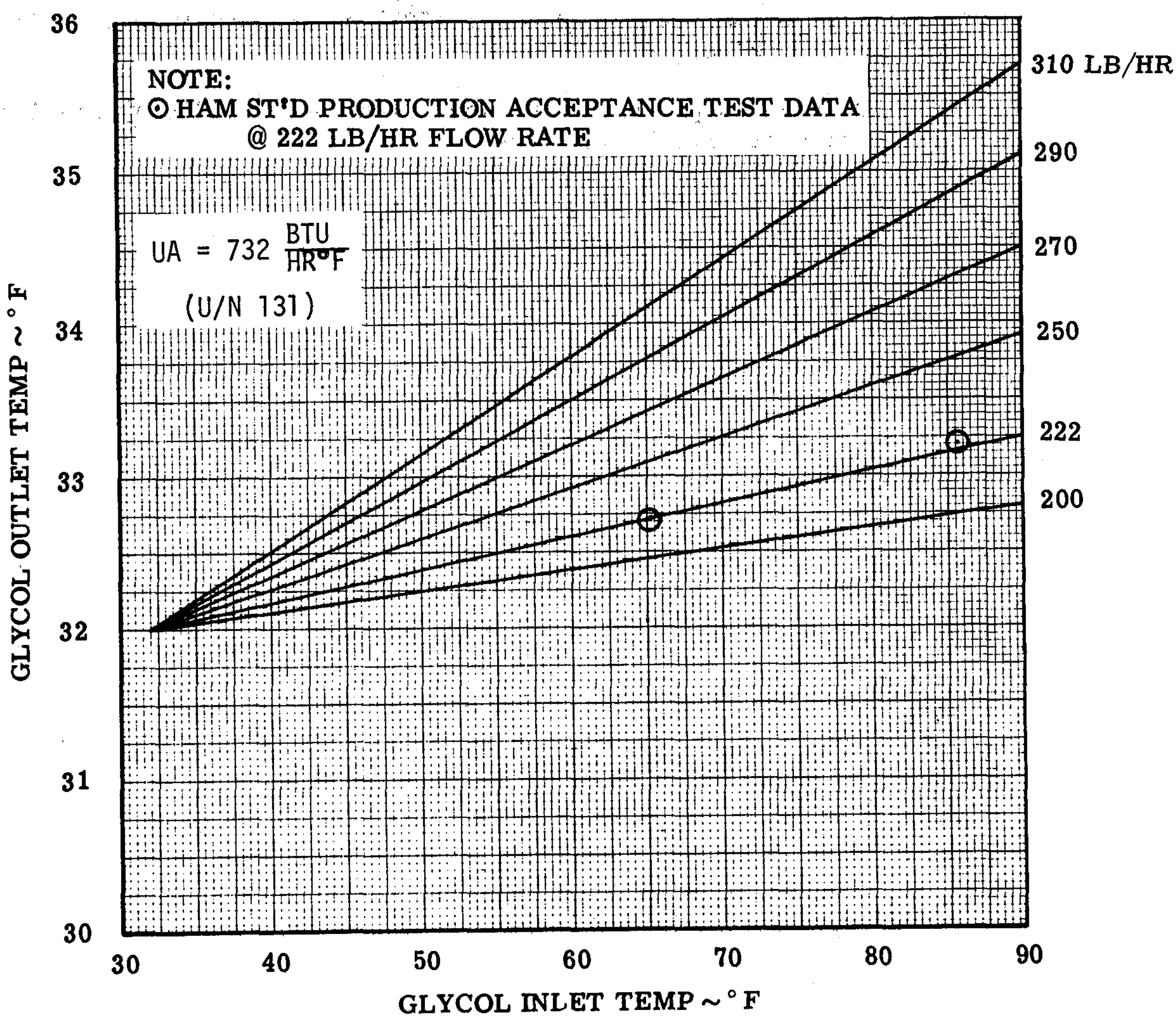

Figure LM7/4.3.8-1 LM-7 Primary HTS Sublimator (209) Acceptance Test Performance

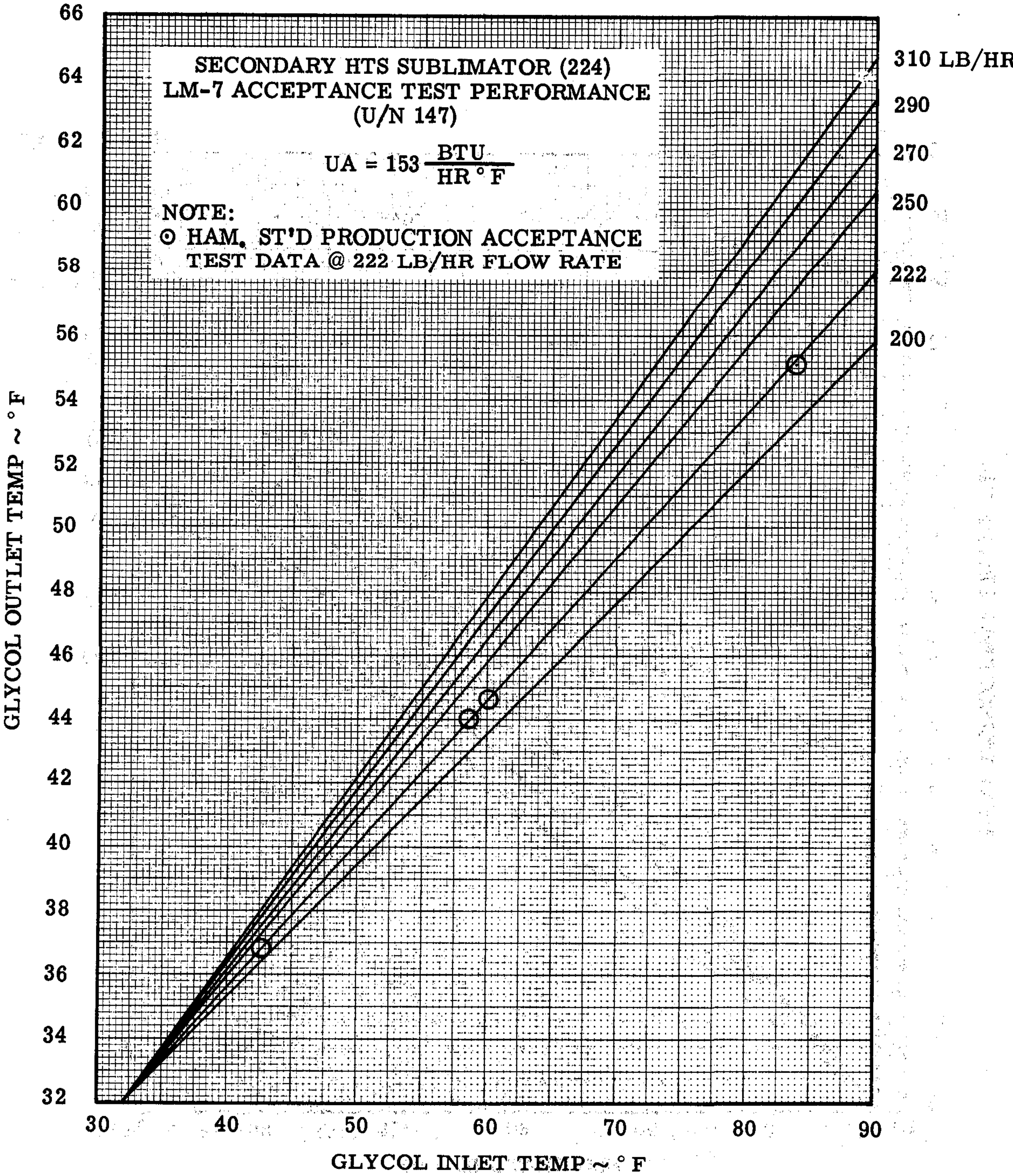

Figure LM7/4.3.8-2 LM-7 Secondary HTS Sublimator (224) Acceptance Test Performance

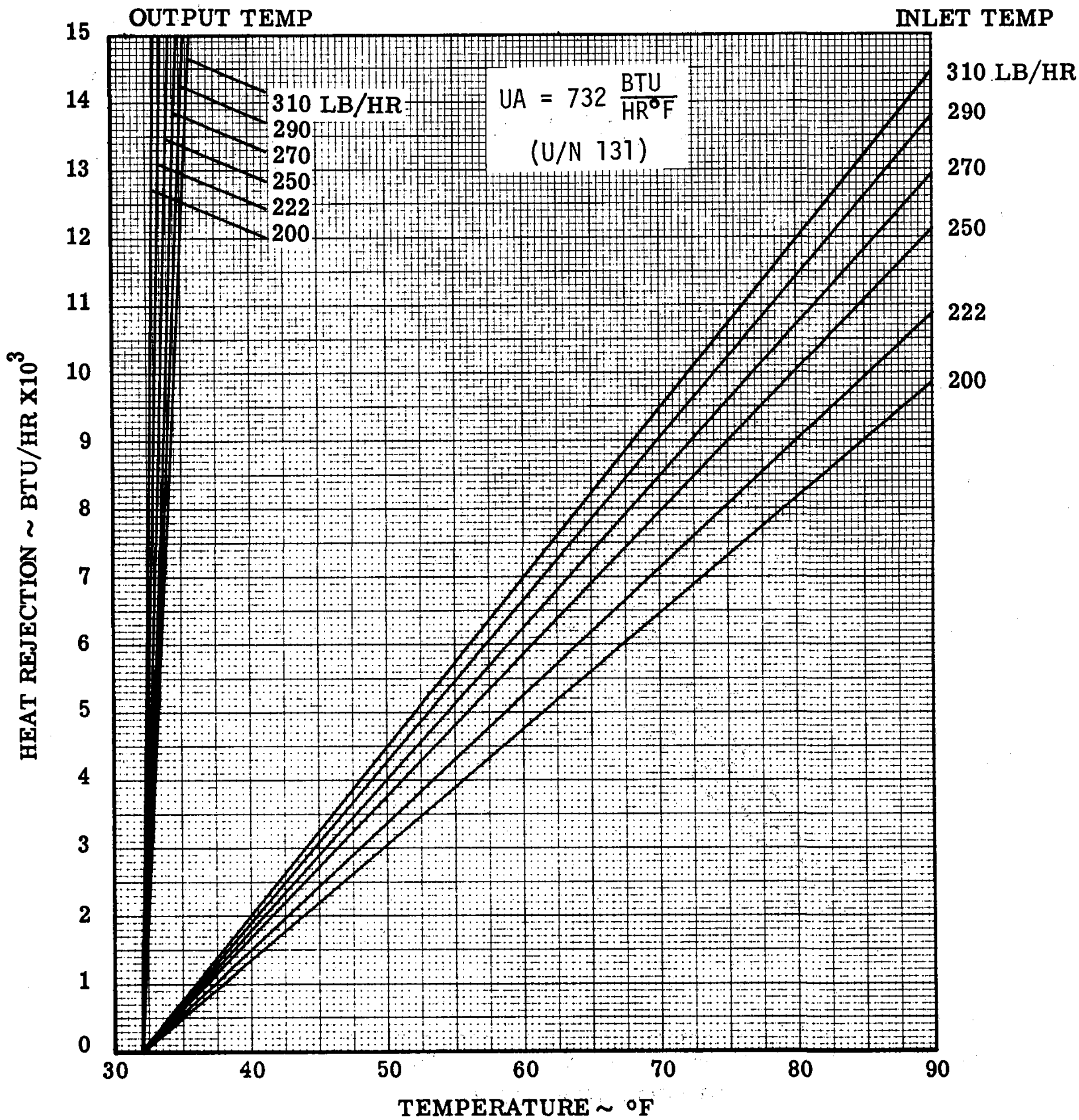

Figure LM7/4.3.8-3 LM-7 Primary HTS Sublimator (209) Heat Rejection Capability

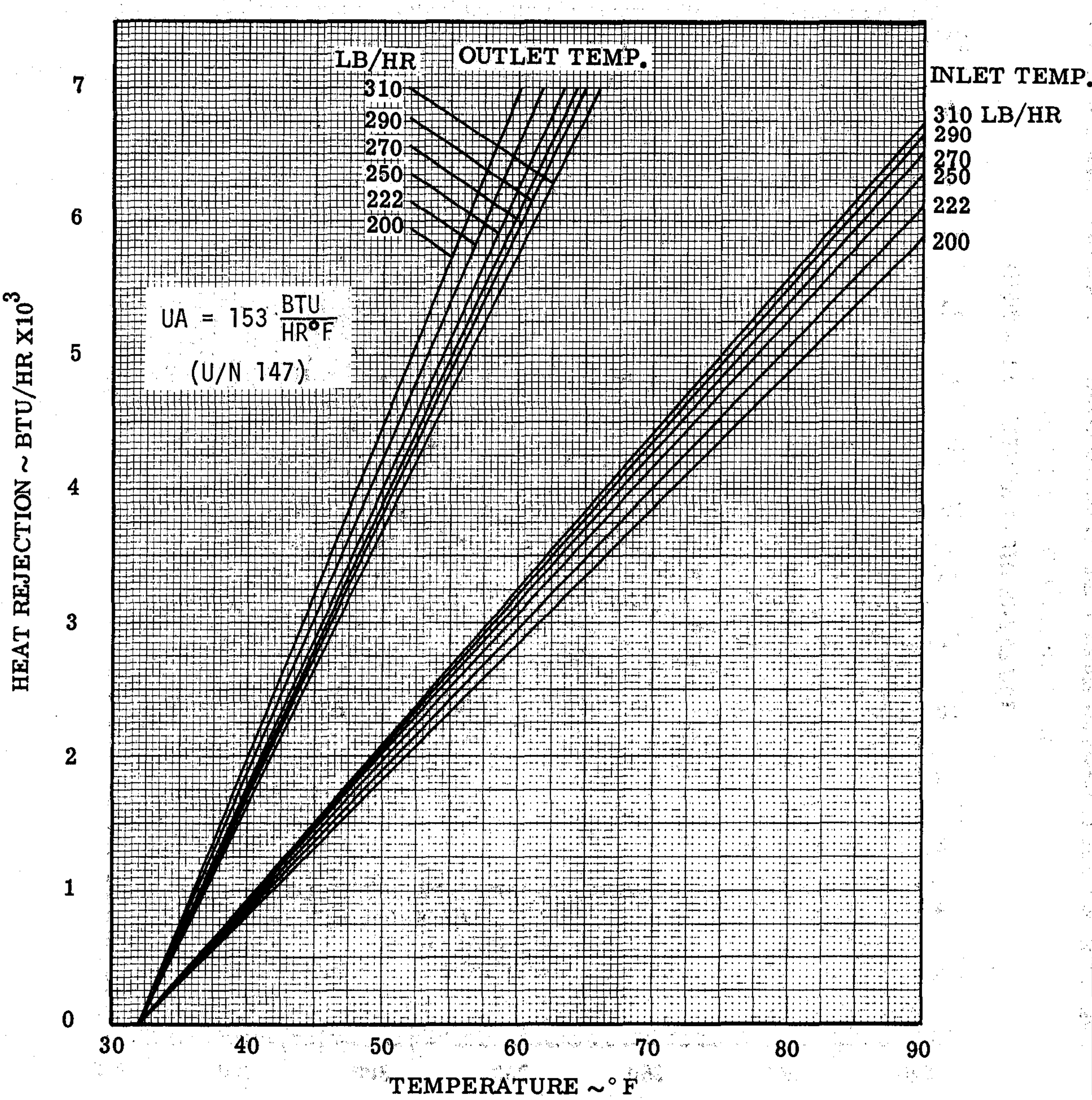

Figure LM7/4.3.8-4 LM-7 Secondary HTS Sublimator (224) Heat Rejection Capability

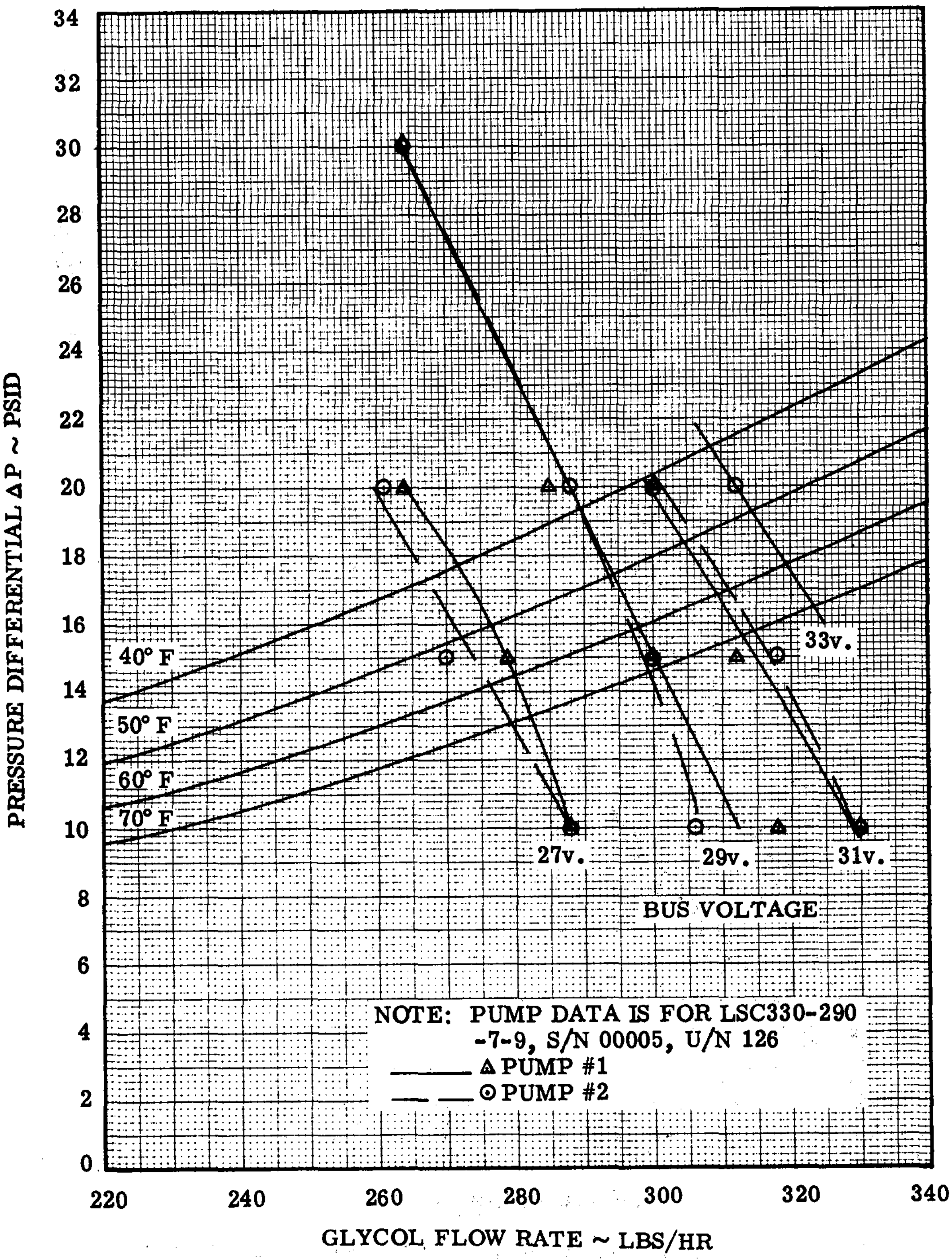

Figure LM7/4.3.8-5 LM-7 System and Pump Characteristics

LM7/4.3.11 Duty Cycle of LM Heaters

The estimated average heater powers of the LM heaters for the H-2 Mission are presented in Table LM7/4.3.11-1. The mission phases or definable spacecraft operations occur as shown in the headings of the table.

Antenna (S-band steerable, rendezvous radar, landing radar) heater requirements were determined from a review and application of the following:

(a) Vendor thermal studies

(b) Acceptance and qualification test data

(c) LM-3, LM-4, LM-5, and LM-6 flight data

Guidance equipment (IMU, ASA) heater requirements were determined from a combination of the following:

(a) Calculations using vehicle structure temperature and coolant temperatures when applicable

(b) Review and application of LM-3, LM-4, LM-5, and LM-6 flight data

Window and AOT heaters are nonthermostatically controlled, constant-power devices. Table LM7/4.3.11-1 lists the nominal heater powers of these items and indicates worst-case usage for the H-2 Mission. The window heaters will be energized at the discretion of the astronaut when fogging is noted.

The RCS thruster heater requirements were determined from the following:

(a) Thermal studies

(b) Review and application of LM-3, LM-4, LM-5, and LM-6 flight data

Lunar stay estimates of heater duty cycle for antenna heaters and RCS thruster heaters are based on a low sun elevation angle at landing (7°) and did not consider any shadowing or vehicle tilting due to irregular terrain.

Table LM7/4.3.11-1. Average Heater Power during Mission Phases

Heaters	Launch & Boost LM Power 00:30 to 02:35 watts	Translunar Coast		Lunar Orbit & Descent		Lunar Stay	Ascent & Lunar Orbit 137:09 to 143:04 watts
		LM Power 02:35 to 03:40 watts	CSM Power 03:40 to 77:25 watts	CSM Power 77:25 to 96:45 watts	LM Power 96:45 to 103:42 watts	LM Power 103:42 to 137:09 watts	
S-Band Steerable Antenna	2	4	4	2	2 (Note 1)	2	2 (Note 1)
Rendezvous Radar Antenna	6	8	8	6	8 (Note 1)	8/2 (Note 5)	8 (Note 1)
Landing Radar Ant	8	20	20	10	10 (Note 1)	-	-
ASA	7	7	7	7	17 (Note 3)	55	17 (Note 3)
IMU	15	15	15	15	14.5 (Note 3)	25	14.5 (Note 3)
Fwd Window (CDR)	0	0	0	0	61.8 (Note 4)	61.8 (Note 4)	61.8 (Note 4)
Fwd Window (SE)	0	0	0	0	61.8 (Note 4)	61.8 (Note 4)	61.8 (Note 4)
Docking Window	0	0	0	0	24.0 (Note 4)	24.0 (Note 4)	24.0 (Note 4)
AOT	0	0	0	0	5.0	5.0	5.0
RCS Thruster	0	0	0	0	(Note 2)	40.0	20.0
Total Average Power/Phase, watt			54	40			
Average current at 28vdc, Amps			1.93	1.43			

(see following page for notes)

Table LM7/4.3.11-1 (Continued)

Notes:

(1) Heater duty cycle estimates are for periods when antennas are activated. Duty cycles are estimated to be zero when the antennas are active.

(2) RCS thrusters require 746 watts for one-half-hour warmup followed by a 140 watt average until undocking and a 20-watt average for the remainder of this phase.

(3) Total ASA power is 55 watts; 38-watts instrument power plus 17-watts heater power. Total IMU power is 73.5 watts; 59-watts instrument power plus 14.5 watts heater power.

(4) Window heaters are normally zero since they are energized only when fogging is noted.

(5) The average RR antenna heater power will vary with the heater mode selected. It is estimated to be 8 watts if the antenna is in the operate mode for the duration of the lunar stay period. It is estimated to be 2 watts if the antenna is in the standby mode for the first part of the stay period (approximately 85%) and in the operate mode for the remainder of the stay period (approximately 15%). However, it should be noted that use of the standby heater mode during lunar stay is in violation of SODB Constraint RR-2(b).

LM7/4.3.12.2.1 GAC Study Performed on Aft Equipment Bay Electronic Replaceable Assemblies

Three contingency situations were analyzed (Cases #1, #2, and #3) in determining the thermal response of equipment during no coolant flow operation using the new network. Each case was analyzed for each of three structural temperatures: 40°F, 70°F and 100°F. Table LM7/4.3.12-4 shows which figures are allocated per ERA.

Case #1 simulates a lift-off from the lunar surface at full power with no coolant flow, immediately following a normal descent and touchdown. The loss of both coolant loops is assumed to have occurred at touchdown. Liftoff is assumed to have occurred immediately upon touching down.

This case provides high initial temperatures for this aft rack equipment since most of them were assumed to have been operating for a long time prior to the assumed loss of the coolant loops (see Table LM7/4.3.12-1). These relatively high initial temperatures (see Table LM7/4.3.12-2), combined with the fact that most assemblies are assumed to be operating following liftoff (Table LM7/4.3.12-1), result in the lowest reliable operating times of the three cases considered (see summary of results, Table LM7/4.3.12-3 and Figure LM7/4.3.12-1 through Figure LM7/4.3.12-22).

Case #2 simulates a liftoff from the lunar surface at full power with no coolant flow following a normal stay on the lunar surface. Liftoff is assumed to have occurred immediately upon simultaneously losing both coolant loops.

This case provides low initial temperatures for the aft rack equipment since most of them were assumed to have been off for a long time prior to the assumed loss of the coolant loops (see Table LM7/4.3.12-1).

These relatively low initial temperatures (Table LM7/4.3.12-2), combined with the fact that most assemblies are assumed to be operating following liftoff (Table LM7/4.3.12-1), result in reliable operating times generally between those of Cases #1 and #3. (See Figure LM7/4.3.12-23 through Figure LM7/4.3.12-44).

Case #3 simulates a liftoff from the lunar surface at low (survival) power with no coolant flow, immediately following a normal stay on the lunar surface. Liftoff is assumed to have occurred immediately upon simultaneously losing both coolant loops.

LM7/4.3.12.2.1 Continued

This case provides low initial temperatures for the aft rack equipment since most of them were assumed to have been off for a long time (during lunar stay) prior to the assumed loss of the coolant loops (same as Case 2). These relatively low initial temperatures (see Table LM7/4.3.12-2), combined with the fact that many assemblies are assumed to be off following liftoff (Table LM7/4.3.12-1), result in the highest reliable operating times of the three cases considered (see summary of results, Table LM7/4.3.12-3 and Figures LM7/4.3.12-45 through Figure LM7/4.3.12-66).

The three cases described above are illustrative of the type of flight simulations which may be performed using the network defined in enclosure (2) of LMO 510-1555, 11 March 1970.

TABLE LM7/4.3.12-1

Equipment Assumed Operating For Cases #1, #2, and #3

Prior to Loss of Coolant Flow			Following Loss of Coolant Flow		
Case #1	Case #2	Case #3	Case #1	Case #2	Case #3
AEA	CWEA	CWEA	AEA	AEA	BATT #5
ATCA	GPI #2	GPI #2	ATCA	ATCA	BATT #6
CWEA	PCMTEA	PCMTEA	BATT #5	BATT #5	CWEA
DUA	SBX	SBX	BATT #6	BATT #6	ECA #3
GPI #2	SCEA #1	SCEA #1	CWEA	CWEA	ECA #4
PCMTEA	SCEA #2	SCEA #2	DUA	DUA	PCMTEA
RREA	SPA	SPA	ECA #3	ECA #3	RTTA
RTTA	VHF "A"	VHF "A"	ECA #4	ECA #4	SBPA
SBPA	VHF "B"	VHF "B"	GPI #2	GPI #2	
			PCMTEA	PCMTEA	SBX
SBX			RREA	RREA	SCEA #1
SCEA #1			RTTA	RTTA	SCEA #2
SPA			SBPA	SBPA	SPA
VHF "A"			SBX	SBX	VHF "A"
VHF "B"			SCEA #1	SCEA #1	VHF "B"
			SCEA #2	SCEA #2	
			SPA	SPA	
			VHF "A"	VHF "A"	
			VHF "B"	VHF "B"	

Table LM 7/4.3.12-2

Equipment Temperatures at Time Coolant Flow is Lost*

Node #	Case #1			Cases #2 and #3		
	40^oF Structure (^oF)	70^oF Structure (^oF)	100^oF Structure (^oF)	40^oF Structure (^oF)	70^oF Structure (^oF)	100^oF Structure (^oF)
53	79.7	85.3	91.2	39.8	45.5	51.4
260	66.4	69.6	72.9	36.3	39.6	42.9
261	39.0	40.0	41.1	32.9	34.0	35.1
262	60.3	65.7	71.3	39.6	45.1	50.7
636	87.6	93.2	99.1	38.6	44.3	50.2
637	61.7	67.3	73.2	44.4	50.1	56.1
638	60.0	65.6	71.0	44.3	49.9	55.8
639	48.9	52.2	55.1	40.5	43.8	47.2
640	44.4	50.3	53.2	36.0	39.3	42.7
641	34.0	35.0	35.9	32.8	33.8	34.7
642	34.8	35.7	36.8	32.8	33.8	34.8
643	46.4	49.6	52.9	36.3	39.6	42.9
644	58.7	64.3	69.7	43.0	48.6	54.5
645	46.4	49.6	52.9	36.3	39.6	42.9
646	71.4	76.9	82.7	40.0	45.6	51.4
647	75.7	81.2	87.0	49.8	55.4	61.2
648	89.1	94.8	100.7	40.3	46.0	52.0
652	96.1	101.8	107.7	40.0	45.7	51.7
653	74.0	79.6	85.5	56.9	62.6	68.6
654	64.3	70.0	75.9	47.3	53.0	58.9
806	68.4	74.0	79.9	38.4	44.1	50.0
807	71.1	76.7	82.6	38.7	44.4	50.4
808	59.0	64.6	70.5	40.3	46.0	52.0
809	56.9	62.5	68.4	41.0	46.7	52.6
810	59.0	64.6	70.5	43.1	48.8	54.7
811	58.3	63.9	68.8	42.8	48.4	54.2
812	56.8	62.4	68.3	40.9	46.6	52.5
813	56.1	61.7	66.6	40.6	46.2	52.0
814	54.6	60.2	65.6	39.1	44.7	50.5
815	34.2	35.2	36.5	32.9	33.9	34.9

*Only the temperatures of nodes with non-zero heat capacity need be specified.

Table LM 7/4.3.12-2 (continued)

Node #	Case #1 40°F Structure (°F)	Case #1 70°F Structure (°F)	Case #1 100°F Structure (°F)	Cases #2 and #3 40°F Structure (°F)	Cases #2 and #3 70°F Structure (°F)	Cases #2 and #3 100°F Structure (°F)
816	55.9	61.5	66.4	40.4	46.0	51.8
817	35.5	36.5	37.4	34.2	35.2	36.2
818	34.2	35.2	36.1	32.9	33.9	34.9
819	33.8	34.7	35.7	32.7	33.6	34.5
820	33.8	34.3	35.7	32.7	33.6	34.5
821	35.7	36.7	37.8	32.9	34.0	35.1
822	35.7	36.7	37.8	32.9	34.0	35.1
823	57.0	62.4	68.0	39.6	45.1	50.7
824	35.7	36.7	37.8	32.9	34.0	35.1
825	57.0	62.4	68.0	39.6	45.1	50.7
826	64.1	69.5	75.1	39.6	45.1	50.7
827	66.1	71.7	77.6	40.4	46.1	52.1
828	63.7	69.1	74.7	43.3	48.8	54.4
829	65.7	71.3	77.2	44.1	49.8	55.8
830	70.3	75.9	81.8	40.4	46.1	52.1
831	69.5	75.2	81.1	40.2	45.9	51.9
832	68.9	74.5	80.4	50.3	56.0	62.0
833	58.9	64.6	70.5	40.9	46.6	52.6
834	72.7	78.4	84.3	40.2	45.9	51.9
835	70.4	76.0	81.9	39.8	45.5	51.4
836	64.5	70.2	76.1	46.5	52.2	58.2
837	62.2	67.8	73.7	46.1	51.8	57.7
838	62.0	67.7	73.6	44.0	49.7	55.7
839	59.7	65.3	71.2	43.6	49.3	55.2

Table LM 7/4.3.12-3

Summary of Allowable Equipment Operating Times

Predicted for Cases #1, #2, and #3

Equipment	Case 1			Case 2			Case 3		
	40° F (Hrs.)	70° F (Hrs.)	100° F (Hrs.)	40° F (Hrs.)	70° F (Hrs.)	100° F (Hrs.)	40° F (Hrs.)	70° F (Hrs.)	100° F (Hrs.)
AEA	1.6	1.5	1.3	2.4	2.2	2.1	---	---	---
AEA Diode Ass'y	2.6	2.5	2.3	3.4	3.2	3.1	---	---	---
ATCA	2.5	2.3	2.1	3.3	3.1	2.9	---	---	---
ATCA Resistor Ass'y	2.1	2.0	1.9	2.8	2.6	2.5	---	---	---
BATT #5	4.8	4.7	4.6	5.0	4.9	4.8	8.+	8.+	8.+
BATT #6	4.9	4.7	4.7	5.1	5.0	4.9	8.+	8.+	8.+
CWEA	4.6	4.3	4.0	5.5	5.2	5.0	8.+	8.+	8.+
DUA	3.2	3.0	2.9	4.0	3.8	3.6	---	---	---
ECA #3	4.6	4.4	4.2	5.3	5.1	4.9	8.+	8.+	8.+
ECA #4	6.5	6.2	5.9	7.2	6.8	6.7	8.+	8.+	8.+
GPI #1	---	---	---	---	---	---	---	---	---
GPI #2	2.0	1.9	1.8	2.6	2.4	2.3	---	---	---
PCMTEA	5.8	5.5	5.3	6.6	6.4	6.2	8.+	8.+	8.+
RREA	1.1	1.0	0.9	1.7	1.6	1.5	---	---	---
RTTA	3.5	3.3	3.0	3.4	3.2	3.9	5.5	5.1	4.8
SBPA	1.1	1.0	0.9	1.8	1.7	1.6	1.8	1.7	1.6
SBX	2.4	2.2	2.0	3.0	2.9	2.7	3.9	3.6	3.4
SCEA #1	4.0	3.7	3.5	4.8	4.6	4.4	8.+	8.+	8.+
SCEA #2	6.8	6.5	6.3	7.5	7.3	7.1	8.+	8.+	8.+
SPA	4.1	3.9	3.6	4.9	4.7	4.4	6.6	6.2	5.9
VHF"A"	1.8	1.7	1.6	2.4	2.2	2.1	4.4	4.0	3.6
VHF "B"	4.2	3.9	3.7	5.0	4.8	4.6	7.4	7.0	6.6
VHF Diplexer	2.2	2.1	1.9	2.8	2.6	2.5	8.+	8.+	8.+

TABLE LM7/4.3.12-4

TEMPERATURE RISE FIGURES FOR AEB EQUIPMENT

Equipment	Case 1	Case 2	Case 3
AEA	LM7/4.3.12-1	LM7/4.3.12-23	LM7/4.3.12-45
AEA DIODE ASS'Y	-2	-24	-46
ATCA	-3	-25	-47
ATCA RES ASS'Y	-4	-26	-48
BATT #5	-5	-27	-49
BATT #6	-6	-28	-50
CWEA	-7	-29	-51
DUA	-8	-30	-52
ECA #3	-9	-31	-53
ECA #4	-10	-32	-54
GPI #1	-11	-33	-55
GPI #2	-12	-34	-56
PCMTEA	-13	-35	-57
RREA	-14	-36	-58
RTTA	-15	-37	-59
SBPA	-16	-38	-60
SBX	-17	-39	-61
SCEA #1	-18	-40	-62
SCEA #2	-19	-41	-63
SPA	-20	-42	-64
VHF XCVRS	-21	-43	-65
VHF DIPLEXER	-22	-44	-66

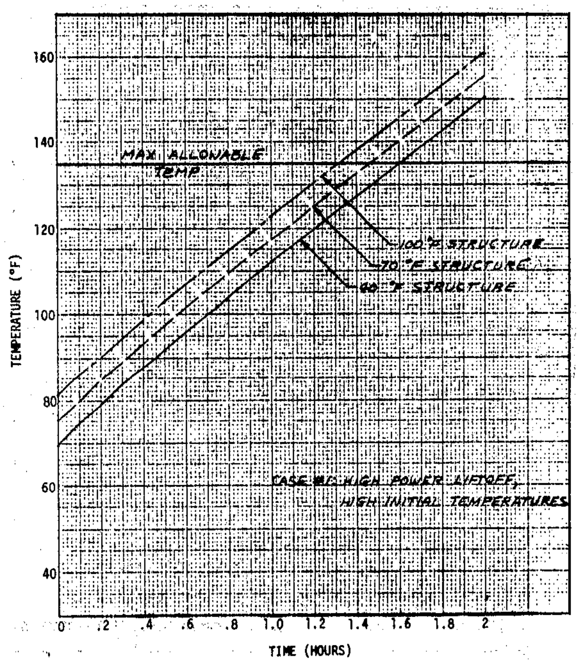

Figure LM7/4.3.12-1. Temperature Rise of the AEA Following Loss of Coolant/Coolant Circulation

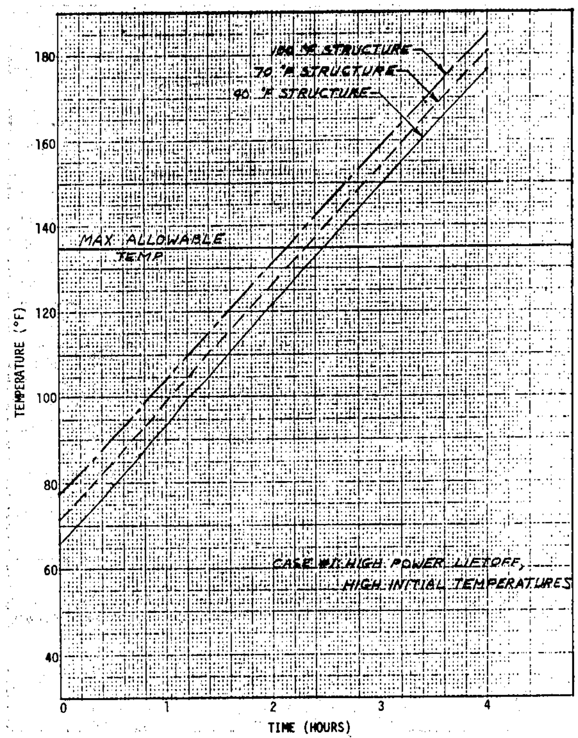

Figure LM7/4.3.12-3. Temperature Rise of the ATCA Following Loss of Coolant/Coolant Circulation

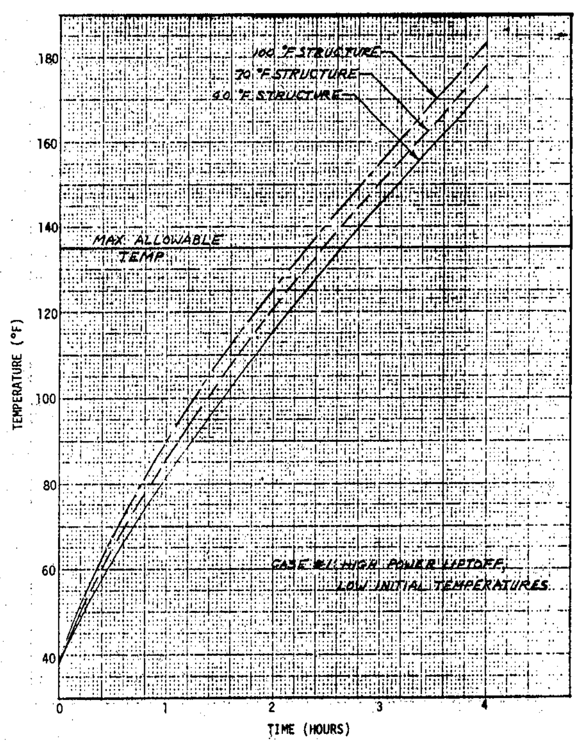

Figure LM7/4.3.12-2. Temperature Rise of the AEA Diode Assembly Following Loss of Coolant/Coolant Circulation

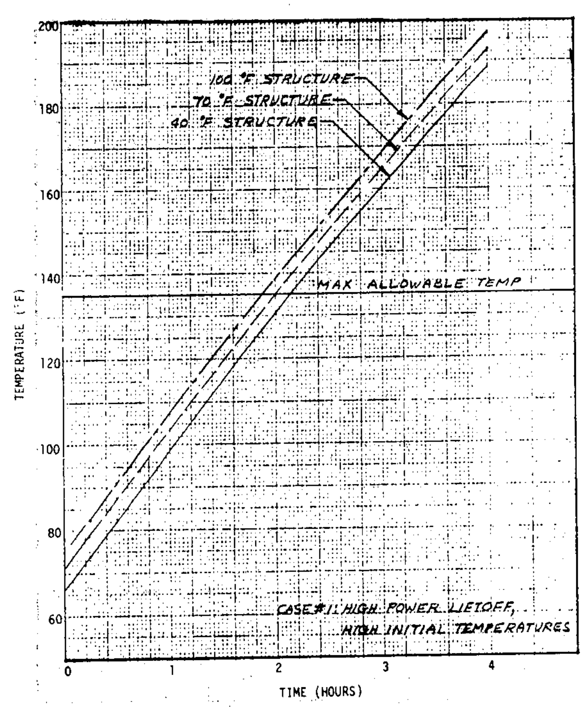

Figure LM7/4.3.12-4. Temperature Rise of the ATCA Res. Ass'y. Following Loss of Coolant/Coolant Circulation

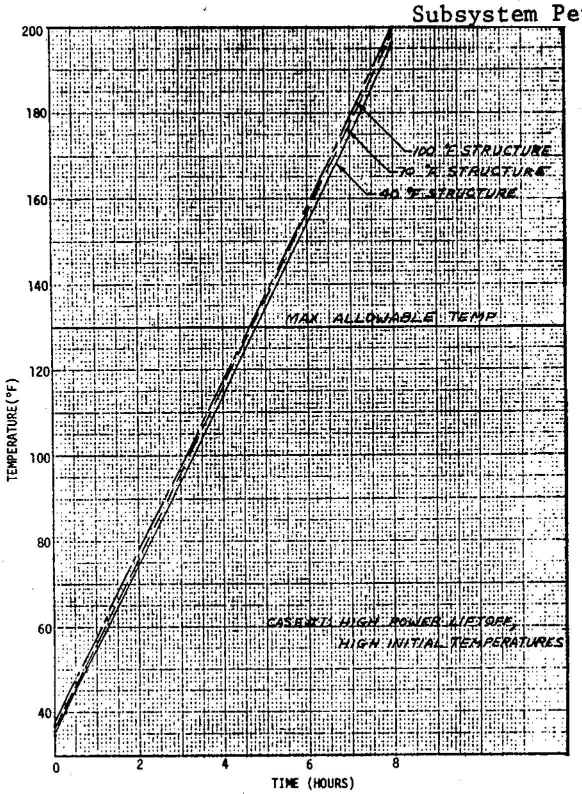

Figure LM7/4.3.12-5. Temperature Rise of the Battery #5 Following Loss of Coolant/Coolant Circulation

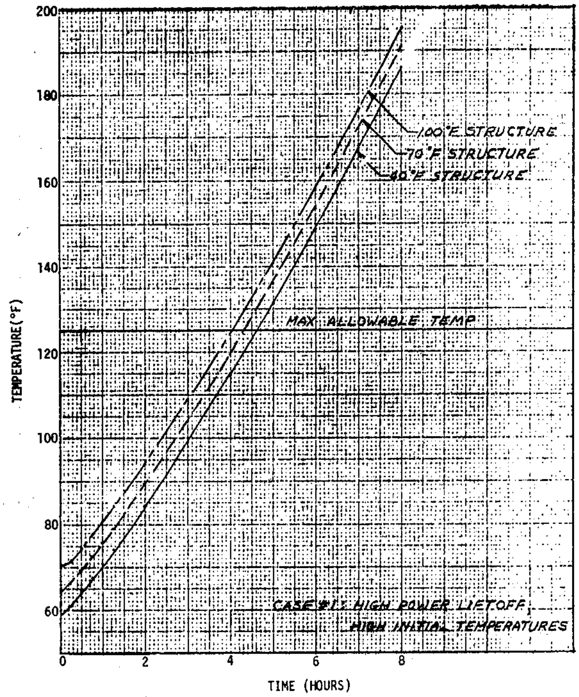

Figure LM7/4.3.12-7. Temperature Rise of the CWEA Following Loss of Coolant/Coolant Circulation

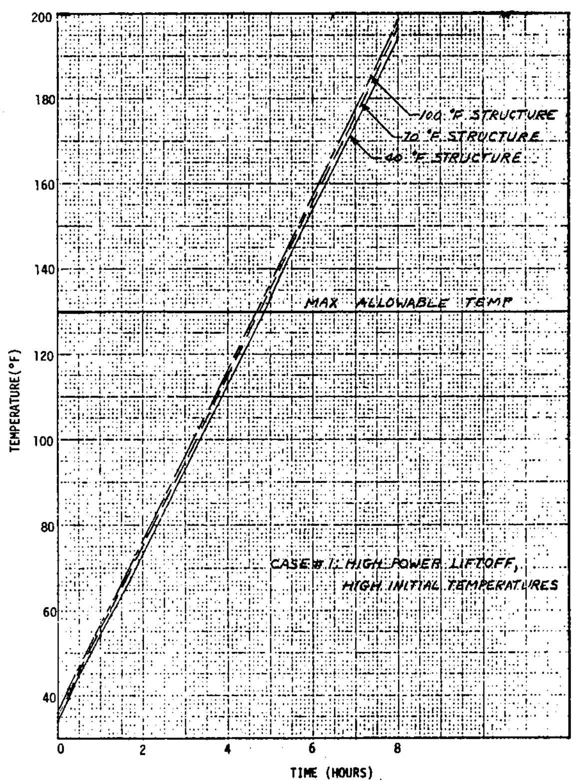

Figure LM7/4.3.12-6. Temperature Rise of the Battery #6 Following Loss of Coolant/Coolant Circulation

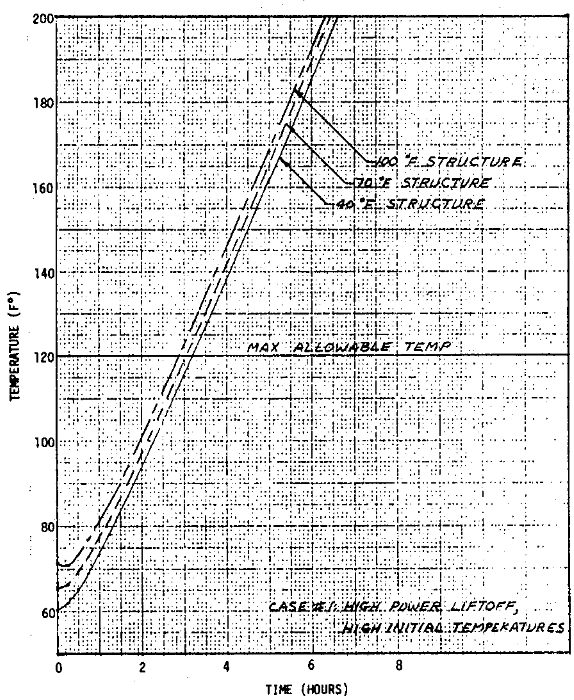

Figure LM7/4.3.12-8. Temperature Rise of the DUA Following Loss of Coolant/Coolant Circulation

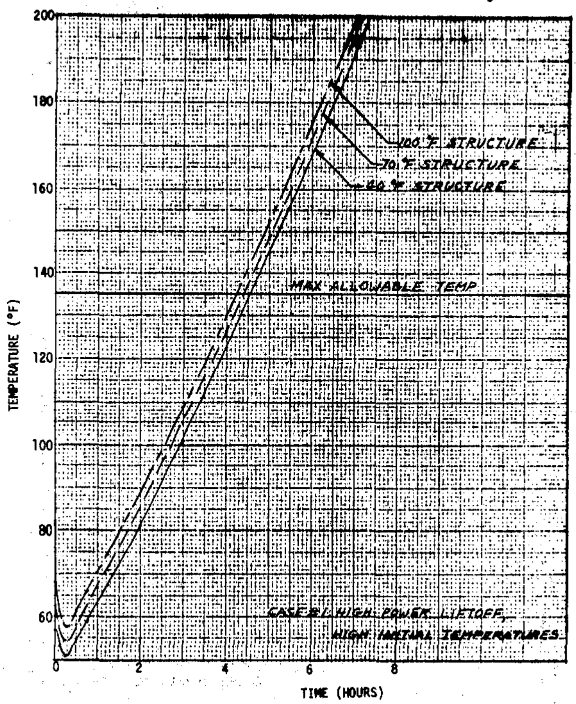

Figure LM7/4.3.12-9. Temperature Rise of the ECA #3 Following Loss of Coolant/Coolant Circulation

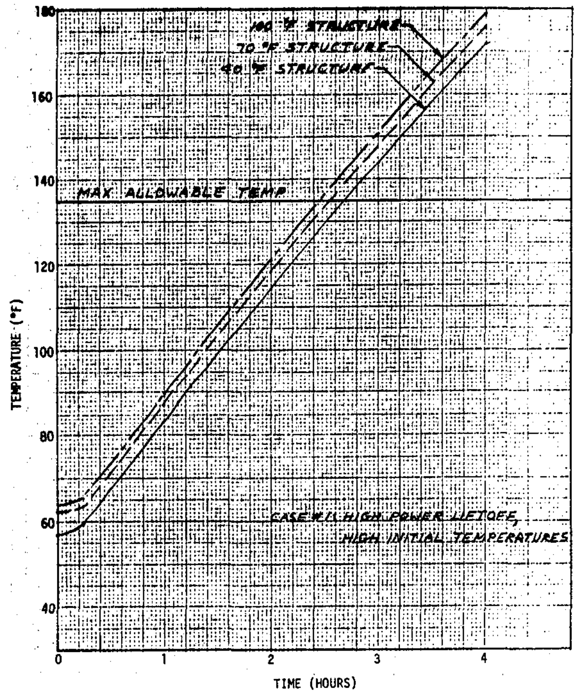

Figure LM7/4.3.12-11. Temperature Rise of the GPI #1 Following Loss of Coolant/Coolant Circulation

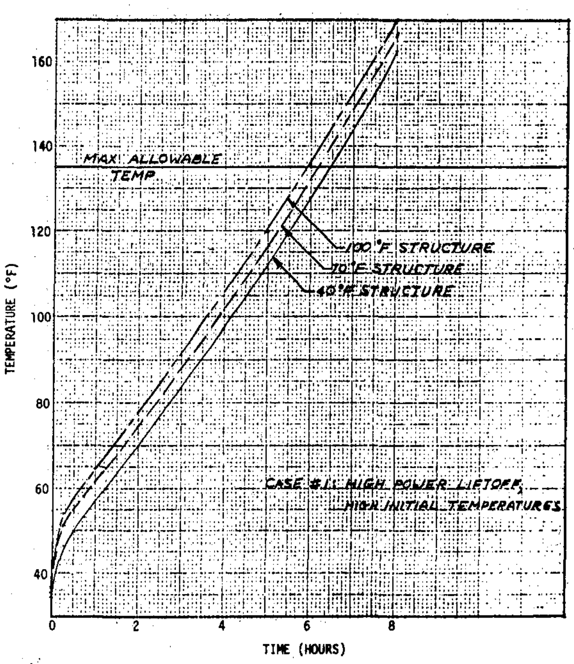

Figure LM7/4.3.12-10. Temperature Rise of the ECA #4 Following Loss of Coolant/Coolant Circulation

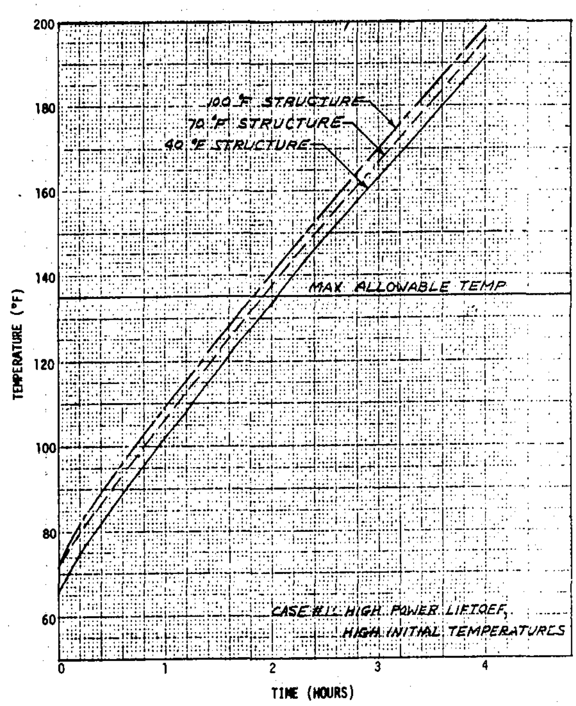

Figure LM7/4.3.12-12. Temperature Rise of the GPI #2 Following Loss of Coolant/Coolant Circulation

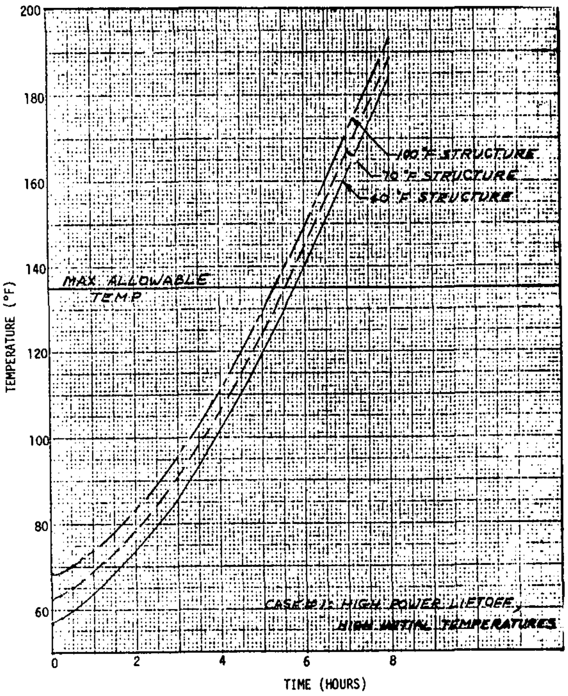

Figure LM7/4.3.12-13. Temperature Rise of the PCMTEA Following Loss of Coolant/Coolant Circulation

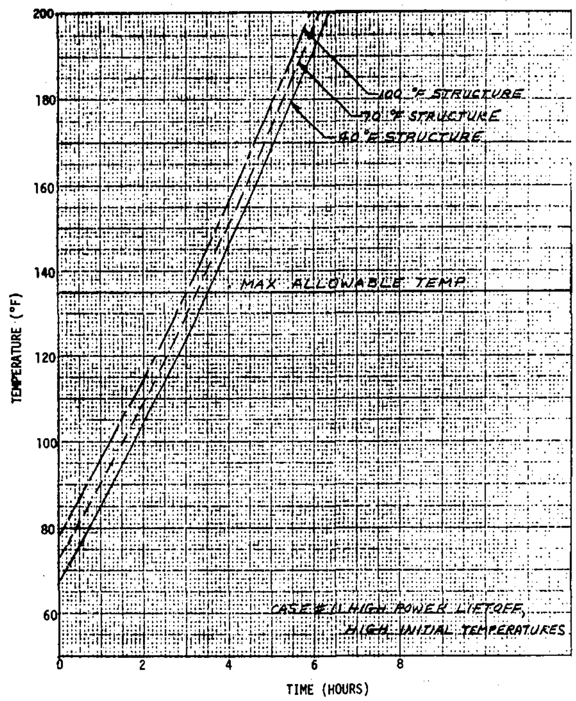

Figure LM7/4.3.12-15. Temperature Rise of the RTTA Following Loss of Coolant/Coolant Circulation

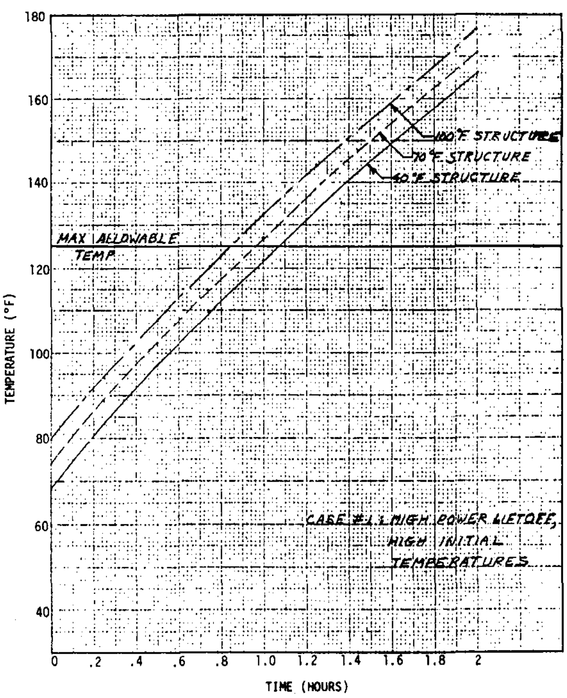

Figure LM7/4.3.12-14. Temperature Rise of the RREA Following Loss of Coolant/Coolant Circulation

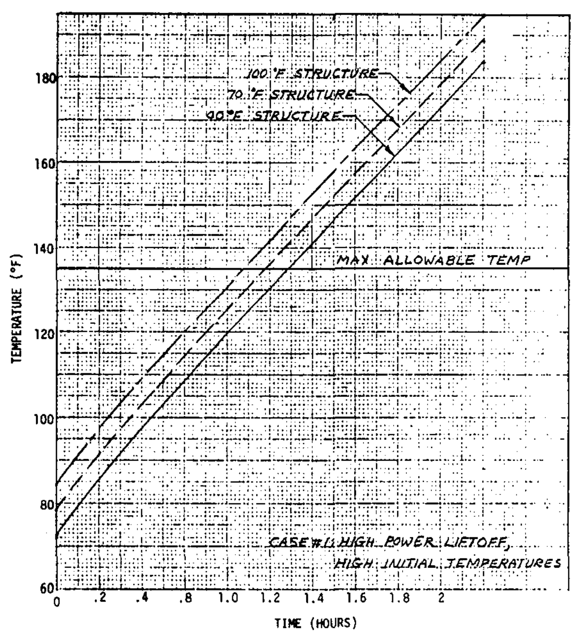

Figure LM7/4.3.12-16. Temperature Rise of the SBPA Following Loss of Coolant/Coolant Circulation

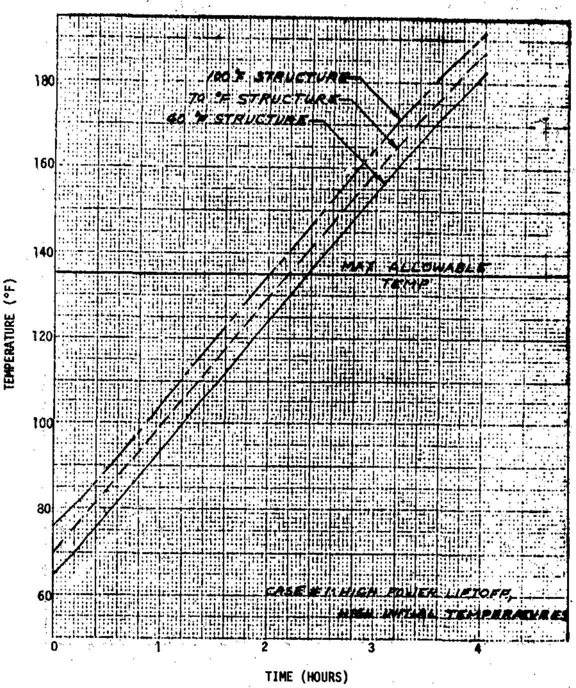

Figure LM7/4.3.12-17. Temperature Rise of the SBX Following Loss of Coolant/Coolant Circulation

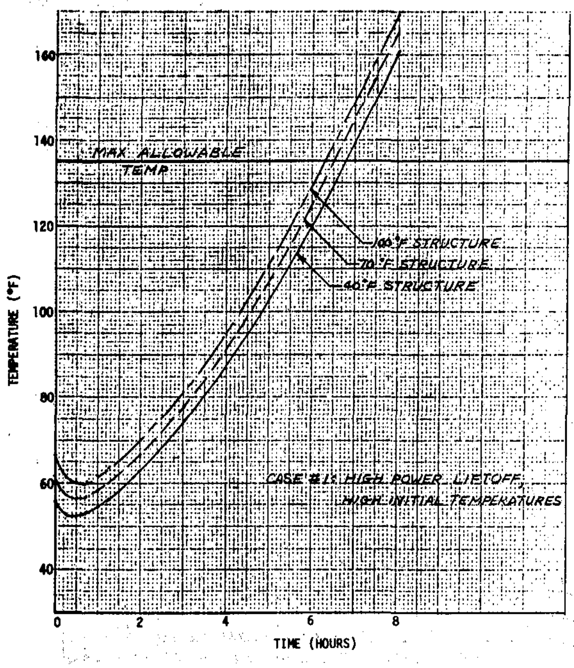

Figure LM7/4.3.12-19. Temperature Rise of the SCEA #2 Following Loss of Coolant/Coolant Circulation

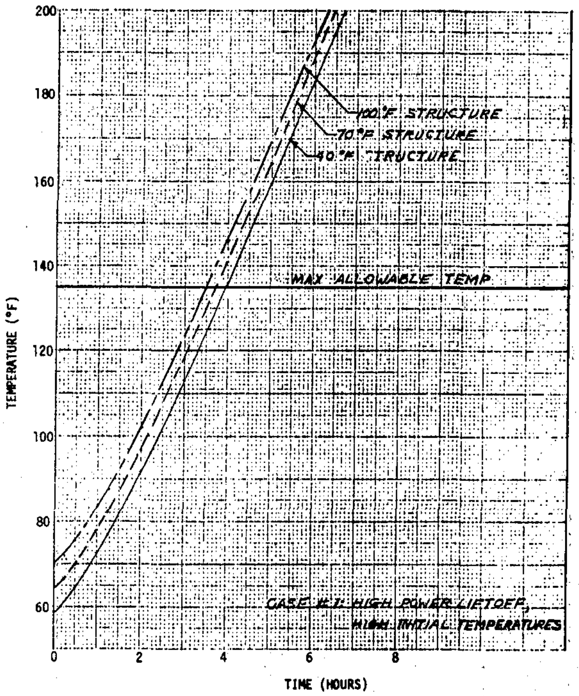

Figure LM7/4.3.12-18. Temperature Rise of the SCEA #1 Following Loss of Coolant/Coolant Circulation

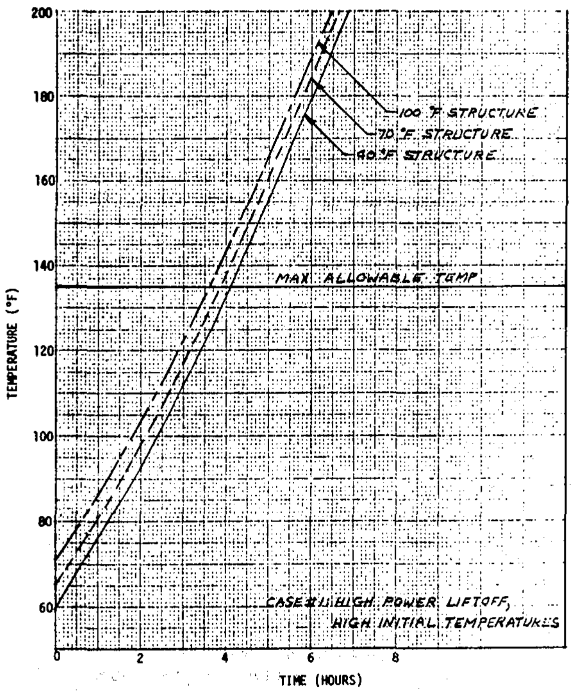

Figure LM7/4.3.12-20. Temperature Rise of the SPA Following Loss of Coolant/Coolant Circulation

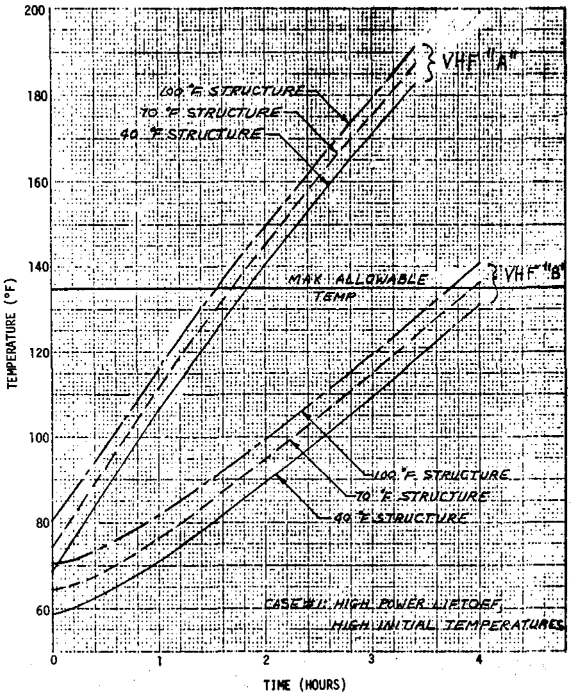

Figure LM7/4.3.12-21. Temperature Rise of the VHF XCVRS Following Loss of Coolant/Coolant Circulation

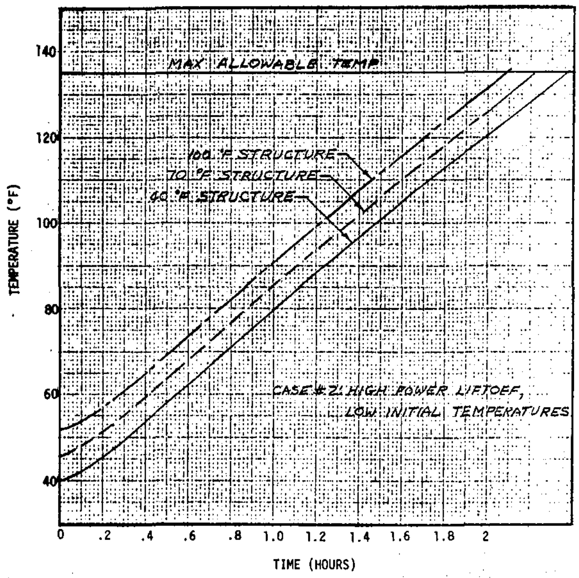

Figure LM7/4.3.12-23. Temperature Rise of the AEA Following Loss of Coolant/Coolant Circulation

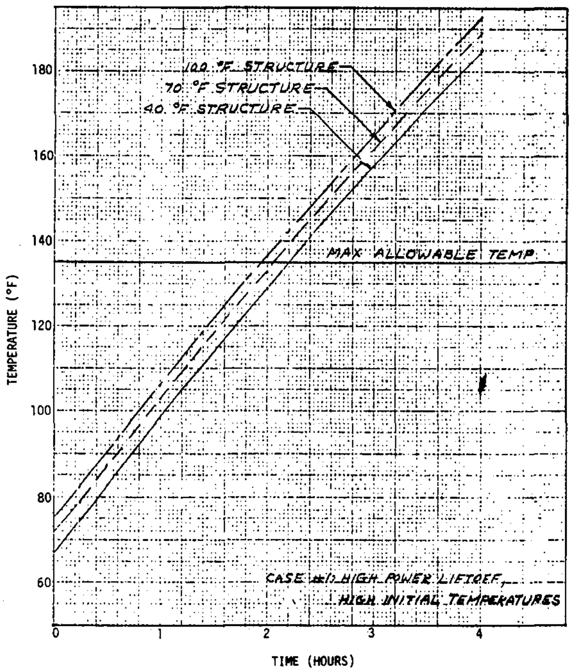

Figure LM7/4.3.12-22. Temperature Rise of the VHF Diplexer Following Loss of Coolant/Coolant Circulation

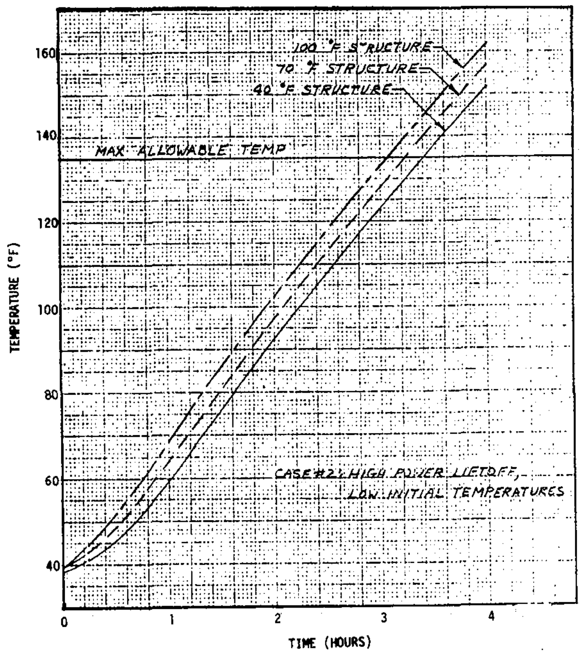

Figure LM7/4.3.12-24. Temperature Rise of the AEA Diode Assembly Following Loss of Coolant/Coolant Circulation

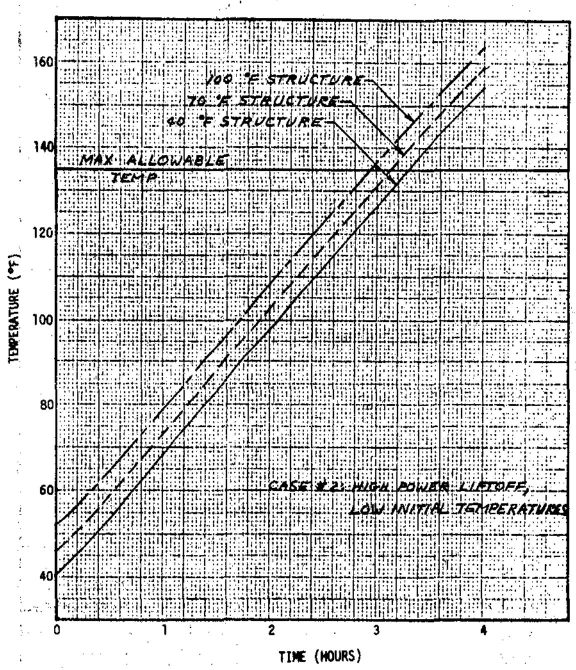

Figure LM7/4.3.12-25. Temperature Rise of the ATCA Following Loss of Coolant/Coolant Circulation

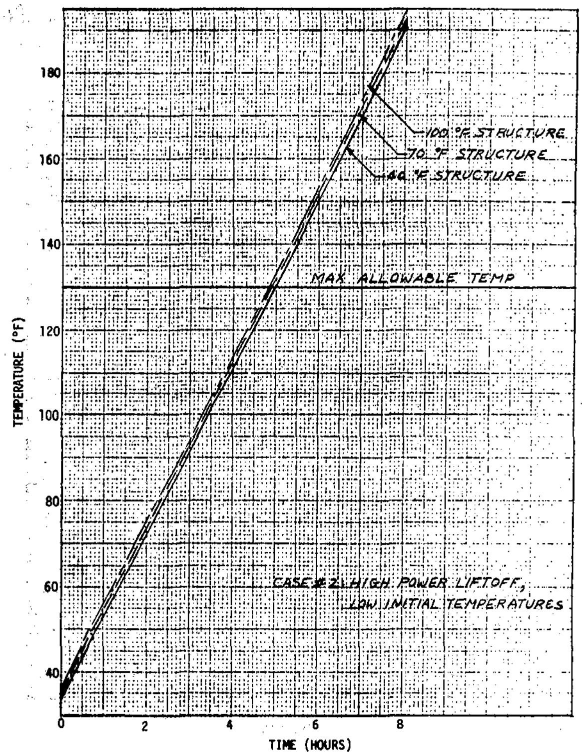

Figure LM7/4.3.12-27. Temperature Rise of the Battery #5 Following Loss of Coolant/Coolant Circulation

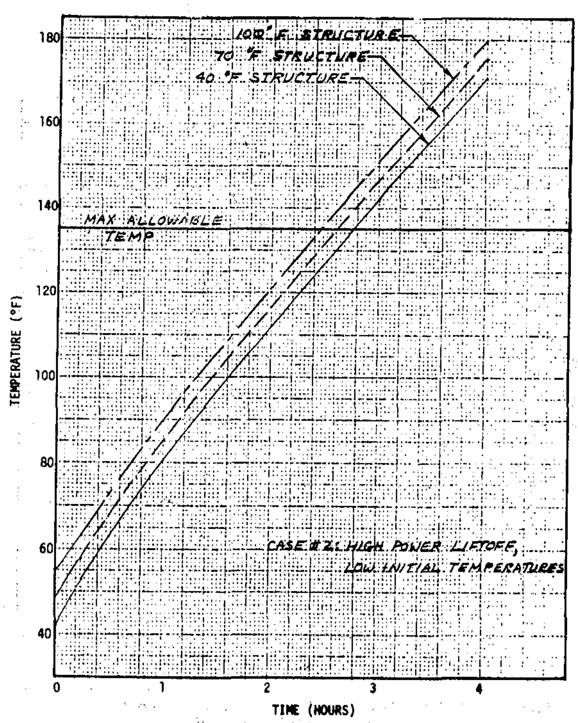

Figure LM7/4.3.12-26. Temperature Rise of the ATCA Res. Assembly Following Loss of Coolant/Coolant Circulation

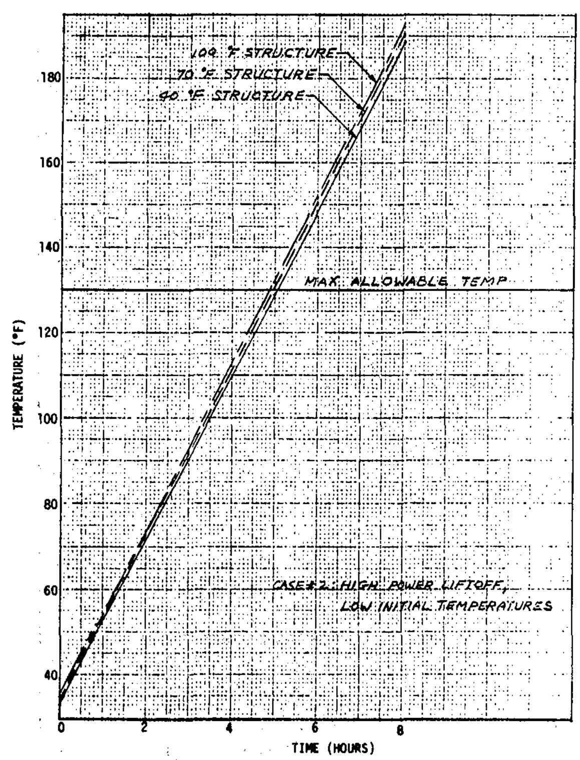

Figure LM7/4.3.12-28. Temperature Rise of the Battery #6 Following Loss of Coolant/Coolant Circulation

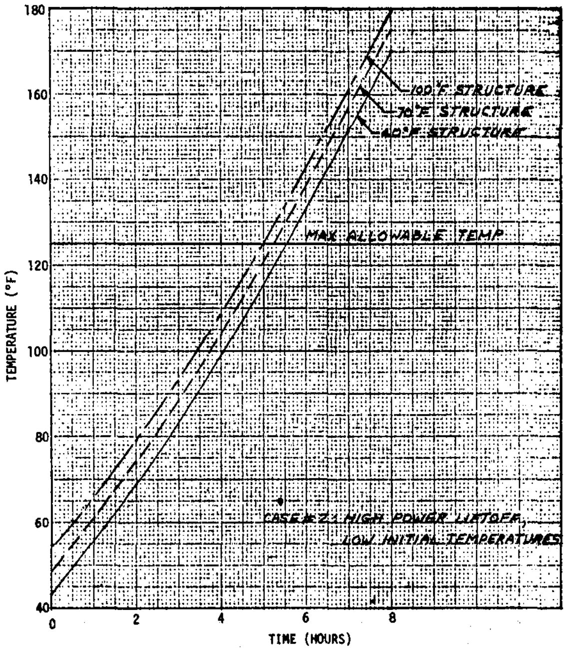

Figure LM7/4.3.12-29. Temperature Rise of the CWEA Following Loss of Coolant/Coolant Circulation

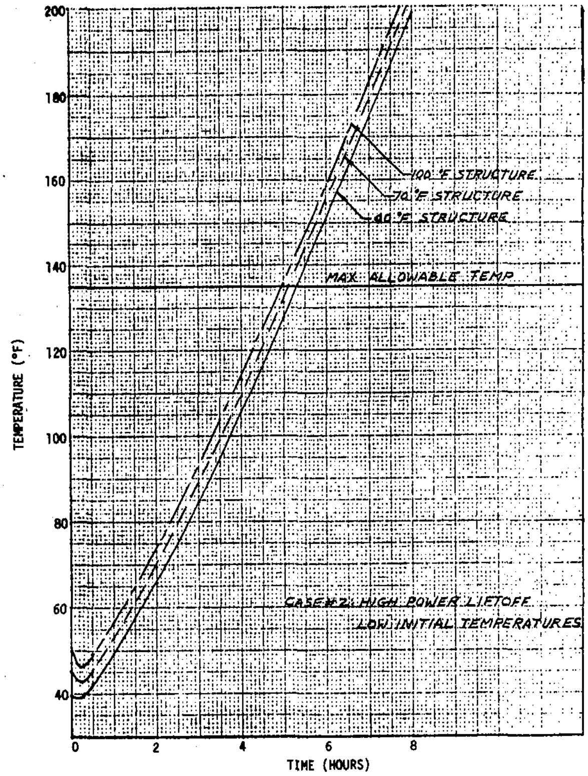

Figure LM7/4.3.12-31. Temperature Rise of the ECA #3 Following Loss of Coolant/Coolant Circulation

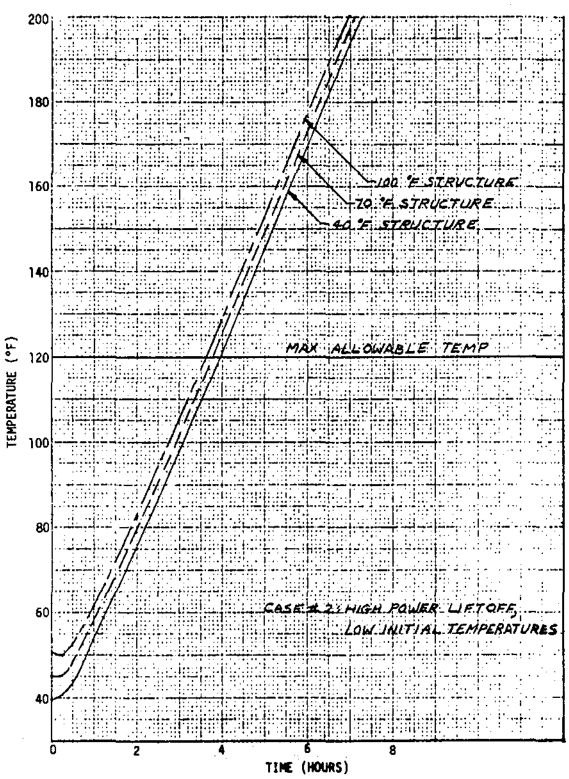

Figure LM7/4.3.12-30. Temperature Rise of the DUA Following Loss of Coolant/Coolant Circulation

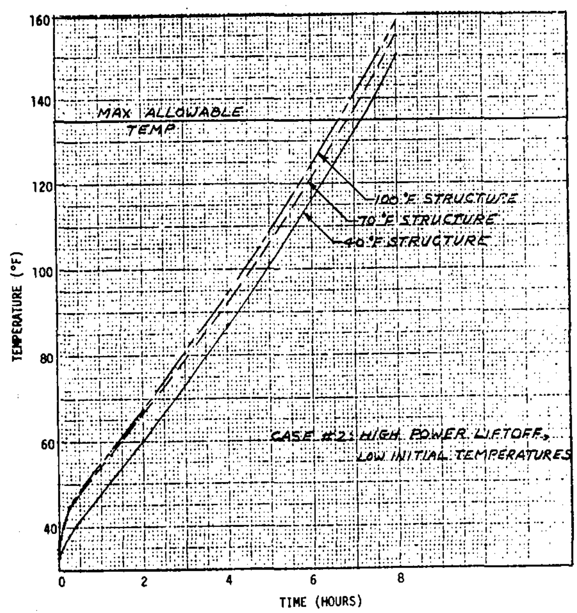

Figure LM7/4.3.12-32. Temperature Rise of the ECA #4 Following Loss of Coolant/Coolant Circulation

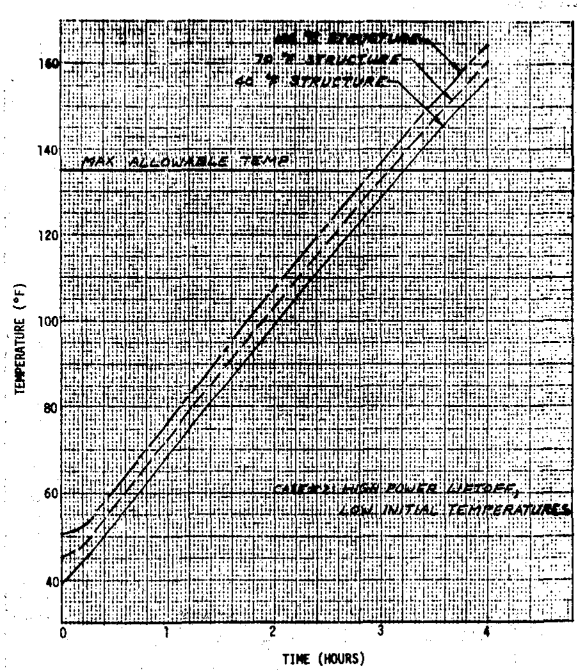

Figure LM7/4.3.12-33. Temperature Rise of the GPI #1 Following Loss of Coolant/Coolant Circulation

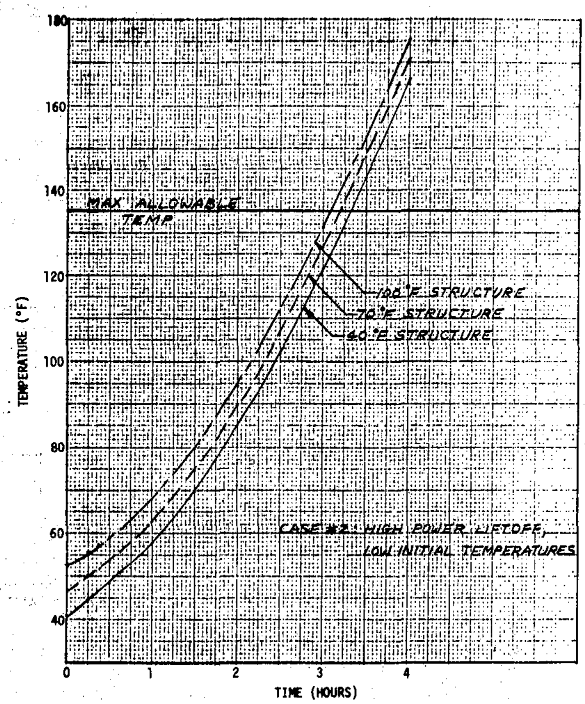

Figure LM7/4.3.12-35. Temperature Rise of the PCMTEA Following Loss of Coolant/Coolant Circulation

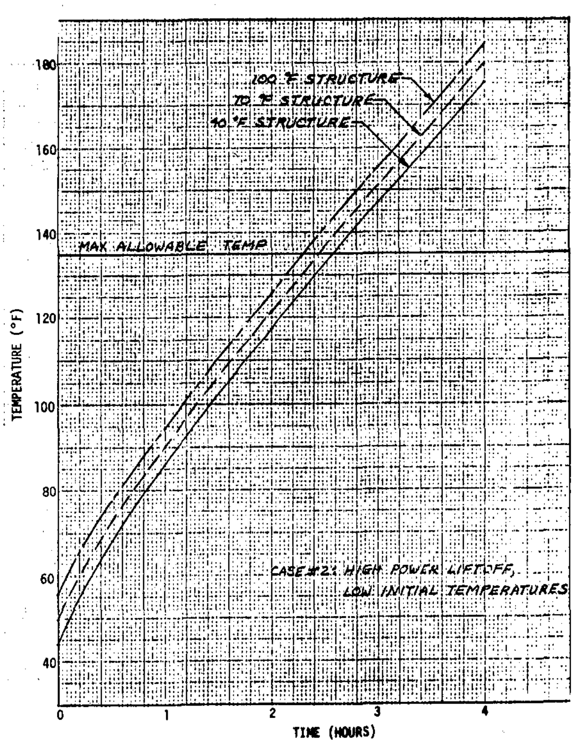

Figure LM7/4.3.12-34. Temperature Rise of the GPI #2 Following Loss of Coolant/Coolant Circulation

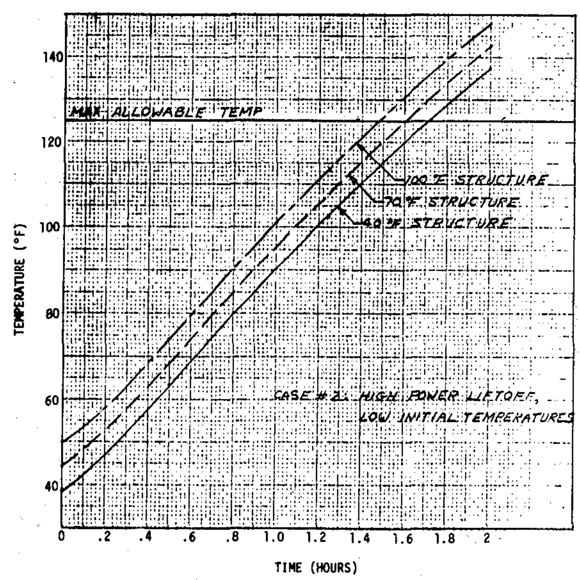

Figure LM7/4.3.12-36. Temperature Rise of the RREA Following Loss of Coolant/Coolant Circulation

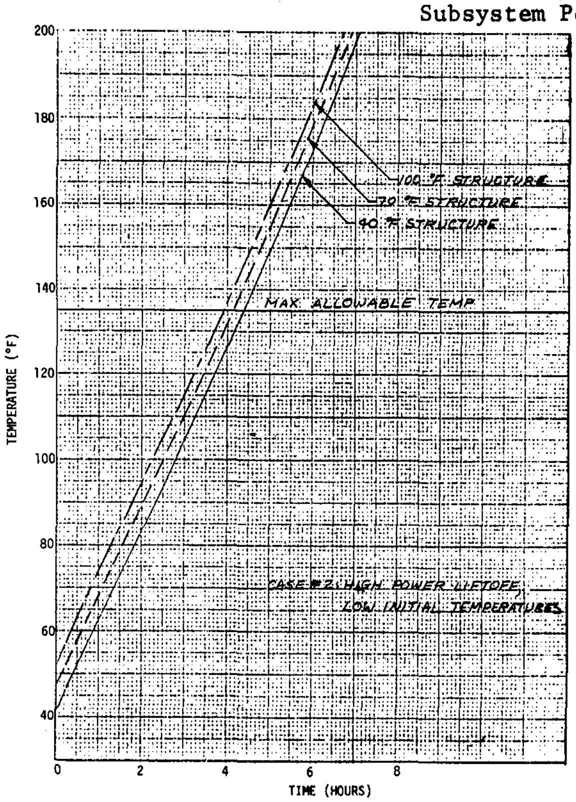

Figure LM7/4.3.12-37. Temperature Rise of the RTTA Following Loss of Coolant/Coolant Circulation

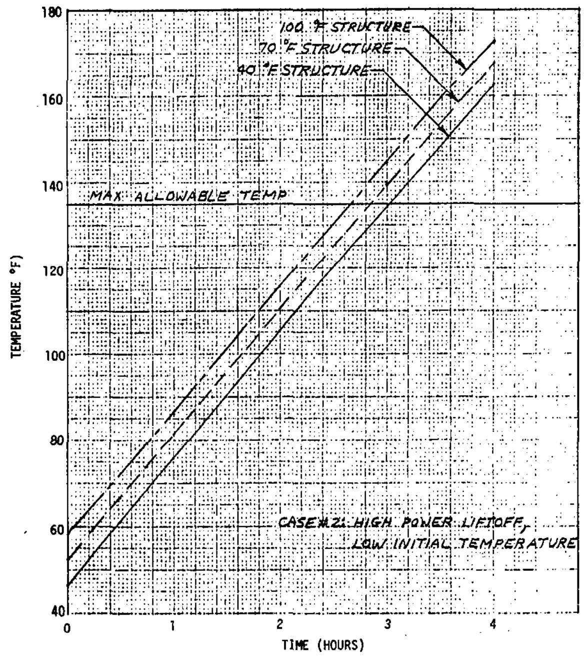

Figure LM7/4.3.12-39. Temperature Rise of the SBX Following Loss of Coolant/Coolant Circulation

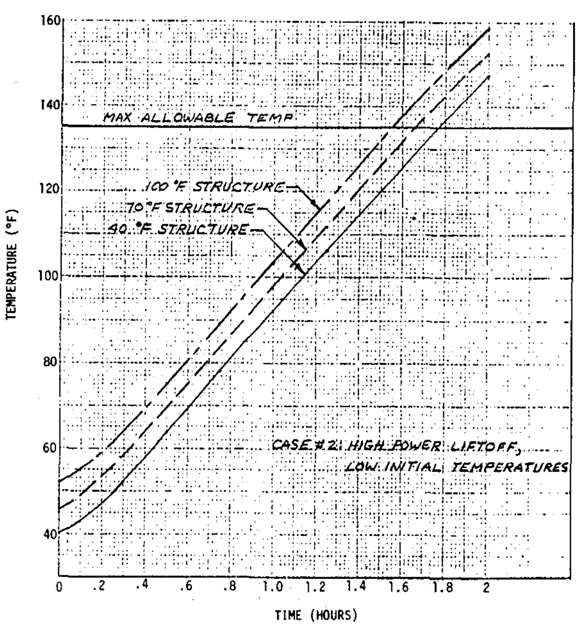

Figure LM7/4.3.12-38. Temperature Rise of the SBPA Following Loss of Coolant/Coolant Circulation

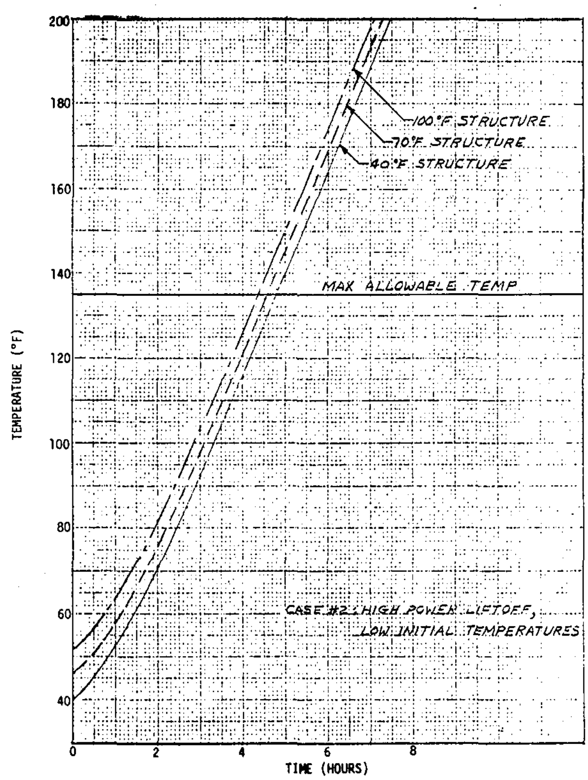

Figure LM7/4.3.12-40. Temperature Rise of the SCEA #1 Following Loss of Coolant/Coolant Circulation

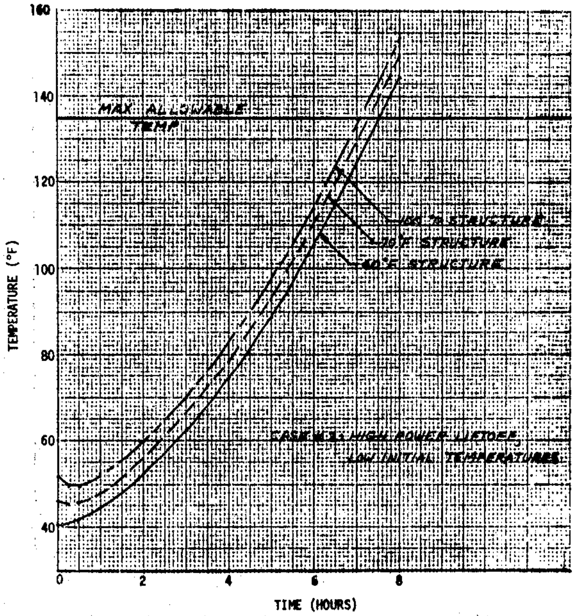

Figure LM7/4.3.12-41. Temperature Rise of the SCEA #2 Following Loss of Coolant/Coolant Circulation

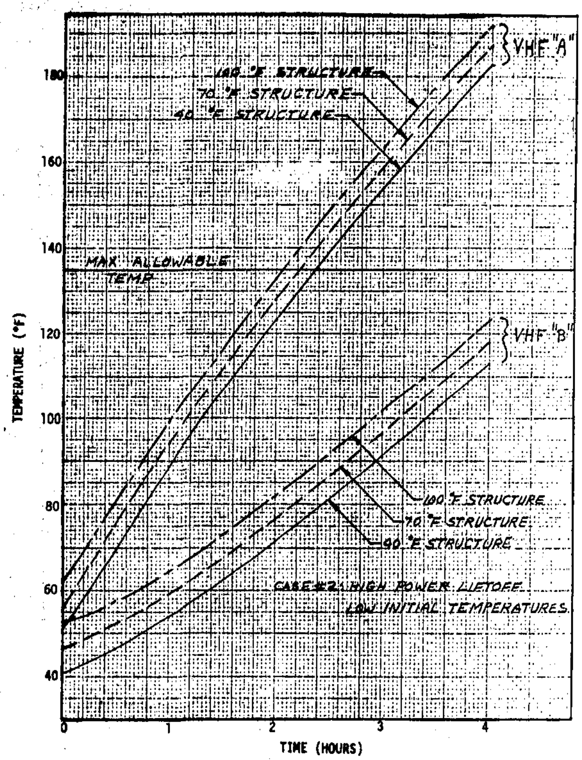

Figure LM7/4.3.12-43. Temperature Rise of the VHF Xcvrs Following Loss of Coolant/Coolant Circulation

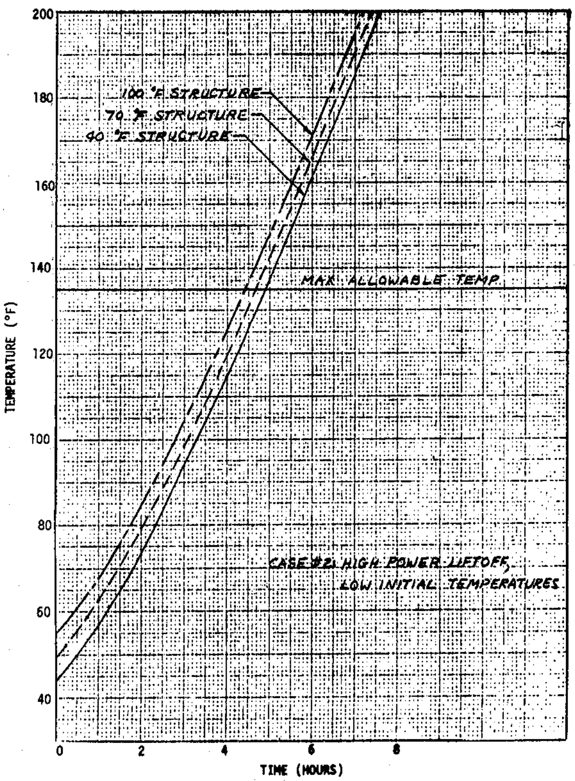

Figure LM7/4.3.12-42. Temperature Rise of the SPA Following Loss of Coolant/Coolant Circulation

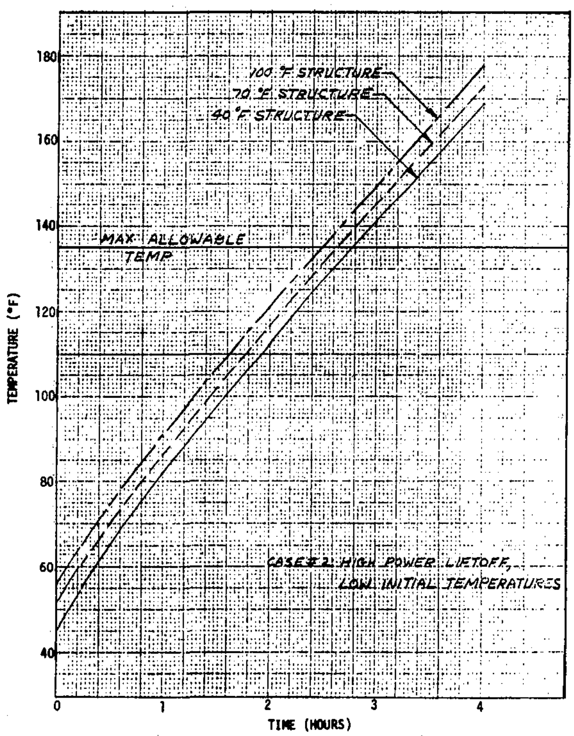

Figure LM7/4.3.12-44. Temperature Rise of the VHF Diplexer Following Loss of Coolant/Coolant Circulation

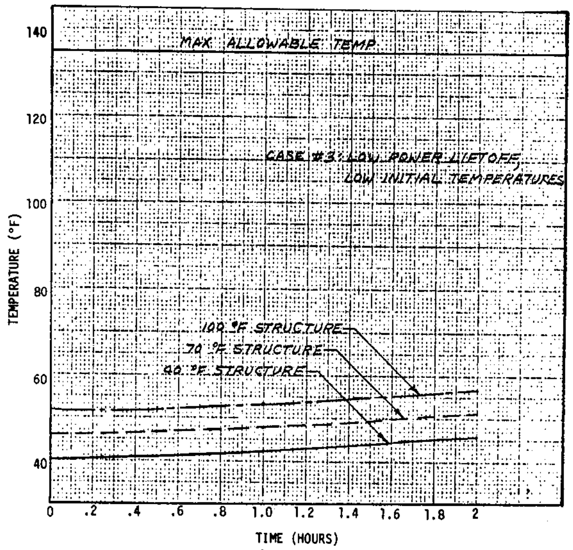

Figure LM7/4.3.12-45. Temperature Rise of the AEA Following Loss of Coolant/Coolant Circulation

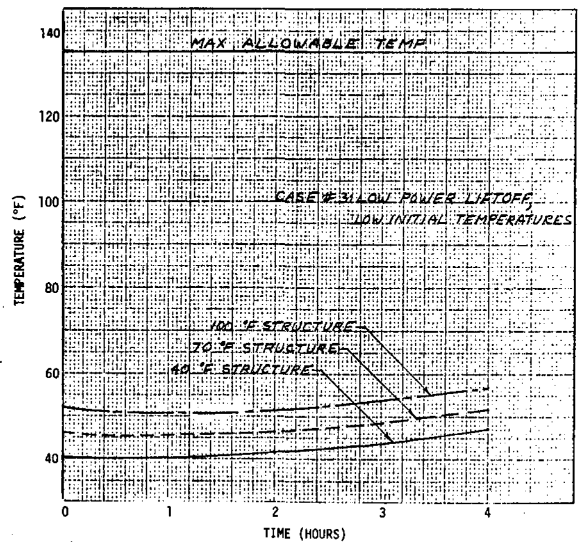

Figure LM7/4.3.12-47. Temperature Rise of the ATCA Following Loss of Coolant/Coolant Circulation

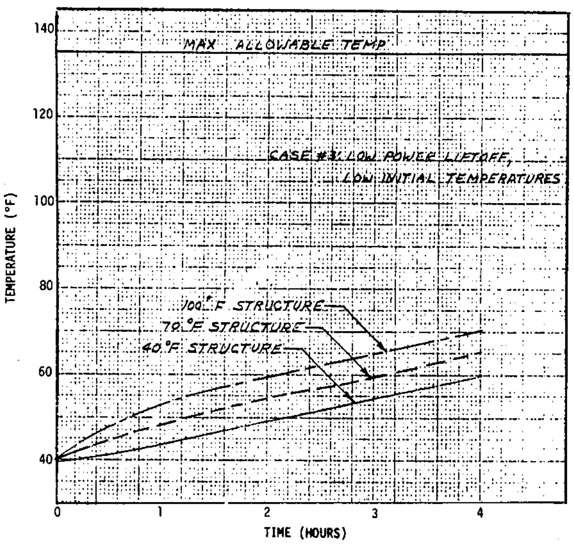

Figure LM7/4.3.12-46. Temperature Rise of the AEA Diode Ass'y. Following Loss of Coolant/Coolant Circulation

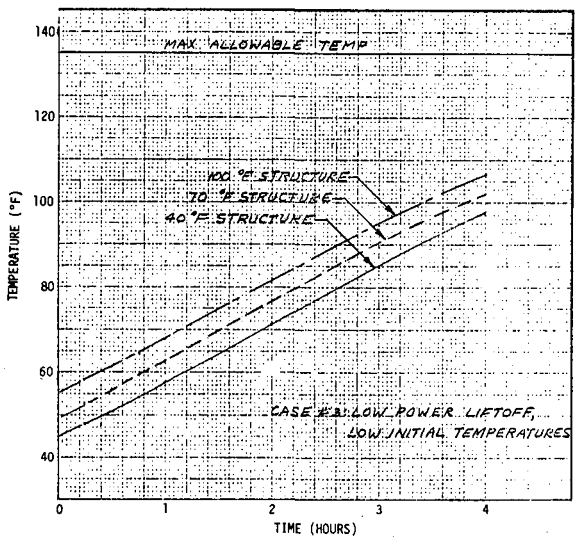

Figure LM7/4.3.12-48. Temperature Rise of the ATCA Res. Ass'y. Following Loss of Coolant/Coolant Circulation

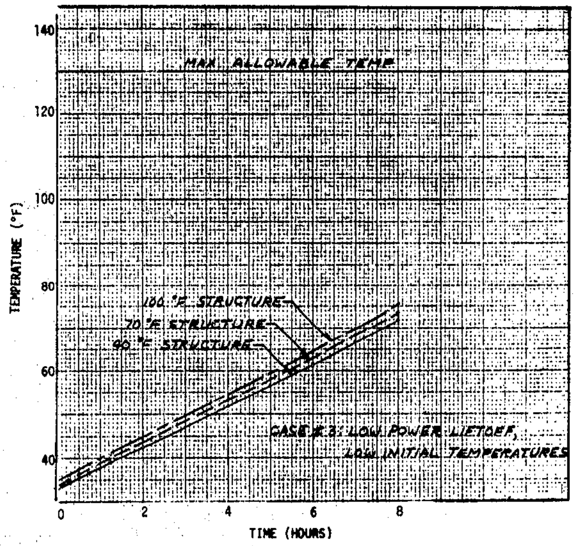

Figure LM7/4.3.12-49. Temperature Rise of the Batt #5 Following Loss of Coolant/Coolant Circulation

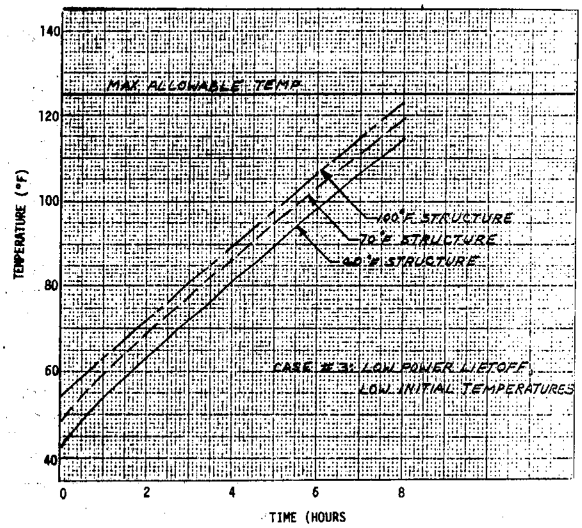

Figure LM7/4.3.12-51. Temperature Rise of the CWEA Following Loss of Coolant/Coolant Circulation

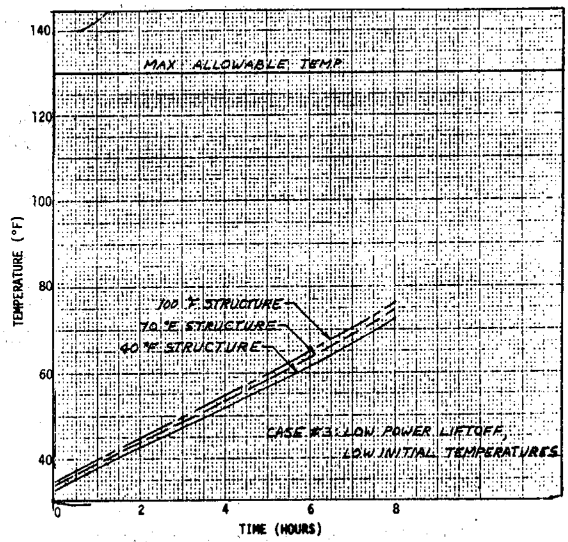

Figure LM7/4.3.12-50. Temperature Rise of the Batt #6 Following Loss of Coolant/Coolant Circulation

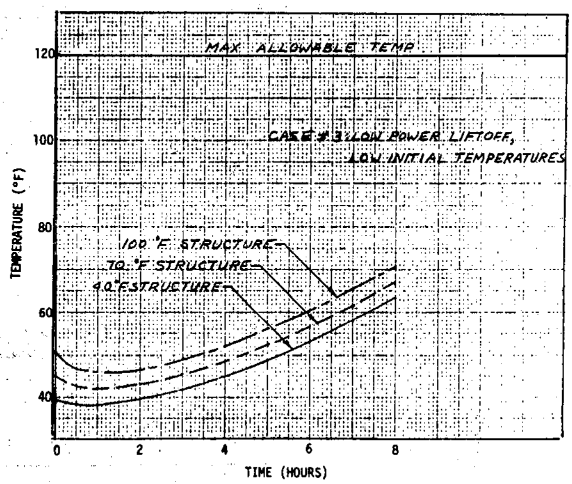

Figure LM7/4.3.12-52. Temperature of the DUA Following Loss of Coolant/Coolant Circulation

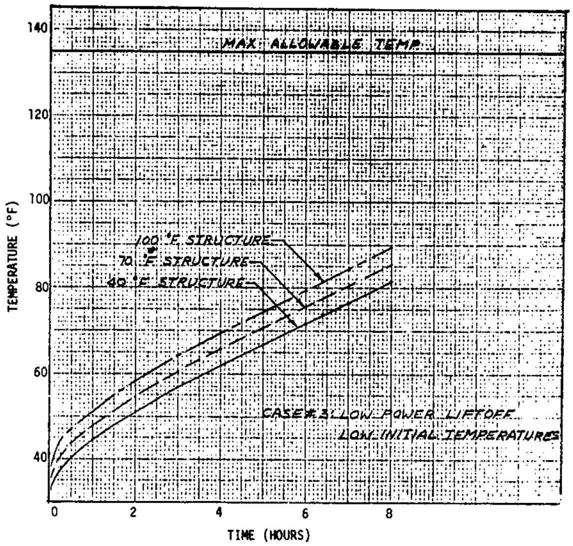

Figure LM7/4.3.12-53. Temperature Rise of the ECA #3 Following Loss of Coolant/Coolant Circulation

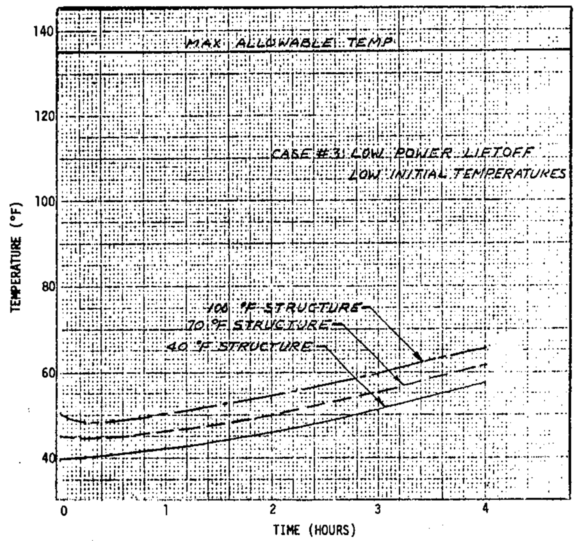

Figure LM7/4.3.12-55. Temperature of the GPI #1 Following Loss of Coolant/Coolant Circulation

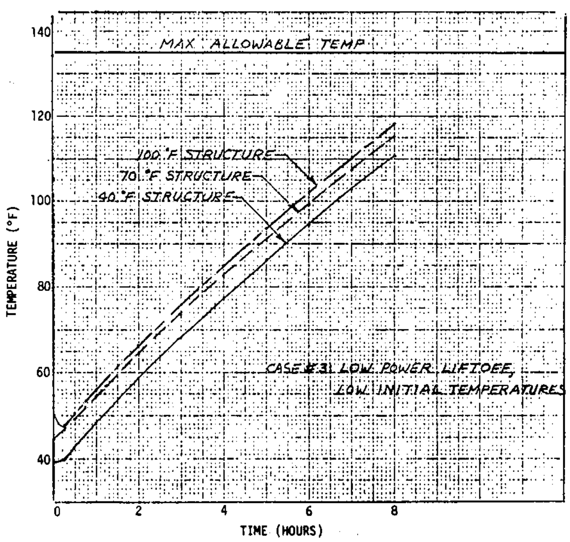

Figure LM7/4.3.12-54. Temperature Rise of the ECA #4 Following Loss of Coolant/Coolant Circulation

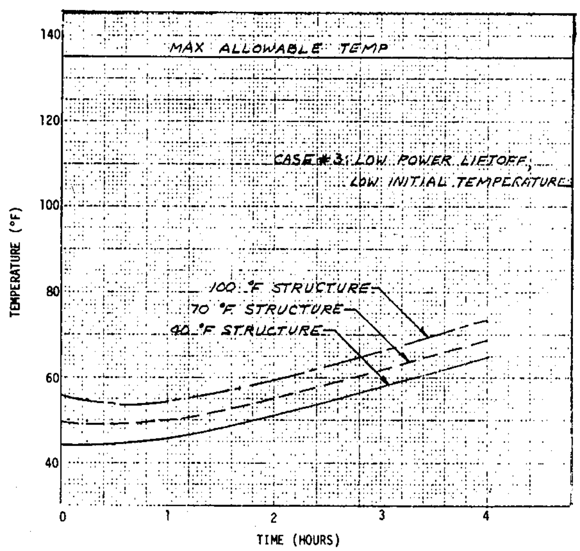

Figure LM7/4.3.12-56. Temperature Rise of the GPI #2 Following Loss of Coolant/Coolant Circulation

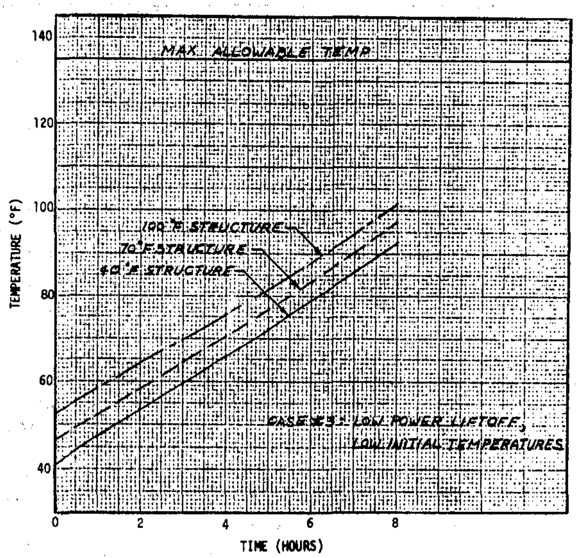

Figure LM7/4.3.12-57. Temperature Rise of the PCMTEA Following Loss of Coolant/Coolant Circulation

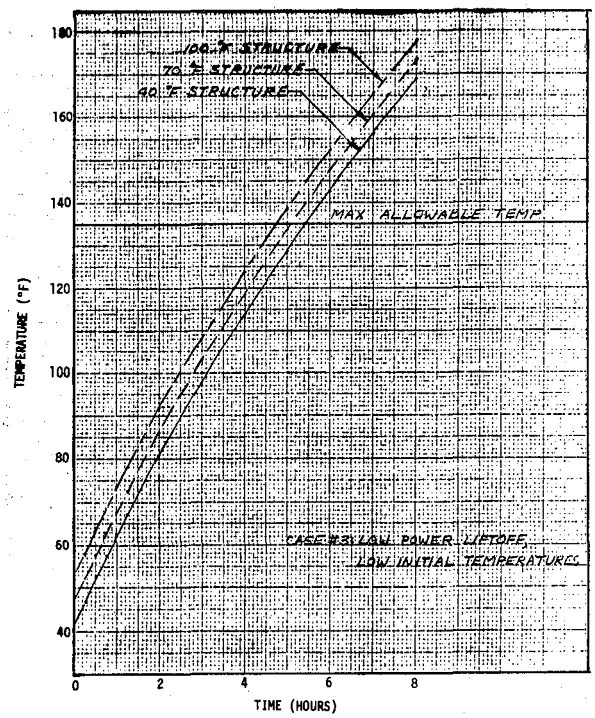

Figure LM7/4.3.12-59. Temperature Rise of the RTTA Following Loss of Coolant/Coolant Circulation

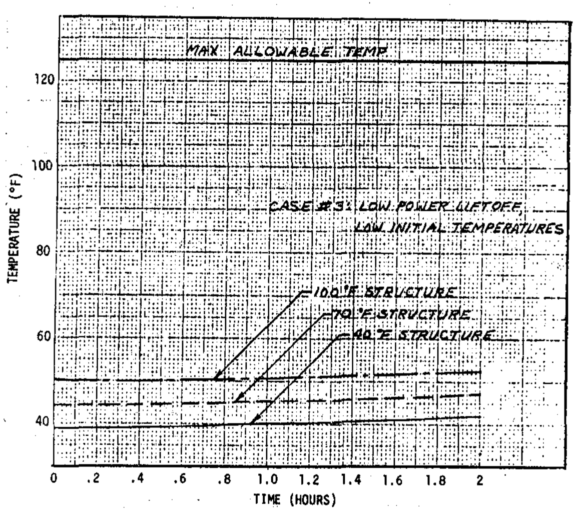

Figure LM7/4.3.12-58. Temperature Rise of the RREA Following Loss of Coolant/Coolant Circulation

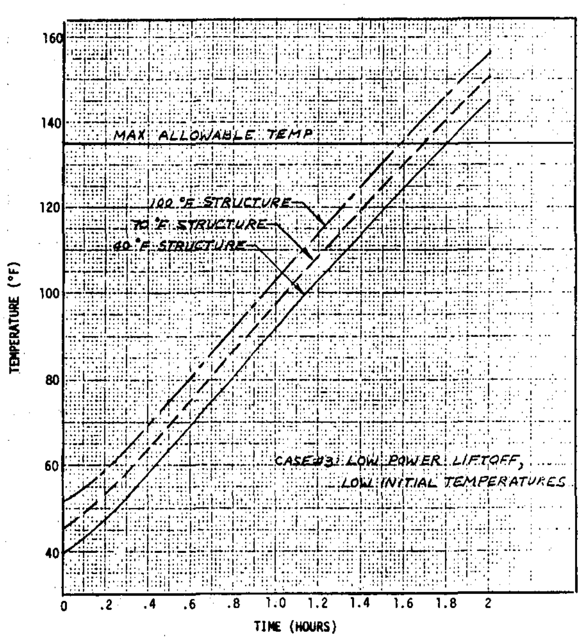

Figure LM7/4.3.12-60. Temperature Rise of the SBPA Following Loss of Coolant/Coolant Circulation

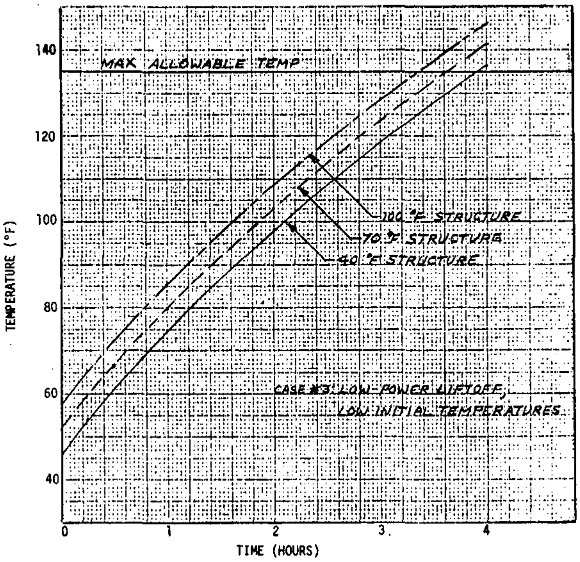

Figure LM7/4.3.12-61. Temperature Rise of the SBX Following Loss of Coolant/Coolant Circulation

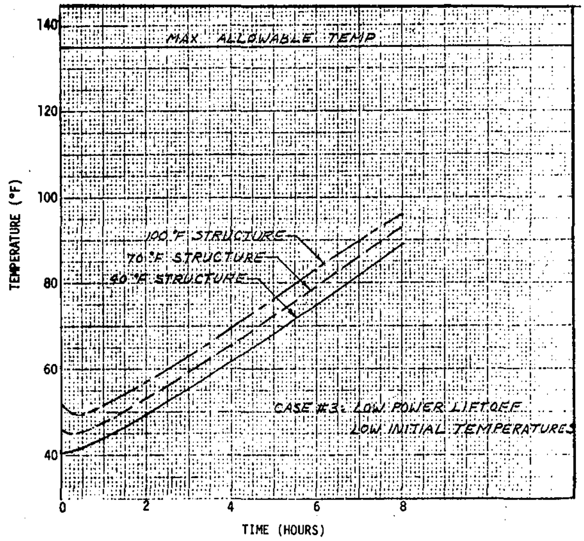

Figure LM7/4.3.12-63. Temperature Rise of the SCEA #2 Following Loss of Coolant/Coolant Circulation

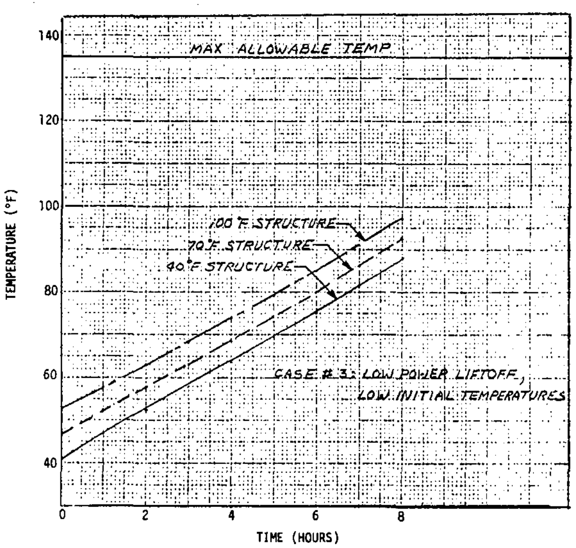

Figure LM7/4.3.12-62. Temperature Rise of the SCEA #1 Following Loss of Coolant/Coolant Circulation

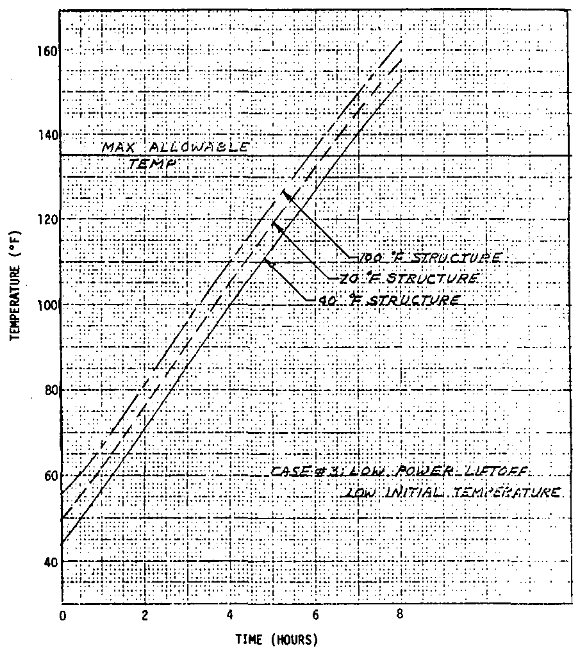

Figure LM7/4.3.12-64. Temperature Rise of the SPA Following Loss of Coolant/Coolant Circulation

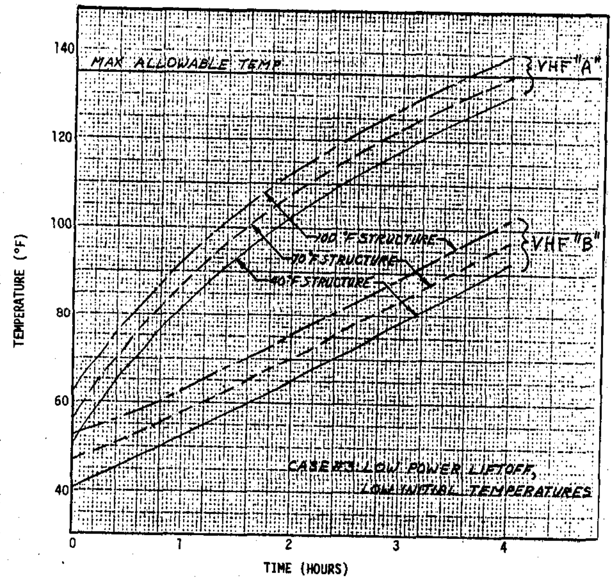

Figure LM7/4.3.12-65. Temperature Rise of the VHF Xcvrs Following Loss of Coolant/Coolant Circulation

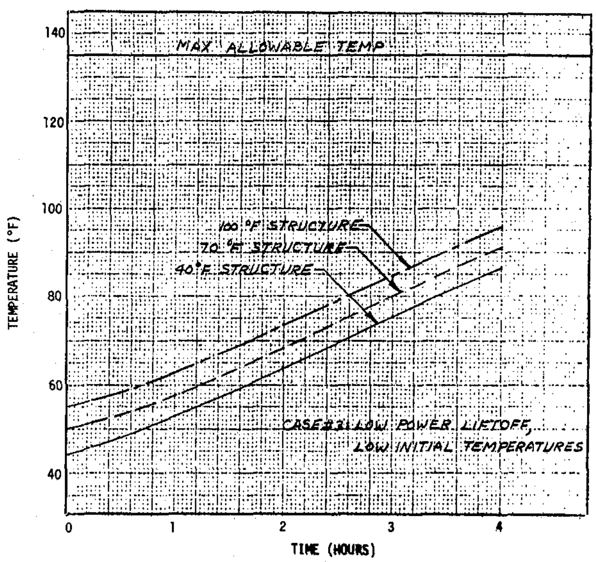

Figure LM7/4.3.12-66. Temperature Rise of the VHF Diplexer Following Loss of Coolant/Coolant Circulation

LM7/4.5.1.1 Uncertainty of LM IMU Alignment from CSM IMU

The measured alignment angles associated with a talkover alignment of the LM IMU from the CSM IMU are listed in Table LM7/4.5.1-2. The contributions to the uncertainty in the talkover alignment of the LM IMU are listed in Table LM7/4.5.1-3. The RSS 1-σ total uncertainties are summarized as follows:

LM Axis	1-σ RSS, arc min
Yaw (about X-axis)	±15.8 (0.264 deg)
Pitch (about Y-axis)	±4.0 (0.067 deg)
Roll (about Z-axis)	±4.0 (0.067 deg)

The above values do not include thermal effects or bending or torque effects from any cause (i.e., RCS jet firing). Also, the effect of the maximum allowable CG offset in the X-axis of 0.2 inch was not included.

LM7/4.5.1.4 Guidance Computer Erasable Memory Constants (NASA DATA SOURCE)

The following listings pertain to the LM Guidance Computer (LGC) pad loaded erasable memory constants. Mission time computed constants, such as state vectors, etc., are not included.

Table LM7/4.5.1-1 contains a tabular listing of the erasable load, both mission tape parameters and launch tape parameters. The remarks column contains a short description of the use of the constant.

The number in the "Rev" column denotes the number of revisions to the value of the corresponding parameter that have been incorporated in publications of the Apollo 13 erasable load.

A single or double star (* or **) in the "Rev" column denotes that it is also in the inflight erasable load. These parameters would have to be verified or reloaded in order to completely initialize the LGC in orbit. A single star denotes loading by ground uplink; a double star denotes loading by the astronaut via the DSKY.

(NASA DATA SOURCE)

Table LM7/4.5.1-1 FINAL H2 PRELAUNCH ERASABLE LOAD (LM131A REV 1)

REV	MNEMONIC	ADDR	OCTAL	SF	ENGINEERING VALUE	VALUE IN AGC UNITS
	FLAGWRD3+ 0	0077	12000	-0		
1	FLAGWRD8+ 0	0104	06000	-0		
	FLGWRD10+ 0	0106	00000	-0		
1	MASS + 0	1243	07401	16	3.387230000+004 LBS	1.536421683+004 KGS
	MASS + 1	1244	00000	0	0.000000000+000 LBS	0.000000000+000 KGS
1**	LEMMASS + 0	1326	07401	16	3.387230000+004 LBS	1.536421683+004 KGS
1**	CSMMASS + 0	1327	10246	16	3.758030000+004 LBS	1.704613734+004 KGS
*	E3J22R2M+ 0	1347	12160	58	9.204790479+016	9.204790479+016 M5/CS2
*	E32C31RM+ 0	1350	03363	80	1.312892560+023	1.312892560+023 M6/CS2
*	RADSKAL + 0	1351	00000	21	0.000000000+000	0.000000000+000 LRB/M/CS
		1352	00000			

UNITS ARE LR LOW SCALE ALTITUDE BITS/METER/CS

(NASA DATA SOURCE)

Table LM7/4.5.1-1 FINAL H2 PRELAUNCH ERASABLE LOAD (LM131A REV 1) (Continued)

REV	MNEMONIC	ADDR	OCTAL	SF	ENGINEERING VALUE	VALUE IN AGC UNITS
	* SKALSKAL+	0 1353	00000	0	0.000000000+000	0.000000000+000
2	* ELBIAS +	0 1356	00044	-1	4.000000000-001 DEG	1.111111111-003 REV
1	* PBIASX +	0 1452	03641	-3	1.490020752-004	1.490020752-002
1	* PIPASCFX+	0 1453	64417	-9		-6.999969482-004
1	* PBIASY +	0 1454	74272	-3	-1.419830322-004	-1.419830322-002
1	* PIPASCFY+	0 1455	54401	-9		-1.189947128-003
1	* PBIASZ +	0 1456	03775	-3	1.560211182-004	1.560211182-002
1	* PIPASCFZ+	0 1457	72727	-9		-3.099441528-004
1	* NBDX +	0 1460	00063	-5		9.727478027-005
1	* NBDY +	0 1461	00015	-5		2.479553223-005
1	* NBDZ +	0 1462	77762	-5		-2.479553223-005
1	* ADIAX +	0 1463	77627	-6		-9.918212890-005
1	* ADIAY +	0 1464	00202	-6		1.239776611-004

(NASA DATA SOURCE)

Table LM7/4.5.1-1 FINAL H2 PRELAUNCH ERASABLE LOAD (LM131A REV 1) (Continued)

REV		MNEMONIC			ADDR	OCTAL	SF	ENGINEERING VALUE	VALUE IN AGC UNITS
1	*	ADIAZ	+	0	1465	77713	-6		-4.959106445-005
1	*	ADSRAX	+	0	1466	77745	-6		-2.479553223-005
1	*	ADSRAY	+	0	1467	00266	-6		1.735687256-004
1	*	ADSRAZ	+	0	1470	00000	-6		0.000000000+000
	*	GCOMPSW	+	0	1477	00000	-0		
		TETCSM	+	0	1570	37777	-0		
		TETLEM	+	0	1642	37777	-0		
	*	X789	+	0	1700	00000	5	0.000000000+000	0.000000000+000 RADIANS
					1701	00000			
	*	X789	+	2	1702	00000	5	0.000000000+000	0.000000000+000 RADIANS
					1703	00000			
	*	X789	+	4	1704	00000	5	0.000000000+000	0.000000000+000 RADIANS
					1705	00000			

(NASA DATA SOURCE)

Table LM7/4.5.1-1 FINAL H2 PRELAUNCH ERASABLE LOAD (LM131A REV 1) (Continued)

REV	MNEMONIC	ADDR	OCTAL	SF	ENGINEERING VALUE	VALUE IN AGC UNITS
1 *	TEPHEM + 0	1706	00011	42	2.460678000+007	2.460678000+009 CS
		1707	05253			
		1710	33560			
1 *	AZO + 0	1711	30623	0	2.788765975+002 DEG	7.746572159-001 REV
		1712	37367			
1 *	-AYO + 0	1713	00000	0	1.311868428-002 DEG	3.644078970-005 REV
		1714	23066			
1 *	AXO + 0	1715	00000	0	1.552999018-002 DEG	4.313886166-005 REV
		1716	26474			
2	REFSMMAT+ 0	1733	11227	1	5.809470490-001	5.809470490-001
		1734	03621			
2	REFSMMAT+ 2	1735	64303	1	-7.260797396-001	-7.260797396-001
		1736	76432			

(NASA DATA SOURCE)

Table LM7/4.5.1-1 FINAL H2 PRELAUNCH ERASABLE LOAD (LM131A REV 1) (Continued)

REV	MNEMONIC	ADDR	OCTAL	SF	ENGINEERING VALUE	VALUE IN AGC UNITS
2	REFSMMAT+ 4	1737 1740	72072 64034	1	-3.678434119-001	-3.678434119-001
2	REFSMMAT+ 6	1741 1742	77664 50201	1	-9.245857596-003	-9.245857596-003
2	REFSMMAT+ 8	1743 1744	70531 72041	1	-4.577863067-001	-4.577863067-001
2	REFSMMAT+10	1745 1746	16162 31571	1	8.890141919-001	8.890141919-001
2	REFSMMAT+12	1747 1750	62764 63727	1	-8.138888478-001	-8.138888478-001
2	REFSMMAT+14	1751 1752	67624 76002	1	-5.130691305-001	-5.130691305-001
2	REFSMMAT+16	1753 1754	73506 53045	1	-2.726628333-001	-2.726628333-001

(NASA DATA SOURCE)

Table LM7/4.5.1-1 FINAL H2 PRELAUNCH ERASABLE LOAD (LM131A REV 1) (Continued)

REV	MNEMONIC	ADDR	OCTAL	SF	ENGINEERING VALUE	VALUE IN AGC UNITS
*	RANGEVAR+ 0	1770	01351	-12	1.111111111-005	1.111111111-005
		1771	24734			
*	RATEVAR + 0	1772	02354	-12	1.877777000-005	1.877777000-005
		1773	04750			
*	RVARMIN + 0	1774	00410	12	7.104180875+002 FT2	6.600000000+001 M2
*	VVARMIN + 0	1775	00165	-12	1.877764172-001 FT2/SEC2	1.744500000-006 M2/CS2
*	WRENDPOS+ 0	2000	05750	14	1.000000000+004 FT	3.048000000+003 M
*	WRENDVEL+ 0	2001	00763	0	1.000000000+001 FT/SEC	3.048000000-002 M/CS
*	WSHAFT + 0	2002	17270	-5	1.500000000+001 MILLIRAD	1.500000000-002 RADIANS
*	WTRUN + 0	2003	17270	-5	1.500000000+001 MILLIRAD	1.500000000-002 RADIANS
*	RMAX + 0	2004	00023	19	2.000000000+003 FT	6.096000000+002 M
*	VMAX + 0	2005	00001	7	2.000000000+000 FT/SEC	6.096000000-003 M/CS
*	WSURFPOS+ 0	2006	00000	14	0.000000000+000 FT	0.000000000+000 M

(NASA DATA SOURCE)

Table LM7/4.5.1-1 FINAL H2 PRELAUNCH ERASABLE LOAD (LM131A REV 1) (Continued)

REV	MNEMONIC		ADDR	OCTAL	SF	ENGINEERING VALUE	VALUE IN AGC UNITS
	* WSURFVEL	+ 0	2007	00000	0	0.000000000+000 FT/SEC	0.000000000+000 M/CS
	* SHAFTVAR	+ 0	2010	00103	-12	1.000000000+000 MILIRAD2	1.000000000-006 RADIANS2
	* TRUNVAR	+ 0	2011	00103	-12	1.000000000+000 MILIRAD2	1.000000000-006 RADIANS2
1	* 504LM	+ 0	2012 2013	77772 46750	0	-3.529451787-004	-3.529451787-004
1	* 504LM	+ 2	2014 2015	77773 57473	0	-2.753883600-004	-2.753883600-004
1	* 504LM	+ 4	2016 2017	00006 06361	0	3.785528243-004	3.785528243-004
	* AGSK	+ 0	2020 2021	04225 10400	28	1.000000000+002 HR	3.600000000+007 CS
2	* RLS	+ 0	2022 2023	00311 31177	27	5.423410433+006	1.653055500+006 M

Table LM7/4.5.1-1 FINAL H2 PRELAUNCH ERASABLE LOAD (LM131A REV 1) (Continued)

REV	MNEMONIC		ADDR	OCTAL	SF	ENGINEERING VALUE	VALUE IN AGC UNITS
2 *	RLS	+ 2	2024 2025	77700 55774	27	-1.708351378+006	-5.207055000+005 M
2 *	RLS	+ 4	2026 2027	77762 55732	27	-3.645751312+005	-1.111225000+005 M
3 *	TLAND	+ 0	2400 2401	04347 20441	28	1.037433811+002 HR	3.734761720+007 CS
*	RBRFG	+ 0	2402 2403	77776 76044	24	-3.562050000+003 FT	-1.085712840+003 M
*	RBRFG	+ 2	2404 2405	00000 00000	24	0.000000000+000 FT	0.000000000+000 M
*	RBRFG	+ 4	2406 2407	77773 75347	24	-1.370571000+004 FT	-4.177500408+003 M
*	VBRFG	+ 0	2410 2411	77766 74245	10	-1.869030500+002 FT/SEC	-5.696804964-001 M/CS

Table LM7/4.5.1-1 FINAL H2 PRELAUNCH ERASABLE LOAD (LM131A REV 1) (Continued)

REV	MNEMONIC		ADDR	OCTAL	SF	ENGINEERING VALUE	VALUE IN AGC UNITS
*	VBRFG	+ 2	2412 2413	00000 00000	10	0.000000000+000 FT/SEC	0.000000000+000 M/CS
*	VBRFG	+ 4	2414 2415	77773 45722	10	-9.873819000+001 FT/SEC	-3.009540031-001 M/CS
*	ABRFG	+ 0	2416 2417	77774 54701	-4	-4.502495000-001 FT/SEC2	-1.372360476-005 M/CS2
*	ABRFG	+ 2	2420 2421	00000 00000	-4	0.000000000+000 FT/SEC2	0.000000000+000 M/CS2
*	ABRFG	+ 4	2422 2423	77663 77104	-4	-9.515097500+000 FT/SEC2	-2.900201718-004 M/CS2
*	VBRFG*	+ 0	2424 2425	77765 45231	13	-1.777287420+003 FT	-5.417172056+000
*	ABRFG*	+ 0	2426 2427	77067 72634	-4	-5.709058500+001 FT/SEC2	-1.740121031-003 M/CS2

(NASA DATA SOURCE)

Table LM7/4.5.1-1 FINAL H2 PRELAUNCH ERASABLE LOAD (LM131A REV 1) (Continued)

REV	MNEMONIC	ADDR	OCTAL	SF	ENGINEERING VALUE	VALUE IN AGC UNITS
*	JBRFG* + 0	2430 2431	77545 63177	-21	-1.474273600-002 FT/SEC3	-4.493585933-009 M/CS3
1 *	GAINBRAK+ 0	2432 2433	37777 37777	0	9.999999963-001	9.999999963-001
*	TCGFBRAK+ 0	2434	00567	17	3.000000000+001 SEC	3.000000000+003 CS
*	TCGIBRAK+ 0	2435	25762	17	9.000000000+002 SEC	9.000000000+004 CS
*	RAPFG + 0	2436 2437	00000 00624	24	8.292750000+001 FT	2.527630200+001 M
*	RAPFG + 2	2440 2441	00000 00000	24	0.000000000+000 FT	0.000000000+000 M
*	RAPFG + 4	2442 2443	77777 77635	24	-2.016050000+001 FT	-6.144920400+000 M
*	VAPFG + 0	2444 2445	77777 77400	10	-3.190000000-001 FT/SEC	-9.723120000-004 M/CS

Contract No. NAS 9-1100
Primary No. 664

(NASA DATA SOURCE)

Table LM7/4.5.1-1 FINAL H2 PRELAUNCH ERASABLE LOAD (LM131A REV 1) (Continued)

REV	MNEMONIC		ADDR	OCTAL	SF	ENGINEERING VALUE		VALUE IN AGC UNITS	
*	VAPFG	+ 2	2446	00000	10	0.000000000+000	FT/SEC	0.000000000+000	M/CS
			2447	00000					
*	VAPFG	+ 4	2450	00000	10	3.123300000-001	FT/SEC	9.519818400-004	M/CS
			2451	00372					
*	AAPFG	+ 0	2452	00002	-4	2.998200000-001	FT/SEC2	9.138513600-006	M/CS2
			2453	14522					
*	AAPFG	+ 2	2454	00000	-4	0.000000000+000	FT/SEC2	0.000000000+000	M/CS2
			2455	00000					
*	AAPFG	+ 4	2456	77774	-4	-4.016500000-001	FT/SEC2	-1.224229200-005	M/CS2
			2457	71233					
*	VAPFG*	+ 0	2460	00000	13	5.621940000+000	FT/SEC	1.713567312-002	M/CS2
			2461	01062					
*	AAPFG*	+ 0	2462	77754	-4	-2.409900000+000	FT/SEC2	-7.345375200-005	M/CS2
			2463	67646					

(NASA DATA SOURCE)

Table LM7/4.5.1-1 FINAL F2 PRELAUNCH ERASABLE LOAD (LM131A REV 1) (Continued)

REV	MNEMONIC	ADDR	OCTAL	SF	ENGINEERING VALUE	VALUE IN AGC UNITS
	* JAPFG* + 0	2464 2465	00612 30722	-21	3.769542000-002 FT/SEC3	1.148956402-008 M/CS3
	* GAINAPPR+ 0	2466 2467	00000 00000	0	0.000000000+000	0.000000000+000
	* TCGFAPPR+ 0	2470	00113	17	6.000000000+000 SEC	6.000000000+002 CS
	* TCGIAPPR+ 0	2471	04704	17	2.000000000+002 SEC	2.000000000+004 CS
2	* VIGN + 0	2472 2473	00416 15755	10	5.545364400+003 FT/SEC	1.690227069+001 M/CS
2	* RIGNX + 0	2474 2475	77730 51505	24	-1.333715400+005 FT	-4.065164539+004 M
2	* RIGNZ + 0	2476 2477	77121 73554	24	-1.445069500+006 FT	-4.404571836+005 M
	* KIGNX/B4+ 0	2500 2501	77255 41625	4	-3.310000000-001	-3.310000000-001

(NASA DATA SOURCE)

Table LM7/4.5.1-1 FINAL F2 PRELAUNCH ERASABLE LOAD (LM131A REV 1) (Continued)

REV	MNEMONIC	ADDR	OCTAL	SF	ENGINEERING VALUE	VALUE IN AGC UNITS
	* KIGNY/B8+ 0	2502 2503	73754 52751	-16	-5.869400000-007 FT/FT2	-1.925656168-006 M-1
	* KIGNV/P4+ 0	2504 2505	72516 57777	18	-4.380000000+002 SEC	-4.380000000+004 CS
	* LOWCRIT + 0	2506	04114	14	5.985000000+003 LBF	2.124374401+003 DPSTROTP
	* HIGHCRIT+ 0	2507	04454	14	6.615000000+003 LBF	2.347992759+003 DPSTROTP
1	* TAUHZ + 0	2510	07640	11	5.000000000+000 SEC	5.000000000+002 CS
1	* QHZ + 0	2511	14632	0	4.000244141-001	4.000244141-001
1	* AHZLIM + 0	2512	00017	-4	1.877311646+000 FT/SEC2	5.722045898-005 M/CS2
1	* TOOFEW + 0	2513	00003	14		3.000000000+000
1	* HLROFF + 0	2514 2515	00000 00364	24	5.003280840+001 FT	1.525000000+001 M
1	* 2LATE466+ 0	2516 2517	00000 00226	28	1.500000000+000 SEC	1.500000000+002 CS

(NASA DATA SOURCE)

Table LM7/4.5.1-1 FINAL H2 PRELAUNCH ERASABLE LOAD (LM131A REV 1) (Continued)

REV	MNEMONIC	ADDR OCTAL	SF	ENGINEERING VALUE	VALUE IN AGC UNITS
4	* DELQFIX + 0	2520 00000 2521 01717	24	2.000000000+002 FT	6.096000000+001 M
	* LRALPHA + 0	2522 01042	-1	6.000000000+000 DEG	1.666666668-002 REV
	* LRBETA1 + 0	2523 04211	-1	2.400000000+001 DEG	6.666666672-002 REV
	* LRALPHA2+ 0	2524 01042	-1	6.000000000+000 DEG	1.666666668-002 REV
	* LRBETA2 + 0	2525 00000	-1	0.000000000+000 DEG	0.000000000+000 REV
	* LRVMAX + 0	2526 01414	7	2.000000000+003 FT/SEC	6.096000000+000 M/CS
	* LRVF + 0	2527 00116	7	2.000000000+002 FT/SEC	6.096000000-001 M/CS
	* LRWVZ + 0	2530 11463	0	3.000000000-001	3.000000000-001
	* LRWVY + 0	2531 11463	0	3.000000000-001	3.000000000-001
	* LRWVX + 0	2532 11463	0	3.000000000-001	3.000000000-001
	* LRWVFZ + 0	2533 06315	0	2.000000000-001	2.000000000-001
	* LRWVFY + 0	2534 06315	0	2.000000000-001	2.000000000-001

(NASA DATA SOURCE)

Table LM7/4.5.1-1 FINAL H2 PRELAUNCH ERASABLE LOAD (LM131A REV 1) (Continued)

REV	MNEMONIC	ADDR	OCTAL	SF	ENGINEERING VALUE	VALUE IN AGC UNITS
	* LRWVFX + 0	2535	06315	0	2.000000000-001	2.000000000-001
	* LPWVFF + 0	2536	03146	0	1.000000000-001	1.000000000-001
	* RODSCALE+ 0	2537	14370	-7	1.000000000+000 FT/SEC	3.048000000-003 M/CS
	* TAURCD + 0	2540 2541	11300 00000	9	1.500000000+000 SEC	1.500000000+002 CS
	* LAG/TAU + 0	2542 2543	15164 01420	0	4.133330000-001	4.133330000-001
	* MINFORCE+ 0	2544 2545	00001 27631	12	9.800000000+002 LBF	4.359257183-001 KG M/CS2
	* MAXFORCE+ 0	2546 2547	00013 06551	12	6.300000000+003 LBF	2.802379617+000 KG M/CS2
1	* J1PARM + 0	2550 2551	07015 12075	23	6.042735900+006 FT	1.841825902+006 M

(NASA DATA SOURCE)

Table LM7/4.5.1-1 FINAL H2 PRELAUNCH ERASABLE LOAD (LM131A REV 1) (Continued)

REV		MNEMONIC		ADDR	OCTAL	SF	ENGINEERING VALUE	VALUE IN AGC UNITS
1	*	K1PARM	+ 0	2552	75534	23	-3.174389100+005 FT/RAD	-6.079319804+005 M/REV
				2553	64200			
1	*	J2PARM	+ 0	2554	07017	23	6.046910400+006 FT	1.843098290+006 M
				2555	31511			
1	*	K2PARM	+ 0	2556	73337	23	-6.245998500+005 FT/RAD	-1.196180467+006 M/REV
				2557	66560			
1	*	THETCRIT	+ 0	2560	76361	0	-1.718327700+001 DEG	-4.773132504-002 REV
				2561	77023			
1	*	RAMIN	+ 0	2562	03326	24	5.880484940+006 FT	1.792371810+006 M
				2563	13475			
	*	YLIM	+ 0	2564	00016	24	8.200000000+000 N.MI.	1.518640000+004 M
				2565	32446			
	*	ABTRDOT	+ 0	2566	00007	7	1.950000000+001 FT/SEC	5.943600000-002 M
				2567	23346			

(NASA DATA SOURCE)

Table LM7/4.5.1-1 FINAL H2 PRELAUNCH ERASABLE LOAD (LM131A REV 1) (Continued)

REV	MNEMONIC	ADDR	OCTAL	SF	ENGINEERING VALUE	VALUE IN AGC UNITS
*	COSTHET1+ 0	2570 2571	00000 00000	2	0.000000000+000	0.000000000+000
*	COSTHET2+ 0	2572 2573	06733 07535	2	8.660254037-001	8.660254037-001
*	DLAND + 0	2634 2635	00000 00000	24	0.000000000+000 FT	0.000000000+000 M
*	DLAND + 2	2636 2637	00000 00000	24	0.000000000+000 FT	0.000000000+000 M
*	DLAND + 4	2640 2641	00000 00000	24	0.000000000+000 FT	0.000000000+000 M
*	HIASCENT+ 0	3000	02324	16	1.090000000+004 LBS	4.944156833+003 KG
1**	ROLLTIME+ 0	3001	05454	14	2.860000000+001 SEC	2.860000000+003 CS
1**	PITTIME + 0	3002	04513	14	2.379000000+001 SEC	2.379000000+003 CS

(NASA DATA SOURCE)

Table LM7/4.5.1-1 FINAL H2 PRELAUNCH ERASABLE LOAD (LM131A REV 1) (Continued)

REV		MNEMONIC		ADDR	OCTAL	SF	ENGINEERING VALUE	VALUE IN AGC UNITS
	*	DKTRAP	+ 0	3003	77001	-3	-3.888888889-003	-3.888888889-003 REV/SEC
	*	DKCMEGAN	+ 0	3004	00012	14	1.000000000+001	1.000000000+001
	*	DKKACSN	+ 0	3005	00074	14	6.000000000+001	6.000000000+001
	*	LMTRAP	+ 0	3006	77001	-3	-3.888888889-003	-3.888888889-003 REV/SEC
	*	LMCMEGAN	+ 0	3007	00000	14	0.000000000+000	0.000000000+000
	*	LMKACSN	+ 0	3010	00074	14	6.000000000+001	6.000000000+001
	*	DKDB	+ 0	3011	00200	15	2.560000000+002	2.560000000+002 REV-1
2	*	IGNACSQ	+ 0	3012	02555	-2	7.630000000+000 DEG/SEC2	2.119444446-002 REV/SEC2
1	*	IGNACSP	+ 0	3013	00150	-2	5.700000000-001 DEG/SEC2	1.583333335-003 REV/SEC2
	*	DOWNTORK	+ 0	3113	00000	5		0.000000000+000 JET SEC
	*	DOWNTORK	+ 1	3114	00000	5		0.000000000+000 JET SEC
	*	DOWNTORK	+ 2	3115	00000	5		0.000000000+000 JET SEC
	*	DOWNTORK	+ 3	3116	00000	5		0.000000000+000 JET SEC

(NASA DATA SOURCE)

Table LM7/4.5.1-1 FINAL H2 PRELAUNCH ERASABLE LOAD (LM131A REV 1) (Continued)

REV	MNEMONIC	ADDR	OCTAL	SF	ENGINEERING VALUE	VALUE IN AGC UNITS
	* DOWNTORK+ 4	3117	00000	5		0.000000000+000 JET SEC
	* DOWNTORK+ 5	3120	00000	5		0.000000000+000 JET SEC
1	* VELBIAS + 0	3371 3372	00001 36331	6	2.500000000+000 FT/SEC	7.620000000-003 M/CS
1	* AZBIAS + 0	3373	77201	-1	-4.200000000+000 DEG	-1.166666667-002 REV
	* ATIGINC + 0	3400 3401	00001 03120	28	3.000000000+000 MIN	1.800000000+004 CS
	* PTIGINC + 0	3402 3403	00001 03120	28	3.000000000+000 MIN	1.800000000+004 CS
	* AOTAZ + 0	3404	65244	-1	-6.007800000+001 DEG	-1.668833335-001 REV
	* AOTAZ + 1	3405	77770	-1	-7.400000000-002 DEG	-2.055555557-004 REV
	* AOTAZ + 2	3406	12514	-1	5.990100000+001 DEG	1.663916668-001 REV
	* AOTAZ + 3	3407	25247	-1	1.199570000+002 DEG	3.332138892-001 REV

(NASA DATA SOURCE)

Table LM7/4.5.1-1 FINAL H2 PRELAUNCH ERASABLE LOAD (LM131A REV 1) (Continued)

REV	MNEMONIC	ADDR	OCTAL	SF	ENGINEERING VALUE	VALUE IN AGC UNITS
*	AOTAZ + 4	3410	37775	-1	1.799640000+002 DEG	4.999000004-001 REV
*	AOTAZ + 5	3411	52521	-1	-1.200480000+002 DEG	-3.334666669-001 REV
*	AOTEL + 0	3412	10011	-1	4.509500000+001 DEG	1.252638890-001 REV
*	AOTEL + 1	3413	10012	-1	4.511300000+001 DEG	1.253138890-001 REV
*	AOTEL + 2	3414	10014	-1	4.512800000+001 DEG	1.253555557-001 REV
*	AOTEL + 3	3415	10013	-1	4.512500000+001 DEG	1.253472223-001 REV
*	AOTEL + 4	3416	10012	-1	4.510700000+001 DEG	1.252972223-001 REV
*	AOTEL + 5	3417	10010	-1	4.509200000+001 DEG	1.252555557-001 REV
*	LRHMAX + 0	3420	35610	14	5.000000000+004 FT	1.524000000+004 M
*	LRWH + 0	3421	13146	0	3.500000000-001	3.500000000-001
*	ZOOMTIME+ 0	3422	05050	14	2.600000000+001 SEC	2.600000000+003 CS
*	TENDBRAK+ 0	3423	01407	17	6.200000000+001 SEC	6.200000000+003 CS
*	TENDAPPR+ 0	3424	00226	17	1.200000000+001 SEC	1.200000000+003 CS

(NASA DATA SOURCE)

Table LM7/4.5.1-1 FINAL H2 PRELAUNCH ERASABLE LOAD (LM131A REV 1) (Continued)

REV	MNEMONIC	ADDP OCTAL		SF	ENGINEERING VALUE	VALUE IN AGC UNITS
*	DELTTFAP+ 0	3425	75632	17	-9.000000000+001 SEC	-9.000000000+003 CS
*	LEADTIME+ 0	3426	77743	17	2.200000000+000 SEC	-2.200000000+002 CS
*	RPCRTIME+ 0	3427	01407	17	6.200000000+001 SEC	6.200000000+003 CS
*	RPCRTQSW+ 0	3430	57777	1	-1.000000000+000	-1.000000000+000
*	INEWA + 0	3431	20000	28		1.342177280+008
		3432	00000			

A LARGE NUMBER TO PREVENT RECYCLING THE LAMBERT SOLUTICN

Table LM7/4.5.1-2

Measured Hardware Alignments Contributing to Alignment of LM IMU from CSM IMU

Measurement	Alignment Arc Min About X-Axis	Y-Axis (About Z-Axis)	Z-Axis (About Y-Axis)
COMMAND MODULE			
Displacement of CSM IMU axes with respect to local vertical.*	-	+3.30	-4.80
Displacement of CSM Nav. base axes with respect to docking ring.*	+62.8	-	-
Displacement of docking ring axes with respect to local vertical.*	-	-0-	-3.0
LUNAR MODULE			
	(LM Yaw)	(LM Roll)	(LM Pitch)
Displacement of docking ring with respect to nav. base axes.**	-	-3.28	-0.75
Displacement of nav. base with respect to IMU.***	-1.63	+4.43	+1.22

*OCP K0070V2 and K3128-1, 7/10/69. In lieu of S/C axes the local vertical was used as the common reference axis.

**Spacecraft Operational Data Book, Volume II, LM Data Book, Rev 2, Para. LM7/4.5.1.5.2

***Spacecraft Operational Data Book, Volume II, LM Data Book, Rev 2, Para. LM7/4.5.2.1.2. Data stated as IMU relative to nav. base, therefore, values tabulated above are negative of SODB values because the desired sense of displacement is from nav. base to IMU.

Table LM7/4.5.1-3

Hardware Contributions to Uncertainty of LM IMU Alignment from CSM IMU

Source of Uncertainty	1-σ Uncertainty, Arc Min		
	About LM X-Axis	About LM Y-Axis	About LM Z-Axis
CM IMU to CM Docking Ring	0.2 (1)	0.2 (1)	0.2 (1)
CM Docking Angle Scale	0.2 (1)	-	-
CM-LM Docking Ring Alignment	-	4.0 (2)	4.0 (2)
LM Docking Angle Pointer	5.0 (3)	-	-
Docking Angle Determination	15.0 (4)	-	-
LM Docking Ring to LM Nav Base	-	Negl. (5)	Negl. (5)
LM Nav Base to LM IMU	Negl. (5)	Negl. (5)	Negl. (5)
RSS 1-σ Uncertainty, Arc Min	15.8	4.0	4.0
Arc Deg	0.264	0.067	0.067

REFERENCES

(1) Estimates based on methods used in OCP K0070V2 and K3128-1, 7/10/69, to measure these alignments. See Table LM7/4.5.1-2.

(2) Apollo ICD MH 01-05053-416 (The included angle measured between the planes of the docking interfaces of the CM and LM will not exceed 0.2 deg.)

(3) Apollo ICD MH 01-05128-116 (60 deg. ±5 arc min.)

(4) Telecon R. Schweickart, NASA astronaut (±0.5 deg., considered to be 2-σ)

(5) Uncertainty in measured alignment considered negligible. See Table LM7/4.5.1-2.

LM7/4.5.1.5.2 **Assembly Alignment Data of Spacecraft Docking Mating Surfaces to the Navigation Base.**

Angular Alignment of the Docking Ring Seal Surface Relative to the Navigation Base Axes

About Z	About Y
$-0^{\circ}\ 3'\ 17''$	$-0^{\circ}\ 0'\ 45''$

Sign Convention for Docking Ring Surface Plane Tilt

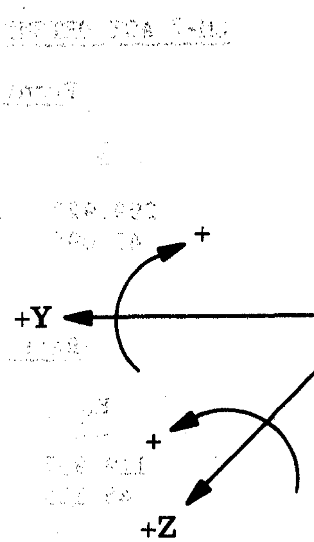

(Right Hand Rule)

Note: All data shown is for an unpressurized LM at ambient conditions. (REF: LAV-566-109 Dated August 8, 1968)

LM7/4.5.1.5.3 AOT Alignment Data

The azimuth and elevation angles for the rear right, rear left and the close (rear) detent positions of the AOT (relative to the AOT mounting surface) are tabulated below for LM-7 (AOT Designation 614, Serial No. 20). These rear detent angles have been calculated using measured azimuth and elevation angles of the front detent positions. The uncertainty associated with these calculated angles is ±2 arc minutes.

The front 3 detent angles are measured, relative to the AOT mounting surface, at Kollsman Instrument Corporation and have a measurement uncertainty of ±30 arc seconds. For information, these measured angles are included in the tabulation. To verify these measured values, an AOT functional test has been performed on the spacecraft.

LM-7 AOT DETENT DATA

	Front (Measured)		
Data	L	F	R
Azim. (Deg)	299.922	359.926	59.901
Elev. (Deg)	45.095	45.113	45.128

	Rear (Calculated)		
Data	R_R	C_L	L_R
Azim. (Deg)	119.957	179.964	239.952
Elev. (Deg)	45.125	45.107	45.092

The above data is for an unpressurized vehicle at ambient conditions.

LM7/4.5.2.1 Abort Sensor Assembly

The LM-7 ASA set-point temperature, as read by T/M No. GI-3301, is set T_{SET} = 120.3°F (STANDBY and OPERATE modes). The nominal temperature reading in the OFF mode is 119.6°F. The temperature maintenance limits are specified in paragraph 4.5.2.1.

(Note: This unit can be expected to show temperature fluctuations within a band of 119.6°F to 123.2°F during ECS glycol flow in the OFF mode).

LM7/4.5.2.1.2 AGS Angular Mounting Error

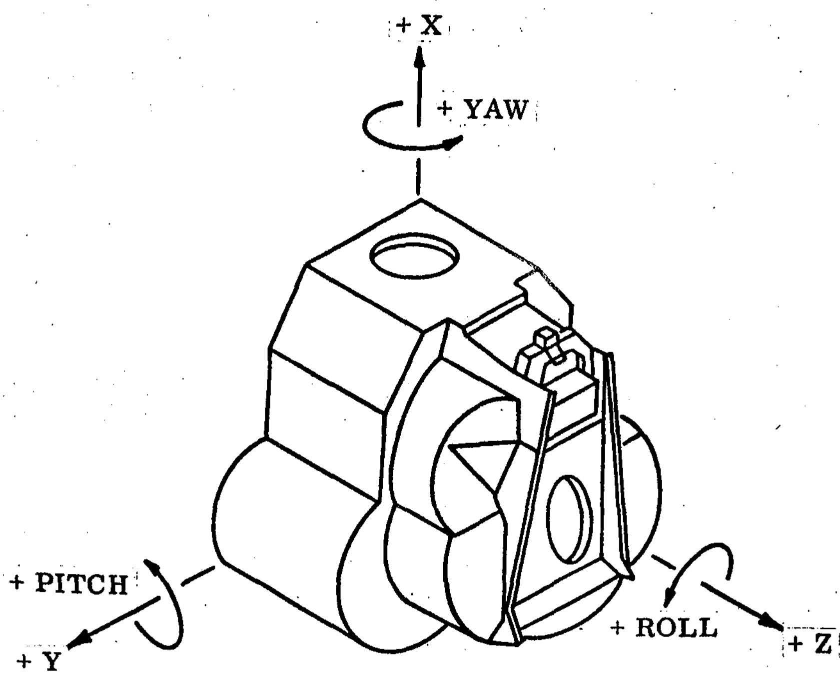

The measured mechanical alignment error of the ASA mounting surface as compared to the NAV. Base Gage (Vehicle Coordinate System) and the IMU is shown below:

	ASA/NAV. Base	IMU/NAV. Base	ASA/IMU
Pitch:	-00° 01' 49"	-00° 01' 13"	-00° 00' 36"
Roll:	-00° 04' 26"	-00° 04' 26"	00° 00' 00"
Yaw:	+00° 01' 38"	+00° 01' 38"	00° 00' 00"

(Ref.: LDW 280-51067, dated 12 November 1968)

LM7/4.5.2.2 Abort Electronics Assembly (NASA DATA SOURCE)

The following listings pertain to the Abort Electronics Assembly Memory Constants.

Table LM7/4.5.2-1 contains a glossary of the constants. The glossary is divided into six groups:

Group 1 - PARAMETERS TO BE SPECIFIED DURING THE MISSION
Group 2 - AGS HARDWARE DEPENDENT CONSTANTS
Group 3 - VEHICLE DEPENDENT CONSTANTS
Group 4 - MISSION DEPENDENT CONSTANTS
Group 5 - EQUATION DEPENDENT CONSTANTS
Group 6 - DEDA CONVERSION FACTORS

Table LM7/4.5.2-2 contains the current values in both octal and decimal, with units.

The CONVERSION FACTOR's are multipliers used to convert the constant from the given engineering units to the equivalent value in the units internally used in the AEA. The number in the SCALE column defines the binary scaling of each constant, i.e., the number of bits in the computer word (excluding the sign bit) to the left of the binary point. A computer word consists of a sign bit and 17 data bits. The actual computer value of a constant is listed in the AEA OCT. column in octal digits. Since the computer word has a finite number of bits, a given input value cannot, in general, be represented exactly in the computer. The AEA VALUE column contains the result of reconverting the AEA octal value to the decimal value in engineering units, using the conversion factor mentioned above.

An asterisk by the name of the constants indicates that these constants are dependent on the hardware to be used during a mission.

Table LM7/4.5.2-1. Glossary of AGS Constants

(NASA DATA SOURCE)

GROUP 1 - PARAMETERS TO BE SPECIFIED DURING THE MISSION

NAME	DESCRIPTION OF LMDAP INPUT	INTERNAL AEA UNITS	LMDAP INPUT UNITS
1J	Desired TPI time for CSI computation	SEC	MIN
4J	Time increment from node to TPF (in TPI mode)	SEC	MIN
17J	Radar range rate	FPS	FPS
18J	Radar range	FT	FT
25J	DEDA altitude update	FT	FT
28J1	Component of External V input in $\underline{V}_1$ Direction	FPS	FPS
28J2	Component of External V input in $\underline{W}_1$ Direction	FPS	FPS
28J3	Component of External V input in $\underline{U}_1$ Direction	FPS	FPS
1J1	LM Update State Vector - X Inertial Position	FT	FT
1J2	Y Inertial Position	FT	FT
1J3	Z Inertial Position	FT	FT
1J4	X Inertial Velocity	FPS	FPS
1J5	Y Inertial Velocity	FPS	FPS
1J6	Z Inertial Velocity	FPS	FPS
1J7	LM Update State Vector Epoch Time	SEC	MIN
2J1	CSM Update State Vector - X Inertial Position	FT	FT
2J2	Y Inertial Position	FT	FT
2J3	Z Inertial Position	FT	FT
2J4	X Inertial Velocity	FPS	FPS
2J5	Y Inertial Velocity	FPS	FPS
2J6	Z Inertial Velocity	FPS	FPS
2J7	CSM Update State Vector Epoch Time	SEC	MIN

Table LM7/4.5.2-1. Glossary of AGS Constants (Continued)

(NASA DATA SOURCE)

GROUP 2 - AGS HARDWARE DEPENDENT CONSTANTS

NAME	DESCRIPTION OF LMDAP INPUT	INTERNAL AEA UNITS	LMDAP INPUT UNITS
1K1P*	X axis gyro drift bias	RAD/20MS (Compen.)	DEG/HR (Bias)
1K6P*	Y axis gyro drift bias	RAD/20MS (Compen.)	DEG/HR (Bias)
1K11P*	Z axis gyro drift bias	RAD/20MS (Compen.)	DEG/HR (Bias)
	A positive gyro drift bias causes a gyro output of more than 32 pulses per millisecond (640 pulses per 20 milliseconds) for no ASA rotation. The range of each of the biases is ± 10 deg/hr.		
1K3*	X axis gyro scale factor deviation	NO-UNITS(Deviation)	NO-UNITS (Deviation)
1K8*	Y axis gyro scale factor deviation	NO-UNITS(Deviation)	NO-UNITS (Deviation)
1K13*	Z axis gyro scale factor deviation	NO-UNITS(Deviation)	NO-UNITS (Deviation)
	A positive scale factor deviation exists when a gyro's scale factor is greater than 2^{-16} radians per pulse. The range of each deviation is ± .78 percent.		
1K14*	Compensation constant for X gyro spin axis mass unbalance drift	RAD/FPS	DEG/HR/G
	A positive gyro spin axis mass unbalance exists when a positive ASA acceleration in the direction of the X gyro input axis results in a negative X gyro output (less than 640 pulses per 20 milliseconds) with no rotation. The range of the bias is ± 10 deg/hr/g.		

*These constants are dependent on the hardware to be used during a mission.

Table LM7/4.5.2-1. Glossary of AGS Constants (Continued)

(NASA DATA SOURCE)

GROUP 2 - (CONTINUED)

NAME	DESCRIPTION OF LMDAP INPUT	INTERNAL AEA UNITS	LMDAP INPUT UNITS
1K18P*	X axis accelerometer scale factor deviation	FPS/PULSE (Scale Factors)	NO-UNITS (Deviation)
1K20P*	Y axis accelerometer scale factor deviation	FPS/PULSE	NO-UNITS (Deviation)
1K22P*	Z axis accelerometer scale factor deviation	FPS/PULSE	NO-UNITS (Deviation)
	A positive accelerometer scale factor deviation exists when the measured accelerometer's scale factor is greater than the nominal value of + .003125 fps/pulse. The range of this input is ± 24 percent.		
1K19P*	X axis accelerometer bias	FPS/20MS(Compen.)	MICRO G (Bias)
1K21P*	Y axis accelerometer bias	FPS/20MS(Compen.)	MICRO G (Bias)
1K23P*	Z axis accelerometer bias	FPS/20MS(Compen.)	MICRO G (Bias)
	A positive accelerometer bias results in an accelerometer output of more than 32 pulses per millisecond (640 pulses per 20 milliseconds). The range of each of these biases is ± 2000 μg.		
1K26	X axis azimuth alignment gain constant (lunar align)	NO-UNITS	NO-UNITS
1K27	Lunar align leveling alignment constant	RAD/FPS	RAD/FPS
1K28	Lunar align leveling alignment constant	NO-UNITS	NO-UNITS
1K29	Lunar align stop error criterion	RAD	RAD
1K30	Gyro calibrate time	2-SEC	2-SEC
1K33	Gyro calibration gain constant	NO-UNITS	NO-UNITS
1K34	Gyro calibration gain constant	1/20MS	1/20MS
1K35	Navigation sensed velocity threshold	FT/SEC	FT/SEC
1K36	Accelerometer calibration gain constant	NO-UNITS	NO-UNITS

*These constants are dependent on the hardware to be used during a mission.

Table LM7/4.5.2-1. Glossary of AGS Constants (Continued)
(NASA DATA SOURCE)

GROUP 2 - (CONTINUED)

NAME	DESCRIPTION OF LMDAP INPUT	INTERNAL AEA UNITS	LMDAP INPUT UNITS
1K37	Accelerometer calibration time	2-SEC	2-SEC
6K2	Radar filter initialization value of P_{11} and P_{22}	FT^2	FT^2
6K4	Radar filter initialization value of P_{33} and P_{44}	$(FPS)^2$	$(FPS)^2$
6K5	Radar filter factor in r_y update	NO-UNITS	NO-UNITS
6K6	Radar filter factor in V_y update	NO-UNITS	NO-UNITS
6K8	Radar filter term in q_{11}	$(FT/SEC)^2$	$(FT/SEC)^2$
6K9	Radar filter factor in q_{11} and q_{22}	$(RAD)^2$	$(RAD)^2$
6K10	Radar filter factor in q_{11} and q_{22}	FT^2	FT^2

Table LM7/4.5.2-1. Glossary of AGS Constants (Continued)
(NASA DATA SOURCE)

GROUP 3 - VEHICLE DEPENDENT CONSTANTS

NAME	DESCRIPTION OF LMDAP INPUT	INTERNAL AEA UNITS	LMDAP INPUT UNITS
1K9	Ullage counter limit	COUNTS	COUNTS
4K2	Coefficient in T_B computation	SEC/FT	SEC/FT
4K3	Coefficient in T_B computation	$(SEC/FT)^2$	$(SEC/FT)^2$
4K7	Cant angle of engine about Y-axis	RAD	RAD
4K8	Cant angle of engine about Z-axis	RAD	RAD
4K21	Limit on body attitude errors	RAD	RAD
4K23	Time to maintain attitude hold momentarily after staging	40-MSEC	40-MSEC
4K25	Ascent engine cutoff impulse compensation	FPS	FPS
4K26	V_G threshold for engine cutoff	FPS	FPS
4K27	Hover Abort overflow protection	FPS	FPS
4K34	Lower limit on a_T	FT/SEC^2	FT/SEC^2
4K35	Ullage threshold	FT/SEC^2	FT/SEC^2

Table LM7/4.5.2-1. Glossary of AGS Constants (Continued)
(NASA DATA SOURCE)

GROUP 4 - MISSION DEPENDENT CONSTANTS

NAME	DESCRIPTION OF LMDAP INPUT	INTERNAL AEA UNITS	LMDAP INPUT UNITS
1K4	Altitude/Altitude rate interpolation factor	NO-UNITS	NO-UNITS
2K1	Lunar gravitational constant	FT^3/SEC^2	FT^3/SEC^2
2K2	Reciprocal of 2K1	SEC^2/FT^3	SEC^2/FT^3
2K4	-2K1 ΔT (ΔT = 2 sec)	FT^3/SEC	FT^3/SEC
3K4	Sine of central angle limit in TPI	NO-UNITS	NO-UNITS
4K4	Coefficient in linear expression for $\dot{r}_f$	1/SEC	1/SEC
4K5	Quantity in linear expression for $\dot{r}_f$	FT	FT
4K6	Upper limit on $\dot{r}_f$	FPS	FPS
4K10	Factor in LM desired semi-major axis α_L (O.I.)	FT/RAD	FT/RAD
4K12	Acceleration check for lower limit of $\ddot{r}_d$	FT/SEC^2	FT/SEC^2
5K14	Upper limit on $\dddot{r}_d$	FT/SEC^3	FT/SEC^3
5K16	Upper limit on $\dddot{y}_d$	FT/SEC^3	FT/SEC^3
5K17	Lower limit on $\dddot{y}_d$	FT/SEC^3	FT/SEC^3
5K18	Lower limit on $\dddot{r}_d$	FT/SEC^3	FT/SEC^3
5K20	Lower limit on $\dddot{r}_d$	FT/SEC^3	FT/SEC^3
5K26	Velocity-to-be-gained threshold	FPS	FPS
K55	Scale factor for $\dot{r}$ display	NO-UNITS	NO-UNITS
WBX	X component of unit vector for guidance steering	NO-UNITS	NO-UNITS
WBY	Y component of unit vector for guidance steering	NO-UNITS	NO-UNITS
WBZ	Z component of unit vector for guidance steering	NO-UNITS	NO-UNITS
2J	Cotangent of desired LOS angle at TPI for CSI computation	NO-UNITS	NO-UNITS

Table LM7/4.5.2-1. Glossary of AGS Constants (Continued)
(NASA DATA SOURCE)

GROUP 4 - (CONTINUED)

NAME	DESCRIPTION OF LMDAP INPUT	INTERNAL AEA UNITS	LMDAP INPUT UNITS
3J	Rendezvous offset time for TPI computation	SEC	MIN
5J	Landing site radius	FT	FT
6J	Desired LM transfer time for TPI routine	SEC	MIN
7J	Term in LM desired semi-major axis α_L (O.I.)	FT	FT
8J	One-half lower limit of apolune radius	FT	FT
10J	Alternate value for 7J (late descent abort)	FT	FT
11J	Alternate value for 4K10 (late descent abort)	FT/RAD	FT/RAD
12J	Threshold value for THETAF (CSM/LM phase angle)	RAD	RAD
16J	Orbit insertion targeted injection altitude	FT	FT
21J	Vertical pitch steering altitude threshold	FT	FT
22J	Vertical pitch steering altitude rate threshold	FPS	FPS
23J	Orbit insertion targeted injection radial rate	FPS	FPS
29J	Radar filter update time initialization value	SEC	MIN
6J1, 6J2, 6J3	Inertial negative lunar rotation rate vector at predicted landing site	RAD/20 MS	RAD/20 MS

Table LM7/4.5.2-1. Glossary of AGS Constants (Continued)
(NASA DATA SOURCE)

GROUP 5 - EQUATION DEPENDENT CONSTANTS

NAME	DESCRIPTION OF LMDAP INPUT	INTERNAL AEA UNITS	LMDAP INPUT UNITS
1K24	FDAI computation singularity region	NO-UNITS	NO-UNITS
2K3	q value set if overflow occurs in e^2 computation of LM orbit parameters	FT	FT
2K11	Set value of V_T if no valid TPI solution	FPS	FPS
2K14	Initial p perturbation	FT	FT
2K17	Number of p-iteration minus 3	COUNTS	COUNTS
2K18	Partial derivative protector in p-iterator routine	SEC	SEC
2K19	Δp limiter	FT	FT
2K20	p-iterator convergence check	SEC	SEC

Table LM7/4.5.2-1. Glossary of AGS Constants (Continued)
(NASA DATA SOURCE)

GROUP 6 - DEDA CONVERSION FACTORS

NAME	DESCRIPTION OF LMDAP INPUT
BACCSF	Convert .001 ft/sec^2 to fps/20 msec at B1
BM13SF	Convert .01°/hr to rad/20 msec at B13
B23SF	Convert 100 ft to ft at B23
B18SF	Convert .1 min to sec at B18
B13VSF	Convert .1 fps to fps at B13
B3SF	Convert .01° to rad at B3
B23RSF	Convert .1 nmi to ft at B23
B13SF	Convert .01 min to sec at B13

Table LM7/4.5.2-2. Constants
(NASA DATA SOURCE)

NAME	LOC.	SCALE	CONVERSION FACTOR	AEA OCT.	AEA VALUE	UNITS
1J	0275	18	.60000 02	000000	.00000000 00	MIN
4J	0306	13	.60000 02	000000	.00000000 00	MIN
17J	0503	13	.10000 01	000000	.00000000 00	FPS
18J	0316	23	.10000 01	000000	.00000000 00	FT
25J	0223	23	.10000 01	000000	.00000000 00	FT
28J1	0450	13	.10000 01	000000	.00000000 00	FPS
28J2	0451	13	.10000 01	000000	.00000000 00	FPS
28J3	0452	13	.10000 01	000000	.00000000 00	FPS
1J1	0240	23	.10000 01	000000	.00000000 00	FT
1J2	0241	23	.10000 01	000000	.00000000 00	FT
1J3	0242	23	.10000 01	000000	.00000000 00	FT
1J4	0260	13	.10000 01	000000	.00000000 00	FPS
1J5	0261	13	.10000 01	000000	.00000000 00	FPS
1J6	0262	13	.10000 01	000000	.00000000 00	FPS
1J7	0254	18	.60000 02	000000	.00000000 00	MIN
2J1	0244	23	.10000 01	000000	.00000000 00	FT
2J2	0245	23	.10000 01	000000	.00000000 00	FT

Table LM7/4.5.2-2. AGS Constants (Continued)

(NASA DATA SOURCE)

	NAME	LOC.	SCALE	CONVERSION FACTOR	AEA OCT.	AEA VALUE	UNITS
	2J3	0246	23	.10000 01	000000	.00000000 00	FT
	2J4	0264	13	.10000 01	000000	.00000000 00	FPS
	2J5	0265	13	.10000 01	000000	.00000000 00	FPS
	2J6	0266	13	.10000 01	000000	.00000000 00	FPS
	2J7	0272	18	.60000 02	000000	.00000000 00	MIN
*	1K1P	0544	-13	-.96963-07	777772	.57629721-01	DEG/HR
*	1K6P	0545	-13	-.96963-07	000037	-.29775356 00	DEG/HR
*	1K11P	0546	-13	-.96963-07	000061	-.47064272 00	DEG/HR
*	1K3	0550	-7	.10000 01	035332	.89800358-03	NO-UNITS
*	1K8	0551	-7	.10000 01	034404	.86998940-03	NO-UNITS
*	1K13	0552	-7	.10000 01	061157	.15019774 -02	NO-UNITS
*	1K14	0537	-14	.15091-06	000440	.88867836 00	DEG/HR/G
*	1K18P	0534	-8	.31250-02	314665	.26130676-03	NO-UNITS
*	1K20P	0535	-8	.31250-02	314427	-.12454987-02	NO-UNITS
*	1K22P	0536	-8	.31250-02	314503	-.82588196 -03	NO-UNITS
*	1K19P	0540	1	-.64254-06	777775	.71243251 02	MICRO-G
*	1K21P	0541	1	-.64254-06	000001	-.23747750 02	MICRO-G

Table LM7/4.5.2-2. AGS Constants (Continued)
(NASA DATA SOURCE)

	NAME	LOC.	SCALE	CONVERSION FACTOR	AEA OCT.	AEA VALUE	UNITS
*	1K23P	0542	1	-.64254-06	777776	.47425501 02	MICRO-G
	1K26	0626	8	.10000 01	561111	-.14285742 03	NO-UNITS
	1K27	0627	-4	.10000 01	262132	.43499947-01	RAD/FPS
*	1K28	0630	7	.10000 01	327443	.10778418 03	NO-UNITS
	1K29	0631	-4	.10000 01	004061	.99992752-03	RAD
	1K30	0617	17	.10000 01	000226	.15000000 03	2-SEC
	1K33	0632	-3	.10000 01	243656	.79999924-01	NO-UNITS
	1K34	0633	-15	.10000 01	247613	.19999919-04	1/20MS
	1K35	0634	7	.10000 01	000400	.25000000 00	FT/SEC
	1K36	0635	0	.10000 01	777651	-.66375733-03	NO-UNITS
	1K37	0621	17	.10000 01	000017	.15000000 02	2-SEC
	6K2	0457	30	.10000 01	027657	.99999744 08	FT2
	6K4	0456	10	.10000 01	031000	.10000000 03	FT2/SEC2
	6K5	0656	0	.10000 01	505075	-.73000336 00	NO-UNITS
	6K6	0522	8	.10000 01	777605	-.24023437 00	NO-UNITS
	6K8	0304	10	.10000 01	000034	.21875000 00	FT2/SEC2
	6K9	0611	-15	.10000 01	376057	.30290103-04	NO-UNITS

Contract No. NAS 9-1100
Primary No. 664

Table LM7/4.5.2-2. AGS Constants (Continued)

(NASA DATA SOURCE)

	NAME	LOC.	SCALE	CONVERSION FACTOR	AEA OCT.	AEA VALUE	UNITS
	6K10	0517	28	.10000 01	005754	.62504960 07	FT2
*	1K9	0616	17	.10000 01	000005	.50000000 01	COUNTS
*	4K2	0654	-12	.10000 01	713267	-.50203875-04	SEC/FT
*	4K3	0655	-25	.10000 01	016336	.16802915-08	SEC2/FT2
*	4K7	0566	0	.10000 01	006547	.26176453-01	RAD
*	4K8	0602	0	.10000 01	000000	.00000000 00	RAD
	4K21	0666	2	.10000 01	020603	.26181030 00	RAD
*	4K23	0622	17	.10000 01	000076	.62000000 02	40MSEC
*	4K25	0657	13	.10000 01	000066	.33750000 01	FPS
*	4K26	0454	13	.10000 01	002140	.70000000 02	FPS
*	4K27	0473	13	.10000 01	406000	-.80000000 04	FPS
	4K34	0660	7	.10000 01	002000	.10000000 01	FT/SEC2
	4K35	0661	7	.10000 01	000146	.99609375-01	FT/SEC2
	1K4	0624	0	.10000 01	031463	.99998474-01	NO-UNITS
	2K1	0636	48	.10000 01	235407	.17318811 15	FT3/SEC2
	2K2	0637	-47	.10000 01	320020	.57740271-14	SEC2/FT3
	2K4	0674	49	.10000 01	542371	-.34637623 15	FT3/SEC

Contract No. NAS 9-1100
Primary No. 664

Table LM7/4.5.2-2. AGS Constants (Continued)
(NASA DATA SOURCE)

	NAME	LOC.	SCALE	CONVERSION FACTOR	AEA OCT.	AEA VALUE	UNITS
	3K4	0613	1	.10000 01	026164	.17364502 00	NO-UNITS
	4K4	0565	-7	.10000 01	203045	.40000081-02	1/SEC
*	4K5	0227	23	.10000 01	257014	.57351680 07	FT
	4K6	0527	13	.10000 01	002400	.80000000 02	FPS
*	4K10	0662	20	.10000 01	662400	-.31744000 06	FT/RAD
	4K12	0506	7	.10000 01	012000	.50000000 01	FT/SEC2
	5K14	0560	-2	.10000 01	000000	.00000000 00	FT/SEC3
*	5K16	0561	-2	.10000 01	012173	.10000229-01	FT/SEC3
*	5K17	0601	-2	.10000 01	765605	-.10000229-01	FT/SEC3
	5K18	0564	-2	.10000 01	631463	-.10000038 00	FT/SEC3
	5K20	0523	-2	.10000 01	000000	.00000000 00	FT/SEC3
	5K26	0466	13	.10000 01	000360	.15000000 02	FPS
	K55	0607	0	.10000 01	377777	.99999237 00	NO UNITS
*	WBX	0514	1	.10000 01	700000	-.50000000 00	NO-UNITS
*	WBY	0515	1	.10000 01	621114	-.86602783 00	NO-UNITS
	WBZ	0516	1	.10000 01	000000	.00000000 00	NO-UNITS
	2J	0605	7	.10000 01	003775	.19970703 01	NO-UNITS

Table LM7/4.5.2-2. AGS Constants (Continued)
(NASA DATA SOURCE)

NAME	LOC.	SCALE	CONVERSION FACTOR	AEA OCT.	AEA VALUE	UNITS
3J	0312	13	.60000 02	000000	.00000000 00	MIN
* 5J	0231	23	.10000 01	255704	.56977920 07	FT
* 6J	0307	13	.60000 02	120500	.43000000 02	MIN
* 7J	0224	23	.10000 01	270322	.60427520 07	FT
* 8J	0225	23	.10000 01	131565	.29402240 07	FT
* 10J	0226	23	.10000 01	270423	.60469120 07	FT
* 11J	0673	20	.10000 01	547405	-.62460000 06	FT/RAD
* 12J	0305	3	.10000 01	766316	-.29992676 00	RAD
16J	0232	23	.10000 01	001652	.60032000 05	FT
21J	0233	23	.10000 01	000607	.25024000 05	FT
22J	0464	13	.10000 01	001440	.50000000 02	FPS
* 23J	0465	13	.10000 01	000470	.19500000 02	FPS
* 29J	0274	18	.60000 02	756330	-.30000000 03	MIN
* 6J1	0640	-14	.10000 01	000007	.32596290-08	RAD/20MS
6J2	0641	-14	.10000 01	777616	-.53085387-07	RAD/20MS
* 6J3	0642	-14	.10000 01	000007	.32596290-08	RAD/20MS
1K24	0625	1	.10000 01	000071	.86975098-03	NO-UNITS

Table LM7/4.5.2-2. AGS Constants (Continued)
(NASA DATA SOURCE)

NAME	LOC.	SCALE	CONVERSION FACTOR	AEA OCT.	AEA VALUE	UNITS
2K3	0216	23	.10000 01	040000	.10485760 07	FT
2K11	0526	13	.10000 01	273400	.60000000 04	FPS
2K14	0217	23	.10000 01	001415	.49984000 05	FT
2K17	0620	17	.10000 01	000005	.50000000 01	COUNTS
2K18	0447	13	.10000 01	000360	.15000000 02	SEC
2K19	0230	23	.10000 01	017205	.50003200 06	FT
2K20	0453	13	.10000 01	000040	.20000000 01	SEC
BM13SF	0676	0	.10000 01	365706	.96049499 00	
B23SF	0677	0	.10000 01	243656	.63999939 00	
B18SF	0700	0	.10000 01	125253	.33333588 00	
B13VSF	0701	0	.10000 01	240000	.62500000 00	
B3SF	0702	0	.10000 01	131415	.34970856 00	
B23RSF	0703	0	.10000 01	032756	.10533142 00	
B13SF	0704	0	.10000 01	032525	.10416412 00	
BACCSF	0446	0	.10000 01	303240	.76293945 00	

LM7/4.5.3.2.2.3 LM-7 DPS Thrust Response At TTCA Minimum and Maximum Positions

The KSC calibration data for the commander's (CMDR) and LM pilot's (LMP) TTCA's are given below.*

TTCA POSITION	THRUST OUTPUT			
	CMDR		LMP	
	TTCA	DECA	TTCA	DECA
Minimum	10.8 %	11.4 %	11.3 %	11.8 %
Maximum	111.3 %	Saturated	109.2 %	Saturated

*TCP No. 0045, Combined Systems Test

The output calibration for all TTCA's is:

$$V_{TTCA} = 0.024852\ \%F_{COMM} + 0.29160$$

where V_{TTCA} = TTCA output voltage, VRMS

$\%F_{COMM}$=Commanded thrust position, %.

The output calibration for the LM-7 DECA is:

$$V_{DECA} = TCV = 0.122176\ \%F_{STD} + 1.3806$$

where V_{DECA} = DECA output voltage to the DPS throttle actuator (TCV), VDC

$\%F_{STD}$ = Commanded thrust at standard values of propellant interface conditions, % (of 10,500 lbf)

Using the above equations and the DPS preflight performance data (Para. LM7/4.7.1) the voltages and thrust values were determined for the above TTCA and DECA calibration data for the CMDR TTCA.

THIS COLUMN NASA DATA SOURCE ↓

TTCA OPERATING POSITION	TTCA COMMANDED THRUST, %	TTCA OUTPUT, VRMS	DECA OUTPUT, VDC	PREDICTED THRUST, LBF
Minimum	10.8	0.56	2.773	1329
Maximum* (Throttle-up	111.3	3.058	>14.6	9852
Maximum** (Throttle-down	111.3	3.058	>14.6	9918

*At 26 sec burn time.
**At 390 sec burn time.

LM7/4.5.3.4.3 GDA Drive Rates

Measurement		
Time of Travel	- pitch 57.5 sec - roll 57.4 sec	These times are the average of 2 measurements made on LM-7 at KSC.
Angular Rate	- pitch .2104°/sec - roll .2108°/sec	

Note: Computed Angle of Travel = 12.1° (in either axis)

LM7/4.5.4.2 Rendezvous Radar Mechanical Alignment

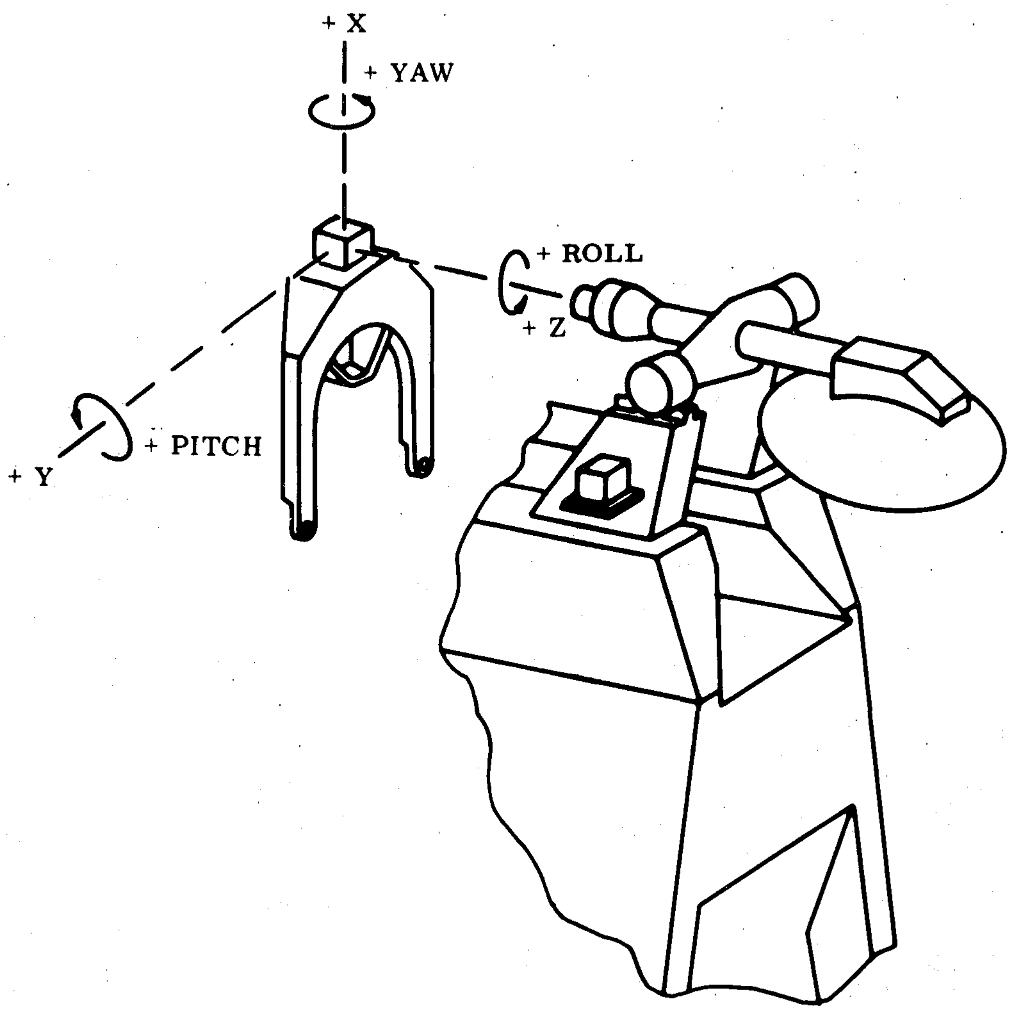

The Rendezvous Radar Antenna Assembly alignment for LM-7 with respect to the Vehicle Coordinate System (Nav. Base Gage) is shown below:

Pitch:	+00° 00' 35"
Roll:	-00° 05' 15"
Yaw:	+00° 00' 18"

(Ref.: LMO-566-215, dated Sept. 1969)

LM7/4.5.4.3 RR Timeline Operation

Figures LM7/4.5.4-10 and LM7/4.5.4-11 show the predicted RR management temperature profile for the LM-7 mission from undocking to touchdown, and from lunar ascent to the completion of the rendezvous sequence. The predicted management curves have been extrapolated from the LM-6 mission data. The RR operating time during the undocking to touchdown phase is limited to one eight-minute checkout phase. No antenna overheating problem due to operation is expected. It is felt that the temperature profile of the high power multiplier chain (HPMC) or gyro are not necessary for this phase of the mission. The RR operating times and operational trajectories for the lunar stay and the lunar ascent to docking phase are almost identical to those for LM-6 and antenna temperatures are expected to be similar to those experienced during the LM-6 mission. Predicted temperature responses of the HPMC and the gyro package for the ascent to docking phase are shown in Figure LM7/4.5.4-11.

The management curves and temperature profiles shown are based on an April 11, 1970, launch date and the following operational timeline:

H-2 MISSION RR TIMELINE (Time in Hrs:Min G.E.T.)

RR "ON"	RR "OFF"
98:49	99:01
99:51	99:59
137:30	140:46

Short ON periods for antenna reorientations, and antenna ON periods less than 30 minutes followed by an OFF period of several hours do not influence critical thermal parameters, and have not been included in this analysis.

The rendezvous radar antenna assembly (RRAA) temperature sensor (GN7723T) should be monitored continuously while the RR is on to assure that the temperature rise does not exceed predicted values. If the RRAA temperature exceeds the management curve of Figures LM7/4.5.4-10 and LM7/4.5.4-11 the RR should be turned off as soon as its use is no longer required. This procedure will assure that there is sufficient in-limit operating time to accomplish mandatory RR operation.

LM7/4.5.4.4.11 RR and T AGC Voltage Versus Range

Figure LM7/4.5.4-6 shows the expected AGC voltage levels versus range and signal level of RR No. 32 with T No. 36. The use of curves instead of nomographs permits a better visualization of the interaction of the variables and also avoids the difficulty of trying to design a nomograph to fit empirical data on non-linearly interrelated variables.

LM7/4.5.4.4.11.1 RR and T AGC Voltage Versus Range and LOS Angle

Figures LM7/4.5.4-7 and LM7/4.5.4-8 show RR AGC readings at several ranges between 0.2 n mi and 400 n mi, as a function of the angle between the LOS and the antenna boresight. The data are shown for angles out to ±10° in both the shaft and trunnion axes, except where very low signal levels would produce low AGC readings which would be of little value.

LM7/4.5.4.4.12 Rendezvous Radar Self-Test

Figure LM7/4.5.4-1 shows the effects of environment on the RR self-test parameters of range and range rate.

The following are the expected RR self-test parameters for RR 32. Radar temperature variations and meter display tolerances result in ranges rather than single values for certain of the expected readouts.

1) Test Monitor:

Self Test AGC	+1.61 VDC (Nominal @ approximately 90°F)
XMTR PWR	+2.37 VDC (Nominal @ approximately 90°F)
SHAFT ERR	+2.04 to + 2.83 VDC (@ 1/2 cps)
TRUN ERR	+2.10 to +2.70 VDC (@ 1/2 cps)

2) Range/Range Rate Meter:

Range R .	193 to 197 n mi
Range Rate R	-467 to -507 ft/sec

3) LGC DSKY Display: V16N78

R_1 Range R .	195 to 196 n mi
R_2 Range Rate R	-469 to -509 ft/sec
R_3 No Display	0

LM7/4.5.4.4.13 RR Power Monitor Calibration

Figure LM7/4.5.4-9 shows the power monitor calibration for RR No. 32, giving power in dBm versus dc volts.

LM7/4.5.4.4.16 Allowable Vehicle Accelerations During RR Power Off Periods

Figures LM7/4.5.4-2 through LM7/4.5.4-5 show the maximum allowable LM body accelerations for any angular position of the RR antenna trunnion and shaft axes under which the antenna will not move from a fixed position with no power applied to the RR. The effect of varying the antenna temperature is also indicated in the figures.

The antenna shaft axis will always be parallel to the LM Y-axis. Therefore, LM body accelerations about the LM Y-axis can be used directly. However, as the shaft axis rotates, the trunnion axis will be parallel to the LM X-axis at 0° shaft position and parallel to the LM Z-axis at -90° shaft position. For other shaft positions, the allowable LM acceleration about the LM axes must be converted to the acceleration about the trunnion axis at the appropriate shaft position.

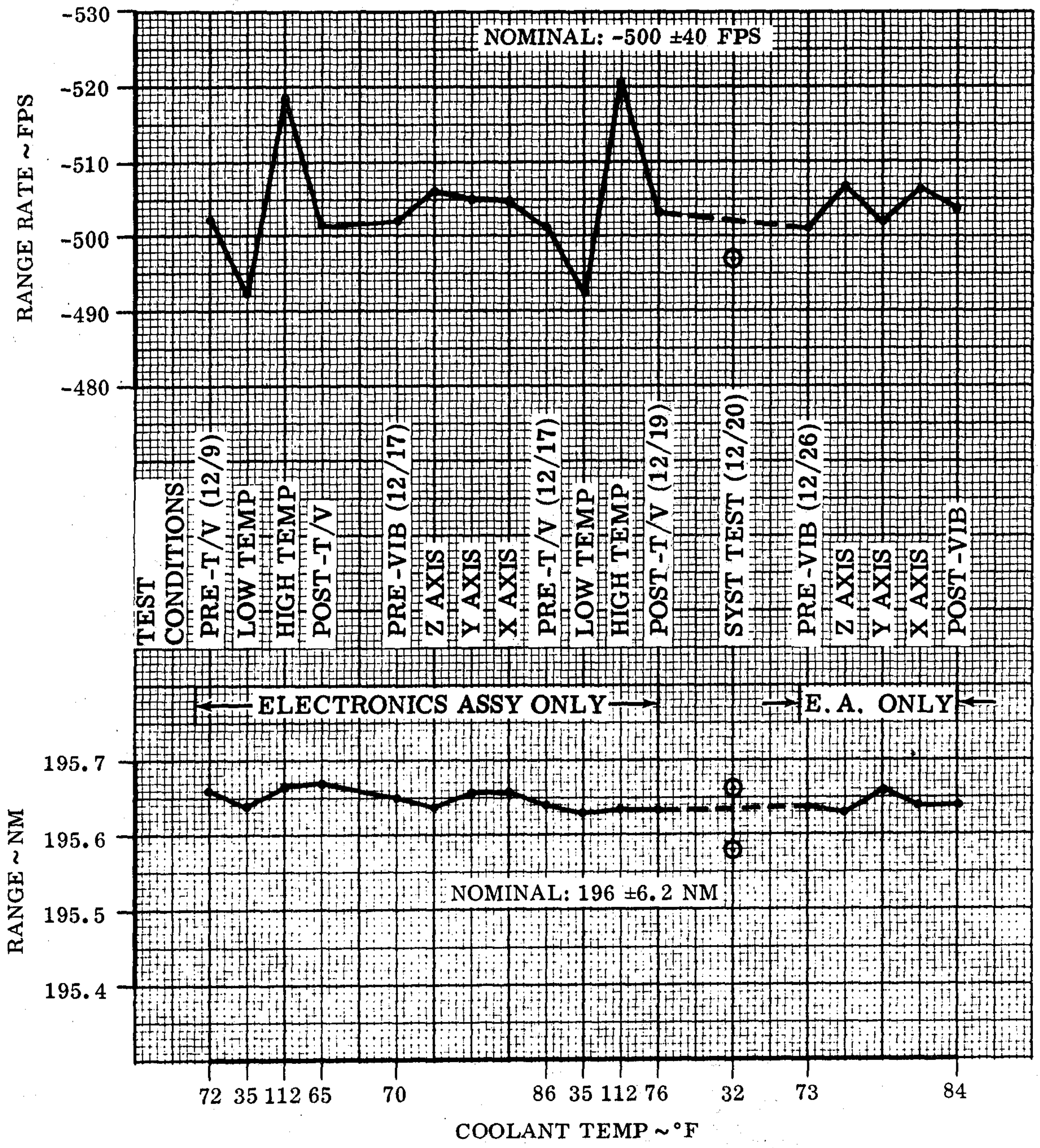

Figure LM7/4.5.4-1. Environmental Effects on RR Self Test Parameters
(See Para. 4.5.4.4.12)

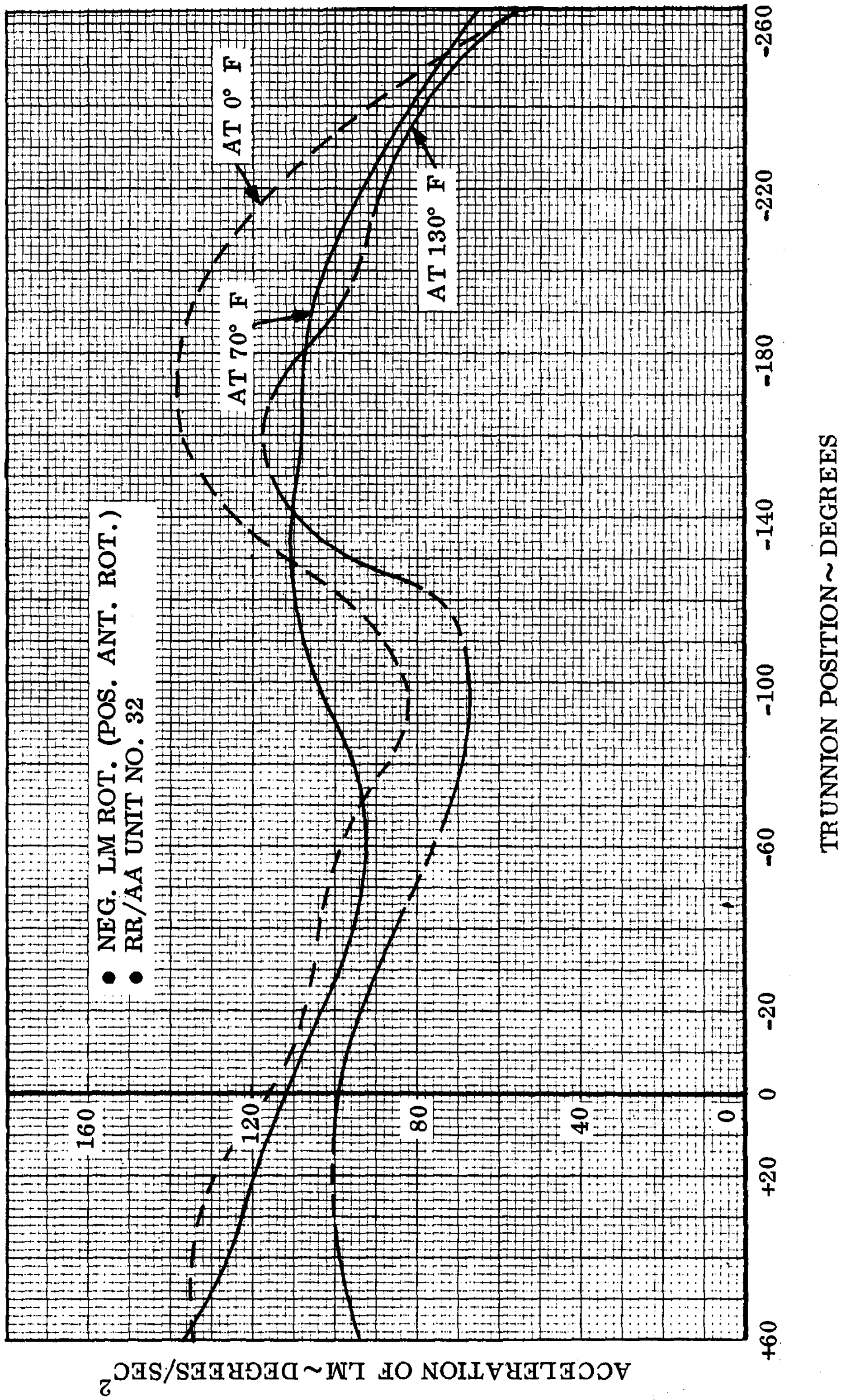

Figure LM7/4.5.4-2. Allowable Acceleration Trunnion Axis

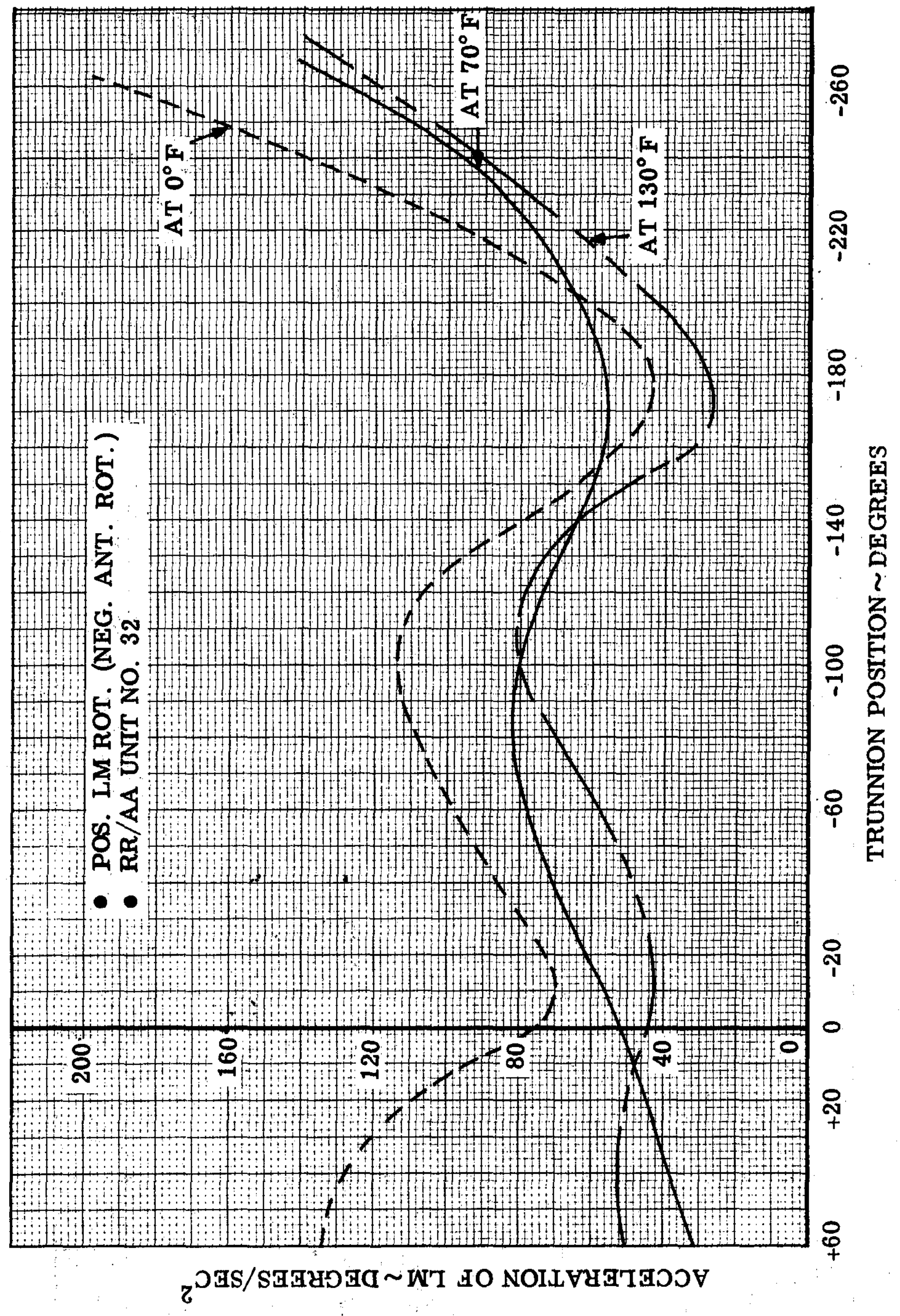

Figure LM7/4.5.4-3. Allowable Acceleration Trunnion Axis

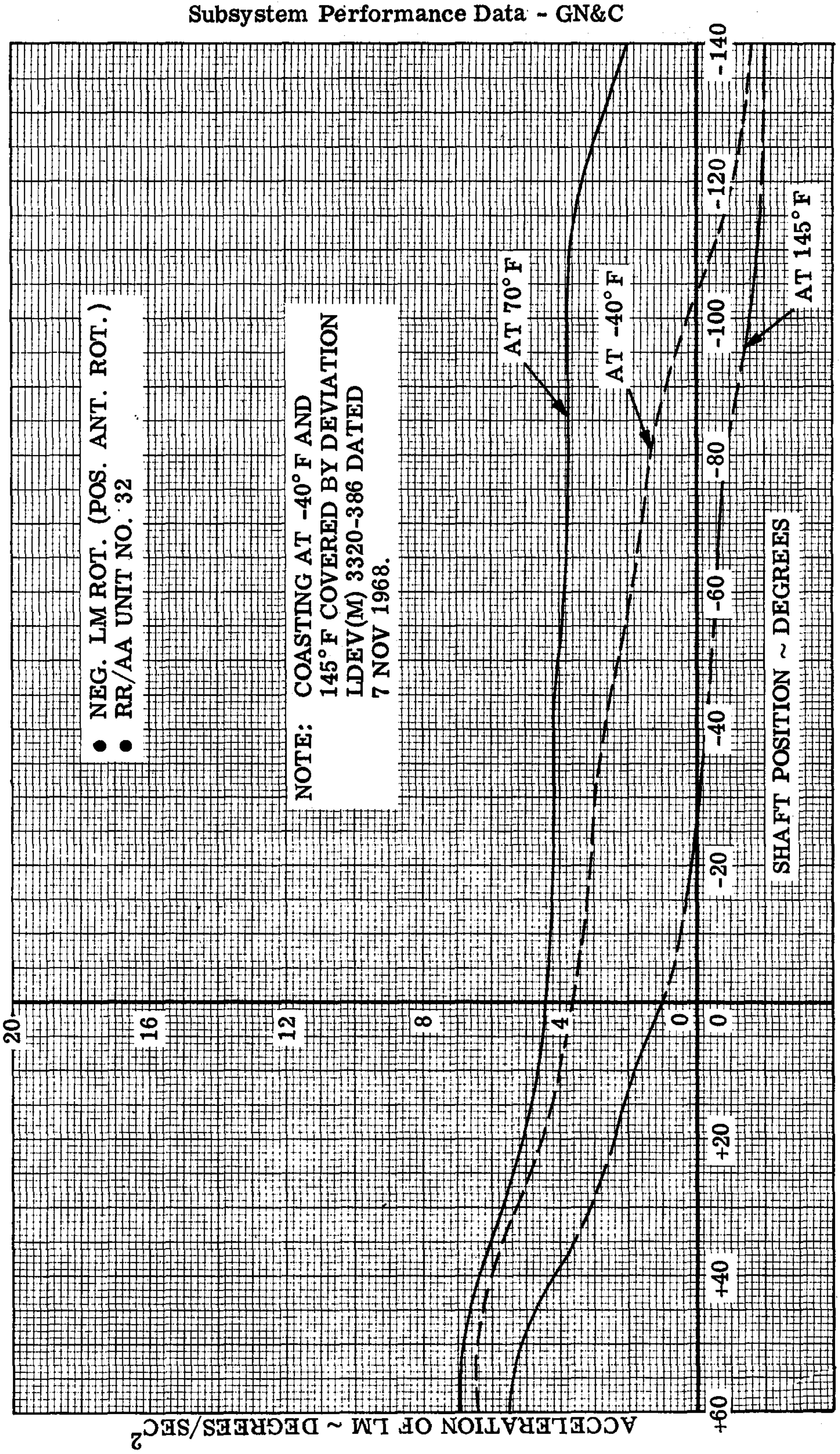

Figure LM7/4.5.4-4. Allowable Acceleration Shaft Axis

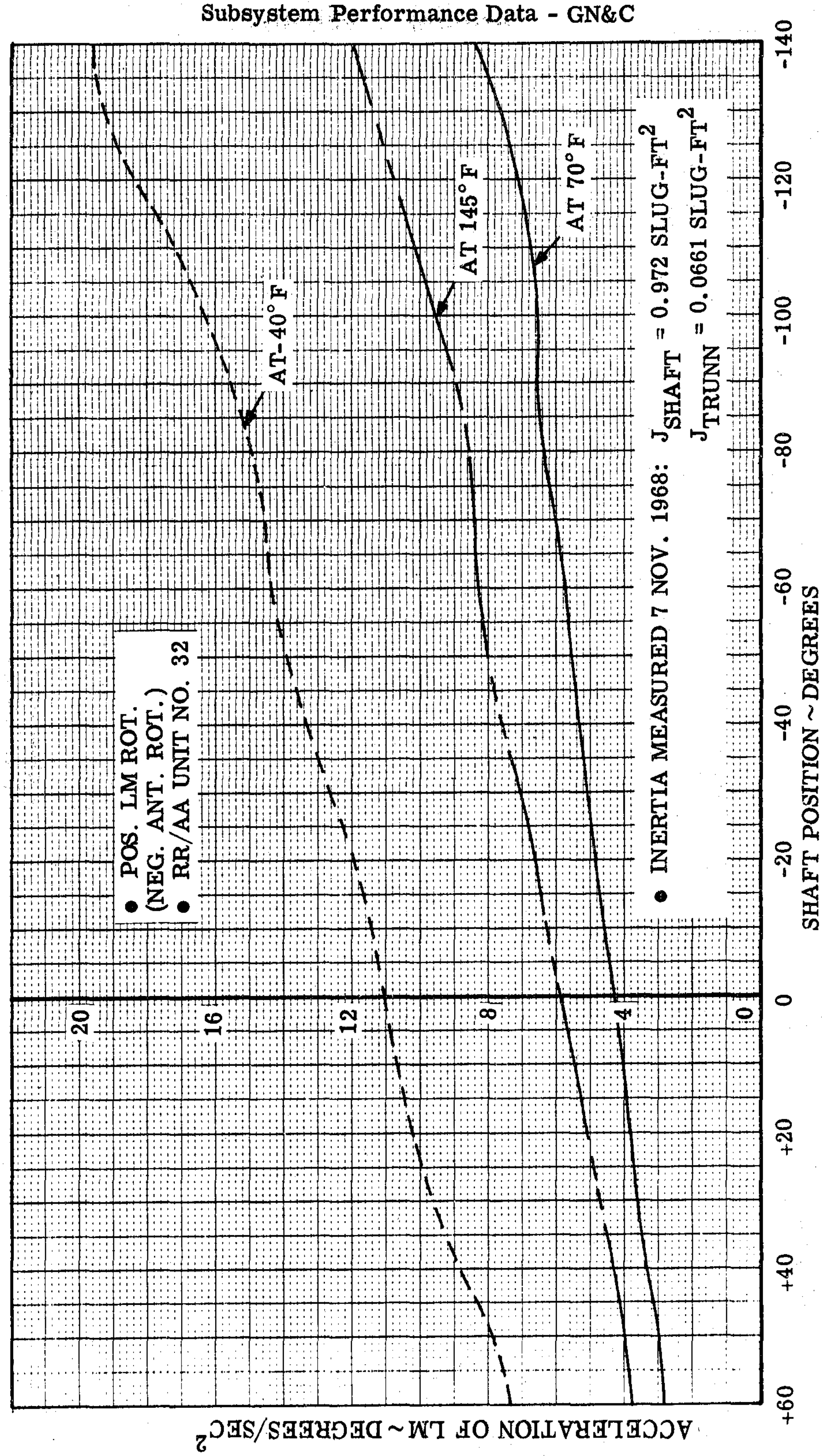

Figure LM7/4.5.4-5. Allowable Acceleration Shaft Axis

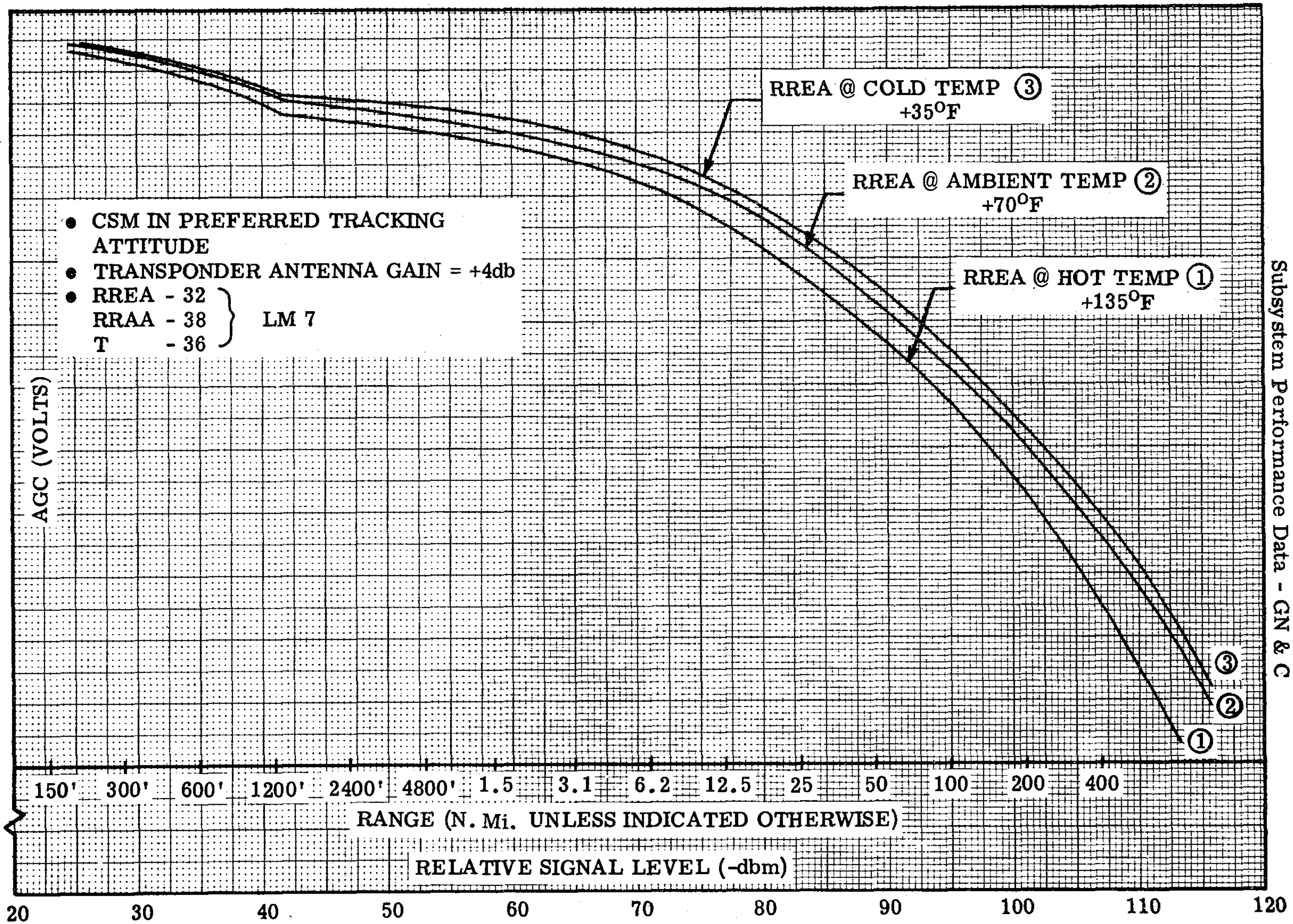

Figure LM7/4.5.4-6. LM7 RR AGC versus Signal Level and Range with T 36 (See Para. 4.5.4.4.11)

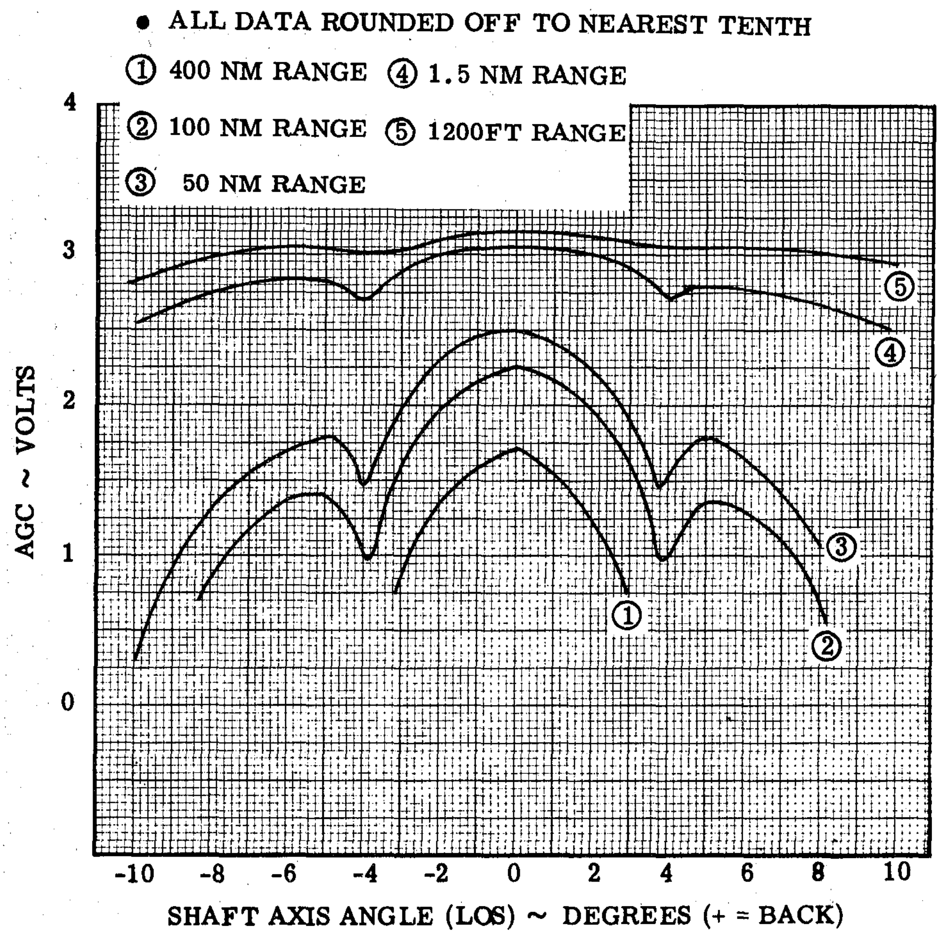

Figure LM7/4.5.4-7. AGC Versus Shaft Axis Angles
(See Para. 4.5.4.4.11.1)

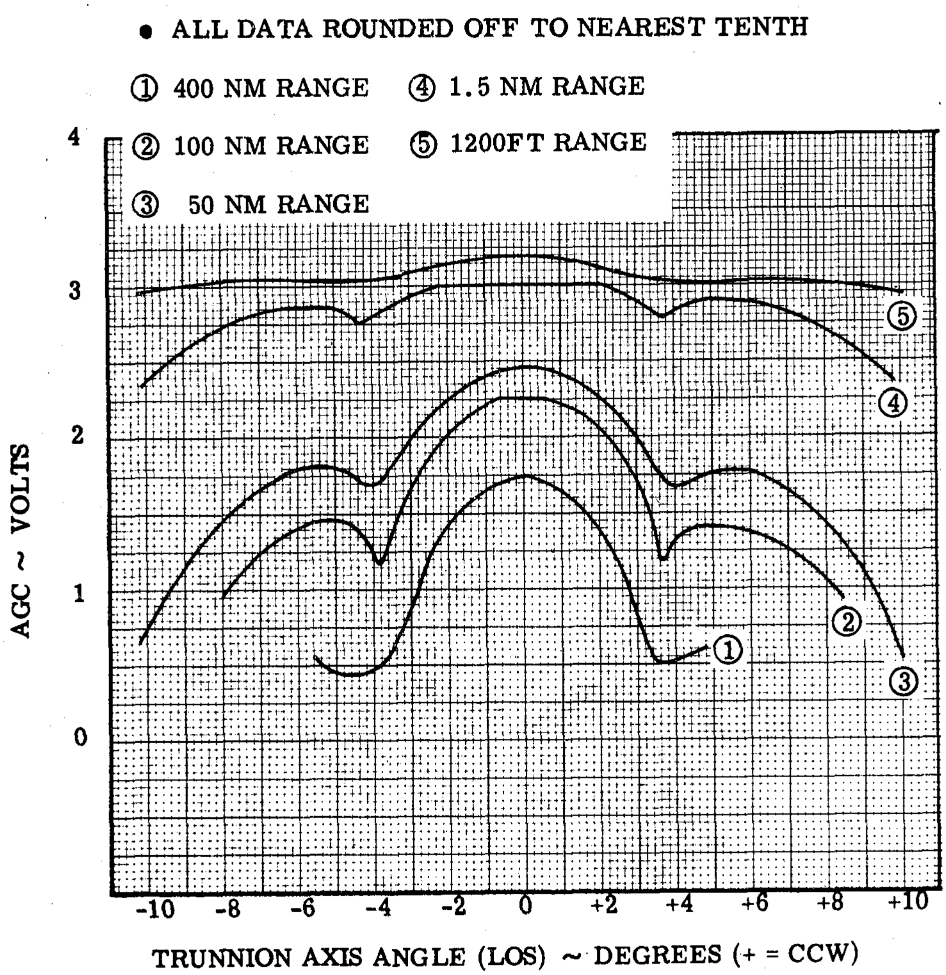

Figure LM7/4.5.4-8. AGC Versus Trunnion Axis Angle
(See Para. 4.5.4.4.11.1)

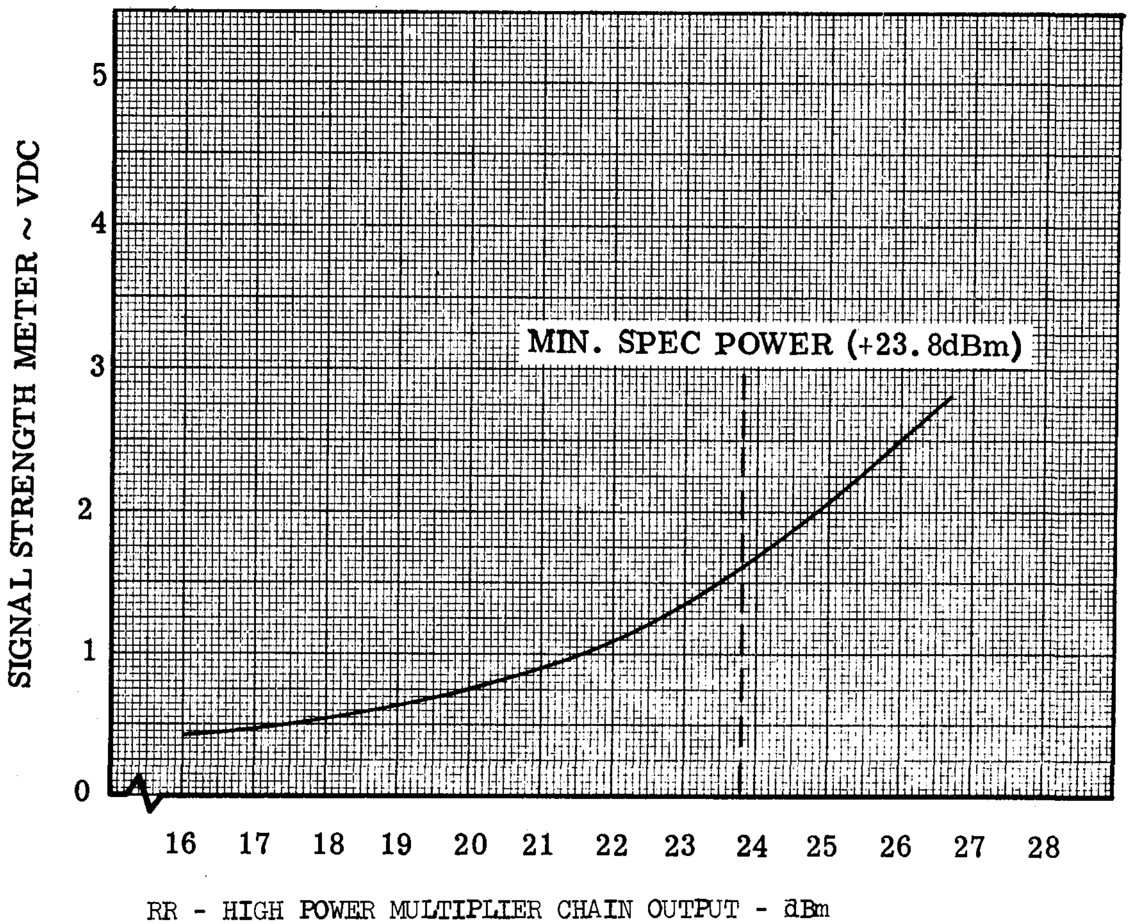

Figure LM7/4.5.4-9. Power Monitor Meter Voltage Vs. RF Power (See Para. LM7/4.5.4.4.13)

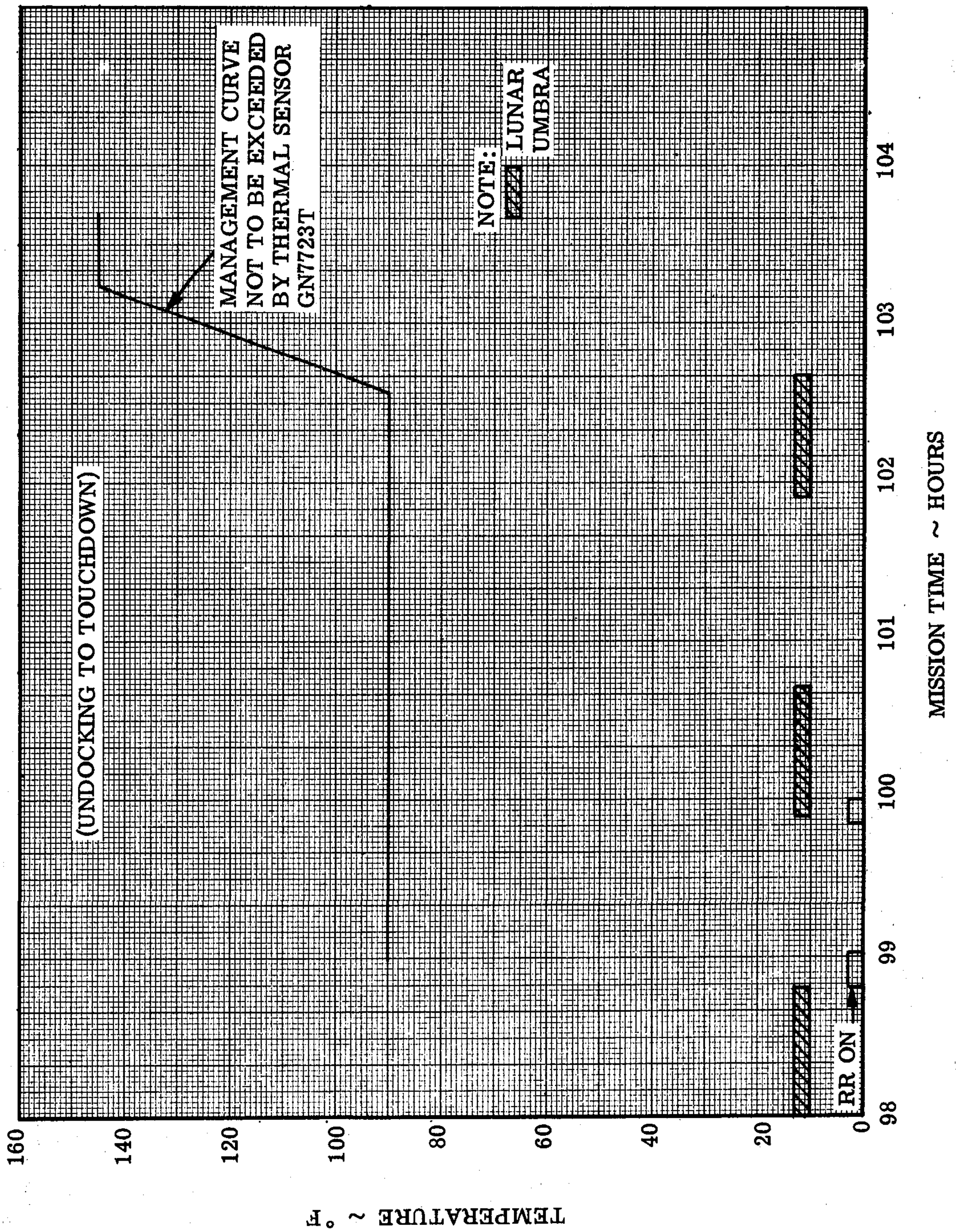

Figure LM7/4.5.4-10. Predicted RR Temperature Management Curve For Final Flight Plan Timeline

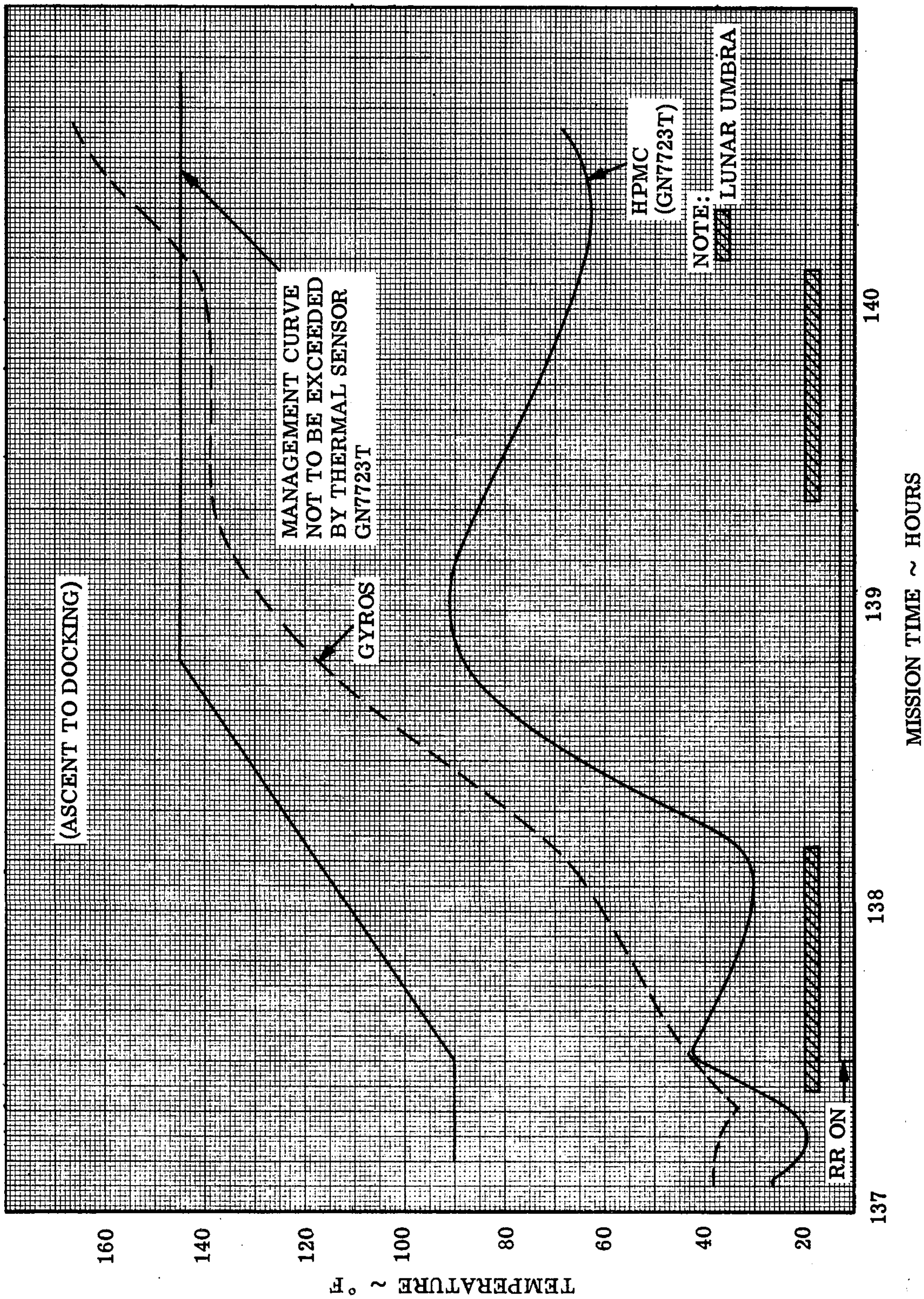

Figure LM7/4.5.4-11. Predicted RR Temperature Management Curve For Final Flight Plan Timeline

LM7/4.5.5.1.16 LR Power Monitor

The following is a calibration of the RF Power Monitor Meter with LR P-42.

Transmitter	Power (dBm)	Power (MW)	Monitor (Vdc)	Calibration
Velocity	23.5	224	3.40	15.2×10^{-3} V/MW
Altimeter	21.4	138	3.90	28.3×10^{-3} V/MW

Note: The power in milliwatts is at the output of the antenna assembly, and includes all losses.

LM7/4.5.5.1.17 Loss of LR Lock as a Function of Vehicle Pitch and Roll for an Apollo 13 Type Trajectory

Figures LM7/4.5.5-1 through LM7/4.5.5-4 describe the LR loss of lock as a function of vehicle pitch and roll for the nominal descent trajectory for antenna positions 1 and 2, respectively.

LM7/4.5.5.1.18 Expected Altitude of LR Velocity and Range Initial "Data Good" Indication

Figures LM7/4.5.5-5 and LM7/4.5.5-6 describe the signal-to-noise (S/N) ratio as a function of altitude of LR beams 1, 2, and 3 (i.e., the velocity beams). The minimum S/N threshold required for lock-on and the range sweep limit are also indicated. Figure LM7/4.5.5-6 includes the same data for beam 4 (range beam). The effect of minimum transmitter power on acquisition altitude is also indicated for each beam.

Note: The band on range acquisition altitude is due to variations in the following items:

a) Radar temperature
b) Signal-to-noise (S/N) uncertainties

LM7/4.5.5.1.21 LR Predicted Accuracy

Figure LM7/4.5.5-7 shows the predicted LR accuracy as a function of time from ignition and of altitude, for an Apollo 13 type descent trajectory.

LM7/4.5.5.2 Landing Radar Antenna Assembly Temperature Profile

Figure LM7/4.5.5-8 presents the landing radar antenna assembly typical high temperature and low temperature profiles for the LM-7 Mission H-2.

LM7/4.5.5.3.1 **Landing Radar Mechanical Alignment**

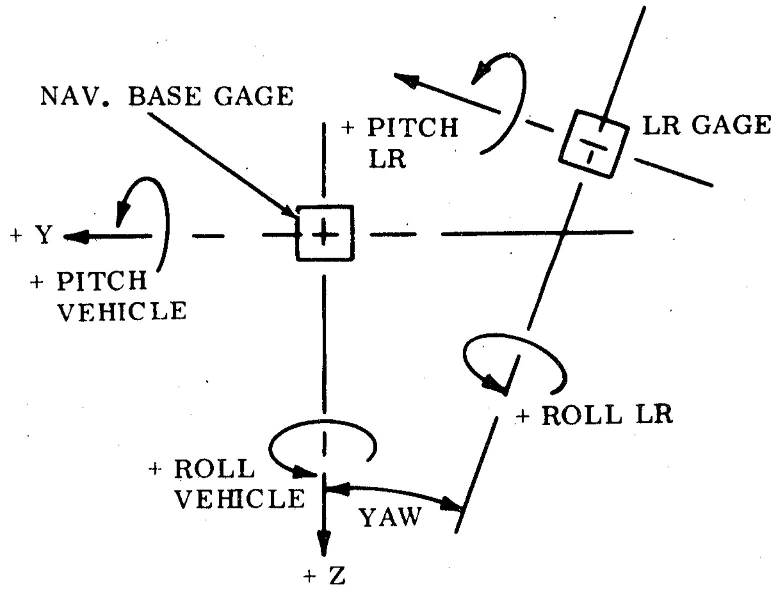

The Landing Radar Antenna Assembly alignment for LM-7 with respect to the Vehicle Coordinate System (Nav. Base Gage) is shown below:

	Position #1	Position #2
Pitch:	-24° 00' 40"	+00° 03' 34"
Roll:	-00° 00' 33"	-00° 00' 34"
Yaw:	-06° 07' 56"	-06° 08' 03"

(Ref.: LMO-566-215, dated Sept. 1969)

LM7/4.5.5.4 Landing Radar Self-Test

The following are the expected LR self-test parameters for P-42. Radar temperature variations and meter display tolerances results in ranges rather than single values for the expected readouts.

1) Test Monitor

ALT XMTR	3.9 Vdc (Nominal Ambient Temp)
VEL XMTR	3.4 Vdc (Nominal Ambient Temp)

2) ALT/ALT Rate Meter:

ALT H	7900 to 8100 ft
ALT Rate $\dot{H}$	-478 to -482 ft/sec

3) LGC DSKY Display:

V16N66

R1 Slant Range	08276 to 08296 ft
R2 Antenna Position	+00001
R3 No Display	0

V16N67

R1 V_{xA}	-00493 to -00497 ft/sec
R2 V_{yA}	01860 to 01864 ft/sec
R3 V_{zA}	01329 to 01333 ft/sec

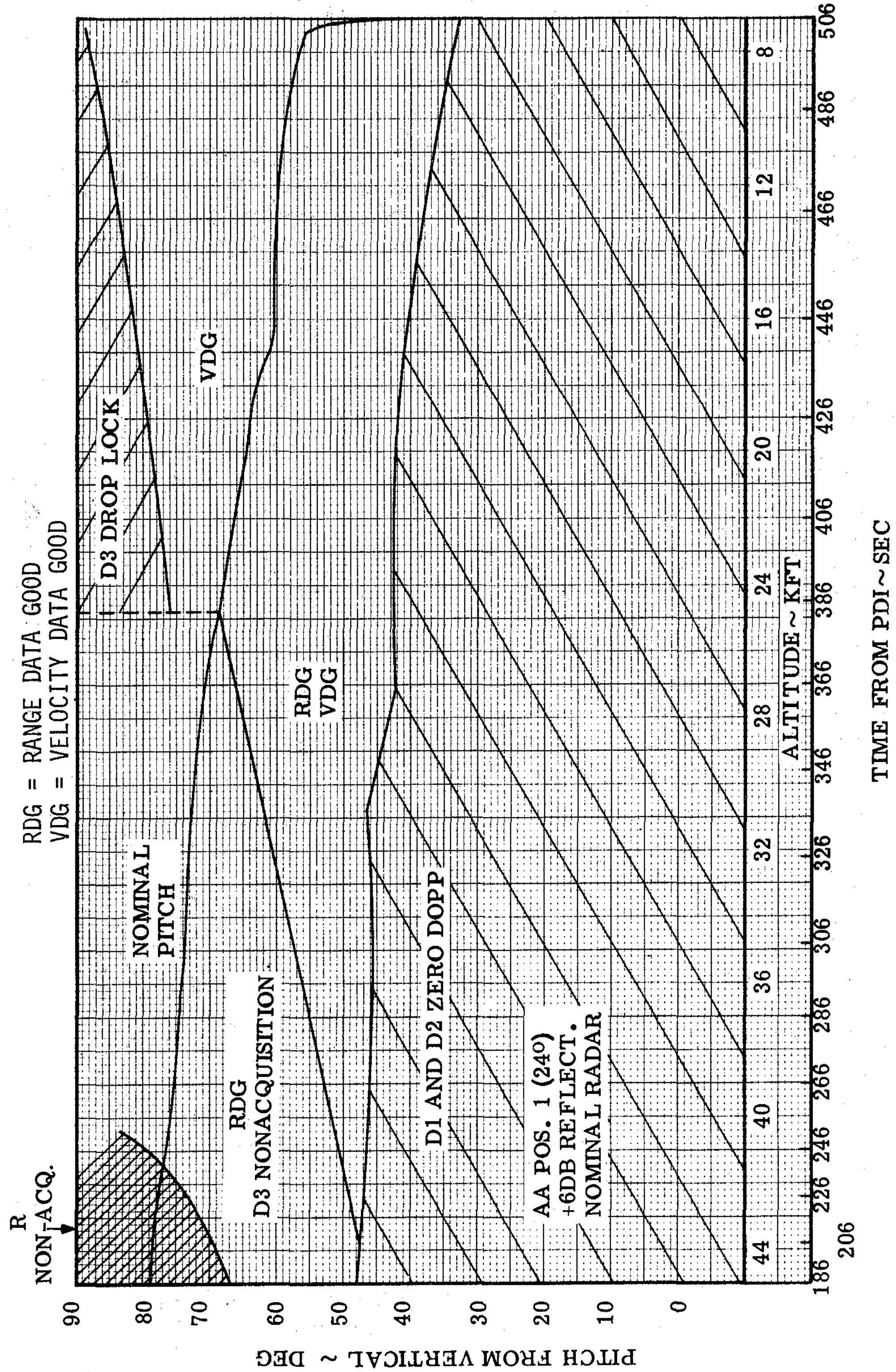

Figure LM7/4.5.5-1. LR Loss of Lock vs Pitch Angle (Antenna Position 1)

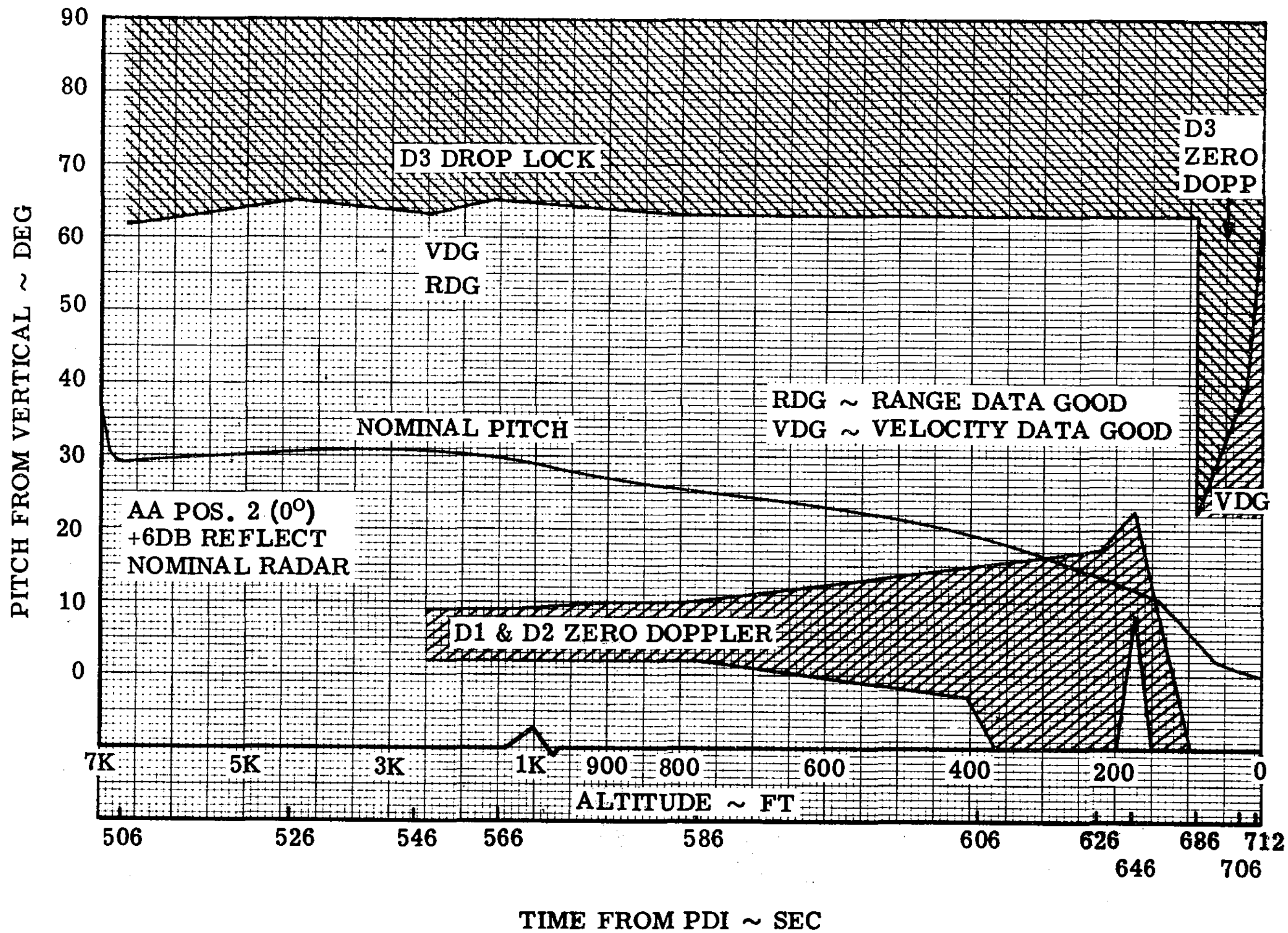

Figure LM7/4.5.5-2. LR Loss of Lock vs. Pitch Angle (Antenna Position 2)

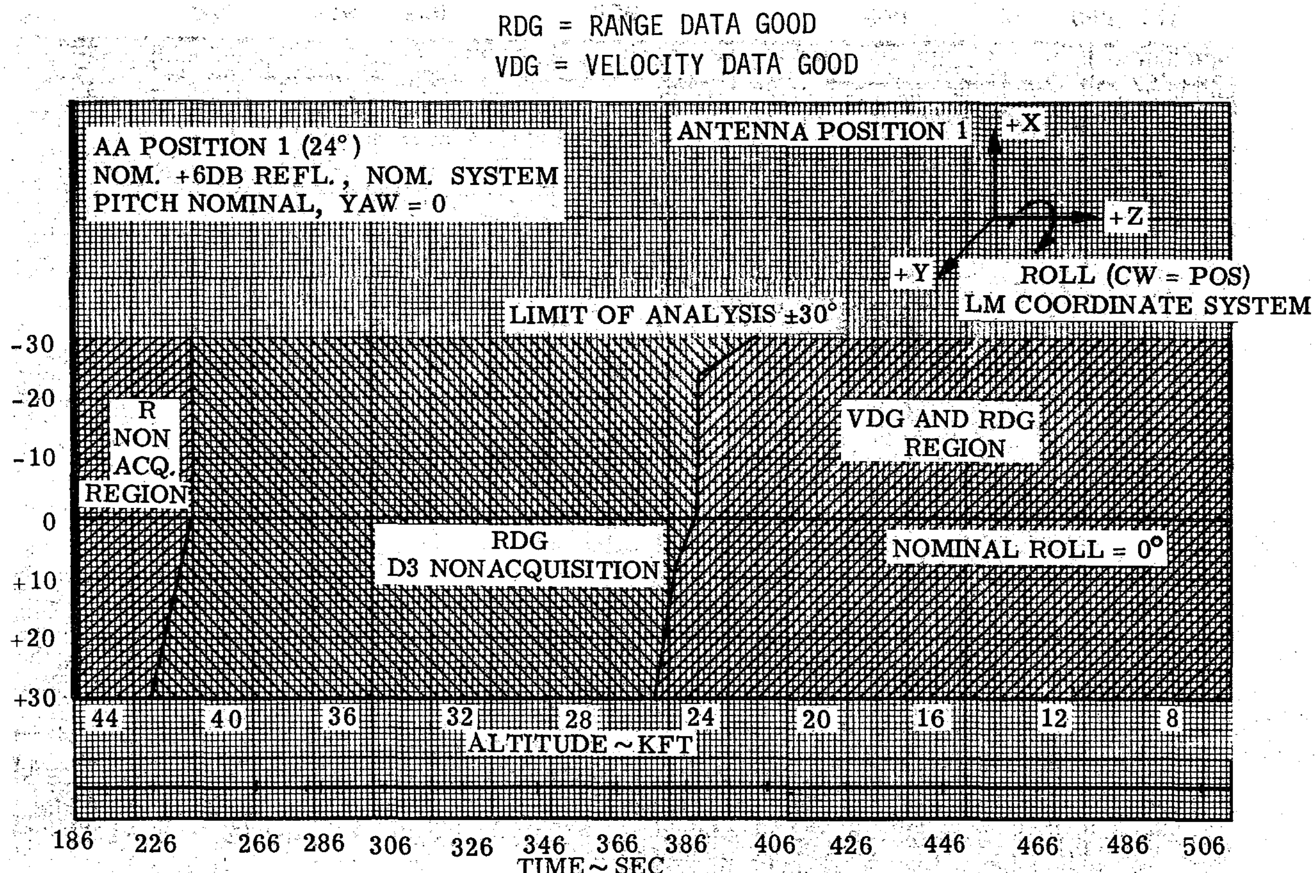

Figure LM7/4.5.5-3. LR Loss of Lock versus Roll Angle

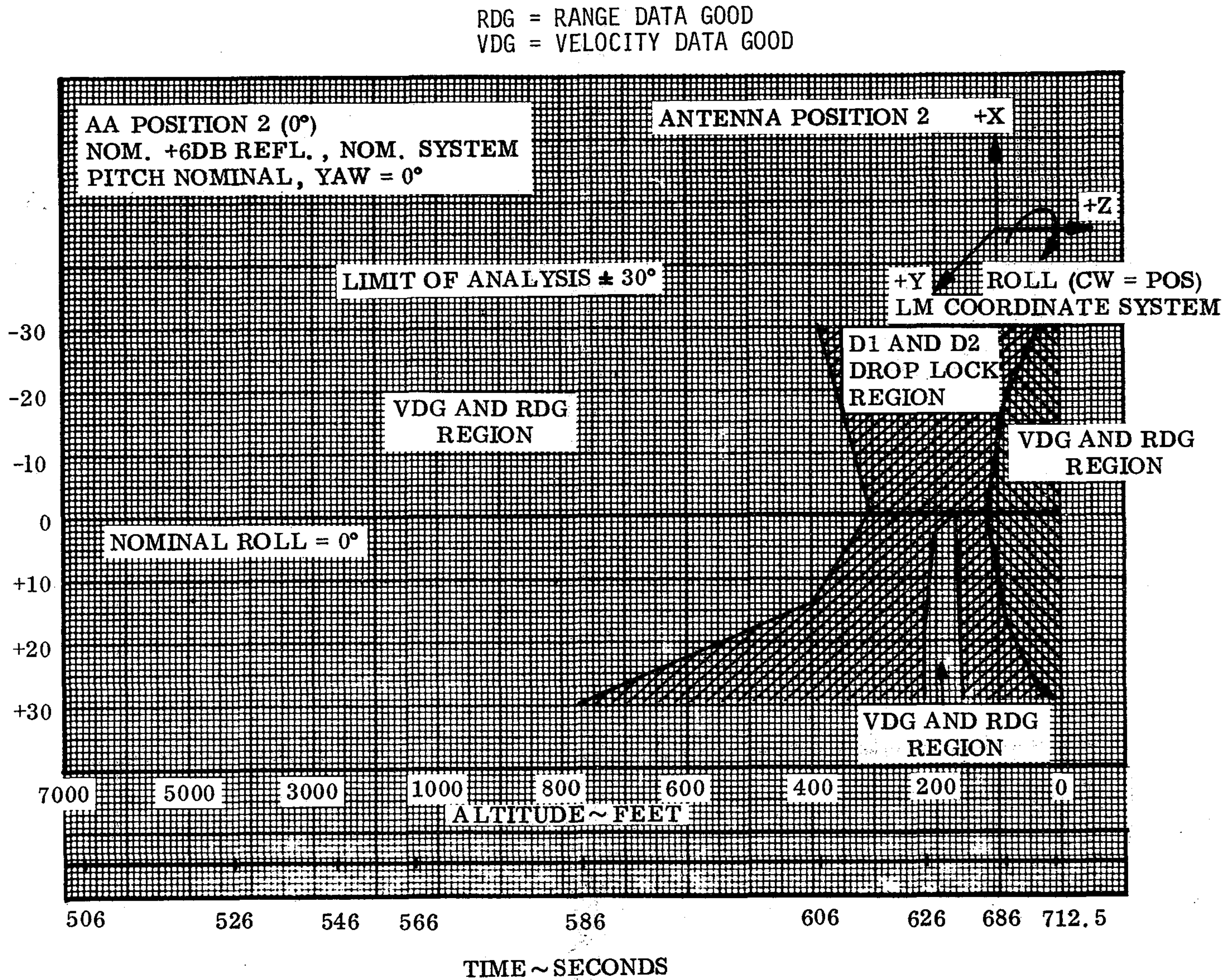

Figure LM7/4.5.5-4. LR Loss of Lock versus Roll Angle

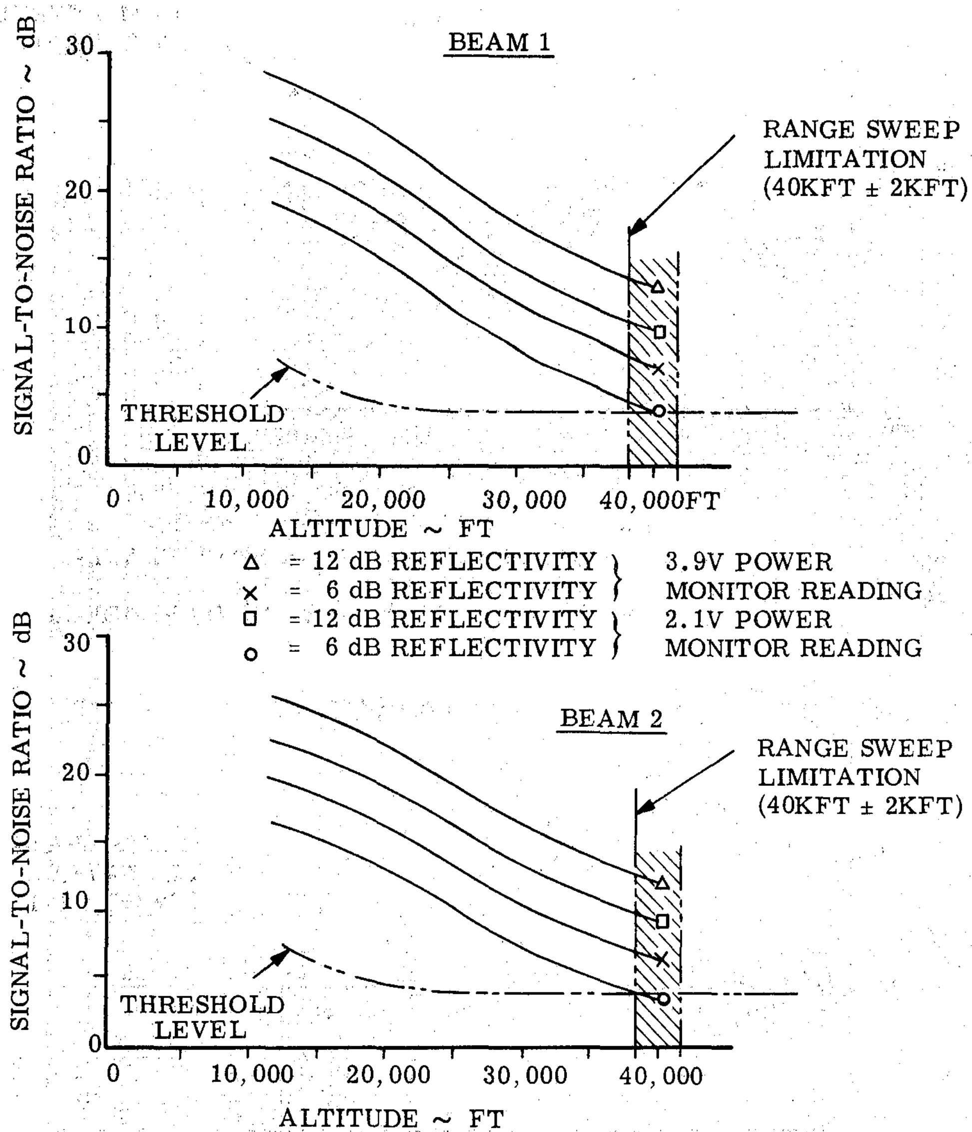

Figure LM7/4.5.5-5. Landing Radar Lock-ON Capability

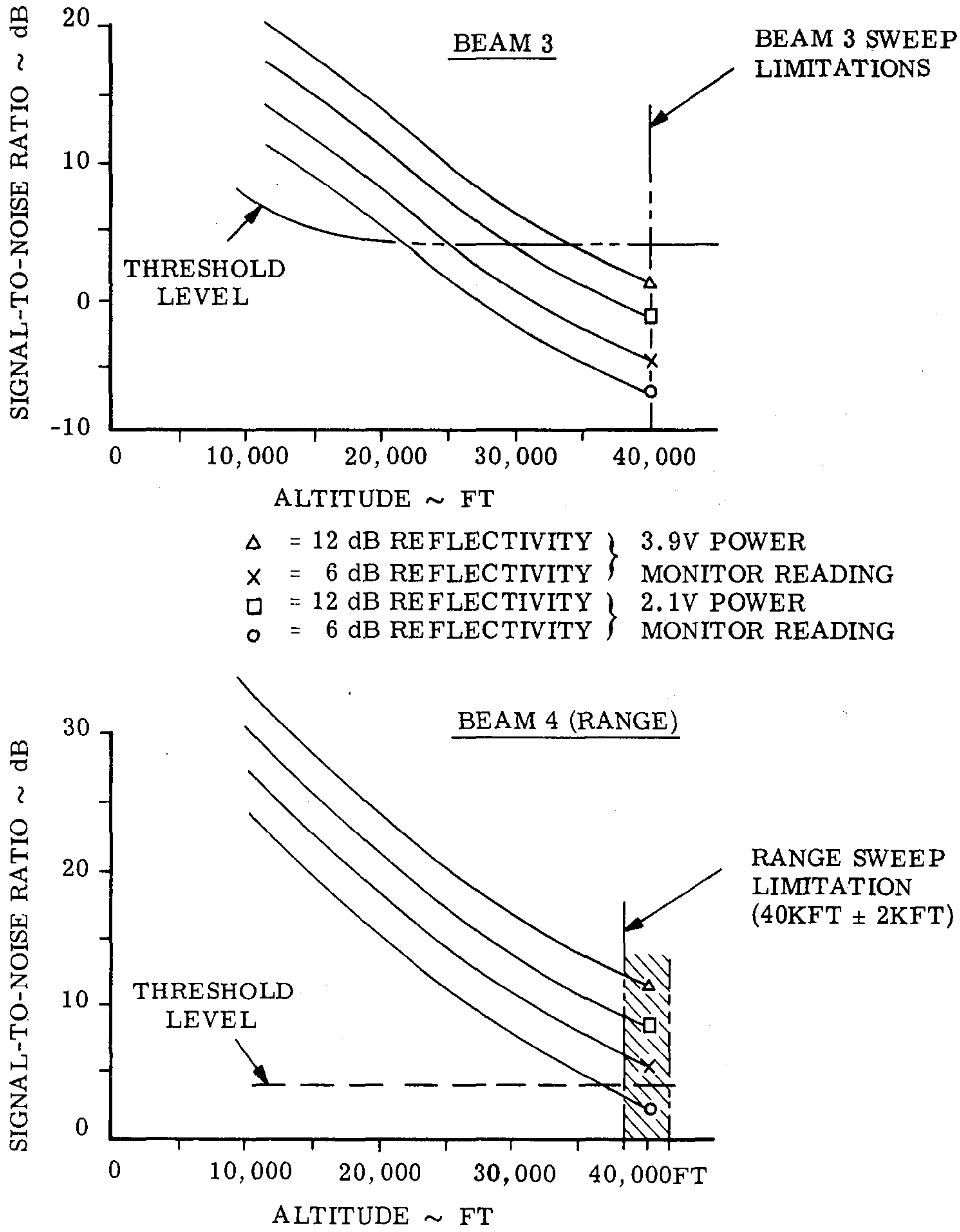

Figure LM7/4.5.5-6. Landing Radar Lock-ON Capability

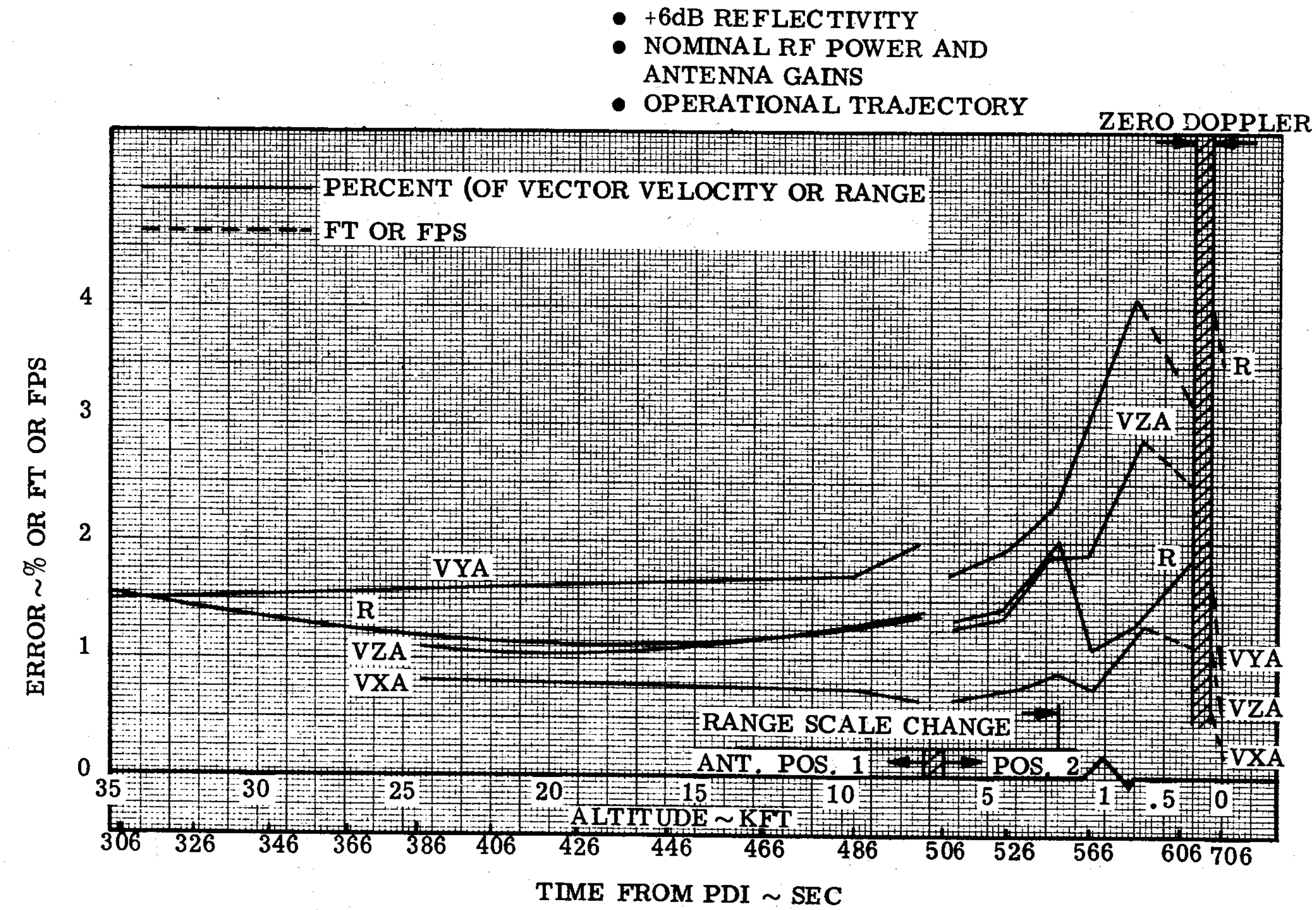

Figure LM7/4.5.5-7. Landing Radar Accuracy

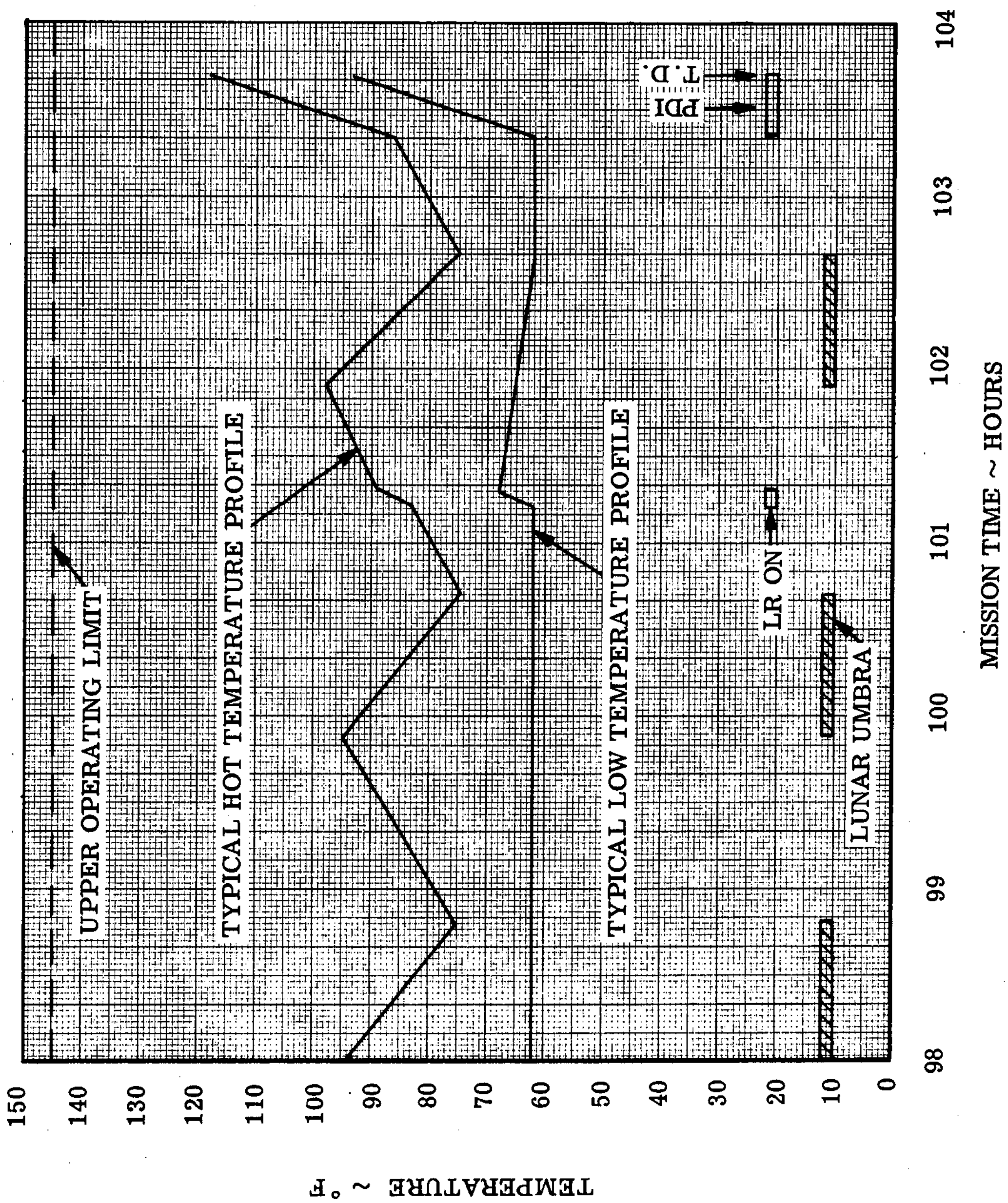

Figure LM7/4.5.5-8. Landing Radar Antenna Assembly Flight Measurement GN7563T LM-7/H-2 Mission

LM7/4.6.1 Mission H2 (LM-7) APS Preflight Analysis

The APS mission duty cycle used in the following analysis is a lunar liftoff with the APS burning to depletion while the planned APS mission duty cycle will be a manned burn initiated from the lunar surface and of a duration to achieve the required vehicle ΔV of approximately 6044 fps.

The vehicle weight characteristics and loaded propellant quantities were obtained from Reference 1. Table LM7/4.6.1-1 is a summary of APS physical characteristics.

It should be noted that the effect of the Reaction Control System on APS performance has been neglected in this analysis. The RCS will affect APS performance in the following manner:

1) RCS propellant consumption (APS/RCS interconnect closed) will alter vehicle weight;

2) RCS propellant consumption through the APS/RCS interconnect will decrease the propellant available to the APS and thus shorten the APS burn time available and decrease the ΔV capability. Also, since the RCS operates at a mixture ratio different from that of the APS, the mixture ratio from the APS tanks will be changed. (The mixture ratio of the ascent engine will not be significantly changed).

The engine performance characterization consists of C* (characteristic exhaust velocity), C_f (thrust coefficient), A_t (throat area), and interface-to-chamber fluid flow resistances defined as functions of engine test data, and (where applicable) predicted values of P_c (chamber pressure), μ (mixture ratio), T (propellant temperature), t_b (engine burn time), t_{acc} (accumulated time on chamber), and helium saturation into the propellants.

The helium regulator characterization used was the nominal Class I - primary regulator expected performance.

The liquid propellant bulk temperatures at the start of the APS burn were assumed to be 70°F for both oxidizer and fuel.

The nominal mixture ratio of 1.605 is for non-saturated propellant conditions prior to ignition. If the tanks are pressurized earlier than is now planned, causing helium saturation of the propellants, the mixture ratio will shift to 1.599.

LM7/4.6.1 Continued

Graphs from the simulation of the LM-7 APS nominal performance under the assumptions and conditions discussed above are presented in Figures LM7/4.6.1-1 through LM7/4.6.1-9. Figure LM7/4.6.1-2 presents the predicted ablative chamber throat area as a function of burn time. The time-varying characteristic of this parameter is included because of its influence in imparting a time-varying character to other propulsion parameters.

APS performance data at three time points have been tabulated and are presented in Table LM7/4.6.1-2. The burnout time presented in this table is the burn-time available assuming no RCS usage of APS propellant through the interconnect.

An uncertainty propagation dispersion analysis was conducted using root-sum-squaring techniques to determine APS performance dispersions. The uncertainties associated with the basic parameters defining propulsion system operation are listed in Table LM7/4.6.1-3. The values given in Table LM7/4.6.1-3 have been derived from Rocketdyne and Grumman inputs by the methods discussed in Reference 2. These values express the uncertainty of the various parameters as 3-sigma at a 50 percent confidence level. These values were used as input to establish the performance dispersions included as part of Table LM7/4.6.1-2. Also presented in Table LM7/4.6.1-2 are average values of the various parameters taken over the duty cycle. The column labeled "Total Standard Deviation" is the standard deviation which must be used in conjunction with the given average values when one is concerned with the engine performance at any given time during the burn. This total standard deviation is the result of combining the error associated with predicting the parameter (as in Table LM7/4.6.1-2, column labeled "Uncertainties/Standard Deviation") with the error resulting from use of a constant (average) value. For consumable analysis purposes values of specific impulse and mixture ratio uncertainty should be obtained from Table LM7/4.6.1-2 (column labeled "Uncertainties/Standard Deviation").

The data presented herein are valid for nominal system conditions. The values of propulsion system parameters presented herein do not represent boundary conditions of operation for the system, and therefore, should not be used as limit values.

The recommended values of mixture ratio shift resulting from APS malfunctions are: -0.018, +0.010 mixture ratio units from the nominal value.

References

1. CSM/LM Spacecraft Operational Data Book, Volume III, Mass Properties, SNA-8-D-027(III) REV 2, Amendment 70, 10 October 1969.

2. "Propulsion Systems Dispersion Analysis and Optimum Propellant Management," TRW Technical Report 11176-H060-R0-00, R. K. M. Seto, 28 October 1968.

TABLE LM7/4.6.1-1

LM-7 APS ENGINE AND FEED SYSTEM PHYSICAL CHARACTERISTICS

Engine[1]	
Engine No.	Rocketdyne S/N 0005C
Injector No.	Rocketdyne S/N 4097714
Initial Chamber Throat Area (in^2)	16.331
Nozzle Exit Area (in^2)	749.760
Initial Expansion Ratio	45.910
Injector Resistance (lb_f-sec^2/lb_m-ft^5) @ time zero and 70^oF	
Oxidizer	12666.
Fuel	20569.
Feed System	
Total Volume (Pressurized, Check Valves to engine interface) (ft^3)[2]	
Oxidizer	37.01
Fuel	37.03
Resistance, Tank Bottom to Engine Interface (lb_f-sec^2/lb_m-ft^5) at 70^oF[3]	
Oxidizer	2531.52
Fuel	4037.76

(1) Rocketdyne Log Book, "Acceptance Test Data Package for Rocket Engine Assembly-Ascent LM-Part No. RS000580-001-00, Serial No. 0005," 20 November 1968.

(2) NASA memorandum EP23-46-69, "Propellant Load Parameters for the DPS and APS of LM-5 through LM-9, and the Estimated Parameters for LM-10 and Subsequent", from EP/Chief, Propulsion and Power Division to PD/Chief, Systems Engineering Division.

(3) GAC Memorandum LMO-271-844, "A/S Hydraulic Resistance LM 7, 8, 9", W. Salter, 6 December 1969.

Table LM7/4.6.1-2 Mission H2 APS Preflight Performance Prediction Summary

PARAMETER	NOMINAL PERFORMANCE			UNCERTAINTIES	AVERAGE VALUES	
	Start of Burn T = 10 secs	"Mid-Tank" T = 225 secs	End of Burn T = 462.4 secs.	Standard Deviation (3σ)	Integrated Average	Total (1) Standard Deviation (3σ)
Specific Impulse (ISP), lb_f-sec/lb_m	309.6	309.8	309.2	3.66	309.7	3.87
Thrust (FVAC), lb_f	3496.	3466.	3464.	103.2	3471.	109.0
Mixture Ratio (MR)	1.610	1.605	1.600	0.029	1.605	0.029
Chamber Pressure (PC), psia	123.1	123.7	122.4	3.19	123.4	3.38
Oxidizer Flowrate (WDTOE), lb_m/sec	6.965	6.893	6.894	0.1956	6.906	0.2088
Fuel Flowrate (WDTFE), lb_m/sec	4.325	4.295	4.310	0.1223	4.303	0.1257
Usable Oxidizer (WOX), lb_m	3124.	1636.	0.	--	--	--
Usable Fuel (WFL), lb_m	1956.	1031.	10.	--	--	--
ΔV (DVTP), ft/sec	106.	2705.	6658.	--	--	--

(1) Note that the dispersions in this column are for the average values only.

TABLE LM7/4.6.1-3

APS SIMULATION PARAMETER UNCERTAINTIES

PARAMETER	THREE STANDARD DEVIATIONS (3σ)	THREE STANDARD DEVIATIONS(%)
Characteristic Exhaust Velocity (C*), ft/sec†	61.8	1.08
Specific Impulse (I_{sp})†, lb_f-sec/lb_m	3.66	1.18
Mixture Ratio (O/F)†	0.029**	1.81
Propellant Feed System Oxidizer Resistance, lb_f-sec^2/lb_m-ft^5	29.37	1.16
Propellant Feed System Fuel Resistance, lb_f-sec^2/lb_m-ft^5	38.4	0.95
Propellant Tank Ullage Pressures, psia	4.0	2.22
Propellant Tank Ullage ΔP, psia	0.5	----
Propellant bulk Temperatures, ^oF	5.0	7.14
Propellant Bulk ΔT, ^oF	1.5	----
Ablative Engine Throat Area, in^2	0.639	3.91

†Engine parameters at standard interface conditions include characterization uncertainties, instrumentation uncertainties, and engine repeatability.

**The total propulsion system mixture ratio uncertainty is approximately 82% of the mixture ratio uncertainty.

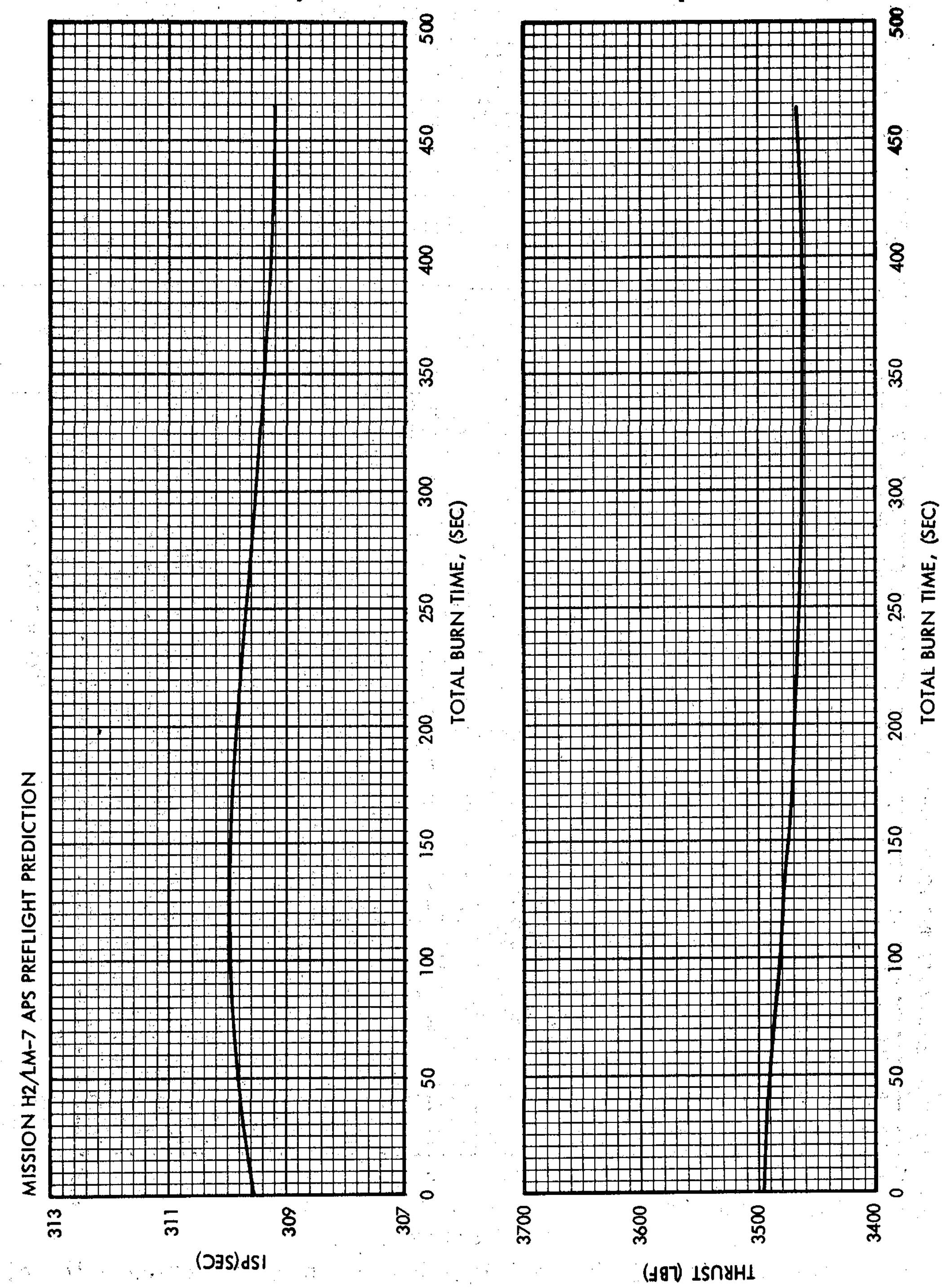

Figure LM7/4.6.1-1 Mission H2 APS Preflight Performance Prediction - Thrust and Specific Impulse Vs. Time

(NASA DATA SOURCE)

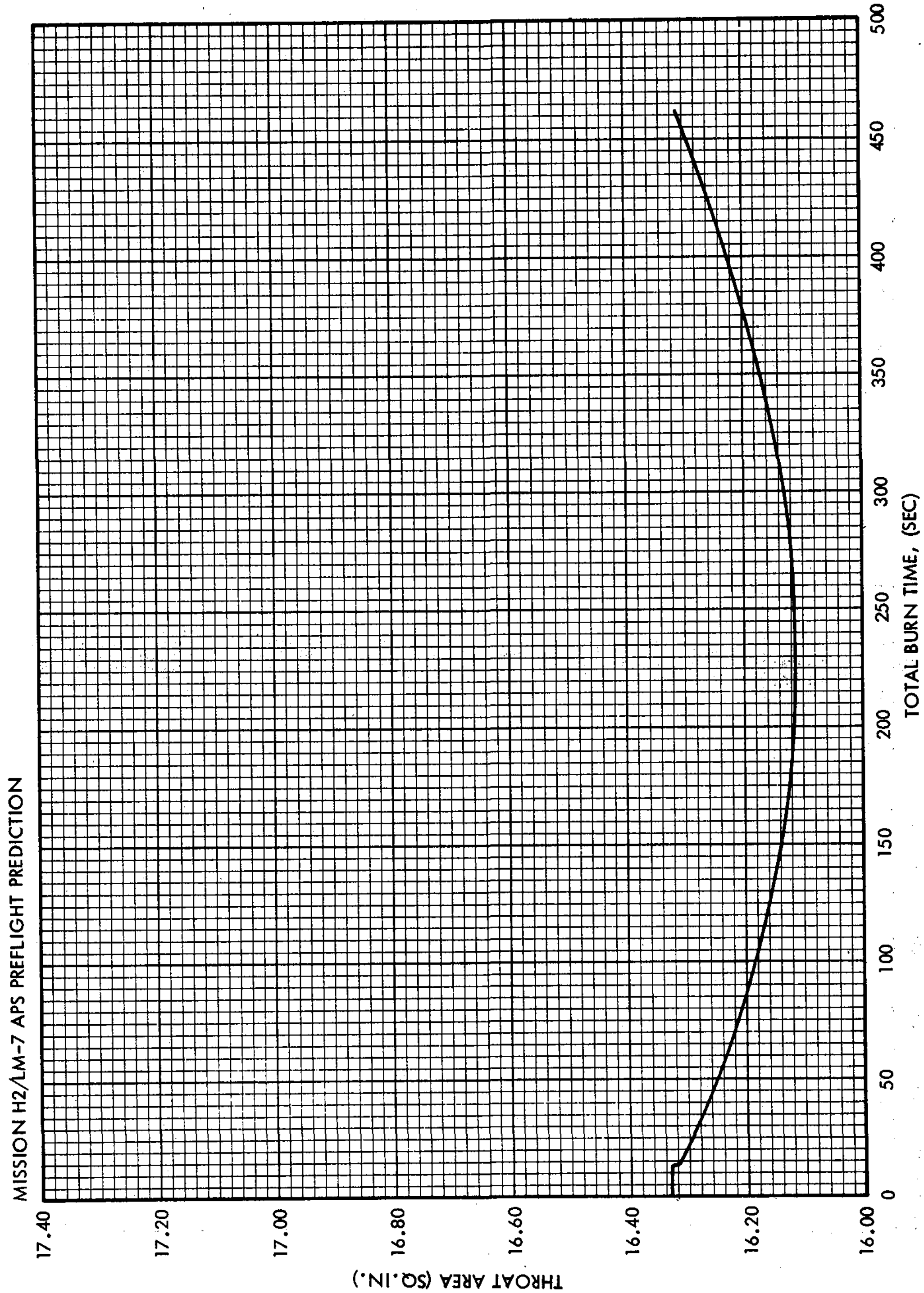

Figure LM7/4.6.1-2 Mission H2 APS Preflight Performance Prediction - Throat Area Vs. Time

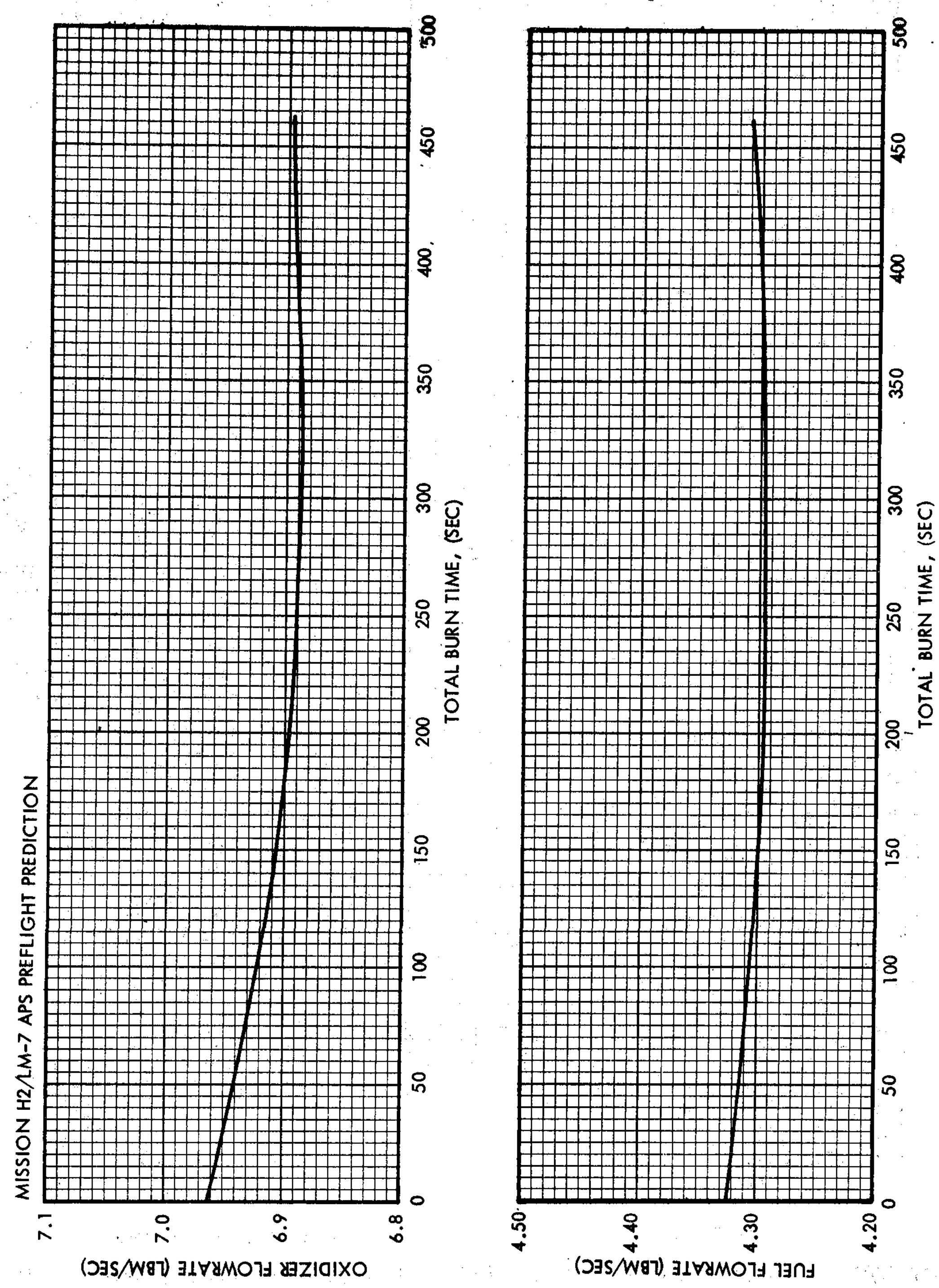

Figure LM7/4.6.1-3 Mission H2 APS Preflight Performance Prediction - Oxidizer and Fuel Flowrates Vs. Time

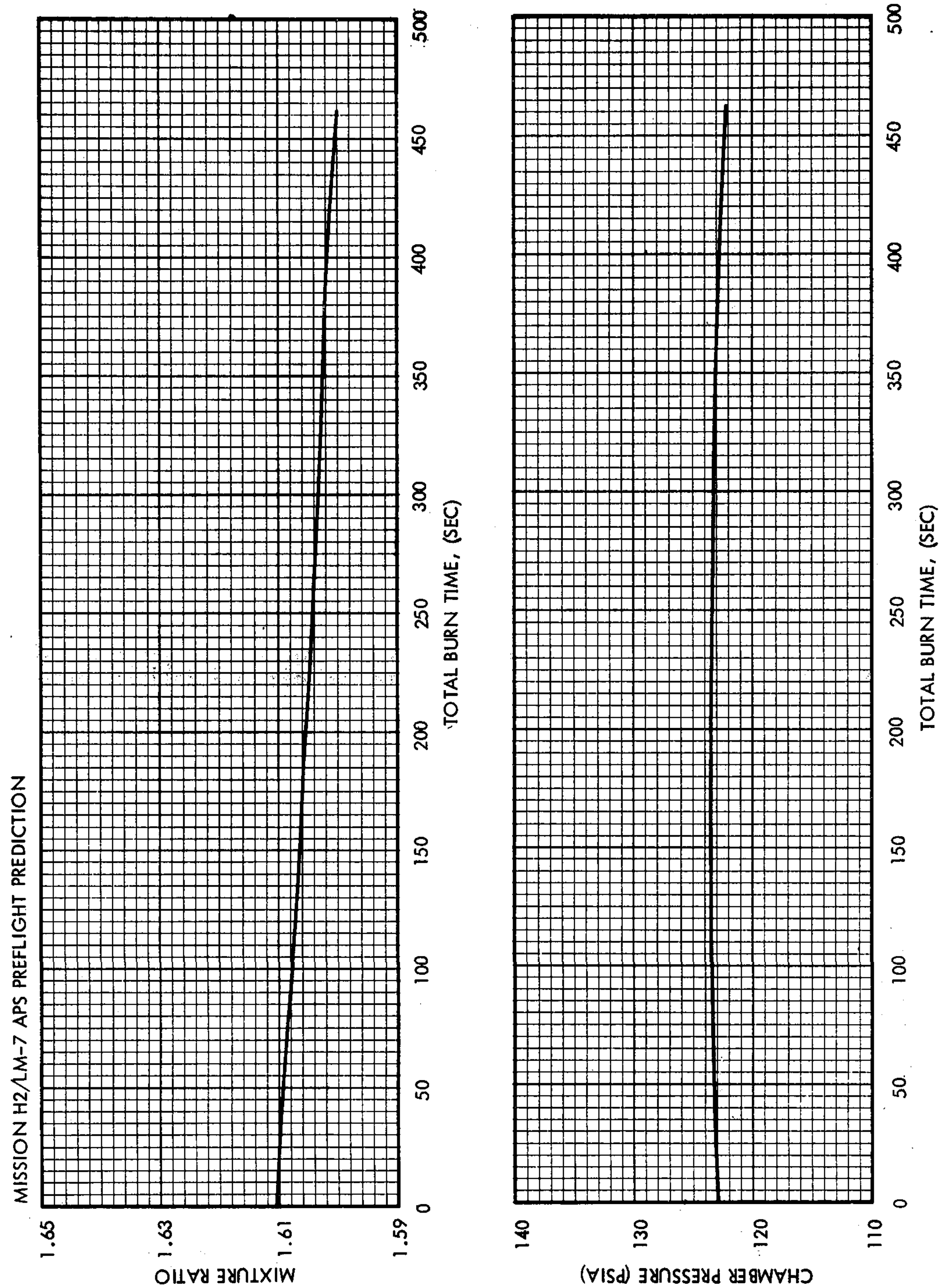

Figure LM7/4.6.1-4 Mission H2 APS Preflight Performance Prediction - Chamber Pressure and Mixture Ratio Vs. Time

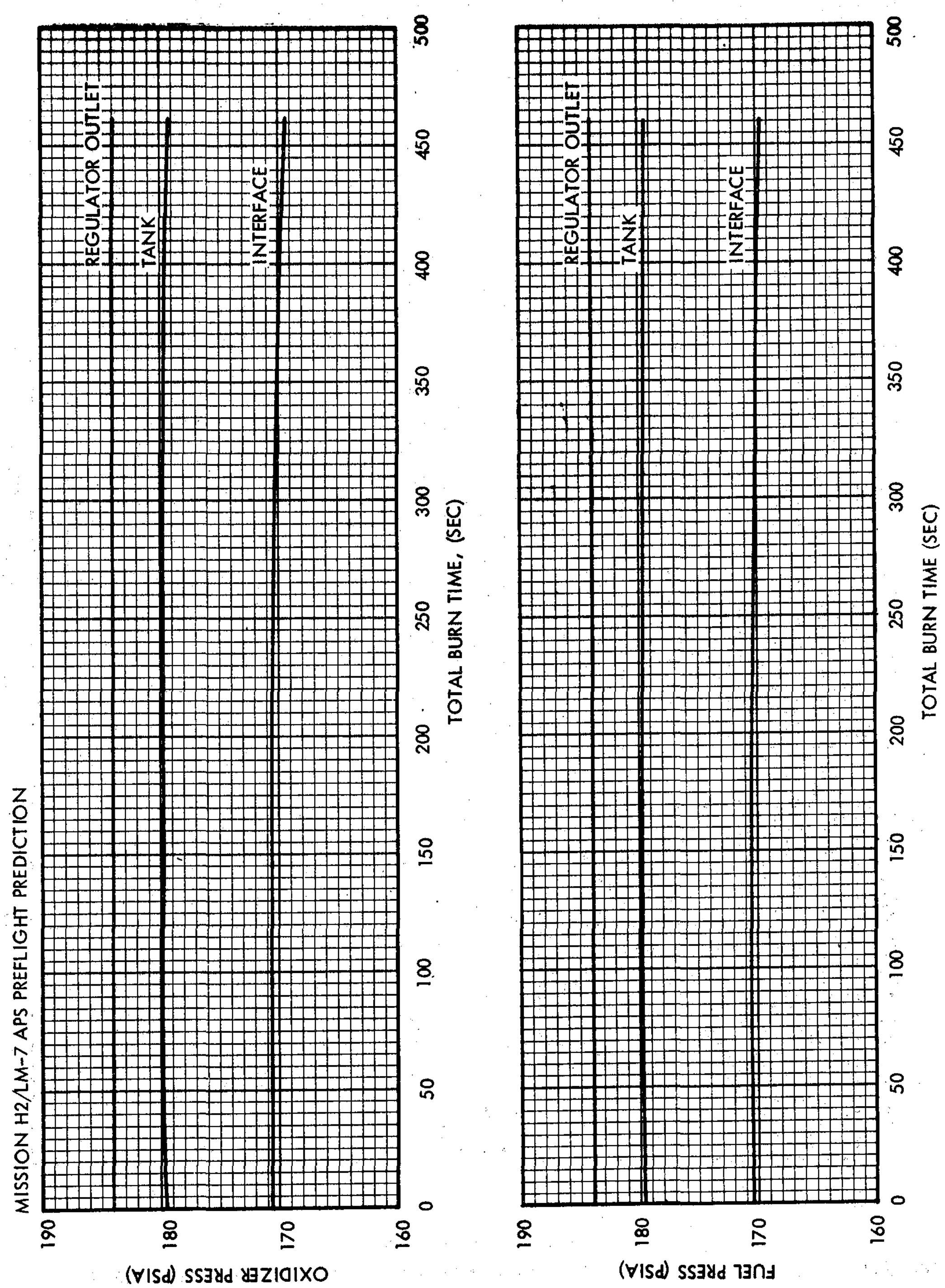

Figure LM7/4.6.1-5 Mission H2 APS Preflight Performance Prediction - Fuel and Oxidizer System Pressures Vs. Time

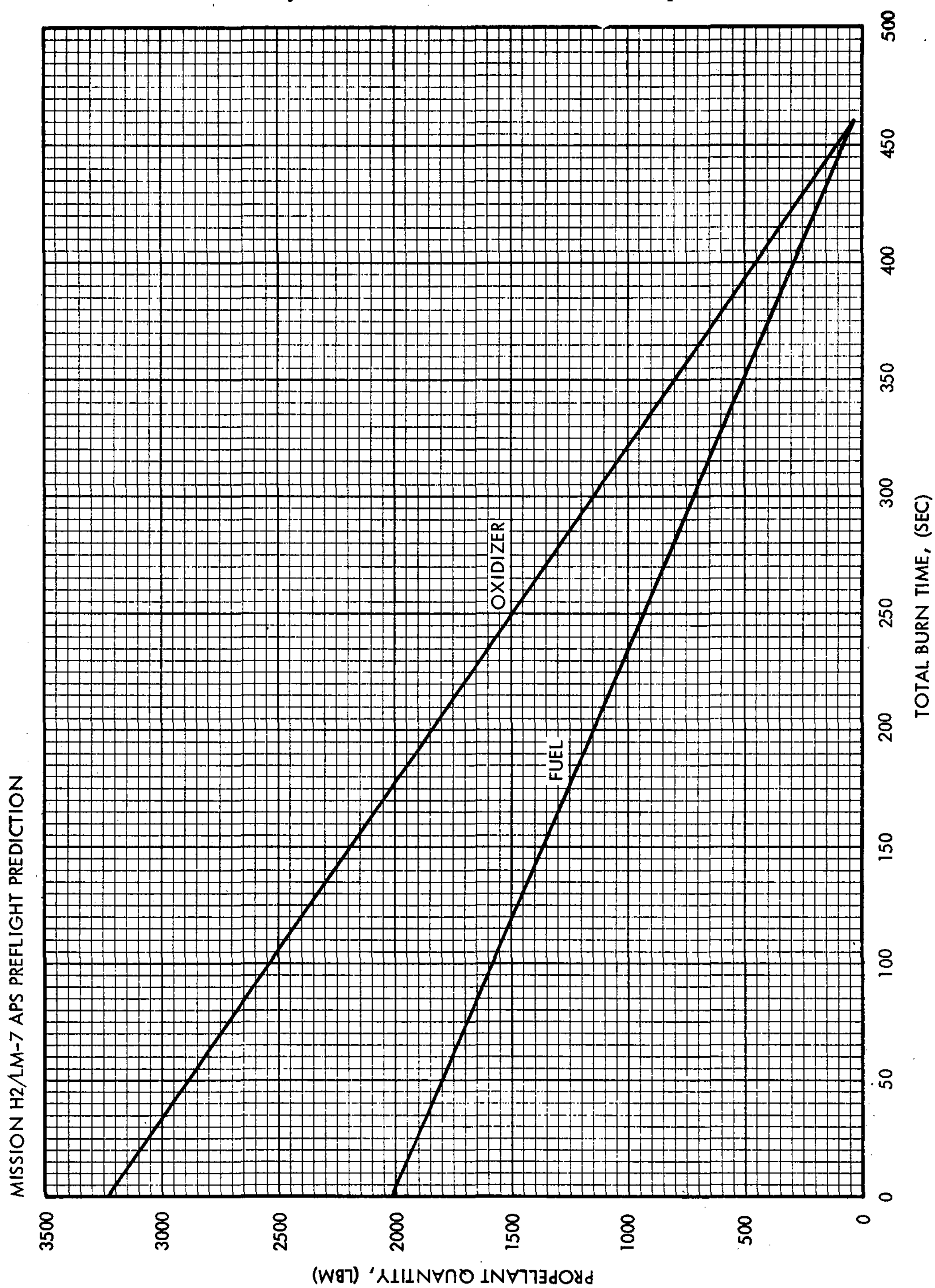

Figure LM7/4.6.1-6 Mission H2 APS Preflight Performance Prediction - Propellant Quantities Vs. Time

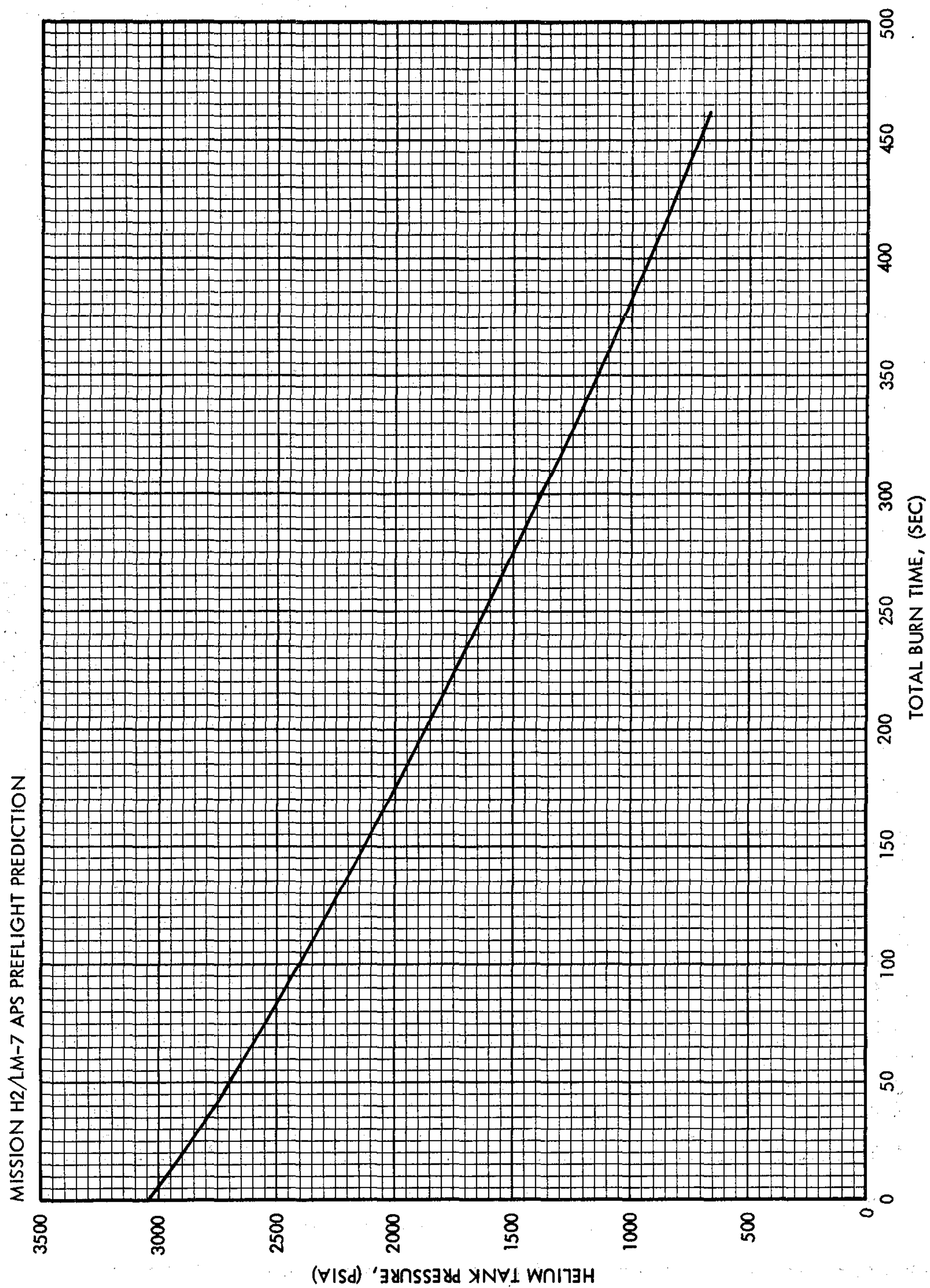

Figure LM7/4.6.1-7 Mission H2 APS Preflight Performance Prediction - Helium Tank Pressure Vs. Time

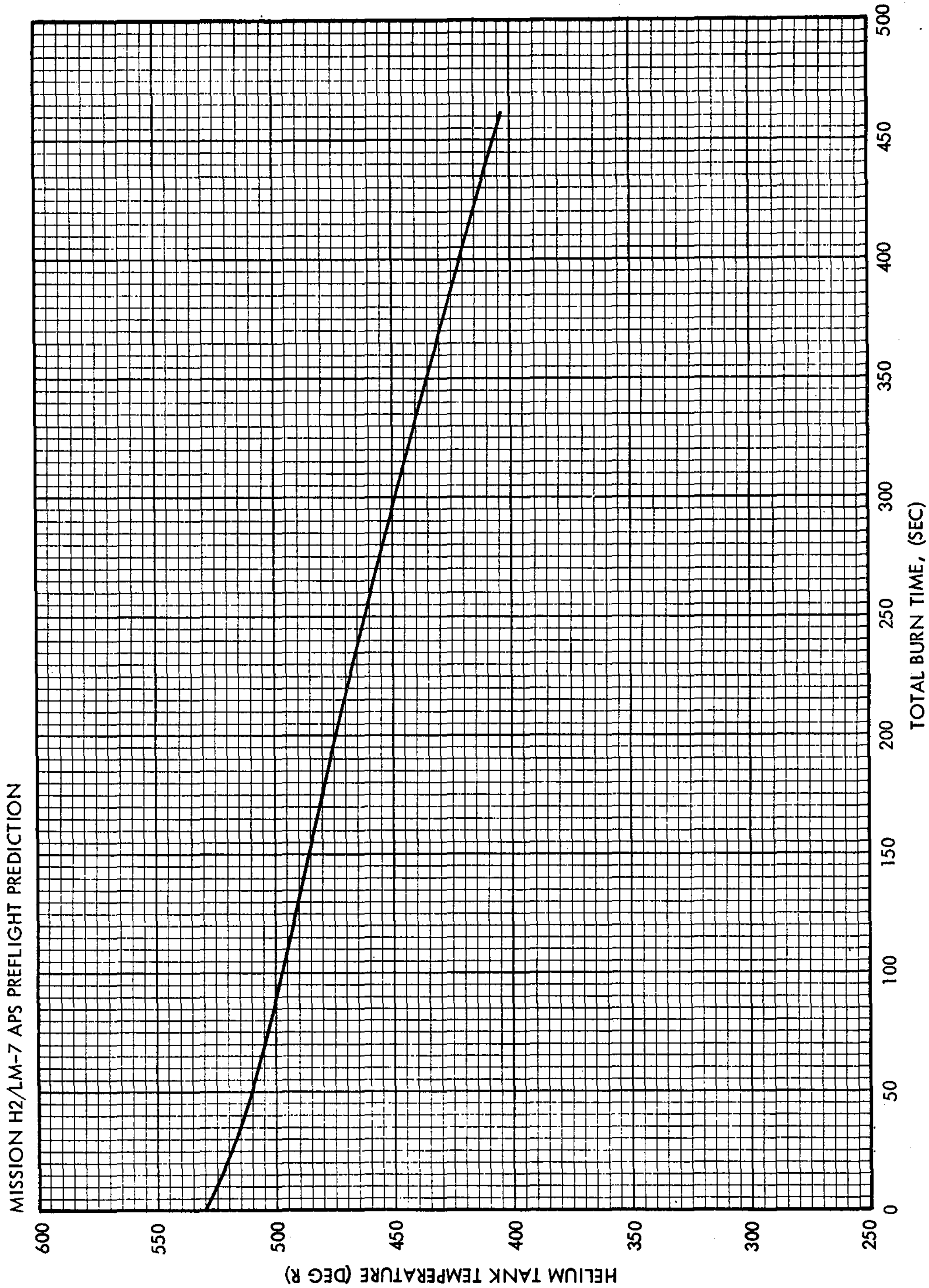

Figure LM7/4.6.1-8 Mission H2 APS Preflight Performance Prediction - Helium Tank Temperature Vs. Time

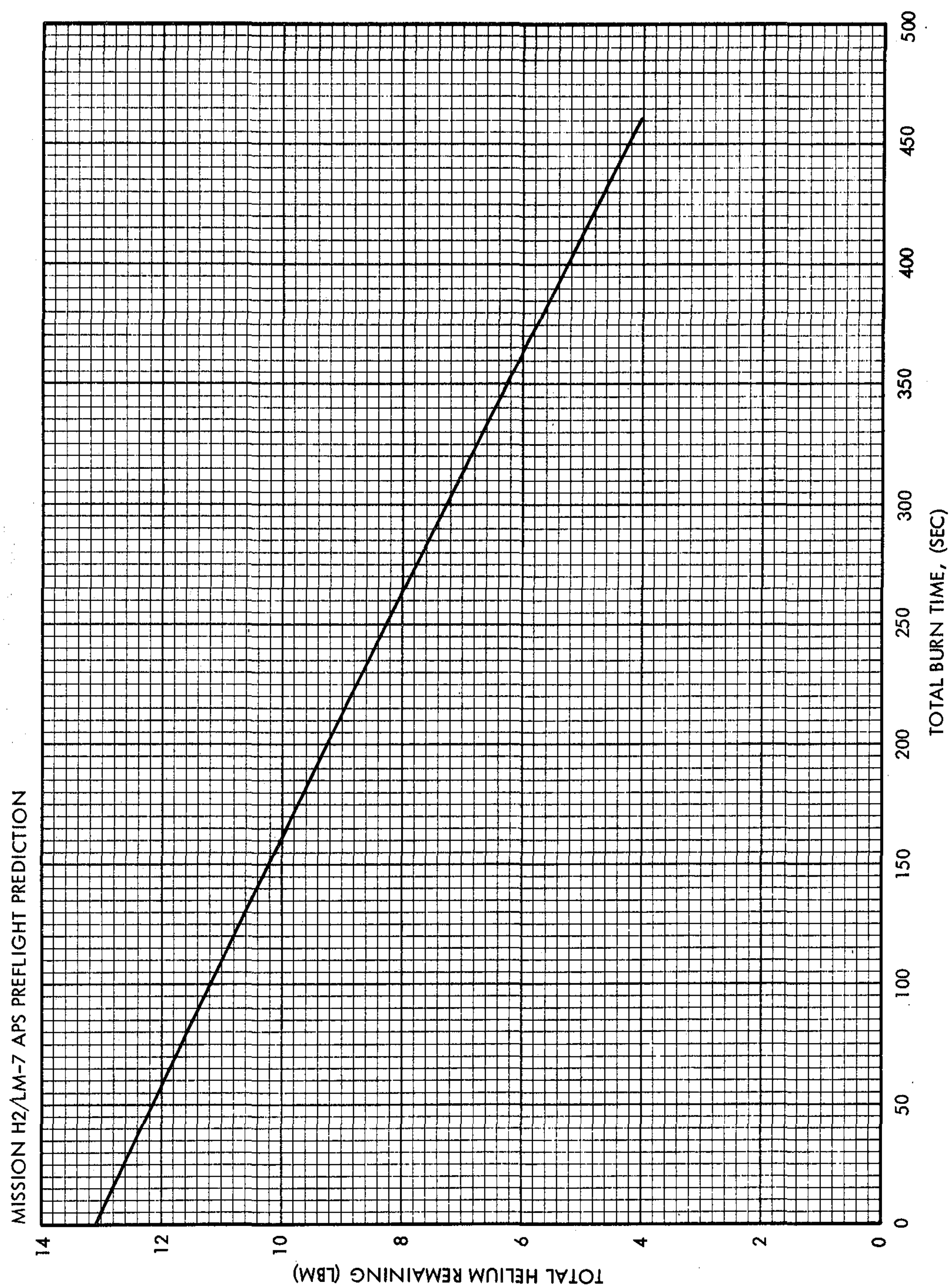

Figure LM7/4.6.1-9 Mission H2 APS Preflight Performance Prediction - Total Helium Remaining Vs. Time

LM7/4.6.8 Thrust Vector Change with Burn Time

The initial thrust vector displacement on Engine Number 0005C is Z = -0.014 inches, Y = -0.007 inches.

LM7/4.6.12 Ascent Engine Regulator Performance

Figure LM7/4.6.12-1 shows performance characteristics for the LM7 Class I primary regulator, Serial No. 159. This is a flight prediction based on KSC checkout at 3400 psia inlet pressure.

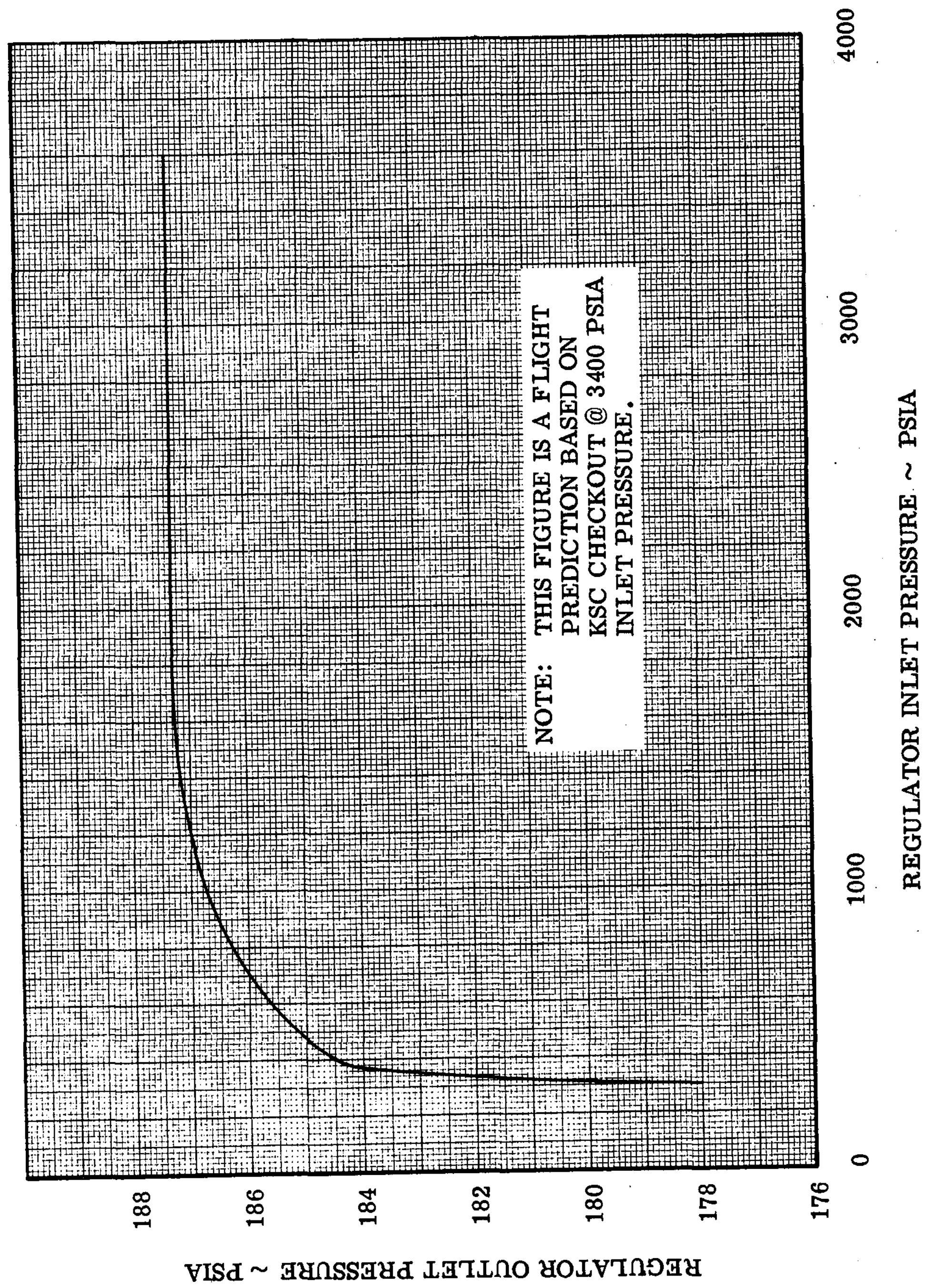

Figure LM7/4.6.12-1. Ascent Engine Regulator Performance

LM7/4.7.1 Mission H2 (LM-7) DPS Preflight Analysis (NASA DATA SOURCE)

The data presented herein are valid only for the system at nominal conditions and do not represent the boundary conditions of operation for the system. Therefore, these values should not be used as limit values.

The nominal mission duty cycle for the Mission H2/LM-7 DPS is presented in Figure LM7/4.7.1-1. The spacecraft weight and propellant loading used in the simulation are given in Table LM7/4.7.1-1. Descent engine and feed system physical characteristics are shown in Table LM7/4.7.1-2.

It should be noted that all performance parameters presented are for DPS operation only, and do not include RCS contributions to thrust or velocity gain. The predicted RCS propellant usage was simulated during the burns as a weight change.

The helium regulator characteristics used to establish the DPS propellant tank ullage pressures were derived from GAEC PIT data. Propellant temperatures measured during Missions F and G were assumed to be representative of those to be expected during Mission H2.

A summary of the Mission H2 (LM-7) performance prediction is given in Table LM7/4.7.1-3 and Figures LM7/4.7.1-1 through LM7/4.7.1-9. Figures LM7/4.7.1-10 and LM7/4.7.1-11 present the vehicle and engine related effective specific impulse as functions of burn time. A prediction of the supercritical helium tank pressure and mass profiles are presented in Figures LM7/4.7.1-12 and LM7/4.7.1-13. The dispersions associated with thrust, specific impulse, and mixture ratio are given in Figures LM7/4.7.1-14 through LM7/4.7.1-16, respectively.

The vehicle effective specific impulse for the descent burn was 300.2 seconds. This value includes the effect of approximately 81 lbm of consumables which are expelled from the spacecraft during the time from PDI to lunar touchdown. The value of the engine effective specific impulse, which does not include the effect of the consumables other than propellant, was 302.3 seconds. It should be noted that the effective specific impulse is not only a function of engine performance but is dependent on vehicle initial mass, mass changes with time, and velocity requirements. Substantial deviations from the conditions of the simulation will invalidate the use of this effective specific impulse. The 1-sigma variation in effective engine specific impulse is ±1.698 seconds for the simulation. The effective vehicle mixture ratio is 1.6014 and the 1-sigma variation is ±0.0075.

The LM-7 DPS shutoff valve malfunction characterization data are as follows: an AB valve malfunction will result in shifts of +0.012, +0.22 seconds, and -217 lbf for mixture ratio, specific impulse, and

LM7/4.7.1 (Continued)

thrust, respectively; while a CD valve malfunction will result in shifts of 0.0, -0.12 seconds, and -227 lbf, respectively, for the given parameters. These data are applicable to FTP operation only.

During the nominal mission, the low level sensor should not be activated prior to the nominal touchdown time (684 seconds after descent burn ignition). If the vehicle is hovering the oxidizer low level sensor should be activated at approximately 737 ±3 seconds (assuming nominal CG shifts (See Table LM7/4.7.1-1). The approximate hover time from the low level signal to oxidizer depletion is predicted to be 116±4 seconds or 853 ±4 seconds after engine ignition. The dispersion in time is based on the dispersion in the oxidizer level at low level sensor activation (See Paragraph LM7/4.7.5).

The data presented herein are valid only for the systems at nominal conditions and do not represent the boundary conditions of operation for the system. Therefore, these values should not be used as limit values.

A docked LM-7 Descent Propulsion System (DPS) burn-to-propellant depletion simulation was made using the Descent Ascent Monte Carlo Program (DAMP).

It was assumed that at engine ignition, the LM was docked with the CSM. The mission duty cycle consisted of a minimum throttle (approximately 12.7% of full thrust) segment of 26 seconds with the remainder of the burn at the Fixed Throttle Position (FTP). The burn was terminated when either the usable oxidizer or fuel was depleted.

The initial spacecraft weight was assumed to be 73,733.4 lbm with 11,290.6 lbm and 7,033.4 lbm of tanked oxidizer and fuel, respectively. Depletion occurs when the tanked quantities reach 98.6 lbm for oxidizer or 33.5 lbm for fuel.

At 583.0 seconds after ignition, oxidizer depletion occurred with approximately 34.8 lbm of usable fuel remaining. The velocity change for the burn was 2745 ft/sec. The effective engine specific impulse, which neglects consumables other than propellants that are expelled from the spacecraft during the burn, was 303.01 seconds. The effective vehicle specific impulse was 301.76 seconds. The average mixture ratio was 1.5994.

Figures LM7/4.7.1-17 through LM7/4.7.1-27 present DPS engine parameters for the burn.

Chamber pressure versus commanded thrust for zero, nominal, 3-σ maximum predicted, and maximum allowable throat erosion (30%) is shown in Figure LM7/4.7.1-28.

Table LM7/4.7.1-1

LM-7 DESCENT PROPULSION SYSTEM

WEIGHT CHARACTERISTICS[1]

SPACECRAFT WEIGHTS (lbm)

DPS Stage Inert		4523.0
Loaded Propellant		18434.8
DPS Oxidizer	11351.1	
DPS Fuel	7083.7	
Loaded APS Stage and Crew		10914.5
LM Weight at Separation		33872.3

UNUSABLE PROPELLANTS

	Oxidizer	Fuel
TRAPPED PROPELLANT	(60.4)	(35.2)
Fill Lines	0.2	0.1
Engine	12.2	6.4
Balance Lines	11.3	7.3
Branch Lines	17.0	8.0
Common Lines	19.0	8.1
Isolation SQ Bypass and Miscellaneous	0.7	0.7
Heat Exchanger	0.0	4.6
LOST PROPELLANT	(2.6)	(2.8)
Start Transient (Two cycles)	1.3	1.0
Shutdown Transient (Two cycles)	1.3	1.8
RESIDUALS IN TANKS	(87.6)	(35.4)
Tank Wetting	2.0	2.0
Zero-G Can	8.6	5.2
Center of Gravity (Thrust Vector)	42.0	15.0
Unporting Prevention	16.0	10.7
Propellant Vapor	19.0	2.5
PROPELLANT USABLE FOR BURN TO DEPLETION	(-27.5)	(-16.7)
Lines	-27.5	-12.1
Heat Exchange	0.0	-4.6
TOTAL UNUSABLES	123.1	56.7
	179.8	

Note: Unusables are defined as that propellant which is physically unavailable to the engine.

[1] These mass properties were used for the purpose of this analysis. Reference should be made to Volume III, Spacecraft Operational Data Book, for current official mass properties data.

Table LM7/4.7.1-2

LM-7 Descent Propulsion Engine
and Feed System Physical Characteristics

ENGINE	
Engine Number	1041
Chamber Throat Area, In^2	53.120[1]
Nozzle Exit Area, In^2	2569.7[4]
Nozzle Expansion Ratio	47.7[4]
Oxidizer Interface to Chamber Resistance at FTP $\frac{lbf-sec^2}{lbm-ft^5}$	3886.5[3]
Fuel Interface to Chamber Resistance at FTP $\frac{lbf-sec^2}{lbm-ft^5}$	6262.4[3]
Fuel Film Coolant Tapoff Point to Combustion Chamber $\frac{lbf-sec^2}{lbm-ft^5}$	465069[3]
FEED SYSTEM	
Oxidizer Propellant Tanks, Total Ambient Volume, Ft^3	126.0[4]
Fuel Propellant Tanks, Total Ambient Volume, Ft^3	126.0[4]
Oxidizer Tank to Interface Resistance, $\frac{lbf-sec^2}{lbm-ft^5}$	425.42[2]
Fuel Tank to Interface Resistance, $\frac{lbf-sec^2}{lbm-ft^5}$	674.53[2]

[1]TRW No. 01827-6191-R000, TRW LM Descent Engine Serial No. 1041 Acceptance Test Performance Report, Paragraph 5.3.1, 4 October 1968.

[2]GAEC Cold Flow Tests.

[3]TRW No. 4728.2.69-7, LM-7, Engine Serial No. 1041 Descent Engine Characteristic Equations, March 1969.

[4]Approximate values.

Table LM7/4.7.1-3 Mission H2 DPS Preflight Performance Prediction Summary

PARAMETER	Start of Descent Burn	36 Seconds of Descent Burn				356 Seconds of Descent Burn				416 Seconds of Descent Burn	506 Seconds of Descent Burn	684 Seconds Touchdown
	Nominal Performance	Nominal Performance	Standard Deviation (1σ)	Standard Deviation (%)	3σ Minimum	Nominal Performance	Standard Deviation (1σ)	Standard Deviation (%)	3σ Minimum	Nominal Performance	Nominal Performance	Nominal Performance
Throttle Position(%)	12.65*	93.84 (FTP)	FTP	FTP	FTP	94.41 (FTP)	FTP	FTP	FTP	57.36	60.14	26.94
ISP (lbf-sec/lbm)	294.64	303.97	1.239	0.408	300.25	302.00	1.277	0.423	298.17	302.26	303.11	295.49
F (lbf)	1329*	9854.	40.6	0.412	9732	9913	44.5	0.449	9780	6023	6315	2829
MR (o/f)	1.5989	1.6033	0.0039	0.243	1.5916	1.6011	0.0038	0.237	1.5897	1.6004	1.6017	1.6002
P_c (psia)												
$\dot{W}_o$ (lbm/sec)	2.774	19.964	0.122	0.611	19.598	20.205	0.139	0.688	19.788	12.264	12.825	5.891
$\dot{W}_f$ (lbm/sec)	1.735	12.452	0.072	0.578	12.236	12.620	0.080	0.634	12.380	7.663	8.007	3.681
WO (lbm)	11291	11027	11.45	0.104	10993	4598	45.88	0.998	4460	3596	2485	1018
WF (lbm)	7049	6884	6.93	0.101	6863	2872	27.38	0.953	2790	2245	1551	634

*TCV = 2.773 VDC

Table LM7/4.7.1-3. (Continued)
Mission H2 Final DPS Preflight Performance Prediction
Summary (Performance During Hover-To-Depletion)

Parameter	768 seconds	853 seconds Depletion (Ox)
	Nominal Performance	Nominal Performance
Throttle Position %	25.66	24.43
ISP	294.56	293.40
F	2694	2565
MR	1.6025	1.6055
Pc	--	--
$\dot{W}o$	5.632	5.387
$\dot{W}f$	3.515	3.355
WO	530.65	62.09
WF	329.60	37.45

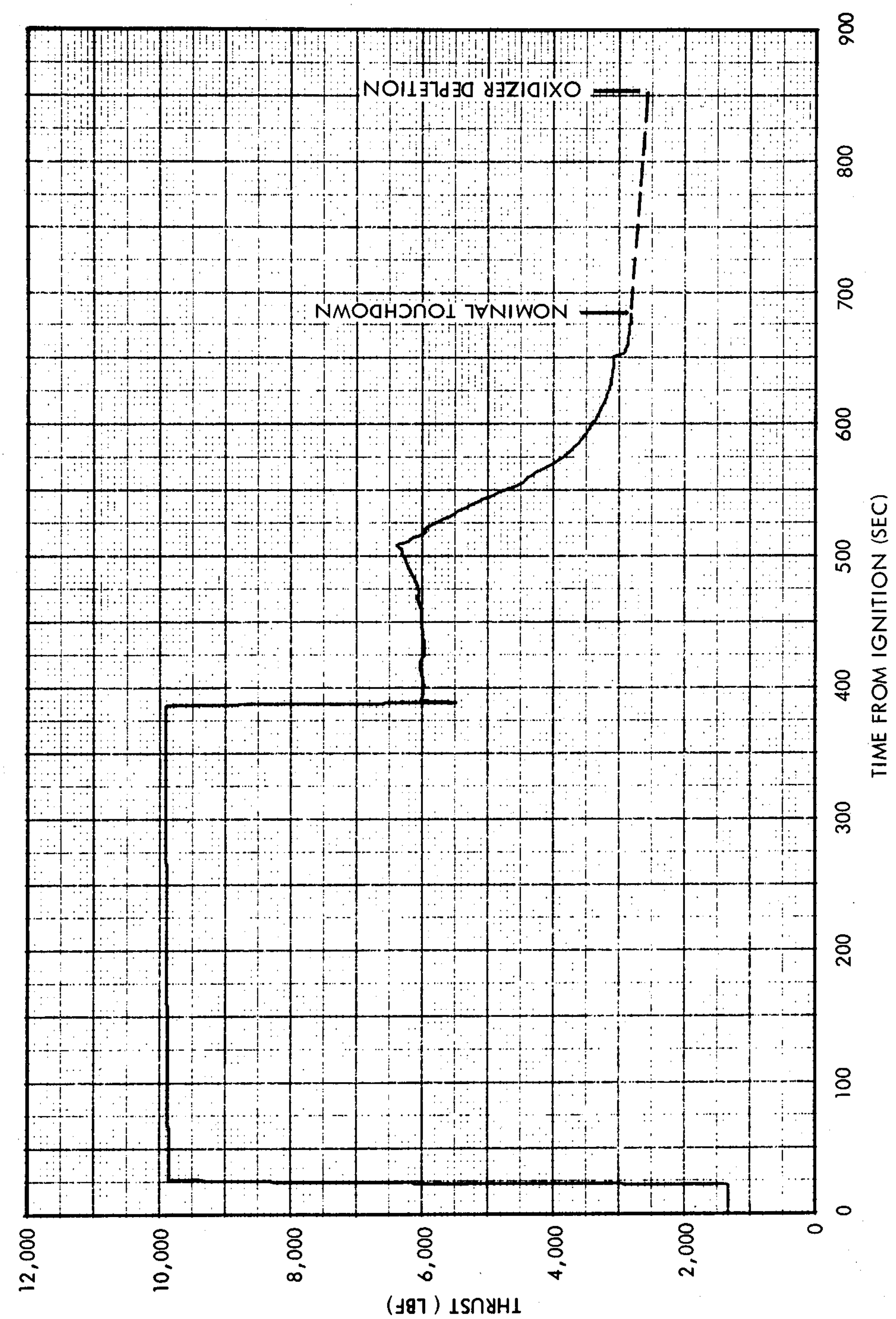

Figure LM7/4.7.1-1 Mission H2 Final DPS Preflight Performance Prediction - Thrust Vs. Time

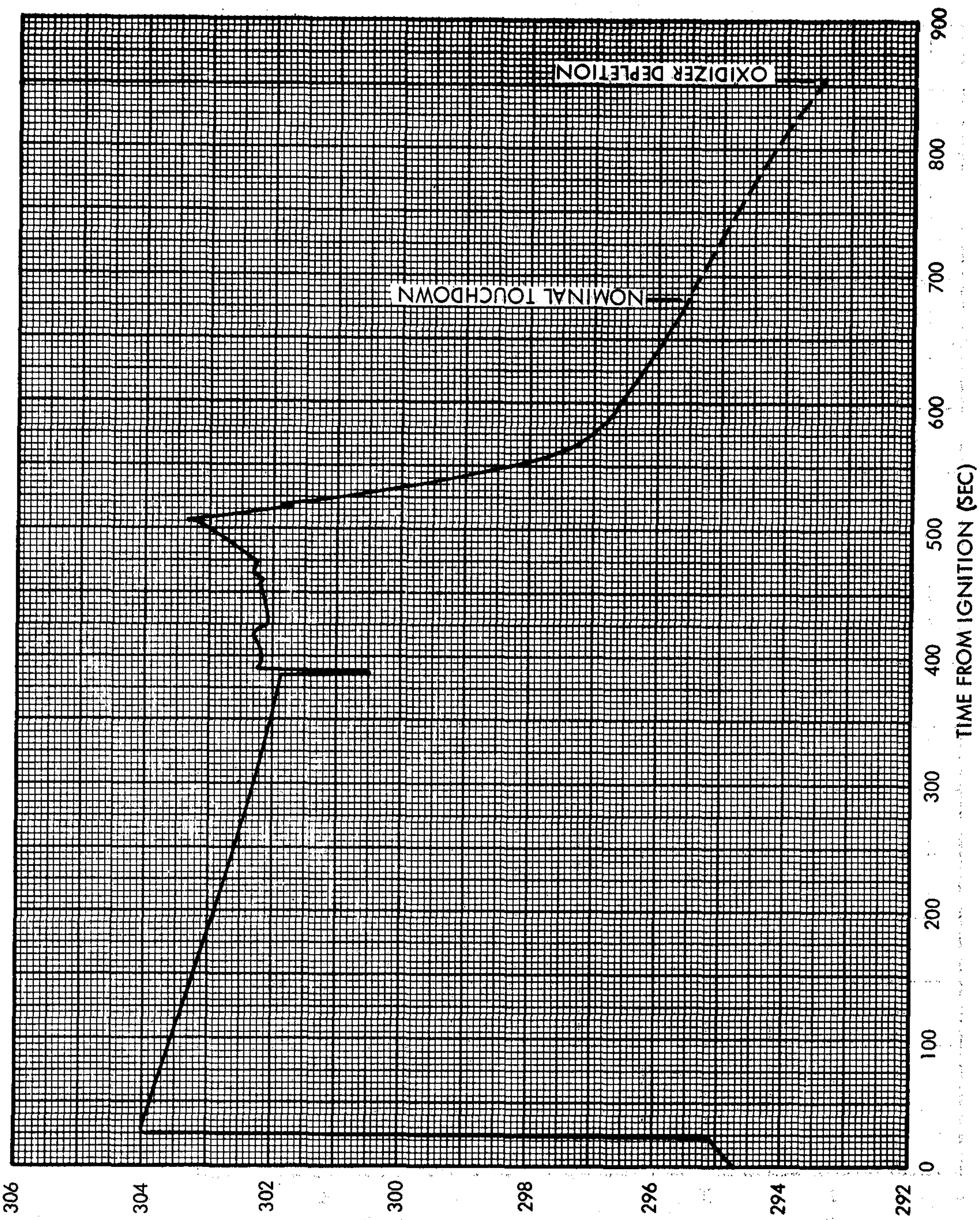

Figure LM7/4.7.1-2 Mission H2 Final DPS Preflight Performance Prediction - Specific Impulse Vs. Time

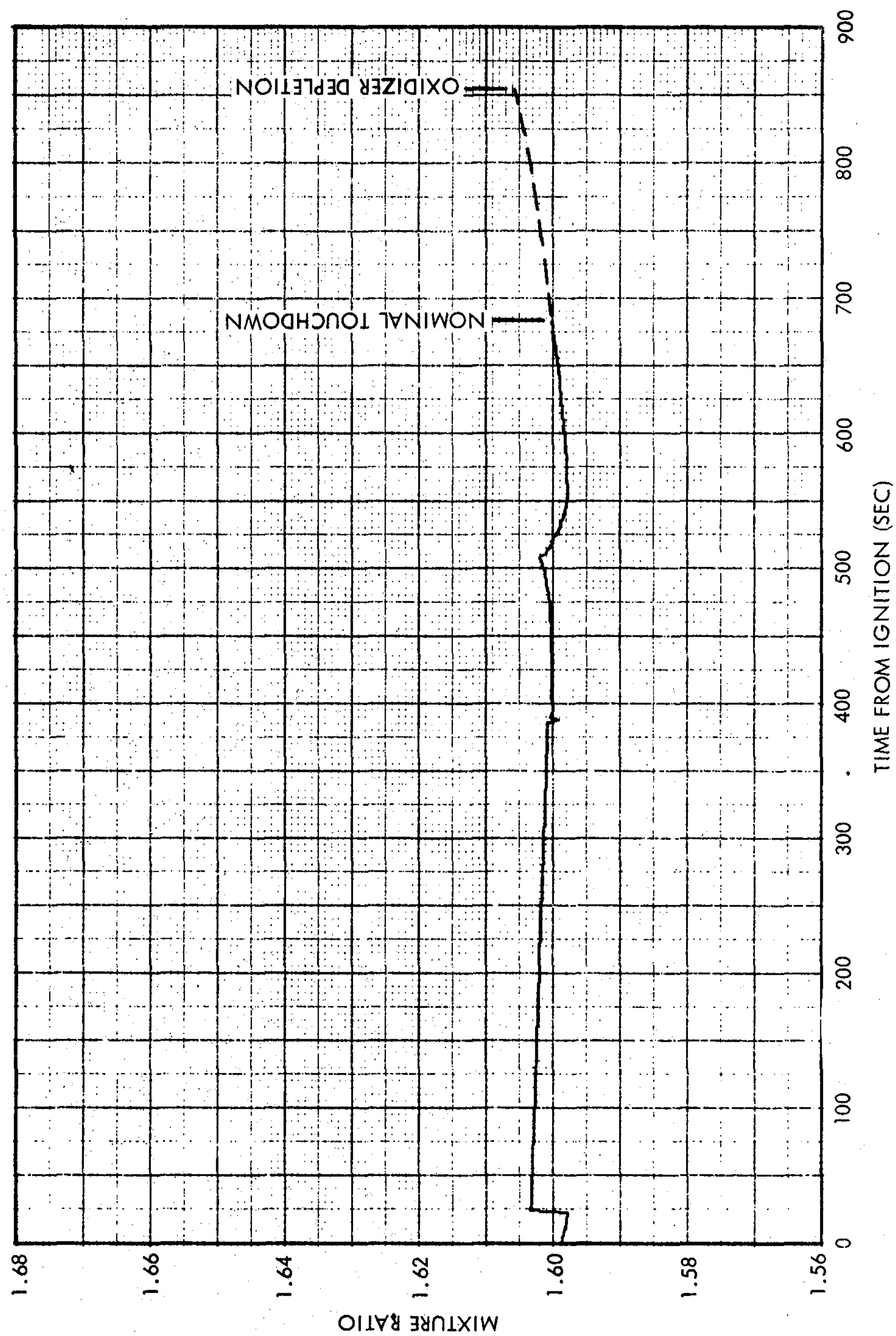

Figure LM7/4.7.1-3 Mission H2 Final DPS Preflight Performance Prediction - Mixture Ratio Vs. Time

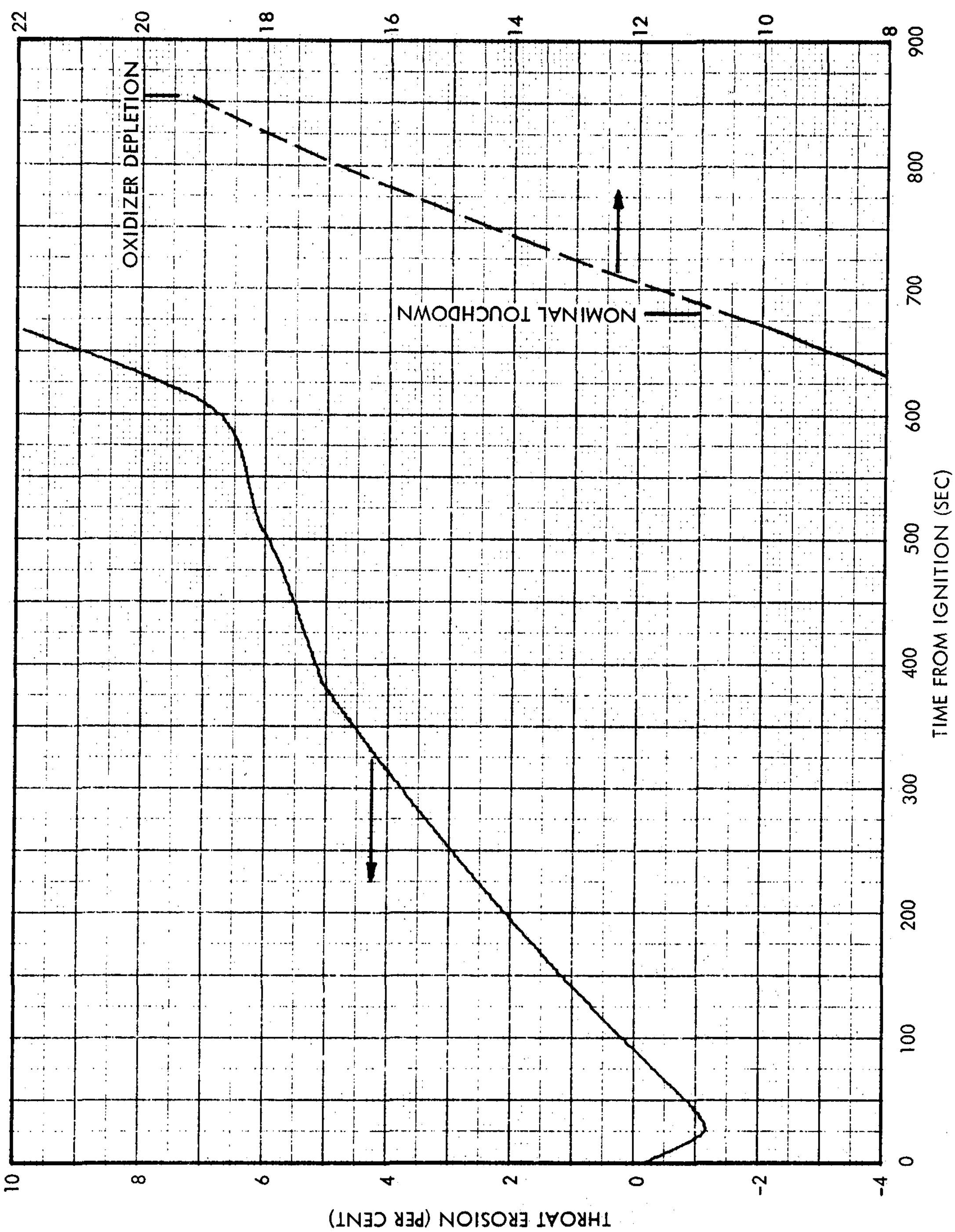

Figure LM7/4.7.1-4 Mission H2 Final DPS Preflight Performance Prediction - Throat Erosion Vs. Time

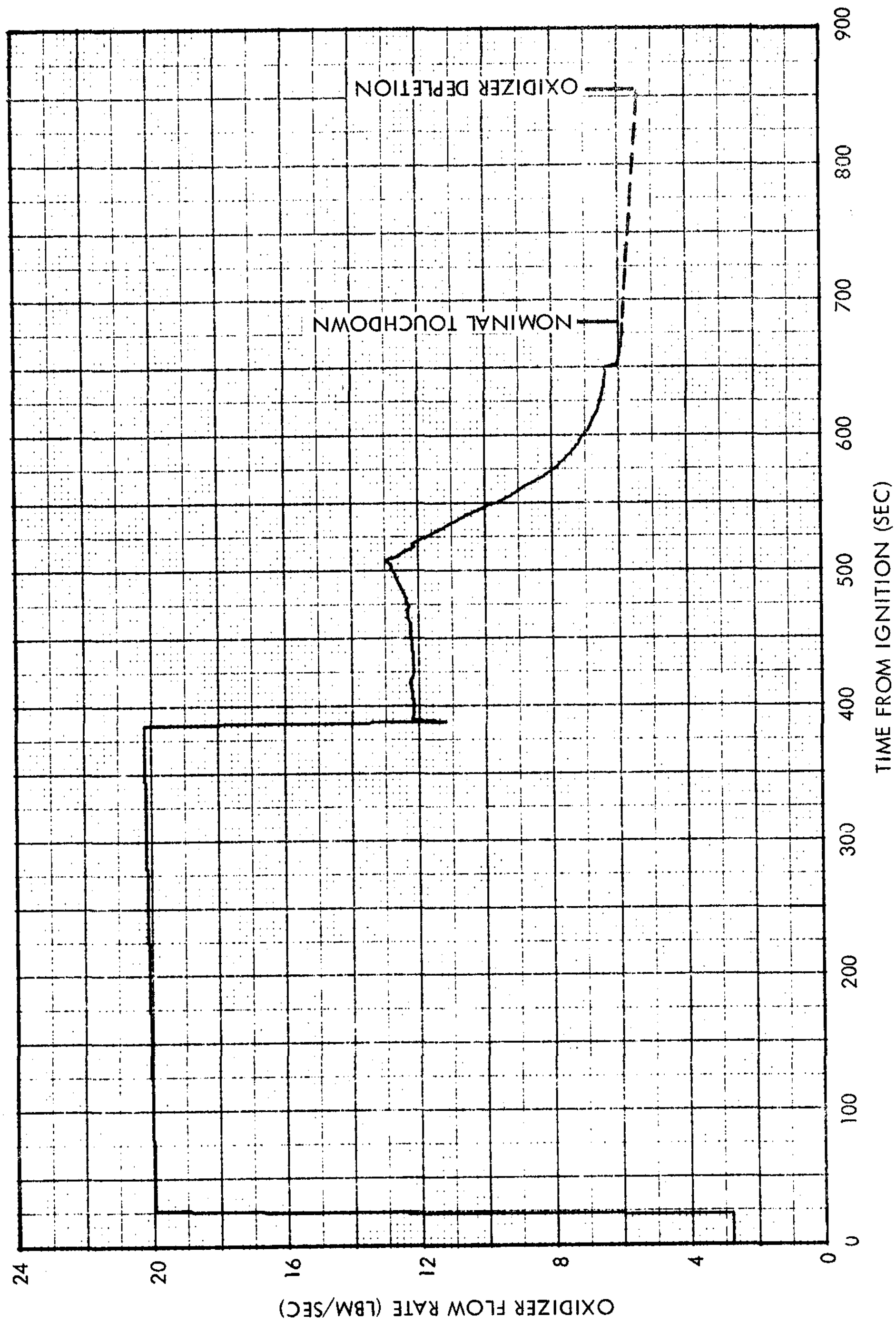

Figure LM7/4.7.1-5 Mission H2 Final DPS Preflight Performance Prediction - Oxidizer Flow Rate Vs. Time

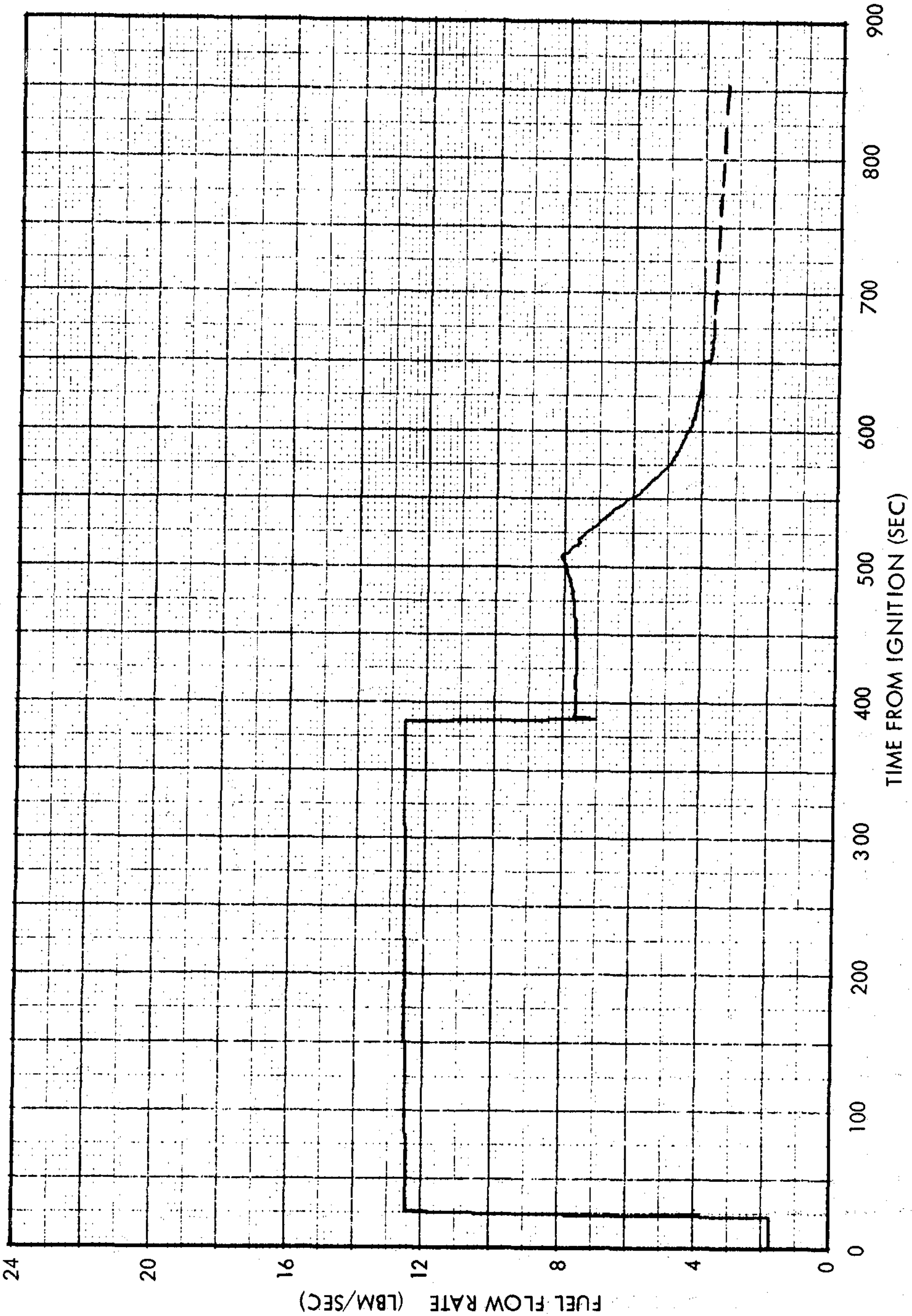

Figure LM7/4.7.1-6 Mission H2 Final DPS Preflight Performance Prediction - Fuel Flow Rate Vs. Time

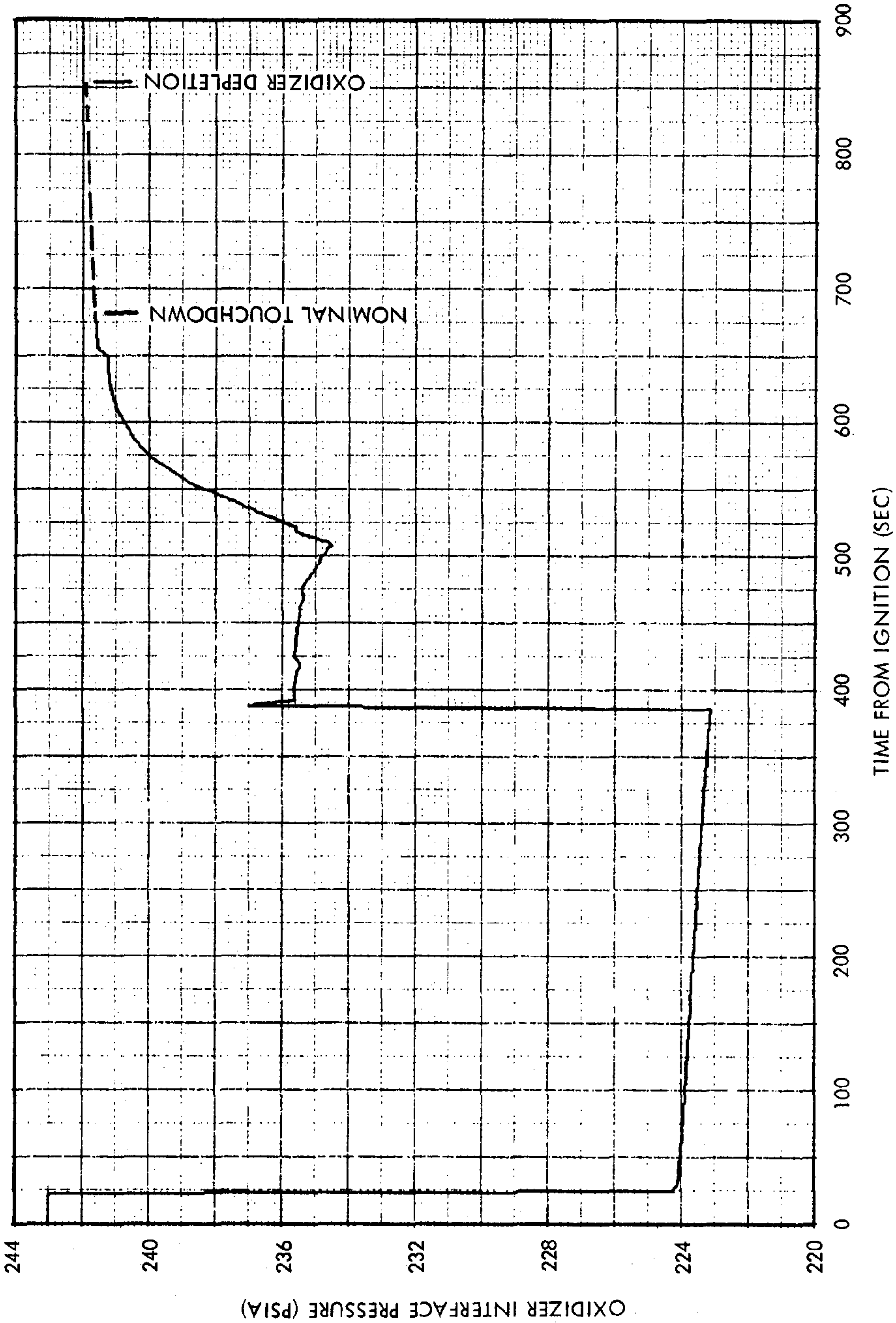

Figure LM7/4.7.1-7 Mission H2 Final DPS Preflight Performance Prediction - Oxidizer Interface Pressure Vs. Time

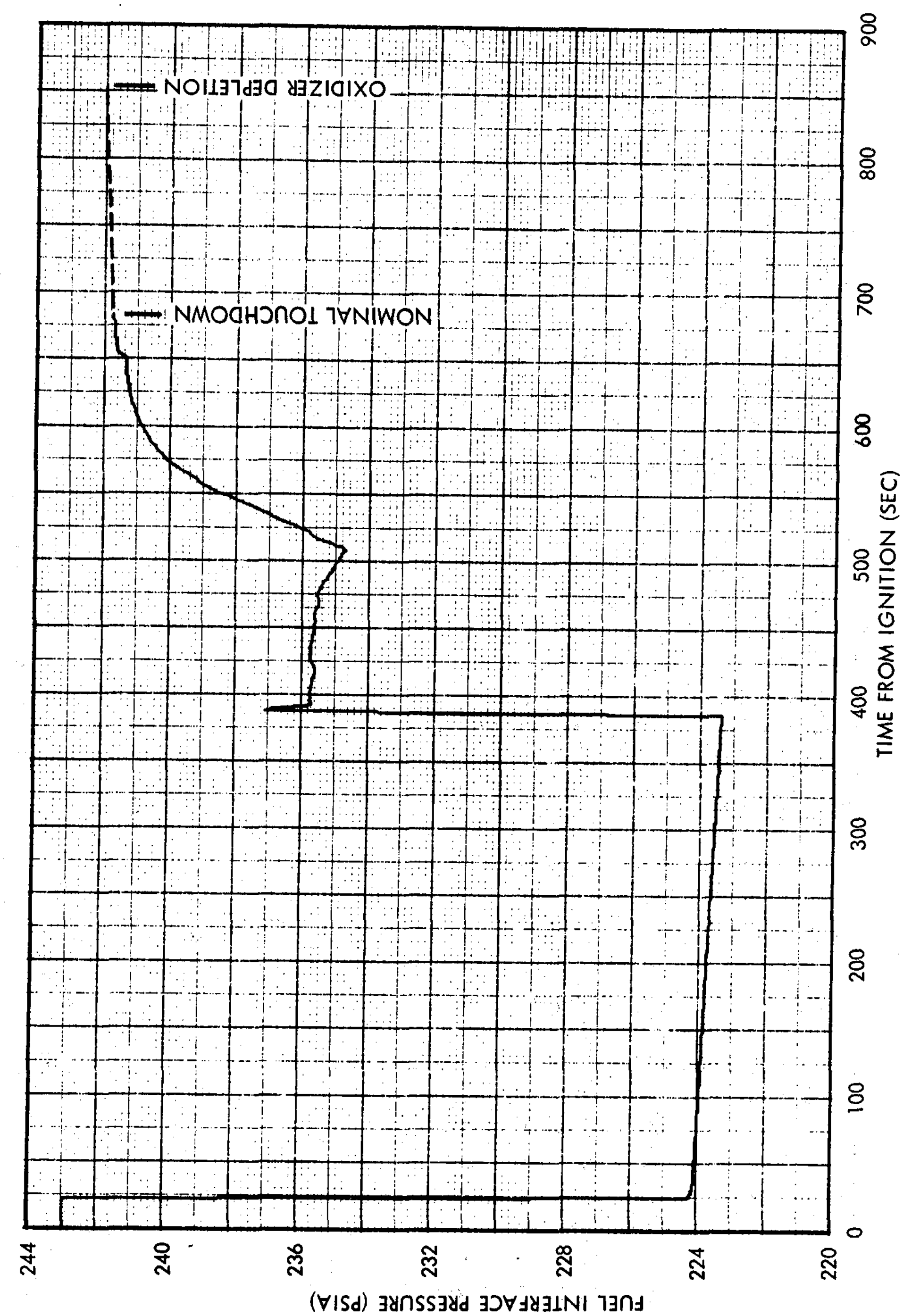

Figure LM7/4.7.1-8 Mission H2 Final DPS Preflight Performance Prediction - Fuel Interface Pressure Vs. Time

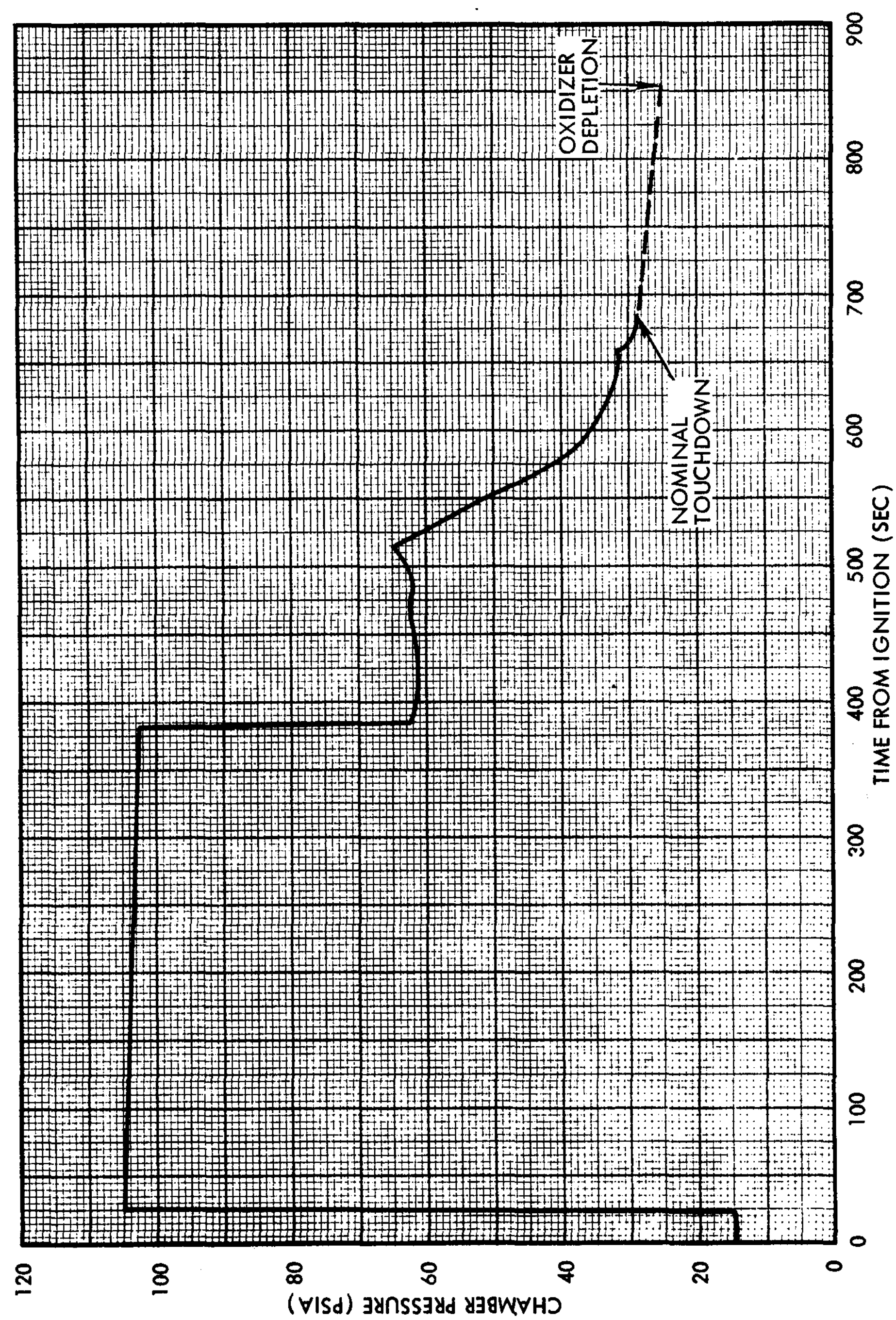

Figure LM7/4.7.1-9 Mission H2 Final DPS Preflight Performance Prediction - Chamber Pressure Vs. Time

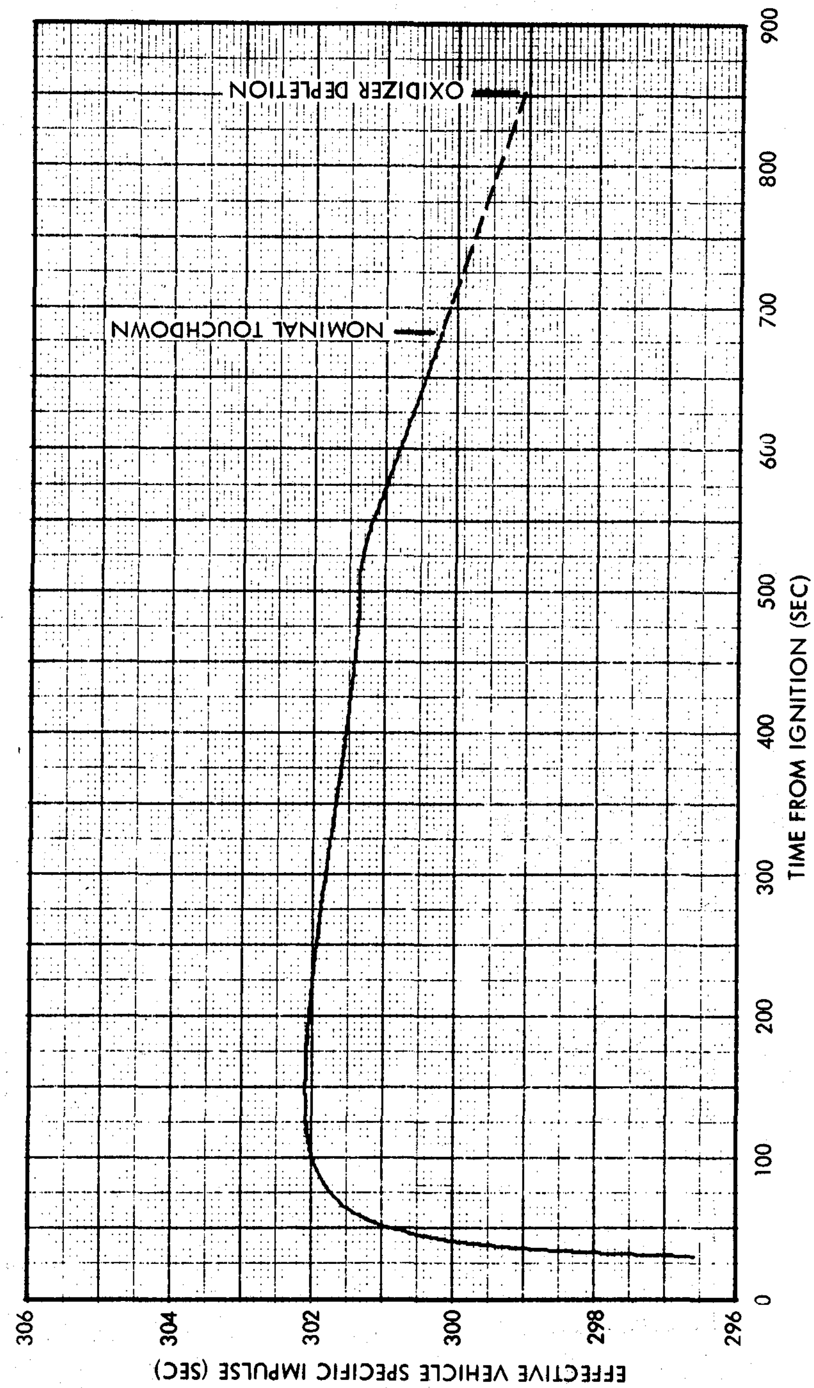

Figure LM7/4.7.1-10 Mission H2 Final DPS Preflight Performance Prediction - Effective Vehicle Specific Impulse Vs. Time

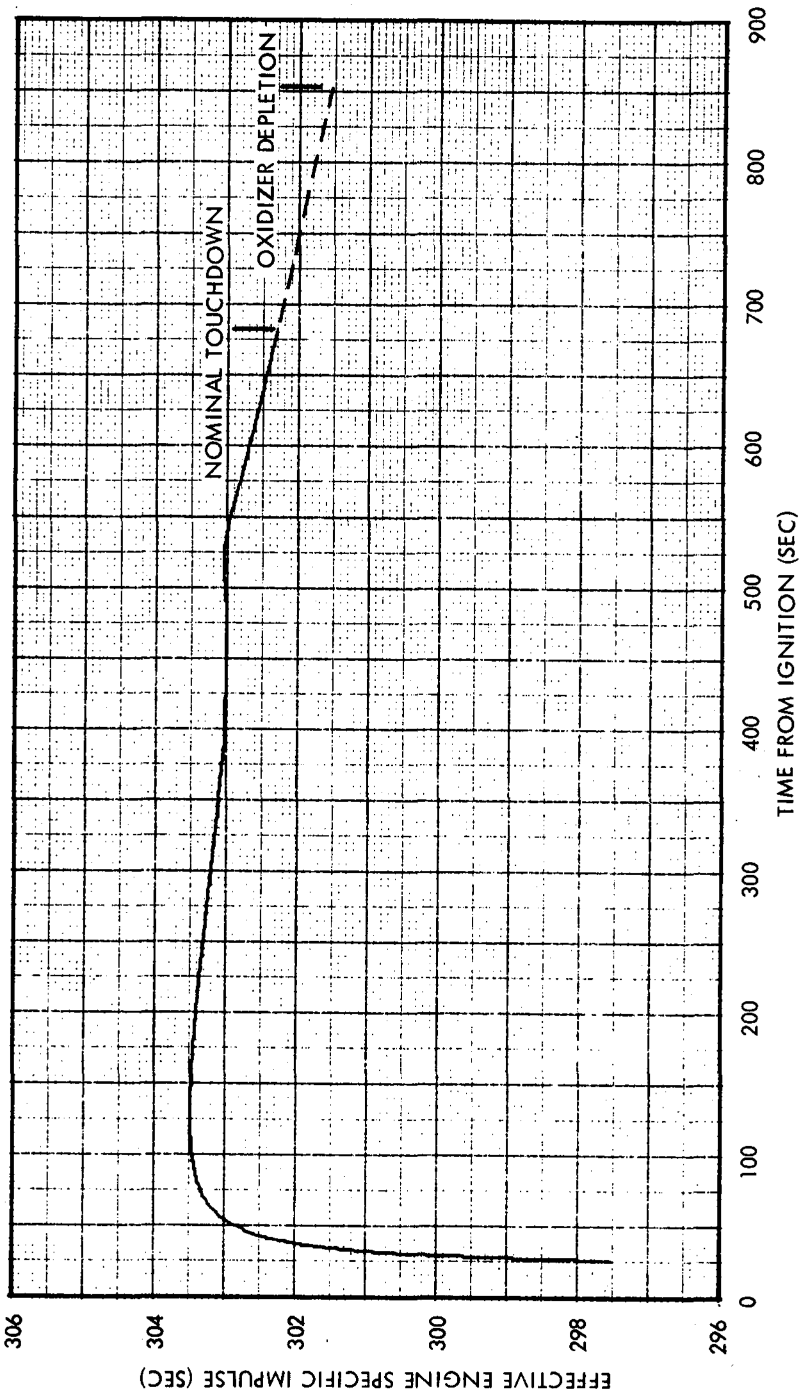

Figure LM7/4.7.1-11 Mission H2 Final DPS Preflight Performance Prediction - Effective Engine Specific Impulse Vs. Time

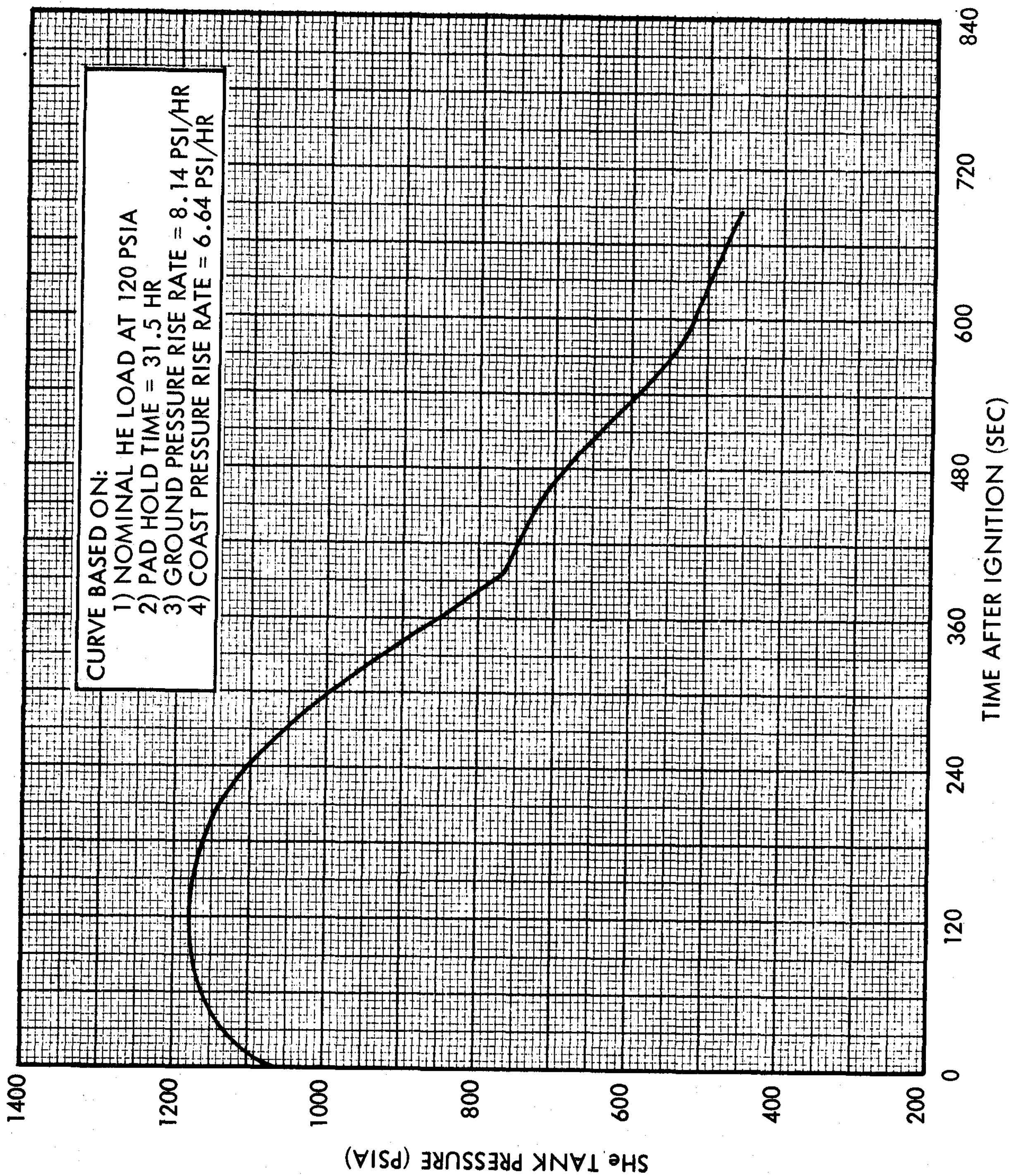

Figure LM7/4.7.1-12 Mission H2 Final DPS Preflight Performance Prediction - Supercritical Helium Bottle Pressure Vs. Time

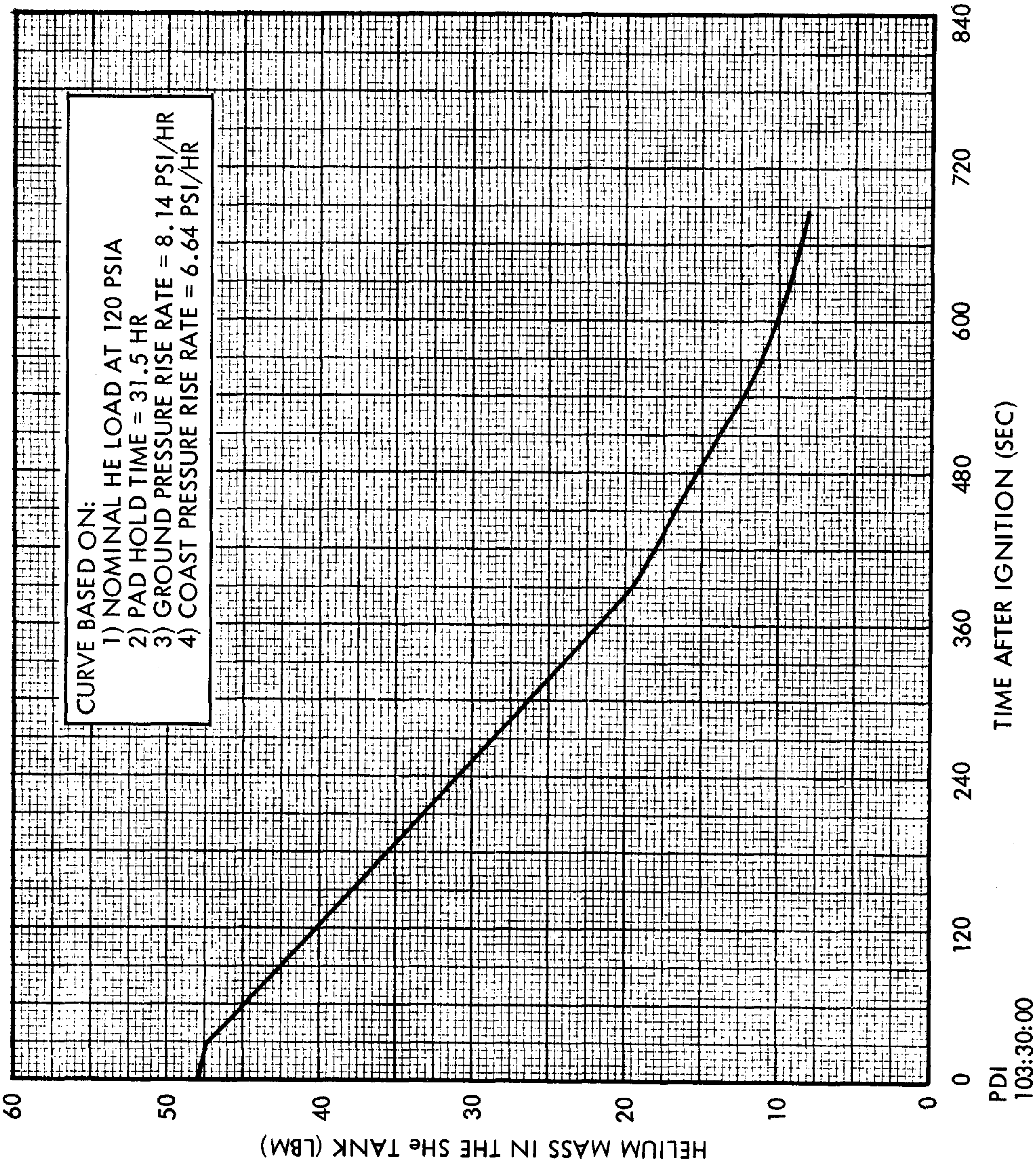

Figure LM7/4.7.1-13 Mission H2 DPS Preflight Performance Prediction - Supercritical Helium Mass Vs. Time

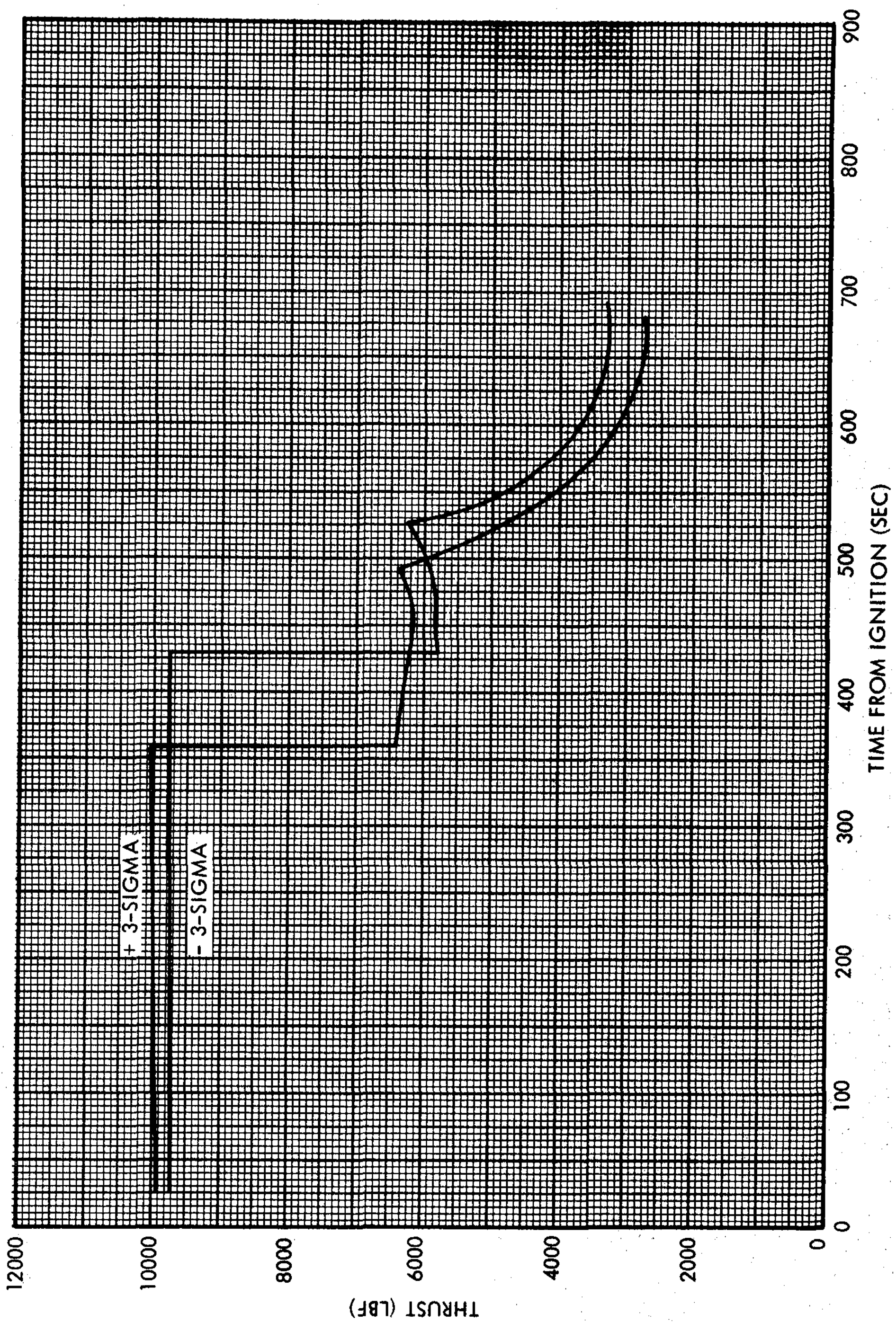

Figure LM7/4.7.1-14 Mission H2 DPS Preflight Performance Prediction - Thrust Dispersion Vs. Time

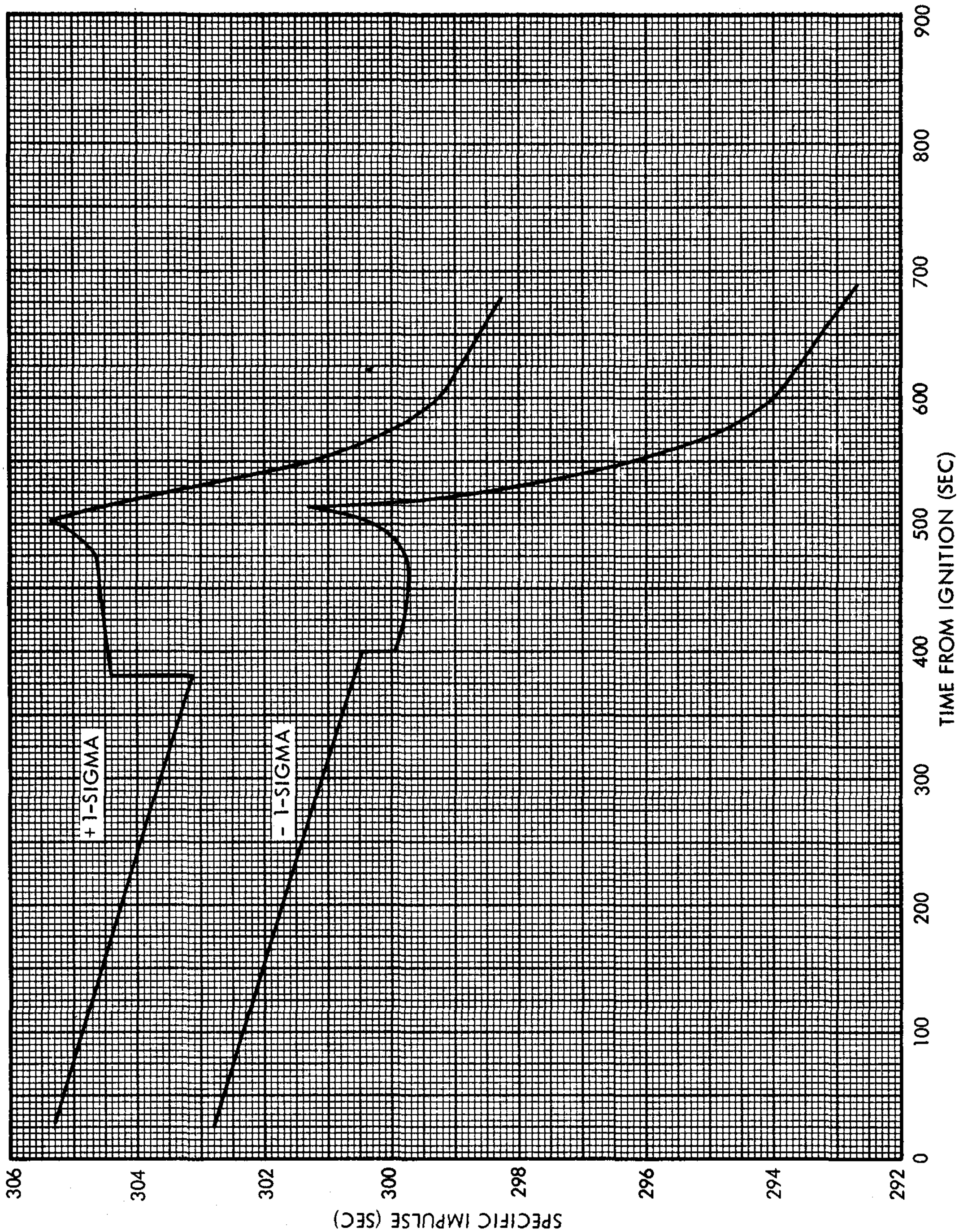

Figure LM7/4.7.1-15 Mission H2 Final DPS Preflight Performance Prediction - Specific Impulse Dispersion Vs. Time

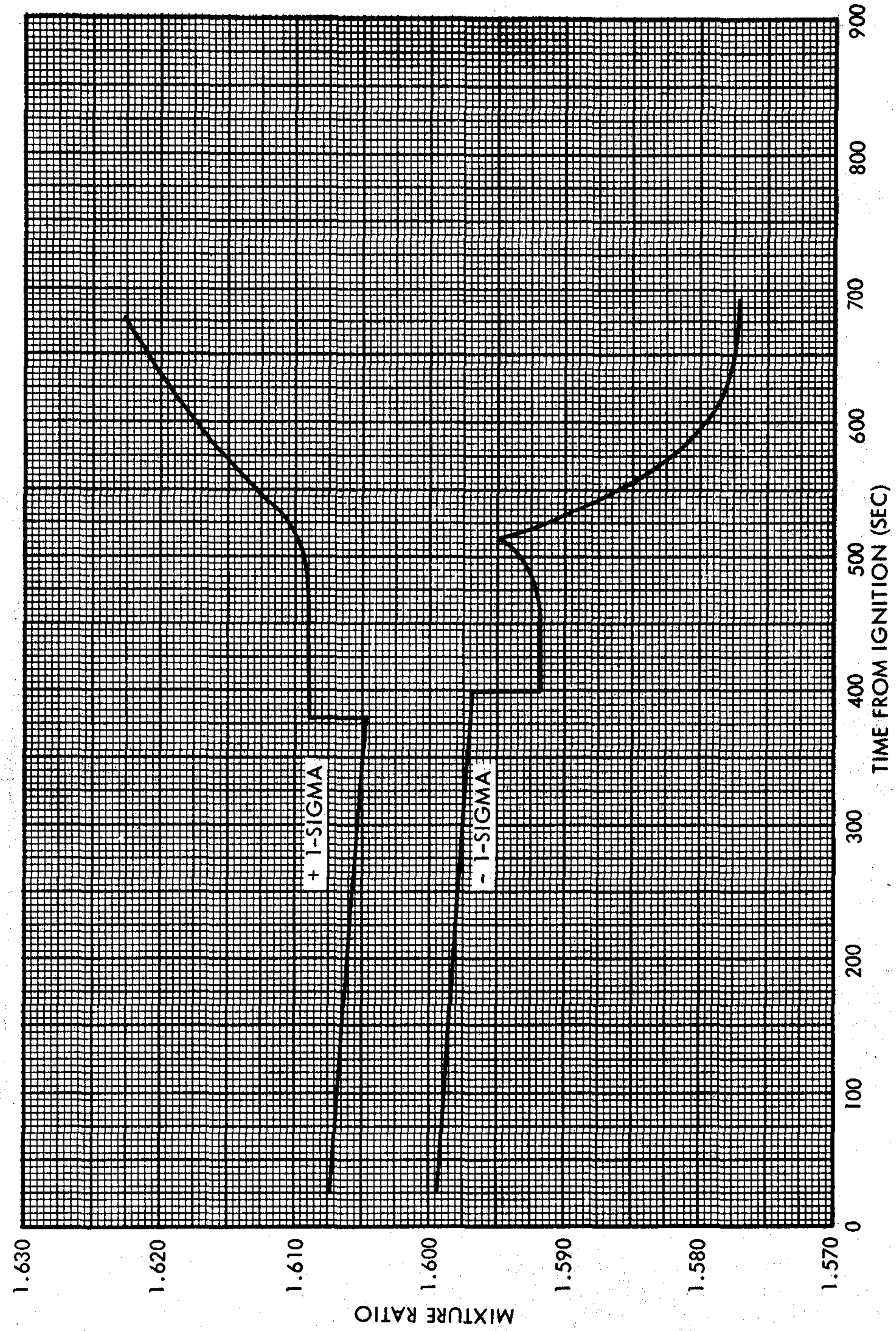

Figure LM7/4.7.1-16 Mission H2 Final DPS Preflight Performance Prediction - Mixture Ratio Dispersion Vs. Time

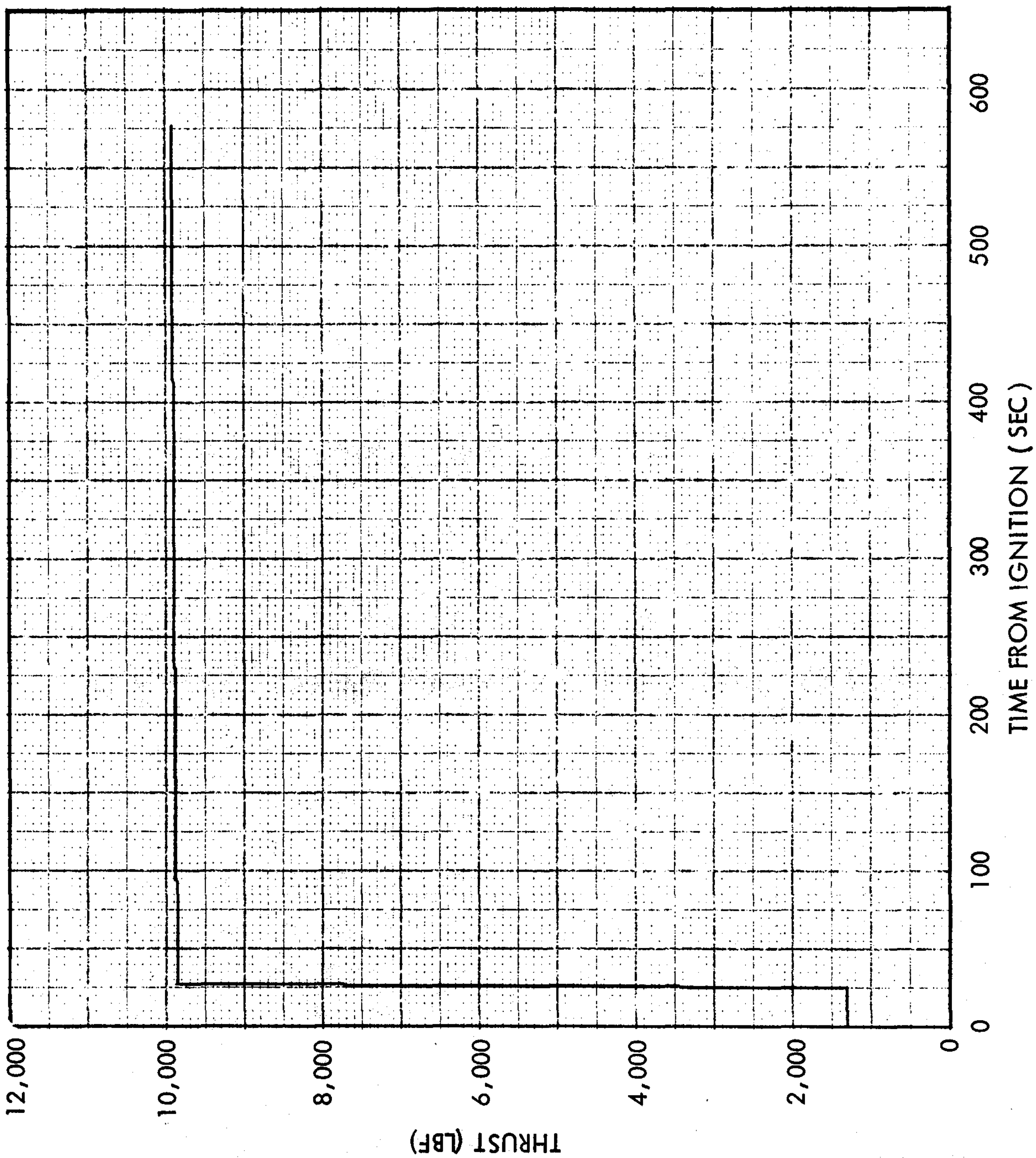

Figure LM7/4.7.1-17 Mission H2 DPS Preflight Performance Prediction - Docked FTP Burn-to-Depletion - Thrust Vs. Time

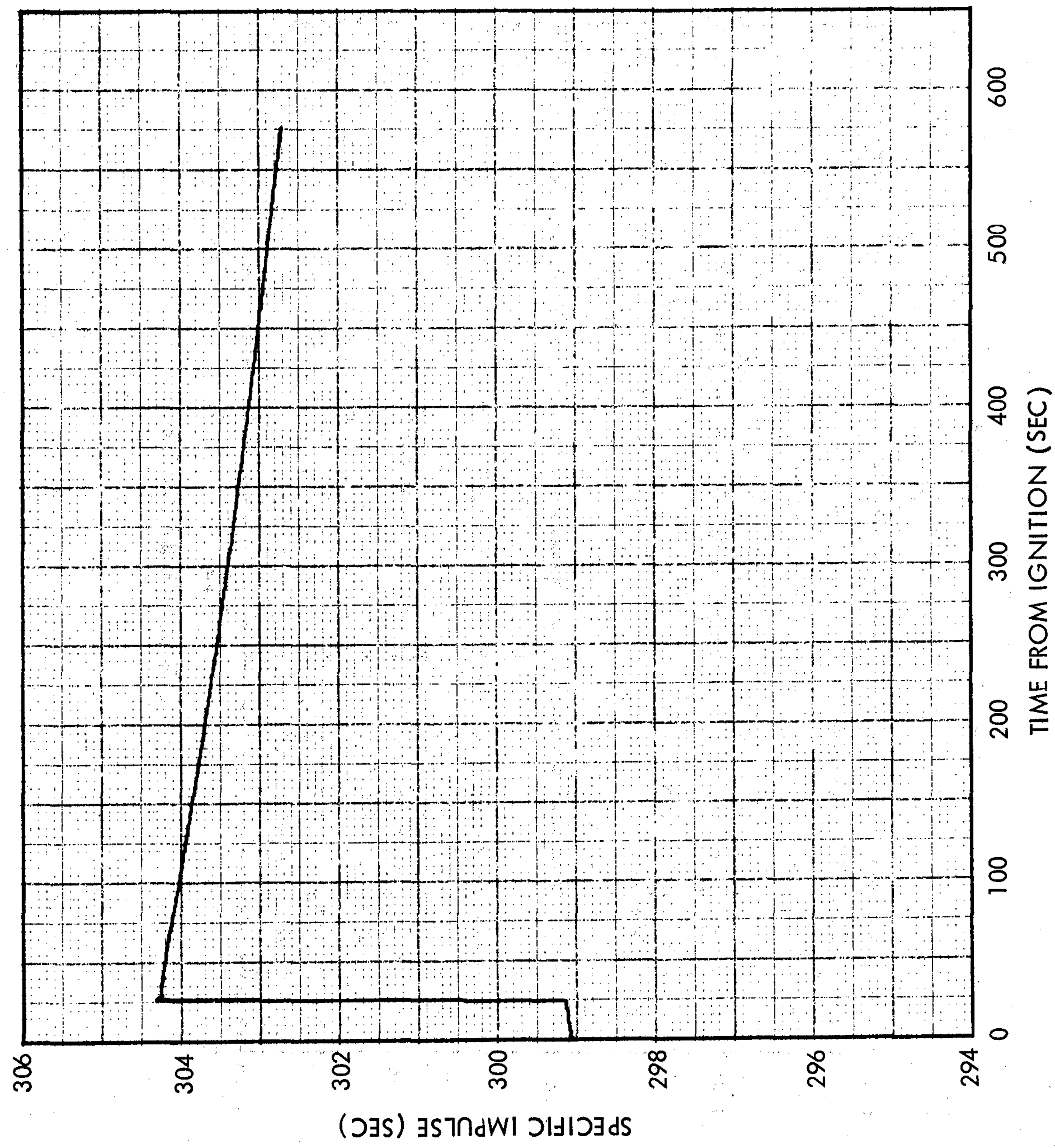

Figure LM7/4.7.1-18 Mission H2 DPS Preflight Performance Prediction - Docked FTP Burn-to-Depletion - Specific Impulse Vs. Time

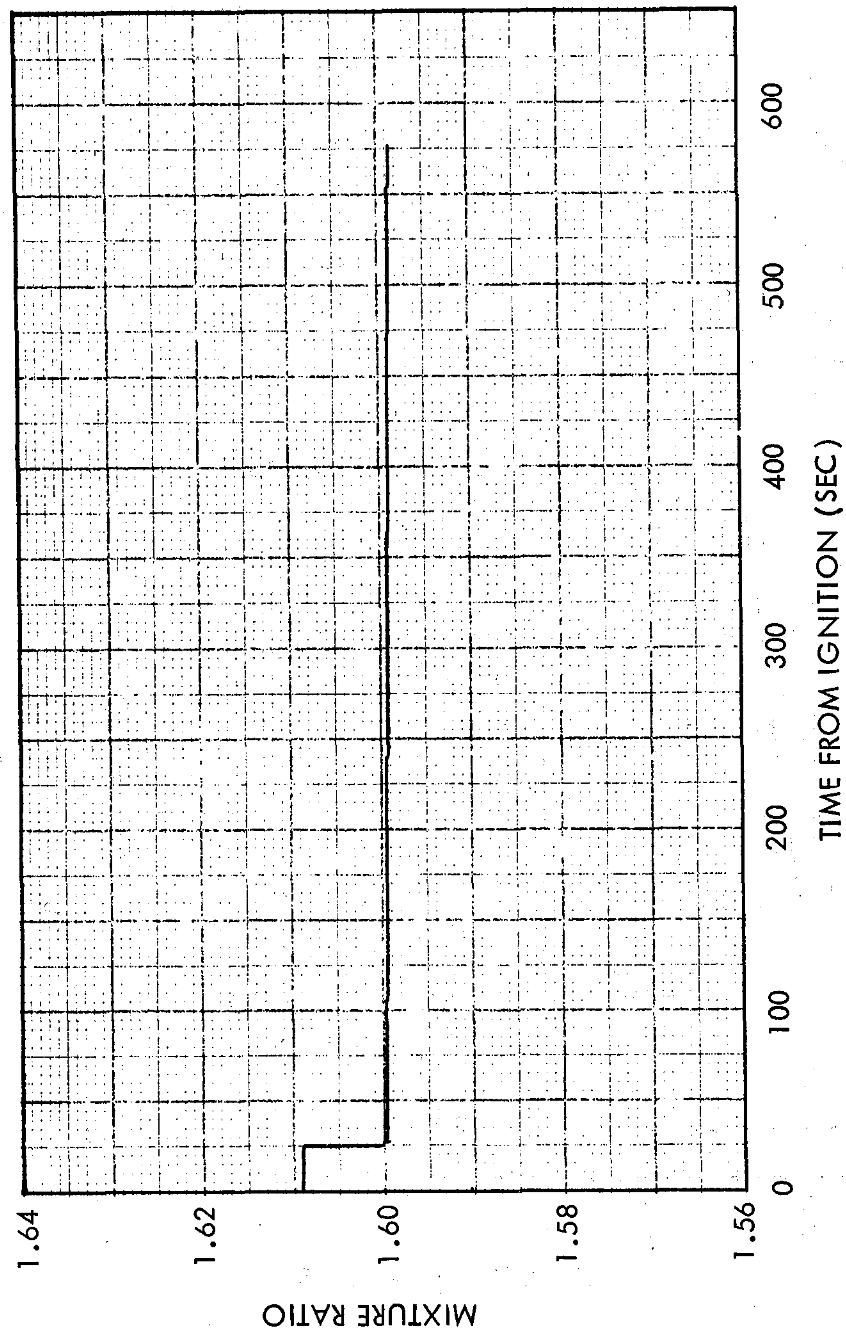

Figure LM7/4.7.1-19 Mission H2 DPS Preflight Performance Prediction - Docked FTP Burn-to-Depletion - Mixture Ratio Vs. Time

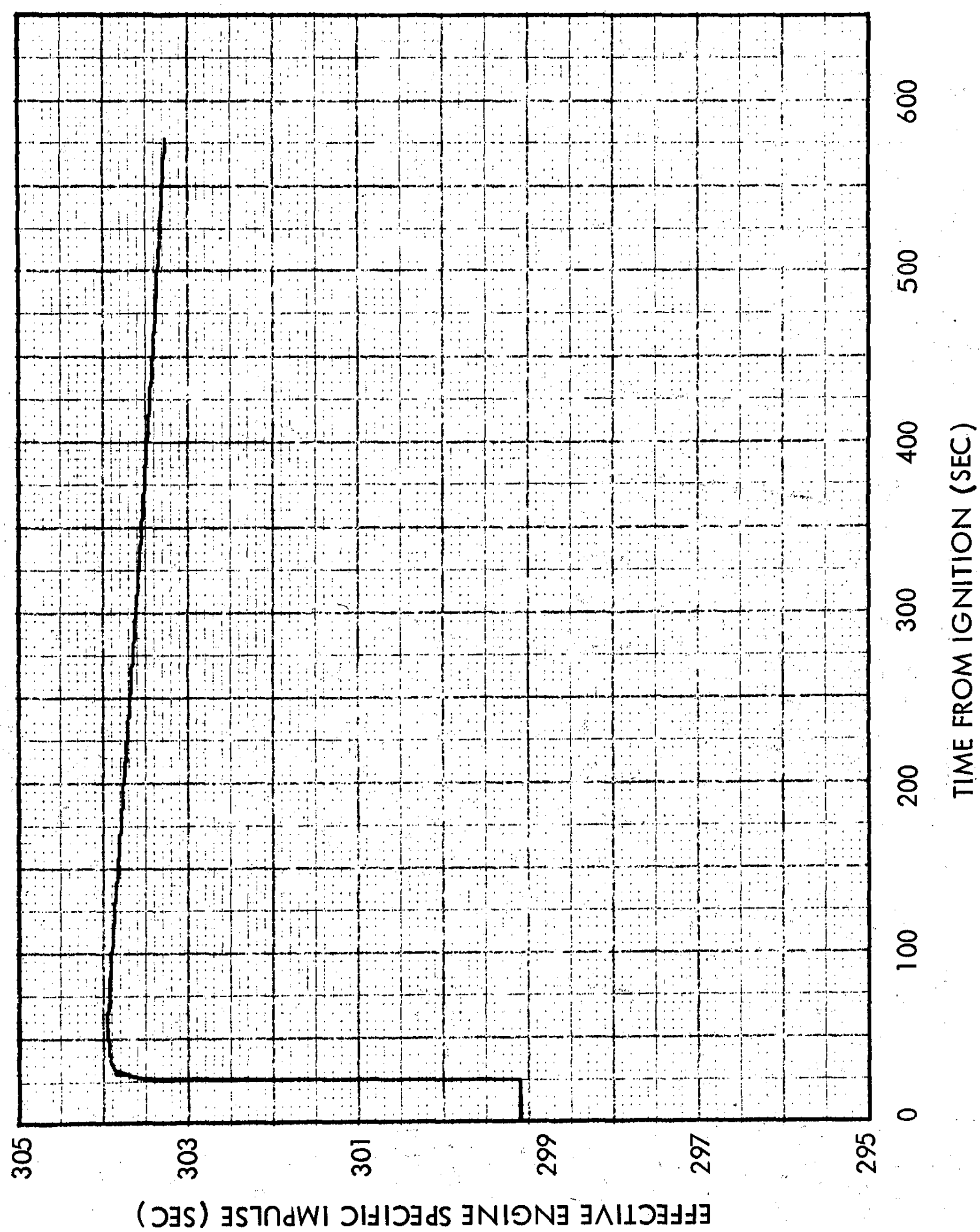

Figure LM7/4.7.1-20 Mission H2 DPS Preflight Performance Prediction - Docked FTP Burn-to-Depletion - Effective Engine Isp Vs. Time

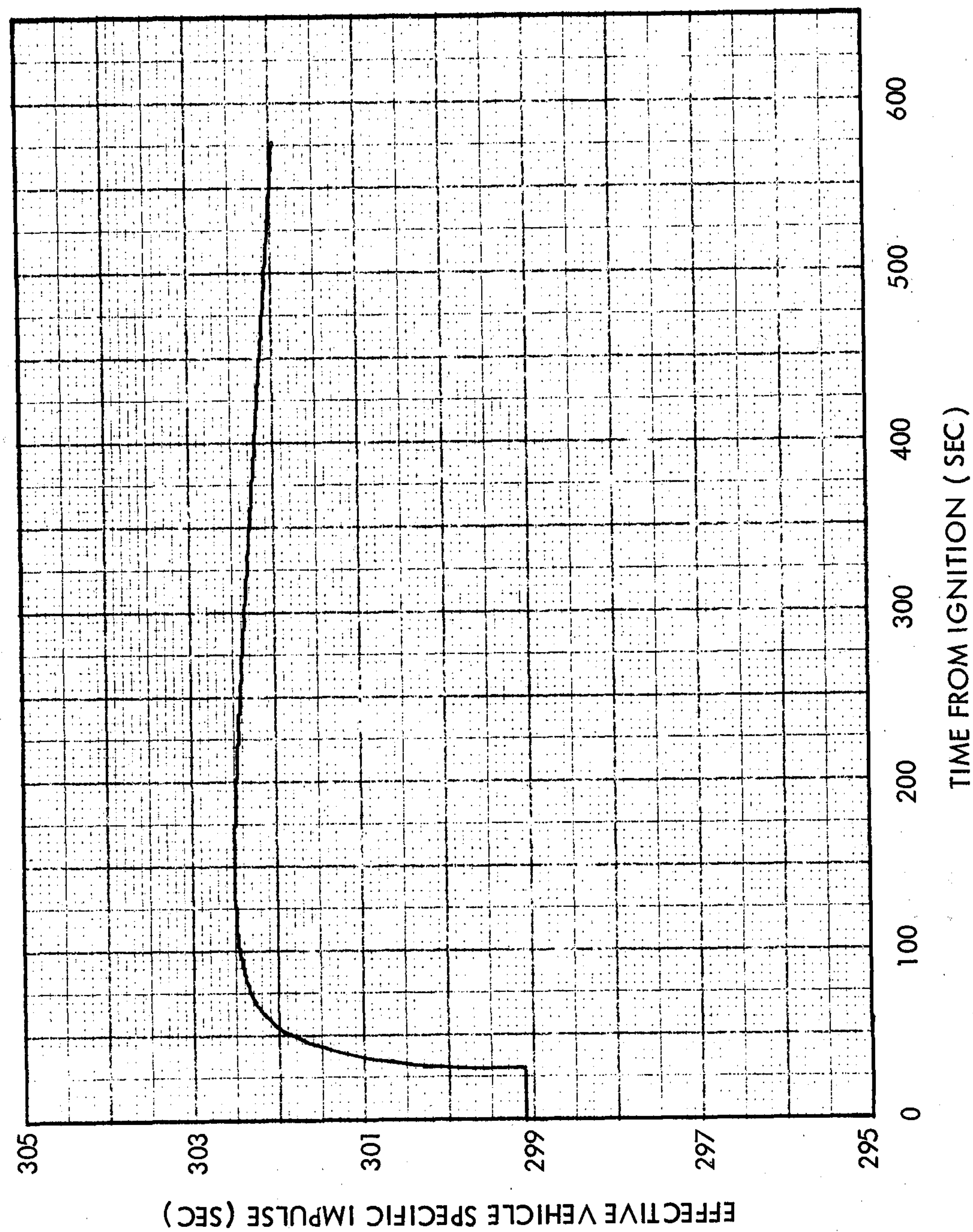

Figure LM7/4.7.1-21 Mission H2 DPS Preflight Performance Prediction - Docked FTP Burn-to-Depletion - Effective Vehicle Isp Vs. Time

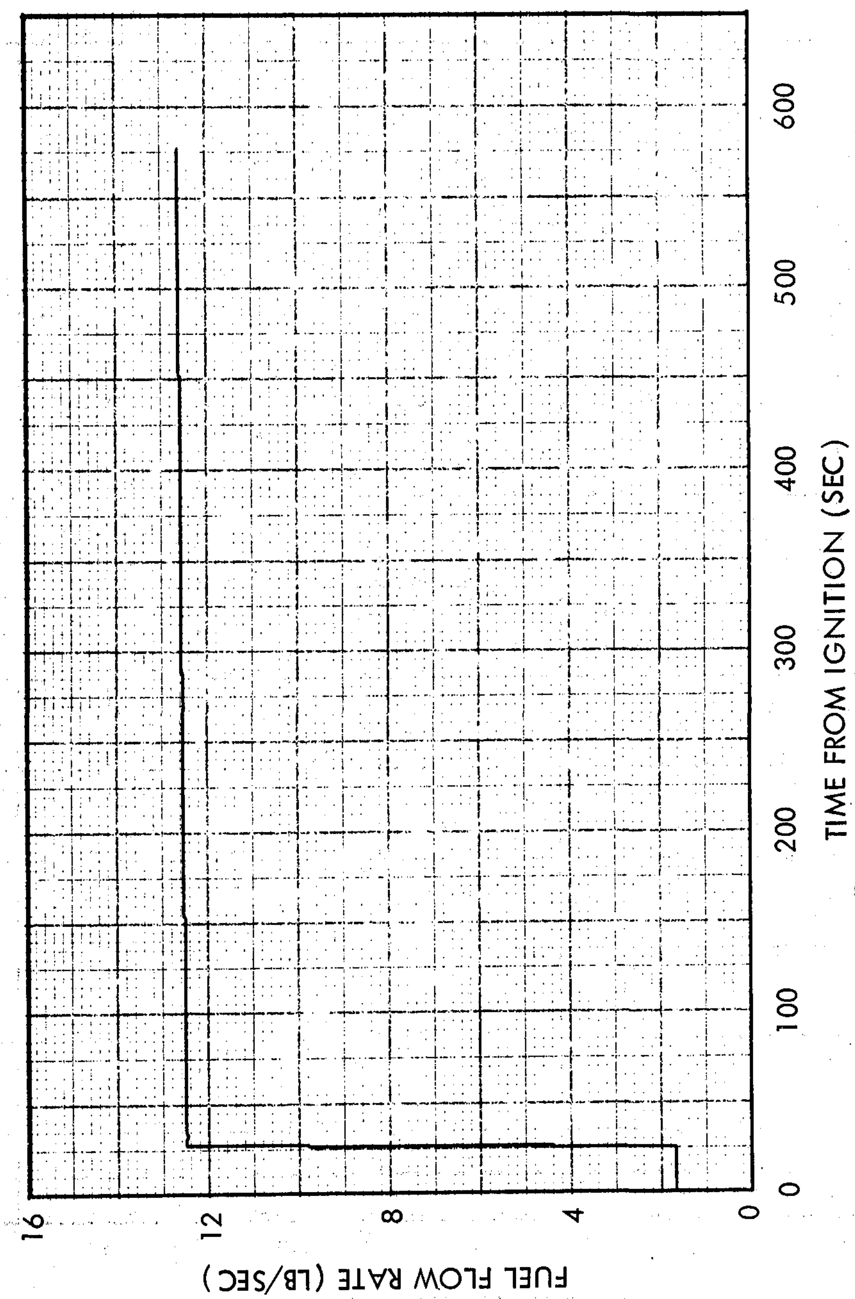

Figure LM7/4.7.1-22 Mission H2 DPS Preflight Performance Prediction - Docked FTP Burn-to-Depletion - Fuel Flow Rate Vs. Time

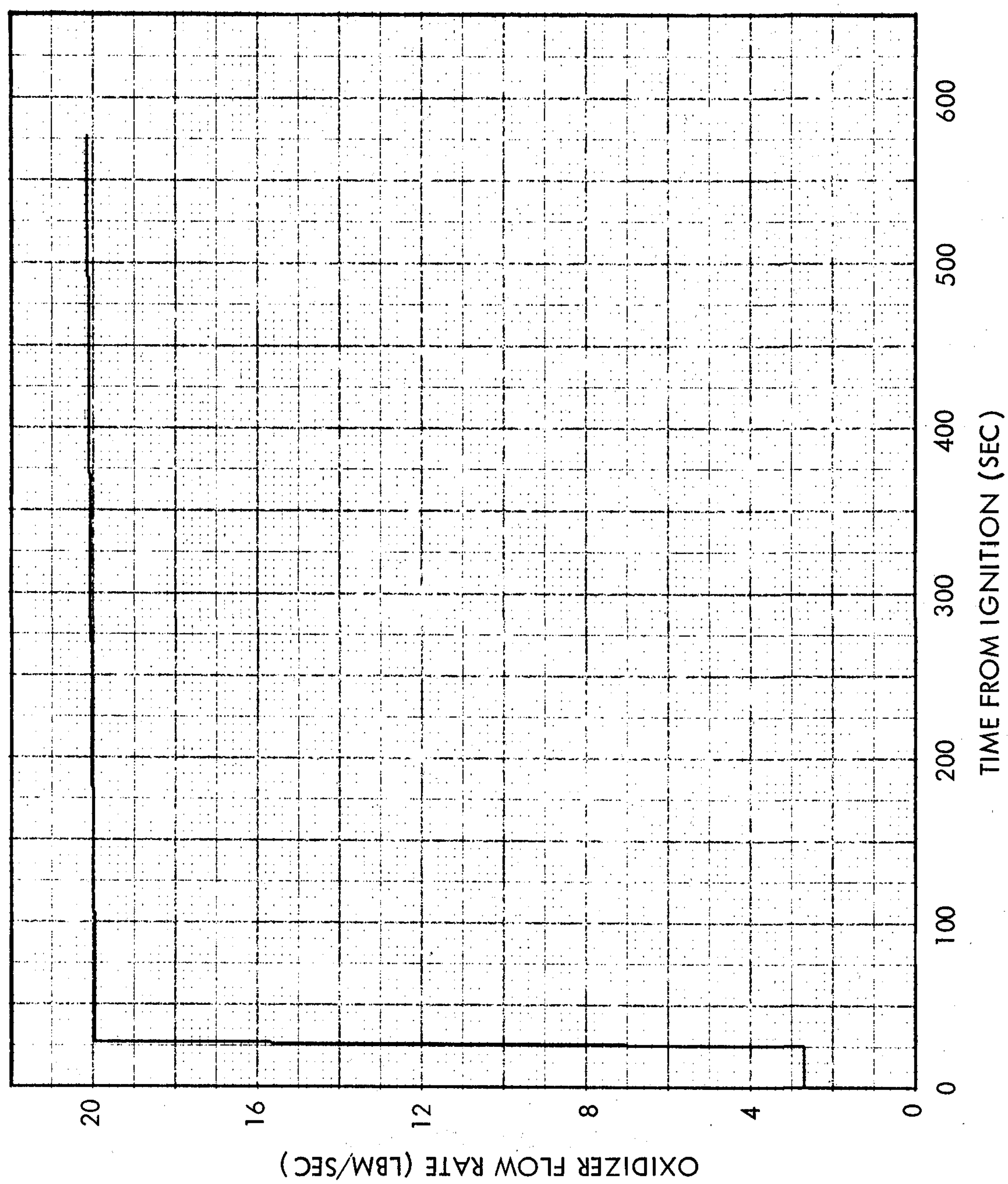

Figure LM7/4.7.1-23 Mission H2 DPS Preflight Performance Prediction - Docked FTP Burn-to-Depletion - Oxidizer Flow Rate Vs. Time

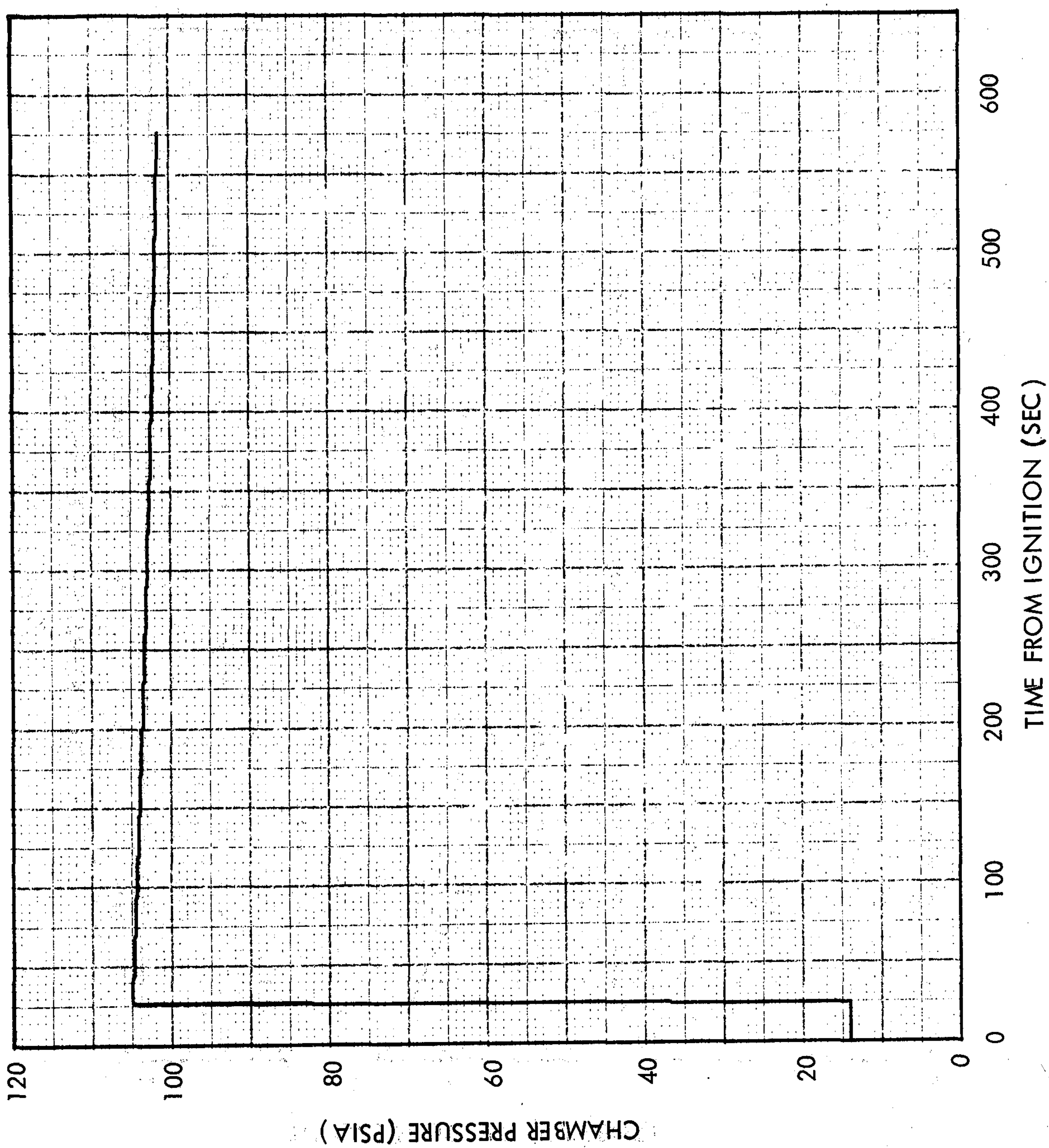

Figure LM7/4.7.1-24 Mission H2 DPS Preflight Performance Prediction - Docked FTP Burn-to-Depletion - Chamber Pressure Vs. Time

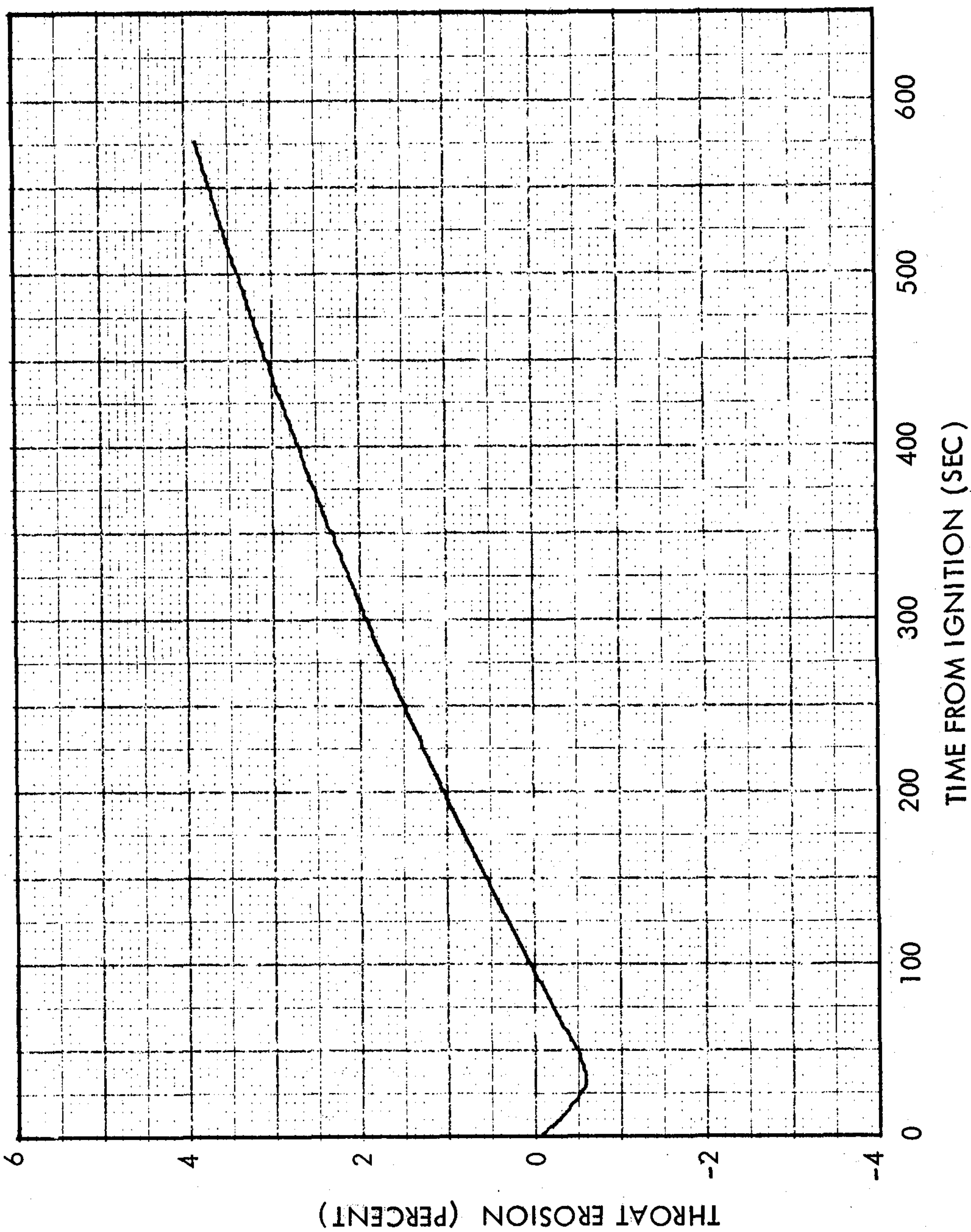

Figure LM7/4.7.1-25 Mission H2 DPS Preflight Performance Prediction - Docked FTP Burn-to-Depletion - Throat Erosion Vs. Time

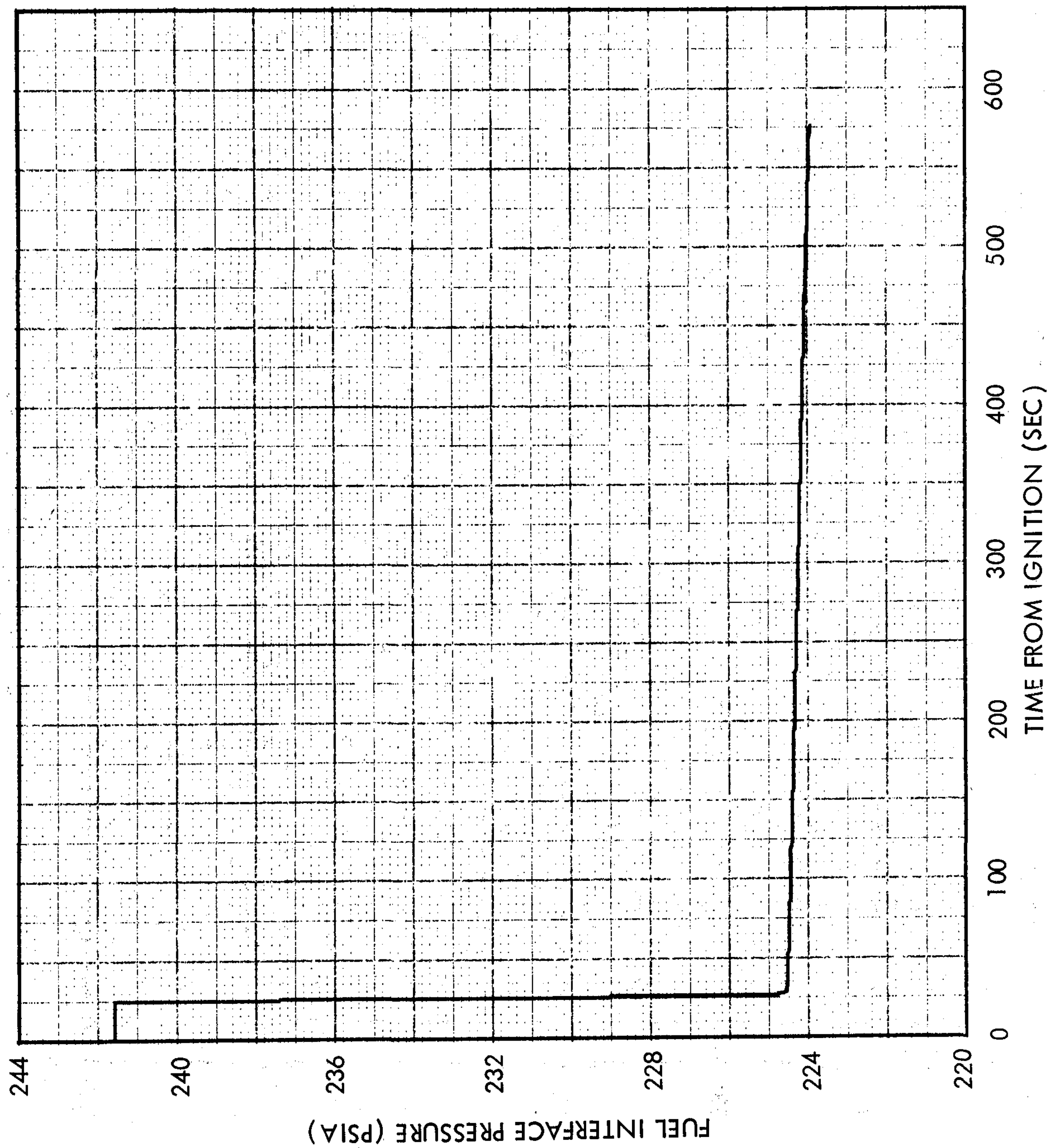

Figure LM7/4.7.1-26 Mission H2 DPS Preflight Performance Prediction - Docked FTP Burn-to-Depletion - Fuel Interface Pressure Vs. Time

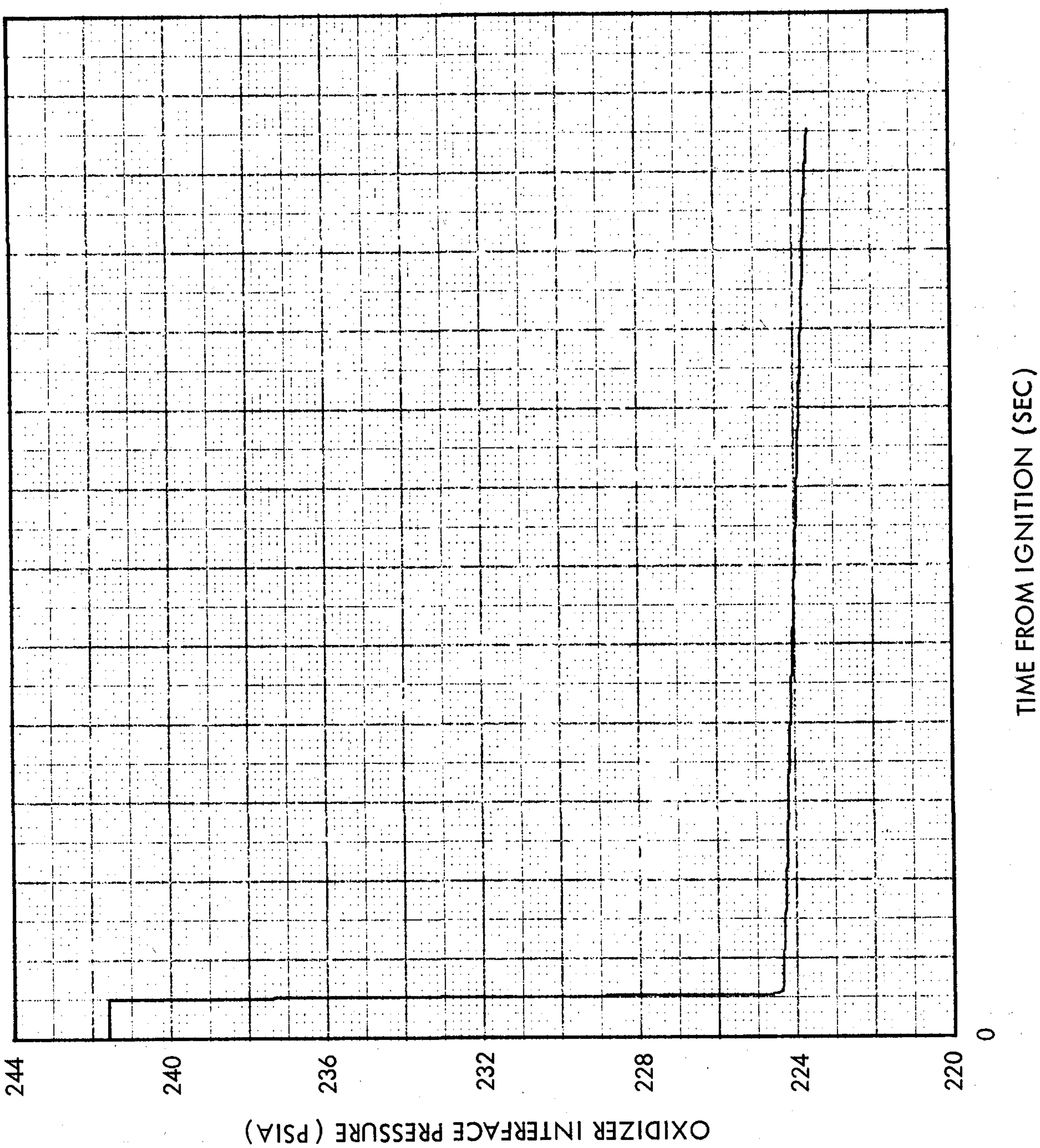

Figure LM7/4.7.1-27 Mission H2 DPS Preflight Performance Prediction - Docked FTP Burn-to-Depletion - Oxidizer Interface Pressure Vs. Time

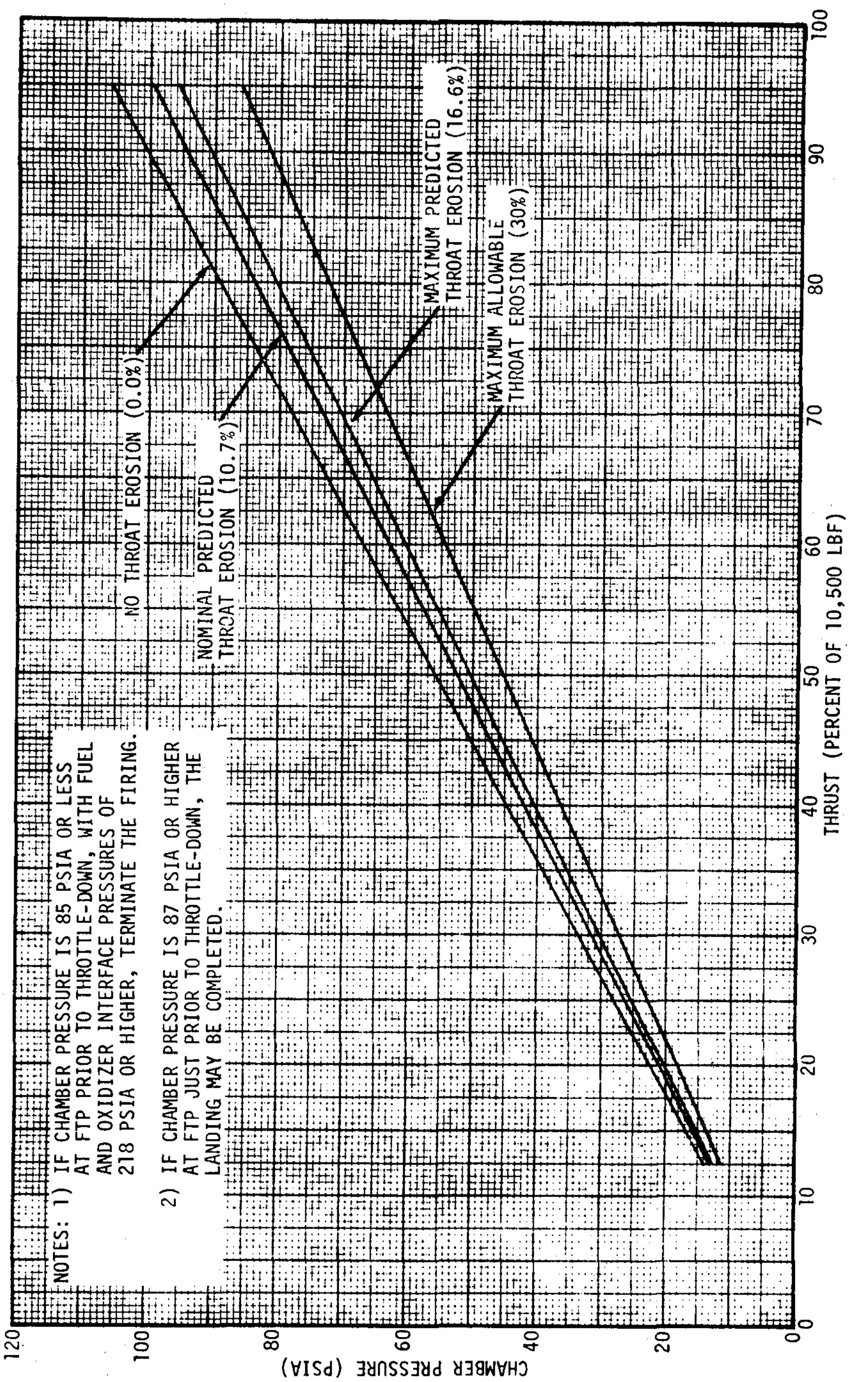

Figure LM7/4.7.1-28 Mission H2 DPS Preflight Performance Prediction - Chamber Pressure Vs. Commanded Thrust for Zero, Nominal, Maximum Predicted and Maximum Allowable Throat Erosion

LM7/4.7.5 DPS Propellant Tank Low Level Sensor Operation

Data from GAC give the propellant quantities remaining in the DPS tanks (at 70°F) at the time of low level sensor actuation as:

Tank	Quantity
Fuel	202±9.9 lbm per tank
Oxidizer	322±13.4 lbm per tank

The propellants in the feed lines and heat exchanger should be added, and the propellants in the zero-g can and for unporting prevention should be deducted from the above quantities. Values for these are taken from the Spacecraft Operational Data Book, Volume III, Rev 2, 20 August 1969, Section 5.6:

Component	Fuel, lbm	Oxidizer, lbm
Feed Lines	+12.1	+27.5
Heat Exchanger	+ 4.6	-0-
Zero-G Can	- 5.2	- 8.6
Unporting Prevention	-10.7	-16.0
Total	+ 0.8	+ 2.9

The propellant quantity corrections tabulated above should be applied regardless of whether depletion occurs from a single tank or both tanks of a pair simultaneously. This is so because in both cases the trapped quantities will be used or not used identically (helium ingestion upon depletion of a single tank effectively shuts off the undepleted tank). Also, since at the time of low level sensor actuation it is not possible to determine whether or not both tanks of a pair are at the same propellant level (they both could be at the high or at the low level), the single tank dispersions should be summed to arrive at the dispersions for both tanks of a pair taken together.

Based upon the above statements and data the propellant quantities available after low level sensor actuation are as follows:

Fuel	404.8±19.8 lbm
Oxidizer	646.9±26.8 lbm

The mean values of fuel and oxidizer flow rate during hover from low level sensor actuation to depletion were calculated to be:

Fuel Flow Rate: 3.465 lbm/sec

Oxidizer Flow Rate: 5.555 lbm/sec

(Spacecraft Operational Data Book, Volume II, Rev. 2, 1 September 1969, Para. LM7/4.7.1).

Using the above flow rates and propellant quantities the burn time from low level sensor actuation to depletion was calculated to be 116.8 seconds for fuel and 116.5 seconds for oxidizer. Both the burn times given above are slightly on the conservative side in as much as use of a mean flow rate is conservative by approximately 1.6 seconds compared to integrating along a thrust-time curve.

The dispersions associated with the burn times given above are ±5.7 seconds for fuel and ±4.8 seconds for oxidizer. Therefore, the minimum burn times from low level sensor actuation to depletion were calculated to be 111.1 seconds for fuel and 111.7 seconds for oxidizer.

Because there are two fuel and two oxidizer tanks, each with a low level sensor with the dispersion given in the first paragraph, the RSS dispersion for the two tanks of a pair represents a more likely case than the maximum dispersion case given immediately above. The RSS dispersions for the total fuel and total oxidizer available at low level sensor activation were calculated to be ±14.0 and ±19.0 lbm, respectively. The burn time dispersions associated with these quantities are ±4.0 seconds for fuel and ±3.4 seconds for oxidizer. Thus, the RSS minimum burn times were calculated to be 112.8 seconds for fuel and 113.1 seconds for oxidizer.

The above burn time calculations do not take into account the uncertainty about the nominal predicted flow rates.

LM7/4.7.6.1 DPS Engine Thrust Vector Alignment

The gimbal trim angles for the DPS engine may be calculated using the equations provided in Paragraph 4.7.6.1. The thrust vector angles of the DPS engine at the start of the DOI burn are given in the Spacecraft Operational Data Book, Volume III, Mass Properties, Revision 2, as:

$$\delta\theta_T = -0.983 \text{ degrees}$$

$$\delta\psi_T = -0.082 \text{ degrees}$$

These values, together with a startup thrust of 1332 pounds, were then used to calculate the gimbal trim angles:

$$\delta\theta = -1.044 \text{ degrees}$$

$$\delta\psi = -0.021 \text{ degrees}$$

These are the recommended launch pad settings for the DPS gimbal trim angles at the start of the DOI burn.

The trim angles are set using the LM Guidance Computer (LGC), and must be expressed referenced to the positive gimbal stops. To accomplish this, 6.05 degrees were added to the trim angles above.

This results in

$$\delta\theta' = 5.006 \text{ degrees}$$

$$\delta\psi' = 6.029 \text{ degrees}$$

both referred to the positive gimbal stops.

The LGC has a nominal drive rate of 0.2000 degrees/second hard-wired into it. Therefore, all actual gimbal angles must be converted to equivalent angles based on the hard-wired drive rate using the actual gimbal drive rates in both pitch and roll. Where entered via the LGC erasable memory load, the angles must be expressed as drive times (from the positive stops). Where entered or displayed on the DSKY the equivalent angles must be expressed as degrees of arc.

LM7/4.7.6.1 DPS Engine Thrust Vector Alignment (Continued)

The GDA drive rates are listed below.

Functional Axis	Drive Rate
Pitch (X-Z plane)	0.2104 deg/sec
Roll (X-Y plane)	0.2108 deg/sec

The gimbal trim data to be entered in the LGC erasable memory load are then obtained as follows:

$$\text{PITTIME} = \frac{\delta\theta'}{0.2104} = 23.79 \text{ seconds}$$

$$\text{ROLLTIME} = \frac{\delta\psi'}{0.2108} = 28.60 \text{ seconds}$$

The corresponding angles to be entered or read from the DSKY are obtained as follows:

$$\text{P-TRIM} = \delta\theta' \left(\frac{0.2000}{0.2104}\right) = 4.758 \text{ degrees}$$

$$\text{R-TRIM} = \delta\psi' \left(\frac{0.2000}{0.2108}\right) = 5.720 \text{ degrees}$$

LM7/4.7.12.1 DPS Propellant Tank Venting For Lunar Landing Mission (NASA DATA SOURCE)

The thermal profile of the DPS propellant tanks after lunar touchdown is dependent upon engine burn time, distance of the descent stage from the lunar surface (i.e., length of landing gear stroke), and the quantity of residual propellant in the specific tank. The fracture mechanics allowable pressure limits are dependent upon the temperature, pressurization history of each tank and the burst disc pressure (measured value of 267 psid for the LM-7 tanks).

In Figure LM7/4.7.12-1 curve "A" represents the fracture mechanics maximum allowable pressure for a landing of maximum thermal severity, i.e., maximum burn time, maximum landing gear stroke and zero residual oxidizer. Curve "B" represents the fracture mechanics maximum allowable pressure for a "cold" landing, i.e., minimal landing gear stroke with ample descent stage clearance and 145 lbm residual oxidizer in the tank. Curve "C" represents the predicted oxidizer tank ullage pressure for landing of maximum thermal severity, i.e., maximum burn time, maximum landing gear stroke and zero residual oxidizer.

For a landing of maximum thermal severity, represented by curves "A" and "C" in Figure LM7/4.7.12-1, Grumman Aerospace Corporation recommends abort within two hours if the oxidizer tanks can not be vented.

However, curve "B" also represents the fracture mechanics maximum allowable pressure for a landing of maximum thermal severity if there is no flaw in the oxidizer tanks greater than 85 percent of that screened for by proof-pressurization testing. In as much as the 85 percent limit is acceptable, abort is not required except as discussed below.

Both curves "A" and "B" assume no failures of the insulation system. Under flight conditions this may be assumed if the monitored oxidizer tank pressure remains within the bounds of curve "C" in Figure LM7/4.7.12-1. If the limits of curve "C" are exceeded, then it must be assumed that severe insulation damage has occurred and abort is recommended.

In the event of failure of the LM-7 fuel tanks to vent, abort is not necessary to avoid violation of the fracture mechanics limits.

(NASA DATA SOURCE)

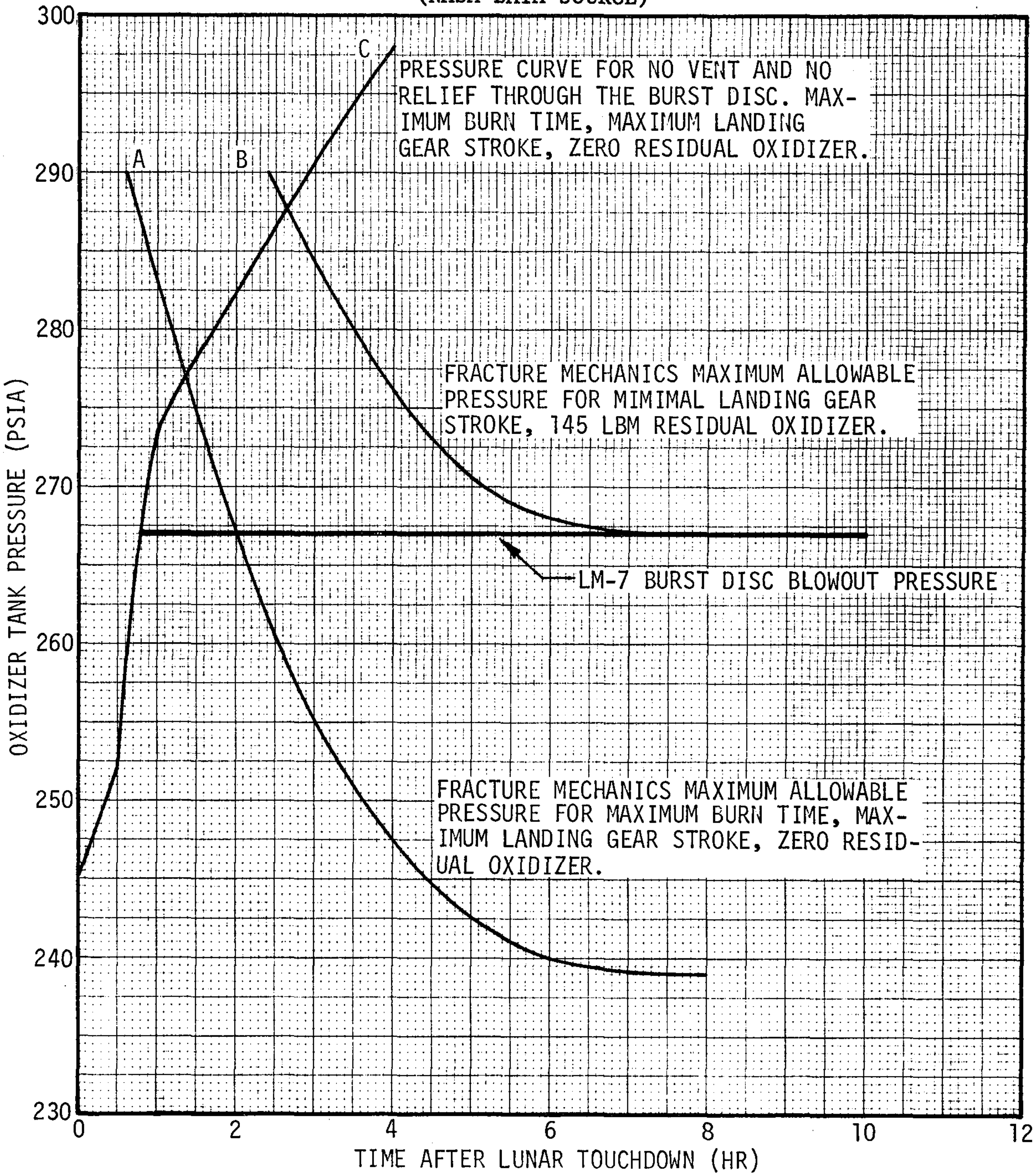

LM7/4.7.12-1. Mission H2 LM DPS Oxidizer Tank Ullage Pressure and Maximum Allowable Tank Pressure Vs. Time After Lunar Touchdown

LM7/4.7.15 Descent Engine Regulator Performance

Figure LM7/4.7.15-1 shows performance characteristics for LM-7 descent engine regulator, Serial No. 121.

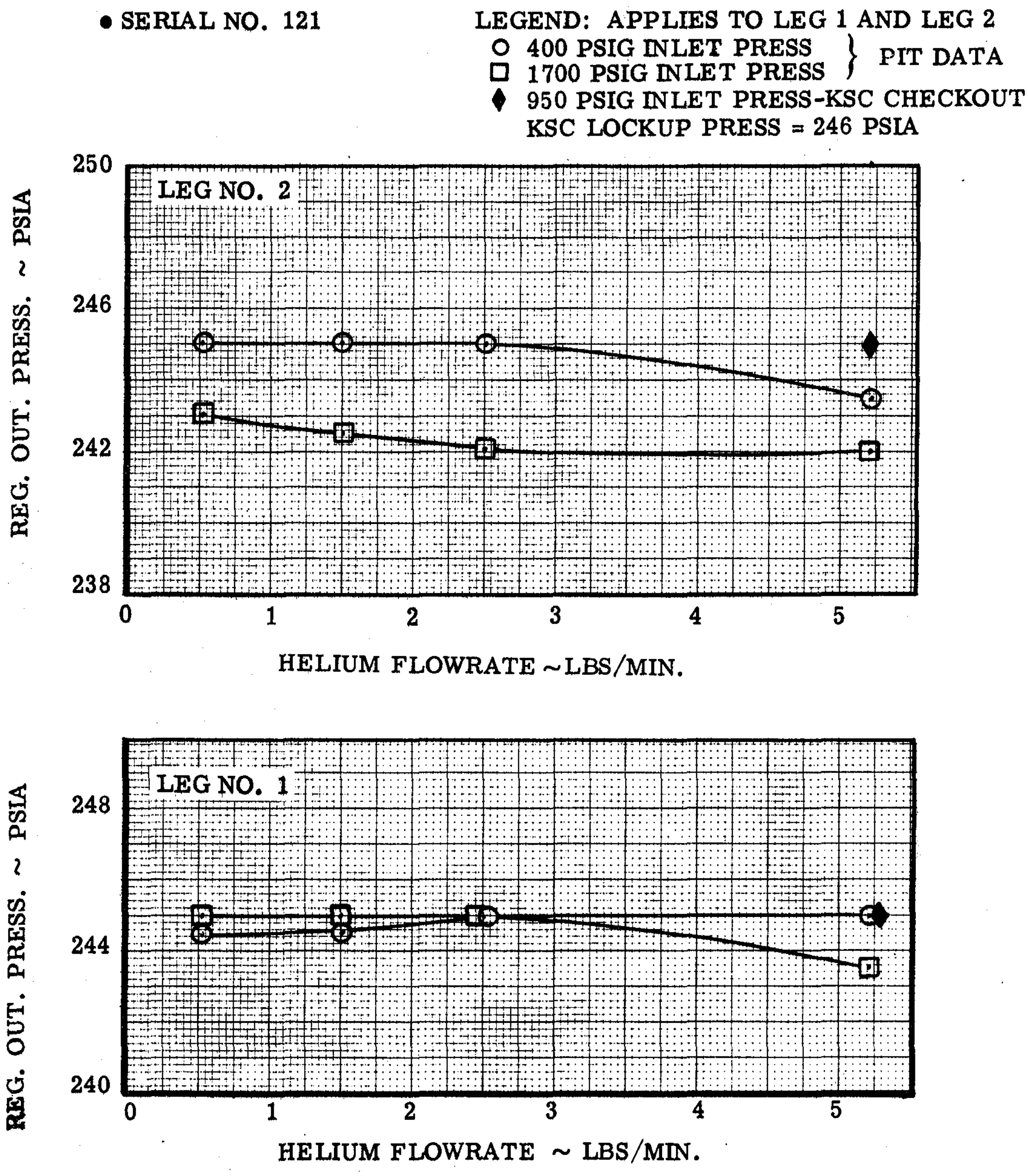

Figure LM7/4.7.15-1. Descent Engine Regulator Performance

LM7/4.8.6.1 Multiple Steady State Firings Heating Effects

Figure LM7/4.8.6-1 shows the plume impingement limits of the -X and +X RCS thrusters in terms of allowable thruster activity at various duty cycles as a function of elapsed time. The primary -X firing constraint curve represents the attainment of maximum allowable S-Band Steerable Antenna parts temperature for a start temperature of 75°F as well as the worst case antenna positioning. The -X firing jets constraint curve is also presented for the EVA antenna and for the S-Band Steerable Antenna assuming a 35°F start temperature.

The primary +X firing constraint curve is a combination of plume impingement capabilities of plume deflectors and the front of the Scientific Equipment Bay and the side of Quad III (SHe Tank). Exceeding these will cause failure of the item indicated.

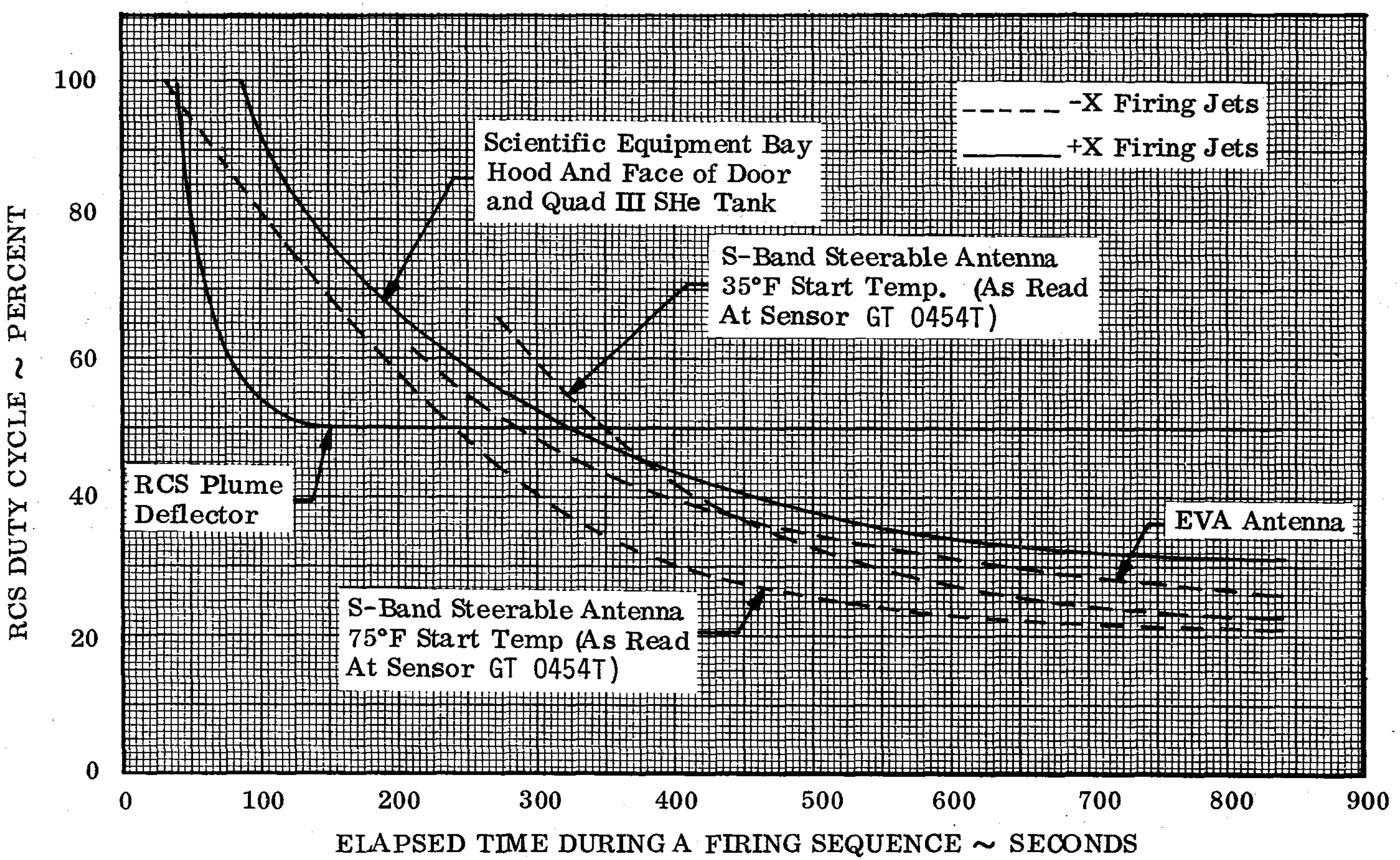

Figure LM7/4.8.6-1. LM7 Plume Impingement Capability-Unstaged (See Para. LM7/4.8.6.1)

LM7/4.8.14 RCS Performance Limitations as a Result of Gimbal Drive Actuator (+ Pitch or + Roll) Failure During Powered Descent

LM7/4.8.14.1 Plume Impingement Constraints due to GDA Failure.

Figure LM7/4.8.14-1 shows the maximum allowable GDA offset angles as limited by the RCS impingement constraints for the affected vehicle hardware. These curves were developed from the LM-7 RCS plume impingement capability curve (See Figure LM7/4.8.6-1).

In the event of a GDA failure during powered descent, RCS plume impingement may constrain the mission. Figure LM7/4.8.14-2 represents the maximum allowable accumulated RCS firing time at any juncture during powered descent for GDA failure at several different times. The curves reflect the duty cycle which causes failure of the plume deflectors.

LM7/4.8.14.2 Additional RCS Propellant Consumption as a Result of Gimbal Drive Actuator Failure During DPS Operation

Figures LM7/4.8.14-3 and LM7/4.8.14-4 present the maximum allowable GDA pitch and roll angles at time of failure, considering the margin of RCS propellant at landing and the RCS limited torque authority (see Paragraph 4.8.14.2). Figure LM7/4.8.14-5 presents the nominal GDA angles during DPS operation.

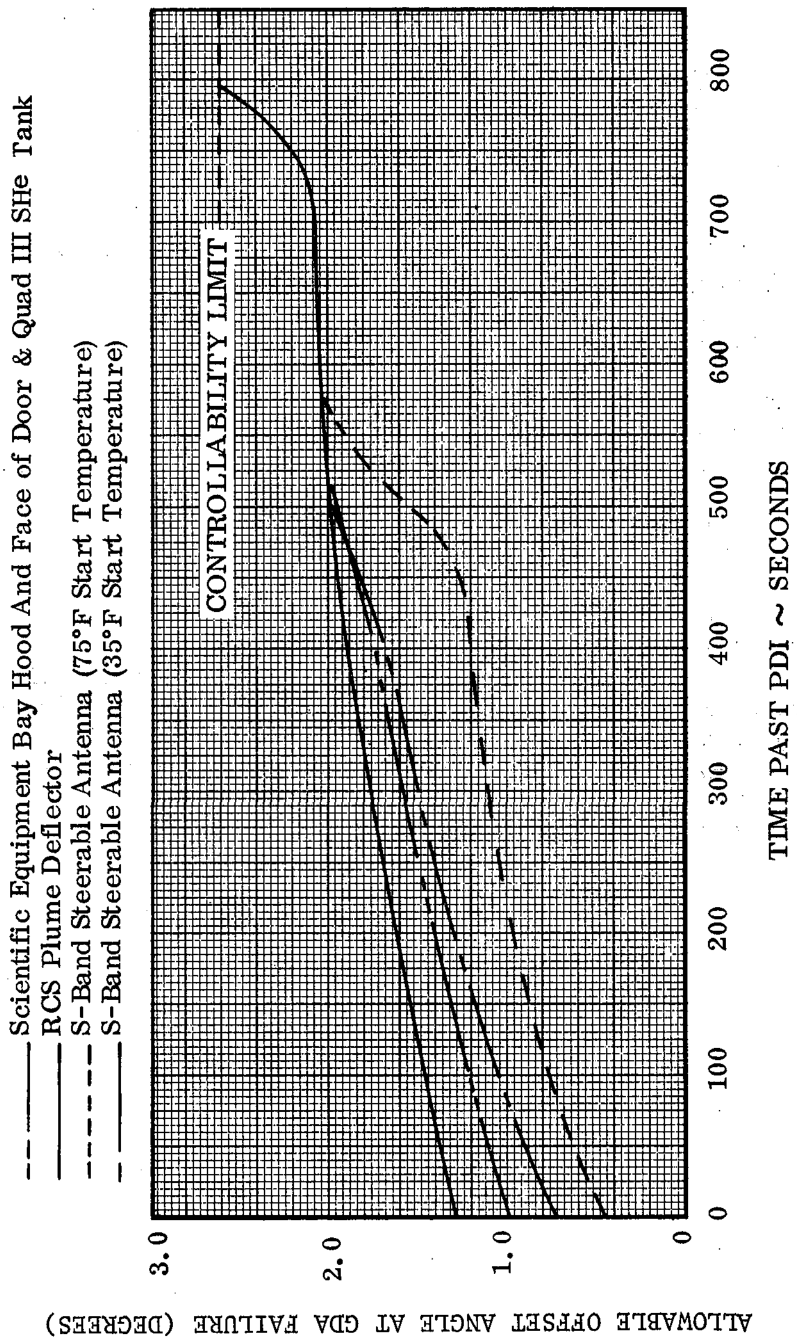

Figure LM7/4.8.14-1. Allowable GDA Offset Angle (at GDA Failure) during Powered Descent (as Determined by RCS Plume Impingement Limit) (See Para. LM7/4.8.14.1)

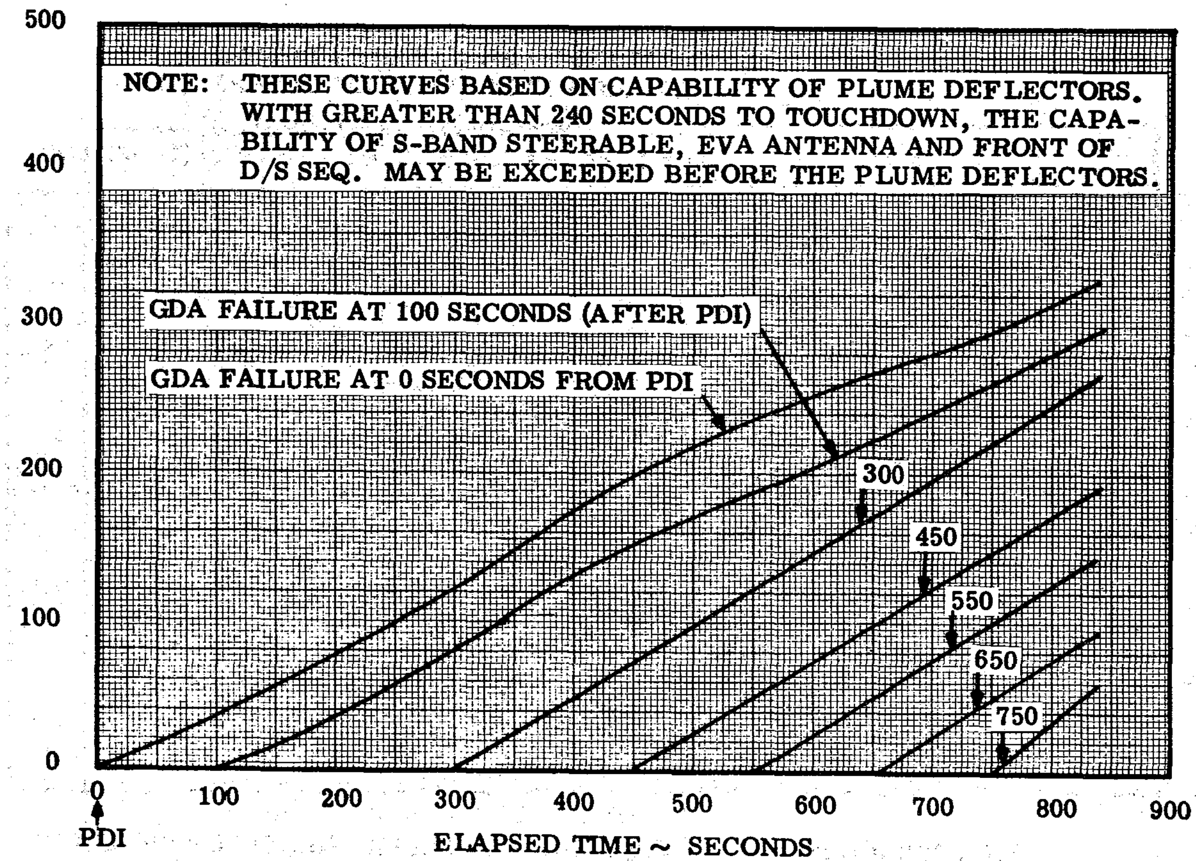

Figure LM7/4.8.14-2. Allowable RCS +X Firing Time vs Time From Powered Descent Initiation (See Para. LM7/4.8.14.1)

CURVES BASED ON MAXIMUM ALLOWABLE DEVIATIONS FOR RCS PROPELLANT AND CONTROLLABILITY RED LINES AS A FUNCTION OF ELAPSED BURN TIME

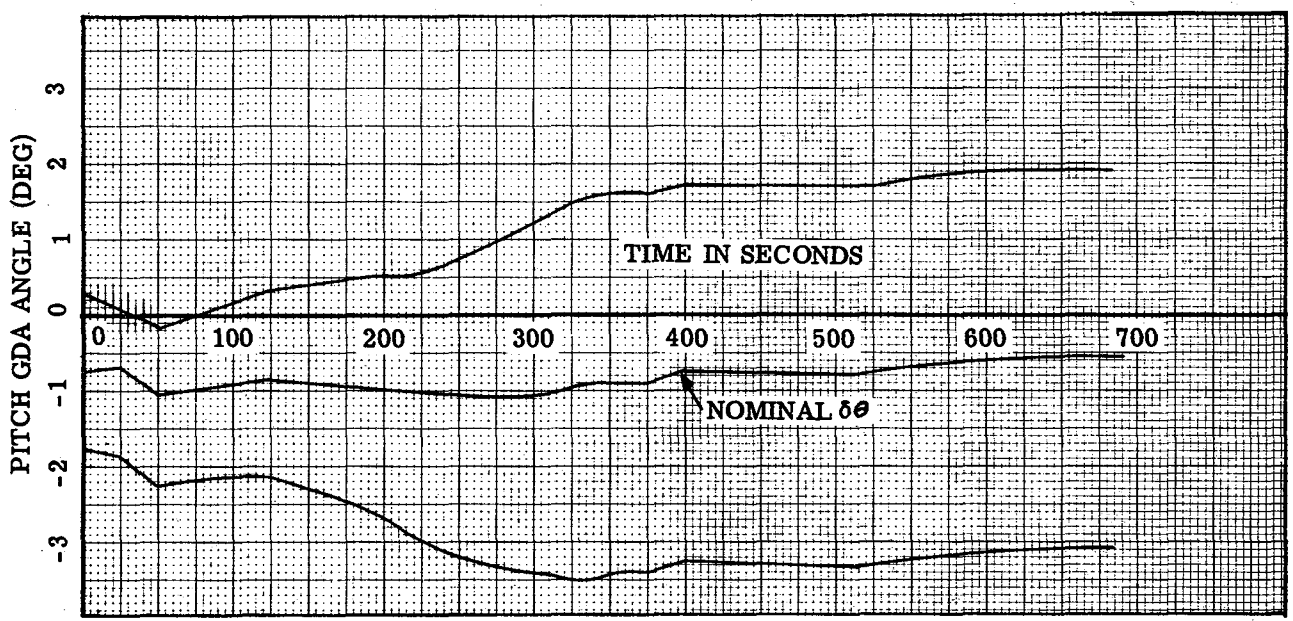

NOTES: (1) ASSUMES 140 LBM RCS PROPELLANT REMAINING AT TOUCHDOWN

(2) THRUST VECTOR CHANGES DUE TO THROAT EROSION NOT INCLUDED

Figure LM7/4.8.14-3. Maximum Allowable Pitch GDA Failure Angle Vs. Time During Powered Descent (See Para. LM7/4.8.14.2)

CURVES BASED ON MAXIMUM ALLOWABLE DEVIATIONS FOR RCS PROPELLANT AND CONTROLLABILITY RED LINES AS A FUNCTION OF ELAPSED BURN TIME

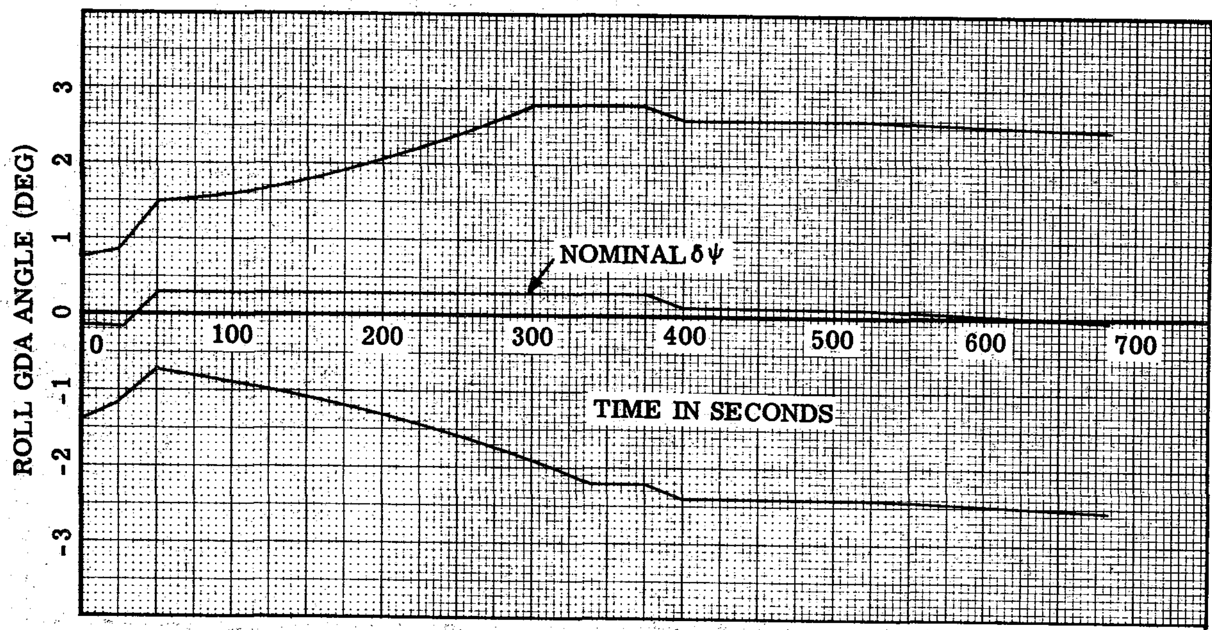

NOTES: (1) ASSUMES 140 LBM RCS PROPELLANT REMAINING AT TOUCHDOWN

(2) THRUST VECTOR CHANGES DUE TO THROAT EROSION NOT INCLUDED

Figure LM7/4.8.14-4. Maximum Allowable Roll GDA Failure Angle Vs. Time During Powered Descent (See Para. LM7/4.8.14.2)

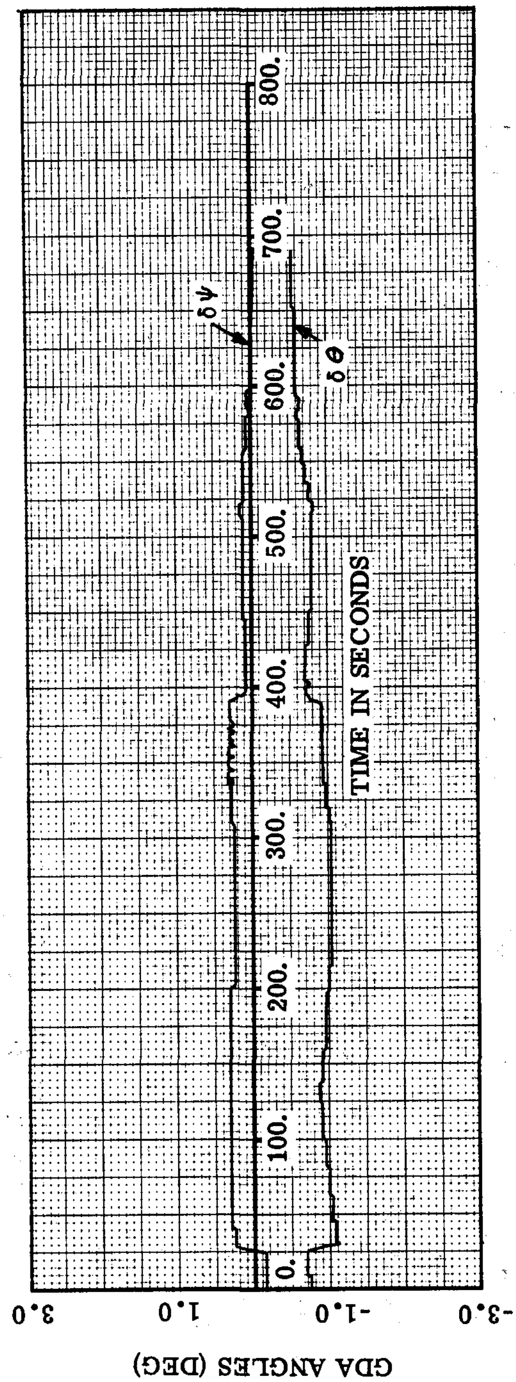

Figure LM7/4.8.14-5. Nominal Expected Gimbal Angles (δθ, δψ) as a Function of DPS Burn Time During Powered Descent (See Para. LM7/4.8.14.2)

This appendix will not be updated and the data presented are only valid up to the Apollo 14 launch date, 31 January 1971. Consequently, revisions subsequent to the Apollo 14 flight may introduce data into the basic text of the data book that conflicts with the data in this appendix. Maintaining or deleting this appendix for LM-8 in the SODB is entirely at the option of the user.

Volume II LM Data Book
APPENDIX LM-8

TABLE OF CONTENTS

Changes to baseline data specific to LM-8 are included in this appendix.

1.0	No change
2.0	No change
3.1	Communications Constraints (TBS)
3.2	Crew/Equipment Constraints (TBS
3.3	Environmental Control Subsystem Constraints
3.6	APS Subsystem Constraints
3.7	DPS Subsystem Constraints
3.8	Reaction Control Subsystem Constraints
3.10	Thermal Constraints
4.2.4	Thermal Variations for the MESA
4.2.5	Thermal Variation of the Sample Return Containers after Removal from the MESA
4.2.6	Thermal Response of the Lunar Surface Color TV Camera
4.3.2.2	Leakage
4.3.2.6	Cabin Regulator Check
4.3.3	Lithium Hydroxide Consumption
4.3.4	Water Consumption (TBS)
4.3.8.1	Heat Transport Section Water Sublimators
4.3.11	Duty Cycle of LM Heaters
4.5.1.1	Uncertainty of LM IMU Alignment from CSM IMU
4.5.1.4	Guidance Computer Erasable Constants
4.5.1.5.2	Assembly Alignment Data of Spacecraft Docking Mating Surfaces to the Navigation Base
4.5.1.5.3	AOT Alignment Data
4.5.2.1	Abort Sensor Assembly
4.5.2.1.2	AGS Angular Mounting Error
4.5.2.2	Abort Electronic Assembly
4.5.3.2.2.3	DPS Thrust Response at TTCA Minimum and Maximum Positions
4.5.3.4.3	GDA Drive Rates
4.5.4.2	RR Mechanical Alignment
4.5.4.3	RR Timeline Operations
4.5.4.4.11	RR and T AGC Voltage Versus Range
4.5.4.4.11.1	RR and T AGC Voltage Versus Range and LOS Angle
4.5.4.4.12	RR Self-Test
4.5.4.4.13	RR Power Monitor Calibration
4.5.4.4.16	Allowable Vehicle Acceleration During RR Power Off Periods
4.5.5.1.16	LR Power Monitor
4.5.5.1.17	Loss of LR Lock as a Function of Vehicle Pitch and Roll for Nominal Trajectory
4.5.5.1.18	Expected Altitude of LR Velocity and Range Initial "Data Good" Indication
4.5.5.1.21	LR Predicted Accuracy
4.5.5.2	LR Temperature Profile
4.5.5.3.1	LR Mechanical Alignment

Volume II LM Data Book
APPENDIX LM-8

TABLE OF CONTENTS

Changes to baseline data specific to LM-8 are included in this appendix.

4.5.5.4	Landing Radar Self-Test
4.6.1	APS Preflight Analysis
4.6.8	Thrust Vector Changes with Burn Time
4.6.12	Ascent Engine Regulator Performance
4.7.1	DPS Preliminary Preflight Prediction
4.7.2	Supercritical Helium Tank Pressure
4.7.5	DPS Propellant Tank Low Level Sensor Operation
4.7.6.1	DPS Engine Thrust Vector Orientation
4.7.12.1	DPS Propellant Tank Venting for Lunar Landing Mission
4.7.15	Descent Engine Regulator Performance
4.8.6.1	Multiple Steady State Firings Heating Effects (TBS)
4.8.14	RCS Performance Limitations as a Result of Gimbal Drive Actuator (+ Pitch or + Roll) Failure During Powered Descent
4.8.14.1	Plume Impingement Constraints due to GDA Failure
4.8.14.2	Additional RCS Propellant Consumption as a Result of Gimbal Drive Actuator Failure During DPS Operation
5.0	No change
6.0	No change
7.0	No change
8.0	No change

LM8/3.3 ENVIRONMENTAL CONTROL SUBSYSTEM

OPERATIONAL LIMITATION OR PROCEDURE	RATIONALE
LM8/ECS-23 D/S GOX Tank Pressure - Temperature Limit Relationship	
The D/S GOX tank pressure-temperature limits should not exceed those shown in Figure LM8/3.3.1-1.	Due to the possibility of hydrogen induced flaw growth in the tank material, the fracture mechanics limit of 2520 psi is set so that the failure mode is tank leakage rather than a catastrophic rupture.
LM8/ECS-24 Descent GOX Tank Venting	
Descent GOX tank pressure limits for no-venting conditions are shown in Figure LM8/3.3-2. Predicted pressure curves for hot and nominal mission are also shown.	Violation of venting requirements (Max. Allowable Indication for No-Venting) could result in exceeding the fracture flaw mechanics limitations and could result in tank failure (See LM8/ECS-23).

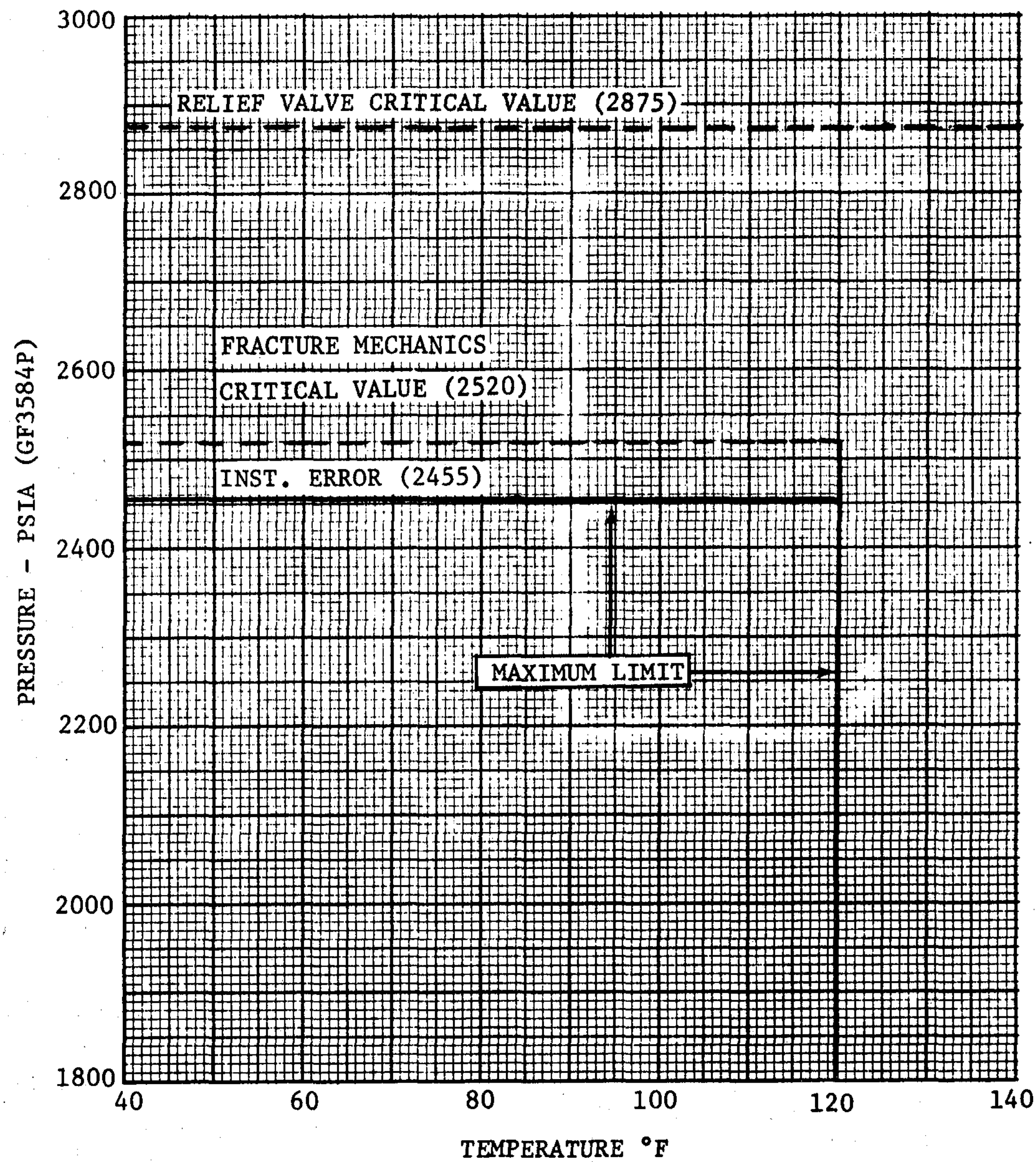

Figure LM8/3.3.1-1. Descent GOX Tank Pressure - Temperature Limitations

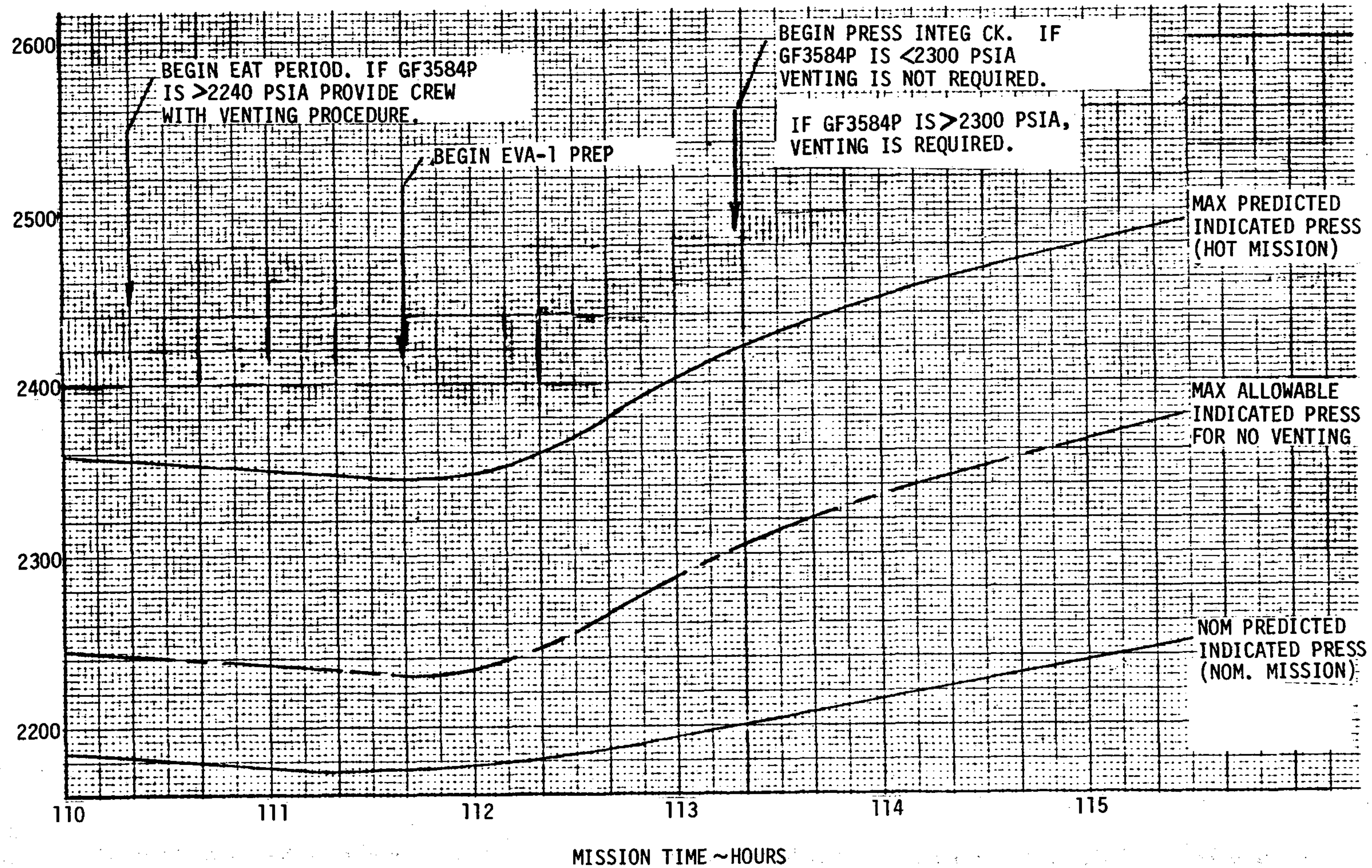

Figure LM8/3.3.1-2. Descent GOX Pressure GF3584P

NOTE:

1 - *INCLUDES INSTR. ERROR
2 - NO LEAKAGE ALLOWED
3 - 2007 LBS TARGET LOAD
4 - MAX. PRESS. DECAY DEFINED BY SOLUBILITY CURVE. HOWEVER, EXCESSIVE DECAY RATES MUST BE EVALUATED CONSIDERING SOLUBILITY EFFECTS FOR INTERMEDIATE POINTS.

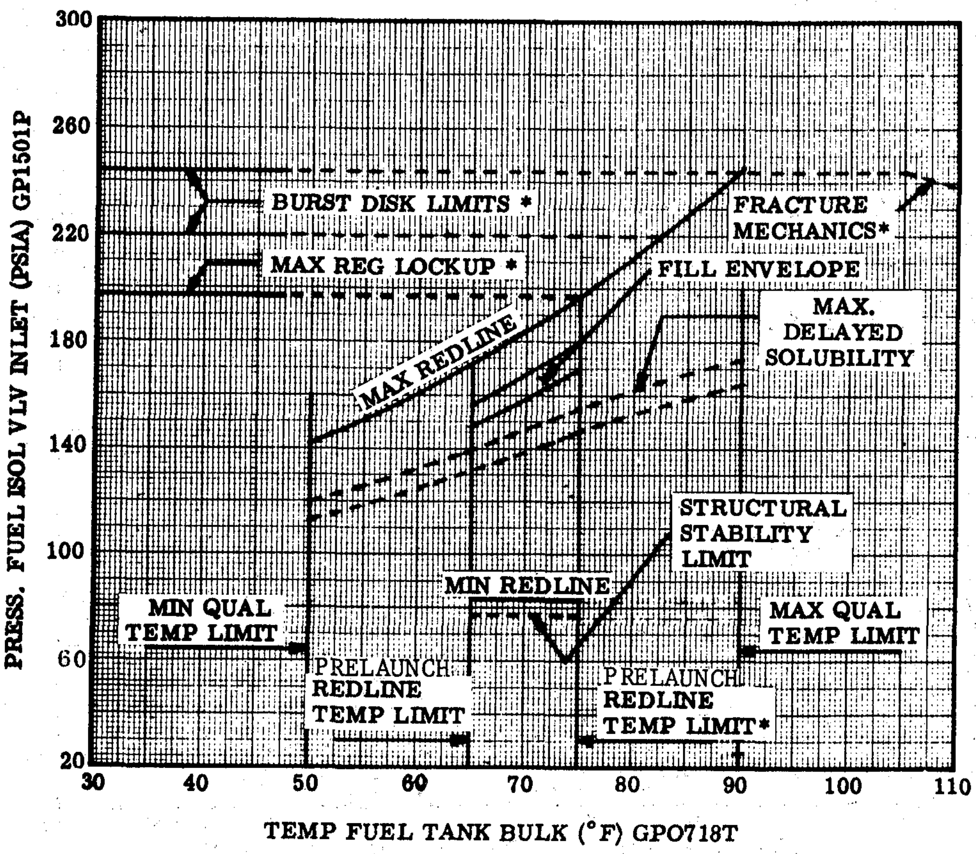

Figure LM8/3.6.1-2. APS Fuel Tank Pressure-Temperature Limitations (See Paragraph LM8/APS-1)

NOTE:

1 - *INCLUDES INSTR. ERROR
2 - NO LEAKAGE ALLOWED
3 - 3218 LBS TARGET LOAD
4 - MAX. PRESS. DECAY DEFINED BY SOLUBILITY CURVE. HOWEVER, EXCESSIVE DECAY RATES MUST BE EVALUATED CONSIDERING SOLUBILITY EFFECTS FOR INTERMEDIATE POINTS.

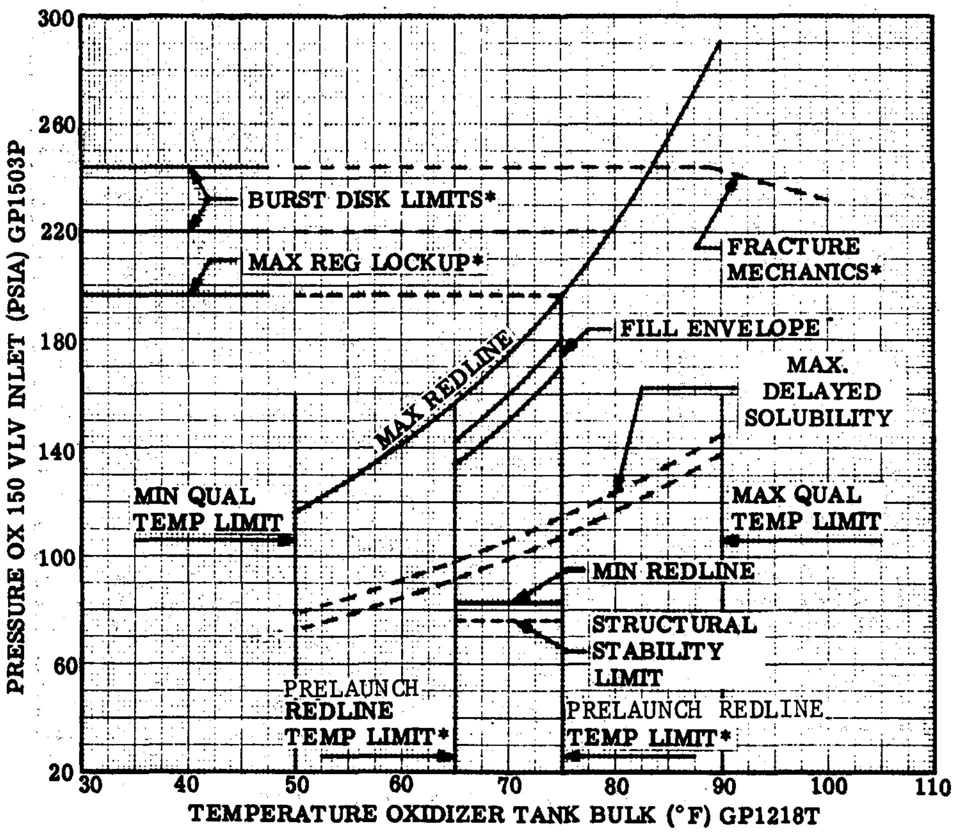

Figure LM8/3.6.1-3. APS Oxidizer Tank Pressure-Temperature Limitations
(See Paragraph LM8/APS-1)

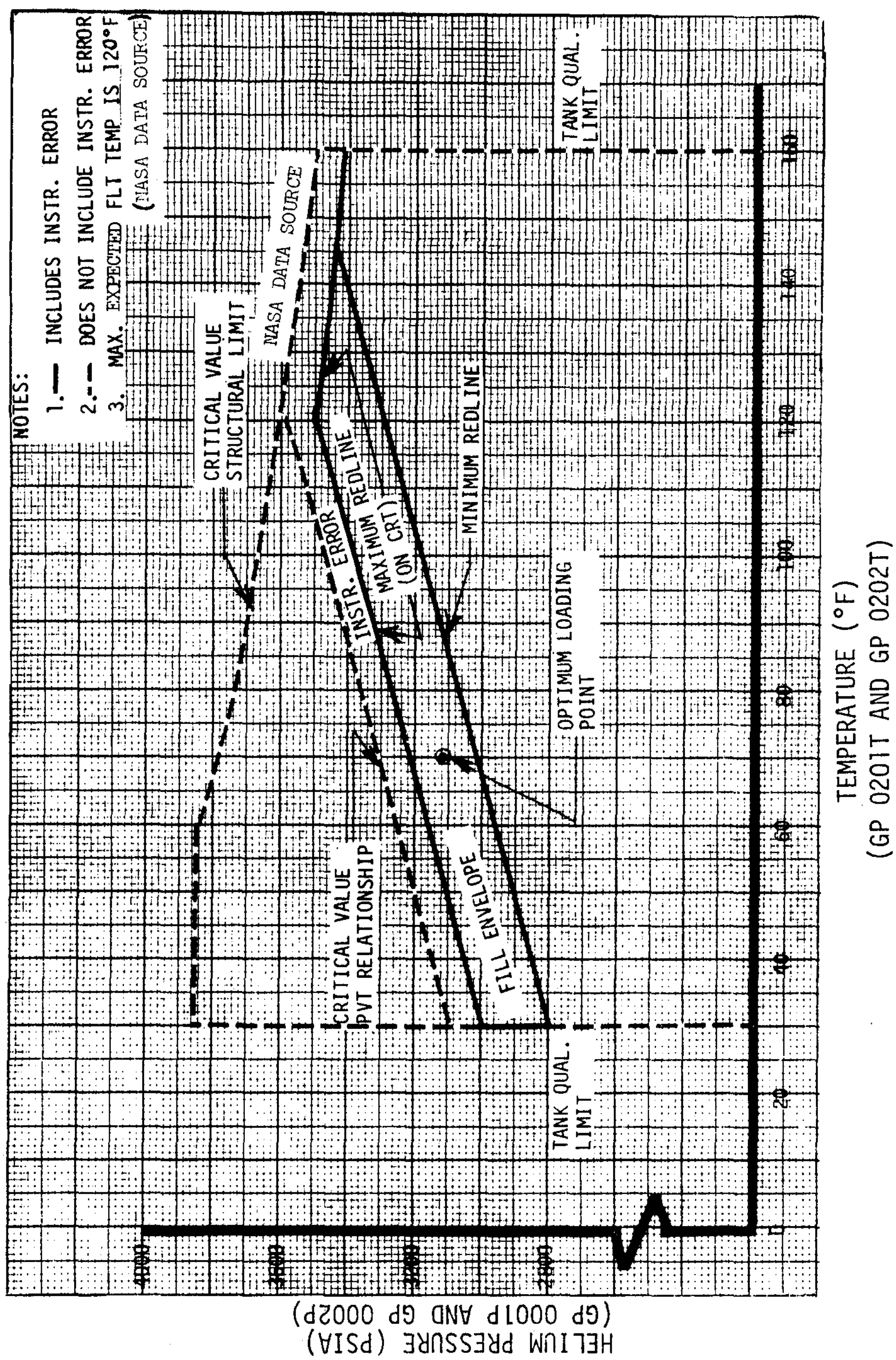

Figure LM8/3.6.1-4. APS Helium Tank Pressure-Temperature Limitations (See Paragraph LM8/APS-9)

LED-540-54

LM8/3.7 PROPULSION - DPS

OPERATIONAL LIMITATION OR PROCEDURE	RATIONALE
LM8/DPS-2 Engine Life	
Using Figure LM8/3.7.1-6, the maximum engine life burn time is that which does not exceed 35% throat erosion.	May exceed the engine thrust chamber heating and erosion limits.
LM8/DPS-6 Propellant Tank Pressure - Temperature Limit Relationship	
The propellant tank pressure should not exceed the values given in Figures LM8/3.7.1-1, LM8/3.7.1-3 and LM8/3.7.1-4.	Reliability is reduced below the allowable value.
LM8/DPS-8 Non-Throttling Range Engine Operation	
See Table LM8/3.7.1-1.	Off-nominal mixture ratios may result, or the thrust chamber may burn through.
LM8/DPS-20 Ambient Helium Storage Tank Pressure-Temperature Limitations	
Ambient helium tank pressure limitations are given in Figure LM8/3.7.1-5.	If the maximum is exceeded, reliability is reduced below allowable value.
LM8/DPS-24 Chamber Pressure Decay at Throttle Down	
For a nominal MDC, the DPS chamber pressure decay from start to end of FTP is not expected to exceed 10.7 psi with normal engine combustion and erosion rates. If it does exceed 10.7 psi a reduction in maximum allowable burn times (prior to depletion) of 15 sec per psi decay exceeding the pressure decay limit must be made. The expected chamber pressures are also presented in Table LM8/3.7.1-2 for reference.	The reference chamber pressure decay corresponds to the maximum FTP erosion that will allow completion of mission with less than 35% erosion under worst case conditions.
LM8/DPS-25 Supercritical Helium Tank Pressure	
The helium tank pressure should not exceed the value given in Figure LM8/3.7.1-2.	Reliability is reduced below allowable value.

Table LM 8/3.7.1-1 Non-Throttling Range Engine Operation

VEHICLE	ENGINE S/N	NOMINAL CONDITIONS		WORST CASE CONDITIONS *	
		Predicted Erosion **	Permissible Time In Non-Throttling Region ***	Predicted Erosion **	Permissible Time In Non-Throttling Region ***
LM-8	1032	21.9%	110 sec.	34.9%	0.85 sec.

* Worst Case erosions are applicable for MDC performed with cold propellant and high mixture ratios. (FTP 0/F = 1.63, 25% Thrust 0/F = 1.65, Propellant Bulk Temperature = 50° F)

** Predicted erosion is to propellant depletion with zero time in non-throttling range.

***Operating time in the non-throttling range is based on the expected engine erosion rate (0.12%/sec) in the event of a loss in manual throttle command during FTP operation. Operation at any other point in the non-throttling range should be based on erosion rates defined in Figure LM8/3.7.1-6.

NOTE: The permissible time in the non-throttling region is based on limiting the total mission duty cycle erosion to 35%, including normal and non-throttling range operations.

MDC - Mission Duty Cycle

Table LM8/3.7.1-2. Non-throttling Range Chamber Pressures, Decays, and Erosion

Engine Characteristics	LM-8 S/N 1032
Allowable Erosion at End of FTP	13%
Swelling at Initiation of FTP	1.8%
FTP Limit Erosion, Initial Swelling Plus 13%	14.8%
Limit Chamber Pressure Decay, Limit Erosion x 0.725 psi/percent	10.7 psi
Predicted Chamber Pressure at Initiation of FTP	105.1 psia
Predicted Chamber Pressure at Termination of FTP	97.4 psia
Predicted Limit Chamber Pressure at Termination of FTP	94.4 psia

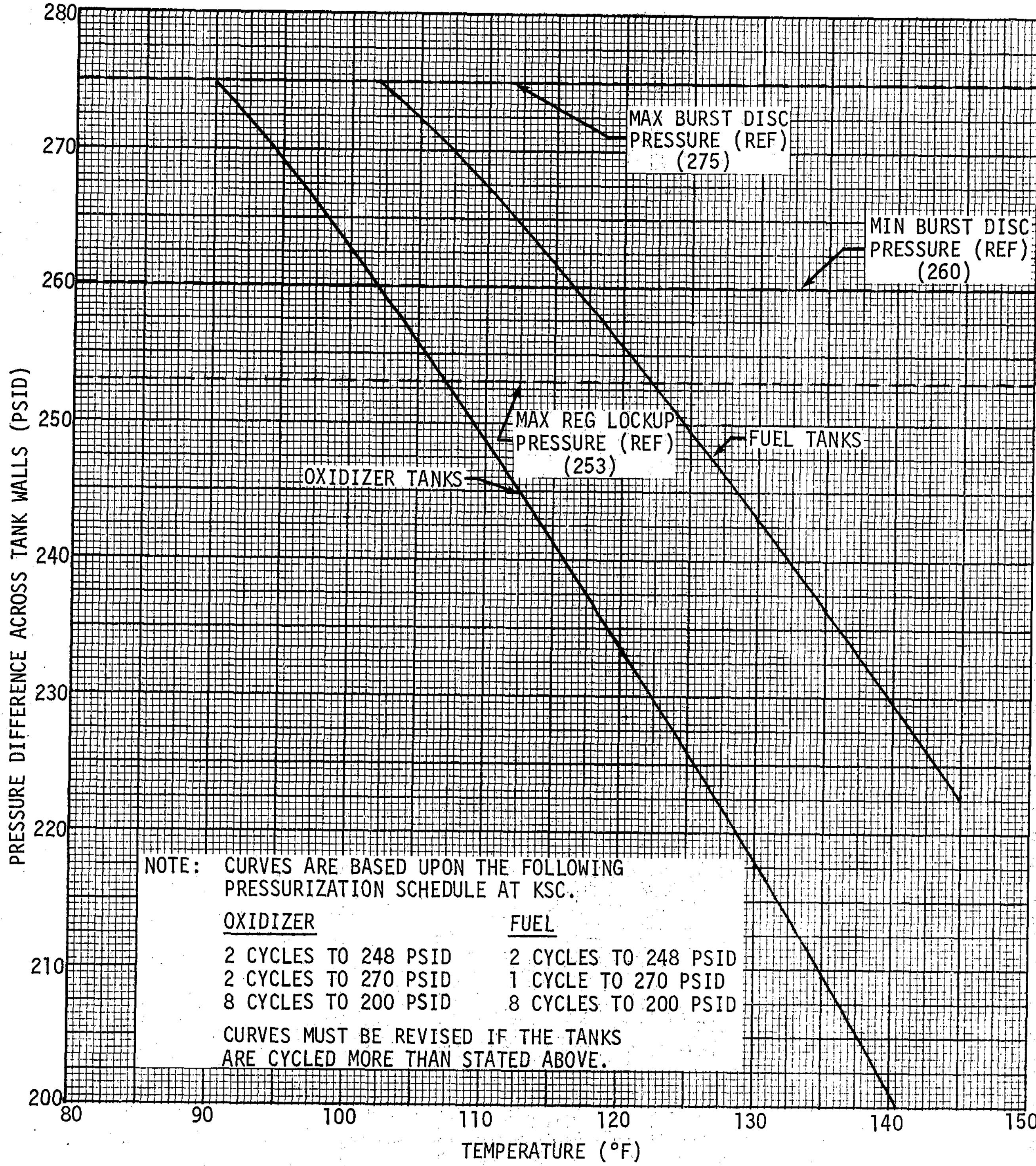

Figure LM8/3.7.1-1. Maximum Allowable Pressure-Temperature Limit Relationship for LM-8 Descent Stage Propellant Tanks

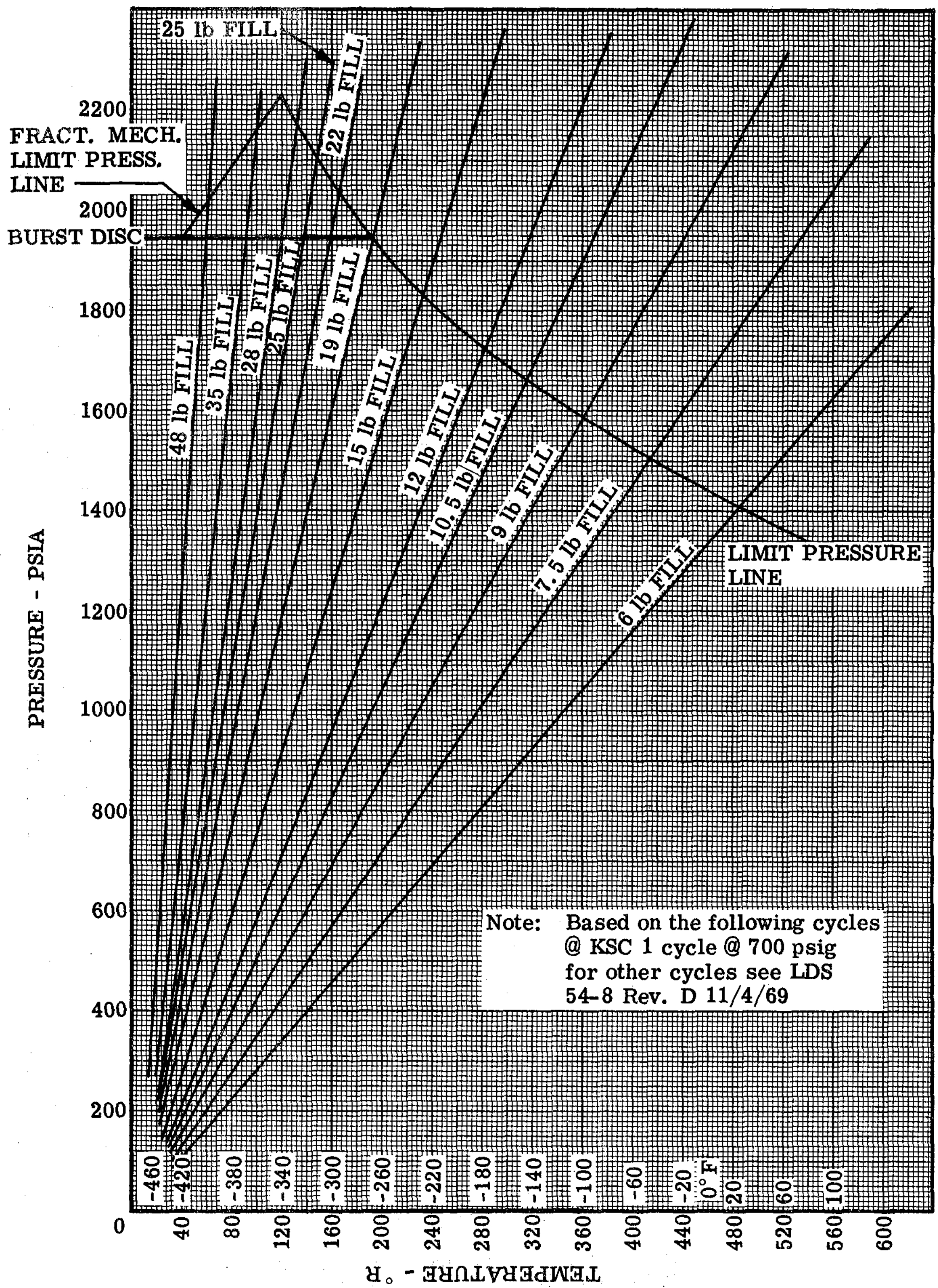

Figure LM8/3.7.1-2. SHe Tank Fracture Mechanics Limits

NOTE:
1. *INCLUDES INSTR. ERROR
2. NO LEAKAGE ALLOWED
3. 7073 LBS TARGET LOAD
4. MAX. EXPECTED PRESS. DECAY IS DEFINED BY THE MAX. DELAYED SOLUBILITY CURVES. THE DETECTION OF EXCESSIVE PRESS. DECAY DURING PRELAUNCH OPERATIONS MUST BE EVALUATED WITH RESPECT TO POSSIBLE LEAKAGE.
5. INITIAL FILL POINTS FALLING OUTSIDE THE DESIRED FILL ENVELOPE MUST BE EVALUATED IN REAL TIME TO INSURE THAT THE TOTAL SOLUBILITY AT DPS PRESSURIZATION WILL NOT PRODUCE A DELTA-P OF 50 PSID (USE "AS READ" CRT NUMBERS TO DETERMINE DELTA-P).

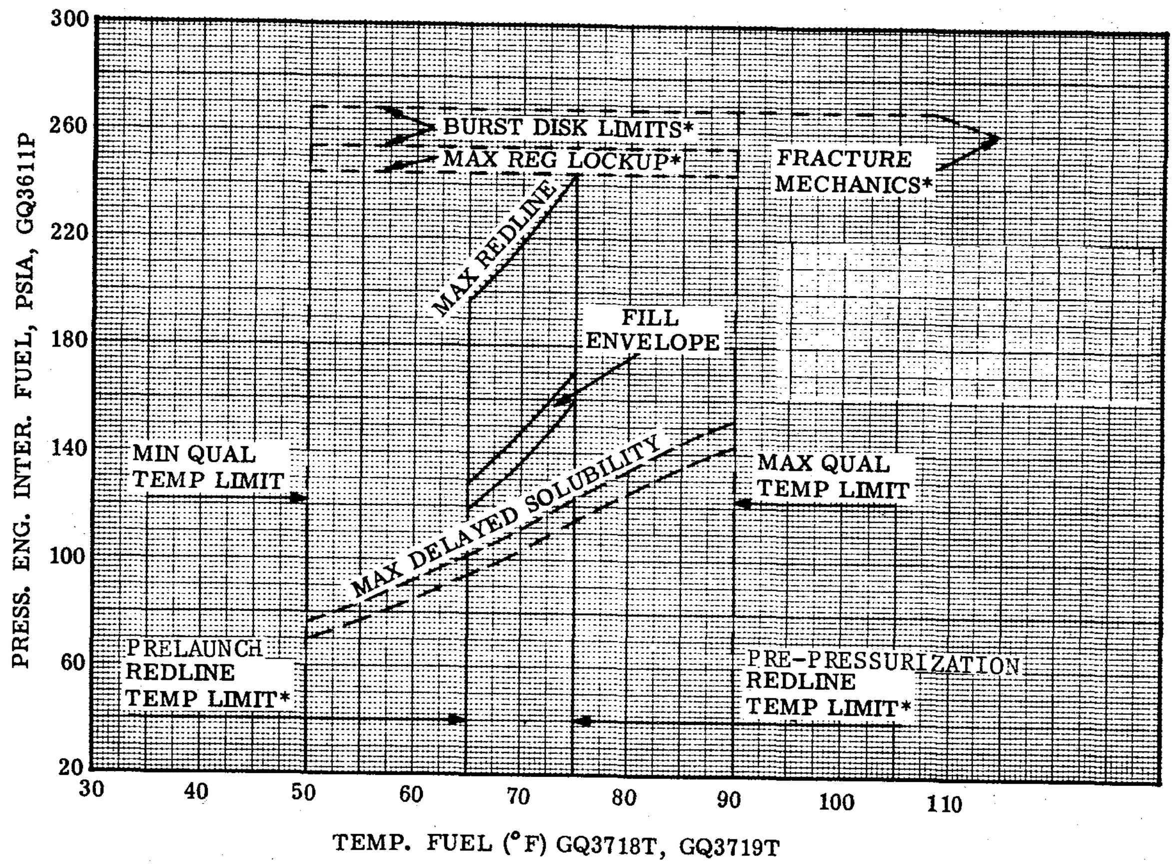

Figure LM8/3.7.1-3. DPS Fuel Tank Press.-Temp. Limitations
(See Paragraph LM8/DPS-6)

NOTE:

1 - *INCLUDES INSTR. ERROR
2 - NO LEAKAGE ALLOWED
3 - 11342 LBS TARGET LOAD
4 - MAX. EXPECTED PRESS. DECAY IS DEFINED BY THE MAX. DELAYED SOLUBILITY CURVES. THE DETECTION OF EXCESSIVE PRESS. DECAY DURING PRELAUNCH OPERATIONS MUST BE EVALUATED WITH RESPECT TO POSSIBLE LEAKAGE.
5 - INITIAL FILL POINTS FALLING OUTSIDE THE DESIRED FILL ENVELOPE MUST BE EVALUATED IN REAL TIME TO INSURE THAT THE TOTAL SOLUBILITY AT DPS PRESSURIZATION WILL NOT PRODUCE A DELTA-P OF 50 PSID (USE "AS READ" CRT NUMBERS TO DETERMINE DELTA-P).

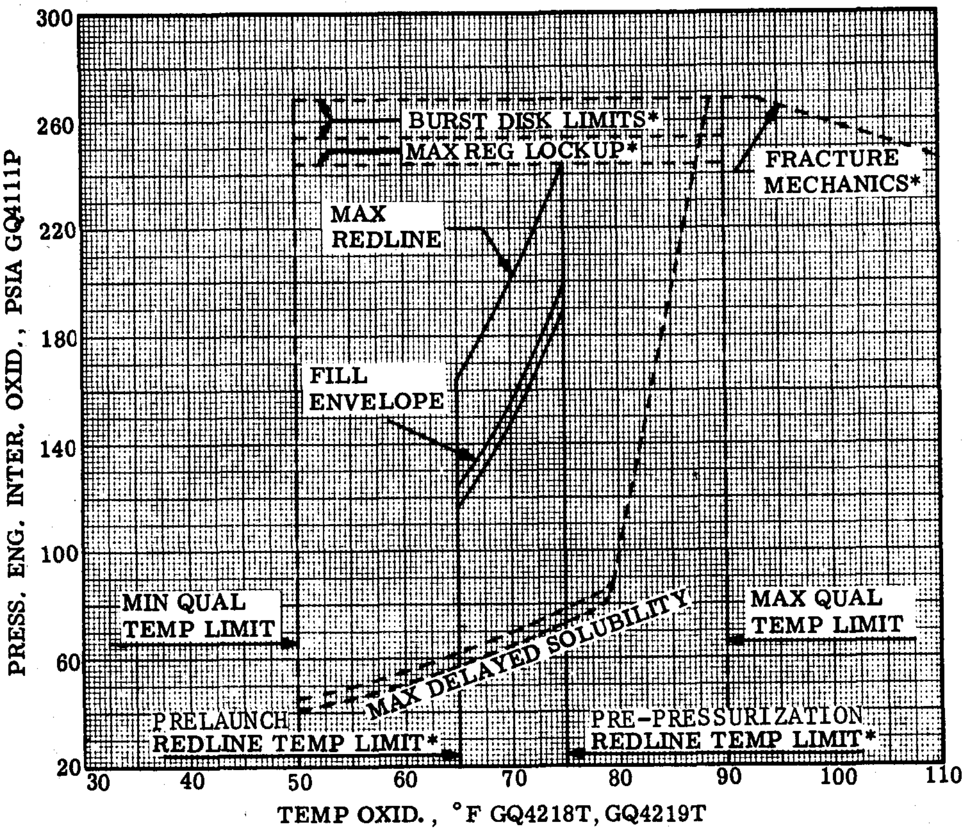

Figure LM8/3.7.1-4. DPS Oxidizer Tank Press.-Temp. Limitations (See Paragraph LM8/DPS-6)

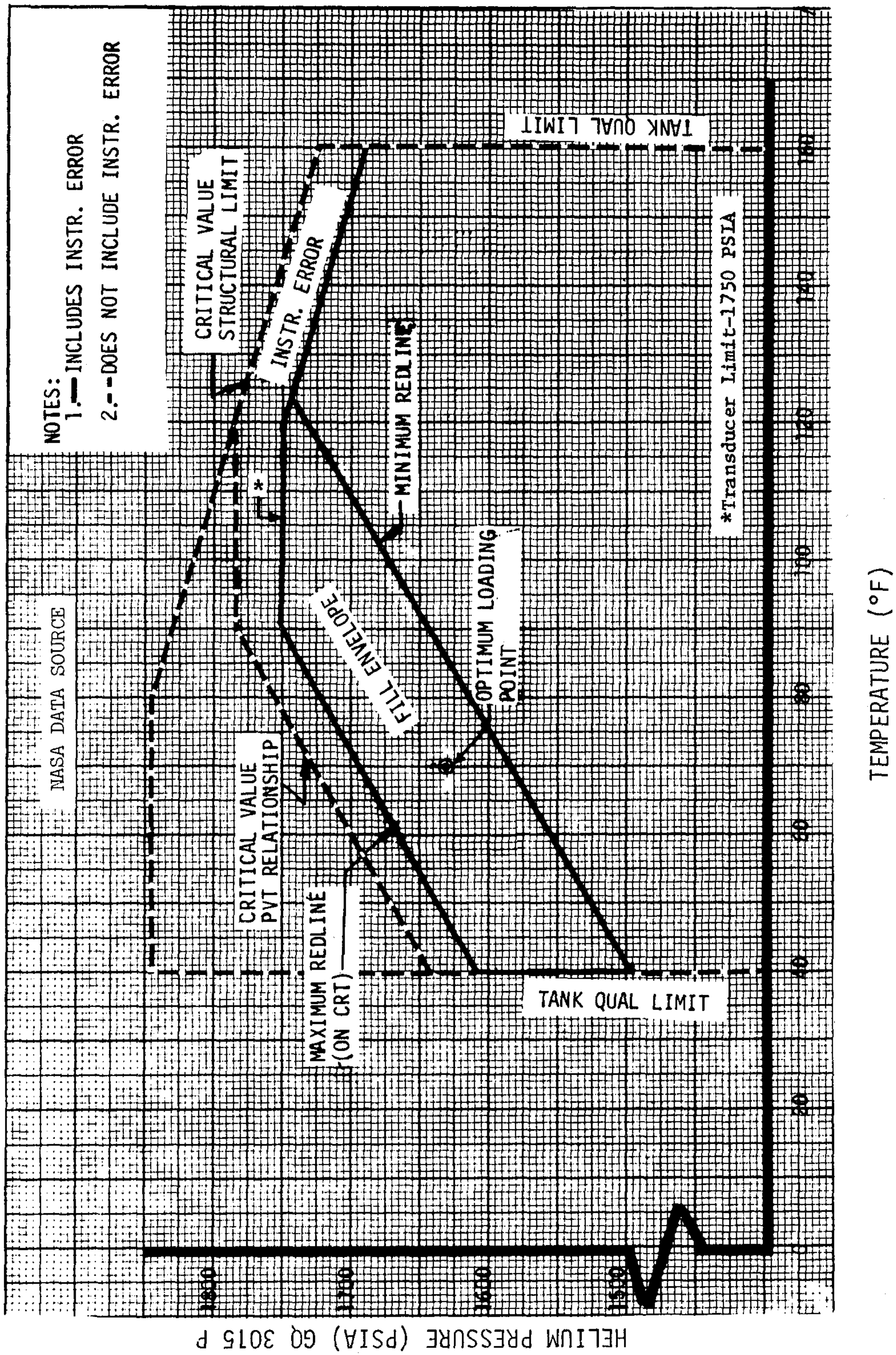

Figure LM8/3.7.1-5. DPS Ambient Helium Tank Pressure-Temperature Limitations (See Para. LM8/DPS-20)

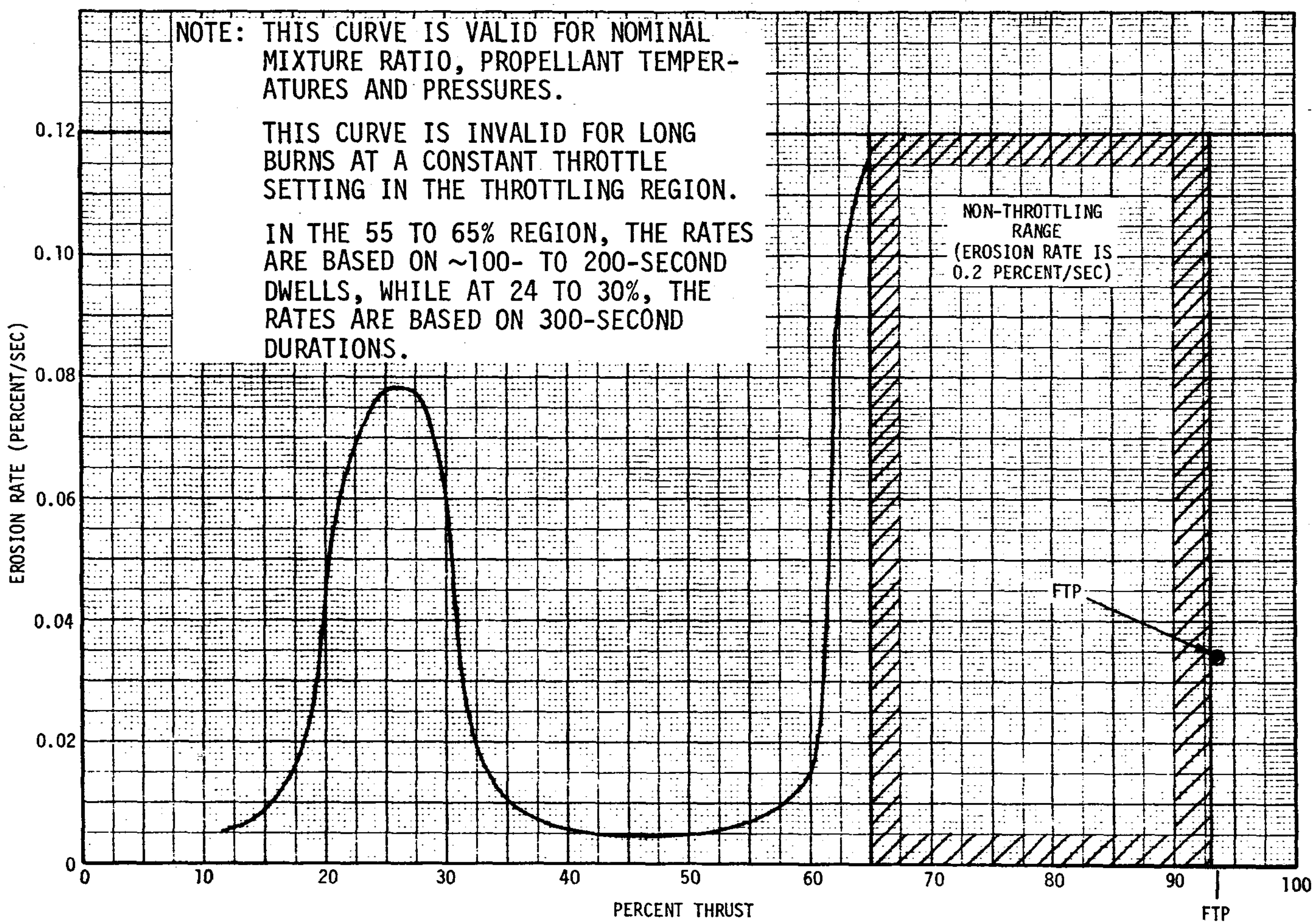

LM8/3.7.1-6. LM8 Descent Engine Throat Erosion Rate Versus Thrust Level for Uneroded Throat

LM8/3.8 REACTION CONTROL SUBSYSTEM

LM8/RCS-13 Propellant Tank Pressure-Temperature Limit Relationship

The propellant tank pressure should not exceed the values given in Figure LM8/3.8.1-1.

Reliability is reduced below the allowable value.

LM8/RCS-17 RCS Helium Bottle Pressure-Temperature Limitations

RCS helium bottle pressure-temperature limitations are given in Figure LM8/3.8.1-2.

If the maximum is exceeded, reliability is reduced below allowable values.

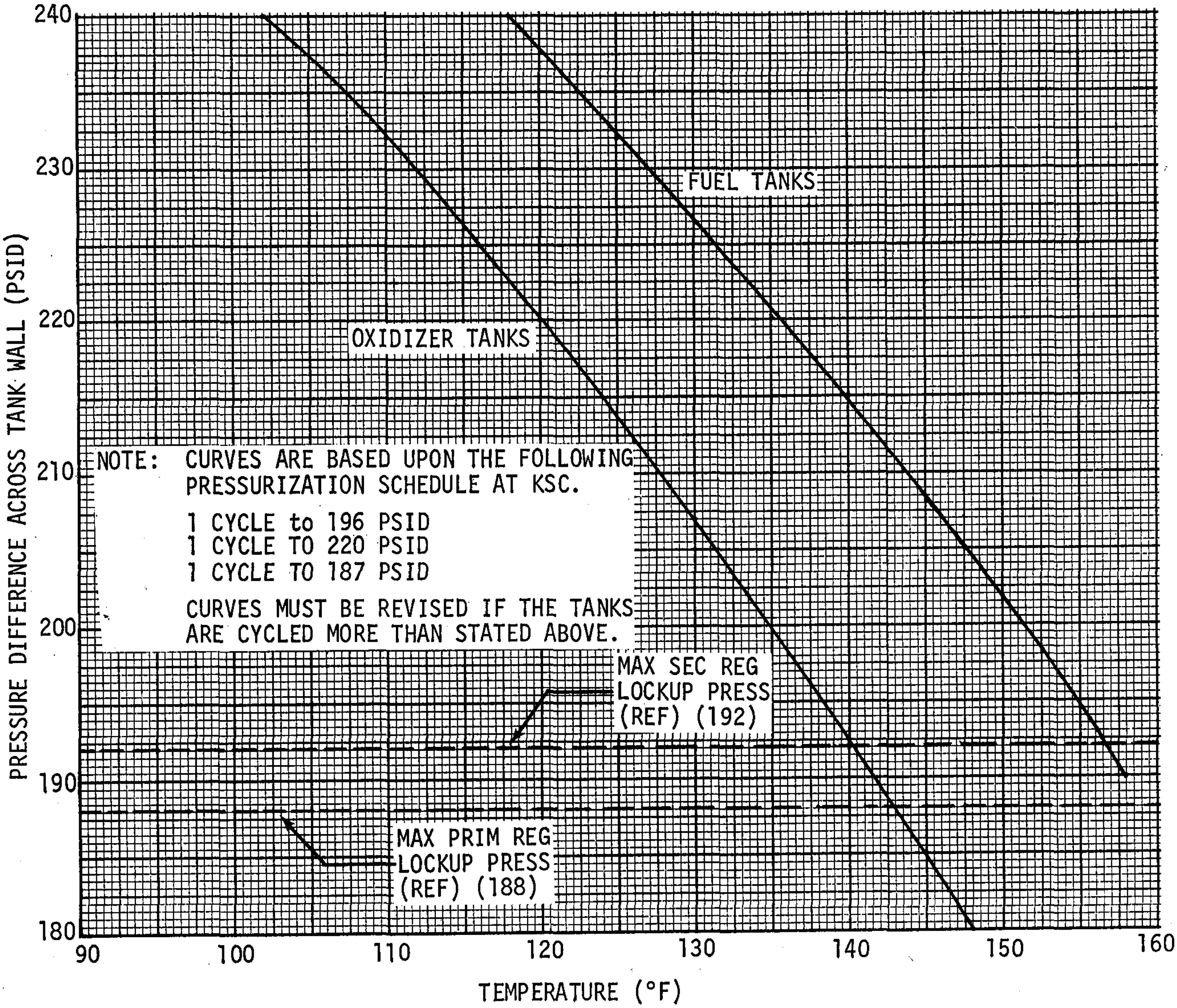

Figure LM8/3.8.1-1. Maximum Allowable Pressure-Temperature Limit Relationship for LM-8 RCS Propellant Tanks

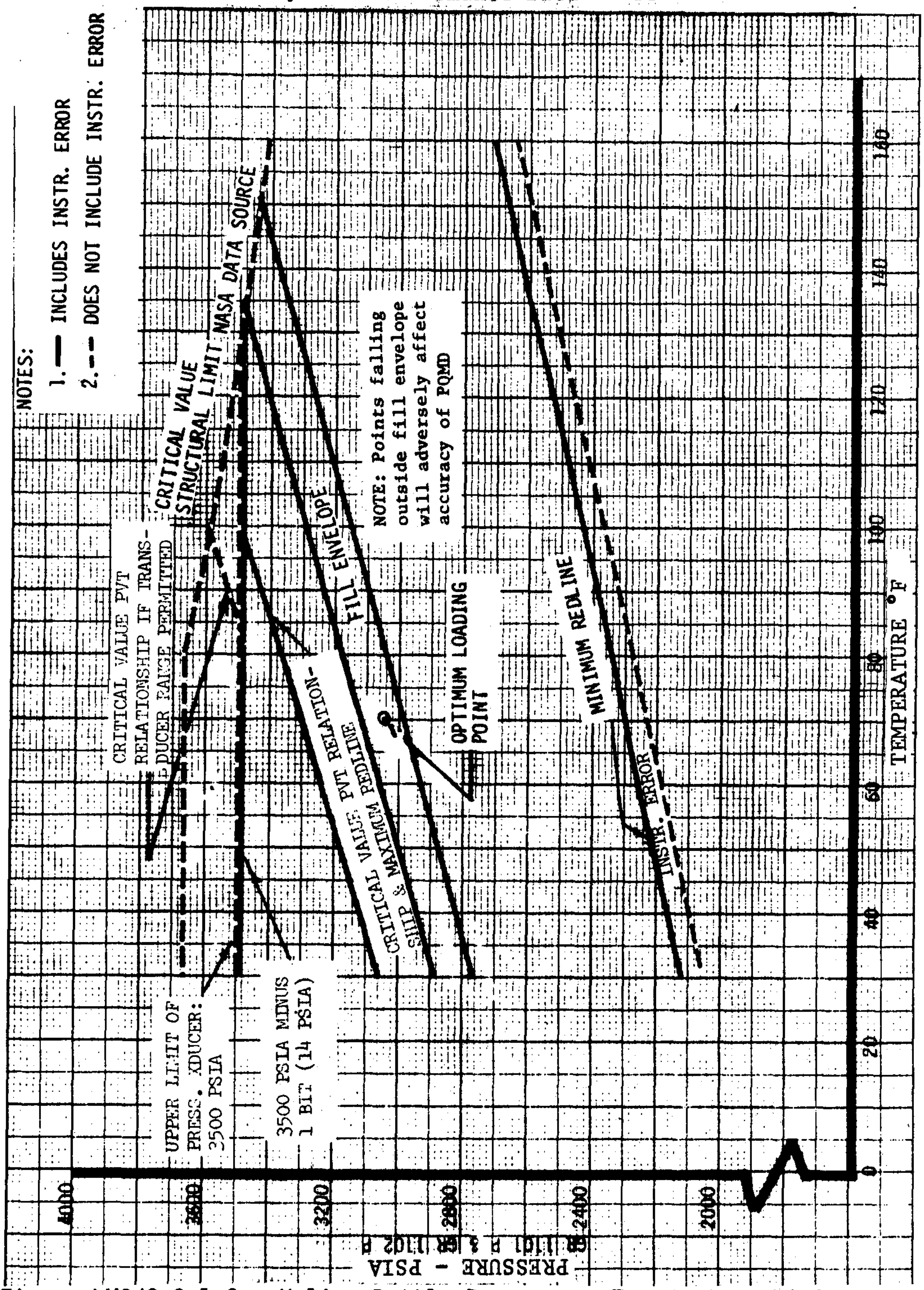

Figure LM8/3.8.1-2. Helium Bottle Pressure - Temperature Limitations (See Para. LM8/RCS-17)

LM8/3.10.1 System Temperature Limitations

Fracture mechanics limits for the APS, DPS, and RCS fuel and oxidizer tanks are presented in Tables LM8/3.10.1-1, LM8/3.10.1-2, and LM8/3.10.1-3, respectively.

Table LM8/3.10.1-1. Ascent Propulsion Subsystem (APS) Limitations

COMPONENT	TEMPERATURE LIMITS (°F)		LOW LIMIT REASON	HIGH LIMIT REASON	MEASUREMENT	
	LOW	HIGH			NUMBER	LOCATION
Fuel Tank		136		Fracture mechanics. Based upon secondary regulator lockup at 205 psid.	GP0718T	Fuel Tank Bulk
Oxidizer Tank		119			GP1218T	Ox Tank Bulk

NOTES:
1. Measurement number readings are valid only when tanks are at least 75% full.
2. See Figure LM8/3.6.1-1 for APS fracture mechanics pressure-temperature relationship curves.
3. See Table 3.10-6 for other APS temperature limitations.

Table LM8/3.10.1-2. Descent Propulsion Subsystem (DPS) Limitations

COMPONENT	TEMPERATURE LIMITS (°F)		LOW LIMIT REASON	HIGH LIMIT REASON	MEASUREMENT	
	LOW	HIGH			NUMBER	LOCATION
Fuel Tank		102		Fracture mechanics. Based upon burst disc pressure of 275 psid.	GQ3718T GQ3719T	Tank #1 Bulk Tank #2 Bulk
Oxidizer Tank		90			GQ4218T GQ4219T	Tank #1 Bulk Tank #2 Bulk

NOTES:
1. Measurement number readings are valid only when tanks are at least 75% full.
2. See Figure LM8/3.7.1-1 for DPS fracture mechanics pressure-temperature relationship curves.
3. See Table 3.10-7 for other DPS temperature limitations.

Table LM8/3.10.1-3. Reaction Control Subsystem (RCS) Limitations

COMPONENT	TEMPERATURE LIMITS (°F)		LOW LIMIT REASON	HIGH LIMIT REASON	MEASUREMENT	
	LOW	HIGH			NUMBER	LOCATION
<u>Fuel Tank</u>				Tank spec. limit and no engine firing experience above 100°F/Fracture mechanics. Based upon secondary regulator lock-up at 192 psid post-LOI.		
System A		100/147			GR2121T	Fuel Tank Outlet
System B		100/147			GR2122T	Fuel Tank Outlet
<u>Oxidizer Tank</u>				Tank spec. limit and no engine firing experience above 100°F/Fracture mechanics. Based upon secondary regulator lock-up at 192 psid post-LOI		
System A		100/130			GR2121T	Fuel Tank Outlet
System B		100/130			GR2122T	Fuel Tank Outlet

NOTES: 1. See Figure LM8/3.8.1-1 for RCS fracture mechanics pressure-temperature relationship curves.

2. See Table 3.10-8 for other RCS temperature limitations.

LM8/4.2.4 Thermal Variations of the MESA

Figures LM8/4.2.4-1 through LM8/4.2.4-3 indicate the thermal response of the MESA and temperature sensitive stowed equipment utilizing the following MESA and equipment optical properties.

	MESA STRUCTURE	ALSSC	LiOH	ALSRC			ETB
				Exterior	Interior	Closeout	
α	0.20	--	--	0.30	0.40	0.43	0.35
ε	0.29	0.9	0.85	0.05	0.40	0.88	0.80

Data are provided for nominal, hot, and cold conditions. The nominal case is for a 12° sun angle and 60°F temperature at deployment. The hot case is for a 33° sun angle and 80°F temperature at deployment with sun incident on the MESA. The cold case is for a 3° sun angle and 40°F temperature at MESA deployment.

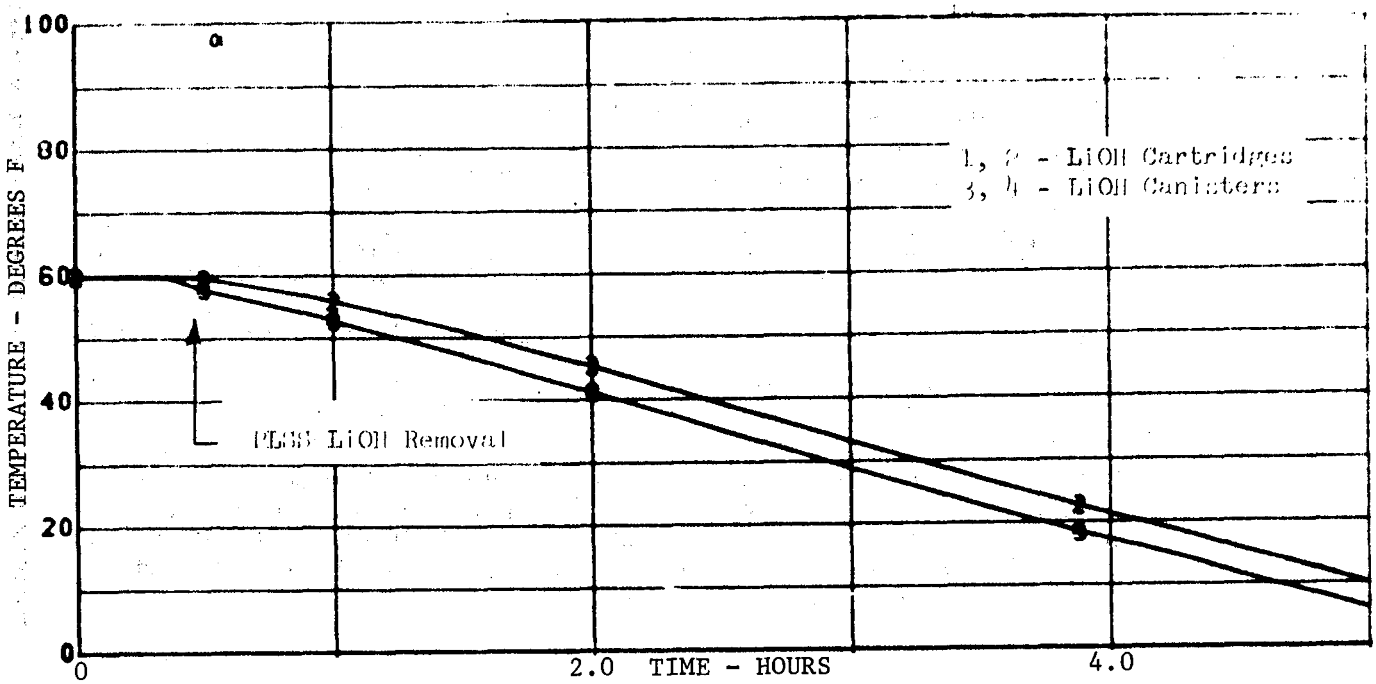

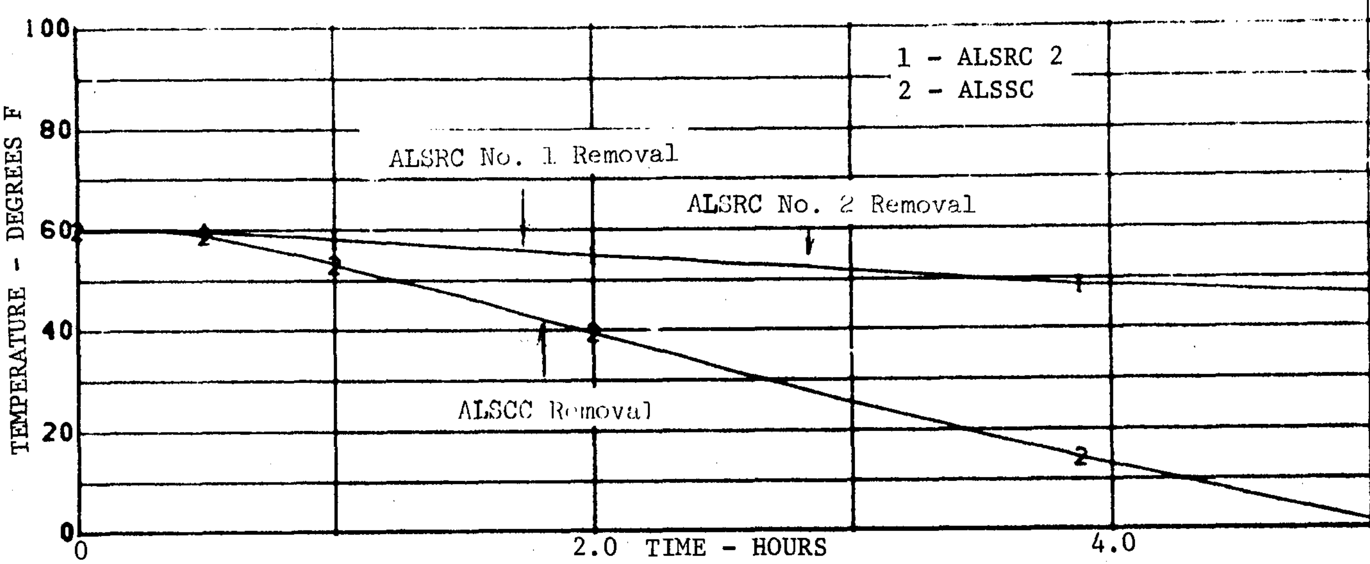

Figure LM8/4.2.4-1. MESA Thermal Analysis - Nominal Case

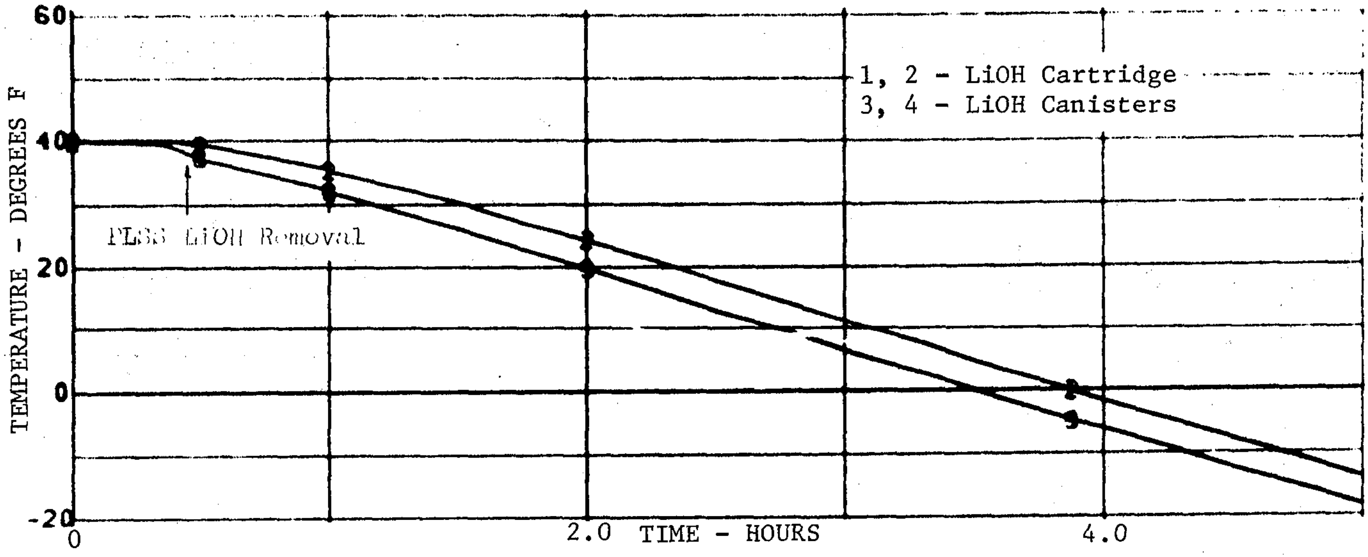

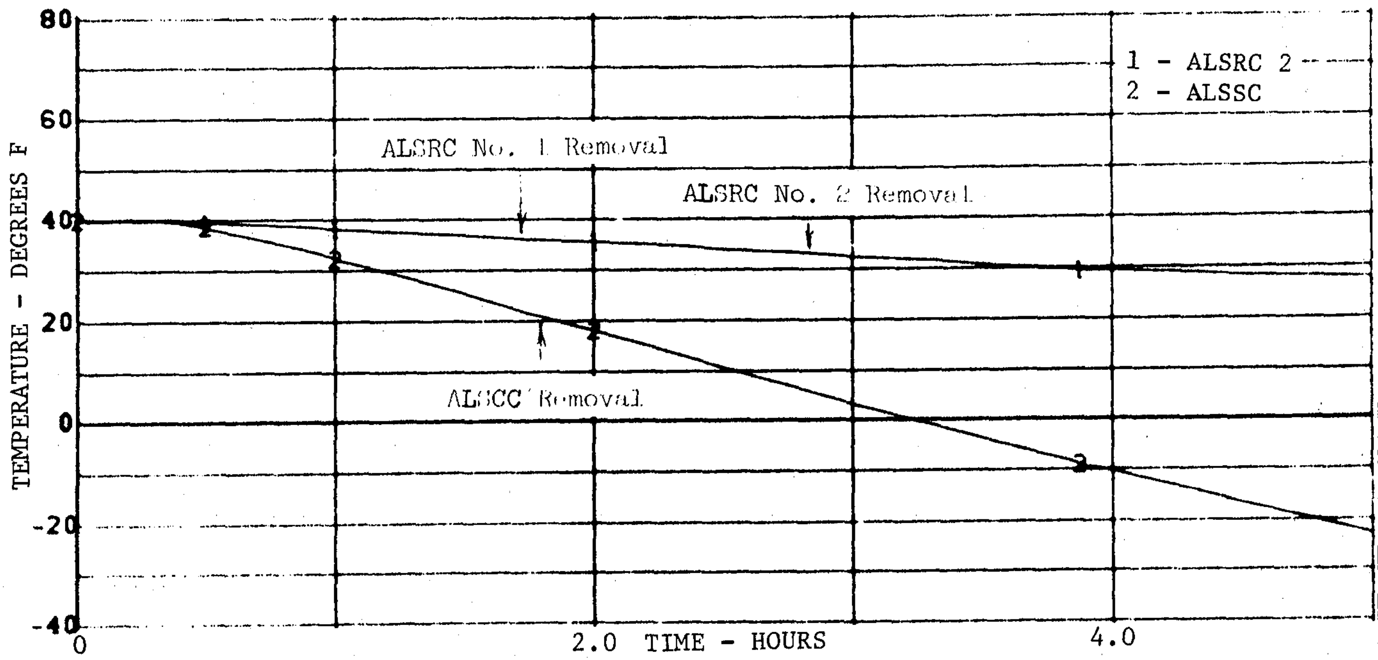

Figure LM8/4.2.4-2. MESA Themal Analysis - Cold Case

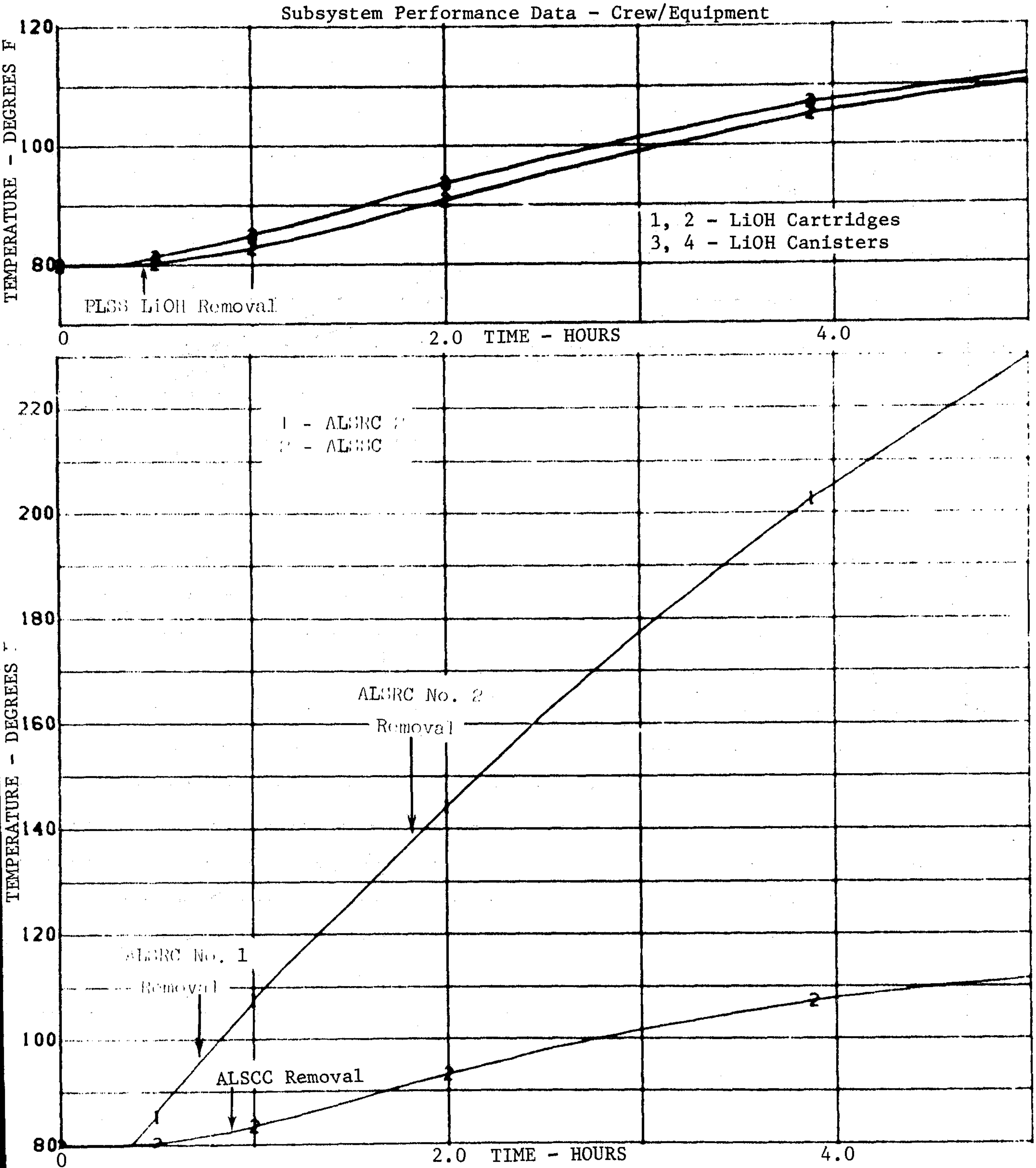

Figure LM8/4.2.4-3. MESA Thermal Analysis - Hot Case

LM8/4.2.5 Thermal Variation of the Sample Return Containers after Removal from the MESA (NASA DATA SOURCE)

The temperature response of the Sample Return Containers (SRC's) for the nominal timeline under nominal, cold, and hot conditions is shown on Figures LM8/4.2.5-1 through LM8/4.2.5-3.

(NASA DATA SOURCE)

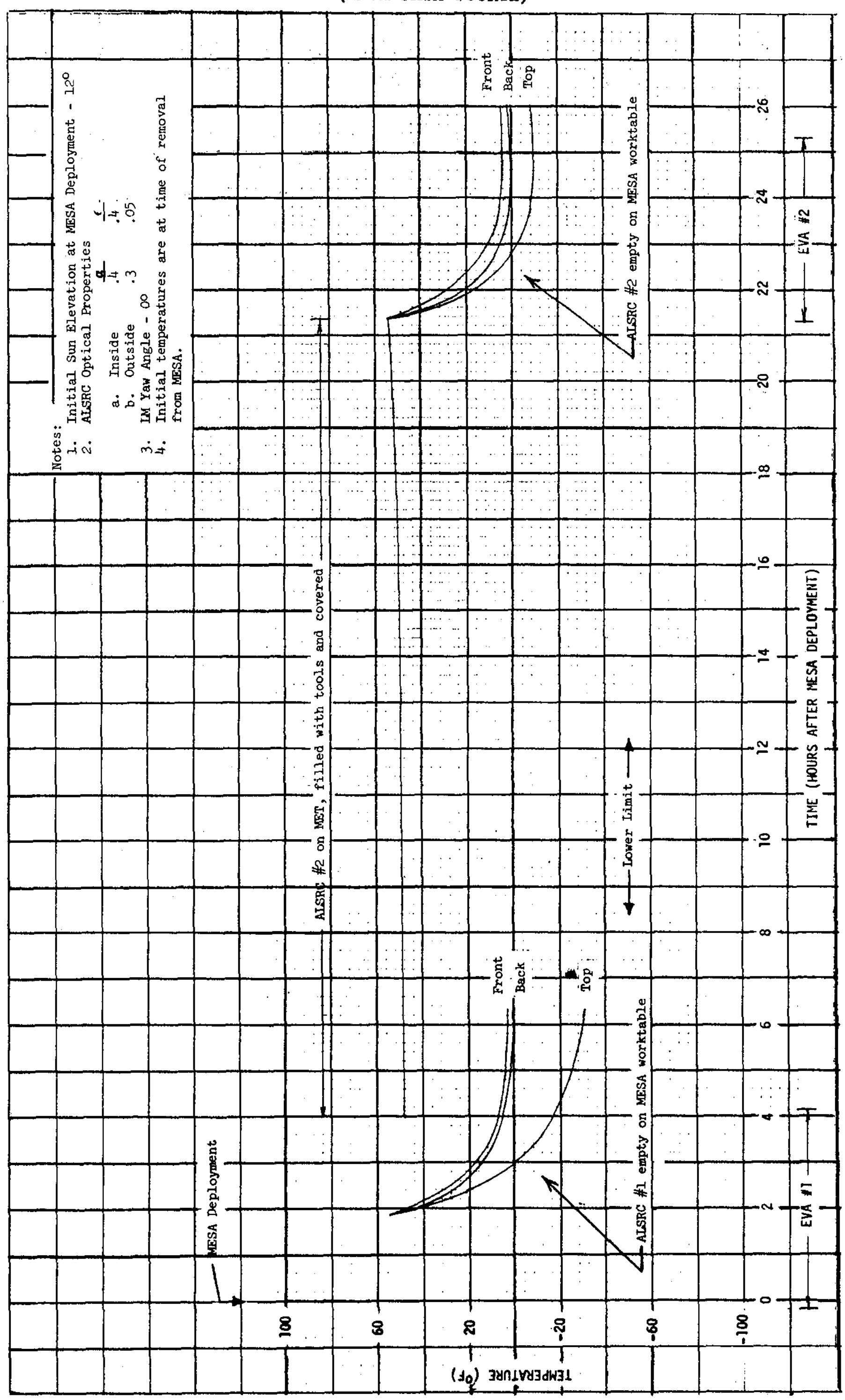

Figure LM8/4.2.5-1. Lunar Sample Return Container-Nominal Conditions

(NASA DATA SOURCE)

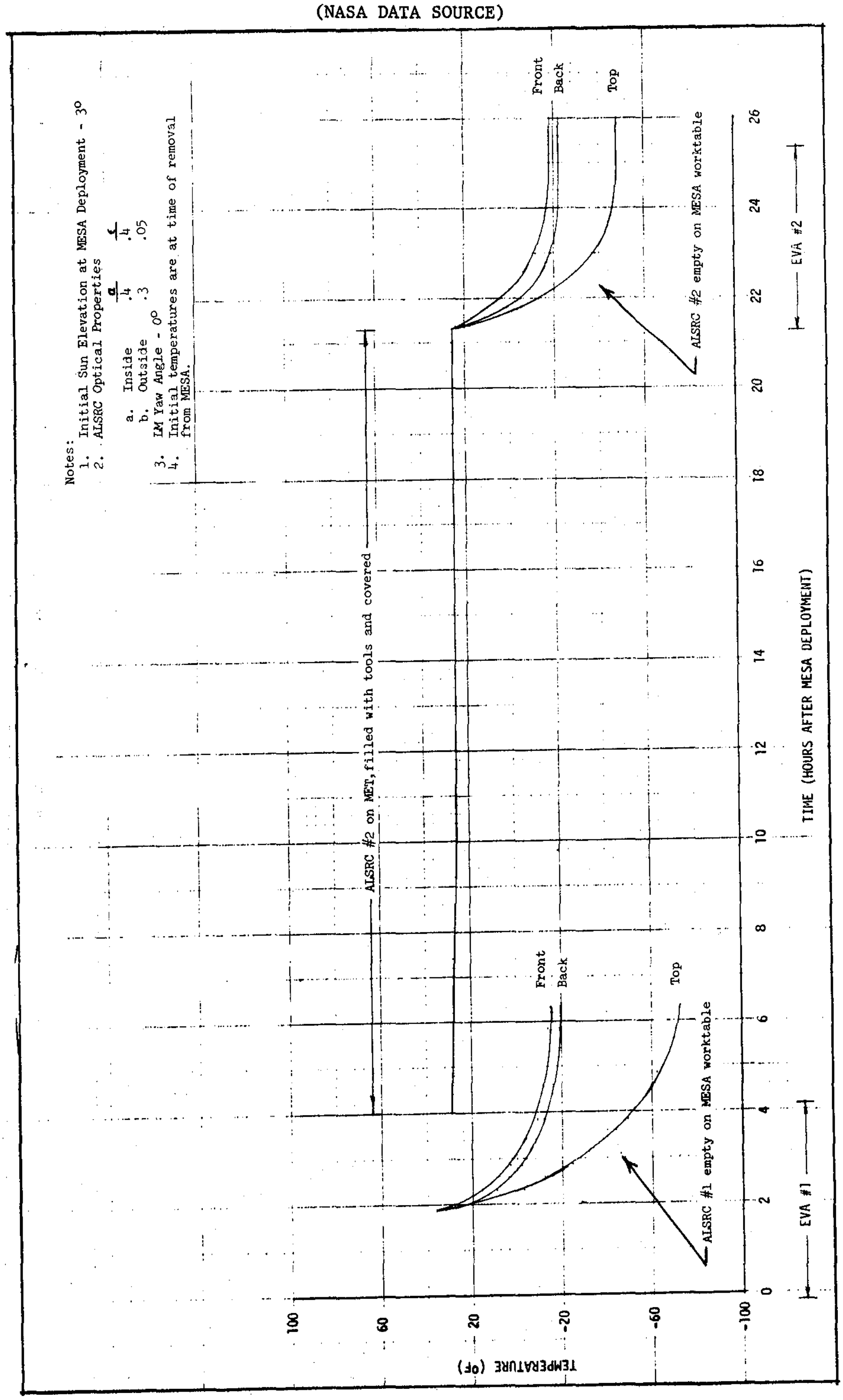

Figure LM8/4.2.5-2. Lunar Sample Return Container-Cold Conditions

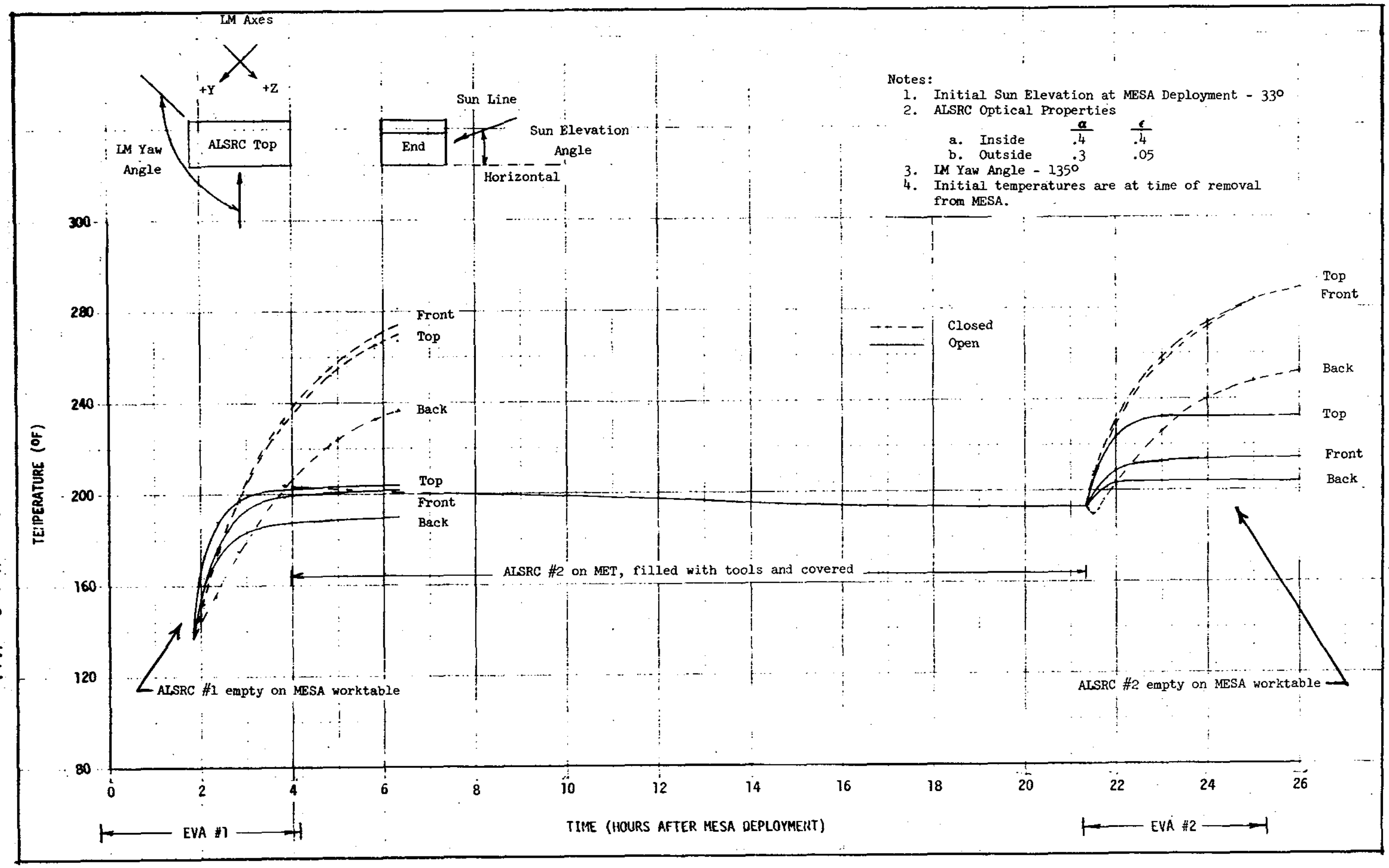

Figure LM8/4.2.5-3. Lunar Sample Return Container-Hot Conditions

LM8/4.2.6 Thermal Response of the Lunar Surface Color TV Camera (NASA DATA SOURCE)

Figure LM8/4.2.6-1 indicates the color TV camera thermal response while operating in the insulated MESA. The initial temperature at camera activation is 50°F.

Figure LM8/4.2.6-2 indicates the color TV camera thermal response while operating on the lunar surface with an initial camera temperature of 70°F at camera deployment, 10° sun angle, and local lunar surface slope of 15° into the sun.

(NASA DATA SOURCE)

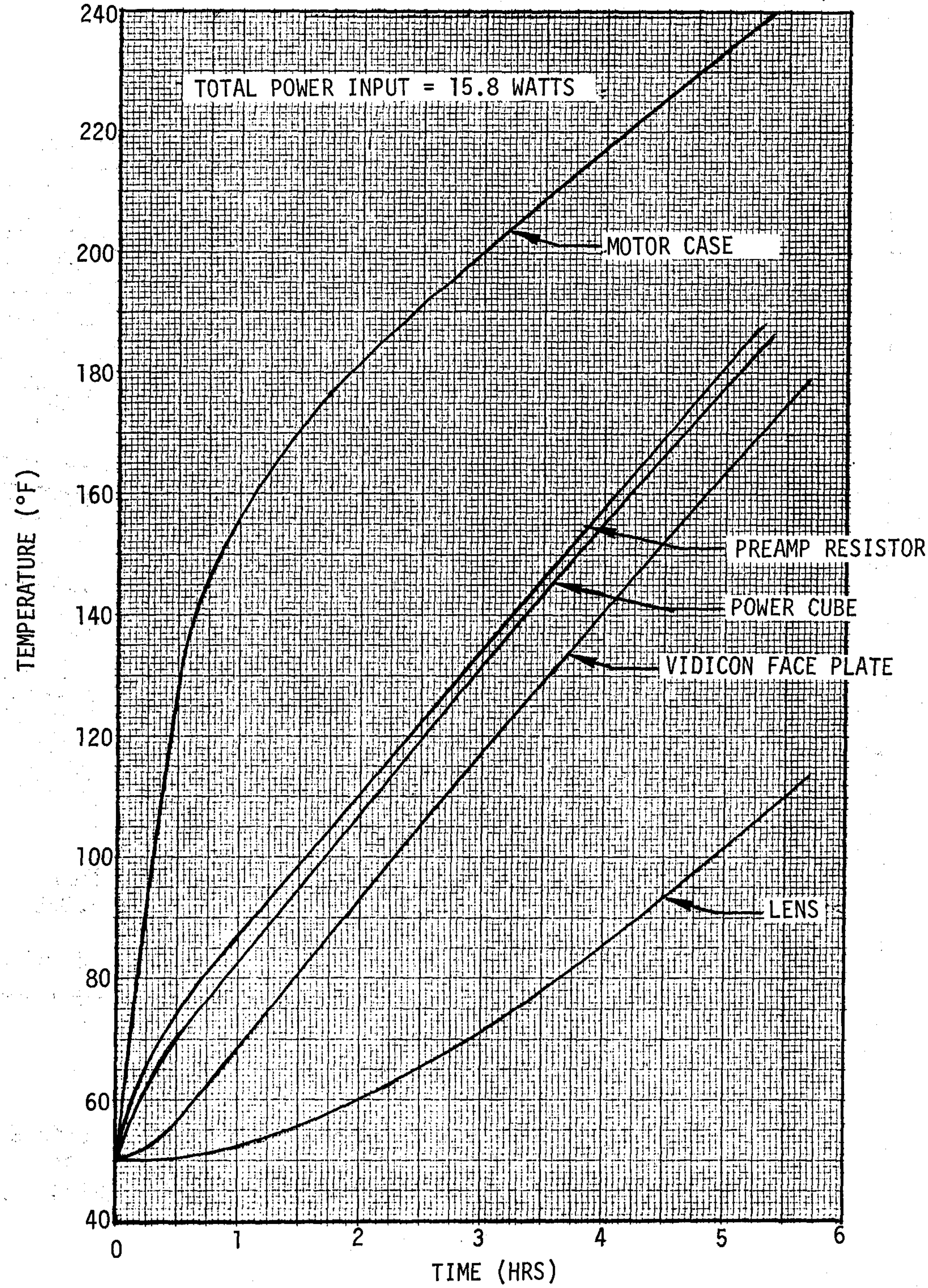

Figure LM8/4.2.6-1. Thermal Response of the Lunar Surface Color TV Camera while Operating in the Insulated MESA (See Para. LM8/4.2.6)

(NASA DATA SOURCE)

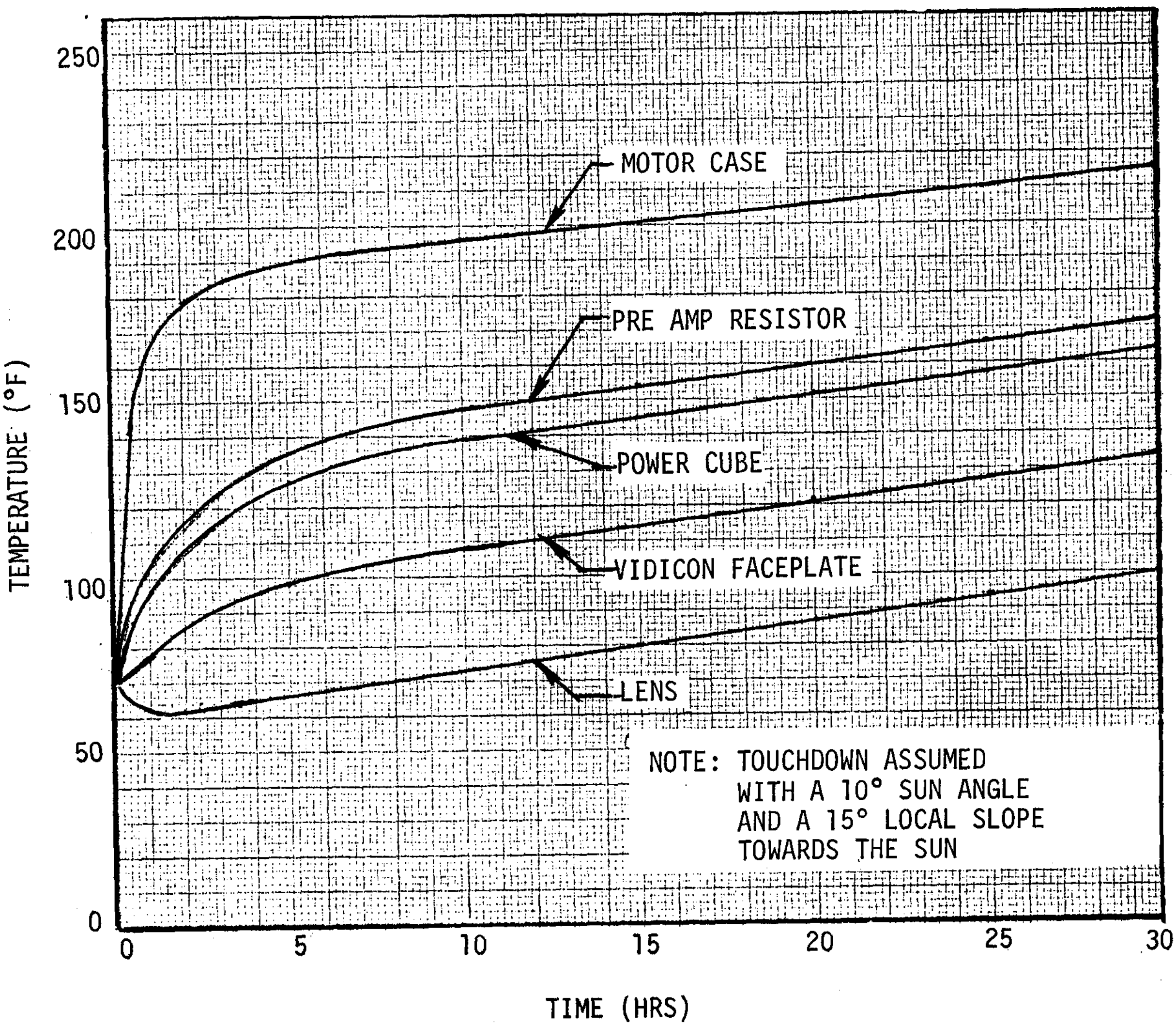

Figure LM8/4.2.6-2. Thermal Response of the Lunar Surface Color TV Camera While Operating on the Lunar Surface (See Para. LM8/4.2.6)

LM8/4.3.2.2 Leakage

Figure LM8/4.3.2-1 presents a band for LM-8 cabin leak rate as a function of cabin pressure over the range 3.0 to 5.2 psia, based on orifice-type and capillary-type leakage. A normal expected leak rate vs. pressure curve has also been included.

LM8/4.3.2.6 Cabin Regulator Check

Each check of the cabin regulators consumes approximately 0.5 lb of oxygen. The 0.5 lb is consumed primarily during the partial cabin repressurization (4.5 psia to 5.0 psia) at the conclusion of the regulator check.

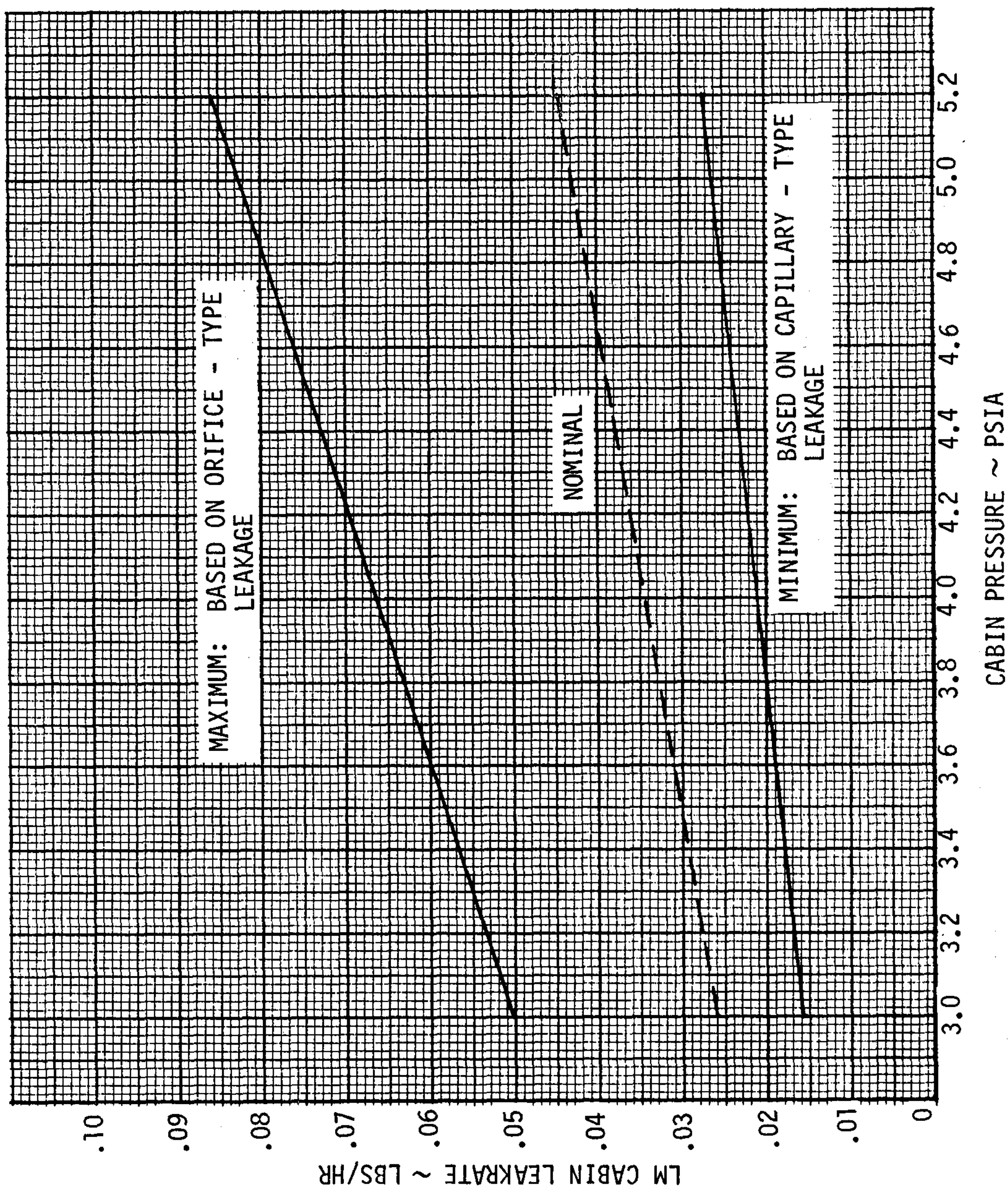

Figure LM8/4.3.2-1. Cabin Leak Rate Vs. Cabin Pressure (See Para. LM8/4.3.2.2)

LM8/4.3.3 Mission CO_2 Partial Pressure and LiOH Remaining

Figure LM8/4.3.3-1 presents CO_2 partial pressure versus mission time for the nominal mission showing the effect of sensor, PCM and CRT errors.

Figure LM8/4.3.3-2 presents CO_2 partial pressure versus mission time for the worst qualified cartridge showing the effect of sensor, PCM and CRT errors.

Figure LM8/4.3.3-3 presents the total LiOH hours remaining versus mission time. All the aforementioned graphs are based on Apollo 14 Final Flight Plan dated 2 December 1970.

The Flight Plan usage on the first cartridge is 23.8 hours and on the second cartridge is 11.0 hours. The average metabolic rates for these times are 461 BTU/hr/man and 595 BTU/hr/man, respectively.

Overall average metabolic rate for LM activities is 504 BTU/hr/man.

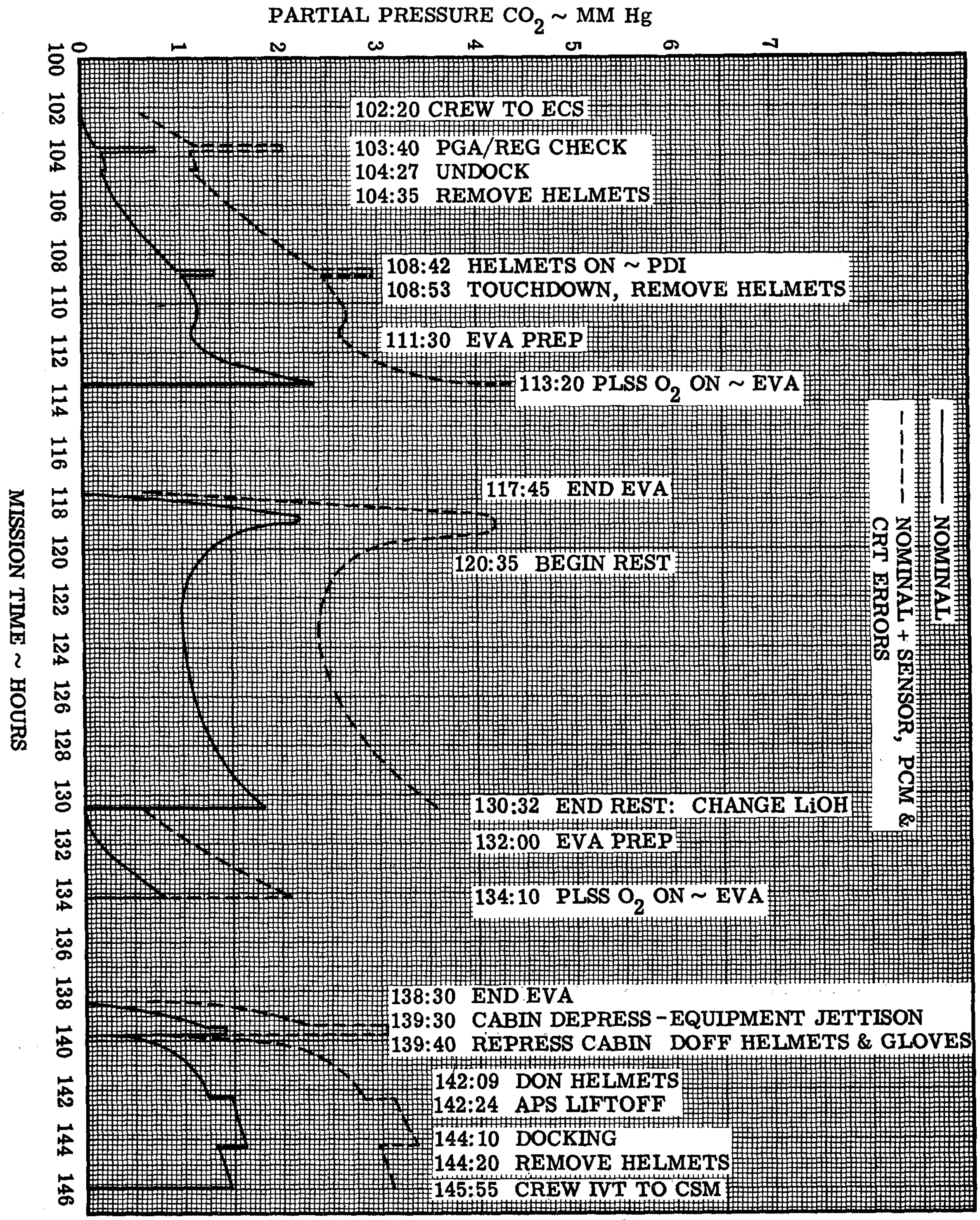

Figure LM8/4.3.3-1. LM-8 H-3 Mission CO2 Partial Pressure ~GF1521P
(See Para. LM8/4.3.3)

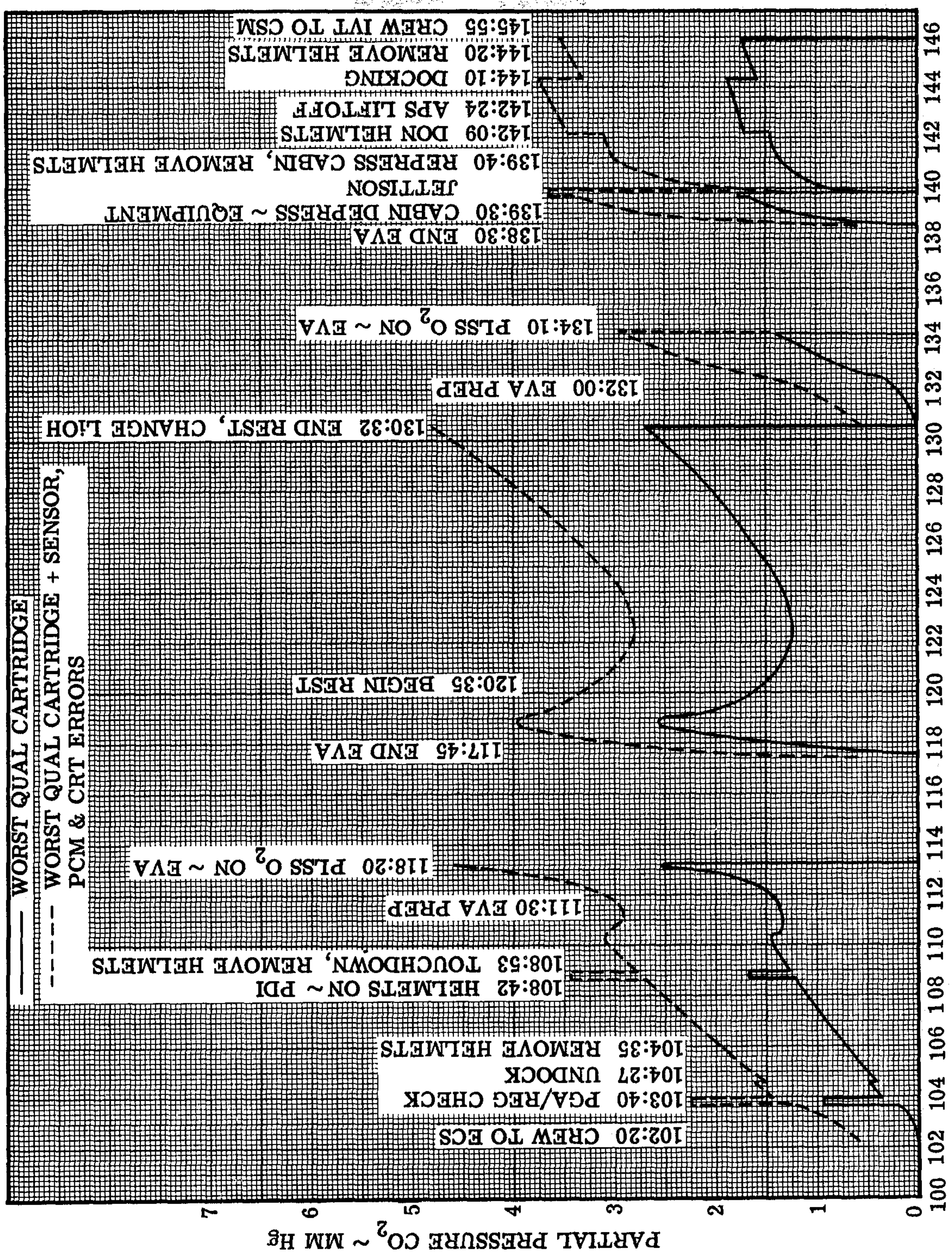

Figure LM8/4.3.3-2. LM-8 H-3 Mission CO2 Partial Pressure - GF1521P (See Para. LM8/4.3.3)

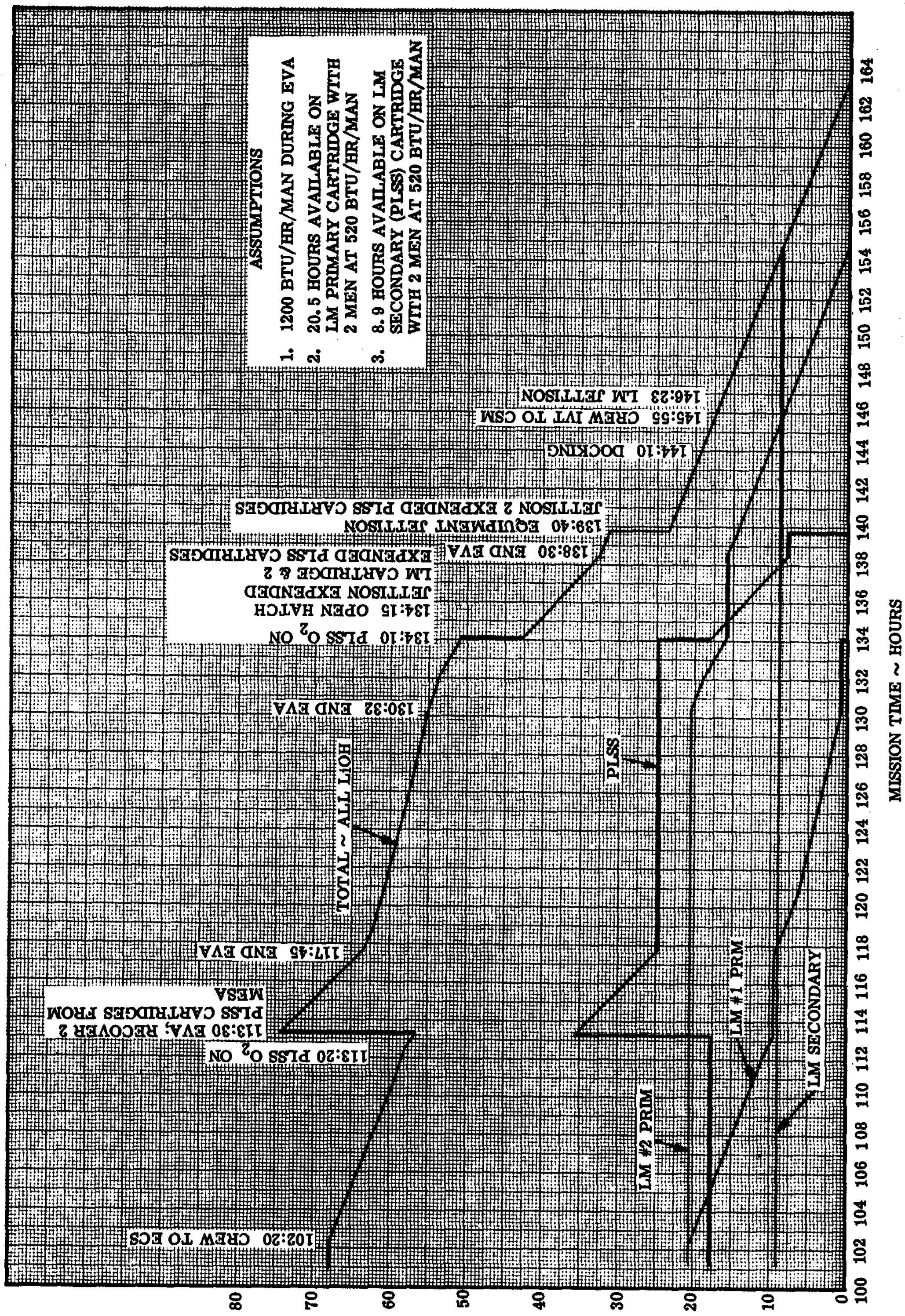

Figure LM8/4.3.3-3. LM-8 H-3 Mission Hours of LiOH Available for Use in LM (see para. LM8/4.3.3)

LM8/4.3.8 Environmental Control Equipment

LM8/4.3.8.1 Heat Transport Section Water Sublimators

Figures LM8/4.3.8-1 and LM8/4.3.8-2 present glycol outlet temperature as a function of glycol inlet temperature for primary HTS sublimator (209) and secondary HTS sublimator (224), respectively.

Figures LM8/4.3.8-3 and LM8/4.3.8-4 represent heat rejection capabilities for primary HTS sublimator (209) and secondary HTS sublimator (224), respectively.

Figure LM8/4.3.8-5 presents pump load line and HTS Δp characteristics as a function of glycol flow rate.

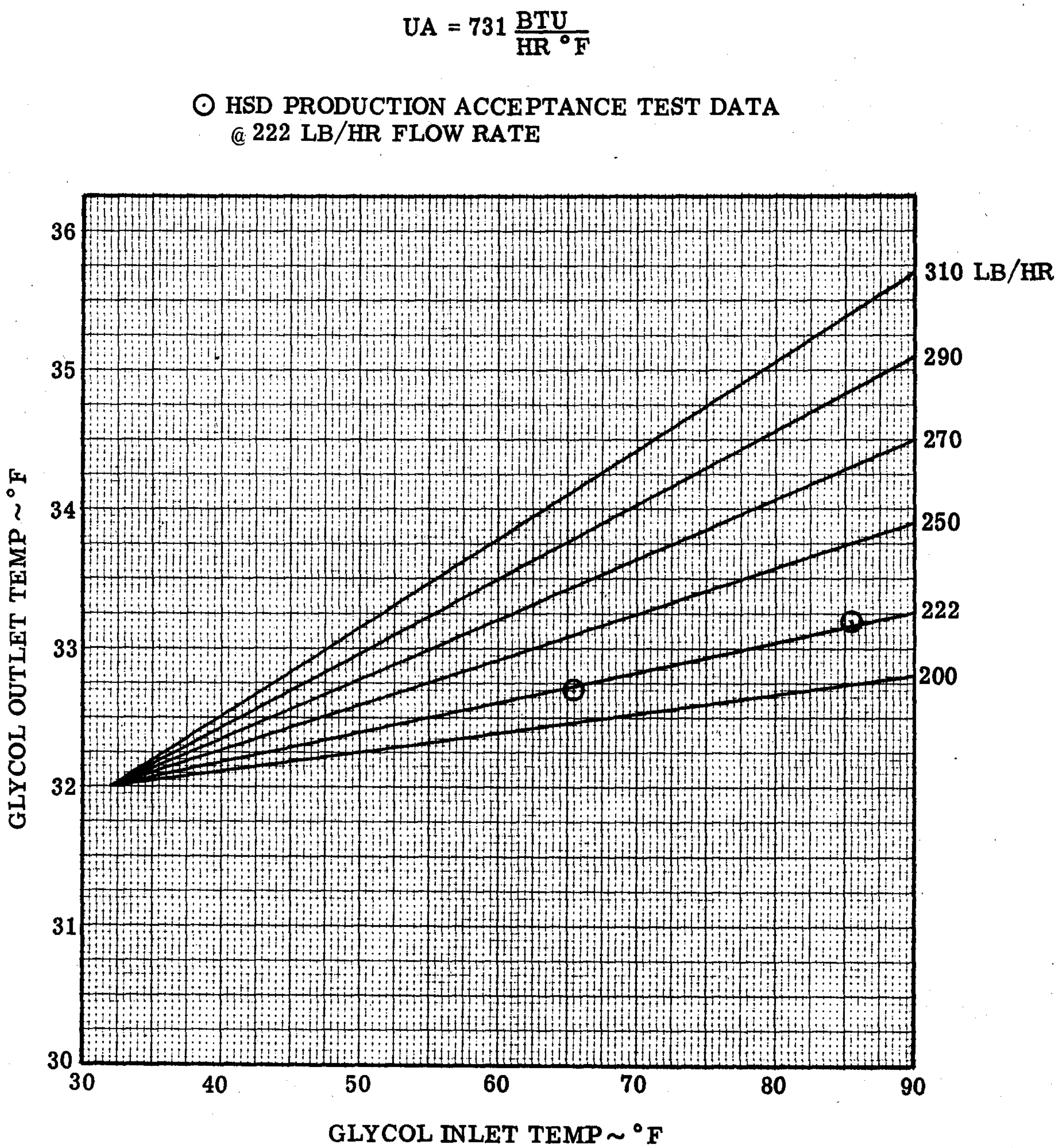

Figure LM8/4.3.8-1. Primary HTS Sublimator (209) LM-8 Acceptance Test Performance (U/N 138)

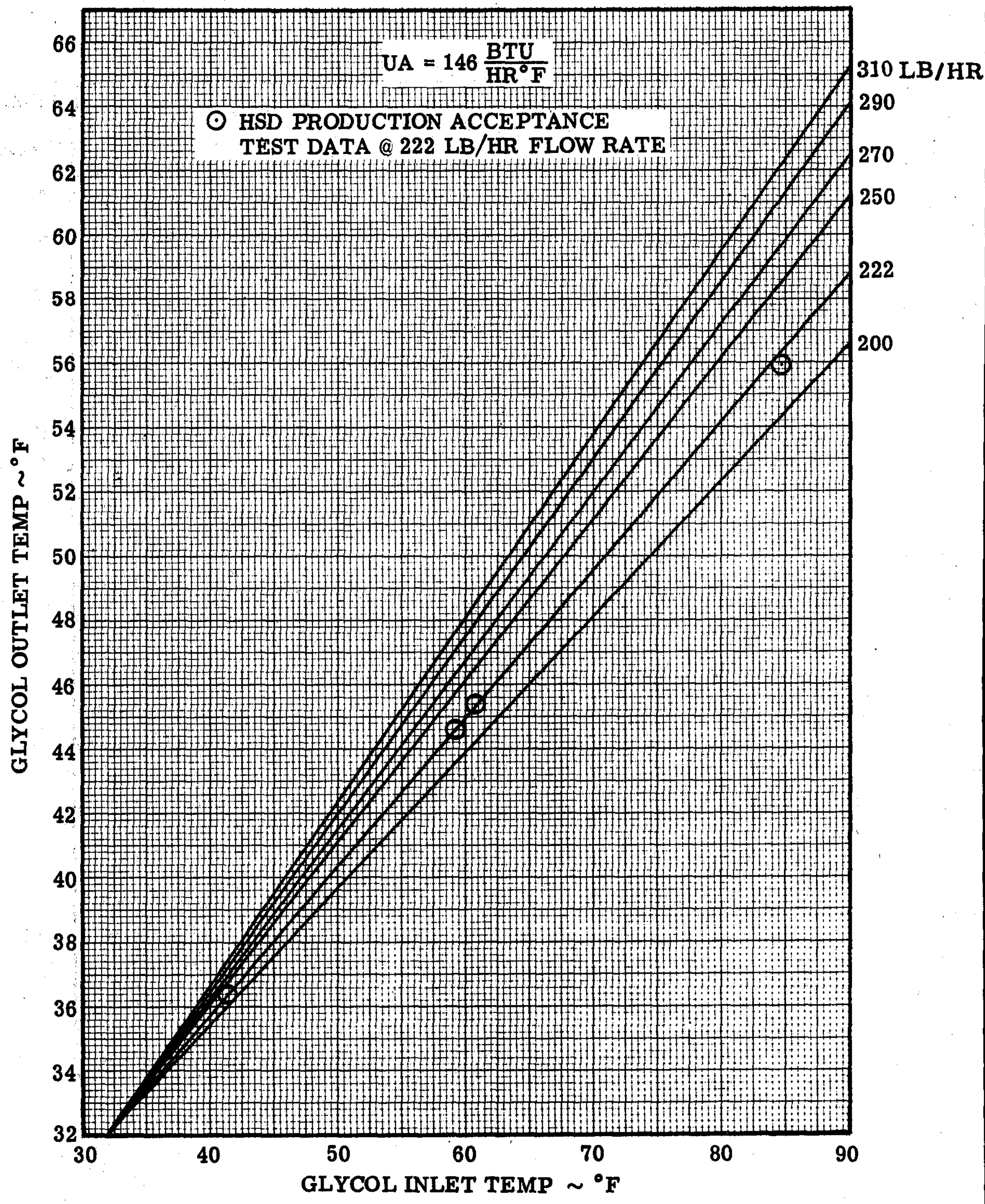

Figure LM8/4.3.8-2. Secondary HTS Sublimator (224) LM-8 Acceptance Test Performance (U/N 141)

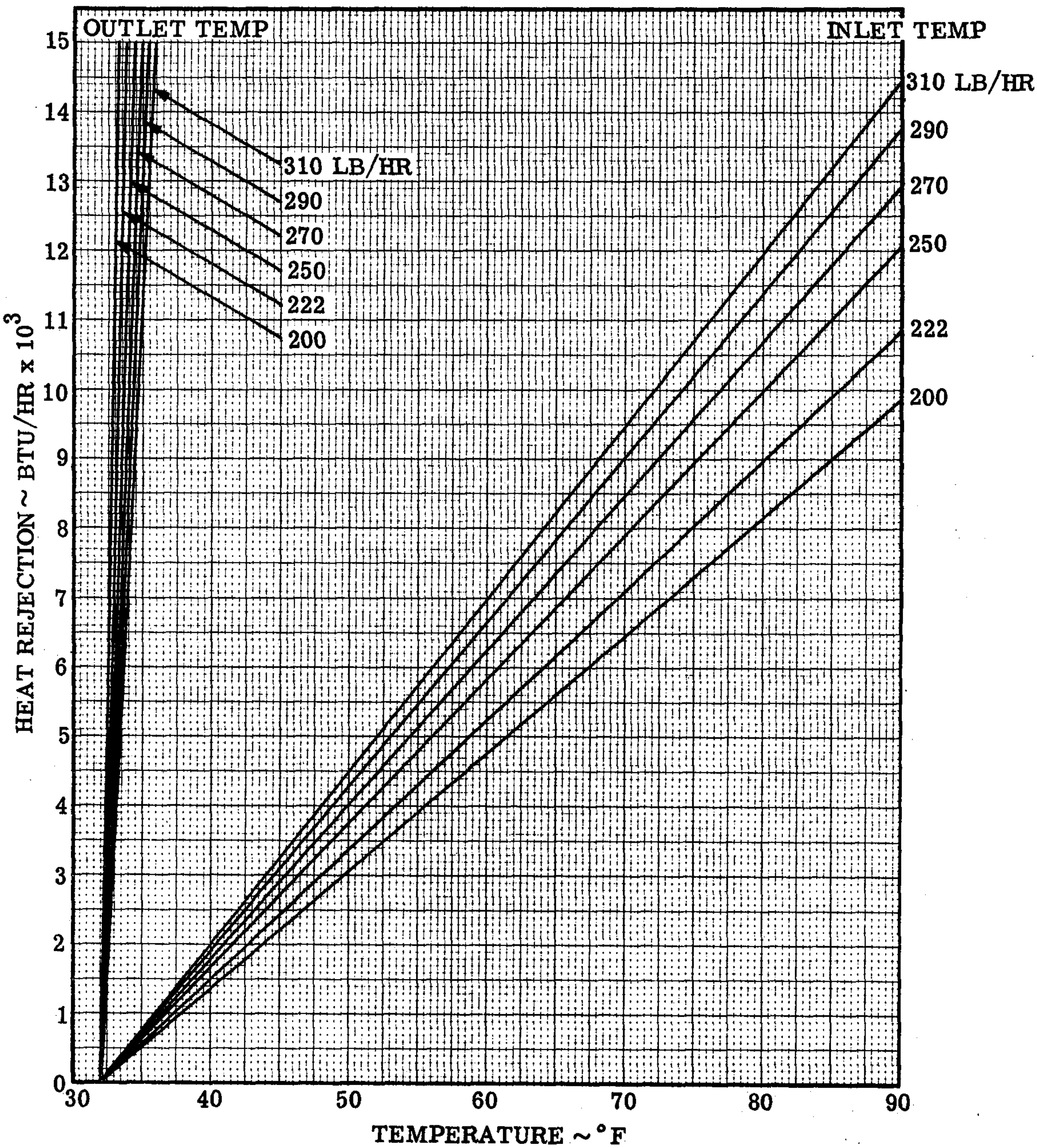

Figure LM8/4.3.8-3. LM-8 Primary HTS Sublimator (209) Heat Rejection Capability for UA = $731 \frac{BTU}{HR\ °F}$ (U/N 138)

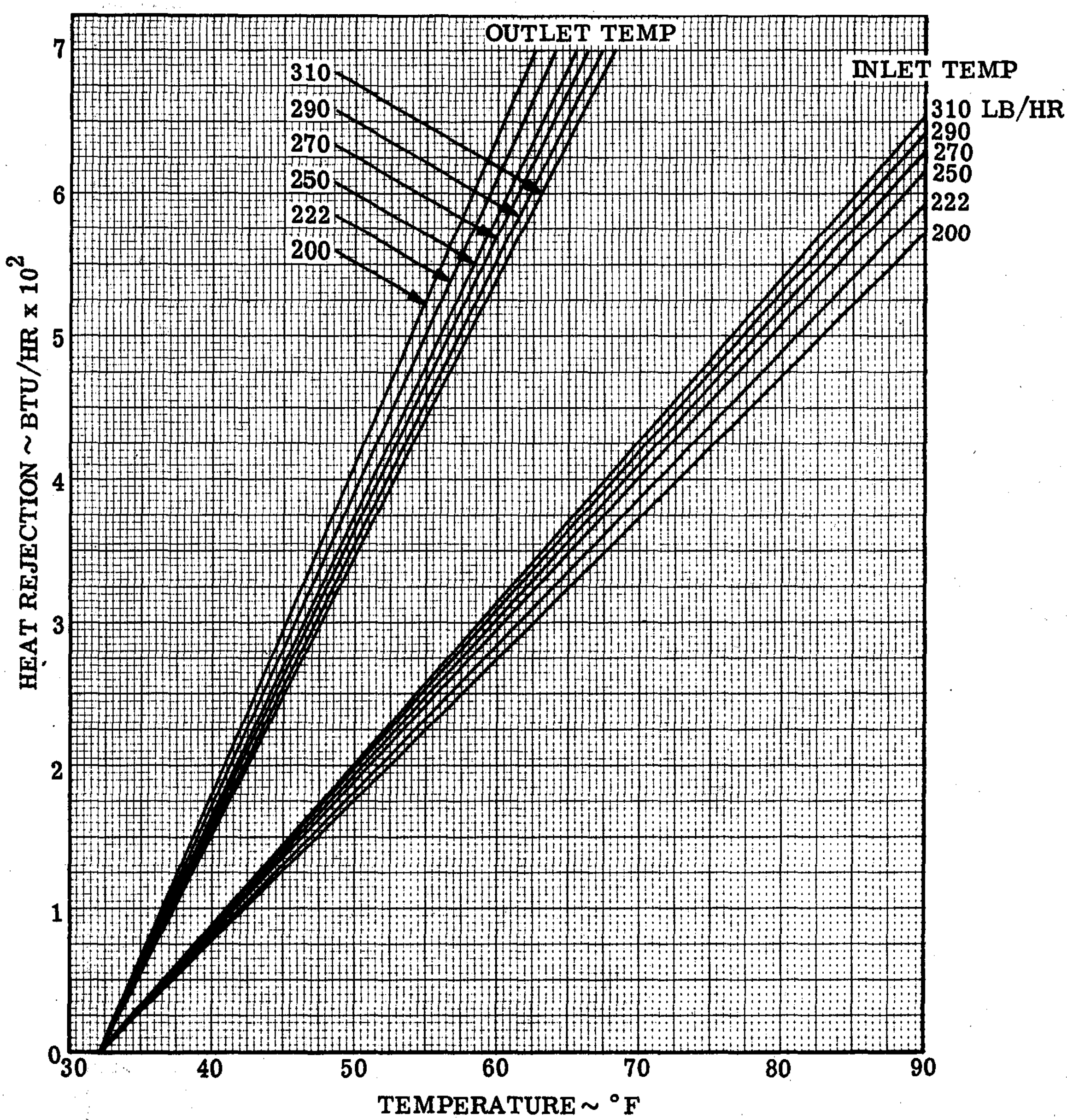

Figure LM8/4.3.8-4. LM-8 Secondary HTS Sublimator (224) Heat Rejection Capability for UA = 146 $\frac{BTU}{HR\ °F}$

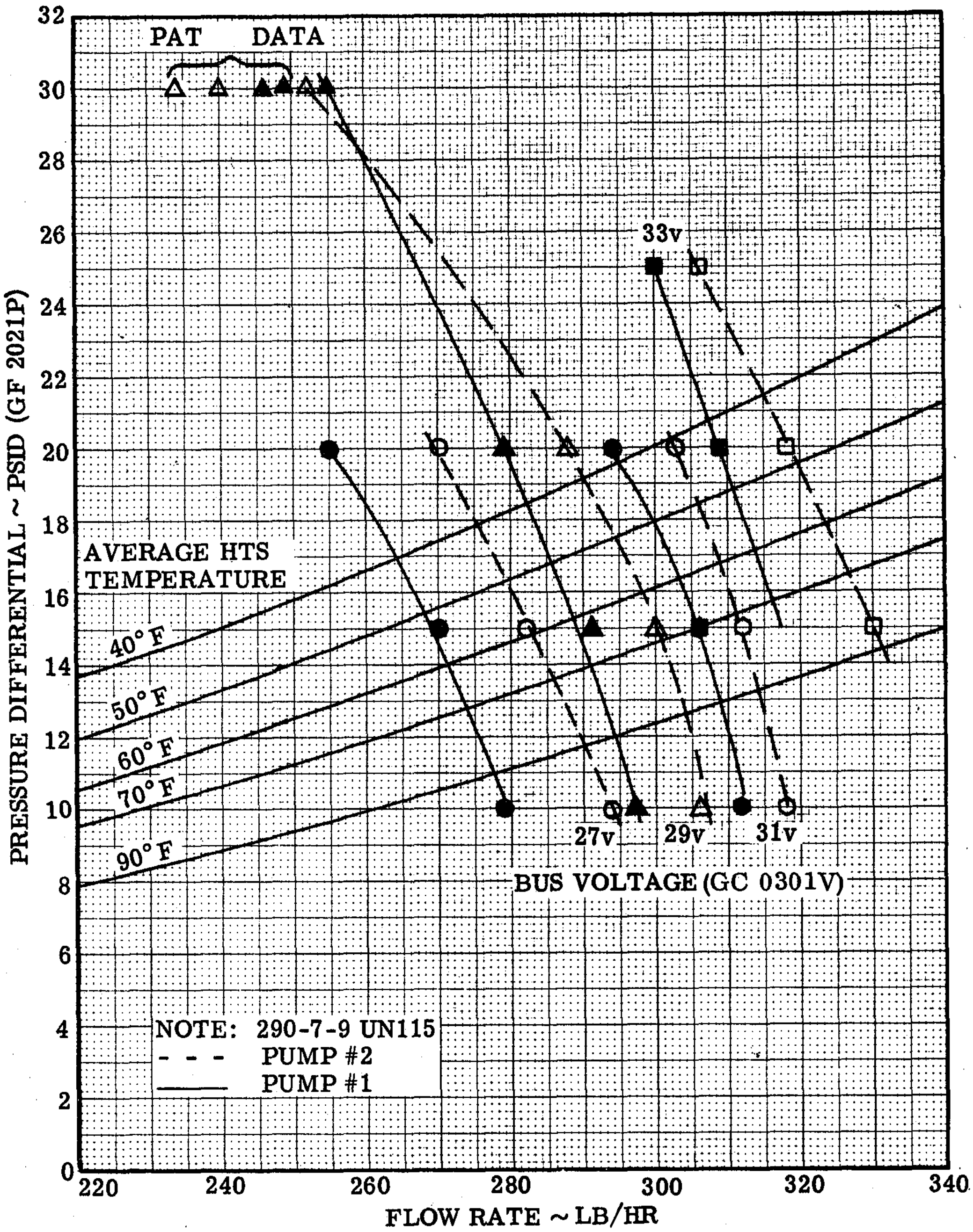

Figure LM8/4.3.8-5. LM-8 HTS System and Pump Characteristics

LM8/4.3.11 Duty Cycle of LM Heaters

The estimated average heater powers of the LM heaters for the LM-8/H-3 Mission are presented in Table LM8/4.3.11-1. The mission phases or definable spacecraft operations occur as shown in the headings of the table per Apollo 14 Flight Plan, AS 509/CSM 110/LM-8, 2 December 1970.

Antenna (S-band steerable, rendezvous radar, landing radar), heater requirements were determined from a review and application of the following:

(a) Vendor thermal studies (see LMO 510-1193).

(b) Acceptance and qualification test data (see LMO 510-1193).

(c) LM-3, LM-4, LM-5, and LM-6 flight data

Guidance equipment (IMU, ASA) heater requirements were determined from a combination of the following:

(a) Calculations using vehicle structure temperature and coolant temperatures when applicable

(b) Review and application of LM-3, LM-4, LM-5, and LM-6 flight data

Window and AOT heaters are nonthermostatically controlled, constant-power devices. Table LM8/4.3.11-1 lists the nominal heater powers of these items and indicates worst-case usage for the H-3 Mission. The window heaters will be energized at the discretion of the astronaut when fogging is noted.

The RCS thruster heater requirements were determined from the following:

(a) Thermal studies

(b) Review and application of LM-3, LM-4, LM-5, and LM-6 flight data

Lunar stay estimates of heater duty cycle for antenna heaters and RCS thruster heaters are based on a low sun elevation angle at landing (7°) and did not consider any shadowing or vehicle tilting due to irregular terrain.

Table LM8/4.3.11-1. Average Heater Power during Mission Phases

Heaters	Launch & Boost	Translunar Coast		Lunar Orbit & Descent		Lunar Stay	Ascent & Lunar Orbit
	LM Power -00:30 to 02:31 watts	LM Power 02:31 to 03:25 watts	CSM Power 03:25 to 82:38 watts	CSM Power 82:38 to 101:59 watts	LM Power 101:59 to 108:54 watts	LM Power 108:54 to 142:24 watts	142:24 to 146:23 watts
S-Band Steerable Antenna	2	4	4	2	2 (Note 1)	2	2 (Note 1)
Rendezvous Radar Antenna	6	8	8	6	8 (Note 1)	8/2 (Note 5)	8 (Note 1)
Landing Radar Ant	8	20	20	10	10 (Note 1)	-	-
ASA	7	7	7	7	17 (Note 3)	55	17 (Note 3)
IMU	15	15	15	15	14.5 (Note 3)	25	14.5 (Note 3)
Fwd Window (CDR)	0	0	0	0	61.8 (Note 4)	61.8 (Note 4)	61.8 (Note 4)
Fwd Window (SE)	0	0	0	0	61.8 (Note 4)	61.8 (Note 4)	61.8 (Note 4)
Docking Window	0	0	0	0	24.0 (Note 4)	24.0 (Note 4)	24.0 (Note 4)
AOT	0	0	0	0	5.0	5.0	5.0
RCS Thruster	0	0	0	0	(Note 2)	40.0	20.0
Total Average Power/Phase, watt			54	40			
Average current at 28vdc, Amps			1.93	1.43			

(see following page for notes)

Table LM8/4.3.11-1 (Continued)

Notes:

(1) Heater duty cycle estimates are for periods when antennas, are de-activated. Duty cycles are estimated to be zero when the antennas are active.

(2) 764 watts for 1/2 hour warmup followed by a 140 watt average until undocking and a 20 watt average for the remainder of this phase.

(3) Total ASA power is 55 watts; 38 watts instrument power plus 17 watts heater power. Total IMU power is 74.5 watts; 59 watts instrument power plus 14.5 watts heater power.

(4) Window heaters are normally zero since they are energized only when fogging is noted.

(5) The average RR antenna heater power will vary with the heater mode selected. It is estimated to be 2 watts for 85% of the stay period (standby heater mode) and 8 watts for the remainder of the stay period (operate heater mode).

LM8/4.3.12.7. Loss of Ascent Stage Water During Lunar Stay (NASA DATA SOURCE)

For the case of loss of ascent stage water, at least one hour prior to ascent (i.e., 141.4 hours GET), the limits for heat stored by a crewman and for equipment temperature are not violated until after docking at 144.16 hours GET. However, between docking and separation (146.47 hours GET), limits for the following are exceeded:

Crewman heat stored	(Figures 4.3.12-40, -41)
SBPA	(Figure 4.3.12-3)
DSEA	(Figure 4.3.12-6)
DUA	(Figure 4.3.12-11)
ASA	(Figure 4.3.12-15)
Batteries	(Figures 4.3.12-21, -22)
TLE	(Figure 4.3.12-23)
IMU	(Figure 4.3.12-25
LGC	(Figures 4.3.12-26, -29, -32)

This simulation is based on the LM-8 nominal timeline and does not incorporate minimum power or equipment cycling procedures specifically designed to control the thermal response of the spacecraft.

The responses of the coldplate equipment and selected ECS parameters are shown in Figures LM8/4.3.12-1 through LM8/4.3.12-46. An index to these figures is given in Table LM8/4.3.12-1.

The predictions are based on the following conditions and assumptions:

1. LM8 nominal trajectory and timeline from lunar liftoff through rendezvous.

2. Normal equipment operation timeline.

3. Utilization of descent water by the heat transport system (HTS) until liftoff.

4. Simultaneous operation of the primary and secondary HTS from one hour prior to ascent through rendezvous; primary and secondary sublimator dry-out is simulated after liftoff.

Table LM8/4.3.12-1. Index to Figures (NASA DATA SOURCE)

Figure No.	Description
4.3.12-1	Signal Processor (SP)
4.3.12-2	S-Band Transceiver
4.3.12-3	S-Band Power Amplifier (SBPA)
4.3.12-4	VHF Transceiver
4.3.12-5	Pulse Code Modulation and Timing Electronics (PCMTEA)
4.3.12-6	Data Storage Electronics Assembly (DSEA)
4.3.12-7	Caution and Warning Electronics Assembly (CWEA)
4.3.12-8	Signal Conditioning Electronics Assembly (SCEA) No. 1
4.3.12-9	Signal Conditioning Electronics Assembly (SCEA) No. 2
4.3.12-10	Rendezvous Radar Electronics (RRE)
4.3.12-11	Digital Uplink Assembly (DUA)
4.3.12-12	Attitude and Translation Control Assembly (ATCA)
4.3.12-13	Gimbal Angle Sequencing Transformation Assembly (GASTA)
4.3.12-14	Rate Gyro Assembly (RGA)
4.3.12-15	Abort Sensor Assembly (ASA)
4.3.12-16	Abort Electronics Assembly (AEA)
4.3.12-17	Inverter No. 1
4.3.12-18	Inverter No. 2
4.3.12-19	A/S Electrical Control Assembly (ECA) No. 3
4.3.12-20	A/S Electrical Control Assembly (ECA) No. 4
4.3.12-21	A/S Battery No. 5 and 6
4.3.12-22	A/S Battery No. 6
4.3.12-23	Tracking Light Electronics (TLE)
4.3.12-24	Lighting Control Assembly (LCA)
4.3.12-25	Inertial Measurement Unit (IMU) Stable Element
4.3.12-26	LM Guidance Computer (LGC) Coldplate
4.3.12-27	LM Guidance Computer (LGC) Right Front Face
4.3.12-28	LM Guidance Computer (LGC) Electronic Module
4.3.12-29	LM Guidance Computer (LGC) Electronic Module
4.3.12-30	LM Guidance Computer (LGC) Logic Module
4.3.12-31	LM Guidance Computer (LGC) Logic Module
4.3.12-32	LM Guidance Computer (LGC) Power Supply
4.3.12-33	LM Guidance Computer (LGC) Power Supply
4.3.12-34	Coupling Data Unit (CDU) Lanyard Logic Module
4.3.12-35	Coupling Data Unit (CDU) Lanyard Logic Module
4.3.12-36	Coupling Data Unit (CDU) Power Supply Module
4.3.12-37	Power and Servo Assembly (PSA) 800 Cycle
4.3.12-38	Power and Servo Assembly (PSA) 800 Cycle
4.3.12-39	Pulse Torque Assembly (PTA) PIPA Calibration
4.3.12-40	Reference Heat Stored, Astronaut No. 1
4.3.12-41	Reference Heat Stored, Astronaut No. 2
4.3.12-42	Average Cabin Structure
4.3.12-43	Primary Sublimator Coolant Inlet
4.3.12-44	Primary Sublimator Coolant Outlet
4.3.12-45	Suit Inlet
4.3.12-46	Low Temperature Electronics (LTE) Coolant Inlet

(NASA DATA SOURCE)

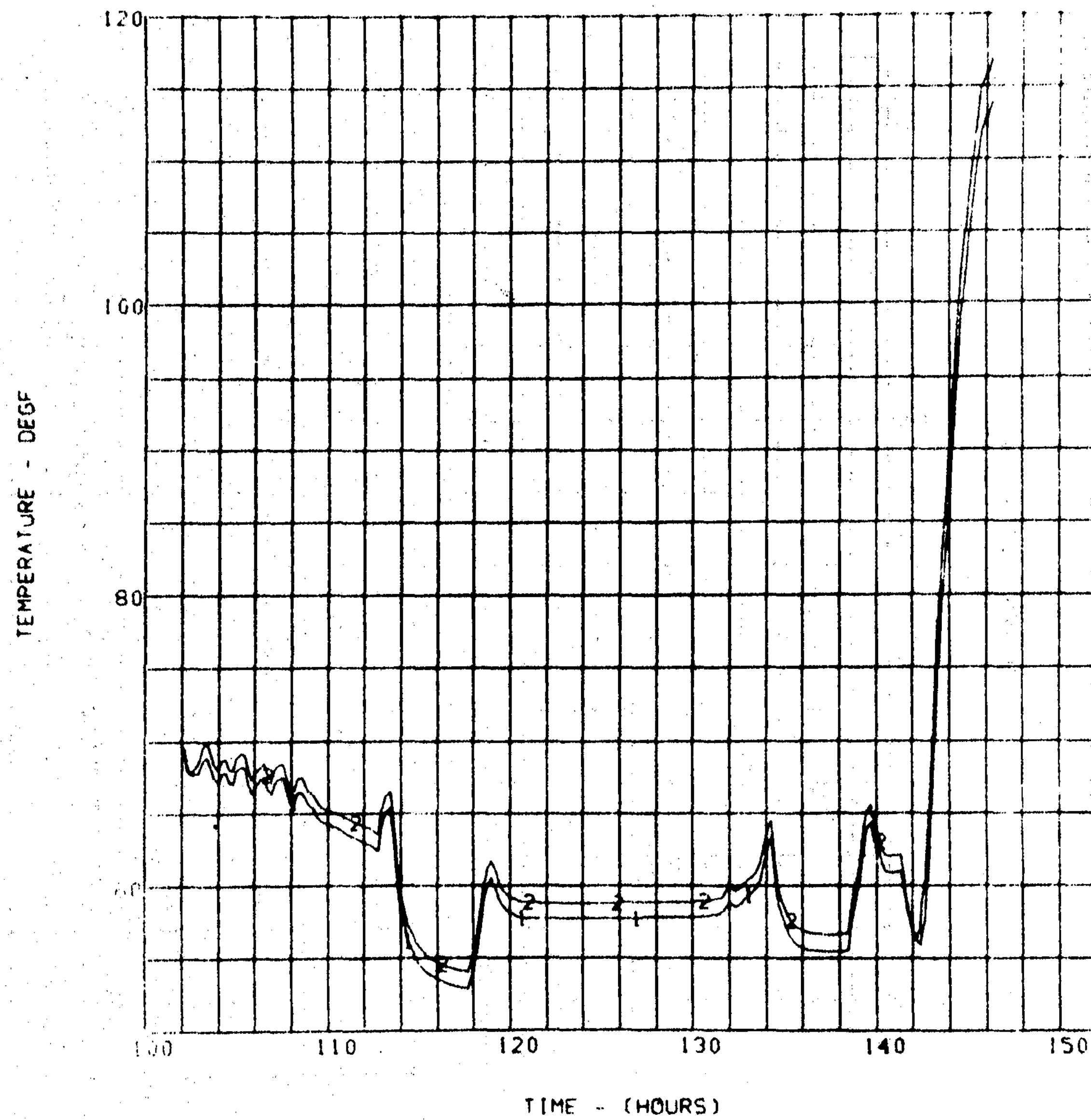

Figure LM8/4.3.12-1. LM8 A/S water Tank Failure Simulation
(1) 50ST Signal Proc. Flange-AEB Limit 135 Deg.
(2) 51ST Signal Proc. Flange-AEB Limit 135 Deg.
(See Para. 4.3.12.7)

(NASA DATA SOURCE)

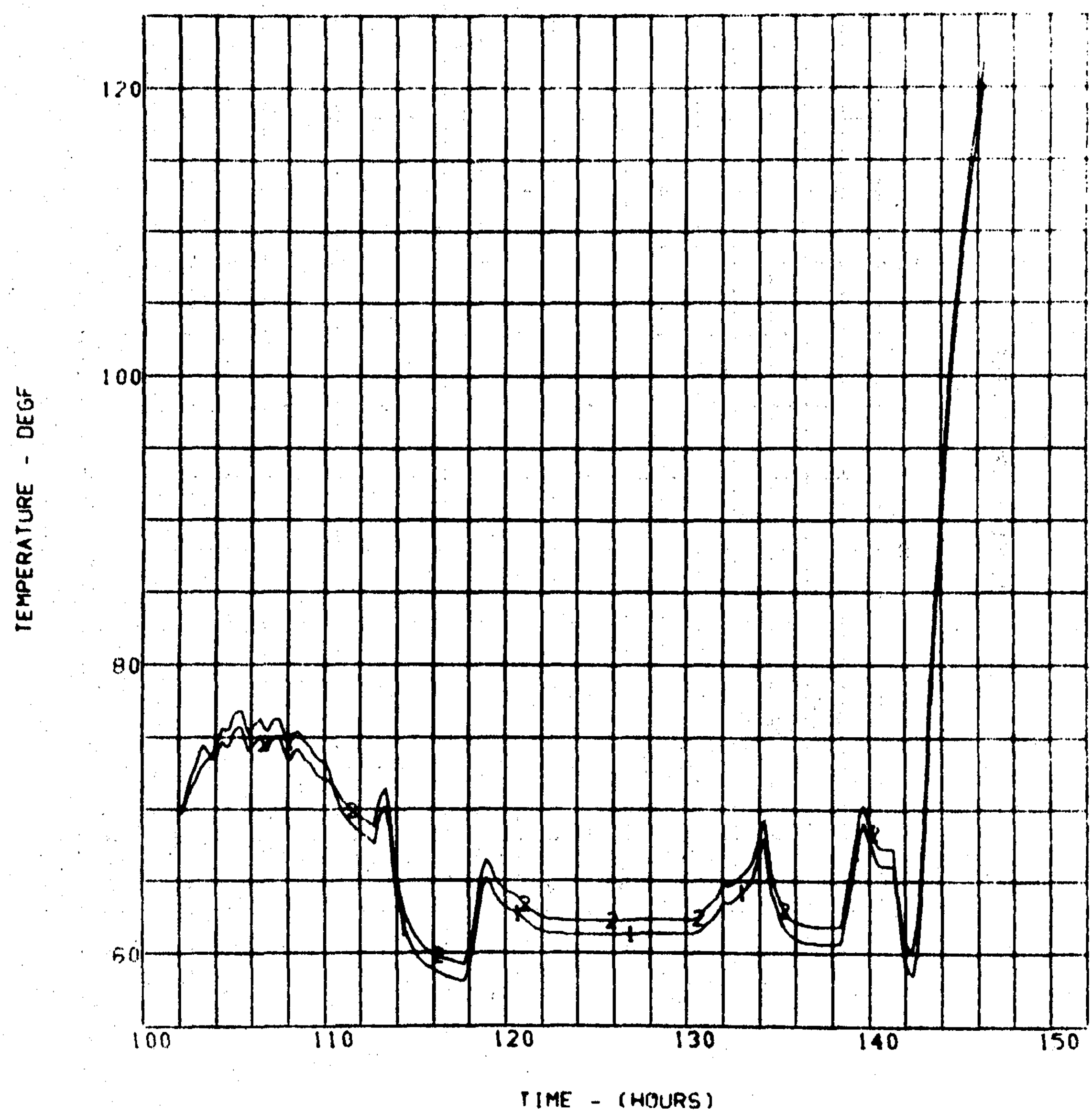

Figure LM8/4.3.12-2. LM8 A/S Water Tank Failure Simulation
(1) 48ST S-Band Trans. Flange-AEB Limit 135 Deg.
(2) 49ST S-Band Trans. Flange-AEB Limit 135 Deg.
(See Para. 4.3.12.7)

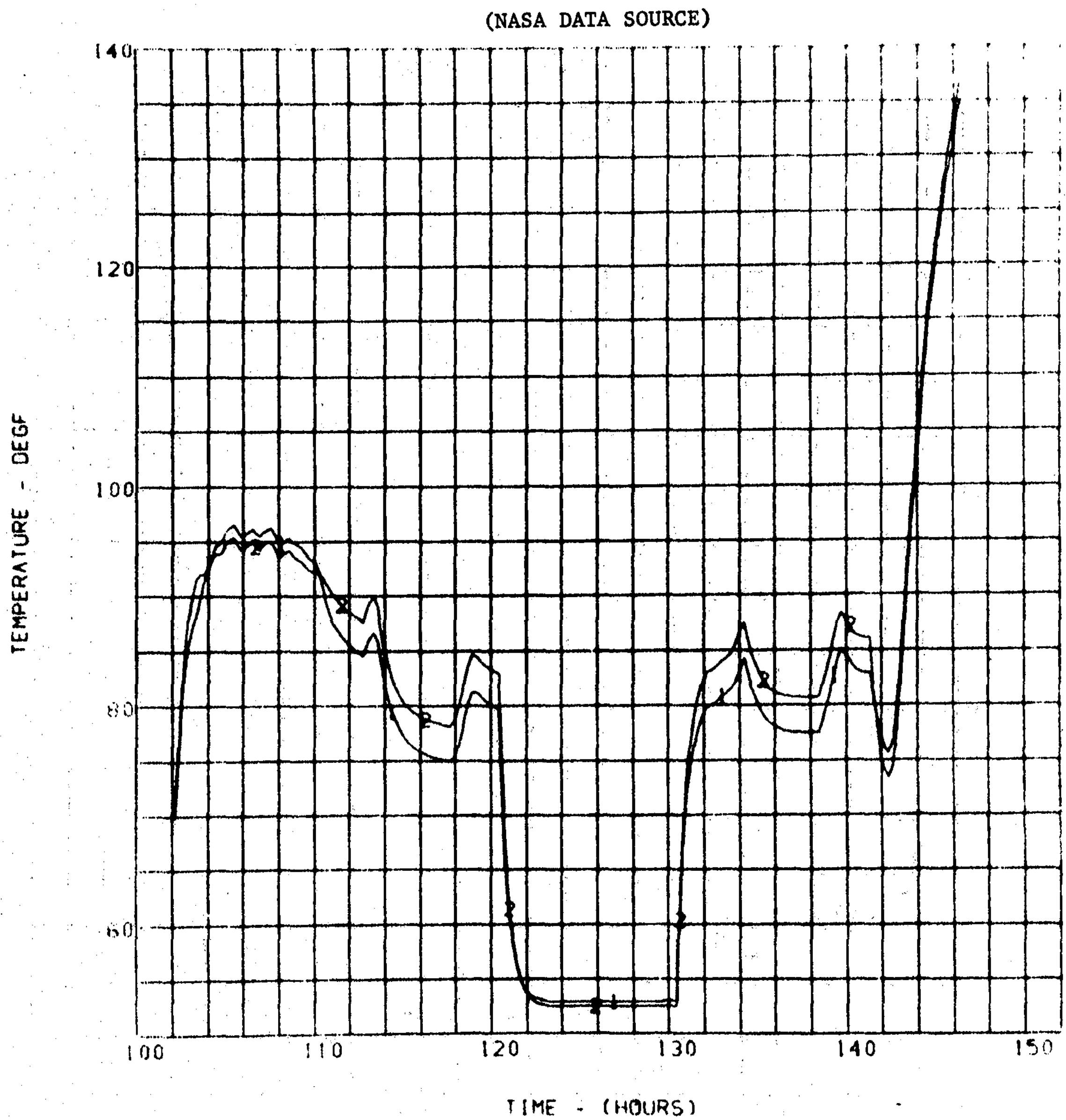

Figure LM8/4.3.12-3. LM8 A/S Water Tank Failure Simulation
(1) 46ST S-Band Power Amp. Flange-AEB Limit 135 Deg.
(2) 47ST S-Band Power Amp. Flange-AEB Limit 135 Deg.
(See Para. 4.3.12.7)

(NASA DATA SOURCE)

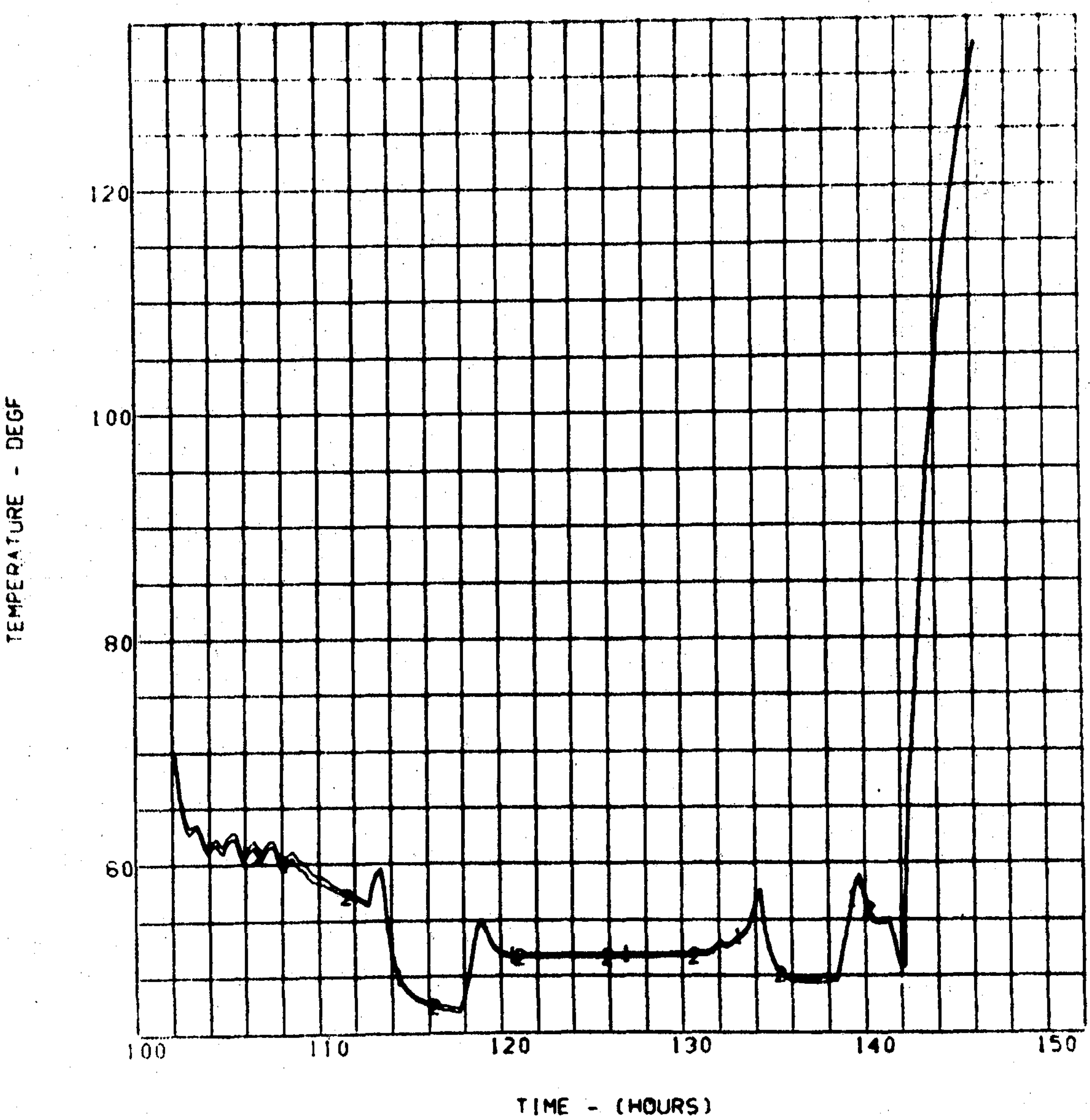

Figure LM8/4.3.12-4. LM8 A/S Water Tank Failure Simulation
(1) 44ST VHF SCVR-Right Side-AEB Limit 135 Deg.
(2) 45ST VHF XCVR-Left Side-AEB Limit 135 Deg.
(See Para. 4.3.12.7)

(NASA DATA SOURCE)

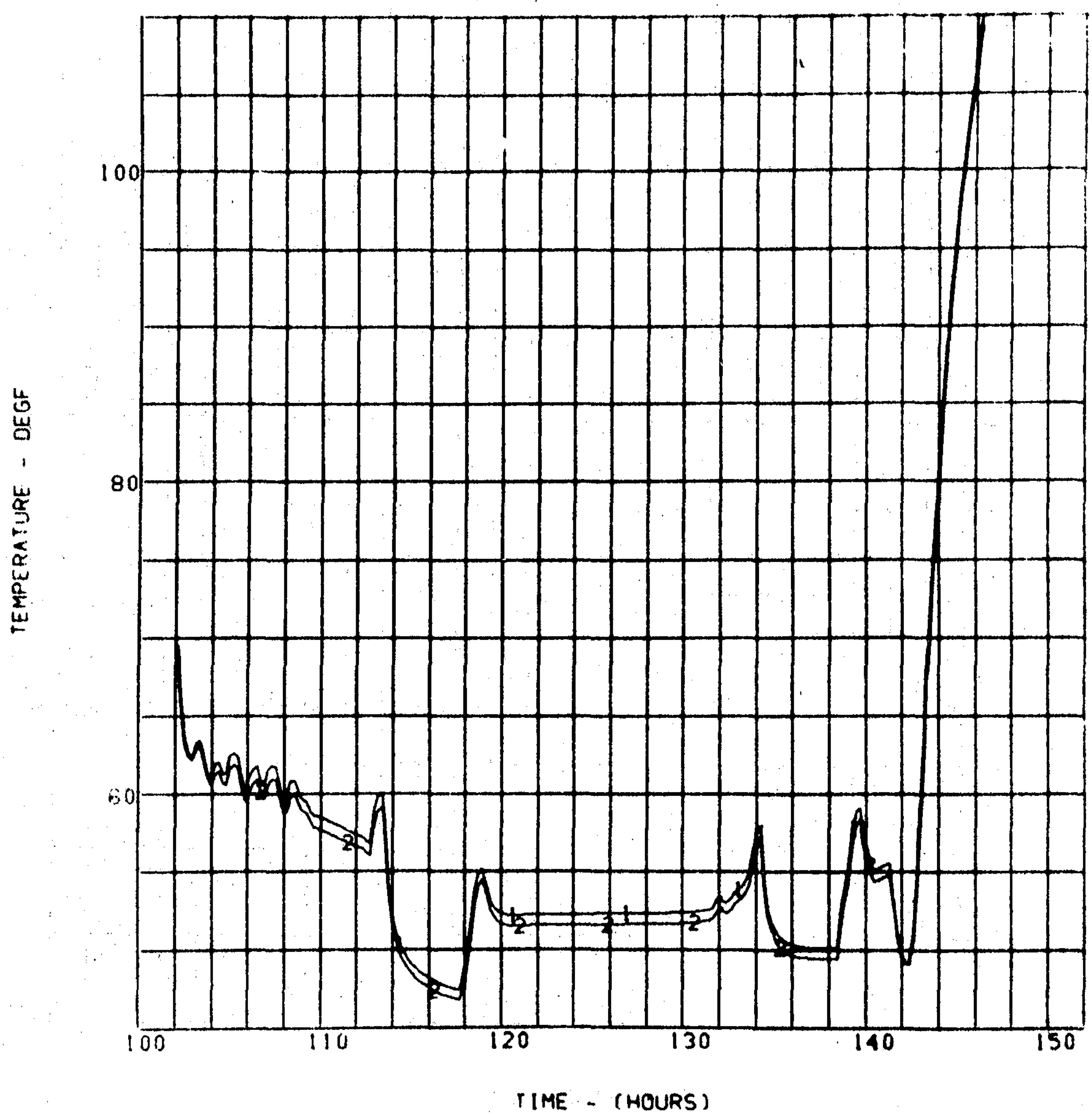

Figure LM8/4.3.12-5. LM8 A/S Water Tank Failure Simulation
(1) PCMTEA Flange Limit 135 Degrees
(2) PCMTEA Flange Limit 135 Degrees
(See Para. 4.3.12.7)

(NASA DATA SOURCE)

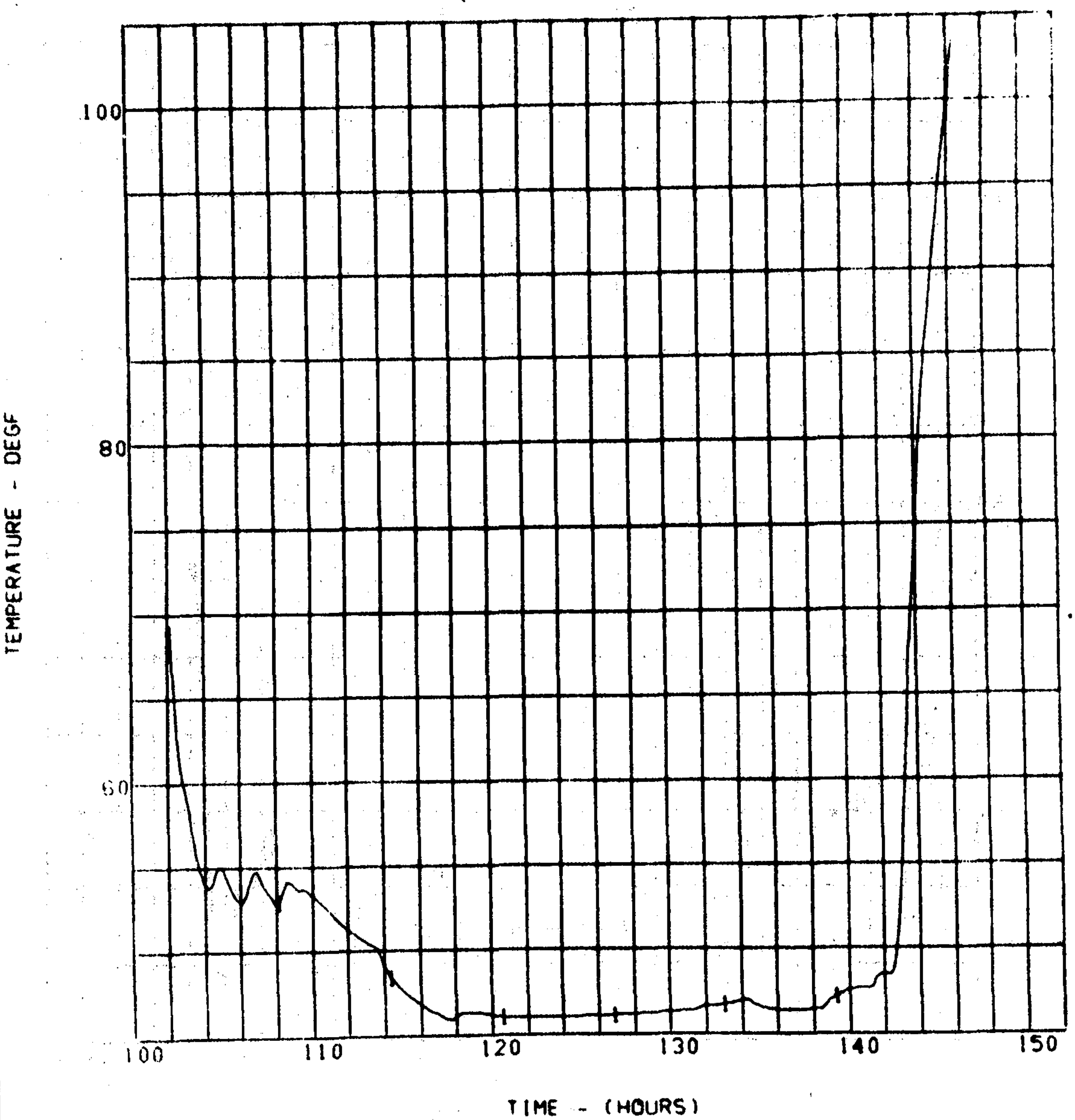

Figure LM8/4.3.12-6. LM8 A/S Water Tank Failure Simulation
(1) DSEA Limit 85 Deg.
(See Para. 4.3.12.7)

(NASA DATA SOURCE)

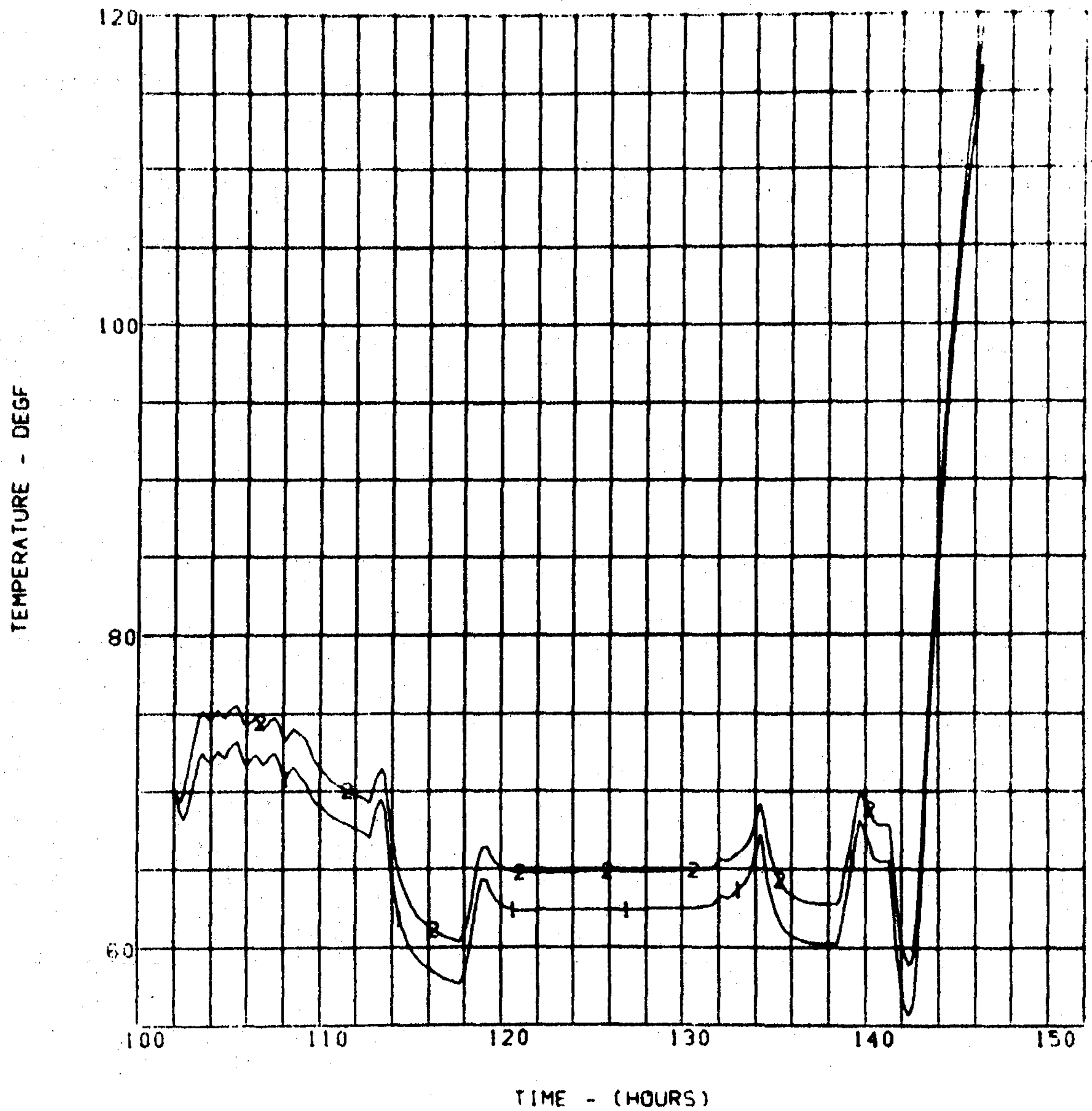

Figure LM8/4.3.12-7. LM8 A/S Water Tank Failure Simulation
(1) CWEA Flange Limit 125 Deg.
(2) CWEA Flange Limit 125 Deg.
(See Para. 4.3.12.7)

(NASA DATA SOURCE)

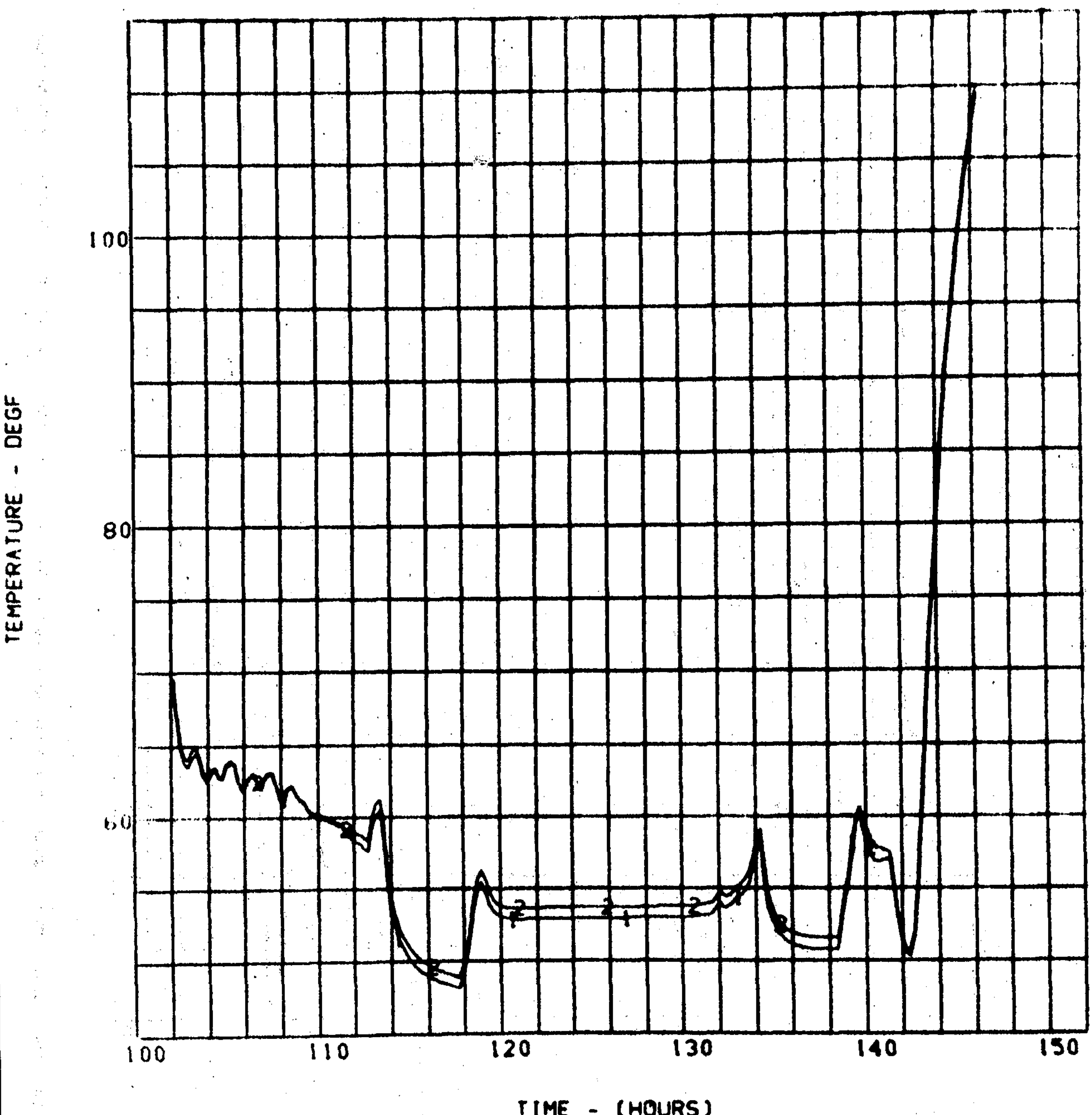

Figure LM8/4.3.12-8. LM8 A/S Water Tank Failure Simulation
(1) SCEA No. 1 Flange Limit 135 Deg.
(2) SCEA No. 1 Flange Limit 135 Deg.
(See Para. 4.3.12.7)

(NASA DATA SOURCE)

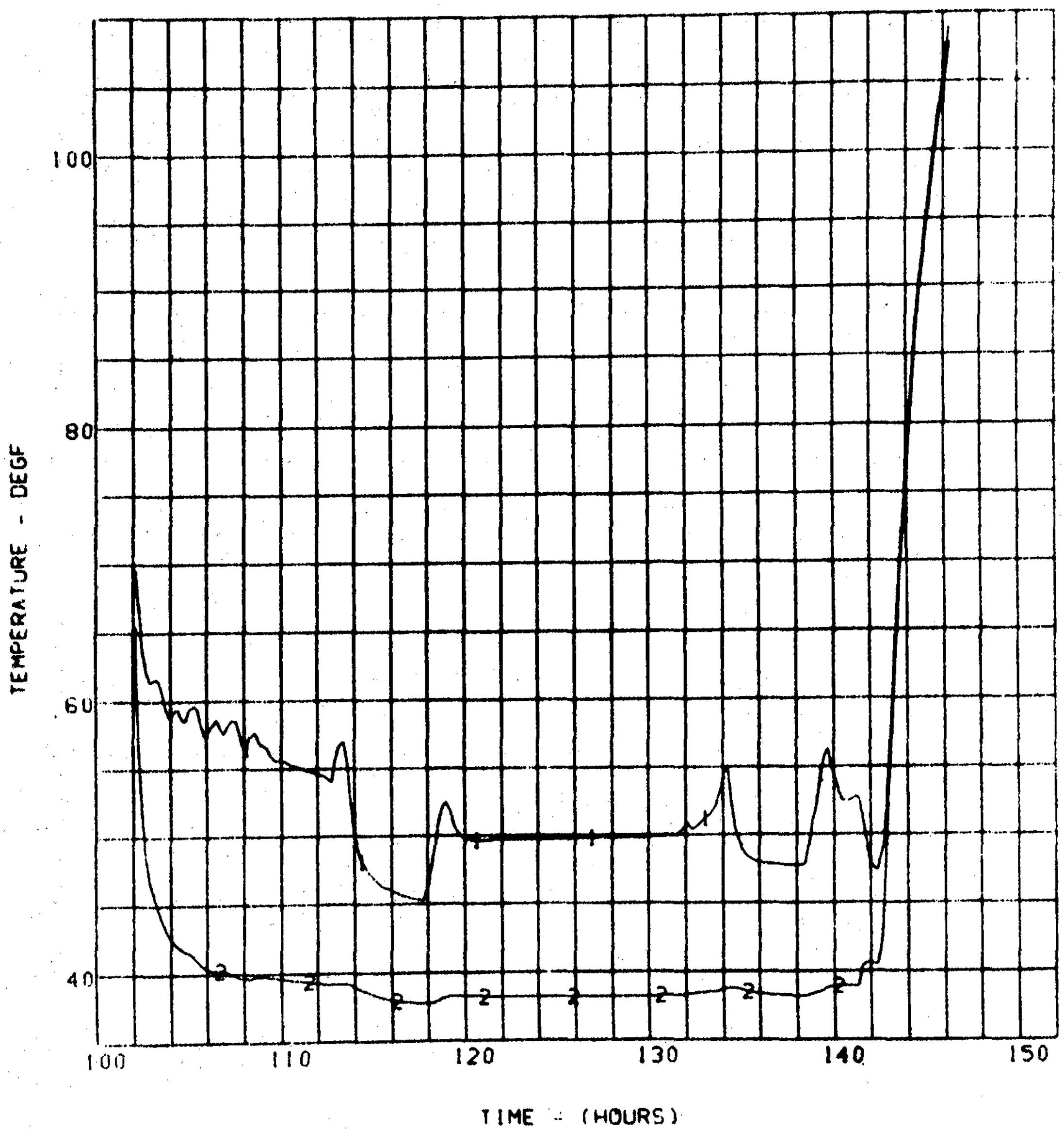

Figure LM8/4.3.12-9. LM8 A/S Water Tank Failure Simulation
(1) SCEA No. 2 Flange Limit 135 Deg.
(2) SCEA No. 2 Flange Limit 135 Deg.
(See Para. 4.3.12.7)

(NASA DATA SOURCE)

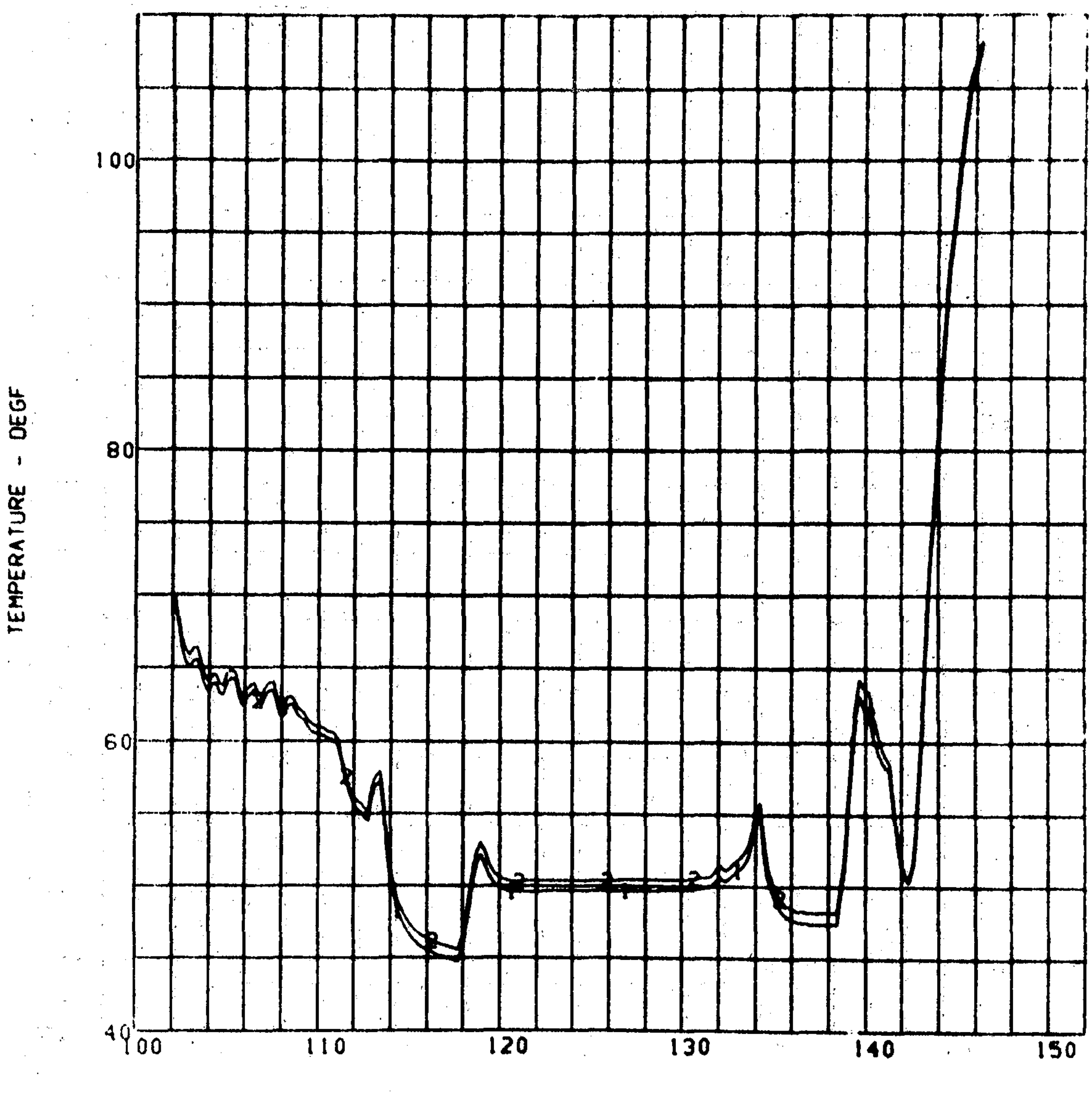

Figure LM8/4.3.12-10. LM8 A/S Water Tank Failure Simulation
(1) 10ST RRE Flange-AEB Limit 125 Deg.
(2) 11ST RRE Flange-AEB Limit 125 Deg.
(See Para. 4.3.12.7)

(NASA DATA SOURCE)

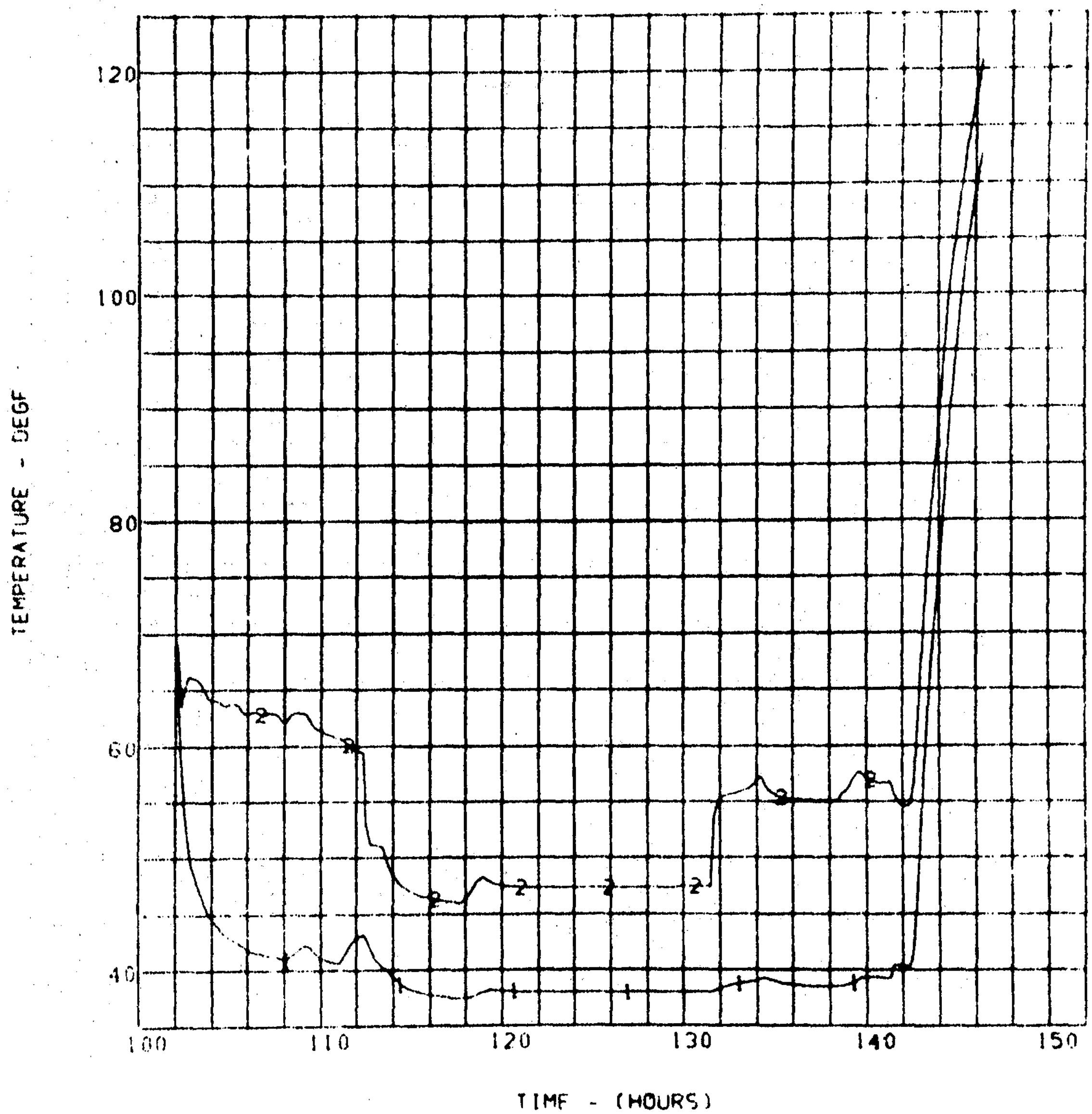

Figure LM8/4.3.12-11. LM8 A/S Water Tank Failure Simulation
(1) SL101 DUA Flange Limit 120 Deg.
(2) SL102 DUA Flange Limit 120 Deg.
(See Para. 4.3.12.7)

(NASA DATA SOURCE)

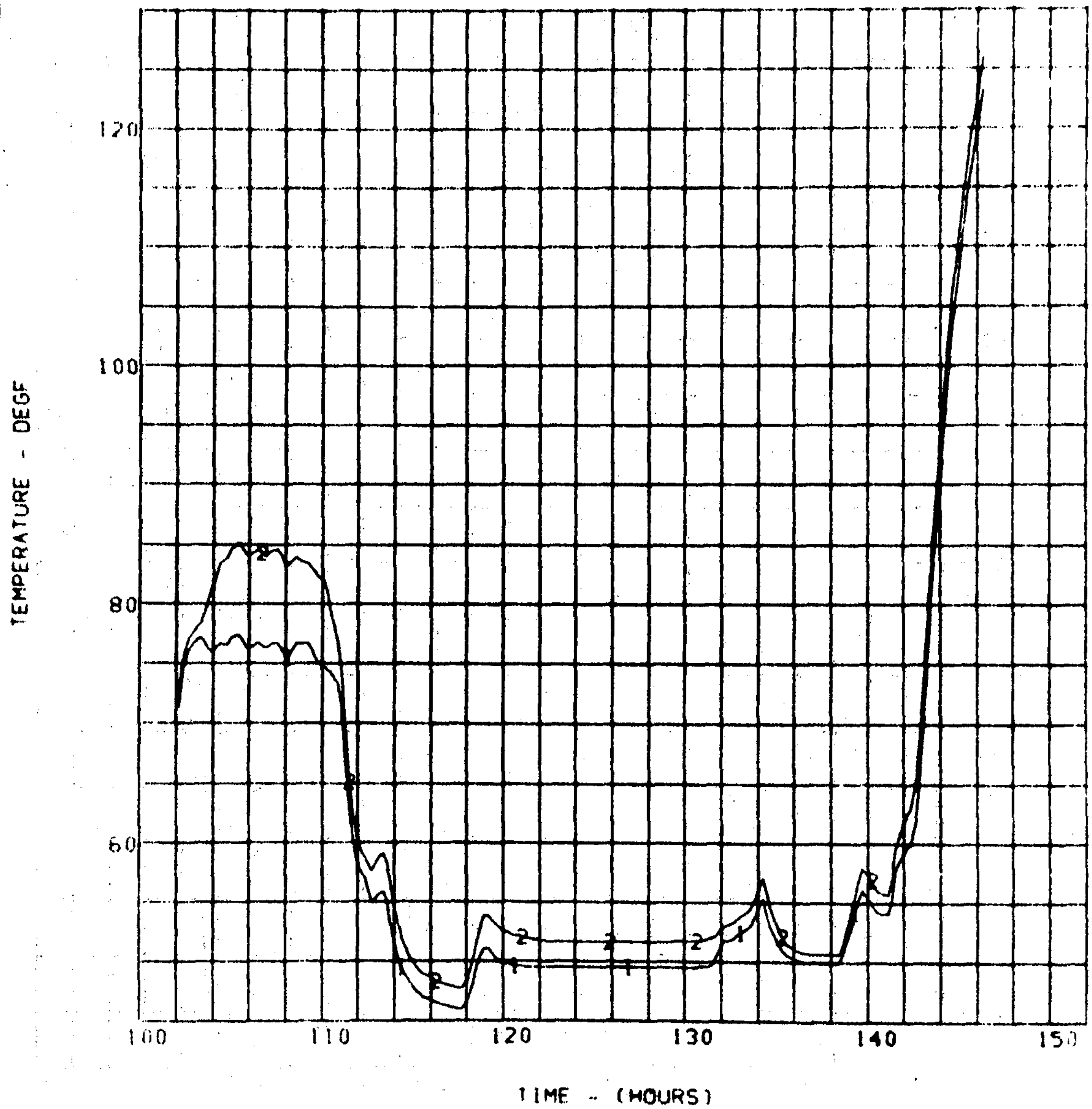

Figure LM8/4.3.12-12. LM8 A/S Water Tank Failure Simulation
(1) 38ST ATCA Flange-AEB Limit 135 Deg.
(2) 39ST ATCA Flange-AEB Limit 135 Deg.
(See Para. 4.3.12.7)

(NASA DATA SOURCE)

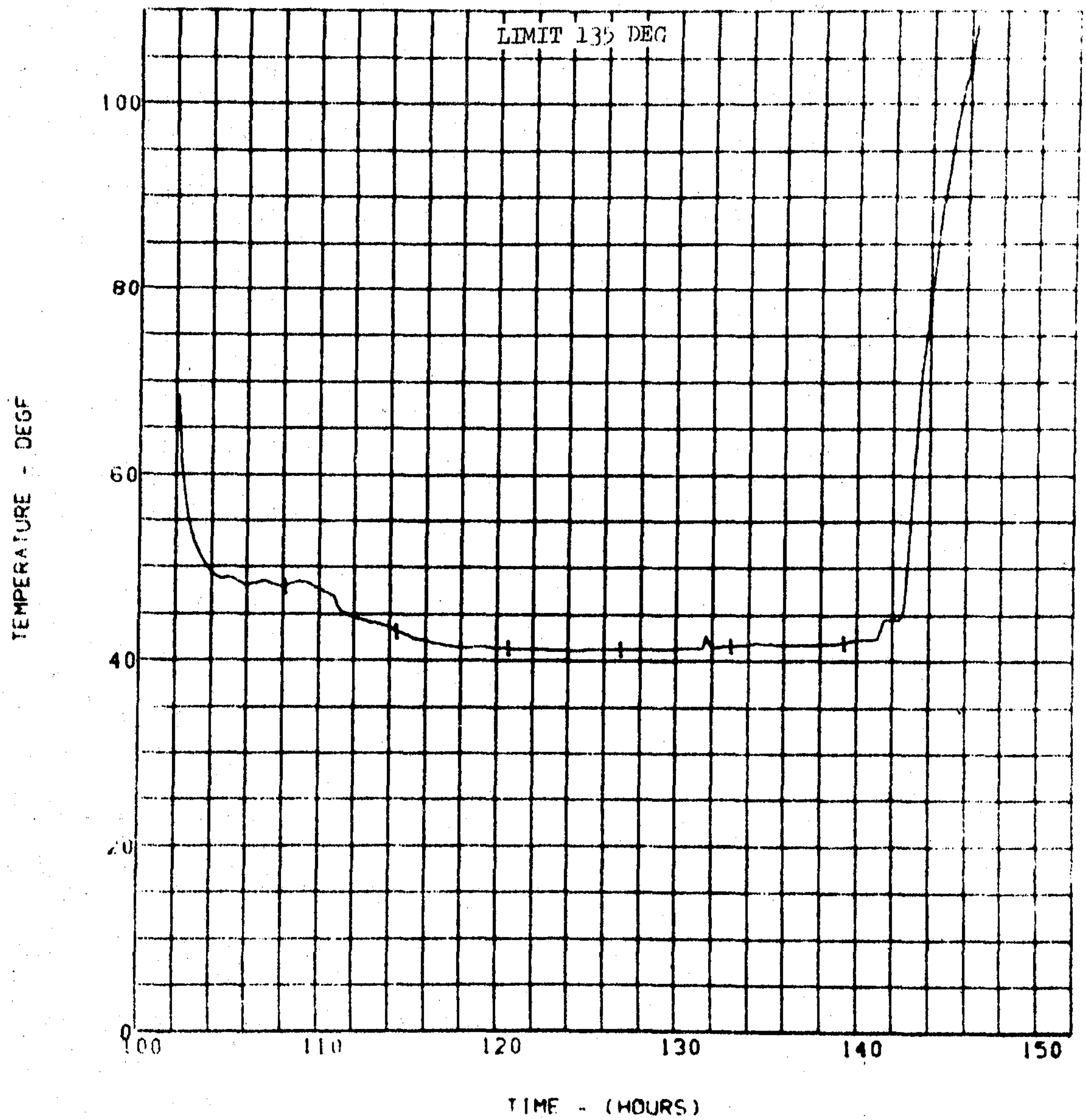

Figure LM8/4.3.12-13. LM8 A/S Water Tank Failure Simulation
(1) 245ST GASTA. Front of Fwd. Rt. Instrument Panel
(See Para. 4.3.12.7)

(NASA DATA SOURCE)

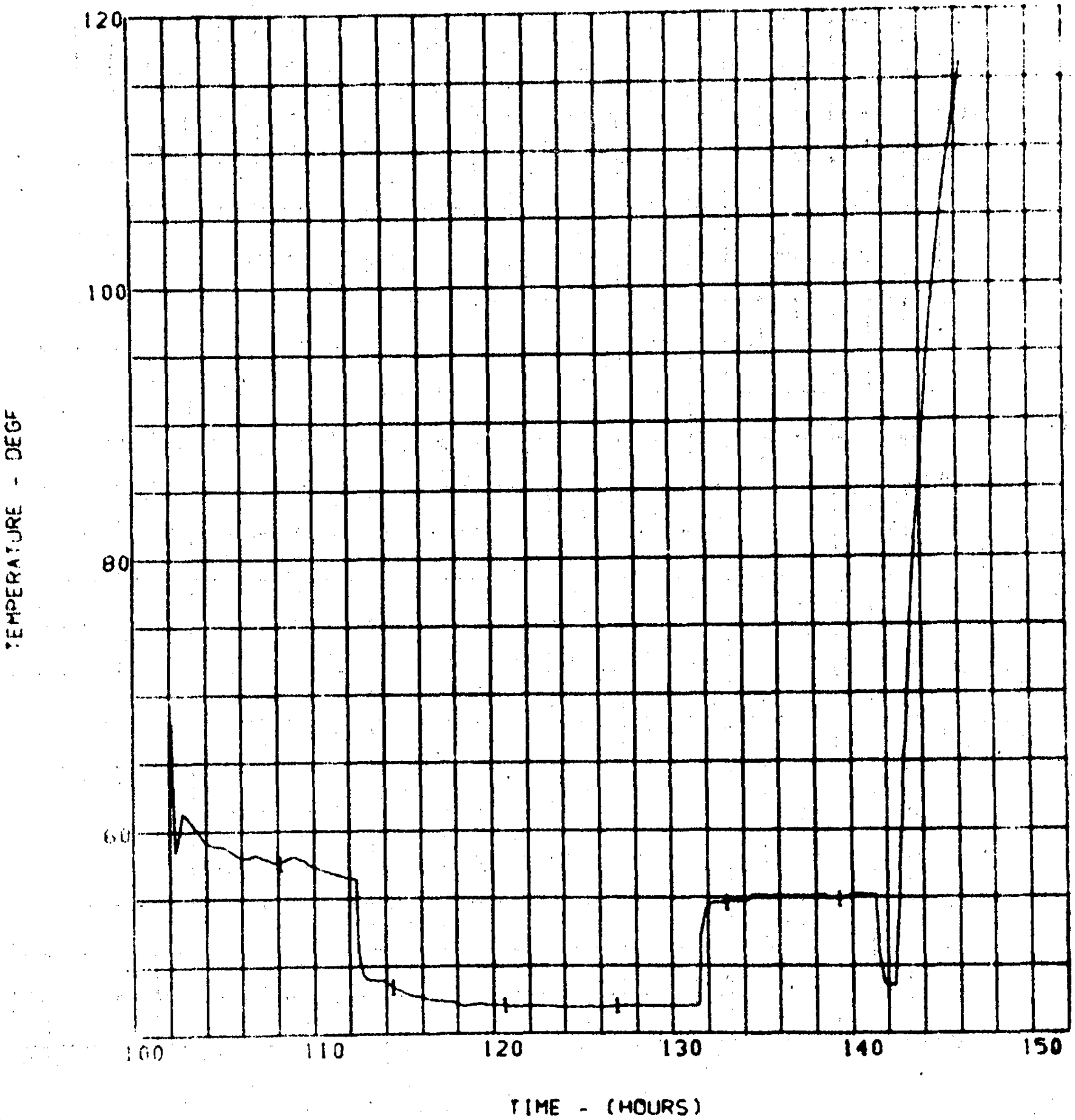

Figure LM8/4.3.12-14. LM8 A/S Water Tank Failure Simulation
(1) 224ST RGA Front of +Z27 Bulkhead
Top Limit 135 Deg.
(See Para. 4.3.12.7)

(NASA DATA SOURCE)

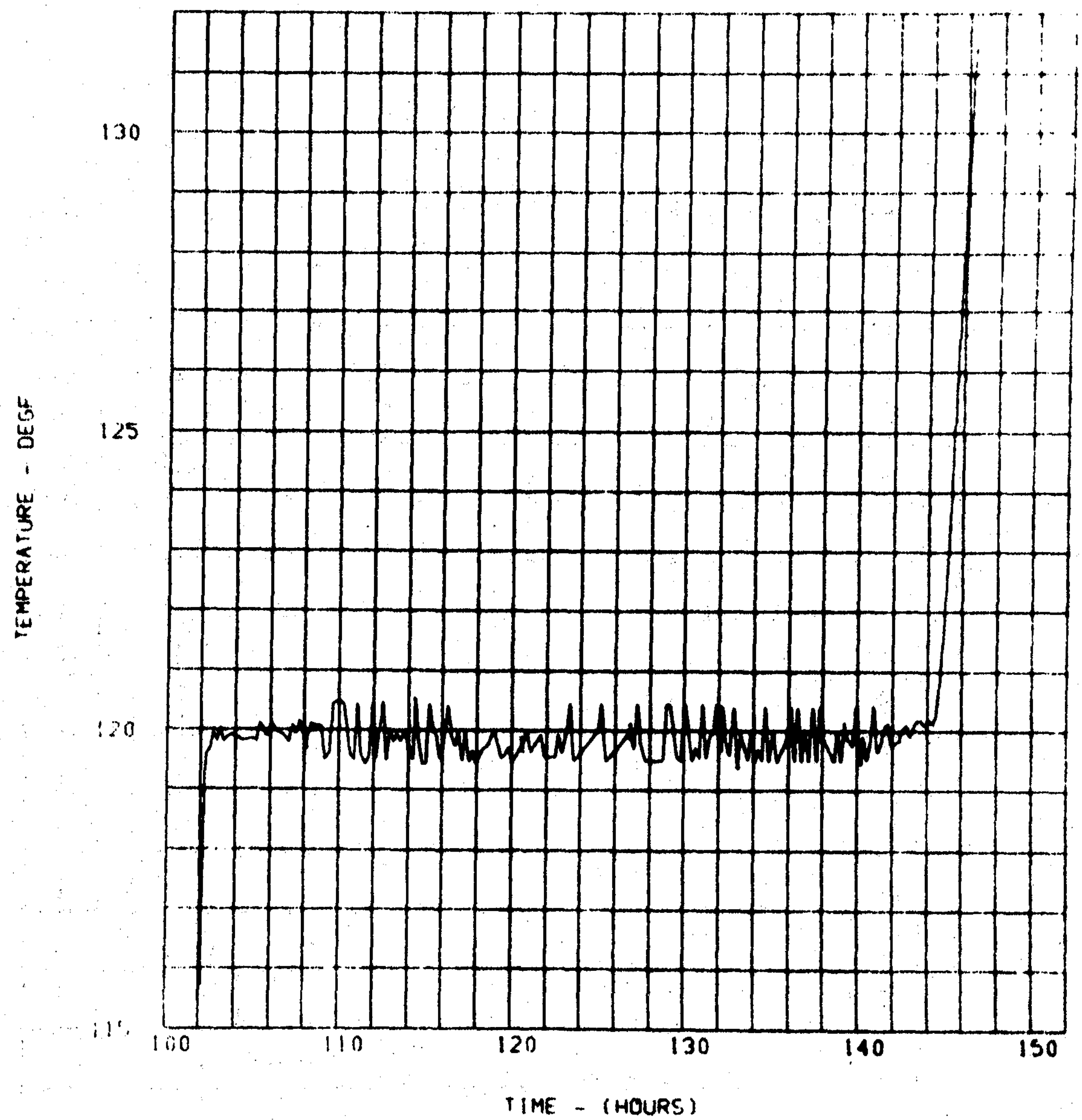

Figure LM8/4.3.12-15. LM8 A/S Water Tank Failure Simulation
(1) 222ST ASA Block. Limit 123 Deg.
(See Para. 4.3.12.7)

(NASA DATA SOURCE)

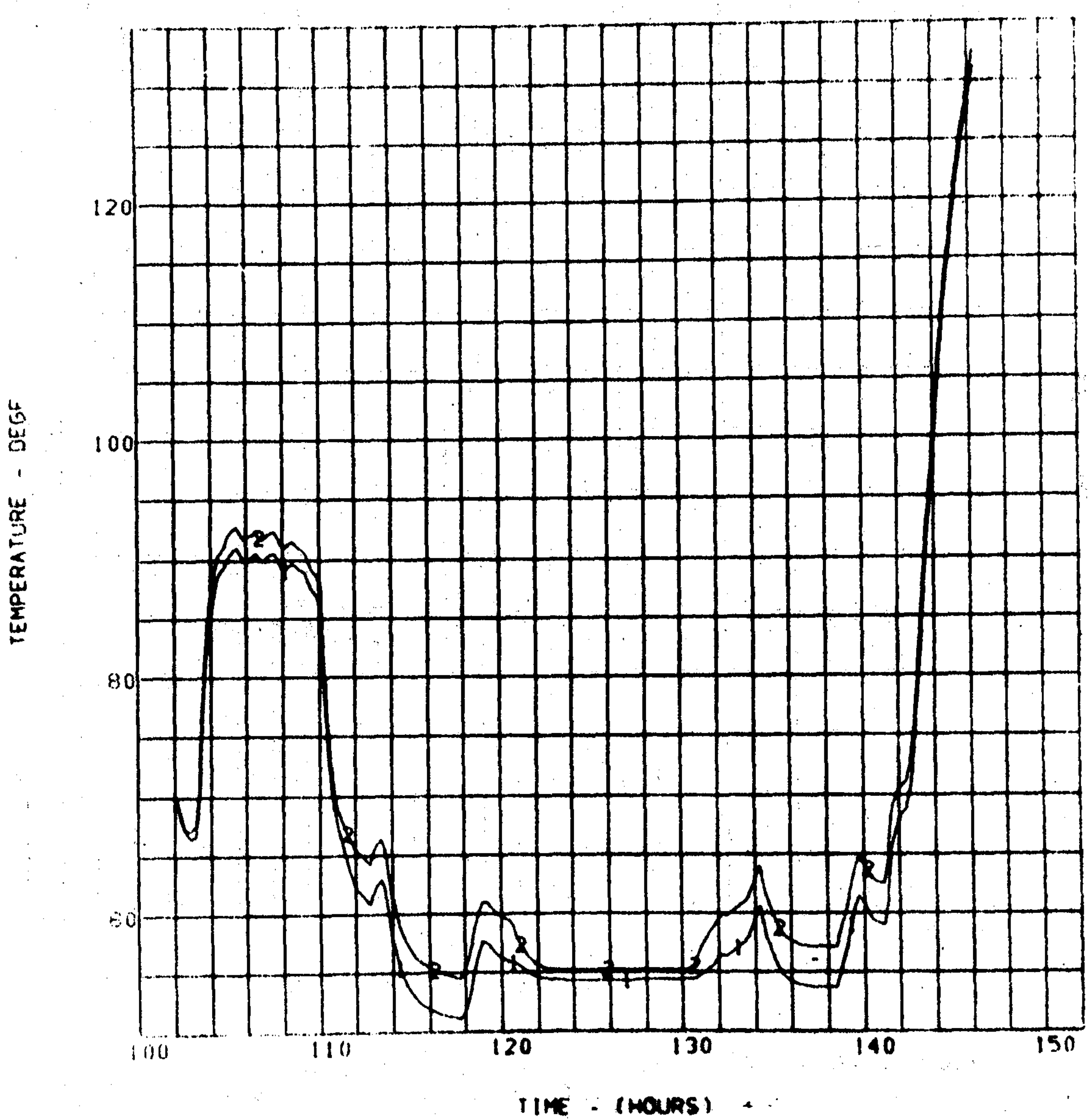

Figure LM8/4.3.12-16. LM8 A/S Water Tank Failure Limitation
(1) 42ST AEA Flange-AEB Limit 135 Deg.
(2) 43ST AEA Flange-AEB Limit 135 Deg.
(See Para. 4.3.12.7)

(NASA DATA SOURCE)

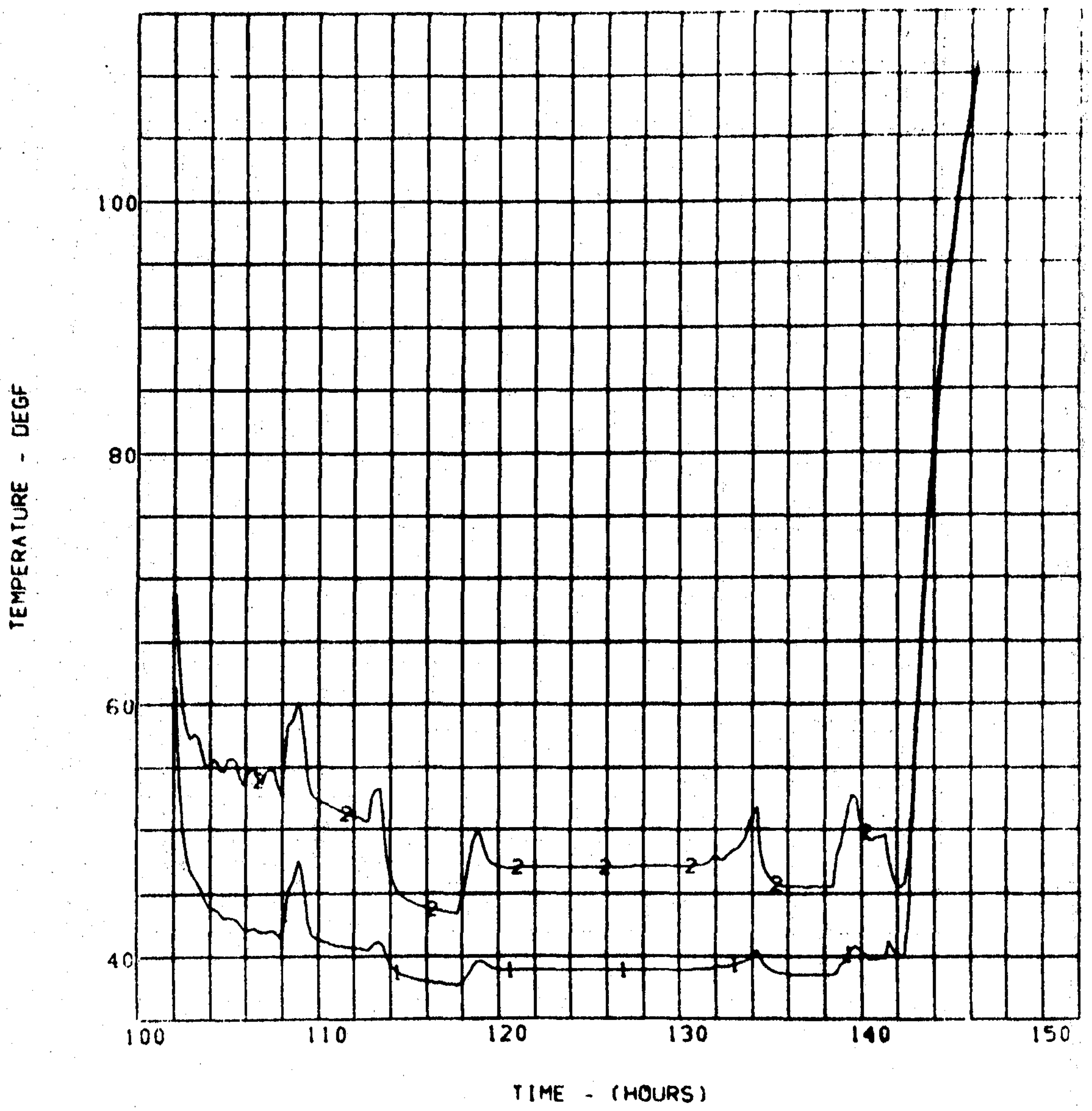

Figure LM8/4.3.12-17. LM8 A/S Water Tank Failure Simulation
(1) 36ST INV No. 1 Flange-AEB Limit 135 Deg.
(2) 37ST INV No. 1 Flange-AEB Limit 135 Deg.
(See Para. 4.3.12.7)

(NASA DATA SOURCE)

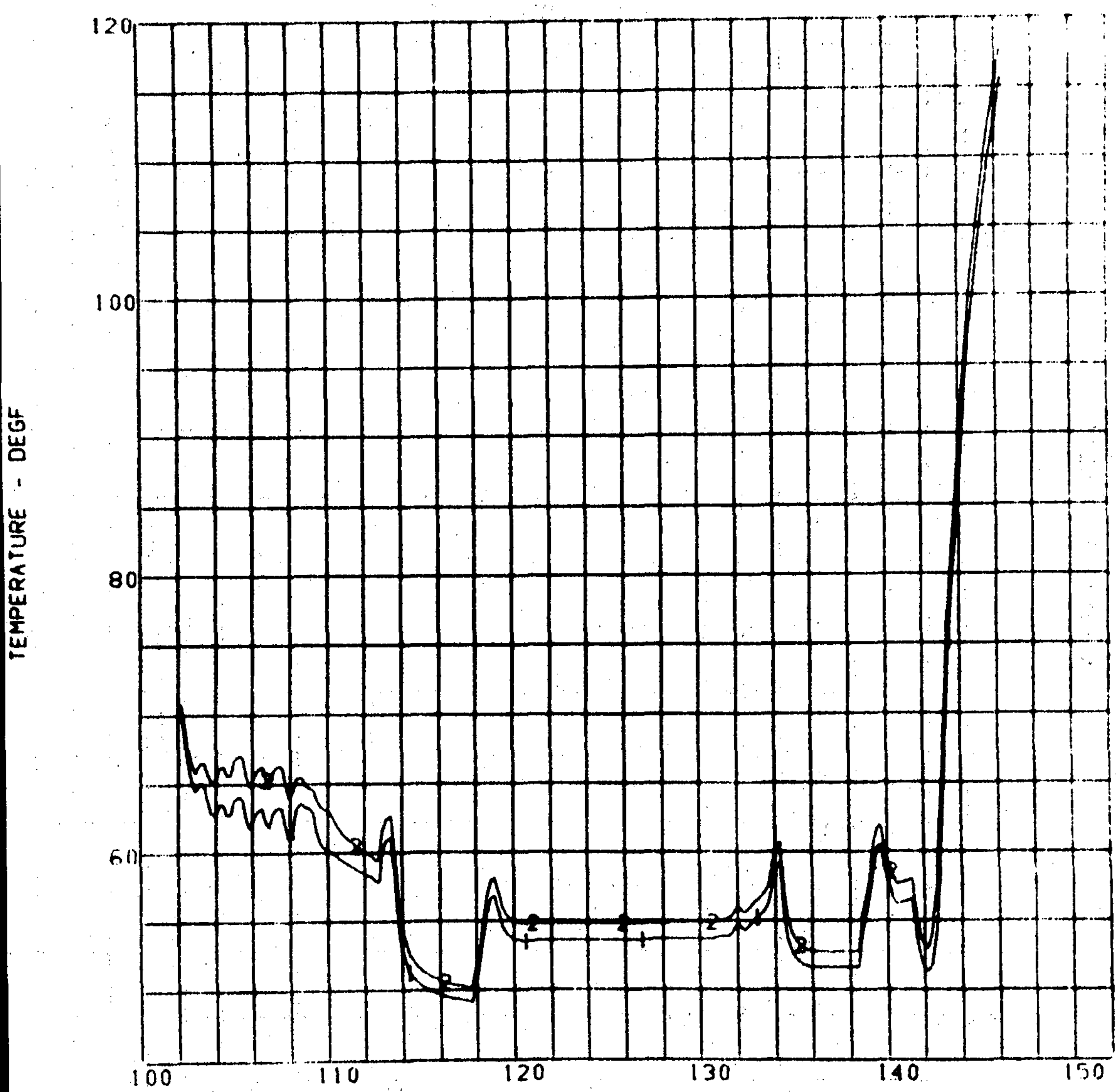

Figure LM8/4.3.12-18. LM8 A/S Water Tank Failure Simulation
(1) 40ST INV No. 2 Flange-AEB Limit 135 Deg.
(2) 41ST INV No. 2 Flange-AEB Limit 135 Deg.
(See Para. 4.3.12.7)

(NASA DATA SOURCE)

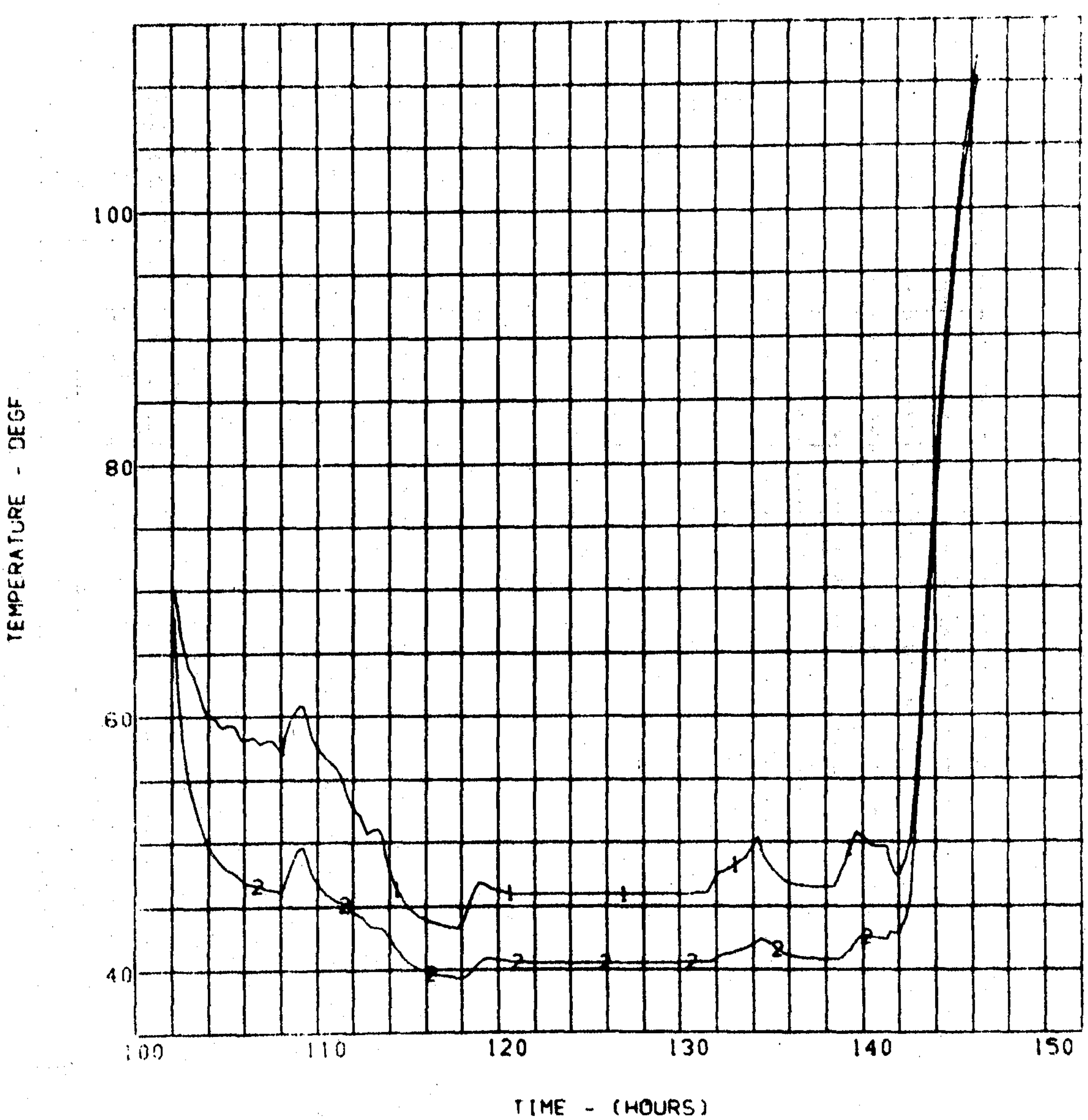

Figure LM8/4.3.12-19. LM8 A/S Water Tank Failure Simulation
(1) 35ST A/S ECA No. 3 Flange-AEB Limit 135 Deg.
(2) 34ST A/S ECA No. 3 Flange-AEB Limit 135 Deg.
(See Para. 4.3.12.7)

(NASA DATA SOURCE)

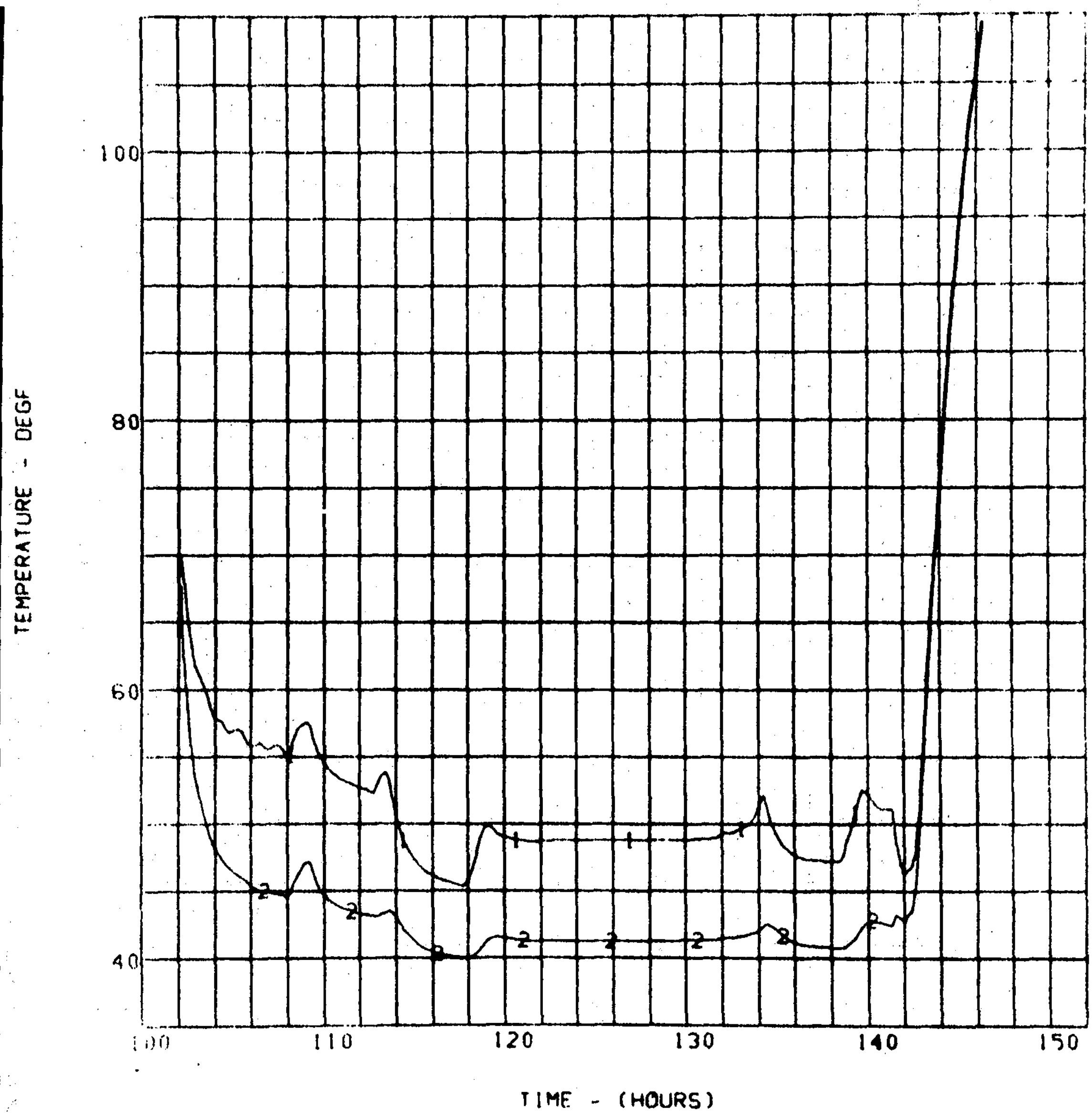

Figure LM8/4.3.12-20. LM8 A/S Water Tank Failure Simulation
(1) 18ST A/S ECA No. 4 Flange-AEB Limit 135 Deg.
(2) 19ST A/S ECA No. 4 Flange-AEB Limit 135 Deg.
(See Para. 4.3.12.7)

(NASA DATA SOURCE)

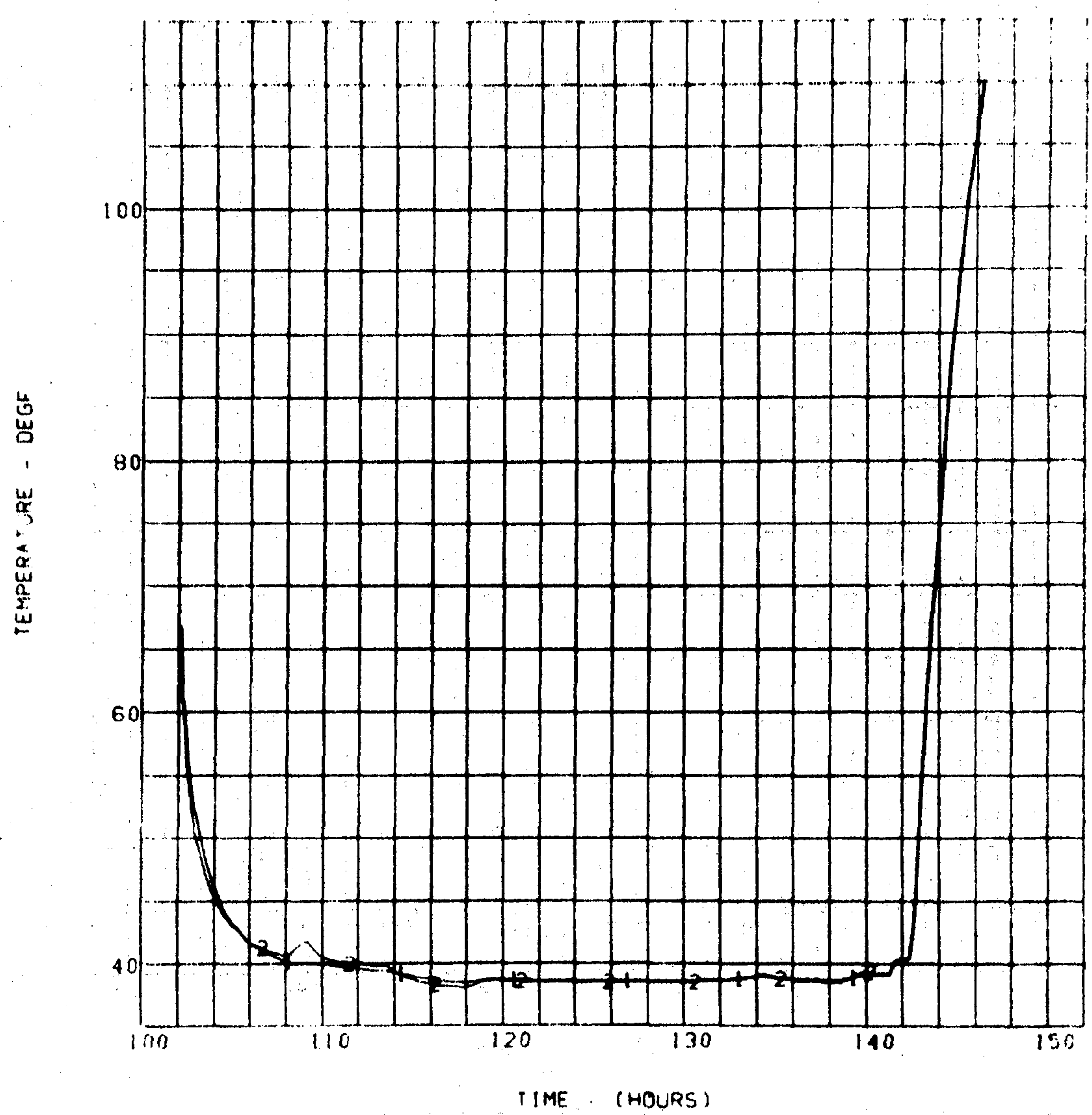

Figure LM8/4.3.12-21. LM8 A/S Water Tank Failure Simulation
(1) 24ST A/S Batt. No. 5 Flange-AEB Limit 100 Deg.
(2) 33ST A/S Batt. No. 6 Flange-AEB Limit 100 Deg.
(See Para. 4.3.12.7)

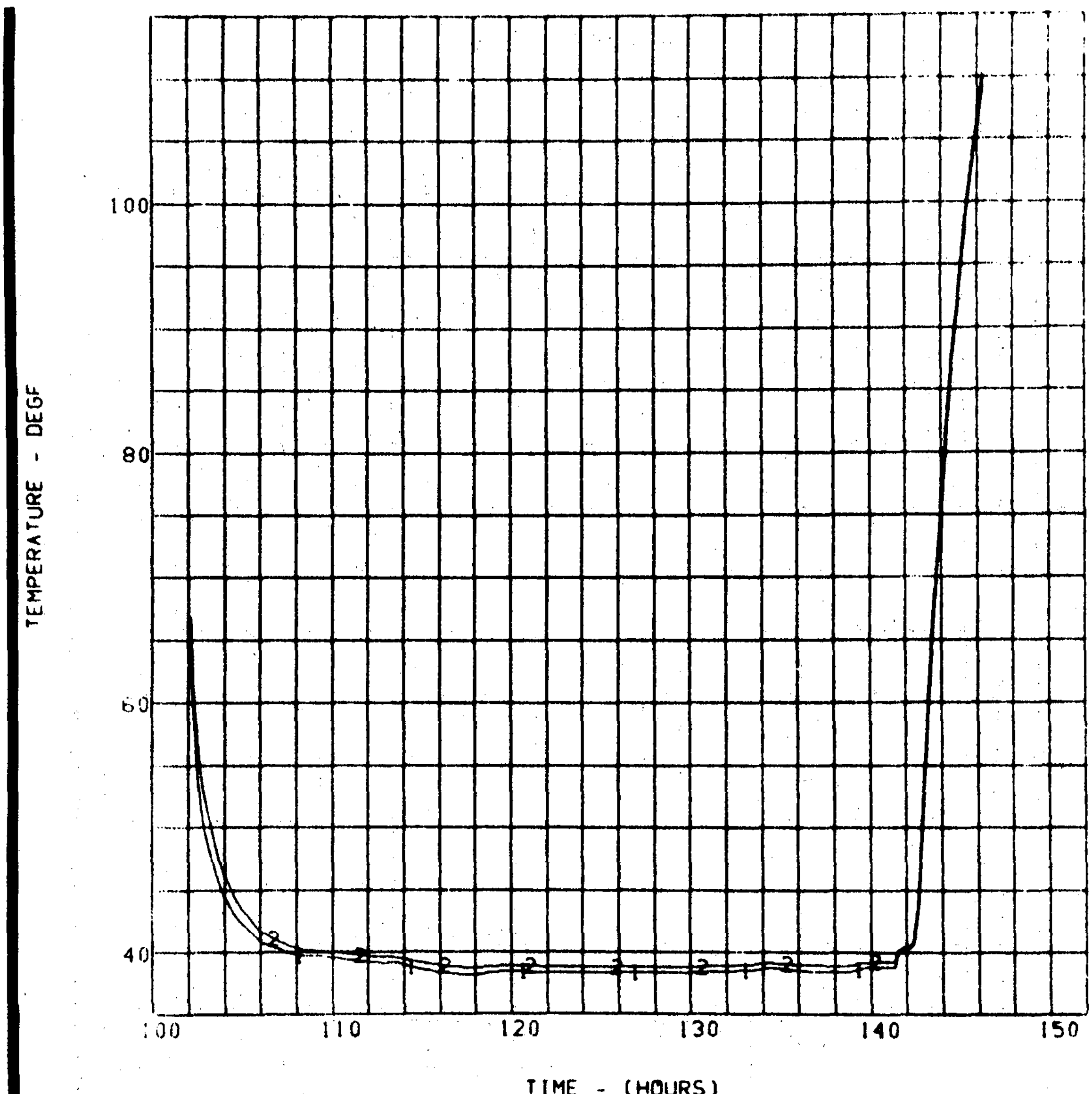

Figure LM8/4.3.12-22. LM8 A/S Water Tank Failure Simulation
(1) 22ST A/S Batt. No. 6 Flange-AEB Limit 100 Deg.
(2) 23ST A/S Batt. No. 6 Flange-AEB Limit 100 Deg.
(See Para. 4.3.12.7)

(NASA DATA SOURCE)

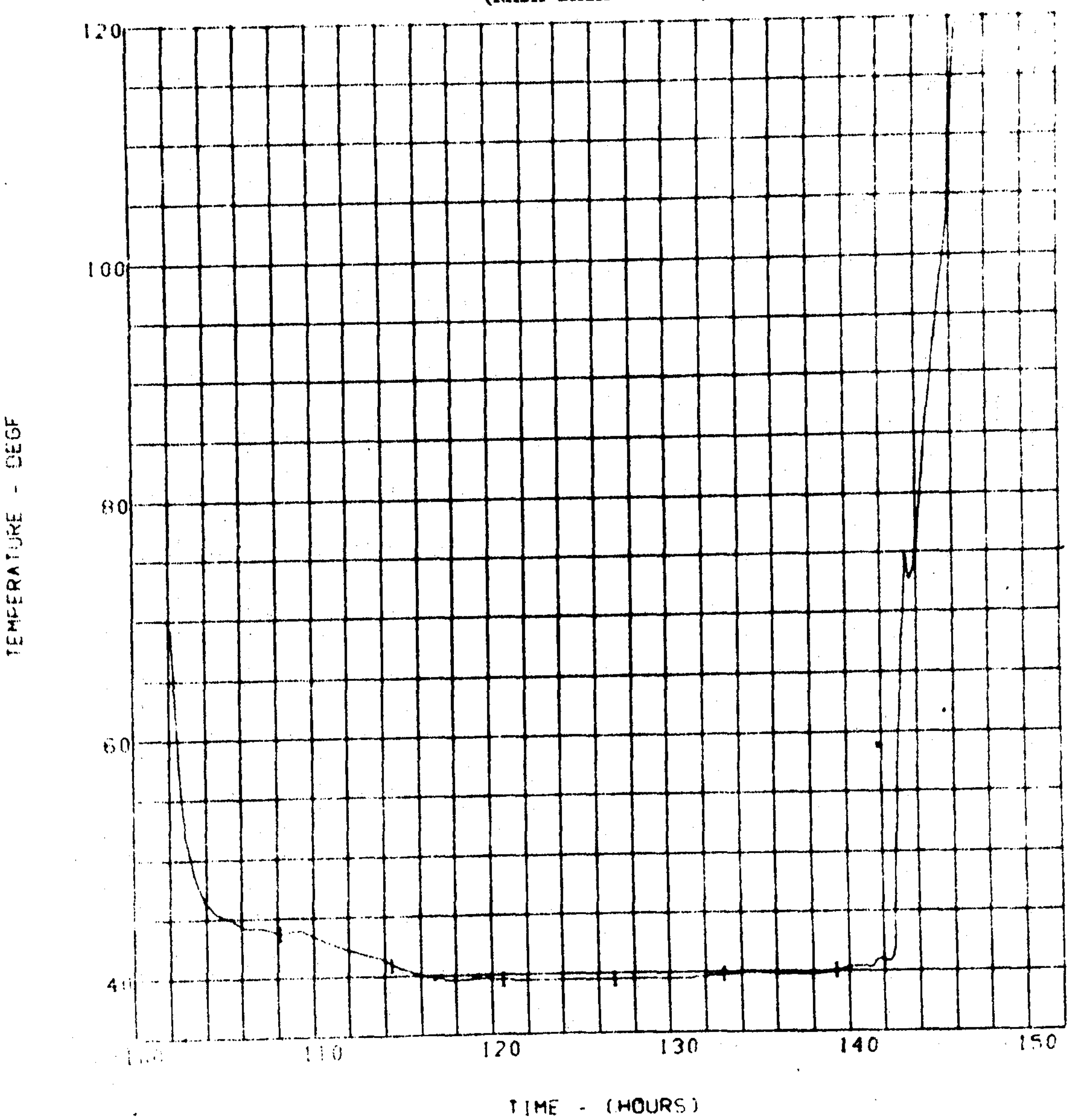

Figure LM8/4.3.12-23. LM8 A/S Water Tank Failure Simulation
(1) TLE Limit 115 Deg.
(See Para. 4.3.12.7)

(NASA DATA SOURCE)

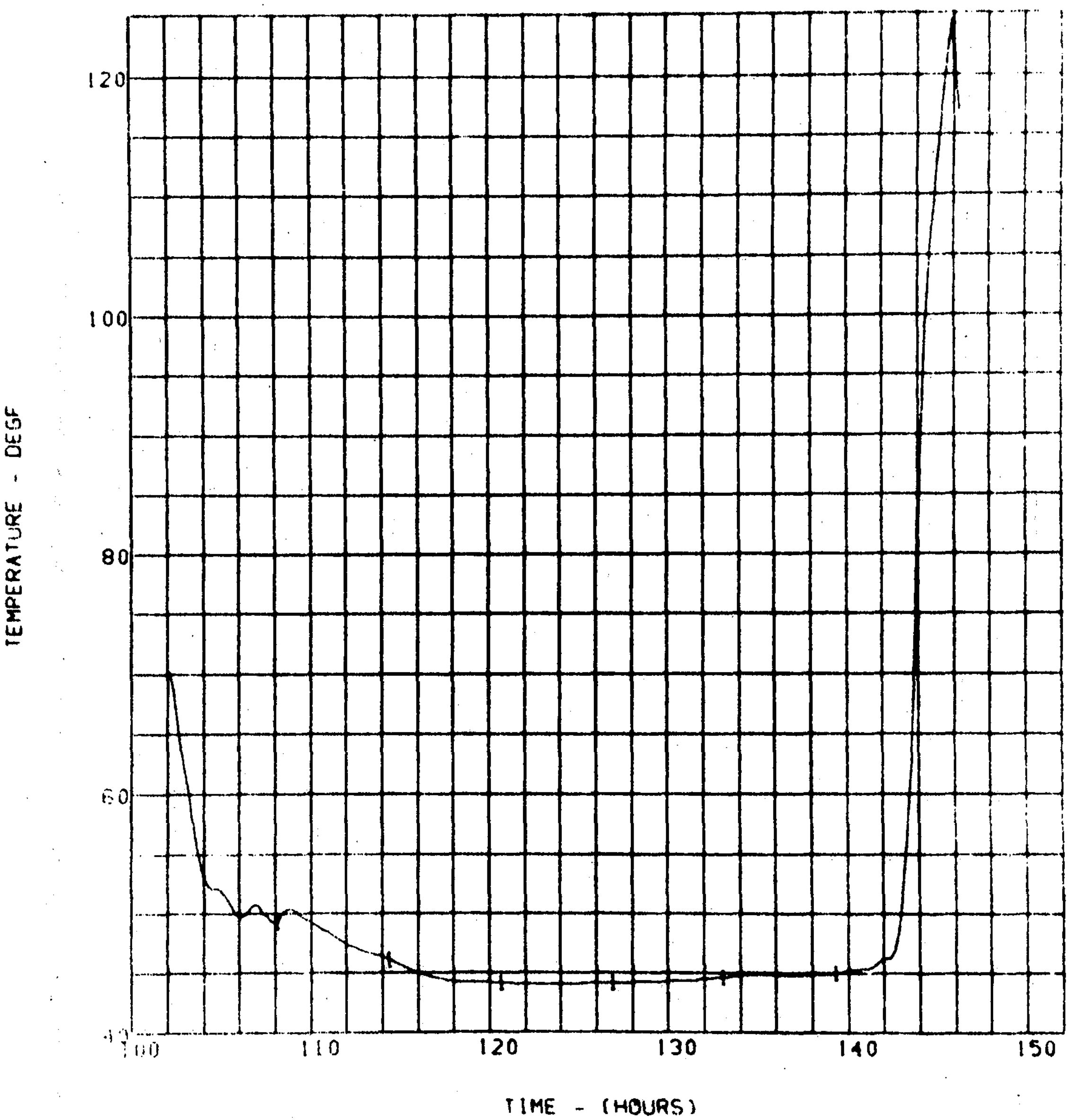

Figure LM8/4.3.12-24. LM8 A/S Water Tank Failure Simulation
(1) 246ST LCA Under Cabin Floor Limit 135 Deg.
(See Para. 4.3.12.7)

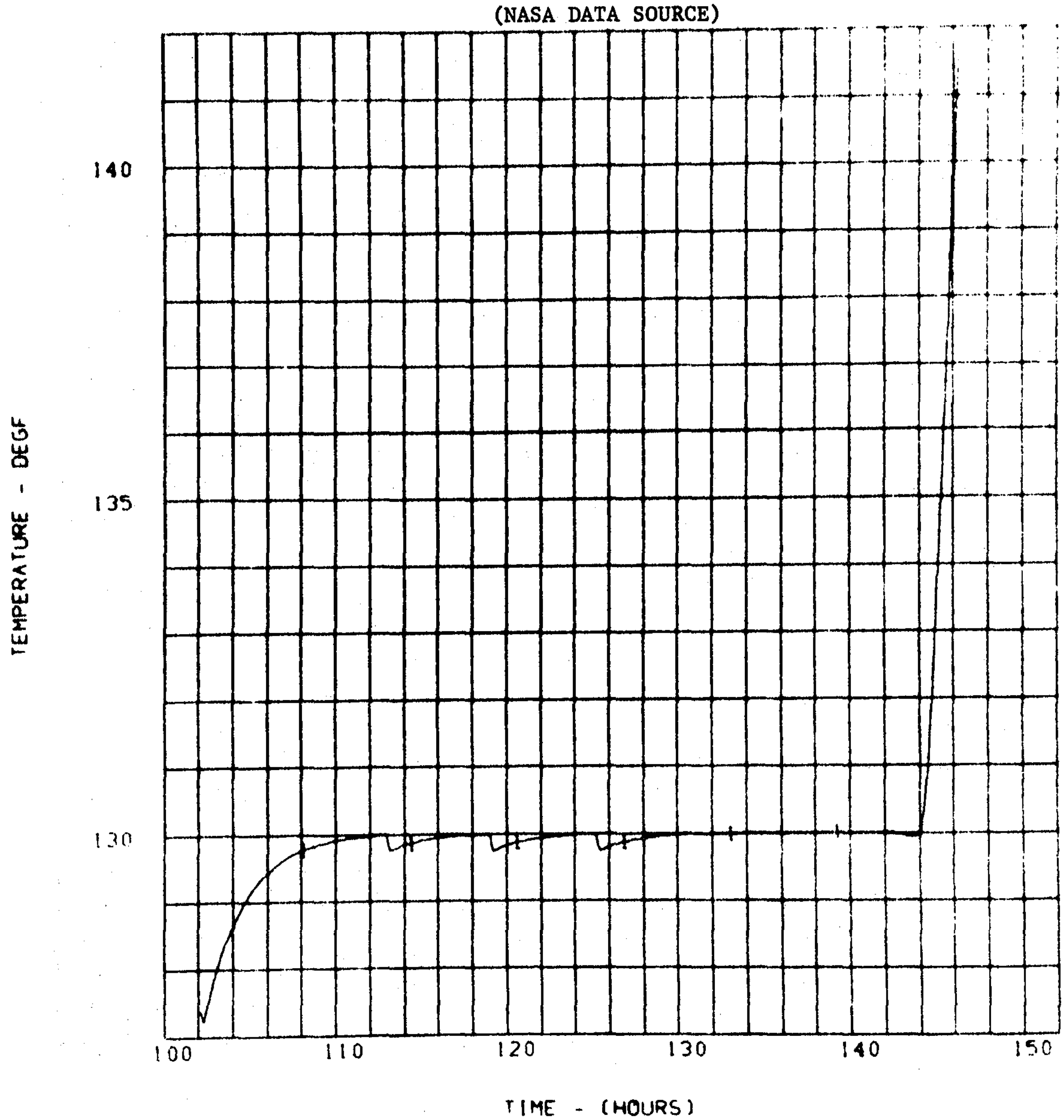

Figure LM8/4.3.12-25. LM8 A/S Water Tank Failure Simulation
(1) 317ST IMU Stable Element Limit 132 Deg.
(See Para. 4.3.12.7)

(NASA DATA SOURCE)

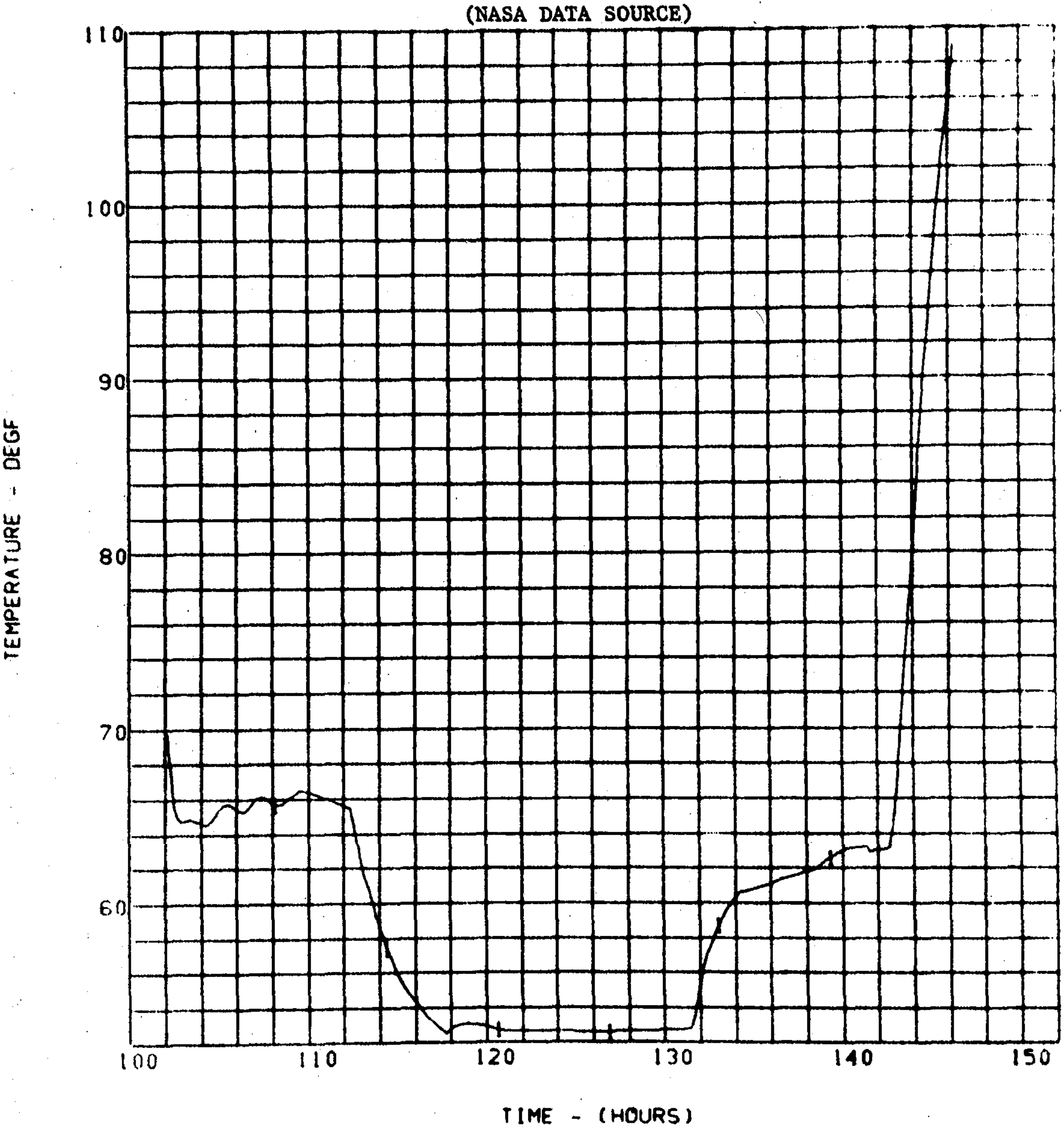

Figure LM8/4.3.12-26. LM8 A/S Water Tank Failure Simulation
(1) 429TL LGC Limit 105 Deg.
(See Para. 4.3.12.7)

(NASA DATA SOURCE)

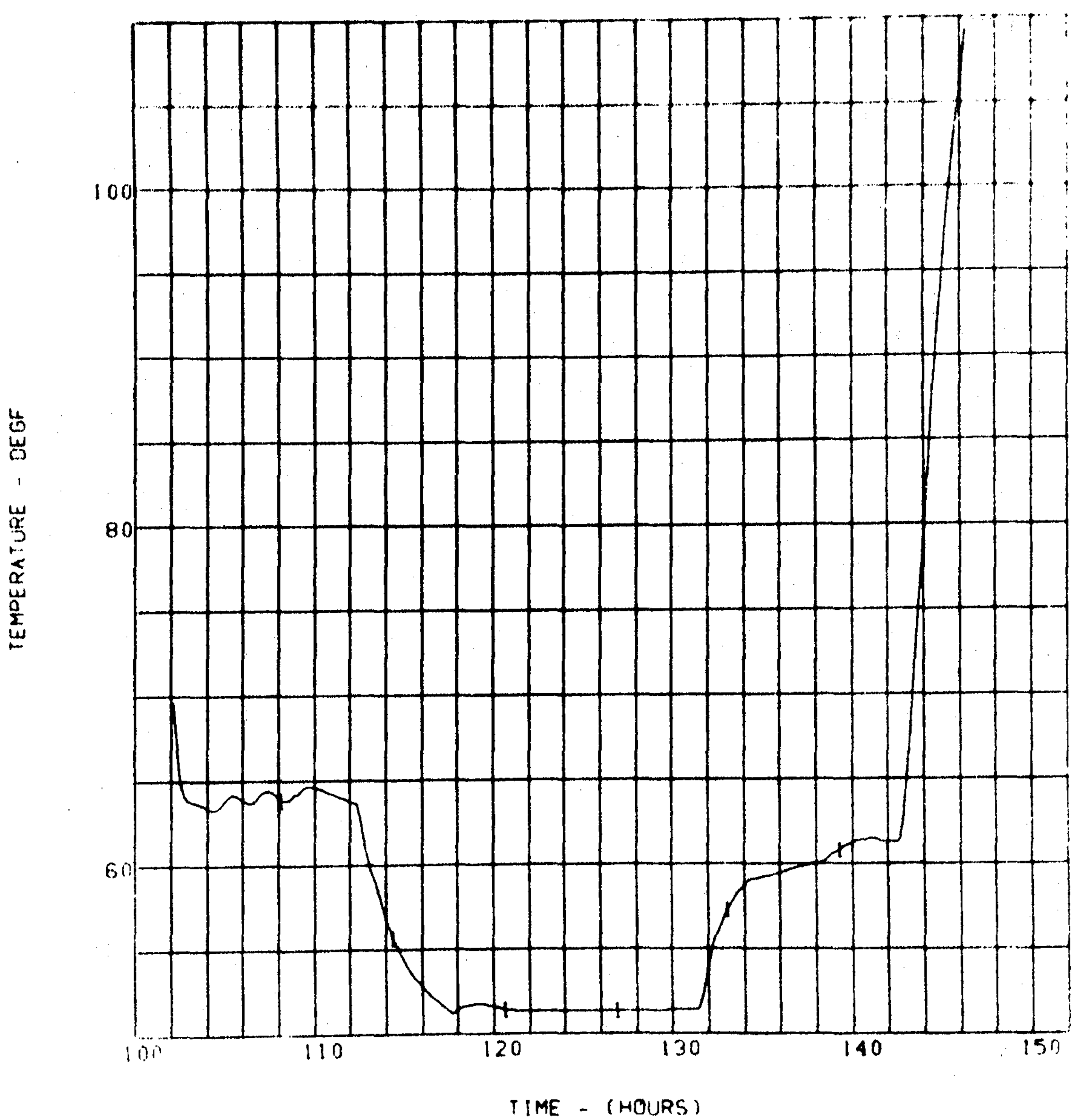

Figure LM8/4.3.12-27. LM8 A/S Water Tank Failure Simulation
(1) 458TT LGC Right Front Face. Limit 210 Deg.
(See Para. 4.3.12.7)

(NASA DATA SOURCE)

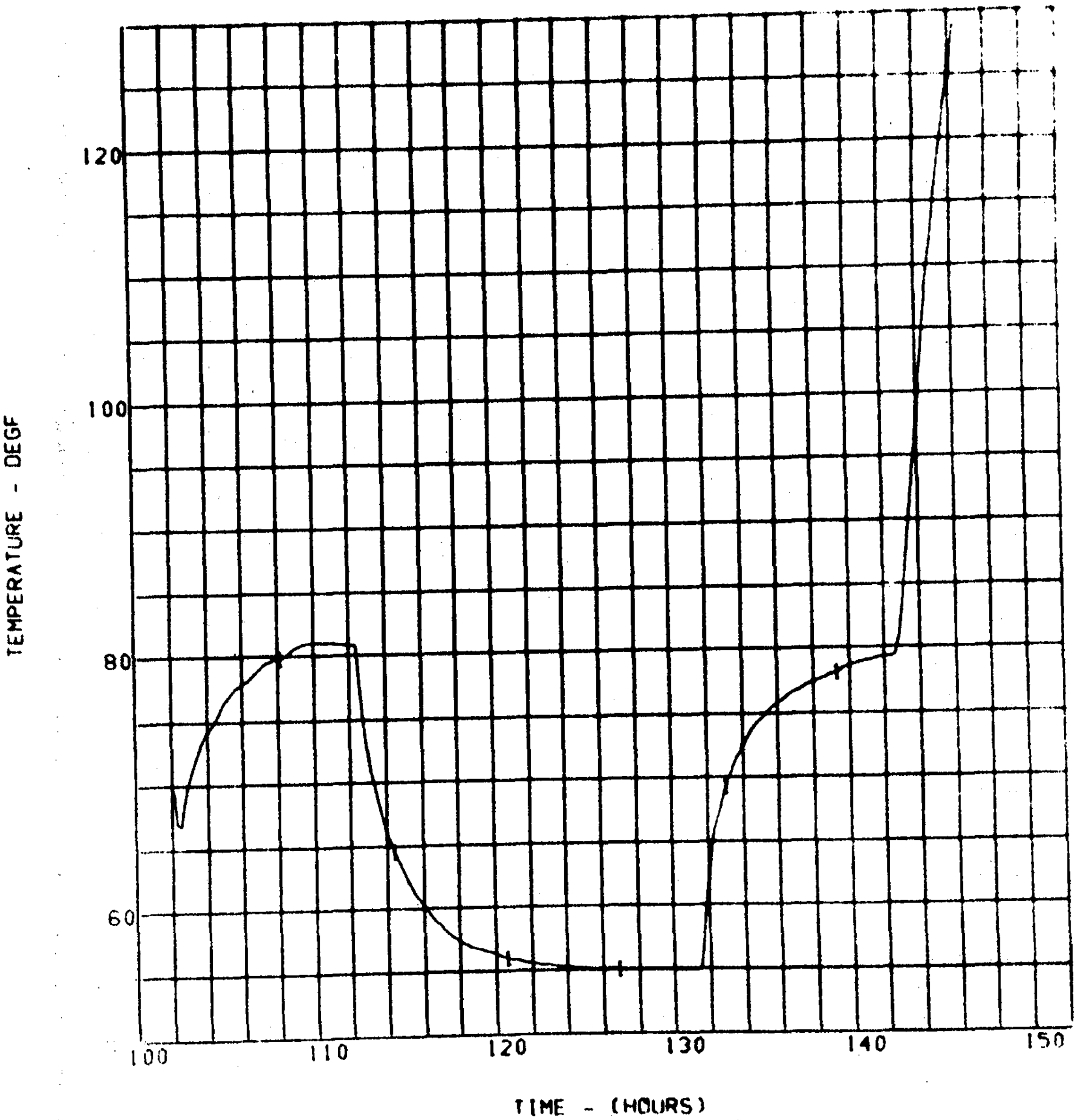

Figure LM8/4.3.12-28. LM8 A/S Water Tank Failure Simulation
(1) 110ST LGC Electronic Module Limit 160 Deg.
(See Para. 4.3.12.7)

(NASA DATA SOURCE)

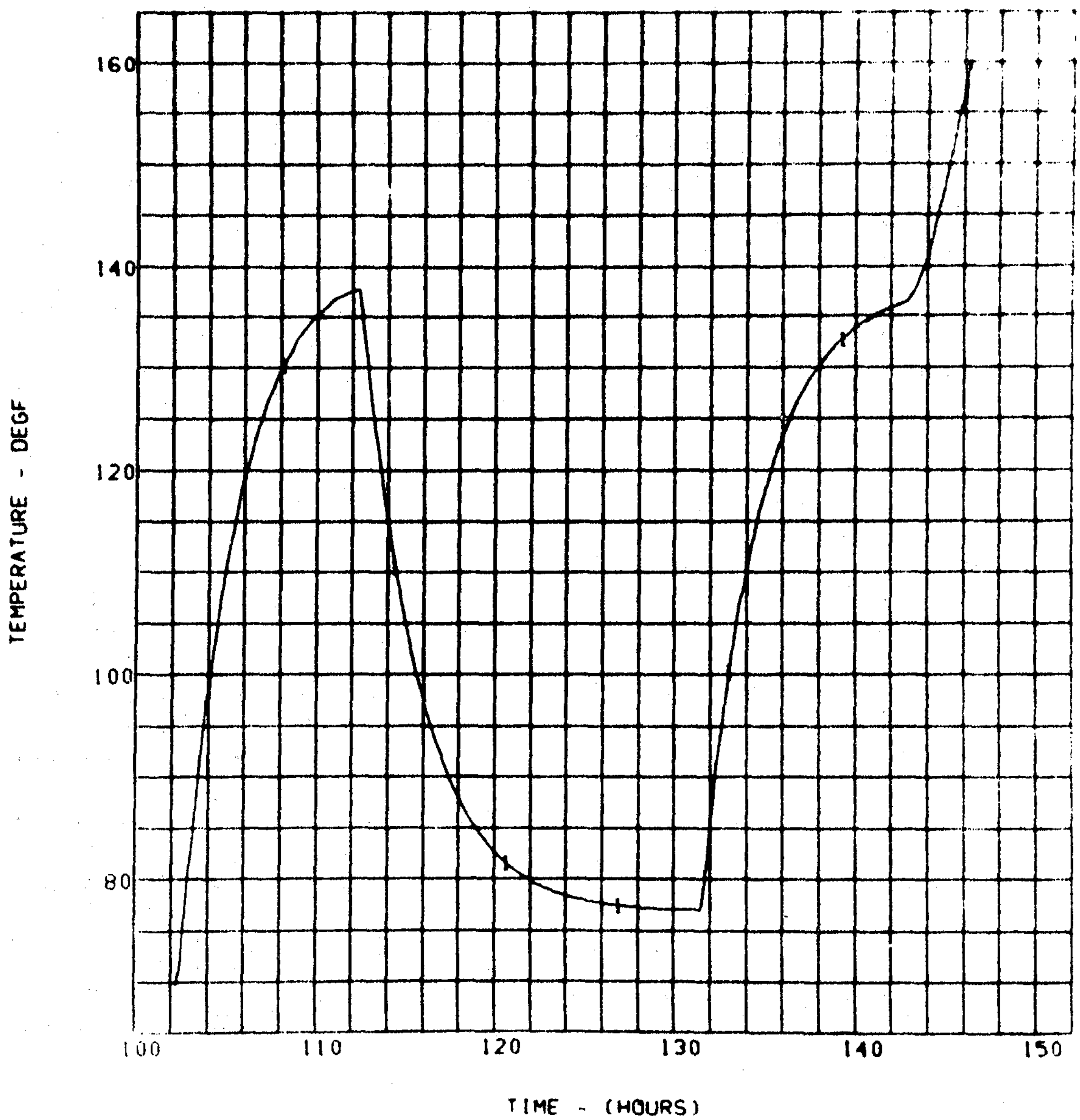

Figure LM8/4.3.12-29. LM8 A/S Water Tank Failure Simulation
(1) 109ST LGC Electronic Module Limit 160 Deg.
(See Para. 4.3.12.7)

(NASA DATA SOURCE)

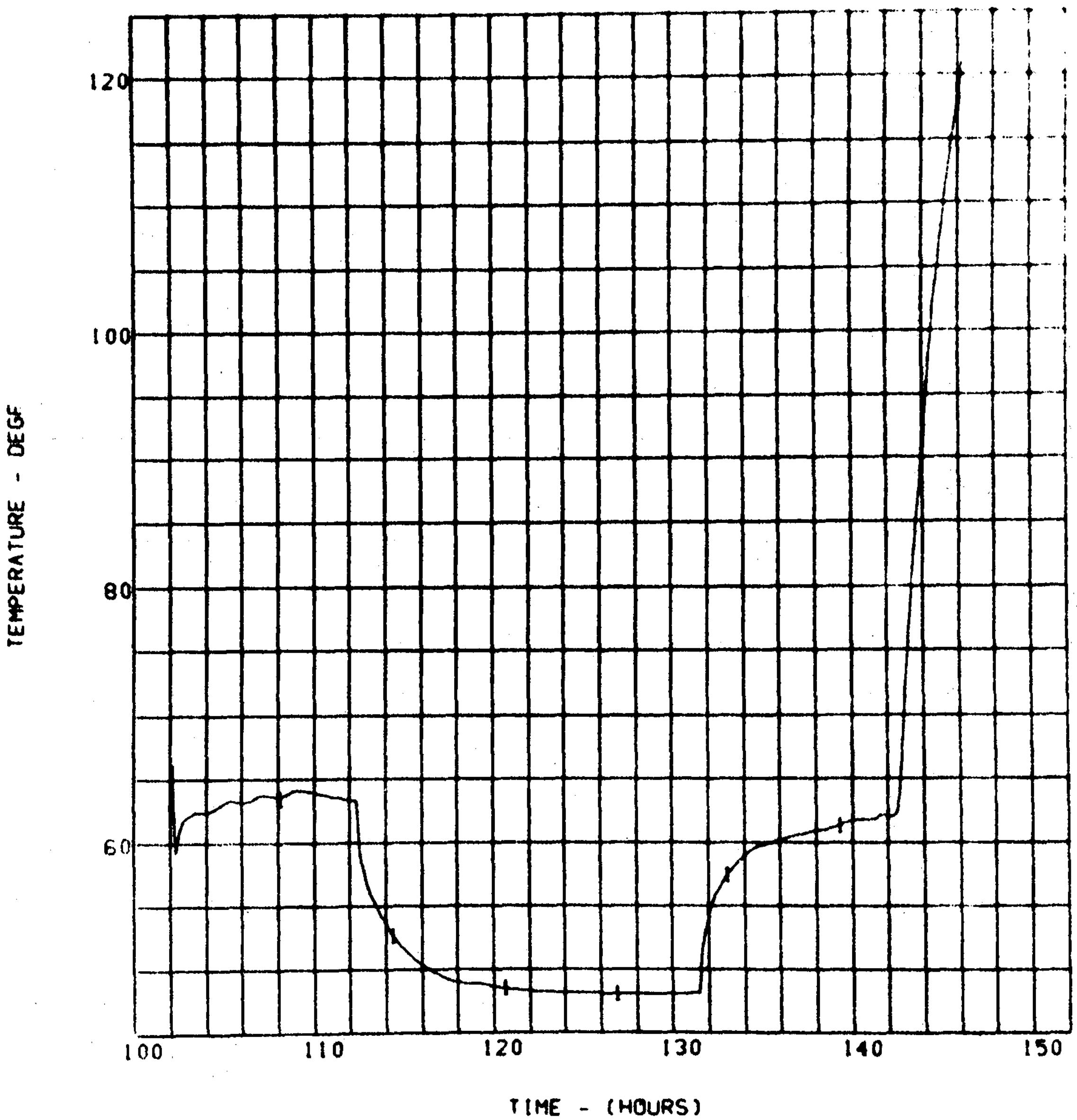

Figure LM8/4.3.12-30. LM8 A/S Water Tank Failure Simulation
(1) 108ST LGC Logic Module Limit 140 Deg.
(See Para. 4.3.12.7)

(NASA DATA SOURCE)

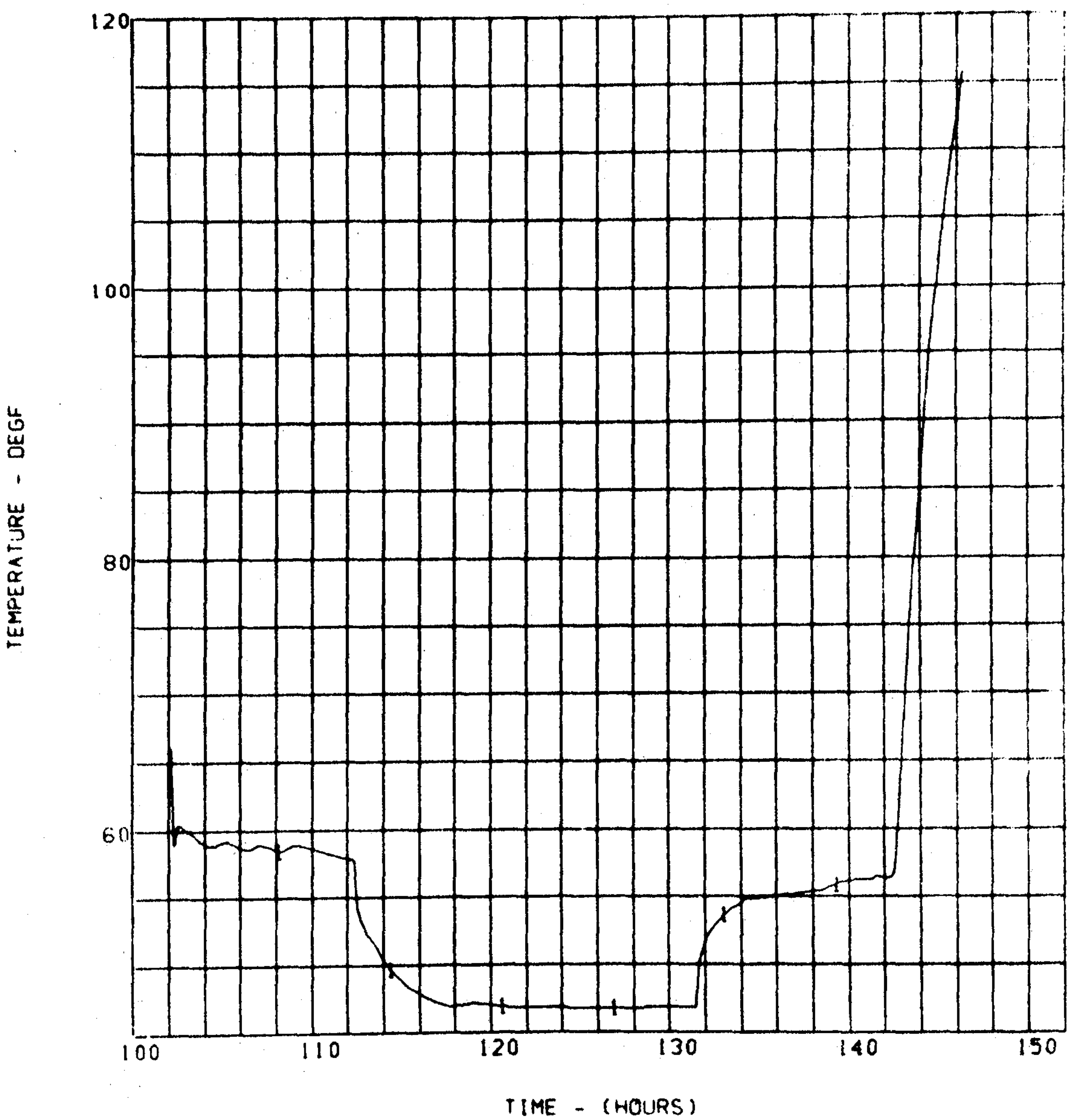

Figure LM8/4.3.12-31. LM8 A/S Water Tank Failure Simulation
(1) 105ST LGC Logic Module Limit 140 Deg.
(See Para. 4.3.12.7)

(NASA DATA SOURCE)

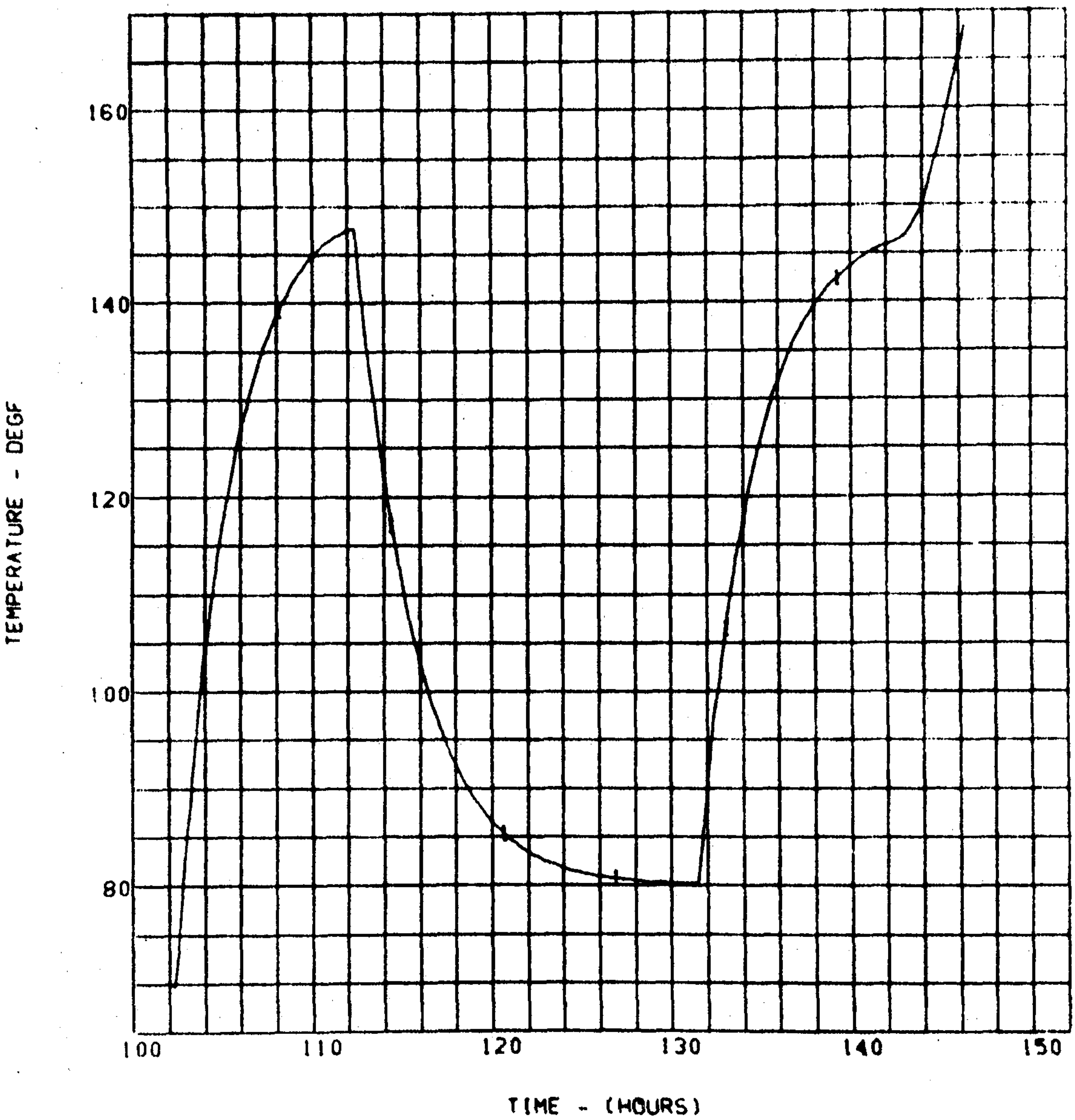

Figure LM8/4.3.12-32. LM8 A/S Water Tank Failure Simulation
(1) 107ST LGC Power Supply Limit 160 Deg.
(See Para. 4.3.12.7)

(NASA DATA SOURCE)

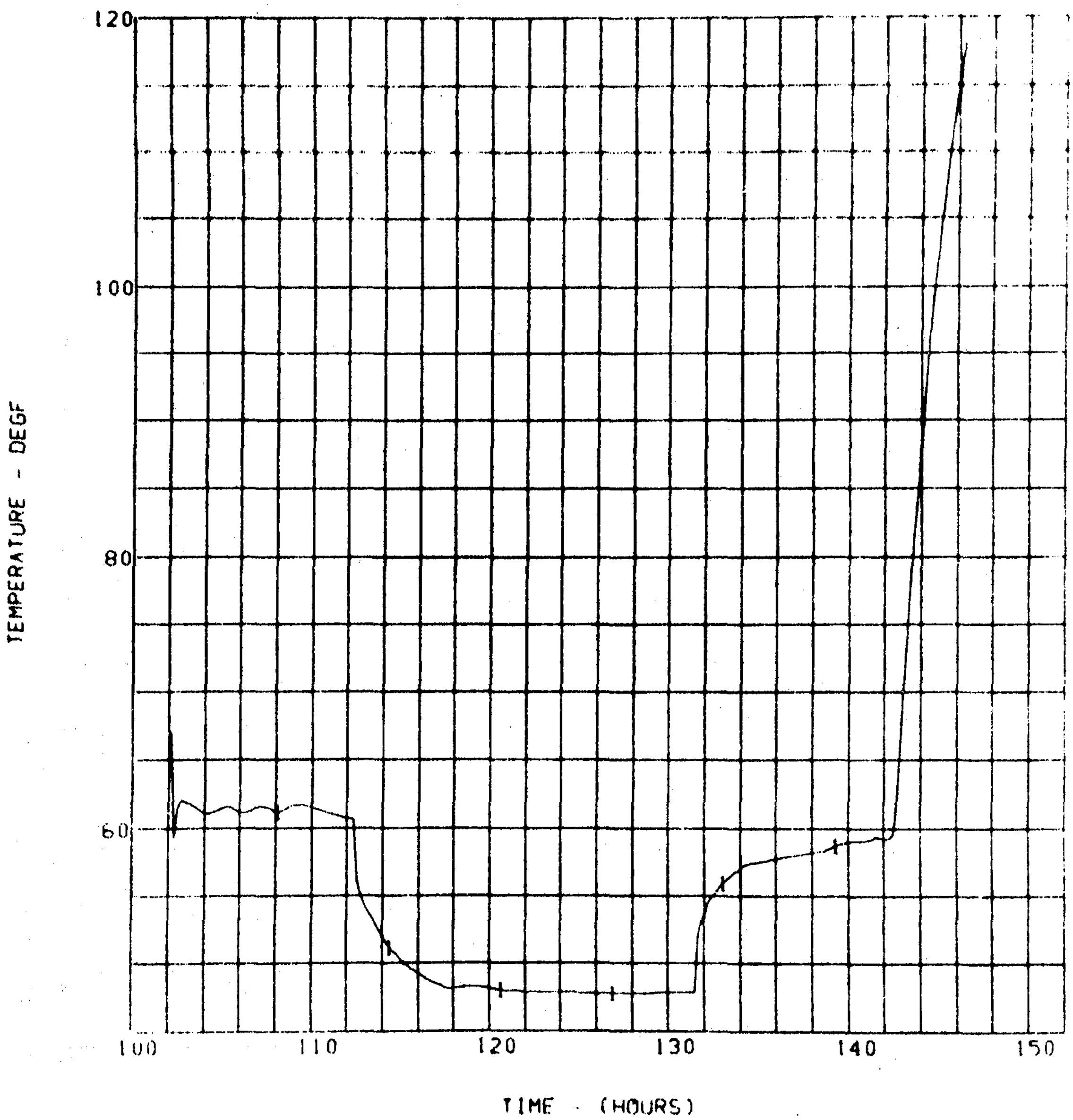

Figure LM8/4.3.12-33. LM8 A/S Water Tank Failure Simulation
(1) 106ST LGC Power Supply Limit 160 Deg.
(See Para. 4.3.12.7)

(NASA DATA SOURCE)

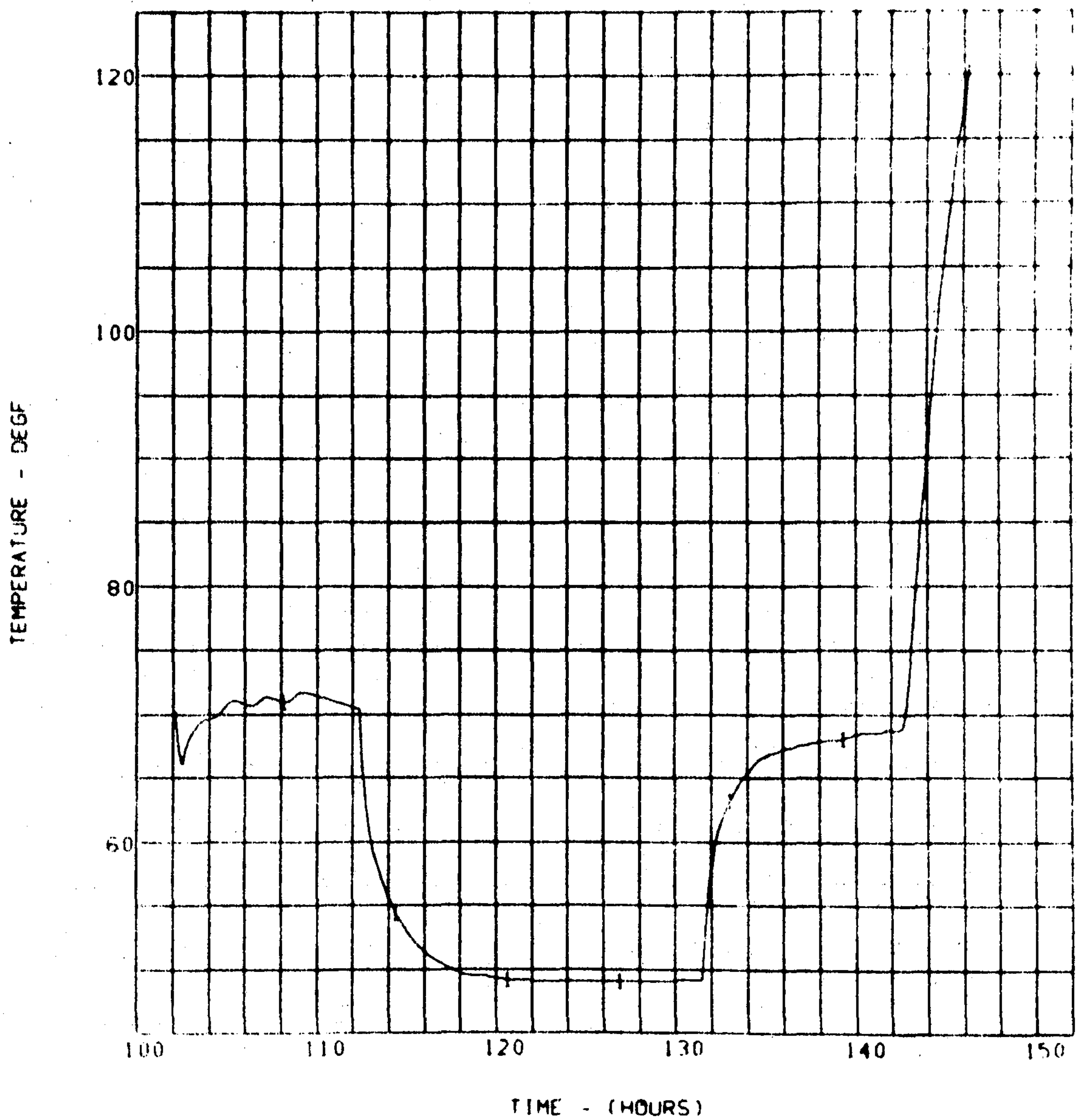

Figure LM8/4.3.12-34. LM8 A/S Water Tank Failure Simulation
(1) 122SL CDU Lanyward Logic Module Limit 220 Deg.
(See Para. 4.3.12.7)

(NASA DATA SOURCE)

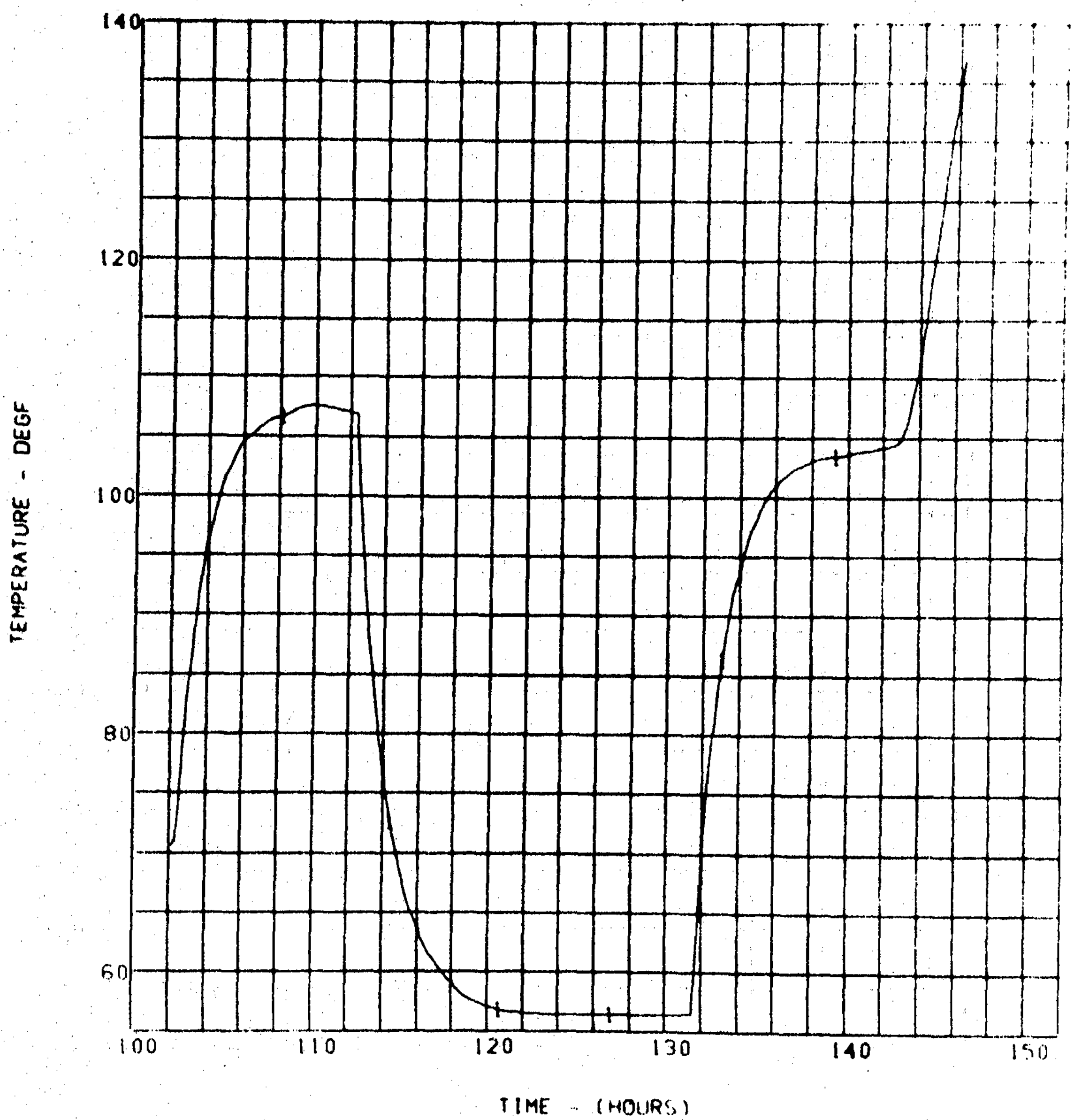

Figure LM8/4.3.12-35. LM8 A/S Water Tank Failure Simulation
(1) 121SL CDU Lanyard Logic Module Limit 220 Deg.
(See Para. 4.3.12.7)

(NASA DATA SOURCE)

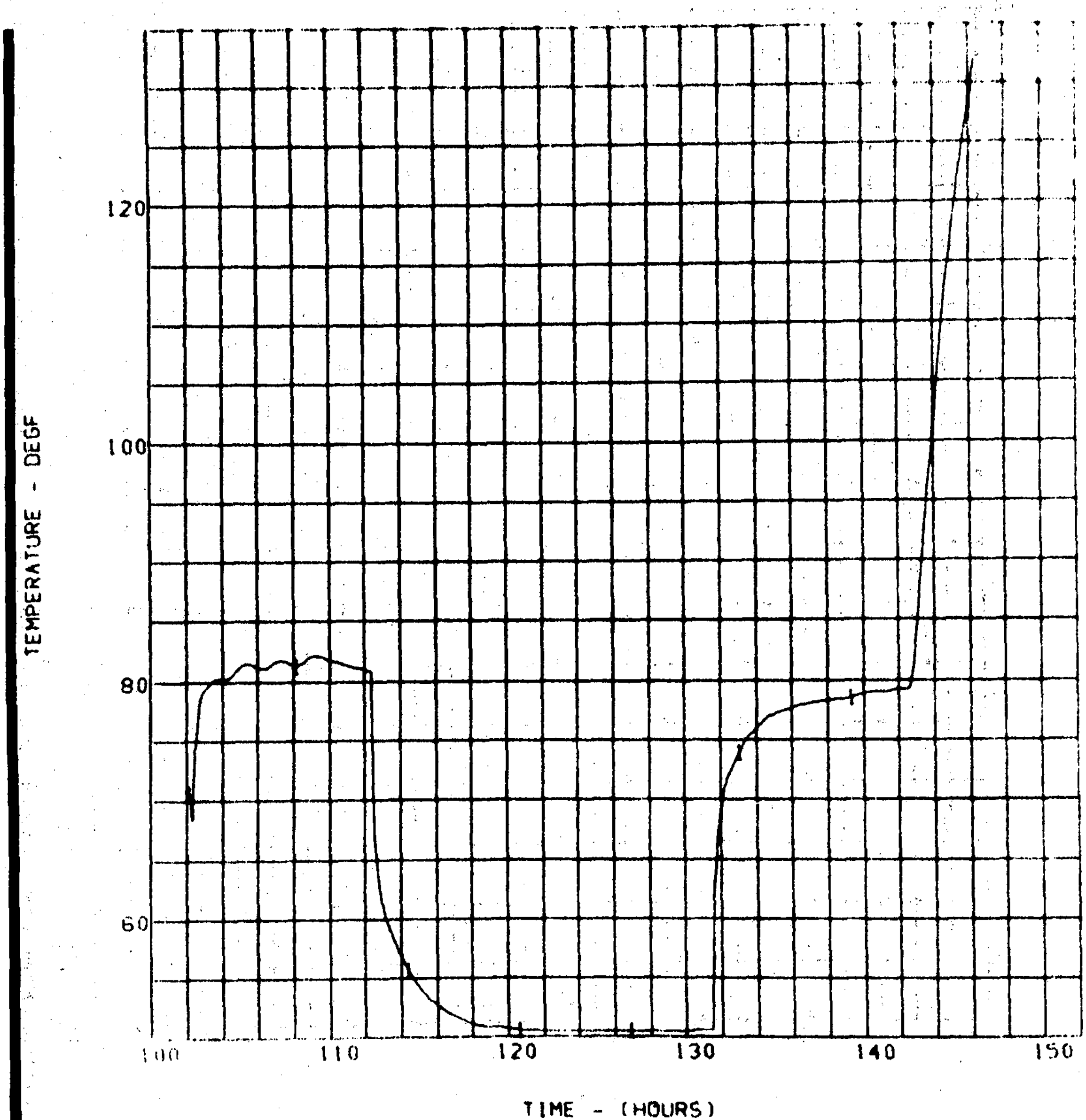

Figure LM8/4.3.12-36. LM8 A/S Water Tank Failure Simulation
(1) 120SL CDU Power Supply Module Limit 220 Deg.
(See Para. 4.3.12.7)

(NASA DATA SOURCE)

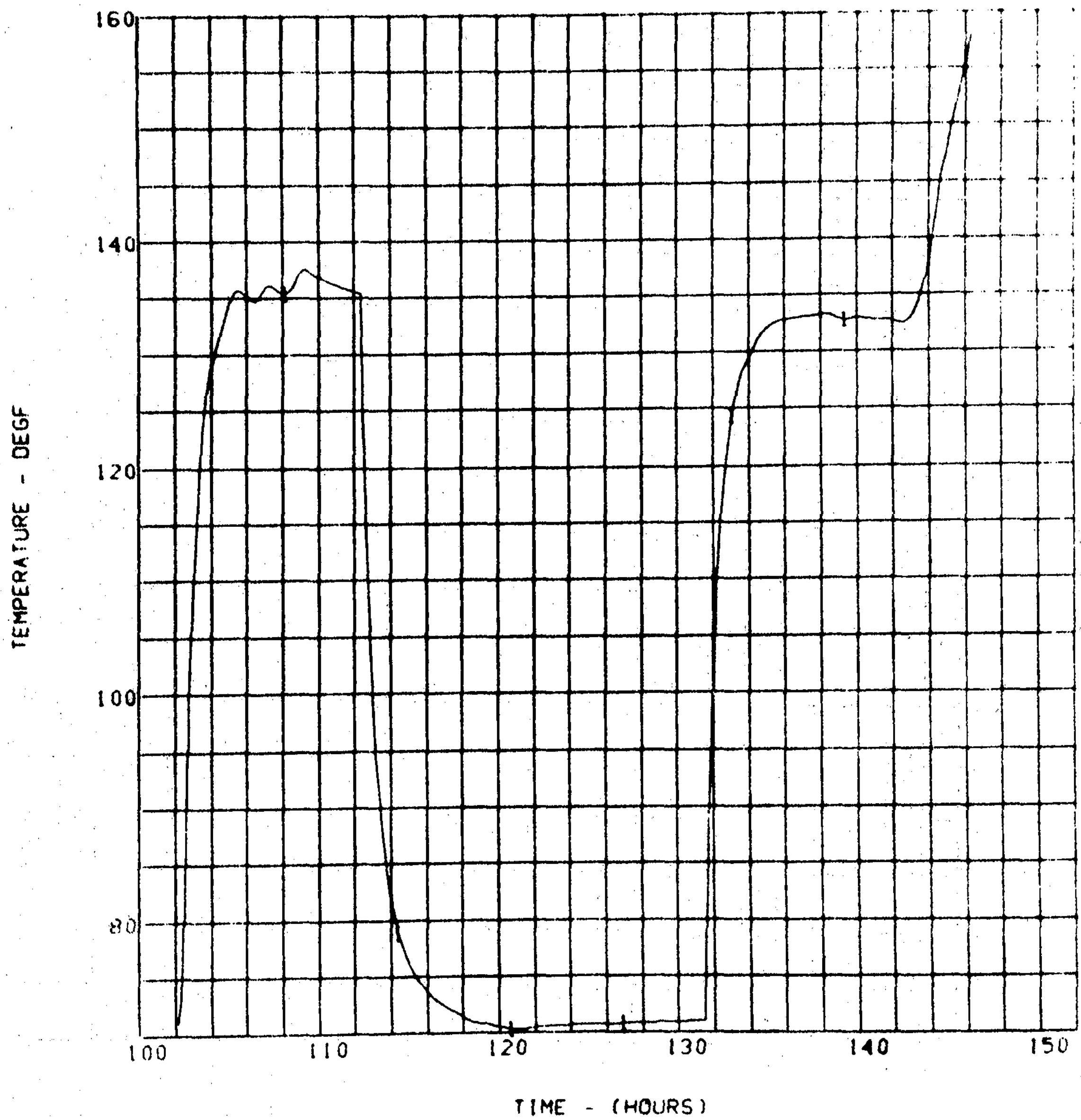

Figure LM8/4.3.12-37. LM8 A/S Water Tank Failure Simulation
(1) 113SL PSA 800 Cycle 5 PS Limit 220 Deg.
(See Para. 4.3.12.7)

(NASA DATA SOURCE)

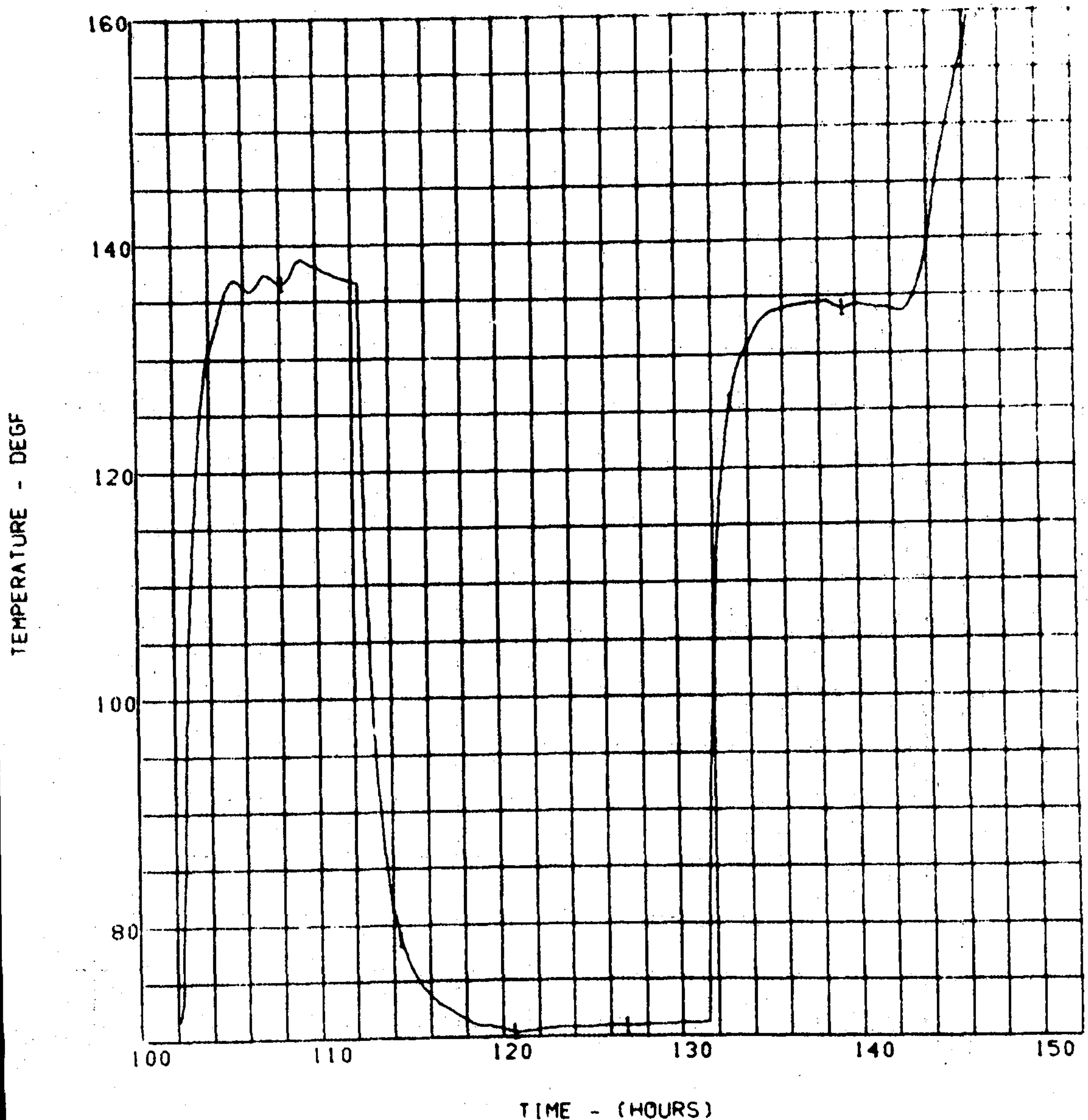

Figure LM8/4.3.12-38. LM8 A/S Water Tank Failure Simulation
(1) 112ST PSA 800 Cycle 5 PS Limit 220 Deg.
(See Para. 4.3.12.7)

(NASA DATA SOURCE)

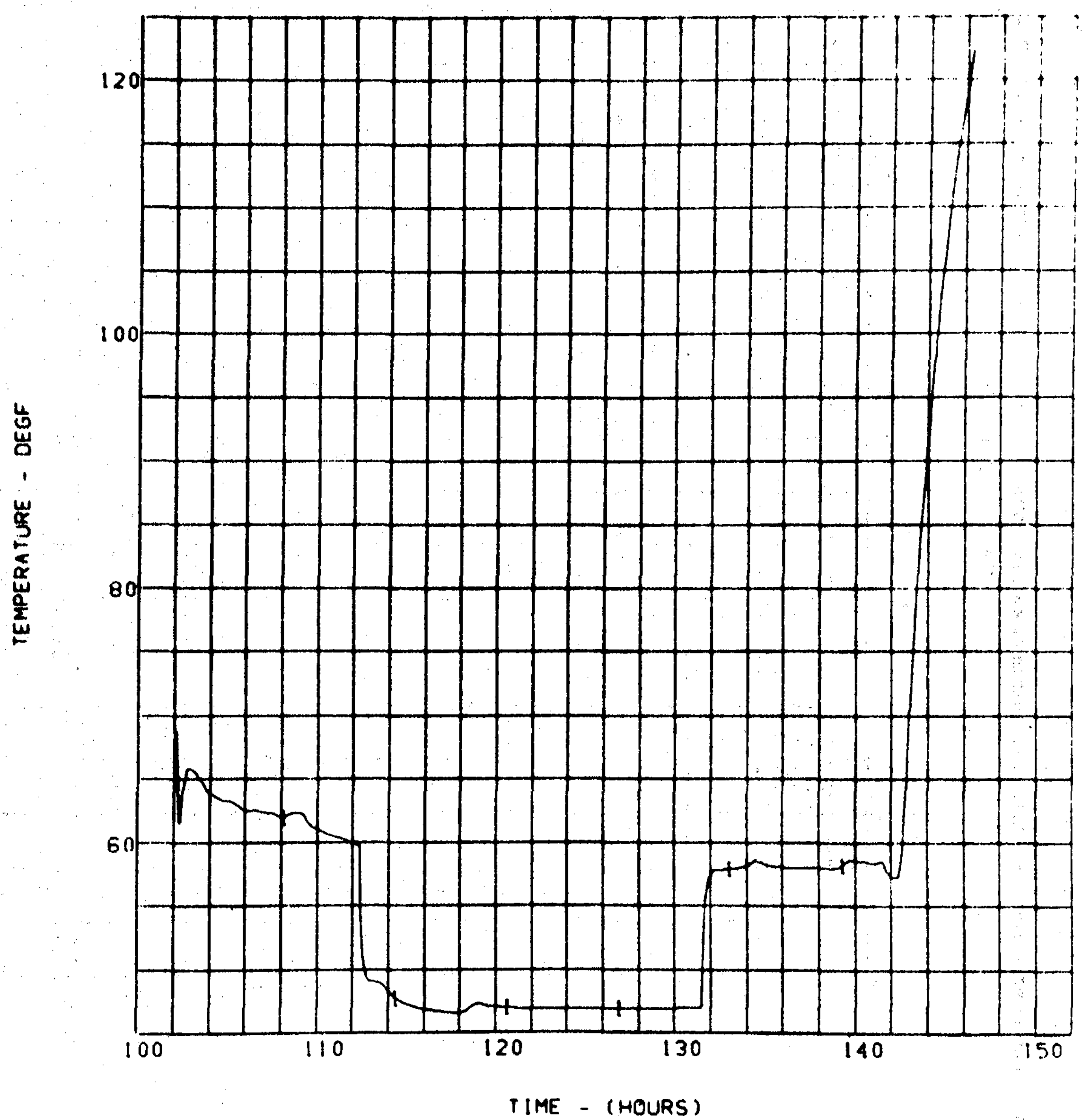

Figure LM8/4.3.12-39. LM8 A/S Water Tank Failure Simulation
(1) 220ST PTA 3 PIPA Cal.Limit 185 Deg.
(See Para. 4.3.12.7)

(NASA DATA SOURCE)

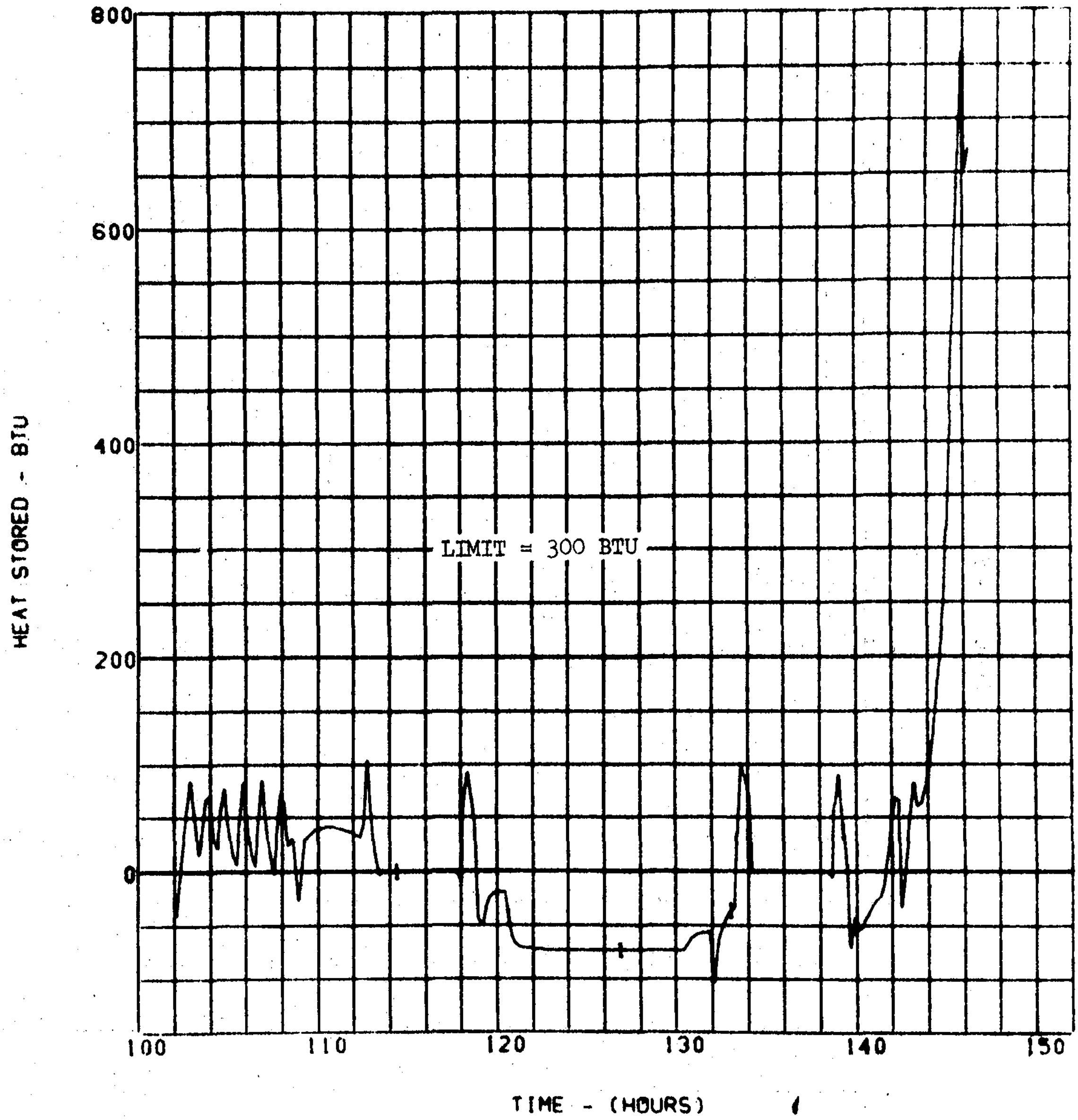

Figure LM8/4.3.12-40. LM8 A/S Water Tank Failure Simulation
(1) Reference Q Stored for Astronaut No. 1
(See Para. 4.3.12.7)

(NASA DATA SOURCE)

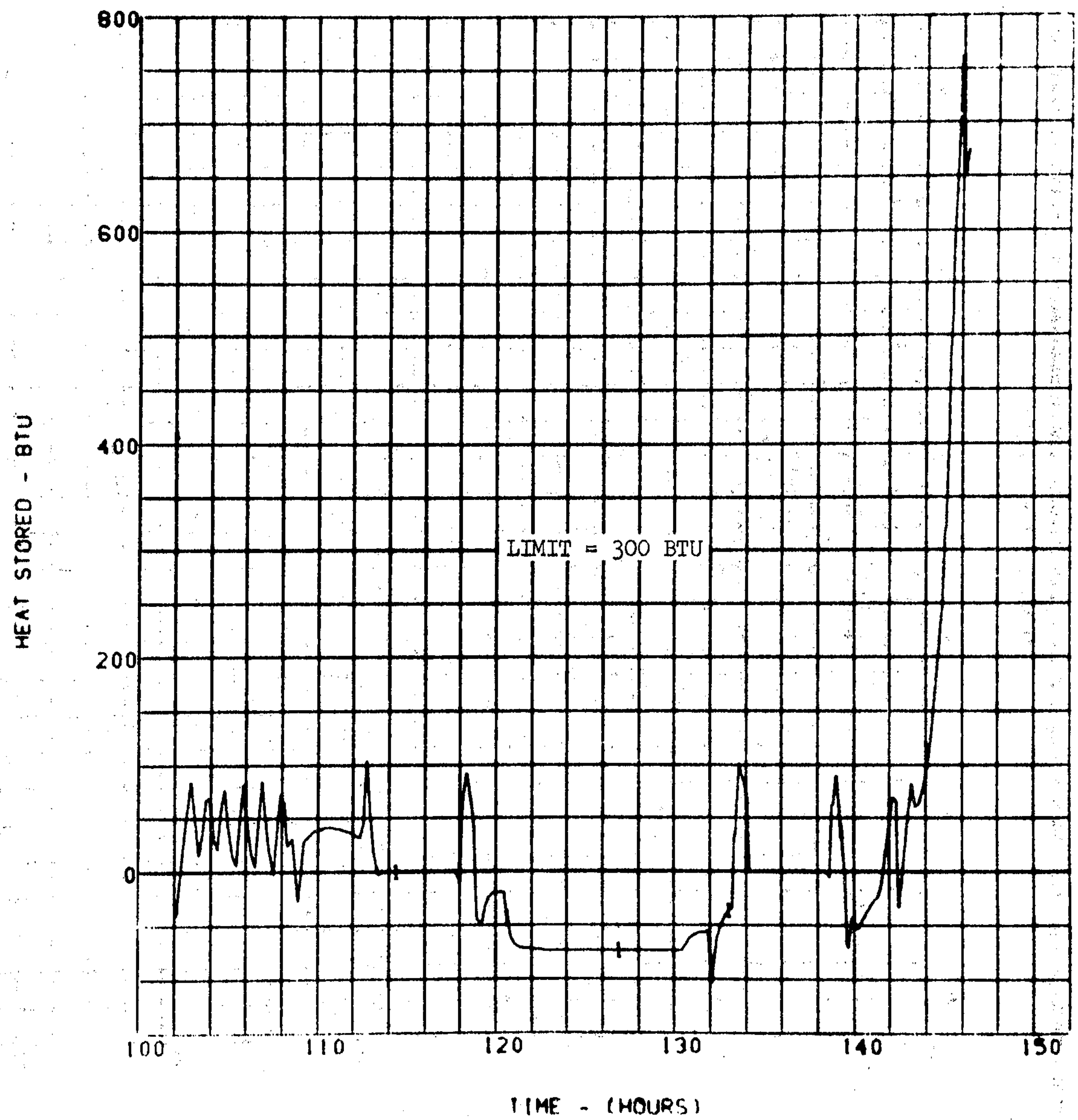

Figure LM8/4.3.12-41. LM8 A/S Water Tank Failure Simulation
(1) Reference Q Stored for Astronaut No. 2
(See Para. 4.3.12.7)

(NASA DATA SOURCE)

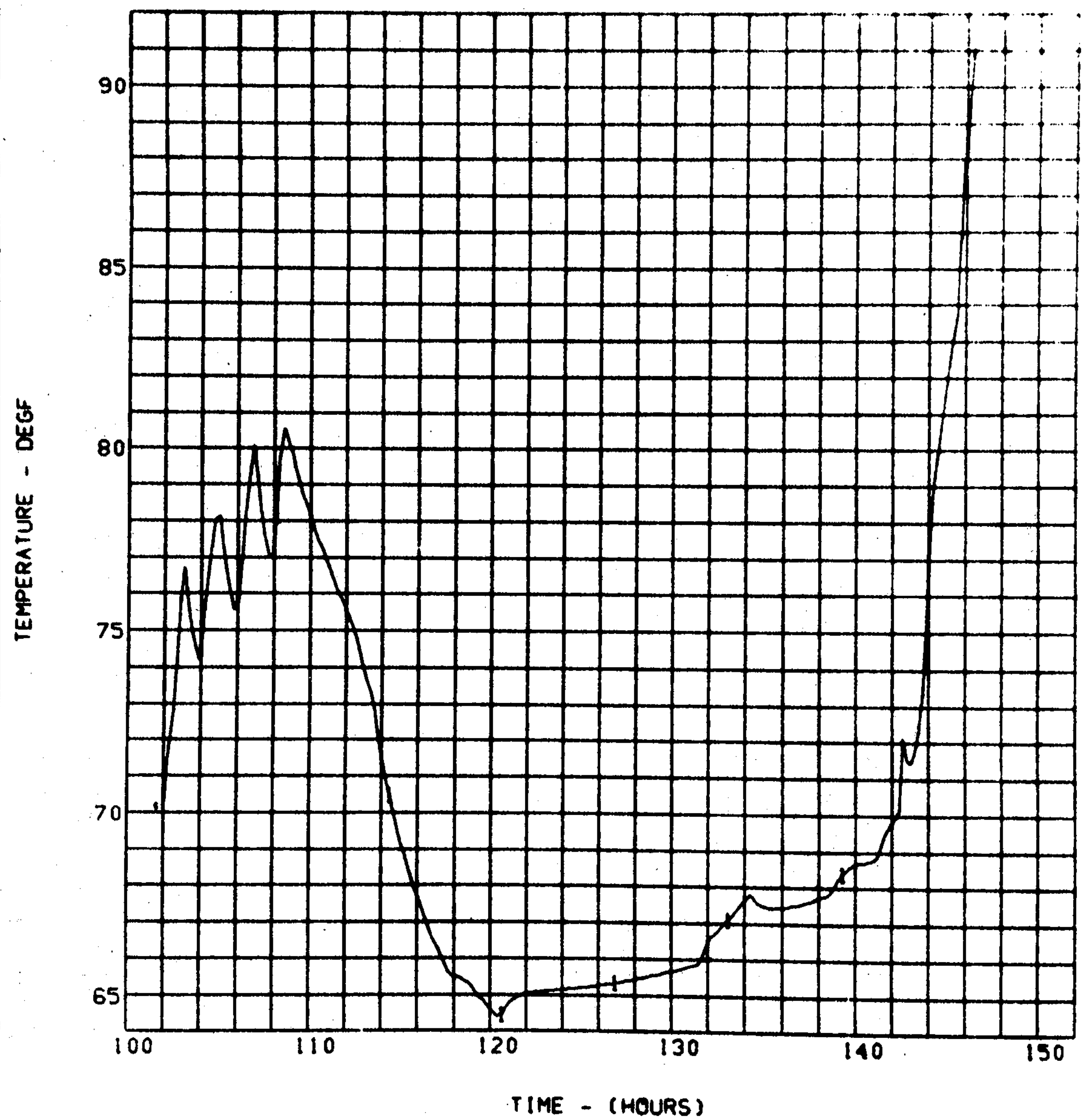

Figure LM8/4.3.12-42. LM8 A/S Water Tank Failure Simulation
(1) 580TL AVE Cabin Structure
(See Para. 4.3.12.7)

(NASA DATA SOURCE)

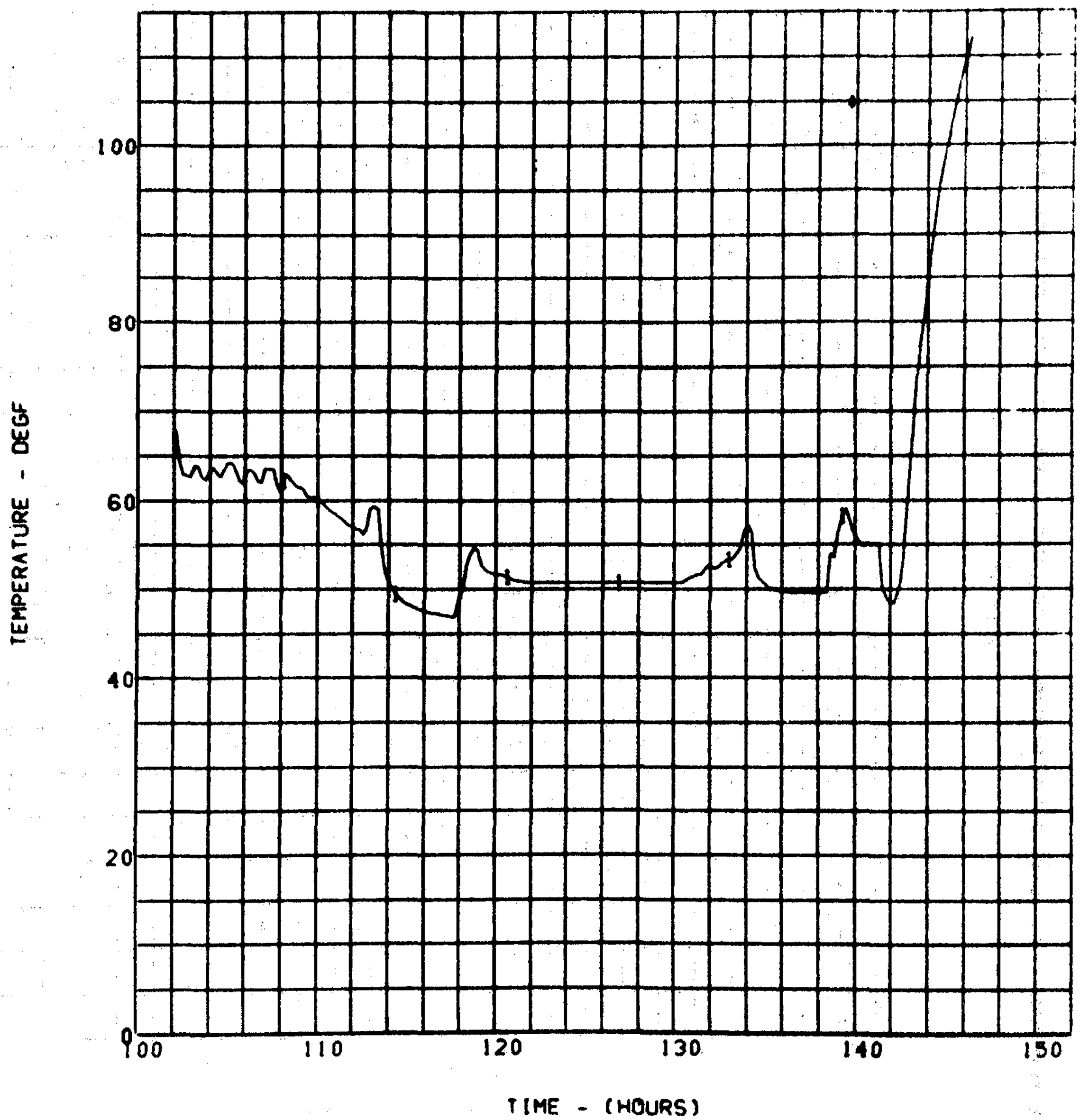

Figure LM8/4.3.12-43. LM8 A/S Water Tank Failure Simulation
(1) Sublimator Coolant Inlet (FL214 GF2531T)
(See Para. 4.3.12.7)

(NASA DATA SOURCE)

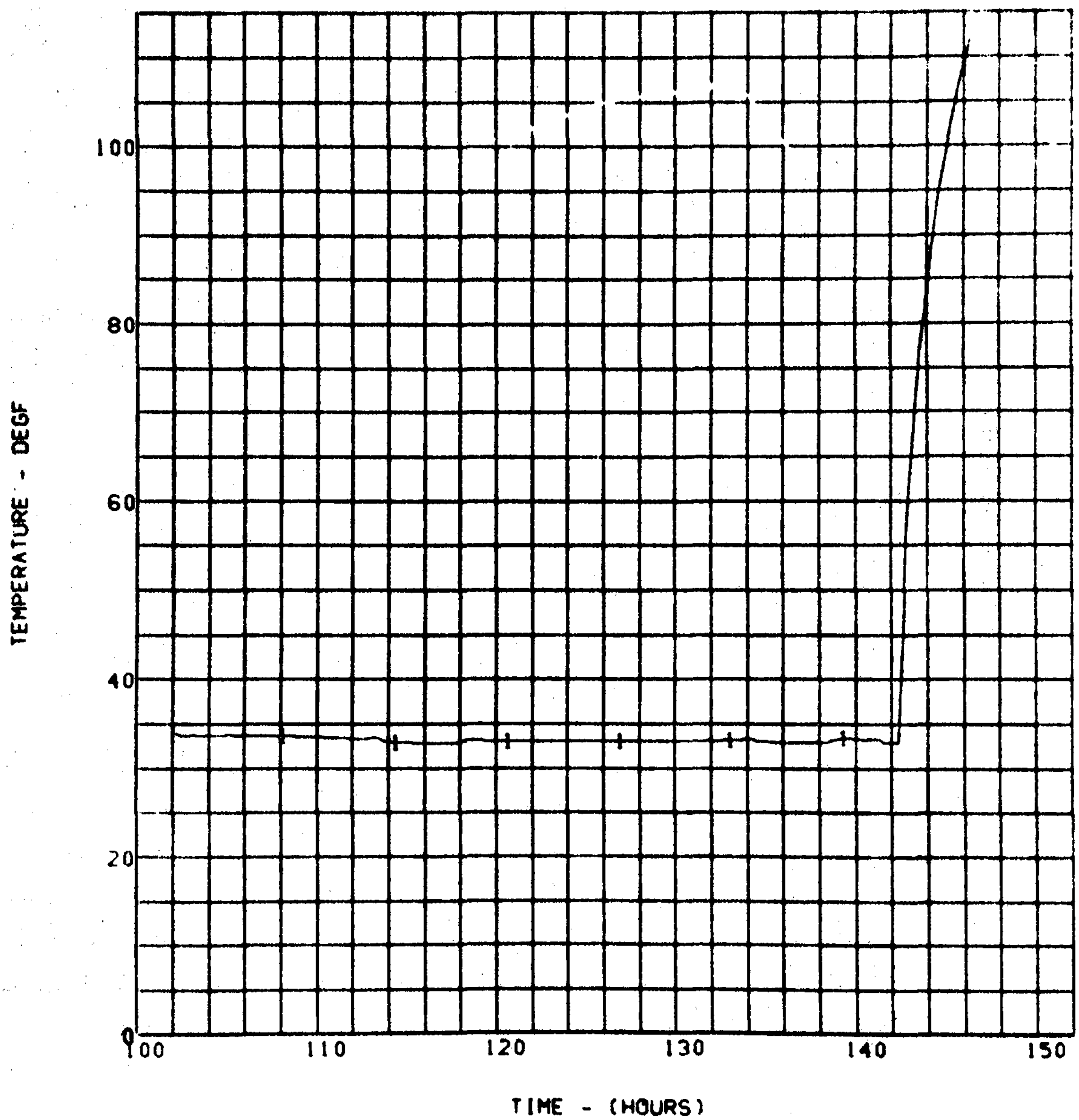

Figure LM8/4.3.12-44. LM8 A/S Water Tank Failure Simulation
(1) Sublimator Coolant Outlet (FL156 GF2581T)
(See Para. 4.3.12.7)

(NASA DATA SOURCE)

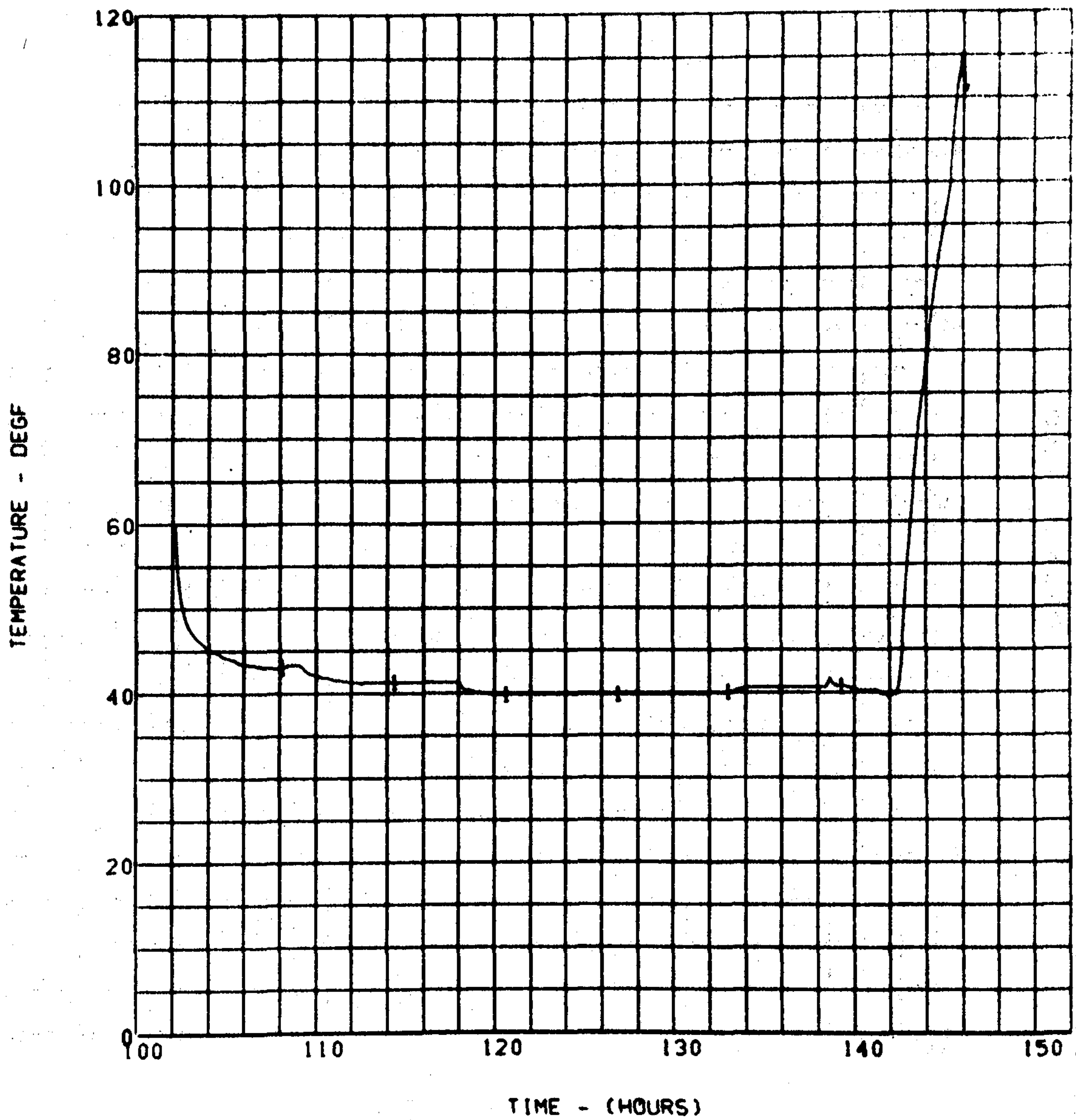

Figure LM8/4.3.12-45. LM8 A/S Water Tank Failure Simulation
(1) Suit Inlet (FL328 GF1281T)
(See Para. 4.3.12.7)

(NASA DATA SOURCE)

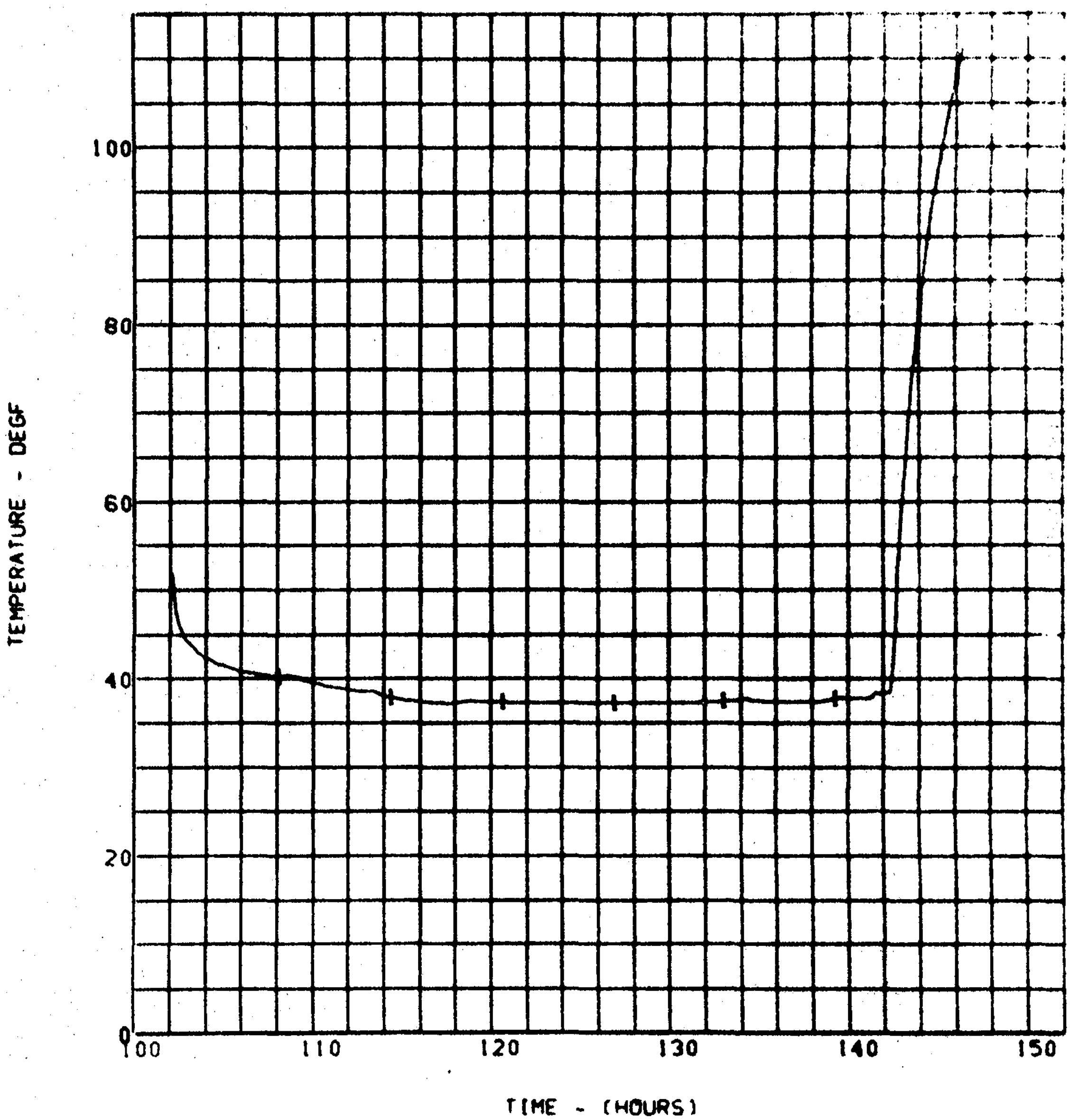

Figure LM8/4.3.12-46. LM8 A/S Water Tank Failure Simulation
(1) LTE Coolant Inlet (FL181 GF9998U)
(See Para. 4.3.12.7)

LM8/4.5.1.1 Uncertainty of LM IMU Alignment from CSM IMU

The measured alignment angles associated with a talkover alignment of the LM IMU from the CSM IMU are listed in Table LM8/4.5.1-1. The contributions to the uncertainty in the talkover alignment of the LM IMU are listed in Table LM8/4.5.1-2. The RSS 1-σ total uncertainties are summarized as follows:

LM Axis	1-σ RSS, arc min
Yaw (about X-axis)	±15.8 (0.264 deg)
Pitch (about Y-axis)	±4.0 (0.067 deg)
Roll (about Z-axis)	±4.0 (0.067 deg)

The above values do not include thermal effects or bending or torque effects from any cause (i.e., RCS jet firing). Also, the effect of the maximum allowable CG offset in the X-axis of 0.2 inch was not included.

LM8/4.5.1.4 Guidance Computer Erasable Memory Constants (NASA DATA SOURCE)

The following listings pertain to the LM Guidance Computer (LGC) pad loaded erasable memory constants. Mission time computed constants, such as state vectors, etc., are not included.

Table LM8/4.5.1-3 contains a tabular listing of the erasable load, both mission tape parameters and launch tape parameters. The remarks column contains a short description of the use of the constant.

The number in the "Rev" column denotes the number of revisions to the value of the corresponding parameter that have been incorporated in publications of the Apollo 14 erasable load.

A single or double star (* or **) in the "Rev" column denotes that it is also in the inflight erasable load. These parameters would have to be verified or reloaded in order to completely initialize the LGC in orbit. A single star denotes loading by ground uplink; a double star denotes loading by the astronaut via the DSKY.

LM8/4.5.1.5.2 **Assembly Alignment Data of Spacecraft Docking Mating Surfaces to the Navigation Base.**

Angular Alignment of the Docking Ring Seal Surface Axes Relative to the Navigation Base Axes

Alignment	Ambient Press. (Initial)	+5.2 psid	+2.6 psid	Ambient Press. (Final)
About Y	-3'40"	-4'50"	-5'22"	-5'40"
About Z	+1'15"	+2'45"	+1'43"	+0'57"

Average Ambient Pressure Readings: About Y = -4'40"
About Z = +1'06"

Sign Convention for Docking Ring Surface Plane Tilt

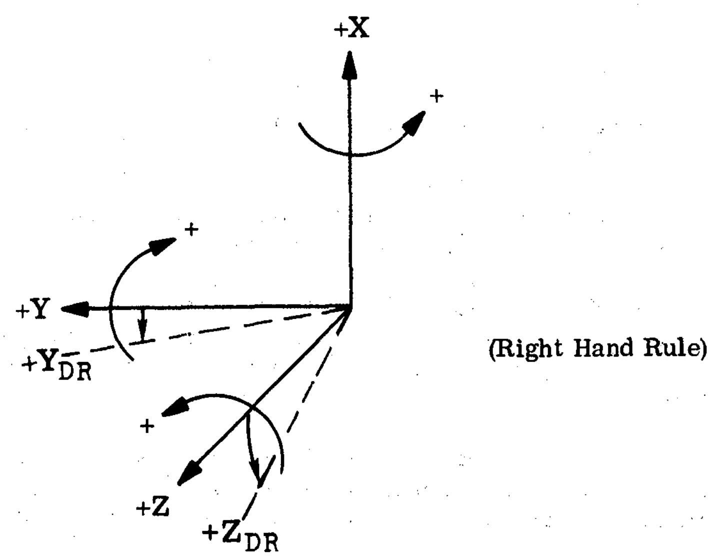

Note: Ambient Pressure = 14.7 psia

LM8/4.5.1.5.3 AOT Alignment Data

The azimuth and elevation angles for the rear right, rear left and the close (rear) detent positions of the AOT (relative to the AOT mounting surface) are tabulated below for LM-8 (AOT Designation 615, Serial No. 21). These rear detent angles have been calculated using measured azimuth and elevation angles of the front detent positions. The uncertainty associated with these calculated angles is ±2 arc minutes.

The front 3 detent angles are measured, relative to the AOT mounting surface, at Kollsman Instrument Corporation and have a measurement uncertainty of ±30 arc seconds. For information, these measured angles are included in the tabulation. To verify these measured values, an AOT functional test has been performed on the spacecraft.

LM-8 AOT DETENT DATA

	Front (Measured)		
Data	L	F	R
Azim. (Deg)	300.246	0.214	60.177
Elev. (Deg)	45.097	45.119	45.114

	Rear (Calculated)		
Data	R_R	C_L	L_R
Azim. (Deg)	120.252	180.233	240.204
Elev. (Deg)	45.086	45.064	45.069

The above data is for an unpressurized vehicle at ambient conditions.

Table LM8/4.5.1-1

Measured Hardware Alignments Contributing to Alignment of LM IMU from CSM IMU

Measurement	Alignment Arc Min About X-Axis	 Y-Axis (About Z-Axis)	 Z-Axis (About Y-Axis)
COMMAND MODULE			
Displacement of CSM IMU axes with respect to local vertical.*	-	-2.4	-7.8
Displacement of CSM Nav. base axes with respect to docking ring.*	+13.8	-	-
Displacement of docking ring axes with respect to local vertical.*	-	-5.5	+8.5
LUNAR MODULE			
	(LM Yaw)	(LM Roll)	(LM Pitch)
Displacement of docking ring with respect to nav. base axes.**	-	+2.75	-4.83
Displacement of nav. base with respect to IMU.***	+4.18	+0.98	+4.42

*TPS 110-S/C-076 and K3128, 12/16/70. In lieu of S/C axes the local vertical was used as the common reference axis.

**Spacecraft Operational Data Book, Volume II, LM Data Book, Rev 2, Para. LM8/4.5.1.5.2

***Spacecraft Operational Data Book, Volume II, LM Data Book, Rev 2, Para. LM8/4.5.2.1.2. Data stated as IMU relative to nav. base, therefore, values tabulated above are negative of SODB values because the desired sense of displacement is from nav. base to IMU.

Table LM8/4.5.1-2

Hardware Contributions to Uncertainty of LM IMU Alignment from CSM IMU

Source of Uncertainty	1-σ Uncertainty, Arc Min		
	About LM X-Axis	About LM Y-Axis	About LM Z-Axis
CM IMU to CM Docking Ring	0.2 (1)	0.2 (1)	0.2 (1)
CM Docking Angle Scale	0.2 (1)	-	-
CM-LM Docking Ring Alignment	-	4.0 (2)	4.0 (2)
LM Docking Angle Pointer	5.0 (3)	-	-
Docking Angle Determination	15.0 (4)	-	-
LM Docking Ring to LM Nav Base	-	Negl. (5)	Negl. (5)
LM Nav Base to LM IMU	Negl. (5)	Negl. (5)	Negl. (5)
RSS 1-σ Uncertainty, Arc Min	15.8	4.0	4.0
Arc Deg	0.264	0.067	0.067

<u>REFERENCES</u>

(1) Estimates based on methods used in TPS 110-S/C-076 and K3128, 12/16/70, to measure these alignments. See Table LM8/4.5.1-1.

(2) Apollo ICD MH 01-05053-416 (The included angle measured between the planes of the docking interfaces of the CM and LM will not exceed 0.2 deg.)

(3) Apollo ICD MH 01-05128-116 (60 deg. ±5 arc min.)

(4) Telecon R. Schweickart, NASA astronaut (±0.5 deg., considered to be 2-σ)

(5) Uncertainty in measured alignment considered negligible. See Table LM8/4.5.1-1.

LM8/4.5.4.2 Rendezvous Radar Mechanical Alignment

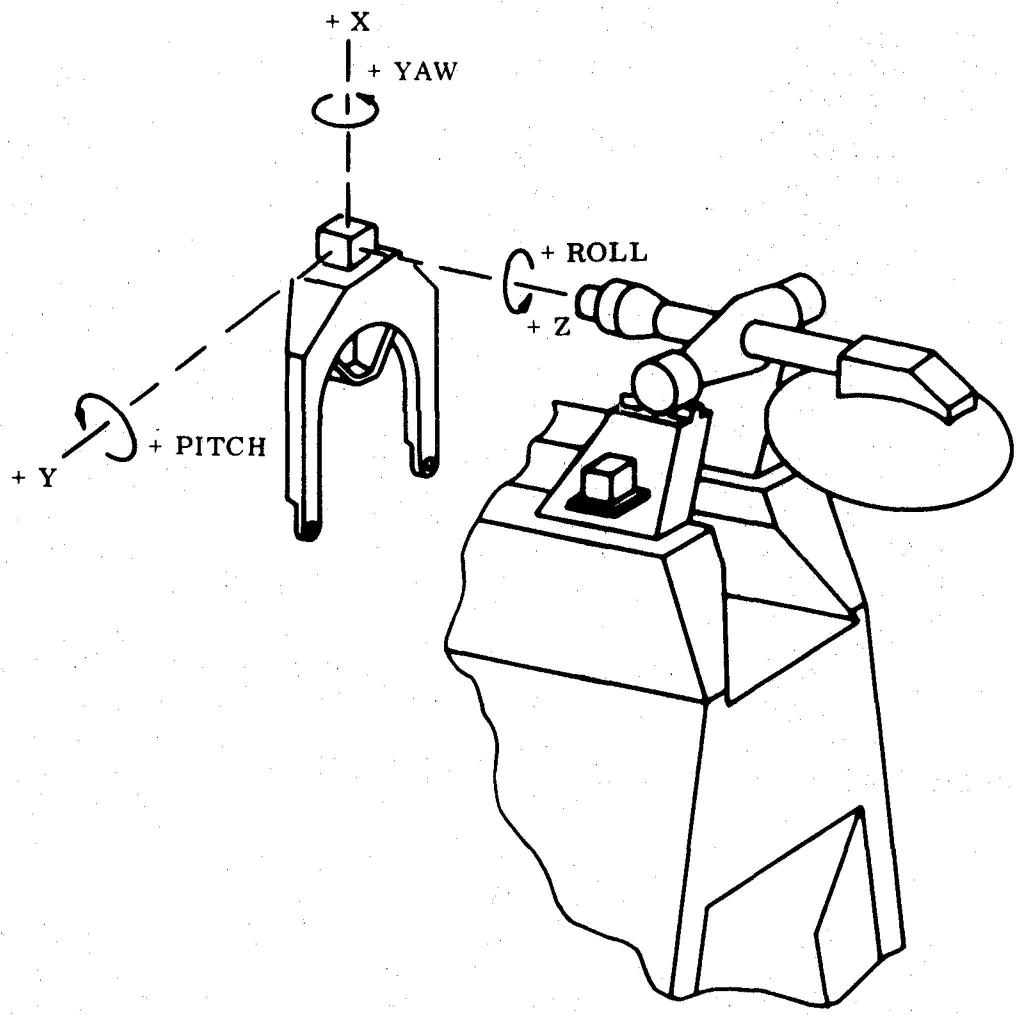

The Rendezvous Radar Antenna Assembly alignment for LM-8 with respect to the Vehicle Coordinate System (Nav. Base Gage) is shown below:

Pitch:	-00° 02' 45"
Roll:	-00° 03' 18"
Yaw:	+00° 00' 05"

(Ref.: LMO-566-215, dated Sept. 1969)

LM8/4.5.4.3 RR Timeline Operation

Figures LM8/4.5.4-1 and LM8/4.5.4-2 show the proposed RR management temperature profile for the LM-8 mission from undocking to touchdown and from lunar ascent to the completion of the rendezvous sequence. The management curves are the same as LM-6 and LM-7 except the times have been corrected to the LM-8 timeline. The RR operating time during the undocking-to-touchdown phase is limited to one seven-minute checkout phase. No antenna over-heating due to this operation is expected. The RR operation for the lunar ascent to docking phase is considerably different than that for LM-6. The RR operating time is considerably shorter (direct ascent vs. concentric ascent) than for LM-6. No antenna over-heating due to this operation is expected. Since high-power multiplier chain (HPMC) and gyro temperatures are expected to be significantly below their maximum allowable values (management curves) for the LM-8 RR operating profile it was considered unnecessary to perform a detailed analysis to obtain predicted HPMC and gyro mission temperature profiles.

The management curves shown are based on a January 31, 1971, launch date and the following operational timeline:

H-3 Mission RR Timeline (Time in Hrs: Min. GET)

RR "ON"	RR "OFF"
104:00	104:12
105:03	105:07
142:32	144:04

Short "ON" periods for antenna reorientations, and antenna "ON" periods less than 30 minutes followed by an "OFF" period of several hours do not influence critical thermal parameters, and have not been included in this evaluation.

The rendezvous radar antenna assembly temperature sensor (GN 7723T) should be monitored continuously while the RR is on to assure that the temperature rise does not exceed the management curve. If the RRAA temperature exceeds the management curve of Figures LM8/4.5.4-1 and LM8/4.5.4-2, the RR should be turned off if its use is not required. This procedure will assure that there is sufficient in-limit operating time to accomplish mandatory operation.

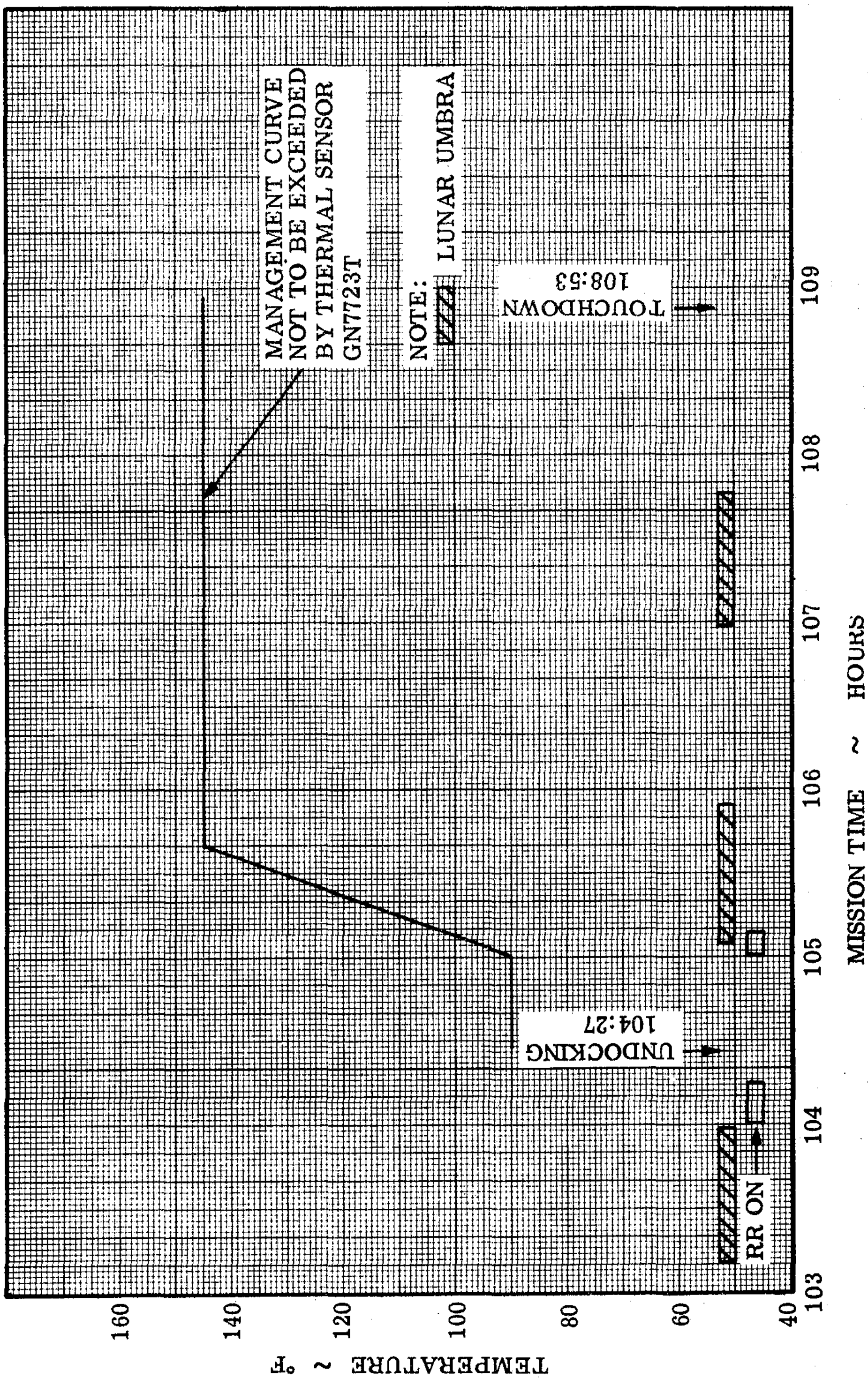

Figure LM8/4.5.4-1. Predicted RR Temperature Management Curve (Undocking to Touchdown) (See Para. LM8/4.5.4.3)

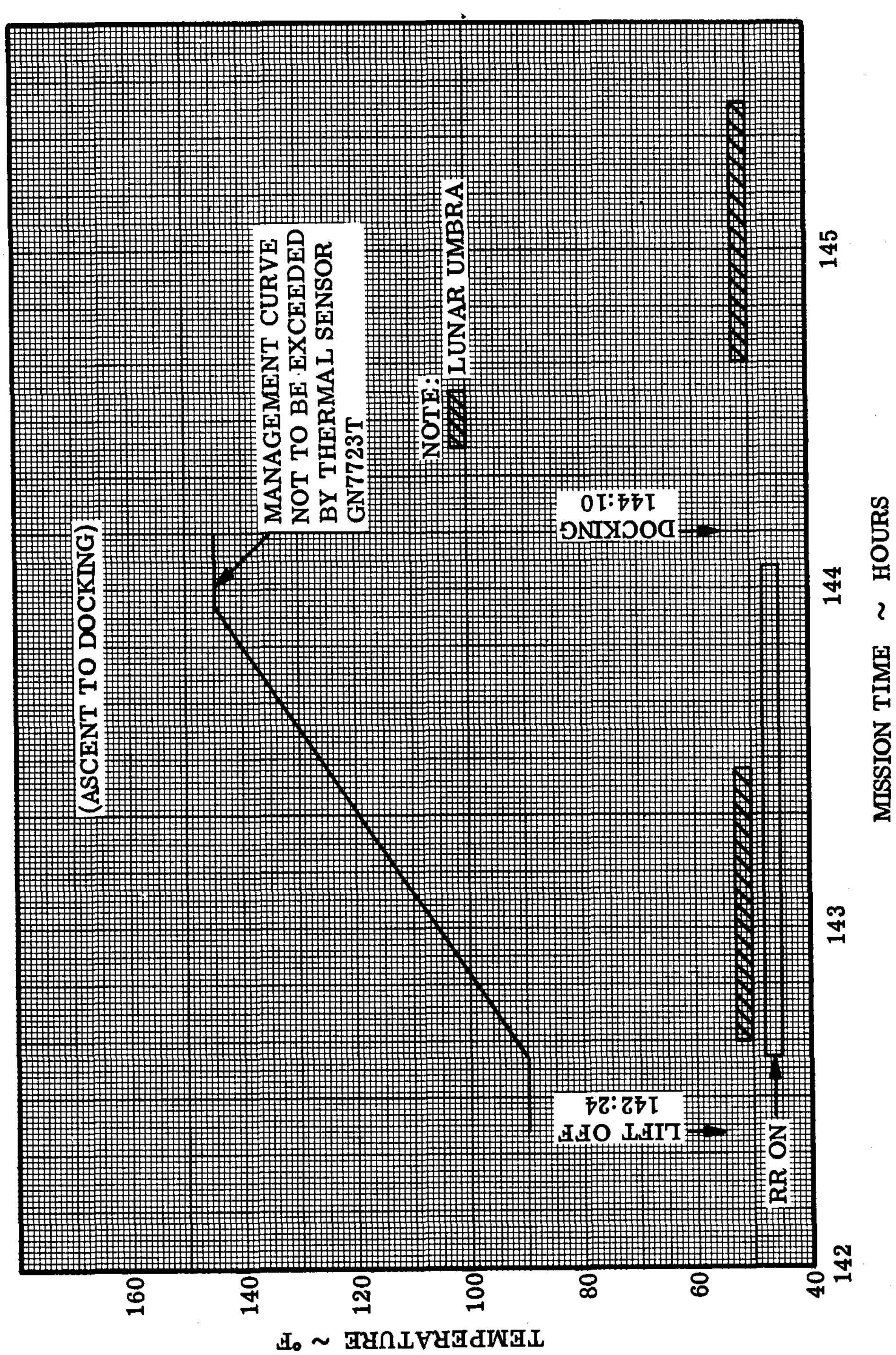

Figure LM8/4.5.4 -2. Predicted RR Temperature Management Curve For Final Flight Plan Timeline (See Para. LM8/4.5.4.3)

LM8/4.5.5.1.16 LR Power Monitor

The following is a calibration of the Power Monitor with LR P-44. These data were obtained from KSC testing during TCP 0045 and include antenna losses.

Transmitter	Power (DBM)	Power (MW)	Monitor (VDC)	Calibration
Velocity	24.3	269	3.85	14.3×10^{-3} V/MW
Altimeter	22.5	178	3.85	21.6×10^{-3} V/MW

LM8/4.5.5.1.17 Loss of LR Lock as a Function of Vehicle Pitch and Roll for an Apollo 14 Type Trajectory

Figures LM8/4.5.5-1 through LM8/4.5.5-4 describe the LR loss of lock as a function of vehicle pitch and roll for the nominal descent trajectory for antenna positions 1 and 2, respectively.

LM8/4.5.5.1.18 Expected Altitude of LR Velocity and Range Initial "Data Good" Indication

Figures LM8/4.5.5-5 and LM8/4.5.5-6 describe the signal-to-noise (S/N) ratio as a function of altitude of LR beams 1, 2, and 3 (i.e., the velocity beams). The minimum S/N threshold required for lock-on and the range sweep limit are also indicated. Figure LM8/4.5.5-6 includes the same data for beam 4 (range beam). The effect of minimum transmitter power on acquisition altitude is also indicated for each beam.

Note: The band on range acquisition altitude is due to variations in the following items:

a) Radar temperature
b) Signal-to-noise (S/N) uncertainties

LM8/4.5.5.1.21 LR Predicted Accuracy

Figure LM8/4.5.5-7 shows the predicted LR accuracy as a function of time from ignition and of altitude, for an Apollo 14 type descent trajectory.

LM8/4.5.5.2 Landing Radar Antenna Assembly Temperature Profile

Figure LM8/4.5.5-8 presents the landing radar antenna assembly typical high-temperature and low-temperature profiles for the LM-8 mission.

Table LM8/4.5.1-1

Measured Hardware Alignments Contributing to Alignment of LM IMU from CSM IMU

TBS

Table LM8/4.5.1-2

Hardware Contributions to Uncertainty of LM IMU Alignment from CSM IMU

TBS

(NASA DATA SOURCE)

Table LM8/4.5.1-3. FINAL H-3 PRELAUNCH ERASABLE LOAD LUMINARY 178

REV	MNEMONIC	ADDR	OCTAL	SF	ENGINEERING VALUE	VALUE IN AGC UNITS
	FLAGWRD3+ 0	0077	12000	-0		
	FLAGWRD8+ 0	0104	06000	-0		
	FLGWRD10+ 0	0106	00000	-0		
1	MASS + 0	1243	07441	16	3.415020000+004 LBS	1.549027015+004 KG
	MASS + 1	1244	00000	0	0.000000000+000 LBS	0.000000000+000 KG
1**	LEMMASS + 0	1326	07441	16	3.415020000+004 LBS	1.549027015+004 KG
1**	CSMMASS + 0	1327	10056	16	3.652450000+004 LBS	1.656723452+004 KG
1 *	E3J22R2M+ 0	1347	12160	58	9.204790479+016 M5/CS2	9.204790479+016 M5/CS2
1 *	E32C31RM+ 0	1350	03363	80	1.312892560+023 M6/CS2	1.312892560+023 M6/CS2
1 *	ELBIAS + 0	1353	00045	-1	4.100000000-001 DEG	1.138888889-003 REV
*	TOOFEW + 0	1354	00003	14	3.000000000+000 UNITLESS	3.000000000+000 UNITLESS
1 *	PBIASX + 0	1452	03250	-3	1.300000000+000 CM/SEC2	1.300000000-002 PIPS/CS
1 *	PIPASCFX+ 0	1453	60336	-9	-9.500000000+002 PPM	-9.500000000-004 PIPS/PIP

Contract No. NAS 9-1100
Primary No. 664

(NASA DATA SOURCE)

Table LM8/4.5.1-3. FINAL H-3 PRELAUNCH ERASABLE LOAD LUMINARY 178 (Continued)

REV		MNEMONIC			ADDR	OCTAL	SF	ENGINEFRING VALUE		VALUE IN AGC UNITS	
1	*	PBIASY	+	0	1454	04163	-3	1.650000000+000	CM/SEC2	1.650000000-002	PIPS/CS
1	*	PIPASCFY	+	0	1455	41414	-9	-1.860000000+003	PPM	-1.860000000-003	PIPS/PIP
1	*	PBIASZ	+	0	1456	03436	-3	1.390000000+000	CM/SEC2	1.390000000-002	PIPS/CS
1	*	PIPASCFZ	+	0	1457	65013	-9	-6.700000000+002	PPM	-6.700000000-004	PIPS/PIP
	*	NBDX	+	0	1460	00163	-5	9.000000000-001	MERU	2.190514165-004	G PUL/CS
1	*	NBDY	+	0	1461	77246	-5	-2.700000000+000	MERU	-6.571542496-004	G PUL/CS
1	*	NBDZ	+	0	1462	77731	-5	-3.000000000-001	MERU	-7.301713884-005	G PUL/CS
1	*	ADIAX	+	0	1463	00116	-6	3.000000000+000	MERU/G	7.445676024-005	GPUL/PIP
1	*	ADIAY	+	0	1464	77307	-6	-1.200000000+001	MERU/G	-2.978270410-004	GPUL/PIP
1	*	ADIAZ	+	0	1465	00234	-6	6.000000000+000	MERU/G	1.489135205-004	GPUL/PIP
	*	ADSRAX	+	0	1466	00000	-6	0.000000000+000	MERU/G	0.000000000+000	GPUL/PIP
1	*	ADSRAY	+	0	1467	00116	-6	3.000000000+000	MERU/G	7.445676024-005	GPUL/PIP
1	*	ADSRAZ	+	0	1470	00202	-6	5.000000000+000	MERU/G	1.240946004-004	GPUL/PIP

Contract No. NAS 9-1100
Primary No. 664

(NASA DATA SOURCE)

Table LM8/4.5.1-3. FINAL H-3 PRELAUNCH ERASABLE LOAD LUMINARY 178 (Continued)

REV	MNEMONIC	ADDR	OCTAL	SF	ENGINEERING VALUE	VALUE IN AGC UNITS
*	GCOMPSW + 0	1477	00000	14	0.000000000+000 UNITLESS	0.000000000+000 UNITLESS
	TETCSM + 0	1570	37777	28	2.684354550+008 CS	2.684354550+008 CS
		1571	37777			
	TETLEM + 0	1642	37777	28	2.684354550+008 CS	2.684354550+008 CS
		1643	37777			
*	X789 + 0	1700	00000	3	0.000000000+000 RADIANS	0.000000000+000 RADIANS
		1701	00000			
*	X789 + 2	1702	00000	3	0.000000000+000 RADIANS	0.000000000+000 RADIANS
		1703	00000			
*	X789 + 4	1704	00000	3	0.000000000+000 RADIANS	0.000000000+000 RADIANS
		1705	00000			
1 *	TEPHEM + 0	1706	00006	42	5.156383333+003 HR	1.856298000+009 CS
		1707	35223			
		1710	16020			

(NASA DATA SOURCE)

Table LM8/4.5.1-3. FINAL H-3 PRELAUNCH ERASABLE LOAD LUMINARY 178 (Continued)

REV	MNEMONIC	ADDR	OCTAL	SF	ENGINEERING VALUE	VALUE IN AGC UNITS
*	-AYO + 0	1711	00000	0	2.949684858-005 RADIANS	2.949684858-005 RADIANS
		1712	17356			
1 *	AXO + 0	1713	00000	0	3.619492054-005 RADIANS	3.619492054-005 RADIANS
		1714	22764			
2	REFSMMAT+ 0	1731	67061	1	-5.564556300-001 UNITLESS	-5.564556300-001 UNITLESS
		1732	60375			
2	REFSMMAT+ 2	1733	64033	1	-7.466666000-001 UNITLESS	-7.466666000-001 UNITLESS
		1734	51650			
2	REFSMMAT+ 4	1735	72126	1	-3.644806200-001 UNITLESS	-3.644806200-001 UNITLESS
		1736	45456			
2	REFSMMAT+ 6	1737	02656	1	1.775381300-001 UNITLESS	1.775381300-001 UNITLESS
		1740	14434			
2	REFSMMAT+ 8	1741	67336	1	-5.353885100-001 UNITLESS	-5.353885100-001 UNITLESS
		1742	43072			

(NASA DATA SOURCE)

Table LM8/4.5.1-3. FINAL H-3 PRELAUNCH ERASABLE LOAD LUMINARY 178 (Continued)

REV	MNEMONIC	ADDR	OCTAL	SF	ENGINEERING VALUE	VALUE IN AGC UNITS
2	REFSMMAT+10	1743	15154	1	8.257356400-001 UNITLESS	8.257356400-001 UNITLESS
		1744	15512			
2	REFSMMAT+12	1745	63006	1	-8.116879500-001 UNITLESS	-8.116879500-001 UNITLESS
		1746	64677			
2	REFSMMAT+14	1747	06242	1	3.947760500-001 UNITLESS	3.947760500-001 UNITLESS
		1750	00131			
2	REFSMMAT+16	1751	06706	1	4.304817500-001 UNITLESS	4.304817500-001 UNITLESS
		1752	20152			
*	RANGEVAR+ 0	1766	01351	-12	1.111111111-005 UNITLESS	1.111111111-005 UNITLESS
		1767	24734			
*	RATEVAR + 0	1770	02354	-12	1.877777778-005 UNITLESS	1.877777778-005 UNITLESS
		1771	04761			
*	RVARMIN + 0	1772	00410	12	7.104180875+002 FT2	6.600000000+001 M2

Contract No. NAS 9-1100
Primary No. 664

(NASA DATA SOURCE)

Table LM8/4.5.1-3. FINAL H-3 PRELAUNCH ERASABLE LOAD LUMINARY 178 (Continued)

REV	MNEMONIC	ADDR	OCTAL	SF	ENGINEERING VALUE	VALUE IN AGC UNITS
*	VVARMIN + 0	1773	00165	-12	1.877764172-001 FT2/SEC2	1.744500000-006 M2/CS2
*	WRENDPOS+ 0	2000	05750	14	1.000000000+004 FT	3.048000000+003 M
*	WRENDVEL+ 0	2001	00763	0	1.000000000+001 FT/SEC	3.048000000-002 M/CS
*	WSHAFT + 0	2002	17270	-5	1.500000000+001 MILLIRAD	1.500000000-002 RADIANS
*	WTRUN + 0	2003	17270	-5	1.500000000+001 MILLIRAD	1.500000000-002 RADIANS
*	RMAX + 0	2004	00023	19	2.000000000+003 FT	6.096000000+002 M
*	VMAX + 0	2005	00001	7	2.000000000+000 FT/SEC	6.096000000-003 M/CS
*	WSURFPOS+ 0	2006	00000	14	0.000000000+000 FT	0.000000000+000 M
*	WSURFVEL+ 0	2007	00000	0	0.000000000+000 FT/SEC	0.000000000+000 M/CS
*	SHAFTVAR+ 0	2010	00103	-12	1.000000000+000 MILIRAD2	1.000000000-006 RADIANS2
*	TRUNVAR + 0	2011	00103	-12	1.000000000+000 MILIRAD2	1.000000000-006 RADIANS2
*	504LM + 0	2012	77772	0	-3.436505795-004 RADIANS	-3.436505795-004 RADIANS
		2013	53647			

(NASA DATA SOURCE)

Table LM8/4.5.1-3. FINAL H-3 PRELAUNCH ERASABLE LOAD LUMINARY 178 (Continued)

REV	MNEMONIC	ADDR	OCTAL	SF	ENGINEERING VALUE	VALUE IN AGC UNITS
	* 504LM + 2	2014 2015	00002 12573	0	1.425556839-004 RADIANS	1.425556839-004 RADIANS
	* 504LM + 4	2016 2017	00001 35676	0	1.180097461-004 RADIANS	1.180097461-004 RADIANS
	* RLS + 0	2020 2021	00311 31727	27	5.423974738+006 FT	1.653227500+006 M
	* RLS + 2	2022 2023	77700 60177	27	-1.706456693+006 FT	-5.201280000+005 M
	* RLS + 4	2024 2025	77762 55276	27	-3.650410105+005 FT	-1.112645000+005 M
1	* TLAND + 0	2026 2027	04531 10427	28	1.089202417+002 HR	3.921128700+007 CS
	* VELBIAS + 0	2400 2401	00001 36331	6	2.500000000+000 FT/SEC	7.620000000-003 M/CS

(NASA DATA SOURCE)

Table LM8/4.5.1-3. FINAL H-3 PRELAUNCH ERASABLE LOAD LUMINARY 178 (Continued)

REV	MNEMONIC		ADDR	OCTAL	SF	ENGINEERING VALUE	VALUE IN AGC UNITS
*	RBRFGX	+ 0	2402 2403	77777 57065	24	-1.773725000+003 FT	-5.406313800+002 M
*	RAPFGX	+ 0	2404 2405	00000 00717	24	9.491910105+001 FT	2.893134200+001 M
*	RBRFGZ	+ 0	2406 2407	77773 66000	24	-1.448802690+004 FT	-4.415950600+003 M
*	RAPFGZ	+ 0	2410 2411	77777 77662	24	-1.572079987+001 FT	-4.791699800+000 M
*	VBRFGX	+ 0	2412 2413	77767 71517	10	-1.681864567+002 FT/SEC	-5.123884800-001 M/CS
*	VAPFGX	+ 0	2414 2415	00000 03201	10	2.083579987+000 FT/SEC	6.350751800-003 M/CS
*	VBRFGZ	+ 0	2416 2417	77774 46700	10	-7.761436680+001 FT/SEC	-2.365685900-001 M/CS

(NASA DATA SOURCE)

Table LM8/4.5.1-3. FINAL H-3 PRELAUNCH ERASABLE LOAD LUMINARY 178 (Continued)

REV	MNEMONIC		ADDR	OCTAL	SF	ENGINEERING VALUE	VALUE IN AGC UNITS
	* VAPFGZ	+ 0	2420	00000	10	8.303187992-001 FT/SEC	2.530811700-003 M/CS
			2421	01227			
	* ABRFGX	+ 0	2422	77772	-4	-6.472360236-001 FT/SEC2	-1.972775400-005 M/CS2
			2423	72405			
	* AAPFGX	+ 0	2424	00004	-4	5.402850066-001 FT/SEC2	1.646788700-005 M/CS2
			2425	12111			
	* ABRFGZ	+ 0	2426	77674	-4	-8.414381890+000 FT/SEC2	-2.564703600-004 M/CS2
			2427	70443			
	* AAPFGZ	+ 0	2430	77776	-4	-2.354229987-001 FT/SEC2	-7.175693000-006 M/CS2
			2431	43634			
	* VBRFG*	+ 0	2432	77767	13	-1.397058596+003 FT/SEC	-4.258234600+000 M/CS
			2433	57361			
1	* VAPFG*	+ 0	2434	00000	13	1.494573786+001 FT/SEC	4.555460900-002 M/CS
			2435	02725			

(NASA DATA SOURCE)

Table LM8/4.5.1-3. FINAL H-3 PRELAUNCH FRASABLE LOAD LUMINARY 178 (Continued)

REV	MNEMONIC	ADDR	OCTAL	SF	ENGINEERING VALUE	VALUE IN AGC UNITS
*	ABRFG* + 0	2436	77154	-4	-5.048629265+001 FT/SEC2	-1.538822200-003 M/CS2
		2437	63330			
*	AAPFG* + 0	2440	77764	-4	-1.412537992+000 FT/SEC2	-4.305415800-005 M/CS2
		2441	66653			
*	JBRFG* + 0	2442	00126	-21	8.257294947-003 FT/SEC3	2.516823500-009 M/CS3
		2443	17216			
*	JAPFG* + 0	2444	00730	-21	4.509242126-002 FT/SEC3	1.374417000-008 M/CS3
		2445	07700			
1 *	GAINBRAK+ 0	2446	37777	0	9.999999963-001 UNITLESS	9.999999963-001 UNITLESS
		2447	37777			
*	GAINAPPR+ 0	2450	00000	0	0.000000000+000 UNITLESS	0.000000000+000 UNITLESS
		2451	00000			
*	TCGFBRAK+ 0	2452	00567	17	3.000000000+001 SEC	3.000000000+003 CS

(NASA DATA SOURCE)

Table LM8/4.5.1-3. FINAL H-3 PRELAUNCH FRASABLE LOAD LUMINARY 178 (Continued)

REV	MNEMONIC	ADDR	OCTAL	SF	ENGINFFRING VALUF	VALUF IN AGC UNITS
	* TCGIBRAK+ 0	2453	25762	17	9.000000000+002 SEC	9.000000000+004 CS
	* TCGFAPPR+ 0	2454	00113	17	6.000000000+000 SEC	6.000000000+002 CS
	* TCGIAPPR+ 0	2455	04704	17	2.000000000+002 SEC	2.000000000+004 CS
1	* VIGN + 0	2456 2457	00416 17516	10	5.546447179+003 FT/SEC	1.690557100+001 M/CS
1	* RIGNX + 0	2460 2461	77726 47151	24	-1.403457283+005 FT	-4.277737800+004 M
1	* RIGNZ + 0	2462 2463	77113 76041	24	-1.464979987+006 FT	-4.465259000+005 M
	* KIGNX/B4+ 0	2464 2465	77122 76151	4	-4.190000000-001 UNITLESS	-4.190000000-001 UNITLESS
	* KIGNY/B8+ 0	2466 2467	71613 74336	-16	-9.049999985-007 FT/FT2	-2.969160100-006 M-1

(NASA DATA SOURCE)

Table LM8/4.5.1-3. FINAL H-3 PRELAUNCH ERASABLE LOAD LUMINARY 178 (Continued)

REV	MNEMONIC		ADDR	OCTAL	SF	ENGINEERING VALUE		VALUE IN AGC UNITS	
*	KIGNV/B4	+ 0	2470 2471	72206 57777	18	-4.700000000+002	SEC	-4.700000000+004	CS
*	LOWCRIT	+ 0	2472	04114	14	5.985007886+003	LBF	2.124377200+003	DPSTRCTF
*	HIGHCRIT	+ 0	2473	04454	14	6.615008568+003	LBF	2.347995800+003	DPSTRCTF
*	TAUHZ	+ 0	2474	07640	11	5.000000000+000	SEC	5.000000000+002	CS
*	QHZ	+ 0	2475	14632	0	4.000000000-001	UNITLESS	4.000000000-001	UNITLESS
*	AHZLIM	+ 0	2476	00617	-4	1.938979987+000	FT/SEC2	5.910011000-005	M/CS2
*	2LATE466	+ 0	2477 2500	00000 00226	28	1.500000000+000	SEC	1.500000000+002	CS
*	DELQFIX	+ 0	2503 2504	00000 64606	24	5.000000000+002	FT	1.524000000+002	M
*	LRVMAX	+ 0	2511	01717	7	2.499999967+003	FT/SEC	7.619999000+000	M/CS
*	LRVF	+ 0	2512	00116	7	1.999999967+002	FT/SEC	6.095999900-001	M/CS

(NASA DATA SOURCE)

Table LM8/4.5.1-3. **FINAL H-3 PRELAUNCH ERASABLE LOAD LUMINARY 178** (Continued)

REV	MNEMONIC		ADDR	OCTAL	SF	ENGINEERING VALUE	VALUE IN AGC UNITS
*	LRWVZ	+ 0	2513	11463	0	3.000D00000-001 UNITLESS	3.000000000-001 UNITLESS
*	LRWVY	+ 0	2514	11463	0	3.000000000-001 UNITLESS	3.000000000-001 UNITLESS
*	LRWVX	+ 0	2515	11463	0	3.000000000-001 UNITLESS	3.000000000-001 UNITLESS
*	LRWVFZ	+ 0	2516	06315	0	2.000000000-001 UNITLESS	2.000000000-001 UNITLESS
*	LRWVFY	+ 0	2517	06315	0	2.000000000-001 UNITLESS	2.000000000-001 UNITLESS
*	LRWVFX	+ 0	2520	06315	0	2.000000000-001 UNITLESS	2.000000000-001 UNITLESS
*	LRWVFF	+ 0	2521	03146	0	1.000000000-001 UNITLESS	1.000000000-001 UNITLESS
*	ABSC0	+ 0	2522	67111	18	-2.379999967+005 FT	-7.254239900+004 M
*	ABSC1	+ 0	2523	75701	18	-5.700000000+004 FT	-1.737360000+004 M
*	ABSC2	+ 0	2524	76132	18	-4.900000000+004 FT	-1.493520000+004 M
*	ABSC3	+ 0	2525	77452	18	-1.120000000+004 FT	-3.413760000+003 M
*	ABSC4	+ 0	2526	77640	18	-5.000000000+003 FT	-1.524000000+003 M
*	SLOPE0	+ 0	2527	77774	6	-1.105000000-002 RADIANS	-1.105000000-002 RADIANS

(NASA DATA SOURCE)

Table LM8/4.5.1-3. **FINAL H-3 PRELAUNCH ERASABLE LOAD LUMINARY 178** (Continued)

REV	MNEMONIC		ADDR	OCTAL	SF	ENGINEERING VALUE		VALUE IN AGC UNITS	
*	SLOPE1	+ 0	2530	77743	6	-1.088000000-001	RADIANS	-1.088000000-001	RADIANS
*	SLOPE2	+ 0	2531	00011	6	3.704000000-002	RADIANS	3.704000000-002	RADIANS
*	SLOPE3	+ 0	2532	77753	6	-7.903000000-002	RADIANS	-7.903000000-002	RADIANS
*	SLOPE4	+ 0	2533	77774	6	-1.200000000-002	RADIANS	-1.200000000-002	RADIANS
*	RODSCALE	+ 0	2534	14370	-7	1.000000000+000	FT/SEC	3.048000000-003	M/CS
*	TAUROD	+ 0	2535	11300	9	1.500000000+000	SEC	1.500000000+002	CS
			2536	00000					
*	LAG/TAU	+ 0	2537	07356	0	2.333300000-001	UNITLESS	2.333300000-001	UNITLESS
			2540	34075					
*	MINFORCE	+ 0	2541	00001	12	9.799999814+002	LBF	4.359257100-001	KG M/CS2
			2542	27631					
*	MAXFORCE	+ 0	2543	00013	12	6.299999961+003	LBF	2.802379600+000	KG M/CS2
			2544	06551					

(NASA DATA SOURCE)

Table LM8/4.5.1-3. **FINAL H-3 PRELAUNCH ERASABLE LOAD LUMINARY 178** (Continued)

REV	MNEMONIC		ADDR	OCTAL	SF	ENGINEERING VALUE	VALUE IN AGC UNITS
*	J1PARM	+ 0	2545 2546	07017 32346	23	6.046952700+006 FT	1.843111183+006 M
*	K1PARM	+ 0	2547 2550	75545 64662	23	-3.150277900+005 FT/RAD	-6.033144086+005 M/REV
*	J2PARM	+ 0	2551 2552	07020 32012	23	6.048609900+006 FT	1.843616297+006 M
*	K2PARM	+ 0	2553 2554	73324 53775	23	-6.276302600+005 FT/RAD	-1.201984051+006 M/REV
*	THETCRIT	+ 0	2555 2556	76347 56551	0	-1.741421853+001 DEG	-4.837282929-002 REV
*	RAMIN	+ 0	2557 2560	03326 07515	24	5.880068250+006 FT	1.792244803+006 M
*	YLIM	+ 0	2561 2562	00016 32446	24	8.200000000+000 N.MI.	1.518640000+004 M

(NASA DATA SOURCE)

Table LM8/4.5.1-3. FINAL H-3 PRELAUNCH ERASABLE LOAD LUMINARY 178 (Continued)

REV	MNEMONIC	ADDR	OCTAL	SF	ENGINEERING VALUE	VALUE IN AGC UNITS
*	ABTRDOT + 0	2563	00007	7	1.950000000+001 FT/SEC	5.943600000-002 M/CS
		2564	22346			
*	COSTHET1+ 0	2565	00000	2	0.000000000+000 UNITLESS	0.000000000+000 UNITLESS
		2566	00000			
*	COSTHET2+ 0	2567	06733	2	8.660254037-001 UNITLESS	8.660254037-001 UNITLESS
		2570	07535			
*	DLAND + 0	2631	00000	24	0.000000000+000 FT	0.000000000+000 M
		2632	00000			
*	DLAND + 2	2633	00000	24	0.000000000+000 FT	0.000000000+000 M
		2634	00000			
*	DLAND + 4	2635	00000	24	0.000000000+000 FT	0.000000000+000 M
		2636	00000			
*	HIASCENT+ 0	3000	02324	16	1.090000000+004 LBS	4.944156833+003 KG

(NASA DATA SOURCE)

Table LM8/4.5.1-3. FINAL H-3 PRELAUNCH ERASABLE LOAD LUMINARY 178 (Continued)

REV	MNEMONIC	ADDR	OCTAL	SF	ENGINEERING VALUE	VALUE IN AGC UNITS
2**	ROLLTIME+	0 3001	05120	14	2.640000000+001 SEC	2.640000000+003 CS
2**	PITTIME +	0 3002	04221	14	2.193000000+001 SEC	2.193000000+003 CS
*	DKTRAP +	0 3003	77001	-3	-3.888888889-003 REV/SEC	-3.888888889-003 REV/SEC
*	DKOMEGAN+	0 3004	00012	14	1.000000000+001 UNITLESS	1.000000000+001 UNITLESS
*	DKKAOSN +	0 3005	00074	14	6.000000000+001 UNITLESS	6.000000000+001 UNITLESS
*	LMTRAP +	0 3006	77001	-3	-3.888888889-003 REV/SEC	-3.888888889-003 REV/SEC
*	LMOMEGAN+	0 3007	00000	14	0.000000000+000 UNITLESS	0.000000000+000 UNITLESS
*	LMKAOSN +	0 3010	00074	14	6.000000000+001 UNITLESS	6.000000000+001 UNITLESS
1 *	DKDB +	0 3011	00200	15	2.560000000+002 REV-1	2.560000000+002 REV-1
1 *	IGNAOSQ +	0 3012	02111	-2	6.027000000+000 DEG/SEC2	1.674166667-002 REV/SEC2
1 *	IGNAOSR +	0 3013	77774	-2	-1.600000000-002 DEG/SEC2	-4.444444445-005 REV/SEC2
*	DOWNTORK+	0 3113	00000	5	0.000000000+000 JET SEC	0.000000000+000 JET SEC
*	DOWNTORK+	1 3114	00000	5	0.000000000+000 JET SEC	0.000000000+000 JET SEC

(NASA DATA SOURCE)

Table LM8/4.5.1-3. FINAL H-3 PRELAUNCH ERASABLE LOAD LUMINARY 178 (Continued)

REV	MNEMONIC	ADDR	OCTAL	SF	ENGINEERING VALUE	VALUE IN AGC UNITS
	* DOWNTORK+ 2	3115	00000	5	0.000000000+000 JET SEC	0.000000000+000 JET SEC
	* DOWNTORK+ 3	3116	00000	5	0.000000000+000 JET SEC	0.000000000+000 JET SEC
	* DOWNTORK+ 4	3117	00000	5	0.000000000+000 JET SEC	0.000000000+000 JET SEC
	* DOWNTORK+ 5	3120	00000	5	0.000000000+000 JET SEC	0.000000000+000 JET SEC
	* AGSK + 0	3371 3372	04225 10400	28	1.000000000+002 HR	3.600000000+007 CS
1	* AZBIAS + 0	3373	77725	-1	-4.600000000-001 DEG	-1.277777778-003 REV
	* ATIGINC + 0	3400 3401	00001 03120	28	3.000000000+000 MIN	1.800000000+004 CS
	* PTIGINC + 0	3402 3403	00001 03120	28	3.000000000+000 MIN	1.800000000+004 CS
1	* AOTAZ + 0	3404	65301	-1	-5.975400000+001 DEG	-1.659833333-001 REV
1	* AOTAZ + 1	3405	00023	-1	2.140000000-001 DEG	5.944444445-004 REV

(NASA DATA SOURCE)

Table LM8/4.5.1-3. **FINAL H-3 PRELAUNCH ERASABLE LOAD LUMINARY 178** (Continued)

REV		MNEMONIC		ADDR	OCTAL	SF	ENGINEERING VALUE		VALUE IN ACC UNITS	
1	*	AOTAZ	+ 2	3406	12545	-1	6.017700000+001	DEG	1.671583333-001	REV
1	*	AOTAZ	+ 3	3407	25302	-1	1.202520000+002	DEG	3.340333334-001	REV
1	*	AOTAZ	+ 4	3410	40025	-1	-1.797670000+002	DEG	-4.993527778-001	REV
1	*	AOTAZ	+ 5	3411	52550	-1	-1.197960000+002	DEG	-3.327666667-001	REV
1	*	AOTEL	+ 0	3412	10011	-1	4.509700000+001	DEG	1.252694445-001	REV
1	*	AOTEL	+ 1	3413	10013	-1	4.511900000+001	DEG	1.253305556-001	REV
1	*	AOTEL	+ 2	3414	10012	-1	4.511400000+001	DEG	1.253166667-001	REV
1	*	AOTEL	+ 3	3415	10010	-1	4.508600000+001	DEG	1.252388889-001	REV
1	*	AOTEL	+ 4	3416	10006	-1	4.506400000+001	DEG	1.251777778-001	REV
1	*	AOTEL	+ 5	3417	10006	-1	4.506900000+001	DEG	1.251916667-001	REV
	*	LRHMAX	+ 0	3420	35610	14	5.000000000+004	FT	1.524000000+004	M
	*	LRWH	+ 0	3421	13146	0	3.500000000-001	UNITLESS	3.500000000-001	UNITLESS
	*	ZOOMTIME	+ 0	3422	05050	14	2.600000000+001	SEC	2.600000000+003	CS

(NASA DATA SOURCE)

Table LM8/4.5.1-3. FINAL H-3 PRELAUNCH ERASABLE LOAD LUMINARY 178 (Continued)

REV	MNEMONIC	ADDR	OCTAL	SF	ENGINEERING VALUE	VALUE IN AGC UNITS
	* TENDBRAK+	0 3423	01407	17	6.200000000+001 SEC	6.200000000+003 CS
	* TENDAPPR+	0 3424	00226	17	1.200000000+001 SEC	1.200000000+003 CS
	* DELTTFAP+	0 3425	75632	17	-9.000000000+001 SEC	-9.000000000+003 CS
1	* LEADTIME+	0 3426	77743	17	-2.200000000+000 SEC	-2.200000000+002 CS
	* RPCRTIME+	0 3427	01407	17	6.200000000+001 SEC	6.200000000+003 CS
	* RPCRTQSW+	0 3430	57777	1	-1.000000000+000 UNITLESS	-1.000000000+000 UNITLESS
	* TNEWA +	0 3431 3432	20000 00000	28	1.342177280+008 CS	1.342177280+008 CS
	* LRWH1 +	0 3756	13146	0	3.500000000-001 UNITLESS	3.500000000-001 UNITLESS

LM8/4.5.2.1 Abort Sensor Assembly

The LM-8 ASA set-point temperature, as read by T/M #GI-3301, is T_{SET} = 121.0°F (STANDBY and OPERATE modes). The nominal temperature reading in the "OFF" mode is 119.6°F. The temperature maintenance limits are specified in Paragraph 4.5.2.1.

LM8/4.5.2.1.2 AGS Angular Mounting Error

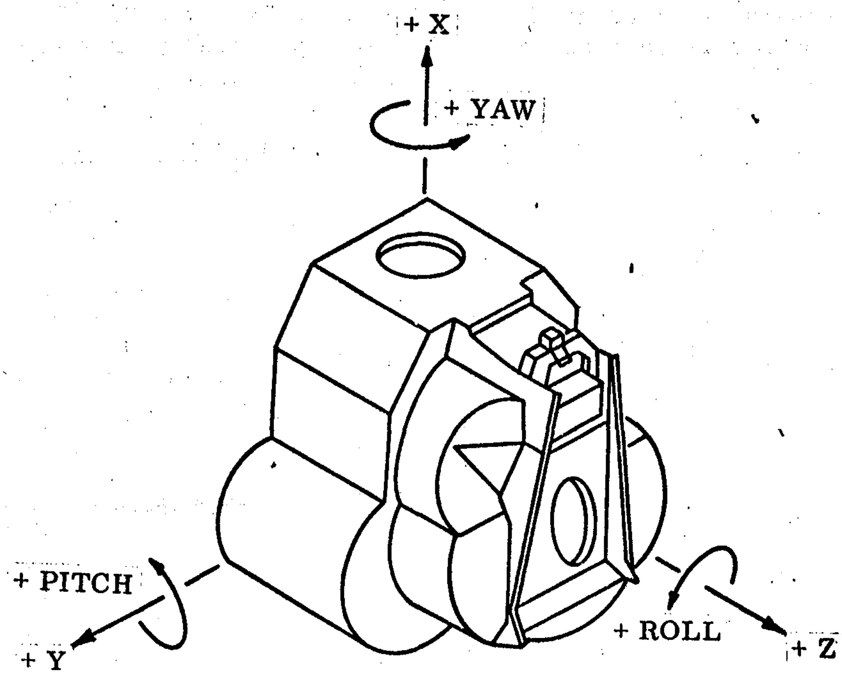

The measured mechanical alignment error of the ASA mounting surface as compared to the NAV. Base Gage (Vehicle Coordinate System) and the IMU is shown below:

	ASA/NAV. Base	IMU/NAV. Base	ASA/IMU
Pitch:	-00° 05' 19"	-00° 04' 25"	-00° 00' 54"
Roll:	+00° 00' 21"	-00° 00' 59"	+00° 01' 20"
Yaw:	-00° 04' 18"	-00° 04' 11"	-00° 00' 07"

(Ref.: LDW 280-51067, dated 21 March 1969)

LM8/4.5.2.2 Abort Electronics Assembly (NASA DATA SOURCE)

The following listings pertain to the Abort Electronics Assembly Memory Constants.

Table LM8/4.5.2-1 contains a glossary of the constants. The glossary is divided into six groups:

Group 1 - PARAMETERS TO BE SPECIFIED DURING THE MISSION
Group 2 - AGS HARDWARE DEPENDENT CONSTANTS
Group 3 - VEHICLE DEPENDENT CONSTANTS
Group 4 - MISSION DEPENDENT CONSTANTS
Group 5 - EQUATION DEPENDENT CONSTANTS
Group 6 - DEDA CONVERSION FACTORS

Table LM8/4.5.2-2 contains the current values in both octal and decimal, with units.

The CONVERSION FACTOR's are multipliers used to convert the constant from the given engineering units to the equivalent value in the units internally used in the AEA. The number in the SCALE column defines the binary scaling of each constant, i.e., the number of bits in the computer word (excluding the sign bit) to the left of the binary point. A computer word consists of a sign bit and 17 data bits. The actual computer value of a constant is listed in the AEA OCT. column in octal digits. Since the computer word has a finite number of bits, a given input value cannot, in general, be represented exactly in the computer. The AEA VALUE column contains the result of reconverting the AEA octal value to the decimal value in engineering units, using the conversion factor mentioned above.

An asterisk by the name of the constants indicates that these constants are dependent on the hardware to be used during a mission.

Table LM8/4.5.2-1. Glossary of AGS Constants

(NASA DATA SOURCE)

GROUP 1 - PARAMETERS TO BE SPECIFIED DURING THE MISSION

NAME	DESCRIPTION OF LMDAP INPUT	INTERNAL AEA UNITS	LMDAP INPUT UNITS
1J	Desired TPI time for CSI computation	SEC	MIN
4J	Time increment from node to TPF (in TPI mode)	SEC	MIN
17J	Radar range rate	FPS	FPS
18J	Radar range	FT	FT
25J	DEDA altitude update	FT	FT
28J1	Component of External V input in $\underline{V}_1$ Direction	FPS	FPS
28J2	Component of External V input in $\underline{W}_1$ Direction	FPS	FPS
28J3	Component of External V input in $\underline{U}_1$ Direction	FPS	FPS
1J1	LM Update State Vector - X Inertial Position	FT	FT
1J2	Y Inertial Position	FT	FT
1J3	Z Inertial Position	FT	FT
1J4	X Inertial Velocity	FPS	FPS
1J5	Y Inertial Velocity	FPS	FPS
1J6	Z Inertial Velocity	FPS	FPS
1J7	LM Update State Vector Epoch Time	SEC	MIN
2J1	CSM Update State Vector - X Inertial Position	FT	FT
2J2	Y Inertial Position	FT	FT
2J3	Z Inertial Position	FT	FT
2J4	X Inertial Velocity	FPS	FPS
2J5	Y Inertial Velocity	FPS	FPS
2J6	Z Inertial Velocity	FPS	FPS
2J7	CSM Update State Vector Epoch Time	SEC	MIN

Table LM8/4.5.2-1. Glossary of AGS Constants (Continued)
(NASA DATA SOURCE)

GROUP 2 - AGS HARDWARE DEPENDENT CONSTANTS

NAME	DESCRIPTION OF LMDAP INPUT	INTERNAL AEA UNITS	LMDAP INPUT UNITS
1K1P*	X axis gyro drift bias	RAD/20MS (Compen.)	DEG/HR (Bias)
1K6P*	Y axis gyro drift bias	RAD/20MS (Compen.)	DEG/HR (Bias)
1K11P*	Z axis gyro drift bias	RAD/20MS (Compen.)	DEG/HR (Bias)
	A positive gyro drift bias causes a gyro output of more than 32 pulses per millisecond (640 pulses per 20 milliseconds) for no ASA rotation. The range of each of the biases is ± 10 deg/hr.		
1K3*	X axis gyro scale factor deviation	NO-UNITS(Deviation)	NO-UNITS (Deviation)
1K8*	Y axis gyro scale factor deviation	NO-UNITS(Deviation)	NO-UNITS (Deviation)
1K13*	Z axis gyro scale factor deviation	NO-UNITS(Deviation)	NO-UNITS (Deviation)
	A positive scale factor deviation exists when a gyro's scale factor is greater than 2^{-16} radians per pulse. The range of each deviation is ± .78 percent.		
1K14*	Compensation constant for X gyro spin axis mass unbalance drift	RAD/FPS	DEG/HR/G
	A positive gyro spin axis mass unbalance exists when a positive ASA acceleration in the direction of the X gyro input axis results in a negative X gyro output (less than 640 pulses per 20 milliseconds) with no rotation. The range of the bias is ± 10 deg/hr/g.		

*These constants are dependent on the hardware to be used during a mission.

Contract No. NAS 9-1100
Primary No. 664

Table LM8/4.5.2-1. Glossary of AGS Constants (Continued)

(NASA DATA SOURCE)

GROUP 2 - (CONTINUED)

NAME	DESCRIPTION OF LMDAP INPUT	INTERNAL AEA UNITS	LMDAP INPUT UNITS
1K18P*	X axis accelerometer scale factor deviation	FPS/PULSE (Scale)	NO-UNITS (Deviation)
1K20P*	Y axis accelerometer scale factor deviation	FPS/PULSE Factors)	NO-UNITS (Deviation)
1K22P*	Z axis accelerometer scale factor deviation	FPS/PULSE	NO-UNITS (Deviation)
	A positive accelerometer scale factor deviation exists when the measured accelerometer's scale factor is greater than the nominal value of + .003125 fps/pulse. The range of this input is ± 24 percent.		
1K19P*	X axis accelerometer bias	FPS/20MS(Compen.)	MICRO G (Bias)
1K21P*	Y axis accelerometer bias	FPS/20MS(Compen.)	MICRO G (Bias)
1K23P*	Z axis accelerometer bias	FPS/20MS(Compen.)	MICRO G (Bias)
	A positive accelerometer bias results in an accelerometer output of more than 32 pulses per millisecond (640 pulses per 20 milliseconds). The range of each of these biases is ± 2000 μg.		
1K26	X axis azimuth alignment gain constant (lunar align)	NO-UNITS	NO-UNITS
1K27	Lunar align leveling alignment constant	RAD/FPS	RAD/FPS
1K28	Lunar align leveling alignment constant	NO-UNITS	NO-UNITS
1K29	Lunar align stop error criterion	RAD	RAD
1K30	Gyro calibrate time	2-SEC	2-SEC
1K33	Gyro calibration gain constant	NO-UNITS	NO-UNITS
1K34	Gyro calibration gain constant	1/20MS	1/20MS
1K35	Navigation sensed velocity threshold	FT/SEC	FT/SEC
1K36	Accelerometer calibration gain constant	NO-UNITS	NO-UNITS

*These constants are dependent on the hardware to be used during a mission.

Table LM8/4.5.2-1. Glossary of AGS Constants (Continued)
(NASA DATA SOURCE)

GROUP 2 - (CONTINUED)

NAME	**DESCRIPTION OF LMDAP INPUT**	**INTERNAL AEA UNITS**	**LMDAP INPUT UNITS**
1K37	Accelerometer calibration time	2-SEC	2-SEC
6K2	Radar filter initialization value of P_{11} and P_{22}	FT^2	FT^2
6K4	Radar filter initialization value of P_{33} and P_{44}	$(FPS)^2$	$(FPS)^2$
6K5	Radar filter factor in r_y update	NO-UNITS	NO-UNITS
6K6	Radar filter factor in V_y update	NO-UNITS	NO-UNITS
6K8	Radar filter term in q_{11}	$(FT/SEC)^2$	$(FT/SEC)^2$
6K9	Radar filter factor in q_{11} and q_{22}	$(RAD)^2$	$(RAD)^2$
6K10	Radar filter factor in q_{11} and q_{22}	FT^2	FT^2

Table LM8/4.5.2-1. Glossary of AGS Constants (Continued)

(NASA DATA SOURCE)

GROUP 3 - VEHICLE DEPENDENT CONSTANTS

NAME	DESCRIPTION OF LMDAP INPUT	INTERNAL AEA UNITS	LMDAP INPUT UNITS
1K9	Ullage counter limit	COUNTS	COUNTS
4K2	Coefficient in T_B computation	SEC/FT	SEC/FT
4K3	Coefficient in T_B computation	$(SEC/FT)^2$	$(SEC/FT)^2$
4K7	Cant angle of engine about Y-axis	RAD	RAD
4K8	Cant angle of engine about Z-axis	RAD	RAD
4K21	Limit on body attitude errors	RAD	RAD
4K23	Time to maintain attitude hold momentarily after staging	40-MSEC	40-MSEC
4K25	Ascent engine cutoff impulse compensation	FPS	FPS
4K26	V_G threshold for engine cutoff	FPS	FPS
4K27	Hover Abort overflow protection	FPS	FPS
4K34	Lower limit on a_T	FT/SEC^2	FT/SEC^2
4K35	Ullage threshold	FT/SEC^2	FT/SEC^2

Contract No. NAS 9-1100
Primary No. 664

Table LM8/4.5.2-1. Glossary of AGS Constants (Continued)
(NASA DATA SOURCE)

GROUP 4 - MISSION DEPENDENT CONSTANTS

NAME	DESCRIPTION OF LMDAP INPUT	INTERNAL AEA UNITS	LMDAP INPUT UNITS
1K4	Altitude/Altitude rate interpolation factor	NO-UNITS	NO-UNITS
2K1	Lunar gravitational constant	FT^3/SEC^2	FT^3/SEC^2
2K2	Reciprocal of 2K1	SEC^2/FT^3	SEC^2/FT^3
2K4	$-2K1\ \Delta T\ (\Delta T = 2$ sec)	FT^3/SEC	FT^3/SEC
3K4	Sine of central angle limit in TPI	NO-UNITS	NO-UNITS
4K4	Coefficient in linear expression for $\dot{r}_f$	1/SEC	1/SEC
4K5	Quantity in linear expression for $\dot{r}_f$	FT	FT
4K6	Upper limit on $\dot{r}_f$	FPS	FPS
4K10	Factor in LM desired semi-major axis α_L (O.I.)	FT/RAD	FT/RAD
4K12	Acceleration check for lower limit of $\dddot{r}_d$	FT/SEC^2	FT/SEC^2
5K14	Upper limit on $\dddot{r}_d$	FT/SEC^3	FT/SEC^3
5K16	Upper limit on $\dddot{y}_d$	FT/SEC^3	FT/SEC^3
5K17	Lower limit on $\dddot{y}_d$	FT/SEC^3	FT/SEC^3
5K18	Lower limit on $\dddot{r}_d$	FT/SEC^3	FT/SEC^3
5K20	Lower limit on $\dddot{r}_d$	FT/SEC^3	FT/SEC^3
5K26	Velocity-to-be-gained threshold	FPS	FPS
K55	Scale factor for $\dot{r}$ display	NO-UNITS	NO-UNITS
WBX	X component of unit vector for guidance steering	NO-UNITS	NO-UNITS
WBY	Y component of unit vector for guidance steering	NO-UNITS	NO-UNITS
WBZ	Z component of unit vector for guidance steering	NO-UNITS	NO-UNITS
2J	Cotangent of desired LOS angle at TPI for CSI computation	NO-UNITS	NO-UNITS

Table LM8/4.5.2-1. Glossary of AGS Constants (Continued)
(NASA DATA SOURCE)

GROUP 4 - (CONTINUED)

NAME	DESCRIPTION OF LMDAP INPUT	INTERNAL AEA UNITS	LMDAP INPUT UNITS
3J	Rendezvous offset time for TPI computation	SEC	MIN
5J	Landing site radius	FT	FT
6J	Desired LM transfer time for TPI routine	SEC	MIN
7J	Term in LM desired semi-major axis α_L (O.I.)	FT	FT
8J	One-half lower limit of apolune radius	FT	FT
10J	Alternate value for 7J (late descent abort)	FT	FT
11J	Alternate value for 4K10 (late descent abort)	FT/RAD	FT/RAD
12J	Threshold value for THETAF (CSM/LM phase angle)	RAD	RAD
16J	Orbit insertion targeted injection altitude	FT	FT
21J	Vertical pitch steering altitude threshold	FT	FT
22J	Vertical pitch steering altitude rate threshold	FPS	FPS
23J	Orbit insertion targeted injection radial rate	FPS	FPS
29J	Radar filter update time initialization value	SEC	MIN
6J1, 6J2, 6J3	Inertial negative lunar rotation rate vector at predicted landing site	RAD/20 MS	RAD/20 MS

Table LM8/4.5.2-1. Glossary of AGS Constants (Continued)
(NASA DATA SOURCE)

GROUP 5 - EQUATION DEPENDENT CONSTANTS

NAME	DESCRIPTION OF LMDAP INPUT	INTERNAL AEA UNITS	LMDAP INPUT UNITS
1K24	FDAI computation singularity region	NO-UNITS	NO-UNITS
2K3	q value set if overflow occurs in e^2 computation of LM orbit parameters	FT	FT
2K11	Set value of V_T if no valid TPI solution	FPS	FPS
2K14	Initial p perturbation	FT	FT
2K17	Number of p-iteration minus 3	COUNTS	COUNTS
2K18	Partial derivative protector in p-iterator routine	SEC	SEC
2K19	Δp limiter	FT	FT
2K20	p-iterator convergence check	SEC	SEC

Table LM8/4.5.2-1. Glossary of AGS Constants (Continued)
(NASA DATA SOURCE)

GROUP 6 - DEDA CONVERSION FACTORS

NAME	DESCRIPTION OF LMDAP INPUT
BACCSF	Convert .001 ft/sec^2 to fps/20 msec at B1
BM13SF	Convert .01°/hr to rad/20 msec at B13
B23SF	Convert 100 ft to ft at B23
B18SF	Convert .1 min to sec at B18
B13VSF	Convert .1 fps to fps at B13
B3SF	Convert .01° to rad at B3
B23RSF	Convert .1 nmi to ft at B23
B13SF	Convert .01 min to sec at B13

Table LM8/4.5.2-2. AGS Constants

(NASA DATA SOURCE)

NAME	LOC.	SCALE	CONVERSION FACTOR	AEA OCT.	AEA VALUE	UNITS
1J	0275	18	.60000 02	000000	.00000000 00	MIN
4J	0306	13	.60000 02	000000	.00000000 00	MIN
17J	0503	13	.10000 01	000000	.00000000 00	FPS
18J	0316	23	.10000 01	000000	.00000000 00	FT
25J	0223	23	.10000 01	000000	.00000000 00	FT
28J1	0450	13	.10000 01	000000	.00000000 00	FPS
28J2	0451	13	.10000 01	000000	.00000000 00	FPS
28J3	0452	13	.10000 01	000000	.00000000 00	FPS
1J1	0240	23	.10000 01	000000	.00000000 00	FT
1J2	0241	23	.10000 01	000000	.00000000 00	FT
1J3	0242	23	.10000 01	000000	.00000000 00	FT
1J4	0260	13	.10000 01	000000	.00000000 00	FPS
1J5	0261	13	.10000 01	000000	.00000000 00	FPS
1J6	0262	13	.10000 01	000000	.00000000 00	FPS
1J7	0254	18	.60000 02	000000	.00000000 00	MIN
2J1	0244	23	.10000 01	000000	.00000000 00	FT
2J2	0245	23	.10000 01	000000	.00000000 00	FT

Table LM8/4.5.2-2. AGS Constants (Continued)

(NASA DATA SOURCE)

NAME	LOC.	SCALE	CONVERSION FACTOR	AEA OCT.	AEA VALUE	UNITS
2J3	0246	23	.10000 01	000000	.00000000 00	FT
2J4	0264	13	.10000 01	000000	.00000000 00	FPS
2J5	0265	13	.10000 01	000000	.00000000 00	FPS
2J6	0266	13	.10000 01	000000	.00000000 00	FPS
2J7	0272	18	.60000 02	000000	.00000000 00	MIN
1K1P	0544	-13	-.96963-07	777761	.14407430 00	DEG/HR
1K6P	0545	-13	-.96963-07	777757	.16328421 00	DEG/HR
1K11P	0546	-13	-.96963-07	777672	.67234675 00	DEG/HR
1K3	0550	-7	.10000 01	047224	.11990070-02	NO-UNITS
1K8	0551	-7	.10000 01	024160	.61702728-03	NO-UNITS
1K13	0552	-7	.10000 01	025355	.65499544-03	NO-UNITS
1K14	0537	-14	.15091-06	000012	.30856887-01	DEG/HR/G
1K18P	0534	-8	.31250-02	314613	-.13923645-03	NO-UNITS
1K20P	0535	-8	.31250-02	314576	-.26321411-03	NO-UNITS
1K22P	0536	-8	.31250-02	314553	-.44441223-03	NO-UNITS
1K19P	0540	1	-.64254-06	777757	.40371175 03	MICRO-G
1K21P	0541	1	-.64254-06	777777	.23747750 02	MICRO-G

Table LM8/4.5.2-2. AGS Constants (Continued)
(NASA DATA SOURCE)

NAME	LOC.	SCALE	CONVERSION FACTOR	AEA OCT.	AEA VALUE	UNITS
1K23P	0542	1	-.64254-06	000002	-.47495501 02	MICRO-G
1K26	0626	8	.10000 01	561111	-.14285742 03	NO-UNITS
1K27	0627	-4	.10000 01	262132	.43499947-01	RAD/FPS
1K28	0630	7	.10000 01	327443	.10778418 03	NO-UNITS
1K29	0631	-4	.10000 01	004061	.99992752-03	RAD
1K30	0617	17	.10000 01	000226	.15000000 03	2-SEC
1K33	0632	-3	.10000 01	243656	.79999924-01	NO-UNITS
1K34	0633	-15	.10000 01	247613	.19999919-04	1/20MS
1K35	0634	7	.10000 01	000400	.25000000 00	FT/SEC
1K36	0635	0	.10000 01	777651	-.66375733-03	NO-UNITS
1K37	0621	17	.10000 01	000017	.15000000 02	2-SEC
6K2	0457	30	.10000 01	027657	.99999744 08	FT2
6K4	0456	10	.10000 01	031000	.10000000 03	FT2/SEC2
6K5	0656	0	.10000 01	505075	-.73000336 00	NO-UNITS
6K6	0522	8	.10000 01	777605	-.24023437 00	NO-UNITS
6K8	0304	10	.10000 01	000034	.21875000 00	FT2/SEC2
6K9	0611	-15	.10000 01	376057	.30290103-04	NO-UNITS

Table LM8/4.5.2-2. AGS Constants (Continued)

(NASA DATA SOURCE)

NAME	LOC.	SCALE	CONVERSION FACTOR	AEA OCT.	AEA VALUE	UNITS
6K10	0517	28	.10000 01	005754	.62504960 07	FT2
1K9	0616	17	.10000 01	000005	.50000000 01	COUNTS
4K2	0654	-12	.10000 01	713267	-.50203875-04	SEC/FT
4K3	0655	-25	.10000 01	016336	.16802915-08	SEC2/FT2
4K7	0566	0	.10000 01	006547	.26176453-01	RAD
4K8	0602	0	.10000 01	000000	.00000000 00	RAD
4K21	0666	2	.10000 01	020603	.26181030 00	RAD
4K23	0622	17	.10000 01	000076	.62000000 02	40MSEC
4K25	0657	13	.10000 01	000066	.33750000 01	FPS
4K26	0454	13	.10000 01	002140	.70000000 02	FPS
4K27	0473	13	.10000 01	406000	-.80000000 04	FPS
4K34	0660	7	.10000 01	002000	.10000000 01	FT/SEC2
4K35	0661	7	.10000 01	000146	.99609375-01	FT/SEC2
1K4	0624	0	.10000 01	031463	.99998474-01	NO-UNITS
2K1	0636	48	.10000 01	235407	.17318811 15	FT3/SEC2
2K2	0637	-47	.10000 01	320020	.57740271-14	SEC2/FT3
2K4	0674	49	.10000 01	542371	-.34637623 15	FT3/SEC

Contract No. NAS 9-1100
Primary No. 664

Table LM8/4.5.2-2. AGS Constants (Continued)
(NASA DATA SOURCE)

NAME	LOC.	SCALE	CONVERSION FACTOR	AEA OCT.	AEA VALUE	UNITS
3K4	0613	1	.10000 01	026164	.17364502 00	NO-UNITS
4K4	0565	-7	.10000 01	203045	.40000081-02	1/SEC
4K5	0227	23	.10000 01	257014	.57351680 07	FT
4K6	0527	13	.10000 01	002400	.80000000 02	FPS
4K10	0662	20	.10000 01	663056	-.31502400 06	FT/RAD
4K12	0506	7	.10000 01	012000	.50000000 01	FT/SEC2
5K14	0560	-2	.10000 01	000000	.00000000 00	FT/SEC3
5K16	0561	-2	.10000 01	012173	.10000229-01	FT/SEC3
5K17	0601	-2	.10000 01	765605	-.10000229-01	FT/SEC3
5K18	0564	-2	.10000 01	631463	-.10000038 00	FT/SEC3
5K20	0523	-2	.10000 01	000000	.00000000 00	FT/SEC3
5K26	0466	13	.10000 01	000360	.15000000 02	FPS
K55	0607	0	.10000 01	377777	.99999237 00	NO UNITS
WBX	0514	1	.10000 01	700000	-.50000000 00	NO-UNITS
WBY	0515	1	.10000 01	621114	-.86602783 00	NO-UNITS
WBZ	0516	1	.10000 01	000000	.00000000 00	NO-UNITS
2J	0605	7	.10000 01	003775	.19970703 01	NO-UNITS

Table LM8/4.5.2-2. AGS Constants (Continued)
(NASA DATA SOURCE)

NAME	LOC.	SCALE	CONVERSION FACTOR	AEA OCT.	AEA VALUE	UNITS
3J	0312	13	.60000 02	000000	.00000000 00	MIN
5J	0231	23	.10000 01	255704	.56977920 07	FT
6J	0307	13	.60000 02	120500	.43000000 02	MIN
7J	0224	23	.10000 01	270424	.60469760 07	FT
8J	0225	23	.10000 01	131562	.29400320 07	FT
10J	0226	23	.10000 01	270456	.60486400 07	FT
11J	0673	20	.10000 01	546612	-.62763200 06	FT/RAD
12J	0305	3	.10000 01	766214	-.30395508 00	RAD
16J	0232	23	.10000 01	001652	.60032000 05	FT
21J	0233	23	.10000 01	000607	.25024000 05	FT
22J	0464	13	.10000 01	001440	.50000000 02	FPS
23J	0465	13	.10000 01	000470	.19500000 02	FPS
29J	0274	18	.60000 02	756330	-.30000000 03	MIN
6J1	0640	-14	.10000 01	000007	.32596290-08	RAD/20MS
6J2	0641	-14	.10000 01	777620	-.52154064-07	RAD/20MS
6J3	0642	-14	.10000 01	777751	-.10710210-07	RAD/20MS
1K24	0625	1	.10000 01	000071	.86975098-03	NO-UNITS

Contract No. NAS 9-1100
Primary No. 664

Table LM8/4.5.2-2. AGS Constants (Continued)

(NASA DATA SOURCE)

NAME	LOC.	SCALE	CONVERSION FACTOR	AEA OCT.	AEA VALUE	UNITS
2K3	0216	23	.10000 01	040000	.10485760 07	FT
2K11	0526	13	.10000 01	273400	.60000000 04	FPS
2K14	0217	23	.10000 01	001415	.49984000 05	FT
2K17	0620	17	.10000 01	000005	.50000000 01	COUNTS
2K18	0447	13	.10000 01	000360	.15000000 02	SEC
2K19	0230	23	.10000 01	017205	.50003200 06	FT
2K20	0453	13	.10000 01	000040	.20000000 01	SEC
BM13SF	0676	0	.10000 01	365706	.96049499 00	
B23SF	0677	0	.10000 01	243656	.63999939 00	
B18SF	0700	0	.10000 01	125253	.33333588 00	
B13VSF	0701	0	.10000 01	240000	.62500000 00	
B3SF	0702	0	.10000 01	131415	.34970856 00	
B23RSF	0703	0	.10000 01	032756	.10533142 00	
B13SF	0704	0	.10000 01	032525	.10416412 00	
BACCSF	0446	0	.10000 01	303240	.76293945 00	

LM8/4.5.3.2.2.3 LM-8 DPS Thrust Response At TTCA Minimum and Maximum Positions

The KSC calibration data for the commander's (CMDR) and LM pilot's (LMP) TTCA's are given below.*

TTCA POSITION	THRUST OUTPUT			
	CMDR		LMP	
	TTCA	DECA	TTCA	DECA
Minimum	11.4 %	11.3 %	11.8 %	11.8 %
Maximum	110.3 %	Saturated	114.8 %	Saturated

*TCP No. 0045, Combined Systems Test

The output calibration for the LM-8 CMDR's TTCA is:

$$V_{TTCA} = 0.024975\ \%F_{COMM} + 0.2838$$

where V_{TTCA} = TTCA output voltage, VRMS

$\%F_{COMM}$ = Commanded thrust position, %.

The output calibration for the LM-8 DECA (throttling range) is:

$$V_{DECA} = TCV = 0.123767\ \%F_{STD} + 1.3614$$

where V_{DECA} = DECA output voltage to the DPS throttle actuator (TCV), VDC

$\%F_{STD}$ = Commanded thrust at standard values of propellant interface conditions, % (of 10,500 lbf)

Using the above equations and the DPS preflight performance data (Para. LM8/4.7.1) the voltages and thrust values were determined for the above TTCA and DECA calibration data for the CMDR TTCA.

THIS COLUMN NASA DATA SOURCE ↓

TTCA OPERATING POSITION	TTCA COMMANDED THRUST, %	TTCA OUTPUT, VRMS	DECA OUTPUT, VDC	PREDICTED THRUST, LBF
Minimum	11.4	0.567	2.77	1377
Maximum* (Throttle-up	110.3	3.04	>14.6	9790
Maximum** (Throttle-down	110.3	3.04	>14.6	9907

*At 26 sec burn time.
**At 395 sec burn time.

LM8/4.5.3.4.3 GDA Drive Rates

Measurement			
Time of Travel	- pitch	57.60 sec.	These times are the average of 3 measurements made on LM-8 at KSC.
	- roll	56.93 sec.	
Angular Rate	- pitch	0.2101°/sec.	
	- roll	0.2125°/sec.	

NOTE: Computed Angle of Travel = 12.1° in either axis.

LM8/4.5.4.2 Rendezvous Radar Mechanical Alignment

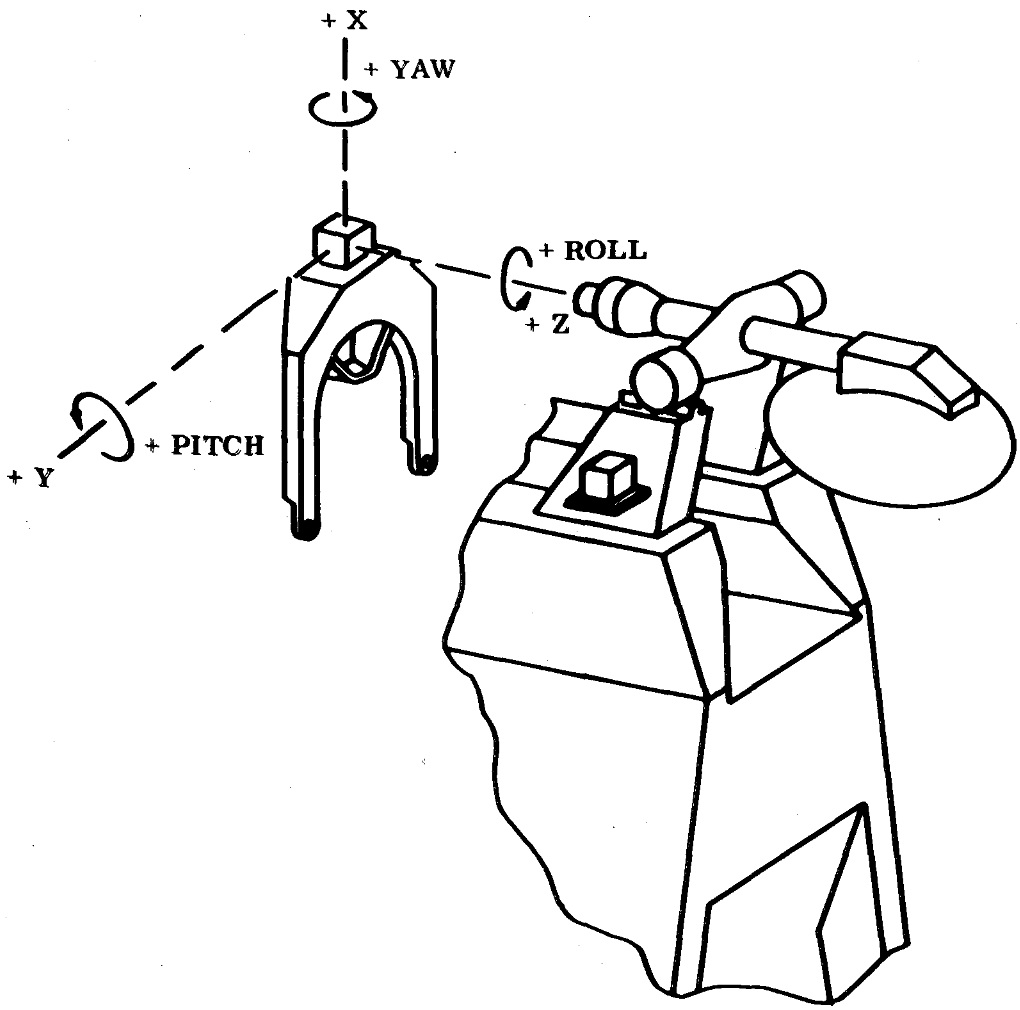

The Rendezvous Radar Antenna Assembly alignment for LM-8 with respect to the Vehicle Coordinate System (Nav. Base Gage) is shown below:

Pitch:	**-00° 02' 45"**
Roll:	**-00° 03' 18"**
Yaw:	**+00° 00' 05"**

(Ref.: LMO-566-215, dated Sept. 1969)

LM8/4.5.4.3 RR Timeline Operation

TBS

LM8/4.5.4.4.11 RR and T AGC Voltage Versus Range

Figure LM8/4.5.4-3 shows the expected AGC voltage levels versus range and signal level for RR No. 30 with T No. 20. The use of curves instead of nomographs permits a better visualization of the interaction of the variables and also avoids the difficulty of trying to design a nomograph to fit empirical data on non-linearly interrelated variables.

LM8/4.5.4.4.11.1 RR and T AGC Voltage Versus Range and LOS Angle

Figures LM8/4.5.4-4 and LM8/4.5.4-5 show RR AGC readings at several ranges between 0.2 nm. and 400 nm., as a function of the angle between the LOS and the antenna boresight. The data are shown for angles out to ±10 degrees in both the shaft and trunnion axes, except where very low signal levels would produce low AGC readings which would be of little value.

LM8/4.5.4.4.12 Rendezvous Radar Self-Test

The following are the measured RR self-test parameters for RR 30. These data were recorded at KSC during FRT Mission-Sim. 0005 and TCP 0045.

1) Test Monitor

SELF-TEST AGC	+1.60 VDC
XMTR PWR	+2.90 VDC
SHAFT ERROR	+2.2 to 2.6 VDC (at 1/2 cps.)
TRUN ERROR	+2.2 to 2.6 VDC (at 1/2 cps.)

2) Range/Range Rate Meter

Range (R)	195.6 NM
Range Rate (R)	-487 ft/sec

3) LGC DSKY Display: V16N78

R_1 (Range)	195.6 NM
R_2 (Range Rate)	-490 ft/sec
R_3 (No Display)	0

LM8/4.5.4.4.13 RR Power Monitor Calibration

Figure LM8/4.5.4-7 shows the power monitor calibration for RR 30, giving power in dBm versus DC volts.

LM8/4.5.4.4.16 Allowable Vehicle Accelerations During RR Power Off Periods

Figures LM8/4.5.4-8 through LM8/4.5.4-11 show the maximum allowable LM body accelerations for any angular position of the RR antenna trunnion and shaft axes under which the antenna will not move from a fixed position with no power applied to the RR. The effect of varying the antenna temperature is also indicated in the figures.

The antenna shaft axis will always be parallel to the LM Y-axis. Therefore, LM body accelerations about the LM Y-axis can be used directly. However, as the shaft axis rotates, the trunnion axis will be parallel to the LM X-axis at 0° shaft position and parallel to the LM Z-axis at -90° shaft position. For other shaft positions, the allowable LM acceleration about the LM axes must be converted to the acceleration about the trunnion axis at the appropriate shaft position.

TBS

Figure LM8/4.5.4-1. Predicted RR Temperature Management Curve For Final Flight Plan Timeline

TBS

Figure LM8/4.5.4-2. Predicted RR Temperature Management Curve For Final Flight Plan Timeline

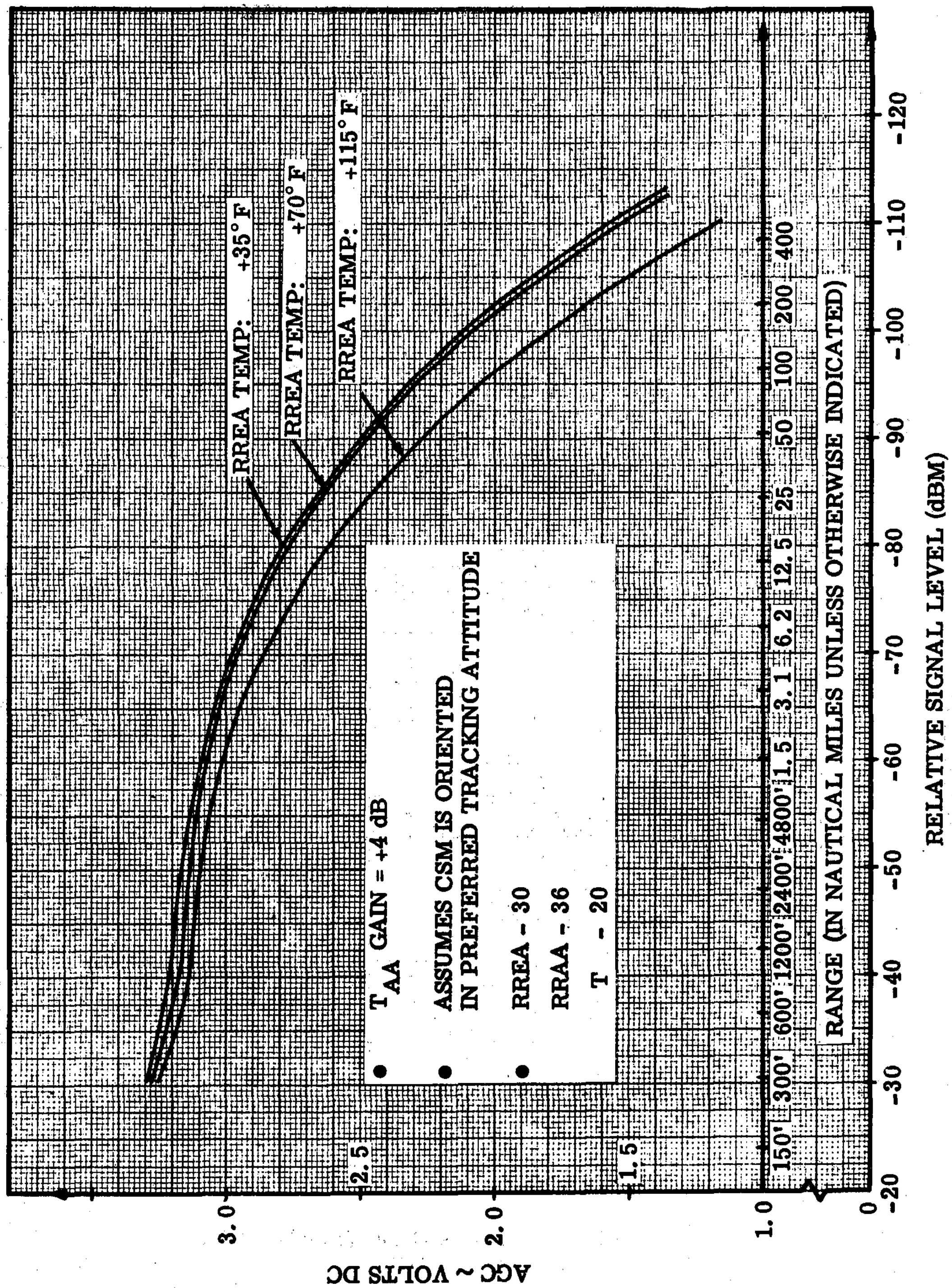

Figure LM8/4.5.4-3. LM-8 AGC Versus Signal Level and Range with T20 (See Para. 4.5.4.4.11)

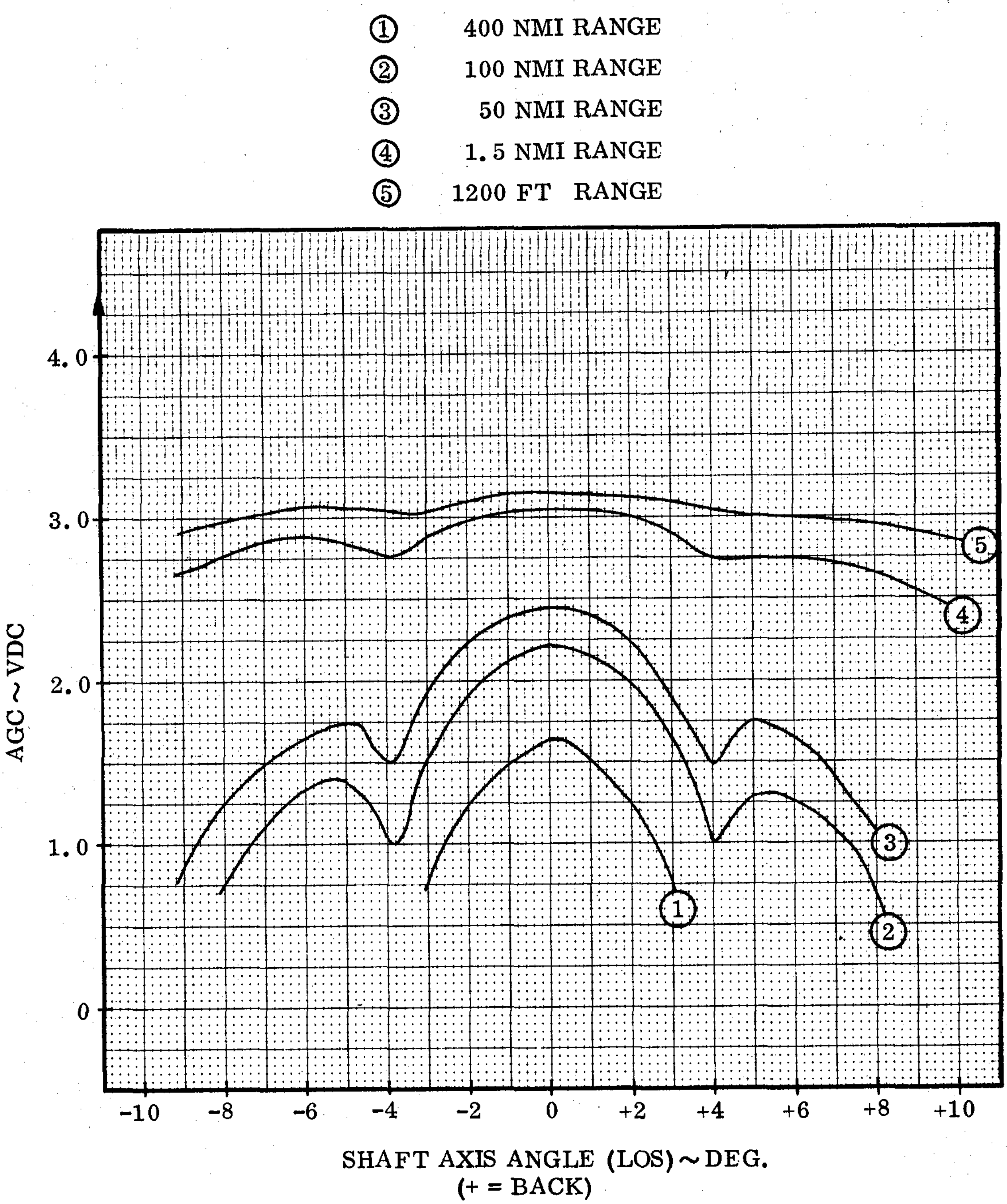

Figure LM8/4.5.4-4. AGC Versus Shaft Axis Angles (LOS) (See Para. 4.5.4.4.11.1)

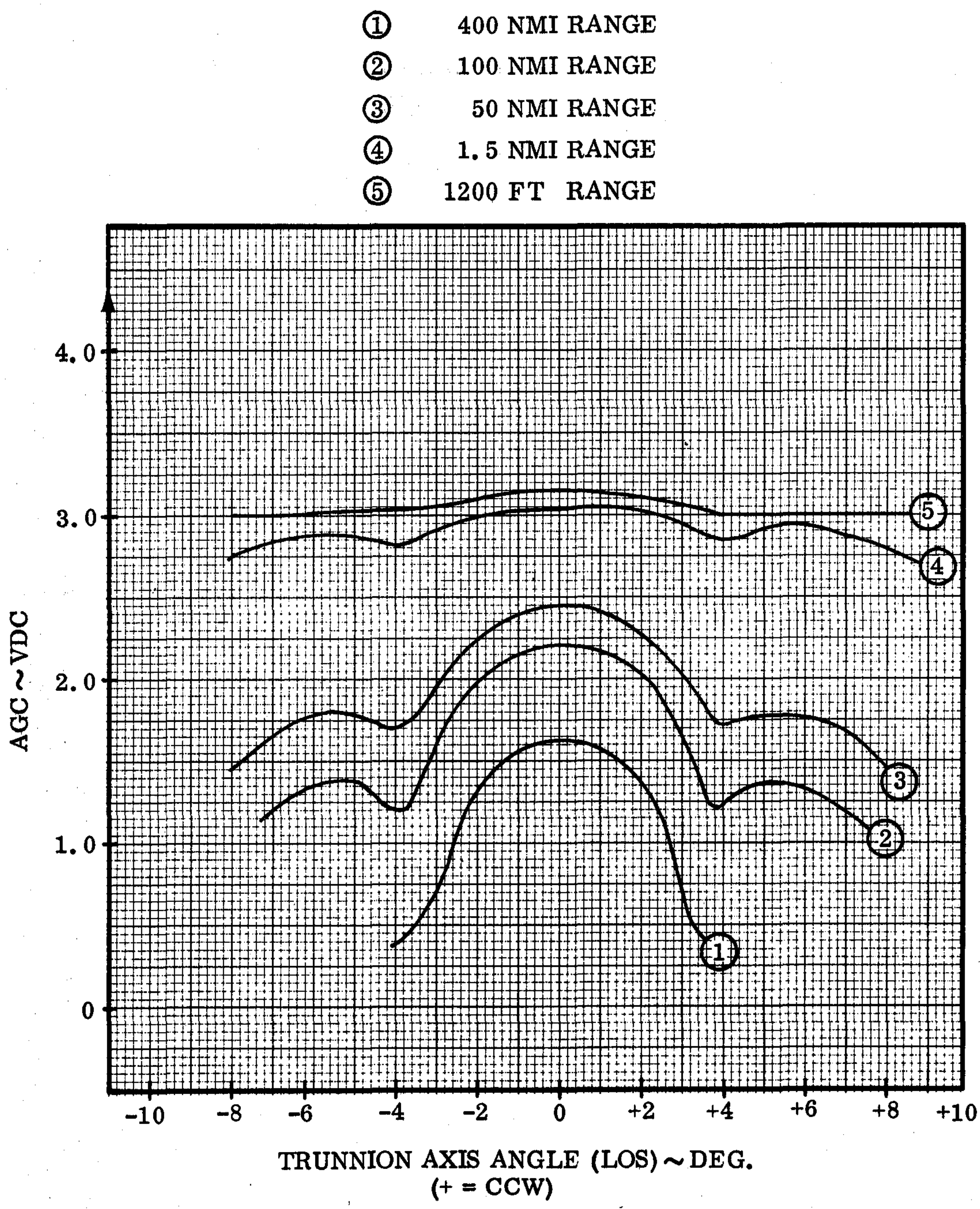

Figure LM8/4.5.4-5. AGC Versus Trunnion Axis (LOS) Angle (See Para. 4.5.4.4.11.1)

TBS

Figure LM8/4.5.4-6. Environmental Effects on RR Self Test Parameters

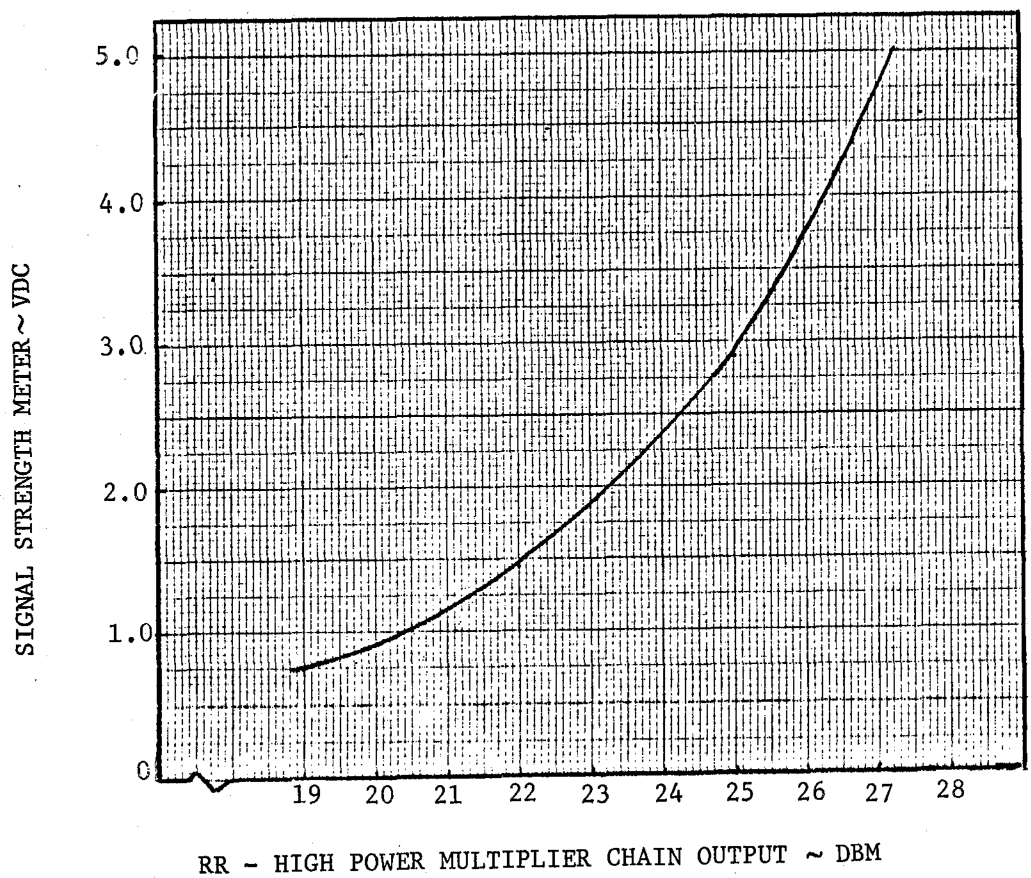

NOTE: HPMC Output Varies Inversely With Temperature

Figure LM8/4.5.4-7 Power Monitor Meter Voltage vs. RF Power

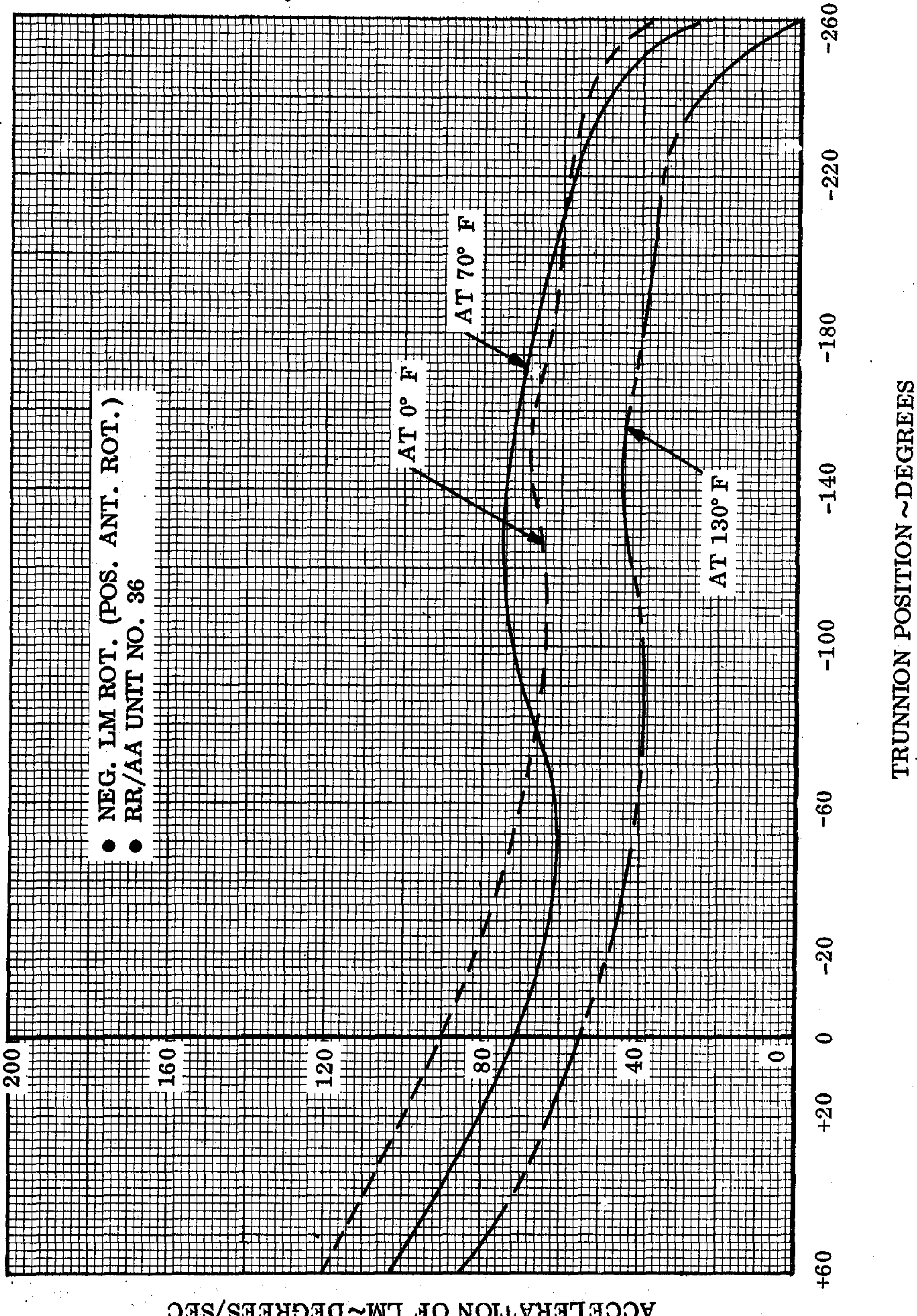

Figure LM8/4.5.4-8. Allowable Acceleration Trunnion Axis
(See Para. LM8/4.5.4.4.16)

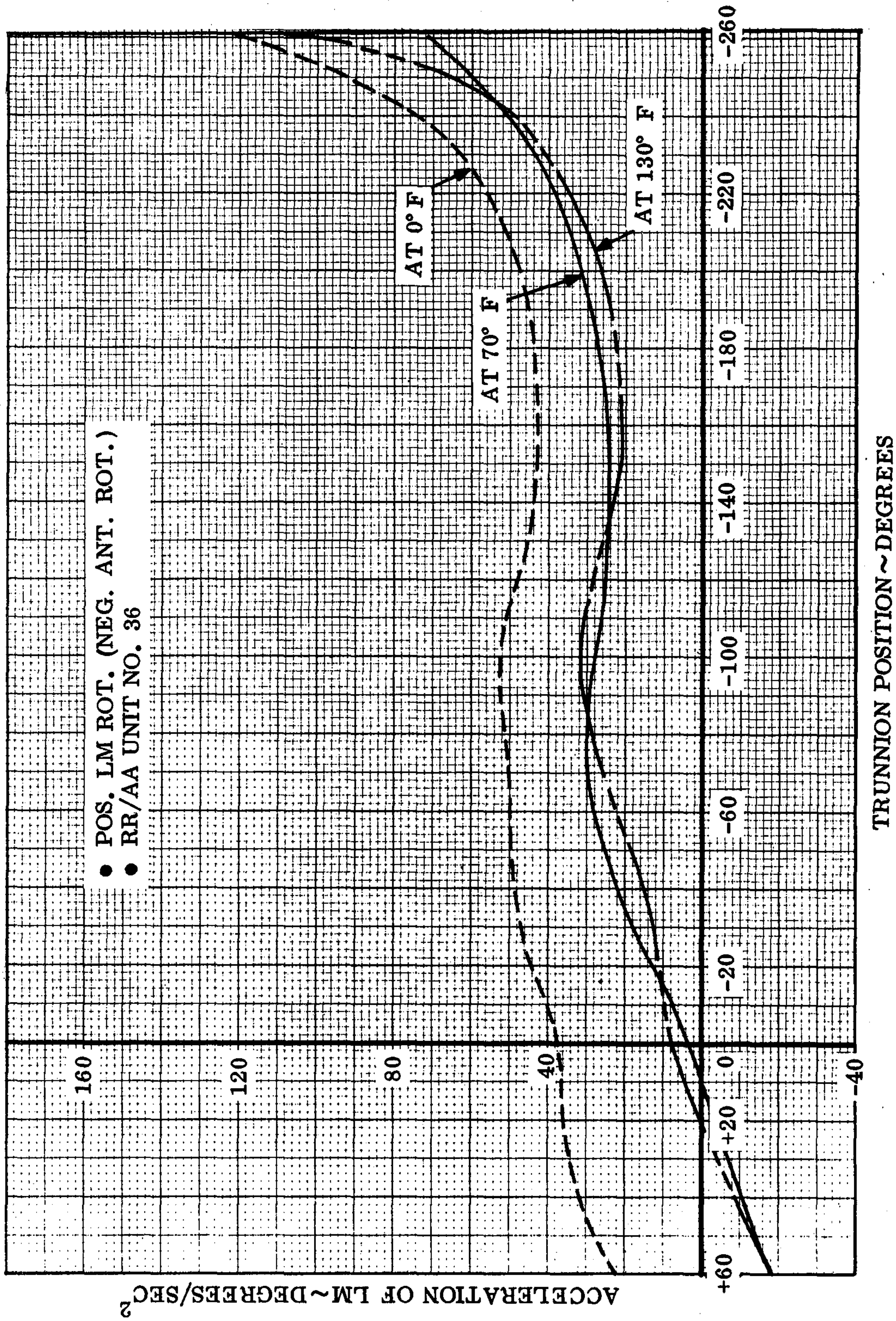

Figure LM8/4.5.4-9. Allowable Acceleration Trunnion Axis
(See Para. LM8/4.5.4.4.16)

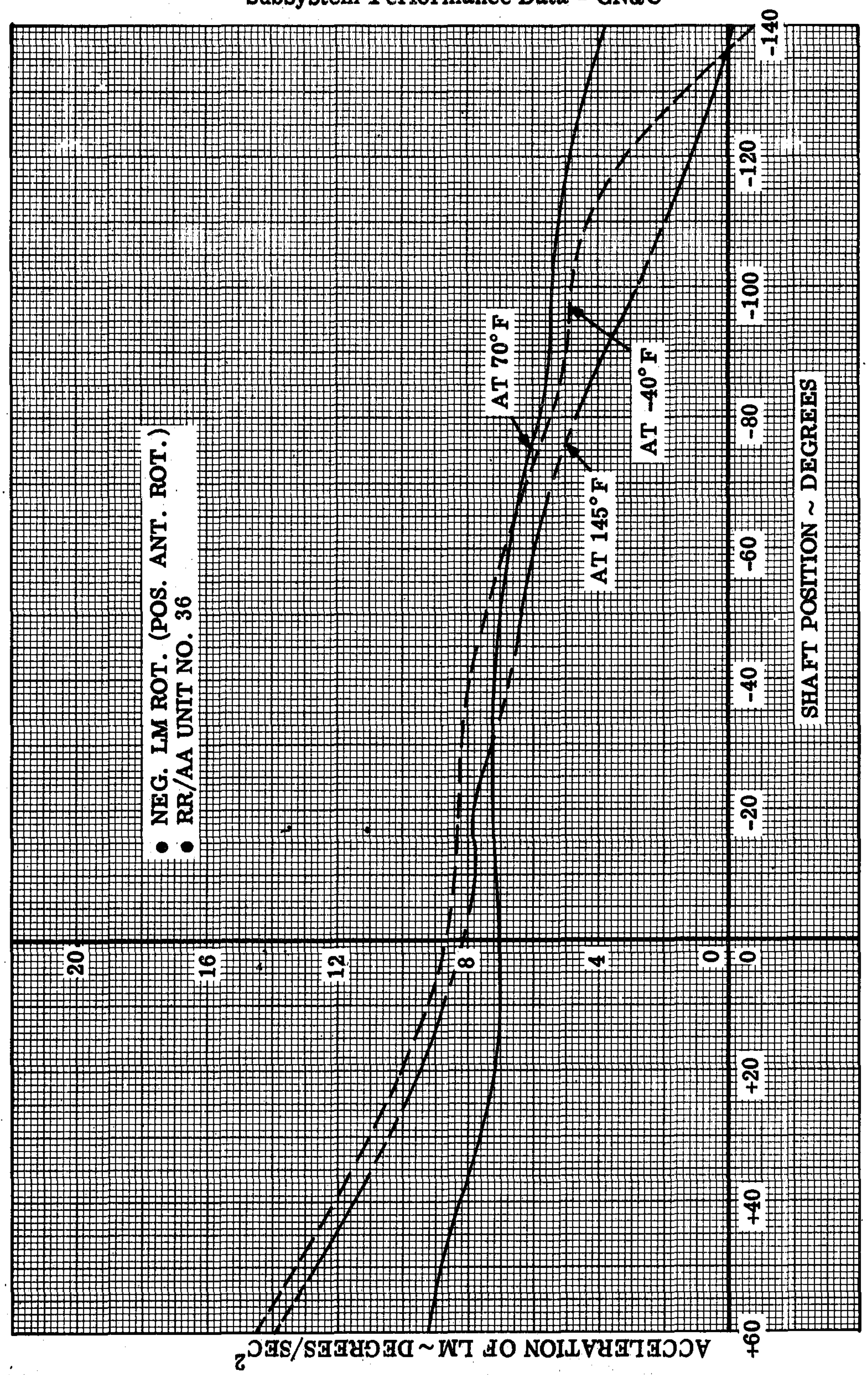

Figure LM8/4.5.4-10. Allowable Acceleration Shaft Axis
(See Para. LM8/4.5.4.4.16)

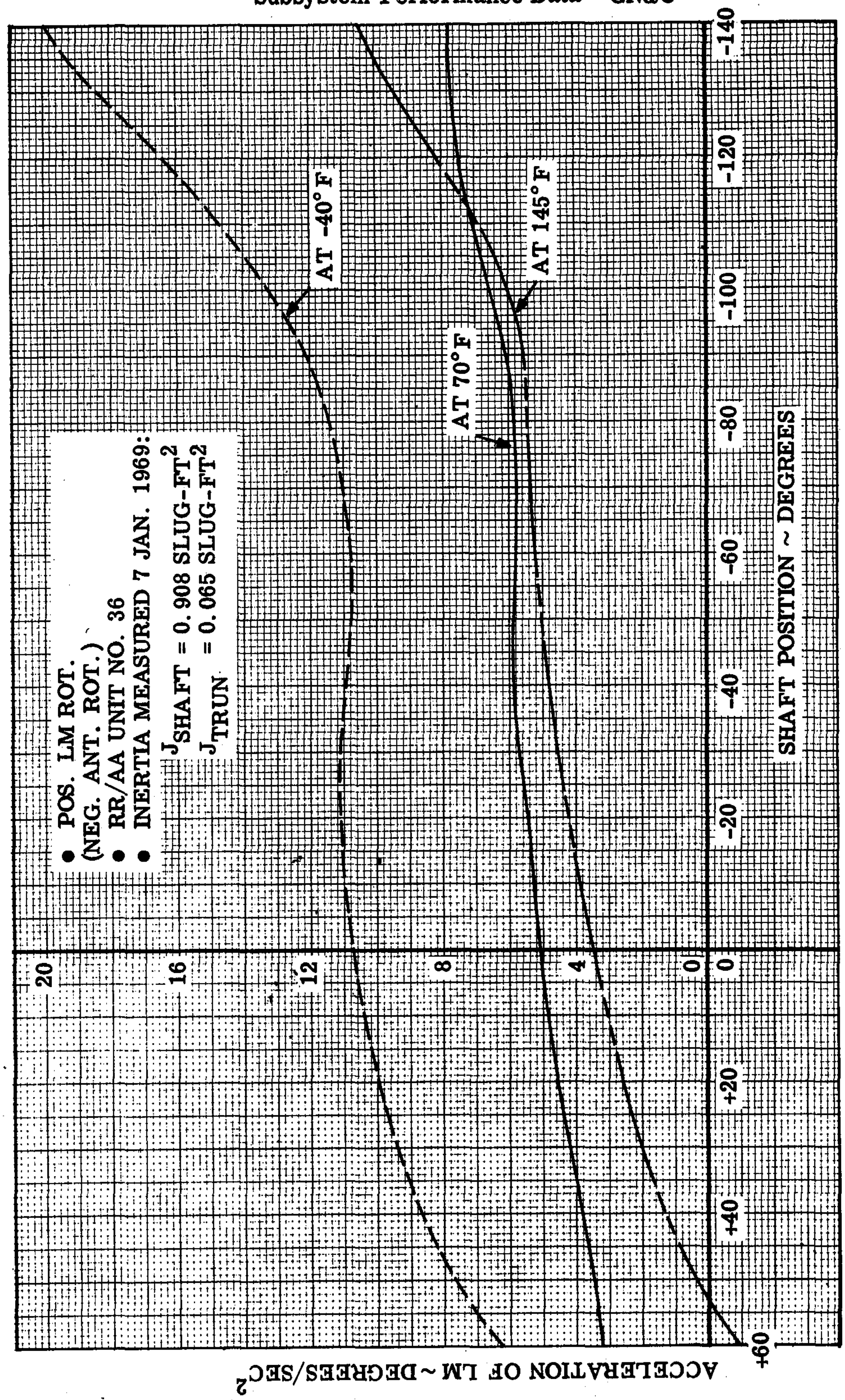

Figure LM8/4.5.4-11. Allowable Acceleration Shaft Axis
(See Para. LM8/4.5.4.4.16)

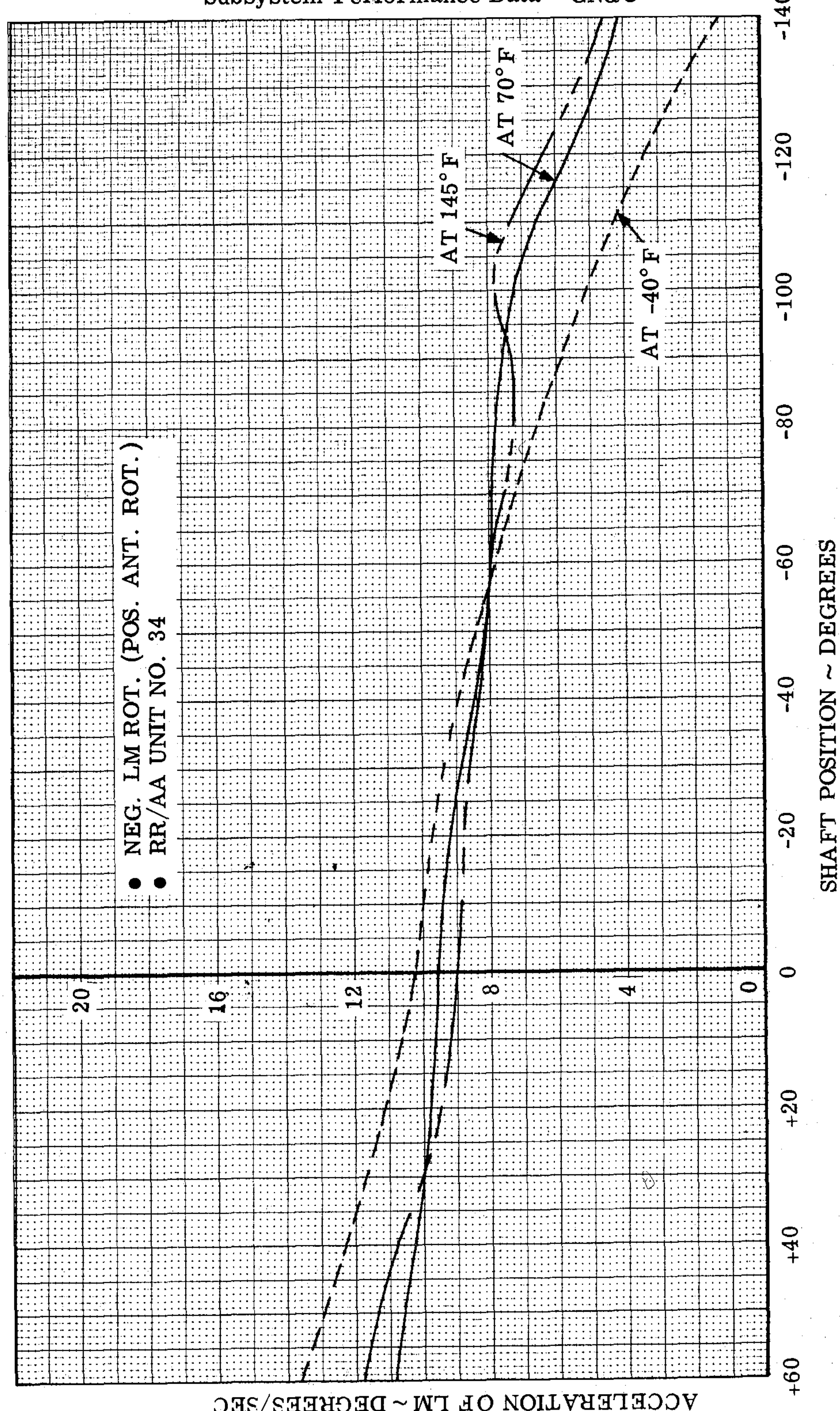

Figure LM8/4.5.4-10. Allowable Acceleration Shaft Axis
(See para. LM8/4.5.4.4.16)

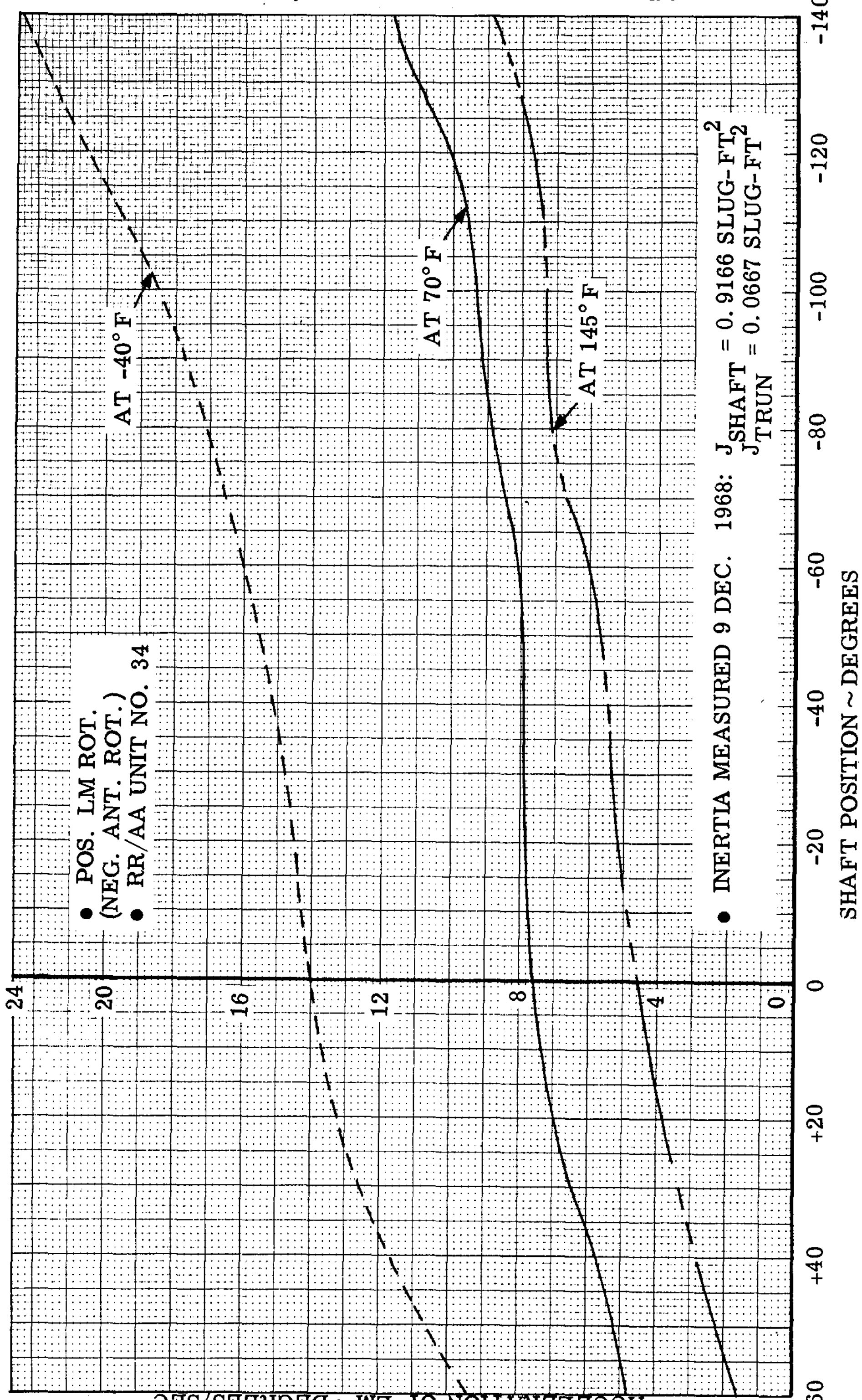

Figure LM8/4.5.4-11. Allowable Acceleration Shaft Axis

(See para. LM8/4.5.4.4.16)

LM8/4.5.5.1.16 LR Power Monitor

The following is a calibration of the Power Monitor with LR P-44. These data were obtained from KSC testing during TCP 0045 and include antenna losses.

Transmitter	Power (DBM)	Power (MW)	Monitor (VDC)	Calibration
Velocity	24.3	269	3.85	14.3×10^{-3} V/MW
Altimeter	22.5	178	3.85	21.6×10^{-3} V/MW

LM8/4.5.5.1.17 Loss of LR Lock as a Function of Vehicle Pitch and Roll for an Apollo 14 Type Trajectory.

TBS

LM8/4.5.5.1.18 Expected Altitude of LR Velocity and Range Initial "Data Good" Indication.

TBS

LM8/4.5.5.1.21 LR Predicted Accuracy

TBS

LM8/4.5.5.2 Landing Radar Antenna Assembly Temperature Profile

TBS

LM8/4.5.5.3 Landing Radar Mechanical Alignment

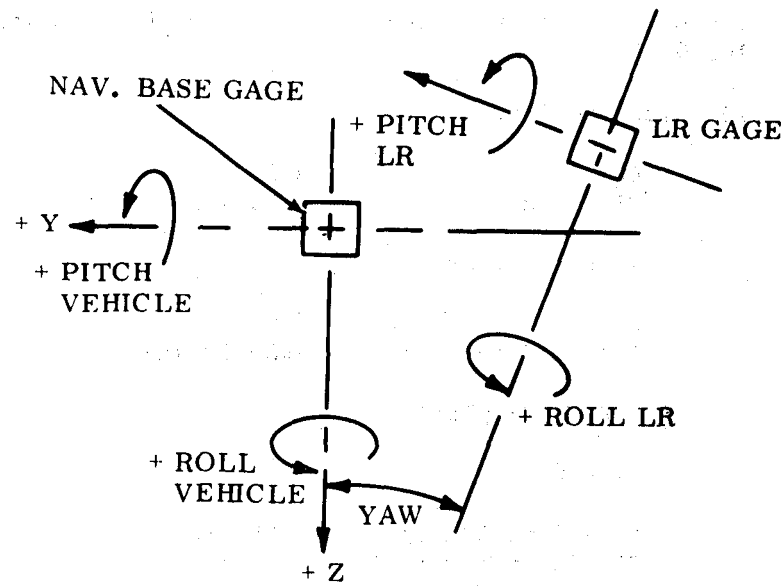

The Landing Radar Antenna Assembly alignment with respect to the Vehicle coordinate System (Nav. Base Gage) is the following:

	Position #2	Position #1
Pitch	-00°01'22"	-24°01'49"
Roll	-00°06'38"	-00°06'15"
Yaw	-05°51'10"	-05°50'40"

The Landing Radar Antenna Assembly alignment with respect to the Inertial Measurement Unit Coordinate System (LR-NB) - (IMU-NB) is the following:

	Position #2	Position #1
Pitch	+00°03'03" (3'03")	-23°57'24" (2'36")
Roll	-00°05'39" (-5'39")	-00°05'16" (-5'16")
Yaw	-05°46'59" (13'01")	-05°46'29" (13'31")

NOTE: The LR/IMU Mechanical Misalignments are indicated in parentheses.

LM8/4.5.5.4 Landing Radar Self Test

The following are the measured LR self test parameters for P-44. These data were recorded at KSC during FRT Mission-Sim. 0005 and TCP 0045.

1) Test Monitor

ALT XMTR	3.85 VDC
VEL XMTR	3.85 VDC

2) ALT/ALT Rate Meter

ALT (R)	8000 ft
ALT Rate ($\dot{R}$)	-480 ft/sec

3) LGC DSKY Display:

V16N66

R_1 (Slant Range)	+8281 ft
R_2 (Antenna Position)	+00001
R_3 (No Display)	0

V16N67

R_1 (Vxa)	-495 ft/sec
R_2 (V_{ya})	+1862 ft/sec
R_3 (V_{za})	+1332 ft/sec

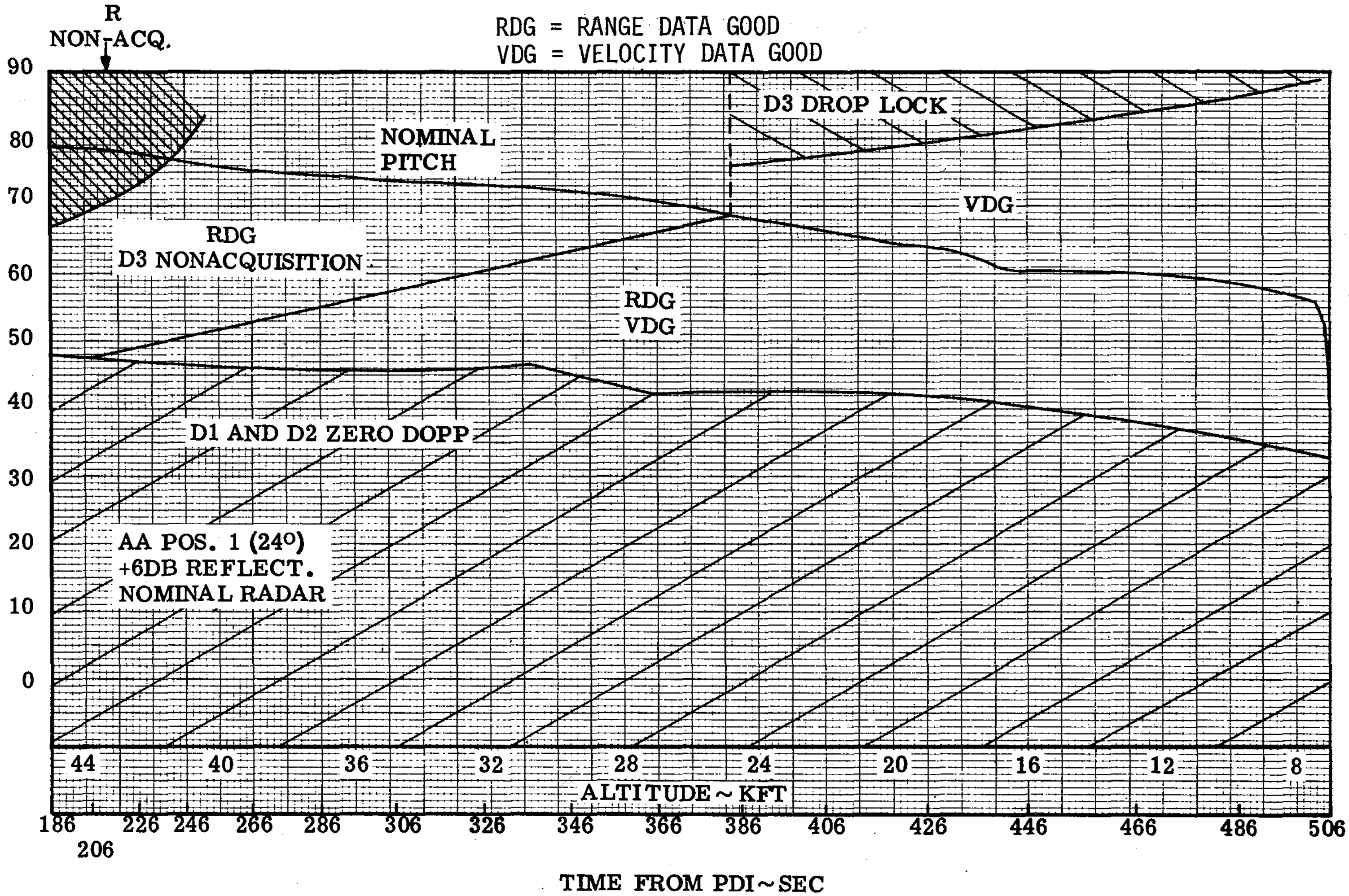

Figure LM8/4.5.5-1. LR Loss of Lock vs Pitch Angle (Antenna Position 1)

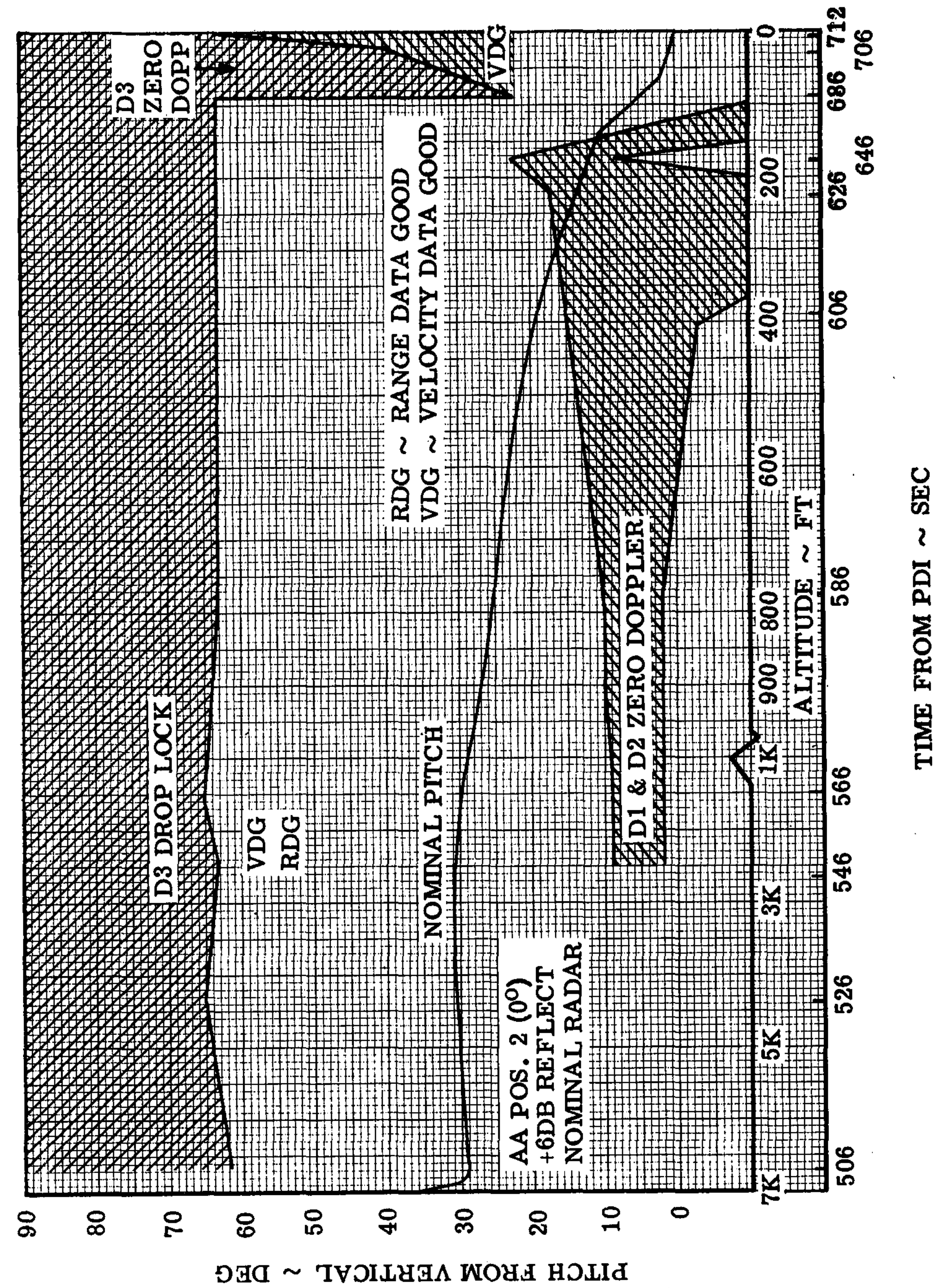

Figure LM8/4.5.5-2 LR Loss of Lock vs. Pitch Angle (Antenna Position 2)

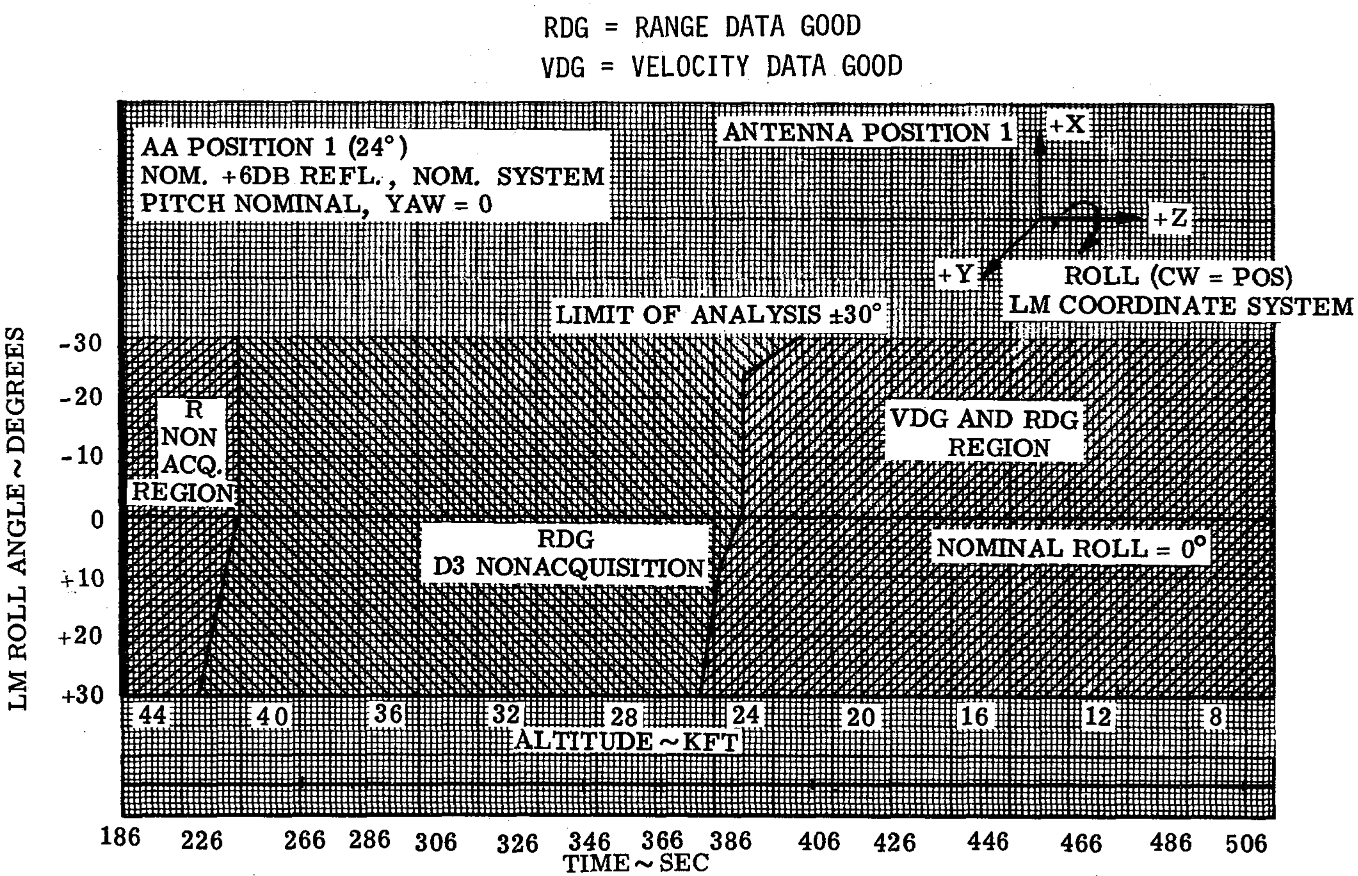

Figure LM8/4.5.5-3 LR Loss of Lock versus Roll Angle

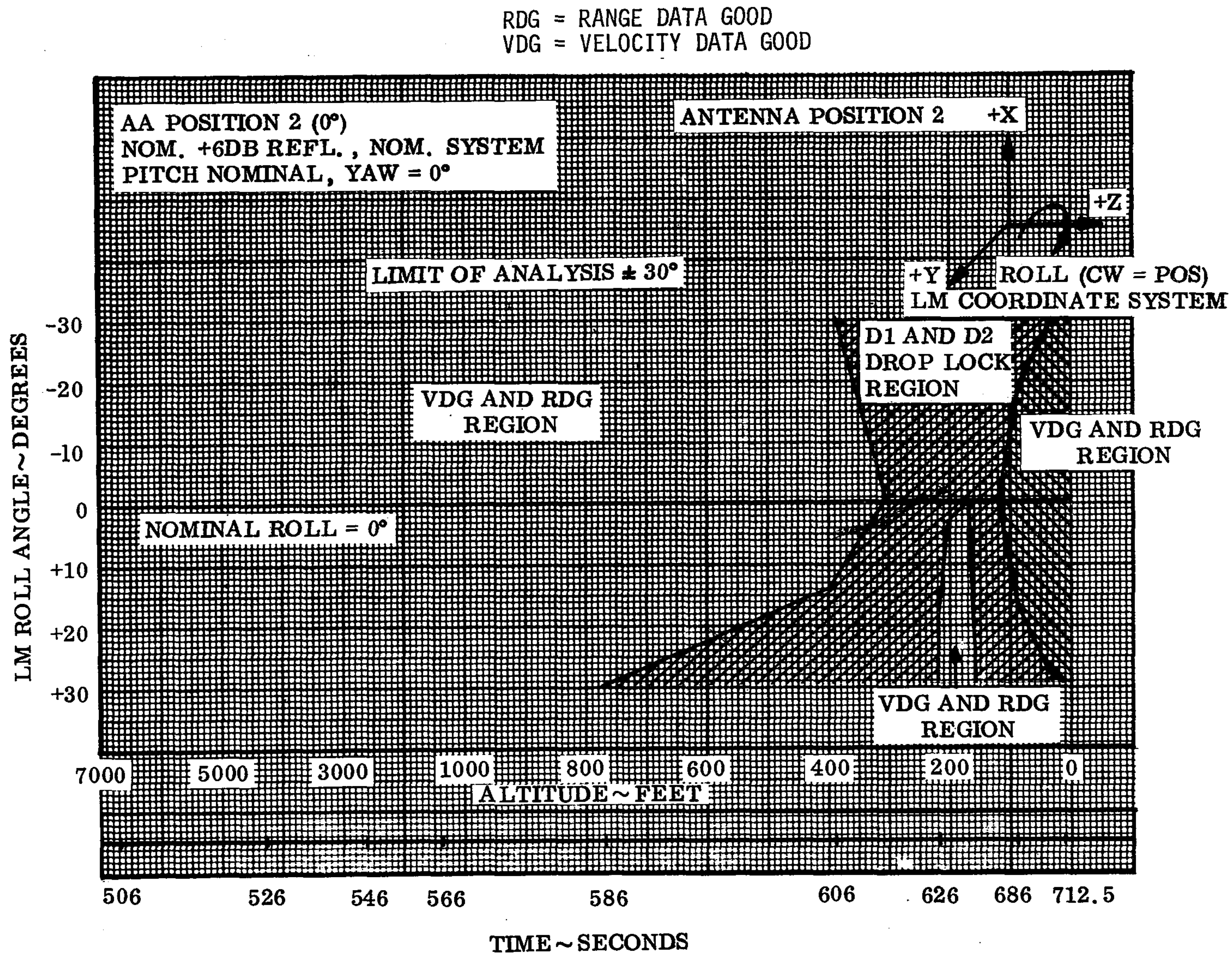

Figure LM8/4.5.5-4. LR Loss of Lock versus Roll Angle

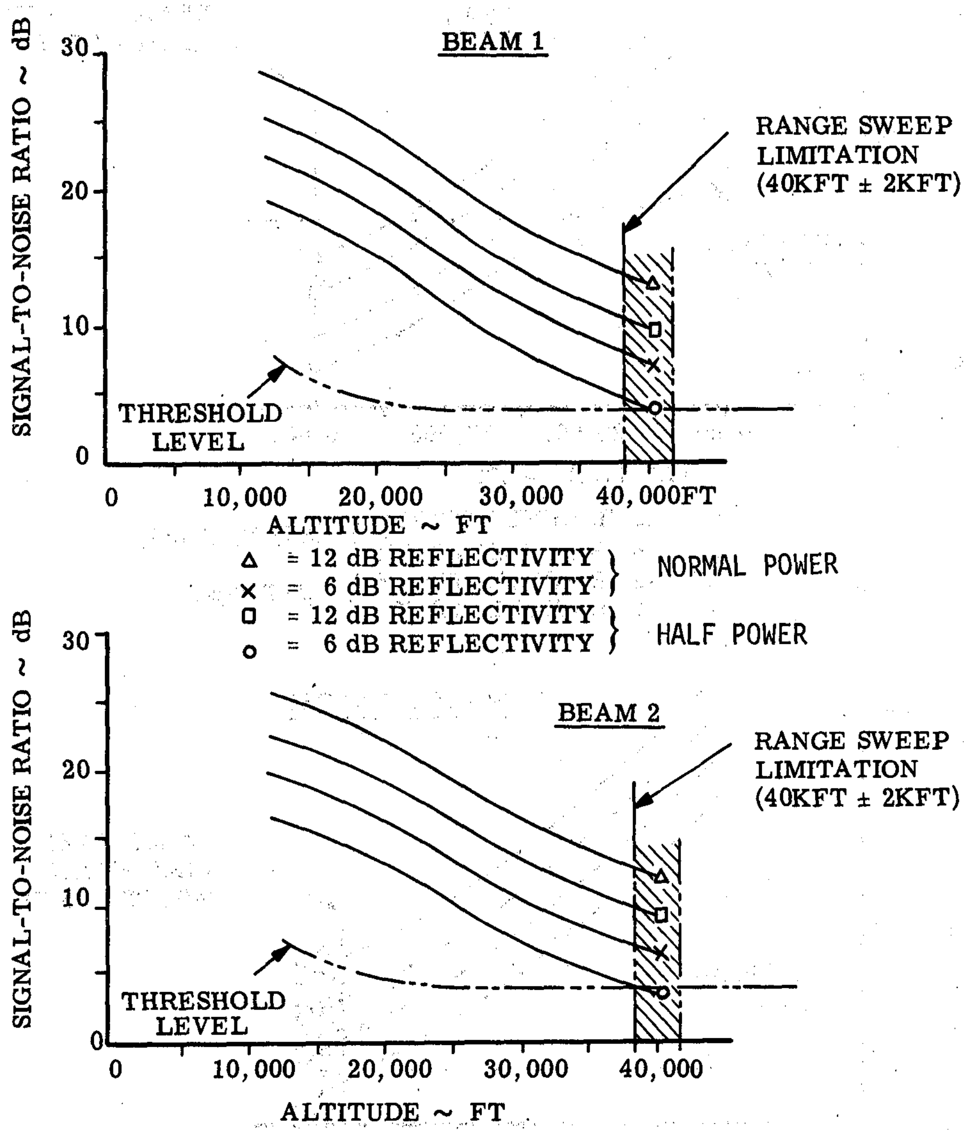

Figure LM8/4.5.5-5. Landing Radar Lock-ON Capability

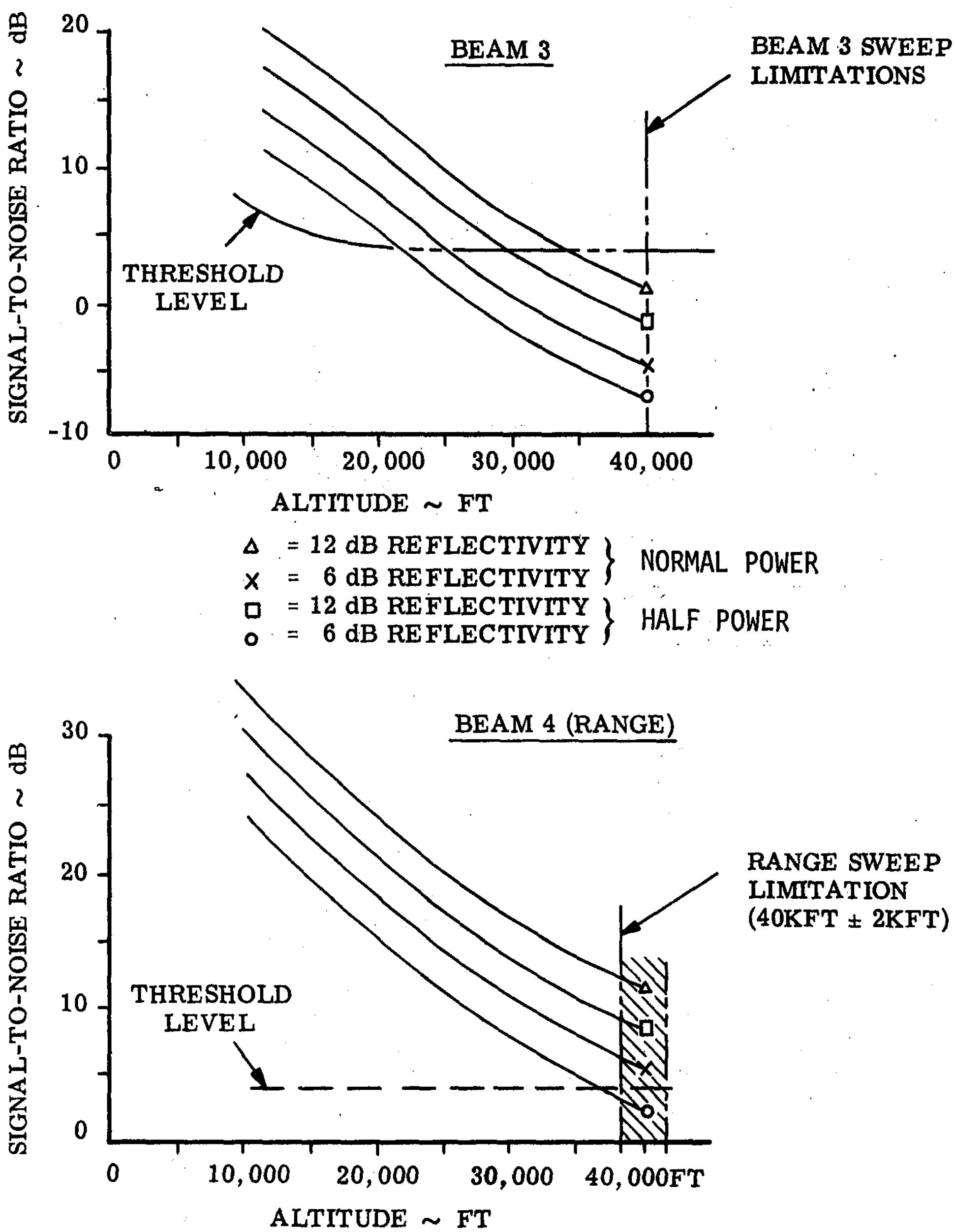

Figure LM8/4.5.5-6. Landing Radar Lock-ON Capability

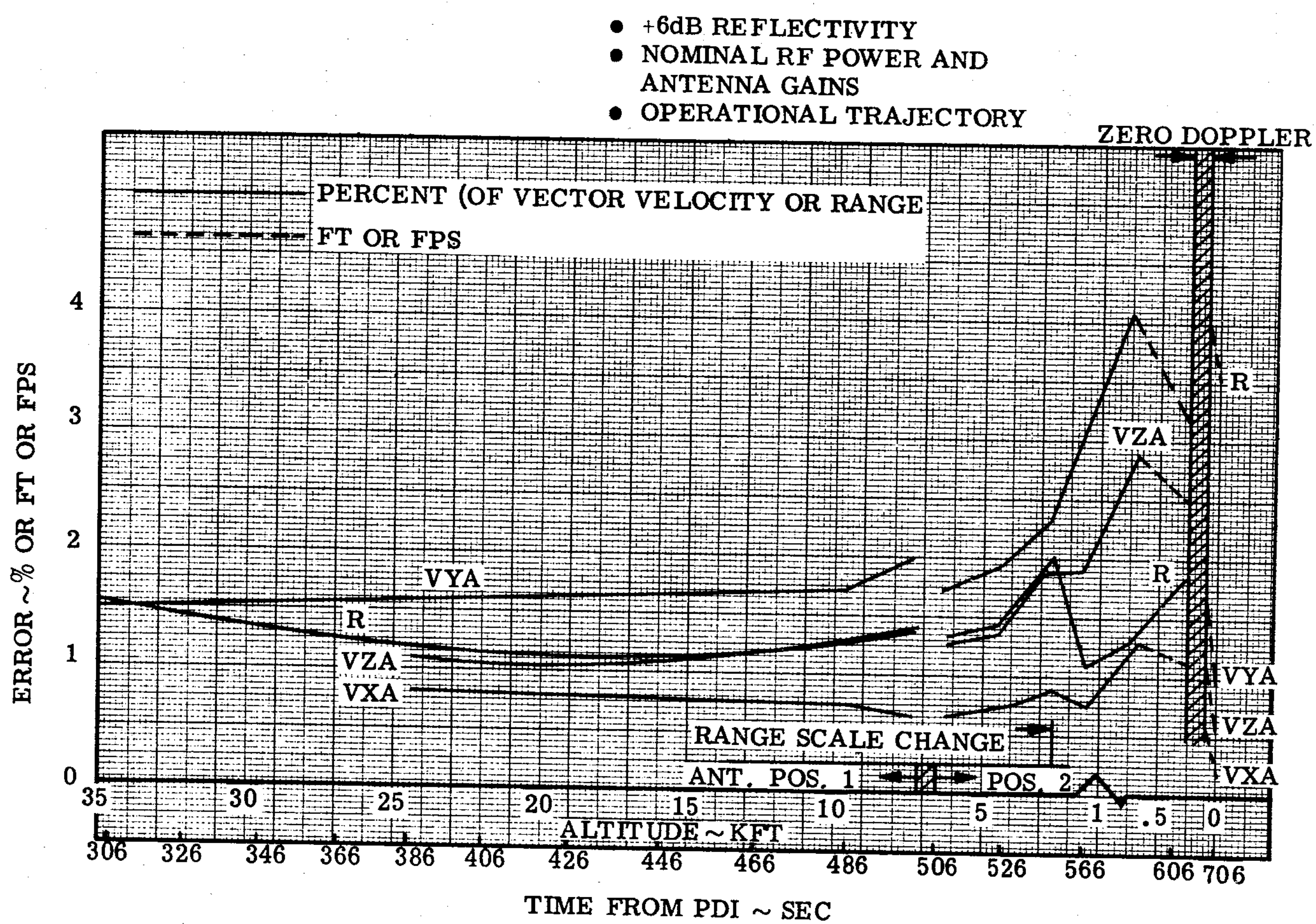

Figure LM8/4.5.5-7. Landing Radar Accuracy

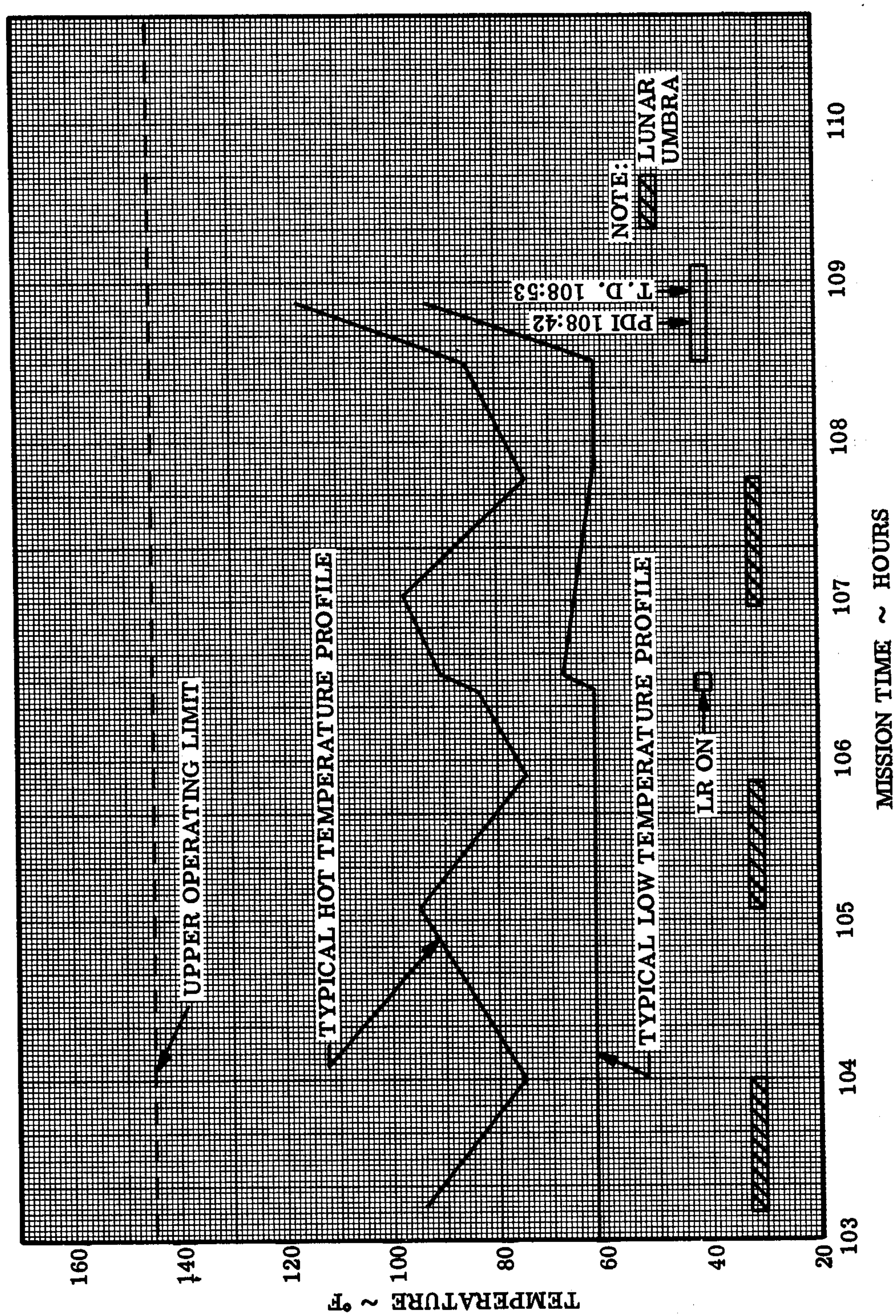

Figure LM8/4.5.5-8. Landing Radar Antenna Assembly Flight Measurement GN7563T LM-8/H-3 Mission (See Para. LM8/4.5.5.2)

LM8/4.6.1 Mission H3 (LM-8) APS Preflight Analysis

The APS mission duty cycle used in the following analysis is a lunar liftoff insertion burn followed by a short Terminal Phase Initiation (TPI) burn. The first and longest burn will be a lunar liftoff to orbit insertion maneuver similar to those accomplished during the Apollo 11 and 12 Missions. The planned vehicle thrust velocity change (ΔV) for that burn is 6053.4 fps. The second burn represents a change from previous APS lunar mission duty cycles in that the APS will perform the TPI burn. The planned ΔV for the TPI maneuver is 77.8 fps. A coast period of approximately 38 minutes between the end of the lunar liftoff burn and ignition of the TPI burn is planned.

The vehicle weight characteristics and loaded propellant quantities were obtained from Reference 1. Table LM8/4.6.1-1 is a summary of APS physical characteristics.

It should be noted that the effect of the Reaction Control System on APS performance has been neglected in this analysis. The RCS will affect APS performance in the following manner:

1) RCS propellant consumption (APS/RCS interconnect closed) will alter vehicle weight;

2) RCS propellant consumption through the APS/RCS interconnect will decrease the propellant available to the APS and thus shorten the APS burn time available and decrease the ΔV capability. Also, since the RCS operates at a mixture ratio different from that of the APS, the mixture ratio from the APS tanks will be changed. (The mixture ratio of the ascent engine will not be significantly changed).

The engine performance characterization consists of C* (characteristic exhaust velocity), C_f (thrust coefficient), A_t (throat area), and interface-to-chamber fluid flow resistances defined as functions of engine test data, and (where applicable) predicted values of P_c (chamber pressure), μ (mixture ratio), T (propellant temperature), t_b (engine burn time), t_{acc} (accumulated time on chamber), and helium saturation into the propellants.

The helium regulator characterization used was the nominal Class I - primary regulator expected performance.

The liquid propellant bulk temperatures at the start of the APS burn were assumed to be 70°F for both oxidizer and fuel.

The nominal mixture ratio of 1.601 is for non-saturated propellant conditions prior to ignition. If the tanks are pressurized earlier than is now planned, causing helium saturation of the propellants, the mixture ratio will shift to 1.595.

LM8/4.6.1 Continued

Graphs from the simulation of the LM-8 APS nominal performance under the assumptions and conditions discussed above are presented in Figures LM8/4.6.1-1 through LM8/4.6.1-9. Figure LM8/4.6.1-2 presents the predicted ablative chamber throat area as a function of burn time. The time-varying characteristic of this parameter is included because of its influence in imparting a time-varying character to other propulsion parameters.

APS performance data at representative time points have been tabulated for both APS burns and are presented in Table LM8/4.6.1-3.

An uncertainty propagation dispersion analysis was conducted using root-sum-squaring techniques to determine APS performance dispersions. The uncertainties associated with the basic parameters defining propulsion system operation are listed in Table LM8/4.6.1-4. The values given in Table LM8/4.6.1-4 have been derived from Rocketdyne and Grumman inputs by the methods discussed in Reference 2. These values express the uncertainty of the various parameters as 3-sigma at a 50 percent confidence level. These values were used as input to establish the performance dispersions included as part of Table LM8/4.6.1-3. Also presented in Table LM8/4.6.1-3 are average values of the various parameters taken over the duty cycle.

The data presented herein are valid for nominal system conditions. The values of propulsion system parameters presented herein do not represent boundary conditions of operation for the system, and therefore, should not be used as limit values.

For propellant budgeting purposes the recommended limit values of mixture ratio shift resulting from APS malfunctions are: -0.018, +0.010 mixture ratio units from the nominal.

References

1. CSM/LM Spacecraft Operational Data Book, Volume III, Mass Properties, SNA-8-D-027(III) REV 2, Amendment 88, 5 October 1970.

2. "Propulsion Systems Dispersion Analysis and Optimum Propellant Management," TRW Technical Report 11176-H060-R0-00, R. K. M. Seto, 28 October 1968.

Table LM8/4.6.1-1. APS Engine and Feed System Physical Characteristics

Engine(1)	
Engine No.	Rocketdyne S/N 0006C
Injector No.	Rocketdyne S/N 4097715
Initial Chamber Throat Area (in^2)	16.336
Nozzle Exit Area (in^2)	749.073
Initial Expansion Ratio	45.854
Injector Resistance (lb_f-sec^2/lb_m-ft^5)@ time zero and 70°F	
Oxidizer	12586.
Fuel	20342.
Feed System	
Total Volume (Pressurized, Check Valves to engine interface)(ft^3)(2)	
Oxidizer	36.89
Fuel	37.00
Resistance, Tank Bottom to Engine Interface (lb_f-sec^2/lb_m-ft^5) at 70°F(3)	
Oxidizer	2580.48
Fuel	4102.56

(1) Rocketdyne Log Book, "Acceptance Test Data Package for Rocket Engine Assembly-Ascent LM-Part No. RS000580-001-00, Serial No. 0006," 3 February 1969.

(2) NASA Memorandum EP23 - 46 - 69, "Propellant Load Parameters for the DPS and APS of LM-5 Through LM-9 and the Estimated Parameters for LM-10 and Subsequent," from EP/Chief, Propulsion and Power Division to PD/CHief, Systems Engineering Division.

(3) GAC Memorandum LMO-271-844, "A/S Hydraulic Resistance LM 7, 8, 9," W. Salter, 6 December 1969.

Table LM8/4.6.1-2. APS Weight Characteristics

Weight APS at Lunar Liftoff lbm:

Inert Weight		5,521.4
APS Propellant Loaded & at Lunar Liftoff[1]		
Oxidizer	3,217.8	
Fuel	2,007.8	
Total APS Propellant		5,225.6
TOTAL		10,747.0[2]

Unusable Propellant, lbm:

	Oxidizer	Fuel
Trapped Propellant[3]		
Fill and Drain Lines	0.8	0.2
Engine (to SOV)	0.3	0.2
Interconnect to RCS	2.3	1.6
Isolation Squib Bypass and Miscellaneous	0.1	0.2
Subtotal	3.5	2.2
Residuals in Tank[3]		
Tank Wetting	1.0	1.0
"0" G Can	2.0	1.2
Thrust Vector Deviation	0.6	0.4
Unporting Prevention	11.3	7.1
Propellant Vapor	13.8	1.0
Subtotal	28.7	10.7
Consumed by RCS through[4] Interconnect	-	-
Transient Operation[3]	3.7	3.1
Subtotal	3.7	3.1
Total Unusable Propellant	35.9	16.0

(1) "CSM/LM Spacecraft Operational Data Book," Volume III, Mass Properties, SNA-8-D-027(III), Revision 2, Amendment 84, 11 August 1970.
(2) "The Spacecraft Operational Trajectory for Apollo 14 (Mission #3)," MSC Internal Note 70-FM-141, September 25, 1970.
(3) "CSM/LM Spacecraft Operational Data Book," Volume III, Mass Properties SNA-8-D-027 (III), Revision 2, Amendment 88, 5 October 1970.
(4) RCS usage of APS propellants has not been included in this simulation.

Table LM8/4.6.1-3
Mission H3 Preflight Performance Prediction Summary
(NASA DATA SOURCE)

PARAMETER	NOMINAL PERFORMANCE					UNCERTAINTIES Three Standard Deviations
	1st Burn				2nd Burn (1)	
	Ignition +10 sec	Ignition +220 sec	Ignition +436 sec	Integrated Average	Ignition +2 sec	
Thrust (FVAC), lbf	3502.	3472.	3470.	3476.	3637.	101.4
Specific Impulse (ISP) lbf-sec/lbm	310.3	310.4	309.9	310.3	307.4	3.50
Mixture Ratio (MR)	1.607	1.601	1.597	1.601	1.682	0.0258
Chamber Pressure (PC) psia	123.4	123.9	122.9	123.6	129.3	3.15
Oxidizer Flowrate (WDTOE), lbm/sec	6.956	6.885	6.886	6.896	7.419	0.193
Fuel Flowrate (WDTFE), lbm/sec	4.329	4.300	4.312	4.307	4.412	0.121
Usable Oxidizer (WOX), lbm	3112.	1660.	234.	--------	159.	------
Usable Fuel (WFL), lbm	1948.	1043.	114.	--------	105.	------
ΔV (DVTP), ft/sec	105.	2610.	6054.	--------	40.	------

(1) These values may be used as the integrated average values for the second burn, however, it should be noted that such values are highly dependent on burn time and until the RCS contribution to total ΔV is known, the main engine burn time is uncertain.

Table LM8/4.6.1-4. APS Simulation Parameters Uncertainties

(NASA DATA SOURCE)

PARAMETER	THREE STANDARD DEVIATIONS (3σ)	THREE STANDARD DEVIATIONS (%)
Characteristic Exhaust Velocity (C*)[(1)], ft/sec	61.8	1.08
Specific Impulse (I_{sp})[(1)], lbf/sec/lbm	3.50	1.13
Engine Oxidizer Resistance, lbf-sec^2/lbm-ft^5	344.	2.7
Engine Fuel Resistance, lbf-sec^2/lbm-ft^5	499.	2.4
Propellant Feed System Oxidizer Resistance, lbf-sec^2/lbm-ft^5	29.37	1.14
Propellant Feed System Fuel Resistance, lbf-sec^2/lbm-ft^5	38.4	0.94
Propellant Tank Ullage Pressures, psia	4.0	2.23
Propellant Tank Ullage ΔP, psia	0.5	----
Propellant Bulk Temperatures, °F	5.0	7.14
Propellant Bulk ΔT, °F	1.5	----
Ablative Engine Throat Area, in^2	0.639	3.91

(1) Engine parameters at standard interface conditions include characterization uncertainties, instrumentation uncertainties, and engine repeatability.

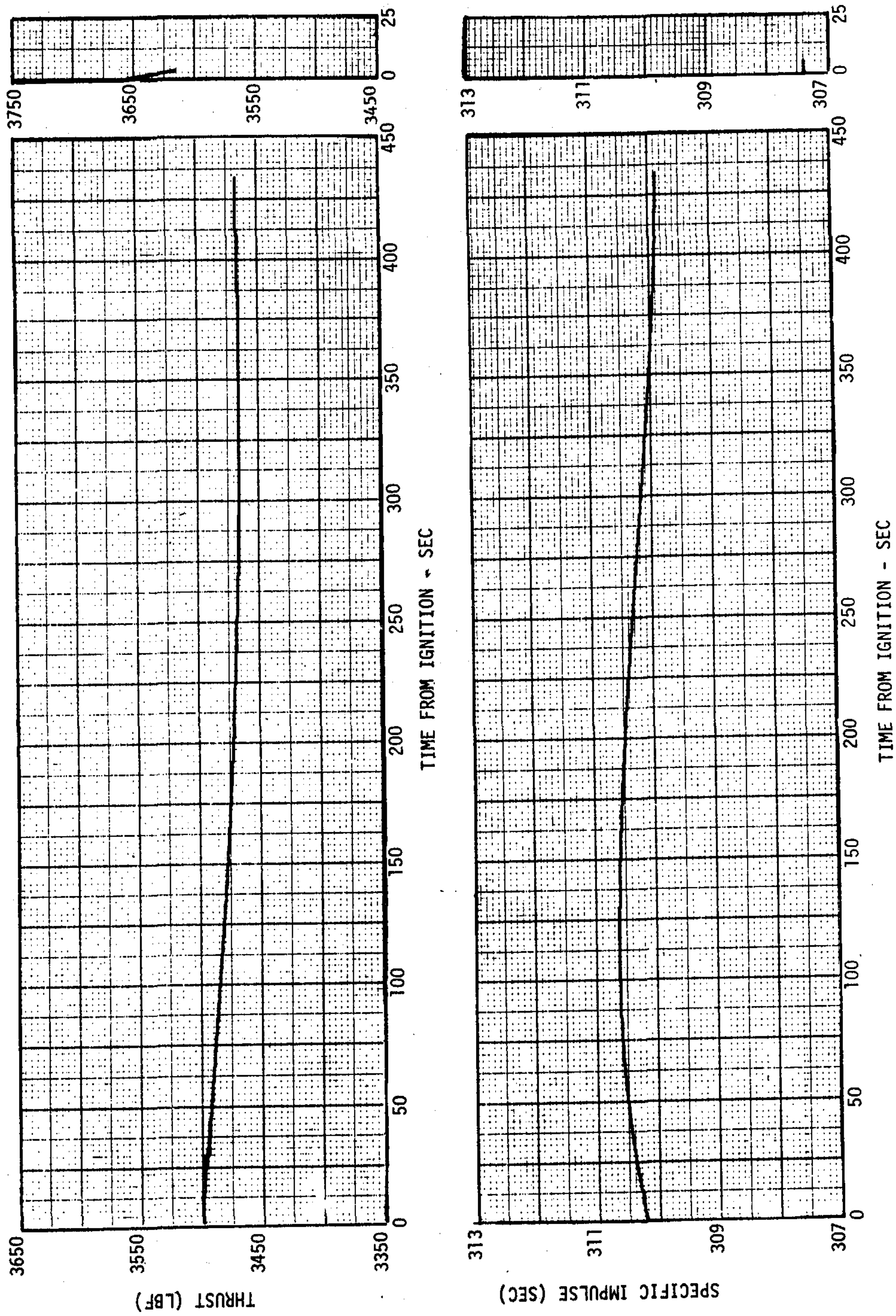

Figure LM8/4.6.1-1 Mission H3 APS Preflight Performance Prediction - Thrust and Specific Impulse Vs. Time

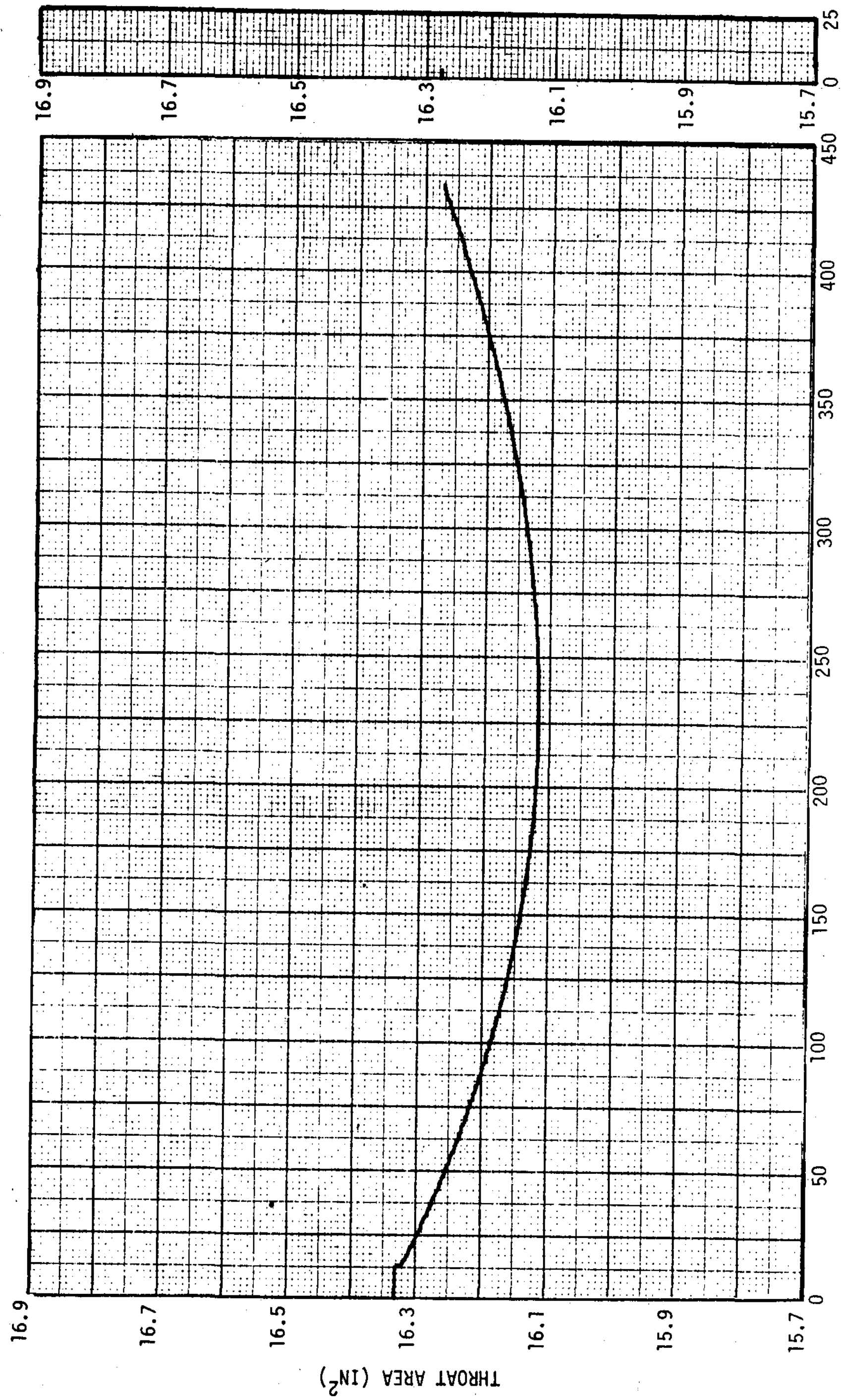

Figure LM8/4.6.1-2 Mission H3 APS Preflight Performance Prediction - Throat Area Vs. Time

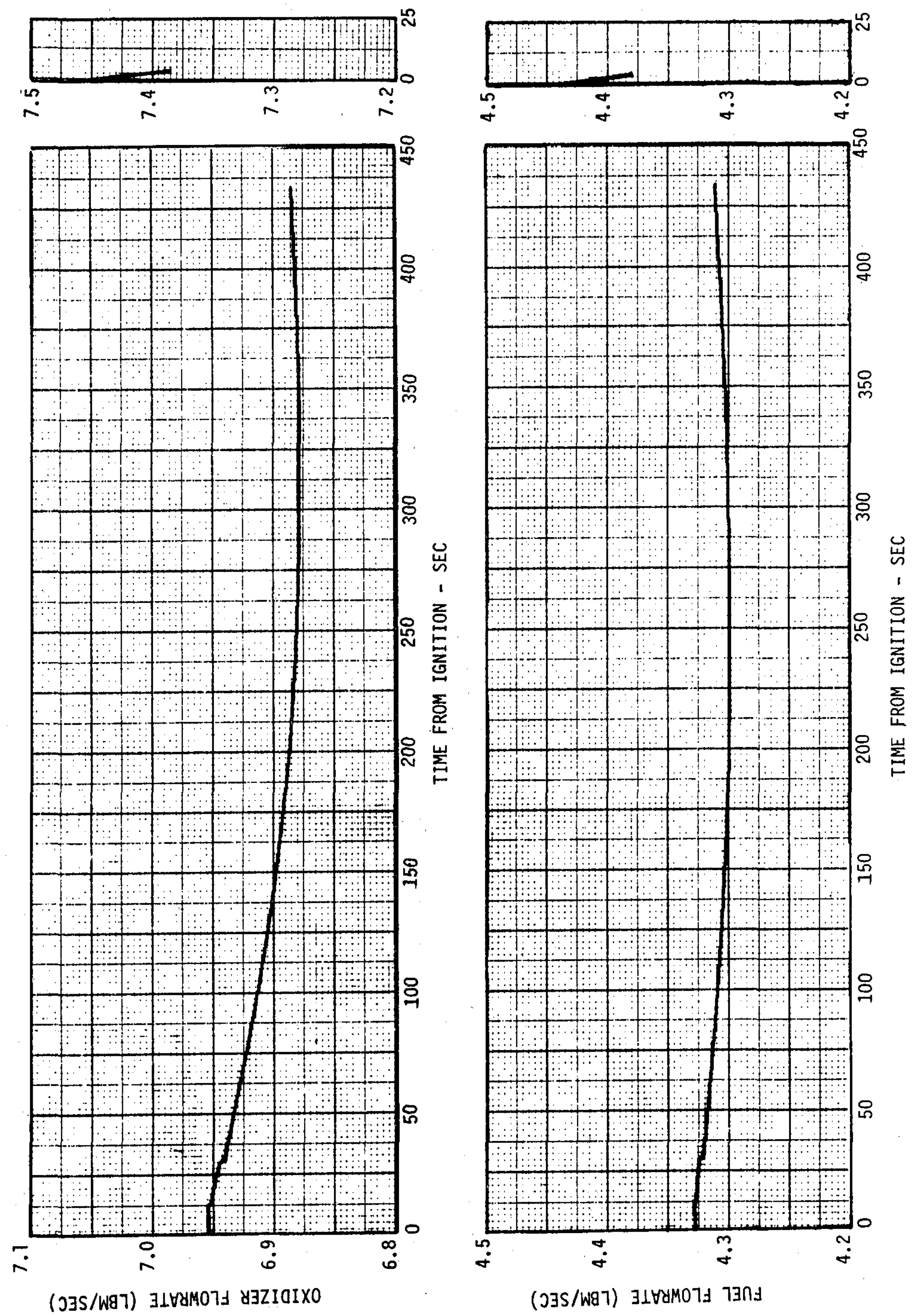

Figure LM8/4.6.1-3 Mission H3 APS Preflight Performance Prediction - Oxidizer and Fuel Flowrates Vs. Time

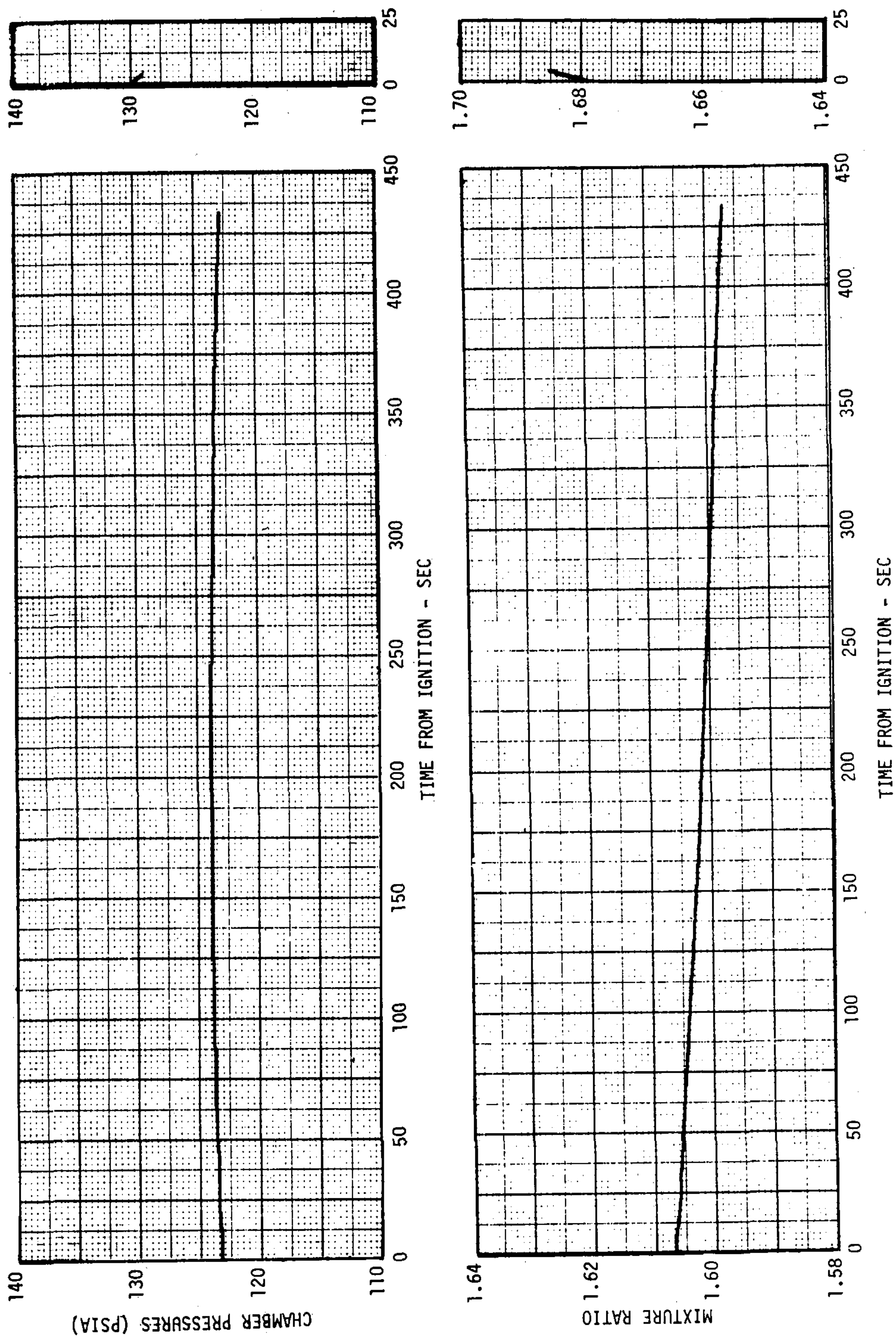

Figure LM8/4.6.1-4 Mission H3 APS Preflight Performance Prediction - Chamber Pressure and Mixture Ratio Vs. Time

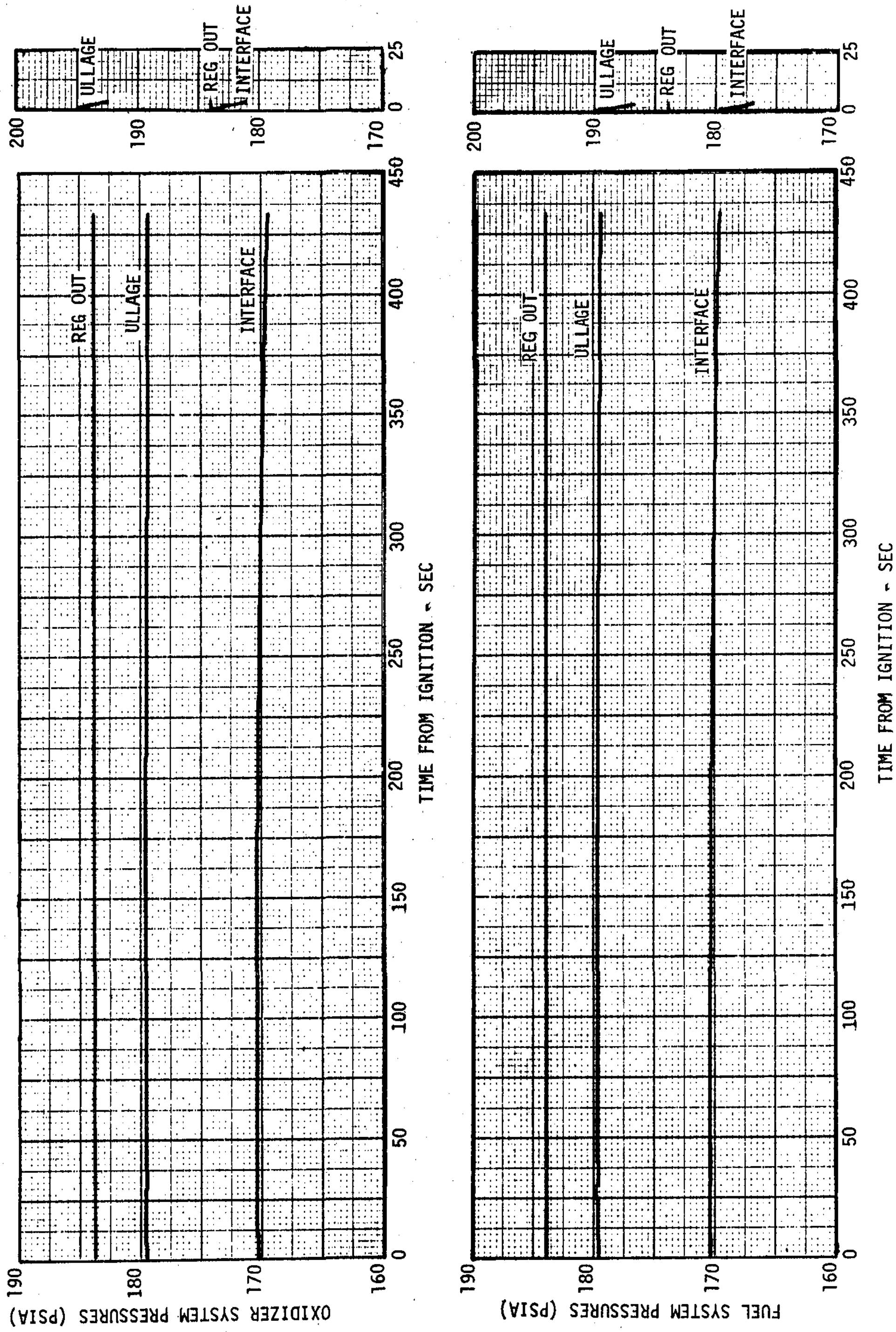

Figure LM8/4.6.1-5 Mission H3 APS Preflight Performance Prediction - Fuel and Oxidizer System Pressures Vs. Time

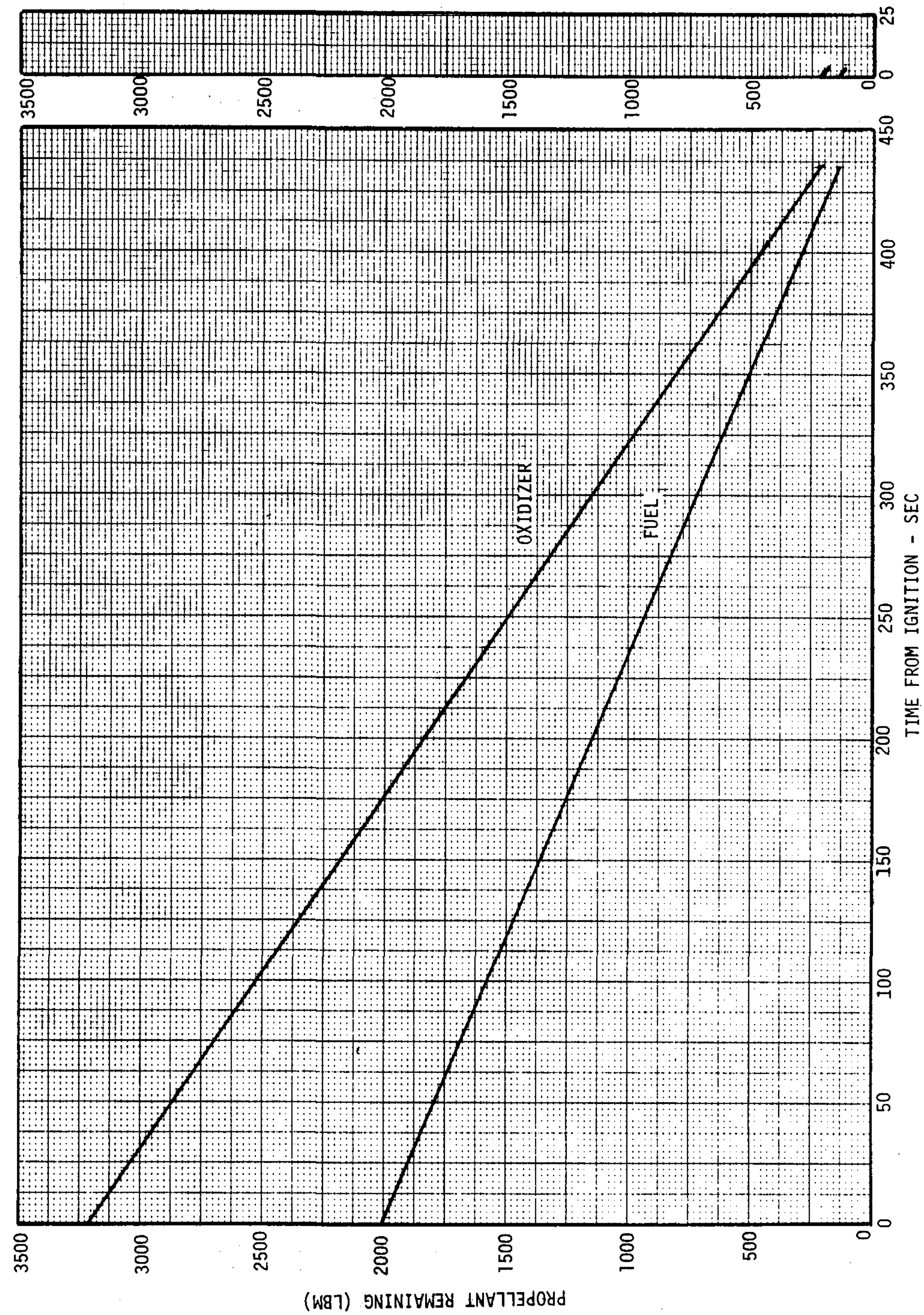

Figure LM8/4.6.1-6 Mission H3 APS Preflight Performance Prediction - Propellant Quantities Vs. Time

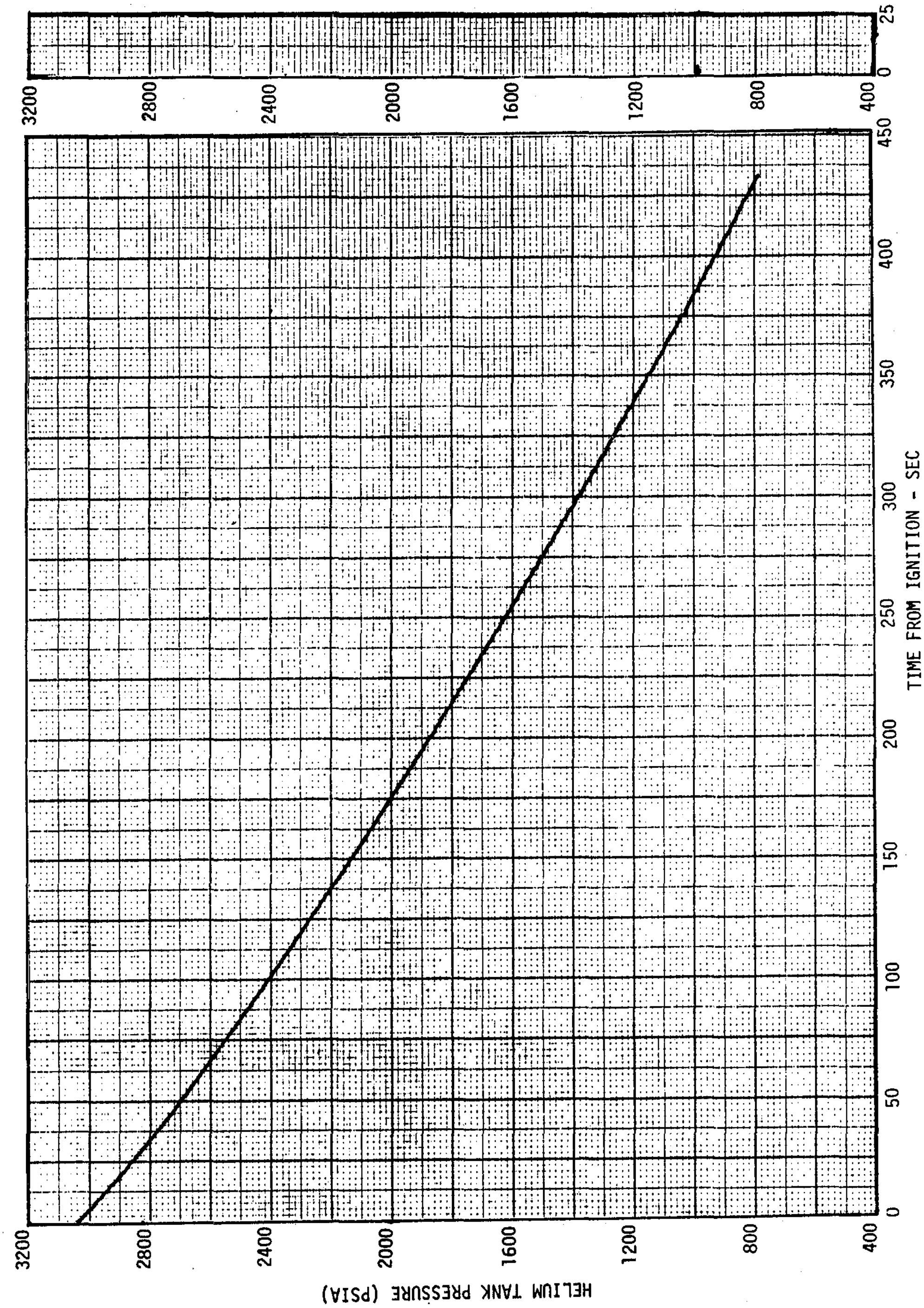

Figure LM8/4.6.1-7 Mission H3 APS Preflight Performance Prediction - Helium Tank Pressure Vs. Time

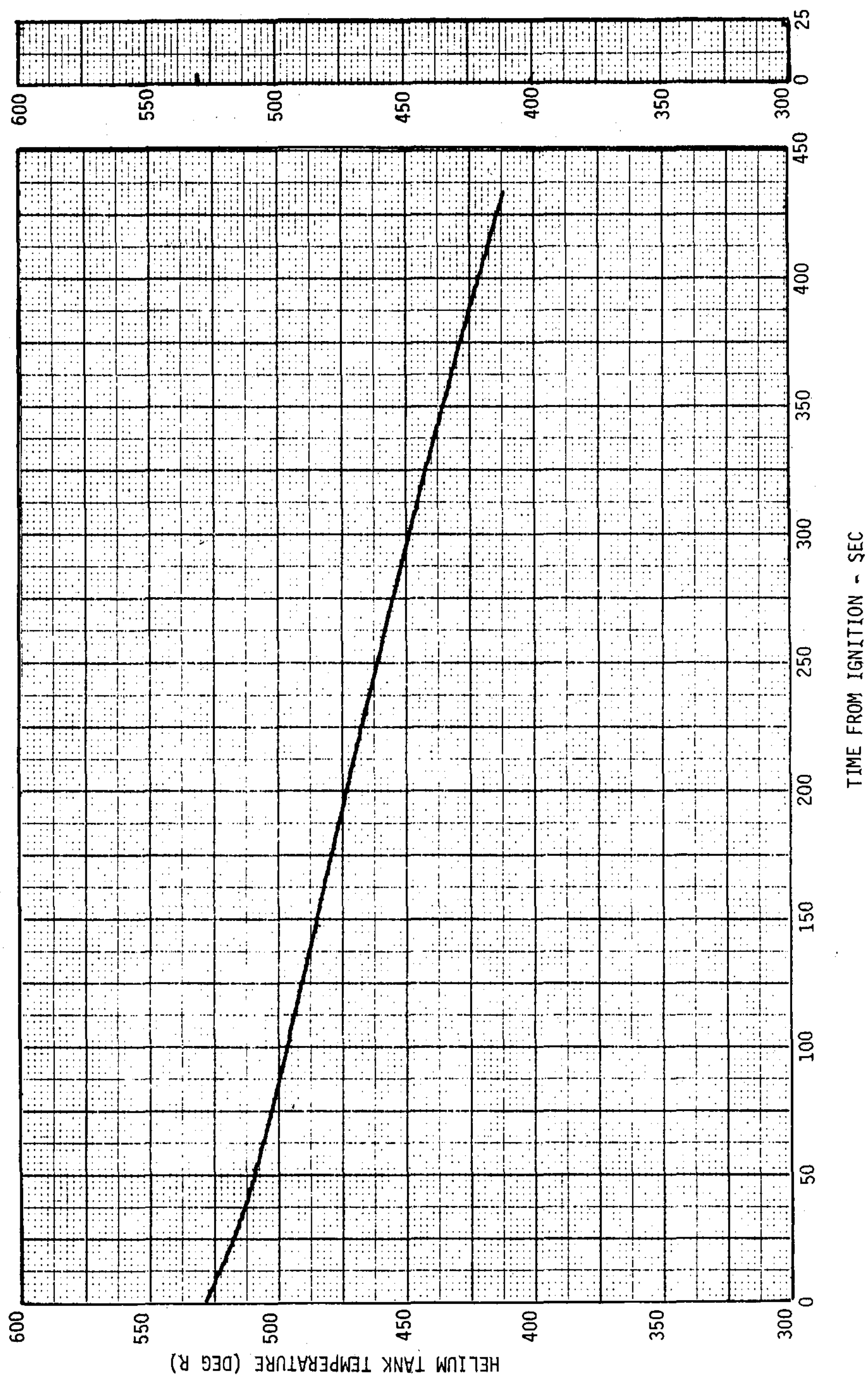

Figure LM8/4.6.1-8 Mission H3 APS Preflight Performance Prediction - Helium Tank Temperature Vs. Time

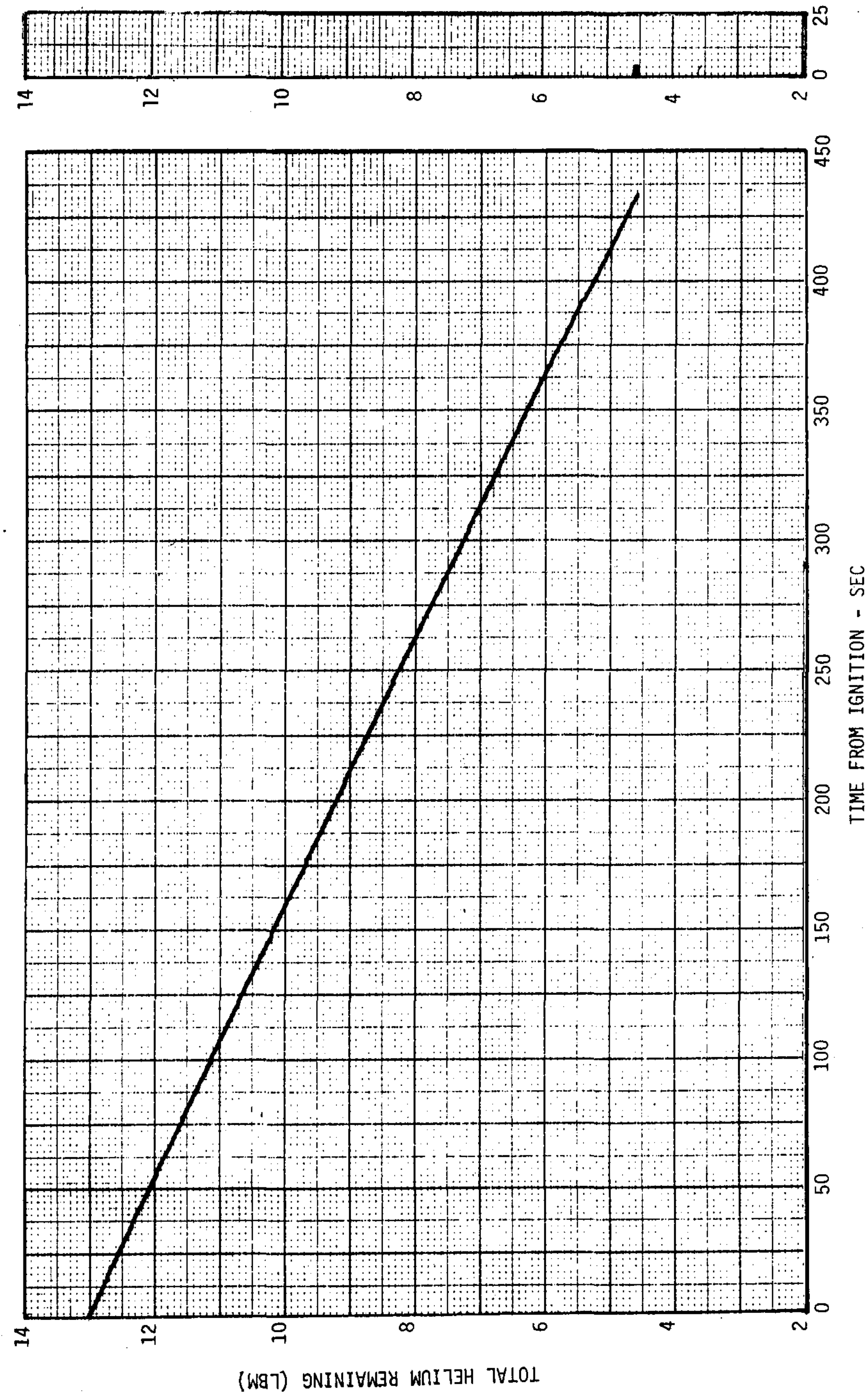

Figure LM8/4.6.1-9 Mission H3 APS Preflight Performance Prediction - Total Helium Remaining Vs. Time

LM8/4.6.8 Thrust Vector Change with Burn Time

The initial thrust vector displacement on Engine Number 0006C is Z = -0.016 inches, Y = -0.027 inches. This information is based on R/D acceptance test # 374-485 conducted on 12/9/68.

LM8/4.6.9 Ascent Propulsion Preflight Thermal Analysis

A change in burn profile is scheduled for LM-8 and subs. A main burn of approximately 440-460 seconds is still required to lift-off from the moon and place the LM ascent stage in a lunar orbit. The engine in addition will perform a short 5 second restart approximately 45 minutes after shutdown. The ascent engine now performs the TPI burn which prior to LM-8 was performed by the RCS engines. The short burn actually cools the injector because of cold propellant flow. The injector (aluminum) is well coupled thermally to the combustion chamber case and therefore the case is slightly cooled also. The cooling of the engine is for a short period of time and after 5-10 minutes temperatures return almost to their pre-restart temperature. The effect of a short restart can be seen in R 7804 Final Report Swip Qual Engine Test of the LM APS Program Vol. I. The analysis presented in LMO 510-1260 is still applicable and will be slightly conservative (higher temperature).

LM8/4.6.12 Ascent Engine Regulator Performance

Figure LM8/4.6.12-1 shows performance characteristics for the LM-8 Class I primary regulator, Serial No. 134. This is a flight prediction based on KSC check-out at 3500 psia inlet pressure.

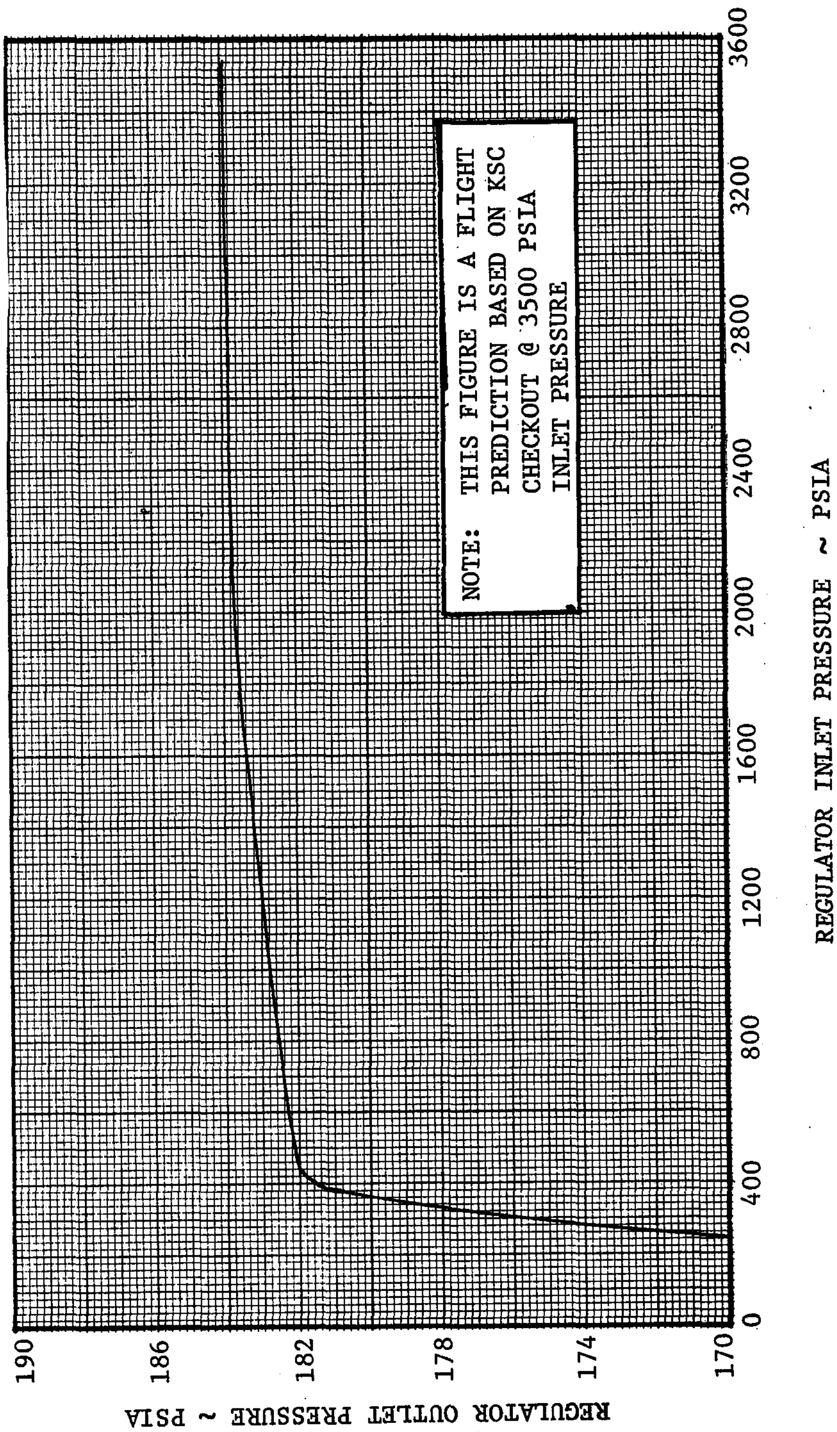

Figure LM8/4.6.12-1. Ascent Engine Regulator Performance

LM8/4.7.1 Mission H3 (LM-8) DPS Preflight Analysis (NASA DATA SOURCE)

The data presented herein are valid only for the system at nominal conditions and do not represent the boundary conditions of operation for the system. Therefore, these values should not be used as limit values.

The nominal mission duty cycle for the Mission H3/LM-8 DPS is presented in Figure LM8/4.7.1-1. The spacecraft weight and propellant loading used in the simulation are given in Table LM8/4.7.1-1. Descent engine and feed system physical characteristics are shown in Table LM8/4.7.1-2.

It should be noted that all performance parameters presented are for DPS operation only, and do not include RCS contributions to thrust or velocity gain. The predicted RCS propellant usage was simulated during the burns as a weight change.

The helium regulator characteristics used to establish the DPS propellant tank ullage pressures were derived from GAEC PIT data. Propellant temperatures measured during Missions G and H1(68°F) were assumed to be representative of those to be expected during Mission H3.

A summary of the Mission H3 (LM-8) performance prediction is given in Table LM8/4.7.1-3 and Figures LM8/4.7.1-1 through LM8/4.7.1-9. Figures LM8/4.7.1-10 and LM8/4.7.1-11 present the vehicle and engine related effective specific impulse as functions of burn time. A prediction of the supercritical helium tank pressure and mass profiles are presented in Figures LM8/4.7.1-12 and LM8/4.7.1-13. The dispersions associated with thrust, specific impulse, and mixture ratio are given in Figures LM8/4.7.1-14 through LM8/4.7.1-16, respectively.

The vehicle effective specific impulse for the descent burn was 300.4 seconds. This value includes the effect of approximately 87 lbm of consumables which are expelled from the spacecraft during the time from PDI to lunar touchdown. The value of the engine effective specific impulse, which does not include the effect of the consumables other than propellant, was 302.5 seconds. It should be noted that the effective specific impulse is not only a function of engine performance but is dependent on vehicle initial mass, mass changes with time, and velocity requirements. Substantial deviations from the conditions of the simulation will invalidate the use of this effective specific impulse. The 1-sigma variation in effective engine specific impulse is ±1.55 seconds for the simulation. The effective vehicle mixture ratio is 1.5983 and the 1-sigma variation is ±0.0075.

The LM-8 DPS shutoff valve malfunction characterization data are as follows: an AB valve malfunction will result in shifts of -0.002, +0.27 seconds, and -207 lbf for mixture ratio, specific impulse, and

LM8/4.7.1 (Continued)

thrust, respectively; while a CD valve malfunction will result in shifts of -0.016, +0.16 seconds, and -198 lbf, respectively, for the given parameters. These data are applicable to FTP operation only.

During the nominal mission, the low level sensor should not be activated prior to the nominal touchdown time (690 seconds after descent burn ignition). If the vehicle is hovering the oxidizer low level sensor should be activated at approximately 710 seconds (assuming a nominal GDA trim angle of 1.06°) (See Table LM8/4.7.1-1). The calculation does not account for dispersion in GDA angle. The approximate hover time from the low level signal to oxidizer depletion is predicted to be 122 seconds or 832 seconds after engine ignition.

A docked LM-8 Descent Propulsion System (DPS) burn-to-propellant depletion simulation was made using the Descent Ascent Monte Carlo Program (DAMP).

It was assumed that at engine ignition, the LM was docked with the CSM. The mission duty cycle consisted of a minimum throttle (approximately 12.9% of full thrust) segment of 6 seconds, 20 seconds at 40% of full throttle, with the remainder of the burn at the Fixed Throttle Position (FTP). The burn was terminated when either the usable oxidizer or fuel was depleted.

The initial spacecraft weight was assumed to be 98,135.5 lbm with 11,307.3 lbm and 7,041.3 lbm of tanked oxidizer and fuel, respectively. Depletion occurs when the tanked quantities reach 102.7 lbm for oxidizer or 14.8 lbm for fuel.

At 576.0 seconds after ignition, oxidizer depletion occurred with approximately 29.9 lbm of usable fuel remaining. The velocity change for the burn was 1,992.9 ft/sec. The effective engine specific impulse, which neglects consumables other than propellants that are expelled from the spacecraft during the burn, was 301.59 seconds. The effective vehicle specific impulse was 300.35 seconds. The average mixture ratio was 1.595.

Figures LM8/4.7.1-17 through LM8/4.7.1-27 present DPS engine parameters for the burn.

Chamber pressure versus commanded thrust for zero, nominal, 3-σ maximum predicted, and maximum allowable throat erosion (35%) is shown in Figure LM8/4.7.1-28.

Table LM8/4.7.1-1

LM-8 Descent Propulsion System Weight Characteristics[1]

Spacecraft Weights (lbm)

DPS Stage Inert		4813.6
Loaded Propellant		18444.2
DPS Oxidizer	11367.8	
DPS Fuel	7076.4	
Loaded APS Stage with Crew		10794.9
LM Weight at P.D.I.		34052.7

UNUSABLE PROPELLANTS

	Oxidizer	Fuel
TRAPPED PROPELLANT	(60.4)[2]	(35.2)[2]
Fill Lines	0.2	0.1
Engine	12.2	6.4
Balance Lines	11.3	7.3
Branch Lines	17.0	8.0
Common Lines	19.0	8.1
Isolated SQ Bypass and Miscellaneous	0.7	0.7
Heat Exchanger	0.0	4.6
RESIDUALS IN TANKS	(102.7)[2]	(14.8)[2]
Tank Wetting	2.0	2.0
Zero-g Can	8.6	5.2
Center of Gravity (Thrust Vector)	98.0	19.0
Engine and Valve Operation	2.6	2.8
Propellant Vapor	19.0	2.5
Heat Exchanger*	-27.5	-16.7
TOTAL UNUSABLES	163.1	50.0

*Considered usable to burn to depletion

Note: Unusables are defined as that propellant which is physically unavailable to the engine.

[1]These mass properties were used for the purpose of this analysis. Reference should be made to Volume III, Spacecraft Operational Data Book, for current official mass properties data.

[2]Parentheses present total for heading

Table LM8/4.7.1-2

LM-8 Descent Propulsion Engine
and Feed System Physical Characteristics

ENGINE	
Engine Number	1032
Chamber Throat Area, In^2	53.379 (1)
Nozzle Exit Area, In^2	2569.7 (3)
Nozzle Expansion Ratio	47.7 (3)
FEED SYSTEM	
Oxidizer Propellant Tanks, Total Ambient (4) Volume, ft^3	126.0 (3)
Fuel Propellant Tanks, Total Ambient Volume, ft^3	126.0 (3)
Oxidizer Tank to Interface Resistance, $\frac{lbf\text{-}ft^5}{lbm\text{-}sec^2}$	431.215 (2)
Fuel Tank to Interface Resistance, $\frac{lbf\text{-}ft^5}{lbm\text{-}sec^2}$	684.787 (2)

(1) TRW Report 01827-6260-R0-00, "TRW LM Descent Engine Serial No. 1032 Acceptance Test Performance Report, Paragraph 6.10," 7 October 1969.

(2) GAEC Cold Flow Tests

(3) Approximate Values

(4) 14.7 psia and 70°F

Table LM8/4.7.1-3 Mission H3 DPS Preflight Performance Prediction Summary

PARAMETER	Start of Descent Burn	28 Seconds of Descent Burn				386 Seconds of Descent Burn				406 Seconds	516 Seconds	690 Seconds Touchdown
	Nominal Performance	Nominal Performance	Standard Deviation (1σ)	Standard Deviation (%)	3σ Minimum	Nominal Performance	Standard Deviation (1σ)	Standard Deviation (%)	3σ Minimum	Nominal Performance	Nominal Performance	Nominal Performance
Throttle Position (%)	13.11 **	93.25 (FTP)	FTP	FTP	FTP	94.32 (FTP)	FTP	FTP	FTP	57.45	52.32	27.08
ISP (lbf-sec/lbm)	295.50	304.59	1.4	0.4	300.39	301.03	1.4	0.4	296.83	303.01	301.60	295.84
F (lbf)	1377	9791	40.2	.41	9670	9904	40.6	.41	9782	6032	5494	2844
MR (o/f)	1.5806	1.5990	.0044	.275	1.5858	1.5956	.0044	.275	1.5824	1.6043	1.5994	1.5972
P_c (psia)	14.5	105.3	--	--	--	98.5	--	--	--	60.7	55.1	27.7
$\dot{W}_o$ (lbm/sec)	2.854	19.777	0.10	.51	19.477	20.224	0.12	.60	19.864	12.264	11.207	5.912
$\dot{W}_f$ (lbm/sec)	1.806	12.368	0.07	.57	12.158	12.675	0.07	.55	12.465	7.645	7.007	3.701
WO*(lbm)	11286	11209	11.6	.10	11174	4046	38.3	.95	3931	3725	2351	970
WF*(lbm)	7028	6979	6.5	.09	6960	2495	22.6	.91	2427	2294	1438	574

*Propellant remaining in the tank

**TCV = 2.77 VDC

Table LM8/4.7.1-3. (Continued)
Mission H3 Final DPS Preflight Performance Prediction
Summary (Performance During Hover-To-Depletion)

Parameter	766 seconds	842 seconds Depletion (Ox)
	Nominal Performance	Nominal Performance
Throttle Position %	25.93	24.83
ISP	294.53	293.08
F	2722	2607
MR	1.5995	1.6023
Pc	25.4	23.2
$\dot{W}o$	5.687	5.477
$\dot{W}f$	3.556	3.418
WO	525.87	102.60
WF	296.16	31.75

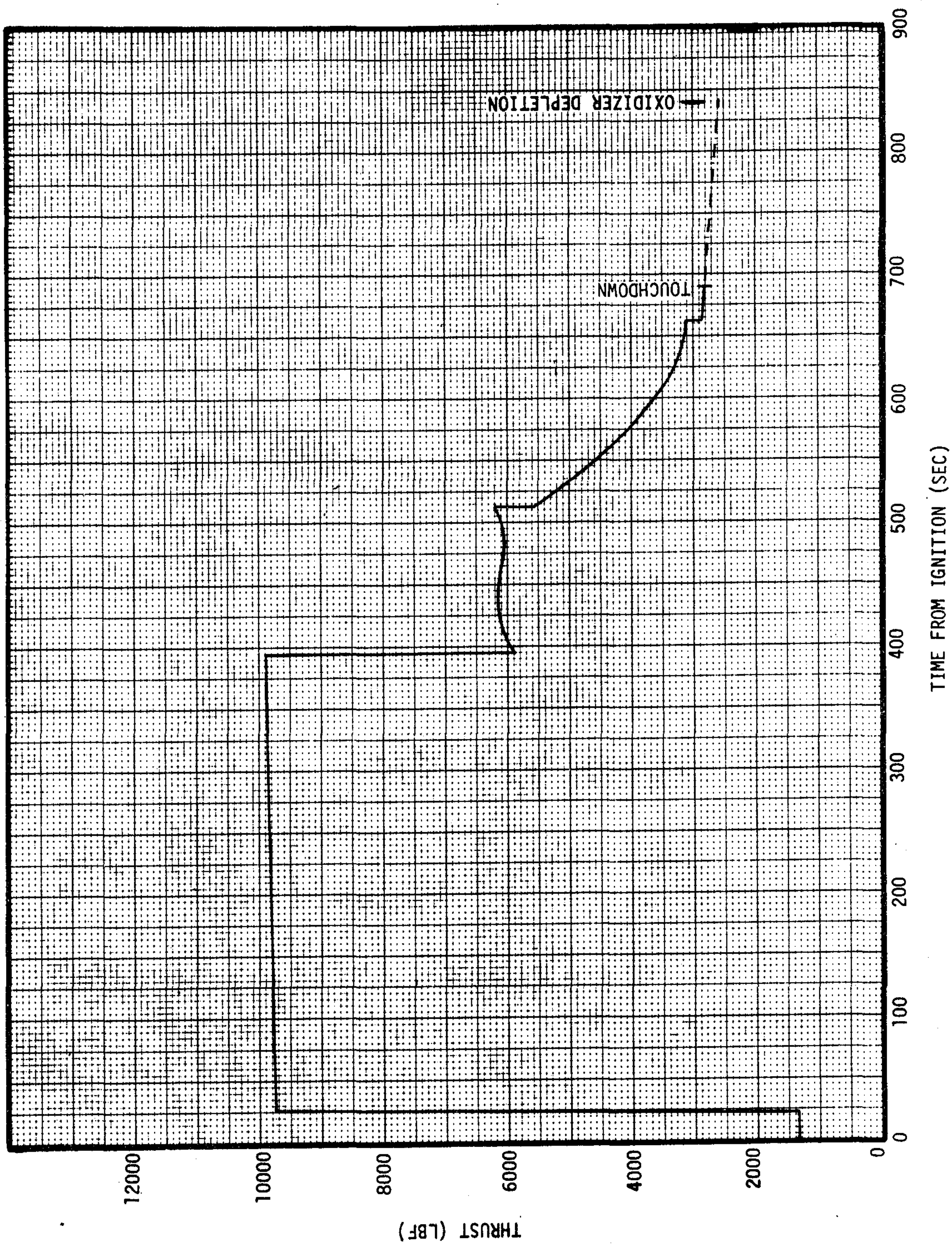

Figure LM8/4.7.1-1 Mission H3 Final DPS Preflight Performance Prediction - Thrust Vs. Time

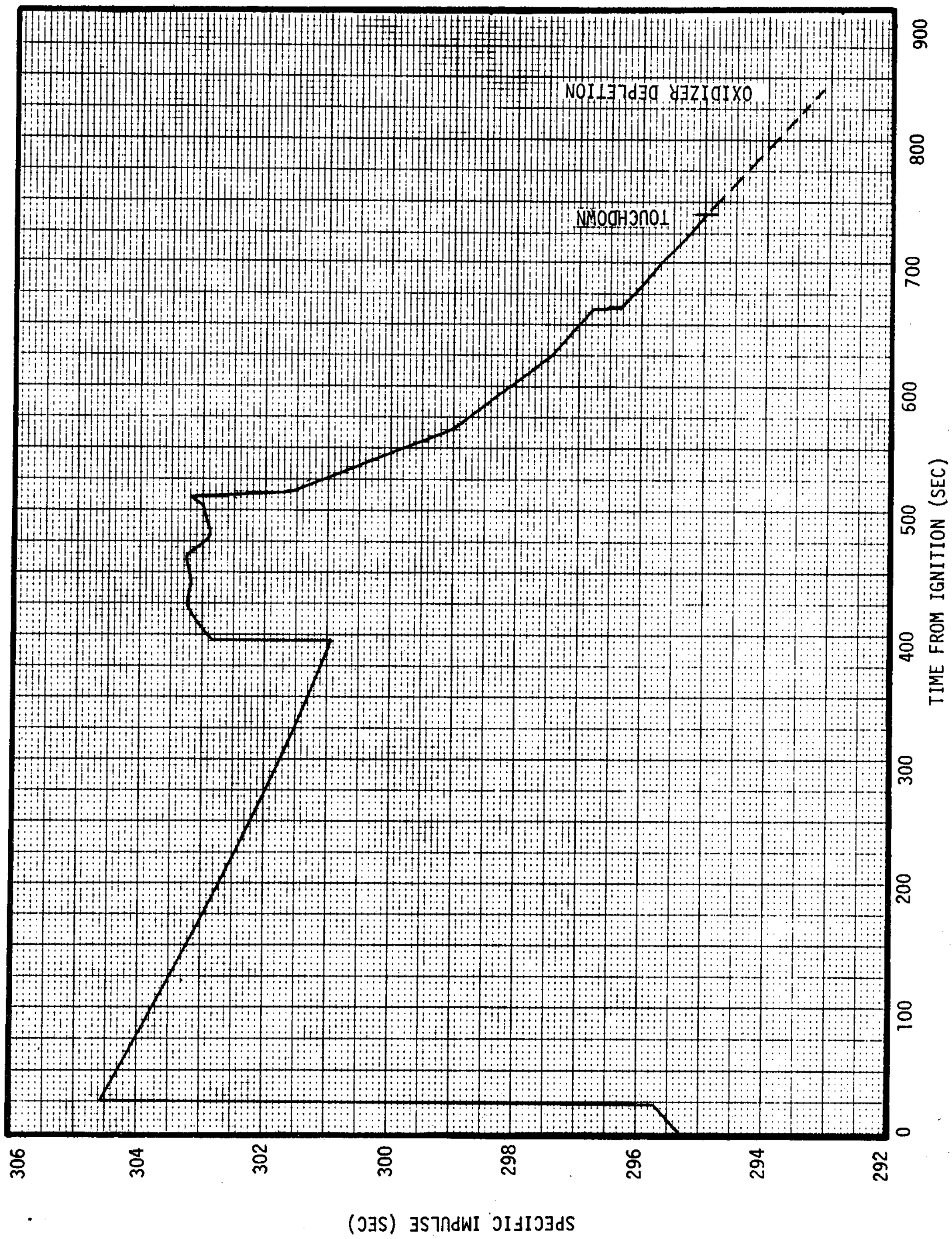

Figure LM8/4.7.1-2 Mission H3 Final DPS Preflight Performance Prediction - Specific Impulse Vs. Time

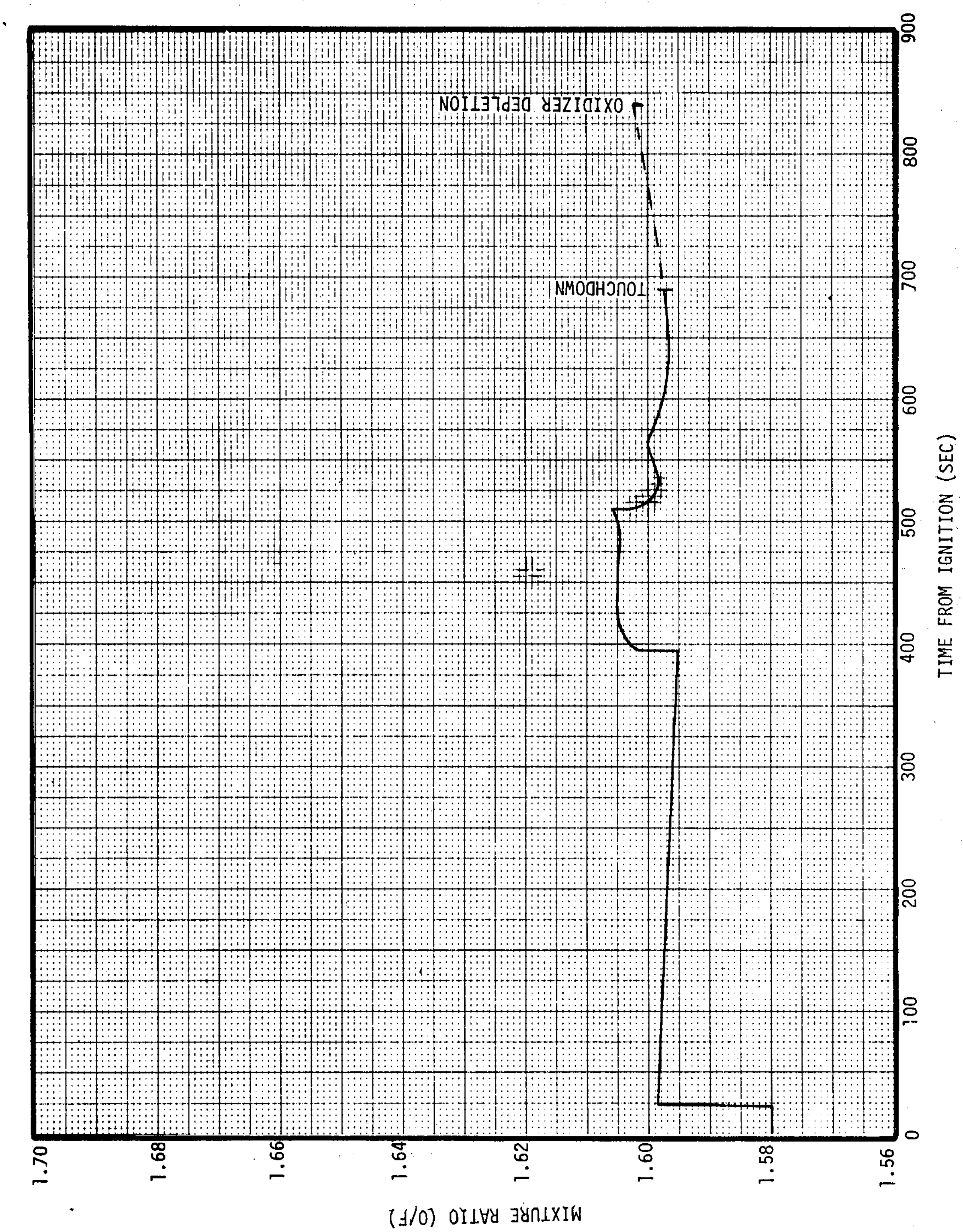

Figure LM8/4.7.1-3 Mission H3 Final DPS Preflight Performance Prediction - Mixture Ratio Vs. Time

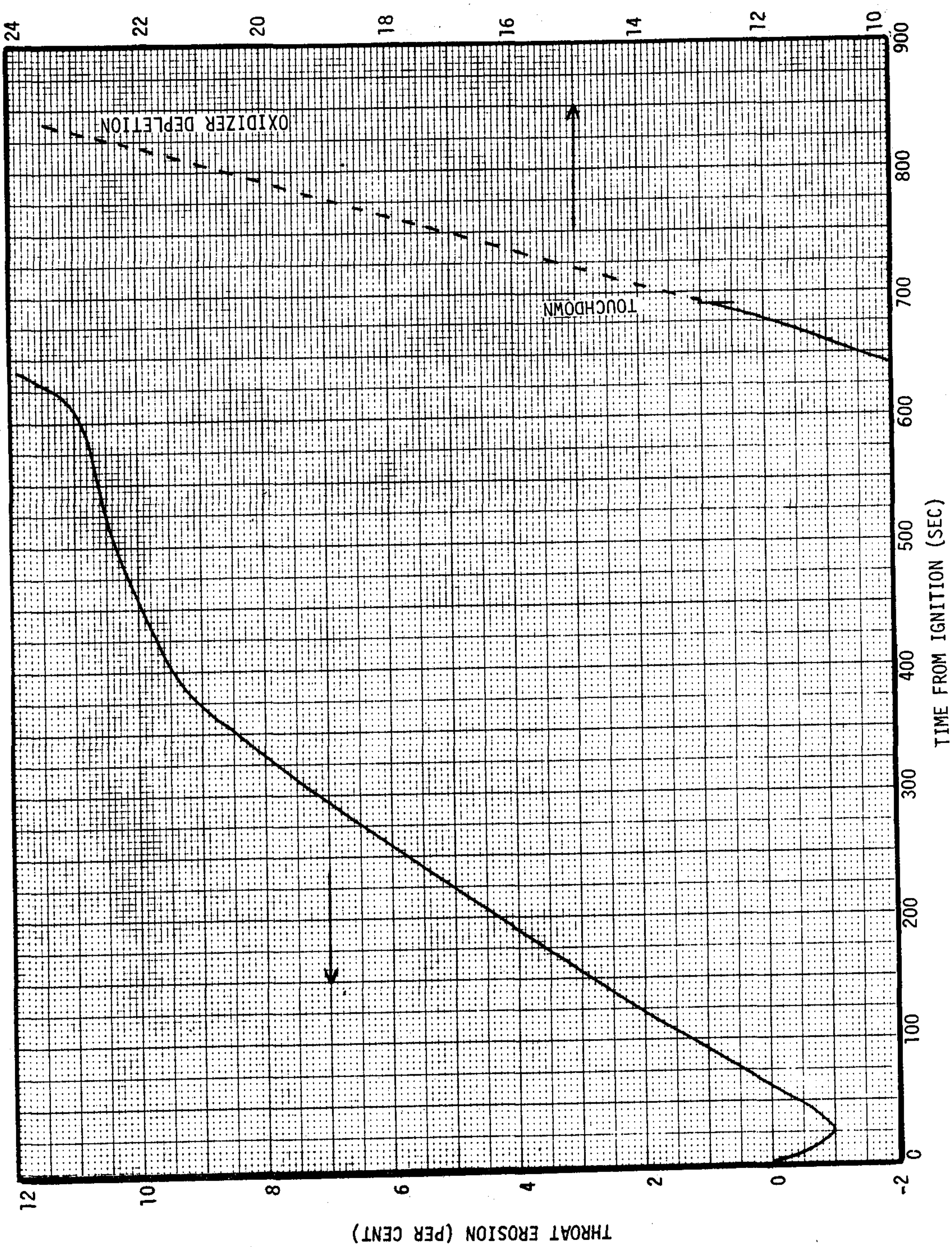

Figure LM8/4.7.1-4 Mission H3 Final DPS Preflight Performance Prediction - Throat Erosion Vs. Time

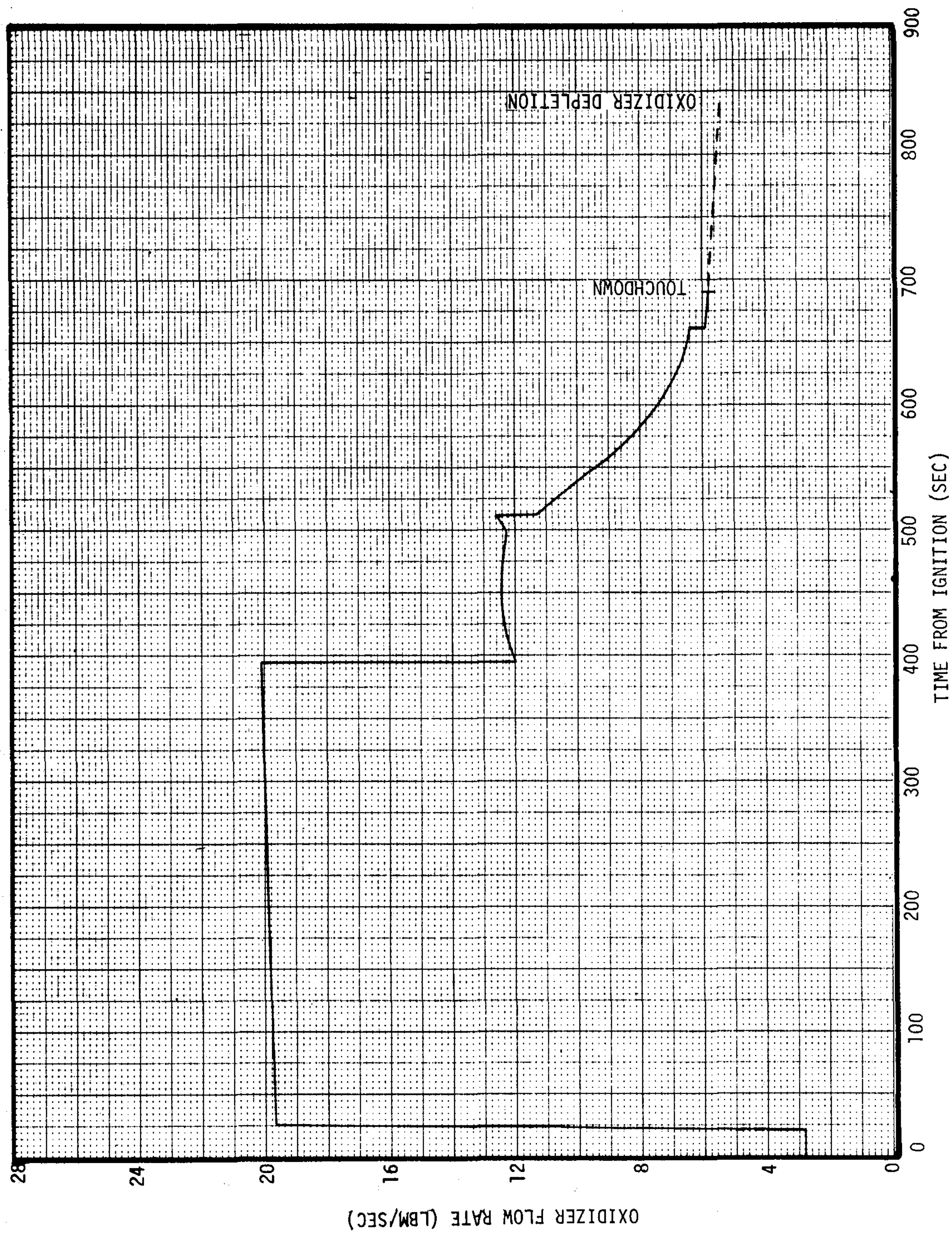

Figure LM8/4.7.1-5 Mission H3 Final DPS Preflight Performance Prediction - Oxidizer Flow Rate Vs. Time

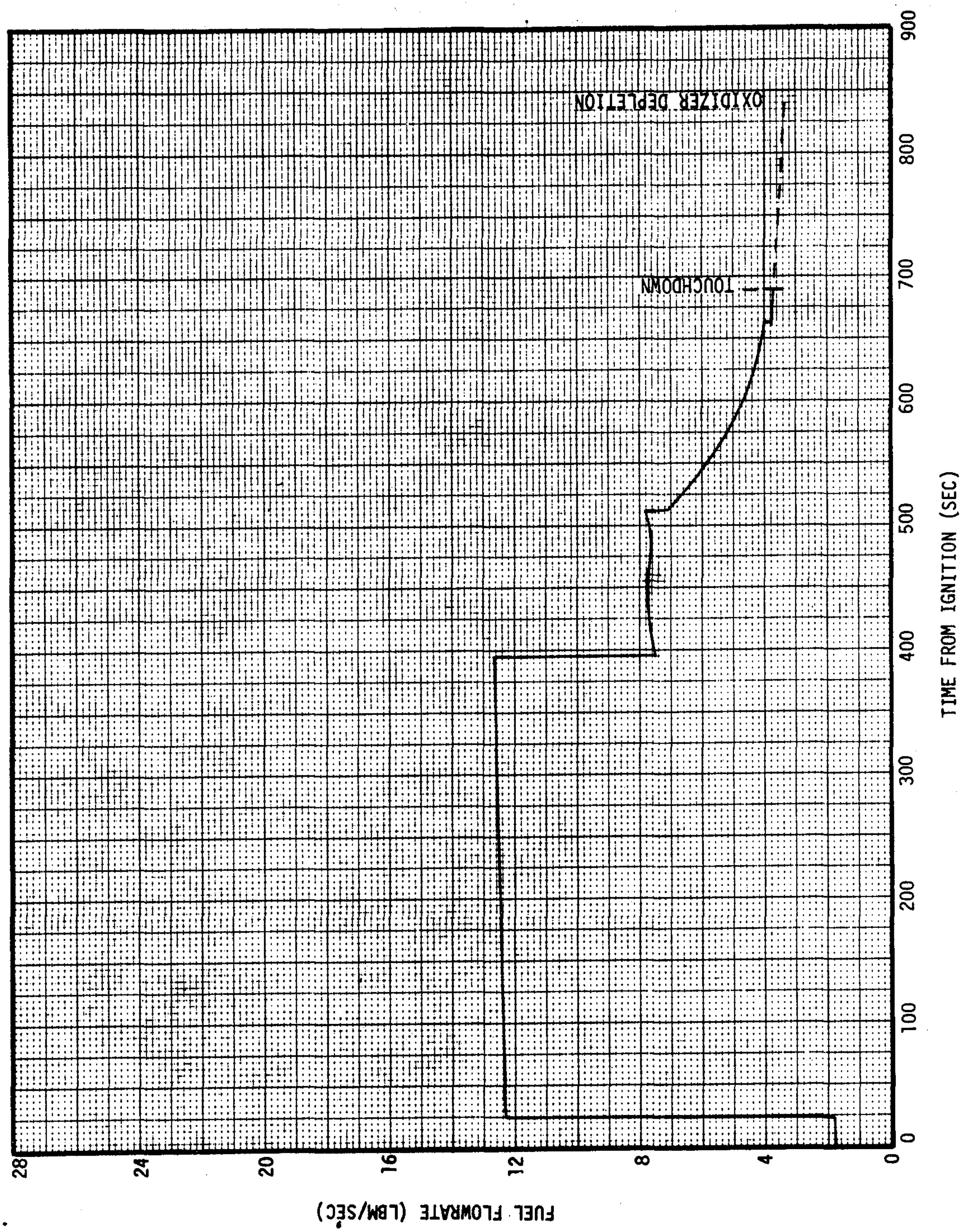

Figure LM8/4.7.1-6 Mission H3 Final DPS Preflight Performance Prediction - Fuel Flow Rate Vs. Time

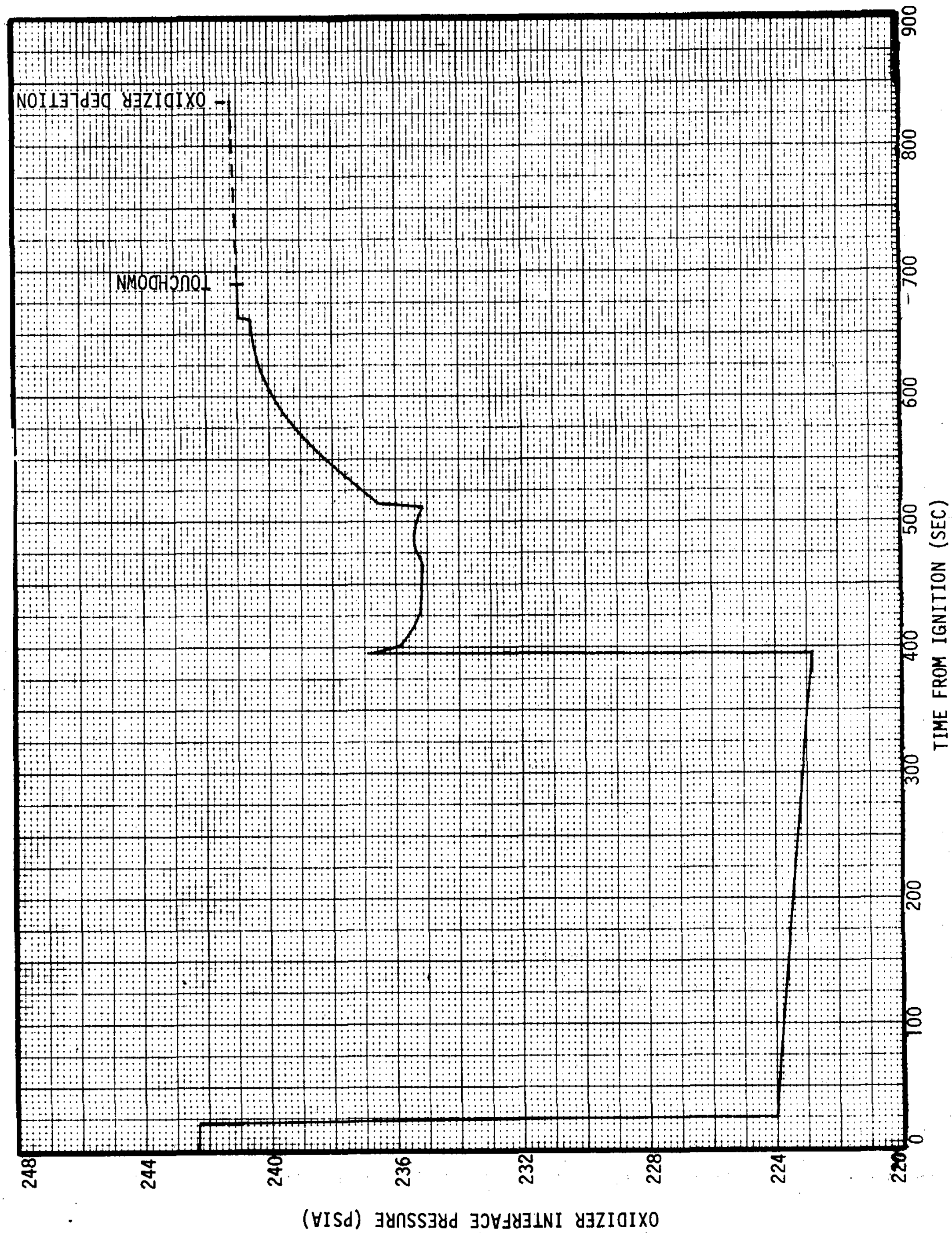

Figure LM8/4.7.1-7 Mission H3 Final DPS Preflight Performance Prediction - Oxidizer Interface Pressure Vs. Time

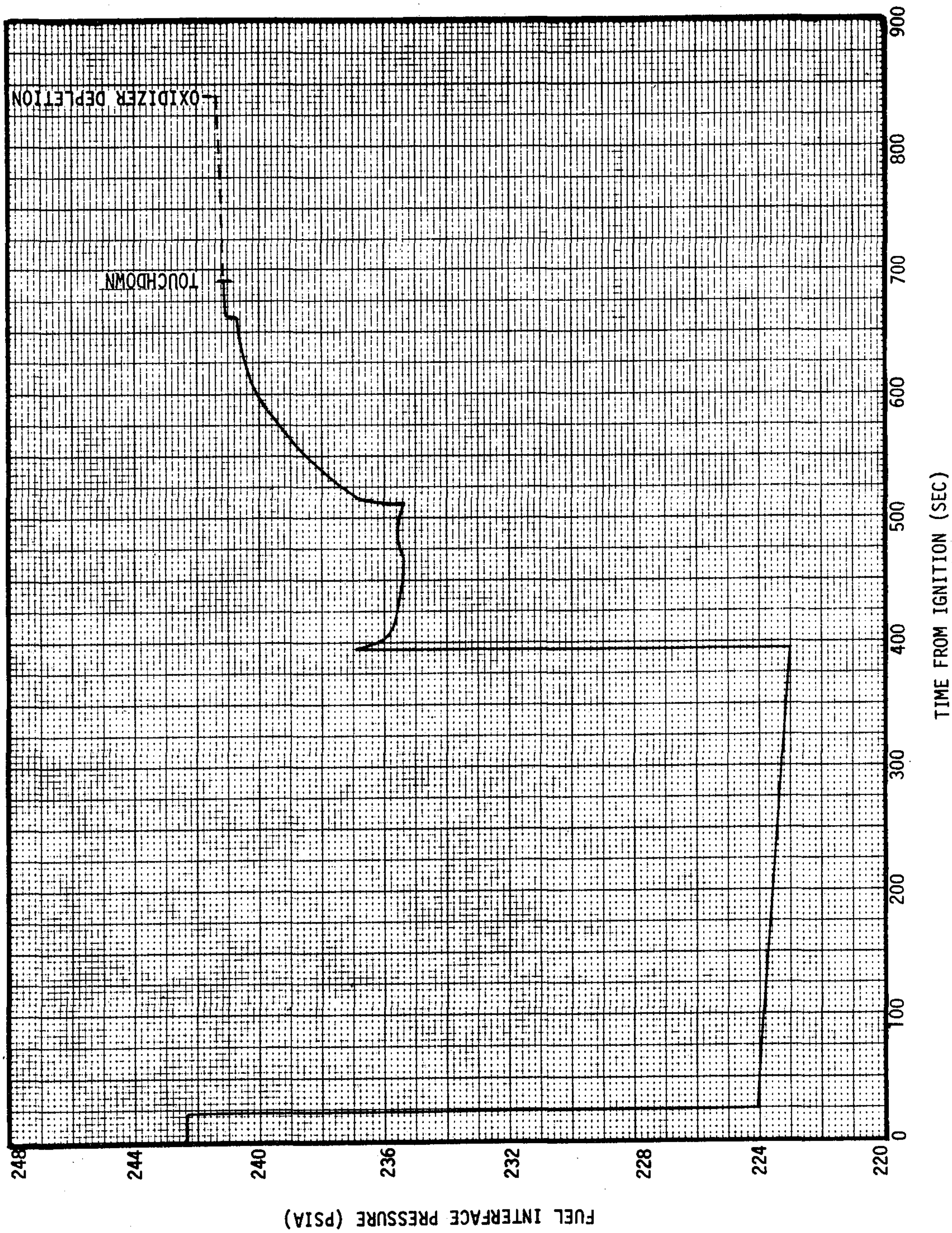

Figure LM8/4.7.1-8 **Mission H3 Final DPS Preflight Performance Prediction - Fuel Interface Pressure Vs. Time**

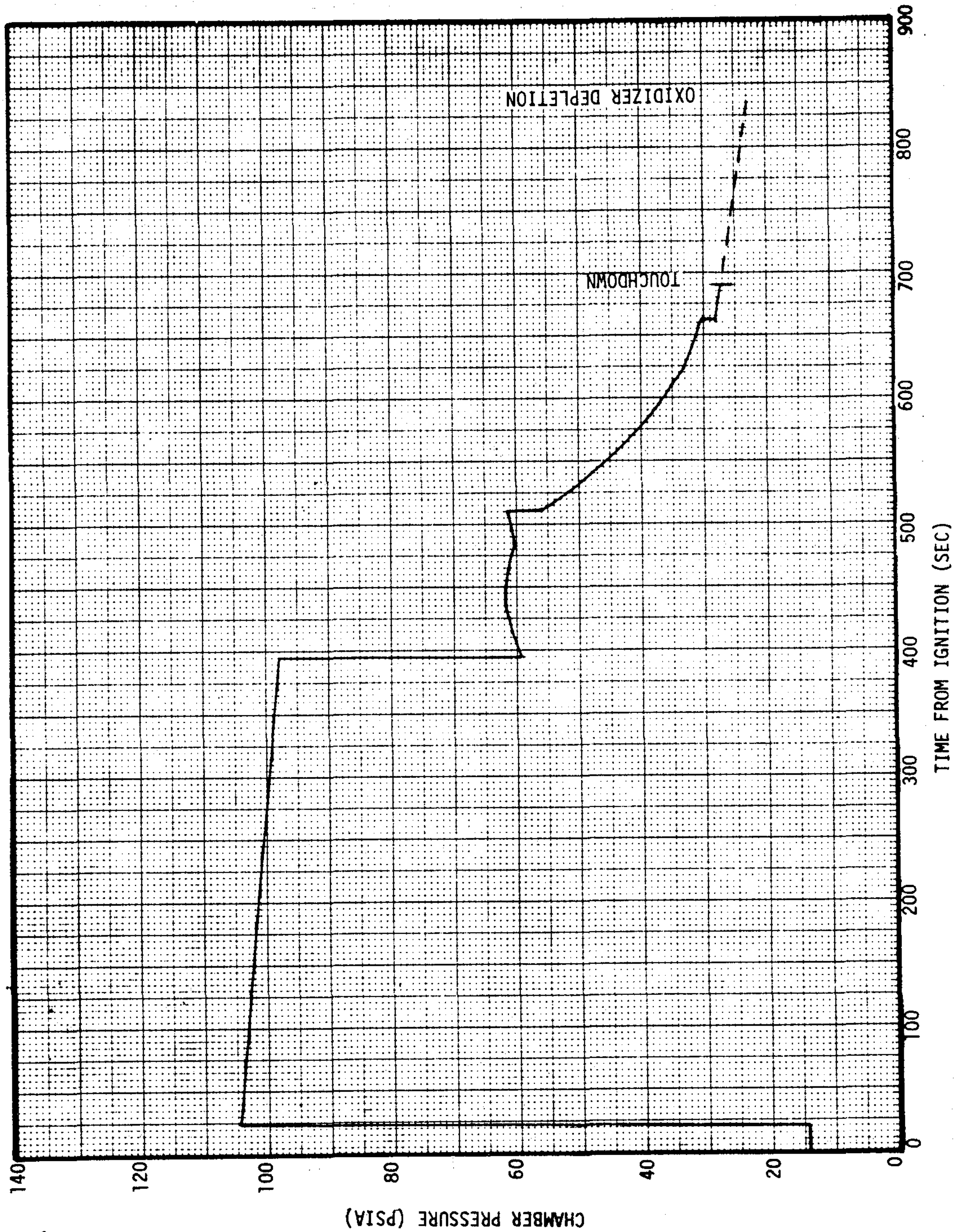

Figure LM8/4.7.1-9 Mission H3 Final DPS Preflight Performance Prediction - Chamber Pressure Vs. Time

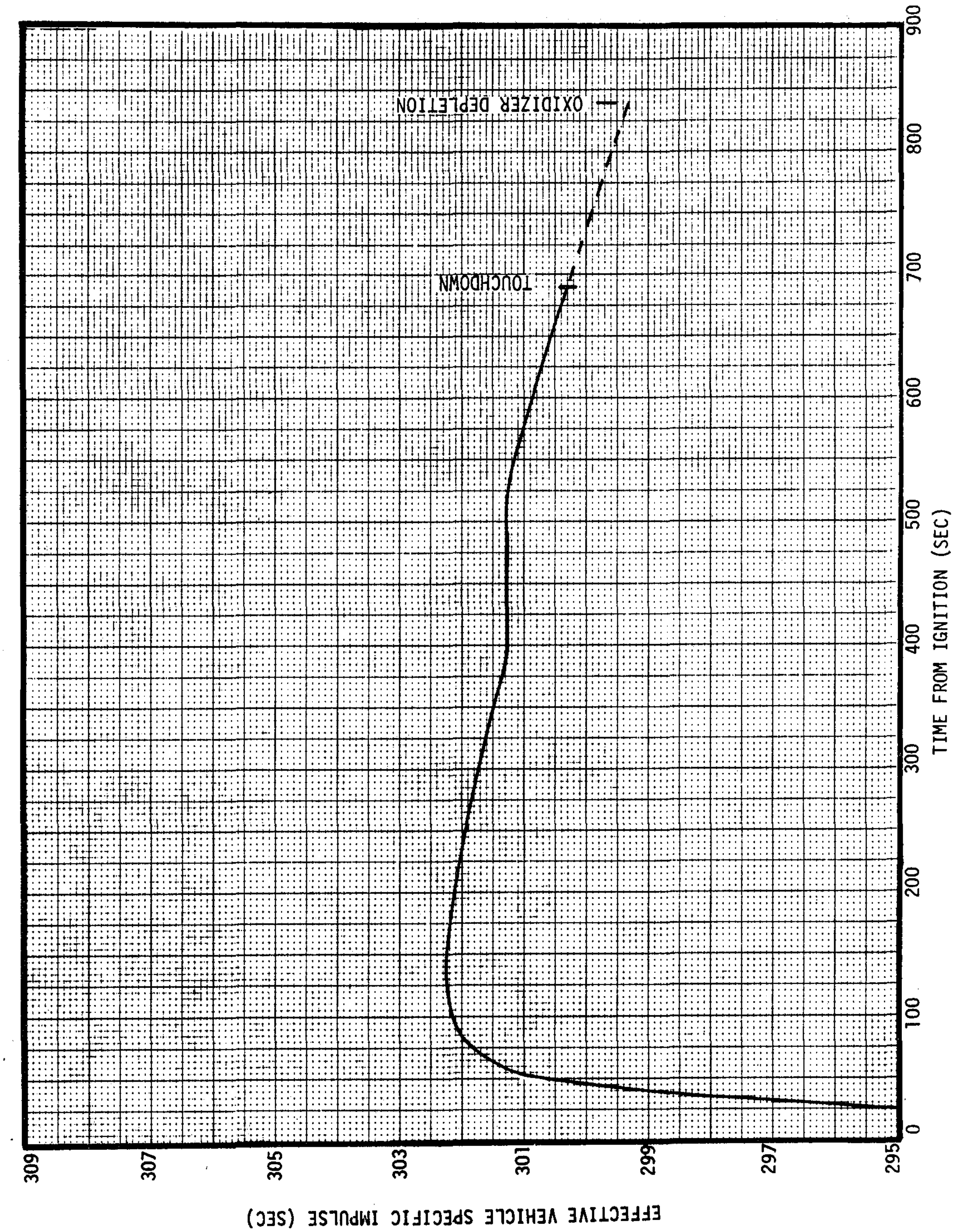

Figure LM8/4.7.1-10 Mission H3 Final DPS Preflight Performance Prediction - Effective Vehicle Specific Impulse Vs. Time

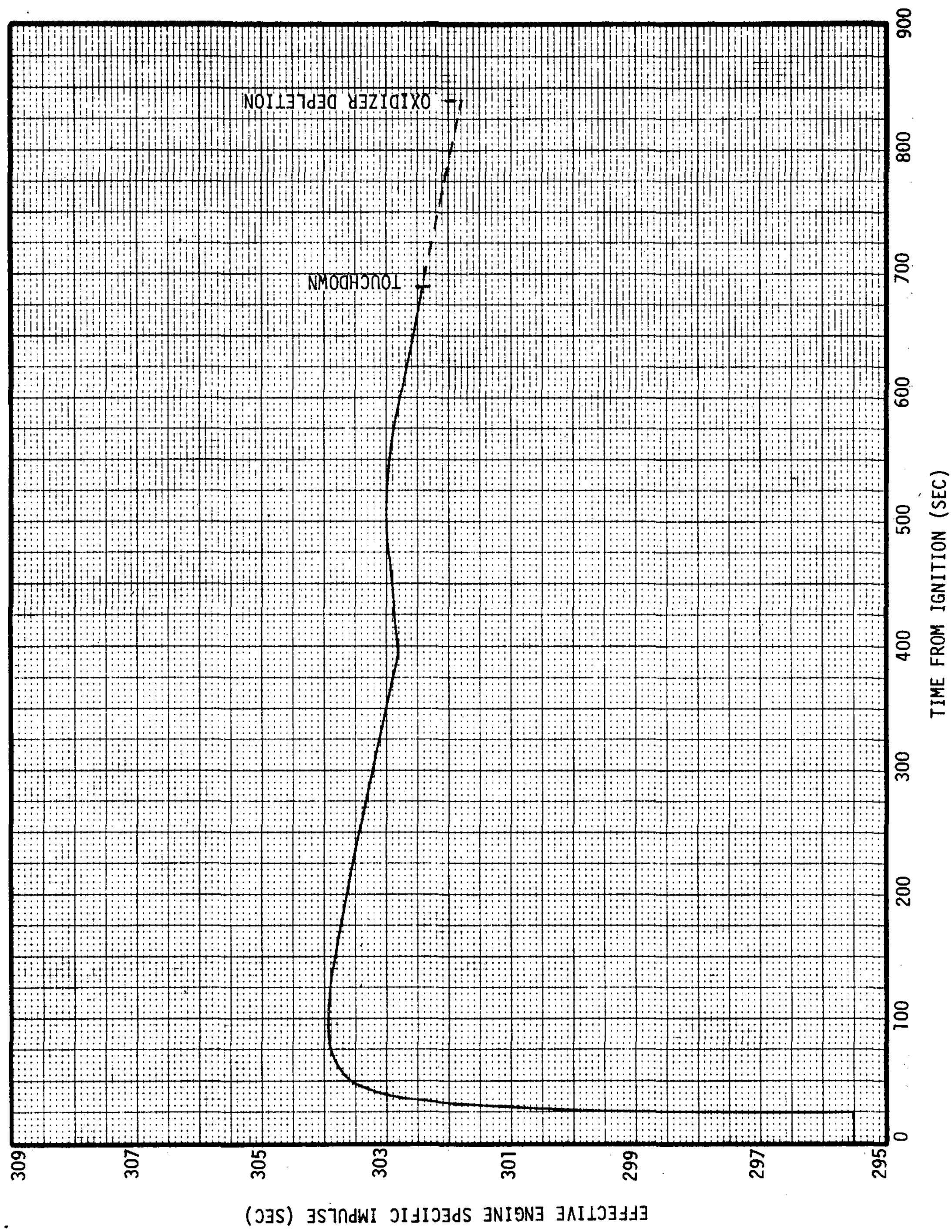

Figure LM8/4.7.1-11 **Mission H3 Final DPS Preflight Performance Prediction - Effective Engine Specific Impulse Vs. Time**

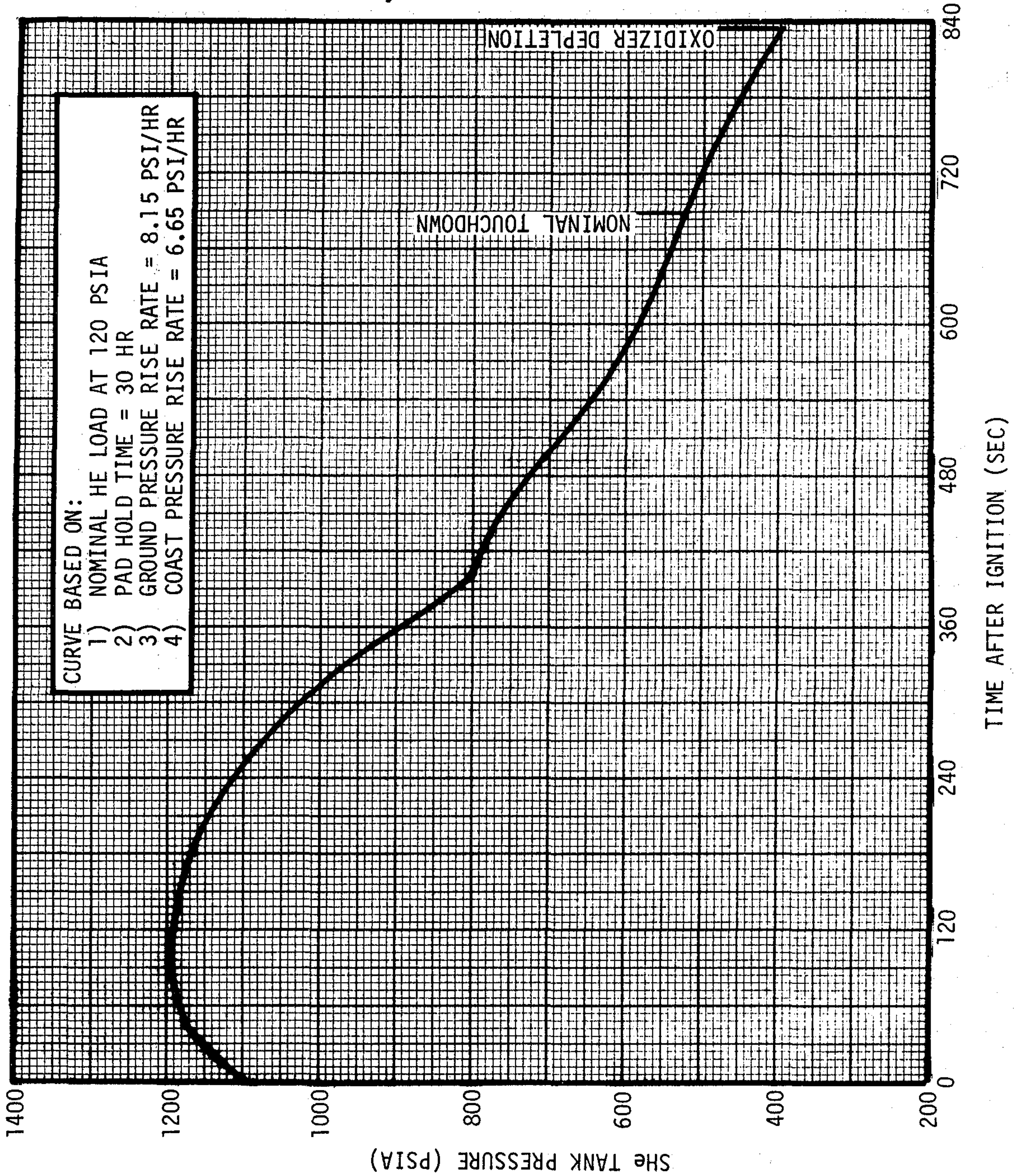

Figure LM8/4.7.1-12 Mission H3 Final DPS Preflight Performance Prediction - Supercritical Helium Bottle Pressure Vs. Time

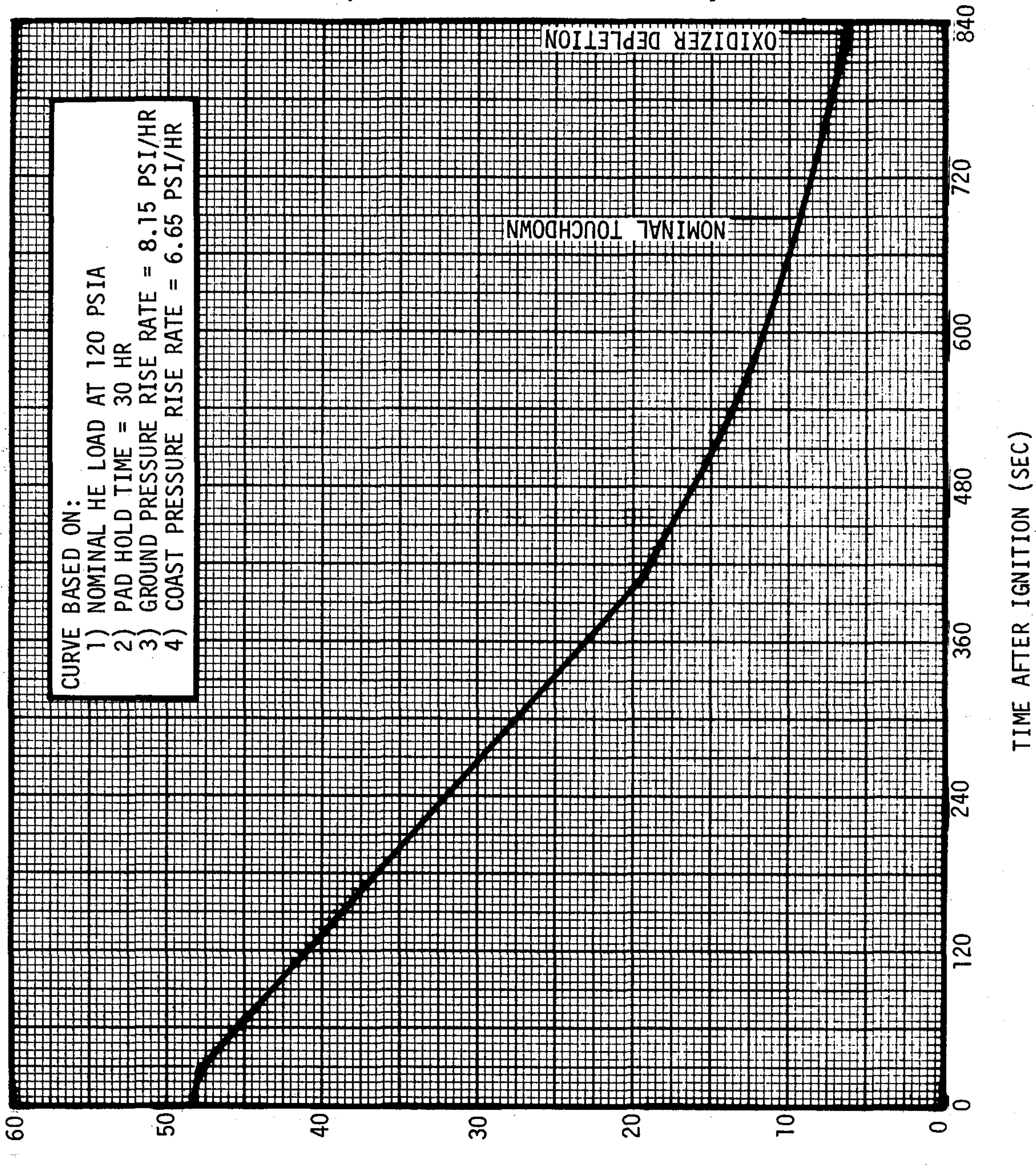

Figure LM8/4.7.1-13 Mission H3 DPS Preflight Performance Prediction - Supercritical Helium Mass Vs. Time

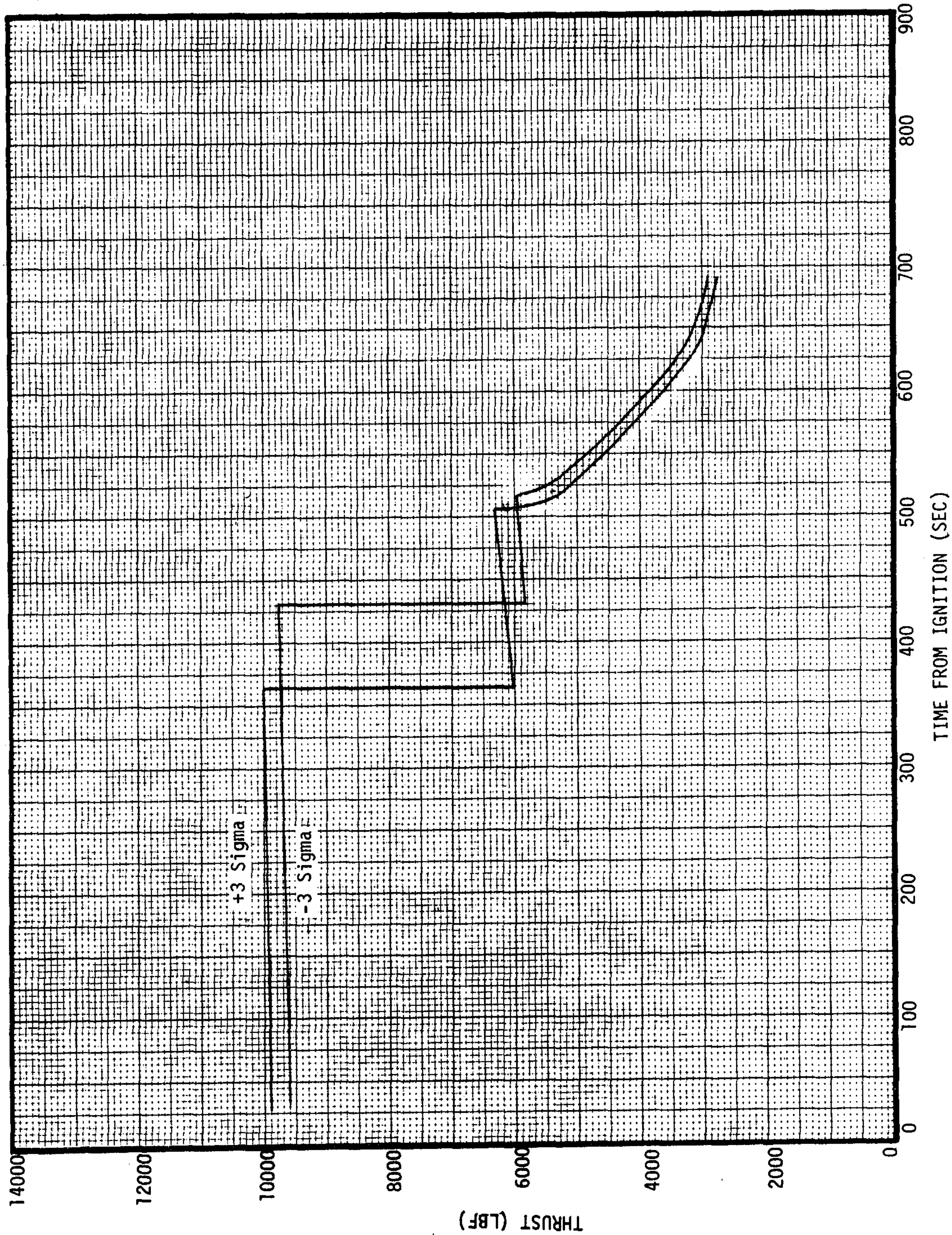

Figure LM8/4.7.1-14 Mission H3 DPS Preflight Performance Prediction - Thrust Dispersion Vs. Time

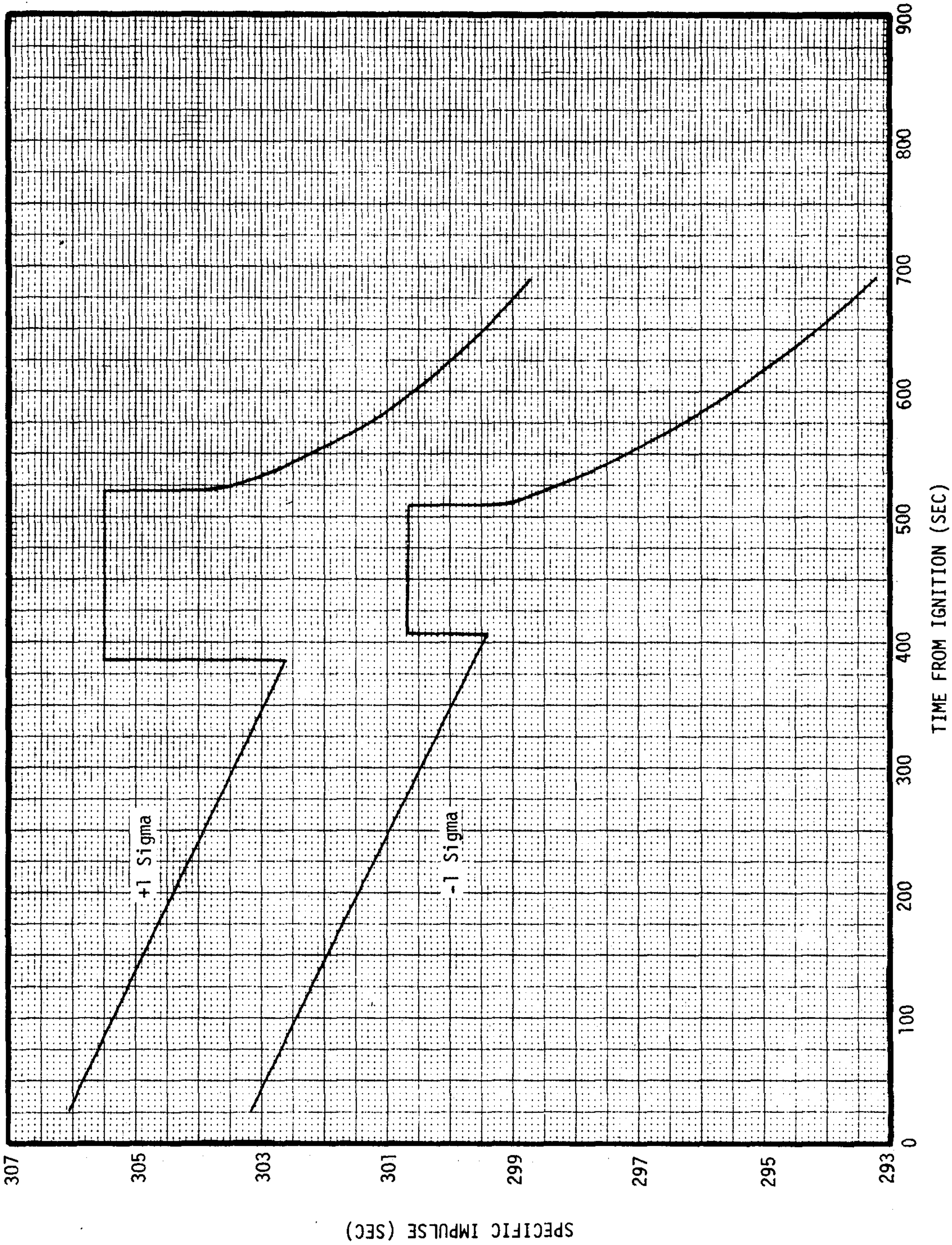

Figure LM8/4.7.1-15 Mission H3 Final DPS Preflight Performance Prediction - Specific Impulse Dispersion Vs. Time

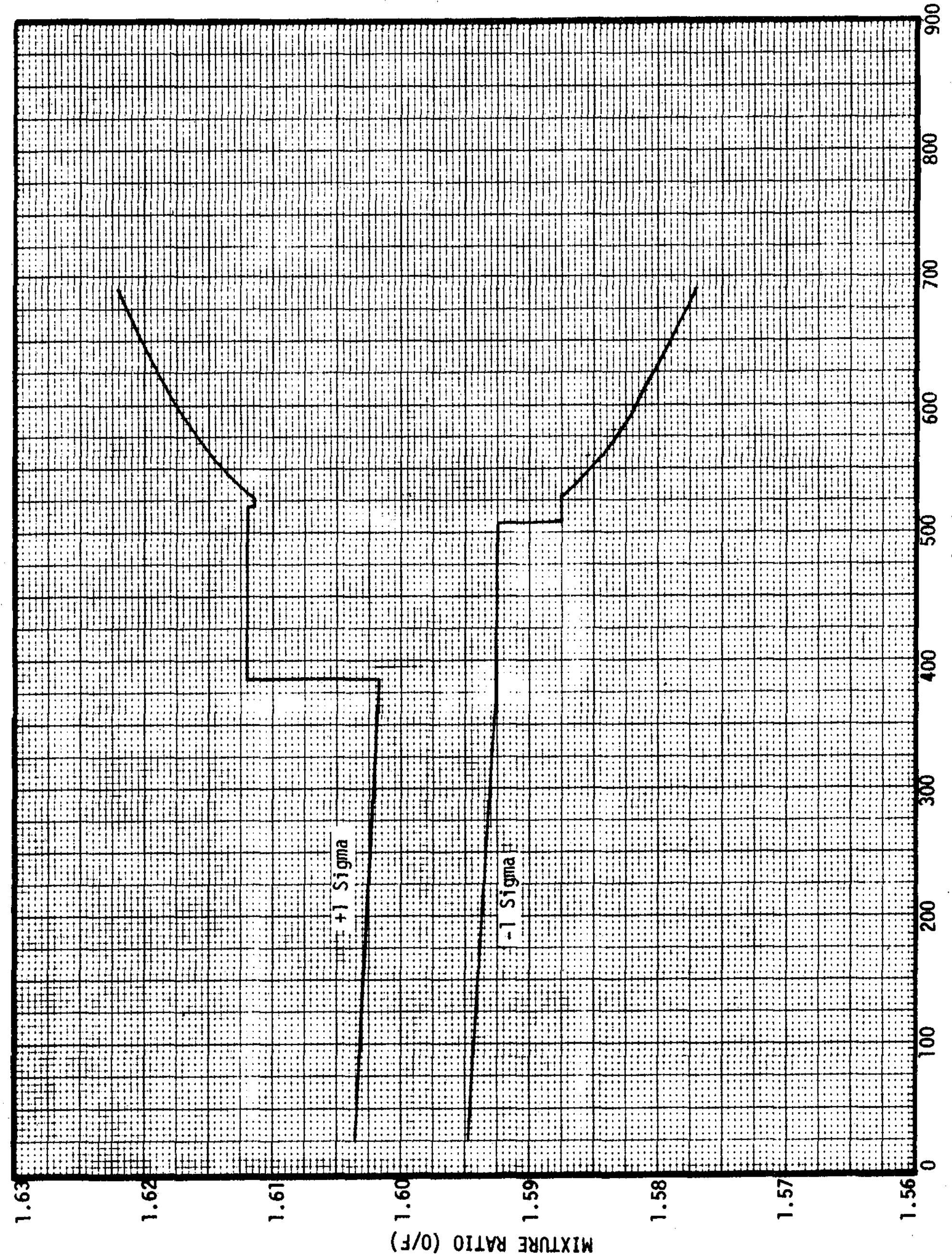

Figure LM8/4.7.1-16 Mission H3 Final DPS Preflight Performance Prediction - Mixture Ratio Dispersion Vs. Time

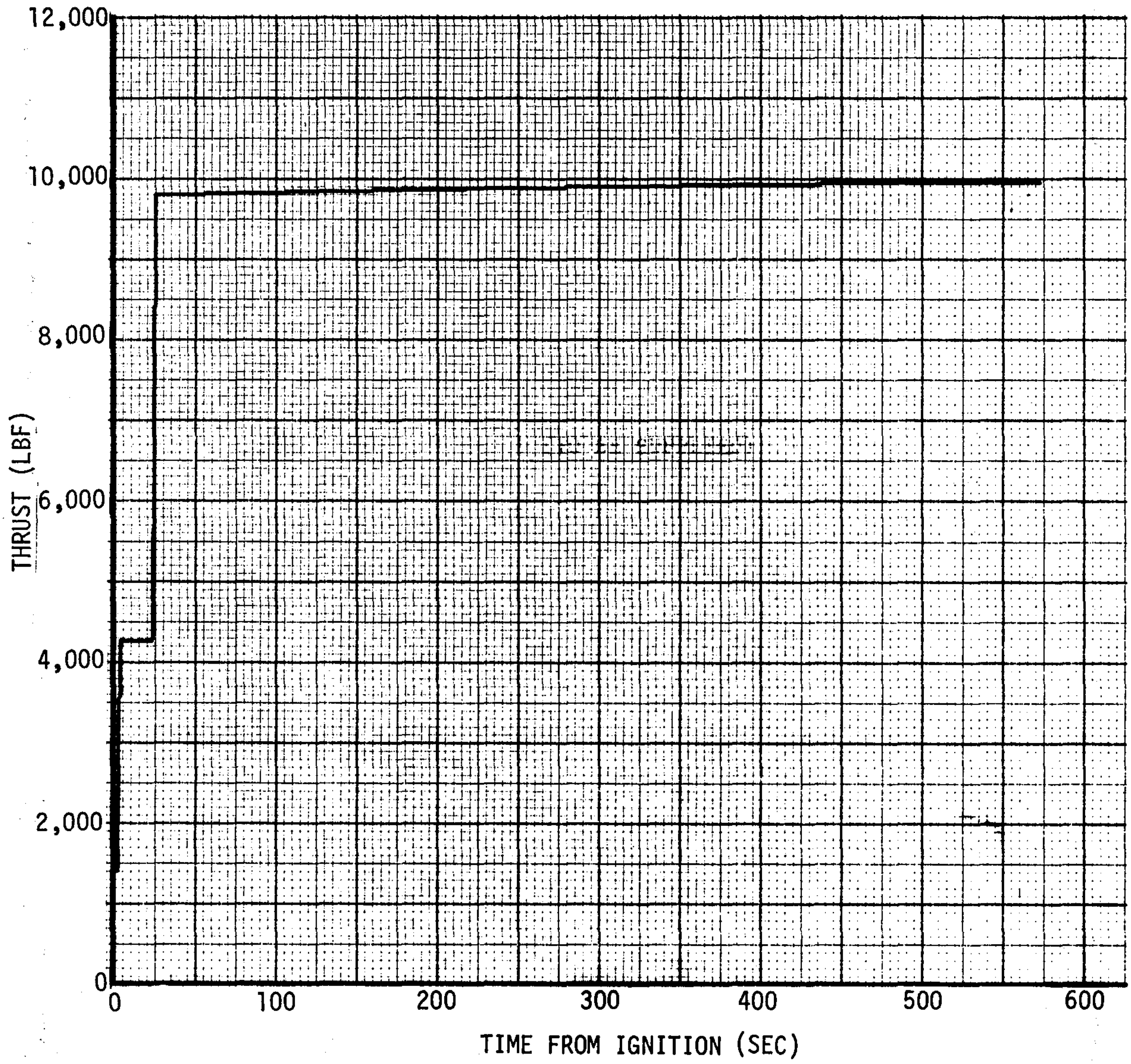

Figure LM8/4.7.1-17 **Mission H3 DPS Preflight Performance Prediction - Docked FTP Burn-to-Depletion - Thrust Vs. Time**

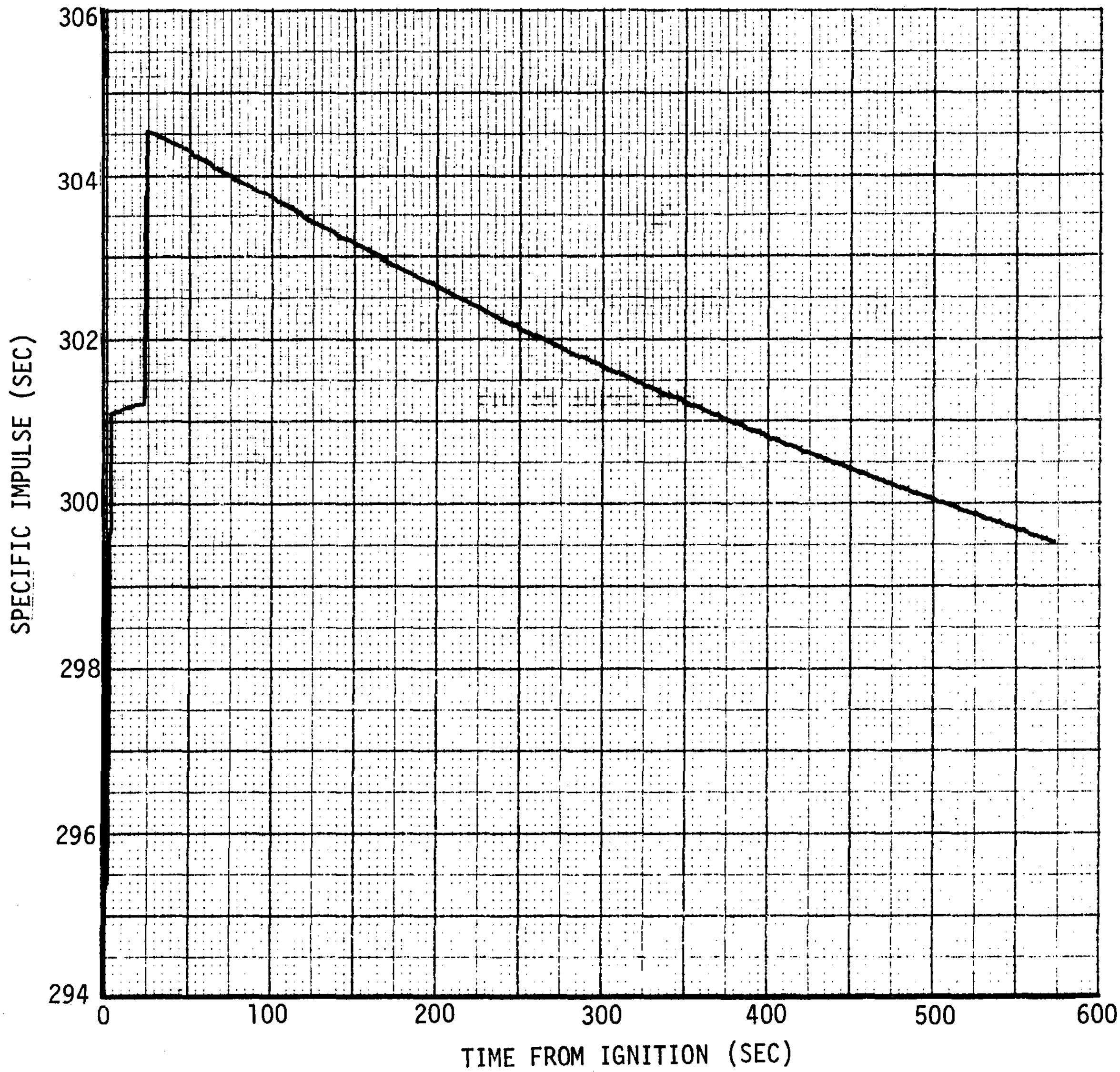

Figure LM8/4.7.1-18 Mission H3 DPS Preflight Performance Prediction - Docked FTP Burn-to-Depletion - Specific Impulse Vs. Time

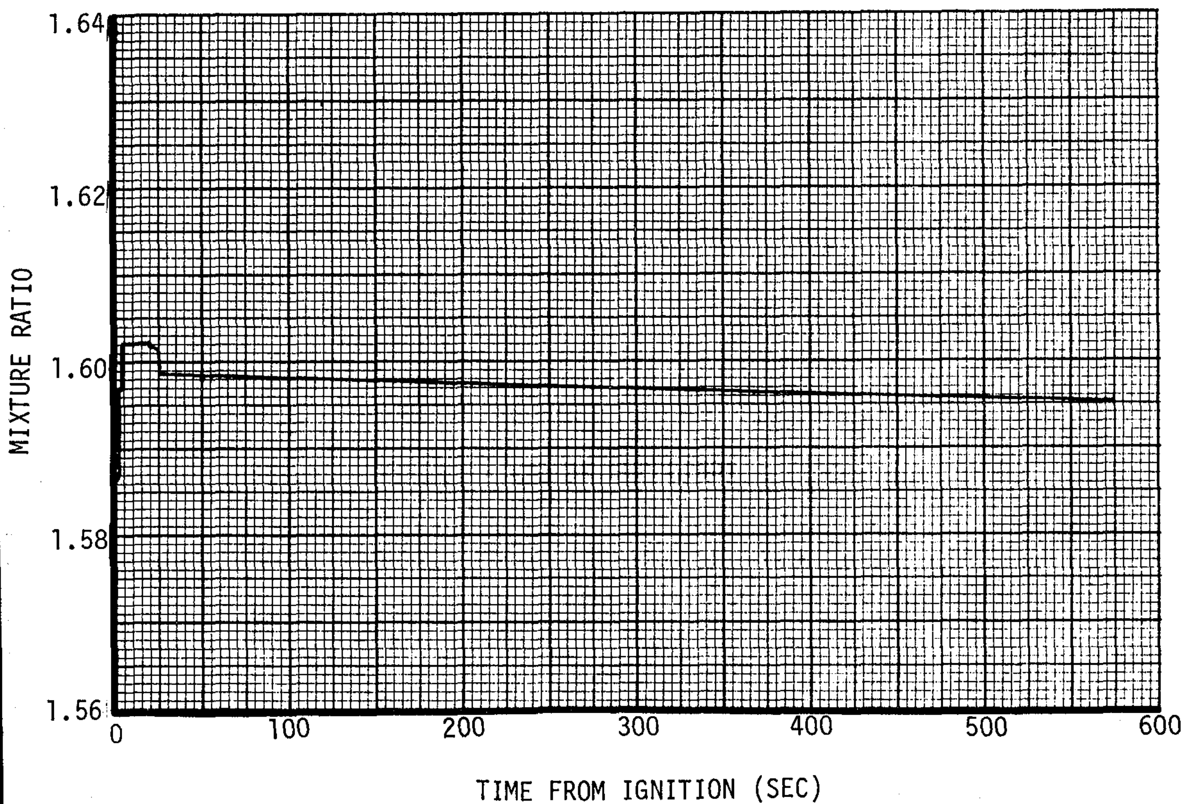

Figure LM8/4.7.1-19 Mission H3 DPS Preflight Performance Prediction - Docked FTP Burn-to-Depletion - Mixture Ratio Vs. Time

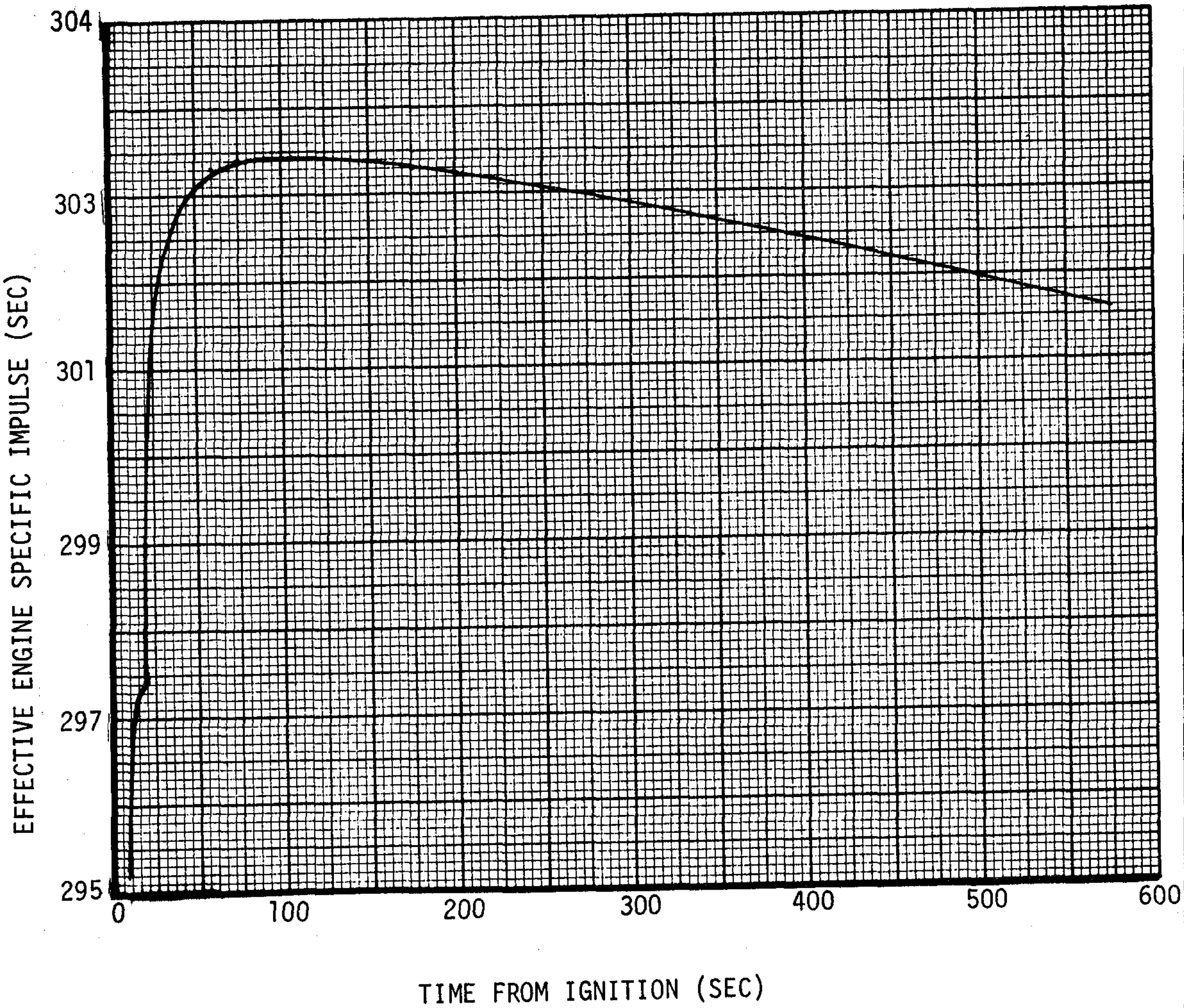

Figure LM8/4.7.1-20 Mission H3 DPS Preflight Performance Prediction - Docked FTP Burn-to-Depletion - Effective Engine Isp Vs. Time

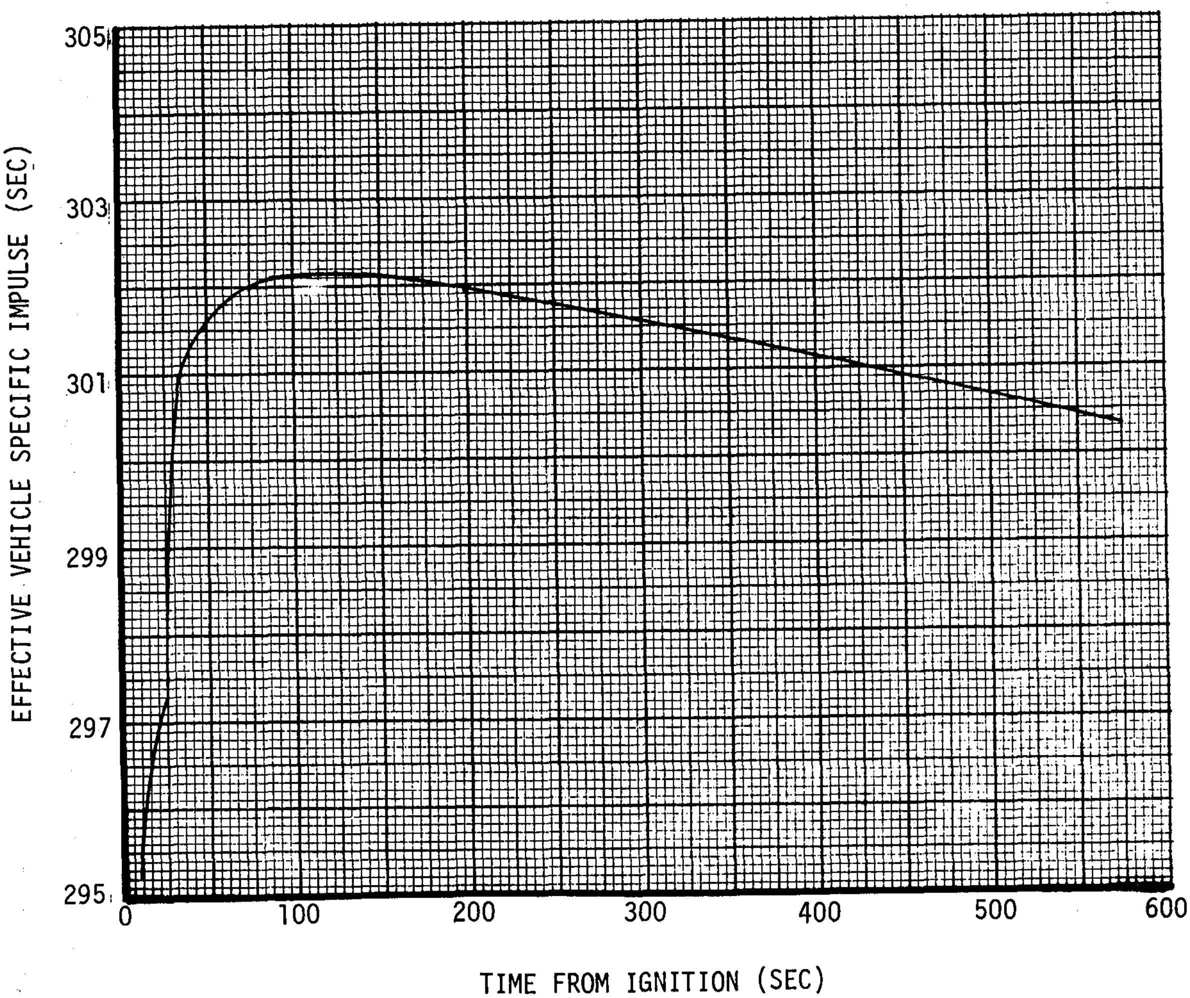

Figure LM8/4.7.1-21 Mission H3 DPS Preflight Performance Prediction - Docked FTP Burn-to-Depletion - Effective Vehicle Isp Vs. Time

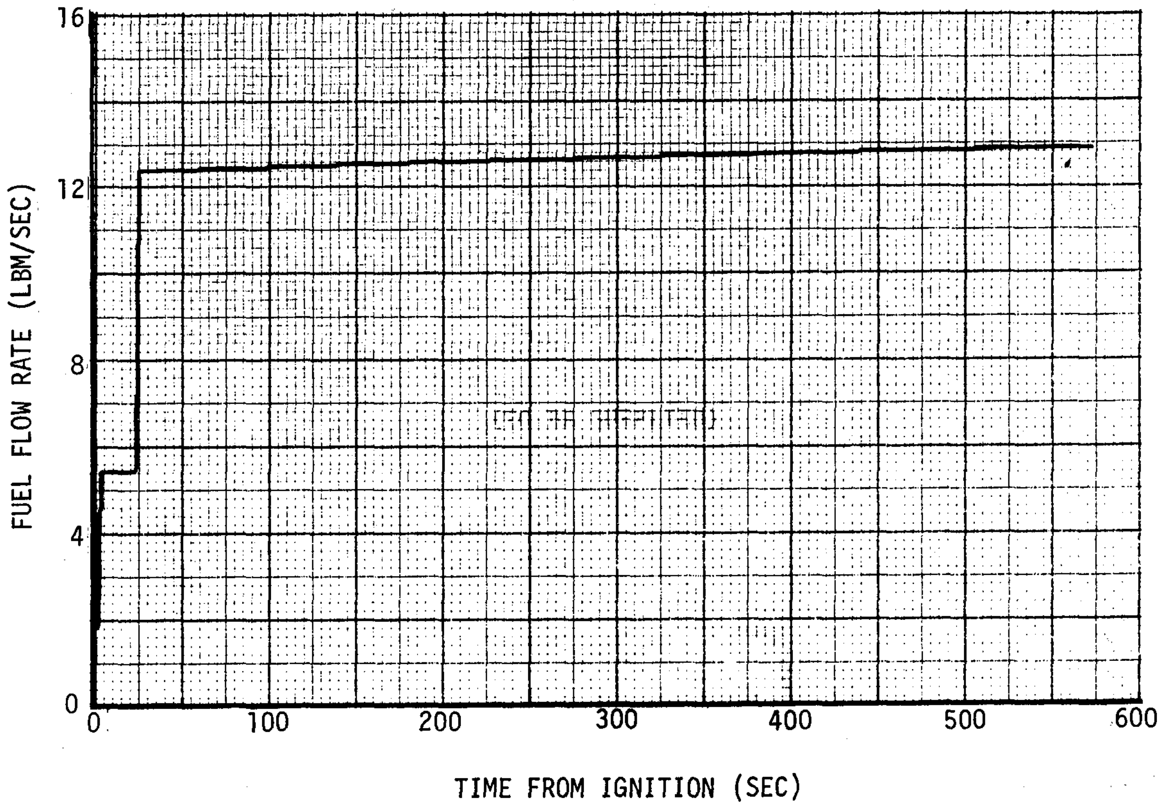

Figure LM8/4.7.1-22 Mission H3 DPS Preflight Performance Prediction - Docked FTP Burn-to-Depletion - Fuel Flow Rate Vs. Time

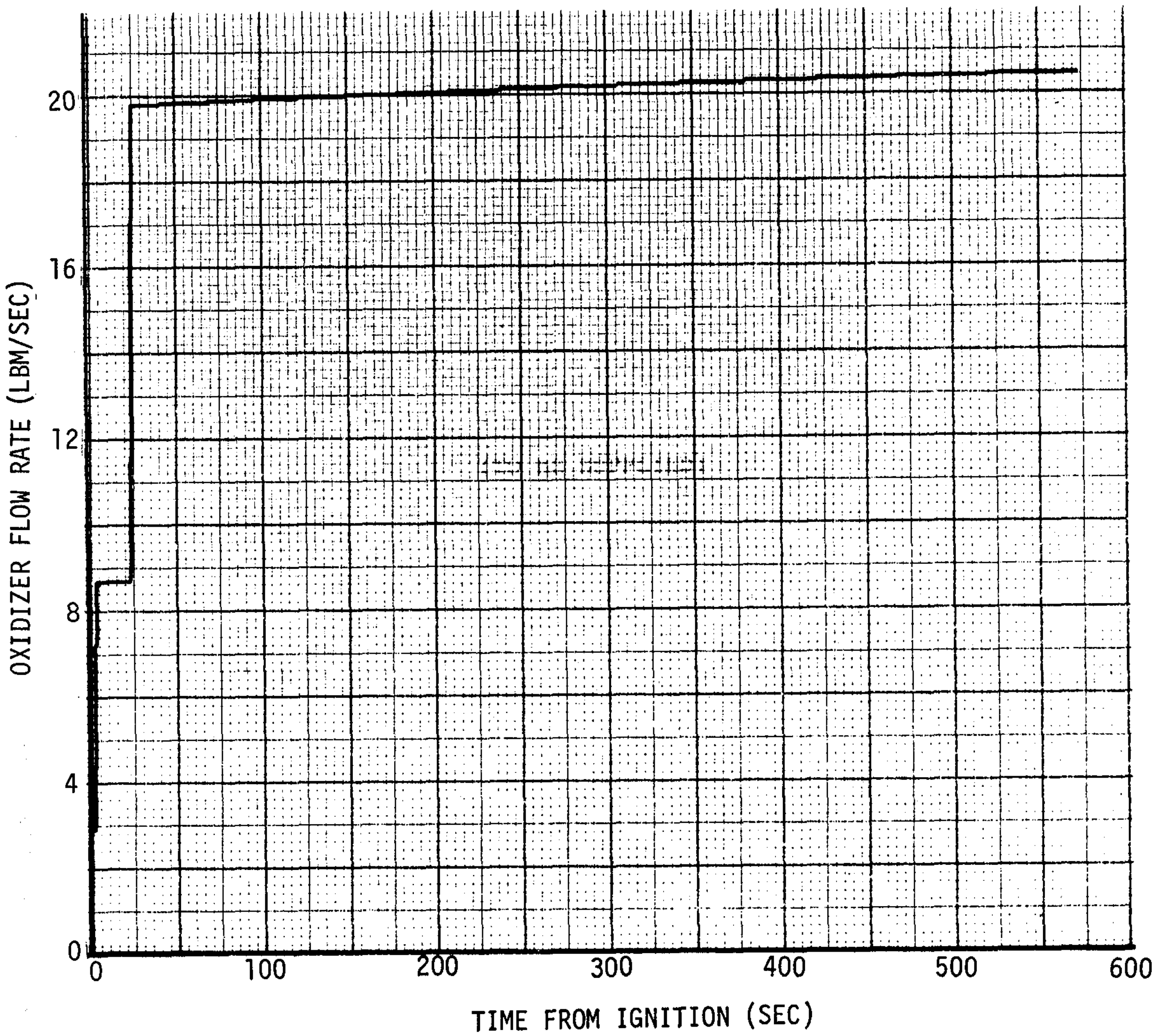

Figure LM8/4.7.1-23 Mission H3 DPS Preflight Performance Prediction - Docked FTP Burn-to-Depletion - Oxidizer Flow Rate Vs. Time

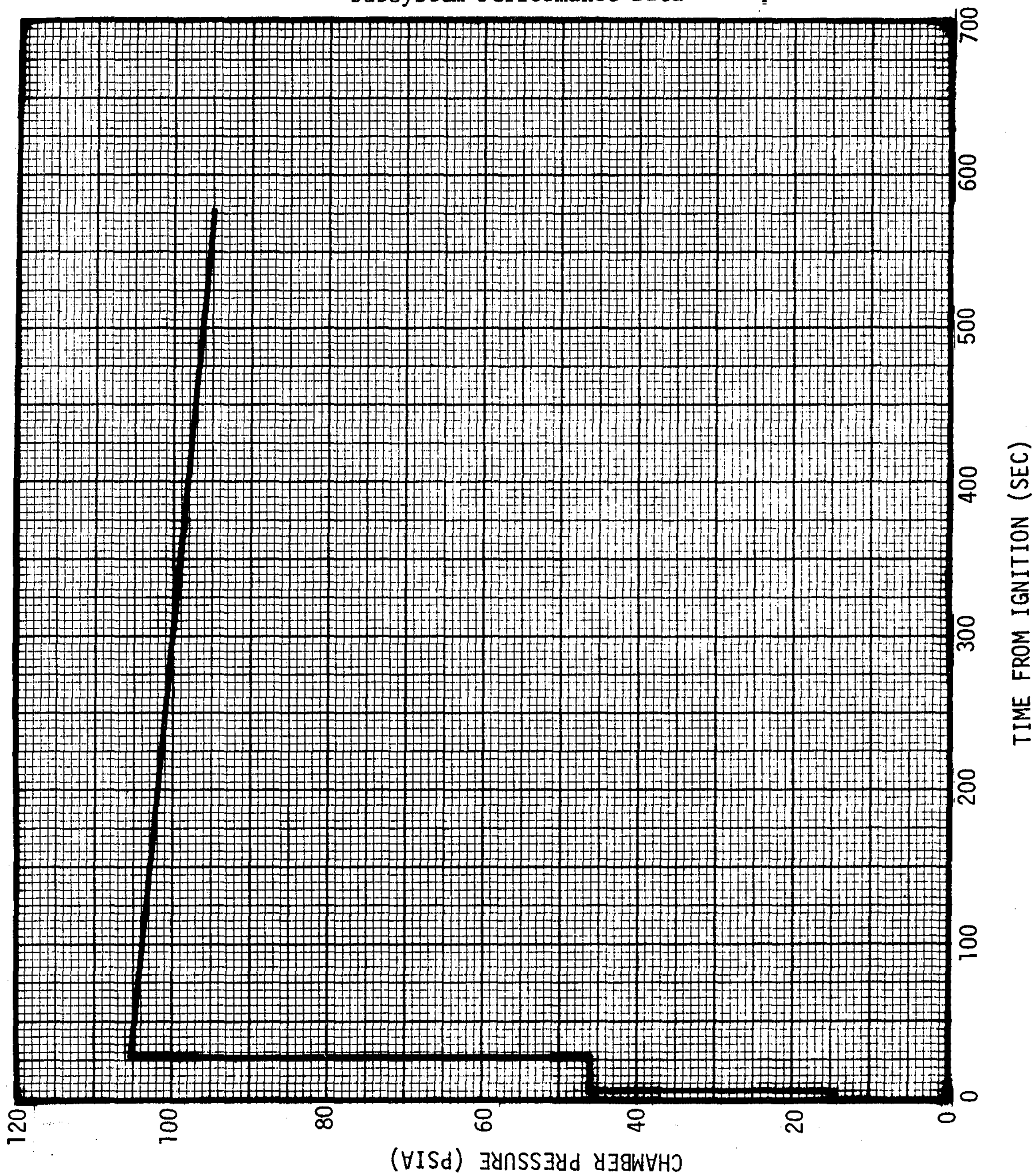

Figure LM8/4.7.1-24 Mission H3 DPS Preflight Performance Prediction - Docked FTP Burn-to-Depletion - Chamber Pressure Vs. Time

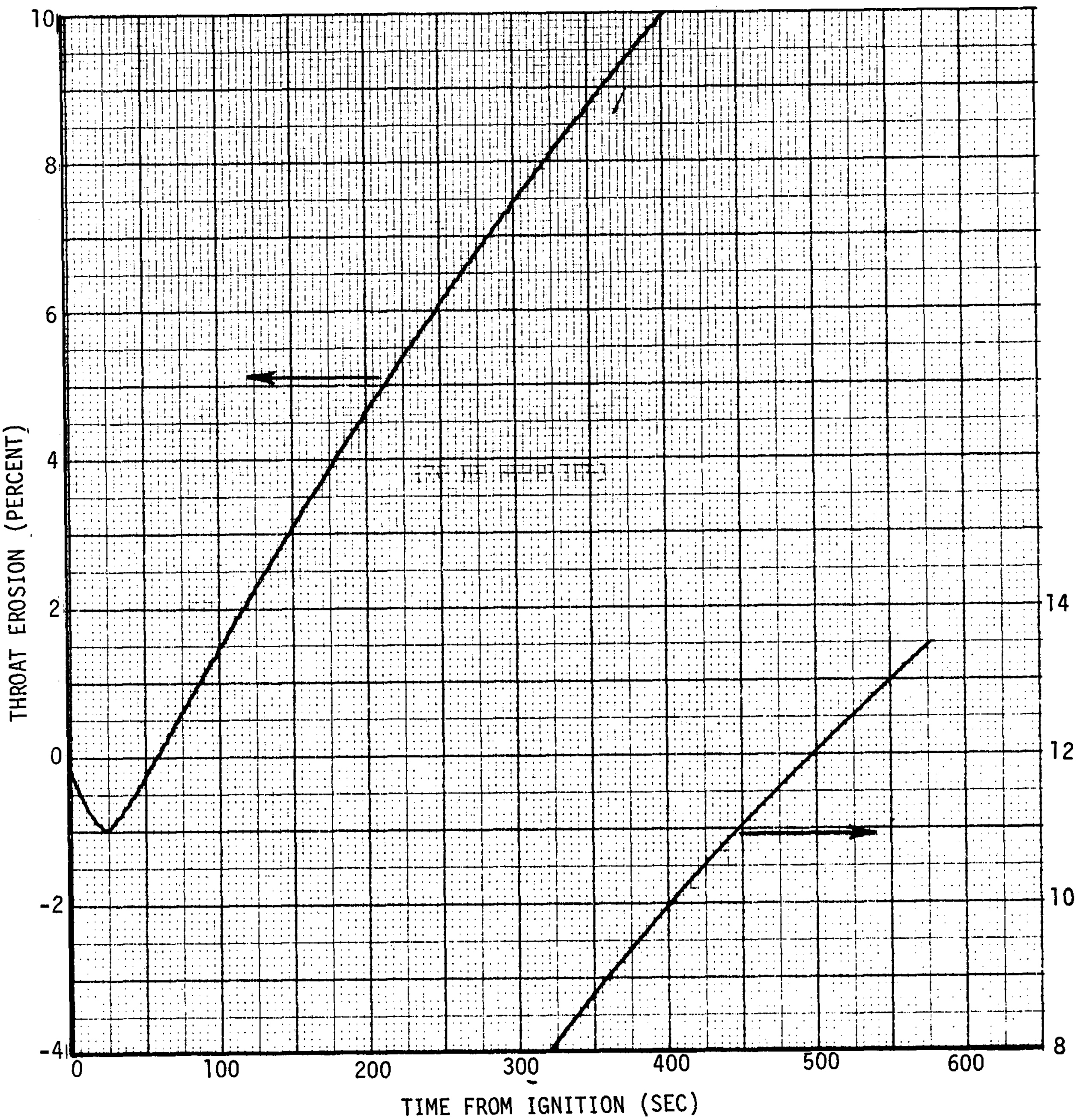

Figure LM8/4.7.1-25 Mission H3 DPS Preflight Performance Prediction - Docked FTP Burn-to-Depletion - Throat Erosion Vs. Time

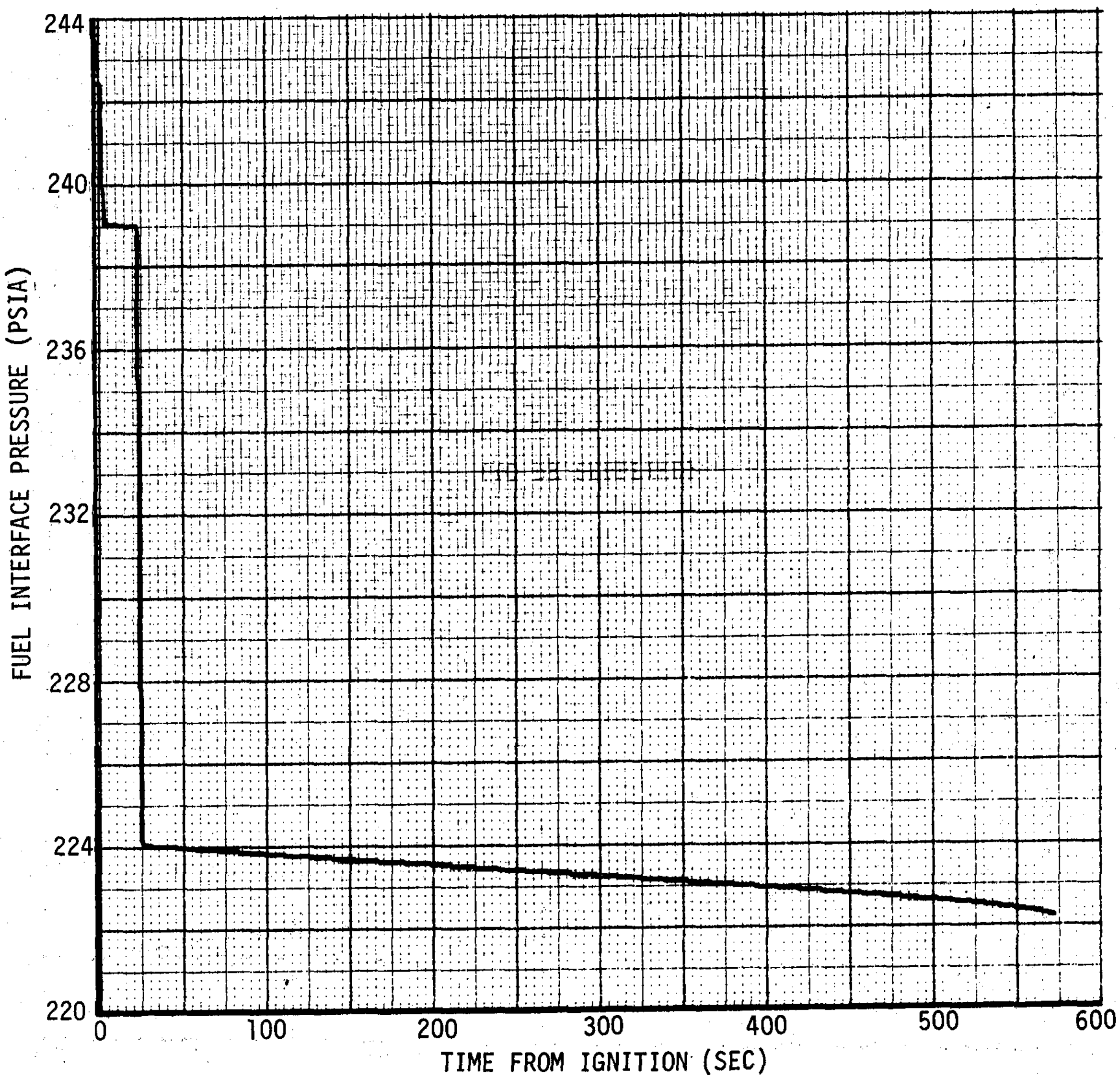

Figure LM8/4.7.1-26 Mission H3 DPS Preflight Performance Prediction - Docked FTP Burn-to-Depletion - Fuel Interface Pressure Vs. Time

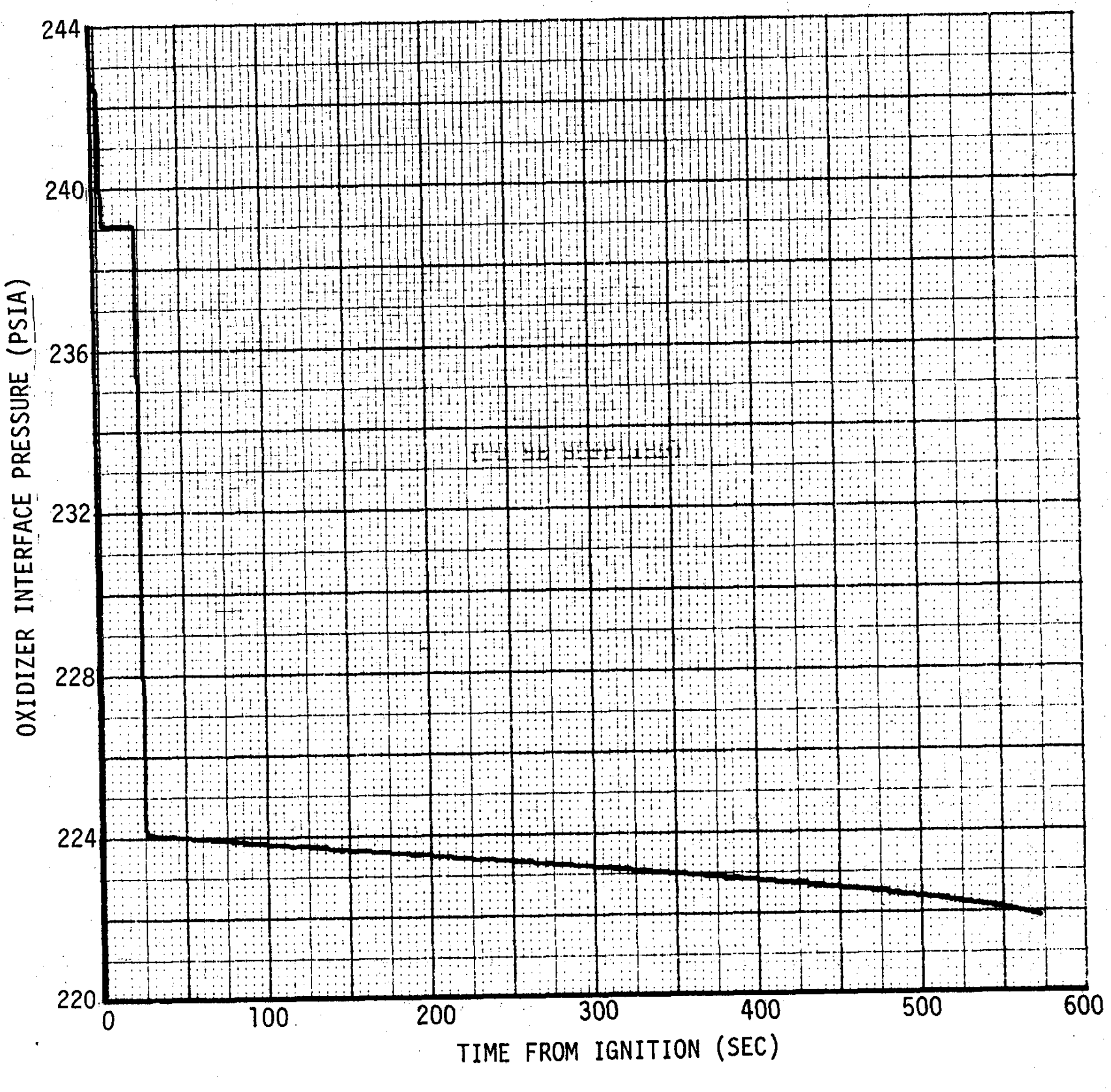

Figure LM8/4.7.1-27 Mission H3 DPS Preflight Performance Prediction - Docked FTP Burn-to-Depletion - Oxidizer Interface Pressure Vs. Time

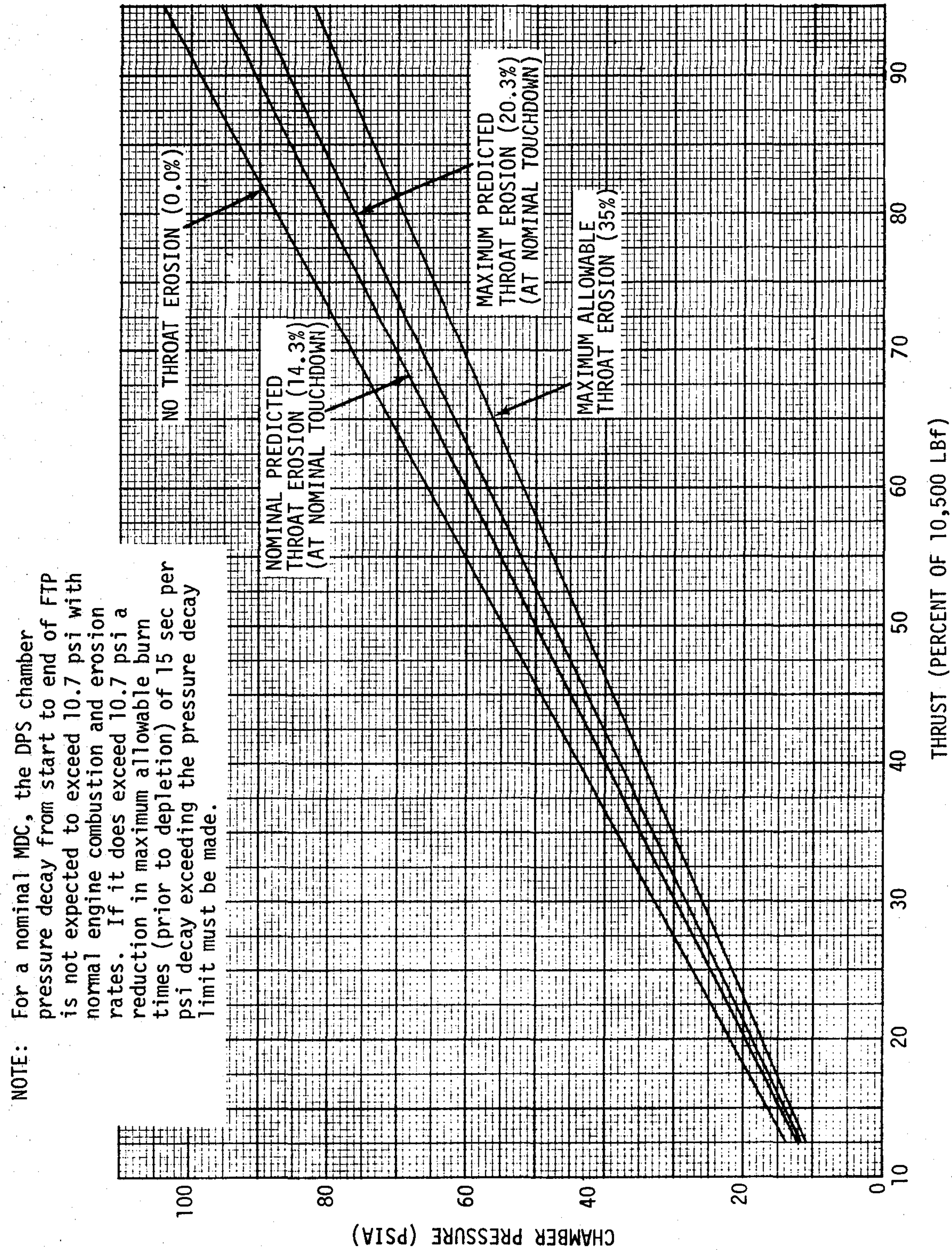

Figure LM8/4.7.1-28 Mission H3 DPS Preflight Performance Prediction - Chamber Pressure Vs. Commanded Thrust for Zero, Nominal, Maximum Predicted and Maximum Allowable Throat Erosion

LM8/4.7.2 Supercritical Helium Tank Pressure

The predicted heat leak pressure rise rates for the LM-8 supercritical helium tanks are shown in Figure LM8/4.7.2-1. Pressure rise rates given in this curve are steady state values and do not account for thermal stabilization just after the burn. These rise rates are therefore independent of mission duty cycle. This data has been obtained from pre-mission screening tests.

The maximum DPS start pressure for the nominal LM-8 mission is 1700 psia. Given a launch SHe pressure and a coast time to PDI the maximum coast rise rate can be found from Figure LM8/4.7.2-2. This rise rate is the highest rise rate for a given coast period in which the maximum allowable SHe pressure during the burn will not be exceeded.

LM8/4.7.5 DPS Propellant Tank Low Level Sensor Operation

Based on measurements of the height of the low level sensor in the propellant tanks made by GAC* the propellant quantities in the tanks at the time of low-level sensor actuation were calculated to be:

Tank	Quantity
Fuel	209.9 ±5.3 lbm per tank
Oxidizer	335.7 ±6.0 lbm per tank

The propellants in the feed lines and heat exchanger should be added, and the propellants in the zero-g-can should be deducted from the above quantities. Values for these are taken from the Spacecraft Operational Data Book, Volume III, Rev 2, 20 August 1969, Section 5.6:

Component	Fuel, lbm	Oxidizer, lbm
Feed Lines	+12.1	+27.5
Heat Exchanger	+ 4.6	-0-
Zero-G-Can	- 5.2	- 8.6
TOTAL	+11.5	+18.9

The propellant quantity corrections tabulated above should be applied regardless of whether depletion occurs from a single tank or both tanks of a pair simultaneously. This is so because in both cases the trapped quantities will be used or not used identically (helium ingestion upon depletion of a single tank effectively shuts off the undepleted tank). Also, since at the time of low level sensor actuation it is not possible to determine whether or not both tanks of a pair are at the same propellant level (they both could be at the high or at the low level), the single tank dispersions should be summed to arrive at the dispersions for both tanks of a pair taken together.

Based upon the above statements and data the propellant quantities available after low level sensor actuation are as follows:

Fuel	431.3 ±10.6 lbm
Oxidizer	690.3 ±12.0 lbm

*Grumman Aerospace Corporation, LM Engineering Memorandum LMO 271-935, 16 September 1970.

The mean values of fuel and oxidizer flow rate during hover from low level sensor actuation to depletion were calculated to be:

Fuel Flow Rate:	3.527 lbm/sec
Oxidizer Flow Rate:	5.643 lbm/sec

(Spacecraft Operational Data Book, Volume II, Rev. 2, 1 September 1969, Para. LM8/4.7.1.)

Using the above flow rates and propellant quantities the burn time from low level sensor actuation to depletion was calculated to be 122.3 seconds for fuel and 122.3 seconds for oxidizer. Both the burn times given above are slightly on the conservative side in as much as use of a mean flow rate is conservative by approximately 1.6 seconds compared to integrating along a thrust-time curve.

The dispersions associated with the burn times given above are ±3.0 seconds for fuel and ±2.1 seconds for oxidizer. Therefore, the minimum burn times from low level sensor actuation to depletion were calculated to be 119.3 seconds for fuel and 120.2 seconds for oxidizer.

Because there are two fuel and two oxidizer tanks, each with a low level sensor with the dispersion given in the first paragraph, the RSS dispersion for the two tanks of a pair represents a more likely case than the maximum dispersion case given immediately above. The RSS dispersions for the total fuel and total oxidizer available at low level sensor activation were calculated to be ±7.5 and ±8.5 lbm, respectively. The burn time dispersions associated with these quantities are ±2.1 seconds for fuel and ±1.5 seconds for oxidizer. Thus, the RSS minimum burn times were calculated to be 119.3 seconds for fuel and 120.8 seconds for oxidizer.

The above burn time calculations do not take into account the uncertainty about the nominal predicted flow rates, or any effects from propellant shosh. In addition, these calculations do not consider the effect of the DPS GDA trim angles on how long after ignition the low level sensor will actuate. Thus, in that sense they are conservative as compared to the data in paragraph LM8/4.7.1, which are based on the nominal predicted GDA trim angles.

LM8/4.7.6.1 DPS Engine Thrust Vector Alignment

The gimbal trim angles for the DPS engine may be calculated using the equations provided in Paragraph 4.7.6.1. The thrust vector angles of the DPS engine at the start of the DOI burn are given in the Spacecraft Operational Data Book, Volume III, Mass Properties, Revision 2, as:

$$\delta\theta_T = -1.510 \text{ degrees}$$

$$\delta\psi_T = -0.347 \text{ degrees}$$

These values, together with a startup thrust of 1300 pounds, were then used to calculate the gimbal trim angles:

$$\delta\theta = -1.570 \text{ degrees}$$

$$\delta\psi = -0.287 \text{ degrees}$$

These are the recommended launch pad settings for the DPS gimbal trim angles at the start of the DOI burn.

The trim angles are set using the LM Guidance Computer (LGC), and must be expressed referenced to the positive gimbal stops. To accomplish this, 6.05 degrees were added to the trim angles above.

This results in

$$\delta\theta' = 4.480 \text{ degrees}$$

$$\delta\psi' = 5.763 \text{ degrees}$$

both referred to the positive gimbal stops.

The LGC has a nominal drive rate of 0.2000 degrees/second hard-wired into it. Therefore, all actual gimbal angles must be converted to equivalent angles based on the hard-wired drive rate using the actual gimbal drive rates in both pitch and roll. Where entered via the LGC erasable memory load, the angles must be expressed as drive times (from the positive stops). Where entered or displayed on the DSKY the equivalent angles must be expressed as degrees of arc.

LM8/4.7.6.1 DPS Engine Thrust Vector Alignment (Continued)

The GDA drive rates are listed below.

Functional Axis	Drive Rate
Pitch (X-Z plane)	0.2099 deg/sec
Roll (X-Y plane)	0.2123 deg/sec

The gimbal trim data to be entered in the LGC erasable memory load are then obtained as follows:

$$\text{PITTIME} = \frac{\delta\theta'}{0.2099} = 21.34 \text{ seconds}$$

$$\text{ROLLTIME} = \frac{\delta\psi'}{0.2123} = 27.15 \text{ seconds}$$

The corresponding angles to be entered or read from the DSKY are obtained as follows:

$$\text{P-TRIM} = \delta\theta' \frac{0.2000}{0.2099} = 4.269 \text{ degrees}$$

$$\text{R-TRIM} = \delta\psi' \frac{0.2000}{0.2123} = 5.429 \text{ degrees}$$

LM8/4.7.12.1 DPS Propellant Tank Contingency Venting

The times to reach fracture mechanics limits (FML) if the lunar dump valve failed to depressurize the tanks shortly after touchdown are presented herein.

The pressure history of the DPS propellant tanks after lunar touchdown is dependent on 1) engine burn time, 2) distance of the descent stage from the lunar surface and 3) residual propellants remaining.

Figures LM8/4.7.12-1 and LM8/4.7.12-2 show the oxidizer and fuel tank pressure time histories under conditions of maximum thermal severity for fracture mechanics limits of 100%, 95% and 85%, and the expected ullage pressure time history when no venting occurs. Figure LM8/4.7.12-3 similarly shows the time history of the oxidizer tank for a nominal landing. No curves are presented for the fuel tank in a thermally nominal landing, since no constraints exist for that case.

For the condition in which no venting occurs the limiting time is the time it takes for the ullage pressure curve to intersect the FML curve. If venting occurs as a result of the cycling of the relief valve, a new limit is established. This new limit is now determined by the time it takes a cycling ullage pressure curve (for the oxidizer and fuel tanks the cycle occurs between 265 psi and 258 psi) to intersect the FML curve at 265 psi.

Table LM8/4.7.12-1 summarizes the times to reach the FML for various contingency cases, and defines the thermally "nominal" and "maximum severity" missions.

LM8/4.7.12.4 Descent Propulsion Preflight Thermal Analysis

The LM-8 descent engine performs essentially the same mission as LM-5 and LM-6; that is, a burn required for lunar landing. The mission duty cycle therefore is very similar to that analyzed in LMO's 510-1408, 510-1421 and 510-1453. These thermal analyses are still applicable to the LM-8 engine. LMO's 510-1421 and 510-1453 are updates to refine the analysis of fuel-bearing components (due to the problem of auto-ignition).

A thermocouple (GQ4220) has been added to the fuel shut-off valve on the LM-8 descent engine. The thermal prediction for this location is presented in Figure LM8/4.7.12-4 and is without any added margin.

TABLE LM8/4.7.12-1. LM-8/DPS PROPELLANT TANKS - MAXIMUM ALLOWABLE STANDBY TIMES FOR THE NO-VENT CASE.

FRACTURE MECHANICS LIMIT	LANDING OF MAXIMUM THERMAL SEVERITY***				LANDING NOMINAL****	
	OXIDIZER TANK SEE FIGURE LM8/4.7.12-1		FUEL TANK SEE FIGURE LM8/4.7.12-2		OXIDIZER TANK SEE FIGURE LM8/4.7.12-3	
	ULLAGE PRESSURE	TIME TO REACH FRACTURE MECHANICS LIMIT	ULLAGE PRESSURE	TIME TO REACH FRACTURE MECHANICS LIMIT	ULLAGE PRESSURE	TIME TO REACH FRACTURE MECHANICS LIMIT
	PSIA	HOURS FROM TOUCH-DOWN	PSIA	HOURS FROM TOUCH-DOWN	PSIA	HOURS FROM TOUCH-DOWN
100%	Pressure Relief 258 - 265 276 (max. allow.)	 2.0 1.2	Pressure Relief 258 - 265 273 (max. allow.)	 ∞ 4.2	Pressure Relief 258 - 265 276 (max. allow.)	 ∞ 2.7
95%	Pressure Relief 258 - 265 281 (max. allow.)	 2.8 1.7	Pressure Relief 258 - 265 280* (max. allow.)	 ∞ ∞	Pressure Relief 258 - 265 282 (max. allow.)	 ∞ 6.1
85%	Pressure Relief 258 - 265 288 (max. allow.)	 ∞ 2.6	Pressure Relief 258 - 265 290 (max. allow. *)	 ∞ ∞	Pressure Relief 258 - 265 290 (max. allow**)	 ∞ ∞

*Maximum pressure predicted at 277 psia.
**Maximum pressure predicted at 288 psia.
***Crushed nozzle
840 seconds burn
Zero residuals
Vapor pressure
Sun angle on +Z (ox), -Y (fuel) 13° above the horizon.

****Nozzle exist 12" above surface
750 seconds burn
211 lb. residual/tank
Vapor pressure
Sun angle on +Z tank 13° above the horizon.

ULLAGE PRESSURE AND ALLOWABLE PRESSURE VS. TIME FROM TOUCHDOWN
LANDING OF MAXIMUM THERMAL SEVERITY LM8 DPS OXIDIZER TANK

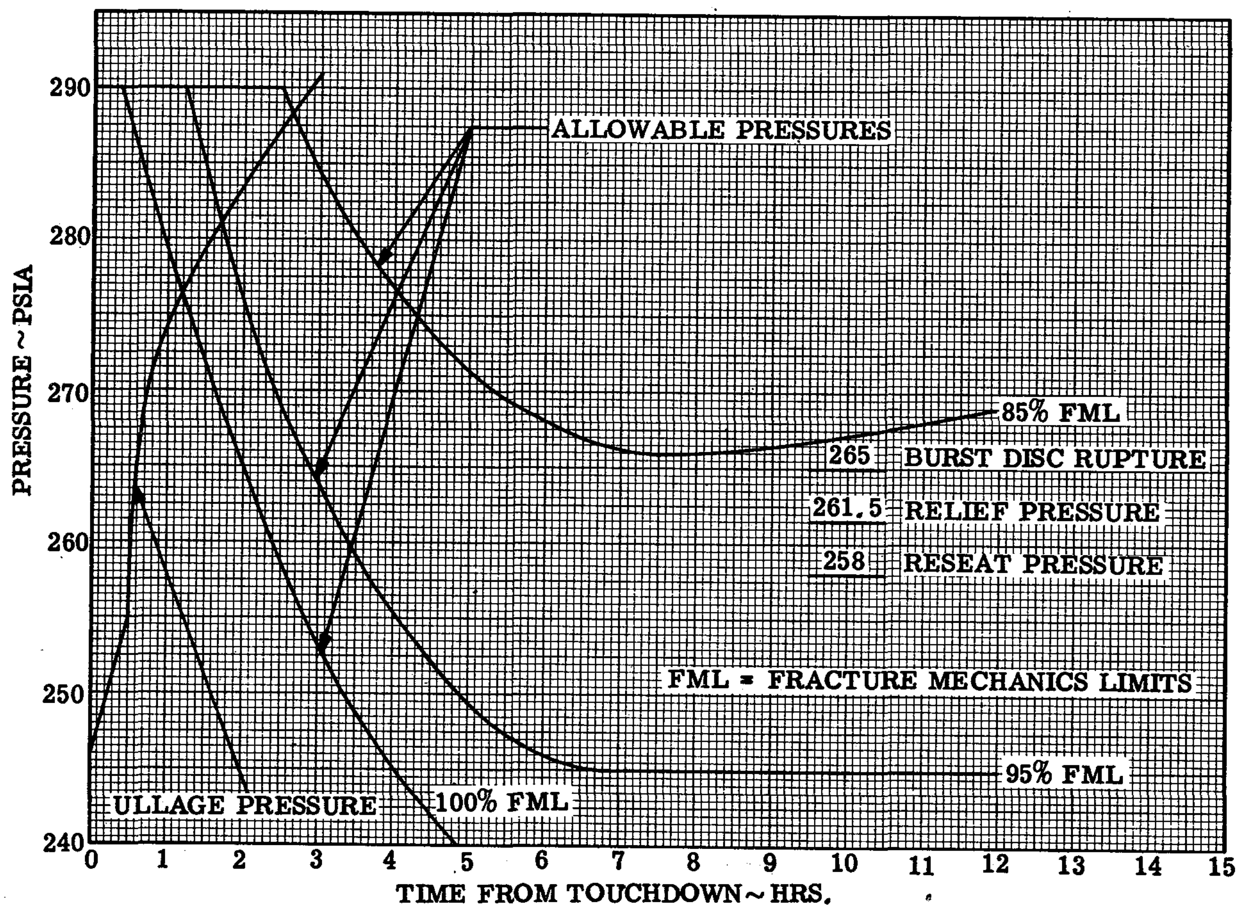

Figure LM8/4.7.12-1, Ullage Pressure and Allowable Pressure Vs. Time from Touchdown

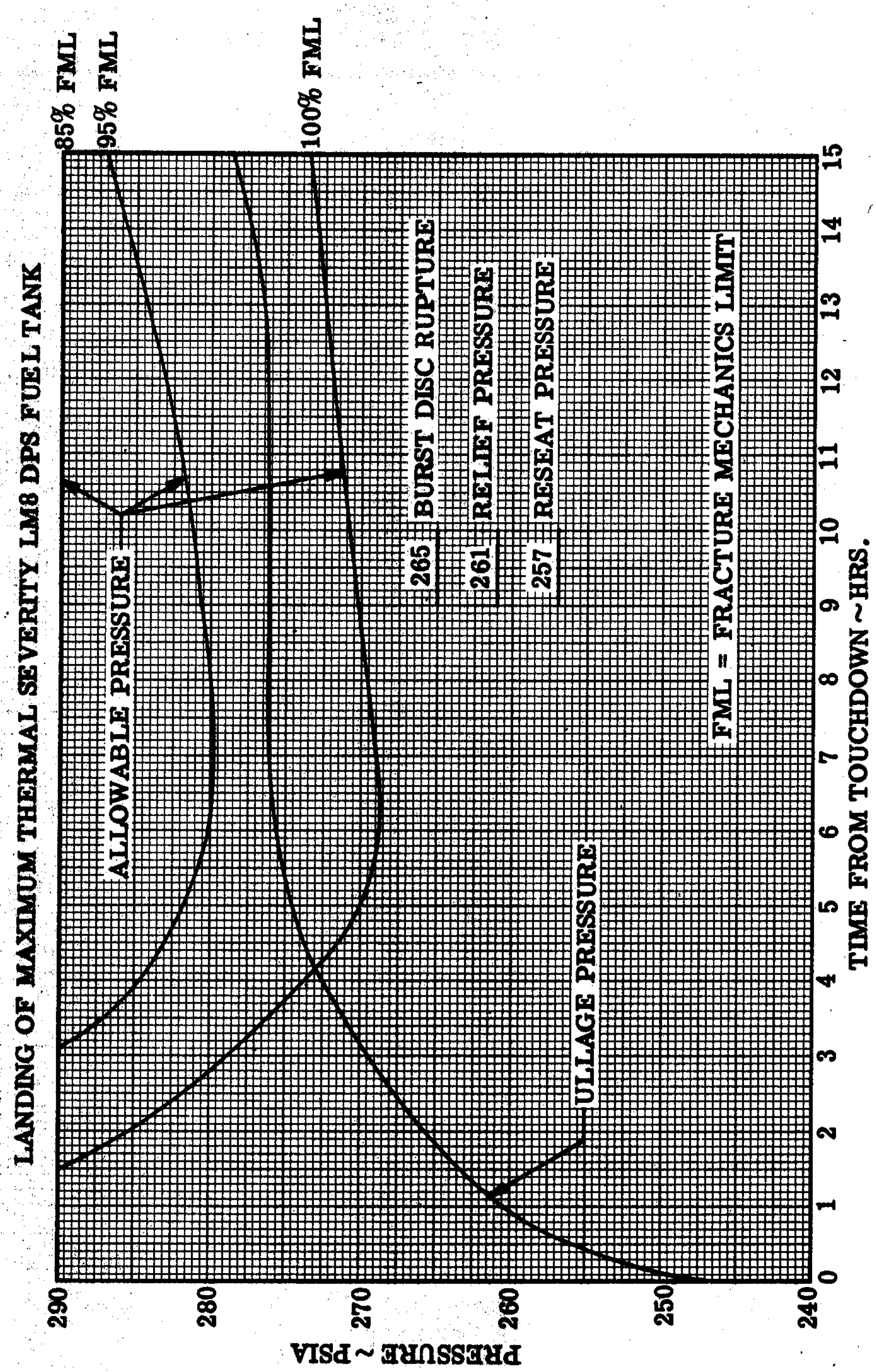

Figure LM8/4.7.12-2. Ullage Pressure and Allowable Pressure Vs. Time from Touchdown

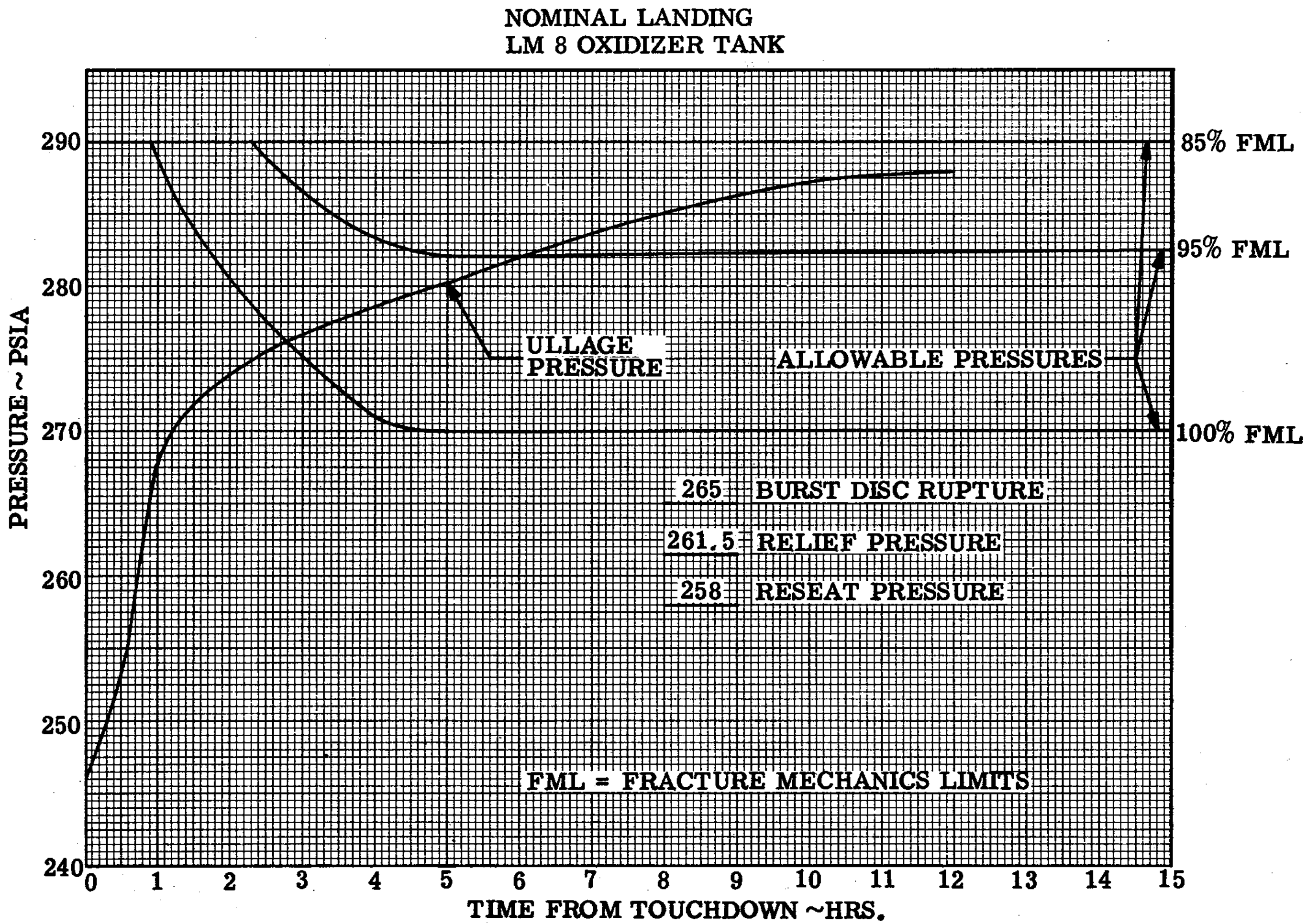

Figure LM8/4.7.12-3. Ullage Pressure and Allowable Pressure Vs. Time from Touchdown

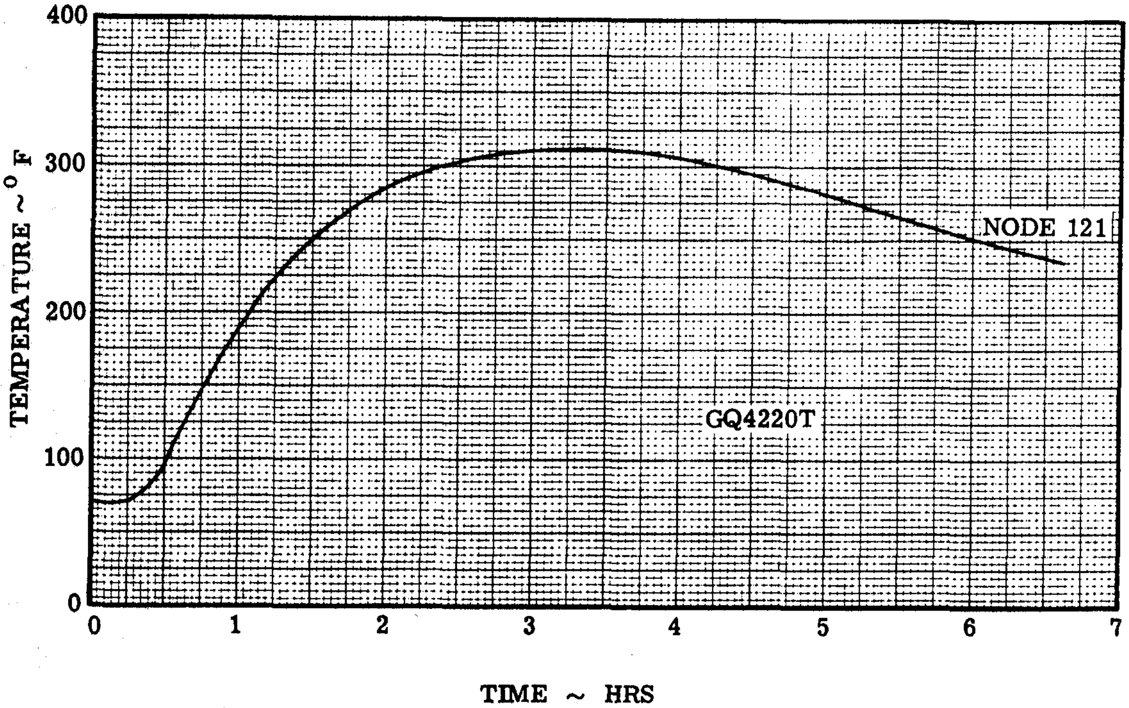

Figure LM8/4.7.12-4. LM-8 Fuel Shut-off Valve Node 121

LM8/4.7.15 Descent Engine Regulator Performance

Figure LM8/4.7.15-1 shows performance characteristics for LM-8 descent engine regulator, Serial No. 116.

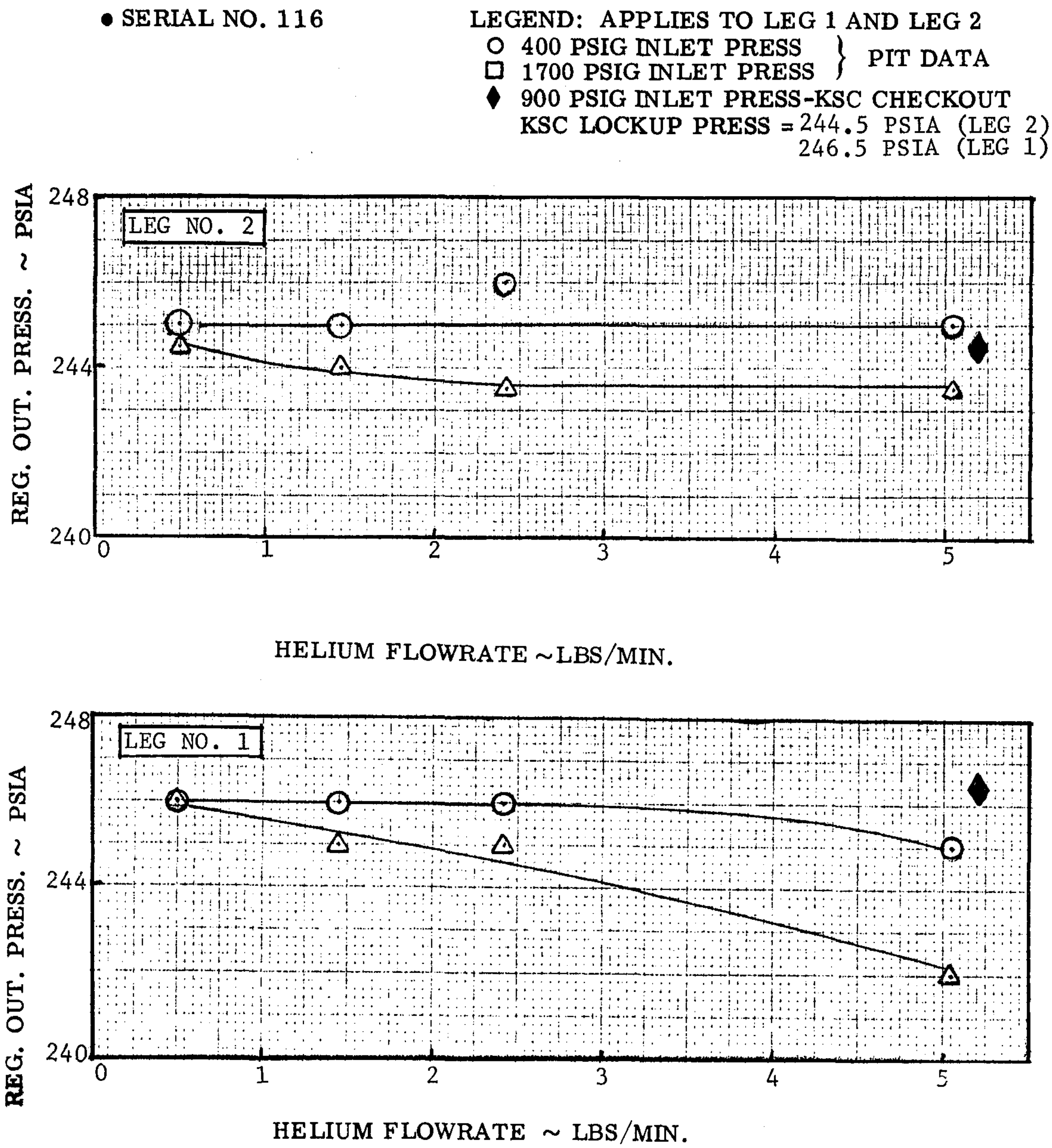

Figure LM8/4.7.15-1. Descent Engine Regulator Performance

LM8/4.8.14 RCS Performance Limitations as a Result of Gimbal Drive Actuator (+ Pitch or + Roll) Failure During Powered Descent

LM8/4.8.14.1 Plume Impingement Constraints Due to GDA Failure

Figure LM8/4.8.14-1 shows the maximum allowable GDA offset angles as limited by the RCS impingement constraints for the affected vehicle hardware. These curves were developed from the LM-8 plume impingement capability curve. (See Figures 4.8-106 through 4.8-119)

In the event of a GDA failure during powered descent, RCS plume impingement may constrain the mission. Figure LM8/4.8.14-2 represents the maximum allowable accumulated RCS firing time at any juncture during powered descent for GDA failure at several different times. The curves reflect the duty cycle which causes failure of the plume deflectors. Note that the attainment of the duty cycle reflected by these curves will exceed the plume impingement capability of the S-band steerable antenna, EVA antenna, scientific equipment bay hood, quad III insulation, and possibly the ladder rung and the primary strut inner cylinder.

LM8/4.8.14.2 Additional RCS Propellant Consumption as a Result of Gimbal Drive Actuator Failure During DPS Operation

Figures LM8/4.8.14-3 and LM8/4.8.14-4 present the maximum allowable GDA pitch and roll angles at time of failure, considering the margin of RCS propellant at landing and the RCS limited torque authority. (See Paragraph 4.8.14.2.)

LM8/4.7.5 Propellant Quantity Gaging

Based on measurements of the height of the low level sensor in the propellant tanks made by GAC* the propellant quantities in the tanks at the time of low-level sensor actuation were calculated to be:

Tank	Quantity
Fuel	209.9 ±5.3 lbm per tank
Oxidizer	335.7 ±6.0 lbm per tank

The propellants in the feed lines and heat exchanger should be added, and the propellants in the zero-g-can should be deducted from the above quantities. Values for these are taken from the Spacecraft Operational Data Book, Volume III, Rev 2, 20 August 1969, Section 5.6:

Component	Fuel, lbm	Oxidizer, lbm
Feed Lines	+12.1	+27.5
Heat Exchanger	+ 4.6	-0-
Zero-G-Can	- 5.2	- 8.6
TOTAL	+11.5	+18.9

The propellant quantity corrections tabulated above should be applied regardless of whether depletion occurs from a single tank or both tanks of a pair simultaneously. This is so because in both cases the trapped quantities will be used or not used identically (helium ingestion upon depletion of a single tank effectively shuts off the undepleted tank). Also, since at the time of low level sensor actuation it is not possible to determine whether or not both tanks of a pair are at the same propellant level (they both could be at the high or at the low level), the single tank dispersions should be summed to arrive at the dispersions for both tanks of a pair taken together.

Based upon the above statements and data the propellant quantities available after low level sensor actuation are as follows:

Fuel	431.3 ±10.6 lbm
Oxidizer	690.3 ±12.0 lbm

*Grumman Aerospace Corporation, LM Engineering Memorandum LMO 271-935, 16 September 1970.

The mean values of fuel and oxidizer flow rate during hover from low level sensor actuation to depletion were calculated to be:

Fuel Flow Rate:	3.527 lbm/sec
Oxidizer Flow Rate:	5.643 lbm/sec

(Spacecraft Operational Data Book, Volume II, Rev. 2, 1 September 1969, Para. LM8/4.7.1.)

Using the above flow rates and propellant quantities the burn time from low level sensor actuation to depletion was calculated to be 122.3 seconds for fuel and 122.3 seconds for oxidizer. Both the burn times given above are slightly on the conservative side in as much as use of a mean flow rate is conservative by approximately 1.6 seconds compared to integrating along a thrust-time curve.

The dispersions associated with the burn times given above are ±3.0 seconds for fuel and ±2.1 seconds for oxidizer. Therefore, the minimum burn times from low level sensor actuation to depletion were calculated to be 119.3 seconds for fuel and 120.2 seconds for oxidizer.

Because there are two fuel and two oxidizer tanks, each with a low level sensor with the dispersion given in the first paragraph, the RSS dispersion for the two tanks of a pair represents a more likely case than the maximum dispersion case given immediately above. The RSS dispersions for the total fuel and total oxidizer available at low level sensor activation were calculated to be ±7.5 and ±8.5 lbm, respectively. The burn time dispersions associated with these quantities are ±2.1 seconds for fuel and ±1.5 seconds for oxidizer. Thus, the RSS minimum burn times were calculated to be 119.3 seconds for fuel and 120.8 seconds for oxidizer.

The above burn time calculations do not take into account the uncertainty about the nominal predicted flow rates, or any effects from propellant slosh. In addition, these calculations do not consider the effect of the DPS GDA trim angles on how long after ignition the low level sensor will actuate. Thus, in that sense they are conservative as compared to the data in paragraph LM8/4.7.1, which are based on the nominal predicted GDA trim angles.

Error values have been computed to be applied to real-time readings for specific quantity values over the range from approximately 14% through depletion. Tables LM8/4.7.5-1, -2, -3, and -4 contain the instantaneous error readings by PCM count for each of the PQGS probes in the 0% to 14% range. Error values for quantities over 14% through 95% will be approximated using sensor performance data over this range. This method is a "worst case" error, but within the data recovery requirements, and simplifies the error application.

The instantaneous channel errors are listed by PCM bit. The errors, as listed, must be applied to the PCM reading and do not include curve-fit error. The curve-fit errors for the range are:

(1)	GQ 3603Q, Fuel No. 1	±.144%
(2)	GQ 3604Q, Fuel No. 2	±.070%
(3)	GQ 4103Q, Ox No. 1	±.056%
(4)	GQ 4104Q, Ox No. 2	±.066%

and must be added algebraically to the uncertainties in Tables LM8/4.7.5-1 through LM8/4.7.5-4, from 1 through 40 PCM bits.

Above 40 PCM bits, due to linear approximation of the PQGS calibration curve, the error will be constant at ±2.4% for all quantities.

Error data contained in Tables LM8/4.7.5-1 through LM8/4.7.5-4, and the errors listed for the Projection Program and Crew Display, are based on the following error sources:

(1)	PQGS Probe	±5 mV (repeatability)
(2)	PQGS Control Unit	±10 mV (PCM or Display output)
(3)	PCM	±15 mV (±15 mV PP application)
(4)	Zero adjust potentiometer error	±15 mV

Projection Program errors listed below are based on an FCD-GAC agreed starting point of 12% indicated quantity and a stop point of 5.8% (124 seconds program duration). The assumed depletion rate was 0.05 percent/second. The errors listed below apply to the mean calculated propellant quantity at the end of the 124-second program.

Tank	Meas. ID	Error (%)
Fuel No. 1	GQ 3603Q	0.502
Fuel No. 2	GQ 3604Q	0.504
Ox No. 1	GQ 4103Q	0.513
Ox No. 2	GQ 4104Q	0.525

In order to provide the crew with a display error, a computation was performed to determine the uncertainty at the threshold of the digital display as it transcends from 3% to 2%. These are listed in Table A below. Table B has been prepared in the event that the exact switching point is not observed by the crew.

Table A

Measurement	Quantity (%) Remaining	
	High	Low
GQ 3603Q, Fuel No. 1	2.93	2.33
GQ 3604Q, Fuel No. 2	2.84	2.23
GQ 4103Q, Ox No. 1	2.70	1.84
GQ 4104Q, Ox No. 2	2.95	2.31

Table B

Measurement	Quantity (%) Remaining	
	High	Low
GQ 3603Q, Fuel No. 1	2.93	1.23
GQ 3604Q, Fuel No. 2	2.84	1.16
GQ 4103Q, Ox No. 1	2.70	0.91
GQ 4104Q, Ox No. 2	2.95	1.23

Table LM8/4.7.5-1
Oxidizer #1 Reading Error by PCM Bit

PCM BITS	PCM QUANTITY	POSITIVE ERROR	NEGATIVE ERROR
1	0.0	0.425	0.0
2	0.222	0.551	-0.222
3	0.543	0.578	-0.467
4	0.891	0.577	-0.577
5	1.239	0.577	-0.577
6	1.587	0.785	-0.577
7	1.935	0.783	-0.577
8	2.492	0.567	-0.786
9	2.834	0.555	-0.588
10	3.176	0.530	-0.567
11	3.497	0.527	-0.546
12	3.815	0.526	-0.527
13	4.132	0.527	-0.527
14	4.450	0.526	-0.527
15	4.767	0.652	-0.527
16	5.085	1.305	-0.527
17	5.664	1.029	-0.789
18	6.493	0.504	-1.297
19	6.797	0.503	-0.668
20	7.100	0.504	-0.503
21	7.404	0.503	-0.504
22	7.707	0.858	-0.503
23	8.011	0.997	-0.504
24	8.751	0.599	-0.940
25	9.125	0.591	-0.946
26	9.467	0.634	-0.567
27	9.847	0.625	-0.606
28	10.232	0.602	-0.638
29	10.595	0.602	-0.616
30	10.958	0.602	-0.602
31	11.321	0.592	-0.602
32	11.684	0.577	-0.602
33	12.032	0.577	-0.588
34	12.380	0.577	-0.578
35	12.727	0.578	-0.577
36	13.075	0.577	-0.577
37	13.423	0.577	-0.577
38	13.771	0.580	-0.577
39	14.119	0.589	-0.577
40	14.472	0.593	-0.582

Table LM8/4.7.5-2
Oxidizer #2 Reading Error by PCM Bit

PCM BITS	PCM QUANTITY	POSITIVE ERROR	NEGATIVE ERROR
1	0.0	0.748	0.0
2	0.515	0.584	-0.515
3	0.868	0.570	-0.585
4	1.215	0.561	-0.580
5	1.553	0.745	-0.565
6	1.891	0.741	-0.561
7	2.412	0.554	-0.744
8	2.746	0.552	-0.682
9	3.080	0.542	-0.554
10	3.408	0.539	-0.548
11	3.733	0.538	-0.539
12	4.057	0.539	-0.538
13	4.382	0.538	-0.539
14	4.706	0.575	-0.538
15	5.031	1.343	-0.539
16	5.483	1.164	-0.666
17	6.467	0.452	-1.326
18	6.739	0.453	-0.926
19	7.012	0.452	-0.452
20	7.285	0.452	-0.453
21	7.557	0.452	-0.452
22	7.830	0.929	-0.453
23	8.269	0.847	-0.619
24	8.902	0.538	-0.979
25	9.226	0.579	-0.619
26	9.558	0.622	-0.546
27	9.933	0.616	-0.596
28	10.307	0.609	-0.621
29	10.674	0.610	-0.613
30	11.042	0.609	-0.610
31	11.409	0.584	-0.609
32	11.770	0.561	-0.603
33	12.108	0.562	-0.574
34	12.447	0.562	-0.562
35	12.785	0.562	-0.561
36	13.124	0.562	-0.562
37	13.463	0.561	-0.562
38	13.801	0.566	-0.561
39	14.140	0.580	-0.562
40	14.488	0.585	-0.571

Table LM8/4.7.5-3
Fuel #1 Reading Error by PCM Bit

PCM BITS	PCM QUANTITY	POSITIVE ERROR	NEGATIVE ERROR
1	0.0	0.747	0.0
2	0.519	0.574	-0.519
3	0.865	0.575	-0.575
4	1.212	0.574	-0.575
5	1.558	0.761	-0.575
6	1.971	0.653	-0.641
7	2.423	0.506	-0.747
8	2.728	0.506	-0.545
9	3.033	0.506	-0.506
10	3.338	0.506	-0.506
11	3.643	0.506	-0.506
12	3.948	0.506	-0.506
13	4.253	0.506	-0.506
14	4.558	0.575	-0.506
15	4.886	0.621	-0.529
16	5.261	0.773	-0.599
17	5.635	0.870	-0.621
18	6.245	0.586	-0.857
19	6.616	0.540	-0.780
20	6.942	0.540	-0.541
21	7.267	0.545	-0.540
22	7.594	0.952	-0.541
23	8.062	0.897	-0.683
24	8.705	0.605	-0.999
25	9.079	0.613	-0.767
26	9.430	0.680	-0.585
27	9.835	0.656	-0.636
28	10.251	0.605	-0.692
29	10.616	0.604	-0.639
30	10.980	0.605	-0.605
31	11.345	0.605	-0.605
32	11.709	0.605	-0.605
33	12.074	0.605	-0.605
34	12.438	0.605	-0.604
35	12.803	0.587	-0.605
36	13.168	0.553	-0.605
37	13.503	0.550	-0.576
38	13.834	0.604	-0.550
39	14.166	0.710	-0.550
40	14.596	0.637	-0.649

Table LM8/4.7.5-4
Fuel #2 Reading Error by PCM Bit

PCM BITS	PCM QUANTITY	POSITIVE ERROR	NEGATIVE ERROR
1	0.0	0.691	0.0
2	0.473	0.548	-0.473
3	0.803	0.548	-0.553
4	1.133	0.548	-0.547
5	1.463	0.734	-0.547
6	1.793	0.746	-0.747
7	2.340	0.501	-0.764
8	2.642	0.501	-0.658
9	2.944	0.501	-0.501
10	3.246	0.502	-0.501
11	3.549	0.501	-0.502
12	3.851	0.501	-0.502
13	4.153	0.501	-0.501
14	4.455	0.501	-0.501
15	4.757	0.557	-0.501
16	5.059	0.805	-0.501
17	5.502	0.878	-0.642
18	6.051	0.657	-0.889
19	6.492	0.545	-0.803
20	6.820	0.546	-0.582
21	7.149	0.545	-0.545
22	7.478	0.899	-0.545
23	7.806	1.024	-0.545
24	8.552	0.625	-0.962
25	8.952	0.572	-0.972
26	9.294	0.660	-0.594
27	9.671	0.692	-0.603
28	10.101	0.629	-0.691
29	10.488	0.610	-0.671
30	10.856	0.609	-0.610
31	11.223	0.615	-0.609
32	11.591	0.627	-0.610
33	11.967	0.631	-0.619
34	12.348	0.630	-0.631
35	12.728	0.614	-0.631
36	13.108	0.572	-0.631
37	13.457	0.561	-0.600
38	13.795	0.571	-0.560
39	14.133	0.610	-0.561
40	14.494	0.627	-0.584

LM8/4.7.6.1 DPS Engine Thrust Vector Alignment

The gimbal trim angles for the DPS engine may be calculated using the equations provided in Paragraph 4.7.6.1. The thrust vector angles of the DPS engine at the start of the PDI burn are given in the Spacecraft Operational Data Book, Volume III, Mass Properties, Revision 2, as:

$$\delta\theta_T = -1.382 \text{ degrees}$$

$$\delta\psi_T = -0.499 \text{ degrees}$$

These values, together with a startup thrust of 1300 pounds, were then used to calculate the gimbal trim angles:

$$\delta\theta = -1.442 \text{ degrees}$$

$$\delta\psi = -0.439 \text{ degrees}$$

These are the recommended launch pad settings for the DPS gimbal trim angles at the start of the PDI burn.

The trim angles are set using the LM Guidance Computer (LGC), and must be expressed referenced to the positive gimbal stops. To accomplish this, 6.05 degrees were added to the trim angles above.

This results in

$$\delta\theta' = 4.608 \text{ degrees}$$

$$\delta\psi' = 5.611 \text{ degrees}$$

both referred to the positive gimbal stops.

The LGC has a nominal drive rate of 0.2000 degrees/second hard-wired into it. Therefore, all actual gimbal angles must be converted to equivalent angles based on the hard-wired drive rate using the actual gimbal drive rates in both pitch and roll. Where entered via the LGC erasable memory load, the angles must be expressed as drive times (from the positive stops). Where entered or displayed on the DSKY the equivalent angles must be expressed as degrees of arc.

LM8/4.7.6.1 DPS Engine Thrust Vector Alignment (Continued)

The GDA drive rates are listed below.

Functional Axis	Drive Rate
Pitch (X-Z plane)	0.2101 deg/sec
Roll (X-Y plane)	0.2125 deg/sec

The gimbal trim data to be entered in the LGC erasable memory load are then obtained as follows:

$$\text{PITTIME} = \frac{\delta\theta'}{0.2101} = 21.93 \text{ seconds}$$

$$\text{ROLLTIME} = \frac{\delta\psi'}{0.2125} = 26.40 \text{ seconds}$$

The corresponding angles to be entered or read from the DSKY are obtained as follows:

$$\text{P-TRIM} = \delta\theta' \left(\frac{0.2000}{0.2101}\right) = 4.386 \text{ degrees}$$

$$\text{R-TRIM} = \delta\psi' \left(\frac{0.2000}{0.2125}\right) = 5.281 \text{ degrees}$$

LM8/4.8.14 RCS Performance Limitations as a Result of Gimbal Drive Actuator (+ Pitch or + Roll) Failure During Powered Descent

LM8/4.8.14.1 Plume Impingement Constraints Due to GDA Failure

Figure LM8/4.8.14-1 shows the maximum allowable GDA offset angles as limited by the RCS impingement constraints for the affected vehicle hardware. These curves were developed from the LM-8 plume impingement capability curve. (See Figures, to be supplied.)

In the event of a GDA failure during powered descent, RCS plume impingement may constrain the mission. Figure LM8/4.8.14-2 represents the maximum allowable accumulated RCS firing time at any juncture during powered descent for GDA failure at several different times. The curves reflect the duty cycle which causes failure of the plume deflectors. Note that the attainment of the duty cycle reflected by these curves will exceed the plume impingement capability of the S-band steerable antenna, EVA antenna, scientific equipment bay hood, quad III insulation, and possibly the ladder rung and the primary strut inner cylinder.

LM8/4.8.14.2 Additional RCS Propellant Consumption as a Result of Gimbal Drive Actuator Failure During DPS Operation

Figures LM8/4.8.14-3 and LM8/4.8.14-4 present the maximum allowable GDA pitch and roll angles at time of failure, considering the margin of RCS propellant at landing and the RCS limited torque authority. (See Paragraph 4.8.14.2.)

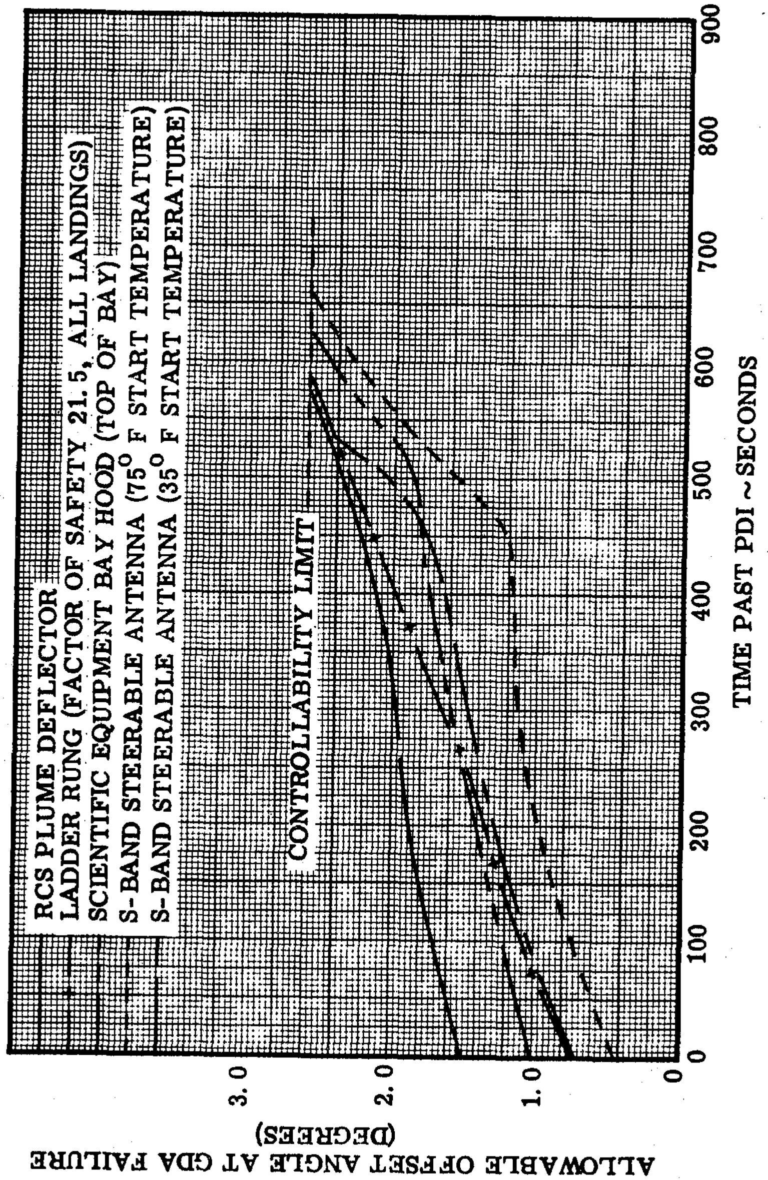

Figure LM8/4.8.14-1. Allowable GDA Offset Angle (at GDA Failure) During Powered Descent (as Determined by RCS Plume Impingement Limit) (See Para. LM8/4.8.14.1)

NOTE: THESE CURVES BASED UPON PLUME IMPINGEMENT CAPABILITY OF PLUME DEFLECTORS. CAPABILITY OF S-BAND STEERABLE ANTENNA, SCIENTIFIC EQUIPMENT BAY HOOD, EVA ANTENNA, QUAD III INSULATION, AND LADDER RUNG MAY BE EXCEEDED IF THESE CYCLES ARE ACHIEVED

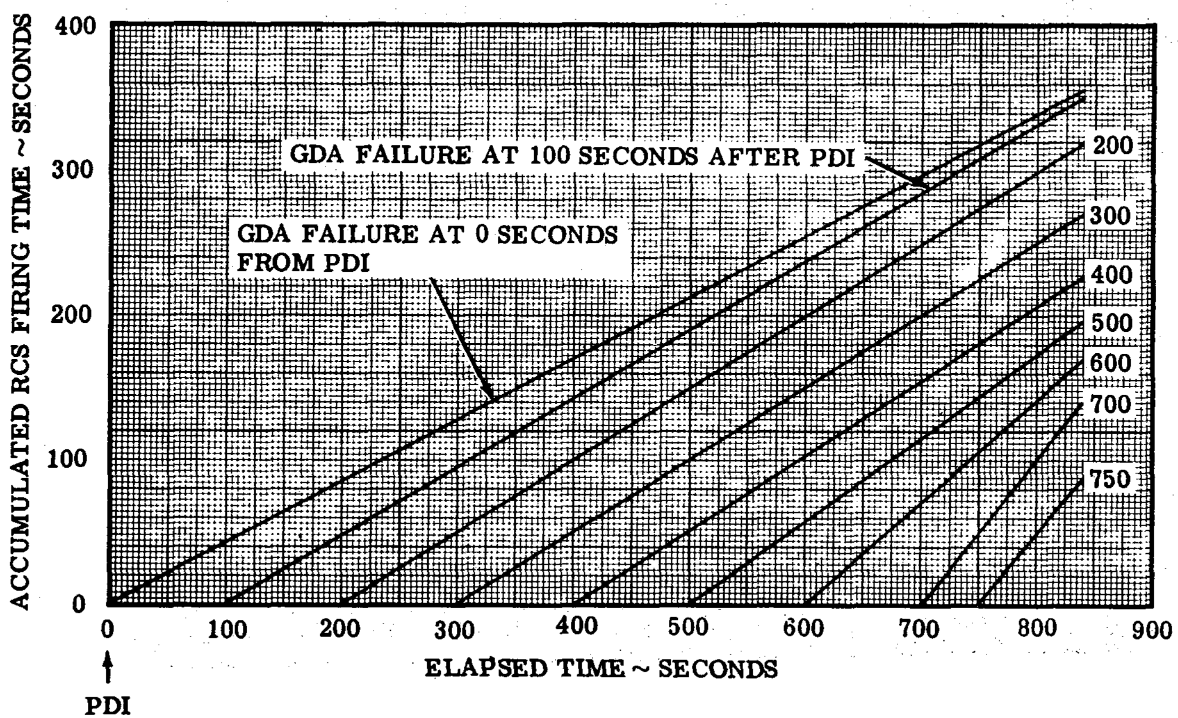

Figure LM8/4.8.14-2. Allowable RCS +X Firing Time vs Time From Powered Descent Initiation (See Para. LM8/4.8.14.1)

- ASSUMES 140 LBM RCS PROPELLANT REMAINING AT TOUCHDOWN
- THRUST VECTOR CHANGES DUE TO THROAT EROSION NOT INCLUDED

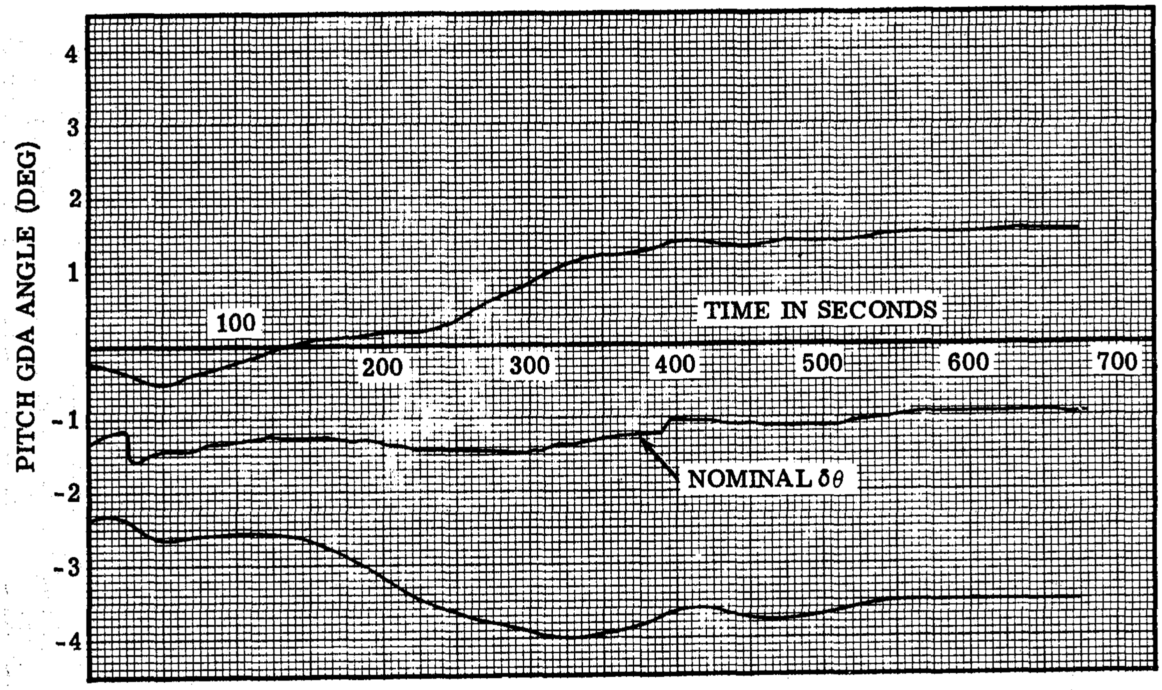

Figure LM8/4. 8. 14-3. Maximum Allowable Pitch GDA Failure Angle vs. Time During Powered Descent LM-8

- ASSUMES 140 LBM RCS PROPELLANT REMAINING AT TOUCHDOWN
- THRUST VECTOR CHANGES DUE TO THROAT EROSION NOT INCLUDED

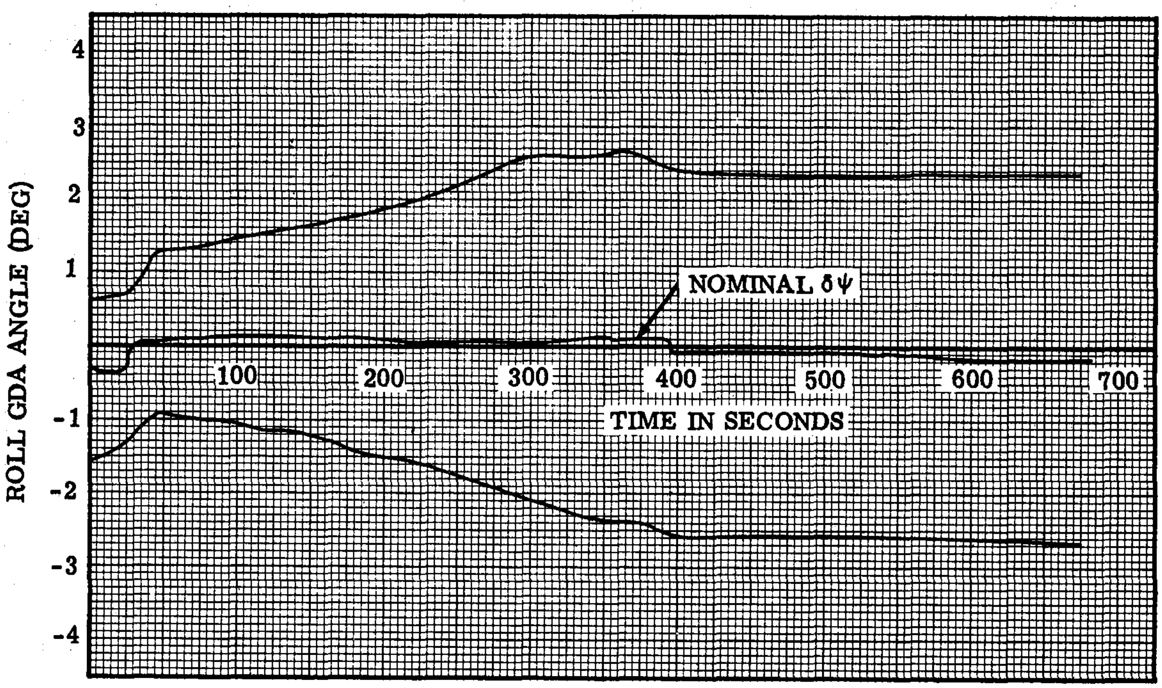

Figure LM8/4. 8. 14-4. Maximum Allowable Roll GDA Failure Angle vs. Time During Powered Descent LM-8

Volume II LM Data Book
APPENDIX LM-9

TABLE OF CONTENTS

Changes to baseline data specific to LM-9 are included in this appendix.

1.0	No change
2.0	No change
3.0	No change
4.5.4.4.16	Allowable Vehicle Acceleration During RR Power Off Periods
5.0	No change
6.0	No change
7.0	No change
8.0	No change

OPERATIONAL LIMITATION OR PROCEDURE	RATIONALE
LM9/DPS-8 Non-Throttling Range Engine Operation	
See Table LM9/3.7.1-1	Off-nominal mixture ratios may result, or the thrust chamber may burn through.

Table LM 9/3.7.1-1 Non-Throttling Range Engine Operation

VEHICLE	ENGINE S/N	NOMINAL CONDITIONS		WORST CASE CONDITIONS *	
		Predicted Erosion **	Permissible Time In Non-Throttling Region ***	Predicted Erosion **	Permissible Time In Non-Throttling Region ***
LM-9	1045	18.6%	82.0 sec.	29.6%	27.0 sec.

* Worst Case erosions are applicable for MDC performed with cold propellants and high mixture ratios. (FTP O/F = 1.63, 25% Thrust O/F = 1.65, Propellant Bulk Temperature = 50° F)

** Predicted erosion is to propellant depletion with zero time in non-throttling range.

*** Operating time in the non-throttling range, as given, is permitted at any time during the lunar landing duty cycle.

Note: The permissible time in the non-throttling region is based on limiting the total mission duty cycle erosion to 35%, including normal and non-throttling range operations.

MDC - Mission Duty Cycle

LM9/4.5.4.4.16 Allowable Vehicle Accelerations During RR Power Off Periods

Figures LM9/4.5.4-1 through LM9/4.5.4-4 show the maximum allowable LM body accelerations for any angular position of the RR antenna trunnion and shaft axes under which the antenna will not move from a fixed position with no power applied to the RR. The effect of varying the antenna temperature is also indicated in the figures.

The antenna shaft axis will always be parallel to the LM Y-axis. Therefore, LM body accelerations about the LM Y-axis can be used directly. However, as the shaft axis rotates, the trunnion axis will be parallel to the LM X-axis at 0° shaft position and parallel to the LM Z-axis at -90° shaft position. For other shaft positions, the allowable LM acceleration about the LM axes must be converted to the acceleration about the trunnion axis at the appropriate shaft position.

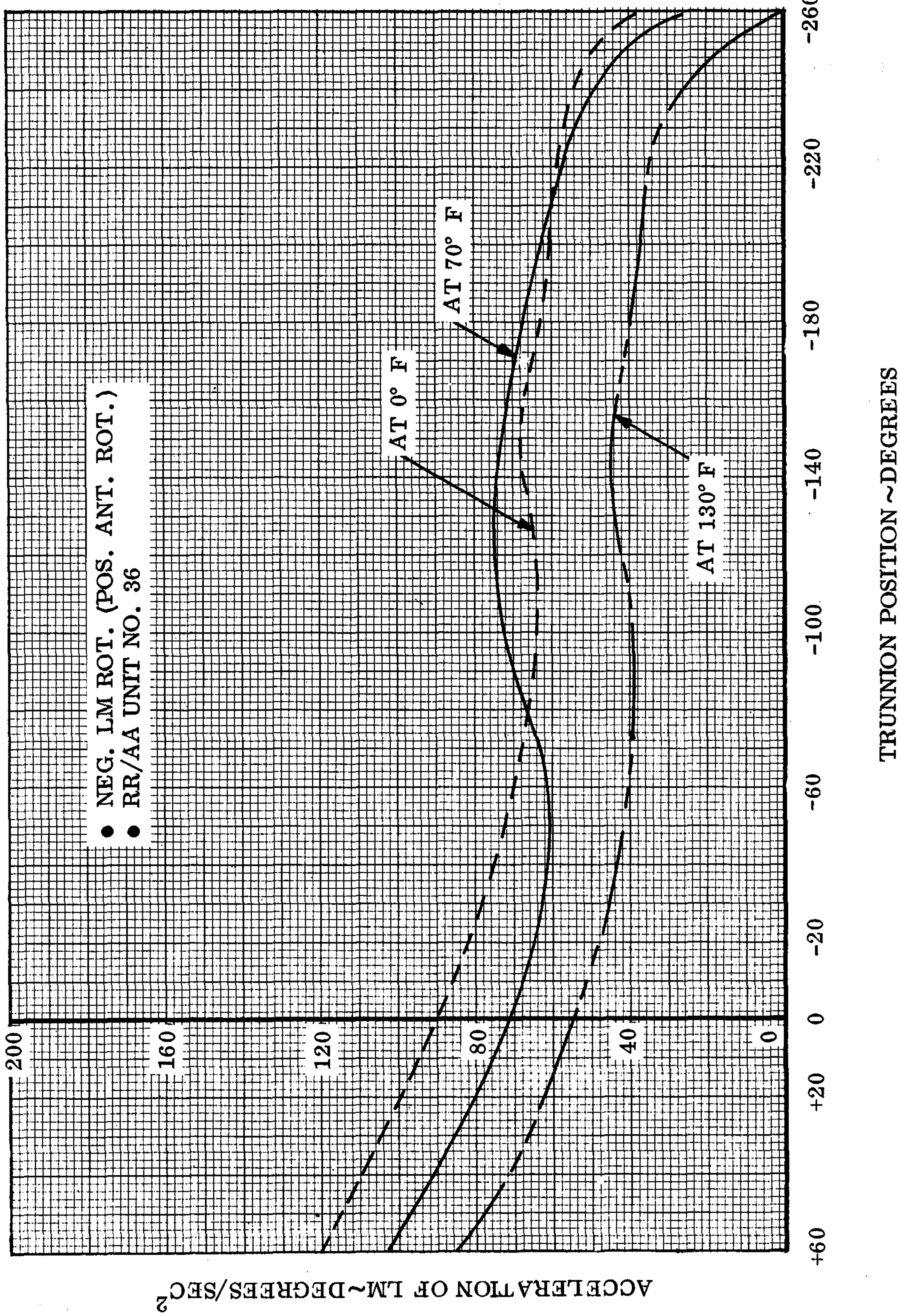

Figure LM9/4.5.4-1. Allowable Acceleration Trunnion Axis

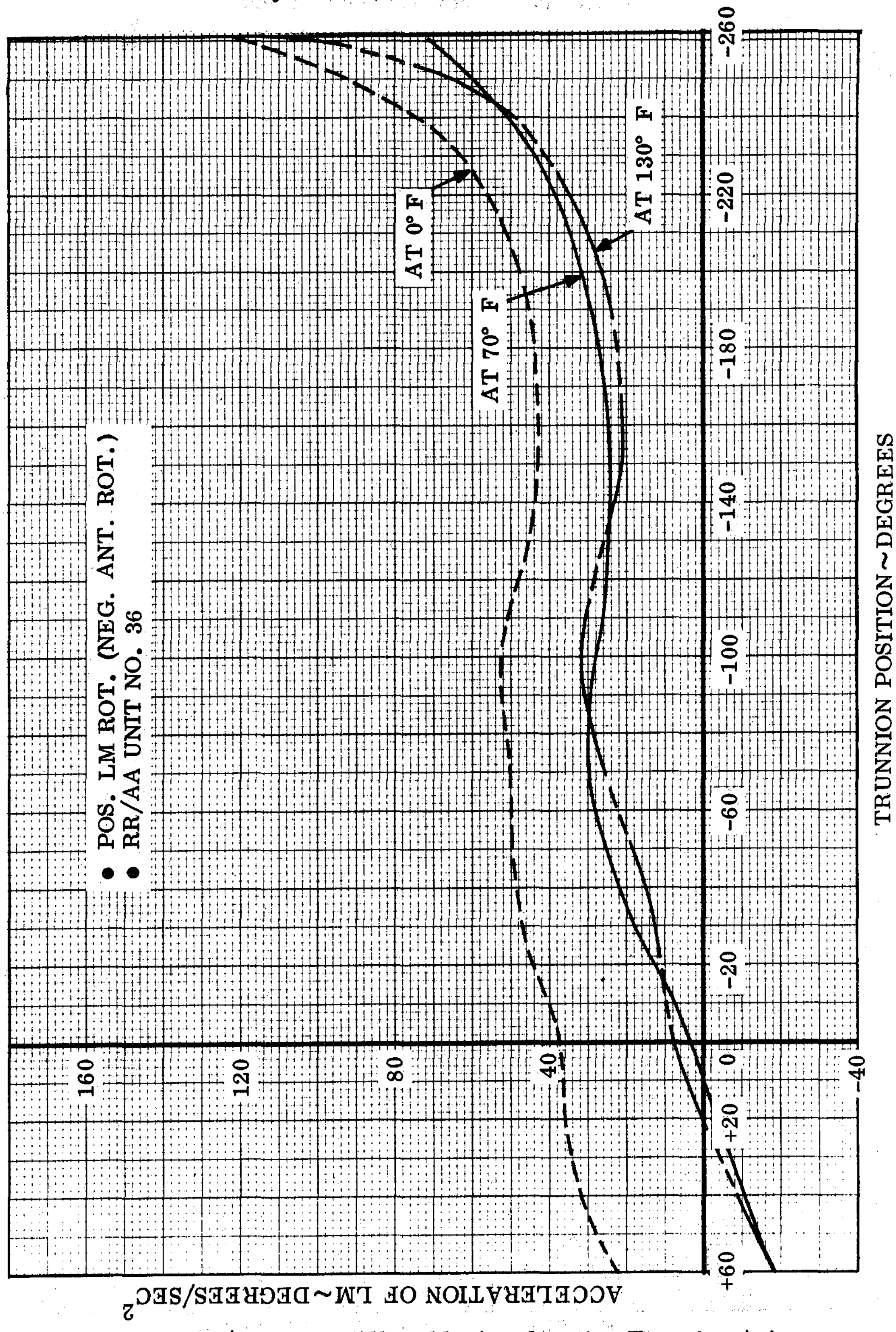

Figure LM9/4.5.4-2. Allowable Acceleration Trunnion Axis

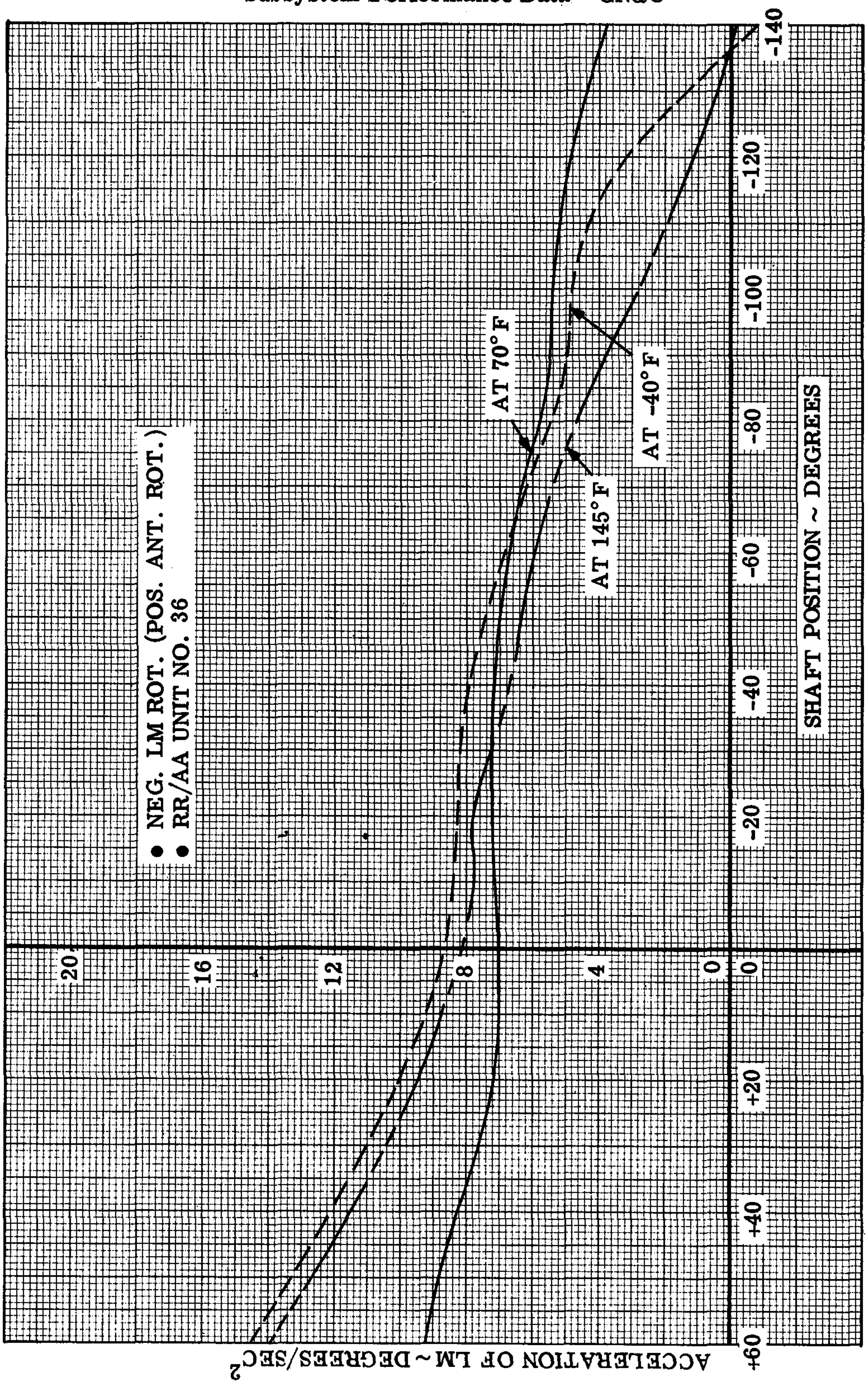

Figure LM9/4. 5. 4-3. Allowable Acceleration Shaft Axis

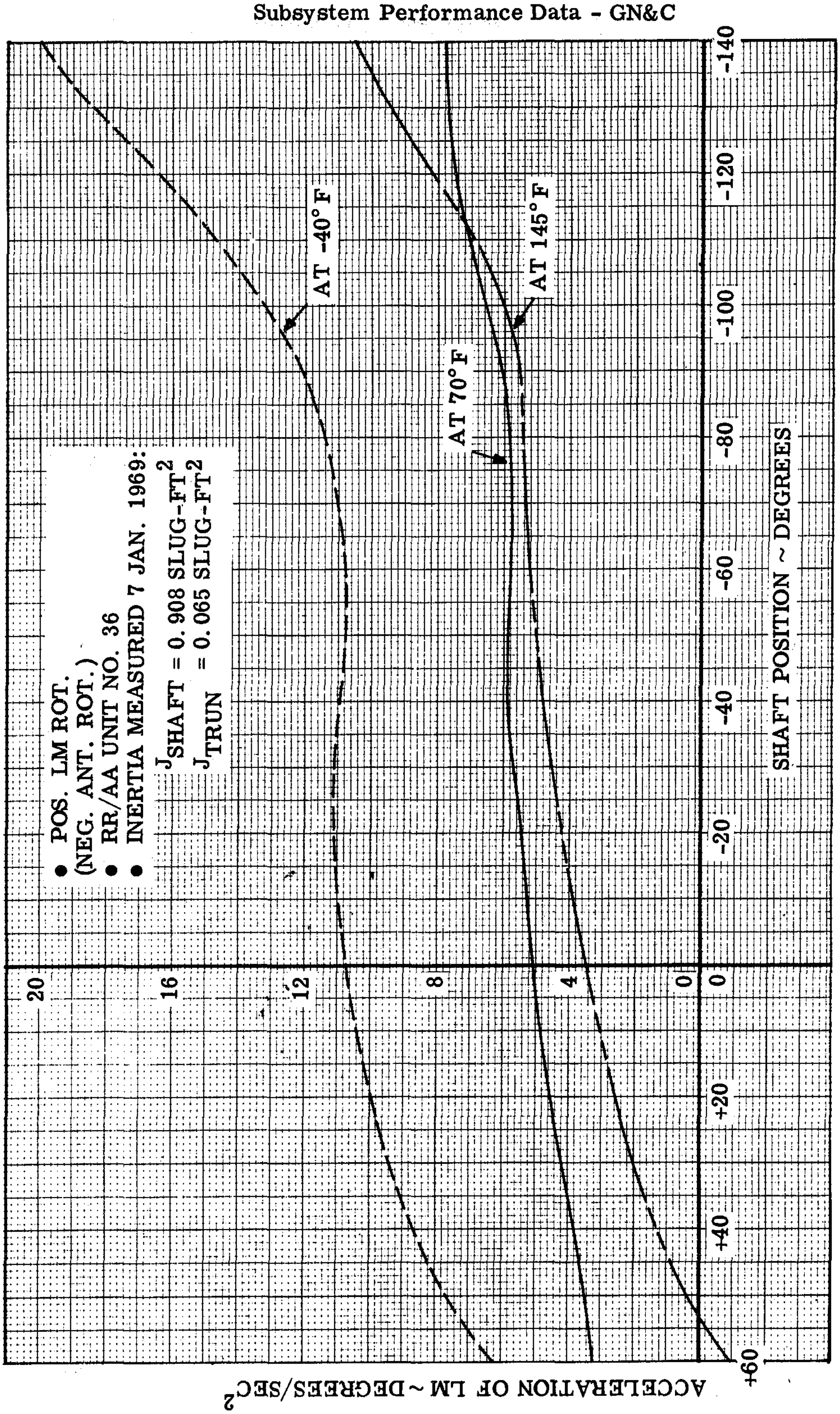

Figure LM9/4.5.4-4. Allowable Acceleration Shaft Axis

Volume II LM Data Book
APPENDIX

This appendix will not be updated and the data presented are only valid up to the Apollo 15 launch date, 26 July 1971. Consequently, revisions subsequent to the Apollo 15 flight may introduce data into the basic text of the data book that conflicts with the data in this appendix. Maintaining or deleting this appendix for LM-10 in the SODB is entirely at the option of the user.

The purpose of the attached listing is to enable each user of the Spacecraft Operational Data Book, Volume 11, Part 1, to ascertain that his data book is presently up-to-date. The listing shows the latest amendment released for each page of the data book. If the original page as released in Revision 2 is applicable, that page is so designated.

If the user determines that he is missing an amendment or any part of an amendment, he should contact George Holland of TRW at HU-8-3530, Ext. 3251. This listing will only be correct prior to the receipt of Amendment 129.

Page numbering key:

F - Front

B - Back

S - Single

F/O - Fold-Out

PAGE NUMBER	AMENDMENT NUMBER
1-1 F	129
1-2 B	Original
1-3 F	78
1-4 B	Original
1-5 F	Original
1-6 B	Original
1-7 F	Original
1-8 B	Original
2-1 F	Original
2-2 B	Original
2-3/2-4 F/O	Original
2-5 F	Original
2-6 B	Original
2-7 F	Original
2-8 B	Original
2-9/2-10 F/O	Original
2-11/2-12 F/O	Original
2-13 S	Original
3.0-1 S	Original
3.1-1 F	60
3.1-2 B	121
3.1-3 F	118
3.1-4 B	125
3.1-5 F	125
3.1-5.1 B	Original
3.1-5.2 S	39
3.1-6 F	Original
3.1-7 B	7
3.1-8 F	Original
3.1-9 B	7
3.1-10 S	Original
3.2-1 F	90
3.2-2 B	107
3.2-3 F	74
3.2-4 B	124
3.2-4.1 F	121
3.2-4.2 B	107
3.2-5 F	Original
3.2-6 B	Original
3.2-7 F	7
3.2-8 B	Original
3.2-9 F	Original
3.2-10 B	Original
3.2-11 F	Original
3.2-12 B	7
3.2-13 F	7
3.2-13.1 B	37
3.2-14 S	Original
3.2-15 F	Original
3.2-16 B	124
3.2-17 S	37

PAGE NUMBER	AMENDMENT NUMBER
3.3-1 F	97
3.3-2 B	Original
3.3-2.1 S	96
3.3-3 F	98
3.3-4 B	Original
3.3-5 F	97
3.3-6 B	98
3.3-6.1 F	109
3.3-6.2 B	111
3.3-6.3 S	111
3.3-7 F	118
3.3-8 B	109
3.3-9 F	109
3.3-10 B	109
3.4-1 F	125
3.4-2 B	22
3.4-2.1 S	97
3.4-3 F	124
3.4-3.1 B	127
3.4-4 F	8
3.4-5 B	8
3.5-1 F	99
3.5-2 B	80
3.5-3 F	121
3.5-4 B	121
3.5-5 F	80
3.5-6 B	80
3.5-7 F	43
3.5-8 B	96
3.5-9 F	112
3.5-10 B	99
3.5-11 F	96
3.5-12 B	43
3.5-12.1 S	93
3.5-13 F	85
3.5-14 B	95
3.5-15 F	45
3.5-16 B	100
3.5-17 F	128
3.5-18 B	Original
3.5-19 S	41
3.5-20 F	80
3.5-21 B	80
3.5-22 F	80
3.5-23 B	80
3.5-24 F	60
3.5-25 B	60
3.5-26 F	60
3.5-27 B	60
3.5-28 F	48
3.5-29 B	30
3.5-30 F	90
3.5-31 B	120

PAGE NUMBER	AMENDMENT NUMBER
3.5-32 F	120
3.5-33 B	Original
3.5-34 S	41
3.5-35 S	93
3.6-1 F	102
3.6-2 B	102
3.6-3 F	118
3.6-4 B	102
3.6-5 F	102
3.6-6 B	102
3.7-1 F	107
3.7-2 B	119
3.7-3 F	101
3.7-4 B	117
3.7-5 F	117
3.7-6 B	107
3.7-6.1 F	107
3.7-6.2 B	107
3.7-6.3 F	107
3.7-6.4 B	120
3.7-6.5 F	120
3.7-6.6 B	Original
3.7-7 F	119
3.7-8 B	117
3.7-9 S	Original
3.7-10 S	119
3.8-1 F	21
3.8-2 B	116
3.8-3 F	100
3.8-4 B	78
3.8-5 F	111
3.8-6 B	Original
3.8-7 F	78
3.8-8 B	78
3.8-9 F	37
3.8-10 B	37
3.8-11 F	78
3.8-12 B	37
3.8-12.1 S	100
3.8-13 S	117
3.9-1 F	Original
3.9-2 B	36
3.9-3 F	114
3.9-4 B	117
3.9-5 F	98
3.9-6 B	117
3.9-7 F	117
3.9-8 B	122

PAGE NUMBER	AMENDMENT NUMBER
3.9-9 F	122
3.9-10 B	122
3.9-11 S	122
3.10-1 F	Original
3.10-2 B	37
3.10-3 F	125
3.10-3.1 B	117
3.10-4 S	57
3.10-5 F	37
3.10-6 B	86
3.10-7 F	121
3.10-8 B	121
3.10-9 F	121
3.10-10 B	37
3.10-11 S	121
3.11-1 F	36
3.11-1.1 B	122
3.11-2 S	116
3.11-3 S	105
4.1 S	121
4.1-1 F	116
4.1-1.1 B	60
4.1-1.2 F	60
4.1-2 B	118
4.1-2.1 S	118
4.1-3 F	121
4.1-4 B	14
4.1-5 F	5
4.1-6 B	Original
4.1-7 F	121
4.1-8 B	121
4.1-9 F	121
4.1-10 B	121
4.1-11 F	121
4.1-12 B	121
4.1-13 F	Original
4.1-14 B	Original
4.1-15 F	Original
4.1-16 B	66
4.1-16.1 F	60
4.1-16.2 B	62
4.1-17 F	Original
4.1-18 B	117
4.1-19 F	117
4.1-19.1 B	60
4.1-19.2 F	60
4.1-19.3 B	60
4.1-19.4 F	118
4.1-19.5 B	118
4.1-19.6 S	118

PAGE NUMBER	AMENDMENT NUMBER
4.1-20/4.1-21 F/O	11
4.1-22/4.1-23 F/O	11
4.1-24/4.1-25 F/O	11
4.1-26/4.1-27 F/O	11
4.1-28 F	Original
4.1-29 B	Original
4.1-30/4.1-31 F/O	11
4.1-32/4.1-33 F/O	11
4.1-34 F	14
4.1-35 B	Original
4.1-36/4.1-37 F/O	11
4.1-38/4.1-39 F/O	11
4.1-40/4.1-41 F/O	11
4.1-42/4.1-43 F/O	11
4.1-44 S	Original
4.2 S	128
4.2-1 F	110
4.2-1.1 B	128
4.2-1.2 S	128
4.2-2 F	110
4.2-3 B	125
4.2-4 F	125
4.2-5 B	125
4.2-6 F	125
4.2-7 B	125
4.2-8 F	128
4.2-9 B	128
4.3 F	115
4.3A B	93
4.3-1 F	119
4.3-2 B	112
4.3-3 F	Original
4.3-4 B	119
4.3-4.1 F	115
4.3-4.2 B	115
4.3-5 F	Original
4.3-6 B	Original
4.3-7 F	88
4.3-8 B	Original
4.3-8.1 F	117
4.3-8.2 B	117
4.3-9 F	13
4.3-10 B	93
4.3-10.1 F	93
4.3-10.2 B	100
4.3-11 F	100
4.3-11.1 B	79
4.3-11.2 S	100
4.3-11.3 F	124

PAGE NUMBER	AMENDMENT NUMBER
4.3-11.4 B	124
4.3-12 S	119
4.3-13 F	117
4.3-14 B	119
4.3-15 F	Original
4.3-16 B	Original
4.3-17 F	Original
4.3-18 B	Original
4.3-19 F	Original
4.3-20 B	Original
4.3-21 F	Original
4.3-22 B	115
4.3-23 F	119
4.3-24 B	119
4.3-25 F	119
4.3-26 B	119
4.3-27 F	13
4.3-28 B	13
4.3-29 F	121
4.3-30 B	121
4.3-31 F	93
4.3-32 B	93
4.3-32.1 F	93
4.3-33 B	93
4.3-33.1 F	100
4.3-33.2 B	100
4.3-33.3 F	100
4.3-33.4 B	100
4.3-33.5 F	124
4.3-33.6 B	124
4.3-33.7 F	124
4.3-33.8 B	67
4.3-33.9 S	124
4.3-34 F	74
4.3-34.1 B	Original
4.3-35 F	111
4.3-36 B	117
4.3-36.1 F	85
4.3-36.2 B	85
4.3-37 F	Original
4.3-38 B	Original
4.3-39 F	Original
4.3-40 B	Original
4.3-41 F	115
4.3-42 B	115
4.3-43 F	115
4.3-44 B	Original
4.3-45 F	Original
4.3-46 B	Original
4.3-47 F	Original
4.3-48 B	Original

PAGE NUMBER	AMENDMENT NUMBER
4.3-49 F	Original
4.3-50 B	Original
4.3-51 F	Original
4.3-52 B	Original
4.3-53 F	94
4.3-54 B	80
4.3-55 F	Original
4.3-56 B	Original
4.3-57 F	Original
4.3-58 B	Original
4.3-59 F	Original
4.3-60 B	Original
4.3-61 F	Original
4.3-62 B	Original
4.3-62.1 S	59
4.3-62.2 F	117
4.3-62.3 B	117
4.3-62.4 F	117
4.3-62.5 B	117
4.3-63 F	114
4.3-64 B	114
4.3-65 F	114
4.3-66 B	114
4.3-66.1 F	93
4.3-66.2 B	93
4.3-66.3 F	93
4.3-66.4 B	93
4.3-66.5 F	93
4.3-66.6 B	93
4.3-66.7 F	93
4.3-66.8 B	93
4.3-66.9 F	93
4.3-66.10 B	93
4.3-66.11 F	93
4.3-66.12 B	93
4.3-66.13 F	93
4.3-66.14 B	93
4.3-66.15 F	93
4.3-66.16 B	93
4.3-66.17 S	93
4.3-66.18 F	105
4.3-66.19 B	105
4.3-66.20 F	105
4.3-66.21 B	105
4.3-66.22 F	105
4.3-66.23 B	124
4.3-66.24 F	124
4.3-66.25 B	124
4.3-66.26 F	105
4.3-66.27 B	105
4.3-66.28 F	105
4.3-66.29 B	105
4.3-66.30 F	105

PAGE NUMBER	AMENDMENT NUMBER
4.3-66.31 B	105
4.3-67 F	Original
4.3-68 B	Original
4.3-69 F	Original
4.3-70 B	Original
4.3-71 F	Original
4.3-72 B	Original
4.3-73 F	Original
4.3-74 B	Original
4.3-75 F	Original
4.3-76 B	Original
4.3-77 F	Original
4.3-78 B	Original
4.3-79 F	Original
4.3-80 B	Original
4.3-81 F	Original
4.3-82 B	Original
4.3-83 F	Original
4.3-84 B	Original
4.3-85 F	Original
4.3-86 B	Original
4.3-87 F	Original
4.3-88 B	Original
4.3-89 F	65
4.3-90 B	65
4.3-91 F	65
4.3-92 B	65
4.3-93 F	65
4.3-94 B	65
4.3-95 F	65
4.3-96 B	65
4.3-97 F	65
4.3-98 B	65
4.3-99 F	65
4.3-100 B	65
4.3-101 F	65
4.3-102 B	65
4.3-103 F	65
4.3-104 B	65
4.3-105 F	65
4.3-106 B	65
4.3-107 F	65
4.3-108 B	65
4.3-109 F	65
4.3-110 B	65
4.3-111 F	65
4.3-112 B	65
4.3-113 S	71
4.3-114 F	67
4.3-115 B	67
4.3-116 F	67
4.3-117 B	67
4.3-118 F	67

PAGE NUMBER	AMENDMENT NUMBER
4.3-119 B	67
4.3-120 F	67
4.3-121 B	67
4.3-122 F	67
4.3-123 B	67
4.3-124 F	67
4.3-125 B	67
4.3-126 F	79
4.3-127 B	79
4.3-128 F	79
4.3-129 B	79
4.3-130 F	124
4.3-131 B	124
4.3-132 F	124
4.3-133 B	124
4.3-134 F	124
4.3-135 B	124
4.3-136 F	124
4.3-137 B	124
4.4 S	124
4.4-1 F	125
4.4-2 B	70
4.4-3 F	Original
4.4-4 B	125
4.4-5 F	Original
4.4-5.1 B	124
4.4-6 S	114
4.4-7 F	127
4.4-8 B	Original
4.4-9 F	114
4.4-10 B	Original
4.4-11 F	114
4.4-12 B	Original
4.4-13 F	121
4.4-14 B	114
4.4-15 F	Original
4.4-16 B	114
4.4-17 F	114
4.4-18 B	Original
4.4-19 F	Original
4.4-20 B	114
4.4-21 F	114
4.4-22 B	114
4.4-23 F	89
4.4-24 B	Original
4.4-25 F	Original
4.4-26 B	114
4.4-27 F	77
4.4-28 B	114
4.4-29 F	114
4.4-30 B	114

PAGE NUMBER	AMENDMENT NUMBER
4.4-31 F	Original
4.4-32 B	114
4.4-33 F	114
4.4-34 B	Original
4.4-35 F	Original
4.4-35.1 B	70
4.4-36 S	Original
4.4-37 F	125
4.4-38 B	125
4.4-39 F	125
4.4-40 B	125
4.4-41 F	125
4.4-42 B	125
4.4-43 F	125
4.4-44 B	Original
4.4-45 F	Original
4.4-46 B	Original
4.4-47 F	Original
4.4-48 B	2-82
4.4-49 F	Original
4.4-50 B	Original
4.4-51 F	Original
4.4-52 B	Original
4.4-53 F	Original
4.4-54 B	Original
4.4-55 F	Original
4.4-56 B	Original
4.4-57 F	Original
4.4-58 B	Original
4.4-59 F	Original
4.4-60 B	Original
4.4-61 F	Original
4.4-62 B	Original
4.4-63 F	Original
4.4-64 B	Original
4.4-65 F	Original
4.4-66 B	46
4.4-67 F	Original
4.4-68 B	46
4.4-69 F	125
4.4-70 B	124
4.4-70.1 S	124
4.4-71 F	125
4.4-72 B	Original
4.4-73 F	Original
4.4-73.1 F	83
4.4-74 S	125
4.4-75 F	125
4.4-76 B	125
4.4-76.1 S	83
4.4-76.2 F	125
4.4-76.3 B	125

PAGE NUMBER	AMENDMENT NUMBER	PAGE NUMBER	AMENDMENT NUMBER
4.4-77 F	Original	4.5-24 B	94
4.4-78 B	Original	4.5-24.1 F	100
4.4-79 F	Original	4.5-24.2 B	100
4.4-80 B	Original	4.5-24.3 F	100
4.4-81 F	Original	4.5-24.4 B	100
4.4-82 B	Original	4.5-25 F	Original
4.4-83 F	Original	4.5-26 B	Original
4.4-84 B	Original	4.5-27 F	Original
4.4-85 F	Original	4.5-28 B	18
4.4-86 B	Original	4.5-28.1 F	126
4.4-87 S	Original	4.5-28.2 B	126
		4.5-28.3 S	115
4.5 F	115	4.5-29 F	77
4.5A B	129	4.5-30 B	77
4.5B F	47	4.5-31 F	77
4.5C B	120	4.5-32 B	77
4.5-1 F	Original	4.5-33 F	Original
4.5-2 B	80	4.5-34 B	Original
4.5-3 F	80	4.5-35 F	Original
4.5-4 B	115	4.5-36 B	Original
4.5-5 F	115	4.5-36.1 F	29
4.5-6 B	29	4.5-36.2 B	67
4.5-7 F	77	4.5-36.3 F	86
4.5-8 B	86	4.5-36.4 B	86
4.5-8.1 F	86	4.5-36.5 F	86
4.5-8.2 B	96	4.5-36.6 B	86
4.5-8.3 F	96	4.5-36.7 F	86
4.5-8.4 B	96	4.5-36.8 B	86
4.5-9 F	Original	4.5-36.9 S	94
4.5-10 B	Original	4.5-37 F	Original
4.5-11 F	Original	4.5-38 B	Original
4.5-12 B	Original	4.5-39 F	Original
4.5-13 F	Original	4.5-40 B	Original
4.5-14 B	97	4.5-41 F	Original
4.5-15 F	4	4.5-42 B	Original
4.5-16 B	3	4.5-43 F	Original
4.5-17 F	97	4.5-44 B	Original
4.5-18 B	95	4.5-45 F	Original
4.5-19 F	Original	4.5-46 B	Original
4.5-20 B	Original	4.5-47 F	Original
4.5-20.1 F	Original	4.5-47.1 B	65
4.5-21 B	128	4.5-47.2 F	65
4.5-21.1 F	47	4.5-47.3 B	86
4.5-21.2 B	47	4.5-47.4 F	86
4.5-21.3 F	47	4.5-47.5 B	86
4.5-21.4 B	47	4.5-47.6 F	86
4.5-21.5 F	47	4.5-47.7 B	86
4.5-21.6 B	47	4.5-48 F	70
4.5-21.7 F	47	4.5-48.1 B	96
4.5-22 B	47	4.5-48.2 F	96
4.5-23 F	55	4.5-48.3 B	96

PAGE NUMBER	AMENDMENT NUMBER
4.5-48.4 F	96
4.5-48.5 B	96
4.5-48.6 F	96
4.5-48.7 B	96
4.5-49 F	Original
4.5-50 B	Original
4.5-51 F	Original
4.5-52 B	Original
4.5-53 F	Original
4.5-54 B	Original
4.5-55 F	Original
4.5-56 B	Original
4.5-57 F	Original
4.5-58 B	Original
4.5-59 F	Original
4.5-60 B	Original
4.5-61 F	Original
4.5-62 B	Original
4.5-63 F	Original
4.5-64 B	Original
4.5-65 F	Original
4.5-66 B	Original
4.5-67 F	Original
4.5-67.1 B	4
4.5-68 S	Original
4.5-69 F	Original
4.5-70 B	Original
4.5-71 F	Original
4.5-72 B	Original
4.5-73 F	Original
4.5-73.1 B	4
4.5-73.2 F	4
4.5-74 B	Original
4.5-75 F	Original
4.5-76 B	Original
4.5-77 F	Original
4.5-78 B	Original
4.5-79 F	Original
4.5-80 B	Original
4.5-81 F	Original
4.5-82 B	Original
4.5-83 F	3
4.5-84 B	3
4.5-84.1 S	47
4.5-84.2 F	83
4.5-84.3 B	83
4.5-84.4 F	83
4.5-84.5 B	83
4.5-85 F	Original
4.5-86 B	Original
4.5-86.1 F	128

PAGE NUMBER	AMENDMENT NUMBER
4.5-86.2 B	128
4.5-86.3 S	128
4.5-87 S	Original
4.5-87.1 F	47
4.5-87.2 B	47
4.5-87.3 F	47
4.5-87.4 B	47
4.5-87.5 F	47
4.5-87.6 B	47
4.5-87.7 F	47
4.5-88 B	24
4.5-89 F	24
4.5-90 B	24
4.5-91 F	Original
4.5-92 B	Original
4.5-93 F	Original
4.5-94 B	Original
4.5-95 F	Original
4.5-96 B	Original
4.5-96.1 S	94
4.5-96.2/ 4.5-96.3 F/O	94
4.5-97 F	Original
4.5-98 B	Original
4.5-98.1 F	105
4.5-98.2 B	105
4.5-98.3 S	105
4.5-98.4 F	100
4.5-98.5 B	100
4.5-99 F	Original
4.5-100 B	Original
4.5-101 F	Original
4.5-102 B	Original
4.6 S	72
4.6-1 F	107
4.6-2 B	107
4.6-2.1 F	97
4.6-2.2 B	97
4.6-3 S	2
4.6-3.1 F	96
4.6-3.2 B	96
4.6-4 F	62
4.6-4.1 B	62
4.6-5 F	58
4.6-5.1 B	Original
4.6-6 S	126
4.6-7 F	103
4.6-8 B	103
4.6-9 F	107
4.6-10 B	12

PAGE NUMBER	AMENDMENT NUMBER
4.6-10.1 S	97
4.6-11 F	Original
4.6-11.1 B	96
4.6-12 F	107
4.6-13 B	107
4.6-14 F	107
4.6-15 B	107
4.6-16/4.6-22 S	107
4.6-23 F	12
4.6-24 B	12
4.6-25 F	12
4.6-26 B	Original
4.6-27 F	Original
4.6-28 B	Original
4.6-29 F	Original
4.6-30 B	Original
4.6-31 F	Original
4.6-32 B	Original
4.6-33 F	Original
4.6-34 B	Original
4.6-34.1 F	69
4.6-34.2 B	69
4.6-34.3 F	69
4.6-34.4 B	69
4.6-34.5 F	72
4.6-34.6 B	72
4.6-34.7 S	69
4.6-34.8 F	72
4.6-34.9 B	72
4.6-34.10 F	72
4.6-34.11 B	72
4.6-34.12 S	97
4.6-35 F	2
4.6-36 B	2
4.6-36.1 S	2
4.6-37 F	19
4.6-38 B	19
4.6-39 F	Original
4.6-40 B	Original
4.6-41 F	Original
4.6-42 B	53
4.6-43 F	53
4.6-44 B	53
4.6-45 F	53
4.6-45.1 B	53
4.6-45.2 F	121
4.6-45.3 B	121
4.6-45.4 S	126
4.6-46 S	Original
4.6-47 F	Original
4.6-48 B	Original
4.6-49 F	Original

PAGE NUMBER	AMENDMENT NUMBER
4.6-50 B	Original
4.6-51 F	Original
4.6-52 B	Original
4.6-53 F	Original
4.6-54 B	Original
4.6-55 F	Original
4.6-56 B	Original
4.6-57 F	Original
4.6-58 B	Original
4.6-59 F	Original
4.6-60 B	Original
4.6-61 F	Original
4.6-62 B	88
4.6-63 F	96
4.6-64 B	Original
4.6-65 F	Original
4.6-66 B	Original
4.7 S	124
4.7-1 F	122
4.7-2 B	122
4.7-3 F	97
4.7-3.1 B	73
4.7-4 S	Original
4.7-4.1 F	122
4.7-5 B	124
4.7-5.1 F	Original
4.7-6 B	118
4.7-7 F	126
4.7-7.1 B	118
4.7-7.2 F	126
4.7-8 B	126
4.7-9 F	115
4.7-10 B	51
4.7-10.1 F	124
4.7-10.2 B	124
4.7-11 F	Original
4.7-12 B	124
4.7-12.1 F	124
4.7-12.2 B	124
4.7-13 F	124
4.7-13.1 B	118
4.7-13.2 S	110
4.7-14 F	110
4.7-15 B	110
4.7-16 F	110
4.7-17 B	110
4.7-18 F	110
4.7-19 B	110
4.7-20 S	110
4.7-21 F	120
4.7-21.1 B	122

PAGE NUMBER	AMENDMENT NUMBER	PAGE NUMBER	AMENDMENT NUMBER
4.7-22 S	120	4.7-50.10 B	53
4.7-23 F	120	4.7-50.11 F	53
4.7-24 B	Original	4.7-50.12 B	53
4.7-25 F	4	4.7-51 F	120
4.7-26 B	4	4.7-51.1 B	114
4.7-27 S	118	4.7-52 F	115
4.7-28 F	73	4.7-53 B	115
4.7-28.1 B	73	4.7-54 F	115
4.7-28.2 F	73	4.7-55 B	115
4.7-28.3 B	73	4.7-56 S	Original
4.7-29 F	Original	4.7-57 F	Original
4.7-30 B	120	4.7-58 B	Original
4.7-31 F	Original	4.7-59 F	Original
4.7-32 B	120	4.7-60 B	Original
4.7-33 F	120	4.7-61 F	Original
4.7-34 B	120	4.7-62 B	Original
4.7-34.1 F	122	4.7-63 F	Original
4.7-34.2 B	95	4.7-64 B	Original
4.7-35 F	Original	4.7-65 F	124
4.7-36 B	Original	4.7-66 B	124
4.7-36.1 S	2		
4.7-37 F	120	4.8 F	100
4.7-38 B	120	4.8A B	59
4.7-39 F	120	4.8-1 F	80
4.7-40 B	53	4.8-2 B	109
4.7-40.1 F	120	4.8-3 F	Original
4.7-40.2 B	120	4.8-4 B	80
4.7-40.3 F	119	4.8-5 F	Original
4.7-40.4 B	70	4.8-6 B	79
4.7-40.5 F	119	4.8-7 F	79
4.7-40.6 B	119	4.8-8 B	Original
4.7-40.7 F	126	4.8-9 F	Original
4.7-40.8 B	126	4.8-10 B	Original
4.7-40.9 F	126	4.8-11 F	Original
4.7-40.10 B	126	4.8-12 B	Original
4.7-40.11 S	116	4.8-13 F	79
4.7-41 F	126	4.8-14 B	Original
4.7-42 B	126	4.8-15 F	Original
4.7-43 F	126	4.8-16 B	Original
4.7-44 B	126	4.8-17 F	Original
4.7-45 F	126	4.8-18 B	95
4.7-46 B	126	4.8-19 F	Original
4.7-47 F	126	4.8-20 B	49
4.7-48 B	126	4.8-20.1 S	73
4.7-49 F	118	4.8-21 F	128
4.7-50 B	53	4.8-21.1 B	128
4.7-50.1 F	53	4.8-21.2 F	128
4.7-50.2 B	53	4.8-21.3 B	100
4.7-50.3 F	53	4.8-21.4 F	116
4.7-50.4 B	53	4.8-21.5 B	128
4.7-50.5 F	53	4.8-21.6 F	128
4.7-50.6 B	53	4.8-21.7 B	100
4.7-50.7 F	53	4.8-22 S	128
4.7-50.8 B	53	4.8-22.1 F	100
4.7-50.9 F	53	4.8-22.2 B	56

PAGE NUMBER	AMENDMENT NUMBER	PAGE NUMBER	AMENDMENT NUMBER
4.8-23 F	110	4.8-67 F	Original
4.8-24 B	Original	4.8-68 B	Original
4.8-25 F	73	4.8-69 F	Original
4.8-26 B	21	4.8-70 B	Original
4.8-26.1 S	38	4.8-71 F	Original
4.8-27 F	53	4.8-72 B	Original
4.8-27.1 B	53	4.8-73 F	Original
4.8-28 S	53	4.8-74 B	Original
4.8-29 F	Original	4.8-75 F	Original
4.8-30 B	53	4.8-76 B	Original
4.8-31 F	Original	4.8-77 F	108
4.8-32 B	Original	4.8-78 B	Original
4.8-33 F	113	4.8-79 F	Original
4.8-34 B	Original	4.8-80 B	Original
4.8-35 F	Original	4.8-81 F	Original
4.8-36 B	21	4.8-82 B	Original
4.8-37 F	21	4.8-83 F	Original
4.8-38 B	21	4.8-84 B	Original
4.8-39 F	21	4.8-85 F	Original
4.8-39.1 B	129	4.8-86 B	Original
4.8-40 F	109	4.8-87 F	Original
4.8-41 B	109	4.8-88 B	Original
4.8-42 F	109	4.8-89 F	Original
4.8-43 B	109	4.8-90 B	Original
4.8-44 F	109	4.8-91 F	Original
4.8-45 B	109	4.8-92 B	Original
4.8-45.1 F	109	4.8-93 F	Original
4.8-45.2 B	109	4.8-94 B	Original
4.8-45.3 F	109	4.8-95 F	Original
4.8-45.4 B	109	4.8-96 B	Original
4.8-46 S	Original	4.8-96.1 F	56
4.8-47 F	Original	4.8-96.2 B	56
4.8-48 B	Original	4.8-97 F	125
4.8-49 F	72	4.8-98 B	Original
4.8-50 B	Original	4.8-99 F	Original
4.8-51 F	Original	4.8-99.1 B	73
4.8-52 B	Original	4.8-100 S	Original
4.8-53 F	Original	4.8-101 F	21
4.8-54 B	72	4.8-102 B	Original
4.8-55 F	79	4.8-103 F	Original
4.8-56 B	Original	4.8-104 B	21
4.8-57 F	Original	4.8-105 F	Original
4.8-58 B	80	4.8-106 B	Original
4.8-59 F	Original	4.8-107 F	21
4.8-60 B	Original	4.8-108 B	Original
4.8-61 F	Original	4.8-109 F	Original
4.8-62 B	Original	4.8-110 B	21
4.8-63 F	Original	4.8-111 F	Original
4.8-64 B	Original	4.8-112 B	Original
4.8-65 F	Original	4.8-113 F	Original
4.8-66 B	Original	4.8-113.1 B	116

PAGE NUMBER	AMENDMENT NUMBER
4.8-114 S	2
4.8-115 F	Original
4.8-116 B	Original
4.8-117 F	2
4.8-118 B	53
4.8-119 F	53
4.8-120 B	15
4.8-121 F	53
4.8-122 B	Original
4.8-123 F	53
4.8-124 B	Original
4.8-125 F	21
4.8-126 B	21
4.8-127 F	Original
4.8-128 B	Original
4.8-129 F	2
4.8-130 B	2
4.8-131 F	112
4.8-132 B	112
4.8-133 F	112
4.8-134 B	112
4.8-135 F	112
4.8-136 B	112
4.8-137 F	112
4.3-138 B	116
4.8-139 F	105
4.8-140 B	105
4.8-141 F	105
4.8-142 B	105
4.8-143 F	105
4.8-144 B	105
4.8-145 F	116
4.8-145.1 B	116
4.8-145.2 F	116
4.8-145.3 B	116
4.8-146 S	105
4.8-147 F	105
4.8-148 B	105
4.8-149 F	105
4.8-150 B	105
4.8-151 F	128
4.8-152 B	128
4.9 S	Original
4.9-1 S	114
5.1-1 F	Original
5.1-2 B	Original
5.1-3 F	Original
5.1-4 B	Original
5.1-5 F	Original
5.1-6 B	Original

PAGE NUMBER	AMENDMENT NUMBER
5.1-7 F	Original
5.1-8 B	Original
5.1-9 S	Original
6.1-1 S	Original
6.1-2 F	104
6.1-3 B	106
7.1-1 F	Original
7.1-2 B	Original
7.1-3 F	Original
7.1-4 B	Original
8.1-1 F	112
8.1-2 B	Original
8.1-3 F	112
8.1-4 B	Original
9.1-1 S	99
9.1-2 F	121
9.1-2.1 B	121
9.1-3 F	121
9.1-3.1 B	99
9.1-3.2 F	99
9.1-3.3 B	99
9.1-3.4 F	99
9.1-3.5 B	99
9.1-3.6 F	99
9.1-4 B	78
9.1-5 F	78
9.1-6 B	78
9.1-7 S	121

Volume II LM Data Book

APPENDIX LM-10

TABLE OF CONTENTS

Changes to baseline data specific to LM-10 are included in this appendix.

1.0	No change
2.0	No change
3.3	Environmental Control Subsystem Constraints
3.6	APS Subsystem Constraints
3.7	DPS Subsystem Constraints
3.8	Reaction Control Subsystem Constraints
3.10	Thermal Constraints
4.2.4	Thermal Variations for the MESA (TBS)
4.2.5	Thermal Variation of the Sample Return Containers after Removal from the MESA (TBS)
4.3.2.2	Leakage
4.3.2.6	Cabin Regulator Check (TBS)
4.3.3	Lithium Hydroxide Consumption
4.3.4.9	Water Quantity Measurement
4.3.8.1	Heat Transport Section Water Sublimators
4.3.11	Duty Cycle of LM Heaters
4.5.1.1	Uncertainty of LM IMU Alignment from CSM IMU
4.5.1.4	Guidance Computer Erasable Constants
4.5.1.5.2	Assembly Alignment Data of Spacecraft Docking Mating Surfaces to the Navigation Base
4.5.1.5.3	AOT Alignment Data
4.5.2.1	Abort Sensor Assembly
4.5.2.1.2	AGS Angular Mounting Error
4.5.2.2	Abort Electronic Assembly
4.5.3.2.2.3	DPS Thrust Response at TTCA Minimum and Maximum Positions
4.5.3.4.3	GDA Drive Rates
4.5.4.2	RR Mechanical Alignment
4.5.4.3	RR Timeline Operations (TBS)
4.5.4.4.11	RR and T AGC Voltage Versus Range
4.5.4.4.11.1	RR and T AGC Voltage Versus Range and LOS Angle
4.5.4.4.12	RR Self-Test
4.5.4.4.13	RR Power Monitor Calibration
4.5.4.4.16	Allowable Vehicle Acceleration During RR Power Off Periods
4.5.5.1.16	LR Power Monitor
4.5.5.1.17	Loss of LR Lock as a Function of Vehicle Pitch and Roll for Nominal Trajectory (TBS)
4.5.5.1.18	Expected Altitude of LR Velocity and Range Initial "Data Good" Indication (TBS)
4.5.5.1.21	LR Predicted Accuracy (TBS)
4.5.5.2	LR Temperature Profile
4.5.5.3	LR Mechanical Alignment

Volume II LM Data Book

APPENDIX LM-10

TABLE OF CONTENTS

Changes to baseline data specific to LM-10 are included in this appendix.

4.5.5.4	Landing Radar Self-Test
4.5.5.5	Landing Radar Reflectivity Model
4.6.1	APS Preflight Analysis
4.6.8	Thrust Vector Changes with Burn Time
4.6.9	Preflight Thermal Analysis of the APS
4.6.12	Ascent Engine Regulator Performance
4.7.1	DPS Preflight Prediction
4.7.2	Supercritical Helium Tank Pressure
4.7.5	DPS Propellant Tank Low Level Sensor Operation
4.7.6.1	DPS Engine Thrust Vector Orientation
4.7.8	Descent Propulsion Pre-Flight Thermal Analyses
4.7.12.1	DPS Propellant Tank Venting for Lunar Landing Mission
4.7.15	Descent Engine Regulator Performance
4.8.14	RCS Performance Limitations as a Result of Gimbal Drive Actuator (+ Pitch or + Roll) Failure During Powered Descent
4.8.14.1	Plume Impingement Constraints Due to GDA Failure
4.8.14.2	Additional RCS Propellant Consumption as a Result of Gimbal Drive Actuator Failure During DPS Operation
5.0	No change
6.0	No change
7.0	No change
8.0	No change

LM10/3.3 ENVIRONMENTAL CONTROL SUBSYSTEM

OPERATIONAL LIMITATION OR PROCEDURE	RATIONALE
LM10/ECS-23 D/S GOX Tank Pressure-Temperature Limit Relationship There are no fracture mechanics constraints on the LM-10 D/S GOX tanks since the fracture limit is above the relief valve critical value. Consequently no venting constraints are required.	

OPERATIONAL LIMITATION OR PROCEDURE	RATIONALE

LM10/3.5 GUIDANCE, NAVIGATION AND CONTROL

LM-10/IMU-6 Glycol Loop Stabilization

Eight-minute water sublimator operation is required prior to IMU operate mode activation.	Erroneous and changing operation during temperature cycling results in erroneous outputs.

OPERATIONAL LIMITATION OR PROCEDURE	RATIONALE
LM10/3.5 GUIDANCE, NAVIGATION AND CONTROL	
LM-10/LGC-1 Glycol Loop Stabilization	
Eight-minute water sublimator operation is required prior to LGC activation.	Erroneous and changing operation during temperature cycling results in erroneous outputs.

OPERATIONAL LIMITATION OR PROCEDURE	RATIONALE
LM10/3.5.2.1 Abort Sensor Assembly	
LM10/ASA-1 Survival Heating	
Continuous heater power is not required from earth launch to LM activation. Note: See restriction on switch from OFF to STBY or OPERATE modes in paragraph 3.5.2.1 ASA-1.	

LM10/3.6 PROPULSION - APS

OPERATIONAL LIMITATION OR PROCEDURE	RATIONALE
LM10/APS-1 Propellant Tank Pressure-Temperature Limit Relationship	
The propellant tank pressures should not exceed the values given in Figure LM10/3.6.1-1, LM10/3.6.1-2 and LM10/3.6.1-3.	Reliability is reduced below the allowable value.
LM10/APS-9 Ambient Helium Storage Tank Pressure	
Helium tank pressure limitations are given in Figure LM10/3.6.1-4.	If maximum is exceeded, reliability is reduced below allowable value. If minimum is exceeded, there will be insufficient helium to complete a lunar mission duty cycle.

NOTE: CURVES ARE BASED UPON THE FOLLOWING PRESSURIZATION SCHEDULE AT KSC.

OXIDIZER	FUEL
1 CYCLE AT 187 PSID	1 CYCLE AT 187 PSID
2 CYCLES AT 185 PSID	1 CYCLE AT 186 PSID
	1 CYCLE AT 188 PSID

CURVES MUST BE REVISED IF THE TANKS ARE CYCLED MORE THAN STATED ABOVE

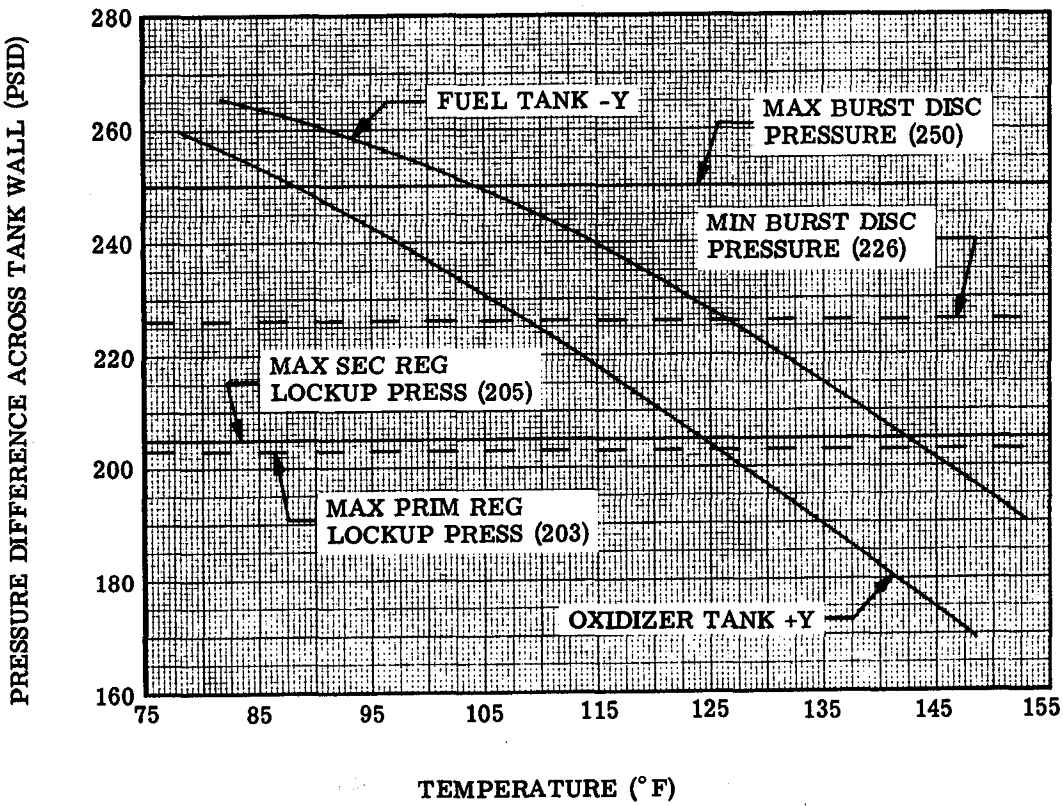

Figure LM10/3.6.1-1. Maximum Allowable Pressure-Temperature Limit Relationship for LM-10 Ascent Stage Propellant Tanks

NOTE: 1 - * INCLUDES INSTR. ERROR
2 - NO LEAKAGE ALLOWED
3 - 2014 LBS TARGET LOAD
4 - MAX. PRESS. DECAY DEFINED BY SOLUBILITY CURVE. HOWEVER, EXCESSIVE DECAY RATES MUST BE EVALUATED CONSIDERING SOLUBILITY EFFECTS FOR INTERMEDIATE POINTS.
5 - ** INCLUDES INSTR. ERROR AND CHECK VALVE CRACKING PRESSURE.

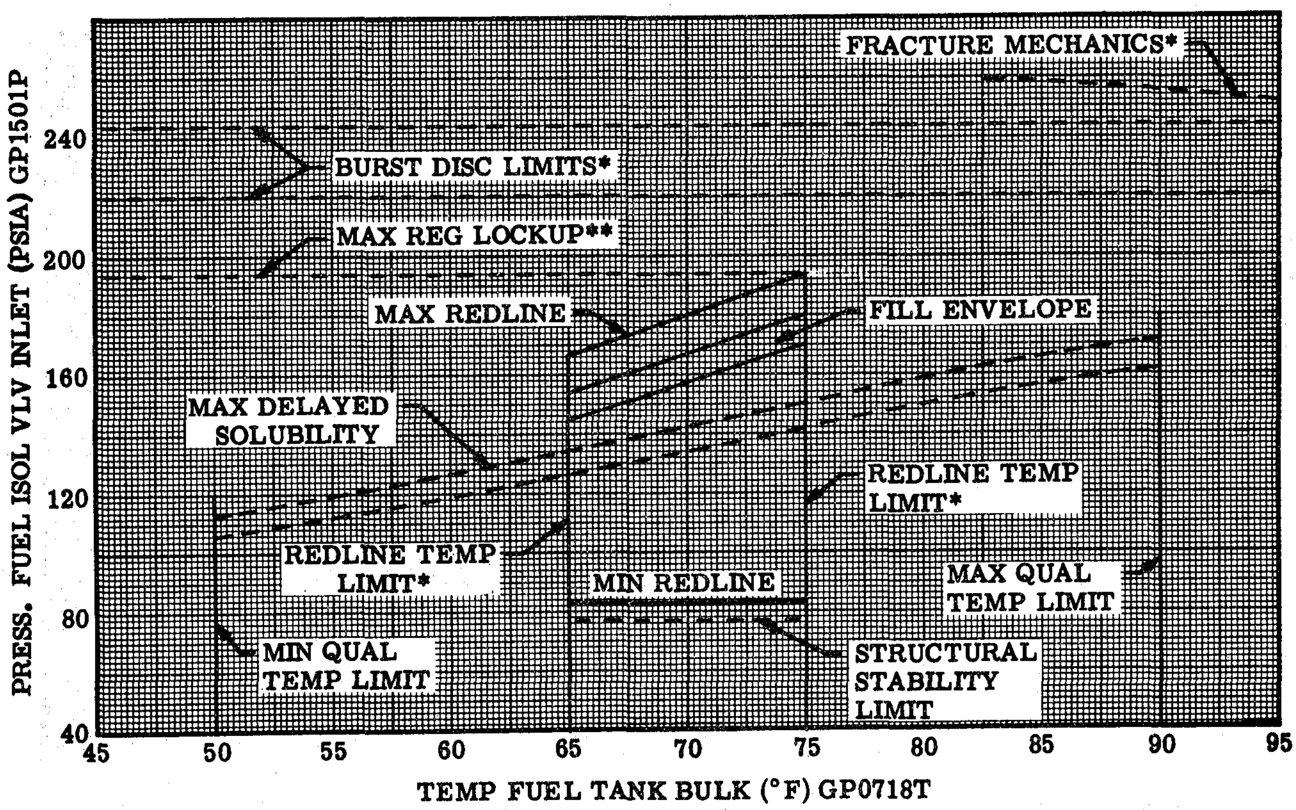

Figure LM10/3.6.1-2. APS Fuel Tank Pressure-Temperature Limitations (See Paragraph LM10/APS-1)

NOTE: 1 - * INCLUDES INSTR. ERROR.
2 - NO LEAKAGE ALLOWED.
3 - 3226 LBS TARGET LOAD.
4 - MAX. PRESS. DECAY DEFINED BY SOLUBILITY CURVE. HOWEVER, EXCESSIVE DECAY RATES MUST BE EVALUATED CONSIDERING SOLUBILITY EFFECTS FOR INTERMEDIATE POINTS.
5 - ** INCLUDES INSTR. ERROR AND CHECK VALVE CRACKING PRESSURE.

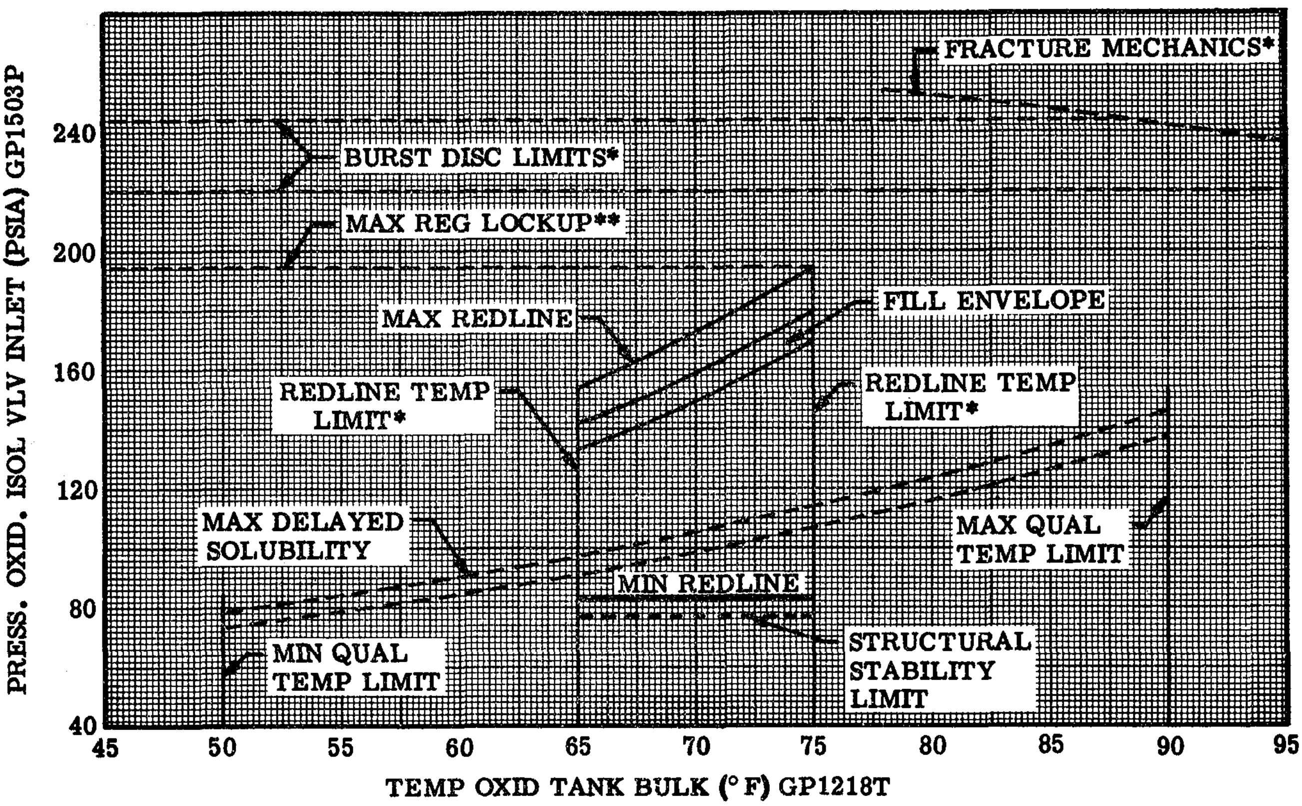

Figure LM10/3.6.1-3. APS Oxidizer Tank Pressure-Temperature Limitations (See Paragraph LM10/APS-1)

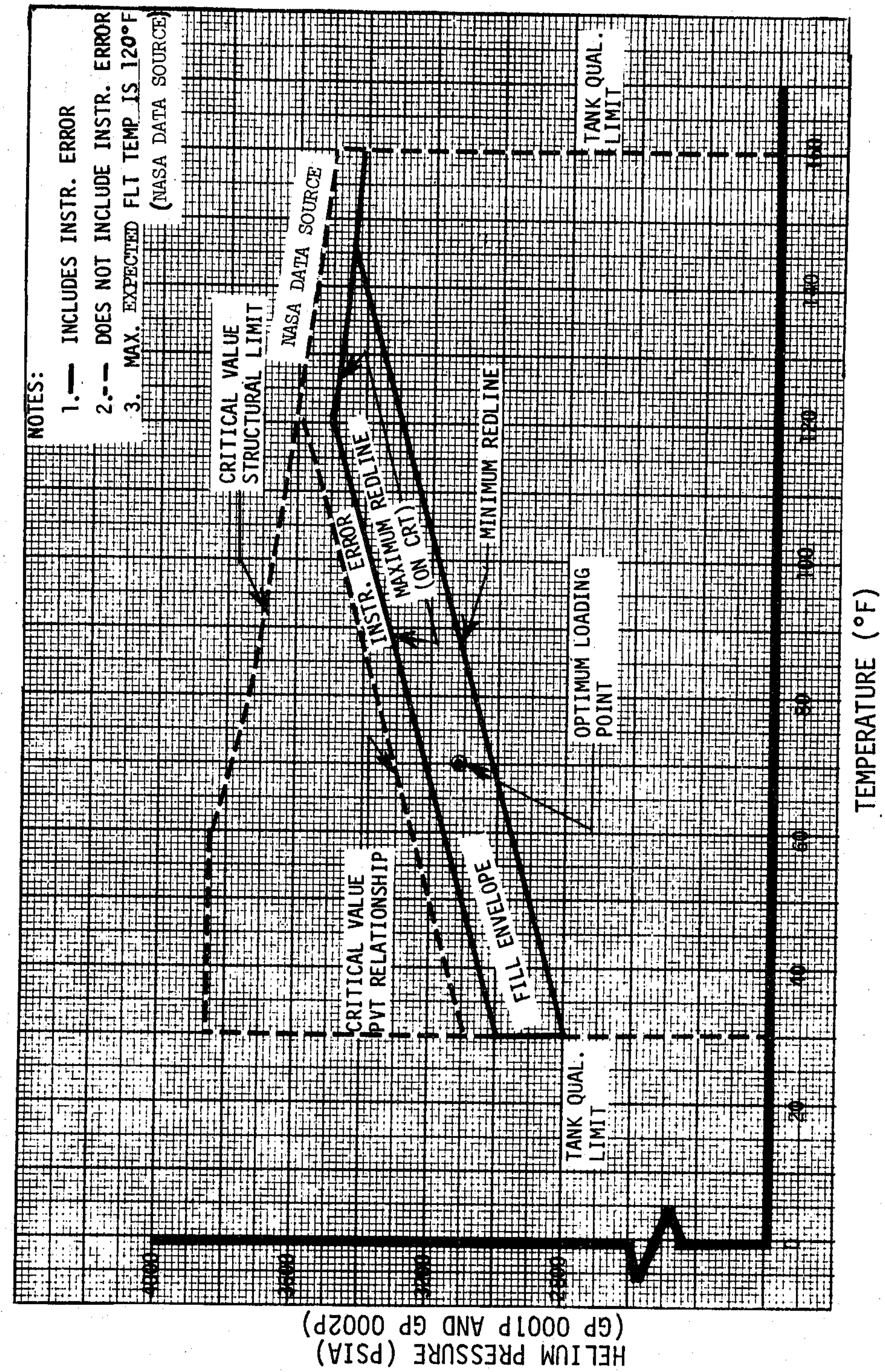

Figure LM10/3.6.1-4. APS Helium Tank Pressure-Temperature Limitations (See Paragraph LM10/APS-9)

LM10/3.7 PROPULSION - DPS

OPERATIONAL LIMITATION OR PROCEDURE	RATIONALE
LM10/DPS-2 Engine Life	
Using Figure LM10/3.7.1-4, the maximum engine life burn time is that which does not exceed 52% throat erosion.	May exceed the engine thrust chamber heating and erosion limits.
LM10/DPS-6 Propellant Tank Pressure-Temperature Limit Relationship	
The propellant tank pressure should not exceed the values given in Figures LM10/3.7.1-1, LM10/3.7.1-2, LM10/3.7.1-5 and LM10/3.7.1-6.	Reliability is reduced below the allowable value.
LM10/DPS-8 Non-Throttling Range Engine Operation	
See Table LM10/3.7.1-1.	Off-nominal mixture ratios may result, or the thrust chamber may burn through.
LM10/DPS-20 Ambient Helium Storage Tank Pressure-Temperature Limitations	
Ambient helium tank pressure limitations are given in Figure LM10/3.7.1-7.	If the maximum is exceeded, reliability is reduced below allowable value.
LM10/DPS-24 Chamber Pressure and Pressure Decay at Throttle-Down	
The DPS chamber pressure decay from start to end of FTP shall not be greater than 22.1 psi for LM-10. The burn must be terminated 20 seconds prior to depletion per psi decay exceeding the 22.1 psi decay limit. The expected chamber pressures are also presented in Table LM10/3.7.1-2 for reference.	The reference chamber pressure decay corresponds to the maximum FTP erosion that will allow completion of mission with less than 52% erosion under worst-case conditions.
LM10/DPS-25 Supercritical Helium Tank Pressure	
The helium tank pressure should not exceed the value given in Figure LM10/3.7.1-3.	Reliability is reduced below the allowable value.

Table LM10/3.7.1-1. Non-Throttling Range Engine Operation

VEHICLE	ENGINE (S/N)	NOMINAL CONDITIONS		WORST CASE CONDITIONS*	
		Predicted Erosion **	Permissible Time In Non-Throttling Region ***	Predicted Erosion **	Permissible Time In Non-Throttling Region ***
LM-10	1046	13.6%	192 Sec.	36.6%	77 Sec.

* Worst Case erosions are applicable for MDC performed with cold propellant and high mixture ratios. (FTP O/F = 1.63, 25% Thrust O/F = 1.65, Propellant Bulk Temperature = 50°F).

** Predicted erosion is to propellant depletion.

*** Operating time in the non-throttling range is based on the worst case expected engine erosion rate (0.20%/sec) in the event of a loss in manual throttle command during FTP operation. Operation at any other point in the non-throttling range should be based on erosion rates defined in Figure LM10/3.7.1-4.

Note: One second of excessive operating time in the non-throttling region requires the hover time to be shortened by 8.8 seconds for the nominal case and 3.1 seconds for the worst case.

EXAMPLE: LM-10 DPS is operated for 90 seconds in non-throttling regime under worst-case off-nominal conditions, or 200 seconds for nominal conditions.

SOLUTION: Engine S/N 1046 is permitted to operate 77 seconds in non-throttling region. Excessive operating time is (90-77) 13 seconds. The hover time must be shortened by (13 X 3.1) 40.3 seconds. For nominal case 192 seconds is permitted. Excessive operating time is (200-192) 8 seconds. The hover time must be shortened by (8 X 8.8) 70.4 seconds. Where 3.1 and 8.8 are the equivalent Δ erosion factors.

Table LM10/3.7.1-2. Non-Throttling Range Chamber Pressures, Decays, and Erosion

Engine Characteristics	LM-10 S/N 1046
Predicted Nominal Delta FTP Erosion	7.6%
Predicted Worst-Case Delta FTP Erosion	13.6%
Maximum Allowable Delta FTP Erosion (29% Plus 1.5% Swelling)	30.5%
Initial Erosion or Swelling at FTP Initiation	- 1.5%
Predicted Chamber Pressure at FTP Initiation	105.3 psia
Predicted Nominal Chamber Pressure at FTP Termination	99.8 psia
Predicted "Worst-Case" Chamber Pressure at FTP Termination	95.4 psia
Minimum Allowable Chamber Pressure at FTP Termination	83.2 psia
Maximum Allowable Chamber Pressure Decay During Braking Phase (FTP Plus Non-Throttling)	22.1 psia

NOTE: CURVES ARE BASED UPON THE FOLLOWING PRESSURIZATION SCHEDULE AT KSC.

OXIDIZER	FUEL
1 CYCLE AT 119 PSID	1 CYCLE AT 245 PSID
1 CYCLE AT 244 PSID	3 CYCLES AT 200 PSID
2 CYCLES AT 200 PSID	

CURVES MUST BE REVISED IF THE TANKS ARE CYCLED MORE THAN STATED ABOVE.

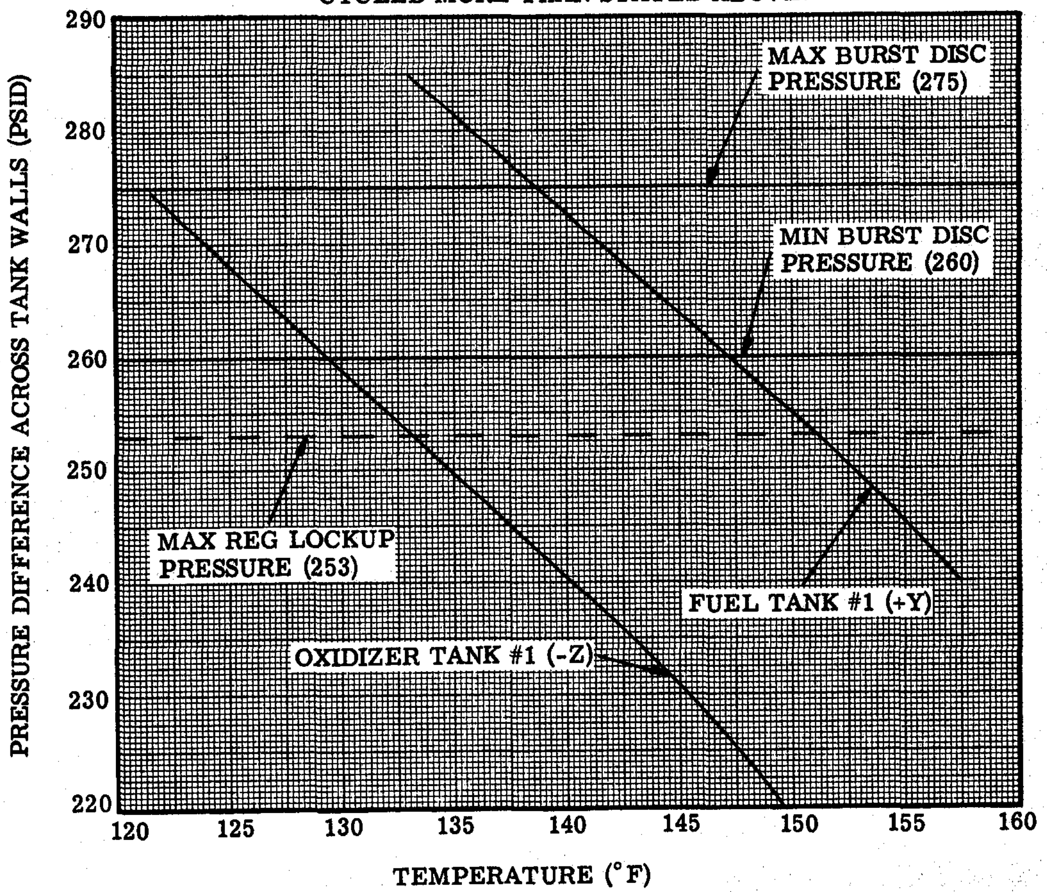

Figure LM10/3.7.1-1. Maximum Allowable Pressure-Temperature Limit Relationship For LM-10 Descent Stage Propellant Tanks #1

NOTE: CURVES ARE BASED UPON THE FOLLOWING PRESSURIZATION SCHEDULE AT KSC.

OXIDIZER	FUEL
1 CYCLE AT 119 PSID	1 CYCLE AT 245 PSID
1 CYCLE AT 244 PSID	3 CYCLES AT 200 PSID
2 CYCLES AT 200 PSID	

CURVES MUST BE REVISED IF THE TANKS ARE CYCLED MORE THAN STATED ABOVE.

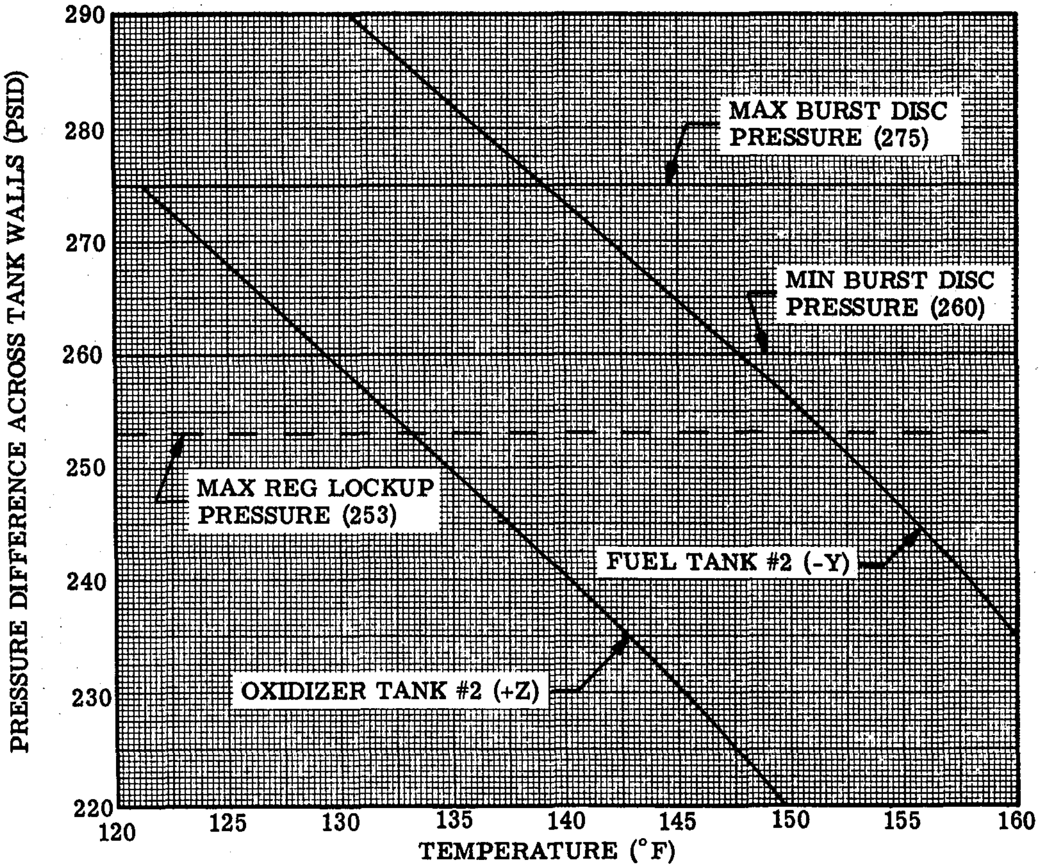

Figure LM10/3.7.1-2. Maximum Allowable Pressure-Temperature Limit Relationship For LM-10 Descent Stage Propellant Tanks #2

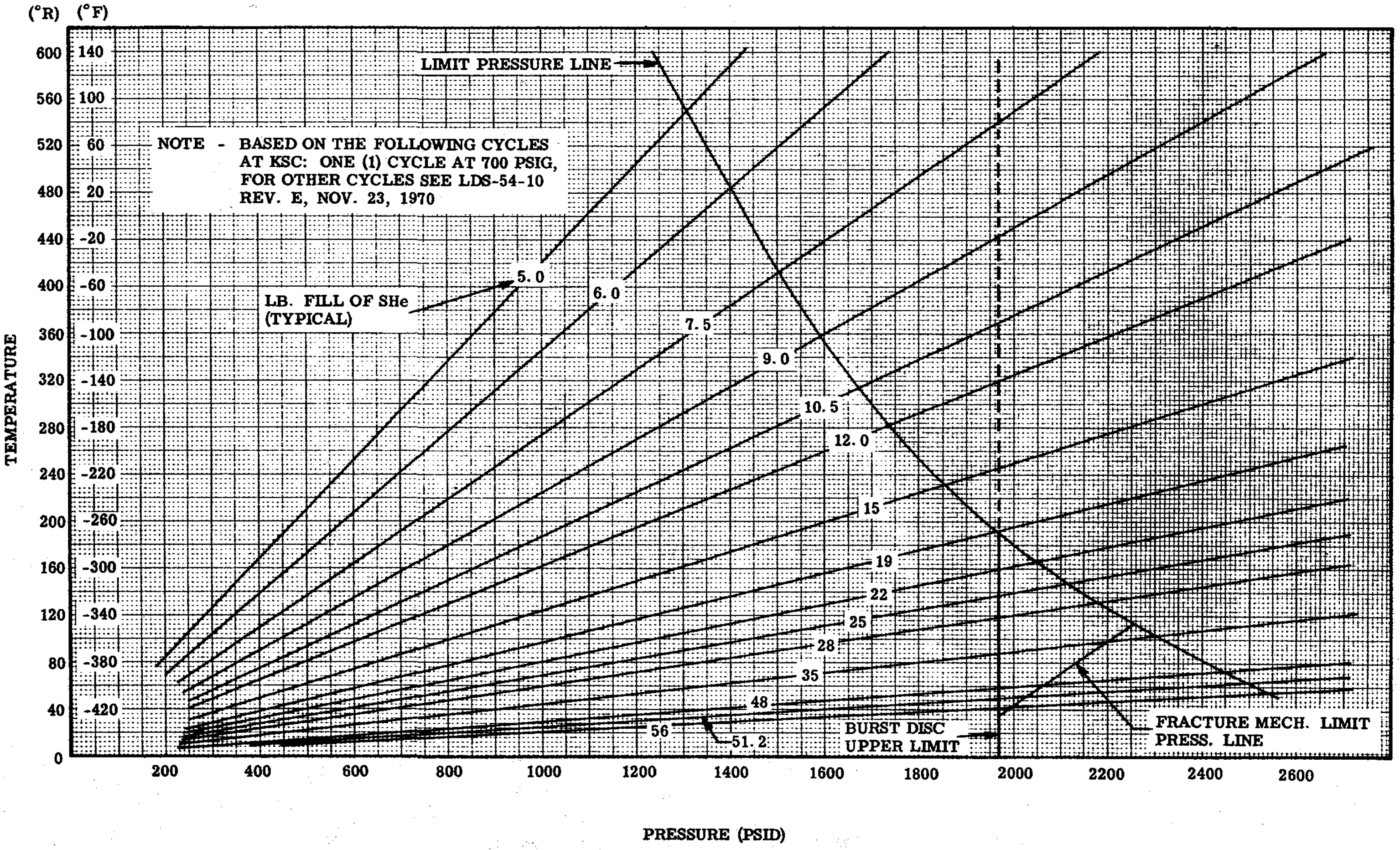

Figure LM10/3.7.1-3. SHe Tank Fracture Mechanics Limits

NOTE: THIS CURVE IS VALID FOR NOMINAL MIXTURE RATIO, PROPELLANT TEMPERATURES AND PRESSURES.

THIS CURVE IS INVALID FOR LONG BURNS AT A CONSTANT THROTTLE SETTING IN THE THROTTLING REGION.

IN THE 55 to 65% REGION, THE RATES ARE BASED ON ~ 100- TO 200-SECOND DWELLS, WHILE AT 24 TO 30%, THE RATES ARE BASED ON 100-SECOND DURATIONS.

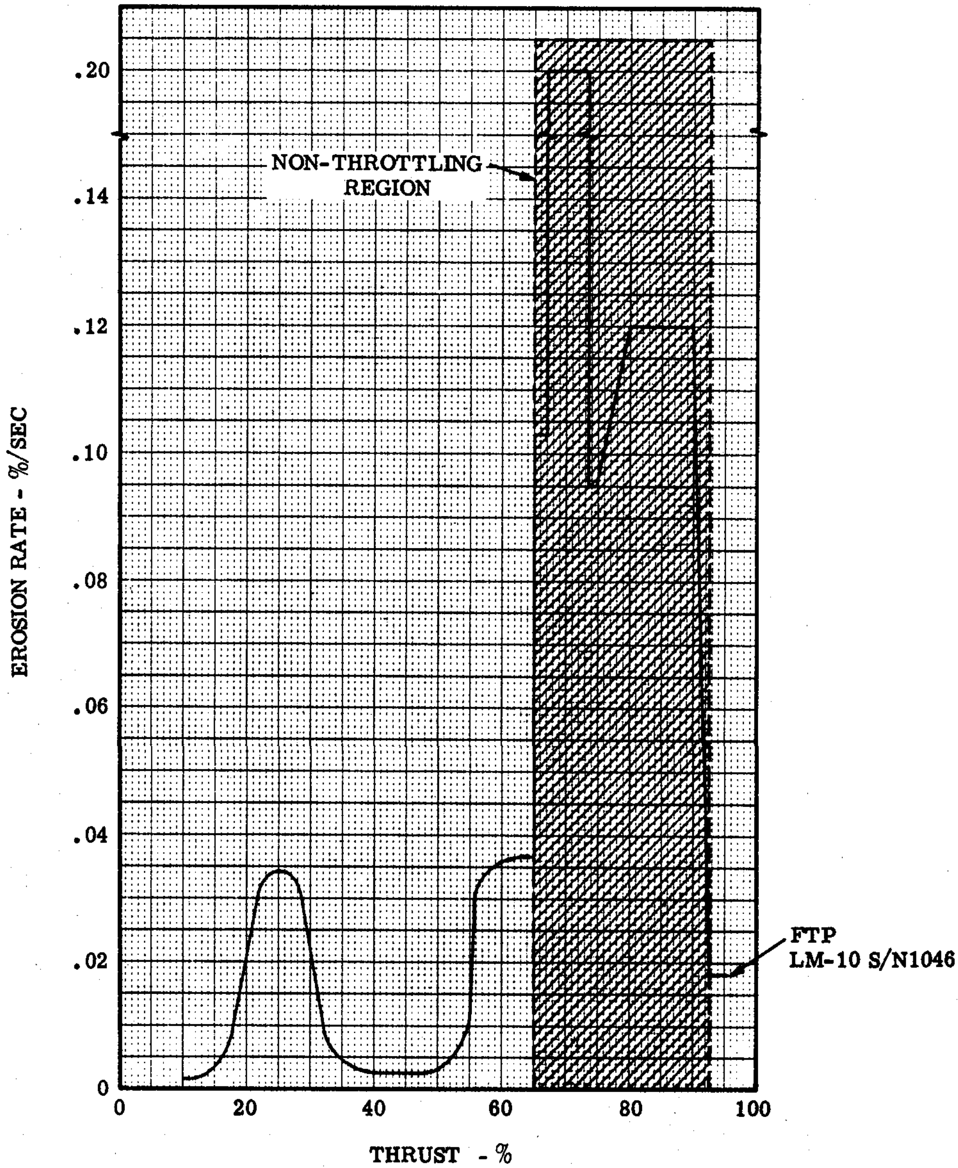

Figure LM10/3.7.1-4. DPS Engine (Quartz Chamber) Nominal Throat Erosion vs Percent Thrust for Uneroded Throat

NOTE:
1 - * INCLUDES INSTR. ERROR.
2 - ** INCLUDES INSTR. ERROR AND CHECK VALVE CRACKING PRESSURE.
3 - NO LEAKAGE ALLOWED.
4 - 7548 lbs TARGET LOAD
5 - MAX. EXPECTED PRESS. DECAY IS DEFINED BY THE MAX DELAYED SOLUBILITY CURVES. THE DETECTION OF EXCESSIVE PRESS. DECAY DURING PRELAUNCH OPERATIONS MUST BE EVALUATED WITH RESPECT TO POSSIBLE LEAKAGE.
6 - INITIAL FILL POINTS FALLING OUTSIDE THE DESIRED FILL ENVELOPE MUST BE EVALUATED IN REAL TIME TO INSURE THAT THE TOTAL SOLUBILITY AT DPS PRESSURIZATION WILL NOT PRODUCE A ΔP OF 50 PSID (USE "AS READ" CRT NUMBERS TO DETERMINE ΔP).

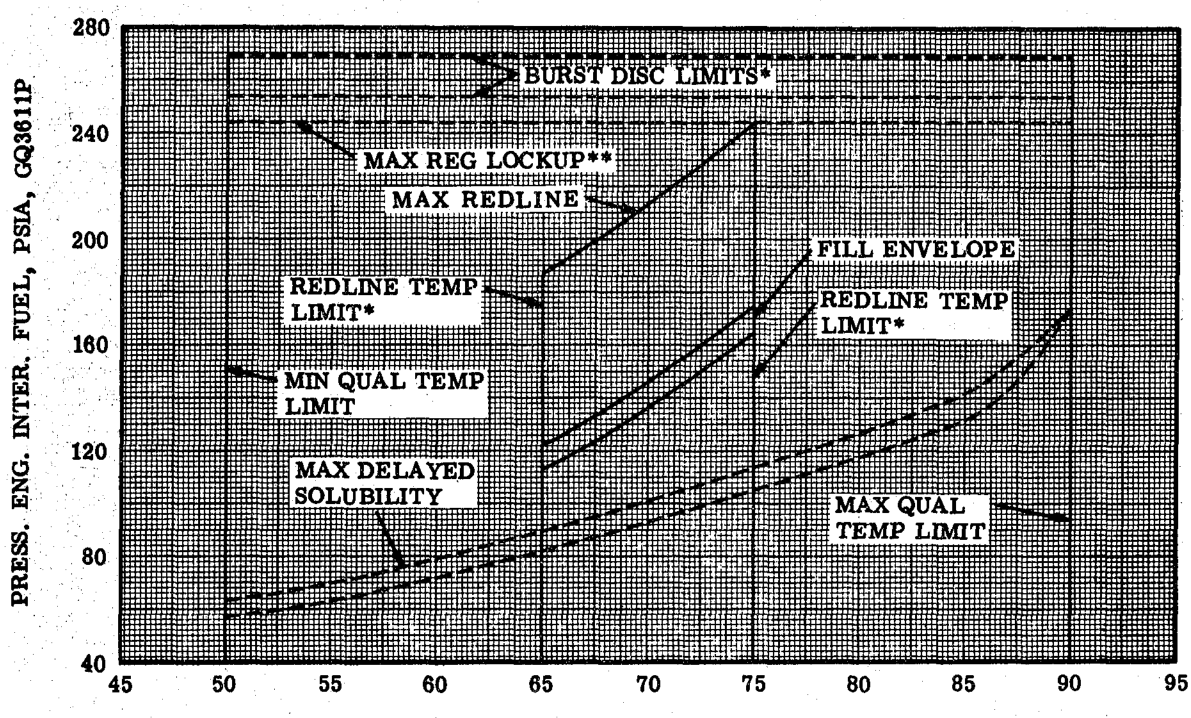

Figure LM10/3.7.1-5. DPS Fuel Tank Pressure-Temperature Limitations (See Paragraph LM10/DPS-6)

NOTE: 1 - * INCLUDES INSTR. ERROR.
2 - ** INCLUDES INSTR. ERROR AND CHECK VALVE CRACKING PRESSURE.
3 - 12024lbs TARGET LOAD.
4 - MAX EXPECTED PRESS. DECAY IS DEFINED BY THE MAX. DELAYED SOLUBILITY CURVES. THE DETECTION OF EXCESSIVE PRESS. DECAY DURING PRELAUNCH OPERATIONS MUST BE EVALUATED WITH RESPECT TO POSSIBLE LEAKAGE.
5 - NO LEAKAGE ALLOWED.
6 - INITIAL FILL POINTS FALLING OUTSIDE THE DESIRED FILL ENVELOPE MUST BE EVALUATED IN REAL TIME TO INSURE THAT THE TOTAL SOLUBILITY AT DPS PRESSURIZATION WILL NOT PRODUCE A ΔP OF 50 PSID (USE "AS READ" CRT NUMBERS TO DETERMINE ΔP).

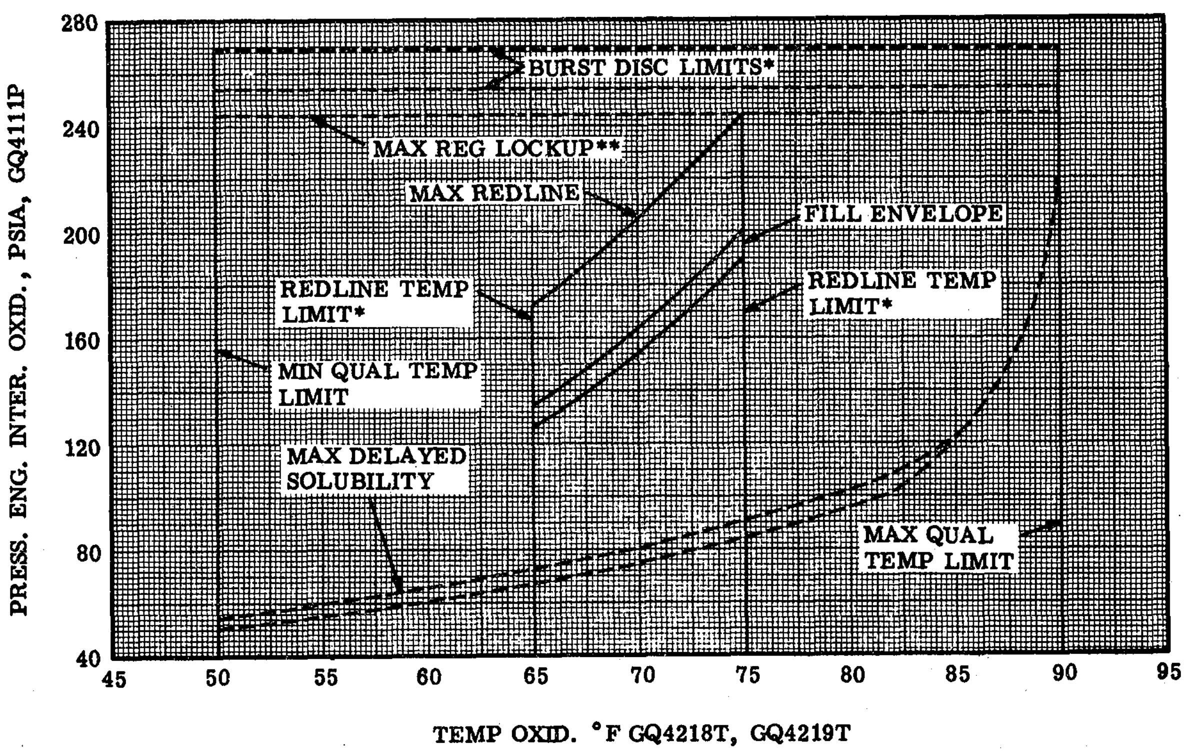

Figure LM10/3.7.1-6. DPS Oxidizer Tank Pressure-Temperature Limitations (See Paragraph LM10/DPS-6)

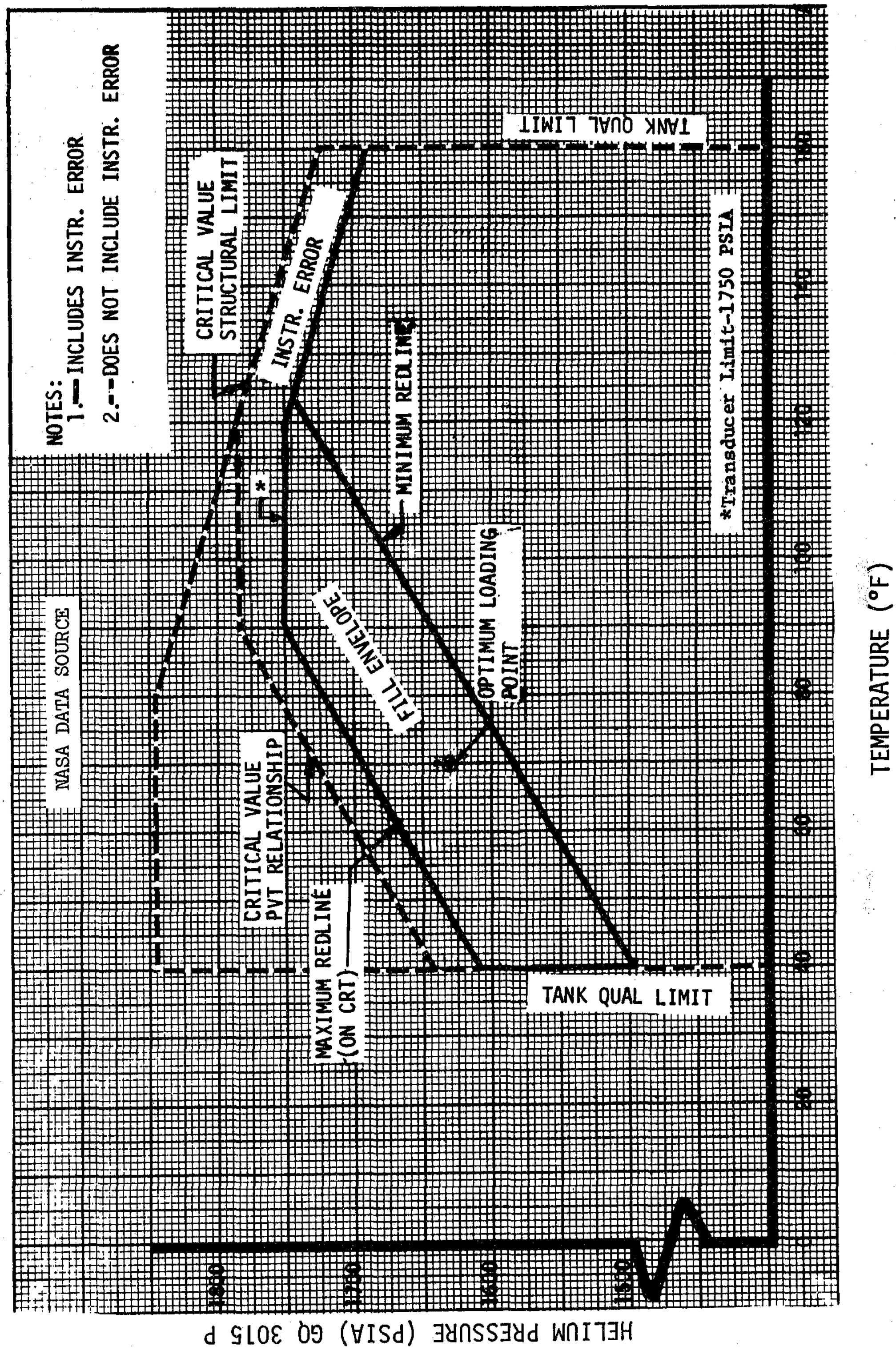

Figure LM10/3.7.1-7. DPS Ambient Helium Tank Pressure-Temperature Limitations (See Paragraph LM10/DPS-20)

LM10/3.8 REACTION CONTROL SUBSYSTEM

OPERATIONAL LIMITATION OR PROCEDURE	RATIONALE
LM10/RCS-13 Propellant Tank Pressure-Temperature Limit Relationship	
The propellant tank pressure should not exceed the values given in Figures LM10/3.8.1-1 and LM10/3.8.1-2.	Reliability is reduced below the allowable value.
LM10/RCS-17 RCS Helium Bottle Pressure-Temperature Limitations	
RCS helium bottle pressure-temperature limitations are given in Figure LM10/3.8.1-3.	If the maximum is exceeded, reliability is reduced below allowable values.

NOTE: CURVES ARE BASED UPON THE FOLLOWING PRESSURIZATION SCHEDULE AT KSC.

1 CYCLE AT 194 PSID
1 CYCLE AT 220 PSID
1 CYCLE AT 187 PSID

CURVES MUST BE REVISED IF THE TANKS ARE CYCLED MORE THAN STATED ABOVE

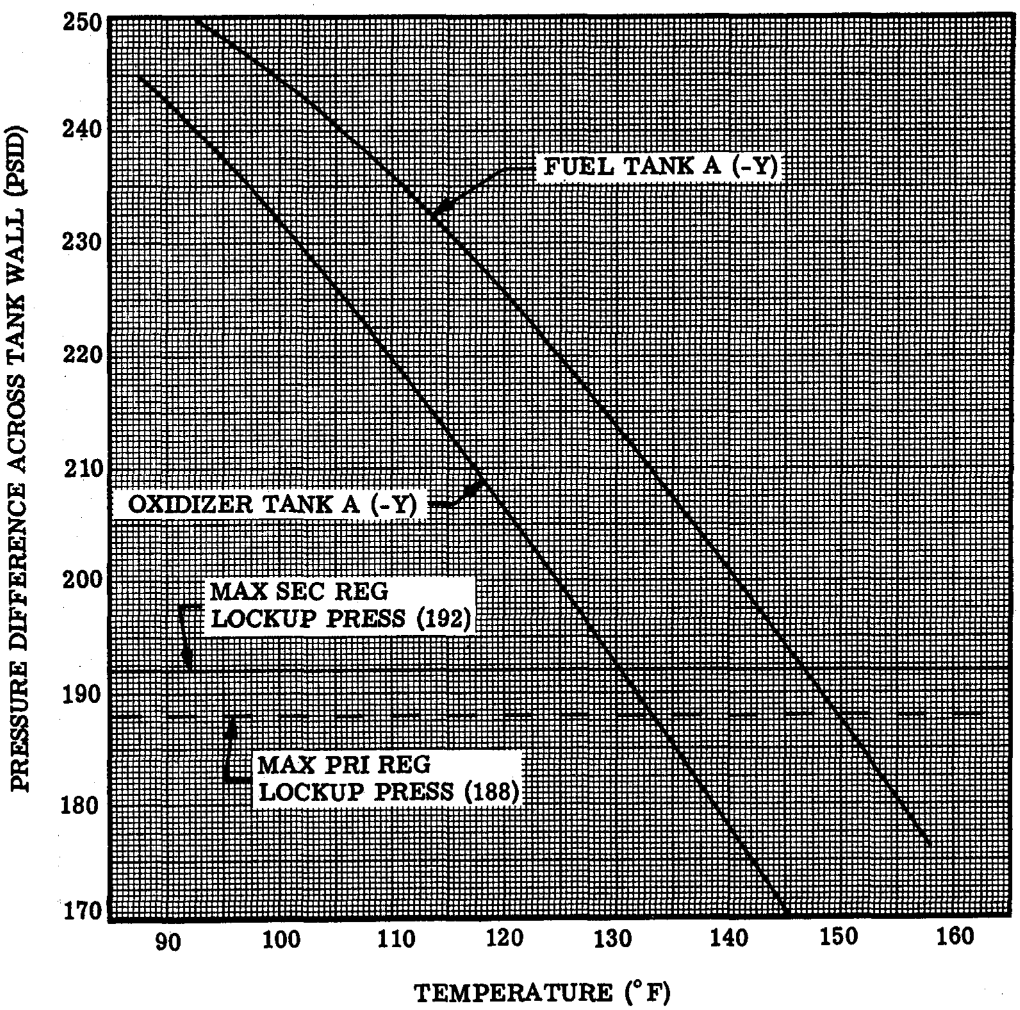

Figure LM10/3.8.1-1. Maximum Allowable Pressure-Temperature Limit Relationship for LM-10 System "A" RCS Propellant Tanks

NOTE: CURVES ARE BASED UPON THE FOLLOWING PRESSURIZATION SCHEDULE AT KSC.

1 CYCLE AT 194 PSID
1 CYCLE AT 220 PSID
1 CYCLE AT 187 PSID

CURVES MUST BE REVISED IF THE TANKS ARE CYCLED MORE THAN STATED ABOVE.

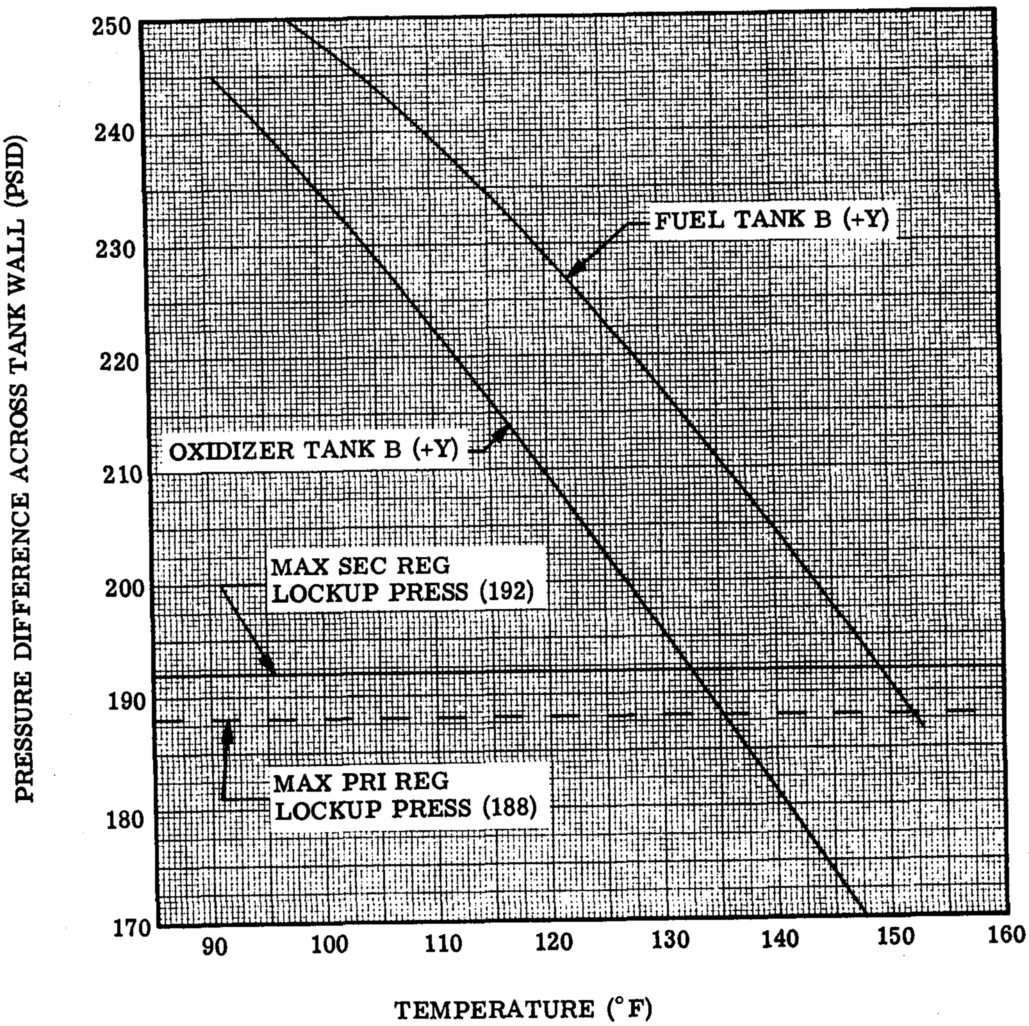

Figure LM10/3.8.1-2. Maximum Allowable Pressure-Temperature Limit Relationship for LM-10 System "B" RCS Propellant Tanks

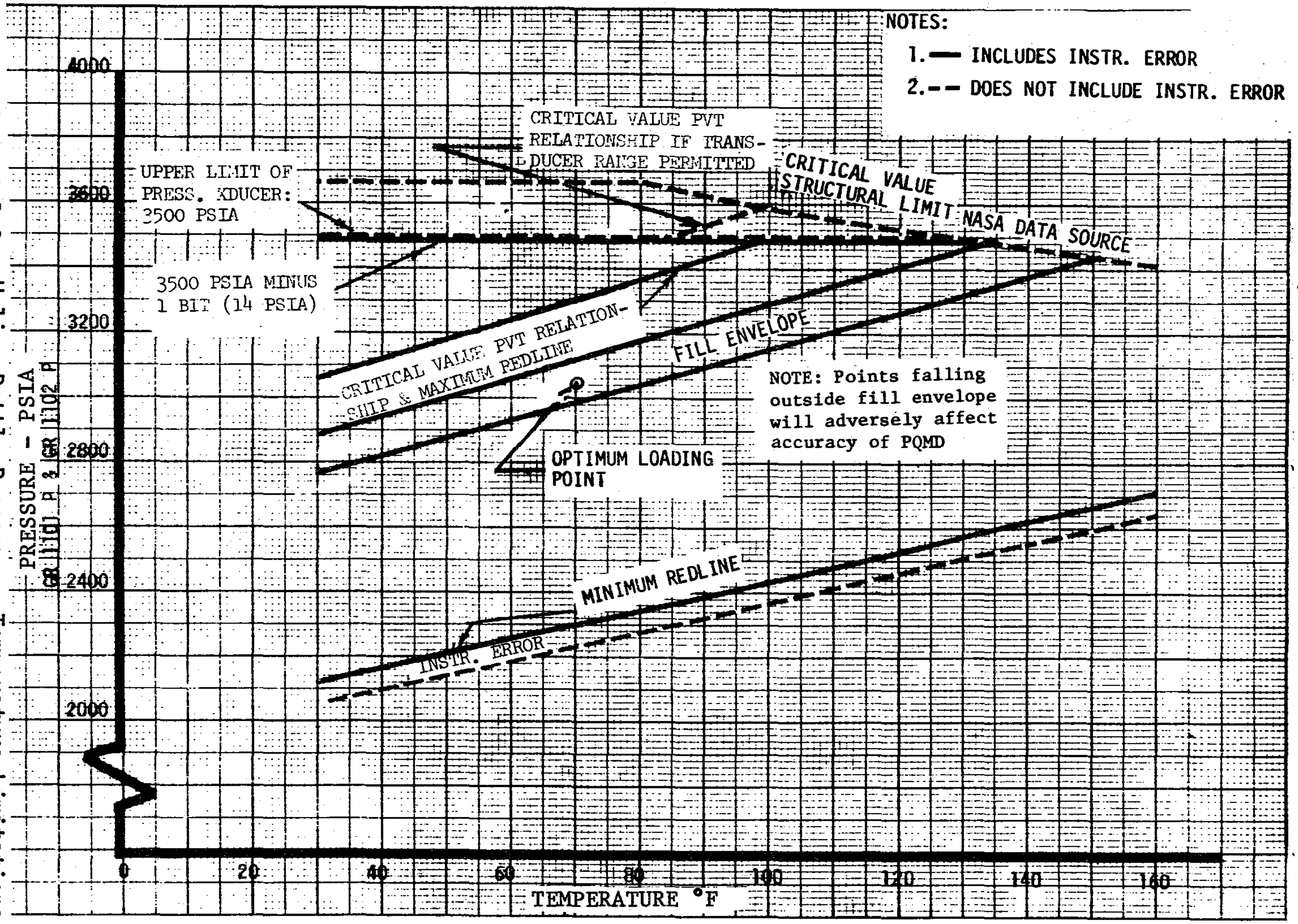

Figure LM10/3.8.1-3. Helium Bottle Pressure - Temperature Limitations
(See Paragraph LM10/RCS-17)

LM10/3.10.1 System Temperature Limitations

Fracture mechanics limits for the APS, DPS, and RCS fuel and oxidizer tanks are presented in Tables LM10/3.10.1-1, LM10/3.10.1-2, and LM10/3.10.1-3, respectively.

Table LM10/3. 10. 1-1. Ascent Propulsion Subsystem (APS) Limitations

COMPONENT	TEMPERATURE LIMITS (°F)		LOW LIMIT REASON	HIGH LIMIT REASON	MEASUREMENT	
	LOW	HIGH			NUMBER	LOCATION
Fuel Tank		142		Fracture mechanics. Based upon secondary regulator lockup at 205 psid.	GP0718T	Fuel Tank Bulk
Oxidizer Tank		124			GP1218T	Ox Tank Bulk

NOTES:
1. Measurement number readings are valid only when tanks are at least 75% full.
2. See Figure LM10/3. 6. 1-1 for APS fracture mechanics pressure-temperature relationship curves.
3. See Table 3. 10-6 for other APS temperature limitations.

Table LM10/3. 10. 1-2. Descent Propulsion Subsystem (DPS) Limitations

COMPONENT	TEMPERATURE LIMITS (°F)		LOW LIMIT REASON	HIGH LIMIT REASON	MEASUREMENT	
	LOW	HIGH			NUMBER	LOCATION
Fuel Tank #1		138.5		Fracture mechanics. Based upon burst disc pressure of 275 psid.	GQ3718T	Tank #1 Bulk
Fuel Tank #2		139.0			GQ3719T	Tank #2 Bulk
Oxidizer Tank #1		121			GQ4218T	Tank #1 Bulk
Oxidizer Tank #2		121			GQ4219T	Tank #2 Bulk

NOTES:
1. Measurement number readings are valid only when tanks are at least 75% full.
2. See Figure LM10/3. 7. 1-1 & LM10/3. 7. 1-2 for DPS fracture mechanics pressure-temperature relationship curves.
3. See Table 3. 10-7 for other DPS temperature limitations.

Table LM10/3. 10. 1-3. Reaction Control Subsystem (RCS) Limitations

COMPONENT	TEMPERATURE LIMITS (°F)		LOW LIMIT REASON	HIGH LIMIT REASON	MEASUREMENT	
	LOW	HIGH			NUMBER	LOCATION
Fuel Tank						
System A		100/146. 5		Tank spec. limit and no engine firing experience above 100°F/ Fracture mechanics. Based upon secondary regulator lock-up at 192 psid post-LOI.	GR2121T	Fuel Tank Outlet
System B		100/149			GR2122T	Fuel Tank Outlet
Oxidizer Tank						
System A		100/130. 5		Tank spec. limit and no engine firing experience above 100°F/ Fracture mechanics. Based upon secondary regulator lock-up at 192 psid post-LOI	GR2121T	Fuel Tank Outlet
System B		100/132. 5			GR2122T	Fuel Tank Outlet

NOTES:
1. See Figure LM10/3. 8. 1-1 & LM10/3. 8. 1-2 for RCS fracture mechanics pressure-temperature relationship curves.
2. See Table 3. 10-8 for other RCS temperature limitations.

LM10/4.1.1 Modes

The circuit margins shown in Table LM10/4.1.1-1 are based upon measured Apollo 15 spacecraft parameters and include those modes commonly used during the mission.

Subsystem Performance Data - Communications

Table LM10/4.1.1-1. LM Circuit Margins (Lunar Stay)

To an MSFN 85-Foot Antenna*		TRP Margin (dB)	
		Steerable	Omni
Mode 1 (PM) [PA On]	HBR Voice EKG & PAM	14.8 15.1 11.1	-8.5 -8.2 -12.2
Mode 7A (PM) [PA Off]	LBR Voice EKG & PAM	8.4 5.2 1.2	-14.9 -18.1 -22.1
Mode 1 (PM) [PA on with CB Pulled]	HBR Voice EKG & PAM	-0.6 -0.3 -4.3	-23.9 -23.6 -27.6
Mode 3 (PM)	LBR: (1) PA Off (2) PA On, CB Pulled	12.6 16.8	-10.7 -6.5
Mode 4 (PM) [PA on with CB Pulled]	LBR BU Voice	15.6 14.0	-7.7 -9.3
Mode 10 (FM) [PA On]	HBR Voice EKG & PAM TV	5.0 5.1 -0.4 -5.0	-18.3 -18.2 -23.7 -28.3
Mode 8 (PM) (rest mode) [PA Off]	HBR (LBR) Voice HLB10M	-2.5**(13.5) 5.0 1.0	-25.8 (-9.8) -18.3 -22.3

*For Parks 210 foot, add 6.5 dB to all margins
For GDS 210 foot, add 8.0 dB to all margins
**HBR not available in this mode during time intervals when astronauts are talking (due to interference). The -2.5 dB margin shown here would correspond to marginal HBR data (a BER of approximately 10^{-2}).

CRITERIA: TM @ 10^{-3} BER; voice @ 70% W.I.: 10-dB required SNR in 1.25-MHz subcarrier pred. NBW (42 KHz) for EKG & PAM in SC PM modes, EKG & PAM in FM modes based on 5% data loss. Omni gain is -3 dB.

LM10/4.2.4 Thermal Variation of the MESA

LM10/4.2.4.1 MESA in Stowed Configuration - Translunar Coast, Lunar Orbit, and Lunar Stay Prior to Deployment

Figure LM10/4.2.4-1 indicates the average thermal response of the MESA for the hot and cold thermal design mission (TDM) and also the LM-10 nominal mission. The hot and cold cases assume worst vehicle orientations and worse case ε effective of blankets, and most severe mission timeline. The nominal LM-10 mission assumes the lastest Apollo-15 timeline and vehicle orientations.

Figure LM10/4.2.4-2 presents the hot and cold case TDM's with failure of translunar heaters (fail "on" in the hot case, "off" in the cold case). The temperature exceeds the 120°F limit for the hot case in 23 hours and the lower limit of 35°F in 55 hours for the cold case.

LM10/4.2.4.2 MESA in Deployed Configuration - Nominal Case Lunar Stay

Figures LM10/4.2.4-3 through 13 present the thermal preflight predictions for various equipment stowed in the MESA. The thermal response of flight sensors GB 0541 T - GB 0543 T is presented in Figure LM10/4.2.4-14.

LM10/4.2.4.3 Failure of MESA Heaters During Lunar Stay, MESA Deployed

Figure LM10/4.2.4-15 indicates the predicted response of the MESA for the following cases:

- Heaters operating normally
- All three heater systems fail "on"
- One heater system fails "on"
- All three heater systems fail "off"
- One or two heater systems fail "off"

All cases assumed the nominal LM-10/Apollo-15 vehicle/MESA landing orientation and timeline.

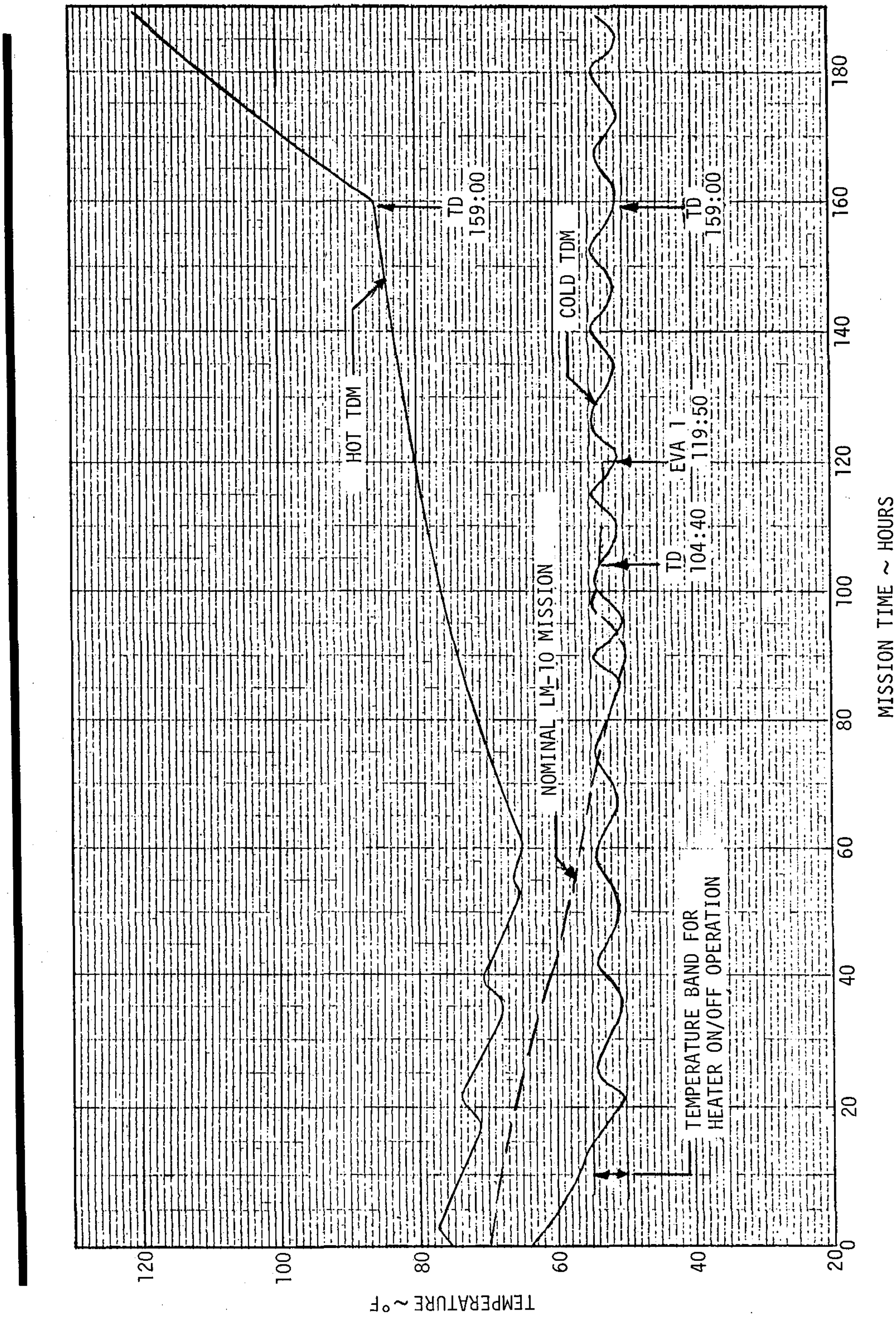

Figure LM10/4.2.4-1. MESA Thermal Analysis - Hot and Cold Cases, Stowed Position

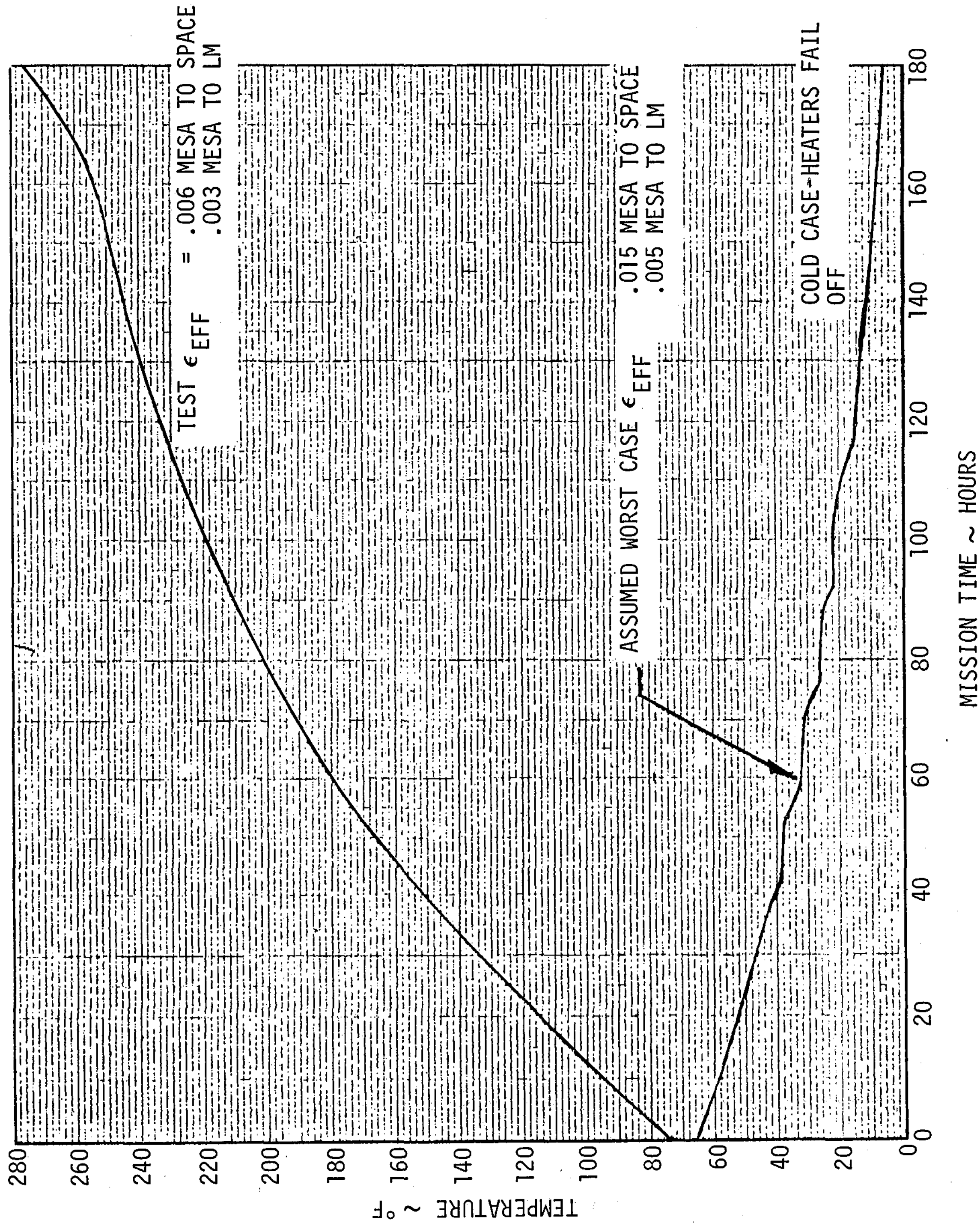

Figure LM10/4.2.4-2. MESA Thermal Analysis - On and Off Heater Failures, Stowed Position

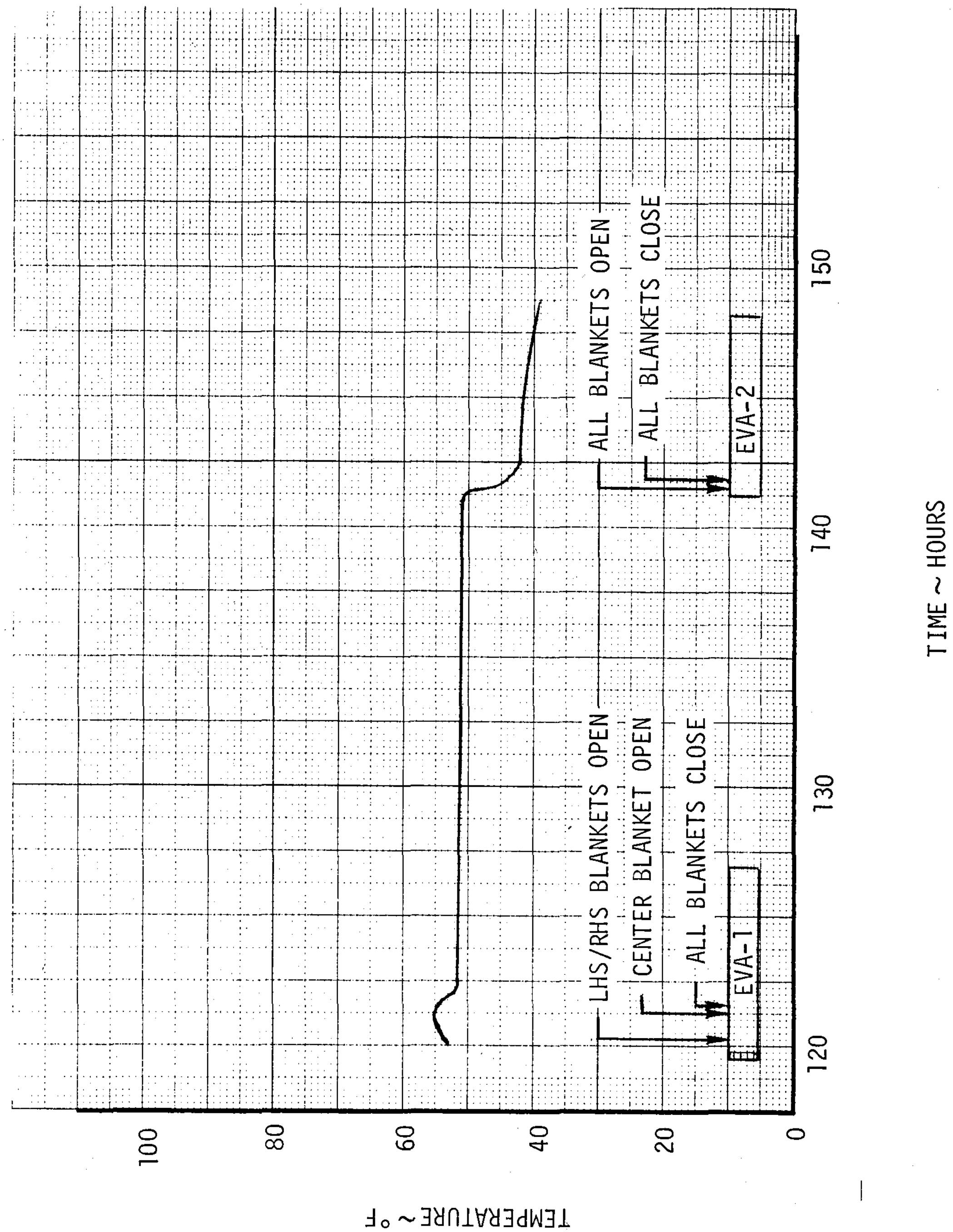

Figure LM10/4.2.4-3. Pallet #2 (Nodes 30 & 31) Temperature

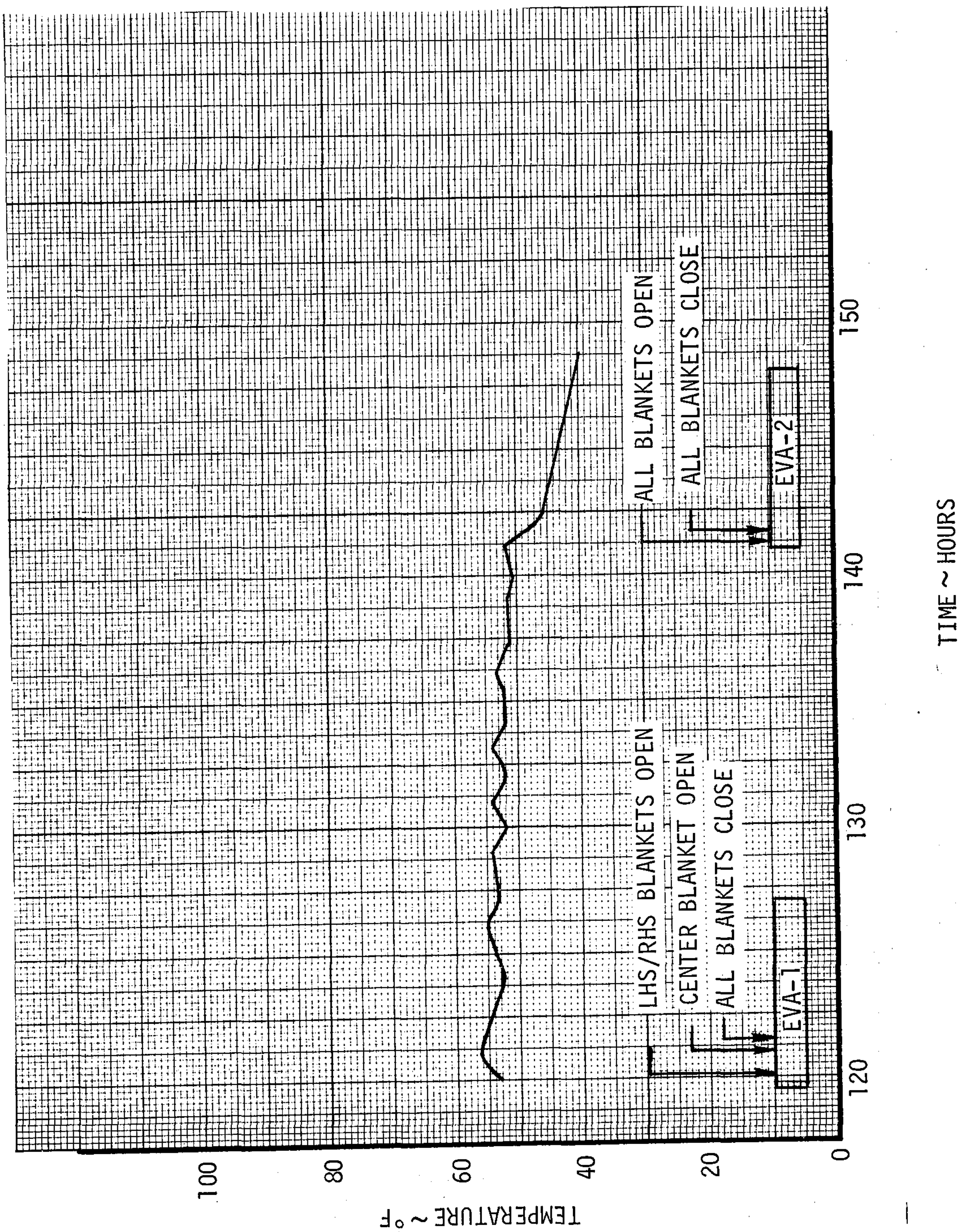

Figure LM10/4.2.4-4. LiOH Canister RHS (Node 45) Temperature

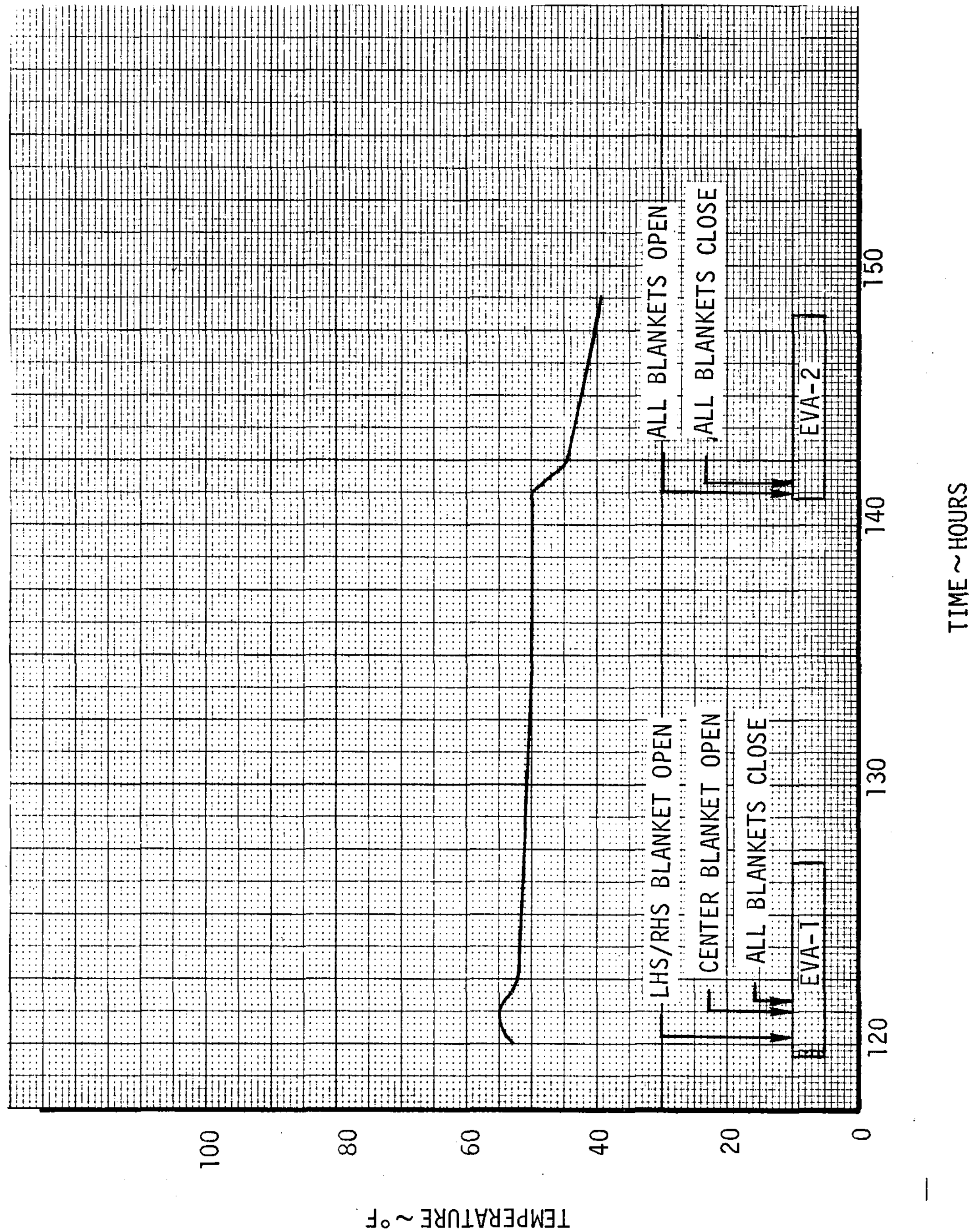

Figure LM10/4.2.4-5. LiOH Canister LHS (Node 44) Temperature

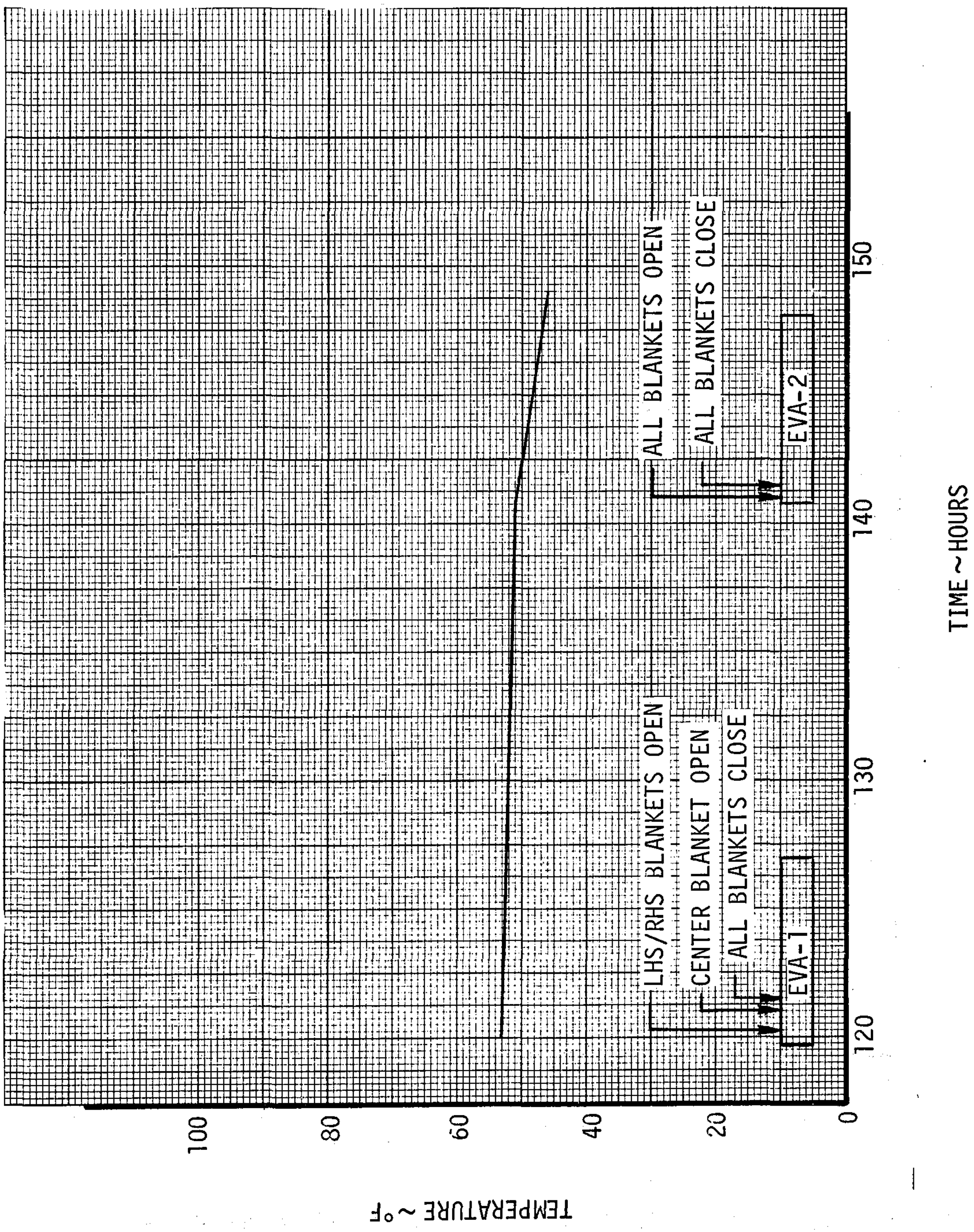

Figure LM10/4.2.4-6. PLSS Battery LHS (Node 32) Temperature

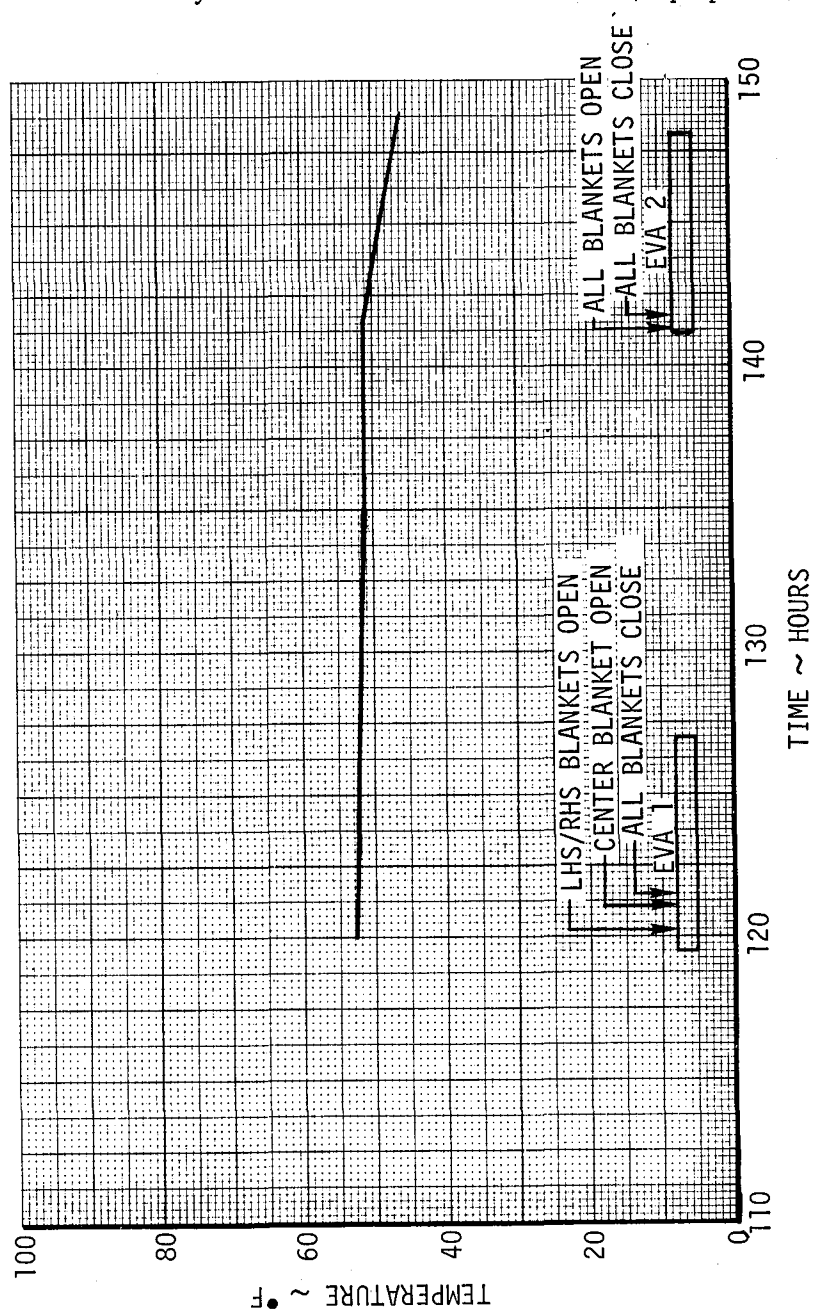

Figure LM10/4.2.4-7. PLSS Battery RHS (Node 33) Temperature

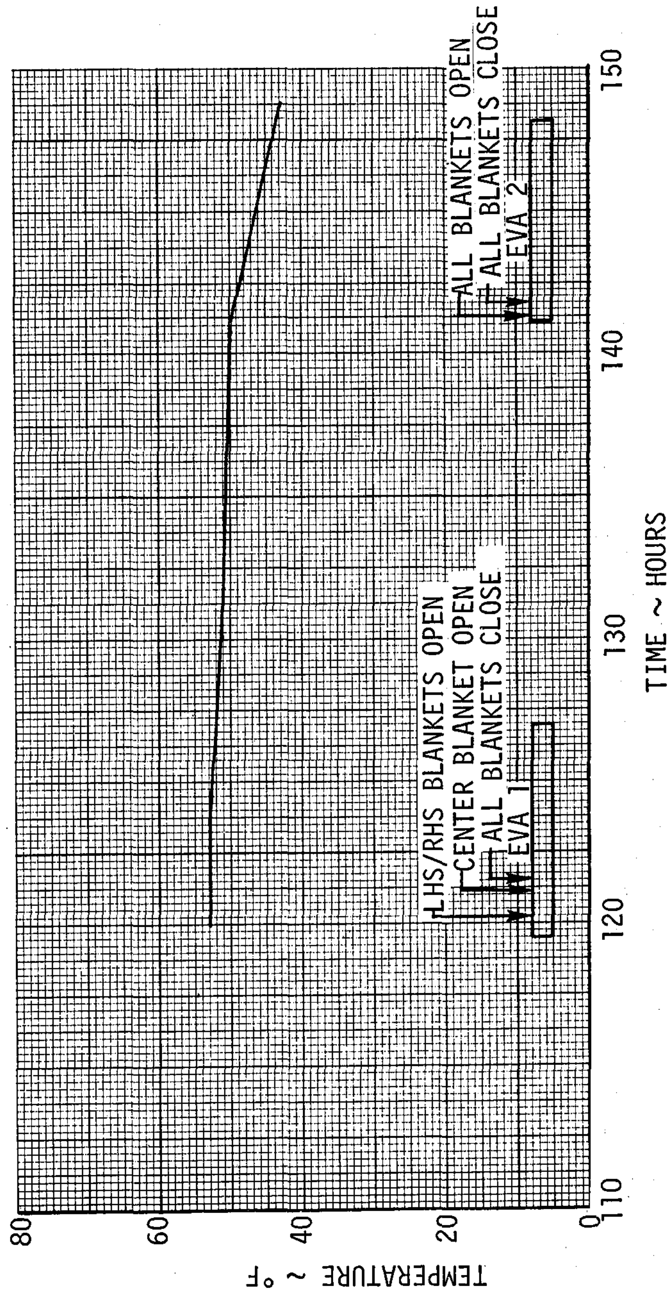

Figure LM10/4.2.4-8. LCRU Battery LHS (Node 5) Temperature

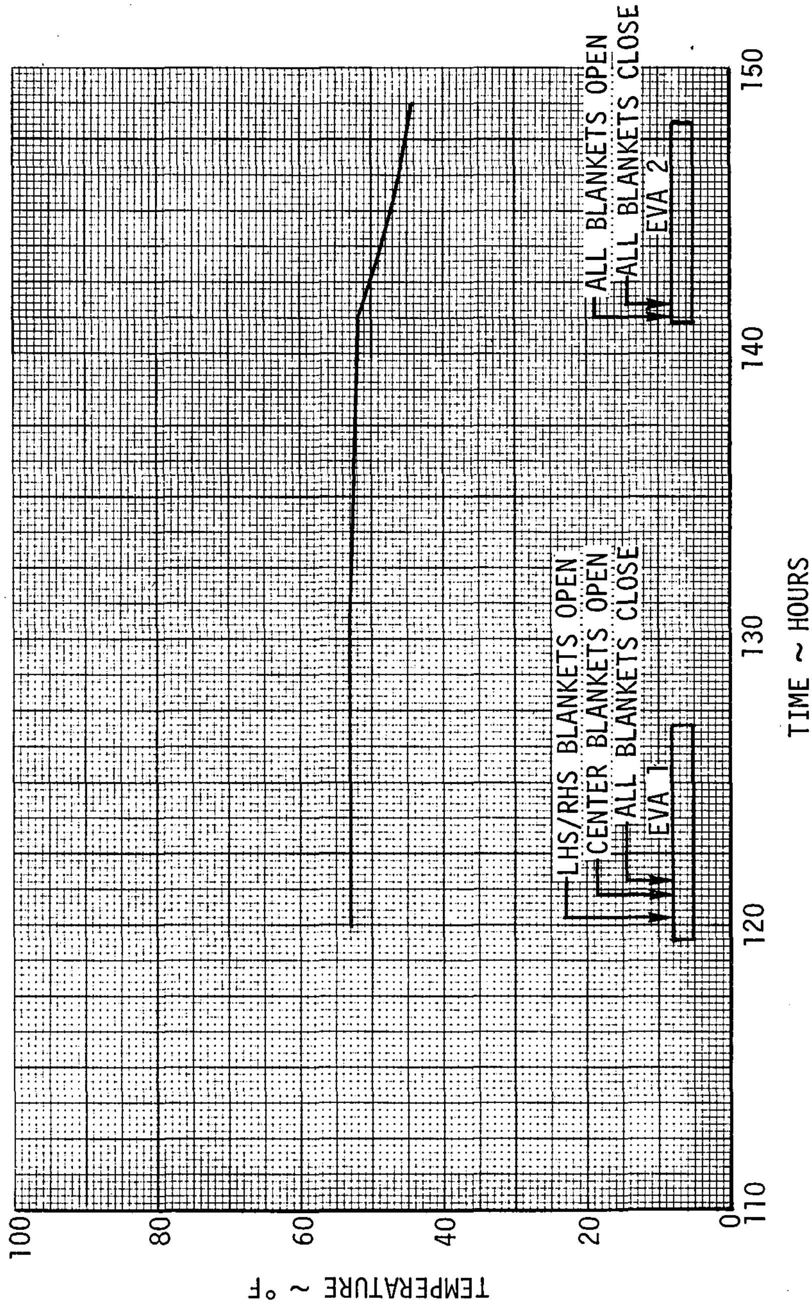

Figure LM10/4.2.4-9. LCRU Battery RHS (Node 4) Temperature

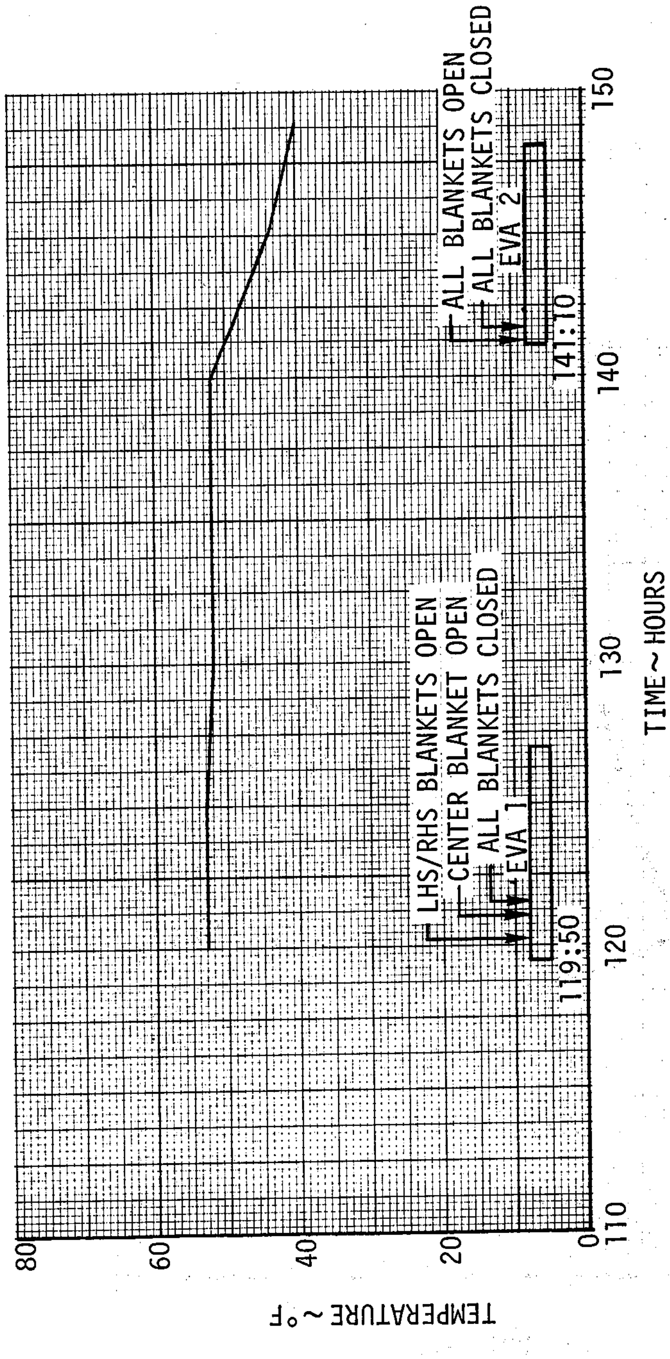

Figure LM10/4.2.4-10. Food Pallet #2 (Nodes 38 and 39) Temperature

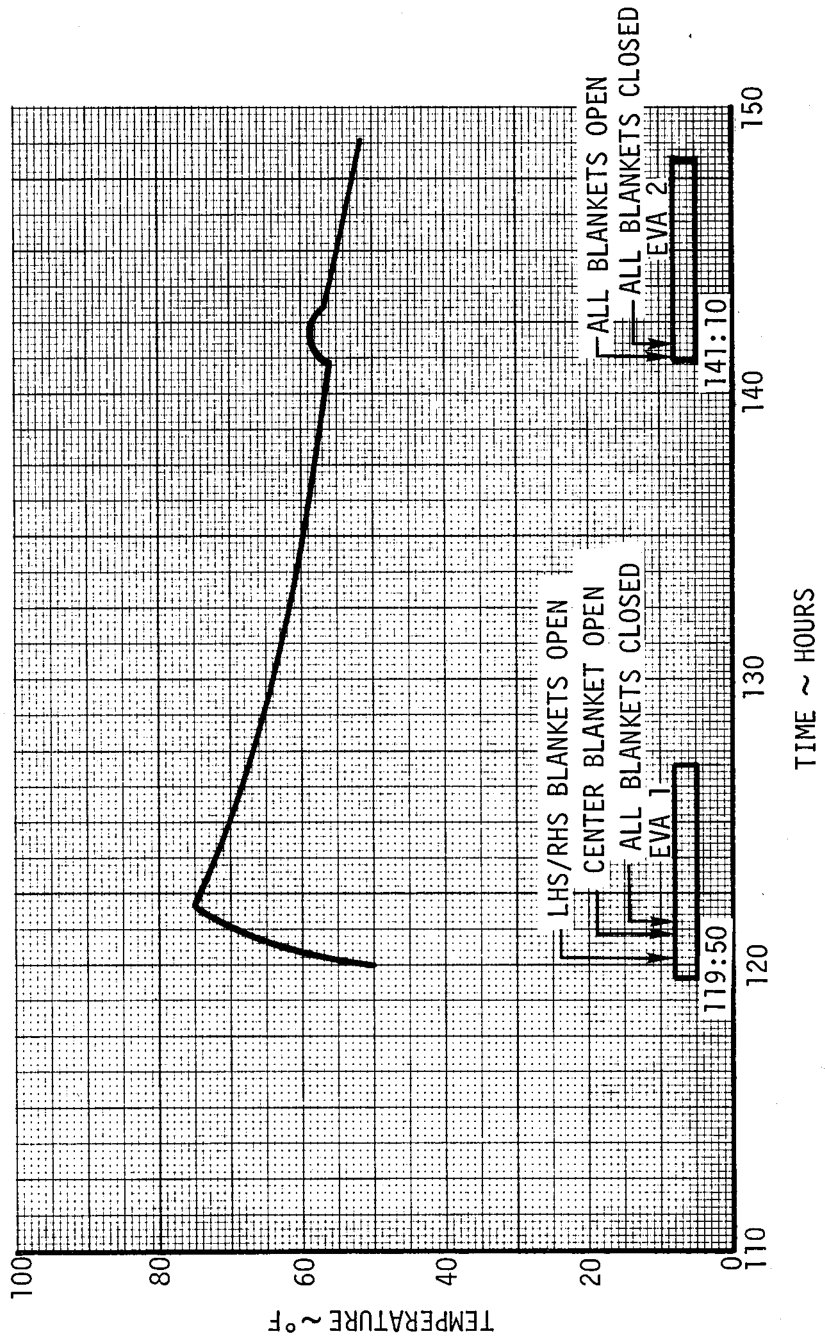

Figure LM10/4.2.4-11. SRC #2 (Nodes 1202 and 1203) Temperature

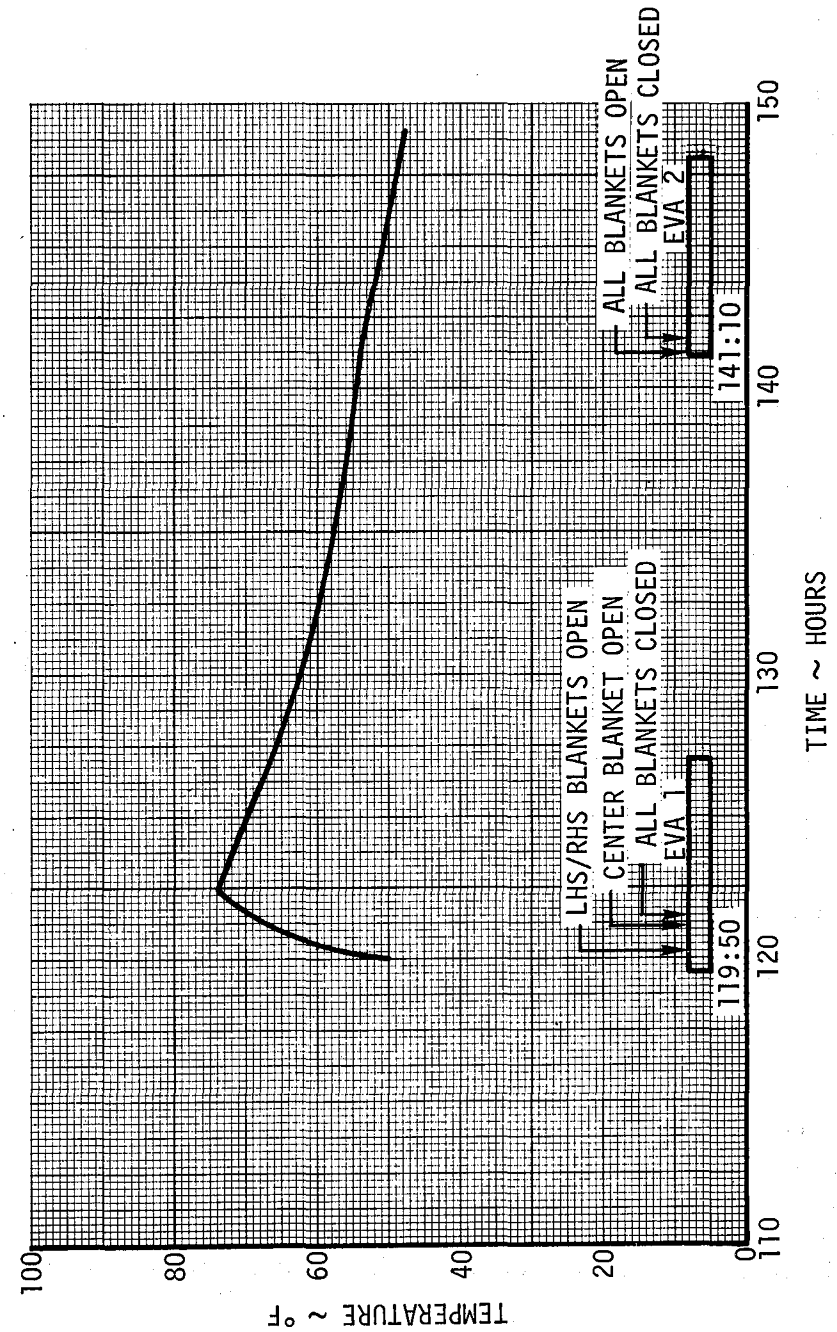

Figure LM10/4.2.4-12. SRC #3 (Nodes 1205 and 1206) Temperature

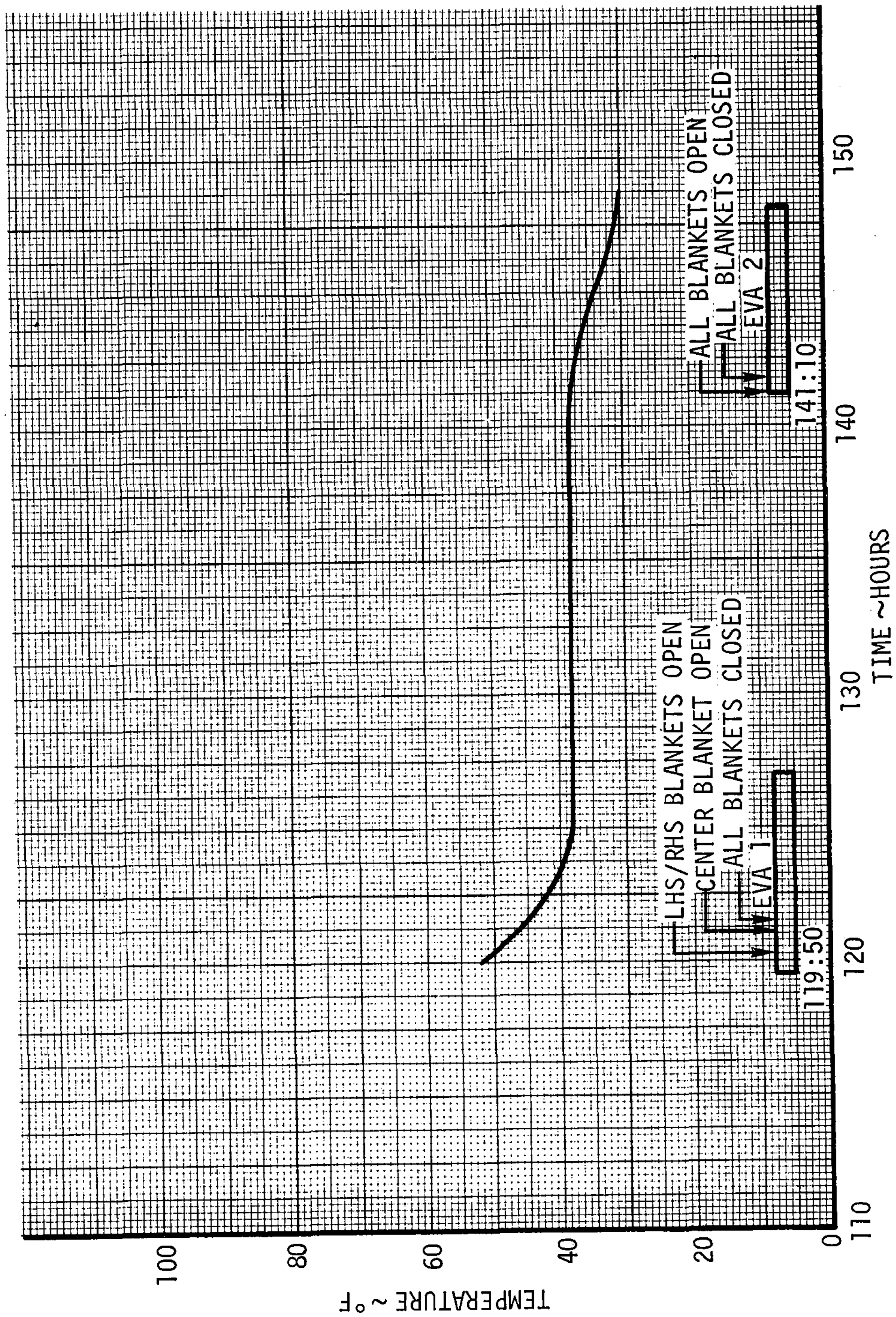

Figure LM10/4.2.4-13. ECS LiOH RHS (Node 1007) Temperature

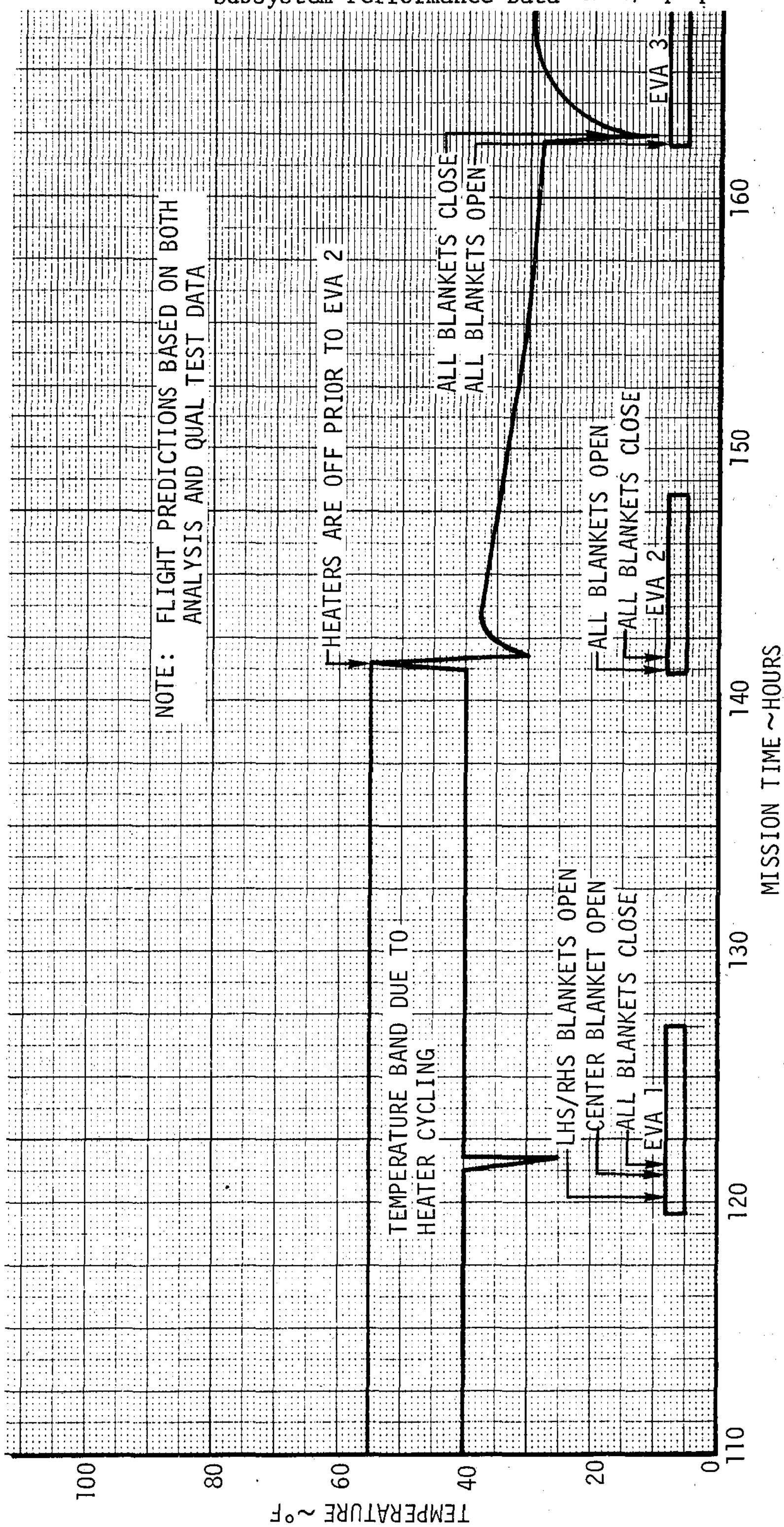

Figure LM10/4.2.4-14. Quad IV MESA Temperature on GB 0541, 0542, and 0543T

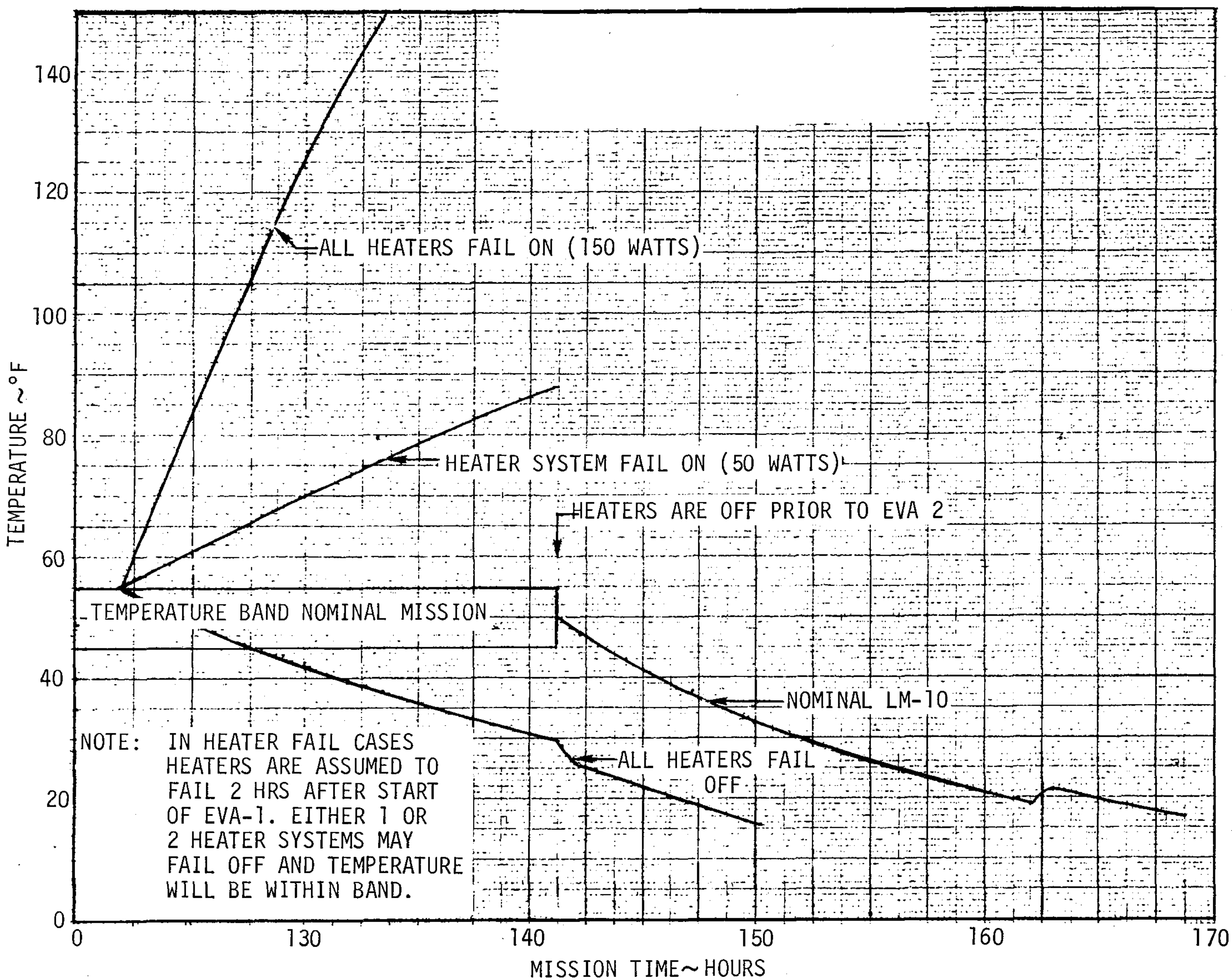

Figure LM10/4.2.4-15. Average MESA Temperature Responses after Deployment

LM10/4.5.4.2 Rendezvous Radar Mechanical Alignment

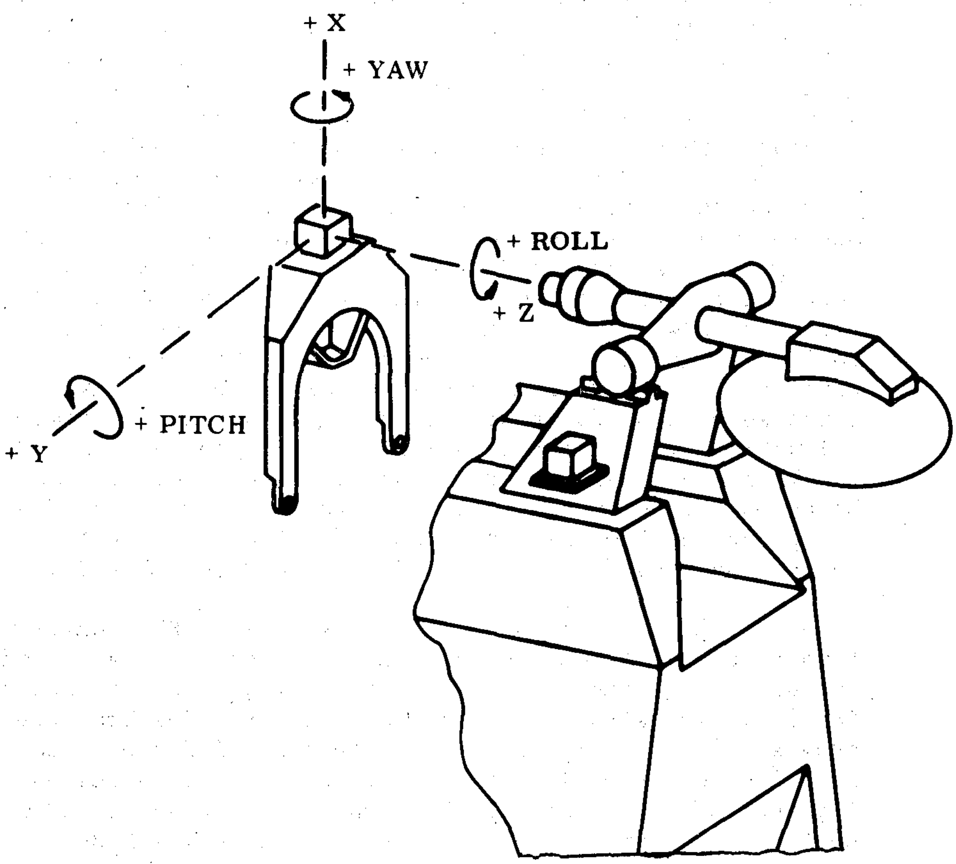

The rendezvous radar antenna assembly alignment for LM-10 with respect to the vehicle coordinate system (nav. base gage) is shown below:

Pitch:	-00° 00' 05"
Roll:	-00° 03' 06"
Yaw:	-00° 00' 55"

LM10/4.5.4.3 RR Timeline Operation

Figures LM10/4.5.4-1 and LM10/4.5.4-2 show the proposed RR management temperature profiles for the LM-10 nominal timeline mission from undocking to touchdown and from lunar ascent to the completion of the rendezvous sequence. The RR operating time during the undocking to touchdown phase is limited to a 10-minute self-test and a two-minute checkout. Since antenna orientations are similar to those of previous missions, it was concluded that RRAA temperatures would remain below 100°F and that there is no danger of an overtemperature condition. For this reason detailed temperatures were not predicted for this mission phase. The RR operation for the lunar ascent is similar to that for LM-8 with a direct ascent planned. Detailed temperature predictions were made however, since the LM-8 flight data were not directly applicable to LM-10 because of LM-10's longer lunar stay time and hence higher liftoff temperature. High power multiplier chain (HPMC) and gyro temperatures were found to be significantly below their maximum allowable values (management curve). It should be noted that the RR antenna temperature response on the lunar surface is based on the antenna boresight in the +X (-90°, Mode II) position except during CSM tracking. Note: Antenna temperature response on the lunar surface is covered by paragraph 4.5.4.3.1.

Figures LM10/4.5.4-12 and LM10/4.5.4-13 show RR management temperature profiles from undocking to touchdown and from lunar ascent to the completion of the rendezvous sequence for a LM-10 mission with a 24-hour launch delay. The predicted lunar stay and ascent temperatures for this mission are higher than for a nominal timeline mission because of the increased heat inputs resulting from a higher sun elevation angle and a hotter lunar surface temperature (the +X position during lunar stay was assumed). The temperatures for the HPMC and gyros however are still found to be below their maximum allowable values (management curve).

The rendezvous radar antenna assembly temperature sensor (GN 7723) should be monitored continuously while the RR is on to assure that the temperature rise does not exceed the management curve. If the RRAA temperature exceeds the management curve, the RR should be turned off if its use is not required. This procedure will assure that there is sufficient in-limit operating time to accomplish mandatory operation.

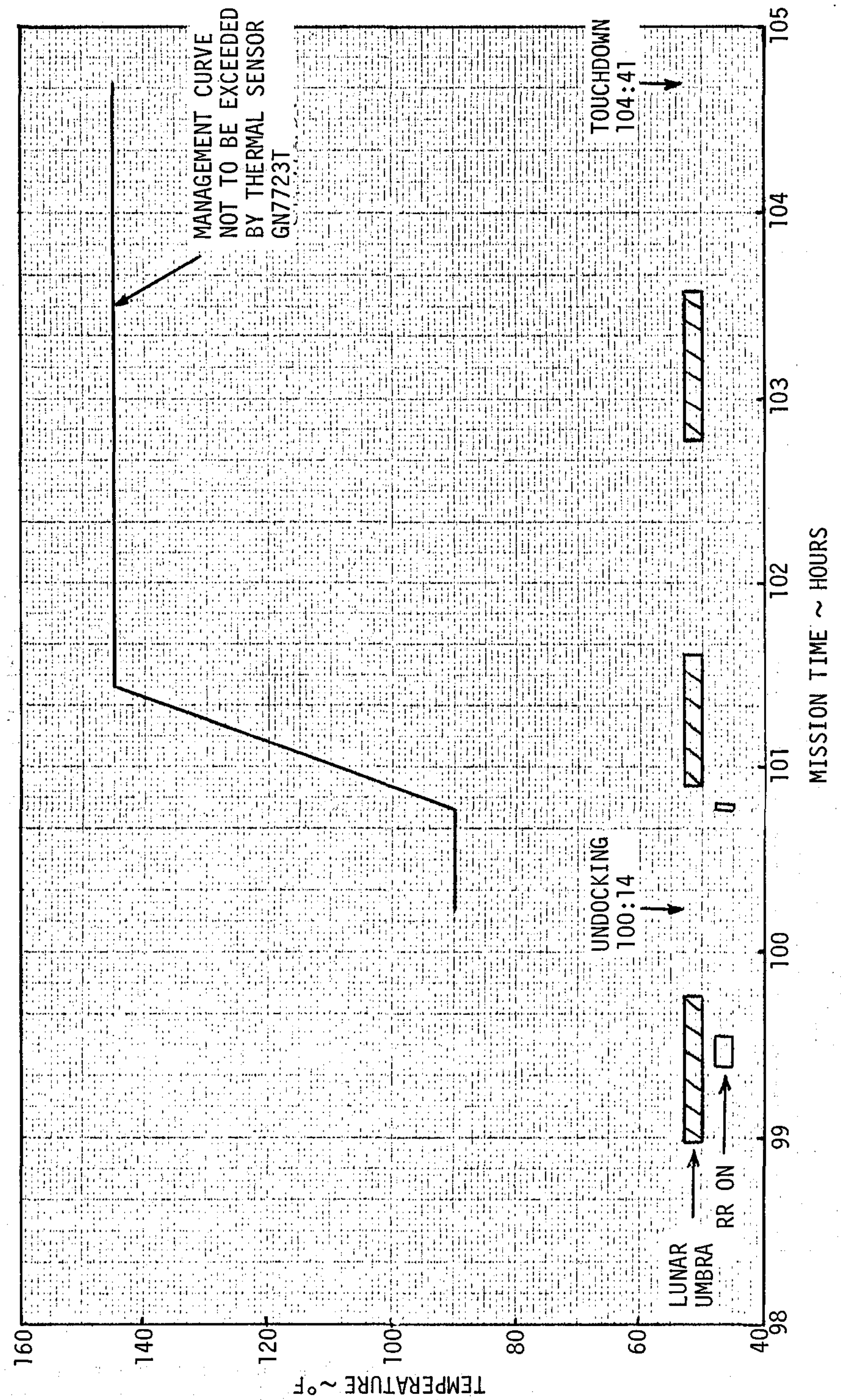

Figure LM10/4.5.4-1. RRAA Temperature Management Curve/LM-10 GN7723T (Undocking to Touchdown) (See Para. LM10/4.5.4.3)

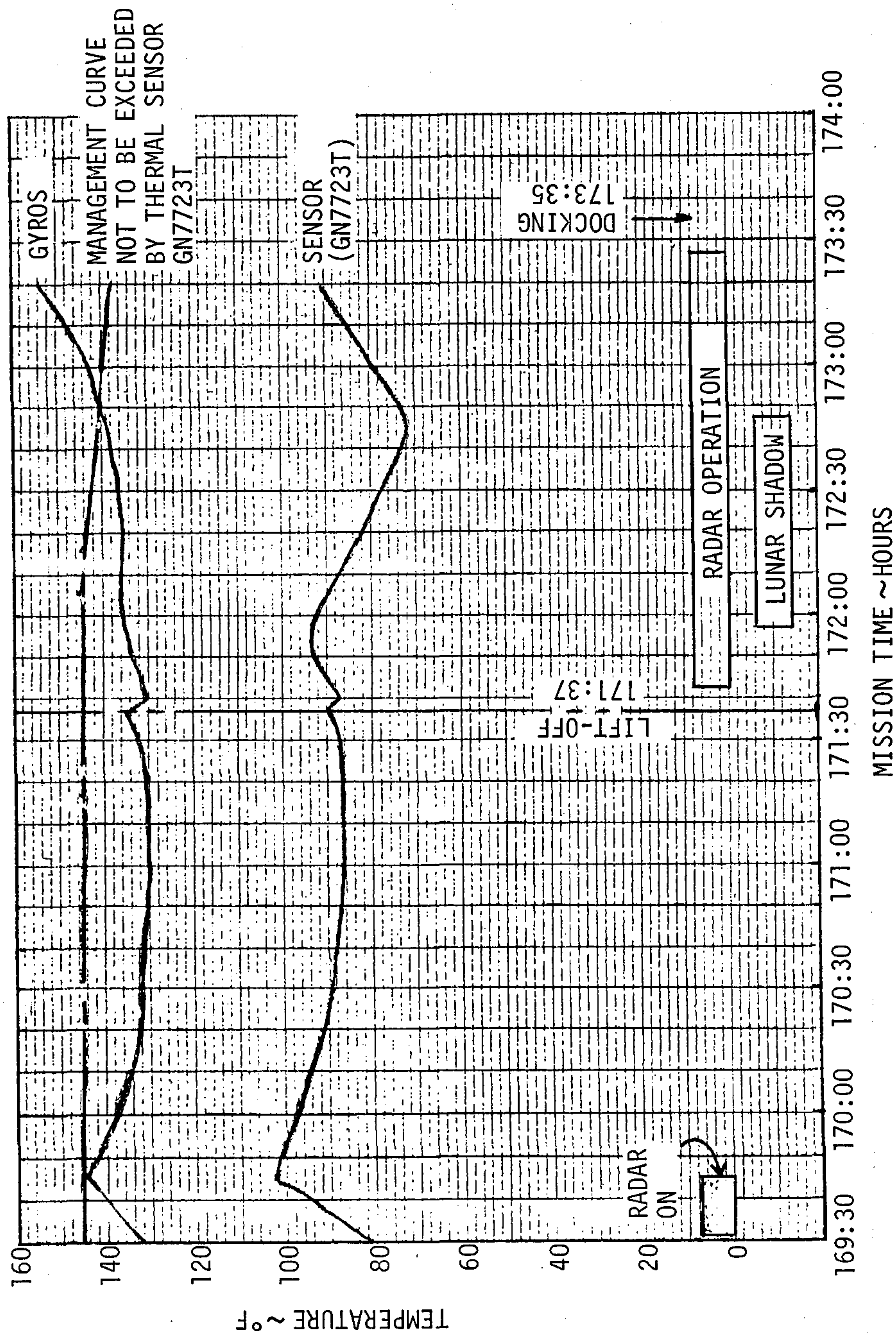

Figure LM10/4.5.4-2. Predicted RR Thermal Response and Management Curve for Final Flight Plan Timeline (Ascent to Docking) (See Para. LM10/4.5.4.3)

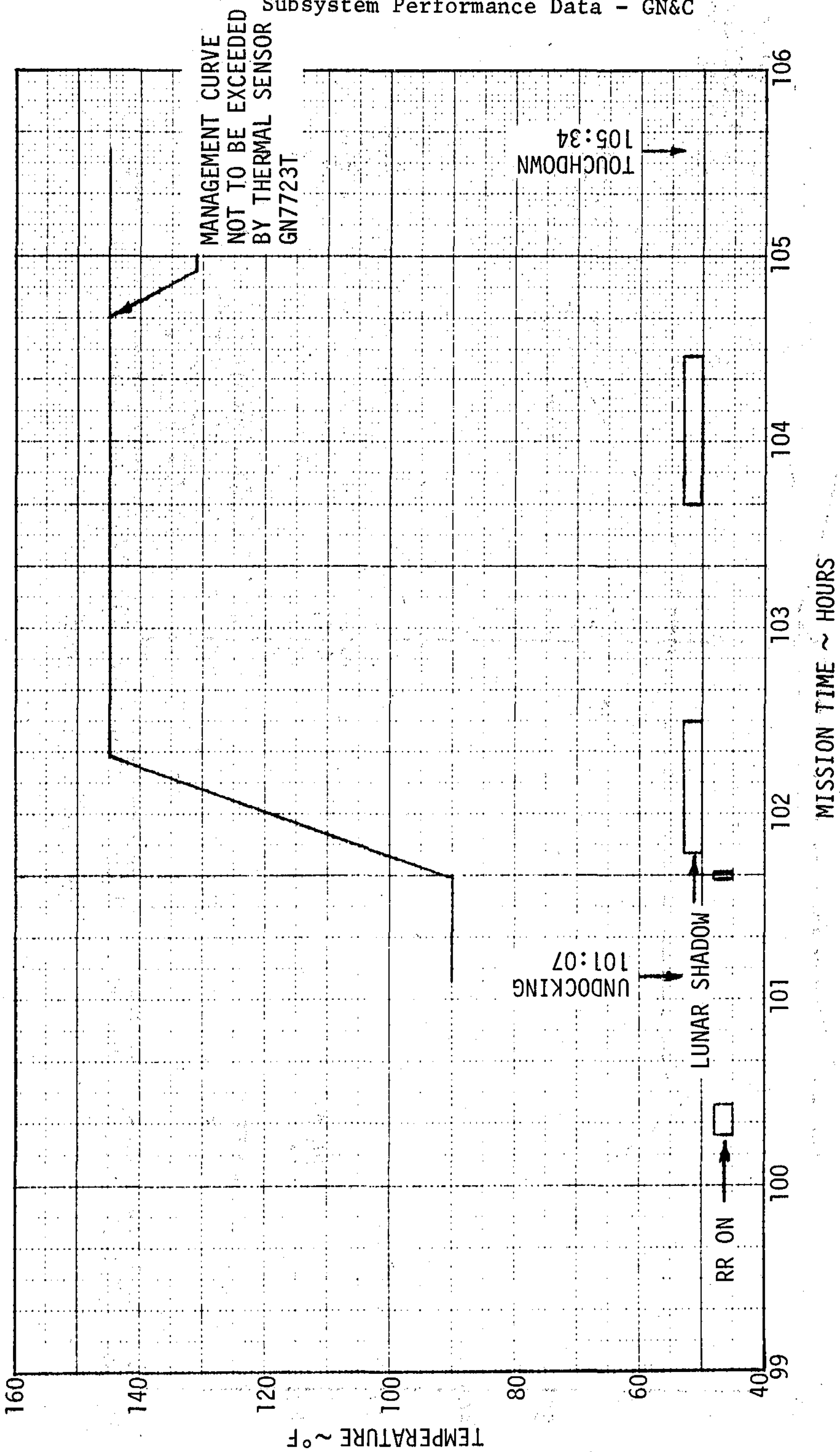

Figure LM10/4.5.4-12. RRAA Temperature Management Curve/LM-10 24-Hour Launch Delay (Undocking to Touchdown) (See Para. LM10/4.5.4.3)

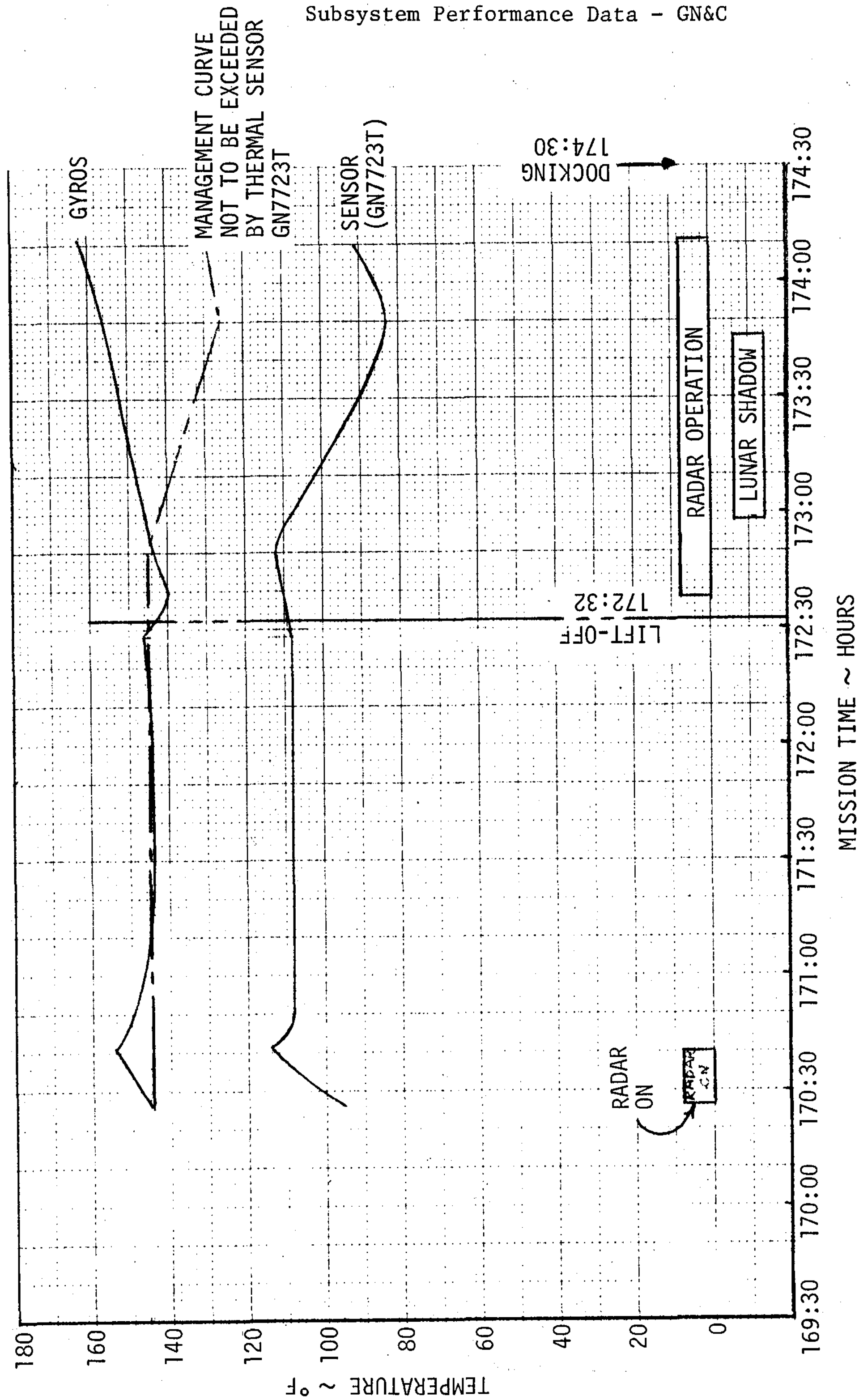

Figure LM10/4.5.4-13. Predicted RR Thermal Response and Management Curve for 24-Hour Launch Delay Timeline (Ascent to Docking) (See Para. LM10/4.5.4.3)

LM10/4.2.8 Data Acquisition Camera (DAC) and Film Canisters Thermal Response (NASA DATA SOURCE)

Figure LM10/4.2.8-1 shows the thermal profile for the DAC for a nominal lunar landing (12.5° sun angle) and for a 24-hour launch delay (24° sun angle). Also, see Table 3.10-2 for DAC temperature limits.

Figure LM10/4.2.8-2 shows the thermal response of the camera magazines located in the LRV (underseat stowage) for a nominal lunar landing (12.5° sun angle).

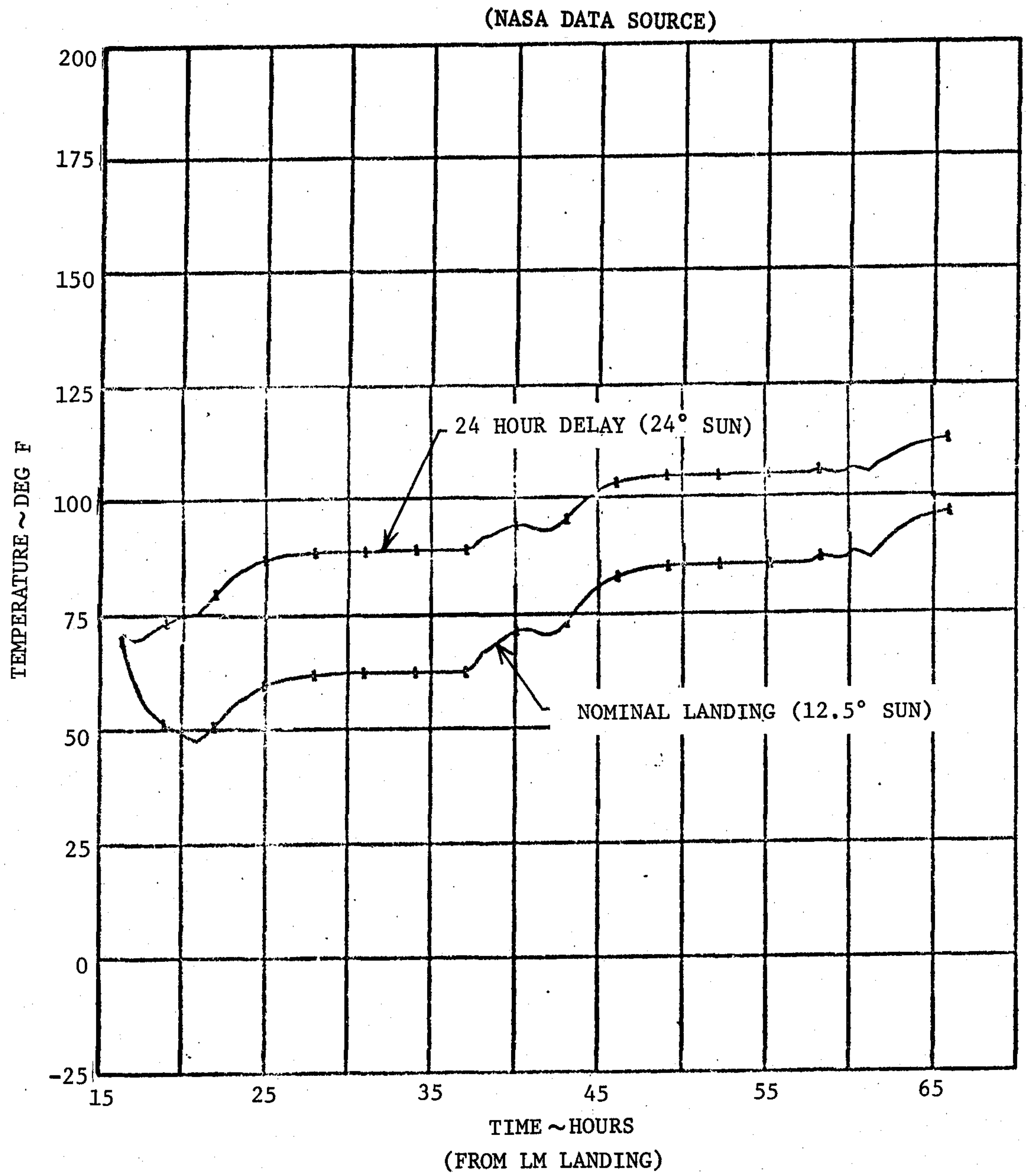

Figure LM10/4.2.8-1. Data Acquisition Camera Thermal Profile

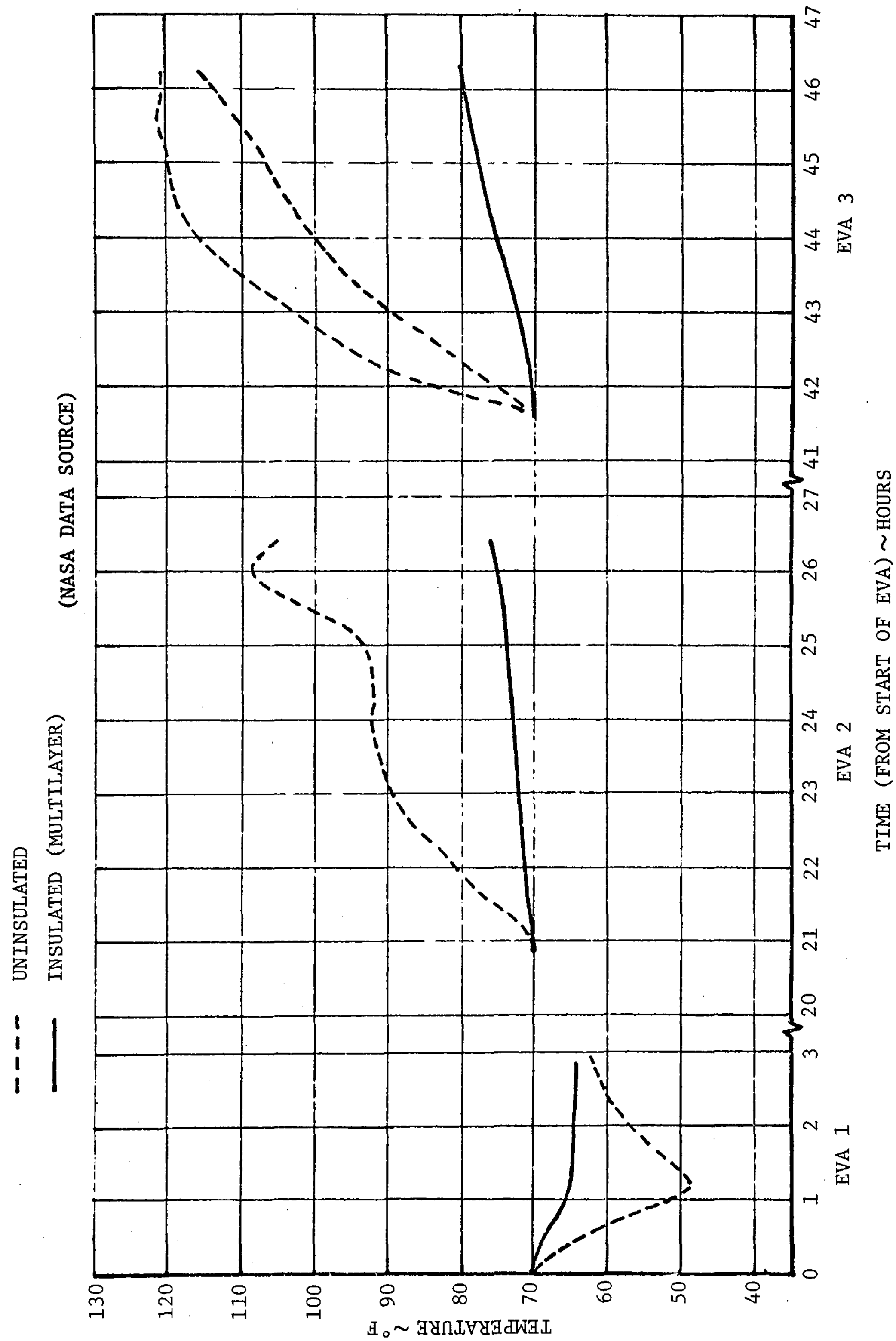

Figure LM10/4.2.8-2. Thermal Response of Camera Magazines (LRV Underseat Stowage) for Apollo 15 Nominal Lunar Landing (12.5° Sun Angle)

LM10/4.2.9 QUAD III STOWAGE TEMPERATURE PREDICTIONS - Nominal Mission

Figure LM10/4.2.9-1 presents the nominal LM-10 Temperature Predictions for the LRV and LR^3 pallets (with mounted equipment). Predictions are generated up to 30 hours after lunar touchdown. The mathematical model used for this study is similar to that used in paragraph 4.2.9 with the following modifications:

(1) External surfaces were modified to more accurately represent the flight configuration.

(2) Updated pallet and mounted equipment thermal capacities.

(3) Updated insulation blanket ϵ_{EFF}.

(4) Nominal external coatings and vehicle orientations were used.

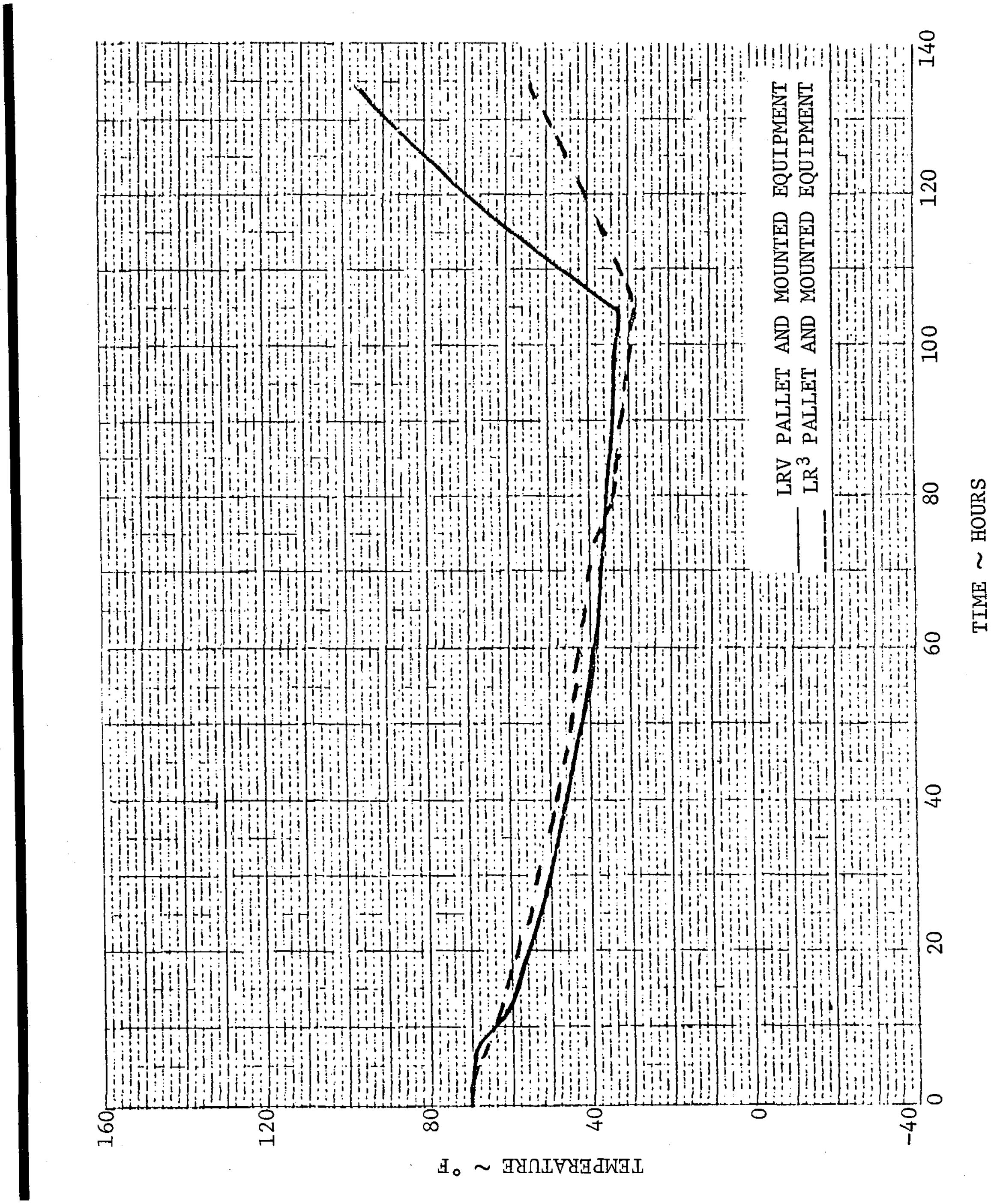

Figure LM10/4.2.9-1 LM-10 Nominal Thermal Response of QUAD III Pallets and Mounted Equipment (See Paragraph LM10/4.2.9)

LM10/4.3.2.2 Leakage

Figure LM10/4.3.2-1 presents a band for LM-10 cabin leak rate as a function of cabin pressure over the range 3.0 to 5.2 psia, based on orifice-type and capillary-type leakage. A normal expected leak rate vs. pressure curve has also been included.

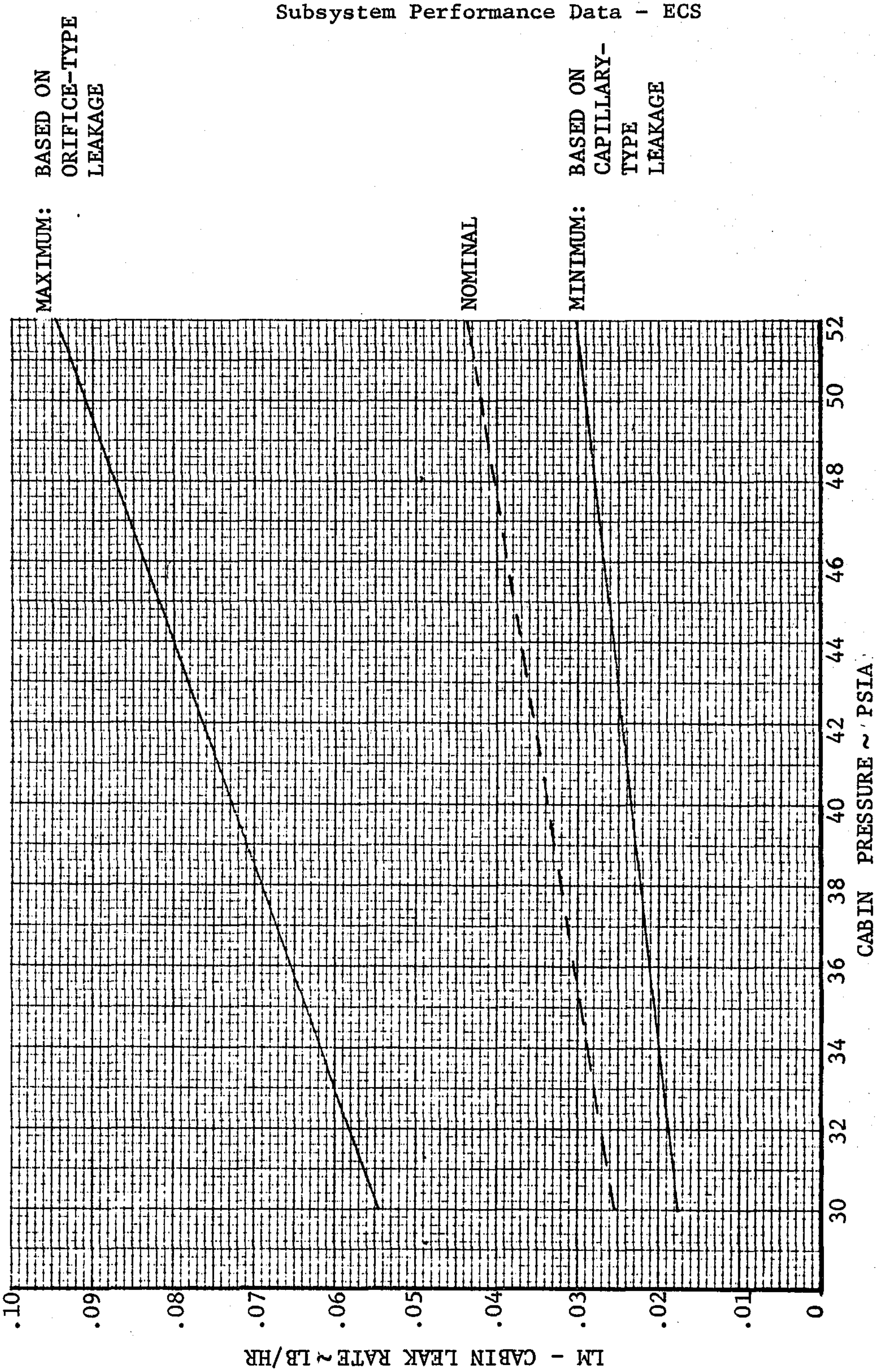

Figure LM10/4.3.2-1. Cabin Leak Rate vs. Cabin Pressure
(See Paragraph LM10/4.3.2.2)

LM10/4.3.3 Mission CO_2 Partial Pressure and LiOH Remaining

Table LM10/4.3.3-1 presents a summation of LM-10 LiOH utilization.

Figures LM10/4.3.3-1 and LM10/4.3.3-1.1 present CO_2 partial pressure versus mission time for the nominal mission showing the effect of sensor, PCM and CRT errors.

Figures LM10/4.3.3-2 and LM10/4.3.3-2.1 present CO_2 partial pressure versus mission time for the worst qualified cartridge showing the effect of sensor, PCM and CRT errors.

Figure LM10/4.3.3-3 presents the total LiOH hours remaining versus mission time. All the aforementioned graphs are based on Apollo 15 Flight Plan, dated 1 June 1971.

Table LM10/4.3.3-1. LM-10 LiOH Utilization

CARTRIDGE	ACTUAL HOURS OPERATION	EQUIVALENT HOURS[1] OPERATION	AVERAGE METABOLIC RATE BTU/HR/MAN	HOURS REMAINING[2] AT CHANGE
1	18.2	16.8	481	4.7
2	20.7	21.3	535	.7
3	18.8	19.0	523	2.3
Mission Totals	57.7	57.1	515	-

1. At 520 BTU/HR/MAN
2. At cartridge change based on spec. life of 20.5 hours at 520 BTU/HR/MAN. Considers CO_2 storage in cabin and dumping of CO_2 during cabin depressurizations.

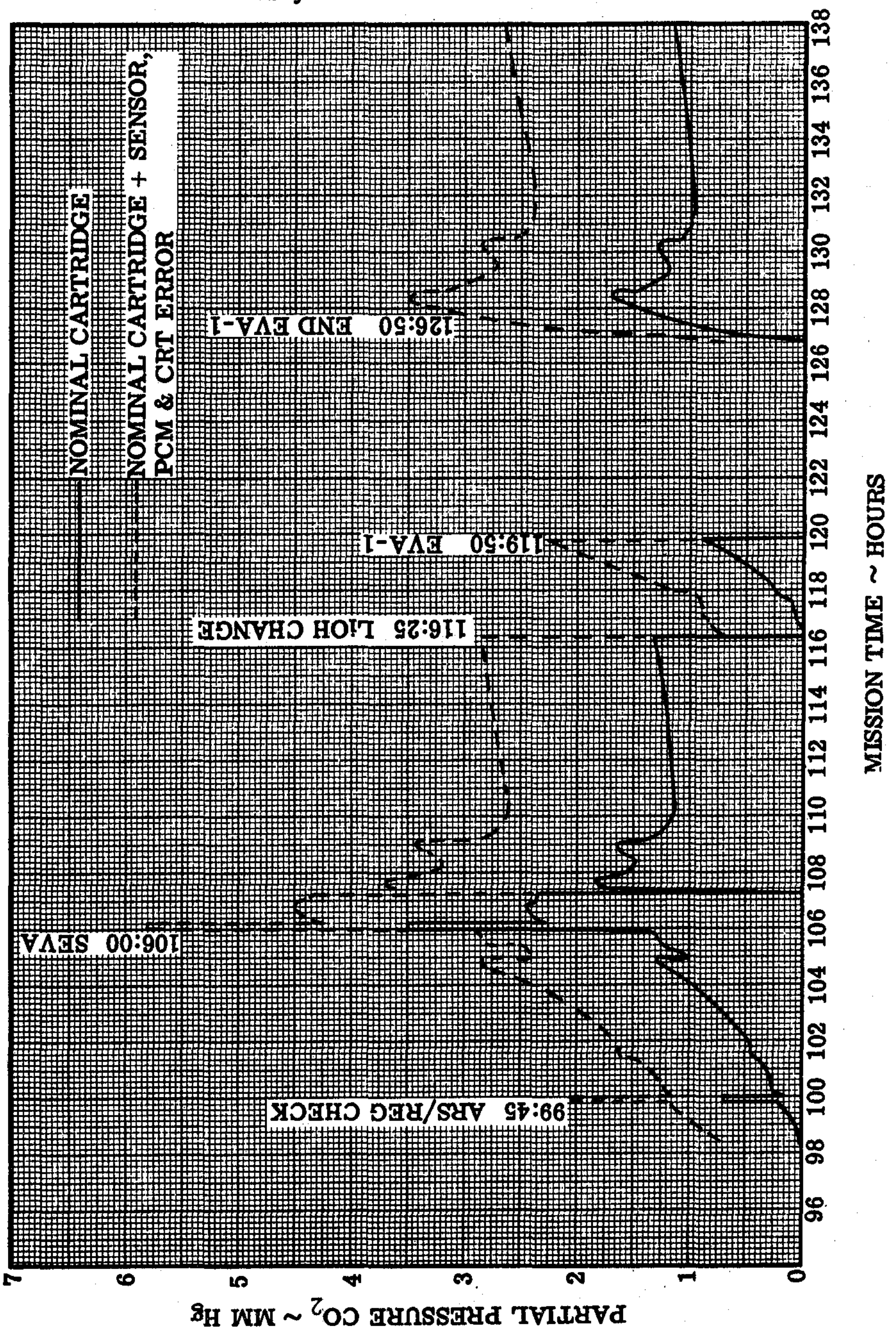

Figure LM10/4.3.3-1. LM-10 J-1 Mission CO_2 Partial Pressure ~ GF1521P (See Para. LM10/4.3.3)

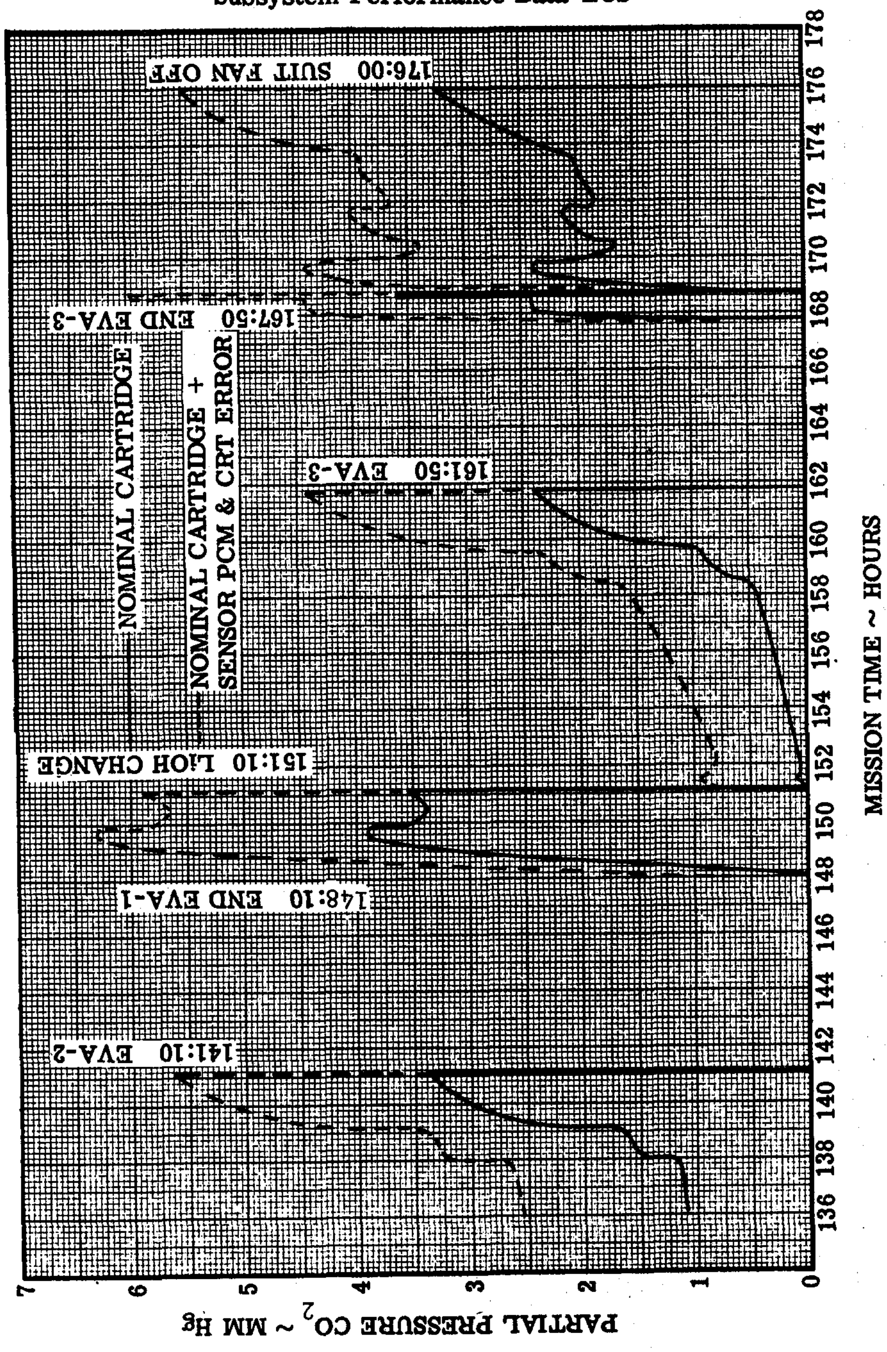

Figure LM10/4.3.3-1.1. LM-10 J-1 Mission CO_2 Partial Pressure ~ GF1521P
(See Para. LM10/4.3.3)

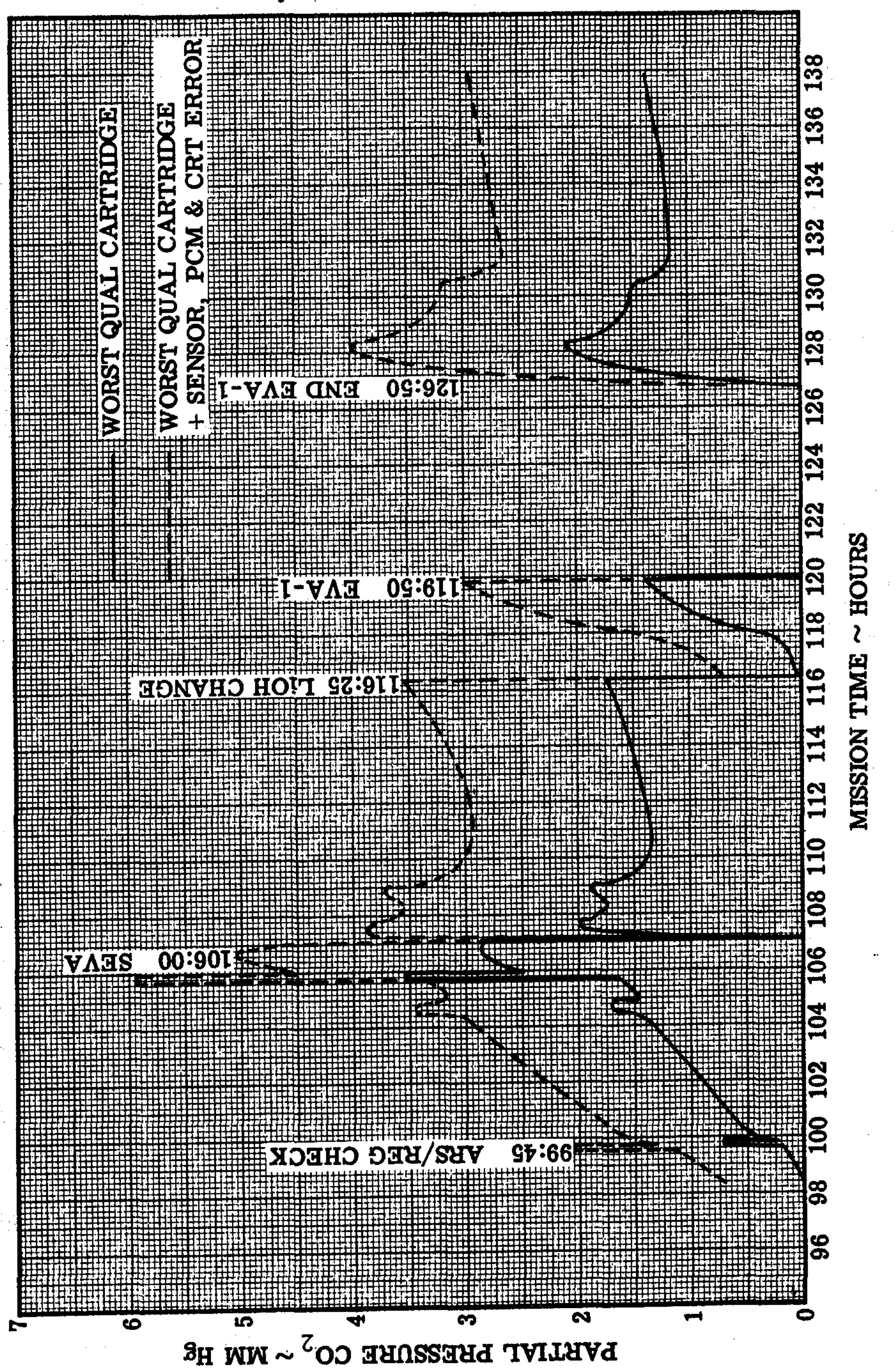

Figure LM10/4.3.3-2. LM-10 J-1 Mission CO_2 Partial Pressure ~ GF1521P
(See Para. LM10/4.3.3)

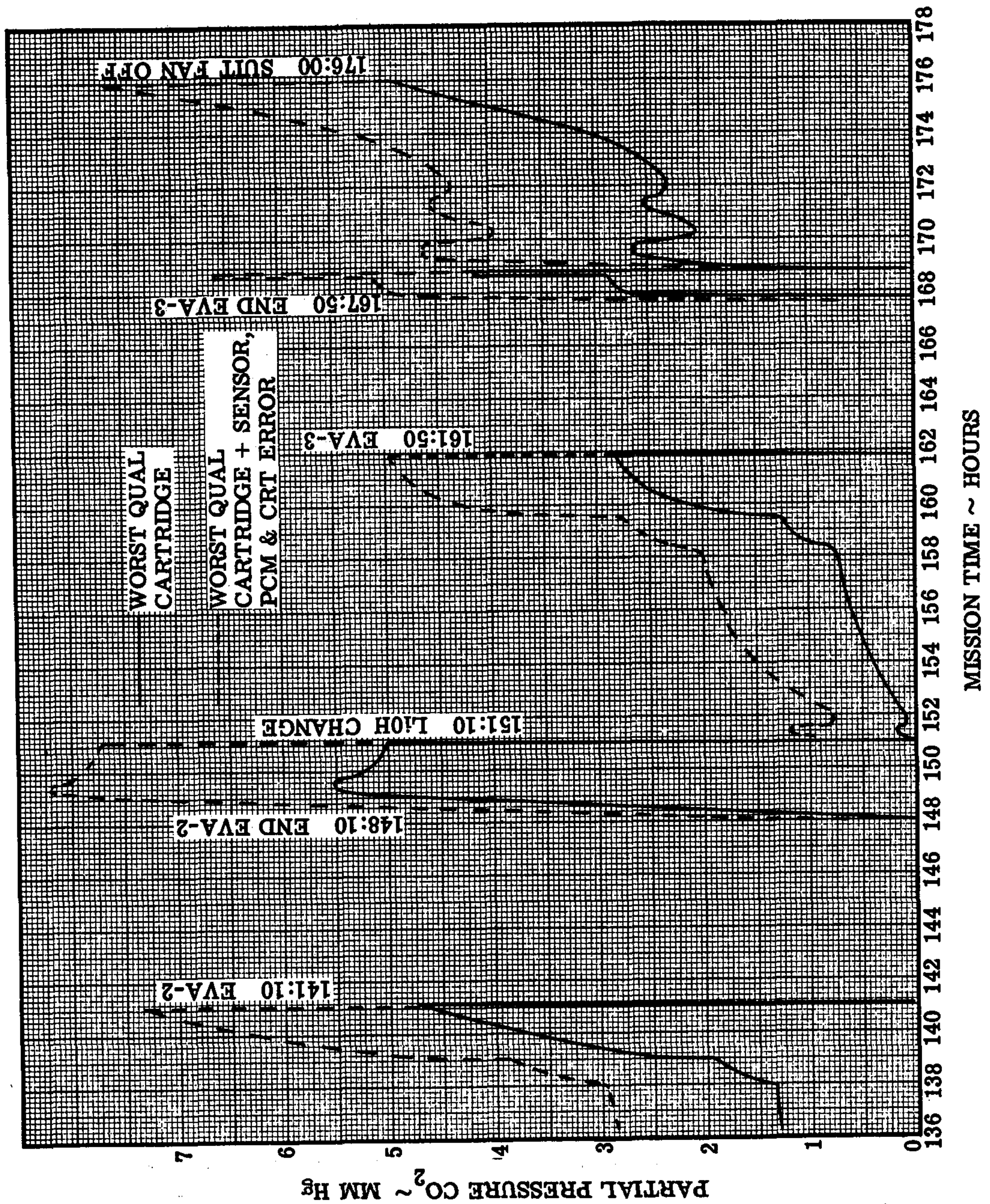

Figure LM10/4.3.3-2.1. LM-10 J-1 Mission CO_2 Partial Pressure ~ GF1521P
(See Para. LM10/4.3.3)

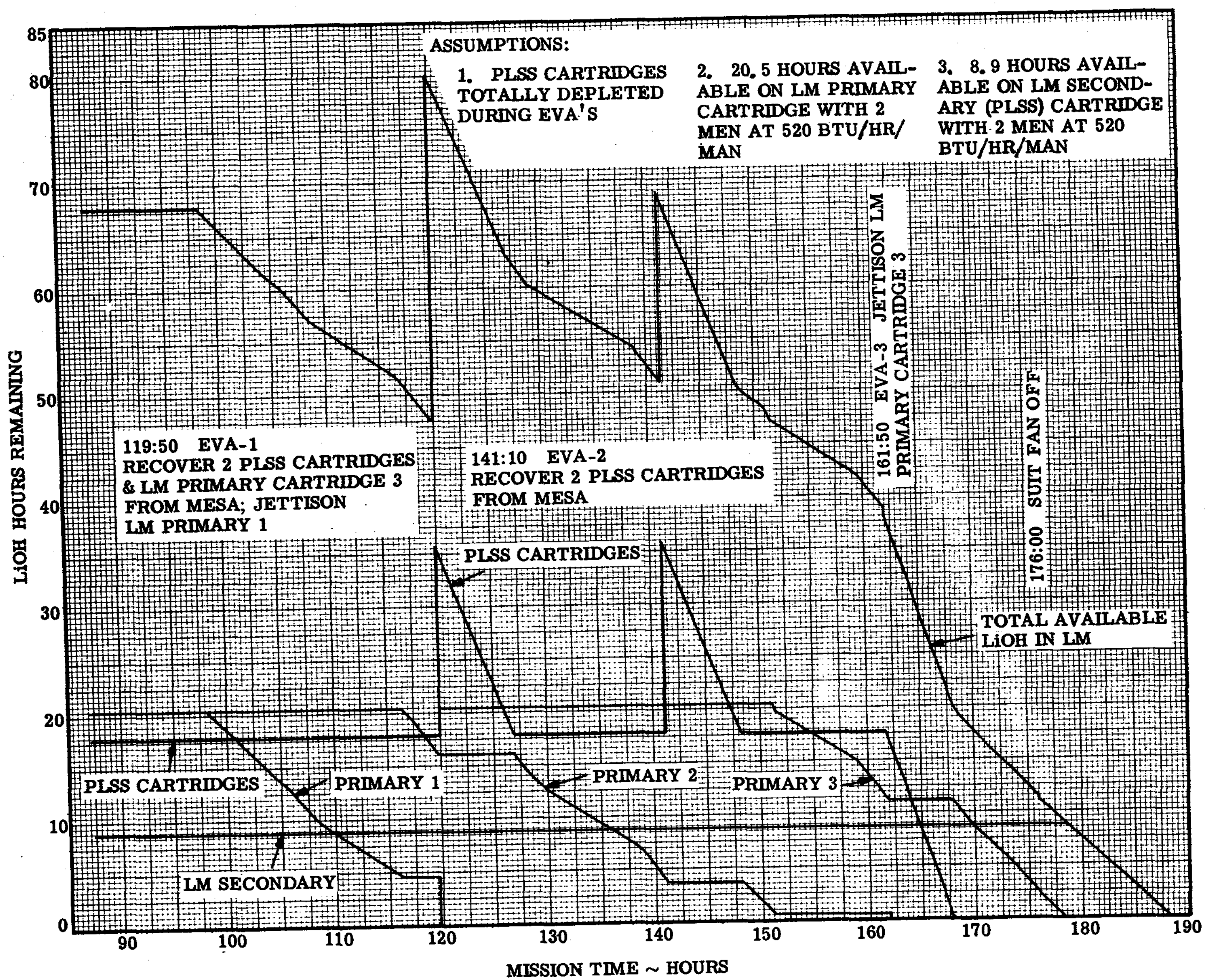

Figure LM10/4.3.3-3. LM-10 J-1 Mission Hours of LiOH Available For Use In LM (See Para. LM10/4.3.3)

LM10/4.3.4 Water Consumption

The following figures present water consumption data and are based on the Apollo 15 Preliminary Flight Plan, dated 20 April 1971.

Figure LM10/4.3.4-1 presents descent water tank pressure (psia) vs. mission time for minimum, nominal and maximum usage.

Figure LM10/4.3.4-2 presents ascent water tank pressure (psia) vs. mission time for minimum, nominal, and maximum usage.

Figure LM10/4.3.4-3 presents descent water tank quantity (lbs/tank) vs. mission time for minimum, nominal and maximum usage.

Figure LM10/4.3.4-4 presents ascent water tank quantity (lbs/tank) versus mission time for minimum, nominal and maximum usage.

LM10/4.3.4.9 Water Quantity Measurement

Figure LM10/4.3.4-5 presents the descent water quantity vs. indicated CRT pressure readings. End-to-end measurement errors are given for 5°F and 10°F temperature uncertainties.

Figure LM10/4.3.4-6 presents the descent water quantity vs. indicated CRT pressure reading (GF4501P). End-to-end measurement errors are given for 5°F and 10°F temperature uncertainties.

Figure LM10/4.3.4-7 presents the descent water quantity vs. cabin meter indicated quantity. End-to-end measurement errors are given for 60°F to 80°F temperature range and one percent error for meter readability.

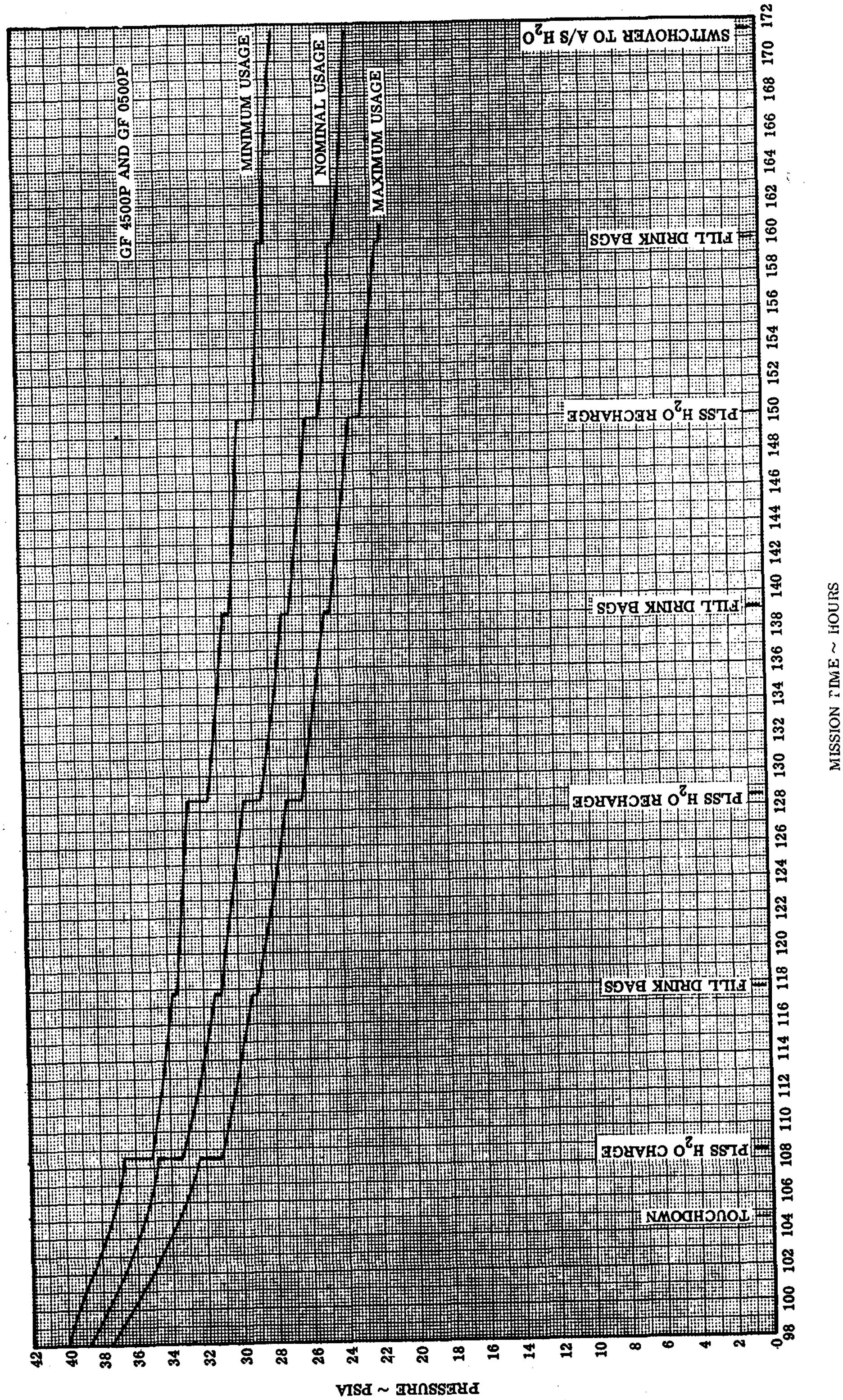

Figure LM10/4. 3. 4-1. LM-10 J-1 Mission Descent Water Tank Pressure - PSI (See Para. LM10/4. 3. 4)

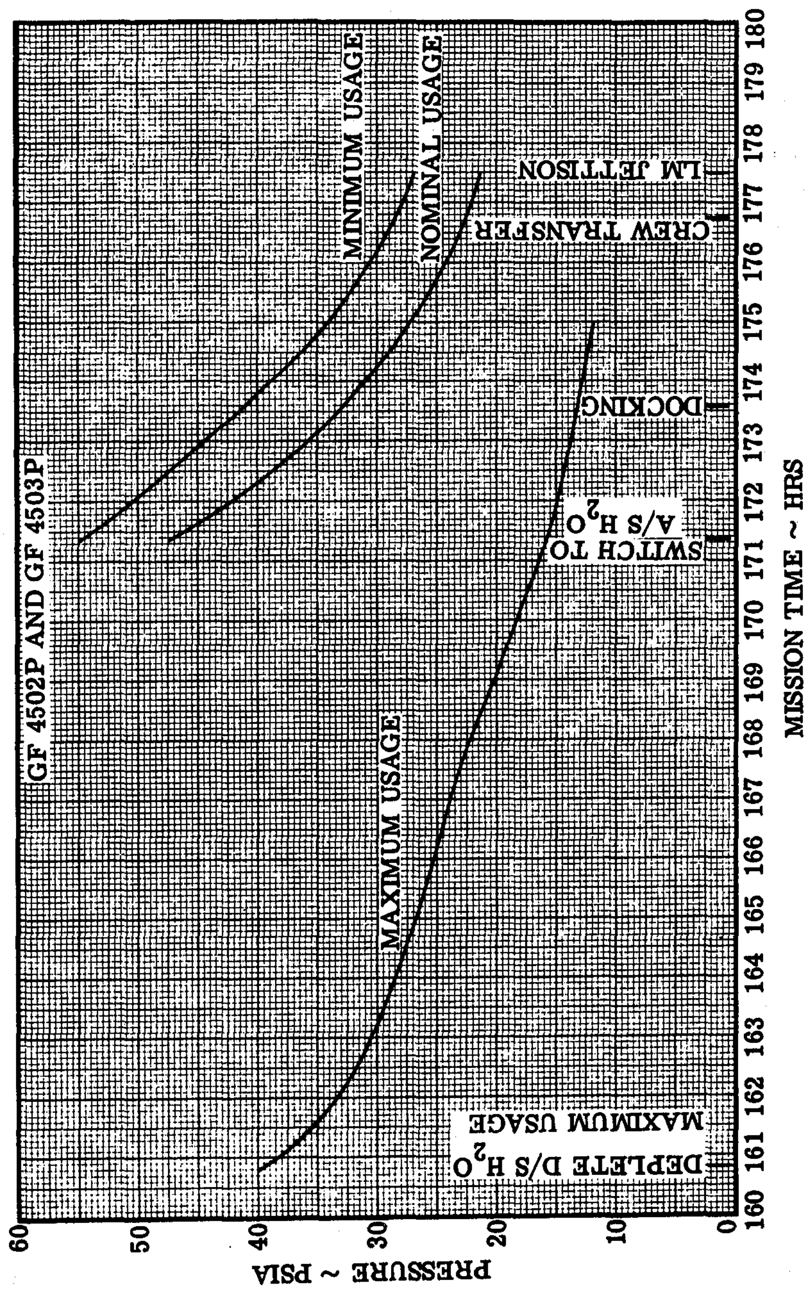

Figure LM10/4.3.4-2. LM-10 J-1 Mission Ascent Water Tank Pressure ~ PSI (See Para. LM10/4.3.4)

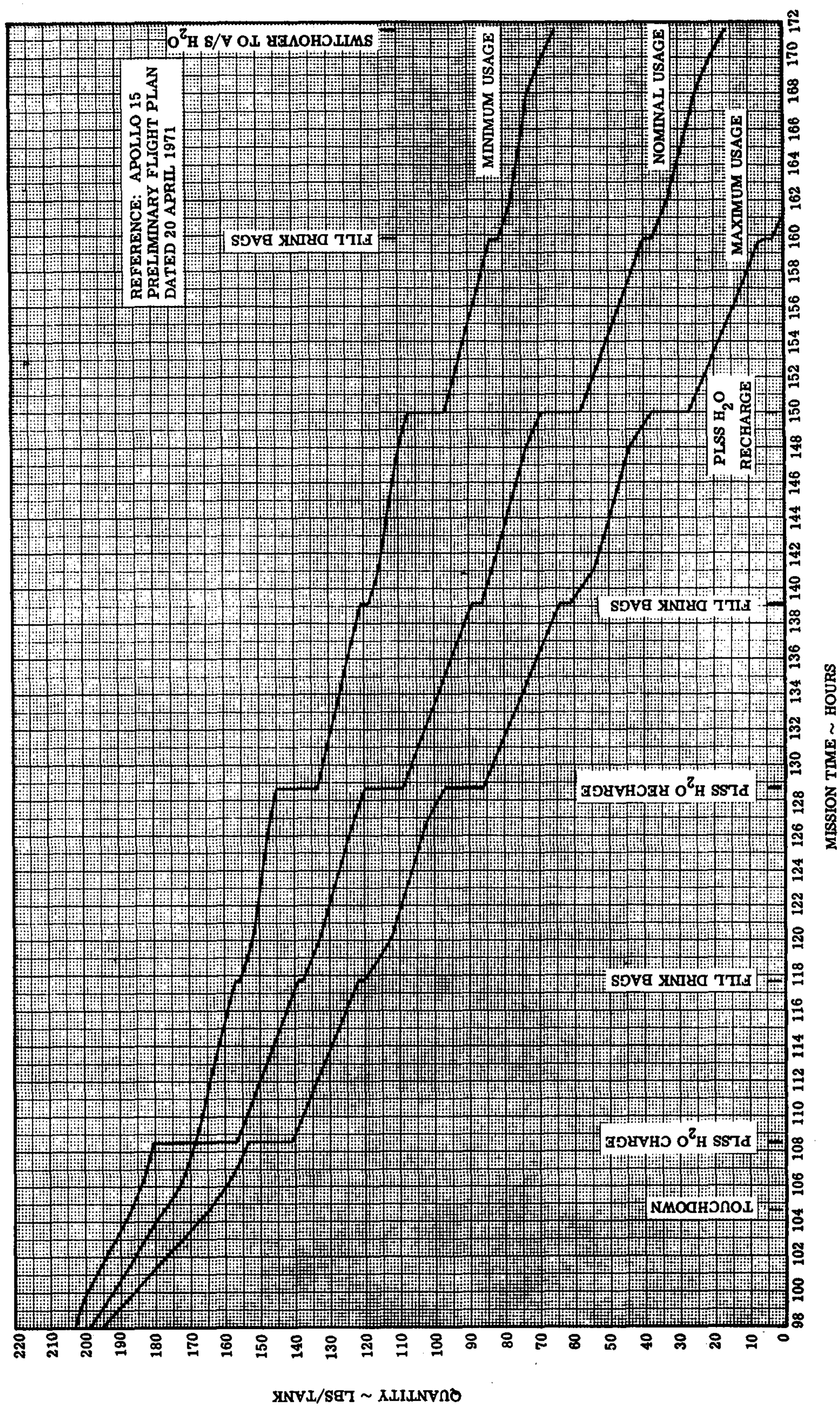

Figure LM10/4. 3. 4-3. LM-10 J-1 Mission Descent Water Tank Quantity - Lbs/Tank (See Para. LM10/4. 3. 4)

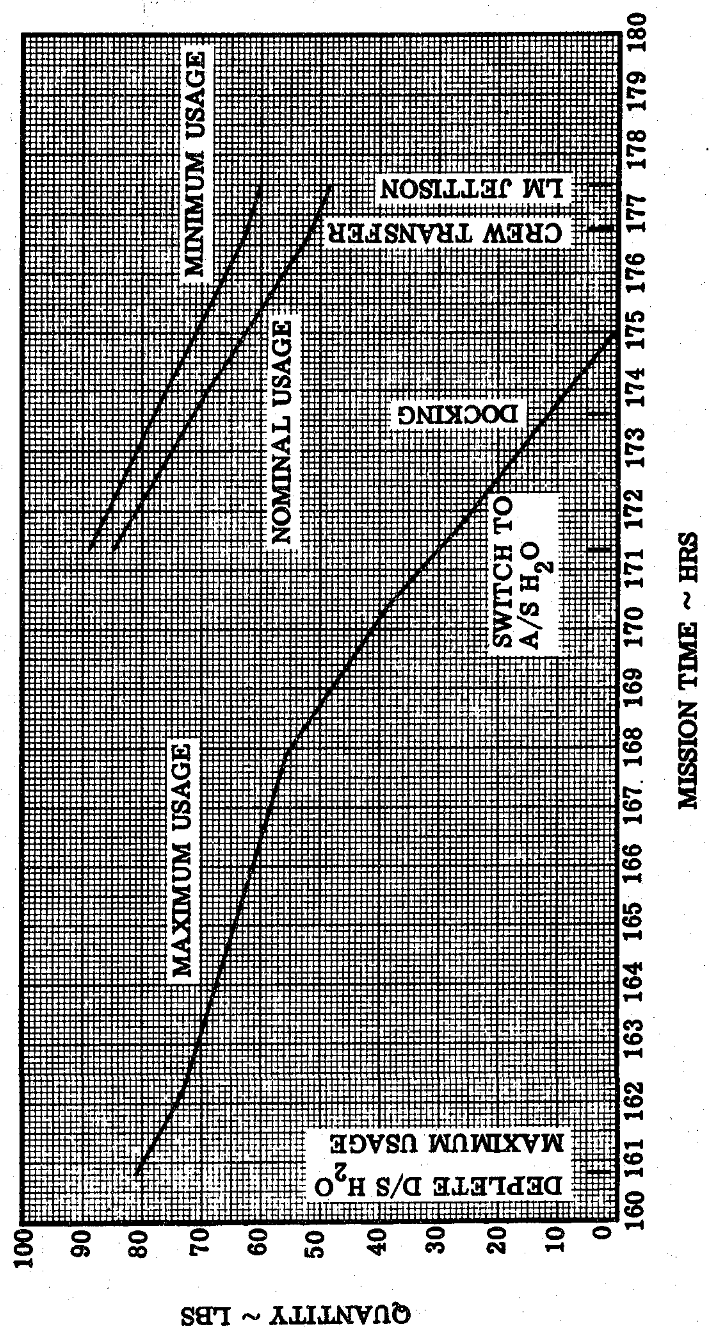

Figure LM10/4.3.4-4. LM-10 J-1 Mission Ascent Water Tank Quantity ~ Lbs/Tank (See Para. LM10/4.3.4)

DESCENT WATER TANK QUANTITY AND MEASUREMENT ERROR
FILL RATIO = 0.4775 : 212 LBS/TANK LOAD

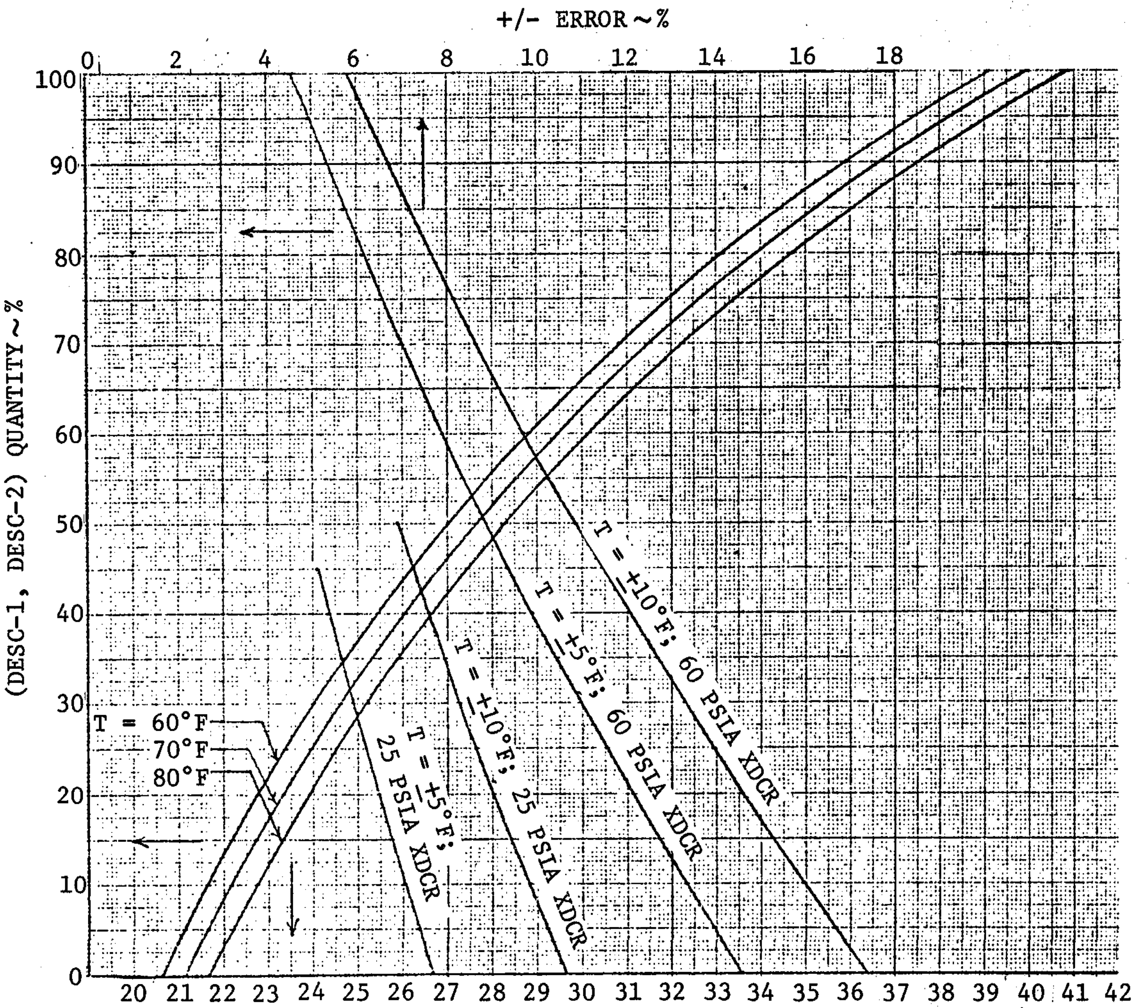

(GF4500P, GF0500P) INDICATED CRT PRESSURE ~ PSIA
(GF4501P + TANK-1, TANK-2, HEAD) CORRECTED CRT PRESSURE ~ PSIA

NOTE:
1. LOAD POINT: 40.00 PSIA @ 70°F
2. FILL WATER ASSUMED SATURATED WITH 14.7 PSIA N_2 PRIOR TO FILL
3. TANK-1 HEAD (1/6 g) = 0.493 - 0.076 (Q/100)
4. TANK-2 HEAD (1/6 g) = 0.638 - 0.076 (Q/100)

Figure LM10/4.3.4-5. Descent H_2O Tank Correction - Usable Water in Tank vs. CRT Readings in PSIA (See Para. LM10/4.3.4.9)

DESCENT WATER TANK QUANTITY AND MEASUREMENT ERROR
FILL RATIO = 0.4775 : 212 LBS/TANK LOAD
LUNAR SURFACE : 1/6g

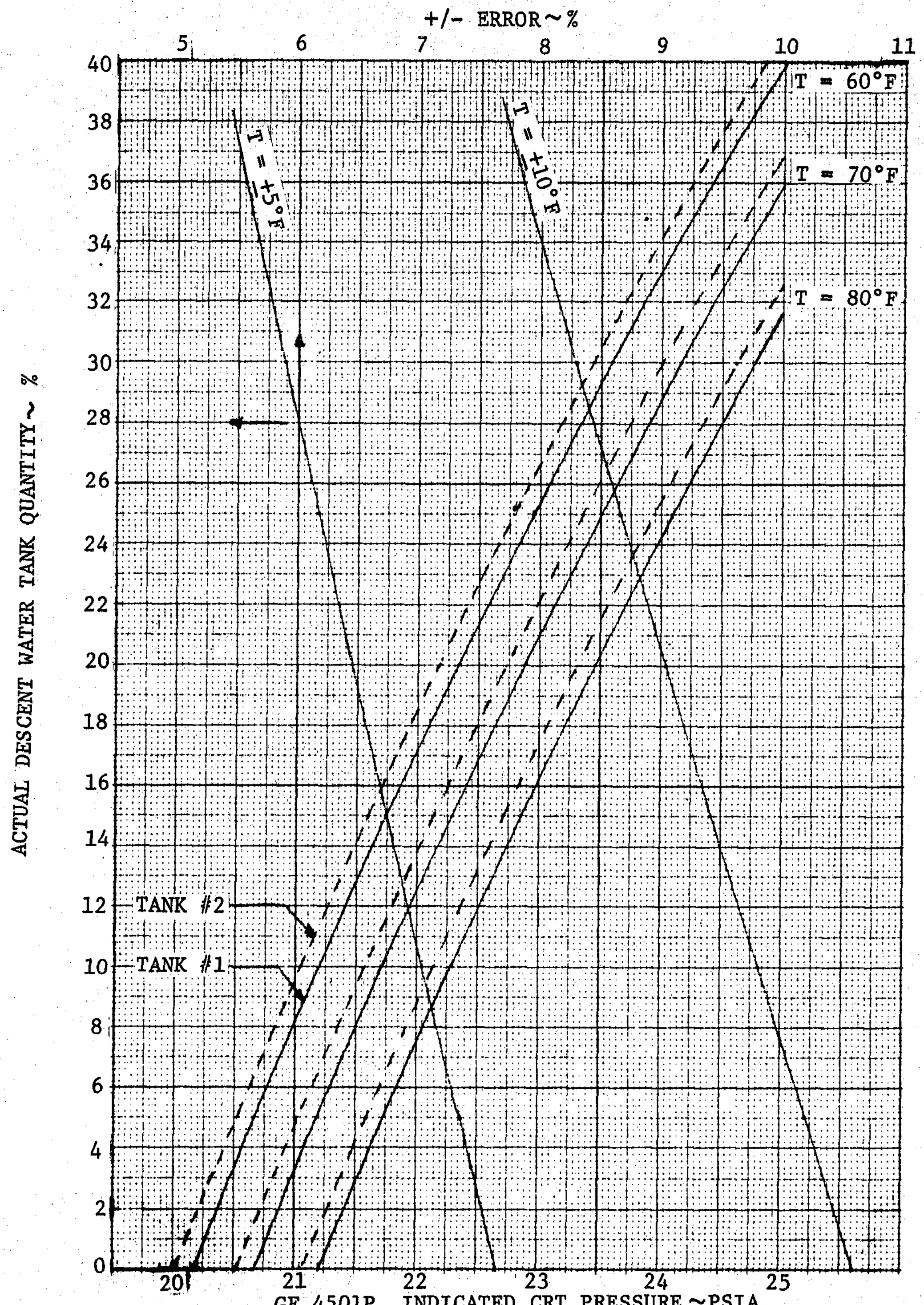

Figure LM10/4.3.4-6. Descent H_2O Tank Correction - Usable Water in Tank vs CRT (GF4501P) Reading in PSIA (See Para. LM10/4.3.4.9)

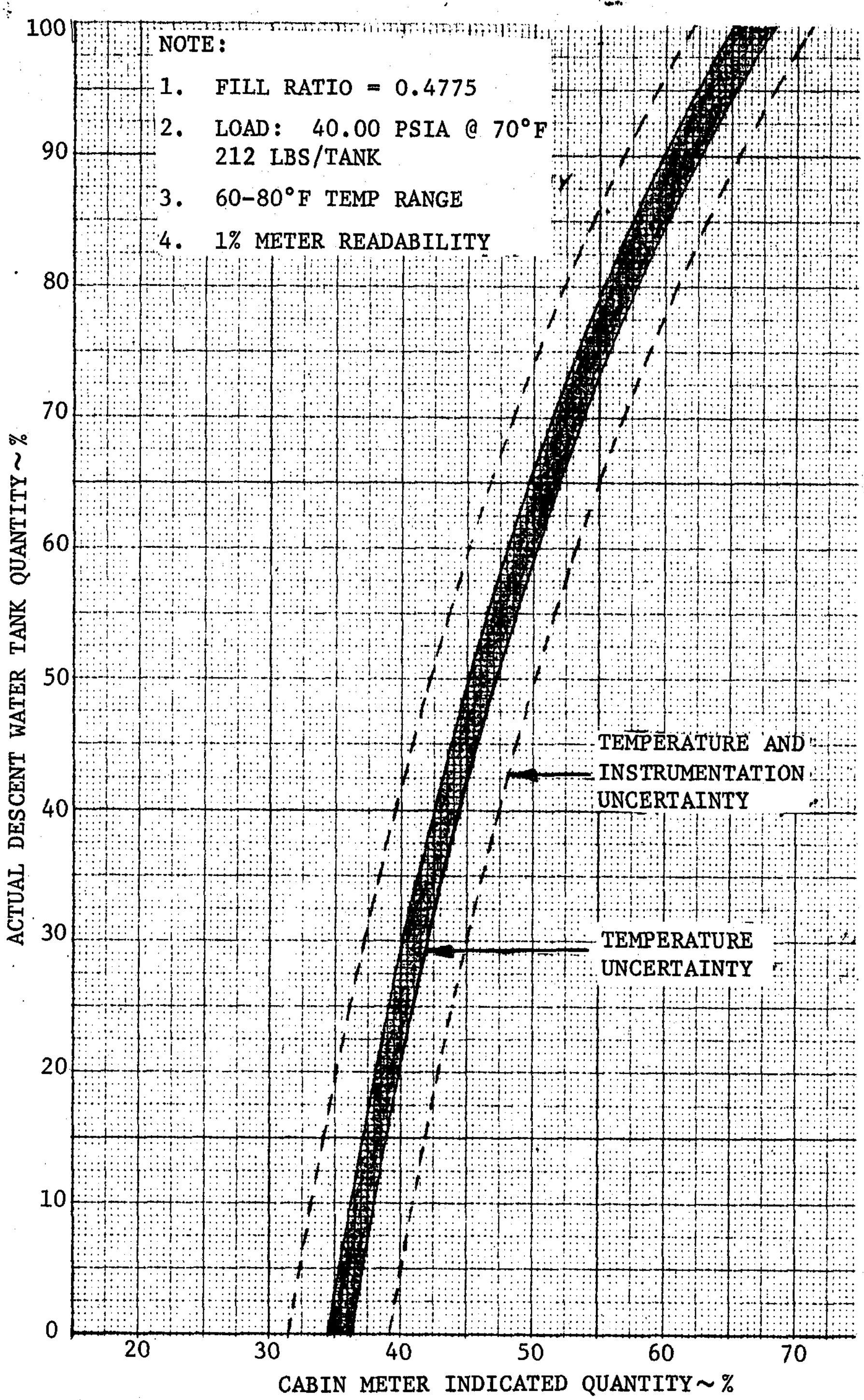

Figure LM10/4.3.4-7. Descent H_2O Tank Quantity vs Cabin Meter Indicated Reading (See Para. LM10/4.3.4.9)

LM10/4.3.8 Environmental Control Equipment

LM10/4.3.8.1 Heat Transport Section Water Sublimators

Figures LM10/4.3.8-1 and LM10/4.3.8-2 present glycol outlet temperature as a function of glycol inlet temperature for primary HTS sublimator (209) and secondary HTS sublimator (224), respectively.

Figures LM10/4.3.8-3 and LM10/4.3.8-4 represent heat rejection capabilities for primary HTS sublimator (209) and secondary HTS sublimator (224), respectively.

Figure LM10/4.3.8-5 presents pump load line and HTS ΔP characteristics as a function of glycol flow rate.

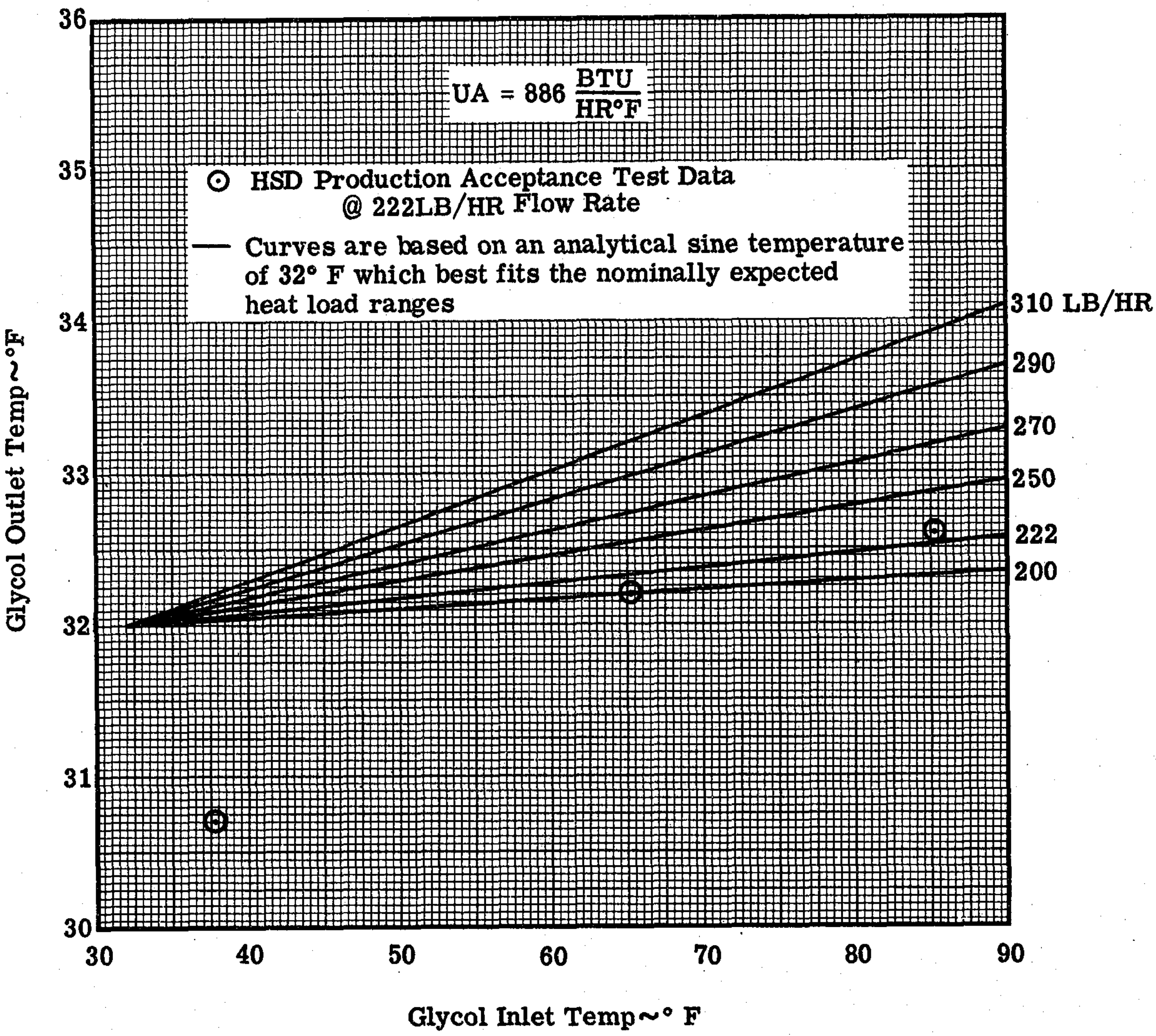

Figure LM10/4.3.8-1. Primary HTS Sublimator (209) LM-10 Acceptance Test Performance (U/N 141)

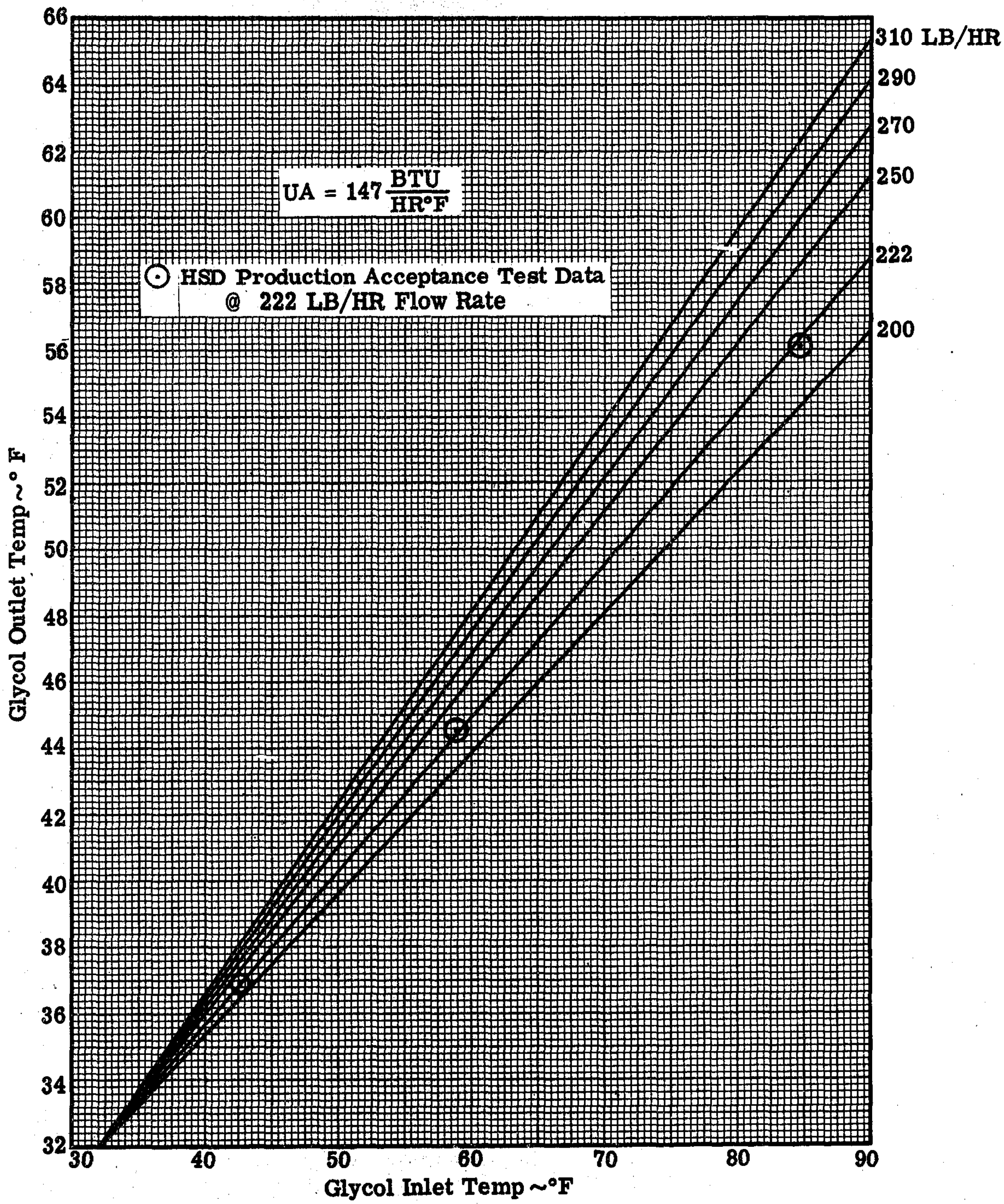

Figure LM10/4.3.8-2. Secondary HTS Sublimator (224) LM-10
Acceptance Test Performance (U/N 142)

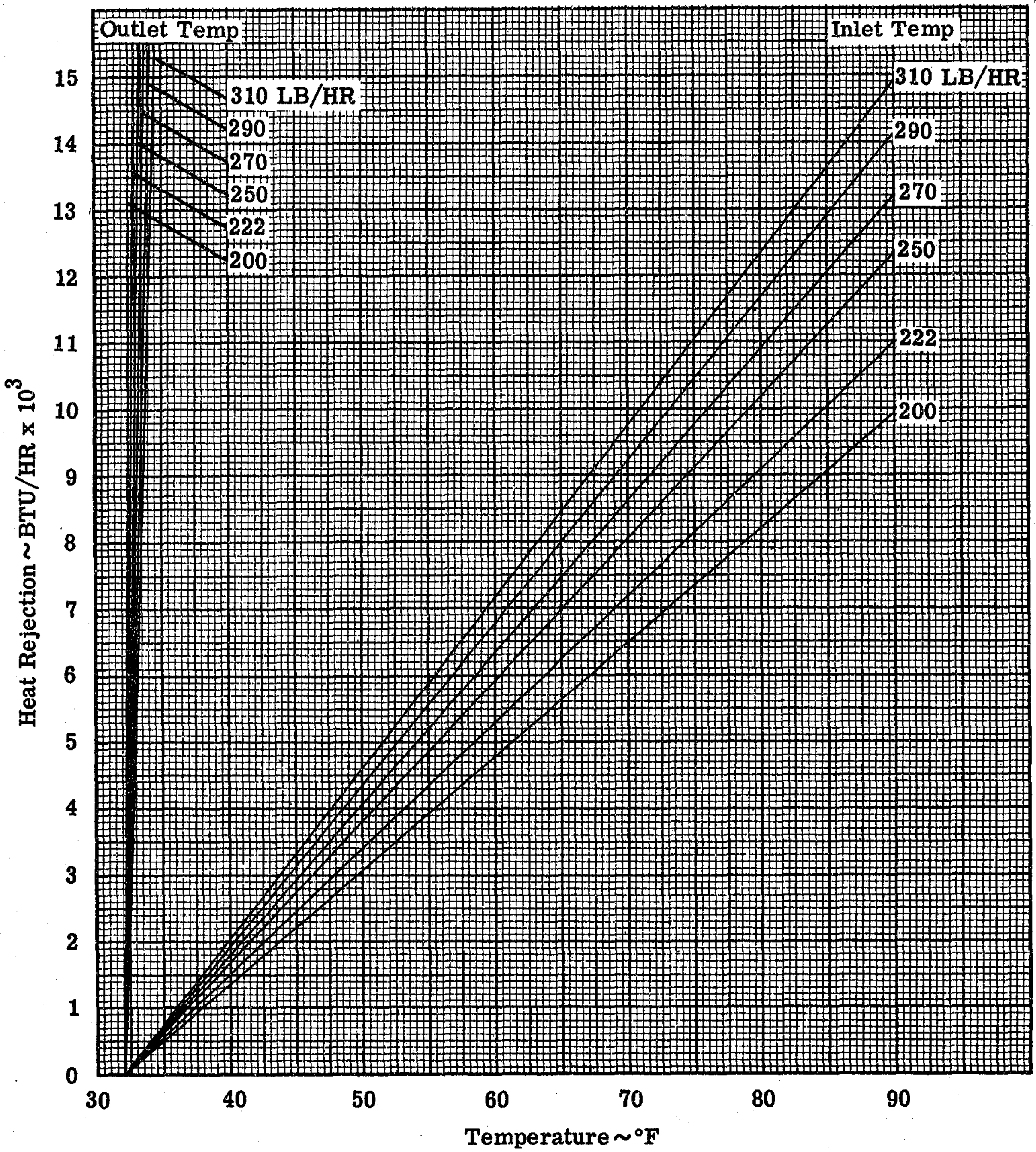

Figure LM10/4.3.8-3. LM-10 Primary HTS Sublimator (209) Heat Rejection Capability For UA = 886 $\frac{BTU}{HR°F}$ (U/N141)

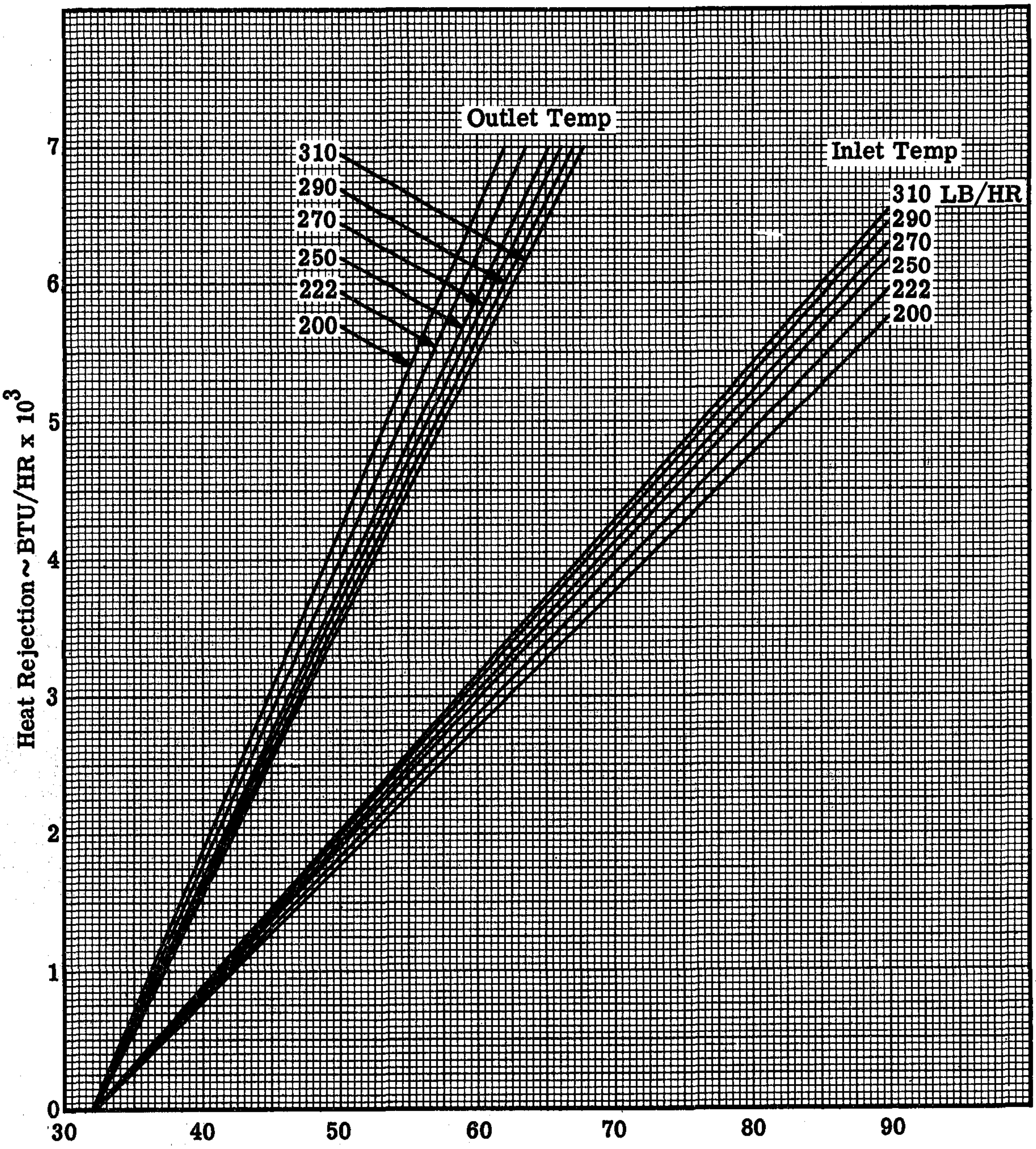

Figure LM10/4.3.8-4. LM-10 Secondary HTS Sublimator (224) Heat Rejection Capability For UA = 147 $\frac{BTU}{HR°F}$ (U/N 142)

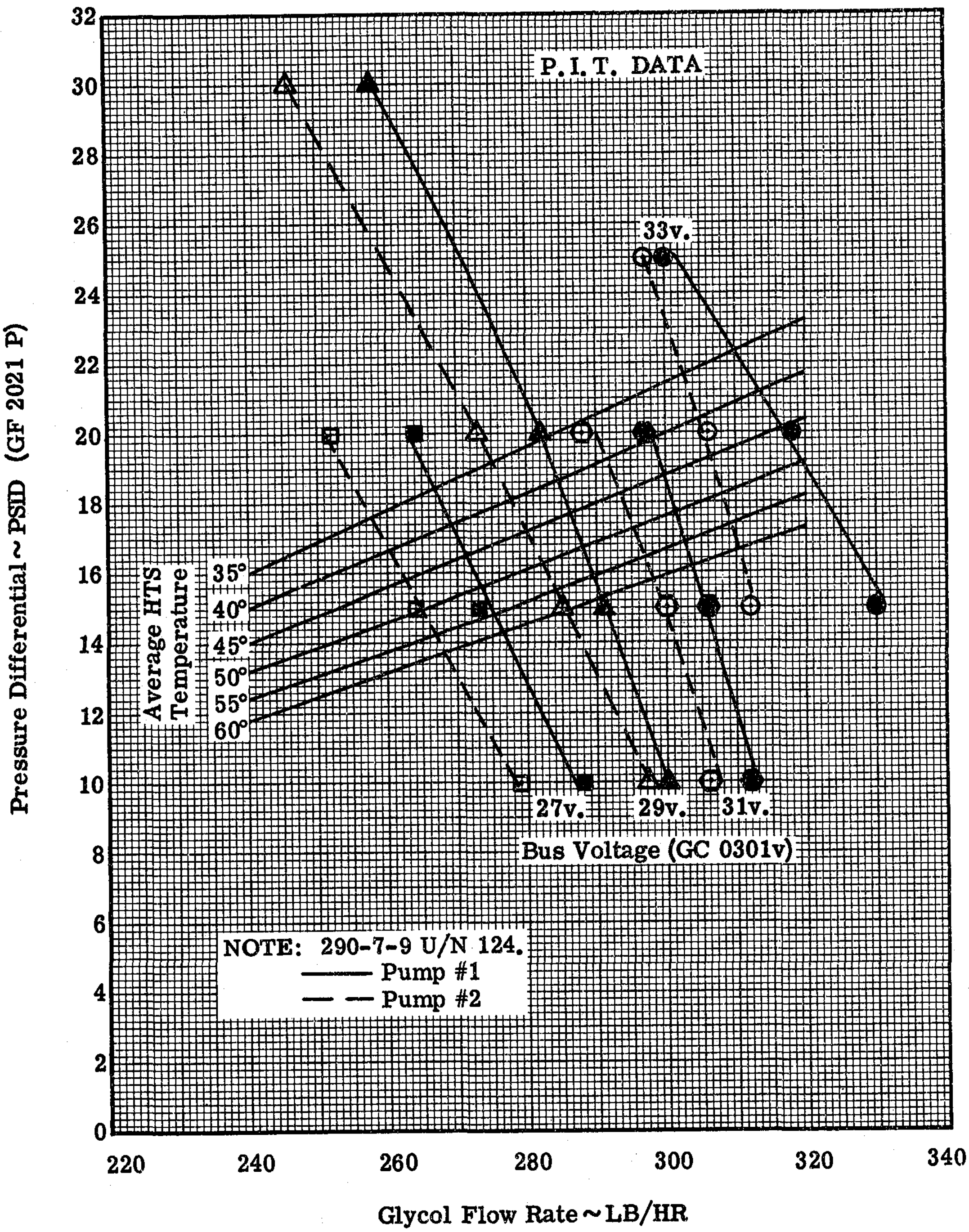

Figure LM10/4.3.8-5. LM-10 HTS System and Pump Characteristics

LM10/4.3.11 Duty Cycle of LM Heaters

The estimated average heater powers of the LM heaters for the LM10/J-1 mission are presented in Table LM10/4.3.11-1. The mission phases or definable spacecraft operations occur as shown in the headings of the table per Apollo 15 Flight Plan, AS 510/CSM 112/LM-10, 20 April 1971.

Antenna (S-band steerable, rendezvous radar, landing radar) heater requirements were determined from a review and application of the following:

(a) Vendor thermal studies (see LMO 510-1193).

(b) Acceptance and qualification test data (see LMO 510-1193).

(c) LM-3 thru LM-8 flight data

Guidance equipment (IMU, ASA) heater requirements were determined from a combination of the following:

(a) Calculations using vehicle structure temperature and coolant temperatures when applicable

(b) Review and application of LM-3 thru LM-8 flight data

Window and AOT heaters are nonthermostatically controlled, constant-power devices. Table LM10/4.3.11-1 lists the nominal heater powers of these items and indicates worst-case usage for the J-1 mission. The window heaters will be energized at the discretion of the astronaut when fogging is noted.

The waste management heater is a nonthermostatically controlled constant power (15 watt nominal) device. Table LM10/4.3.11-1 lists heater requirements and expected usage.

The RCS thruster heater requirements were determined from the following:

(a) Thermal studies

(b) Review and application of LM-3 thru LM-8 flight data

MESA heater requirements have been provided on the basis of test data and analysis, LMO 510-1817 and LMO 510-1722, respectively.

Lunar stay estimates of heater duty cycle for antenna heaters and RCS thruster heaters are based on a low sun elevation angle at landing (≈10° to 13°) and did not consider any shadowing or vehicle tilting due to irregular terrain.

Table LM10/4.3.11-1. Average Heater Power During Mission Phases

Heaters	Launch & Boost LM Power -00:30 to-02:50 Watts	Translunar Coast		Lunar Orbit & Descent		Lunar Stay LM Power 104:41 to-171:37 Watts	Ascent & Lunar LM Power 171:37 to 177:30 Watts
		LM Power 02:50 to-03:45 Watts	CSM Power 03:45 to-78:31 Watts	CSM Power 78:31 to-97:55 Watts	LM Power 97:55 to-104:41 Watts		
S-Band Steer Ant	0	4	4	2	2 (Note 1)	2	2 (Note 1)
Rend. Radar Ant.	0	8	8	6	8 (Note 1)	8/2 (Note 5)	8 (Note 1)
Land. Radar Ant	8	20	20	10	10 (Note 1)	---	---
ASA	7	7	7	7	17 (Note 3)	55	17 (Note 3)
IMU	15	15	15	15	14.5 (Note 3)	25	14.5 (Note 3)
Waste Management	0	0	0	0	0	1.8 (Note 6)	---
Fwd Window (CDR)	0	0	0	0	61.8 (Note 4)	61.8 (Note 4)	61.8 (Note 4)
Fwd Window (SE)	0	0	0	0	61.8 (Note 4)	61.8 (Note 4)	61.8 (Note 4)
Docking Window	0	0	0	0	24.0 (Note 4)	24.0 (Note 4)	24.0 (Note 4)
AOT	0	0	0	0	5.0	5.0	5.0
RCS Thruster	0	0	0	0	(Note 2)	30.0	20.0
MESA	0	0	11.7	17.5	17.5	35/22 (Note 7)	--

Total Average Power/Phase, Watts	65.7	57.5
Average Current at 28 vdc amps	2.35	2.06

Table LM10/4.3.11-1 Average Heater Power During Mission Phases (cont)

NOTES:

(1) Heater duty cycle estimates are for periods when antennas are de-activated. Duty cycles are estimated to be zero when the antennas are active.

(2) 764 watts for 1/2 hour warmup followed by a 140 watt average until undocking and a 20 watt average for the remainder of this phase.

(3) Total ASA power is 55 watts; 38 watts instrument power plus 17 watts heater power. Total IMU power is 74.5 watts; 59 watts instrument power plus 14.5 watts heater power.

(4) Window heaters are normally zero since they are energized only when fogging is noted.

(5) The average RR antenna heater power will vary with the heater mode selected. It is estimated to be 2 watts for 90% of the stay period (standby heater mode) and 8 watts for the remainder of the stay period (operate heater mode).

(6) The average Waste Management heater power was based on a total of 41 transfers with each transfer requiring 12 minutes of heater operation; 5 minutes before transfer, 2 minutes during transfer and 5 minutes after transfer. The 41 transfers were determined on the basis of 6 PLSS condensate transfers plus 35 urine transfers; urine transfers were assumed to occur at the rate of 6 per 24 hours per man over the 67 hour stay phase. Two additional lunar stay urine transfers were included to account for urine passed during the the descent phase.

(7) Two average MESA heater power levels were determined for the overall Lunar Stay period:
   1. 35 watts - heaters active up to EVA3
   2. 22 watts - heaters active up to EVA2

These Lunar Stay average power levels were established based on an average load of 30 watts from touchdown to MESA deployment, 83 watts for the first open blanket period, 67 watts for the subsequent open blanket period and 44 watts between open blanket periods.

LM10/4.4.1.1 Available Electrical Energy

The table below indicates the predicted capacities of the Apollo 15 (descent) flight batteries, and the battery installed in the service module. Also indicated in the table are the ATP cell capacities.

Battery	S/N	**ATP Capacities (Four Cells) (Amp-Hrs)				ATP Avg (Amp-Hrs)	*Predicted Capacity (Amp-Hrs)
Descent #1	105	444.1	456.2	455.5	421.4	444.3	438.1
#2	114	452.2	450.2	447.6	449.5	449.9	445.0
#3	104	453.0	452.3	447.8	452.8	451.5	431.5
#4	115	449.9	458.1	448.3	454.3	452.7	436.5
Lunar Batt	102	431.0	436.4	417.6	432.2	429.1	441.0
SM	103	446.5	453.8	442.7	418.7	440.4	432.2

*Predictions are based on Eagle-Picher computer program, assuming a discharge rate of 25 amps and an initial temperature of 80°F.
**ATP cells are discharged at 25 amps, uncooled at room temperatures.

LM10/4.5.1.1 Uncertainty of LM IMU Alignment from CSM IMU

The measured alignment angles associated with a talkover alignment of the LM IMU from the CSM IMU are listed in Table LM10/4.5.1-1. The contributions to the uncertainty in the talkover alignment of the LM IMU are listed in Table LM10/4.5.1-2. The RSS 1-σ total uncertainties are summarized as follows:

LM Axis	1-σ RSS, arc min
Yaw (about X-axis)	±15.8 (0.264 deg)
Pitch (about Y-axis)	±4.0 (0.067 deg)
Roll (about Z-axis)	±4.1 (0.068 deg)

The above values do not include thermal effects or bending or torque effects from any cause (i.e., RCS jet firing). Also, the effect of the maximum allowable c.g. offset in the X-axis of 0.2 inch was not included.

LM10/4.5.1.4 Guidance Computer Erasable Memory Constants (NASA DATA SOURCE)

The following listings pertain to the LM Guidance Computer (LGC) pad loaded erasable memory constants. Mission time computed constants, such as state vectors, etc., are not included.

Table LM10/4.5.1-3 contains a tabular listing of the erasable load, both mission tape parameters and launch tape parameters.

The number in the "REV" column denotes the number of revisions to the value of the corresponding parameter that have been incorporated in publications of the Apollo 14 erasable load.

A single or double star (* or **) in the "REV" column denotes that it is also in the inflight erasable load. These parameters would have to be verified or reloaded in order to completely initialize the LGC in orbit. A single star denotes loading by ground uplink; a double star denotes loading by the astronaut via the DSKY.

LM10/4.5.1.5.2 Assembly Alignment Data of Spacecraft Docking Mating Surfaces to the Navigation Base.

Angular Alignment of the Docking Ring Seal Surface Axes Relative to the Navigation Base Axes.

Axis	Ambient Pressure (Initial)	+5.2 psid	+2.6 psid	Ambient Pressure (Final)
Roll (Z)	- 3' 47"	- 2' 08"	- 2' 26"	- 2' 35"
Pitch (Y)	- 0' 06"	+ 0' 30"	- 0' 27"	- 0' 15"

Average Ambient Pressure Readings: Roll = -3' 11"
Pitch = -0' 10"

Sign Convention for Docking Ring Surface Plane Tilt

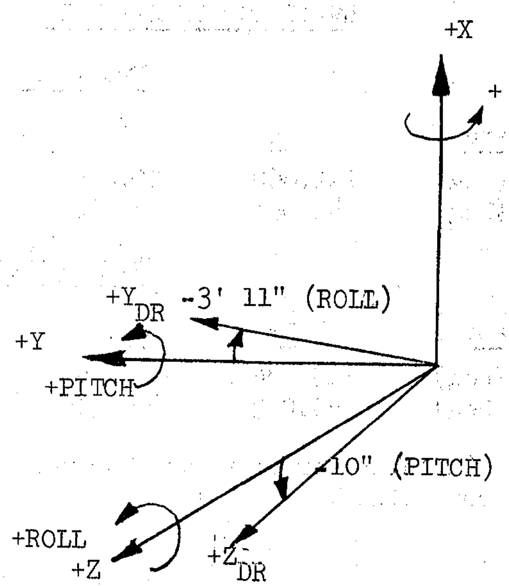

Note: Ambient Pressure = 14.7 psia

LM10/4.5.1.5.3 AOT Alignment Data

The azimuth and elevation angles for the rear right, rear left and the close (rear) detent positions of the AOT (relative to the AOT mounting surface) are tabulated below for LM-10 (AOT Designation 611R, Serial No. 17). These rear detent angles have been calculated using measured azimuth and elevation angles of the front detent positions. The uncertainty associated with these calculated angles is ±2 arc minutes.

The three front detent angles are measured, relative to the AOT mounting surface, at Kollsman Instrument Corporation and have a measurement uncertainty of ±30 arc seconds. For information, these measured angles are included in the tabulation. To verify these measured values, an AOT functional test has been performed on the spacecraft.

LM-10 AOT DETENT DATA

	Front (Measured)		
Data	L	F	R
Azim. (Deg)	299.860	359.883	59.884
Elev. (Deg)	45.061	45.062	45.077

	Rear (Calculated)		
Data	R_R	C_L	L_R
Azim. (Deg)	119.884	179.902	239.910
Elev. (Deg)	45.093	45.092	45.077

The above data is for an unpressurized vehicle at ambient conditions.

Table LM10/4.5.1-1

Measured Hardware Alignments Contributing to Alignment of LM IMU from CSM IMU

Measurement	Alignment Arc Min		
	About X-Axis	Y-Axis (About Z-Axis)	Z-Axis (About Y-Axis
COMMAND MODULE			
Displacement of CSM IMU axes with respect to local vertical*	-	+1.2	-0.6
Displacement of nav. base axes with respect to docking ring*	-2.8	-	-
Displacement of docking ring axes with respect to local vertical*	-	+2.5	+1.0
LUNAR MODULE			
	(LM Yaw)	(LM Roll)	(LM Pitch)
Displacement of docking ring with respect to nav. base axes**	-	-2.13	+0.50
Displacement of nav. base with respect to IMU***	+2.28	-1.33	-0.28

*TCP 112-S/C-070, 3/23/71, K-0048 and K-3128, 2/15/71. In lieu of S/C axes the local vertical was used as the common reference axis.

**Spacecraft Operational Data Book, Volume II, LM Data Book, Rev 2, Para. LM10/4.5.1.5.2

***Spacecraft Operational Data Book, Volume II, LM Data Book, Rev 2, Para. LM10/4.5.2.1.2. Data stated as IMU relative to nav. base, therefore, values tabulated above are negative of SODB values because the desired sense of displacement is from nav. base to IMU.

Table LM10/4.5.1-2

Hardware Contributions to Uncertainty of LM IMU Alignment from CSM IMU

Source of Uncertainty	1-σ Uncertainty, Arc Min About LM X-Axis	 About LM Y-Axis	 About LM Z-Axis
CM IMU to CM Docking Ring	0.2 (1)	0.2 (1)	0.4 (1)
CM Docking Angle Scale	0.2 (1)	-	-
CM-LM Docking Ring Alignment	-	4.0 (2)	4.0 (2)
LM Docking Angle Pointer	5.0 (3)	-	-
Docking Angle Determination	15.0 (4)	-	-
LM Docking Ring to LM Nav Base	-	Negl. (5)	Negl. (5)
LM Nav Base to LM IMU	Negl. (5)	Negl. (5)	Negl. (5)
RSS 1-σ Uncertainty, Arc Min	15.8	4.0	4.1
Arc Deg	0.264	0.067	0.068

REFERENCES

(1) Estimates based on methods used in TCP 112-S/C-070, 3/23/71, K-0048 and K-3128, 2/15/71, to measure these alignments. See Table LM10/4.5.1-1.

(2) Apollo ICD MH 01-05053-416 (The included angle measured between the planes of the docking interfaces of the CM and LM will not exceed 0.2 deg.).

(3) Apollo ICD MH 01-05128-116 (60 deg. ±5 arc min.).

(4) Telecon R. Schweickart, NASA astronaut (±0.5 deg., considered to be 2-σ).

(5) Uncertainty in measured alignment considered negligible. See Table LM10/4.5.1.1.

(NASA DATA SOURCE)

Table LM10/5.4.1-3. FINAL E-LOAD LUM 210 APOLLO-15

REV	MNEMONIC	ADDR	OCTAL	SF	ENGINEERING VALUE		VALUE IN AGC UNITS	
	FLAGWRD3+ 0	0077	12000	0				
	FLAGWRD8+ 0	0104	06000	0				
	FLGWRD10+ 0	0106	00000	0				
**	CHANBKUP+ 0	0374	00011	0				
1	MASS + 0	1243	10101	16	3.6697600000D 04	LBS	1.664575136D 04	KG
	MASS + 1	1244	00000	2	0.0	LBS	0.0	KG
*	LRWH1 + 0	1315	13146	0	3.5000000000D-01	UNITLESS	3.5000000000D-01	UNITLESS
1**	LEMMASS + 0	1326	10101	16	3.6697600000D 04	LBS	1.664575136D 04	KG
1**	CSMMASS + 0	1327	10314	16	3.7921900000D 04	LBS	1.720108450D 04	KG
*	E3J22R2M+ 0	1347	12160	58	9.204790479D 16	M5/CS2	9.204790479D 16	M5/CS2
*	E32C31RM+ 0	1350	03363	80	1.312892560D 23	M6/CS2	1.312892560D 23	M6/CS2
1 *	ELBIAS + 0	1353	00020	-1	1.8000000000D-01	DEG	5.0000000000D-04	REV
*	TOOFEW + 0	1354	00003	14	3.0000000000D 00	UNITLESS	3.000000000D 00	UNITLESS

(NASA DATA SOURCE)

Table LM10/4.5.1-3. ~~FINAL E-LOAD LUM 21C APOLLO-15~~ (Continued)

REV	MNEMONIC		ADDR	OCTAL	SF	ENGINEERING VALUE	VALUE IN AGC UNITS
1	* PBIASX	+ 0	1452	04264	-3	1.700000000D 00 CM/SEC2	1.700000000D-02 PIPS/CS
1	* PIPASCFX	+ 0	1453	57742	-9	-9.800000000D 02 PPM	-9.800000000D-04 PIPS/PIP
1	* PBIASY	+ 0	1454	03470	-3	1.410000000D 00 CM/SEC2	1.410000000D-02 PIPS/CS
1	* PIPASCFY	+ 0	1455	57616	-9	-9.900000000D 02 PPM	-9.900000000D-04 PIPS/PIP
	* PBIASZ	+ 0	1456	03505	-3	1.420000000D 00 CM/SEC2	1.420000000D-02 PIPS/CS
1	* PIPASCFZ	+ 0	1457	50443	-9	-1.430000000D 03 PPM	-1.430000000D-03 PIPS/PIP
1	* NBDX	+ 0	1460	00630	-5	3.200000000D 00 MERU	7.788494810D-04 G PUL/CS
1	* NBDY	+ 0	1461	77646	-5	-7.000000000D-01 MERU	-1.703733240D-04 G PUL/CS
1	* NBDZ	+ 0	1462	00263	-5	1.400000000D 00 MERU	3.407466479D-04 G PUL/CS
1	* ADIAX	+ 0	1463	00202	-6	5.000000000D 00 MERU/G	1.240946004D-04 GPUL/PIP
	* ADIAY	+ 0	1464	77713	-6	-2.000000000D 00 MERU/G	-4.963784016D-05 GPUL/PIP
1	* ADIAZ	+ 0	1465	00266	-6	7.000000000D 00 MERU/G	1.737324406D-04 GPUL/PIP
	* ADSRAX	+ 0	1466	77543	-6	-6.000000000D 00 MERU/G	-1.489135205D-04 GPUL/PIP

(NASA DATA SOURCE)

Table LM10/4.5.1-3. FINAL E-LOAD LUM 210 APOLLO-15 (Continued)

REV	MNEMONIC	ADDR	OCTAL	SF	ENGINEERING VALUE	VALUE IN AGC UNITS
1	* ADSRAY + 0	1467	00150	-6	4.000000000D 00 MERU/G	9.927568032D-05 GPUL/PIP
1	* ADSRAZ + 0	1470	77627	-6	-4.000000000D 00 MERU/G	-9.927568032D-05 GPUL/PIP
	* GCCMPSW + 0	1477	00000	14	0.0 UNITLESS	0.0 UNITLESS
	TETCSM + 0	1570 1571	37777 37777	28	2.684354550D 08 CS	2.684354550D 08 CS
	TETLEM + 0	1642 1643	37777 37777	28	2.684354550D 08 CS	2.684354550D 08 CS
	* X789 + 0	1700 1701	00000 00000	3	0.0 RADIANS	0.0 RADIANS
	* X789 + 2	1702 1703	00000 00000	3	0.0 RADIANS	0.0 RADIANS
	* X789 + 4	1704 1705	00000 00000	3	0.0 RADIANS	0.0 RADIANS

(NASA DATA SOURCE)

Table LM10/4.5.1-3. ~~FINAL E-LOAD LUM 210 APOLLO 15~~ (Continued)

REV	MNEMONIC	ADDR	OCTAL	SF	ENGINEERING VALUE	VALUE IN AGC UNITS
*	TEPHEM + 0	1706	00000	42	6.135666667D 02 HR	2.208840000D 08 CS
		1707	32251			
		1710	26040			
*	-AYO + 0	1711	77777	0	-1.696124673D-05 RADIANS	-1.696124673D-05 RADIANS
		1712	67066			
*	AXO + 0	1713	00000	0	3.089010716D-05 RADIANS	3.089010716D-05 RADIANS
		1714	20144			
*	REFSMMAT+ 0	1731	11244	1	5.825612400D-01 UNITLESS	5.825612400D-01 UNITLESS
		1732	12736			
*	REFSMMAT+ 2	1733	07474	1	4.761850900D-01 UNITLESS	4.761850900D-01 UNITLESS
		1734	35041			
*	REFSMMAT+ 4	1735	12423	1	6.586882200D-01 UNITLESS	6.586882200D-01 UNITLESS
		1736	37124			

(NASA DATA SOURCE)

Table LM10/4.5.1-3. ~~FINAL E-LOAD LUM 210 APOLLO-15~~ (Continued)

REV	MNEMONIC	ADDR	OCTAL	SF	ENGINEERING VALUE	VALUE IN AGC UNITS
*	REFSMMAT+ 6	1737 1740	73772 64052	1	-2.506558100D-01 UNITLESS	-2.506558100D-01 UNITLESS
~~*~~	~~REFSMMAT+ 8~~	~~1741~~ 1742	~~65262~~ 77044	~~1~~	~~-6.656529500D-01 UNITLESS~~	~~-6.656529500D-01 UNITLESS~~
*	REFSMMAT+10	1743 1744	13176 06616	1	7.029067100D-01 UNITLESS	7.029067100D-01 UNITLESS
~~*~~	~~REFSMMAT+12~~	~~1745~~ 1746	~~14275~~ 32203	~~1~~	~~7.731714500D-01 UNITLESS~~	~~7.731714500D-01 UNITLESS~~
*	REFSMMAT+14	1747 1750	66634 76474	1	-5.745902300D-01 UNITLESS	-5.745902300D-01 UNITLESS
~~*~~	~~REFSMMAT+16~~	~~1751~~ 1752	~~73551~~ 41767	~~1~~	~~-2.684250500D-01 UNITLESS~~	~~-2.684250500D-01 UNITLESS~~
*	RANGEVAR+ 0	1766 1767	01351 24734	-12	1.111111111D-05 UNITLESS	1.111111111D-05 UNITLESS

(NASA DATA SOURCE)

Table LM10/4.5.1-3. ~~FINAL E-LOAD LUM 210 APOLLO-15~~ (Continued)

REV	MNEMONIC	ADDR OCTAL	SF	ENGINEERING VALUE	VALUE IN AGC UNITS
*	PATEVAR + 0	1770 02354 ~~1771 04761~~	-12	1.877777778D-05 UNITLESS	1.877777778D-05 UNITLESS
~~*~~	~~RVARMIN + 0~~	~~1772 00410~~	~~12~~	~~7.104180875D 02 FT2~~	~~6.600000000D 01 M2~~
~~*~~	~~VVARMIN + 0~~	~~1773 00165~~	~~-12~~	~~1.877764172D-01 FT2/SEC2~~	~~1.744500000D-06 M2/CS2~~
~~*~~	~~WRENDPOS+ 0~~	~~2000 05750~~	~~14~~	~~1.000000000D 04 FT~~	~~3.048000000D 03 M~~
~~*~~	~~WRENDVEL+ 0~~	~~2001 00763~~	~~0~~	~~1.000000000D 01 FT/SEC~~	~~3.048000000D-02 M/CS~~
~~*~~	~~WSHAFT + 0~~	~~2002 17270~~	~~-5~~	~~1.500000000D 01 MILLIRAD~~	~~1.500000000D-02 RADIANS~~
~~*~~	~~WTRUN + 0~~	~~2003 17270~~	~~-5~~	~~1.500000000D 01 MILLIRAD~~	~~1.500000000D-02 RADIANS~~
~~*~~	~~RMAX + 0~~	~~2004 00023~~	~~19~~	~~2.000000000D 03 FT~~	~~6.096000000D 02 M~~
~~*~~	~~VMAX + 0~~	~~2005 00001~~	~~7~~	~~2.000000000D 00 FT/SEC~~	~~6.096000000D-03 M/CS~~
~~*~~	~~WSURFPOS+ 0~~	~~2006 00000~~	~~14~~	~~0.0 FT~~	~~0.0 M~~
~~*~~	~~WSURFVEL+ 0~~	~~2007 00000~~	~~0~~	~~0.0 FT/SEC~~	~~0.0 M/CS~~
~~*~~	~~SHAFTVAR+ 0~~	~~2010 00103~~	~~-12~~	~~1.000000000D 00 MILLIRAD2~~	~~1.000000000D-06 RADIANS2~~

(NASA DATA SOURCE)

Table LM10/4.5.1-3. ~~FINAL E-LOAD LUM 210 APOLLO-15~~ (Continued)

REV	MNEMONIC	ADDR	OCTAL	SF	ENGINEERING VALUE	VALUE IN AGC UNITS
*	TRUNVAR + 0	2011	00103	-12	1.000000000D 00 MILIRAD2	1.000000000D-06 RADIANS2
*	504LM + 0	2012 2013	77774 51037	0	-2.268552780D-04 RADIANS	-2.268552780D-04 RADIANS
*	504LM + 2	2014 2015	00011 35623	0	6.061308086D-04 RADIANS	6.061308086D-04 RADIANS
*	504LM + 4	2016 2017	77775 53053	0	-1.619607210D-04 RADIANS	-1.619607210D-04 RADIANS
*	RLS + 0	2020 2021	00275 31473	27	5.101198379D 06 FT	1.554845266D 06 M
*	RLS + 2	2022 2023	00014 03666	27	3.257573530D 05 FT	9.929084118D 04 M
*	RLS + 4	2024 2025	00135 02034	27	2.501253767D 06 FT	7.623821483D 05 M

Contract No. NAS 9-1100
Primary No. 664

(NASA DATA SOURCE)

Table LM10/4.5.1-3. ~~FINAL E-LOAD LUM 210 APOLLO-15~~ (Continued)

REV	MNEMONIC	ADDR	OCTAL	SF	ENGINEERING VALUE	VALUE IN AGC UNITS
*	TLAND + 0	2026	04374	28	1.046824861D 02 HR	3.768569500D 07 CS
		2027	04677			
~~*~~	~~N26/PRI + 0~~	~~2371~~	~~00000~~	~~14~~	~~0.0 MIN~~	~~0.0 CS~~
~~*~~	~~N26/2CAD + 0~~	~~2372~~	~~00000~~	~~0~~		~~0.0~~
		2373	00000			
*	VELBIAS + 0	2400	00001	6	2.5000000000D 00 FT/SEC	7.620000000D-03 M/CS
		2401	36331			
~~*~~	~~RBRFGX + 0~~	~~2402~~	~~77777~~	~~24~~	~~-3.118358793D 03 FT~~	~~-9.504757600D 02 M~~
		2403	42227			
*	RAPFGX + 0	2404	00000	24	1.585000000D 02 FT	4.831080000D 01 M
		2405	01405			
~~*~~	~~RBRFGZ + 0~~	~~2406~~	~~77774~~	~~24~~	~~-1.174144094D 04 FT~~	~~-3.578791200D 03 M~~
		2407	60122			

(NASA DATA SOURCE)

Table LM10/4.5.1-3. FINAL E-LOAD LUM 210 APOLLO-15 (Continued)

REV	MNEMONIC		ADDR	OCTAL	SF	ENGINEERING VALUE	VALUE IN AGC UNITS
*	RAPFGZ	+ 0	2410 2411	77777 77572	24	-2.735539993D 01 FT	-8.337925900D 00 M
*	VBRFGX	+ 0	2412 2413	77766 55311	10	-1.964691600D 02 FT/SEC	-5.988379997D-01 M/CS
*	VAPFGX	+ 0	2414 2415	77777 72367	10	-3.534759843D 00 FT/SEC	-1.077394800D-02 M/CS
*	VBRFGZ	+ 0	2416 2417	77767 73603	10	-1.667599672D 02 FT/SEC	-5.082843800D-01 M/CS
*	VAPFGZ	+ 0	2420 2421	00000 00024	10	2.495050000D-02 FT/SEC	7.604912400D-05 M/CS
*	ABRFGX	+ 0	2422 2423	77772 50265	-4	-7.182481299D-01 FT/SEC2	-2.189220300D-05 M/CS2
*	AAPFGX	+ 0	2424 2425	00000 23567	-4	7.717830052D-02 FT/SEC2	2.352394600D-06 M/CS2

Contract No. NAS 9-1100
Primary No. 664

(NASA DATA SOURCE)

Table LM10/4.5.1-3. FINAL E-LOAD LUM 210 APOLLO-15 (Continued)

REV	MNEMONIC	ADDR OCTAL	SF	ENGINEERING VALUE	VALUE IN AGC UNITS
*	ABRFGZ + 0	2426 77675 2427 65140	-4	-8.3C2450459D C0 FT/SEC2	-2.5305869CCD-04 M/CS2
*	AAPFGZ + 0	243C 77773 2431 51173	-4	-5.89627C013D-C1 FT/SEC2	-1.7971831CCD-05 M/CS2
*	VBRFG* + 0	2432 77755 2433 66351	13	-3.0016799870 03 FT/SEC	-9.1491206000 00 M/CS
*	VAPFG* + 0	2434 CCC3C 2435 0CC55	13	4.491C89855D-C1 FT/SEC	1.3688842CCD-03 M/CS
*	ABRFG* + 0	2436 77161 2437 771C6	-4	-4.981470144D C1 FT/SEC2	-1.518352100D-C3 M/CS2
*	AAPFG* + 0	244C 77743 2441 67344	-4	-3.537762139D C0 FT/SEC2	-1.C783099CCD-C4 M/CS2
*	JBRFG* + 0	2442 77541 2443 63456	-21	-1.512365879D-C2 FT/SEC3	-4.609691200D-C9 M/CS3

(NASA DATA SOURCE)

Table LM10/4.5.1-3. FINAL E-LOAD LUM 210 APOLLO-15 (Continued)

REV	MNEMONIC	ADDR	OCTAL	SF	ENGINEERING VALUE	VALUE IN AGC UNITS
	* JAPFG* + 0	2444 2445	00704 04643	-21	4.317359908D-02 FT/SEC3	1.315931300D-08 M/CS3
	* GAINBRAK+ 0	2446 2447	37777 37777	0	9.999999963D-01 UNITLESS	9.999999963D-01 UNITLESS
	* GAINAPPR+ 0	2450 2451	00000 00000	0	0.0 UNITLESS	0.0 UNITLESS
	* TCGFBRAK+ 0	2452	00567	17	3.000000000D 01 SEC	3.000000000D 03 CS
	* TCGIBRAK+ 0	2453	25762	17	9.000000000D 02 SEC	9.000000000D 04 CS
	* TCGFAPPR+ 0	2454	00113	17	6.000000000D 00 SEC	6.000000000D 02 CS
	* TCGIAPPR+ 0	2455	04704	17	2.000000000D 02 SEC	2.000000000D 04 CS
1	* VIGN + 0	2456 2457	00416 22227	10	5.548141010D 03 FT/SEC	1.691073380D 01 M/CS
1	* RIGNX + 0	2460 2461	77717 63636	24	-1.625396686D 05 FT	-4.954209100D 04 M

(NASA DATA SOURCE)

Table LM10/4.5.1-3. ~~FINAL E-LOAD LUM 21C APOLLO-15~~ (Continued)

REV	MNEMONIC	ADDR	OCTAL	SF	ENGINEERING VALUE	VALUE IN AGC UNITS
1	* RIGNZ + 0	2462	77063	24	-1.547120997D 06 FT	-4.715624800D 05 M
		~~2463~~	~~57527~~			
	~~* KIGNX/B4+ 0~~	~~2464~~	~~77251~~	~~4~~	~~-3.340000000D-01 UNITLESS~~	~~-3.340000000D-01 UNITLESS~~
		2465	77371			
	* KIGNY/B8+ 0	2466	76366	-16	-2.206999985D-07 FT/FT2	-7.240813600D-07 M-1
		~~2467~~	~~60601~~			
	~~* KIGNV/B4+ 0~~	~~2470~~	~~71727~~	~~18~~	~~-4.980000000D 02 SEC~~	~~-4.980000000D 04 CS~~
		2471	57777			
	* LOWCRIT + 0	2472	04114	14	5.985007886D 03 LBF	2.124377200D 03 DPSTROTP
	* HIGHCRIT+ 0	2473	04454	14	6.615008567D 03 LBF	2.347995800D 03 DPSTROTP
	* TAUHZ + 0	2474	07640	11	5.000000000D 00 SEC	5.000000000D 02 CS
	* QHZ + 0	2475	14632	0	4.000000000D-01 UNITLESS	4.000000000D-01 UNITLESS
	* AHZLIM + 0	2476	00017	-4	1.938979987D 00 FT/SEC2	5.910011000D-05 M/CS2

Contract No. NAS 9-1100
Primary No. 664

(NASA DATA SOURCE)

Table LM10/4.5.1-3. ~~FINAL E-LOAD LUM 210 APOLLO-15~~ (Continued)

REV	MNEMONIC	ADDR OCTAL	SF	ENGINEERING VALUE	VALUE IN AGC UNITS
*	2LATE466+ 0	2477 00000 ~~2500 00226~~	28	1.5000000000D 00 SEC	1.5000000000D 02 CS
~~*~~	~~DELQFIX + 0~~	~~2503 00000~~ 2504 00750	~~24~~	~~1.0000000000D 02 FT~~	~~3.0480000000D 01 M~~
*	LRVMAX + 0	2511 01717	7	2.4999999567D 03 FT/SEC	7.6199999000D 00 M/CS
*	LRVF + 0	2512 00116	7	1.9999999567D 02 FT/SEC	6.0959999000D-01 M/CS
*	LRWVZ + 0	2513 11463	0	3.0000000000D-01 UNITLESS	3.0000000000D-01 UNITLESS
*	LRWVY + 0	2514 11463	0	3.0000000000D-01 UNITLESS	3.0000000000D-01 UNITLESS
*	LRWVX + 0	2515 11463	0	3.0000000000D-01 UNITLESS	3.0000000000D-01 UNITLESS
*	LRWVFZ + 0	2516 06315	0	2.0000000000D-01 UNITLESS	2.0000000000D-01 UNITLESS
*	LRWVFY + 0	2517 06315	0	2.0000000000D-01 UNITLESS	2.0000000000D-01 UNITLESS
*	LRWVFX + 0	2520 06315	0	2.0000000000D-01 UNITLESS	2.0000000000D-01 UNITLESS
*	LRWVFF + 0	2521 03146	0	1.0000000000D-01 UNITLESS	1.0000000000D-01 UNITLESS

Contract No. NAS 9-1100
Primary No. 664

(NASA DATA SOURCE)

Table LM10/4.5.1-3. FINAL E-LOAD LUM 210 APOLLO-15 (Continued)

REV	MNEMONIC		ADDR	OCTAL	SF	ENGINEERING VALUE		VALUE IN AGC UNITS	
1 *	ABSC0	+ 0	2522	51736	18	-5.9300000000D 05	FT	-1.807464000D 05	M
1 *	ABSC1	+ 0	2523	72551	18	-1.9600000000D 05	FT	-5.974080000D 04	M
1 *	ABSC2	+ 0	2524	74034	18	-1.0600000000D 05	FT	-3.230880000D 04	M
1 *	ABSC3	+ 0	2525	74530	18	-8.9400000000D 04	FT	-2.724912000D 04	M
1 *	ABSC4	+ 0	2526	76723	18	-2.9200000000D 04	FT	-8.900160000D 03	M
1 *	SLOPE0	+ 0	2527	00005	6	2.0968000000D-02	RADIANS	2.096800000D-02	RADIANS
*	SLOPE1	+ 0	2530	00000	6	0.0	RADIANS	0.0	RADIANS
1 *	SLOPE2	+ 0	2531	00060	6	1.8674700000D-01	RADIANS	1.867470000D-01	RADIANS
1 *	SLOPE3	+ 0	2532	77710	6	-2.1478400000D-01	RADIANS	-2.147840000D-01	RADIANS
1 *	SLOPE4	+ 0	2533	00003	6	1.1301400000D-02	RADIANS	1.130140000D-02	RADIANS
*	RODSCALE	+ 0	2534	14370	-7	1.0000000000D 00	FT/SEC	3.048000000D-03	M/CS
*	TAUROD	+ 0	2535	11300	9	1.5000000000D 00	SEC	1.500000000D 02	CS
			2536	00000					

(NASA DATA SOURCE)

Table LM10/4.5.1-3. ~~FINAL E-LOAD LUM 21C APOLLO-15~~ (Continued)

REV	MNEMONIC	ADDR	OCTAL	SF	ENGINEERING VALUE	VALUE IN AGC UNITS
*	LAG/TAU + 0	2537 2540	07356 34075	0	2.333300000D-01 UNITLESS	2.333300000D-01 UNITLESS
*	MINFORCE+ 0	2541 2542	00001 27631	12	9.7599998140 02 LBF	4.359257100D-01 KG M/CS2
*	MAXFORCE+ 0	2543 2544	00013 06551	12	6.2559999610 03 LBF	2.802379600D 00 KG M/CS2
*	J1PARM + 0	2545 2546	07014 11451	23	6.0410278000 06 FT	1.8413052730 06 M
*	K1PARM + 0	2547 2550	75563 52023	23	-3.113752500D C5 FT/RAD	-5.963193749D 05 M/REV
*	J2PARM + 0	2551 2552	07015 01363	23	6.0422821000 06 FT	1.8416875840 06 M
*	K2PARM + 0	2553 2554	73350 64255	23	-6.2221362000 05 FT/RAD	-1.1916105630 06 M/REV

(NASA DATA SOURCE)

Table LM10/4.5.1-3. ~~FINAL E-LOAD LUM 21C APOLLO-15~~ (Continued)

REV	MNEMONIC	ADDR	OCTAL	SF	ENGINEERING VALUE		VALUE IN AGC UNITS	
*	THETCRIT+ 0	2555 2556	76343 42146	0	-1.751069600D 01	DEG	-4.864082223D-02	REV
~~*~~	~~RAMIN + 0~~	~~2557~~ 2560	~~03324~~ 04500	~~24~~	~~5.873031490D 06~~	~~FT~~	~~1.790099998D 06~~	~~M~~
*	YLIM + 0	2561 2562	00016 32446	24	8.200000000D 00	N.MI.	1.518640000D 04	M
~~*~~	~~ABTRDOT + 0~~	~~2563~~ 2564	~~00007~~ 23346	~~7~~	~~1.950000000D 01~~	~~FT/SEC~~	~~5.943600000D-02~~	~~M/CS~~
*	COSTHET1+ 0	2565 2566	00000 00000	2	0.0	UNITLESS	0.0	UNITLESS
~~*~~	~~COSTHET2+ 0~~	~~2567~~ 2570	~~06733~~ 07535	~~2~~	~~8.660254037D-01~~	~~UNITLESS~~	~~8.660254037D-01~~	~~UNITLESS~~
*	DLAND + 0	2631 2632	00000 00000	24	0.0	FT	0.0	M

(NASA DATA SOURCE)

Table LM10/4.5.1-3. ~~FINAL E-LOAD LUM 210 APOLLO-15~~ (Continued)

REV	MNEMONIC	ADDR OCTAL	SF	ENGINEERING VALUE	VALUE IN AGC UNITS
*	CLAND + 2	2633 00000 2634 00000	24	0.0 FT	0.0 M
~~*~~	~~CLAND + 4~~	~~2635 00000~~ 2636 00000	~~24~~	~~0.0 FT~~	~~0.0 M~~
*	HIASCENT+ 0	3000 02324	16	1.090000000D 04 LBS	4.944156833D 03 KG
1**	ROLLTIME+ 0	3001 06246	14	3.238000000D 01 SEC	3.238000000D 03 CS
1**	PITTIME + 0	3002 06112	14	3.146000000D 01 SEC	3.146000000D 03 CS
1 *	DKTRAP + 0	3003 77000	-3	-3.898620605D-03 REV/SEC	-3.898620605D-03 REV/SEC
*	DKOMEGAN+ 0	3004 00012	14	1.000000000D 01 UNITLESS	1.000000000D 01 UNITLESS
*	DKKACSN + 0	3005 00074	14	6.000000000D 01 UNITLESS	6.000000000D 01 UNITLESS
1 *	LMTRAP + 0	3006 77000	-3	-3.898620605D-03 REV/SEC	-3.898620605D-03 REV/SEC
*	LMOMEGAN+ 0	3007 00000	14	0.0 UNITLESS	0.0 UNITLESS
*	LMKACSN + 0	3010 00074	14	6.000000000D 01 UNITLESS	6.000000000D 01 UNITLESS

(NASA DATA SOURCE)

Table LM10/4.5.1-3. FINAL E-LOAD LUM 210 APOLLO-15 (Continued)

REV	MNEMONIC	ADDR OCTAL	SF	ENGINEERING VALUE	VALUE IN AGC UNITS
	* DKCB + 0	3011 00200	15	2.5600000000D 02 REV-1	2.5600000000D 02 REV-1
2	* IGNAOSQ + 0	3012 02075	-2	5.9610000000D 00 DEG/SEC2	1.6558333333D-02 REV/SEC2
2	* IGNAOSR + 0	3013 00036	-2	1.6300000000D-01 DEG/SEC2	4.5277777778D-04 REV/SEC2
	* DOWNTORK+ 0	3113 00000	5	0.0 JET SEC	0.0 JET SEC
	* DOWNTORK+ 1	3114 00000	5	0.0 JET SEC	0.0 JET SEC
	* DOWNTORK+ 2	3115 00000	5	0.0 JET SEC	0.0 JET SEC
	* DOWNTORK+ 3	3116 00000	5	0.0 JET SEC	0.0 JET SEC
	* DOWNTORK+ 4	3117 00000	5	0.0 JET SEC	0.0 JET SEC
	* DOWNTORK+ 5	3120 00000	5	0.0 JET SEC	0.0 JET SEC
	* AGSK + 0	3371 04225 3372 10400	28	1.0000000000D 02 HR	3.6000000000D 07 CS
~~1~~	~~* AZBIAS + 0~~	~~3373 77725~~	~~-1~~	~~-4.6000000000D-01 DEG~~	~~-1.2777777778D-03 REV~~
	~~* ATIGINC + 0~~	~~3400 00001~~ 3401 03120	~~28~~	~~3.0000000000D 00 MIN~~	~~1.8000000000D 04 CS~~

(NASA DATA SOURCE)

Table LM10/4.5.1-3. ~~FINAL E-LOAD LUM 210 APOLLO-15~~ (Continued)

REV	MNEMONIC		ADDR	OCTAL	SF	ENGINEERING VALUE	VALUE IN AGC UNITS
*	PTIGINC	+ 0	3402 3403	00001 03120	28	3.0000000000D 00 MIN	1.8000000000D 04 CS
~~1 *~~	~~ACTAZ~~	~~+ 0~~	~~3404~~	~~65236~~	~~-1~~	~~-6.0140000000D 01 DEG~~	~~-1.6705555556D-01 REV~~
~~1 *~~	~~ACTAZ~~	~~+ 1~~	~~3405~~	~~77765~~	~~-1~~	~~-1.1700000000D-01 DEG~~	~~-3.2500000000D-04 REV~~
~~1 *~~	~~ACTAZ~~	~~+ 2~~	~~3406~~	~~12513~~	~~-1~~	~~5.9884000000D 01 DEG~~	~~1.6634444445D-01 REV~~
~~1 *~~	~~ACTAZ~~	~~+ 3~~	~~3407~~	~~25240~~	~~-1~~	~~1.1988400000D 02 DEG~~	~~3.3301111111D-01 REV~~
~~1 *~~	~~ACTAZ~~	~~+ 4~~	~~3410~~	~~37767~~	~~-1~~	~~1.7990200000D 02 DEG~~	~~4.9972777778D-01 REV~~
~~1 *~~	~~ACTAZ~~	~~+ 5~~	~~3411~~	~~52515~~	~~-1~~	~~-1.2009000000D 02 DEG~~	~~-3.3358333334D-01 REV~~
~~1 *~~	~~ACTEL~~	~~+ 0~~	~~3412~~	~~10000~~	~~-1~~	~~4.5061000000D 01 DEG~~	~~1.2516944445D-01 REV~~
~~1 *~~	~~ACTEL~~	~~+ 1~~	~~3413~~	~~10006~~	~~-1~~	~~4.5062000000D 01 DEG~~	~~1.2517222222D-01 REV~~
~~1 *~~	~~ACTEL~~	~~+ 2~~	~~3414~~	~~10007~~	~~-1~~	~~4.5077000000D 01 DEG~~	~~1.2521388889D-01 REV~~
~~1 *~~	~~ACTEL~~	~~+ 3~~	~~3415~~	~~10010~~	~~-1~~	~~4.5093000000D 01 DEG~~	~~1.2525833333D-01 REV~~
~~1 *~~	~~ACTEL~~	~~+ 4~~	~~3416~~	~~10010~~	~~-1~~	~~4.5092000000D 01 DEG~~	~~1.2525555556D-01 REV~~

(NASA DATA SOURCE)

Table LM10/4.5.1-3. ~~FINAL E-LOAD LUM 210 APOLLO-15~~ (Continued)

REV	MNEMONIC	ADDR	OCTAL	SF	ENGINEERING VALUE	VALUE IN AGC UNITS
1	* ACTEL + 5	3417	10007	-1	4.507700000D 01 DEG	1.252138889D-01 REV
	* LRHMAX + 0	3420	35610	14	5.000000000D 04 FT	1.524000000D 04 M
	* LRWH + 0	3421	13146	0	3.500000000D-01 UNITLESS	3.500000000D-01 UNITLESS
	* ZOOMTIME+ 0	3422	05050	14	2.600000000D 01 SEC	2.600000000D 03 CS
	* TENDBRAK+ 0	3423	01407	17	6.200000000D 01 SEC	6.200000000D 03 CS
	* TENDAPPR+ 0	3424	00226	17	1.200000000D 01 SEC	1.200000000D 03 CS
	* DELTTFAP+ 0	3425	75632	17	-9.000000000D 01 SEC	-9.000000000D 03 CS
	* LEADTIME+ 0	3426	77743	17	-2.200000000D 00 SEC	-2.200000000D 02 CS
	* RPCRTIME+ 0	3427	01407	17	6.200000000D 01 SEC	6.200000000D 03 CS
	* RPCRTQSW+ 0	3430	57777	1	-1.000000000D 00 UNITLESS	-1.000000000D 00 UNITLESS
	* TNEWA + 0	3431	20000	28	1.34217728D 08 CS	1.34217728D 08 CS
		~~3432~~	~~00000~~			

Contract No. NAS 9-1100
Primary No. 664

NASA — MSC — Coml., Houston, Texas

Grumman Aerospace Corporation

LM10/4.5.2.1 Abort Sensor Assembly

The LM-10 ASA set-point temperature, as read by T/M #GI-3301, is T_{SET} = 119.6°F (STANDBY and OPERATE modes). The nominal temperature reading in the OFF mode is also 119.6°F. The temperature maintenance limits are specified in paragraph 4.5.2.1.

LM10/4.5.2.1.2 AGS Angular Mounting Error

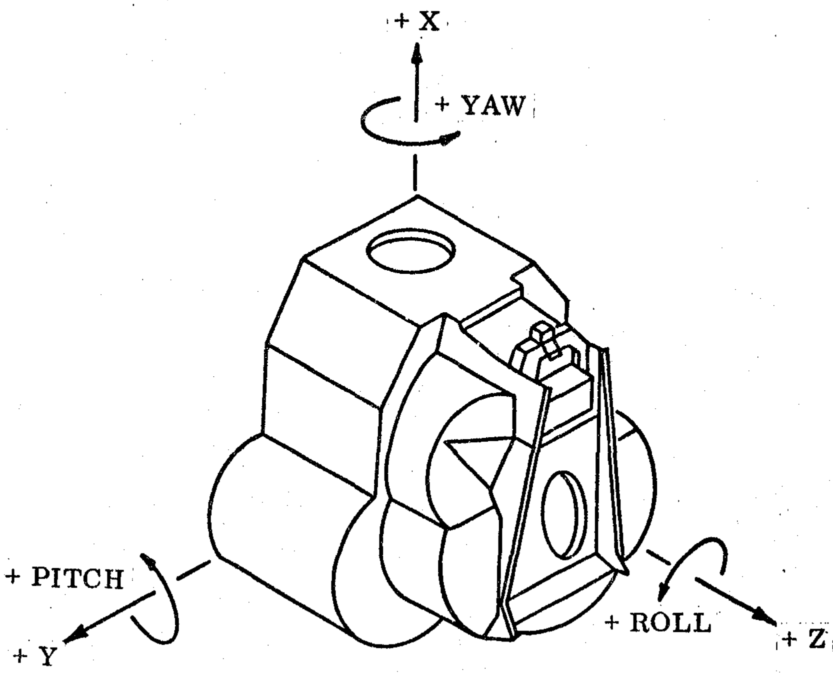

The measured mechanical alignment error of the ASA mounting surface relative to the nav. base gage (vehicle coordinate system) and the IMU is shown below:

	ASA/Nav. Base	IMU/Nav. Base	ASA/IMU
Pitch:	-00° 00' 14"	+ 00° 00' 17"	+ 00° 00' 31"
Roll:	+00° 02' 20"	+ 00° 01' 20"	- 00° 01' 00"
Yaw:	-00° 01' 25"	- 00° 02' 17"	- 00° 00' 52"

LM10/4.5.2.2 Abort Electronics Assembly (NASA DATA SOURCE)

The following listings pertain to the Abort Electronics Assembly Memory Constants.

Table LM10/4.5.2-1 contains a glossary of the constants. The glossary is divided into six groups:

Group 1 - PARAMETERS TO BE SPECIFIED DURING THE MISSION
Group 2 - AGS HARDWARE DEPENDENT CONSTANTS
Group 3 - VEHICLE DEPENDENT CONSTANTS
Group 4 - MISSION DEPENDENT CONSTANTS
Group 5 - EQUATION DEPENDENT CONSTANTS
Group 6 - DEDA CONVERSION FACTORS

Table LM10/4.5.2-2 contains the current values in both octal and decimal, with units.

The CONVERSION FACTOR's are multipliers used to convert the constant from the given engineering units to the equivalent value in the units internally used in the AEA. The number in the SCALE column defines the binary scaling of each constant, i.e., the number of bits in the computer word (excluding the sign bit) to the left of the binary point. A computer word consists of a sign bit and 17 data bits. The actual computer value of a constant is listed in the AEA OCT. column in octal digits. Since the computer word has a finite number of bits, a given input value cannot, in general, be represented exactly in the computer. The AEA VALUE column contains the result of reconverting the AEA octal value to the decimal value in engineering units, using the conversion factor mentioned above.

An asterisk by the name of the constants indicates that these constants are dependent on the hardware to be used during a mission.

Table LM10/4.5.2-1. Glossary of AGS Constants

(NASA DATA SOURCE)

GROUP 1 - PARAMETERS TO BE SPECIFIED DURING THE MISSION

NAME	DESCRIPTION OF LMDAP INPUT	INTERNAL AEA UNITS	LMDAP INPUT UNITS
1J	Desired TPI time for CSI computation	SEC	MIN
4J	Time increment from node to TPF (in TPI mode)	SEC	MIN
17J	Radar range rate	FPS	FPS
18J	Radar range	FT	FT
25J	DEDA altitude update	FT	FT
28J1	Component of External ΔV input in $\underline{V}_1$ Direction	FPS	FPS
28J2	Component of External ΔV input in $\underline{W}_1$ Direction	FPS	FPS
28J3	Component of External ΔV input in $\underline{U}_1$ Direction	FPS	FPS
1J1	LM Update State Vector - X Inertial Position	FT	FT
1J2	Y Inertial Position	FT	FT
1J3	Z Inertial Position	FT	FT
1J4	X Inertial Velocity	FPS	FPS
1J5	Y Inertial Velocity	FPS	FPS
1J6	Z Inertial Velocity	FPS	FPS
1J7	LM Update State Vector Epoch Time	SEC	MIN
2J1	CSM Update State Vector - X Inertial Position	FT	FT
2J2	Y Inertial Position	FT	FT
2J3	Z Inertial Position	FT	FT
2J4	X Inertial Velocity	FPS	FPS
2J5	Y Inertial Velocity	FPS	FPS
2J6	Z Inertial Velocity	FPS	FPS
2J7	CSM Update State Vector Epoch Time	SEC	MIN

Table LM10/4.5.2-1. Glossary of AGS Constants (Continued)
(NASA DATA SOURCE)

GROUP 2 - AGS HARDWARE DEPENDENT CONSTANTS

NAME	DESCRIPTION OF LMDAP INPUT	INTERNAL AEA UNITS	LMDAP INPUT UNITS
1K1P*	X axis gyro drift bias	RAD/20MS (Compen.)	DEG/HR (Bias)
1K6P*	Y axis gyro drift bias	RAD/20MS (Compen.)	DEG/HR (Bias)
1K11P*	Z axis gyro drift bias	RAD/20MS (Compen.)	DEG/HR (Bias)
	A positive gyro drift bias causes a gyro output of more than 32 pulses per millisecond (640 pulses per 20 milliseconds) for no ASA rotation. The range of each of the biases is ± 10 deg/hr.		
1K3*	X axis gyro scale factor deviation	NO-UNITS(Deviation)	NO-UNITS (Dev.)
1K8*	Y axis gyro scale factor deviation	NO-UNITS(Deviation)	NO-UNITS (Dev.)
1K13*	Z axis gyro scale factor deviation	NO-UNITS(Deviation)	NO-UNITS (Dev.)
	A positive scale factor deviation exists when a gyro's scale factor is greater than 2^{-16} radians per pulse. The range of each deviation is ± .78 percent.		
1K14*	Compensation constant for X gyro spin axis mass unblanace drift	RAD/FPS	DEG/HR/G
	A positive gyro spin axis mass unblanace exists when a positive ASA acceleration in the direction of the X gyro input axis results in a negative X gyro output (less than 640 pulses per 20 milliseconds) with no rotation. The range of the bias is ± 10 deg/hr/g.		

*These constants are dependent on the hardware to be used during a mission.

Contract No. NAS 9-1100
Primary No. 664

Table LM10/4.5.2-1. Glossary of AGS Constants (Continued)
(NASA DATA SOURCE)

GROUP 2 - (Continued)

NAME	DESCRIPTION OF LMDAP INPUT	INTERNAL AEA UNITS	LMDAP INPUT UNITS
1K18P*	X axis accelerometer scale factor deviation	FPS/PULSE (Scale Factors)	NO-UNITS (Dev.)
1K20P*	Y axis accelerometer scale factor deviation	FPS/PULSE	NO-UNITS (Dev.)
1K22P*	Z axis accelerometer scale factor deviation	FPS/PULSE	NO-UNITS (Dev.)

A positive accelerometer scale factor deviation exists when the measured accelerometer's scale factor is greater than the nominal value of + .003125 fps/pulse. The range of this input is ± 24 percent.

NAME	DESCRIPTION OF LMDAP INPUT	INTERNAL AEA UNITS	LMDAP INPUT UNITS
1K19P*	X axis accelerometer bias	FPS/20MS (Compen.)	MICRO G (Bias)
1K21P*	Y axis accelerometer bias	FPS/20MS (Compen.)	MICRO G (Bias)
1K23P*	Z axis accelerometer bias	FPS/20MS (Compen.)	MICRO G (Bias)

A positive accelerometer bias results in an accelerometer output of more than 32 pulses per millisecond (640 pulses per 20 milliseconds). The range of each of these biases is ± 2000 µg.

NAME	DESCRIPTION OF LMDAP INPUT	INTERNAL AEA UNITS	LMDAP INPUT UNITS
1K26	X axis azimuth alignment gain constant (lunar align)	NO-UNITS	NO-UNITS
1K27	Lunar align leveling alignment constant	RAD/FPS	RAD/FPS
1K28	Lunar align leveling alignment constant	NO-UNITS	NO-UNITS
1K29	Lunar align stop error criterion	RAD	RAD
1K30	Gyro calibrate time	2-SEC	2-SEC
1K33	Gyro calibration gain constant	NO-UNITS	NO-UNITS
1K34	Gyro calibration gain constant	1/20MS	1/20MS
1K35	Navigation sensed velocity threshold	FT/SEC	FT/SEC
1K36	Accelerometer calibration gain constant	NO-UNITS	NO-UNITS

*These constants are dependent on the hardware to be used during a mission.

Table LM10/4.5.2-1. Glossary of AGS Constants (Continued)
(NASA DATA SOURCE)

GROUP 2 - (Continued)

NAME	DESCRIPTION OF LMDAP INPUT	INTERNAL AEA UNITS	LMDAP INPUT UNITS
1K37	Accelerometer calibration time	2-SEC	2-SEC
6K2	Radar filter initialization value of P_{11} and P_{22}	FT^2	FT^2
6K4	Radar filter initialization value of P_{33} and P_{44}	$(FPS)^2$	$(FPS)^2$
6K5	Radar filter factor in r_y update	NO-UNITS	NO-UNITS
6K6	Radar filter factor in V_y update	NO-UNITS	NO-UNITS
6K8	Radar filter term (range rate variance)	$(FT/SEC)^2$	$(FT/SEC)^2$
6K9	Radar filter factor (angular variance)	$(RAD)^2$	$(RAD)^2$
6K10	Radar filter factor (range variance)	FT^2	FT^2
7K2	Radar filter state vector noise term	$\{FT^2$, FT^2/SEC^2	$\{FT^2$, FT^2/SEC^2
6K11	Conversion for raw radar shaft and trunnion angles to radians	DEG/RAD	DEG/RAD
6K12	Conversion factor for raw radar range to feet at B22	FT/COUNT	FT/COUNT
6K13	Conversion for raw radar range rate to FPS at B13	COUNTS/FPS	COUNTS/FPS
6K14	Radar range rate null	COUNTS	COUNTS

Table LM10/4.5.2-1. Glossary of AGS Constants (Continued)
(NASA DATA SOURCE)

GROUP 3 - VEHICLE DEPENDENT CONSTANTS

NAME	DESCRIPTION OF LMDAP INPUT	INTERNAL AEA UNITS	LMDAP INPUT UNITS
1K9	Ullage counter limit	COUNTS	COUNTS
4K2	Coefficient in T_B computation	SEC/FT	SEC/FT
4K3	Coefficient in T_B computation	$(SEC/FT)^2$	$(SEC/FT)^2$
4K21	Limit on body attitude errors	RAD	RAD
4K23	Time to maintain attitude hold momentarily after staging	40-MSEC	40-MSEC
4K25	Ascent engine cutoff impulse compensation	FPS	FPS
4K26	V_G threshold for engine cutoff	FPS	FPS
4K27	Hover abort overflow protection	FPS	FPS
4K34	Lower limit on a_T	FT/SEC^2	FT/SEC^2
4K35	Ullage threshold	FT/SEC^2	FT/SEC^2

Table LM10/4.5.2-1. Glossary of AGS Constants (Continued)
(NASA DATA SOURCE)

GROUP 4 - MISSION DEPENDENT CONSTANTS

NAME	DESCRIPTION OF LMDAP INPUT	INTERNAL AEA UNITS	LMDAP INPUT UNITS
1K4	Altitude/Altitude rate interpolation factor	NO-UNITS	NO-UNITS
2K1	Lunar gravitational constant	FT^3/SEC^2	FT^3/SEC^2
2K2	Reciprocal of 2K1	SEC^2/FT^3	SEC^2/FT^3
2K4	$-2K1\ \Delta T$ (ΔT = 2 sec)	FT^3/SEC	FT^3/SEC
3K4	Sine of central angle limit in TPI	NO-UNITS	NO-UNITS
4K4	Coefficient in linear expression for $\dot{r}_f$	1/SEC	1/SEC
4K5	Quantity in linear expression for $\dot{r}_f$	FT	FT
4K6	Upper limit on $\dot{r}_f$	FPS	FPS
4K10	Factor in LM desired semi-major axis α_L (O.I.)	FT/RAD	FT/RAD
4K12	Acceleration check for lower limit of $\ddot{r}_d$	FT/SEC^2	FT/SEC^2
5K14	Upper limit on $\dddot{r}_d$	FT/SEC^3	FT/SEC^3
5K16	Upper limit on $\dddot{y}_d$	FT/SEC^3	FT/SEC^3
5K17	Lower limit on $\dddot{y}_d$	FT/SEC^3	FT/SEC^3
5K18	Lower limit on $\dddot{r}_d$	FT/SEC^3	FT/SEC^3
5K20	Lower Limit on $\dddot{r}_d$	FT/SEC^3	FT/SEC^3
5K26	Velocity-to-be-gained threshold	FPS	FPS
K55	Scale factor for $\dot{r}$ display	NO-UNITS	NO-UNITS
WBX	X component of unit vector for guidance steering	NO-UNITS	NO-UNITS
WBY	Y component of unit vector for guidance steering	NO-UNITS	NO-UNITS
WBZ	Z component of unit vector for guidance steering	NO-UNITS	NO-UNITS
2J	Cotangent of desired LOS angle at TPI for CSI computation	NO-UNITS	NO-UNITS

Table LM10/4.5.2-1. Glossary of AGS Constants (Continued)

(NASA DATA SOURCE)

GROUP 4 - (Continued)

NAME	DESCRIPTION OF LMDAP INPUT	INTERNAL AEA UNITS	LMDAP INPUT UNITS
3J	Rendezvous offset time for TPI computation	SEC	MIN
5J	Landing site radius	FT	FT
6J	Desired LM transfer time for TPI routine	SEC	MIN
7J	Term in LM desired semi-major axis, α_L (O.I.)	FT	FT
8J	One-half lower limit of apolune radius	FT	FT
10J	Alternate value for 7J (late descent abort)	FT	FT
11J	Alternate value for 4K10 (late descent abort)	FT/RAD	FT/RAD
12J	Threshold value for THETAF (CSM/LM phase angle)	RAD	RAD
16J	Orbit insertion targeted injection altitude	FT	FT
21J	Vertical pitch steering altitude threshold	FT	FT
22J	Vertical pitch steering altitude rate threshold	FPS	FPS
23J	Orbit insertion targeted injection radial rate	FPS	FPS
6J1, 6J2, 6J3	Inertial negative lunar rotation rate vector at predicted landing site	RAD/20MS	RAD/20MS
7K1	T_{ig} offset time prior to burn	SEC	SEC

Table LM10/4.5.2-1. Glossary of AGS Constants (Continued)

(NASA DATA SOURCE)

GROUP 5 - EQUATION DEPENDENT CONSTANTS

NAME	DESCRIPTION OF LMDAP INPUT	INTERNAL AEA UNITS	LMDAP INPUT UNITS
1K24	FDAI computation singularity region	NO-UNITS	NO-UNITS
2K3	q value set if overflow occurs in e^2 computation of LM orbit parameters	FT	FT
2K11	Set value of V_F if no valid TPI solution	FPS	FPS
2K14	Initial p perturbation	FT	FT
2K17	Number of p-iteration minus 3	COUNTS	COUNTS
2K18	Partial derivative protector in p-iterator routine	SEC	SEC
2K19	Δp limiter	FT	FT
2K20	p-iterator convergence check	SEC	SEC

Contract No. NAS 9-1100
Primary No. 664

Table LM10/4.5.2-1. Glossary of AGS Constants (Continued)
(NASA DATA SOURCE)

GROUP 6 - DEDA CONVERSION FACTORS

NAME	DESCRIPTION OF LMDAP INPUT
BACCSF	Convert .001 ft/sec^2 to fps/20 msec at B1
BM13SF	Convert .01°/hr to rad/20 msec at B13
B23SF	Convert 100 ft to ft at B 23
B18SF	Convert .1 min to sec at B18
B3SF	Convert .01° to rad at B3
B23RSF	Convert .1 nmi to ft at B23
B13SF	Convert .01 min to sec at B13
B13VSF	Convert .1 fps to fps at B13
B22RSF	Convert .01 nmi to ft at B22

Table LM10/4.5.2-2. AGS Constants

(NASA DATA SOURCE)

NAME	LOC.	SCALE	CONVERSION FACTOR	AEA OCT.	AEA VALUE	UNITS
1J	0275	18	.60000 02	000000	.00000000 00	MIN
4J	0306	13	.60000 02	000000	.00000000 00	MIN
17J	0503	13	.10000 01	000000	.00000000 00	FPS
18J	0316	22	.10000 01	000000	.00000000 00	FT
25J	0223	23	.10000 01	000000	.00000000 00	FT
28J1	0450	13	.10000 01	000000	.00000000 00	FPS
28J2	0451	13	.10000 01	000000	.00000000 00	FPS
28J3	0452	13	.10000 01	000000	.00000000 00	FPS
1J1	0240	23	.10000 01	000000	.00000000 00	FT
1J2	0241	23	.10000 01	000000	.00000000 00	FT
1J3	0242	23	.10000 01	000000	.00000000 00	FT
1J4	0260	13	.10000 01	000000	.00000000 00	FPS
1J5	0261	13	.10000 01	000000	.00000000 00	FPS
1J6	0262	13	.10000 01	000000	.00000000 00	FPS
1J7	0254	18	.60000 02	000000	.00000000 00	MIN
2J1	0244	23	.10000 01	000000	.00000000 00	FT
2J2	0245	23	.10000 01	000000	.00000000 00	FT

Table LM10/4.5.2-2. AGS Constants (Continued)

(NASA DATA SOURCE)

NAME	LOC.	SCALE	CONVERSION FACTOR	AEA OCT.	AEA VALUE	UNITS
2J3	0246	23	.10000 01	000000	.00000000 00	FT
2J4	0264	13	.10000 01	000000	.00000000 00	FPS
2J5	0265	13	.10000 01	000000	.00000000 00	FPS
2J6	0266	13	.10000 01	000000	.00000000 00	FPS
2J7	0272	18	.60000 02	000000	.00000000 00	MIN
* 1K1P	0544	-13	-.96963-07	000002	-.19209907-01	DEG/HR
* 1K6P	0545	-13	-.96963-07	000136	-.90286563 00	DEG/HR
* 1K11P	0546	-13	-.96963-07	777771	.67234674-01	DEG/HR
* 1K3	0550	-7	.10000 01	041621	.10309815-02	NO-UNITS
* 1K8	0551	-7	.10000 01	042444	.10550022-02	NO-UNITS
* 1K13	0552	-7	.10000 01	730513	-.12009740-02	NO-UNITS
* 1K14	0537	-14	.15091-06	777751	-.70970841-01	DEG/HR/G
* 1K18P	0534	-8	.31250-02	314267	-.21610260-02	NO-UNITS
* 1K20P	0535	-8	.31250-02	314226	-.24757385-02	NO-UNITS
* 1K22P	0536	-8	.31250-02	315026	.11863708-02	NO-UNITS
* 1K19P	0540	1	-.64254-06	000002	-.47495501 02	MICRO-G
* 1K21P	0541	1	-.64254-06	777773	.11873875 03	MICRO-G

Contract No. NAS 9-1100
Primary No. 664

Table LM10/4.5.2-2. AGS Constants (Continued)

(NASA DATA SOURCE)

	NAME	LOC.	SCALE	CONVERSION FACTOR	AEA OCT.	AEA VALUE	UNITS
*	1K23P	0542	1	-.64254-06	000004	-.94991001 02	MICRO-G
	1K26	0626	8	.10000 01	561111	-.14285742 03	NO-UNITS
	1K27	0627	-4	.10000 01	262132	.43499947-01	RAD/FPS
	1K28	0630	7	.10000 01	326774	.10749609 03	NO-UNITS
	1K29	0631	-4	.10000 01	004061	.99992752-03	RAD
	1K30	0617	17	.10000 01	000226	.15000000 03	2-SEC
	1K33	0632	-3	.10000 01	243656	.79999924-01	NO-UNITS
	1K34	0633	-15	.10000 01	247613	.19999919-04	1/20MS
	1K35	0634	7	.10000 01	000400	.25000000 00	FT/SEC
	1K36	0635	0	.10000 01	777651	-.66375733-03	NO-UNITS
	1K37	0613	17	.10000 01	000017	.15000000 02	2-SEC
	6K2	0457	30	.10000 01	027657	.99999744 08	FT2
	6K4	0456	10	.10000 01	031000	.10000000 03	FT2/SEC2
	6K5	0276	0	.10000 01	505075	-.73000336 00	NO-UNITS
	6K6	0522	-8	.10000 01	676356	-.99998713-03	NO-UNITS
	6K8	0564	10	.10000 01	000034	.21875000 00	FT2/SEC2
	6K9	0565	-4	.10000 01	000100	.30517578-04	RAD2

Table LM10/4.5.2-2. AGS Constants (Continued)
(NASA DATA SOURCE)

	NAME	LOC.	SCALE	CONVERSION FACTOR	AEA OCT.	AEA VALUE	UNITS
*	1K23P	0542	1	-.64254-06	000000	-.00000000 00	MICRO-G
	1K26	0626	8	.10000 01	561111	-.14285742 03	NO-UNITS
	1K27	0627	-4	.10000 01	262132	.43499947-01	RAD/FPS
	1K28	0630	7	.10000 01	326774	.10749609 03	NO-UNITS
	1K29	0631	-4	.10000 01	004061	.99992752-03	RAD
	1K30	0617	17	.10000 01	000226	.15000000 03	2-SEC
	1K33	0632	-3	.10000 01	243656	.79999924-01	NO-UNITS
	1K34	0633	-15	.10000 01	247613	.19999919-04	1/20MS
	1K35	0634	7	.10000 01	000400	.25000000 00	FT/SEC
	1K36	0635	0	.10000 01	777651	-.66375733-03	NO-UNITS
	1K37	0613	17	.10000 01	000017	.15000000 02	2-SEC
	6K2	0457	30	.10000 01	027657	.99999744 08	FT2
	6K4	0456	10	.10000 01	031000	.10000000 03	FT2/SEC2
	6K5	0276	0	.10000 01	505075	-.73000336 00	NO-UNITS
	6K6	0522	-8	.10000 01	676356	-.99998713-03	NO-UNITS
	6K8	0564	10	.10000 01	000034	.21875000 00	FT2/SEC2
	6K9	0565	-4	.10000 01	000100	.30517578-04	RAD2

Table LM10/4.5.2-2. AGS Constants (Continued)

(NASA DATA SOURCE)

NAME	LOC.	SCALE	CONVERSION FACTOR	AEA OCT.	AEA VALUE	UNITS
6K10	0566	28	.10000 01	005754	.62504960 07	FT2
7K2	0650	17	.10000 01	000002	.20000000 01	NO-UNITS
6K11	0237	0	.10000 01	121372	.31831360 00	NO-UNITS
6K12	0313	4	.10000 01	226051	.93800049 01	FT/COUNT
6K13	0577	1	.10000 01	464072	-.15928650 01	FPS/COUNT
6K14	0517	14	.10000 01	411500	-.15768000 05	COUNTS
1K9	0616	17	.10000 01	000005	.50000000 01	COUNTS
4K2	0654	-12	.10000 01	713267	-.50203875-04	SEC/FT
4K3	0655	-25	.10000 01	016336	.16802915-08	SEC2/FT2
4K21	0666	2	.10000 01	020603	.26181030 00	RAD
4K23	0622	17	.10000 01	000076	.62000000 02	40MSEC
4K25	0446	13	.10000 01	000072	.36250000 01	FPS
4K26	0454	13	.10000 01	002140	.70000000 02	FPS
4K27	0473	13	.10000 01	406000	-.80000000 04	FPS
4K34	0660	7	.10000 01	002000	.10000000 01	FT/SEC2
4K35	0661	7	.10000 01	000146	.99609375-01	FT/SEC2
1K4	0624	0	.10000 01	031463	.99998474-01	NO-UNITS

Table LM10/4.5.2-2. AGS Constants (Continued)

(NASA DATA SOURCE)

NAME	LOC.	SCALE	CONVERSION FACTOR	AEA OCT.	AEA VALUE	UNITS
6K10	0566	28	.10000 01	005754	.62504960 07	FT2
7K2	0650	17	.10000 01	000002	.20000000 01	NO-UNITS
6K11	0237	0	.10000 01	121372	.31831360 00	NO-UNITS
6K12	0313	4	.10000 01	226051	.93800049 01	FT/COUNT
6K13	0577	1	.10000 01	464072	-.15928650 01	FPS/COUNT
6K14	0517	14	.10000 01	411500	-.15768000 05	COUNTS
1K9	0616	17	.10000 01	000005	.50000000 01	COUNTS
4K2	0654	-12	.10000 01	713267	-.50203875-04	SEC/FT
4K3	0655	-25	.10000 01	016336	.16802915-08	SEC2/FT2
4K21	0666	2	.10000 01	020603	.26181030 00	RAD
4K23	0622	17	.10000 01	000076	.62000000 02	40MSEC
4K25	0446	13	.10000 01	000072	.36250000 01	FPS
4K26	0454	13	.10000 01	002140	.70000000 02	FPS
4K27	0473	13	.10000 01	406000	-.80000000 04	FPS
4K34	0660	7	.10000 01	002000	.10000000 01	FT/SEC2
4K35	0661	7	.10000 01	000146	.99609375-01	FT/SEC2
1K4	0624	0	.10000 01	031463	.99998474-01	NO-UNITS

Table LM10/4.5.2-2. AGS Constants (Continued)

(NASA DATA SOURCE)

NAME	LOC.	SCALE	CONVERSION FACTOR	AEA OCT.	AEA VALUE	UNITS
2K1	0636	48	.10000 01	235407	.17318811 15	FT3/SEC2
2K2	0637	-47	.10000 01	320020	.57740271-14	SEC2/FT3
2K4	0674	49	.10000 01	542371	-.34637623 15	FT3/SEC
3K4	0304	1	.10000 01	026164	.17364502 00	NO-UNITS
4K4	0557	-7	.10000 01	203045	.40000081-02	1/SEC
4K5	0227	23	.10000 01	257015	.57352320 07	FT
4K6	0527	13	.10000 01	002400	.80000000 02	FPS
4K10	0662	20	.10000 01	663766	-.31137600 06	FT/RAD
4K12	0506	7	.10000 01	012000	.50000000 01	FT/SEC2
5K14	0560	-2	.10000 01	000000	.00000000 00	FT/SEC3
5K16	0561	-2	.10000 01	012173	.10000229-01	FT/SEC3
5K17	0611	-2	.10000 01	765605	-.10000229-01	FT/SEC3
5K18	0267	-2	.10000 01	631463	-.10000038 00	FT/SEC3
5K20	0523	-2	.10000 01	000000	.00000000 00	FT/SEC3
5K26	0466	13	.10000 01	000360	.15000000 02	FPS
K55	0607	0	.10000 01	377777	.99999237 00	NO UNITS
WBX	0514	1	.10000 01	655562	-.64279175 00	NO-UNITS

Table LM10/4.5.2-2. AGS Constants (Continued)

(NASA DATA SOURCE)

NAME	LOC.	SCALE	CONVERSION FACTOR	AEA OCT.	AEA VALUE	UNITS
WBY	0515	1	.10000 01	635745	-.76603699 00	NO-UNITS
WBZ	0516	1	.10000 01	000000	.00000000 00	NO-UNITS
2J	0605	7	.10000 01	003775	.19970703 01	NO-UNITS
3J	0312	13	.60000 02	000000	.00000000 00	MIN
5J	0231	23	.10000 01	255526	.56907520 07	FT
6J	0307	13	.60000 02	120500	.43000000 02	MIN
7J	0224	23	.10000 01	270267	.60410240 07	FT
8J	0225	23	.10000 01	131473	.29365120 07	FT
10J	0226	23	.10000 01	270313	.60423040 07	FT
11J	0673	20	.10000 01	550057	-.62221600 06	FT/RAD
12J	0305	3	.10000 01	766161	-.30560303 00	RAD
16J	0232	23	.10000 01	001652	.60032000 05	FT
21J	0233	23	.10000 01	000607	.25024000 05	FT
22J	0464	13	.10000 01	001440	.50000000 02	FPS
23J	0465	13	.10000 01	000470	.19500000 02	FPS
6J1	0640	-14	.10000 01	777716	-.23283064-07	RAD/20MS
6J2	0641	-14	.10000 01	777631	-.47963113-07	RAD/20MS

Table LM10/4.5.2-2. AGS Constants (Continued)
(NASA DATA SOURCE)

NAME	LOC.	SCALE	CONVERSION FACTOR	AEA OCT.	AEA VALUE	UNITS
6J3	0642	-14	.10000 01	000000	.00000000 00	RAD/20MS
7K1	0274	18	.10000 01	000017	.30000000 02	SEC
1K24	0625	1	.10000 01	000071	.86975098-03	NO-UNITS
2K3	0216	23	.10000 01	040000	.10485760 07	FT
2K11	0526	13	.10000 01	273400	.60000000 04	FPS
2K14	0217	23	.10000 01	001415	.49984000 05	FT
2K17	0620	17	.10000 01	000005	.50000000 01	COUNTS
2K18	0447	13	.10000 01	000360	.15000000 02	SEC
2K19	0230	23	.10000 01	017205	.50003200 06	FT
2K20	0453	13	.10000 01	000040	.20000000 01	SEC
BM13SF	0676	0	.10000 01	365706	.96049499 00	
B23SF	0677	0	.10000 01	243656	.63999939 00	
B18SF	0665	0	.10000 01	125253	.33333588 00	
B13VSF	0651	0	.10000 01	240000	.62500000 00	
B3SF	0652	0	.10000 01	131415	.34970856 00	
B23RSF	0653	0	.10000 01	032756	.10533142 00	
B13SF	0643	0	.10000 01	032525	.10416412 00	

Table LM10/4.5.2-2. AGS Constants (Continued)

(NASA DATA SOURCE)

NAME	LOC.	SCALE	CONVERSION FACTOR	AEA OCT.	AEA VALUE	UNITS
B22RSF	0656	0	.10000 01	206645	.52664947 00	
BACCSF	0657	0	.10000 01	303240	.76293945 00	

LM10/4.5.3.2.2.3 LM-10 DPS Thrust Response at TTCA Minimum and Maximum Positions

The KSC calibration data for the commander's (CMDR) and LM pilot's (LMP) TTCA's are given below.*

TTCA POSITION	THRUST OUTPUT			
	CMDR		LMP	
	TTCA	DECA	TTCA	DECA
Minimum	11.3 %	11.4 %	11.3 %	11.8 %
Maximum	112.3 %	Saturated	111.3 %	Saturated

*TCP No. 0045, Combined Systems Test

The output calibration for the LM-10 CMDR's TTCA is:

$$V_{TTCA} = 0.024851\ \%F_{COMM} + 0.2910$$

where V_{TTCA} = TTCA output voltage, VRMS

$\%F_{COMM}$ = Commanded thrust position, %.

The output calibration for the LM-10 DECA (throttling range) is:

$$V_{DECA} = TCV = 0.12995\ \%F_{STD} + 1.1000$$

where V_{DECA} = DECA output voltage to the DPS throttle actuator (TCV), VDC

$\%F_{STD}$ = Commanded thrust at standard values of propellant interface conditions, % (of 10,500 lbf)

Using the above equations and the DPS preflight performance data (Para. LM10/4.7.1) the voltages and thrust values were determined for the above TTCA and DECA calibration data for the CMDR TTCA.

THIS COLUMN NASA DATA SOURCE ↓

TTCA OPERATING POSITION	TTCA COMMANDED THRUST, %	TTCA OUTPUT, VRMS	DECA OUTPUT, VDC	PREDICTED THRUST, LBF
Minimum	11.3	0.572	2.777	1378
Maximum* (Throttle-up	112.3	3.082	>14.6	9899
Maximum** (Throttle-down	112.3	3.082	>14.6	9985

*At 26 sec burn time.
**At 436 sec burn time.

LM10/4.5.3.4.3 GDA Drive Rates

Measurement

Time of Travel	- pitch	57.3 sec.	These times are the average of 2 measurements made on LM-10 at KSC.
	- roll	56.95 sec.	
Angular Rate	- pitch	0.2112°/sec.	
	- roll	0.2125°/sec.	

NOTE: Computed Angle of Travel = 12.1° in either axis.

LM10/4.5.4.2 Rendezvous Radar Mechanical Alignment

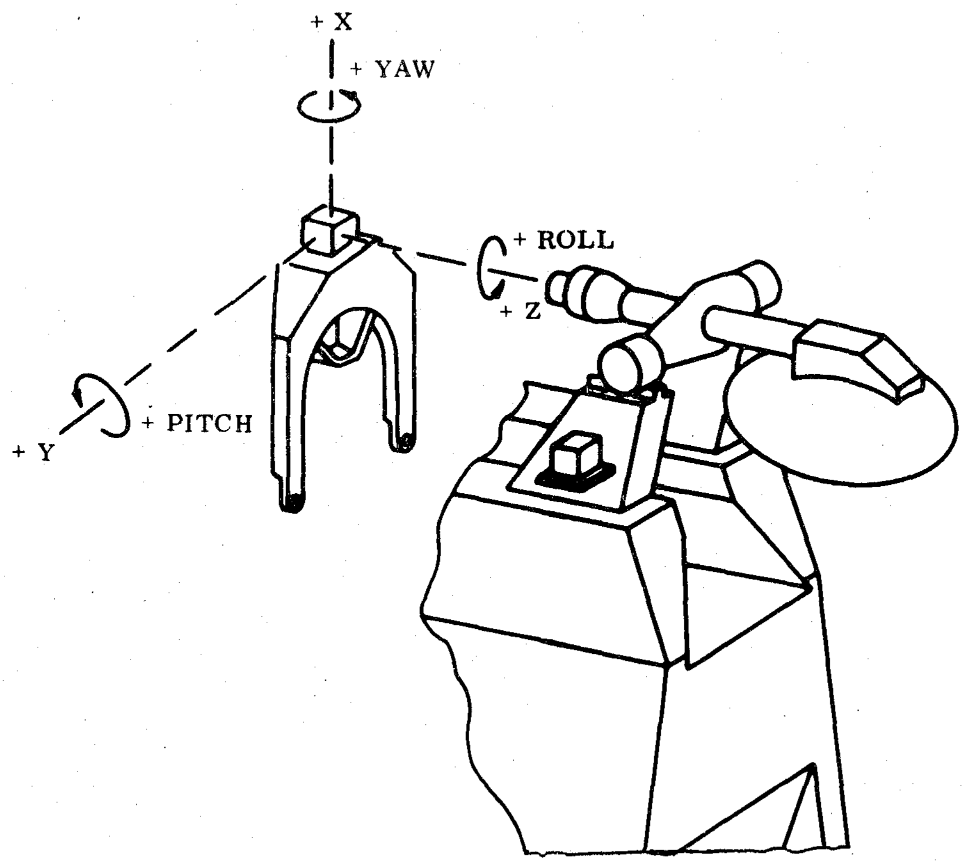

The rendezvous radar antenna assembly alignment for LM-10 with respect to the vehicle coordinate system (nav. base gage) is shown below:

Pitch:	-00° 00' 05"
Roll:	-00° 03' 06"
Yaw:	-00° 00' 55"

LM10/4.5.4.4.11 RR and T AGC Voltage Versus Range

Figure LM10/4.5.4-3 shows the expected AGC voltage levels versus range and signal level for RR No. 38 with T No. 18. The use of curves instead of nomographs permits a better visualization of the interaction of the variables and also avoids the difficulty of trying to design a nomograph to fit empirical data on non-linearly interrelated variables.

LM10/4.5.4.4.11.1 RR and T AGC Voltage Versus Range and LOS Angle

Figures LM10/4.5.4-4 and LM10/4.5.4-5 show RR AGC readings at several ranges between 0.2 nm. and 400 nm., as a function of the angle between the LOS and the antenna boresight. The data are shown for angles out to ±10 degrees in both the shaft and trunnion axes, except where very low signal levels would produce low AGC readings which would be of little value.

LM10/4.5.4.4.12 Rendezvous Radar Self-Test

The following are the measured RR self-test parameters for RR 38. These data were recorded at KSC during FRT Mission-Sim. 0005 and TCP 0045.

1) Test Monitor

SELF-TEST AGC	+1.80 Vdc
XMTR PWR	+3.40 Vdc
SHAFT ERROR	+2.2 to 2.6 Vdc (at 1/2 cps)
TRUN ERROR	+2.15 to 2.5 Vdc (at 1/2 cps)

2) Range/Range Rate Meter

Range (R)	195.5 n mi
Range Rate ($\dot{R}$)	-496.5 ft/sec

3) LGC DSKY Display: V16N78

R_1 (Range)	195.7 n mi
R_2 (Range Rate)	-499 ft/sec
R_3 (No Display)	0

LM10/4.5.4.4.13 RR Power Monitor Calibration

Figure LM10/4.5.4-7 shows the power monitor calibration for RR 38, giving power in dBm versus dc volts.

LM10/4.5.4.4.16 Allowable Vehicle Accelerations During RR Power Off Periods

Figures LM10/4.5.4-8 through LM10/4.5.4-11 show the maximum allowable LM body accelerations for any angular position of the RR antenna trunnion and shaft axes under which the antenna will not move from a fixed position with no power applied to the RR. The effect of varying the antenna temperature is also indicated in the figures.

The antenna shaft axis will always be parallel to the LM Y-axis. Therefore, LM body accelerations about the LM Y-axis can be used directly. However, as the shaft axis rotates, the trunnion axis will be parallel to the LM X-axis at 0° shaft position and parallel to the LM Z-axis at -90° shaft position. For other shaft positions, the allowable LM acceleration about the LM axes must be converted to the acceleration about the trunnion axis at the appropriate shaft position.

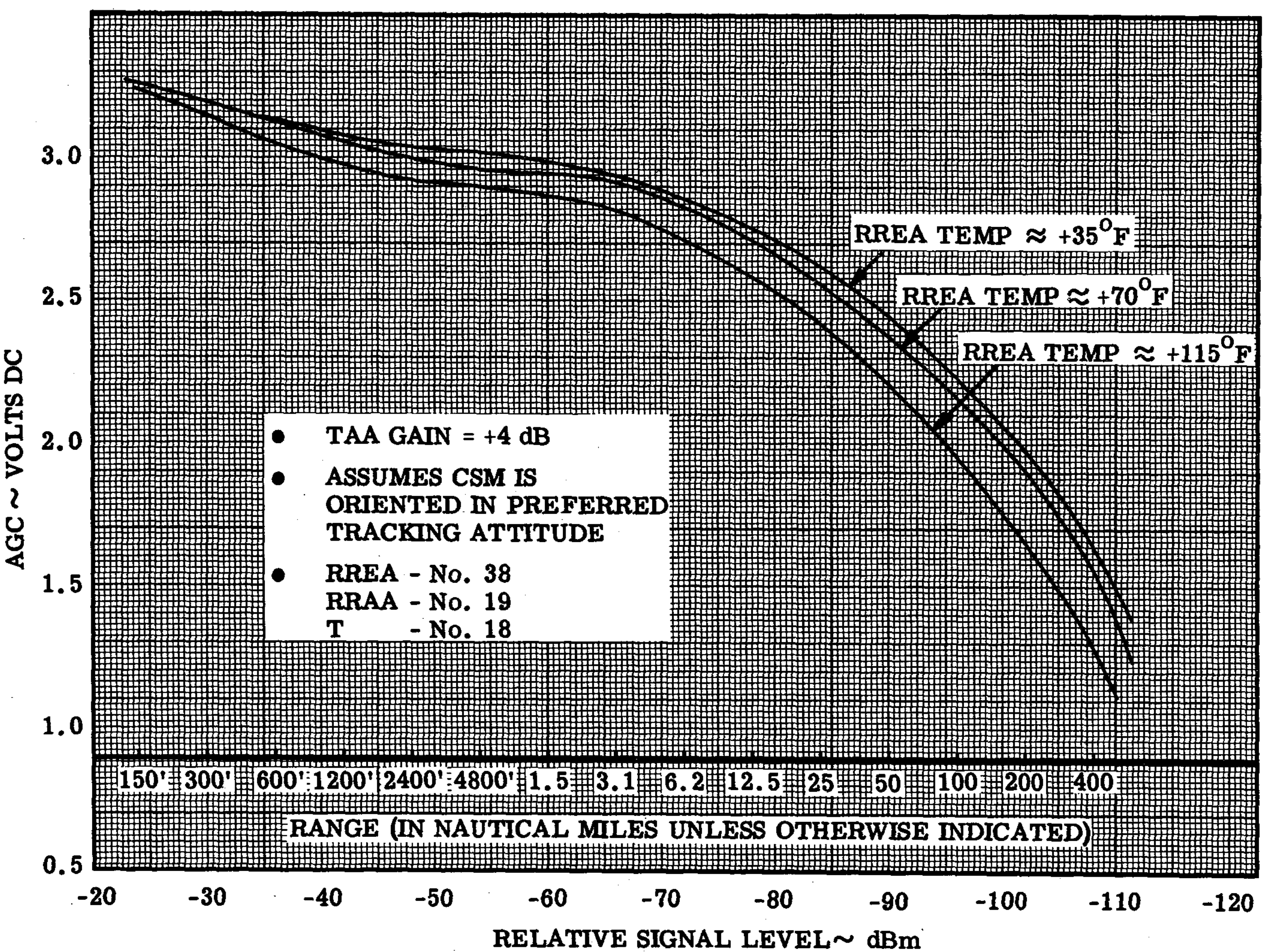

Figure LM10/4.5.4-3. LM-10 RR AGC Versus Signal Level and Range with T (See Para. 4.5.4.11)

1	400 NM RANGE
2	100 NM RANGE
3	50 NM RANGE
4	1.5 NM RANGE
5	1200 FT RANGE

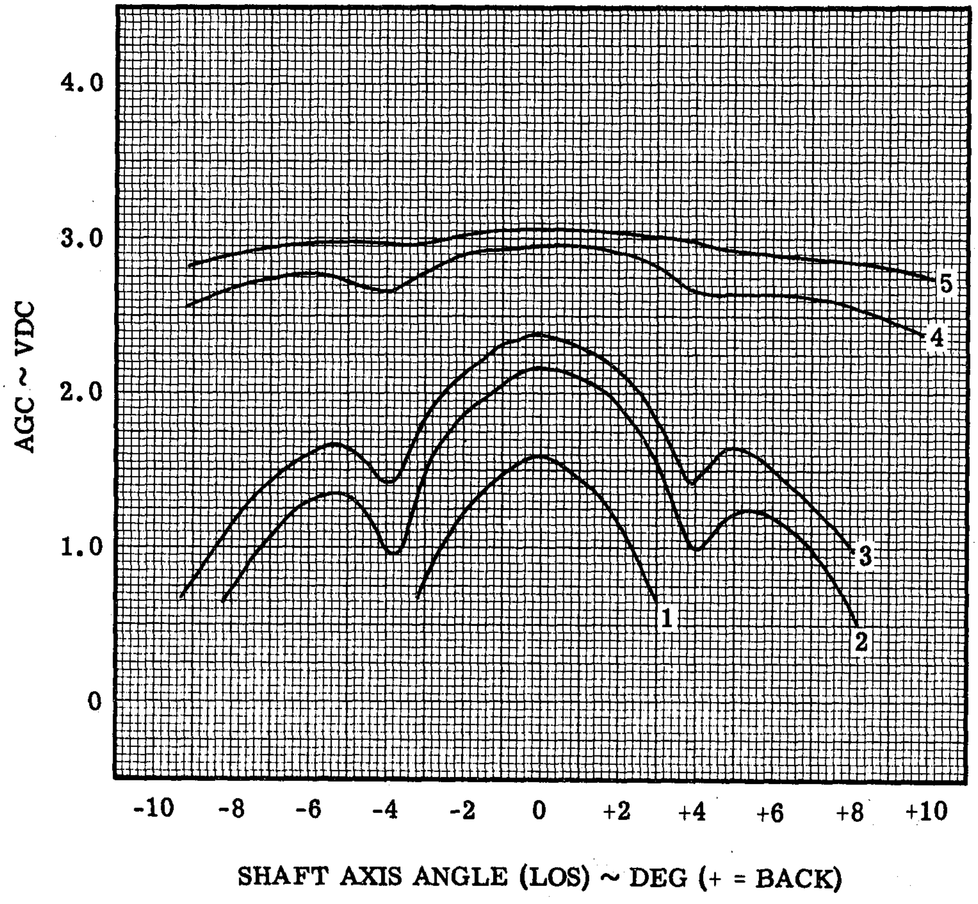

Figure LM10/4.5.4-4. AGC Versus Shaft Axis Angles (LOS)
(See Para. 4.5.4.4.11.1)

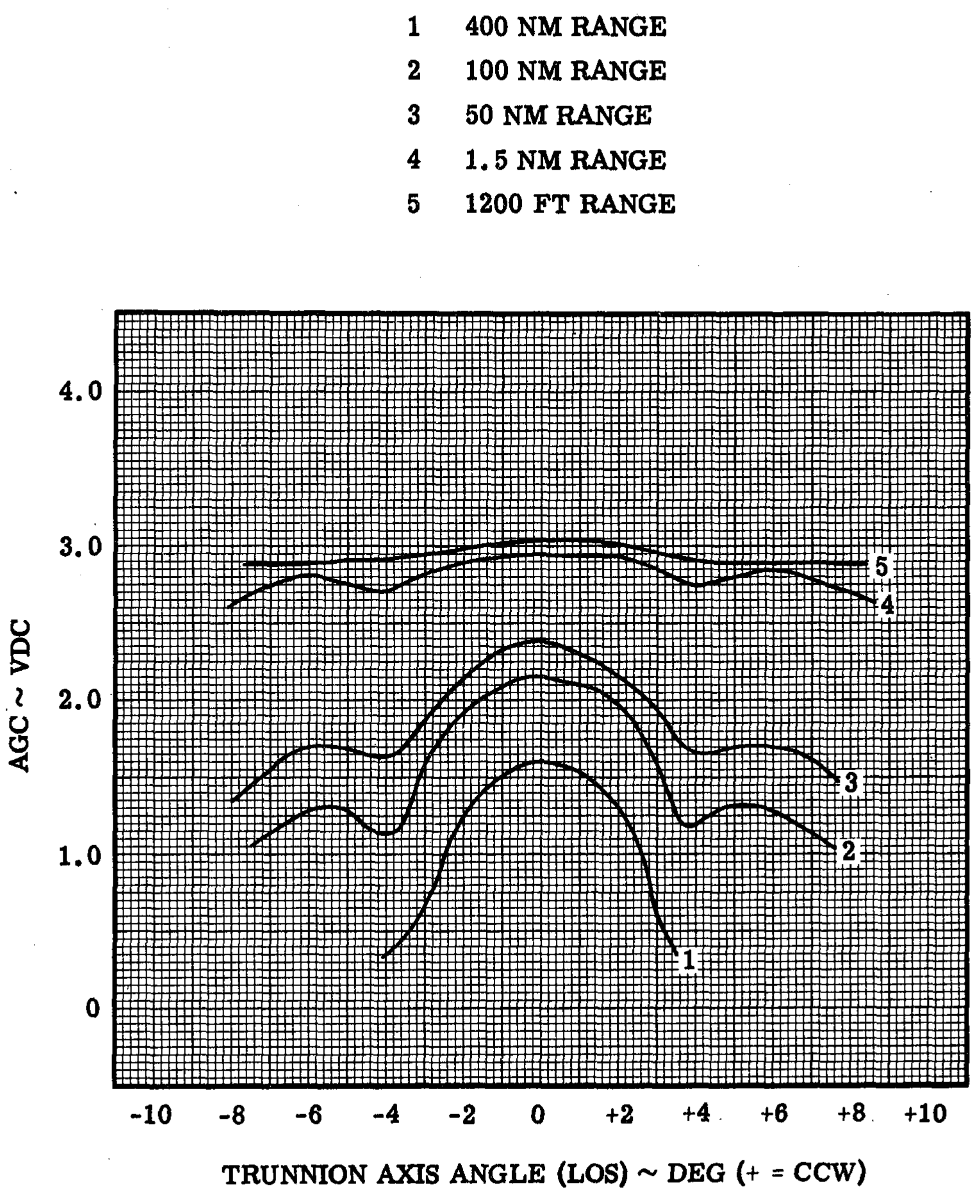

Figure LM10/4.5.4-5. AGC Versus Shaft Axis Angles (LOS)
(See Para. 4.5.4.4.11.1)

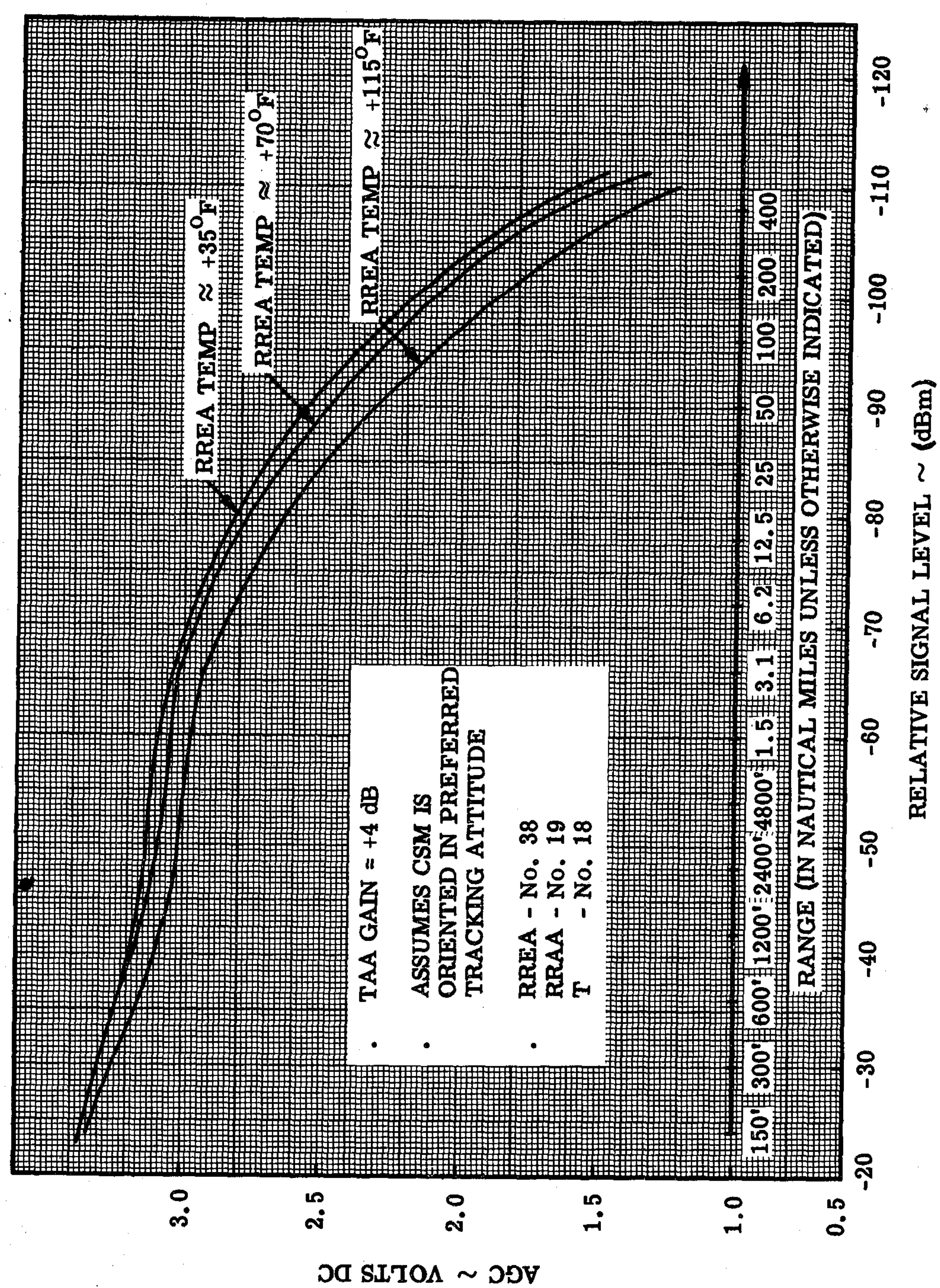

Figure LM10/4.5.4-3. LM-10 RR AGC Versus Signal Level and Range with T (See Para. 4.5.4.4.11)

1 400 NM RANGE
2 100 NM RANGE
3 50 NM RANGE
4 1.5 NM RANGE
5 1200 FT RANGE

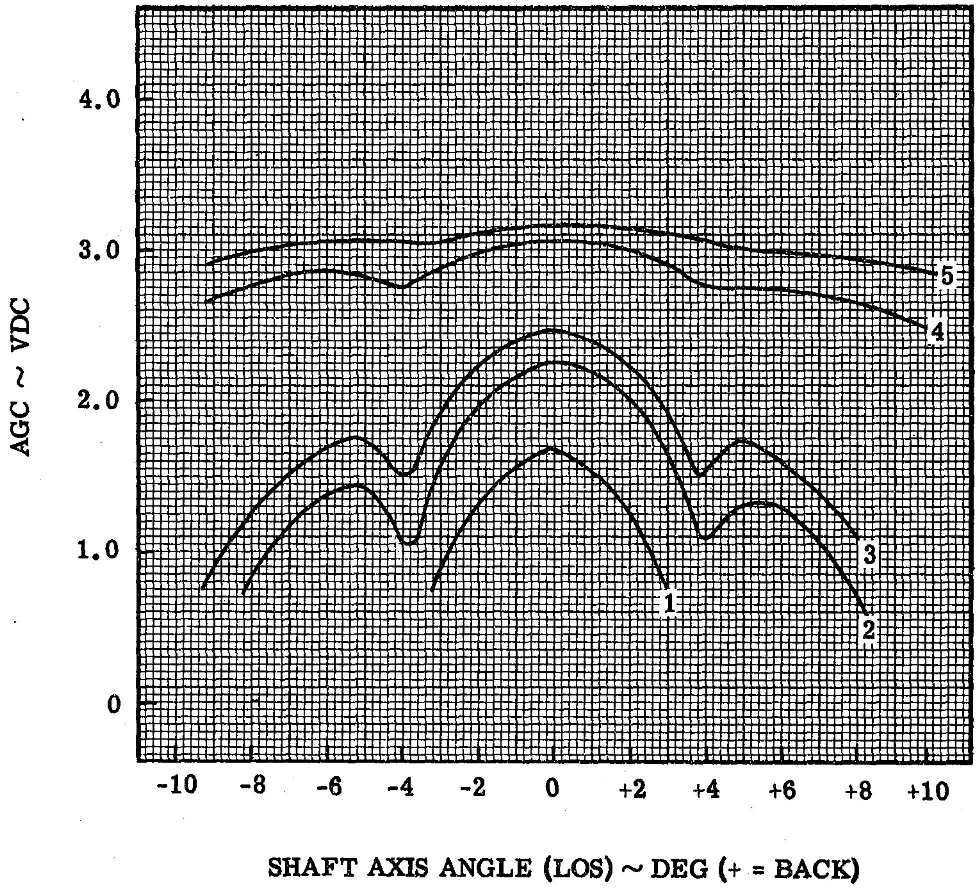

Figure LM10/4.5.4-4. AGC Versus Shaft Axis Angles (LOS)
(See Para. 4.5.4.4.11.1)

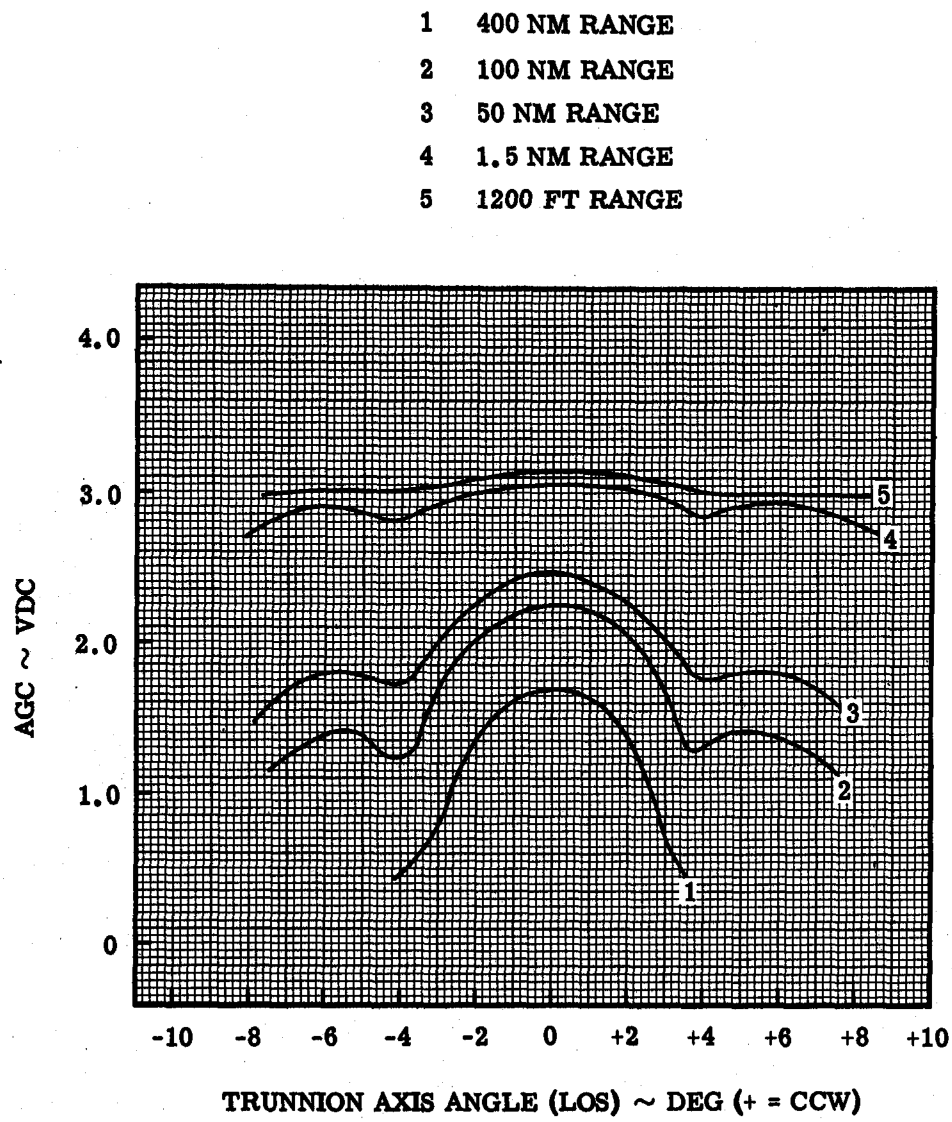

Figure LM10/4.5.4-5. AGC Versus Trunnion Axis (LOS) Angle (See Para. 4.5.4.4.11.1)

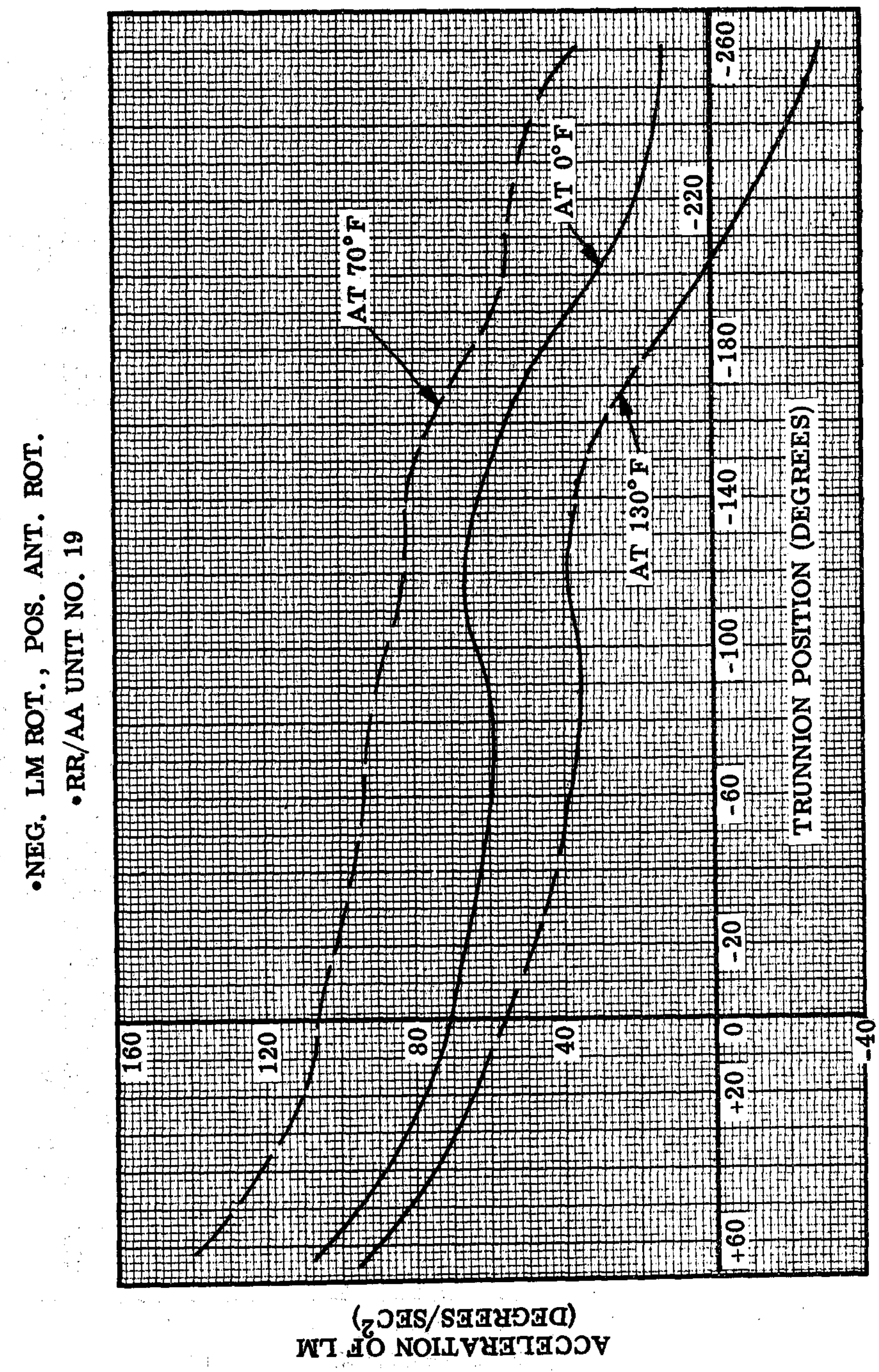

Figure LM10/4. 5. 4-8. Allowable Acceleration Trunnion Axis
(See Para. LM10/4. 5. 4. 4. 16)

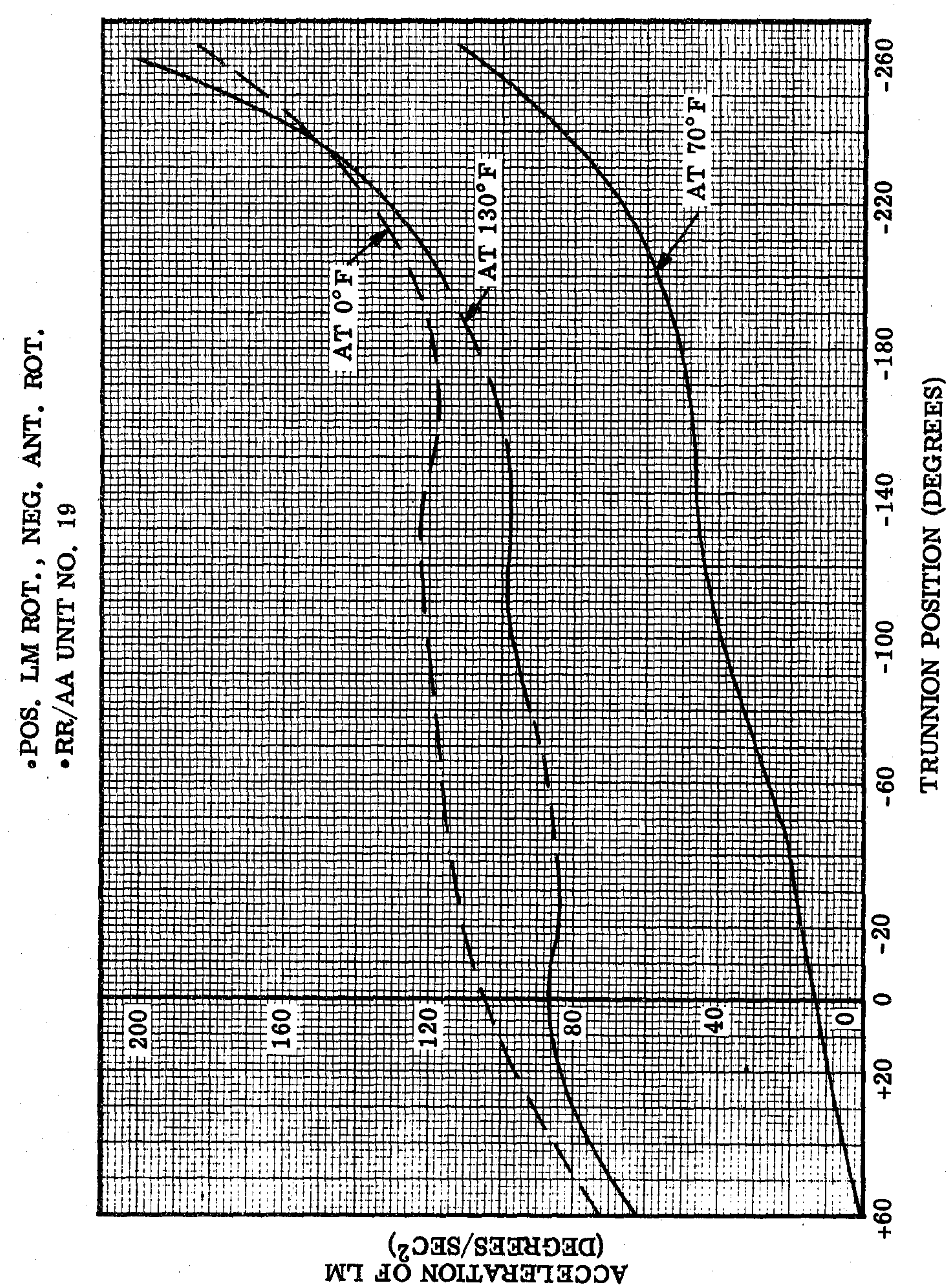

Figure LM10/4.5.4-9 Allowable Acceleration Trunnion Axis
(See Para. LM10/4.5.4.4.16)

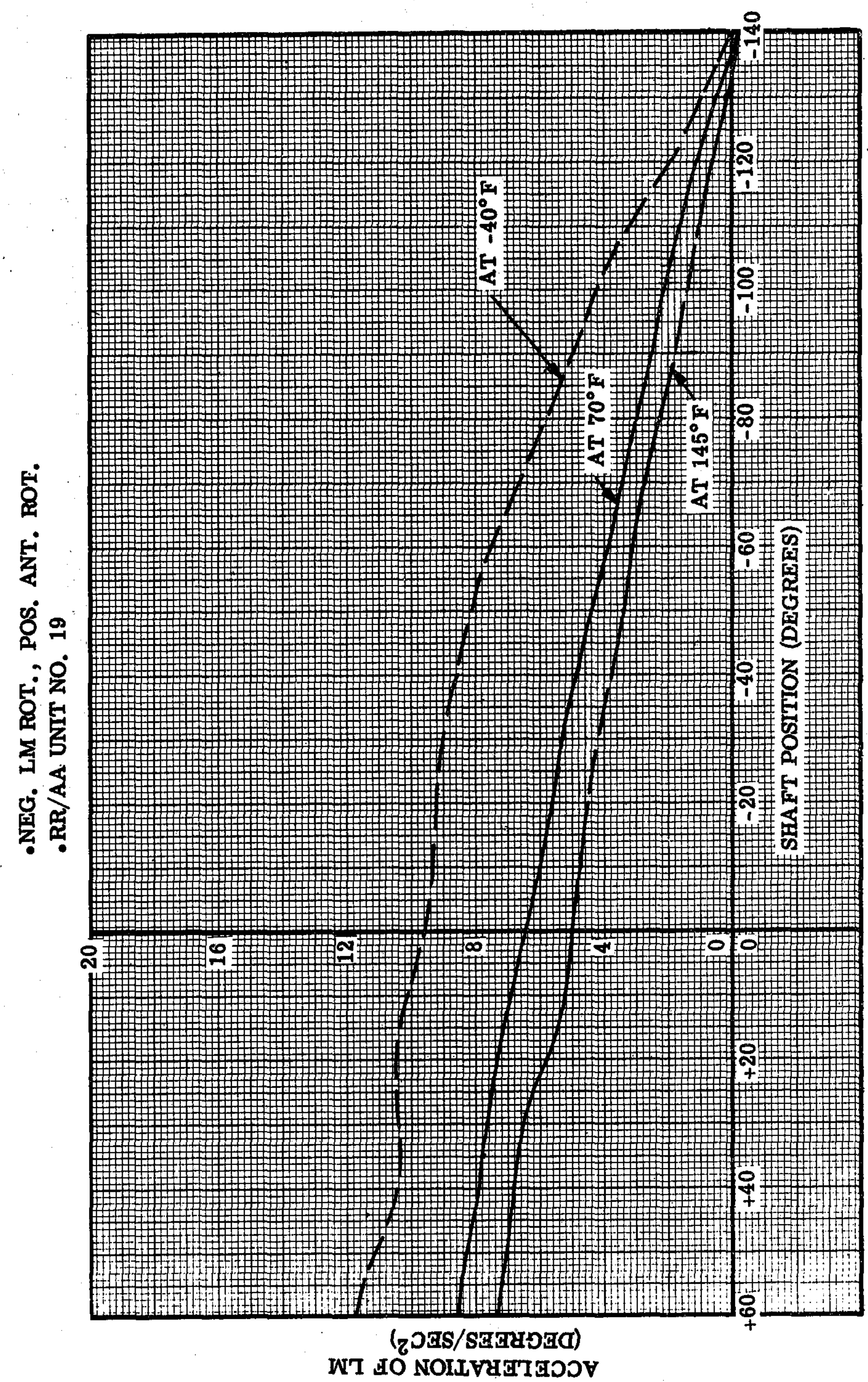

Figure LM10/4. 5. 4-10. Allowable Acceleration Shaft Axis
(See Para. LM10/4. 5. 4. 4. 16)

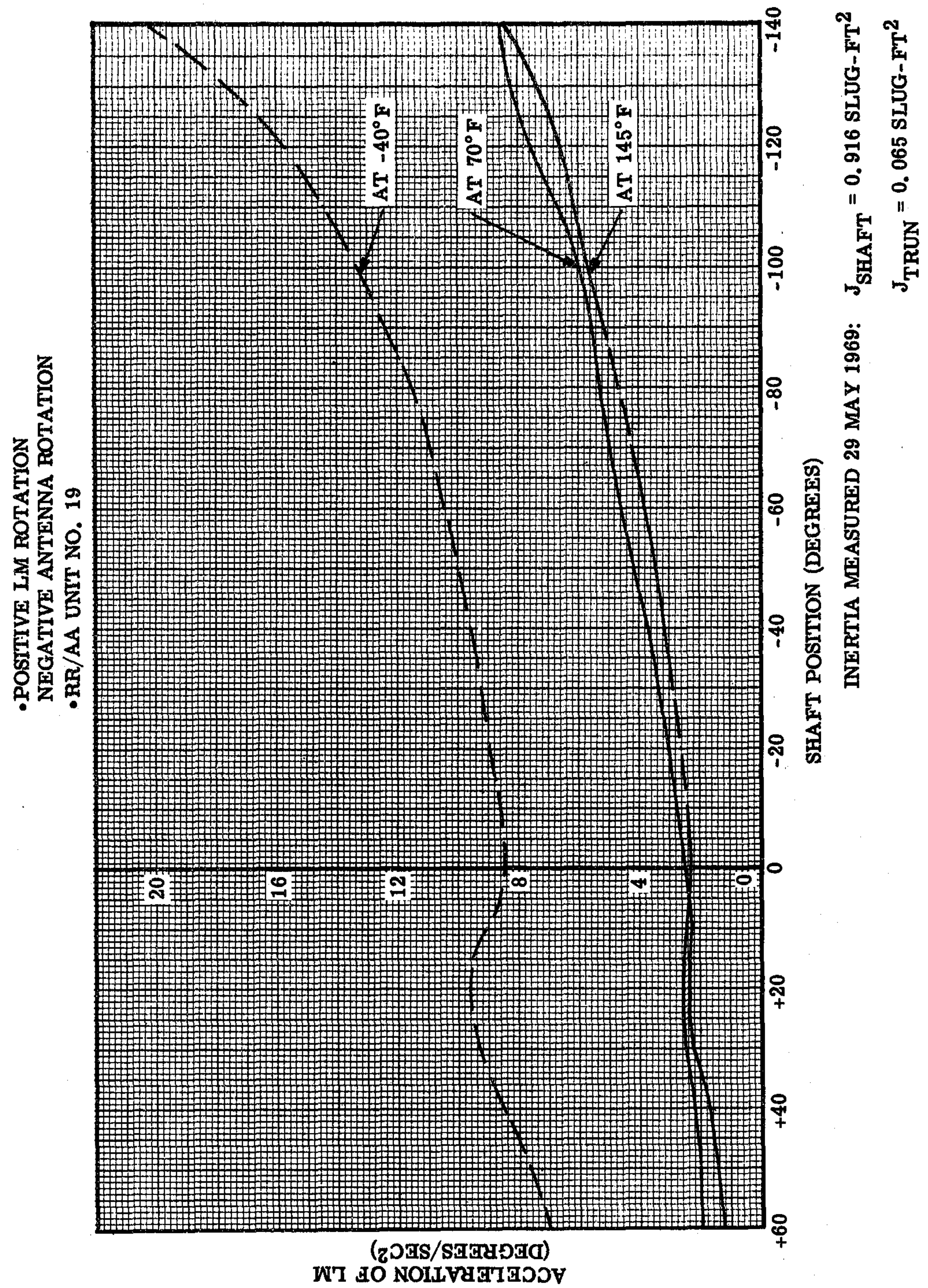

Figure LM10/4.5.4-11. Allowable Acceleration Shaft Axis
(See Para. LM10/4.5.4.4.16)

LM10/4.5.5.1.16 LR Power Monitor

The following is a calibration of the power monitor with LR P-51. These data were obtained from KSC testing during TCP 0045 and include antenna losses.

Transmitter	Power (dBm)	Power (MW)	Monitor (Vdc)	Calibration
Velocity	24.8	302	3.55	11.8×10^{-3} V/MW
Altimeter	21.2	132	3.5	26.5×10^{-3} V/MW

LM10/4.5.5.1.18 Expected Altitude of LR Velocity and Range Initial "Data Good" Indication

Figure LM10/4.5.5-1 presents the expected altitudes of LR velocity and range acquisition for a nominal Apollo 15 trajectory. The data were computed using the measured transmitter power and antenna gain for the Apollo 15 landing radar and +9 dB reflectivity (2 times the +6 dB model given in paragraph 4.5.5.5). The results were that range beam acquisition occurred at an altitude of about 40,800 ft above the landing site and 39,200 ft above the local terrain; while velocity acquisition occurred at an altitude of about 37,600 ft above the landing site and 35,000 ft above the local terrain.

LM10/4.5.5.2 Landing Radar Antenna Assembly Temperature Profile

Figure LM10/4.5.5-8 presents the landing radar antenna assembly typical high-temperature and low-temperature profiles for the LM-10 mission.

LM10/4.5.5.3 Landing Radar Mechanical Alignment

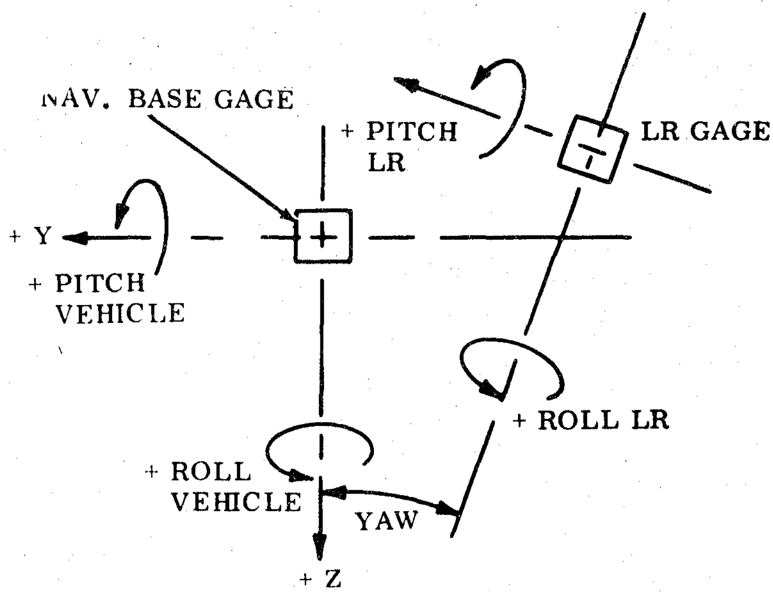

The landing radar antenna assembly alignment with respect to the vehicle coordinate system (nav. base gage) is the following:

	Position #2	Position #1
Pitch	+00°04'06"	-23°51'24"
Roll	-00°01'04"	-00°01'24"
Yaw	-06°07'26"	-06°07'54"

The landing radar antenna assembly alignment with respect to the inertial measurement unit coordinate system (LR-NB) - (IMU-NB) is the following:

	Position #2	Position #1
Pitch	+00°03'49" (3'49")	-23°51'41" (8'19")
Roll	-00°02'24" (-2'24")	-00°02'44" (-2'44")
Yaw	-06°05'09" (-5'09")	-06°05'37" (-5'37")

NOTE: The LR/IMU mechanical misalignments are indicated in parentheses.

LM10/4.5.5.4 Landing Radar Self Test

The following are the measured LR self test parameters for P-51. These data were recorded at KSC during FRT Mission-Sim. 0005 and TCP 0045.

1) Test Monitor

ALT XMTR	+3.50 Vdc
VEL XMTR	+3.55 Vdc

2) ALT/ALT Rate Meter

ALT (R)	8000 ft
ALT Rate ($\dot{R}$)	-480 ft/sec

3) LGC DSKY Display:

V16N66

R_1 (Slant Range)	+08281 ft
R_2 (Antenna Position)	+00001
R_3 (No Display)	0

V16N67

R_1 (Vxa)	-00495 ft/sec
R_2 (Vyz)	+01862 ft/sec
R_3 (Vza)	+01331 ft/sec

LM10/4.5.5.5 Landing Radar Reflectivity Model (NASA DATA SOURCE)

In conjunction with the LR reflectivity model, the following is a description of the Apollo 15 landing site (Hadley) for an approach azimuth of -91°.

Surface Range	Description
5000,000 ft to 106,600 ft	Smooth
106,600 ft to 29,700 ft	Rough
29,700 to landing site	Smooth

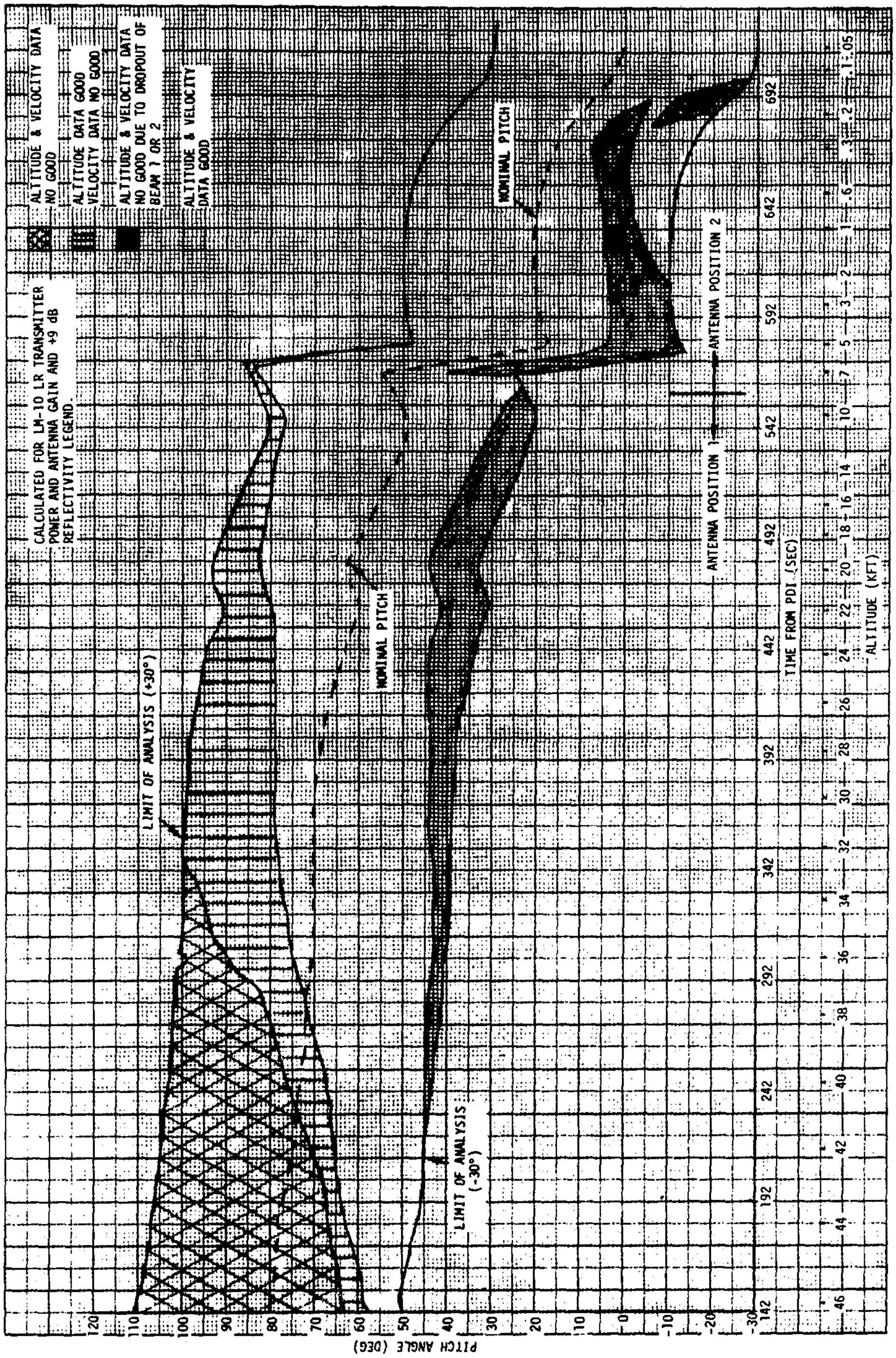

Figure LM10/4.5.5-1. LR Loss of Lock versus Pitch Angle (See Paragraph LM10/4.5.5.1.18)

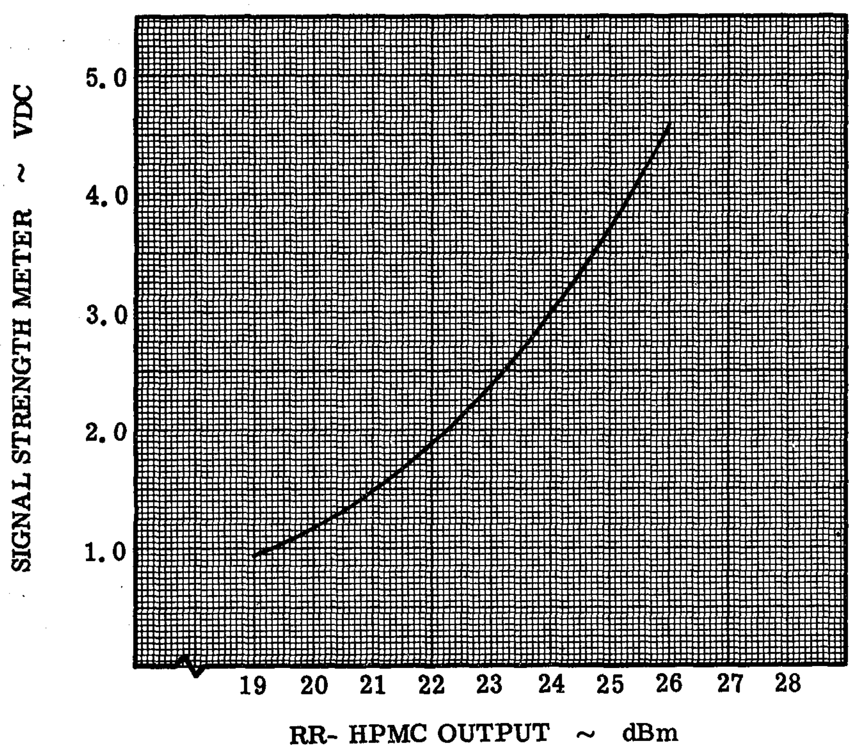

NOTE: HPMC OUTPUT VARIES INVERSELY WITH TEMPERATURE

Figure LM10/4.5.4-7 Power Monitor Meter Voltage vs RR RF Power
(See Para. LM10/4.5.4.4.13)

LM10/4.5.5.1.16 LR Power Monitor

The following is a calibration of the power monitor with LR P-51. These data were obtained from KSC testing during TCP 0045 and include antenna losses.

Transmitter	Power (dBm)	Power (MW)	Monitor (Vdc)	Calibration
Velocity	24.8	302	3.55	11.8×10^{-3} V/MW
Altimeter	21.2	132	3.5	26.5×10^{-3} V/MW

LM10/4.5.5.4 Landing Radar Self Test

The following are the measured LR self test parameters for P-51. These data were recorded at KSC during FRT Mission-Sim. 0005 and TCP 0045.

1) Test Monitor

ALT XMTR	+3.50 Vdc
VEL XMTR	+3.55 Vdc

2) ALT/ALT Rate Meter

ALT (R)	8000 ft
ALT Rate ($\dot{R}$)	-480 ft/sec

3) LGC DSKY Display:

V16N66

R_1 (Slant Range)	+08281 ft
R_2 (Antenna Position)	+00001
R_3 (No Display)	0

V16N67

R_1 (Vxa)	-00495 ft/sec
R_2 (Vyz)	+01862 ft/sec
R_3 (Vza)	+01331 ft/sec

LM10/4.5.5.5 Landing Radar Reflectivity Model (NASA DATA SOURCE)

In conjunction with the LR reflectivity model, the following is a description of the Apollo 15 landing site (Hadley) for an approach azimuth of -91°.

Surface Range	Description
500,000 ft to 106,600 ft	Smooth
106,600 ft to 29,700 ft	Rough
29,700 to landing site	Smooth

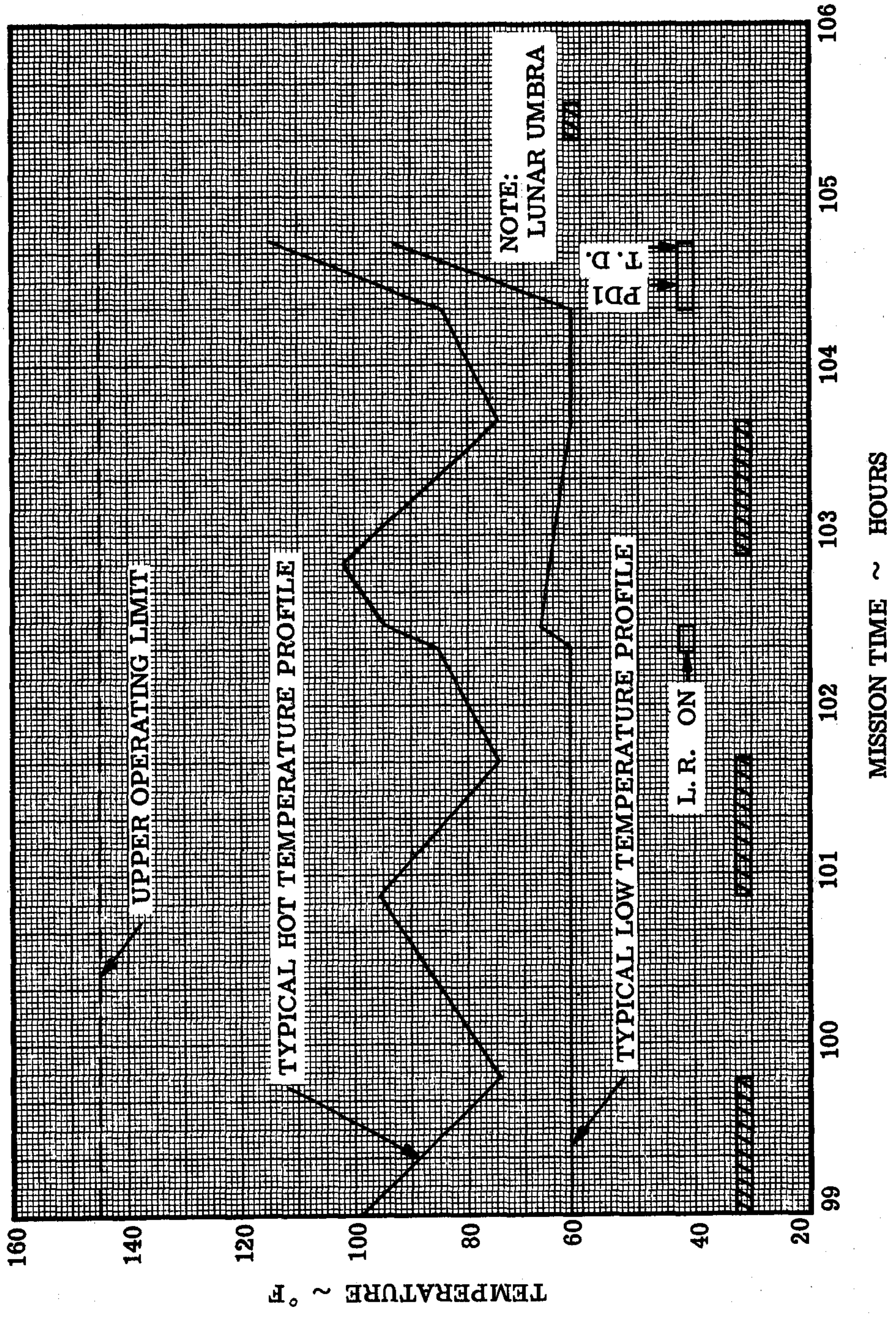

Figure LM 10/4.5.5-8. Landing Radar Antenna Assembly Flight Measurement GN 7563T LM 10 Mission (See Para LM 10/4.5.5.2)

LM10/4.6.1 Mission J-1 (LM-10) APS Preflight Analysis (NASA DATA SOURCE)

The APS mission duty cycle used in the following analysis is a lunar liftoff insertion burn followed by a short terminal phase initiation (TPI) burn. This duty cycle is similar to the Apollo 14 Mission APS duty cycle. The first and longest burn will be a lunar liftoff to orbit insertion maneuver. The planned vehicle thrust velocity change (ΔV) for that burn is 6055.5 fps. The second burn will be performed after a planned coast period of approximately 45 minutes from the end of the lunar liftoff burn. The planned ΔV for the TPI burn is 73.3 fps.

Table LM10/4.6.1-1 is a summary of APS physical characteristics. The vehicle weight characteristics and loaded propellant quantities were obtained from Reference 1 and are presented in Table LM10/4.6.1-2.

It should be noted that the effect of the reaction control system on APS performance has been neglected in this analysis. The RCS will affect APS performance in the following manner:

1) RCS propellant consumption (APS/RCS interconnect closed) will alter vehicle weight;

2) RCS propellant consumption through the APS/RCS interconnect will decrease the propellant available to the APS and thus shorten the APS burn time available and decrease the ΔV capability. Also, since the RCS operates at a mixture ratio different from that of the APS, the mixture ratio from the APS tanks will be changed. (The mixture ratio of the ascent engine will not be significantly changed).

The engine performance characterization consists of C* (characteristic exhaust velocity), C_f (thrust coefficient), A_t (throat area), and interface-to-chamber fluid flow resistances defined as functions of engine test data, and (where applicable) predicted values of P_c (chamber pressure), μ (mixture ratio), T (propellant temperature), t_b (engine burn time), t_{acc} (accumulated time on chamber), and helium saturation into the propellants.

The helium regulator characterization used was the nominal Class I primary regulator expected performance.

The liquid propellant bulk temperatures at the start of the APS burn were assumed to be 70°F for both oxidizer and fuel.

LM10/4.6.1 (Continued)

The nominal mixture ratio of 1.600 is for nonsaturated propellant conditions prior to ignition. If the tanks are pressurized earlier than is now planned, causing helium saturation of the propellants, the mixture ratio will shift to 1.593.

Graphs from the simulation of the LM-10 APS nominal performance under the assumptions and conditions discussed above are presented in Figures LM10/4.6.1-1 through LM10/4.6.1-4.

APS performance data have been tabulated for both APS burns and are presented in Table LM10/4.6.1-3.

An uncertainty propagation dispersion analysis was conducted using root-sum-squaring techniques to determine APS performance dispersions. The uncertainties associated with the basic parameters defining propulsion system operation are listed in Table LM10/4.6.1-4. The values given in Table LM10/4.6.1-4 have been derived from Rocketdyne and Grumman inputs by the methods discussed in Reference 2. These values express the uncertainty of the various parameters as 3-sigma at a 50 percent confidence level. These values were used as input to establish the performance dispersions included as part of Table LM10/4.6.1-3.

The data presented herein are valid for nominal system conditions. The values of propulsion system parameters presented herein do not represent boundary conditions of operation for the system and, therefore, should not be used as limit values.

For propellant budgeting purposes the recommended limit values of mixture ratio shift resulting from APS malfunctions are: -0.018, +0.010 mixture ratio units from the nominal.

References

1. CSM/LM Spacecraft Operational Data Book, Volume III, Mass Properties, SNA-8-D-027(III) REV 2, Amendment 94, 10 December 1970.

2. "Propulsion Systems Dispersion Analysis and Optimum Propellant Management," TRW Technical Report 11176-H060-RO-00, R. K. M. Seto, 28 October 1968.

Table LM10/4.6.1-1. APS Engine and Feed System Physical Characteristics

Engine(1)	
Engine No.	Rocketdyne S/N 0014 C
Injector No.	Rocketdyne S/N 4097734
Initial Chamber Throat Area (in^2)	16.378
Nozzle Exit Area (in^2)	749.531
Initial Expansion Ratio	45.764
Injector Resistance (lb_f-sec^2/lb_m-ft^5)@ time zero and 70°F	
Oxidizer	12420.7
Fuel	19886.7
Feed System	
Total Volume (Pressurized, Check Valves to Engine Interface) (ft^3)(2)	
Oxidizer	36.95
Fuel	37.00
Resistance, Tank Bottom to Engine Interface (lb_f-sec^2/lb_m-ft^5) at 70°F(3)	
Oxidizer	2459.52
Fuel	4065.12

(1) Rocketdyne Log Book, "Acceptance Test Data Package for Rocket Engine Assembly - Ascent LM-Part No. RS000580-001-04, Serial No. 0014," 8 July 1969.

(2) NASA Memorandum EP23 - 46 - 69, "Propellant Load Parameters for the DPS and APS of LM-5 Through LM-9 and the Estimated Parameters for LM-10 and Subsequent," from EP/Chief, Propulsion and Power Division to PD/Chief, Systems Engineering Division.

(3) GAC Memorandum LMO-271-194, "A/S Hydraulic Resistance LM-8 Thru LM-12 As Per NASA/MSC Data Request Under CCA #467," T. Laterra, 26 October 1970.

Table LM10/4.6.1-2 APS Weight Characteristics

Weight APS at Lunar Liftoff, lbm: (1)		
Inert Weight		5,638.7
APS Propellant Loaded & at Lunar Liftoff		
Oxidizer	3,225.8	
Fuel	2,008.6	
Total APS Propellant		5,234.4
TOTAL		10,873.1

Unusable Propellant, lbm:	Oxidizer	Fuel
Trapped Propellant (2)		
Fill and Drain Lines	0.8	0.2
Engine (to SOV)	0.3	0.2
Interconnect to RCS	2.3	1.6
Isolation Squib Bypass and Miscellaneous	0.1	0.2
Subtotal	3.5	2.2
Residuals in Tank (3)		
Tank Wetting	1.0	1.0
"0" G Can	2.0	1.2
Thrust Vector Deviation	0.6	0.4
Unporting Prevention	11.3	7.1
Propellant Vapor	13.8	1.0
Subtotal	28.7	10.7
Consumed by RCS through (4) Interconnect	--	--
Transient Operation (3)	3.7	3.1
Subtotal	3.7	3.1
Total Unusable Propellant	35.9	16.0

(1) "CSM/LM Spacecraft Operational Data Book," Volume III, Mass Properties, SNA-8-D-027(III), Revision 2, Amendment 94, 10 December 1970.
(2) "CSM/LM Spacecraft Operational Data Book," Volume III, Mass Properties, SNA-8-D-027(III), Revision 2, Amendment 82, 18 June 1970.
(3) "CSM/LM Spacecraft Operational Data Book," Volume III, Mass Properties, SNA-8-D-027(III), Revision 2, Amendment 88, 5 October 1970.
(4) RCS usage of APS propellants has not been included in this simulation.

Table LM10/4.6.1-3. Mission J-1 Preflight Performance Prediction Summary

Parameter	First Burn			Second Burn	
	Orbit Insertion Effective Performance	Burn to Depletion Effective Performance	First Burn Dispersions 3 Sigma	TPI Effective Performance	Second Burn Dispersions 3 Sigma
Thrust (lbf)	3491.6	3492.4	106.4	3640.3	130.6
Specific Impulse (sec)	309.9	309.9	3.50	306.9	5.1
Mixture Ratio	1.600	1.601	.026	1.683	.048
Oxidizer Flowrate (lbm/sec)	6.933	6.936	.204	7.440	.281
Fuel Flowrate (lbm/sec)	4.332	4.333	.126	4.421	.131
Oxidizer Remaining at End of Burn (lbm)	180.1	—	—	146.4	—
Fuel Remaining at End of Burn (lbm)	105.4	—	—	85.4	—

Table LM10/4.6.1-4. APS Simulation Parameters Uncertainties

FIRST BURN AND SECOND BURN		
PARAMETER	Three Standard Deviations (3σ)	Three Standard Deviations (%)
Characteristic Exhaust Velocity (C^*)(1), ft/sec	61.8	1.07
Specific Impulse (I_{sp})(1), lbf-sec/lbm	3.50	1.12
Engine Oxidizer Resistance(1), lbf-sec^2/lbm-ft^5	334.	2.7
Engine Fuel Resistance (1), lbf-sec^2/lbm-ft^5	499.	2.5
Propellant Feed System Oxidizer Resistance, lbf-sec^2/lbm-ft^5	29.37	1.19
Propellant Feed System Fuel Resistance, lbf-sec^2/lbm-ft^5	38.4	0.94
Propellant Tank Ullage Pressures, psia	4.0	2.22
Propellant Tank Ullage ΔP,psia	0.5	----
Propellant Bulk Temperatures,°F	5.0	7.14
Propellant Bulk ΔT,°F	1.5	----
Ablative Engine Throat Area,in^2	0.639	3.91
SECOND BURN ONLY (2)		
Specific Impulse Degradation Between First and Second Burn - sec	3.69	1.20
Throat Area - in^2	0.2	1.22
Propellant Tank Pressures - psia		
Oxidizer	5.	2.58
Fuel	2.	1.06

(1) Engine parameters at standard interface conditions include characterization uncertainties, instrumentation uncertainties, and engine repeatability.

(2) Refers to additional uncertainties peculiar to the second burn only.

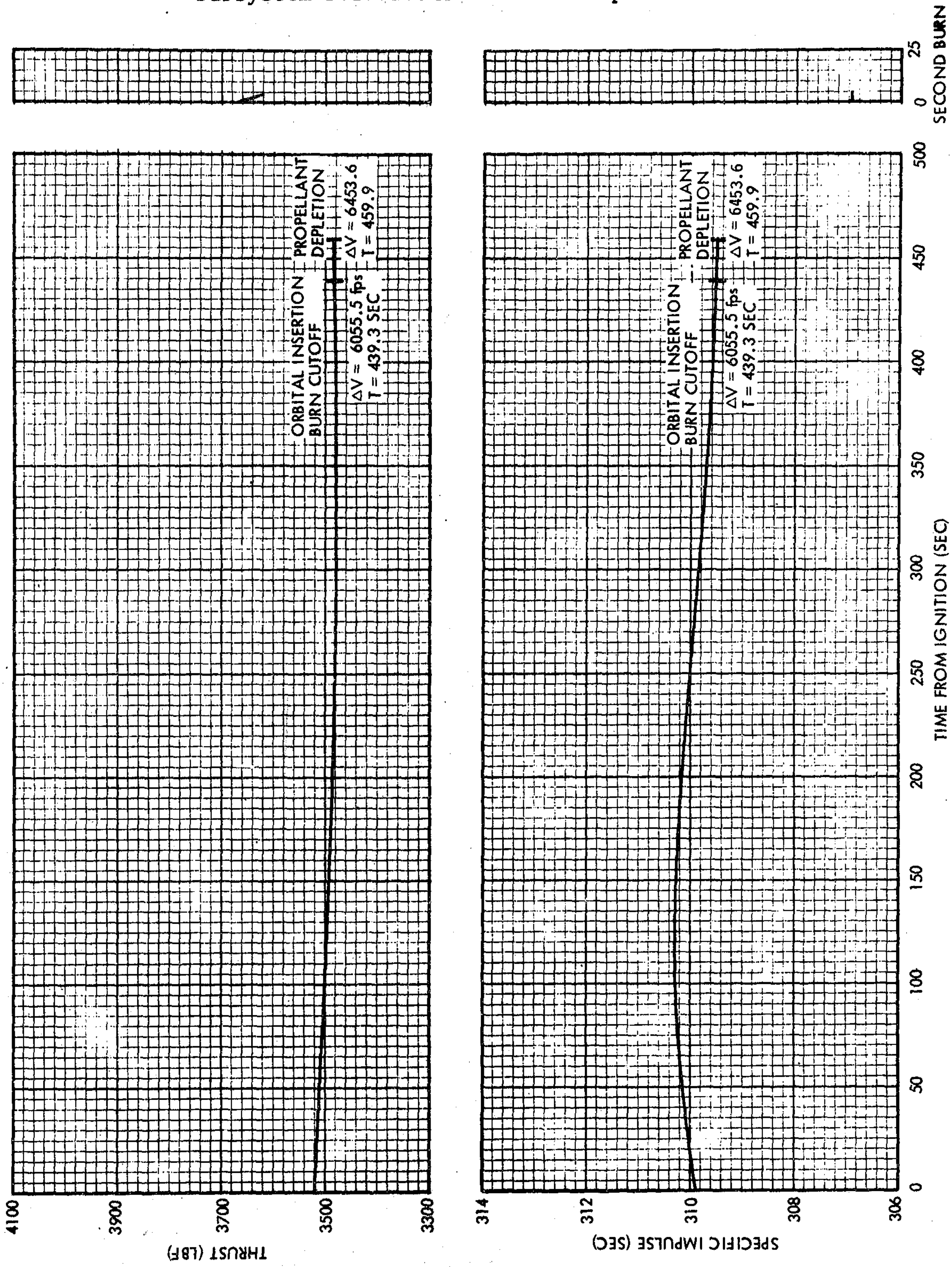

Figure LM10/4.6.1-1. Mission J-1 APS Preflight Performance Prediction - Thrust and Specific Impulse Vs. Time

(NASA DATA SOURCE)

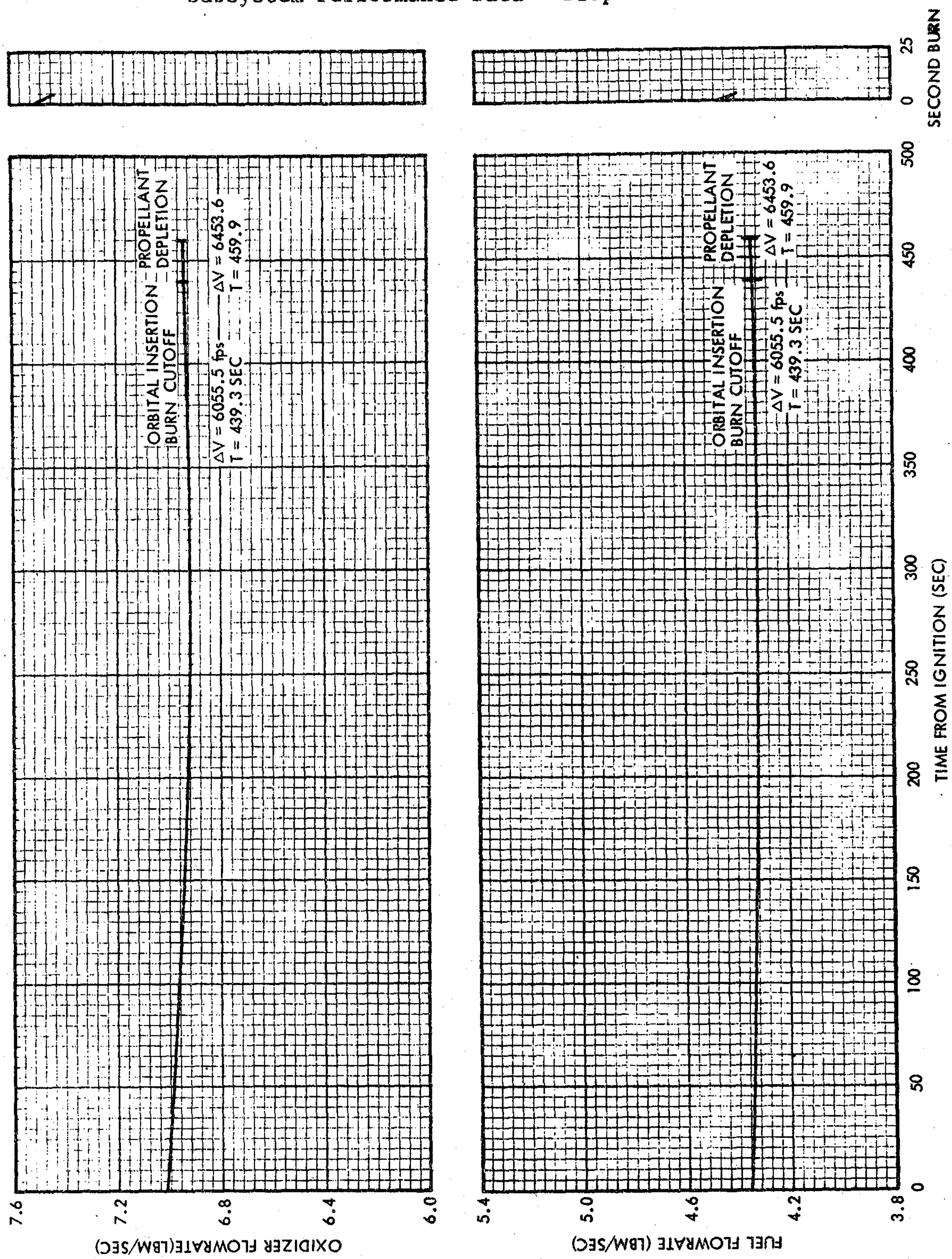

Figure LM10/4.6.1-2. Mission J-1 APS Preflight Performance Prediction - Oxidizer and Fuel Flowrates Vs. Time

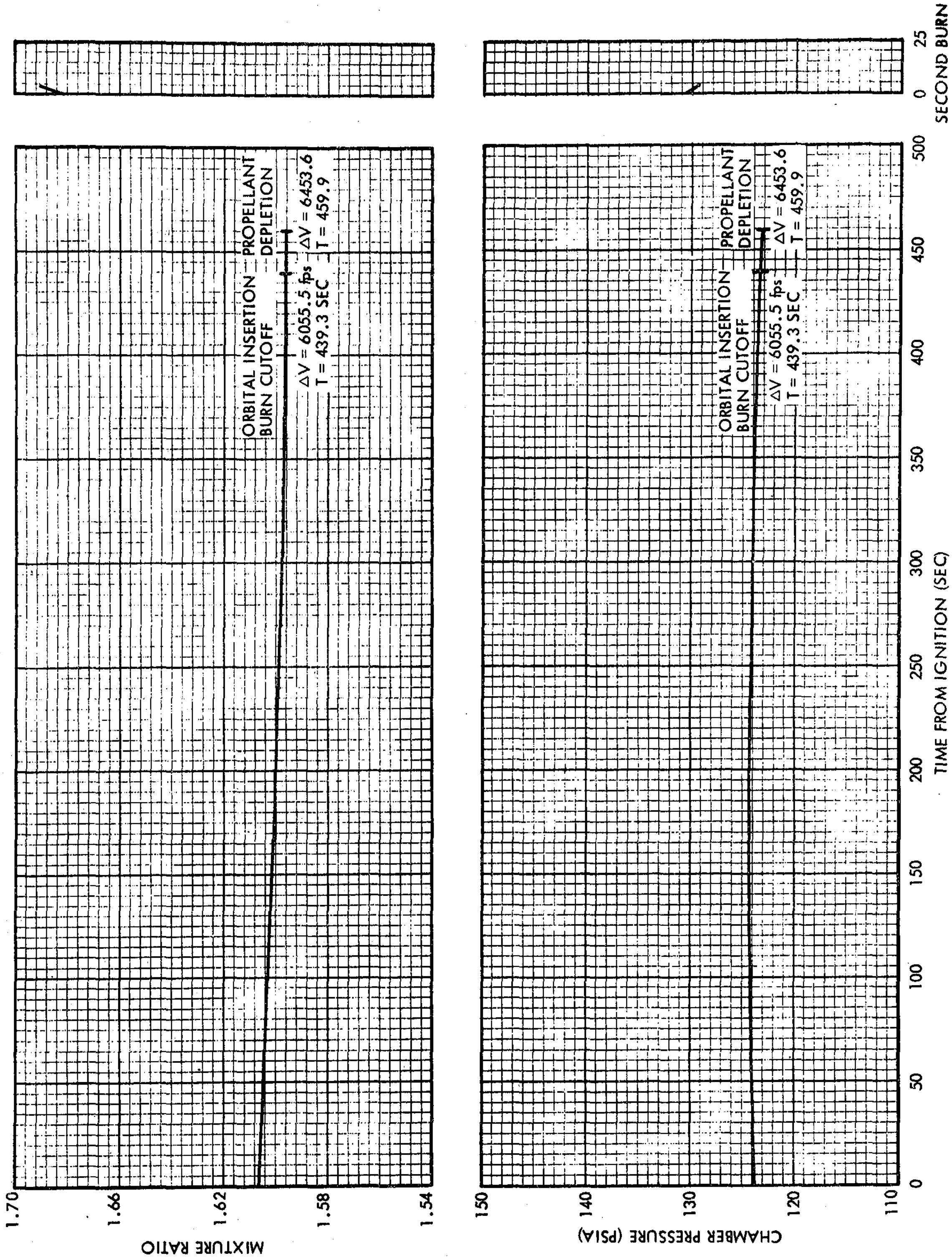

Figure LM10/4.6.1-3. Mission J-1 APS Preflight Performance Prediction - Chamber Pressure and Mixture Ratio Vs. Time

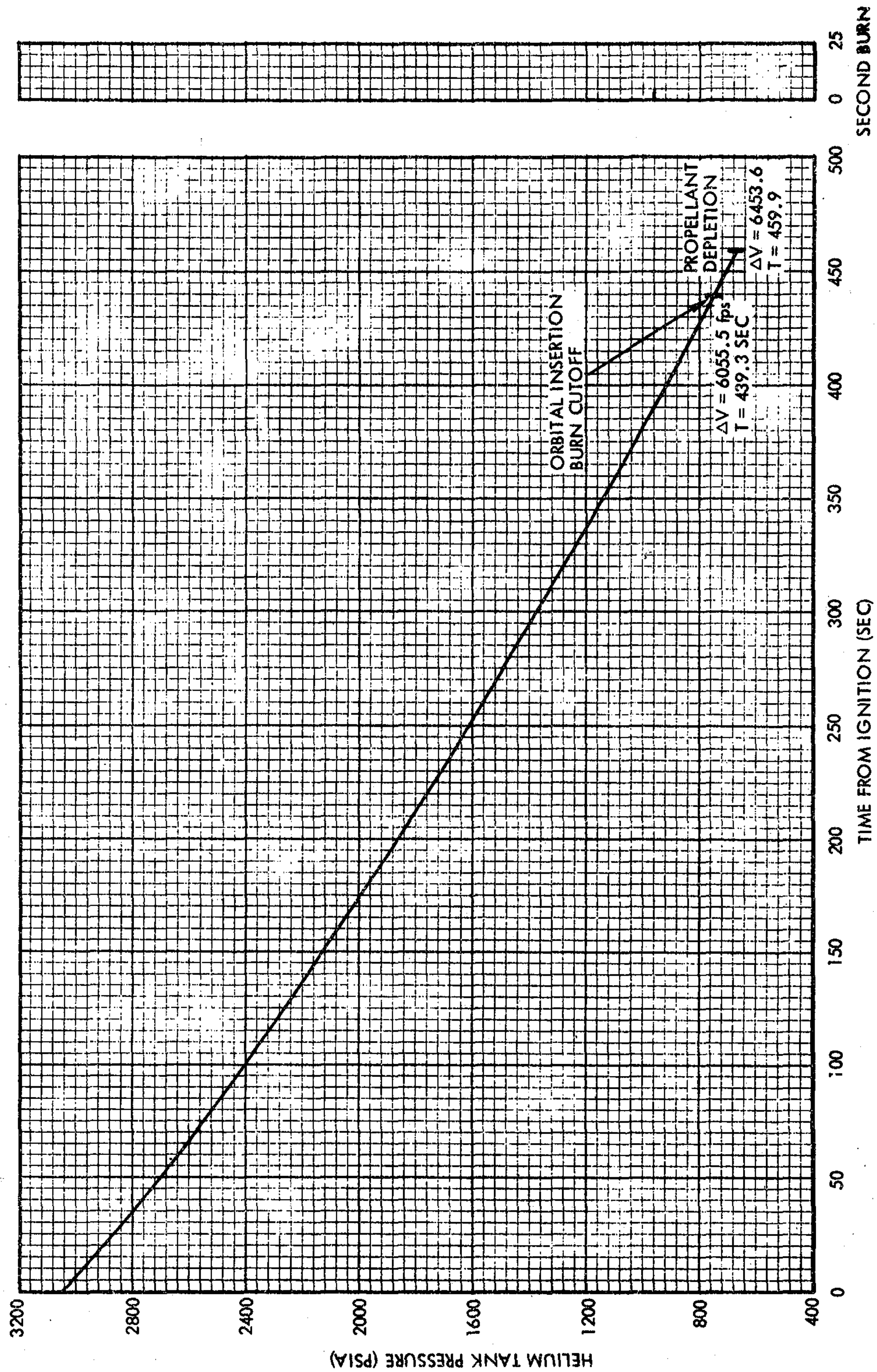

Figure LM10/4.6.1-4. Mission J-1 APS Preflight Performance Prediction - Helium Tank Pressure Vs. Time

LM10/4.6.8 Thrust Vector Change with Burn Time

The initial thrust vector displacement for the LM-10 engine, R/D No. 0014C, is Y = -0.03 inches, Z = -0.027 inches. This information is based on R/D acceptance tests No. 374-194 and 374-195 conducted on 4/8/69 and 4/9/69, respectively.

LM10/4.6.9 Preflight Thermal Analysis of the APS

. The analysis presented in the basic book is still applicable and will be slightly conservative (higher temperature).

LM10/4.6.12 Ascent Propulsion System Regulator Performance

Figure LM10/4.6.12-1 shows performance characteristics for the LM-10 Class I primary regulator, Serial No. 158. This is a flight prediction based on KSC check-out at 3500 psia inlet pressure.

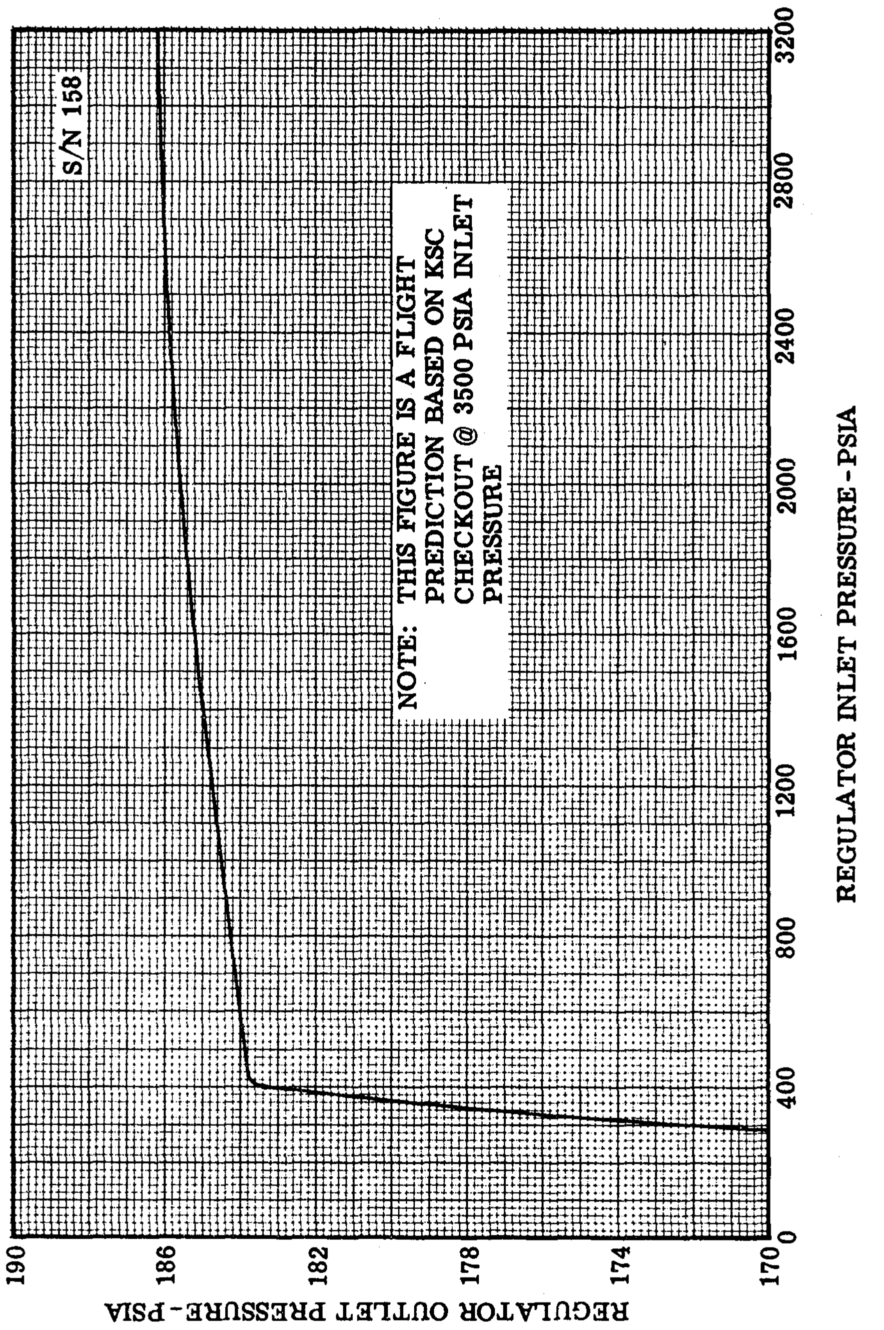

Figure LM10/4.6.12-1. **Ascent Propulsion System Regulation Performance**

LM10/4.7.1 Mission J1 (LM-10) DPS Preflight Analysis (NASA DATA SOURCE)

The data presented herein are valid only for the system at nominal conditions and do not represent the boundary conditions of operation for the system. Therefore, these values should not be used as limit values.

The nominal mission duty cycle for the Mission J1/LM-10 DPS is presented in Figure LM10/4.7.1-1. The spacecraft weight and propellant loading used in the simulation are given in Table LM10/4.7.1-1 (target loads). Descent engine and feed system physical characteristics are shown in Table LM10/4.7.1-2.

It should be noted that all performance parameters presented are for DPS operation only, and do not include RCS contributions to thrust or velocity gain. The predicted RCS propellant usage was simulated during the burns as a weight change.

The helium regulator characteristics used to establish the DPS propellant tank ullage pressures were derived from GAEC PIT data. Propellant temperatures measured during Missions G and H1(68°F) were assumed to be representative of those to be expected during Mission J1.

A summary of the Mission J1 (LM-10) performance prediction is given in Table LM10/4.7.1-3 and Figures LM10/4.7.1-1 through LM10/4.7.1-9. Figure LM10/4.7.1-10 presents the engine related effective specific impulse as a function of burn time. A prediction of the supercritical helium tank pressure and mass profiles are presented in Figures LM10/4.7.1-11 and LM10/4.7.1-12. The dispersions associated with thrust, specific impulse, and mixture ratio are given in Figures LM10/4.7.1-13 through LM10/4.7.1-15, respectively.

The value of the engine effective specific impulse, which does not include the effect of the consumables other than propellant, was 304.8 seconds. It should be noted that the effective specific impulse is not only a function of engine performance but is dependent on vehicle initial mass, mass changes with time, and velocity requirements. Substantial deviations from the conditions of the simulation will invalidate the use of this effective specific impulse. The 1-sigma variation in effective engine specific impulse is ±0.6 seconds for the simulation. The effective vehicle mixture ratio is 1.593 and the 1-sigma variation is ±0.004.

The LM-10 DPS shutoff valve malfunction characterization data are as follows: an AB valve malfunction will result in shifts of +0.006, -0.10 seconds, and -221 lbf for mixture ratio, specific impulse, and

LM10/4.7.1 (Continued)

thrust, respectively; while a CD valve malfunction will result in shifts of -0.011, -0.87 seconds, and -202 lbf, respectively, for the given parameters. These data are applicable to FTP operation only.

During the nominal mission, the low-level sensor should not be activated prior to the nominal touchdown time (718 seconds after descent burn ignition). If the vehicle is hovering the fuel low-level sensor (Tank 2) should be activated at approximately 735 seconds (assuming a nominal GDA trim angle of 0.8°) (See Table LM10/4.7.1-1). The calculation does not account for dispersion in GDA angle. The approximate hover time from the low-level signal to oxidizer depletion is predicted to be 118 seconds or 853 seconds after engine ignition.

A docked LM-10 Descent Propulsion System (DPS) burn-to-propellant depletion simulation was made using the Descent Ascent Monte Carlo Program (DAMP).

It was assumed that at engine ignition, the LM was docked with the CSM. The mission duty cycle consisted of a minimum throttle (approximately 12.9% of full thrust) segment of 6 seconds, 20 seconds at 40% of full throttle, with the remainder of the burn at the fixed throttle position (FTP). The burn was terminated when either the usable oxidizer or fuel was depleted.

The initial spacecraft weight was assumed to be 102,751.8 lbm with 11,974.8 lbm and 7,520.4 lbm of tanked oxidizer and fuel, respectively. Depletion occurs when the tanked quantities reach 38.0 lbm for oxidizer or 18.8 lbm for fuel.

At 611 seconds after ignition, oxidizer depletion occured with approximately 42.0 lbm of usable fuel remaining. The velocity change for the burn was 2,047 ft/sec. The effective engine specific impulse, which neglects consumables other than propellants that are expelled from the spacecraft during the burn, was 304.0 seconds. The effective vehicle specific impulse was 302.8 seconds. The average mixture ratio was 1.595.

Figures LM10/4.7.1-16 through LM10/4.7.1-25 present DPS engine parameters for the burn.

Chamber pressure versus commanded thrust for zero, nominal, 3-σ predicted, and maximum allowable throat erosion (52%) is shown in Figure LM10/4.7.1-26.

Table LM10/4.7.1-1

LM-10 Descent Propulsion System Weight Characteristics[1]

SPACECRAFT WEIGHTS (lbm)

DPS Stage Inert			6153.3
Loaded Propellant			
DPS Oxidizer	12023.7	19571.4	
DPS Fuel	7547.7		
Loaded APS Stage with Crew			10901.6
LM Weight at P.D.I.			36626.3

UNUSUABLE PROPELLANTS

	Oxidizer	Fuel	
OUTSIDE TANKS	(21.4)[2]	(10.9)[2]	
Fill Lines	0.2	0.1	
Engine	12.0	6.0	
Branch Lines	8.5	4.1	
Isolated SQ Bypass and Miscellaneous	0.7	0.7	
INSIDE TANKS	(65.5)[2]	(35.3)[2]	
Tank Wetting	2.0	2.0	
Zero-g Can	7.2	4.5	
Center of Gravity (Thrust Vector)	29.6	16.7	
Engine and Valve Operation	2.6	2.9	
Propellant Vapor	19.0	2.5	
Branch Line Orificing	5.1	6.7	
TOTAL UNUSUABLES	86.9	46.2	133.1

NOTE: Unusables are defined as that propellant which is physically unavailable to the engine.

[1] NASA SNA-8-D-027(III) Rev. 3, "CSM/LM Spacecraft Operational Data Book," Vol. III, Mass Properties, 1 April 1971, Amendment 106, 22 June 1971.

[2] Parentheses present total for heading.

Table LM10/4.7.1-2

LM-10 Descent Propulsion Engine
and Feed System Physical Characteristics

ENGINE	
Engine Number	1046
Chamber Throat Area, In^2	53.495 (1)
Nozzle Exit Area, In^2	2937.6 (3)
Nozzle Expansion Ratio	54.0 (3)
FEED SYSTEM	
Oxidizer Propellant Tanks, Total Ambient (4) Volume, ft^3	135.4 (3)
Fuel Propellant Tanks, Total Ambient Volume, ft^3	135.4 (3)
Oxidizer Tank to Interface Resistance, $\frac{lbf\text{-}ft^5}{lbm\text{-}sec^2}$	413.194 (2)
Fuel Tank to Interface Resistance, $\frac{lbf\text{-}ft^5}{lbm\text{-}sec^2}$	672.674 (2)

(1) TRW IOC 4600.12.10-62, "Acceptance Test Performance Report, S/N 1046," F. E. Amon, 1 April 1970

(2) GAEC Cold Flow Tests

(3) Approximate Values

(4) 14.7 psia and 70°F

Table LM10/4.7.1-3. Mission J-1 Preflight Performance Prediction Summary

PARAMETER	Start of Descent Burn[1]	30 Seconds of Descent Burn				326 Seconds of Descent Burn			
	Nominal Performance	Nominal Performance	Standard Deviation (1σ)	Standard Deviation (%)	3σ Minimum	Nominal Performance	Standard Deviation (1σ)	Standard Deviation (%)	3σ Minimum
Throttle Position (%)	13.21	FTP	FTP	FTP	FTP	FTP	FTP	FTP	FTP
ISP (lbf-sec/lbm)	299.2	306.4	.30	.10	305.5	304.4	.4	.13	303.2
F (lbf)	1378	9899	30.	.29	9809	9962	31.	.29	9869
MR (o/f)	1.603	1.597	.0016	.10	1.592	1.595	.0017	.10	1.590
P_c (psia)	16.44	105.24	---	---	---	101.52	---	---	---
$\dot{W}_o$ (lbm/sec)	2.835	19.87	.060	.30	19.68	20.12	.072	.36	19.90
$\dot{W}_f$ (lbm/sec)	1.769	12.44	.035	.28	12.34	12.61	.044	.35	12.48
WO[2] (lbm)	11925	11837	10.9	.09	11804	5919	19.9	.34	5859
WF[2] (lbm)	7490	7434	6.5	.09	7414	3727	11.2	.30	3693

PARAMETER	426 Seconds	446 Seconds	526 Seconds	586 Seconds	718 Seconds Touchdown
	Nominal Performance	Nominal Performance	Nominal Performance	Nominal Performance	Nominal Performance
Throttle Position (%)	FTP	56.60	55.50	48.46	29.02
ISP (lbf-sec/lbm)	303.7	304.6	303.8	301.3	298.3
F (lbf)	9983	5968	5856	5114	3056
MR (o/f)	1.594	1.584	1.586	1.586	1.583
P_c (psia)	100.20	60.47	58.52	50.94	30.37
$\dot{W}_o$ (lbm/sec)	20.20	12.01	11.82	10.41	6.28
$\dot{W}_f$ (lbm/sec)	12.67	7.58	7.46	6.56	3.97
WO[2] (lbm)	3904	3534	2582	1892	862
WF[2] (lbm)	2463	2231	1631	1196	545

[1]Estimated minimum throttle position and performance at flight interface conditions.
[2]Propellant remaining in the tank (including unusable).

Table LM10/4.7.1-3. (Continued)
Mission J1 Final DPS Preflight Performance Prediction Summary (Performance During Hover-To-Depletion)

Parameter	782 seconds	853 seconds Depletion (Ox)
	Nominal Performance	Nominal Performance
Throttle Position %	27.99	26.92
ISP	298.0	297.5
F	2945	2829
MR	1.584	1.586
Pc	28.96	27.50
$\dot{W}o$	6.059	5.832
$\dot{W}f$	3.826	3.678
WO	461.41	39.12
WF	292.36	25.84

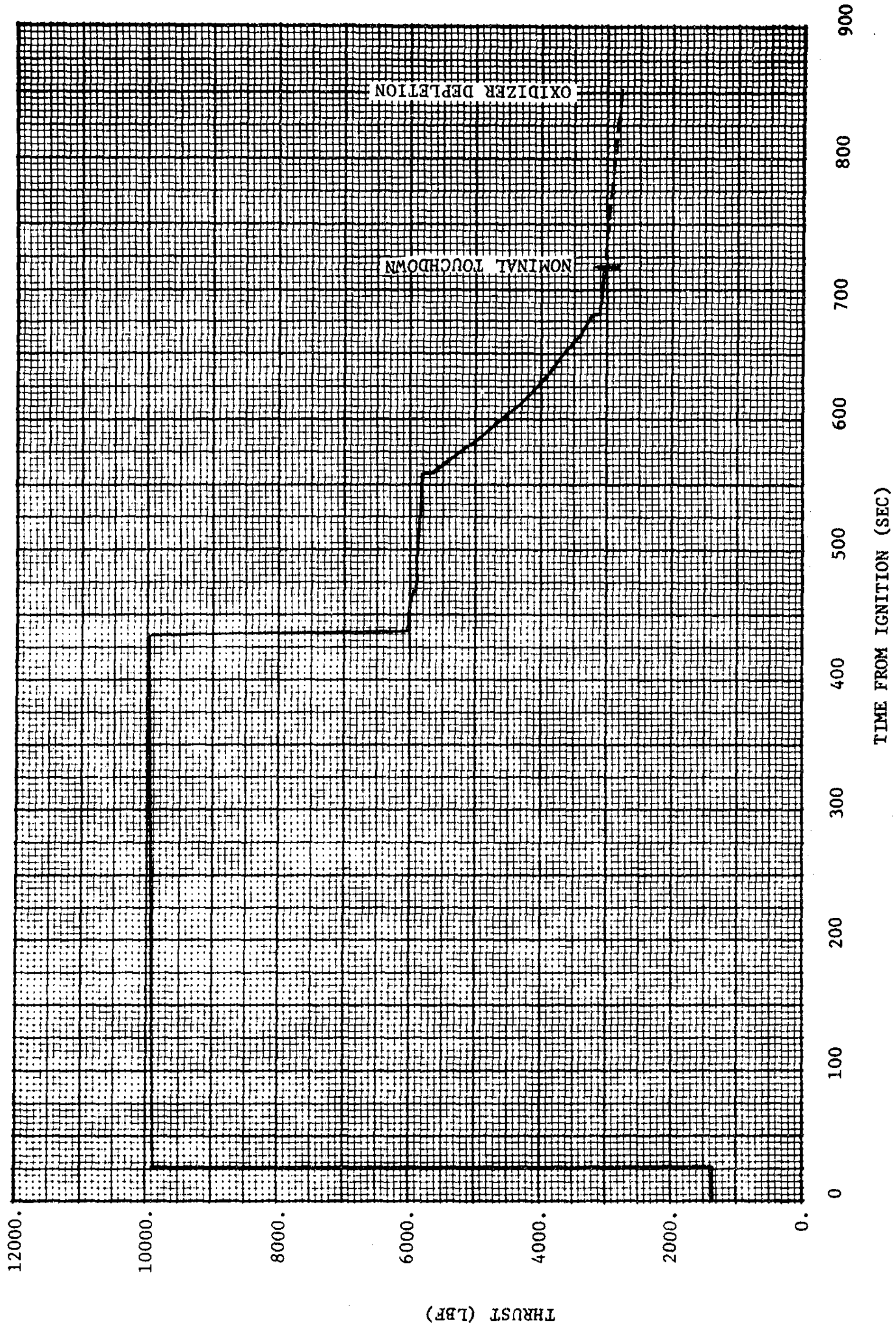

Figure LM10/4.7.1-1 Mission J1 Final DPS Preflight Performance Prediction - Thrust Vs. Time

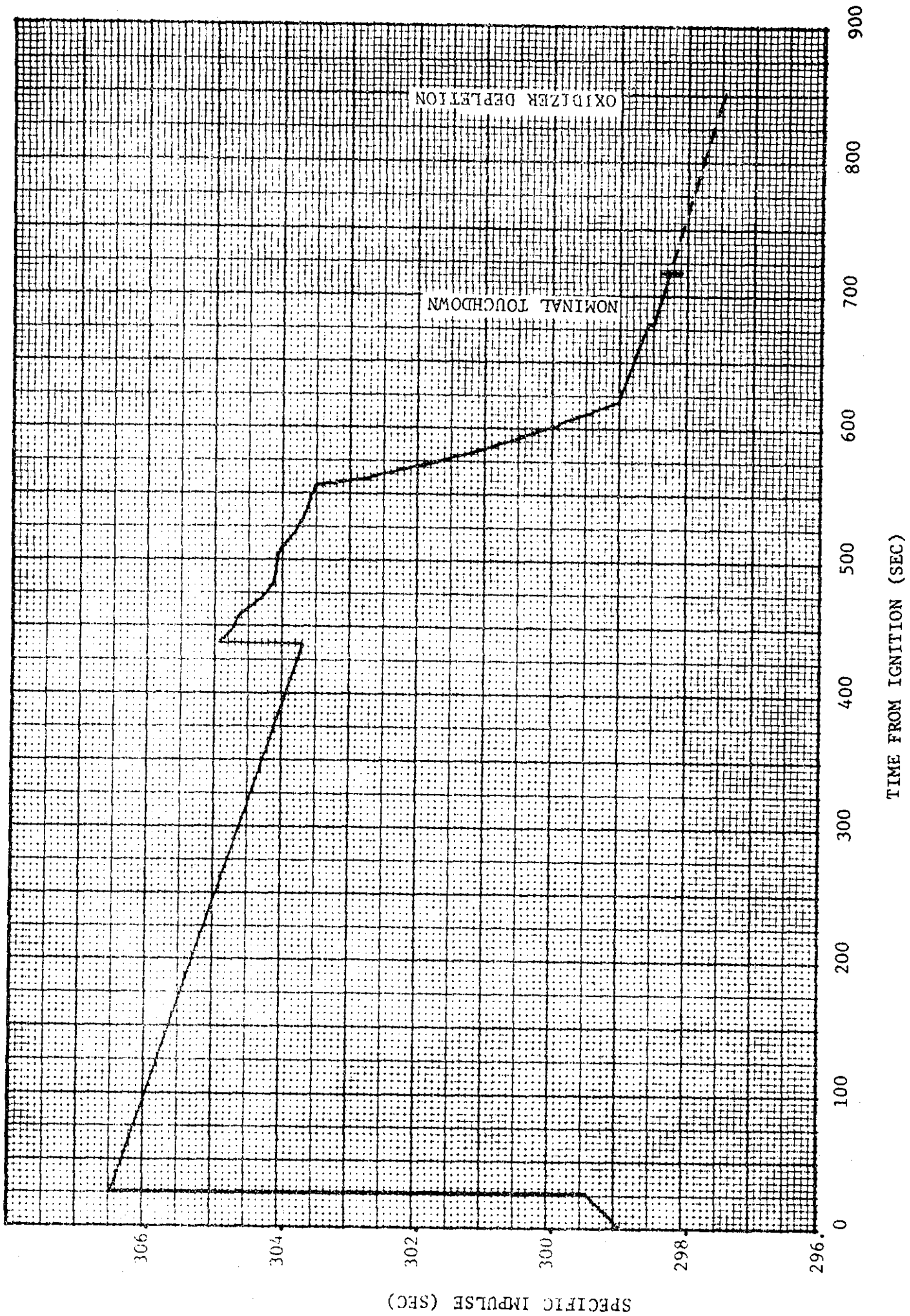

Figure LM10/4.7.1-2 Mission J1 Final DPS Preflight Performance Prediction - Specific Impulse Vs. Time

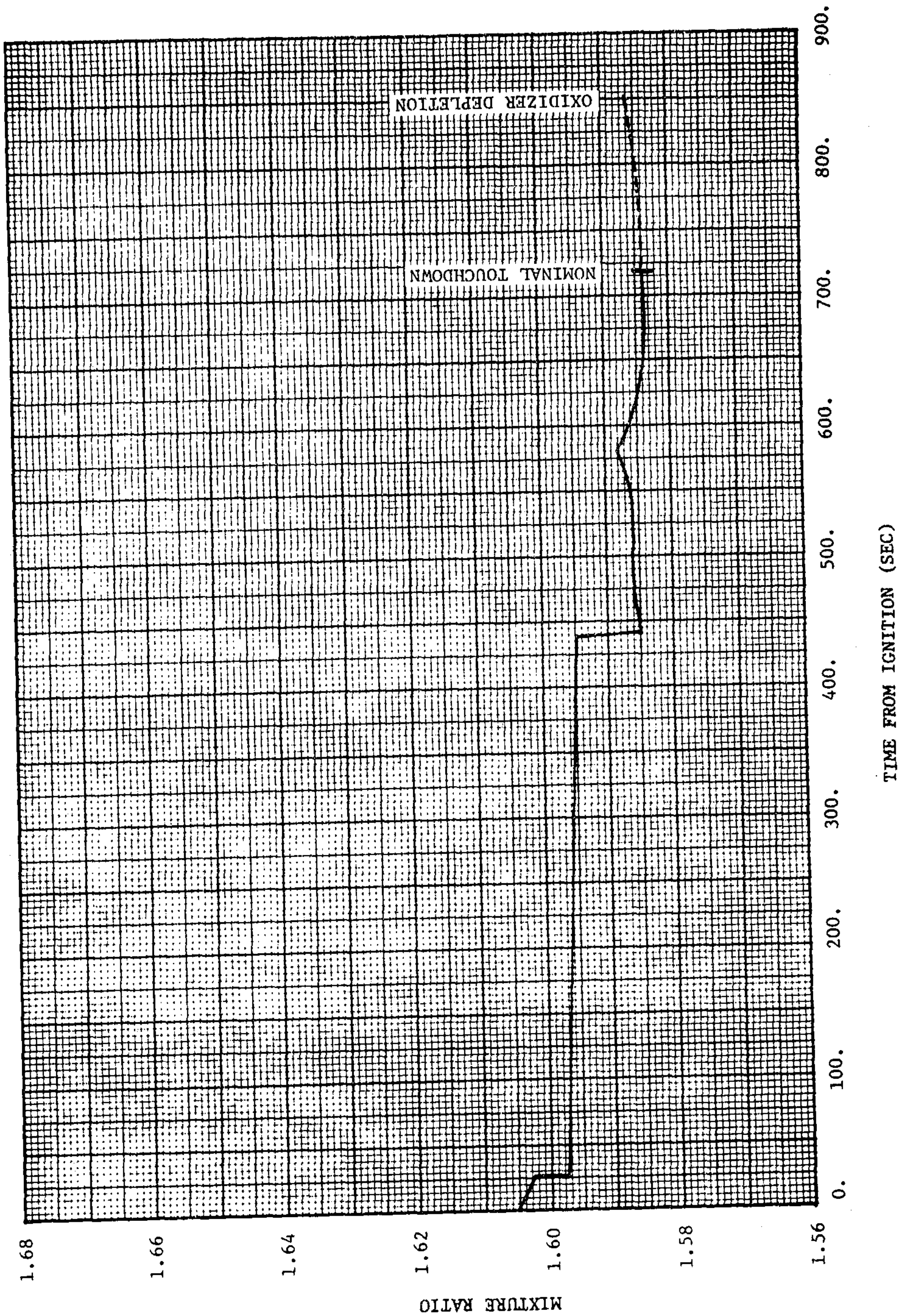

Figure LM10/4.7.1-3 Mission J1 Final DPS Preflight Performance Prediction - Mixture Ratio Vs. Time

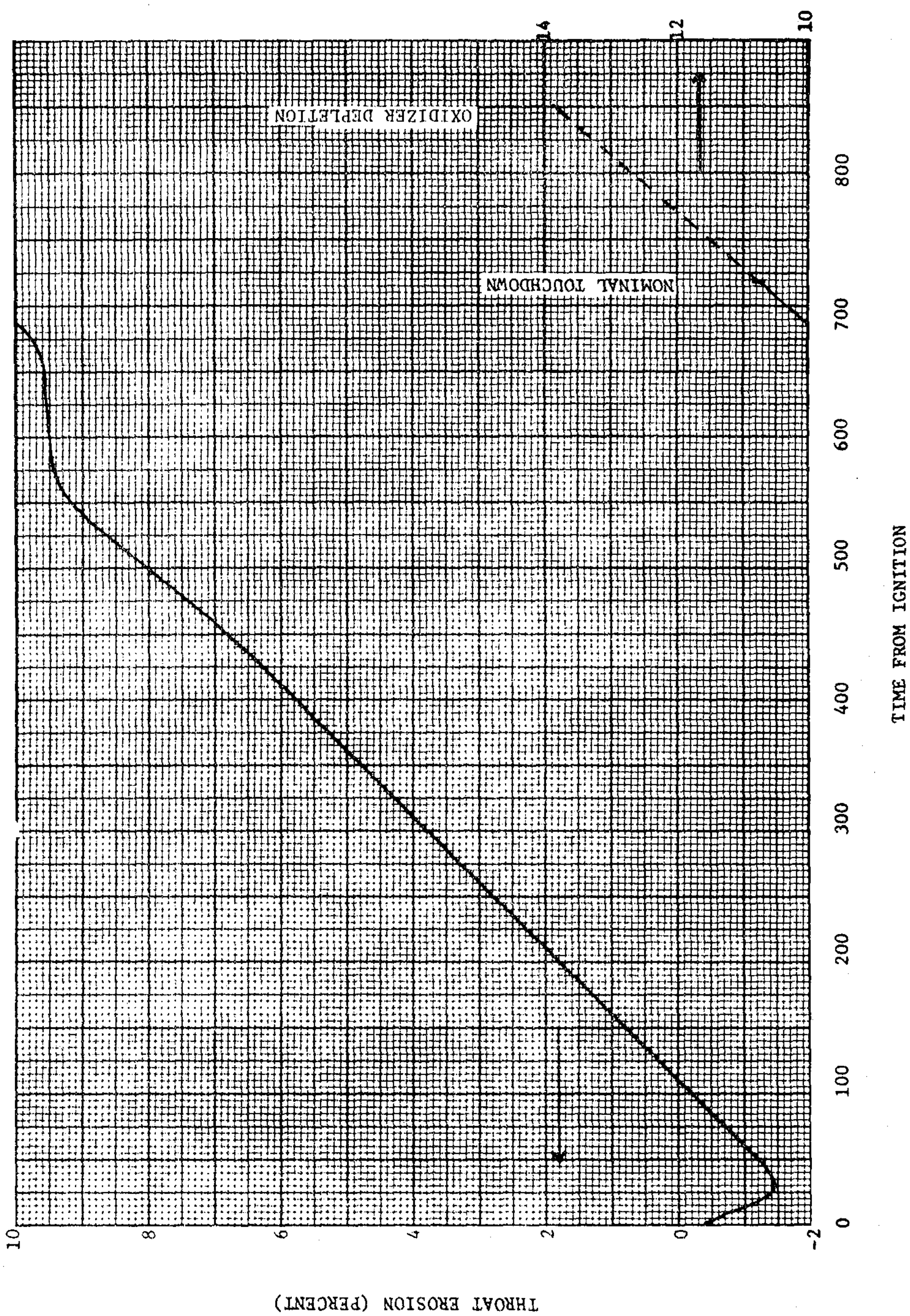

Figure LM10/4.7.1-4 Mission J1 Final DPS Preflight Performance Prediction - Throat Erosion Vs. Time

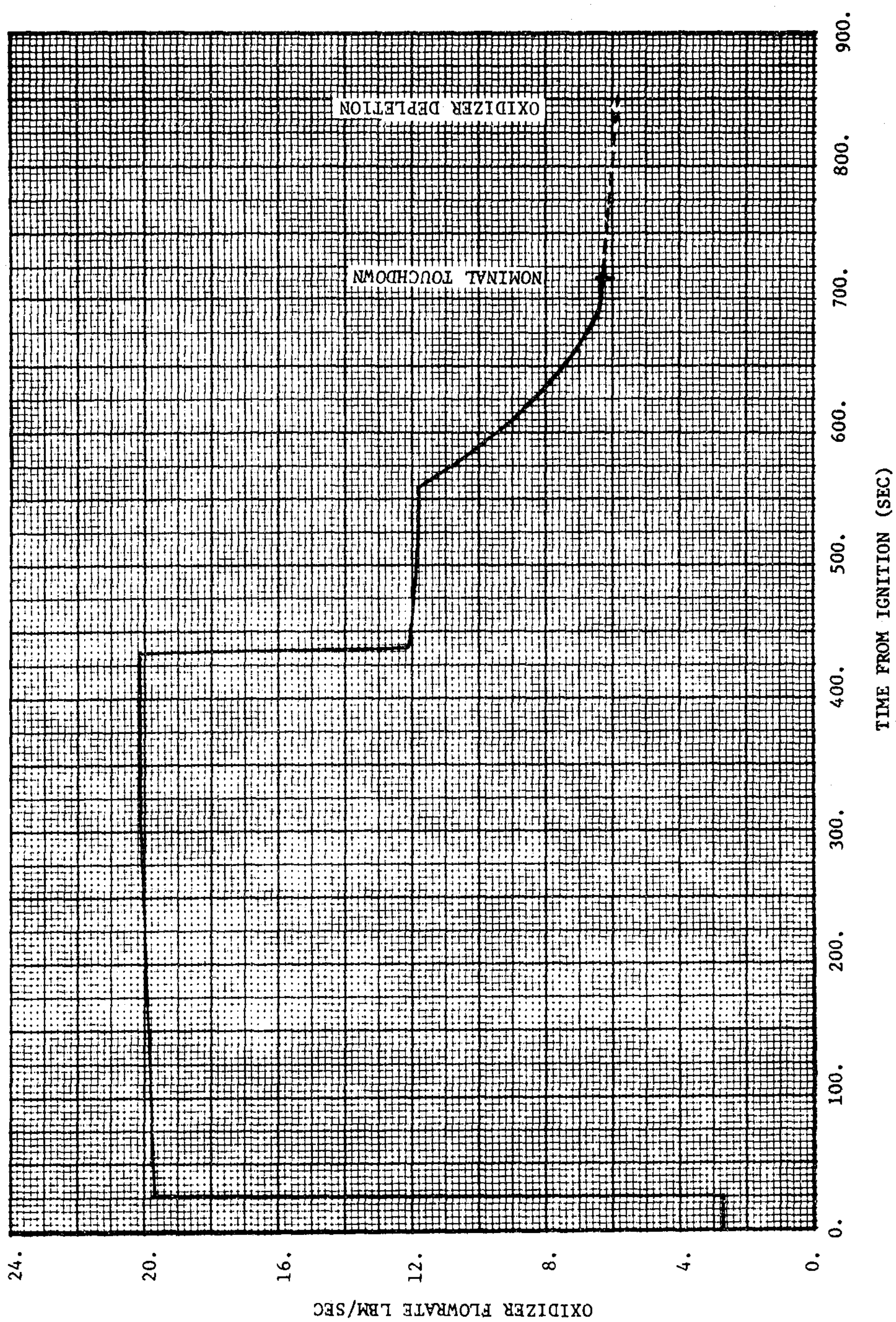

Figure LM10/4.7.1-5 Mission J1 Final DPS Preflight Performance Prediction - Oxidizer Flow Rate Vs. Time

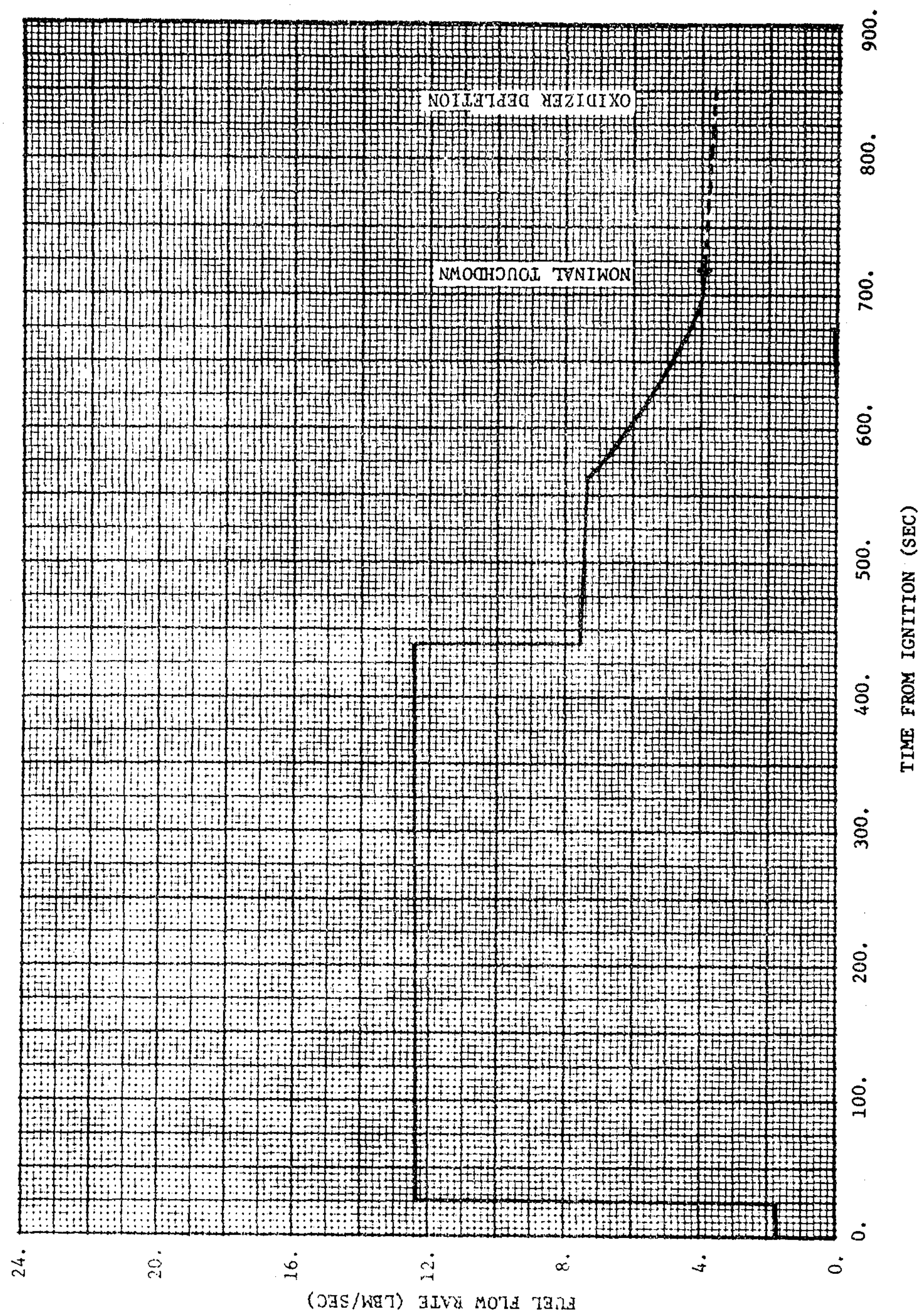

Figure LM10/4.7.1-6 Mission J1 Final DPS Preflight Performance Prediction - Fuel Flow Rate Vs. Time

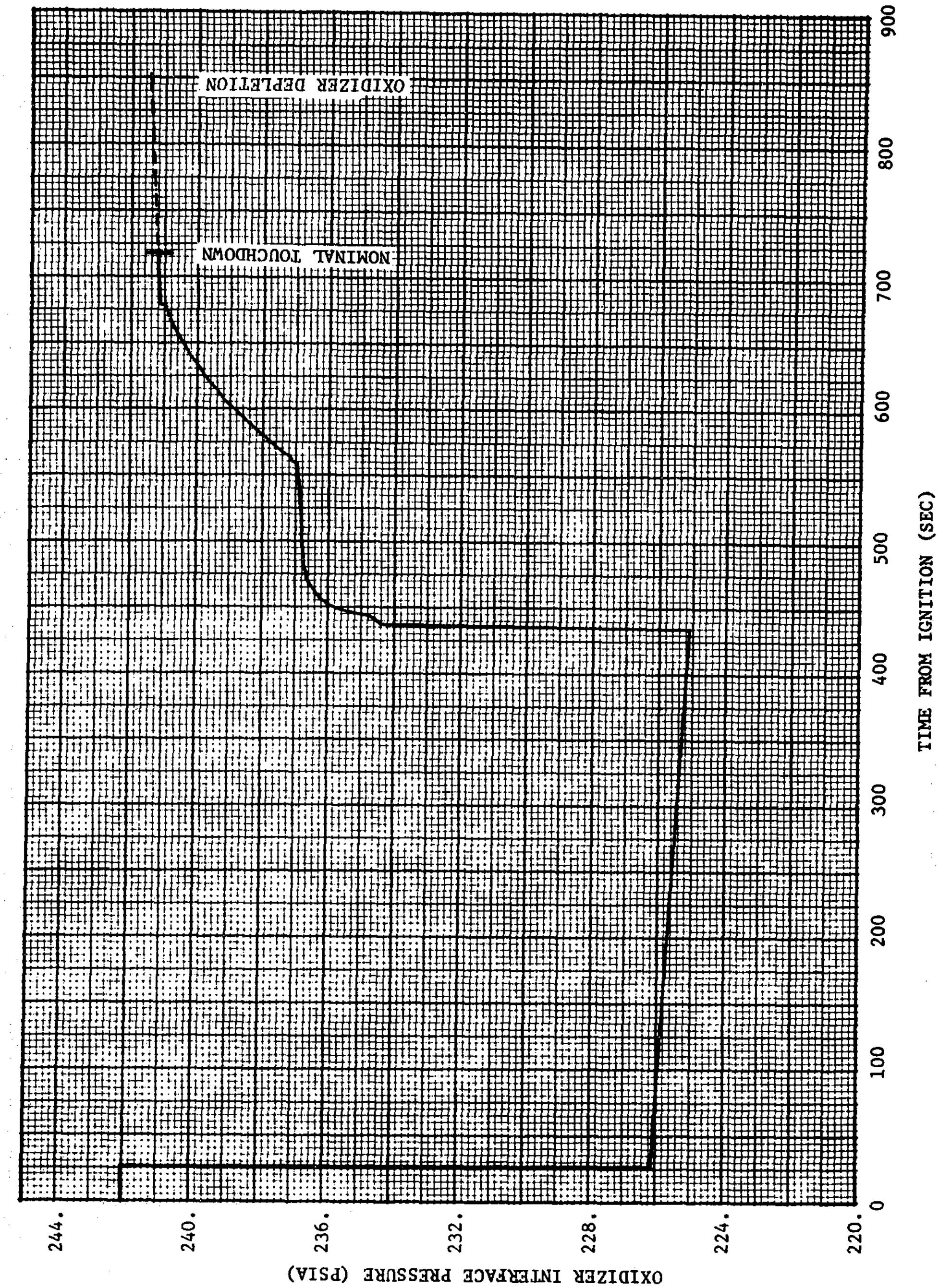

Figure LM10/4.7.1-7 Mission J1 Final DPS Preflight Performance Prediction - Oxidizer Interface Pressure Vs. Time

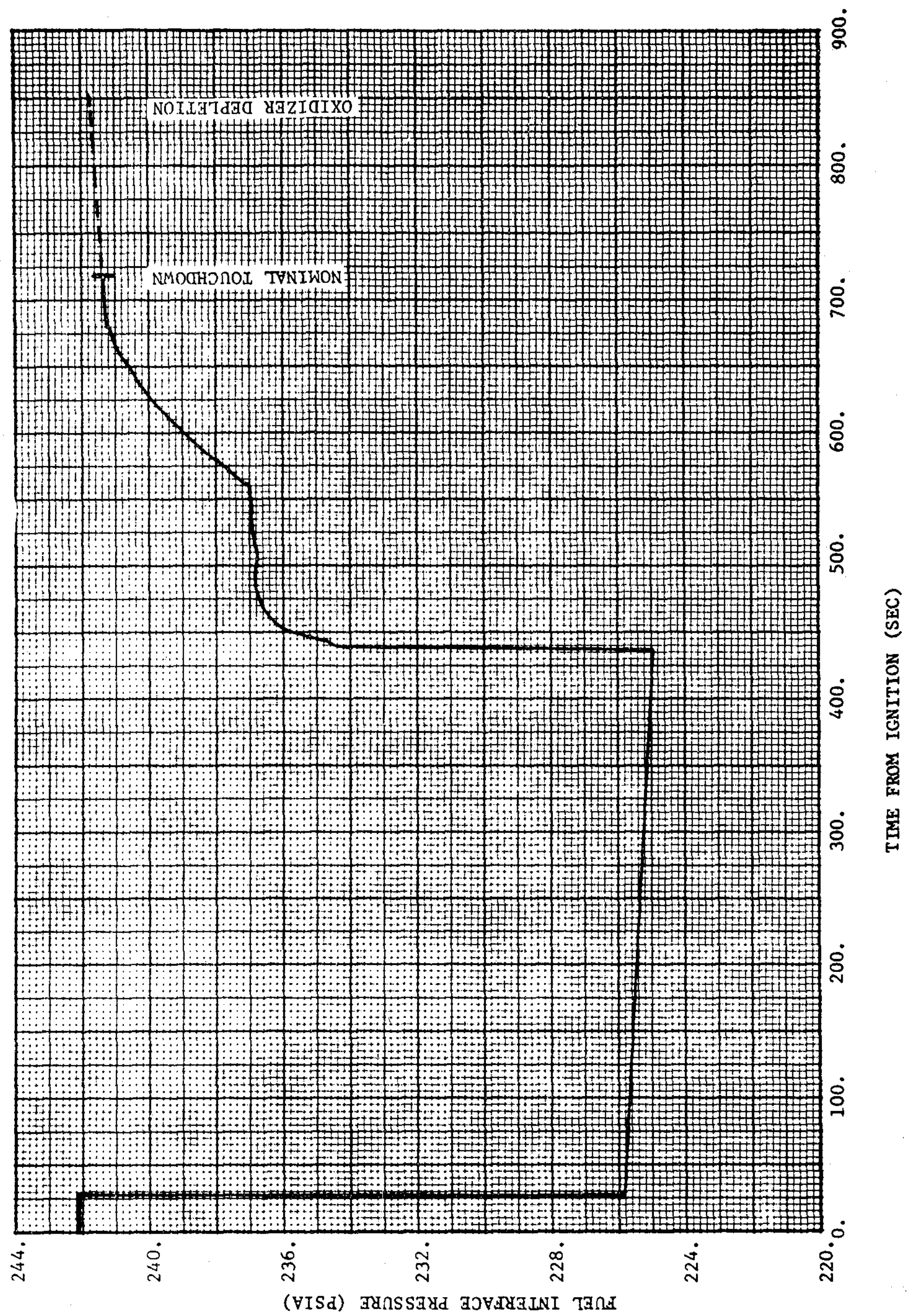

Figure LM10/4.7.1-8 Mission J1 Final DPS Preflight Performance Prediction - Fuel Interface Pressure Vs. Time

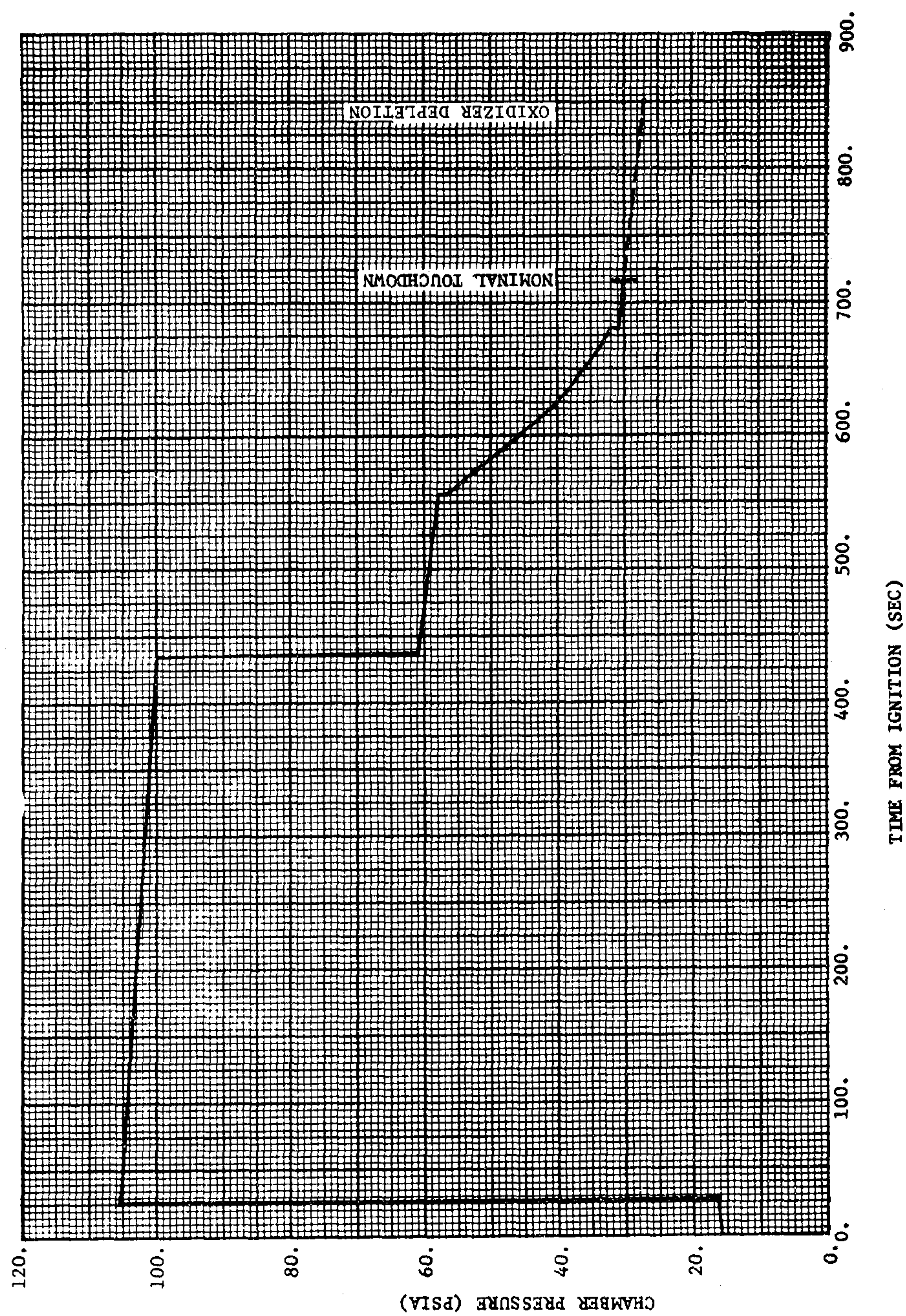

Figure LM10/4.7.1-9 Mission J1 Final DPS Preflight Performance Prediction - Chamber Pressure Vs. Time

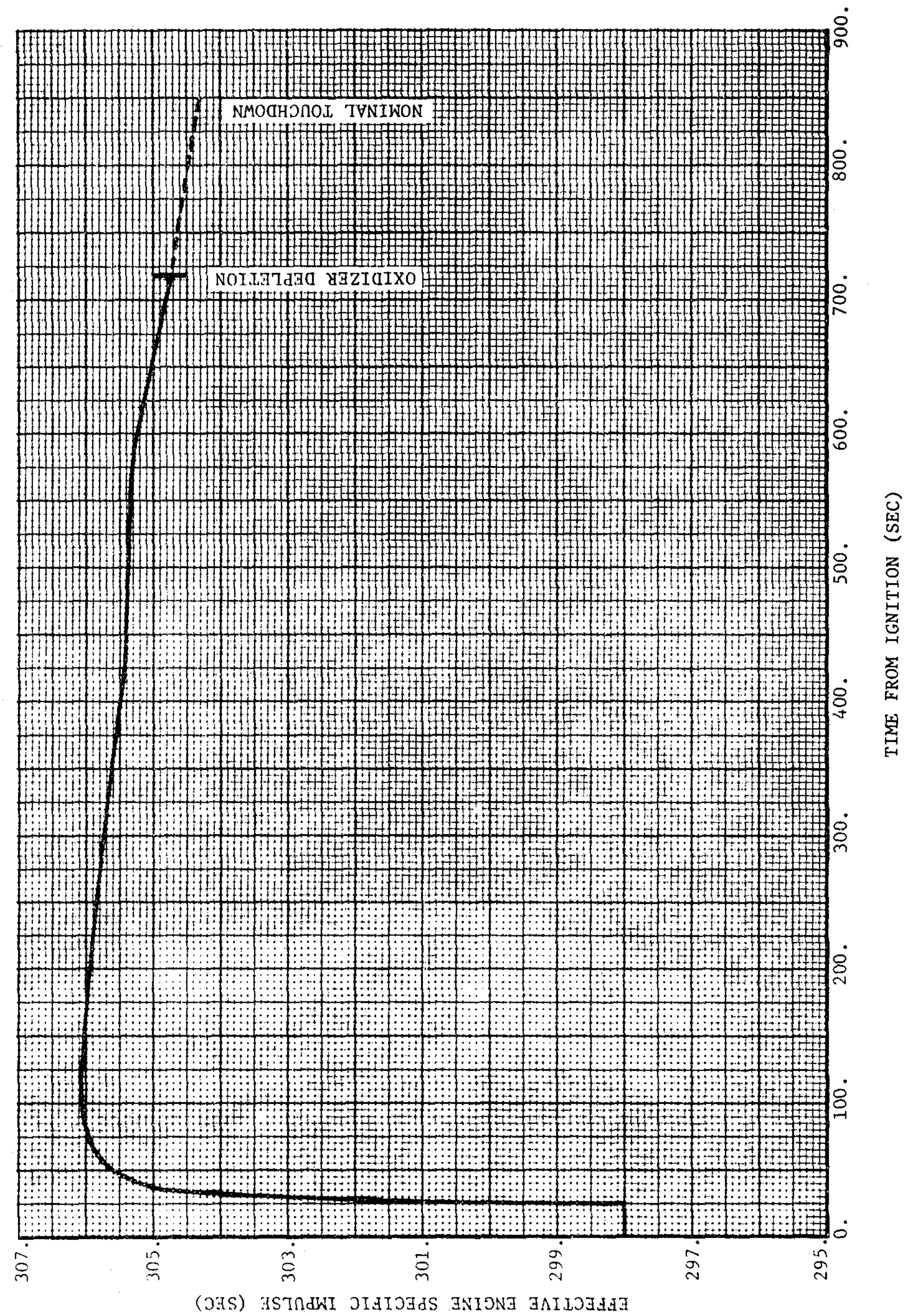

Figure LM10/4.7.1-10 Mission J1 Final DPS Preflight Performance Prediction - Effective Engine Specific Impulse Vs. Time

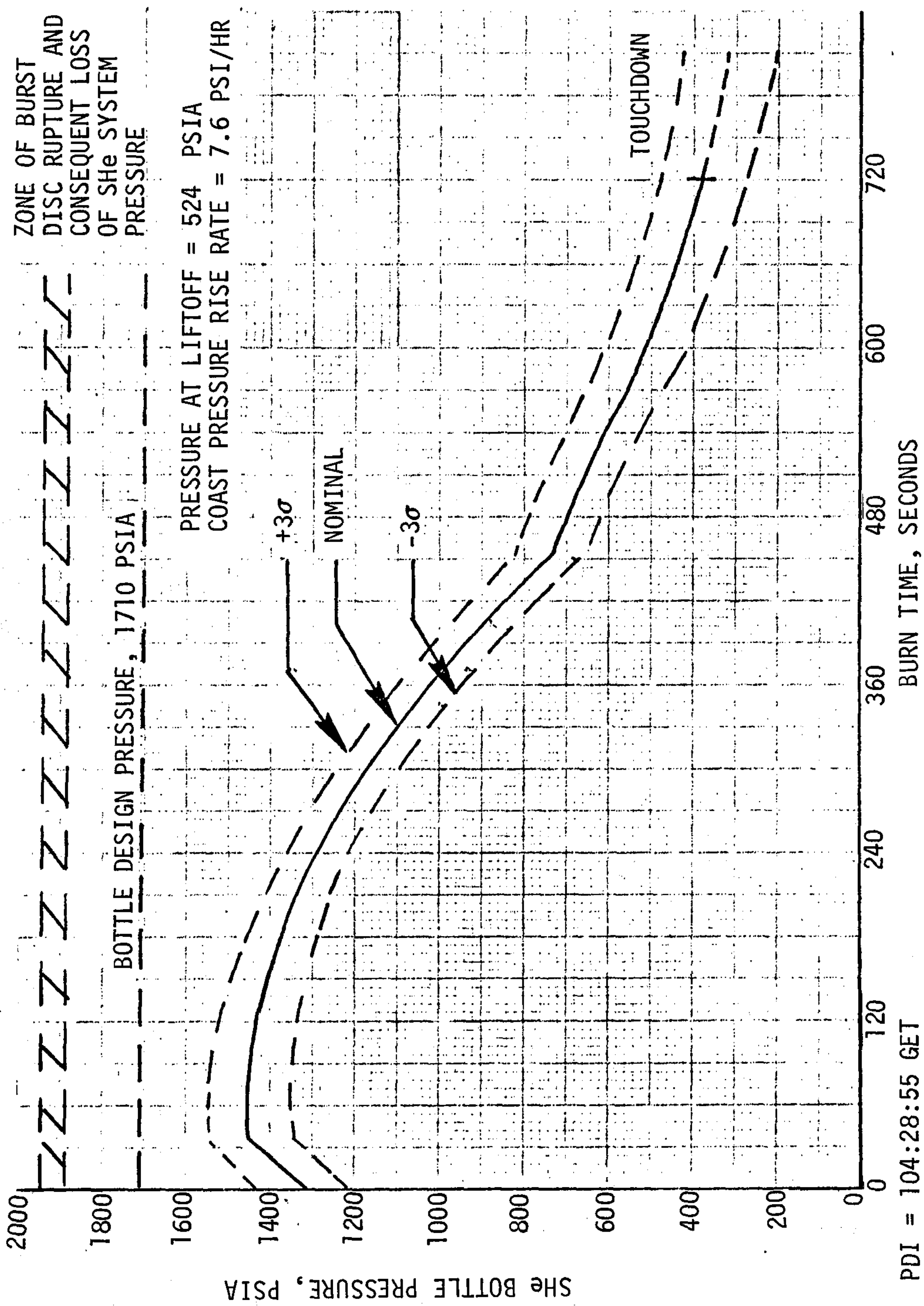

Figure LM10/4.7.1-11 Mission J1 Final DPS Preflight Performance Prediction - Supercritical Helium Bottle Pressure Vs. Time

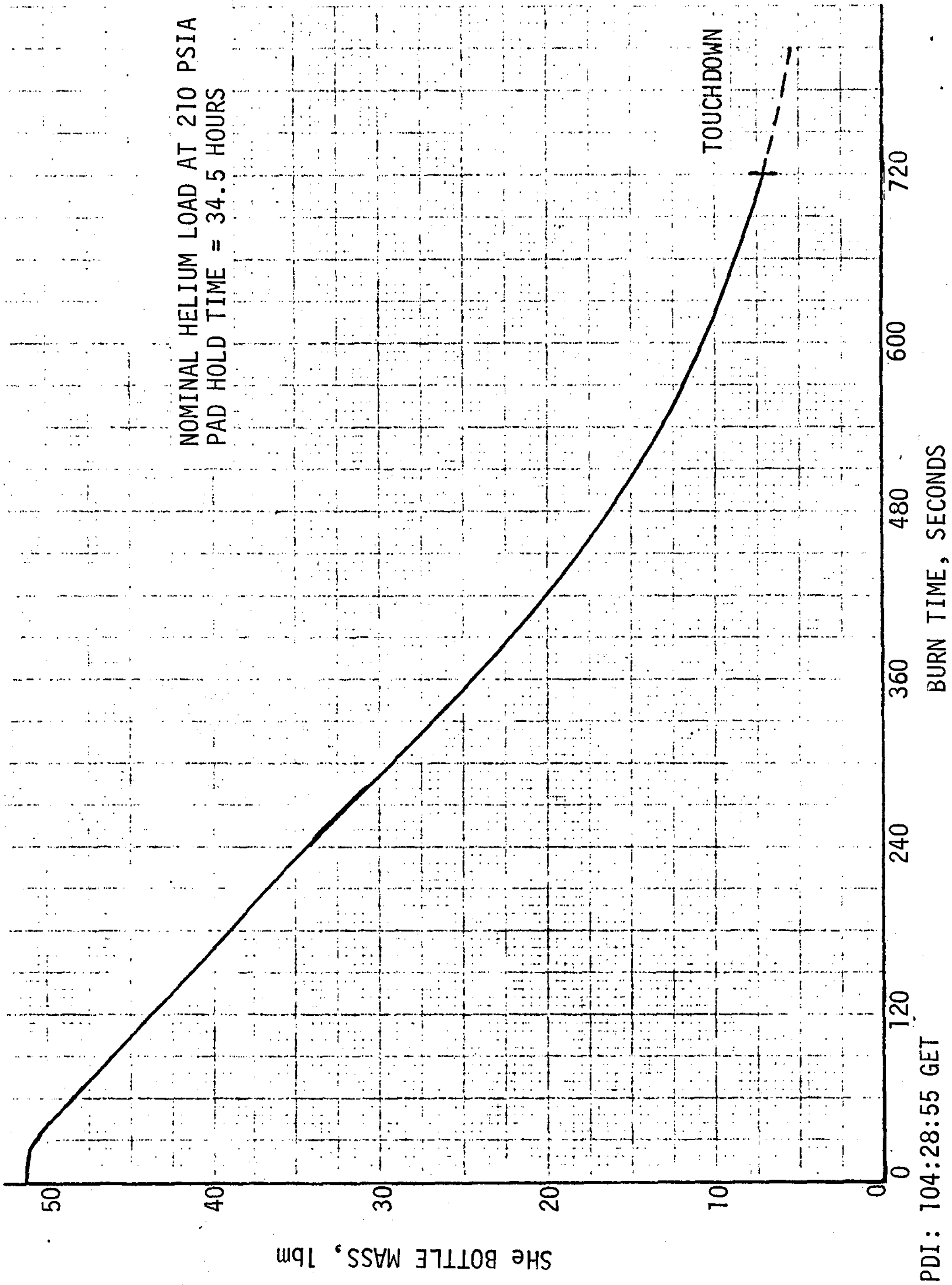

Figure LM10/4.7.1-12 Mission J1 Final DPS Preflight Performance Prediction - Supercritical Helium Mass Vs. Time

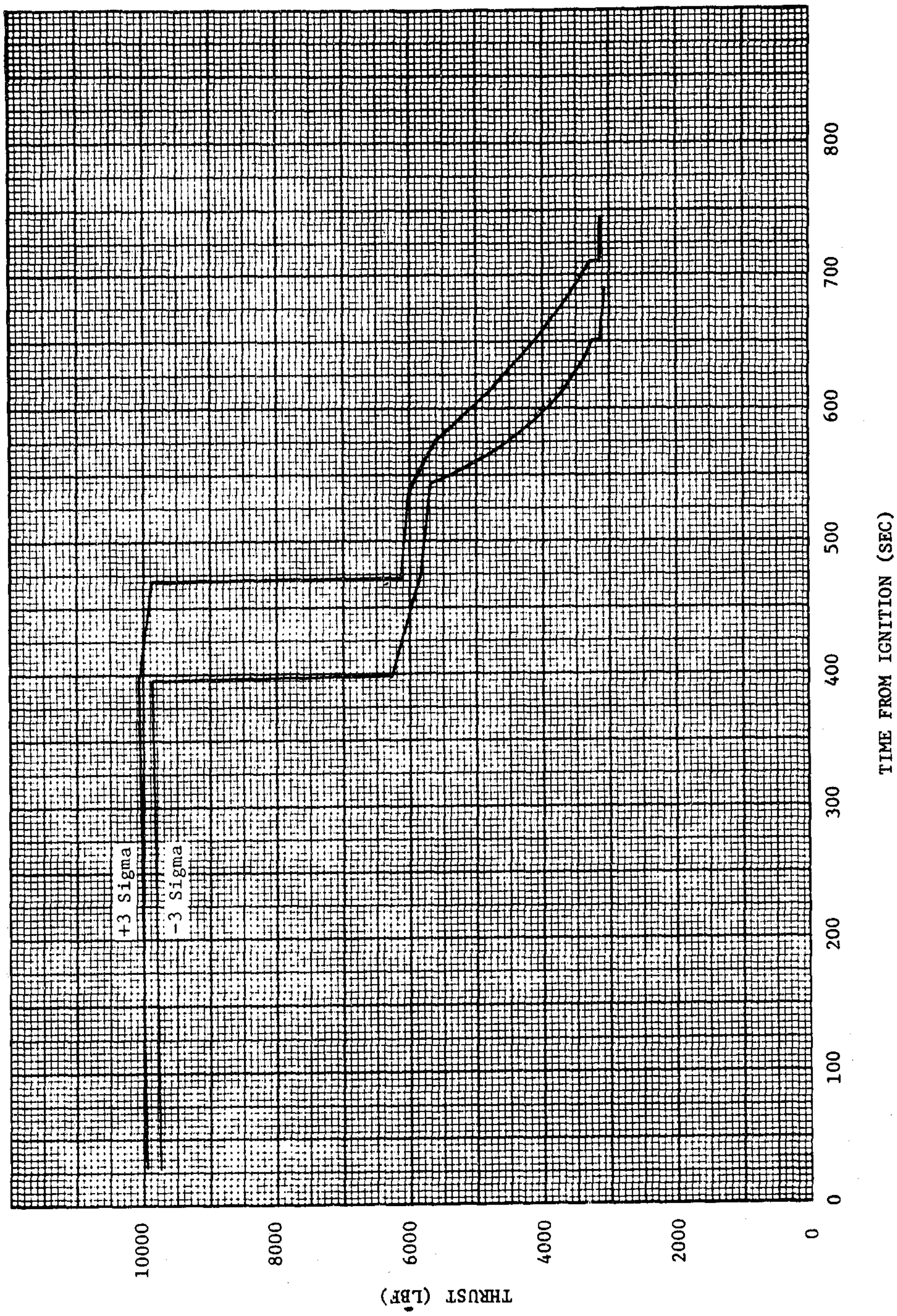

Figure LM10/4.7.1-13 Mission J1 Final DPS Preflight Performance Prediction - Thrust Dispersion Vs. Time

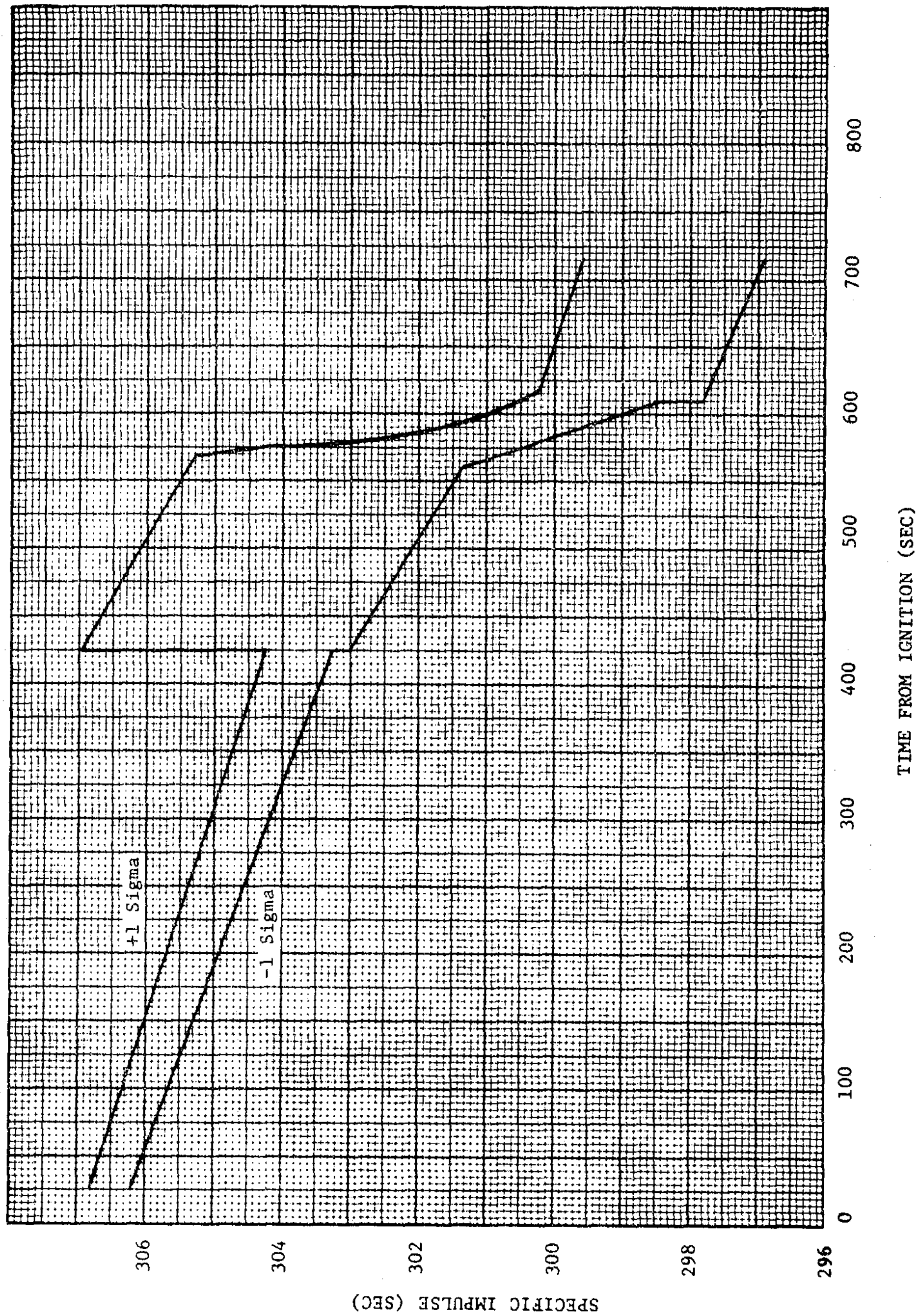

Figure LM10/4.7.1-14 Mission J1 Final DPS Preflight Performance Prediction - Specific Impulse Dispersion Vs. Time

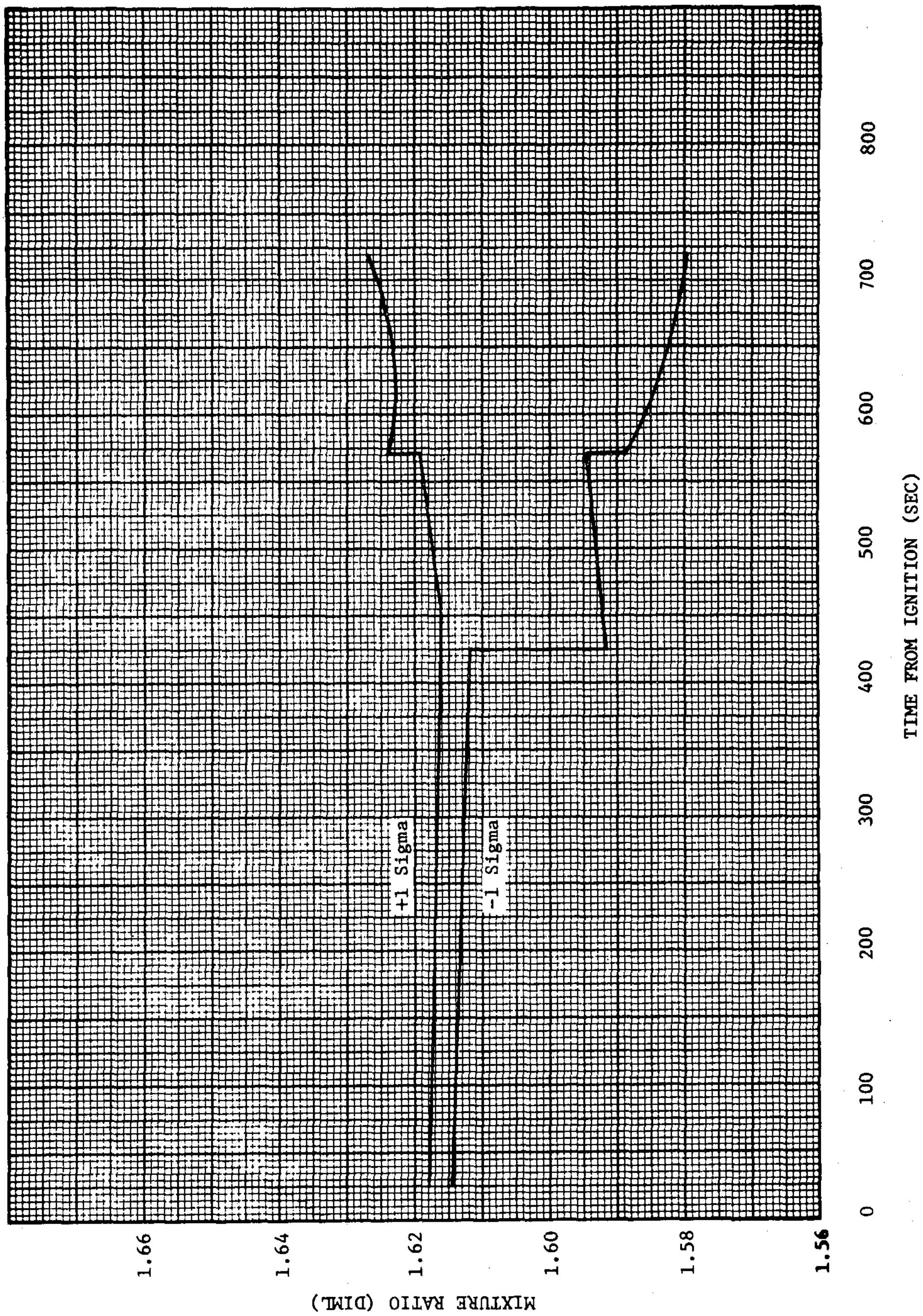

Figure LM10/4.7.1-15 Mission J1 Final DPS Preflight Performance Prediction - Mixture Ratio Dispersion Vs. Time

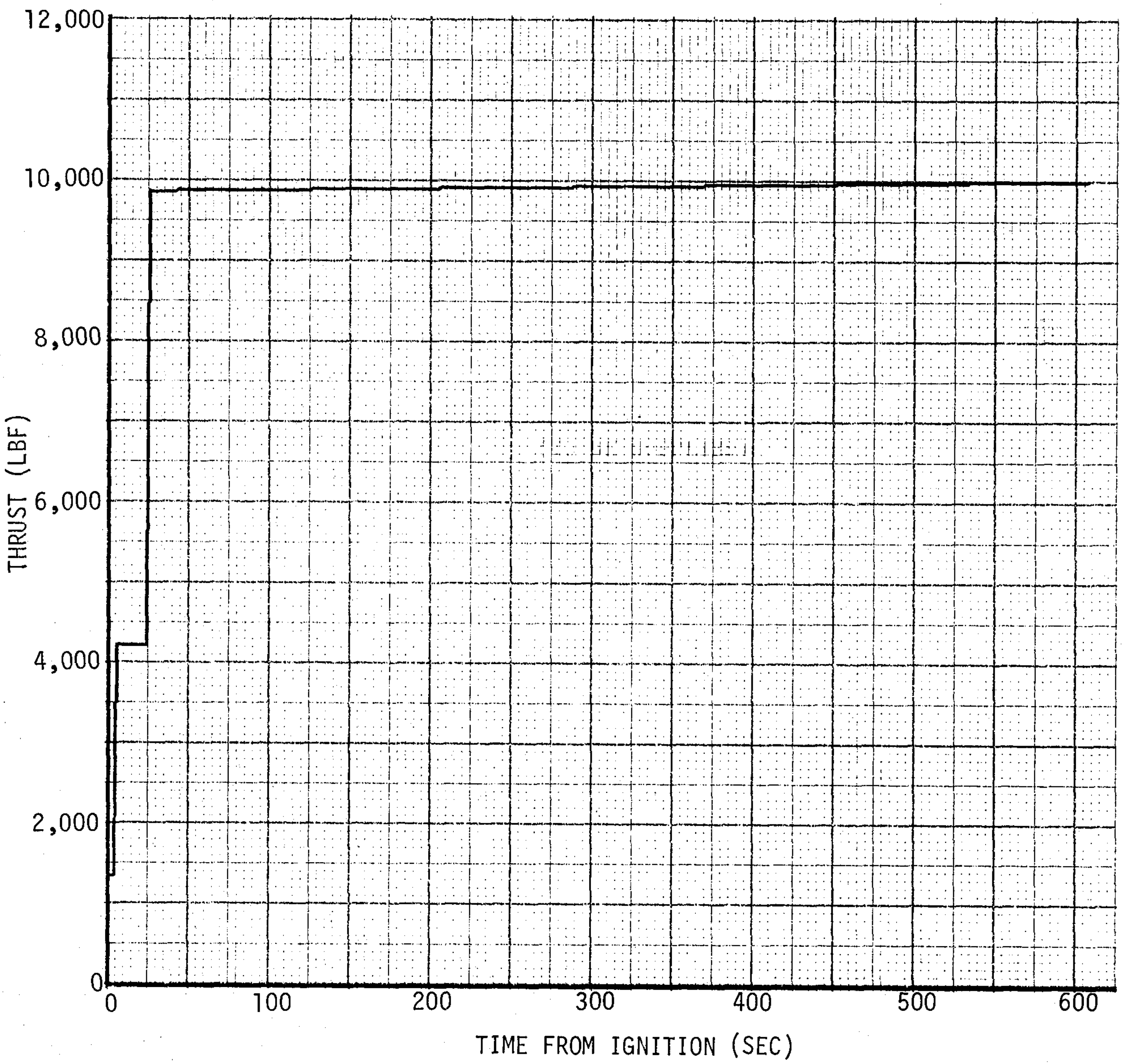

Figure LM10/4.7.1-16 Mission J1 DPS Preflight Performance Prediction - Docked FTP Burn-to-Depletion - Thrust Vs. Time

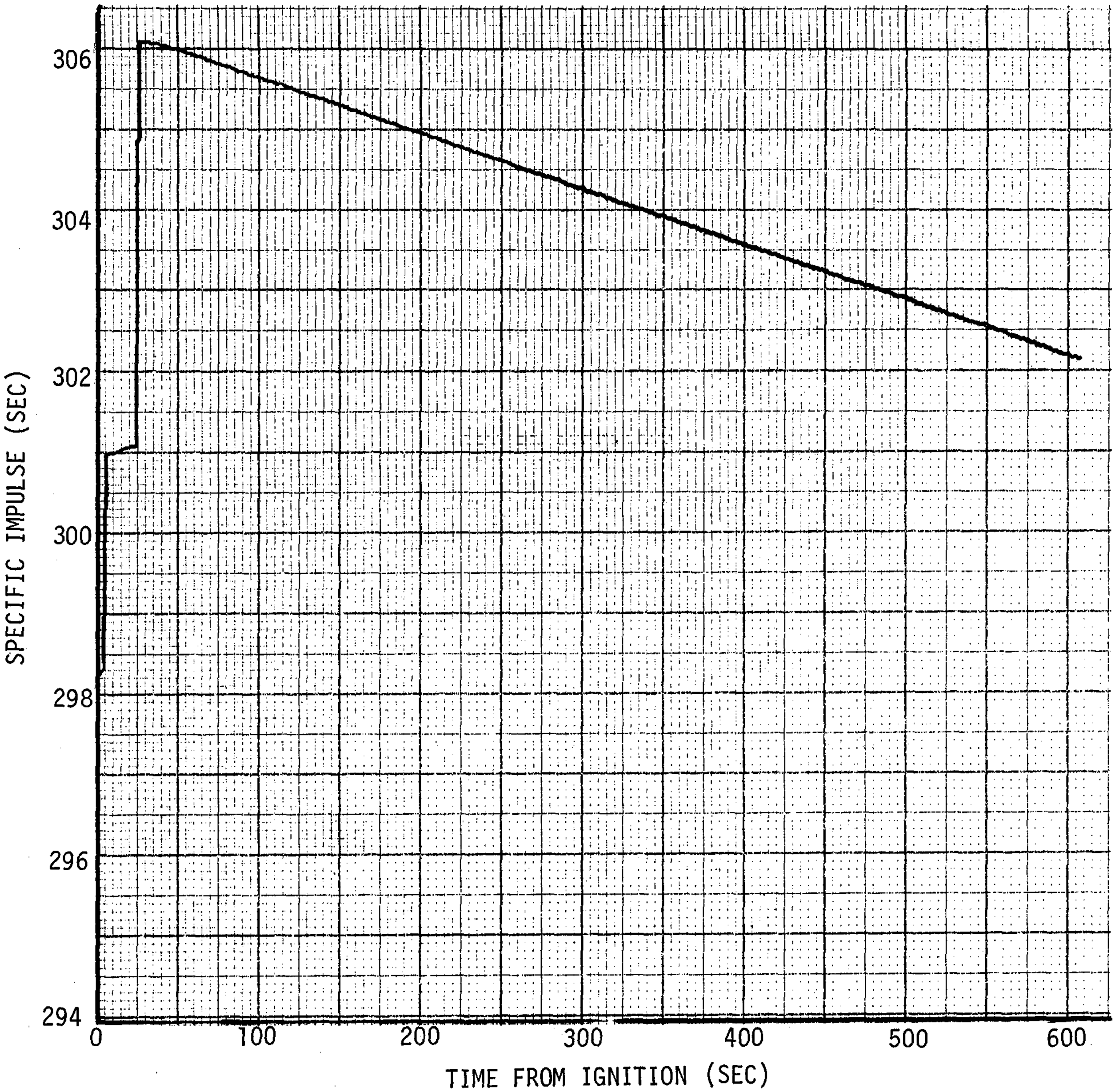

Figure LM10/4.7.1-17 Mission J1 DPS Preflight Performance Prediction - Docked FTP Burn-to-Depletion - Specific Impulse Vs. Time

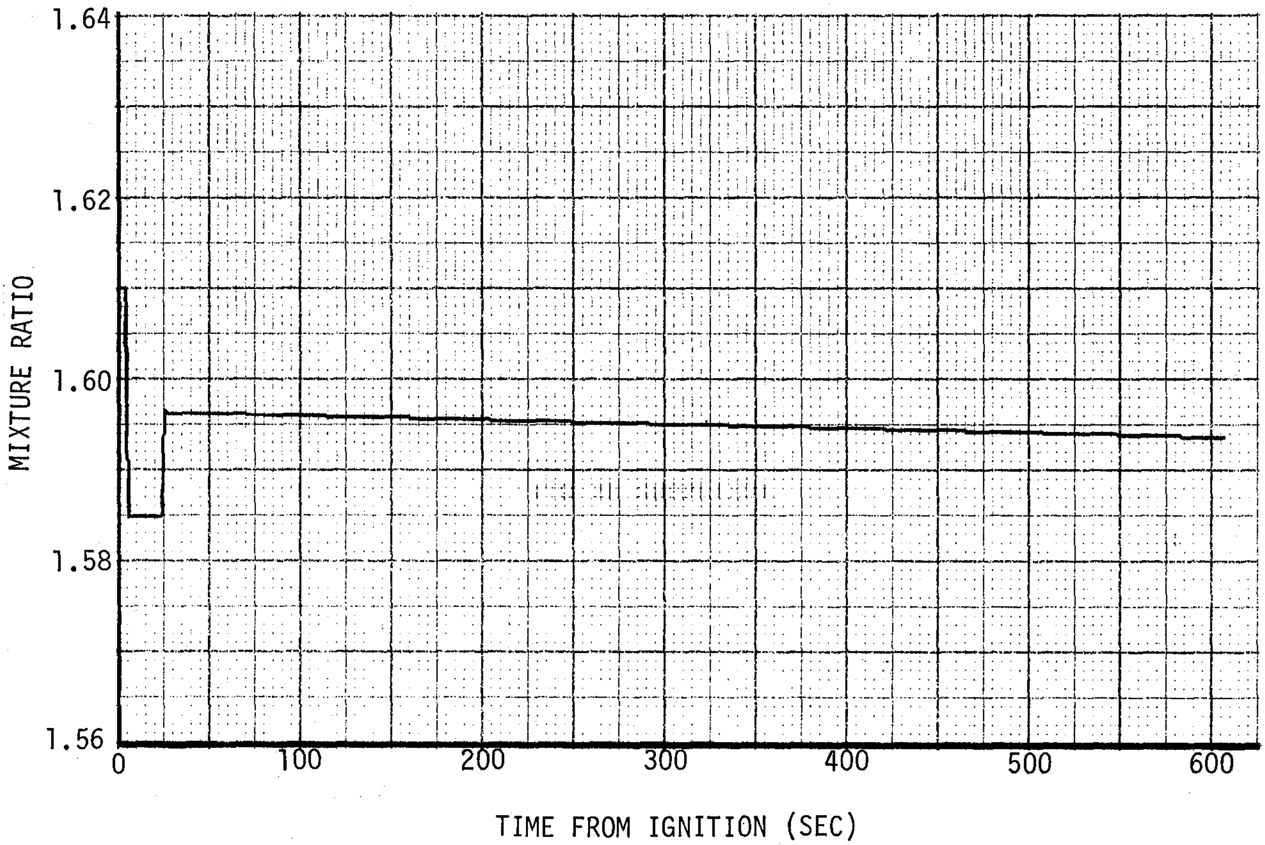

Figure LM10/4.7.1-18 Mission J1 DPS Preflight Performance Prediction - Docked FTP Burn-to-Depletion - Mixture Ratio Vs. Time

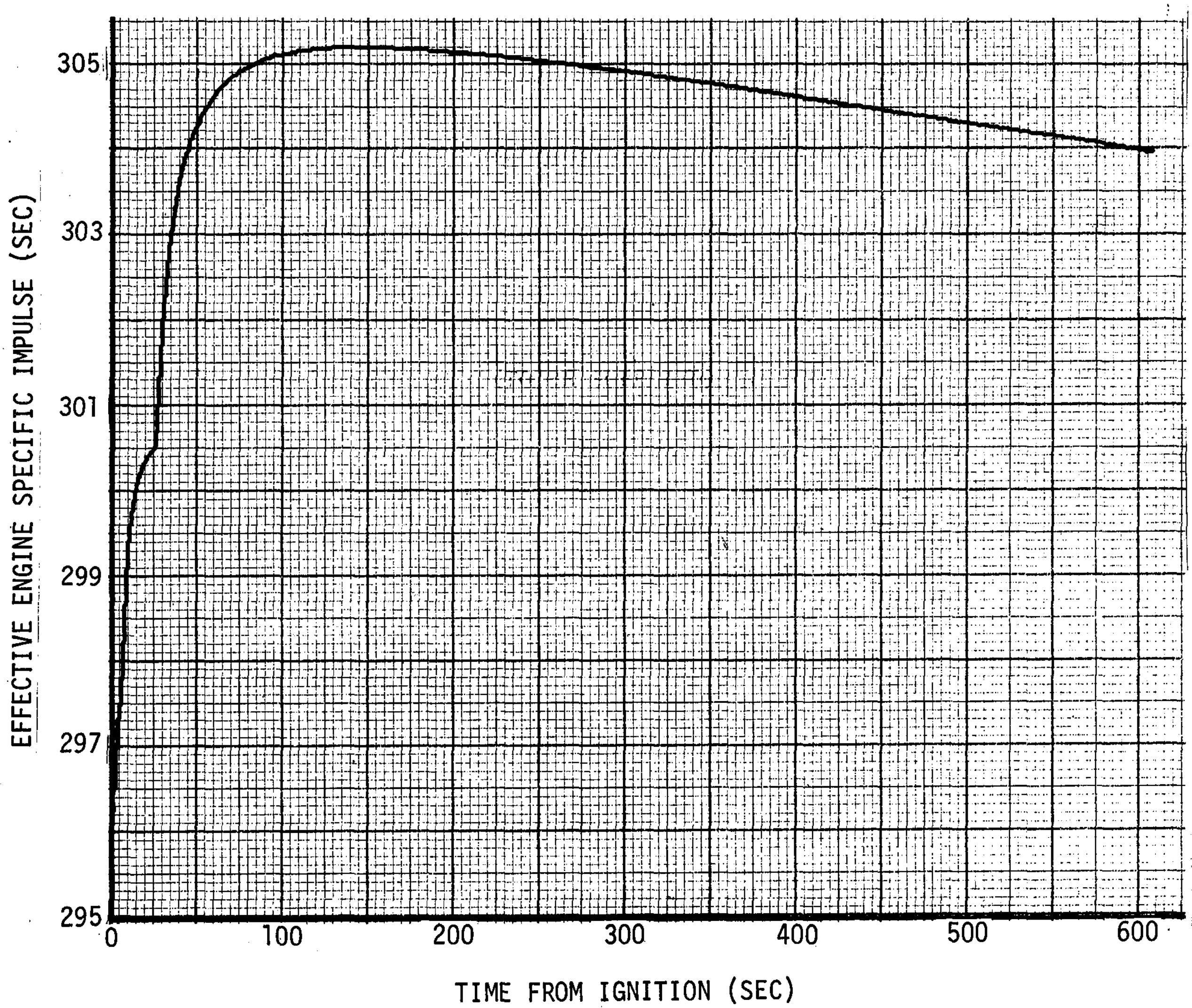

Figure LM10/4.7.1-19 Mission J1 DPS Preflight Performance Prediction - Docked FTP Burn-to-Depletion - Effective Engine Isp Vs. Time

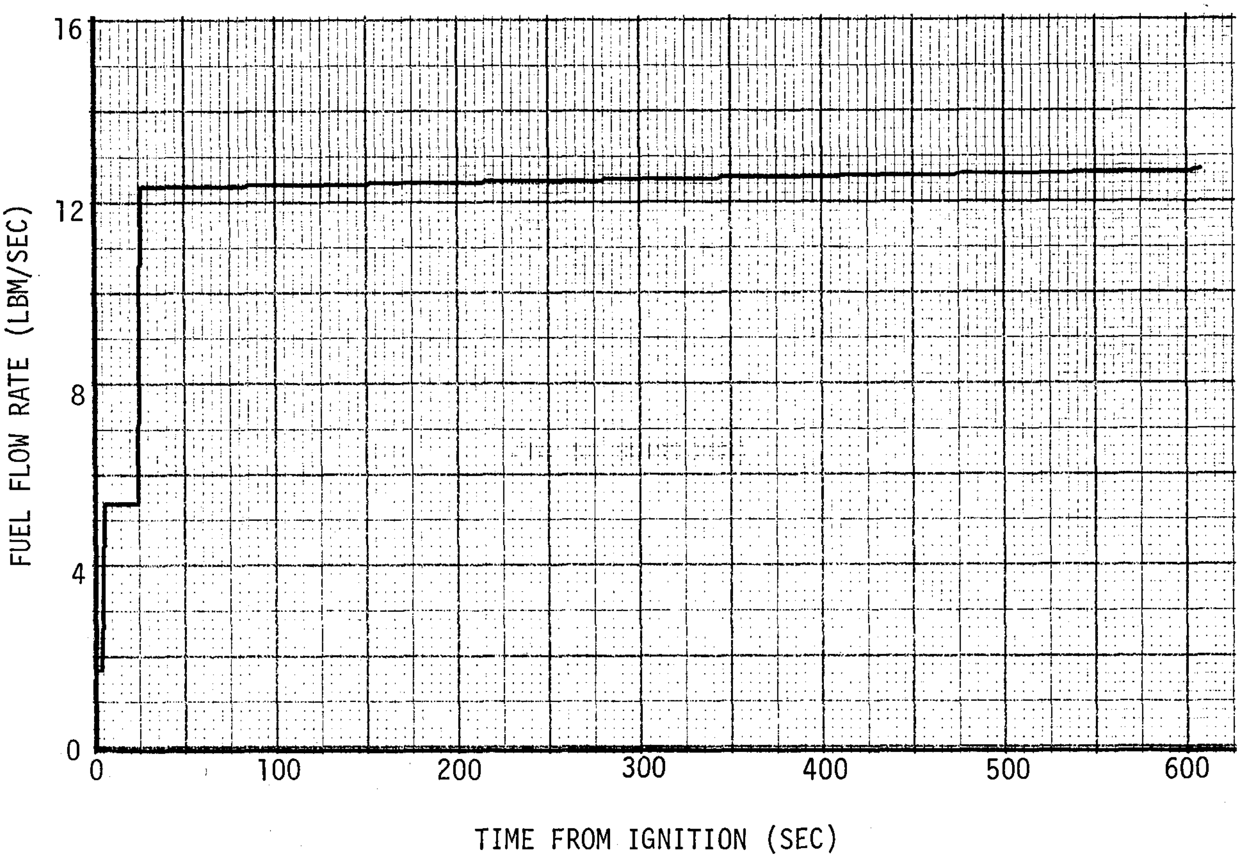

Figure LM10/4.7.1-20 Mission J1 DPS Preflight Performance Prediction - Docked FTP Burn-to-Depletion - Fuel Flow Rate Vs. Time

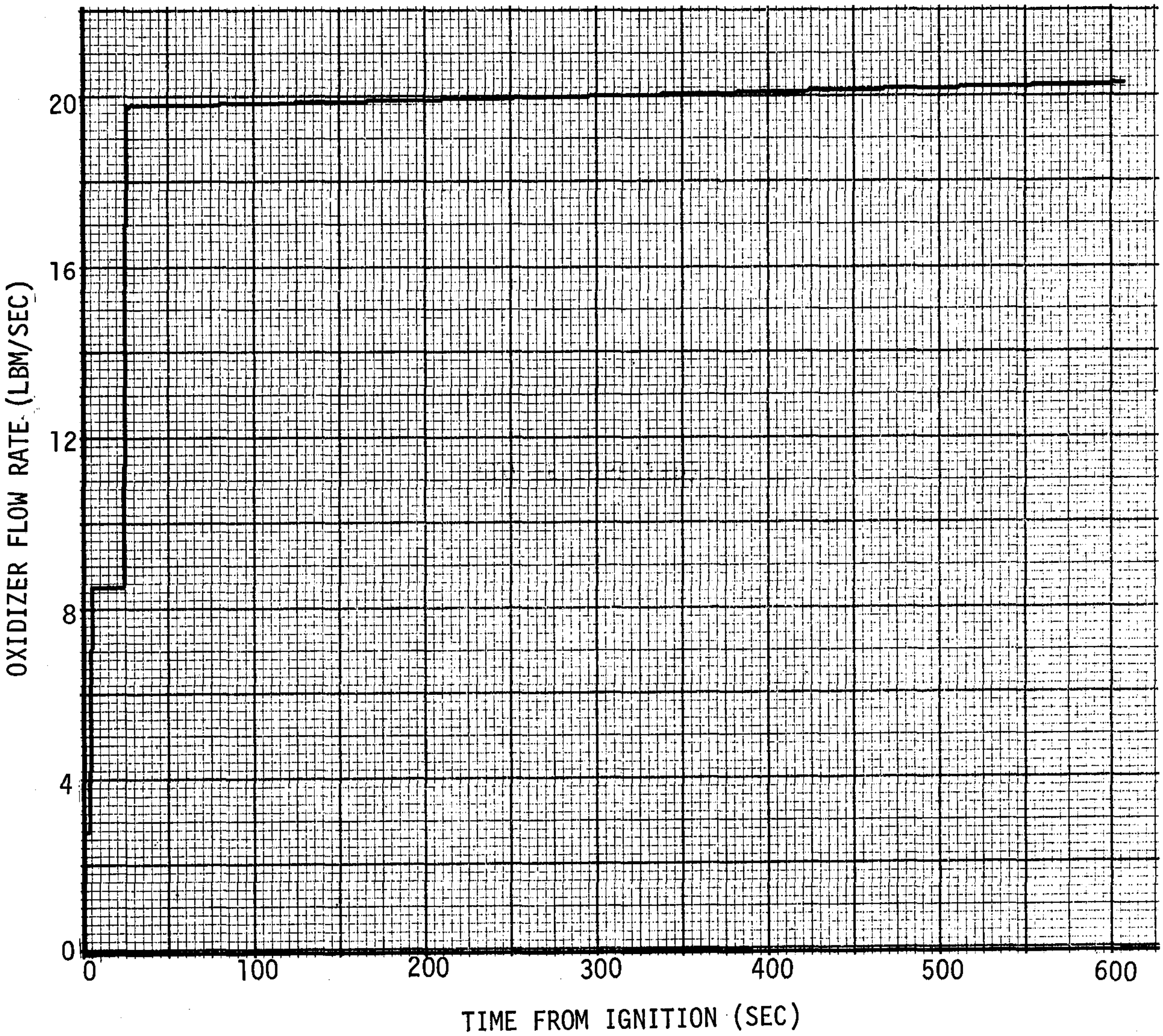

Figure LM10/4.7.1-21 Mission J1 DPS Preflight Performance Prediction - Docked FTP Burn-to-Depletion - Oxidizer Flow Rate Vs. Time

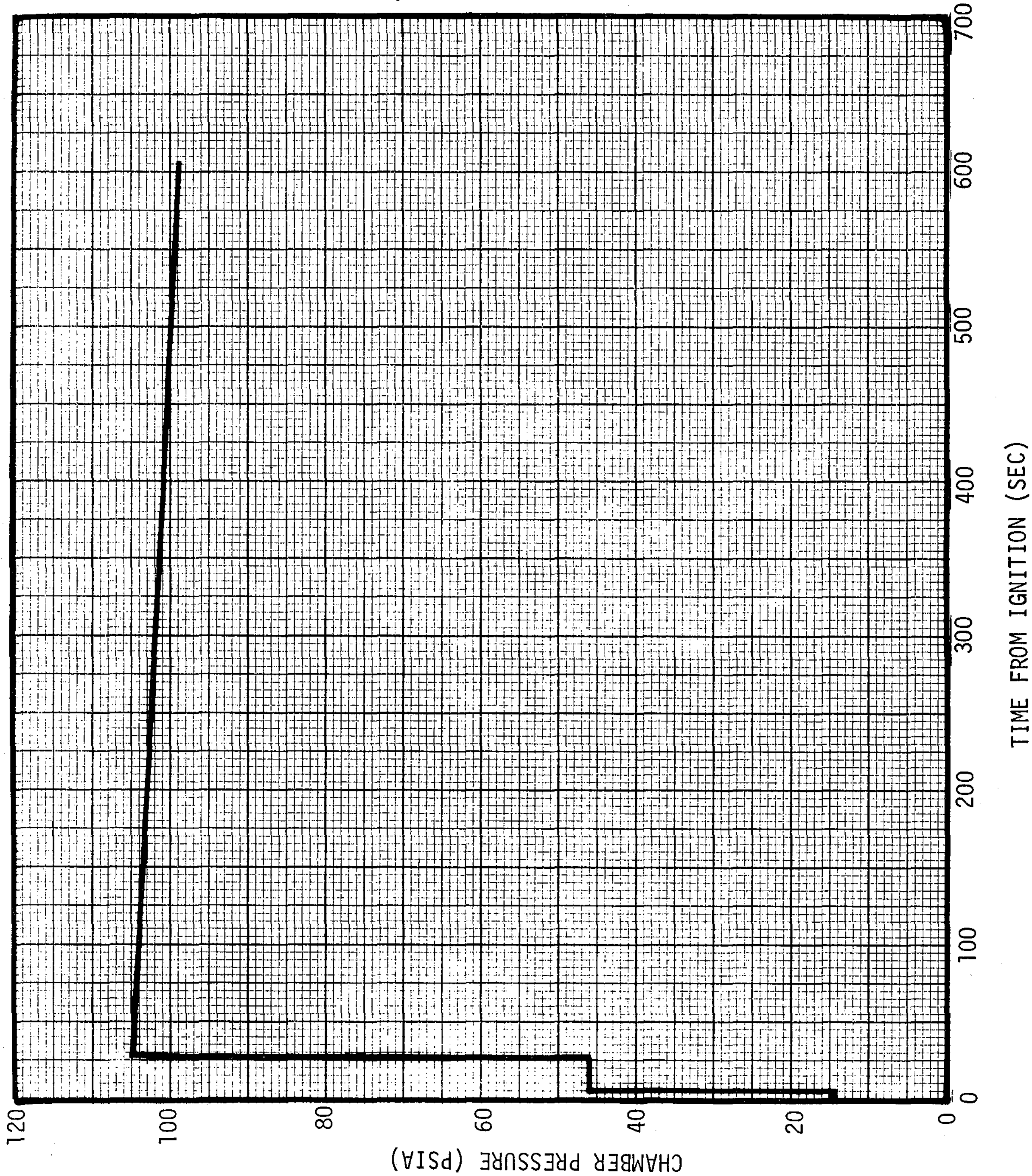

Figure LM10/4.7.1-22 Mission J1 DPS Preflight Performance Prediction - Docked FTP Burn-to-Depletion - Chamber Pressure Vs. Time

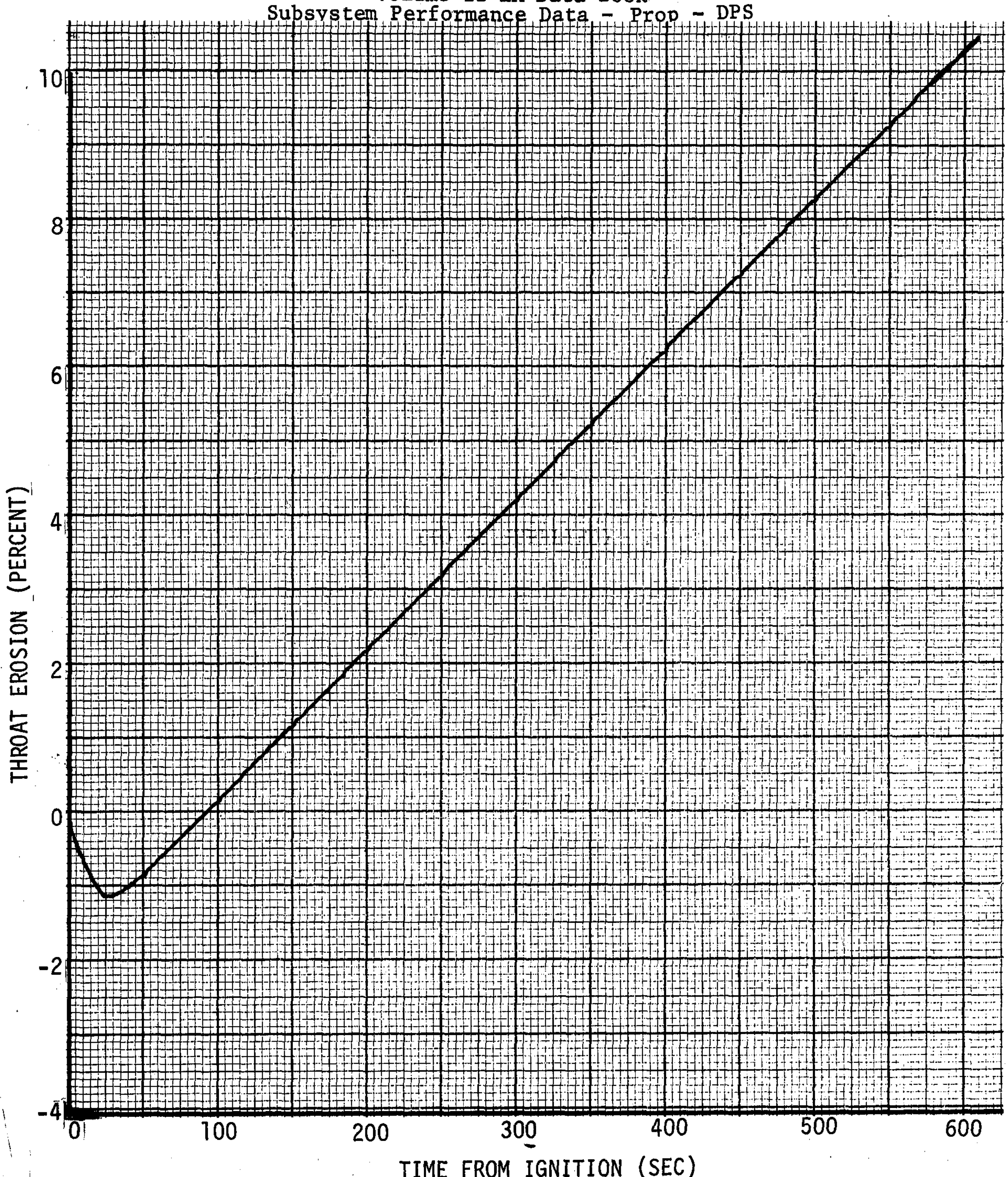

Figure LM10/4.7.1-23 Mission J1 DPS Preflight Performance Prediction - Docked FTP Burn-to-Depletion - Throat Erosion Vs. Time

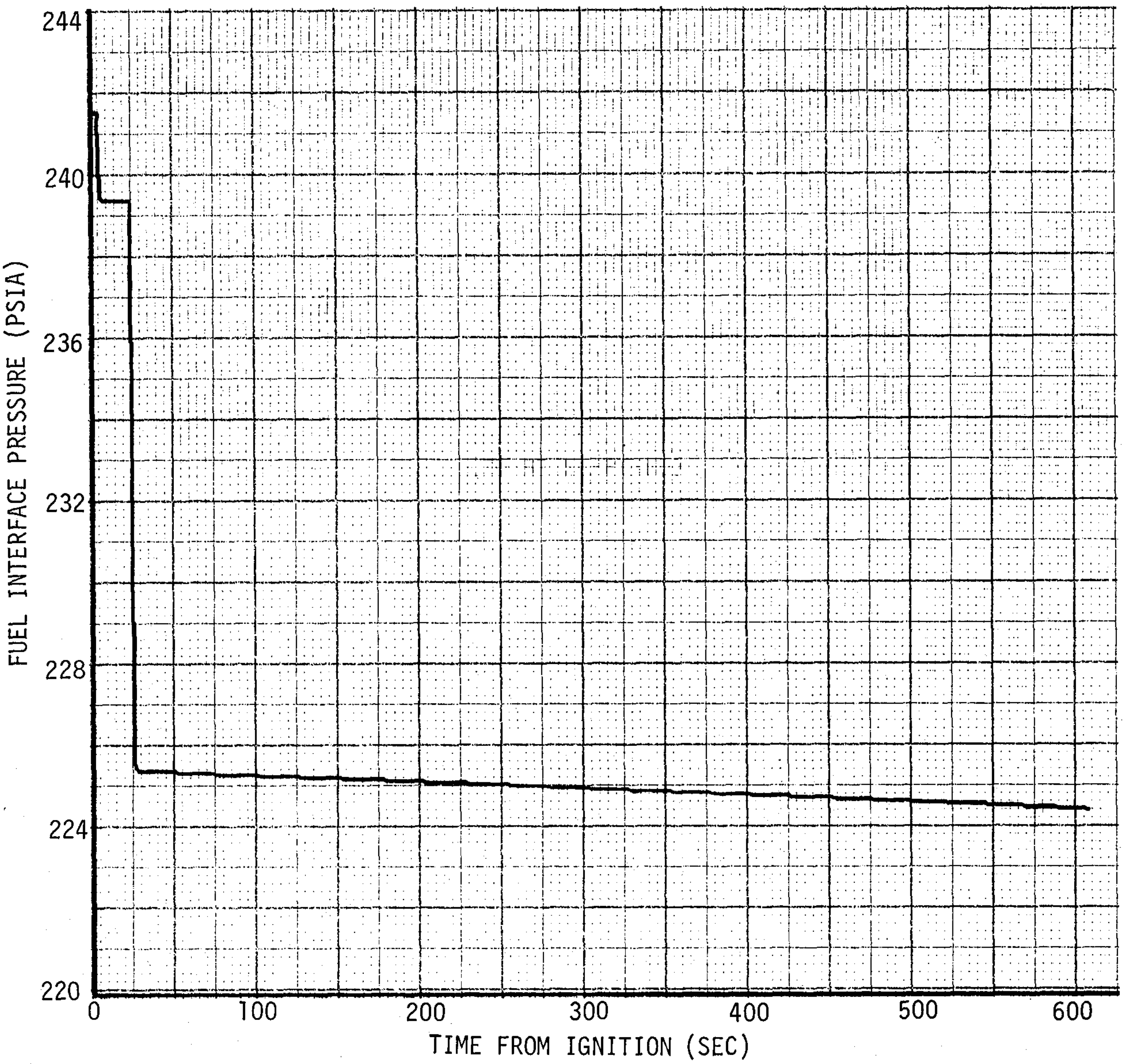

Figure LM10/4.7.1-24 Mission J1 DPS Preflight Performance Prediction - Docked FTP Burn-to-Depletion - Fuel Interface Pressure Vs. Time

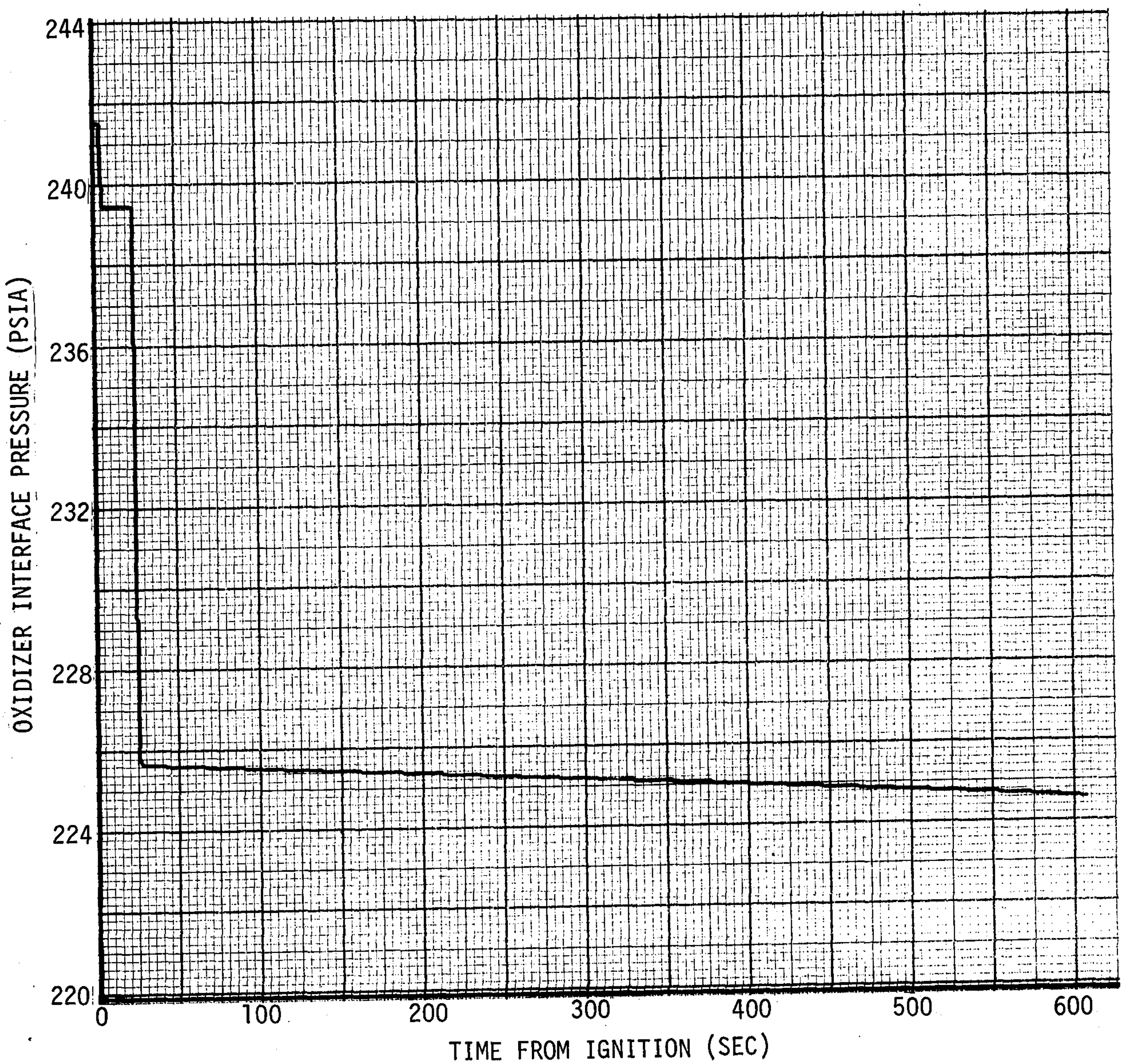

Figure LM10/4.7.1-25 Mission J1 Preflight Performance Prediction - Docked FTP Burn-to-Depletion - Oxidizer Interface Pressure Vs. Time

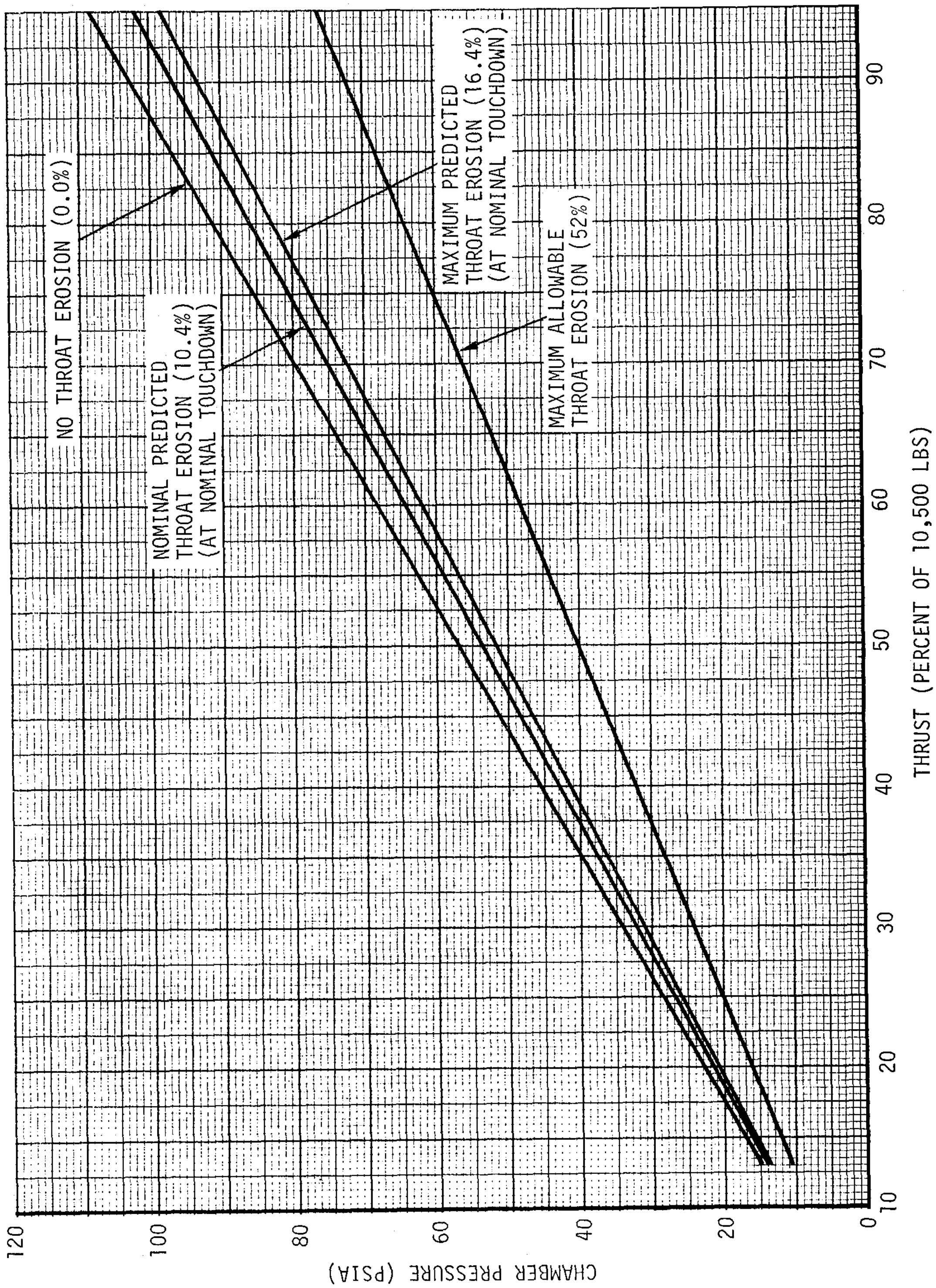

Figure LM10/4.7.1-26 Mission J1 DPS Preflight Performance Prediction - Chamber Pressure Vs. Commanded Thrust for Zero, Nominal, Maximum Predicted and Maximum Allowable Throat Erosion

(TO BE SUPPLIED)

Figure LM10/4.7.1-26 Mission J1 DPS Preflight Performance Prediction - Chamber Pressure Vs. Commanded Thrust for Zero, Nominal, Maximum Predicted and Maximum Allowable Throat Erosion

LM10/4.7.2 Supercritical Helium Tank Pressure

The predicted heat leak pressure rise rates for the LM-10 supercritical helium tanks are shown in Figure LM10/4.7.2-1. Pressure rise rates given in this curve are steady state values and do not account for thermal stabilization just after the burn. These rise rates are therefore independent of mission duty cycle. This data has been obtained from pre-mission screening tests.

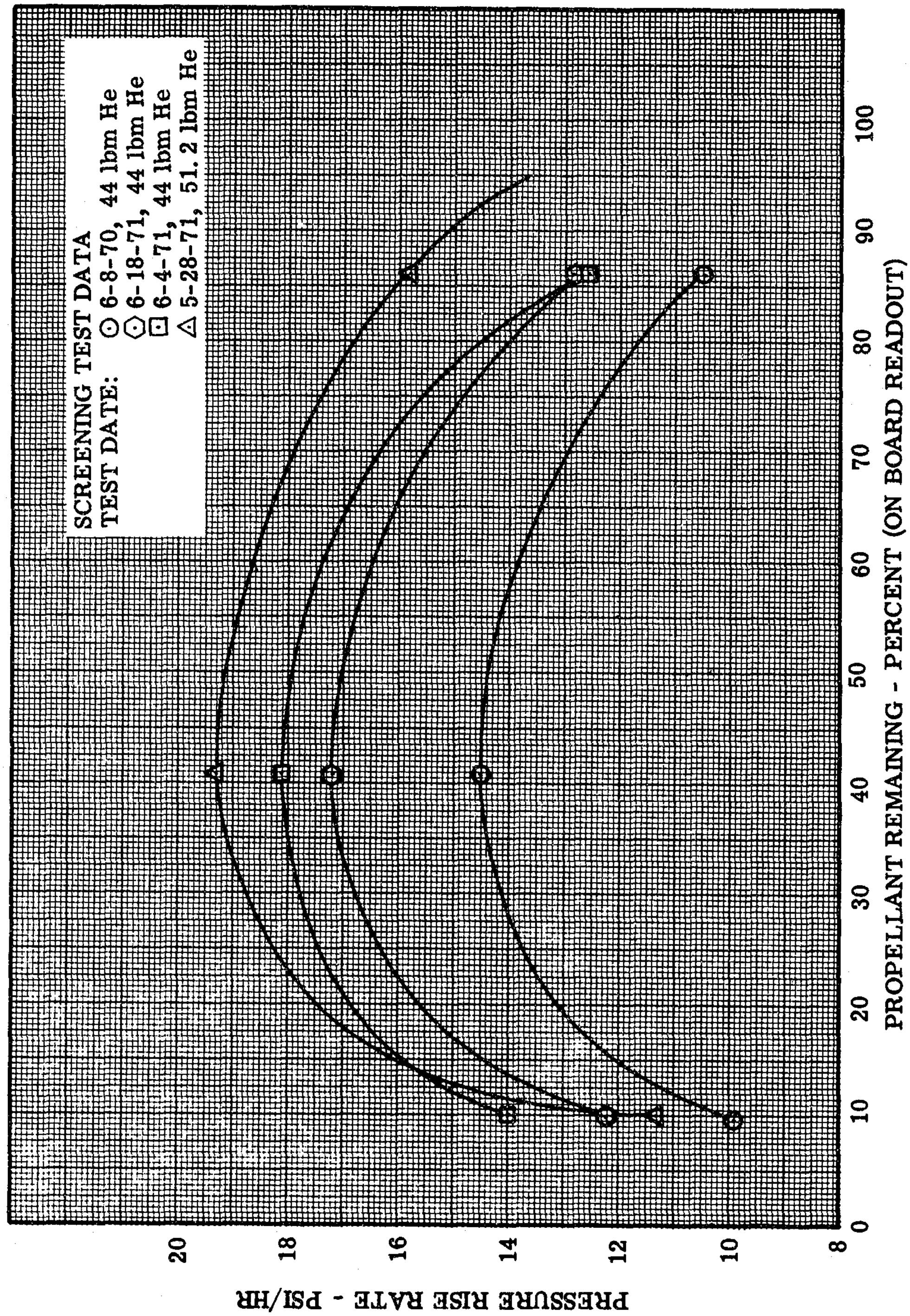

Figure LM10/4.7.2-1 Supercritical Helium Tank Pressure Rise Rate Vs. Percentage of Propellant Remaining

LM10/4.7.5 Propellant Quantity Gaging

Based on measurements of the height of the low level sensor in the propellant tanks made by GAC* the propellant quantities in the tanks at the time of low-level sensor actuation were calculated to be:

Tank	Quantity
Fuel	208.2 ±4.9 lbm per tank
Oxidizer	332.8 ±5.3 lbm per tank

The propellants in the feed lines and heat exchanger should be added, and the propellants in the zero-g-can should be deducted from the above quantities. Values for these are taken from the Spacecraft Operational Data Book, Volume III, Rev 3, 1 April 1971, Section 5.6 (Amendment 106, 6/22/71):

Component	Fuel, lbm	Oxidizer, lbm
Feed Lines	+12.0	+27.5
Heat Exchanger	+ 4.4	-0-
Zero-G-Can	- 4.5	- 7.2
TOTAL	+11.9	+20.3

The propellant quantity corrections tabulated above should be applied regardless of whether depletion occurs from a single tank or both tanks of a pair simultaneously. This is so because in both cases the trapped quantities will be used or not used identically (helium ingestion upon depletion of a single tank effectively shuts off the undepleted tank). Also, since at the time of low level sensor actuation it is not possible to determine whether or not both tanks of a pair are at the same propellant level (they both could be at the high or at the low level), the single tank dispersions should be summed to arrive at the dispersions for both tanks of a pair taken together.

Based upon the above statements and data the propellant quantities available after low level sensor actuation are as follows:

Fuel	428.3 ± 9.8 lbm
Oxidizer	685.9 ±10.6 lbm

*Grumman Aerospace Corporation, LM Engineering Memorandum LMO 271-935, 16 September 1970.

The mean values of fuel and oxidizer flow rate during hover from low level sensor actuation to depletion were calculated to be:

Fuel Flow Rate:	3.798 lbm/sec
Oxidizer Flow Rate:	6.017 lbm/sec

(Spacecraft Operational Data Book, Volume II, Rev. 2, 1 September 1969, Para. LM10/4.7.1.)

Using the above flow rates and propellant quantities the burn time from low level sensor actuation to depletion was calculated to be 112.8 seconds for fuel and 114.0 seconds for oxidizer. Both the burn times given above are slightly on the conservative side in as much as use of a mean flow rate is conservative by approximately 1.6 seconds compared to integrating along a thrust-time curve.

The dispersions associated with the burn times given above are ±2.6 seconds for fuel and ±1.8 seconds for oxidizer. Therefore, the minimum burn times from low level sensor actuation to depletion were calculated to be 110.2 seconds for fuel and 112.2 seconds for oxidizer.

Because there are two fuel and two oxidizer tanks, each with a low level sensor with the dispersion given in the first paragraph, the RSS dispersion for the two tanks of a pair represents a more likely case than the maximum dispersion case given immediately above. The RSS dispersions for the total fuel and total oxidizer available at low level sensor activation were calculated to be ±6.9 and ±7.5 lbm, respectively. The burn time dispersions associated with these quantities are ±1.8 seconds for fuel and ±1.3 seconds for oxidizer. Thus, the RSS minimum burn times were calculated to be 111.0 seconds for fuel and 112.7 seconds for oxidizer.

The above burn time calculations do not take into account the uncertainty about the nominal predicted flow rates, or any effects from propellant slosh. In addition, these calculations do not consider the effect of the DPS GDA trim angles on how long after ignition the low level sensor will actuate. Thus, in that sense they are conservative as compared to the data in paragraph LM10/4.7.1, which are based on the nominal predicted GDA trim angles.

LM10/4.7.5 Propellant Quantity Gaging (Cont.)

Error values have been computed to be applied to real-time readings for specific quantity values over the range from approximately 12% through depletion. Tables LM10/4.7.5-1 through LM10/4.7.5-4 contain the instantaneous error readings by PCM count for each of the PQGS probes in the 0% to 12% range.

Figure LM10/4.7.5-1 provides the instantaneous PQGS errors for quantities above 12%. These data were calculated by the RSS (root-sum-square) of the worst case channel error due to the PQGS control unit, zero adjust potentiometer, PCM, and the PQGS repeatability and height-volume errors.

Error data contained in Tables LM10/4.7.5-1 through LM10/4.7.5-4, and the errors listed for the projection program and crew display are based on the following error sources:

(1)	PQGS Probe	±5 mV (repeatability)
(2)	PQGS Control Unit	±10 mV (PCM or display output)
(3)	PCM	±25 mV (±15 mV PP application)
(4)	Zero Adjust Potentiometer Error	±15 mV

Projection program errors listed below are based on an FCD-GAC agreed starting point of 12% indicated quantity and a stop point of 5.8% (114-second program duration). The assumed depletion rate was 0.054 percent/second. The errors listed below apply to the mean calculated propellant quantity at the end of the 114-second program.

Tank	Meas. ID	Error (%)
Fuel #1	GQ 3603Q	0.486
Fuel #2	GQ 3604Q	0.493
Oxid #1	GQ 4103Q	0.450
Oxid #2	GQ 4104Q	0.448

In order to provide the crew with a display error, a computation was performed to determine the uncertainty at the threshold of the digital display as it transcends from 3% to 2%. These are listed in Table A below. Table B has been prepared in the event that the exact switching point is not observed by the crew.

Table A

Measurement	Quantity (%) Remaining	
	High	Low
GQ 3603Q, Fuel No. 1	2.968	2.369
GQ 3604Q, Fuel No. 2	2.583	1.668
GQ 4103Q, Oxid. No. 1	2.558	1.701
GQ 4104Q, Oxid. No. 2	2.492	1.610

Table B

Measurement	Quantity (%) Remaining	
	High	Low
GQ 3603Q, Fuel No. 1	2.968	1.252
GQ 3604Q, Fuel No. 2	2.583	0.678
GQ 4103Q, Oxid. No. 1	2.558	0.767
GQ 4104Q, Oxid. No. 2	2.492	0.640

Reference: LMO 360-1097, LM-10 PQGS Calibration Data and System Accuracy, dated 22 June 1971.

Table LM10/4.7.5-1 Propellant Quantity Gaging System GQ3603G Fuel Tank No 1 Reading Error By PCM Bit

PCM BITS	PCM QUANTITIES LOW	NOM	HIGH	INSTANTANEOUS POSITIVE	PCM ERROR NEGATIVE
1	0.0	0.000	0.757	0.756	0.000
2	0.0	0.543	1.117	0.574	-0.543
3	0.314	0.892	1.465	0.573	-0.578
4	0.642	1.241	1.793	0.552	-0.599
5	1.003	1.590	2.352	0.761	-0.587
6	1.354	1.987	2.670	0.682	-0.633
7	1.700	2.483	2.985	0.502	-0.783
8	2.243	2.789	3.298	0.509	-0.546
9	2.569	3.096	3.606	0.610	-0.527
10	2.884	3.404	3.914	0.511	-0.519
11	3.199	3.712	4.214	0.502	-0.512
12	3.508	4.020	4.480	0.460	-0.512
13	3.816	4.305	4.750	0.445	-0.489
14	4.124	4.571	5.121	0.550	-0.447
15	4.395	4.877	5.541	0.663	-0.482
16	4.662	5.265	6.104	0.839	-0.604
17	5.003	5.735	6.534	0.799	-0.732
18	5.404	6.118	6.870	0.752	-0.714
19	5.914	6.501	7.205	0.704	-0.587
20	6.428	6.883	7.540	0.657	-0.456
21	6.763	7.266	7.897	0.631	-0.503
22	7.098	7.707	8.669	0.962	-0.608
23	7.434	8.256	9.050	0.794	-0.822
24	7.760	8.805	9.403	0.598	-1.045
25	8.524	9.171	9.806	0.635	-0.647
26	8.937	9.532	10.222	0.689	-0.595
27	9.291	9.948	10.589	0.641	-0.657
28	9.674	10.347	10.956	0.610	-0.673
29	10.090	10.712	11.324	0.612	-0.622
30	10.472	11.077	11.691	0.614	-0.605
31	10.840	11.442	12.057	0.614	-0.603
32	11.207	11.808	12.422	0.614	-0.601
33	11.574	12.173	12.787	0.614	-0.599
34	11.940	12.539	13.153	0.614	-0.598
35	12.306	12.904	13.492	0.588	-0.598
36	12.671	13.270	13.829	0.559	-0.599

Table LM10/4.7.5-2 Propellant Quantity Gaging System GC3604Q Fuel Tank No 2 Reading Error By PCM Bit

PCM BITS	PCM QUANTITIES			INSTANTANEOUS PCM ERROR	
	LOW	NOM	HIGH	POSITIVE	NEGATIVE
1	0.0	0.000	0.757	0.756	0.000
2	0.0	0.131	0.513	0.381	-0.131
3	0.0	0.262	0.917	0.655	-0.262
4	0.0	0.669	1.291	0.622	-0.669
5	0.390	1.082	1.650	0.567	-0.692
6	0.793	1.496	2.224	0.728	-0.703
7	1.176	1.910	2.602	0.692	-0.734
8	1.535	2.308	2.943	0.635	-0.773
9	1.944	2.667	3.286	0.619	-0.723
10	2.493	3.025	3.634	0.609	-0.532
11	2.834	3.384	3.983	0.599	-0.550
12	3.176	3.743	4.313	0.570	-0.567
13	3.524	4.101	4.623	0.521	-0.578
14	3.872	4.419	4.981	0.562	-0.547
15	4.214	4.729	5.388	0.659	-0.514
16	4.524	5.114	5.917	0.803	-0.590
17	4.858	5.584	6.448	0.863	-0.726
18	5.251	5.996	6.778	0.783	-0.745
19	5.708	6.384	7.109	0.725	-0.676
20	6.342	6.773	7.440	0.667	-0.430
21	6.673	7.161	7.805	0.644	-0.488
22	7.004	7.559	8.626	1.067	-0.555
23	7.335	8.162	9.014	0.853	-0.827
24	7.680	8.764	9.368	0.604	-1.084
25	8.469	9.147	9.764	0.616	-0.679
26	8.902	9.490	10.180	0.690	-0.588
27	9.255	9.906	10.561	0.654	-0.651
28	9.632	10.313	10.938	0.625	-0.682
29	10.048	10.692	11.315	0.623	-0.644
30	10.441	11.070	11.691	0.621	-0.629
31	10.818	11.449	12.057	0.608	-0.631
32	11.195	11.819	12.422	0.603	-0.625
33	11.572	12.179	12.787	0.609	-0.607
34	11.940	12.538	13.153	0.615	-0.598
35	12.306	12.897	13.497	0.600	-0.591
36	12.671	13.256	13.839	0.583	-0.585

Table LM10/4.7.5-3 Propellant Quantity Gaging System GC4103Q Oxid Tank No 1 Reading Error By PCM Bit

PCM BITS	PCM QUANTITIES			INSTANTANEOUS PCM ERROR	
	LOW	NOM	HIGH	POSITIVE	NEGATIVE
1	0.0	0.000	0.211	0.211	0.000
2	0.0	0.159	0.627	0.468	-0.159
3	0.0	0.376	0.987	0.611	-0.376
4	0.0	0.743	1.337	0.594	-0.743
5	0.487	1.109	1.684	0.575	-0.622
6	0.872	1.449	2.146	0.697	-0.577
7	1.227	1.789	2.576	0.787	-0.562
8	1.574	2.333	2.909	0.576	-0.759
9	1.926	2.694	3.242	0.548	-0.769
10	2.470	3.025	3.583	0.559	-0.555
11	2.803	3.359	3.925	0.565	-0.556
12	3.136	3.700	4.253	0.553	-0.564
13	3.475	4.041	4.554	0.512	-0.566
14	3.816	4.351	4.877	0.526	-0.535
15	4.157	4.644	5.274	0.631	-0.487
16	4.458	5.112	6.384	1.273	-0.654
17	4.763	5.644	6.685	1.041	-0.882
18	5.122	6.085	6.986	0.901	-0.963
19	6.037	6.504	7.287	0.783	-0.467
20	6.590	6.922	7.590	0.668	-0.333
21	6.890	7.341	7.912	0.571	-0.451
22	7.191	7.678	8.640	0.963	-0.486
23	7.492	8.177	9.034	0.857	-0.684
24	7.804	8.781	9.368	0.586	-0.977
25	8.288	9.141	9.748	0.607	-0.853
26	8.928	9.482	10.153	0.671	-0.554
27	9.262	9.887	10.522	0.636	-0.625
28	9.619	10.283	10.885	0.602	-0.664
29	10.024	10.644	11.248	0.603	-0.620
30	10.407	11.005	11.610	0.605	-0.599
31	10.769	11.366	11.968	0.601	-0.597
32	11.132	11.727	12.325	0.598	-0.594
33	11.495	12.082	12.681	0.599	-0.588
34	11.854	12.438	13.038	0.600	-0.584
35	12.211	12.794	13.386	0.592	-0.583
36	12.568	13.150	13.728	0.578	-0.582

Table LM10/4.7.5-4 Propellant Quantity Gaging System GC4104Q Oxid Tank No 2 Reading Error By PCM Bit

PCM BITS	PCM QUANTITIES			INSTANTANEOUS PCM ERROR	
	LOW	NOM	HIGH	POSITIVE	NEGATIVE
1	0.0	0.000	0.211	0.211	0.000
2	0.0	0.138	0.492	0.353	-0.138
3	0.0	0.282	0.859	0.578	-0.282
4	0.0	0.619	1.222	0.603	-0.619
5	0.390	0.978	1.591	0.613	-0.589
6	0.745	1.337	1.951	0.614	-0.593
7	1.105	1.697	2.511	0.814	-0.592
8	1.473	2.209	2.851	0.641	-0.736
9	1.826	2.631	3.191	0.559	-0.805
10	2.402	2.969	3.526	0.557	-0.567
11	2.742	3.306	3.861	0.555	-0.563
12	3.083	3.641	4.191	0.550	-0.558
13	3.420	3.976	4.484	0.508	-0.556
14	3.755	4.288	4.788	0.500	-0.534
15	4.089	4.573	5.162	0.589	-0.484
16	4.391	4.987	6.244	1.257	-0.596
17	4.684	5.542	6.624	1.083	-0.858
18	5.043	6.014	6.941	0.927	-0.971
19	5.629	6.443	7.258	0.815	-0.814
20	6.524	6.872	7.572	0.700	-0.349
21	6.840	7.302	7.872	0.570	-0.461
22	7.157	7.718	8.406	0.689	-0.561
23	7.474	8.118	9.009	0.892	-0.644
24	7.773	8.558	9.361	0.804	-0.785
25	8.213	9.026	9.741	0.715	-0.813
26	8.897	9.494	10.134	0.641	-0.596
27	9.249	9.881	10.511	0.630	-0.632
28	9.616	10.266	10.883	0.617	-0.651
29	10.009	10.637	11.255	0.618	-0.628
30	10.393	11.008	11.628	0.620	-0.615
31	10.765	11.379	11.994	0.615	-0.614
32	11.137	11.748	12.359	0.611	-0.611
33	11.509	12.109	12.724	0.615	-0.600
34	11.878	12.471	13.090	0.619	-0.593
35	12.243	12.833	13.438	0.605	-0.590
36	12.608	13.194	13.780	0.586	-0.586

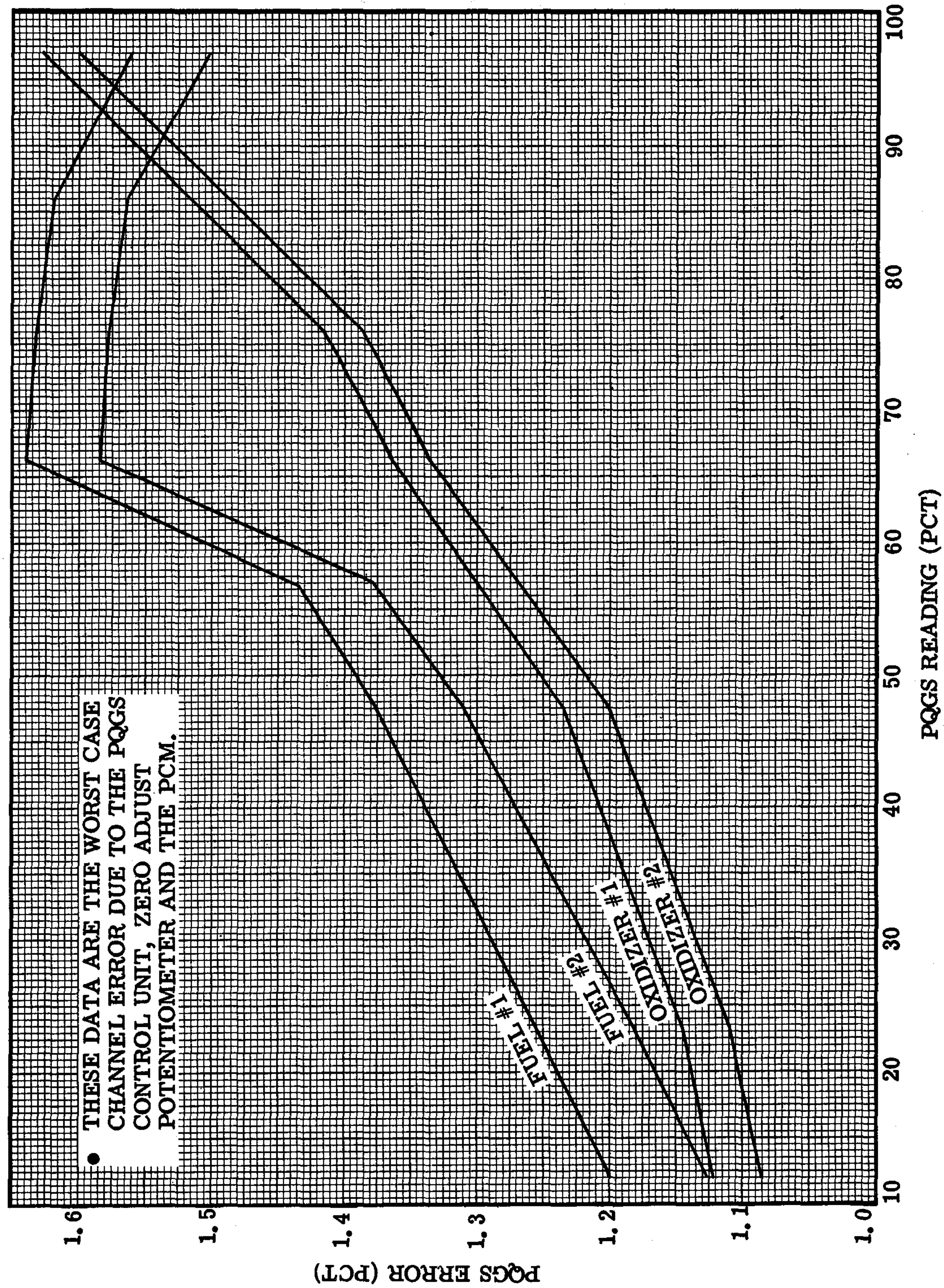

Figure LM10/4.7.5-1 PQGS Error vs. Quantity (Above 12%) (See Para. LM10/4.7.5)

LM10/4.7.6.1 DPS Engine Thrust Vector Alignment

The gimbal trim angles for the DPS engine may be calculated using the equations provided in Paragraph 4.7.6.1. The thrust vector angles of the DPS engine at the start of the PDI burn are given in the Spacecraft Operational Data Book, Volume III, Mass Properties, Revision 3, as:

$$\delta\theta_T = +0.659 \text{ degress}$$

$$\delta\psi_T = +0.767 \text{ degrees}$$

These values, together with a startup thrust of 1300 pounds, were then used to calculate the gimbal trim angles:

$$\delta\theta = +0.595 \text{ degrees}$$

$$\delta\psi = +0.831 \text{ degrees}$$

These are the recommended launch pad settings for the DPS gimbal trim angles at the start of the PDI burn.

The trim angles are set using the LM Guidance Computer (LGC), and must be expressed referenced to the positive gimbal stops. To accomplish this, 6.05 degrees were added to the trim angles above.

This results in

$$\delta\theta' = 6.645 \text{ degrees}$$

$$\delta\psi' = 6.881 \text{ degrees}$$

both referred to the positive gimbal stops.

The LGC has a nominal drive rate of 0.2000 degrees/second hard-wired into it. Therefore, all actual gimbal angles must be converted to equivalent angles based on the hard-wired drive rate using the actual gimbal drive rates in both pitch and roll. Where entered via the LGC erasable memory load, the angles must be expressed as drive times (from the positive stops). Where entered or displayed on the DSKY the equivalent angles must be expressed as degrees of arc.

LM10/4.7.6.1 DPS Engine Thrust Vector Alignment (Continued)

The GDA drive rates are listed below.

Functional Axis	Drive Rate
Pitch (X-Z plane)	0.2112 deg/sec
Roll (X-Y plane)	0.2125 deg/sec

The gimbal trim data to be entered in the LGC erasable memory load are then obtained as follows:

$$\text{PITTIME} = \frac{\delta\theta'}{0.2112} = 31.46 \text{ seconds}$$

$$\text{ROLLTIME} = \frac{\delta\psi'}{0.2125} = 32.38 \text{ seconds}$$

The corresponding angles to be entered or read from the DSKY are obtained as follows:

$$\text{P-TRIM} = \delta\theta' \left(\frac{0.2000}{0.2112}\right) = 6.293 \text{ degrees}$$

$$\text{R-TRIM} = \delta\psi' \left(\frac{0.2000}{0.2125}\right) = 6.476 \text{ degrees}$$

LM10/4.7.8 Descent Propulsion Pre-Flight Thermal Analysis

The LM-10 engine differs from previous DPS engines in that it has a 10" nozzle extension which affects the thermal environment. The clearance between the nozzle exit plane and the lunar surface for the nominal thermal case is 2". Figures LM10/4.7.8-1 through LM10/4.7.8-6 show the soakback temperature response of important engine components and interface boundaries for the descent stage. The nominal burn profile lasts for 785 seconds. Additional engine temperatures are contained in LMO 510-1848.

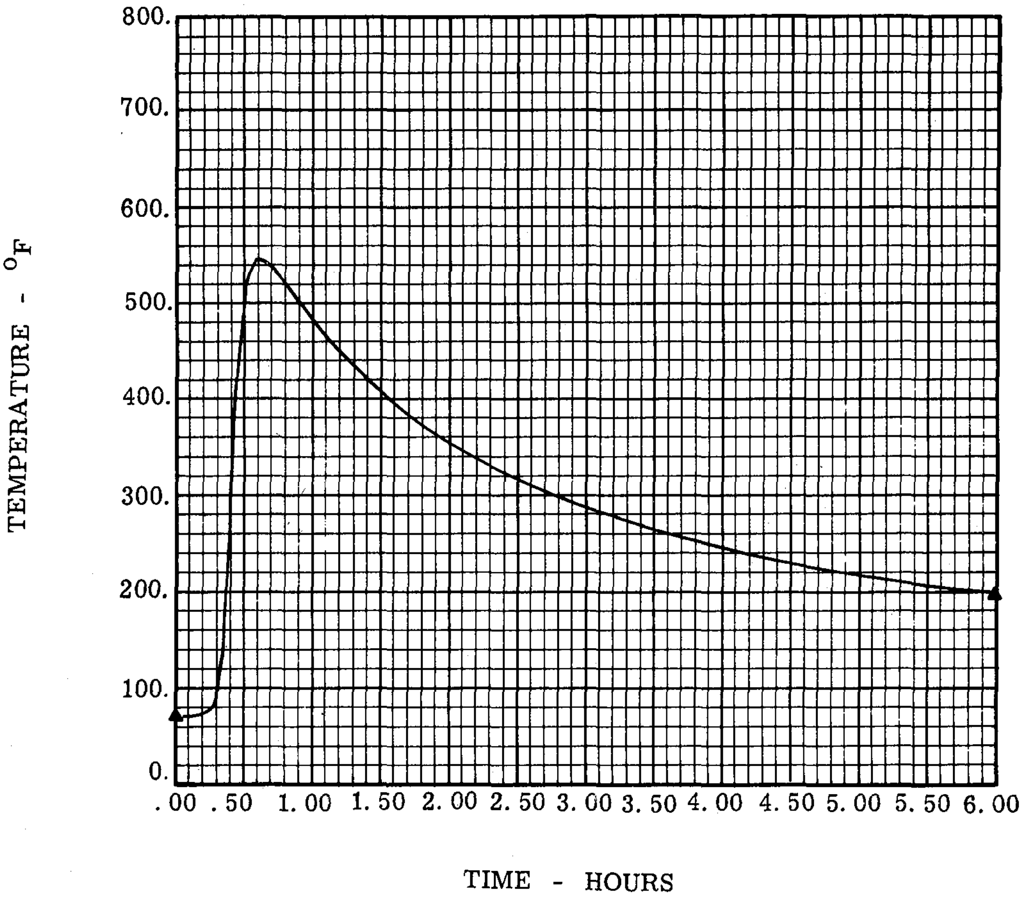

Figure LM10/4.7.8-1. Radiation Heat Shield, Node 82

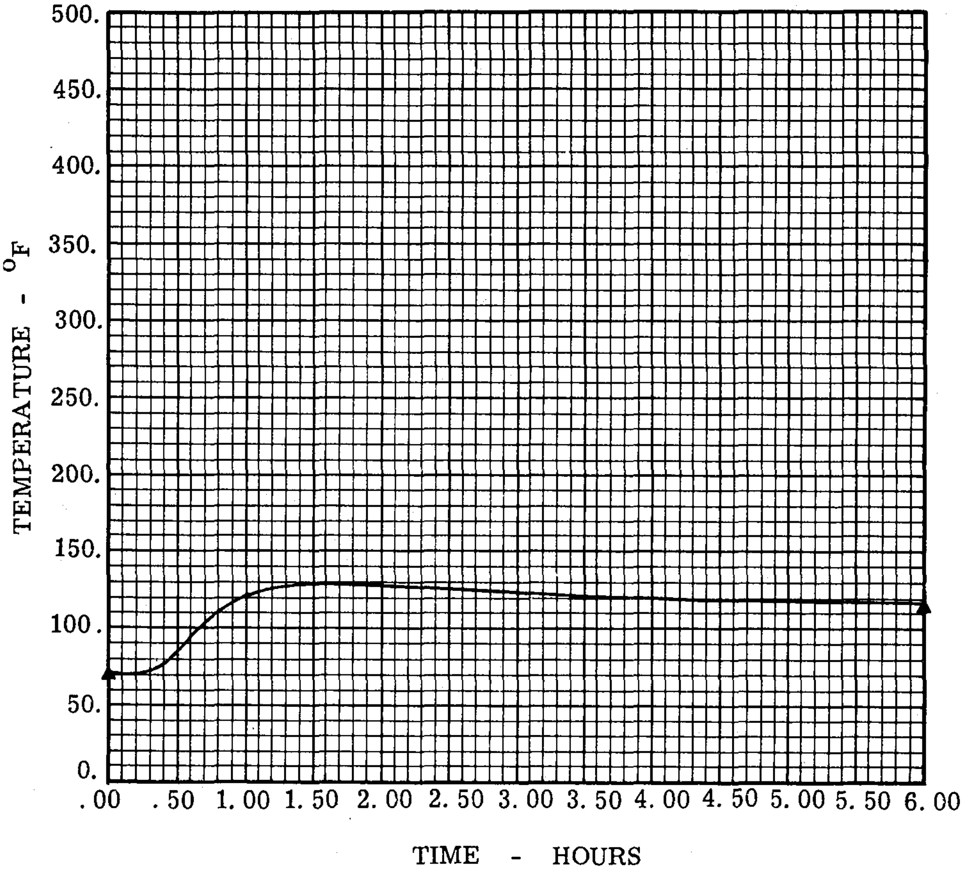

Figure LM10/4.7.8-2. Engine Bay Wall, Node 99

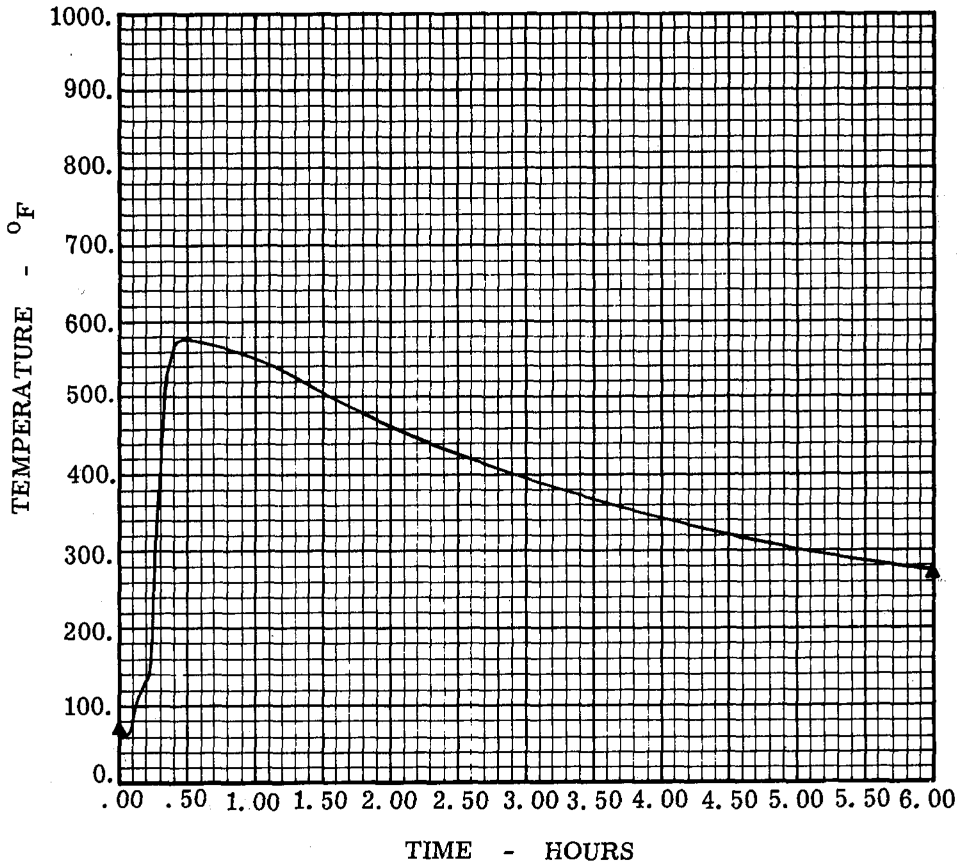

Figure LM10/4.7.8-3. Injector, Node 106

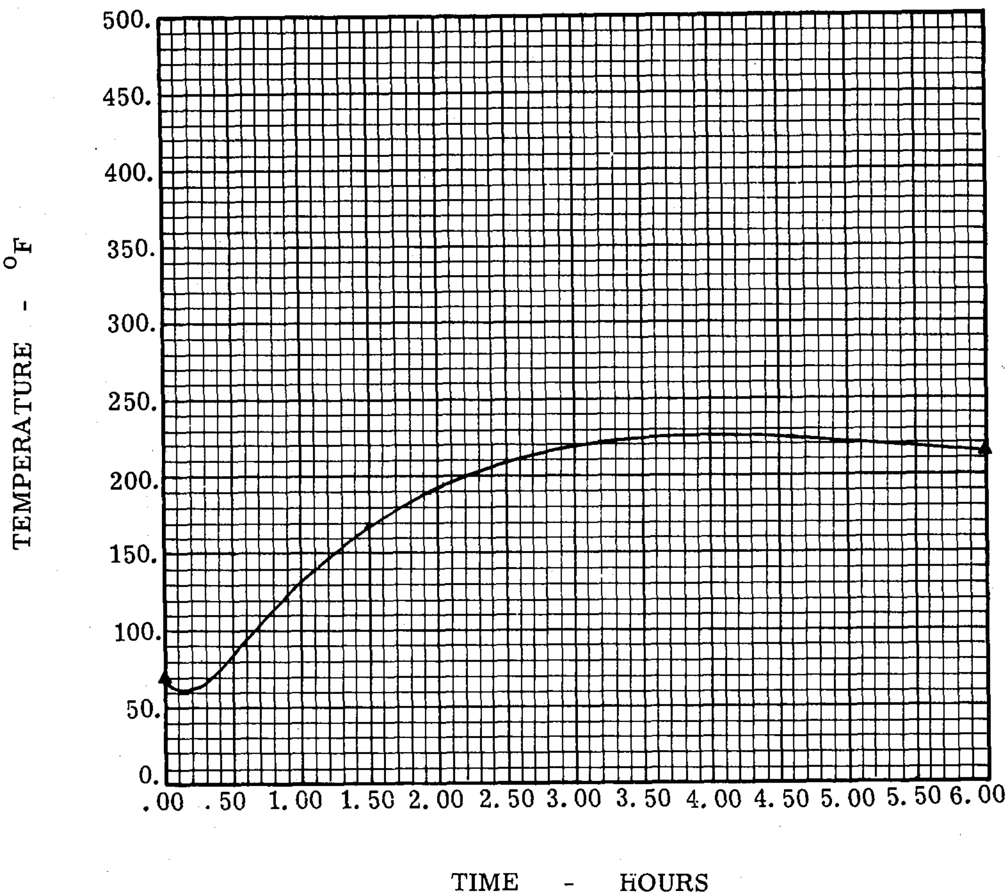

Figure LM10/4.7.8-4. Fuel Shut off Valve, Node 121

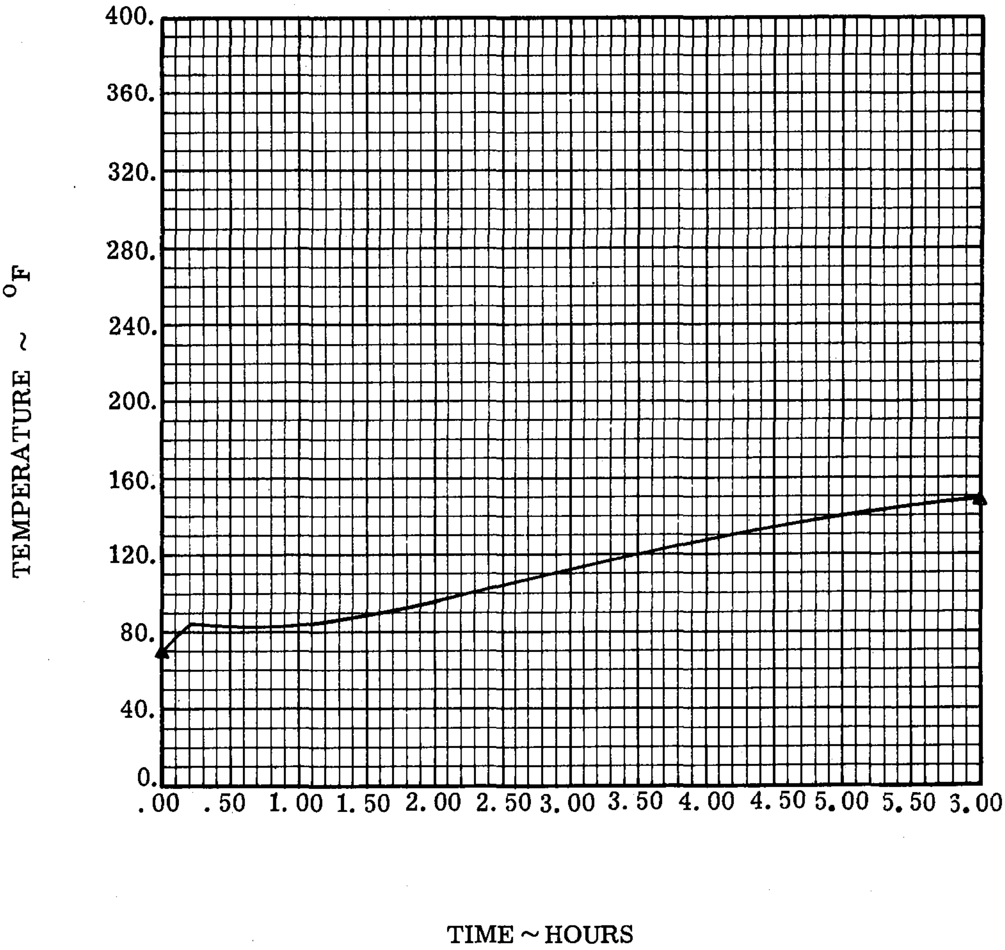

Figure LM10/4.7.8-5. Throttle Actuator, Node 128

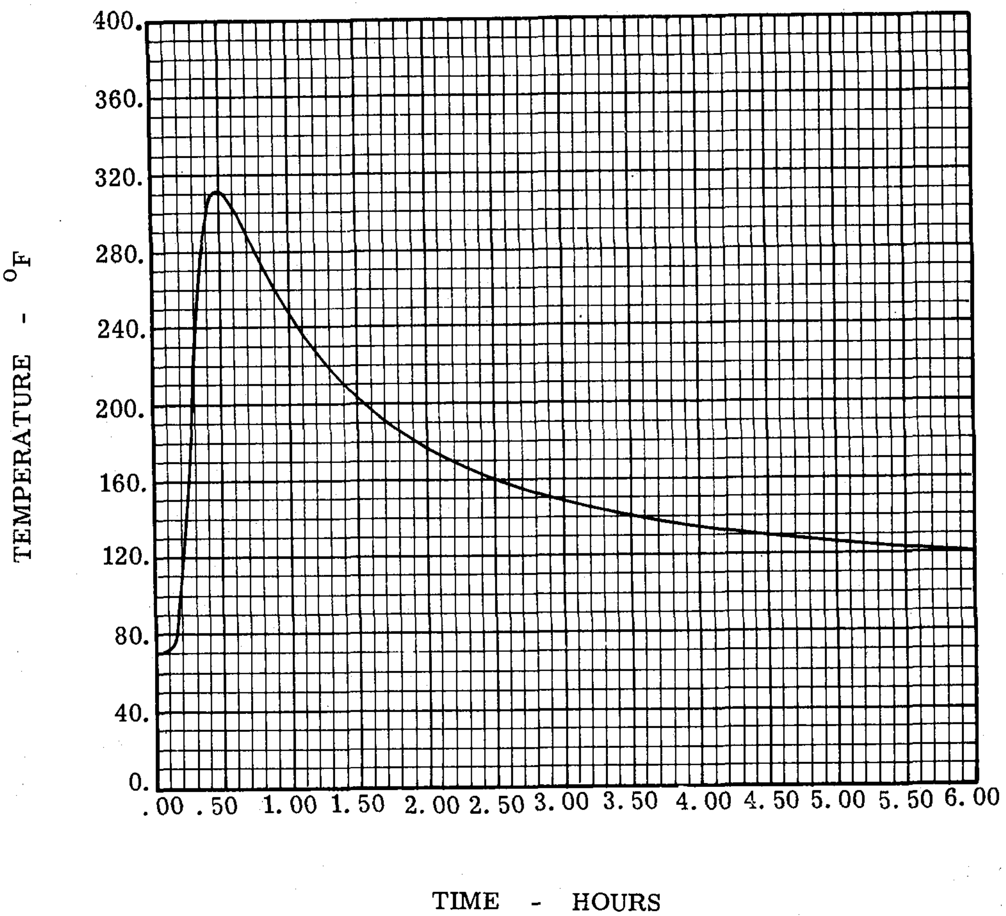

Figure LM10/4.7.8-6. Interior Base Heat Shield, Node 237

LM10/4.7.12.1 DPS Propellant Tank Contingency Venting

The times to reach fracture mechanics limits (FML) if the lunar dump valve failed to depressurize the tanks shortly after touchdown are presented herein.

The pressure history of the DPS propellant tanks after lunar touchdown is dependent on 1) engine burn time, 2) distance of the descent stage from the lunar surface and 3) residual propellants remaining.

Figure LM10/4.7.12-1 shows the oxidizer pressure time history under conditions of maximum thermal severity for fracture mechanics limits of 100% and 95%, and the expected ullage pressure time history when no venting occurs. No curves are presented for the fuel and oxidizer tanks in a thermally nominal landing and fuel maximum severity landing, since no constraints exist for those cases.

For the condition in which no venting occurs the limiting time is the time it takes for the ullage pressure curve to intersect the FML curve.

Table LM10/4.7.12-1 summarizes the time to reach the FML for the oxidizer maximum severity case.

Table LM10/4.7.12-1. LM-10 DPS Propellant Tanks - Maximum Allowable Standby Times For The No-Vent Case

FRACTURE MECHANICS LIMITS	LANDING OF MAXIMUM THERMAL SEVERITY *	
	OXIDIZER TANK SEE FIGURE LM10/4.7.12-1	
	ULLAGE PRESSURE	TIME TO REACH FRACTURE MECHANICS LIMITS
	PSIA	HOURS FROM TOUCHDOWN
100%	Pressure Relief 263 - 268 297.5 (max. allow.)	 ∞ 3.3
95%	Pressure Relief 263 - 268 302.5 (max. allow.)	 ∞ 4.4
85%	Pressure Relief 263 - 268 320 (max. allow.)	 ∞ ∞

* Crushed nozzle
850 seconds burn
Zero residuals
Vapor pressure
Sun angle on -Z (ox), -Y (fuel) 12° above the horizon.

Contract No. NAS 9-1100
Primary No. 664
Grumman Aerospace Corporation

MAXIMUM THERMAL SEVERITY - NO VENT CASE
LM10 DPS OXIDIZER TANK (+Z, NO. 2)

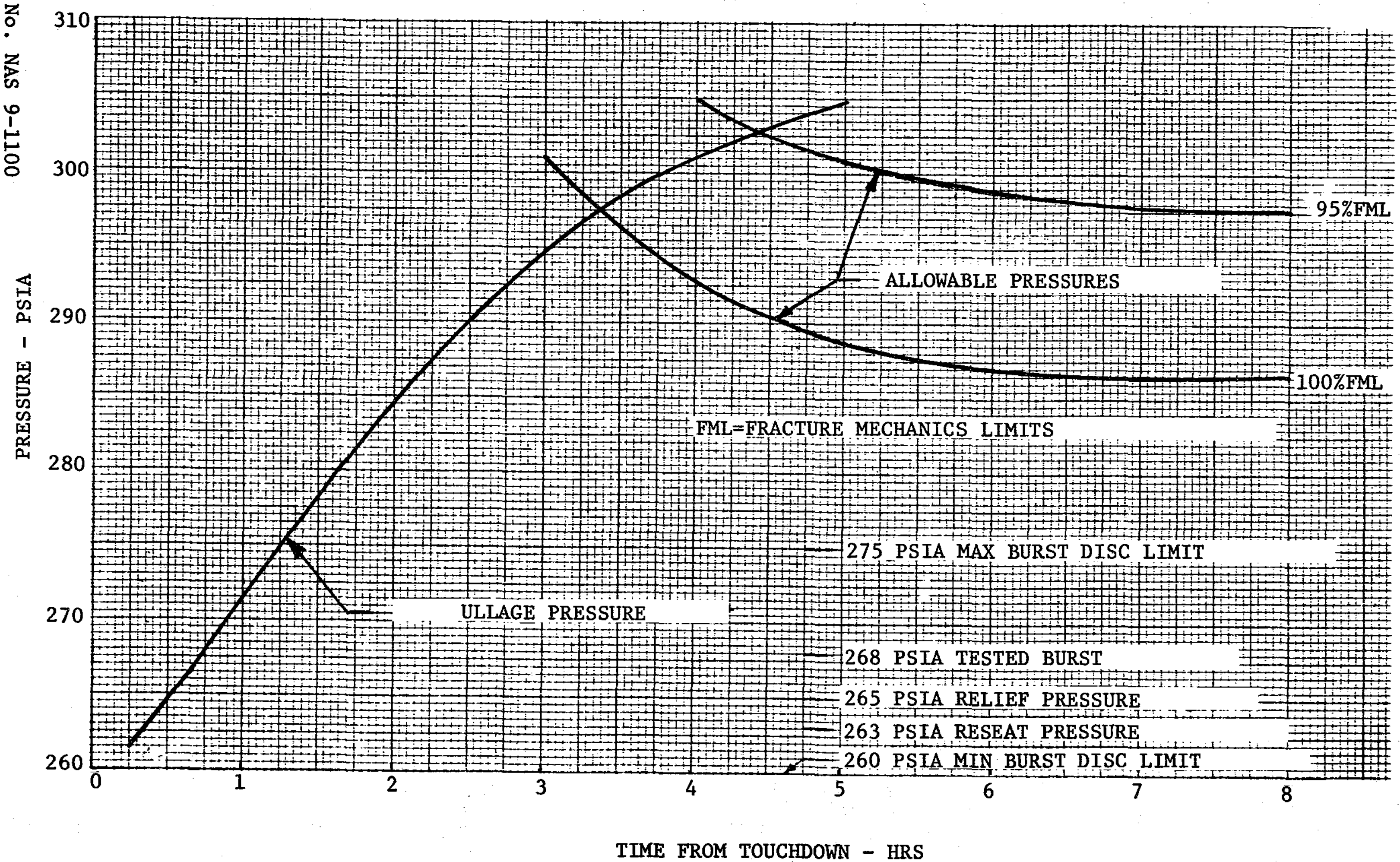

Figure LM10/4.7.12-1. Ullage Pressure and Allowable Pressure vs. Time from Touchdown

LM10/4.7.15 Descent Propulsion System Regulator Performance

Figure LM10/4.7.15-1 shows performance characteristics for LM-10 descent engine regulator, Serial No. 129.

• SERIAL NO. 129

LEGEND: APPLIES TO LEG 1 AND LEG 2
⊡ 400 PSIG INLET PRESS. } PIT DATA
⊙ 1700 PSIG INLET PRESS. }
◇ 900 PSIG INLET PRESS. -KSC CHECKOUT
KSC LOCK-UP PRESS. = 248 PSIA (LEG 2)
246. 5 PSIA (LEG 1)

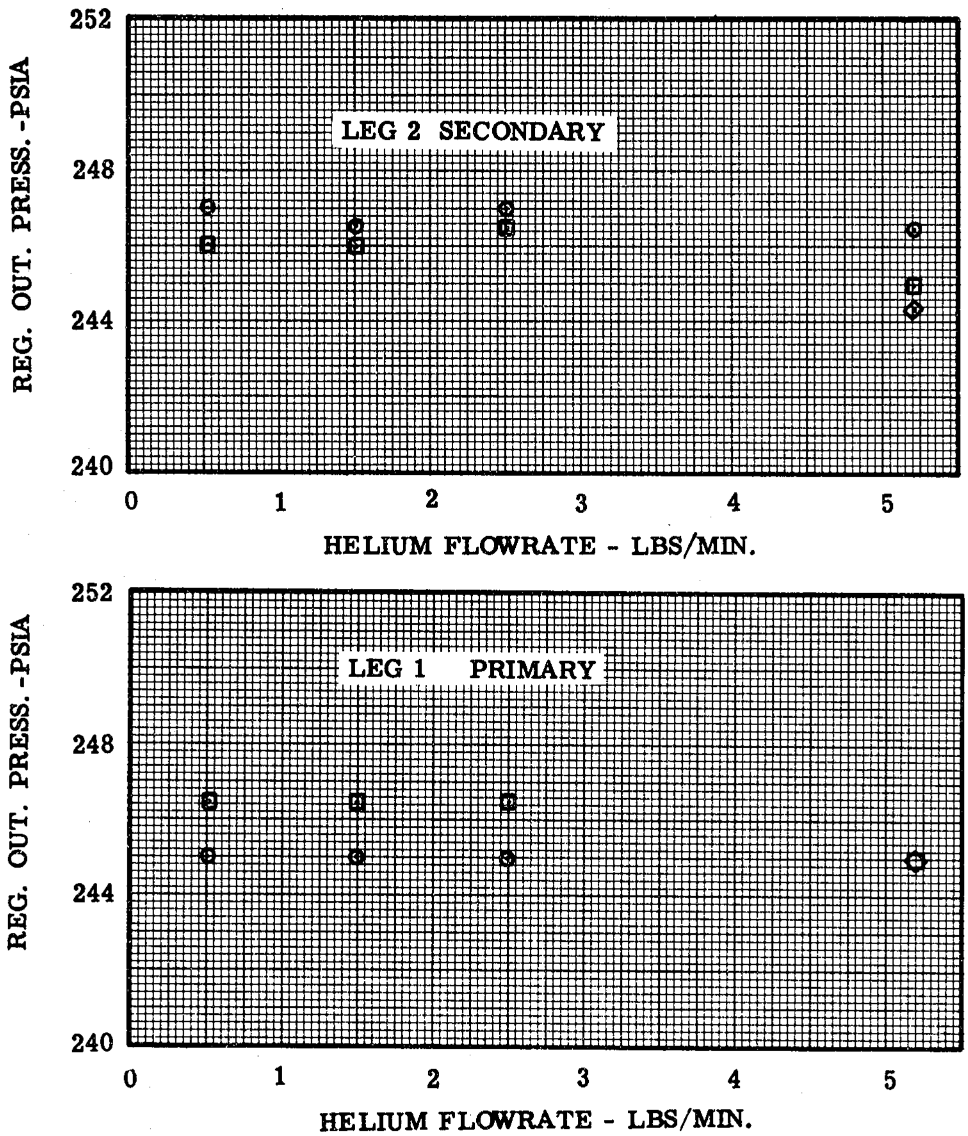

Figure LM10/4. 7. 15-1. Descent Propulsion System Regulator Performance

LM10/4.8.14 RCS Performance Limitations as a Result of Gimbal Drive Actuator (+ Pitch or + Roll) Failure During Powered Descent

LM10/4.8.14.1 Plume Impingement Constraints Due to GDA Failure

Figure LM10/4.8.14-1 shows the maximum allowable GDA offset angles as limited by the RCS impingement constraints for the affected vehicle hardware. These curves were developed from the LM-10 plume impingement capability curves. (See Figures 4.8-106 through 4.8-119.)

In the event of GDA failure during powered descent, RCS plume impingement may constrain the mission. Figure LM10/4.8.14-2 represents the maximum allowable accumulated RCS firing time at any juncture during powered descent for GDA failure at several different times. The curves represent the duty cycles which cause failure of the plume deflectors. Note that the attainment of the duty cycles reflected by these curves will exceed the plume impingement capability of the S-band steerable antenna, EVA antenna, SEQ, ladder rung, and quad III and IV MESA. Figure LM10/4.8.14-3 presents a curve similar to Figure LM10/4.8.14-2 but for the ladder rung assuming a factor of safety of 1.5. Figure LM10/4.8.14-2 is a landing constraint, whereas Figure LM10/4.8.14-3 might be a constraint for an EVA.

LM10/4.8.14.2 Additional RCS Propellant Consumption as a Result of Gimbal Drive Actuator Failure During Powered Descent

Figures LM10/4.8.14-4 and LM10/4.8.14-5 present the maximum allowable GDA pitch and roll angles at time of failure, considering the margin of RCS propellant at landing and the RCS limited torque authority. (See Paragraph 4.8.14.2.)

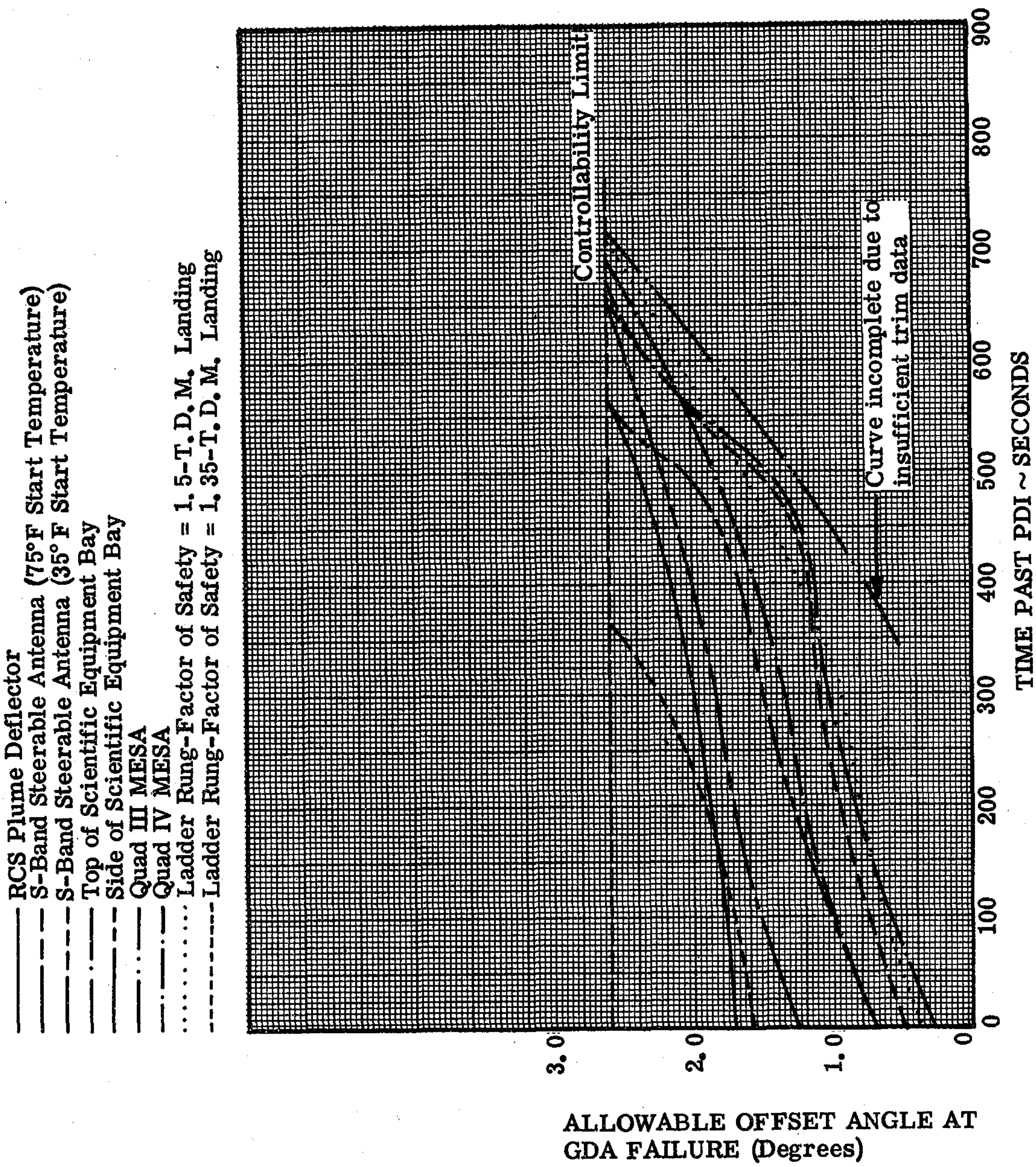

Figure LM10/4.8.14-1. Allowable GDA Offset Angle (at GDA Failure) During Powered Descent (as Determined by RCS Plume Impingement Limit) (See Para. LM10/4.8.14.1)

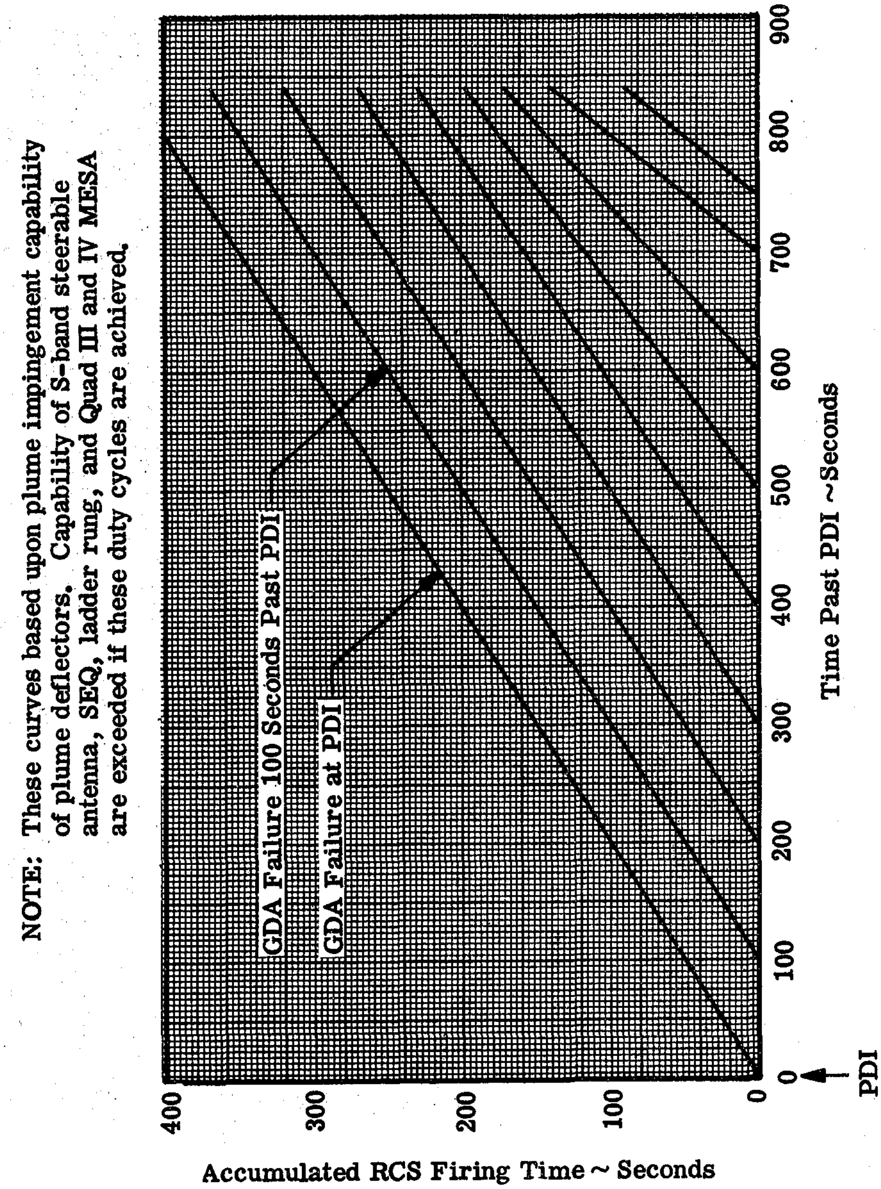

Figure LM10/4.8.14-2. Maximum Allowable Accumulated RCS Firing Time per -X or +X RCS Engine vs Time Past PDI of a GDA Failure (See Para. LM10/4.8.14.1)

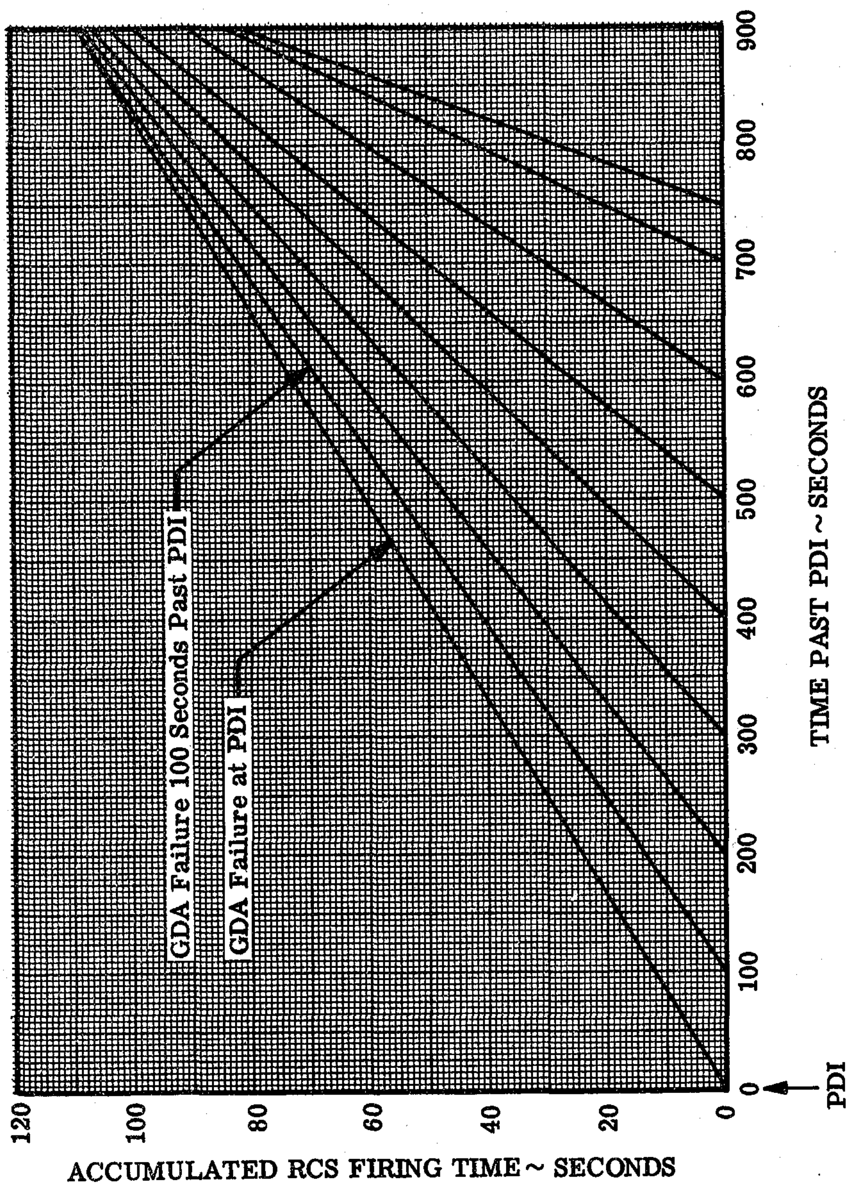

Figure LM10/4.8.14-3. Maximum Allowable Accumulated RCS Firing Time per -X or +X RCS Engine vs Time Past PDI of a GDA Failure for the Ladder Rungs with a Factor of Safety of 1.5

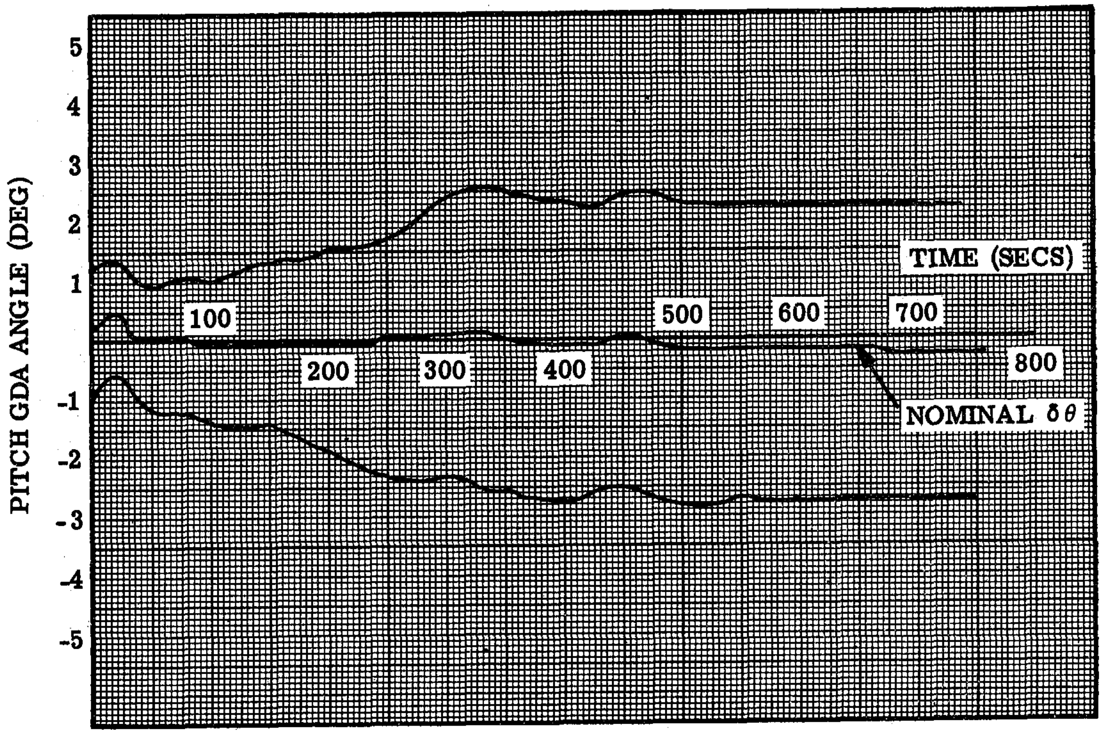

• ASSUMES 140 LBM RCS PROPELLANT REMAINING AT TOUCHDOWN

Figure LM10/4.8-14.4. Maximum Allowable Pitch GDA Failure Angle vs. Time During Powered Descent LM-10

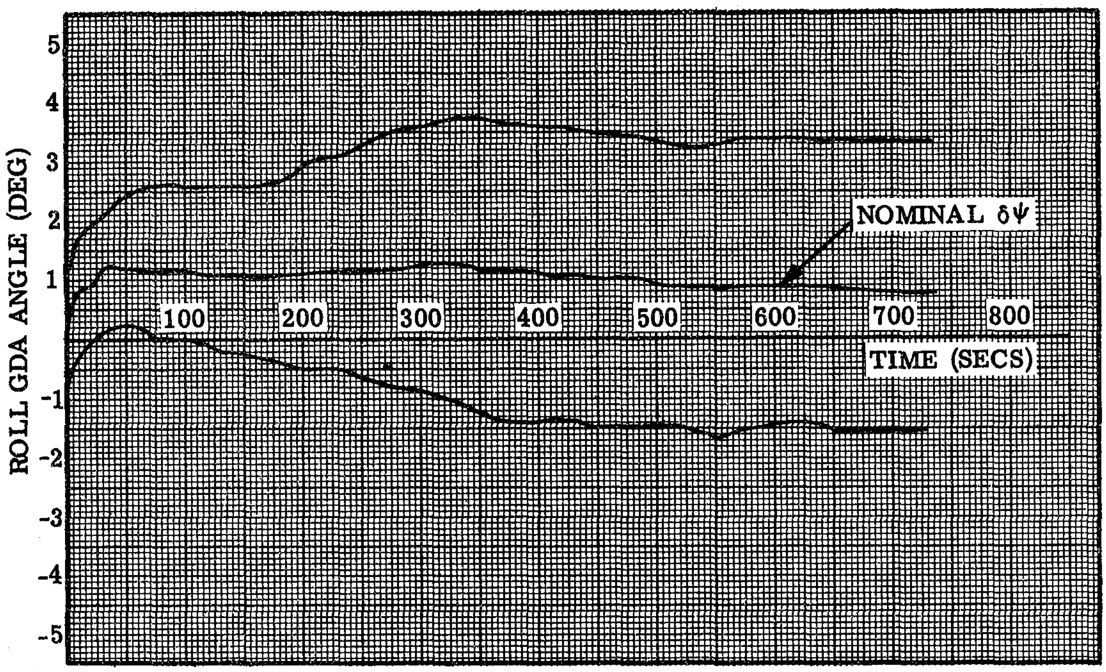

• ASSUMES 140 LBM RCS PROPELLANT REMAINING AT TOUCHDOWN

Figure LM10/4.8-14.5. Maximum Allowable Roll GDA Failure Angle vs. Time During Powered Descent LM-10

LM10/8.1 Descent Tank Slosh Data

Due to the larger volume of the LM-10 descent stage propellant tanks, the slosh parameters have changed from those of the earlier vehicles (see Para. 8.0). Table LM10/8.1-1 presents the slosh parameters for the enlarged tanks.

Table LM10/8.1-1. Descent Stage Propellant Tanks Slosh Functions

Fraction of Propellant in Tank	Ratio:Slosh Mass to Max Prop. Mass	λ, Frequency Parameter	Support Position*
0.0	0.00	1.00	-0.22
0.1	0.08	1.10	-0.22
0.2	0.14	1.16	-0.22
0.3	0.17	1.22	-0.20
0.4	0.19	1.30	-0.17
0.5	0.20	1.34	-0.13
0.6	0.21	1.35	-0.05
0.7	0.20	1.35	0.02
0.8	0.18	1.36	0.10
0.9	0.15	1.52	0.21
1.0	0.00	2.50	0.22

*Support Position is ratio of pendulum support distance (measured from tank center positive toward the top) to the tank diameter.

Reference: LMO-500-721, "Mechanical Model Representation of the LMMP Descent Stage Propellant Sloshing", 1 August 1969.